ISSN:1390-9347

Bionatura

Ibero - American journal of Biotechnology and Life Sciences

2 CIICTAV
CONGRESO INTERNACIONAL
DE INNOVACIÓN, CIENCIA Y TECNOLOGÍA
AMAZONÍA VIVA

Del 22 al 24 de noviembre de 2023

Espoch Sede Orellana · ITSO Universitario · ISPIBMBR · ISTGEA Instituto Superior Tecnológico General Eloy Alfaro · INIAP

Scopus Publons · UCO Universidad Católica de Oriente · CEBA

Bionatura
Ibero-American Journal of Biotechnology and Life Sciences

Editorial

Coexistencia de procesos productivos y de conservación en la Amazonía ecuatoriana

Co-existence of productive and conservation processes in the Ecuadorian Amazonia

Maritza Sánchez-Capa[1*]; *Hilda Fabiola Anguaya Isama*[2]
[1] *Escuela Superior Politécnica de Chimborazo - Sede Orellana, El Coca Ecuador*
[2] *Instituto Superior Tecnológico Martha Bucaram de Roldós, Nueva Loja, Ecuador*
* *Correspondence: maritzac.sanchez@espoch.edu.ec*
Available from. http://dx.doi.org/10.21931/RB/2024.09.01.1

La región amazónica de Ecuador está conforma por las provincias Sucumbíos, Orellana, Napo, Pastaza, Morona Santiago y Zamora Chinchipe, su extensión es de ~120.000 Km^2 [1]. En las dos últimas décadas, la educación superior se ha implementado en cada una de las provincias, buscando responder a las necesidades de profesionales en los diferentes sectores que constituyen las actividades económicas principales de cada provincia. Sucumbíos y Orellana son provincias que sustentan su economía en la producción petrolera, sin embargo, en esta superficie se encuentran áreas protegidas como la reserva de la biósfera YASUNÍ, parque nacional Cuyabeno, reserva Limoncocha, que son áreas con una gran biodiversidad por lo que la coexistencia entre conservación y producción industrial generan una búsqueda consante de alternativas sustentables y sostenibles [2].

Esta editorial muestra alternativas productivas sustentables que involucra los recursos y biodiversidad propios de la región. Este número especial comprenden la publicación de veinte artículos de investigación originales que abordan el uso de los recursos, mejoras en la producción agrícola y uso de tecnologías innovadoras, buscan responder a la necesidad de difundir los trabajos de investigación de los actores locales, nacionales e internacionales para la generación de articulación interinstitucional en pro del desarrollo de la Amazonía ecuatoriana. Estos trabajos fueron presentados en el II Congreso Internacional de Innovación, Ciencia y Tecnología "AMAZONIA VIVA" (CIICTAV) [3].

El CIICTAV es un Congreso que se desarrolla desde el año 2022 en la Amazonía norte del Ecuador, en la provincia de Sucumbíos y Orellana, que busca reunir de manera anual a investigadores cuyos trabajos tengan impacto en la región para que estudiantes, docentes, investigadores, empresarios y todas las personas interesadas en aprender o actualizar conocimientos asociados a las áreas de Ciencias, Ingeniería, Agropecuaria, Servicios, Salud y Educación tengan un espacio para compartir ideas y promover el desarrollo de la región [3].

La producción agropecuaria, después de la producción petrolera es una de las actividades relevantes en la economía de las provincias de Sucumbíos y Orellana esto se refleja en el trabajo Fighting moniliasis in Orellana with sensors and PWA for sustainable agriculture, cuyo objetivo fue mejorar la producción y la calidad del cacao en países tropicales, enfocandose principalmente en el control de la moniliasis, una enfermedad fúngica que afecta a los frutos del cacao y provoca un importante descenso de la producción y la calidad del cultivo. Este trabajo empleó un enfoque multidisciplinar que combinaba sensores, bases de datos MongoDB Compass, aplicaciones web progresivas (PWA) y modelos predictivos, lo que permitió la detección

precoz de la moniliasis para adoptar medidas preventivas y correctivas más precisas, lo que se tradujo en una mejora significativa de la producción y la calidad del cacao [4].

El cacao es uno de los cultivos más relevantes en la región debido a que contribuye con el 8% de las exportaciones de productos no petroleros tradicionales del Ecuador [5] es por eso que trabajos como Cocoa moniliasis prevention using Progressive Web Applications and sensor data in Francisco de Orellana Province y Predictive Model in Production through Progressive Web Applications to Forecast Moniliasis in Cacao,permitieron establecer el método ensemble Boosting con un valor de 1,0 y 4 en estimadores,el algoritmo que muestra un mejor ajuste para la predicción de Moniliasis del cacao y el desarrollo de una aplicación web progresiva que se puso a disposición de los agricultores para su uso público, constituyeron un gran aporte para el sector cacaotero de la región [6].

Otro de los cultivos relevantes en la región amazónica es el de pitahaya tanto amarilla como roja puesto que son productos de exportación no tradicionales y se encuentra dentro del top 10 de exportaciones de mayor crecimiento en Ecuador [5]. Por lo tanto, investigaciones como Biological nematicides as an alternative for control of Meloidogyne incognita populations in yellow pitahaya (Selenicereus megalanthus) que demostró que cuando se aplica P. lilacinum + T. asperellum después de la inoculación de nemátodos, el número de nódulos radiculares disminuye, así como Hylocereus undatus reproductive phenology in the Northern Ecuadorian Amazon que identificó los estadíos fenológicos de Hylocereus undatus para comprender el funcionamiento reproductivo de la planta cultivada en tutores vivos, estableciendo que el periodo desde la aparición de la yema reproductora hasta la recolección del fruto dura 55 días y que los soportes no influyeron en las fases de desarrollo reproductivo, floración y desarrollo del fruto, pero sí afectaron a la fase de maduración del fruto de tal modo que las plantas cultivadas sobre soportes inertes produjeron frutos de mayor diámetro y longitud, mientras que las plantas cultivadas sobre soportes vivos mostraron un mayor contenido en sólidos solubles [7].

Cultivos de menor relevancia económica pero que contribuyen a la seguridad y soberanía alimentaria como naranja agria y pepino [8] también fueron considerados en las investigaciones, es así que el trabajo de Evaluación de parámetros de calidad de naranja (Citrus × sinensis) en tres estados de madurez, a través del análisis de parámetros como peso, morfometría, color, firmeza y sólidos solubles de la fruta estableció que el estado de madurez medio es recomendable para la cosecha, puesto que ofrece un equilibrio entre alto contenido de azúcar, peso y tamaño adecuados para el consumidor. El trabajo Evaluación del desempeño del cultivo de pepino (Cucumis sativus) frente a tres fertilizantes foliares en la parroquia Nuevo Paraíso, Orellana, Ecuador determinó que el fertilizante Evergreen es una opción de fertilización rentable con un costo-beneficio de $1,27 y que contribuye a mejorar las características de planta y fruto [9].

En la producción agroecológica entre las aristas que permiten el desarrollo de una agricultura más limpia es el manejo de plagas a través de factores biológicos y la fertilización con insumos orgánicos y si se considera que los ecosistemas amazónicos por sus condiciones edafoclimáticas y biodiversidad son sensibles, el establecimiento de las alternativas de producción sostenible son indispensables [10]. Es así que el trabajo In vitro evaluation of the inhibitory capacity of three Trichoderma isolates on Ralstonia solanacearum en el que se estableció que el consorcio de aislados de Trichoderma (Trichoderma viride, T. harzianum, T. asperellum) al día 10 tiene 72,61% de porcentaje de frente a R. solanacearum; el trabajo Effect of five concentrations of aqueous extracts of Pleurotus ostreatus P. Kumm and Tagetes minuta L. on the mortality of two nematodes in a laboratory setting que determinó que el extracto acuoso de las flores de T. minuta mostró una baja actividad nematicida, y el extracto acuoso de la hoja de T. minuta mostró la mejor actividad nematicida; y el trabajo "Análisis de la conductividad eléctrica, potencial de hidrógeno, concentraciones de nitrato, potasio y calcio, en cuatro diferentes preparaciones del fertilizante orgánico contrubuyeron con el conocimiento necesario para una producción agrícola más amigable con el ambiente"[10].

En las provincias de Sucumbíos y Orellana la ganadería es la actividad que mayor influencia tiene en la expanción de la frontera agrícola [11,12], en su mayoría la ganadería extensiva, por lo tanto, toda investigación que contribuya a mejorar esta actividad es un aporte importante para le región. La investigación Somatic Cell

Count Evaluation in Early Lactation between Primiparous and Multiparous Bos indicus Cows, es un estudio realizado con vacas Bos indicus que examinó la relación entre el recuento de células somáticas (RCS) y la producción de leche. Se evaluaron ciento cincuenta vacas (Primíparas, PM, 75 y Multíparas, MP 75) en lactación temprana (días en leche, PM =134 ± 3; MP = 136 ± 5), producción de leche (9,88 kg/d, en promedio) de la raza criolla Gyr lechers. Antes de ser asignadas a cada tratamiento, los valores de RCS fueron inferiores a 220.000 células/mL, por término medio. Las vacas MP tuvieron mayor producción de leche que las PM (10,83 vs. 9,18 ± 0,38 kg/d; P = 0,003). Se observaron contenidos bajos de grasa en ambos grupos y la paridad con la lactancia avanzada condicionaron los contenidos de RCS [13].

La conservación de los recursos naturales y la detección oportuna de agentes contaminantes en ecosistemas sensibles como la Amazonía son acciones que promoverán el desarrollo sostenible de la región, por lo que se presentan trabajos de investigación en aras que aportan con conocimiento en esta área.

La Detection of Arsenic and lead ions in water through validation of the electrothermal atomic absorption method es una investigación que consistió en la validación del método de espectrometría electrotérmica para la determinación de arsénico y plomo en muestras de agua, el mismo quegarantiza la calidad de los datos analíticos. El método de validación demostró que el análsiis fue robusto y preciso. Mientras que el trabajo Determination of water quality through the use of bioindicators, physical-chemical and microbiological analysis of the lagoon Santo Domingo of the national park Cotopaxi, province of Pichincha, period 2018 definió que la calidad del agua analizada se encuentra en estado dudoso y/o crítico. Otro aporte importante fue el estudio Determination of the effectiveness of the electrocoagulation process in the treatment of leachate from the controlled landfill site in Francisco de Orellana, investigó la eficiencia de la electrocoagulación para la eliminación de DBO5, DQO, SST, turbidez y color utilizando un reactor a escala de laboratorio. Se utilizaron muestras de lixiviados crudos provenientes del relleno sanitario controlado del cantón Francisco de Orellana, ubicado en la Amazonía ecuatoriana. Se realizó una caracterización fisicoquímica, identificando una reducida presencia de metales pesados y una alta biodegradabilidad, lo que sugiere que se trata de un lixiviado antiguo. Empleando la electrocoagulación en condiciones de 2.5 V y un periodo de 20 minutos existió mayor eficiencia de reducciones de DBO5 (85.23%), DQO (98.20%), SST (11.30%) turbidez (96.52%) y color (90.73%) [9].

En toda la región amazónica coexisten grupos indígenas con el ecosistema n atural como lo indica el trabajo “Valoración de los servicios ecosistémicos del bosque primario de la comunidad Waorani Nampaweno, Orellana, Ecuador” que revela el valor cultural de prácticas como la caza, el respeto a la fauna y el uso de recursos forestales en artesanías y vestimenta. Sin embargo, la colonización y la explotación petrolera amenazan sus formas de vida y la identidad cultural de los Waorani, especialmente entre los jóvenes, poniendo en riesgo su riqueza cultural ancestral. Estudio que hace hincapié a la preservación de estás comunidades y su cosmovisión. En cambio, respecto al manejo de los recursos naturales el estudio “Análisis Multitemporal de Deforestación y Cambio de Cobertura del Suelo en La Joya de los Sachas (1990-2018)” mostró que el incremento de la frontera agrícola ha dejado una huella significativa en la cobertura del suelo de la Joya de los Sachas. A través del geoprocesamiento, se ha evidenciado incrementos significativos de tierras agrícolas y pastizales en los últimos 28 años, siendo las actividades agropecuarias la principal causa de deforestación. La tasa anual de deforestación de 1,300 ha/año genera preocupación y alarma en la generación de planes de manejo y conservación del recurso natural impactado negativamente, pues, si esta tendencia persiste, se proyecta que en aproximadamente 30 años La Joya de los Sachas perderá por completo su cobertura boscosa [14].

Las actividades antropogénicas, el crecimiento población, el índice de pobreza, los modos de vida, el impacto Ambiental y otros, son factores que no garantizan el sumak kawsay “Buen vivir”, en razón de ello se han realizado Investigaciones de innovación con miras a un futuro sostenible, tales son “Analysis of energy poverty in Andean rural households and design of an efficient cooking solution using biomass” “Anthropometric indicators and their relationship with body fat in women with obesity” “Heart Failure Prognostic Algorithm Using Spectral Analysis and Matlab Software”, que desde los hogares rurales de la Reserva de Producción Faunística Chimborazo hasta la batalla contra la obesidad y la predicción de la

insuficiencia cardíaca, los proyectos no solo exploran problemas actuales, sino que también proponen soluciones innovadoras. Desde un diseño eficiente para cocinar con biomasa hasta algoritmos pronósticos utilizando análisis espectral. Investigaciones que prometen marcar la pauta para un futuro más sostenible. En el corazón de estos proyectos yace el compromiso con la ciencia, la comunidad y el bienestar global [14].

El II Congreso Internacional de Innovación, Ciencia y Tecnología "Amazonía Viva" es un evento de académico científico organizado por instituciones de Educación Superior (Escuela Superior Politécnica de Chimborazo, Instituto Tecnológico Superior Universitario Oriente, Instituto Superior Tecnológico Martha Bucaram de Roldos e Instituto Superior Tecnológico General Eloy Alfaro) y otras instituciones (Instituto Nacional de Investigaciones Agropecuarias de Ecuador). El congreso se efectuó los días 22, 23 y 24 de noviembre del 2023, con la participación virtual de 28 ponentes nacionales, 9 conferencistas invitados, entre ellas 7 Internacionales y 2 nacionales, así, también contó con más de 460 asistencias que interactuaron en todo el evento. El desarrollo de cada jornada del evento tuvo lugar a una duración de 4 horas. Además, se desarrollaron 5 talleres presenciales durante los 3 días del evento, con una duración de 2 horas, esto con el fin de conocer y poner en práctica los conocimientos en las áreas como: Contaminación y Muestreo de Suelos, Configuración de sistemas IOT para entornos domóticos, La app Scratch Jr. para el desarrollo del sensamiento

computacional en la primera infancia, Manejo de drones para estudios agromedioambientales y Tecnologías para la producción agropecuaria sostenible en la Amazonía.

Figura 1. Registro fotográfico del II CCICTAV. a) Inauguración del evento. b) Taller presencial

CONCLUSIONES

El II Congreso Internacional de Innovación, Ciencia y Tecnología "Amazonía Viva" destaca la relevancia de la investigación científica y la aplicación de tecnologías innovadoras para abordar los desafíos ambientales en cuanto su conservación mediante la detección de contaminantes, el uso de tecnologías innovadoras para mejorar la salud de las personas, trabajos de investigación que aportan al sector económico, ambiental y social de la región amazónica ecuatoriana.

La región amazónica de Ecuador, específicamente las provincias de Sucumbíos y Orellana, enfrenta el desafío de conciliar la producción industrial, la coexistencia de procesos productivos, en particular la producción petrolera, con la conservación de áreas protegidas de gran biodiversidad, como la reserva de la biósfera YASUNÍ, el parque nacional Cuyabeno y la reserva Limoncocha

El II Congreso Internacional promueve la articulación interinstitucional entre instituciones de educación superior, organismos de investigación y otras entidades, con el fin de brindar un espacio para la presentación y discusión de investigaciones que abordan el uso sostenible de los recursos, mejoras en la producción agrícola y el uso de tecnologías innovadoras, con el objetivo de promover el desarrollo de la Amazonía ecuatoriana.

REFERENCES

1. Secretaría Técnica de la Circunscripción Territorial Especial Amazónica. Plan Integral para la Amazonía 2021-2025 [Internet]. Puyo, Ecuador; 2021 Mar [cited 2023 Sep 4]. Report No.: 001-2022-002. Available from: https://www.secretariadelamazonia.gob.ec/wp-content/uploads/downloads/2022/09/PIA_final-Digital-.pdf
2. Mestanza-Ramón C, Henkanaththegedara SM, Vásconez Duchicela P, Vargas Tierras Y, Sánchez Capa M, Constante Mejía D, et al. In-Situ and Ex-Situ Biodiversity Conservation in Ecuador: A Review of Policies, Actions and Challenges. Diversity (Basel) [Internet]. 2020;12(8). Available from: https://www.mdpi.com/1424-2818/12/8/315
3. CIICTAV. Objetivos. 2023 [cited 2024 Jan 25]. p. 1–1 Congreso Internacional de Innovación, Ciencia y Tecnología "AMAZONIA VIVA" . Available from: https://ciictav.ec/
4. Ponce-Sanchez J, Zurita-Benavides MG, Penuela MC. Reproductive ecology of white cacao (Theobroma bicolor Humb. & Bonpl.) in Ecuador, western Amazonia: floral visitors and the impact of fungus and mistletoe on fruit production. Brazilian journal of botany. 2021;44(2):479–89.
5. Ministerio de producción comercio exterior inversiones y pesca. Boletín de cifras, Comercio exterior mayo 2023. Quito-Ecuador; 2023.
6. Plasencia-Vázquez AH, Vilchez-Ponce CR, Ferrer-Sánchez Y, Veloz-Portillo CE. Effect of climate change on the potential distribution of the fungus (Moniliophthora roreri) and the cultivation of cacao (Theobroma cacao) in continental Ecuador. TERRA LATINOAMERICANA. 2022;40.
7. Vargas-Tierras Y, Diaz A, Caicedo C, Macas J, Suarez-Tapia A, Viera W. Benefits of Legume Species in an Agroforestry Production System of Yellow Pitahaya in the Ecuadorian Amazon. Sustainability. 2021;13(16).
8. Food and Agriculture Organization of the United Nation (FAO). Perspectivas a mediano plazo: perspectivas para la producción y el comercio mundial de bananos y frutas tropicales 2019-2028 [Internet]. Roma; 2020 [cited 2023 Oct 8]. Available from: https://www.fao.org/publications/card/es/c/ca7568es/
9. Das Gupta M. Growth trend and potential of horticulture in Northeast India. JOURNAL OF HORTICULTURAL SCIENCES. 2022;17(2):530–42.
10. Wezel A, Bellon S, Doré T, Francis C, Vallod D, David C. Agroecology as a science, a movement and a practice. A review. Agron Sustain Dev. 2009;29(4):503–15.
11. Alcaldía de Lago Agrio. Plan de desarrollo y ordenamiento territorial del cantón Lago Agrio. 2021.
12. Alcaldía Francisco de Orellana. Plan de desarrollo y ordenamiento territorial del cantón Francisco de Orellana. Francisco de Orellana; 2023.
13. Torres B, Andrade V, Heredia-R M, Toulkeridis T, Estupiñán K, Luna M, et al. Productive Livestock Characterization and Recommendations for Good Practices Focused on the Achievement of the SDGs in the Ecuadorian Amazon. Sustainability. 2022;14(17).
14. Hoelle J. Quantifying cultural values associated with deforestation in the Brazilian Amazon. J Land Use Sci. 2018;13(1–2):166–81.

Received: October 9th 2023/ **Accepte**d: January 15th 2024 / **Published:**15 February 2024

Citation: Sánchez-Capa M; Anguaya Isama H F.Coexistencia de procesos productivos y de conservación en la Amazonía ecuatoriana. Revis Bionatura 2024; 9 (1) 1. http://dx.doi.org/10.21931/RB/2024.09.01.1

Additional information Correspondence should be addressed to *maritzac.sanchez@espoch.edu.ec*
Peer review information. Bionatura thanks anonymous reviewer(s) for their contribution to the peer review of this work using https://reviewerlocator.webofscience.com/

Bionatura
Ibero-American Journal of Biotechnology and Life Sciences

Bionatura ISSN. First 13909355 Ecuador. **Scopus coverage years**: from 2016 to the present

Bionatura
Ibero American Journal of Biotechnology and Life Sciences

Article

Analysis of energy poverty in Andean rural households and design of an efficient cooking solution using biomass

Wladimir A Silva-Castelo [1], *Rafael Córdova-Uvidia* [1*], *Ángel Ordoñez-Echeverria* [1], *Miguel Aquino-Arroba* [2]

[1] *Escuela Superior Politécnica de Chimborazo, Grupo de Investigación y Desarrollo para el Ambiente y Cambio Climático, Riobamba, Ecuador; alesilvacas@gmail.com, angel.ordoniez@espoch.edu.ec,*

[2] *Escuela Superior Politécnica de Chimborazo, Facultad de Mecánica, Riobamba, Ecuador; socrates.aquino@espoch.edu.ec,*

***** *Correspondence: rafael.cordova@espoch.edu.ec Phone: +593987552520*

Available from. http://dx.doi.org/10.21931/RB/2024.09.01.2

ABSTRACT

This work explores energy poverty in the rural households surrounding the Chimborazo Faunal Production Reserve (RPFCH) and proposes an efficient cooking solution using firewood. Energy poverty was evaluated through the multidimensional poverty index (MEPI), including the 10% rule, hidden energy poverty, disproportionate expenses, and a subjective analysis of housing conditions. The research found ten households experiencing moderate energy poverty with a MEPI of 0,1562. An efficient cooking solution was proposed as an improved rocket stove design with an ignition system and forced air at the combustion chamber inlet. This stove utilizes a solar panel and batteries to power the fan. Its thermal efficiency is 13%, including Peltier cells to convert residual heat into DC electricity. The rocket stove's heating capacity is 1,6 kW, which is sufficient for heating a small room and cooking meals. After implementation, a follow-up energy poverty analysis using the same indicators is recommended to evaluate the effectiveness of the proposed solution and its impact on reducing energy poverty.

Keywords: energy poverty; rocket stove; thermal efficiency; room heating; Peltier cell; photovoltaic energy.

INTRODUCTION

Globally, approximately 800 million people lack electricity, and nearly 2,6 billion do not have access to clean cooking fuels, according to the United Nations[1]. Energy poverty is the lack of or limited access to modern technologies for cooking, food refrigeration, water heating, home conditioning, and human group entertainment[2]. The concept and measurement of energy poverty vary based on each country's reality, as in the European Union, where an estimated 35 to 100 million Europeans are afflicted by energy poverty[3].

Energy poverty is significant in developing countries because it helps quantify inequity in energy access and the expenditure residents incur relative to their incomes. The number of studies related to energy poverty in developing countries has increased in the past year due to the interest shown by international organizations like the United Nations (UN), the International Energy Agency (IEA), and the Economic Commission for Latin America and the Caribbean (CEPAL)[4].

Latin America features a varied geography with several isolated populations living in remote rural areas, far from roads and major cities, leading to limited access to energy and technological services[5]. In Ecuador, 0,76%

of the population is without access to electricity, a statistic predominantly seen in rural areas. In addition to electricity, there is a scant supply of liquefied petroleum gas (LPG) due to challenging access and road conditions in the region[5,6]. There is only one macro-level study on energy poverty in Ecuador. The study reveals that rural regions experience greater energy poverty than urban areas[7].

The calculation of Energy Poverty (PE) must be adjusted to the reality of the region being studied, considering the data available in the study area and analyzing some indicators using the Multidimensional Energy Poverty Index (MEPI)[8,9] methodology. The most used indices worldwide are the Ten Percent Rule (TPR), Twice National Median Indicator (2M), Minimum Income Standard (MIS), Low Income, High Cost (LIHC), After Fuel Cost Poverty Indicator (AFCP), Hidden Energy Poverty (HEP), and the European Union Statistics on Income and Living Conditions (EU-SILC)[4, 10 11]. Energy poverty can also be analyzed from two perspectives: i) the difficulty in connecting to or sourcing energy and ii) the lack of energy use for three main reasons - adopting new electrical devices to improve productivity, energy prices, and electricity availability[12].

Around the world, there are 2,7 billion people who depend on biomass, such as firewood, coal, or crop residues, for cooking. In rural areas of developing countries, there is a 90% biomass consumption rate[13]. The use of biomass in food cooking results in 1,6 million people dying each year due to emissions from burning fuels[1]. In Latin America, 54 million people lack a clean cooking system, all primarily dependent on biomass[5;] in Ecuador, firewood consumption in 2016 was 1486 barrels of oil equivalent (BOE)[7].

Improvements in cooking have allowed household tasks to be faster and less polluting, increasing time for other developmental activities and reducing illnesses from pollution. For instance, in Brazil, the likelihood of girls and teenagers completing primary education before turning 18 rose to 59% in 2014. A 2013 study in South Africa found that a woman's probability of finding work increased by 9%, and in Nicaragua, it increased by 23% when the time dedicated to cooking-related household activities was reduced[14]. In 2012, based on data obtained from deaths due to indoor pollution, more than 60% of women and children were exposed to gases produced by cooking with firewood[15].

To quantify energy poverty in the community of Rio Colorado, located in the Faunal Production Reserve (RPFCH), the Multidimensional Energy Poverty Index (MEPI) method was used with four indicators: TPR, HEP, 2M, and a subjective indicator assessing if the house has leaks in the roof, walls, floors, damp foundations, or rotting window frames. After analyzing energy poverty, an efficient cooking solution is proposed using Quality Function Deployment (QFD). This method is based on designing services or products based on the customer's voice, which is translated into technical specifications with the engineer's voice, aiming to reduce energy poverty indicators and diseases caused by pollutants generated from biomass combustion[16].

Nomenclature

Abbreviations

$\dot{m}_{comb}$, Combustion mass flow [kg/s]
$\dot{V}_{comb}$, Combustion volume as a function of time [m^3/s]
$\dot{\rho}_{comb}$, Fuel density [kg/s]
$\dot{m}_{air}$, Air mass flow [kg/s]
m_{comb_c}, Fuel mass flow (actual 90%) [kg/s]
AC, Ratio of air mass to fuel mass
$\dot{Q}$, heat transfer ratio [W]
T_f, temperature of the cold side of the cell
T_∞, room temperature
R_t, thermal resistance
Ra: Rayleigh number
g, gravity
β, coefficient of volumetric expansion
T_{ep}, external wall temperature
T_∞, ambient temperature
Lc, characteristic length of the analyzed surface
v, kinematic viscosity of the fluid
Pr, Prandtl number
Nu, Nusselt number
h, air convection coefficient [W/m^{2}K]
Lc, characteristic length of the analyzed surface [m]
k, thermal conductivity. [W/mK]
ε, the emissivity of steel
σ, Stefan–Boltzmann constant
T_s, surface temperature
Ps, the combined power of solar panels [W]
C, total daily system consumption in watt-hours [Wh]
ε, system efficiency, usually 70%
B, solar battery capacity [A-h]
DOD, depth of discharge (50%)
Tc, rated current of the charge controller [A]
Vs, voltage of the photovoltaic system [V]
Fs, safety factor (1,3)
ω, angular velocity [rad/s]
V_∞, linear fan speed [m/s]

MATERIALS AND METHODS

Energy poverty analysis

For the analysis of energy poverty, it was considered that the concept and measurement vary according to the reality of each country. The Multidimensional Energy Poverty Index (MEPI) methodology was applied. First, the Research and Development Group for the Environment and Climate Change (GIDAC) conducted a study of all the indicators and their weighting. The selection and weighting of the indicators were based on the available data and the region's reality.

Study Area

With the programs ArcGIS, Geoportal and Google Maps, the points to be analyzed in the community of Rio Colorado were delimited; a broader panorama of the area was also observed. All points are shown in Figure 1, and the coordinates of the points can be found in Google Maps through the following link: https://goo.gl/maps/cPf5VYEMLA8p11LcA.

Figure 1. Geographical location of households visited.

Selection and evaluation of indicators

The steps outlined in Figure 2 were followed to select the most appropriate indicator. The analysis and evaluation of the indicators, as well as their weightings, are important[10]. Defining the concept and impact of energy poverty in the area under study is necessary. All those involved should be knowledgeable about the most widely used indicators globally and their advantages and disadvantages.

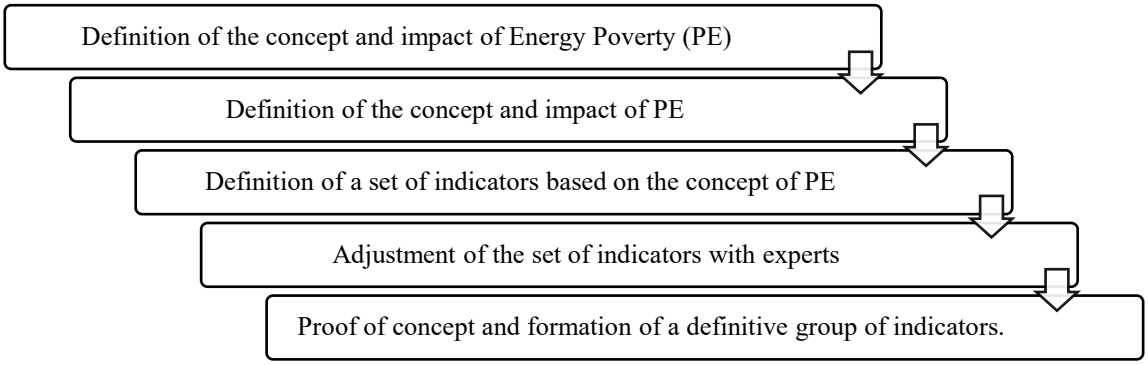

Figure 2. Indicator selection process

When defining the indicators, we selected which ones to use by analyzing data availability and ease of calculation. The following indicators were chosen: 10% Income, Hidden Energy Poverty (HEP), Disproportionate Expenditure (2M), and a subjective indicator analyzing if the house has leaks in the roof, walls, floors, damp foundations, or rotting window frames. To adjust the indicators, we transformed the kg of firewood (4,5 kWh/kg) and liquefied petroleum gas (12,80 kWh/kg)[17]. Finally, surveys were conducted in the community through participatory dialogue.

Using the STAMP principles of Bellagio, a system for evaluating a set of indicators was developed, in which four criteria were analyzed: Objectivity, Transparency, Practicality/Flexibility, and Participation. Several subcriteria were generated from these criteria, which are detailed in Table 1[10].

Criterion	Sub-criterion	Qualification
Objectivity	Indicators reflecting the economic dimensions of the problem are included	X
	Indicators reflecting the social dimensions of the problem are involved.	
	Indicators reflecting the environmental dimensions of the problem are involved.	
Transparency	The methodology for the selection of indicators is presented	X
	Links to data sources are indicated.	X
	Data sources are publicly available.	
Practicality and flexibility	The system for calculating indicators is quite simple.	X
	The set of indicators can be easily adapted to other research	X
	The methodology is presented (or links are shown)	X
Participation	Stakeholders or experts are involved in the indicator selection process.	X
	Stakeholders or experts are involved in determining the weights of the indicators.	X
	Scientific methods are used for the participation of stakeholders or experts (selection, agreement of opinions)	X
TOTAL		9/12

Table 1. Assessment of the set of indicators

Analysis of the cooking method

The technical visits and the analysis of energy poverty in the Rio Colorado Community allowed us to demonstrate the cooking methods and the use of firewood, as shown in Figure 3. Once the cooking problem in the community was identified, the user's voice was obtained through participatory dialogue.

Figure 3. Food cooking method in the Rio Colorado community.

The user's voice allowed the engineer's voice to be obtained and these values to be quantified into accurate data. Additionally, the parameters for increasing the combustion efficiency of wood stoves, lowering their emissions and improving their safety were utilized. [18].

Functional analysis

Figure 4 describes the functions of the efficient cooking solution, starting from level 0 and extending to all parts of the design. Level 0, at this level, what the efficient cooking method does is described, where firewood and air enter, and heat energy for cooking and home heating is produced; power is also generated through a Peltier cell.

Level 1, at this level, the definition of modules emerges, where the first module is the heat energy generated by the stove, and the second module is the electrical energy and the forced air directed to the combustion chamber. Module 1: Combustion chamber, heat energy, gases, ashes, ashtray. Module 2: DC Electricity, battery, fan, external power source.

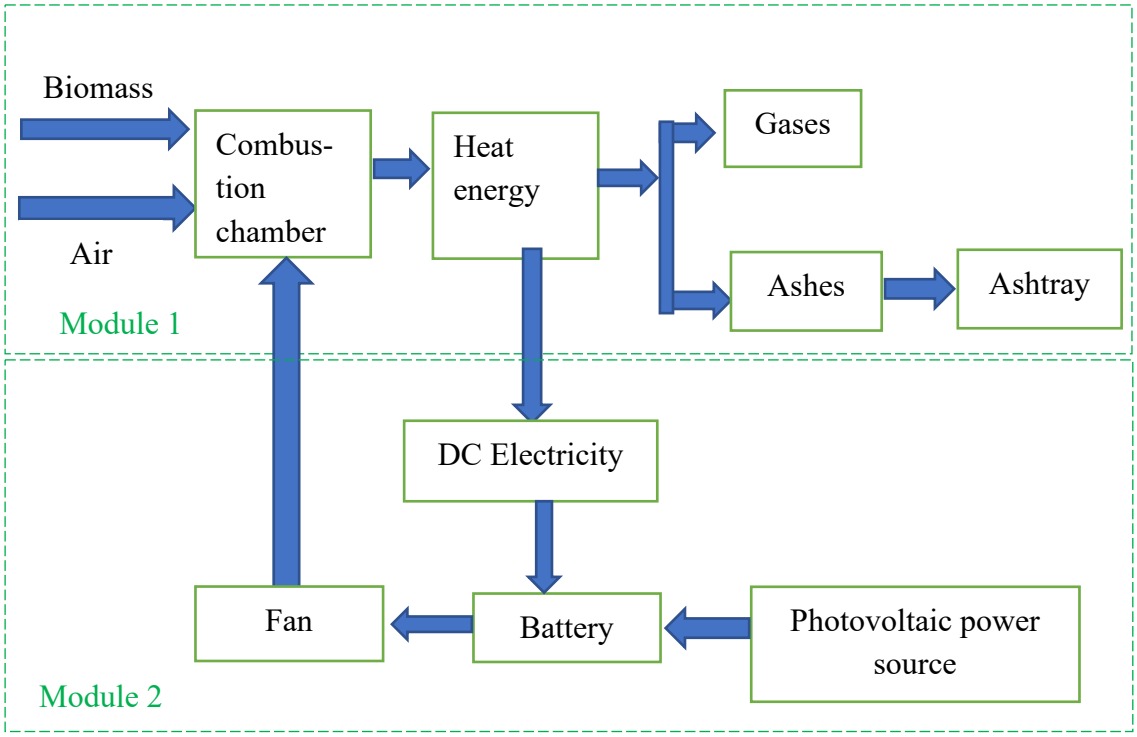

Figure 4. Niveles de análisis funcional

Analysis of Solutions

An analysis was made in Clean Burning Biomass Cook-stoves 2nd Edition 2021, where the main characteristics that a wood stove should have, such as air intake, consumption, and efficiency, were obtained[19]. To corroborate the stove's characteristics, the Quality Function Deployment (QFD) Annex1 and the stove's modules were used. The main factors were obtained: wood input, grate, energy source, and air input. With the help of CAD software (SolidWorks), different solutions were produced, and then the advantages and disadvantages of each solution were analyzed.

Figure 5 shows three options based on the Quality Function Deployment Matrix for the required cooking solution. Figure 5 (a) features a mechanical air controller; air enters below the wood, but the disadvantage is that the user must push the wood. In Figure 5 (b), there's no need to make the wood (entrance at 45°); the air enters the combustion chamber downwards using a fan; its main disadvantages are a single energy source (Peltier cell) and the vertical grate that may prevent ash from descending optimally. Finally, Figure 6 (c) has forced air input, double combustion chamber, dual-energy source, and interchangeable grate; however, it has the disadvantage that if there is no sun or the stove is not used with this method, the battery could be discharged.

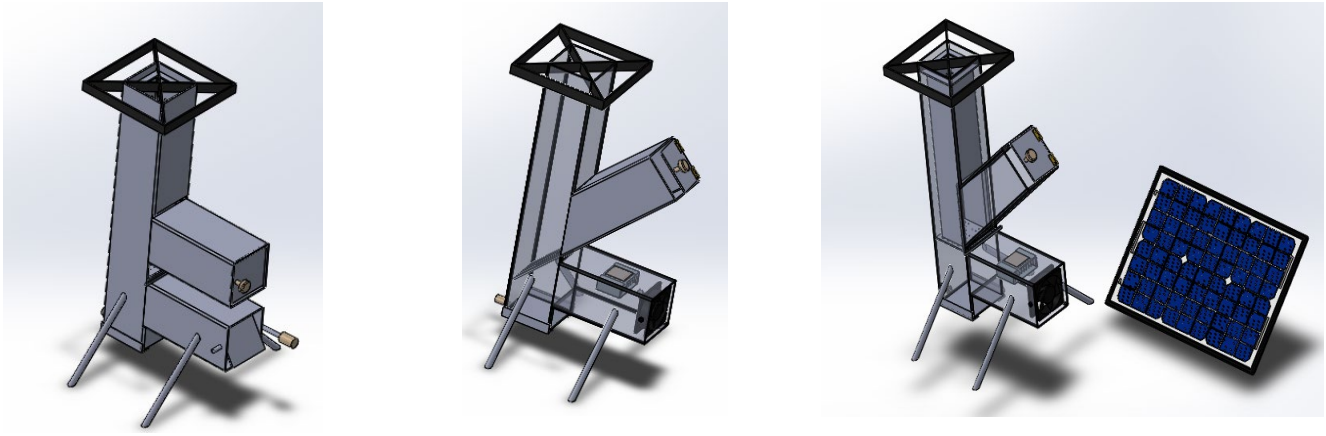

(**a**) (**b**) (**b**)

Figure 5. Possible solutions are (a) natural convection rocket stove, (b) forced convection rocket stove, and (c) forced convection rocket stove powered by a solar panel.

The solution is evaluated using the weighted criteria method. For the application of this method, a value of 1 is utilized to assign higher relevance, 0,5 for equal significance, and 0 when there is less relevance to the criterion being compared.

Low cost: This is important as it is aimed at individuals with scarce economic resources. High efficiency: This will allow the user to cook faster and more efficiently. Low emissions: Emissions need to be quiet because the woodstoves are used in indoor home areas. Energy source: The energy source is crucial, especially in remote areas with no constant network. Minimal maintenance: Maintenance should be as simple as possible, or in its absence, the user should be able to carry it out independently.

With these parameters, each criterion's specific weight was evaluated, where low emissions, high efficiency, low cost, energy source, and minimal maintenance were also analyzed. As a result, Figure 5 (c) was identified as the ideal solution.

Key features of simulation

In the Computational Fluid Dynamics (CFD) analysis, the control volume is isolated, considering the inflow and outflow of combustion gases in 2D. To analyze the mass flow of firewood, equation (1) was used with a combustion volume flow rate. $\dot{V}_{comb}$ of 0,0375 m^3 /h and a $\dot{\rho}_{comb}$ of 780 m^3/kg. The volumetric flow and density values are experimental data obtained from wood in the Sinincay community of Cuenca [20].

$$\dot{m}_{comb} = \dot{V}_{comb} \times \dot{\rho}_{comb} \quad (1)$$

A value of $\dot{m}_{comb}$ of 0,9965 kg/s, the AC value was calculated using a humidity of 20% and a combustion efficiency 0,8. These values were entered into equation (2), and the mass air flow was calculated ($\dot{m}_{aire}$)

$$\dot{m}_{air} = m_{comb_c} \times AC \quad (2)$$

The geometry of the rocket stove was calculated using the Ansys software. The fuels' and air's mass flow are used for combustion in the software. Once these data were obtained, the temperature at the pot's base was determined, which should be greater than or equal to 62,85 °C [21].

A 2D model was created in the Ansys software, using the dimensions shown in Figure 6 (a), to determine the distance at which this temperature is achieved. The geometry values were entered in the Details View section, as shown in Figure 6 (b). The geometry values are based on the general measurements of the rocket stove.

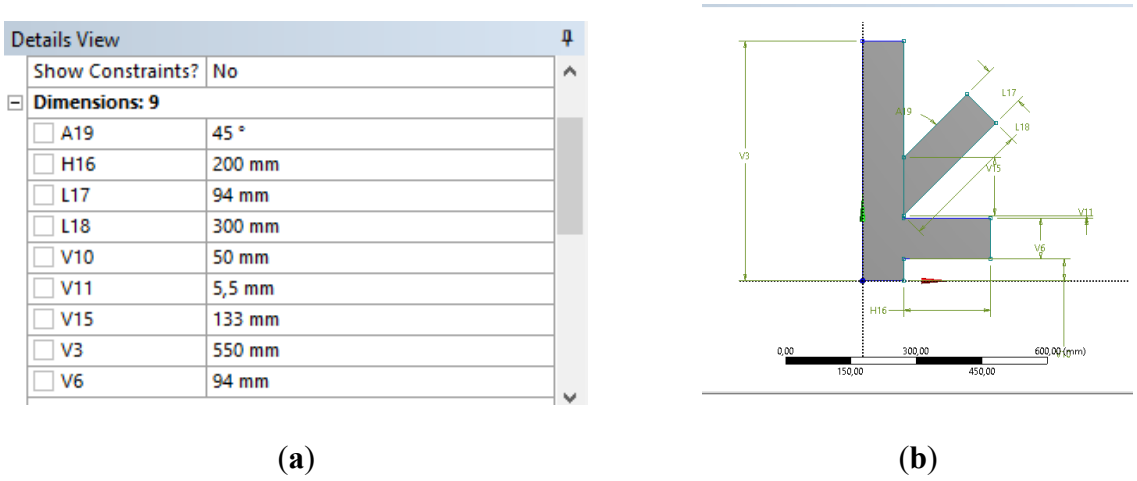

(a) **(b)**

Figure 6. Parameterization of the geometry (a) dimensions entered the program (b) model 2 D analyzed.

The geometry was meshed with a size of 5 mm, and the Fluent CFD was chosen as the reference physics to ensure the meshing matches the simulation requirements. In Figure 7 (a), you can observe the meshing in Ansys, and Figure 7 (b) demonstrates that it meets the minimum meshing requirements. The average value is 0,98079, and the image reveals that most elements have a regular shape, validating the mesh quality.

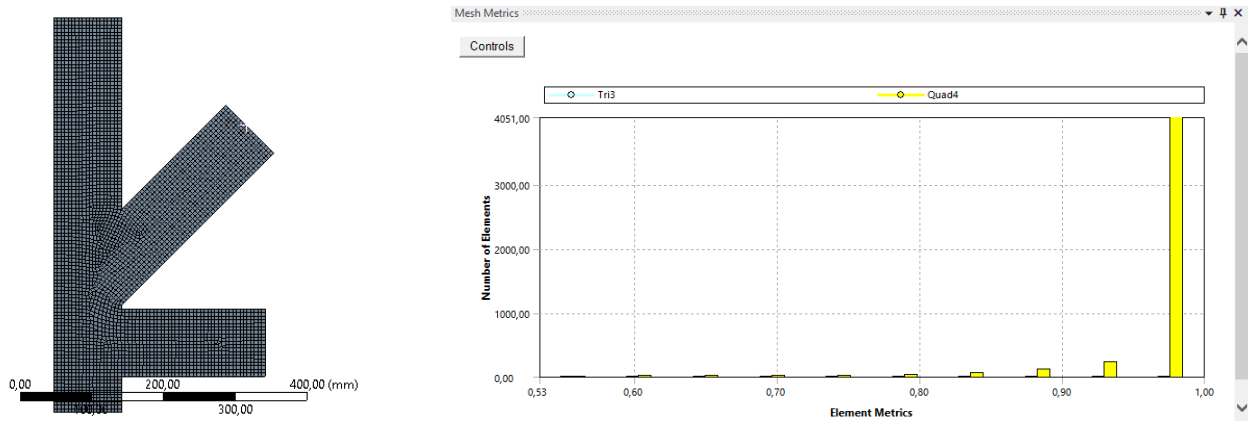

(a) **(b)**

Figure 7. Meshing in Ansys (a) 2D meshing (b) mesh quality

Thermo-Structural Analysis of the Woodstove

In Figure 8 (a), the geometry for the thermo-structural analysis is shown. Some parts that do not affect the structure's resilience were removed. The surface where the temperatures reached during combustion were applied is detailed in Figure 8 (b).

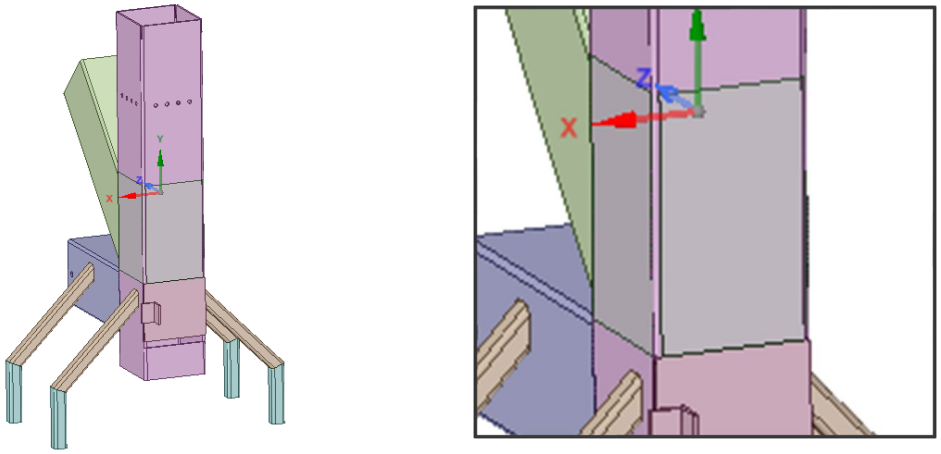

Figure 8. (a) 3D geometry for structural thermal analysis, (b) Thermal limit in the combustion chamber.

The average temperature was obtained in each wall using an infrared thermometer, as shown in Figure 9. A mesh was painted on the walls of the rocket stove, and the points were mapped when the stove reached thermal equilibrium; the average measured temperature was 397 °C.

Figure 9. Measurement of temperatures in the three walls of the combustion chamber

The mechanical method was chosen for the physical mesh analysis, and a mesh size of 7 mm was applied to the entire geometry. To improve the combustion, extra holes were added to promote double combustion. Ansys' inflation command achieved a more optimal and high-quality mesh. The static thermal analysis is performed by communicating two solutions, Steady-State Thermal and Static Structural, where the data are shared for the final analysis. The weight of the pot with water was 5 kg, obtained using a digital scale, as shown in Figure 10.

Figure 10. Weight for structural thermal analysis

Heating power of the wood-burning stove

A significant feature of a wood-burning stove in rural areas of Chimborazo is that, in addition to cooking, it can heat the surrounding environment. To determine whether the wood-burning cooking method heats a room, the calorific power of the stove's walls is calculated, which was obtained using equation (3).

$$\dot{Q}_{wall} = 4\left(\dot{Q}_{p\ convection}\right) + 4\left(\dot{Q}_{p\ radiation}\right) \quad (3)$$

For the calculation of the film temperature in equation (4), the values T_{ep}=377,225°C and an ambient temperature T_{∞}=3 °C were applied.

$$T_p = \frac{T_{ep} + T_{\infty}}{2} \quad (4)$$

With equations (5) to (9) dimensionless numbers $R_a = 319990487{,}1$, $Nu = 86{,}472$, and the coefficients $h = 8{,}0874\frac{W}{m^2k}$ $Q_{convection} = 15{,}758\,W$ $\dot{Q}_{radiation} = 398{,}310\,W$, were obtained. The last 2 values were replaced in Equation 3, getting a value of $\dot{Q}_{walls} = 1{,}656\,kW$, this value is more excellent than 1 kW, which means that the proposed woodstove would be able to heat a small room.

$$R_a = \frac{g \times \beta\left(T_{ep} + T_{\infty}\right) \times Lc^3}{v^2} \times Pr \quad (5)$$

$$Nu = \left\{0{,}825 + \frac{0{,}387(R_a)^{\frac{1}{6}}}{\left[1 + \left[\frac{0{,}492}{Pr}\right]^{\frac{9}{16}}\right]^{\frac{8}{27}}}\right\}^2 \quad (6)$$

$$h = \frac{Nu \times k}{Lc} \quad (7)$$

$$Q_{convection} = h(A_s)(T_s - T_\infty) \quad (8)$$

$$\dot{Q}_{radiation} = \varepsilon \times \sigma \times As \times (T_s^4 - T_{around}^4) \quad (9)$$

Analysis of the photovoltaic system

To determine the electric loads, the fan was analyzed with a voltage of 12 V and an amperage of 0,14 A; both values need to be entered into equation (10) to obtain the power that is required in the system. after doing the calculations, this value totals 1,68 W.

$$Pow = VI \quad (10)$$

Having obtained the power, we analyzed the time of its use. Generally, and according to the data collected in the community, the cooking time is four hours a day. With this data and the power, we applied equation (11) where we obtained $Energy\ consumed = 5{,}04\ Wh/d$ [22]

$$Energy\ consumed = Pow(cooking\ time) \quad (11)$$

The province of Tungurahua in Ecuador has an average irradiation of 5,4 kWh/m^2, equivalent to 5,4 solar hours. This middle irradiation determined the solar panel's necessary power for our air intake system [2].

For the charge controller, an LM7805 voltage regular was used that admits up to 1 A, thus validating the value of the nominal current of 0,33 A, with a 1N4007 diode that prevents the return of the energy of the 3,7 V battery; it also has an MT3608 voltage elevator that is regulated to 12 V at the voltage output. The control of the energy input to the circuit is done with an LED spotlight to the entrance with a resistance of 100 ohms. The system can be seen in Figure 11.

The airflow controller circuit is shown in Figure 12; it was constructed using a TIP 122 transistor, a 10k potentiometer for the transistor base and a 100uF capacitor for the motor. The solar panel can power the circuit or, if there is no sun, by a 12V transformer connected to a battery.

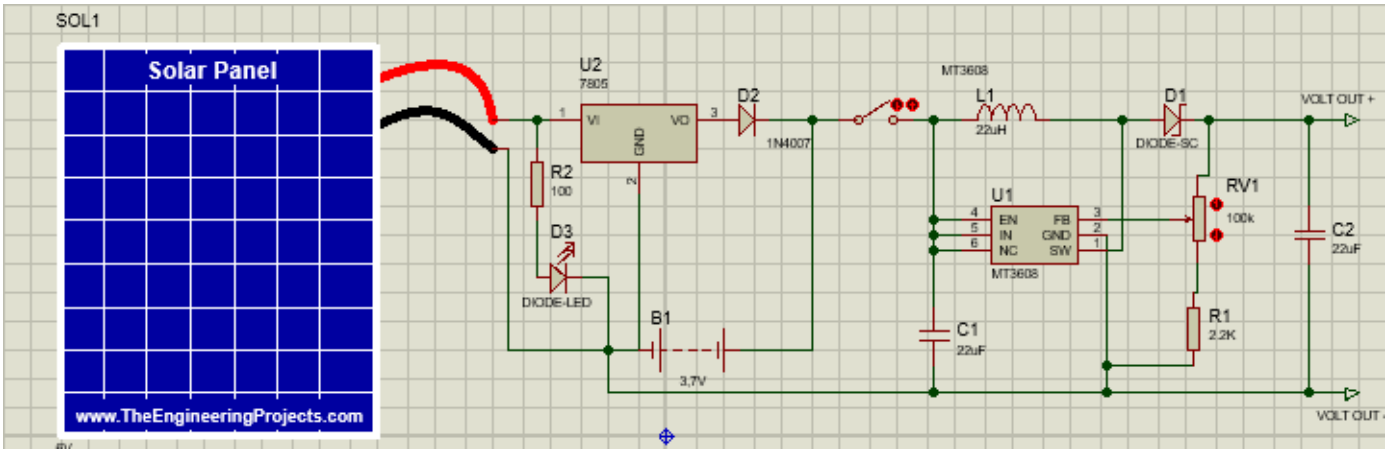

Figure 11. Charge controller circuit

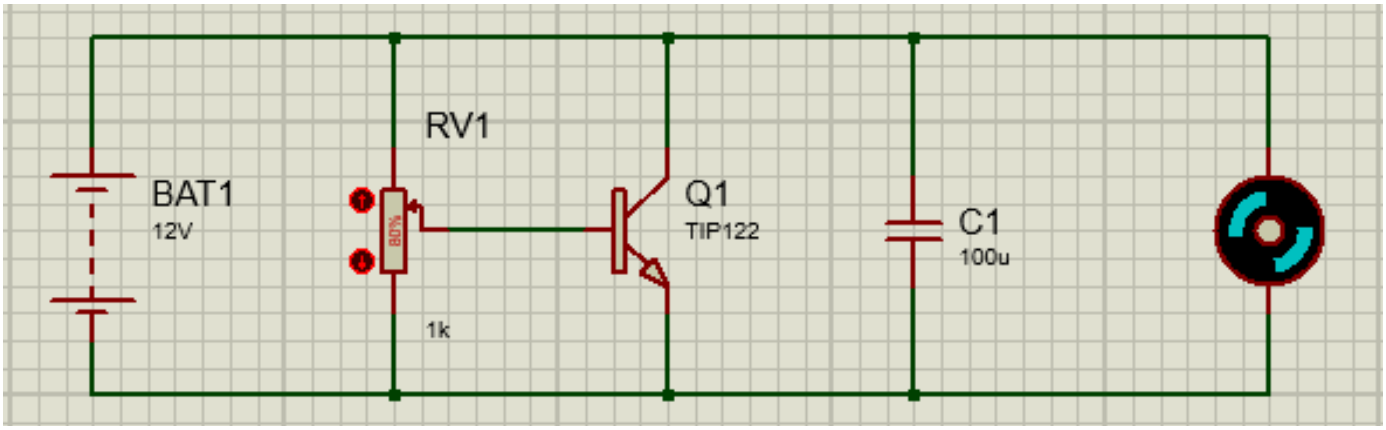

Figure 12. Speed regulator circuit

Calculation of the Peltier cell heatsink.

The community in the Andean area of Ecuador may not have sunlight on some days of the week; therefore, the possibility of installing Peltier cells, which give energy on cloudy days, was analyzed. The Peltier cell examined is TEC1-12705, which works at a maximum temperature of 138 °C.

Figure 16 (a) shows the temperature at the air inlet. The temperature in the selected face of the stove was approximately 75,57 ° C. The fan speed was taken as 6,28 m/s, around 6 m/s. The area's ambient temperature is 10 ° C in the day and 3 ° C at night, giving an average of 6,5 ° C [23].

Three Peltier cells generated a potential difference of 2.5V, so the LM7805 regulator regulates the voltage and powers the 3.5V battery. The fin and fin-free areas were determined; these measurements are shown in Figure 13; the heatsink length is 50 mm with these data areas. $A_{alet} = 0{,}0108\, m^2$ y un $A_{alet} = 2{,}8x10^{-3}m^2$ respectively were calculated.

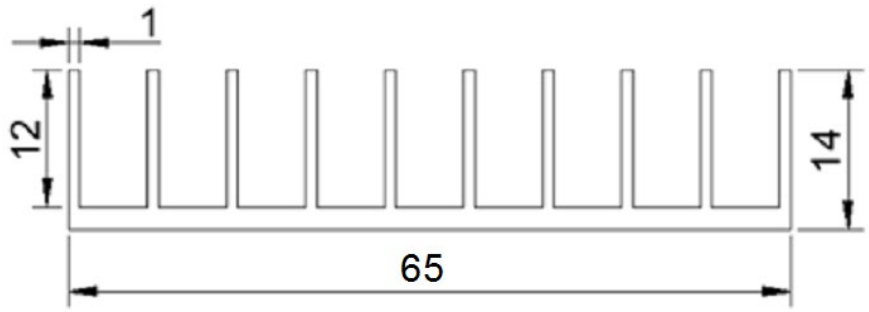

Figure 13. Heat sink

RESULTS

Finally, table 2 shows the results of the energy poverty of all the houses in the community of Rio Colorado were obtained. With the help of Excel, each of the results was weighted. All houses suffer from energy poverty because they all have a value greater than 0,25.

Number of households		C1	C2	C3	C4	C5	C6	C7	C8	C9	C10	Equivalence
k=4	Indicators											
1	10%	0	0	0	1	1	0	1	1	1	0	0,25
2	HEP	0	0	0	0	0	0	0	0	0	0	0,25
3	2M	1	1	1	1	1	1	1	1	1	1	0,25
4	Housing condition	1	1	1	1	1	1	1	1	1	1	0,25
	Energy poverty condition	0,50	0,50	0,50	0,75	0,75	0,50	0,75	0,75	0,75	0,50	
	Energy-poor house	YES	YES	YES	YES	YES	YES	YES	YES	YES	YES	

Table 2. Study of energy poverty in the production reserve of Fauna Chimborazo community Río Colorado (Tungurahua)

Figure 14 shows the four indicators that measure energy poverty. It is observed that the HEP meter does not exist in any of the houses analyzed, and Table 3 shows an MEPI of 0,1562, which is moderate energy poverty.

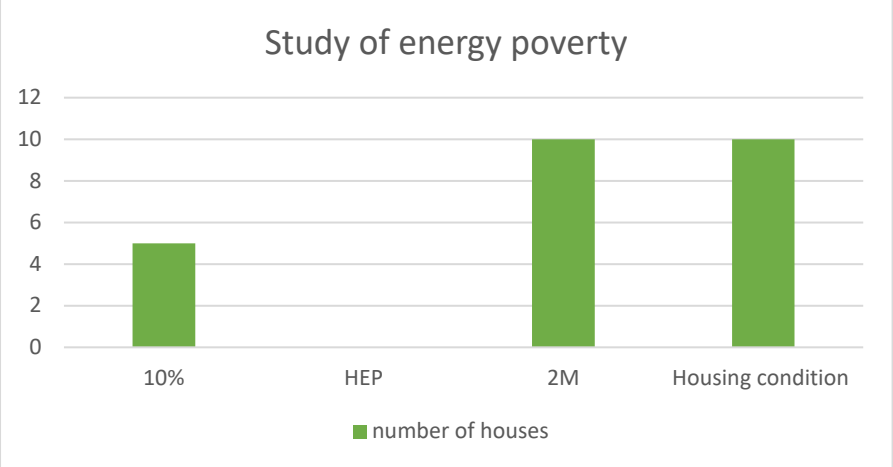

Figure 14. Indicators to measure energy poverty.

Total number of households (n)	**10**		
Households with energy poverty (q)	10		
Total number of indicators (k)	4		
EPIR incidence rate (q/n)	1		
Numerator	C	q	c*q
	0,50	5	2,5
	0,75	5	3,75
	1	0	0
Total, numerator	6,25		
Total, denominator	40		
IEP Intensity	0,15625		
MEPI	0,15625		

Table 3. Energy poverty results and MEPI indicator

Validation of the geometry of the cooking solution.

If the combustion simulation is turbulent, this distance must be reduced. Figure 14 (a) shows a laminar flow that validates the distance from the combustion chamber [24]. The rocket stove can be built and assembled with Ansys analysis verifying the temperature and flow velocity. Finally, the contaminants generated in the combustion were simulated; in Figure 15 (b), the mass fraction of CO_2 with the efficient cooking method (rocket cooker) is observed, with a value of 0,2164.

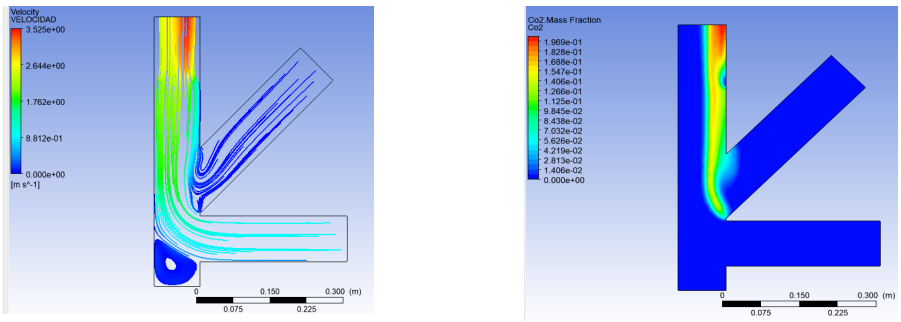

(a) (b)

Figure 15. Ansys Simulation (a) Velocity (b) CO_2 mass fraction

Static thermal simulation

Figure 15 (a) shows the temperature range reached by the kitchen throughout its structure, having a maximum of 344 °C and a temperature of 75 °C. Figure 16 (b) is the deformation analysis, with a maximum of 1,6856mm at the top and 0,38 at the legs of the rocket stove. The von Mises effort has a maximum value of 690 MPa in the small effort concentrators found in the corners of the rocket kitchen, as shown in Figure 15 (c).

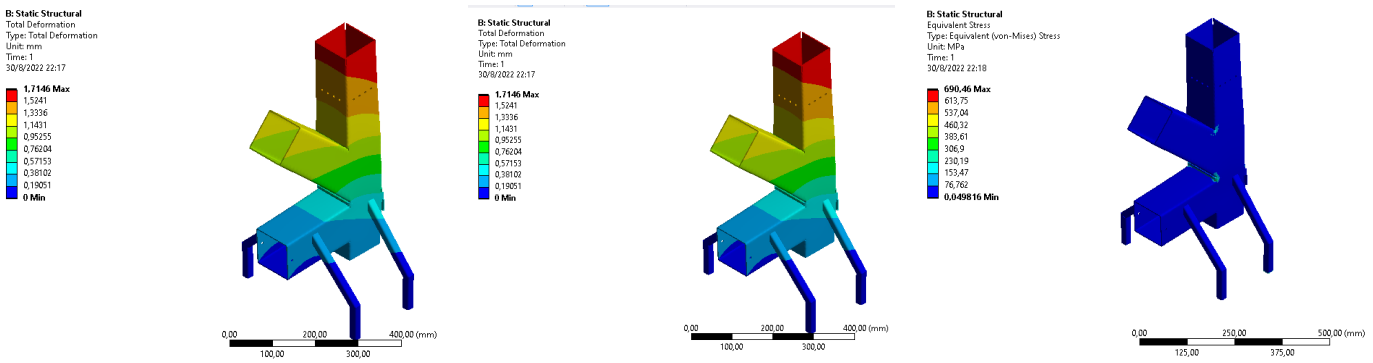

(a) **(b)** **(c)**

Figure 16. Analysis in Ansys (a) temperature (b) strain (c) Von Mises stress

Heat sink simulation and thermoelectric generation

Figure 16 (a) shows the temperature variation in the Peltier cell; at the bottom, a temperature of 75 ° C was placed, and with the wind speed generated from the fan we have a temperature of 38,49 ° C. Figure 17 (b) shows the thermoelectric power generation of the Peltier cell, having a maximum of 2 V of generation. Therefore, three cells of the same characteristics were coupled to generate the 6 V of potential.

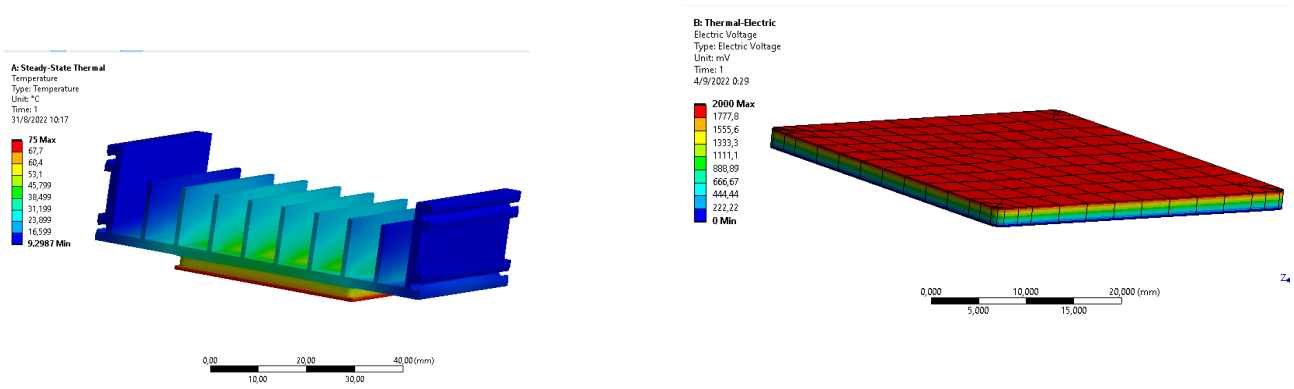

(a) **(b)**

Figure 17. Simulation (a) heat dissipation (b)

Rocket stove efficiency with the WBT method

Table 4 shows the value of thermal efficiency; in this case, we have a value of 13%, which, compared to traditional methods (7%), dramatically exceeds thermal efficiency [25]. The WBT test has 3 phases: cold start, hot start, and medium fire phase; however, a quick test can be performed. The rapid test consists of analyzing the stove only with a cold start and simmering if said stove has little mass [26].

.

Calculation/Results	Units	data	label
Fuel consumed (moist)	g	1,250	f_{cm}
Net change in char during the test	g	(10)	ΔC_c
Equivalent dry fuel consumed	g	981	f_{cd}
Water vaporized from all pots	g	300	w_{cv}
Effective mass of water boiled	g	4,926	w_{cr}
Time to boil Pot #1	min	85	Δt_c
Temp-corr time to boil Pot #1	min	82	Δt^T_c
Thermal efficiency	%	13%	h_c
Buring rate	g/min	11,5	r_{cb}
Specific fuel consumption	g/liter boiled	199	SC_c
Temp-corr sp consumption	g/liter	191,5602547	SC^T_c
Temp-corr sp energy consumption	kJ/liter	3,609	SE^T_C
Firepower	watts	3625	FP_c

Table 4. Calculation of thermal efficiency using WBT

DISCUSSION

Energy poverty in homes in the community of Rio Colorado in the province of Tungurahua, belonging to the RPFC, was analyzed using an MEPI, and a rocket woodstove was designed, which can potentially improve the community's quality of life. Based on the bibliographic study with PSALSAR methodology, PICOC, the most used indicators and methods for the analysis of energy poverty at the macro, meso and micro levels worldwide were found, as well as the methods of measuring energy poverty in developing countries that are applicable in rural communities of Ecuador.

The analysis of energy poverty in the Rio Colorado community revealed that all 10 households studied are experiencing energy poverty. This issue contributes significantly to the community's economic and social challenges. Each household's energy poverty status was determined through a multi-indicator method using four indicators: 10% rule, Housing Energy Poverty (HEP), Two Times Median (2M), and housing conditions. It should be noted that energy poverty is influenced by various factors such as income, energy prices, and the house's energy efficiency.

This evaluation resulted in an energy poverty index incidence rate of 1 and a moderate energy poverty intensity index (MEPI) of 0,1562. Although this intensity level is mild, it emphasizes the pressing need to address the energy poverty situation in this community, enhance the living conditions, and stimulate the potential for economic development. Unlike the index (MEPI) for all of Ecuador, which was 0,013 in 2014, this index has a percentage of 47% in the Sierra region, confirming that the problem exists in Ecuador [7].

Further, the CO_2 mass fraction for this efficient cooking method was found to be 0,2164, which, while not ideal, is significantly less than traditional cooking methods. Reducing CO_2 emissions is crucial in the fight against global warming, and implementing more efficient cooking methods like this could dramatically contribute to emission reduction efforts.

The static thermal simulation shows that the temperature range throughout the rocket stove's structure was within acceptable parameters, with a maximum of 344 °C and a minimum of 75 °C. The deformation and Von-Mises stress analyses showed that the structure can withstand the heat generated during cooking, ensuring the stove is robust and safe to use.

In addition to providing a cooking solution, this study aimed to generate electricity using Peltier cells. The temperature gradient across the Peltier cell ranged from 75 °C to 38,49 °C, which produced 2 V of electrical power per cell. The maximum voltage generated by the TEC1-12708 cell is 2,33 V; therefore, the cell would be causing an optimal voltage by not reaching the maximum nor being below this value [27]. Each household could generate 6 V of electricity using three cell-like kitchens with the same characteristics and provide valuable additional energy resources [28].

The final aspect of the rocket stove's performance, its thermal efficiency, was measured using the Water Boiling Test (WBT). Compared to traditional methods, with a thermal efficiency of around 7%, the rocket stove showed a significantly higher thermal efficiency of 13%. The thermal efficiency is superior to other wood stoves that range from 9 to 12% efficiency [29].

While the results from this investigation are promising, the study is limited by its small sample size. Further research should involve more households and varied geographic conditions to evaluate the solution's scalability and adaptability. Also, a cost-benefit analysis is recommended to assess the financial viability of implementing such rocket stoves on a broader scale.

CONCLUSIONS

This study demonstrates the alarming prevalence of energy poverty in the Rio Colorado community and proposes a promising and practical solution: a rocket wood stove. This solution could potentially address the urgent need for reliable energy sources, significantly improve the living conditions of the inhabitants, and contribute towards sustainable development goals. Further research and efforts are needed to scale this solution to a broader community level.

A MEPI multidimensional energy poverty index was applied to analyze energy poverty after carrying out the indicator selection process with a panel of experts. Each indicator was weighted with a value of 0,25. A participatory dialogue guide was developed, which allowed data to be obtained through field visits to the community.

The study further investigated the implementation of a rocket wood stove as a potential solution, utilizing ANSYS Computational Fluid Dynamics (CFD) software to conduct an in-depth analysis of the fluid velocity and maximum temperatures achieved by the stove. The velocity analysis confirmed a lack of turbulence in the combustion process, leading to efficient and stable operation. Simultaneously, the temperature results, peaking at about 900°C, verified the suitable length of the stove's combustion chamber, ensuring adequate heat for cooking purposes.

Author Contributions: Conceptualization, Wladimir Silva-Castelo, Rafael Córdova-Uvidia.; methodology, Wladimir Silva-Castelo, Rafael Córdova-Uvidia, and Miguel Aquino-Arroba.; software, Wladimir Silva-Castelo, and Miguel Aquino-Arroba; validation, Wladimir Silva-Castelo, Rafael Córdova-Uvidia; formal analysis, Wladimir Silva-Castelo; investigation, Wladimir Silva-Castelo, Rafael Córdova-Uvidia; data curation, Ángel Ordoñez-Echeverria.; writing—original draft preparation, Wladimir Silva-Castelo; writing—review and editing, Rafael Córdova-Uvidia and Miguel Aquino-Arroba.; visualization, Wladimir Silva-Castelo; supervision, Miguel Aquino-Arroba.; project administration, Ángel Ordoñez-Echeverria.; funding acquisition, Ángel Ordoñez-Echeverria. All authors have read and agreed to the published version of the manuscript.

Funding: This research project has received funding from Escuela Superior Politécnica de Chimborazo through project grant No. IDIPI-274

Institutional Review Board Statement: This project has been approved by the resolution of the Polytechnic Council No. 353.CP.2021 and has written authorization from the Bioethics Committee led by Prof. María Viteri dated 7 June 2021.

Informed Consent Statement: Informed consent was obtained from all subjects involved in the study.

Conflicts of Interest: The authors declare no conflict of interest.

REFERENCES

1. ONU. Ending Energy Poverty Saves Lives and Saves the Planet. Available online: https://www.un.org/es/climatechange/damilola-ogunbiyi-ending-energy-poverty (14-02-2022).
2. Griffa, P. B. Exploring the Concept of Energy Poverty. *Cent. Invest. Econ. Plan.* **2019**,*1*,1–4.
3. European Commission. Energy Poverty Advisory Hub Course Plataform. Available online: https://energy-poverty.ec.europa.eu/get-support/trainings-catalogue/epah-introductory-course-introduction-energy-poverty-and-epah_en (13-04-2021).
4. Sy, S. A. & Mokaddem, L. Energy Poverty in Developing Countries: A Review of the Concept and its Measurements. *Energy Res Soc Sci* 2022 89, 102562.
5. Calvo, R., Álamos, N., Marco, B., Anahi, U. & Rubén, C. L. Development of Energy Poverty Indicators in Latin America and the Caribbean. 2020,60.
6. Carrere, J. *et al.* Energy Poverty, its Intensity and Health in Vulnerable Populations in a Southern European city. *Gac Sanit* 2021 35, 438–444.
7. Quishpe, P., Taltavull, P. & Juárez, F. Energy Poverty in Ecuador. *Sustainability (Switzerland)* 2019 11, 1–19.
8. Nussbaumer, P., Bazilian, M. & Modi, V. Measuring Energy Poverty: Focusing on What Matters. *Renewable and Sustainable Energy Reviews* 2012 16, 231–243.
9. Sebastian Levine, J. M. and Y. M. B. A Robust Multidimensional Poverty Profile for Uganda. *Oxford Poverty and Human Development Initiative* 2012, 27.
10. Siksnelyte-Butkiene, I., Streimikiene, D., Lekavicius, V. & Balezentis, T. Energy Poverty Indicators: A Systematic Literature Review and Comprehensive Analysis of Integrity. *Sustain Cities Soc* 2021 67, 102756.
11. Santillán, O. S., Cedano, K. G. & Martínez, M. Analysis of Energy Poverty in 7 Latin American Countries Using Multidimensional Energy Poverty index. *Energies (Basel)* 2020 13,.
12. Ayodele, T. R., Ogunjuyigbe, A. S. O. & Opebiyi, A. A. Electrical Energy Poverty Among Micro-enterprises: Indices Estimation Approach for the City of Ibadan, Nigeria. *Sustain Cities Soc* 2018 37, 344–357.

13. Urmee, T. & Gyamfi, S. A Review of Improved Cook-stove Technologies and Programs. *Renewable and Sustainable Energy Reviews* 2014 33,625–635.
14. UN Enviroment. Global Gender and Environment.2016 doi:10.18356/0b979453-en.
15. WHO. Ambient Air Pollution. 2016.
16. Yacuzzi, E., Martín, F. & Pharma, A. QFD: Concepts, Applications, and New Developments. 2016, 1–37 doi:10.1007/b138775.
17. Mirza, B. & Szirmai, A. Towards a New Measurement of Energy Poverty: A Cross-Community Analysis of Rural Pakistan. *UNU-MERIT Working Paper Series 024* 2010 44, 1–41.
18. Baldwin & Winiarski. Design Principles for Wood-Burning Stoves by Documents Ecoaldeas - Issuu. 1987.
19. Still, D. Earthen Stove Aprovecho Class June 2002. 2002, 18–21.
20. García, G. & Pañi, L. Optimization of the Energy Efficiency of Firewood (Eucalyptus Globulus) as fuel in an Artisanal Brick Kiln Model, Through the Analysis and Modification of Fuel Characteristics, Third Level, Salesian Polytechnic University, Ecuador, 2013, 195.
21. Kshirsagar, M. P. & Kalamkar, V. R. User-Centric Approach for the Design and Sizing of Natural Convection Biomass Cook-stoves for Lower Emissions. *Energy* 2016 115, 1202–1215.
22. Vaca, D. & Ordóñez, F. Research in Alternative Energy. 2019, 12–26.
23. The Weather Channel. Weather Map and Radar. Available online: https://weather.com/es-GT/tiempo/mapas/interactive/l/d0402d7fffa1e3a93baa0a4002cee53c88a61a4db957474bec102e62374a0706 (12-03-2021).
24. Gandigude, A. & Nagarhalli, M. Simulation of Rocket Cook-Stove Geometrical Aspect for its Performance Improvement. *Mater Today Proc* 2018 5, 3903–3908.
25. Recalde, C. *et al.* In-situ Energy and Security Evaluations of Wood Stoves in the High Andean Region of Ecuador. *Espacios* 2018 39.
26. Global Alliance For Clean Cook-stoves. Water boiling test (4.2.3). 2014.
27. Nuwayhid, R. Y., Rowe, D. M. & Min, G. Low-Cost Stove-Top Thermoelectric Generator for Regions with Unreliable Electricity Supply. *Renewable Energy* Available online: www.elsevier.com/locate/renene (13-08-2022) vol. 28.
28. Champier, D. *et al.* Study of a TE (thermoelectric) Generator Incorporated in a Multifunction Wood Stove. *Energy* 2011 36, 1518–1526.
29. Medina, P., Núñez, J., Ruiz-García, V. M. & Beltrán, A. Experimental and Numerical Comparison of CO2 Mass Flow Rate Emissions, Combustion and Thermal Performance for a Biomass Plancha-Type Cookstove. *Energy for Sustainable Development* 2021 63, 153–159.

ANNEXES 1. Quality Function Deployment for efficient firewood cooking solution.

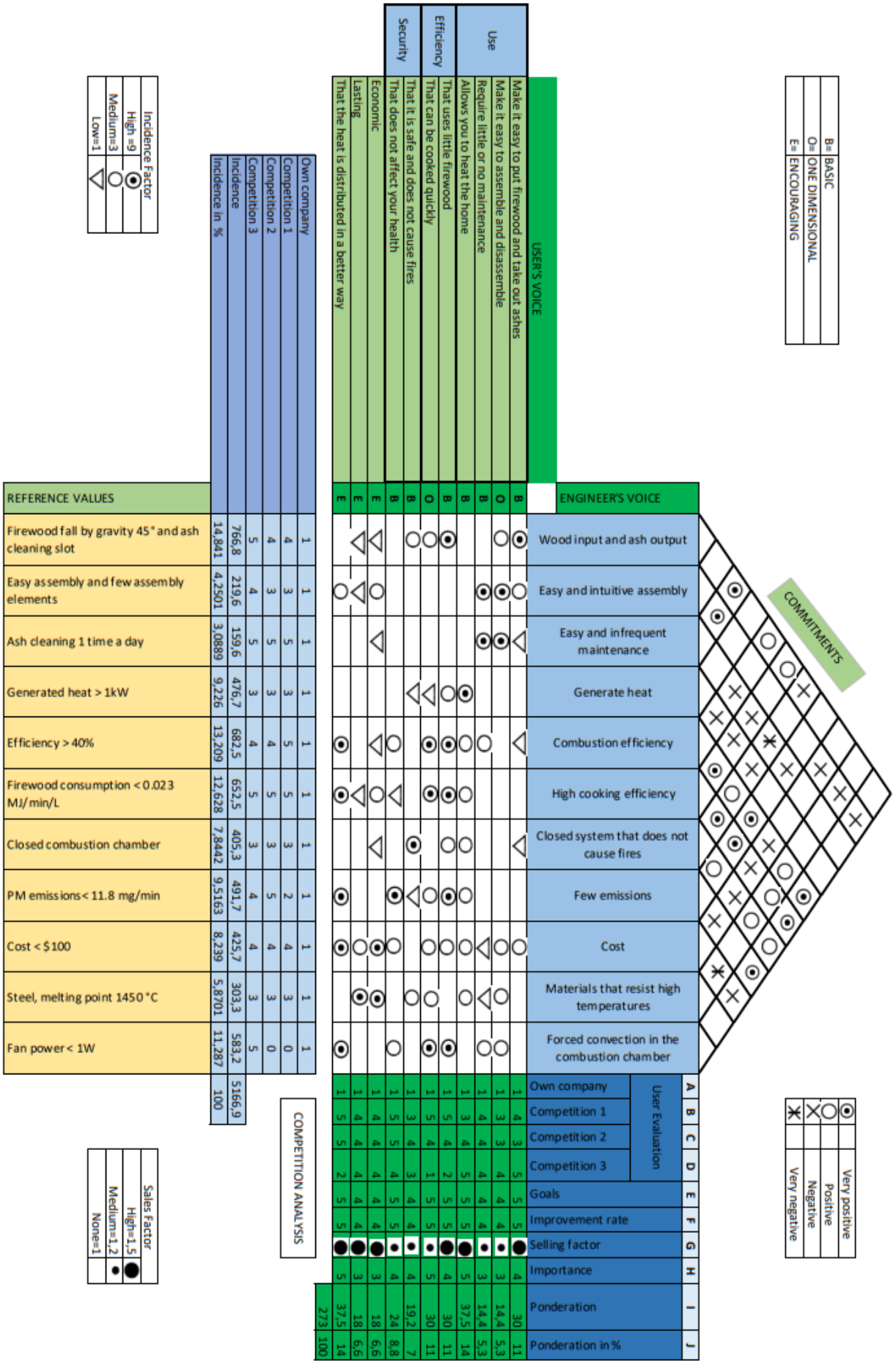

Received: 9 October 2023/ **Accepte**d: 15 January 2024 / **Published:**15 February 2024

Citation. Silva-Castelo W A, Córdova-Uvidia R, Ordoñez-Echeverria Á, Aquino-Arrob*a* M. Analysis of energy poverty in Andean rural households and design of an efficient cooking solution using biomass. Revis Bionatura 2024; 9 (1) 2. http://dx.doi.org/10.21931/RB/2024.09.01.2

Additional information Correspondence should be addressed to *rafael.cordova@espoch.edu.ec*

Peer review information. Bionatura thanks anonymous reviewer(s) for their contribution to the peer review of this work using https://reviewerlocator.webofscience.com/

All articles published by Bionatura Journal are made freely and permanently accessible online immediately upon publication, without subscription charges or registration barriers.
Bionatura ISSN. First 13909355 Ecuador. **Scopus coverage years**: from 2016 to the Present
Publisher's Note: Bionatura stays neutral concerning jurisdictional claims in published maps and institutional affiliations.

Bionatura
Ibero-American Journal of Biotechnology and Life Sciences

Article

Anthropometric indicators and their relationship with body fat in obese women.

Yury Rosales-Ricardo[1*], *Vinicio Caiza-Ruiz*[2], *Sonia Álvarez-Carrión*[3]

[1] *Universidad Nacional de Chimborazo – Ecuador. Facultad de Ciencias de la Salud;Ecuador*
[2] *Universidad Nacional de Chimborazo – Ecuador. Facultad de Ciencias de la Salud.; marcocaiza@unach.edu.ec.*
[3] *Universidad Nacional de Chimborazo – Ecuador. Facultad de Ciencias de la Salud.; salvarez@unach.edu.ec*
* *Correspondence: yuryrr82@gmail.com*
Available from. http://dx.doi.org/10.21931/RB/2024.09.01.3

ABSTRACT

To determine the anthropometric indicator of best correlation with body fat in women with obesity aged 20 to 59 years. A correlational cross-sectional study was conducted. The percentage of body fat was determined (% GC) and lipid profile (LDL, TG, CT), Body Mass Index (BMI), Hip Waist Index (ICC), Waist Height Index (ICE), Conicity Index (CI), Body Adiposity Index (BSI), Hip Height Index (HSI) and Body Weight by Height Index (BWI). Seven hundred and eighty obese women were selected by random cluster sampling. The correlation of the mean % GC with anthropometric indicators was: BMI:0.697, ICC: 0.661, ECI: 0.910, CI: 0.587, ICadE: 0.323, CAI: 0.578, EICP: 0.549. The lipid profile correlation with anthropometric variables and indices was: LDL (BMI: 0.615, ICC: 0.765, ECI: 0.881, CSI: 0.535, ICadE: 0.588, ECDI: 0.492), TG (BMI: 0.690, ICC: 0.776, ICE: 0.855, CI:0.625, CI: 0.572, CIadE: 0.632, EICP: 0.631) Y TC (BMI: 0.699, ICC: 0.715, ECI: 0.829, CI: 0.601, ACI: 0.609, CIadE: 0.709, EICP: 0.500) High correlation between % GC and Waist Circumference. Waist Height Index had a better correlation with Body Fat.

Keywords: obesity; health; women; nutritional status

INTRODUCTION

A country's entire production and service capacity rests on working-age adults. That is why the nutritional evaluation of this group, whose social importance is indisputable, acquires excellent relevance in the study of any population from the point of view of their health status. Anthropometry, an easy-to-apply, inexpensive and non-invasive procedure, has been widely used to estimate nutritional status from a clinical and epidemiological point of view.

The incorporation of women into work, their participation in the economic development of the country and their leading role in the support and development of the family mean that, from a social and financial point of view, their medical attention should be ensured so that the biological changes produced by the decrease in estrogen production in their organism do not turn this transition stage into a disease, for which these women should receive comprehensive medical attention.

Obesity in women has peculiar nuances that are beginning to be understood. The higher prevalence of obesity in women is a product of biological and psychological characteristics, as well as social situations. Pregnancy and menopause favor obesity. Women have a higher prevalence of eating disorders. In addition, the "obesogenic" environment may have a more significant effect on women because the portions they eat are usually greater than their needs [1].

According to the World Health Organization (WHO) [2], obesity is the most prevalent chronic non-communicable disease in the world, which is why it is called "The Epidemic of the 21st Century". Over 3 billion adults were overweight in 2016, 39% of persons (39% of males and 40% of women). In total, 11% of men and 15% of women in the adult population of the world were obese in 2016 [2].

According to the latest concept issued by WHO, obesity is defined as an abnormal or excessive accumulation of fat [2], i.e., describing this as a body weight above values considered normal for height would be incorrect and would depart from the genuine concept of obesity, as body fat is only one component of total body weight.

The indicator used and validated to evaluate obesity in adults is the Body Mass Index (BMI). However, this has several difficulties in the sense that what it considers is overweight and not obesity. On the other hand, other indicators such as waist circumference (WC) and waist height index (WHI) 3 have been less studied in these populations. The EWI in Asian studies (in adults from China) [4] is a better indicator of coronary risk factors, dyslipidemia and type 2 diabetes than other anthropometric indicators such as BMI, WC and waist-hip index in some epidemiological studies [4 - 9]. The results indicated that the EWI could be an optimal anthropometric predictor of metabolic syndrome risk factors. Other less-used indexes at international level, such as the Conicity index 10 or the Body Adiposity Index 11, have reported good results.

Therefore, this study aimed to determine the anthropometric indicator with the best correlation with body fatness in obese women aged 20 to 59.

MATERIALS AND METHODS

Cross-sectional correlational study to determine the relationship between body fat percentile (using three anthropometric methods in isolation and the mean of these) and lipid profile (LDL, TC, TAG) and other existing anthropometric indicators such as Body Mass Index, Waist Circumference, Hip Circumference, Body Weight, Waist Hip Index, Hip Height Index, Taper Index, Conicity Index, Body Weight, Hip Hip Height Index, Hip Height Index, Hip Height Index, Hip Taper Index, Hip Conicity Index and Body Weight, Waist Circumference, Hip Circumference, Body Weight, Waist Hip Index, Hip Height Index, Conicity Index, Body Adiposity Index, based on the correct WHO definition of obesity.

For this purpose, 780 women with obesity were selected using random sampling by clusters. The first conglomerate was the 320 clinics in the 10 health areas of Holguin, Cuba. From there, 20% of these (64 clinics) were selected by simple random sampling. From each clinic, one out of every ten patients with these research characteristics was determined by systematic random sampling. Of these 780 patients, 55 did not present themselves, for a 7 % loss, and another 35 were no longer obese or pre-obese when they introduced themselves or did not want to donate their data to the study, for a 4.4 % loss, which represented a total loss of 11.4 % (90 patients). The final sample consisted of 690 female patients between 20 and 59 years of age with obesity from the 10 health areas of the municipality of Holguín, Cuba. In the consultation of health promotion and physical development of the Provincial Center of Sports Medicine of Holguin, 30 patients were attended weekly, two days per week for 26 weeks.

Anthropometric measurements were performed by an anthropometric technician level II of the International Society for the Advancement of Kineanthropometry (ISAK). Body weight was determined using a previously calibrated electronic scale with a sensitivity of up to 0.1 kg, and height was measured utilizing a stadiometer with a sensitivity of 0.1 cm. A Harpenden caliper with a sensitivity of 0.1 mm and a pressure of 10 mm2 was always used for the triplicate evaluation of the 4 skinfolds (tricipital, bicipital, subscapular and suprailiac muscles). The percent body fat was assessed by first estimating the Body Density using the Durnin-Womersley formula for women between 16 and 72 years of age (measurement of the bicipital, tricipital, subscapular and suprascapular skinfolds) and then taking this result to the Siri equation to determine the fat percentages. All

measurements were performed in triplicate in a non-consecutive manner and using the median as the final value [12].

The lipid profile was found in the clinical area of the Center in conjunction with the Department of Clinical Bioanalysis of the University of Medical Sciences of Holguin.

The author of the research carried out the surveys.

Measurements were taken for both studies (according to the methodology of the International Society for the Development of Cineanthropometry, ISAK) [15]:

The sequence of measurements used:

1. Body weight (BW) in kg.

2. Height (E) in meters

3. Waist circumference (WC) in cm.

4. Circumference of the hip (CCad) in cm.

5. Biceps crease (Pb) in mm.

6. Triceps crease (Pt) in mm.

7. Subscapularis crease (Pse) in mm.

8. Suprailiac crease (Psi) in mm.

Other variables considered:

1- Age in years

2- Associated pathologies

To determine the type of causal obesity (exogenous or endogenous), we used the determination of the possible associated pathologies that could have caused the obesity in the clinical consultation of the Center using the methodology of the SEEDO [12, 15].

It was essential to identify the medications taken by the patient, with particular emphasis on determining the intake of drugs associated with an increase in weight, such as insulin, sulfonylureas, methyglinides, thiazolidinediones, phenothiazines, tricyclic antidepressants, certain antipsychotics, glucocorticoids, megestrol acetate, estrogens, antiepileptics such as valproate and carbamazepine, cyproheptadine and beta-blockers. This suggested the presence of endogenous obesity [12, 15].

From the results of these variables, the following indexes were found:

1- Percent body fat (%BF).

Three methods found this:

A) The above four skinfolds were measured to estimate body density (D) and from there, the percent body fat (%BF) with the Durnin-Womersley and Siri equation, respectively, for the female population of working age (18 to 59 years) for adult Cuban population 16:

$$D = 1.1567 - 0.0717 * \log10 (Pt + Pb + Pse + Psi) \quad (1)$$

$$\% GC = (5.03 / D) - 4.59$$

B) Weltman's formula for obese women aged 20 to 60 years [13, 16]:

% GC= 0.11077 * CC - 0.17666 * E + 0.14354 * PC + 51.033.

C) Lean's more accurate formula for women aged 18 to 83 years [14, 16]:

% GC= 0.232 * CC + 0.657 * Pt + 0.215 * Age - 5.5

In addition to the individual result of each one, the average of the three values was also found to determine the fat percentages and their correlation with the anthropometric indexes that are exposed below much more efficiently:

1- Body Mass Index (BMI)

BMI= WC / E2

2- Waist Hip Index (ICC)

ICC= CC / CCad

3- Height Waist Height Index (ICE)

ICE= CC / E

4- Conicity Index (CI) [17]

CI= CC / (0.109 √ PC / E)

5- Body Adiposity Index (BAI) [18]

BCI= ([CCad]/[E]1.5-18)

6- Hip Height Index (ICadE)

ICadE= CCad / E

Index proposed by the author

The venous blood samples to determine the laboratory variables were taken after an overnight fast of 12-14 hours, and low-lipid diets were processed in duplicate, not exceeding 5% of the variation coefficient. The reagents of national production (Finlay laboratories): total cholesterol (TC): Colestest reagent; triglycerides (TG): Triglitest reagent and low-density lipoproteins (LDL) according to Friedewald's formula (LDL= CT-(HDL + TG * 5).

The results of PC, CC, CCad, BMI, ICC, IAC, IC, ICadE and ICE were correlated with the %GC in their three results, the mean of these three values, and the lipid profile.

The mean (X) and standard deviation (SD) were used for the parametric statistical analysis. The Spearman correlation coefficient was employed to study the level of correlation between variables. A 95% confidence interval was used.

The objectives and procedures of the study were explained in detail to all the participants, and they were provided with the necessary information for their knowledge. In addition, so that they could answer correctly, the interview was carried out as long as the patients expressed their informed consent to participate in the research and also agreed to answer questions involving the sexuality of the couple. This was a research project cited in the no-risk research category.

RESULTS

The final sample of 690 women diagnosed with obesity in all health areas of Holguín municipality, aged between 20 and 59 years, is shown in Table 1.

	X	SD
Age	41.7	± 19.66
% GC	40.3	± 5.93
BMI	36.6	± 4.81
ICC	0.91	± 0.14
ICE	**0.57**	± 0.11
CI	1.49	± 0.19
IAC	33.1	± 3.44
ICadE	0.64	± 0.13

P <0.05

Table 1. Descriptive statistics of the study variables.

In women with obesity, there is a high correlation between Body Fat and Waist Circumference, with a somewhat lower correlation between the former and Body Weight and Height. On the other hand, there is a low correlation with Hip Circumference and Age (Table 2).

	PC	E	CC	CCad	Age
% GC Pc	.612*	.596*	.815**	.390	.284
% GC L	.634*	.570*	.895**	.335	.280
% GC W	.626*	.618*	.874**	.410	.305
X % GC	**.624***	**.595***	**.861****	**.378**	**.290**

P <0.05

Table 2. Correlation of the variables with the % CG. Total sample (n= 690).

Legend: %BF Pc: percent body fat calculated using skinfolds; %BF L: percent body fat using the Lean equation (21); %BF W: percent body fat calculated using the Weltman equation(5); X %BF: mean of the three results; BW: body weight (kg); E: height (meters); WC: waist circumference or circumference (cm);

HC: waist circumference or circumference (cm); HCad: hip circumference or circumference (cm). Degrees of correlation: **: highly significant (.750 - 1); *: significant (.500 - .749).

The Height-Waist Index was the best correlated with Body Fat in the whole population studied, much higher than other validated and much more used indexes (Table 3).

	BMI	**ICC**	**ICE**	**IC**	**BAC**	**ICadE**	**IPCE**
% GC Pc	.715*	.618*	.896**	.560*	.572*	.315	.556*
% GC L	.685*	.680*	.928**	.605*	.570*	.320	.545*
% GC W	.690*	.685*	.905**	.595*	.592*	.335	.553*
X % GC	**.697***	**.661***	**.910****	**.587***	**.578***	**.323**	**.549***

P <0.05

Table 3. Correlations between anthropometric indices and %GC. Total sample (n= 690).

In women with android obesity, the variable that correlated best with Body Fat was by far Waist Circumference. The index was Waist Height (Table 4).

	BMI	**ICC**	**ICE**	**IC**	**IAC**	**ICadE**	**IPCE**
% GC Pc	.715*	.590*	.950**	.585*	.410	.320	.490
% GC L	.685*	.612*	.965**	.598*	.425	.312	.505*
% GC W	.712*	.631*	.958**	.599*	.432	.355	.510*
X % GC	**.706***	**.611***	**.961****	**.594***	**.422**	**.329**	**.502***

P<0.05

Table 4. Index correlations with %GC in obese android women (n=587).

In women with gynecoid obesity, on the other hand, the variable with the best correlation with Body Fat was Hip Circumference and the index was Hip Height, proposed by the author. (Table 5).

.	**BMI**	**ICC**	**ICE**	**IC**	**IAC**	**ICadE**	**IPCE**
% GC Pc	.634*	.605*	.332	.538*	.715*	.890**	.498
% GC L	.642*	.622*	.318	.556*	.733*	.912**	.514*
% GC W	.649*	.612*	.327	.565*	.738*	.919**	.508*
X % GC	**.642***	**.615***	**.326**	**.553***	**.729***	**.907****	**.507***

P<0.05

Table 5. Index correlations with %GC in obese gynaecoid women (n=103).

As for the lipid profile, the highest correlations with this were found in the Waist Hip Index, Waist Circumference, Waist Hip Index, Body Mass Index, Hip Height Index and Taper Index in that order (Table 6).

	PC	CC	CCad	BMI	ICC	ICE	IC	IAC	ICAdE	IPCE
LDL	.306	.815**	.344	.615*	.765*	.881**	.509*	.535*	.588*	.492
TG	.430	.840**	.390	.690*	.776*	.855**	.625*	.572*	.632*	.631*
CT	.422	.787**	.410	.699*	.715*	.829**	.601*	.609*	.709*	.500*

P<0.05

Table 6. Correlation of lipid profile with anthropometric variables and indices. Total sample (n= 690)

DISCUSSION

The main objective of this study was to determine the anthropometric indicator with the best correlation with body fat in obese women aged 20 to 59 years. Skinfolds, present in most studies on body composition as a comparison technique, show a high concordance or correlation with %BF obtained through various techniques such as densitometry, dilutional methods and bioelectrical impedance, which, together with its cost and accessibility, justifies its wide use in this type of studies and can be considered as the gold standard among anthropometric measurements. The Spanish Society for the Study of Obesity (SEEDO) recommends the use of skinfolds and the Siri equation for the assessment of body fat percentage, considering both the global and the specific way of calculating body density with the Durnin-Womersley equation to be valid [19].

This can be seen in a critical study in Brazil where the relationship between anthropometric markers of fat distribution and body fat as measured by bioelectrical impedance or the total number of skinfolds was assessed in 262 women. The body fat determined by skinfold summation and bioelectrical impedance were comparable. The thicknesses of body fat measured by bioelectrical impedance and those calculated by the sum of skinfolds, waist circumference, and waist-to-height ratio were strongly correlated. As for the taper index, a weak correlation was observed for women; the results were similar in our study [20].

Regarding the current research, similar results have been observed in other studies, as shown in the study by Oliveira et al.[21] men had higher BMI, WC, and WHR, whereas women had higher %BF (p 0.001). Males had a greater proportion of changed RCC and %GC for LDL-c and TC. There was a link between BMI and CC (r = 0.97 for men and 0.95 for women; p 0.001). The best association (p 0.001) in men was between CC and CCR (r = 0.82), and in women, it was %GC as well as CC (r = 0.80). Triglycerides (TG) were found to be connected to CC (male: r = 0.992; female: r = 0.95; p 0.001), as well as to CC (male: r = 0.82; female: r = 0.79; p 0.001). In several analyses, BMI was associated with total cholesterol (p = 0.051) in males and weakly associated with TG/HDL-cholesterol (p = 0.062) in females.

In a study conducted in Pernambuco, Brazil,[22,] the diagnosis of MS was found in 65.3% of the patients. There were 81.3% who were inactive and 37.4% who were overweight in 28% of the patients. HOMA-IR and sagittal abdominal diameter (SAD) (p = 0.016), body mass index (p = 0.040), and body fat % (p = 0.016) were found to be correlated. The DAS was the anthropometric indicator that presented the best correlation with IR in hospitalized patients with coronary artery disease.

Another study included a sample of 105 workers. The following were operationalized as clinical variables: abdominal waist measurement, body mass index, skin fold, blood pressure and lipid profile. Pearson's correlation coefficient was calculated with a 95% confidence interval. The results showed a slight increase in total cholesterol in males at the expense of HDL cholesterol, with no changes in the other variables. A higher susceptibility to cardiometabolic risk was seen in non-obese people. There was insufficient concordance with our investigation since the fat mass index did not significantly correlate with the other anthropometric

measures. Individuals with a changed abdominal circumference and the metabolic syndrome diagnostic criteria are closely related. [23].

Domínguez-Reyes et al.[24] evaluated anthropometric measures in a Mexican adult; after abdominal obesity in women, hypertriglyceridemia was the metabolic risk factor with the highest prevalence, followed by hyperglycemia, hypercholesterolemia and high blood pressure, which were more common in men, even though abdominal obesity was more common in women. Waist circumference was the best predictor for presenting one or more metabolic risk factors [area under the curve ABC = 0.85 (95% CI, 0.78-0.92)], followed by BMI [ABC = 0.79 (95% CI, 0.72-0.88)] and finally ICC [ABC = 0.63 (95% CI, 0.52-0.74)]. In addition, it was observed that abdominal obesity doubles the risk of presenting metabolic syndrome. In a different study, the waist-to-height ratio (WHI) was the predictor variable with the highest adjusted OR (7.1 [4.3-11.6]) and the highest area under the curve (0.954 [0.928-0.979]); from an overall cut-off value for discriminating obesity of 0.507, it achieved a sensitivity of 90% and a specificity of 90%, has been an excellent predictor of obesity in children [25].

In other studies, the correlations were: BMI: body fat (0.70) very coincident with our study (0.697), waist (0.70), ICCad (0.48), ICT (0.72); ICCad: body fat (0.38), waist (0.69), endomorphy (0.39), mesomorphy (0.38); ICT: body fat (0.50) slightly different with ours (0.661) and waist (0.96); taper: waist (0.85), ICCad (0.58), ICT (0.85). The indicator with the poorest relationship between obesity and body mass index does not distinguish between different body parts. The waist-hip index presents a high prevalence but a weak relationship with body composition at risk. The waist-height index reflects a distribution of body volume. It suggests the best correlations with the body components at risk, being the most prevalent and adequate index to explain the biological risk associated with myocardial infarction [26].

The main strength of the present study is the quality of its methodology: the use of measurement protocols that were carried out according to the methods of the International Society for the Development of Kineanthropometry (ISAK) and SEEDO to perform the measurements and hence the realization of the respective anthropometric indicators. An ISAK level II anthropometric technician performed the anthropometric measurements. In addition, the sample used was probabilistic, using random cluster sampling, representative of the population.

Despite its strengths, some issues related to our studies deserve attention. It was impossible to measure body fat percentages using the international gold standard measures that would have given greater accuracy in correlation levels with the double indirect anthropometric indicators used. Furthermore, it was not possible to work with populations from other provinces of the country.

CONCLUSIONS

Therefore, it can be concluded that, in women with obesity, in general, there is a high correlation between Body Fat and Waist Circumference. The Waist Height Index was the one that correlated best with Body Fat over the other most commonly used indexes. In women with android obesity, the variable that best correlated with Body Fat was Waist Circumference, and the index was the Waist Height Index. In women with gynecoid obesity, the variable with the best correlation with Body Fat was Hip Circumference, and the index was Hip Height, as proposed by the author. With lipid profile, the highest correlations were found in the Waist Hip Index, Waist Circumference, Waist Hip Index, Body Mass Index, Hip Height Index and Conicity Index.

Author Contributions: A short paragraph specifying their individual contributions must be provided for research articles with several authors. The following statements should be used "Conceptualization, YRR; methodology, YRR, VCR, SAC; software, YRR; validation, YRR; formal analysis: YRR, VCR, SAC; investigation, YRR, VCR, SAC; resources, YRR; data curation, YRR; writing—original draft preparation, YRR; writing—review and editing, YRR, VCR, SAC; visualization, YRR; supervision, YRR; project administration, YRR; funding acquisition, YRR All authors have read and agreed to the published version of the manuscript." Please turn to the CRediT taxonomy for the term explanation. Authorship must be limited to those who have contributed substantially to the work reported.

Funding: "This research received no external funding."

Institutional Review Board Statement: "Not applicable."

Informed Consent Statement: "Not applicable."

Conflicts of Interest: "The authors declare no conflict of interest."

REFERENCES

1. Cano, E. R., Recio, G. M., Saldaña, M. R., Fernández, C. Á., Reyes, A. H., & Luque, R. M. (2020). Comparación de índices antropométricos, clásicos y nuevos, para el cribado de Síndrome Metabólico en población adulta laboral. Revista española de salud pública. 2020; (94), 83.
2. Obesidad y sobrepeso [Internet]. Who.int. [citado el 22 de enero de 2023]. Disponible en: https://www.who.int/es/news-room/fact-sheets/detail/obesity-and-overweight
3. Hsieh T. The waist and height ratio as a simple anthropometric index to identify metabolic risk. Internac J of Obesit. 2003; 27(5): 610-616
4. Shao J, Yu L. Waist-to-Height Ratio, an Optimal Predictor for Obesity and Metabolic Syndrome in Chinese Adults. J Nutr Health Aging. 2010; 14(9):782-5.
5. Ashwell M, Gibson S Waist-to-height ratio as an indicator of 'early health risk': simpler and more predictive than using a 'matrix' based on BMI and waist circumference BMJ Open 2016;6: e010159. doi: 10.1136/bmjopen-2015-010159
6. Sardinha LB, Santos DA, Silva AM, Grøntved A, Andersen LB. A Comparison between BMI, Waist Circumference, and Waist-To-Height Ratio for Identifying Cardio-Metabolic Risk in Children and Adolescents. PLOS ONE. 2016; 11(2): e0149351. https://doi.org/10.1371/journal.pone.0149351
7. Hou X, Chen S, Hu G, Chen P, Wu J, Ma X, Jia W. Stronger associations of waist circumference and waist-to-height ratio with diabetes than BMI in Chinese adults. Diabetes research and clinical practice. 2019; 147:9-18.
8. A Rodrigues, L Mascarenhas, A Gama, I Mourão, H Nogueira, V Rosado, C Padez, Waist-to-height ratio and its association with sedentary behaviour in a sample of Portuguese male children, *European Journal of Public Health*, 2019; 29(1) ckz035.026, https://doi.org/10.1093/eurpub/ckz035.026
9. Lam BCC, Koh GCH, Chen C, Wong MTK, Fallows SJ. Comparison of Body Mass Index (BMI), Body Adiposity Index (BAI), Waist Circumference (WC), Waist-To-Hip Ratio (WHR) and Waist-To-Height Ratio (WHtR) as Predictors of Cardiovascular Disease Risk Factors in an Adult Population in Singapore. PLOS ONE. 2015; 10(4): e0122985. https://doi.org/10.1371/journal.pone.0122985
10. Rachael W Taylor, Ianthe E Jones, Sheila M Williams, Ailsa Goulding, Evaluation of waist circumference, waist-to-hip ratio, and the conicity index as screening tools for high trunk fat mass, as measured by dual-energy X-ray absorptiometry, in children aged 3–19. The American Journal of Clinical Nutrition, 2000; 72(2): 490–495, https://doi.org/10.1093/ajcn/72.2.490
11. Bergman, R. N., Stefanovski, D., Buchanan, T. A., Sumner, A. E., Reynolds, J. C., Sebring, N. G., Xiang, A. H. and Watanabe, R. M. A Better Index of Body Adiposity. Obesity. 2011; 19: 1083-1089. doi:10.1038/oby.2011.38
12. Lecube A, Monereo S, Rubio MÁ, Martínez-de-Icaya P, Martí A, Salvador J, Masmiquel L, Goday A, Bellido D, Lurbe E, García-Almeida JM, Tinahones FJ, García-Luna PP, Palacio E, Gargallo M, Bretón I, Morales-Conde S, Caixàs A, Menéndez E, Puig-Domingo M, Casanueva FF. Prevention, diagnosis, and treatment of obesity. 2016 position statement of the Spanish Society for the Study of Obesity. Endocrinol Diabetes Nutr. 2017 Mar;64 (1):15-22.
13. Cándido A. P. C., Alosta J. P. S., Oliveira C. T., Freitas R. N., Freitas S. N., Machado-Coelho G. L. L.. Anthropometric methods for obesity screening in schoolchildren: the Ouro Preto Study. Nutr. Hosp. 2012 Feb [citado 2018 Jul 05] ; 27(1): 146-153.
14. Lean, EJ. Waist circumference as a measure for indicating need for weight management, BMJ, 1995; 311:158-161.
15. Ferreyro, F., Esparza, F. y Jones, M., Eds. Kinanthropometry XV. International Society for the Advancement of Kinanthopometry Conference. World Conference in Knanthropometry and Body Composition ISAK-UADY 2016, Ediciones de la Universidad Autónoma de Yucatán, Mérida, Mexico. 284 p.

16. Carvajal W, Deturnel Y, Echevarría I, Martínez M, Castillo ME. Protocolo de valoración de la composición corporal para el control cineantropométrico del entrenamiento deportivo. Documento de consenso del Departamento de Cineantropometría del Instituto de Medicina del Deporte de Cuba. Revista. Cubana de. Medicina del. Deporte y la Cultura. Física 2010; 5(3).
17. Valdez R, Seidell JC, Ahn YI, Weiss KM. A new index of abdominal adiposity as an indicator of risk for cardiovascular disease. A cross-population study. Int J Obes Relat Metab Disord. 1993 Feb;17(2):77-82.
18. Bergman RN, Stefanovski D, Buchanan TA, Sumner AE, Reynolds JC, Sebring NG, Xiang AH, Watanabe RM. A better index of body adiposity. Obesity (Silver Spring). 2011 May; 19(5):1083-9
19. Martín Moreno Vicente, Gómez Gandoy Juan Benito, Antoranz González María Jesús. Medición de la grasa corporal mediante impedancia bioeléctrica, pliegues cutáneos y ecuaciones a partir de medidas antropométricas. Análisis comparativo. Rev. Esp. Salud Publica . 2001 Mayo; 75(3): 221-236.
20. Diniz-Araujo. Evaluación de la grasa corporal por impedancia bioeléctrica y su correlación con indicadores antropométricos. Nutr. Hosp. 2012; 27(6)
21. Oliveira M, Arruda M, Fagundes R, Martins L, Moreira E, Trindade E. Relación de indicadores antropométricos con factores de riesgo para enfermedad cardiovascular. Arq. Bras. Cardiol. 2010 Ap; 94(4): 478-485.
22. Pessoa L, Araújo Tavares CM, Freire Clementino MC, Freire Lustosa M, Batista RA, Calado Brito D. Asociación de los indicadores antropométricos y de composición corporal en la predicción de la resistencia a la insulina en pacientes con enfermedad de las arterias coronarias. Nutr. Hosp. 2016 Ago; 33(4): 825-831.
23. Cedeño Morales R, Castellanos González M, Benet Rodríguez M, Mass Sosa L, Mora Hernández C, Parada Arias JC. Indicadores antropométricos para determinar la obesidad, y sus relaciones con el riesgo cardiometabólico. Revista Finlay; 2015; 5(1): 12-23
24. Domínguez-Reyes T, Quiroz-Vargas I, Salgado-Bernabé AB, Salgado-Goytia L, Muñoz-Valle JF, Parra-Rojas I. Las medidas antropométricas como indicadores predictivos de riesgo metabólico en una población mexicana. Nutr. Hosp. 2017 Feb; 34(1):96-101. Disponible en: http://scielo.isciii.es/scielo.php?script=sci_arttext&pid=S0212-16112017000100015&lng=es. http://dx.doi.org/10.20960/nh.983.
25. Vaquero-Álvarez M, Romero-Saldaña M, Valle-Alonso F, Llorente J, Cantarero. Estudio de la obesidad en una población infantil rural y su relación con variables antropométricas. Atención Primaria;2019; 51 (6): 341-349
26. Martín-Castellanos A, Cabañas MD, Martín P, Barca FJ. The body composition in myocardial infarction males. Novel findings in both the association and relationship between anthropometric indicators of risk. JONNPR. 2017;2(9):388-398. DOI: 10.19230/jonnpr.1547

Received: 9 October 2023/ **Accepte**d: 15 January 2024 / **Published:**15 February 2024

Citation. Rosales-Ricardo Y, Caiza-Ruiz V, Álvarez-Carrión S. Anthropometric indicators and their relationship with body fat in obese women. Revis Bionatura 2024; 9 (1) 3. http://dx.doi.org/10.21931/RB/2024.09.01.3

Additional information Correspondence should be addressed to *yuryrr82@gmail.com*

Peer review information. Bionatura thanks anonymous reviewer(s) for their contribution to the peer review of this work using https://reviewerlocator.webofscience.com/

Bionatura ISSN. First 13909355 Ecuador. **Scopus coverage years**: from 2016 to the Present

Bionatura
Ibero-American Journal of Biotechnology and Life Sciences

Article

Biological nematicides as an alternative for control of *Meloidogyne incognita* populations in yellow pitahaya (S*selenicereus megalanthus*).

Yadira Vargas[1]*, *Jimmy Pico*[1], *Neiver Manobanda*[2], *Angel Garcia*[1], *Jessica Sanmiguel*[1].

[1] *Estación Experimental Central de la Amazonía, Instituto Nacional de Investigaciones Agropecuarias, La Joya de los Sachas, Ecuador; jimmy.pico@iniap.gob.ec; angel.garcia@iniap.gob.ec..; jessica.sanmiguel@iniap.gob.ec.*
[2] *Tesista, Escuela Superior Politécnica de Chimborazo, Extensión Norte Amazónica;manobandaneiver1999@gmail.com*
* *Correspondence: yadira.vargas@iniap.gob.ec; +593 0991900401.*
Available from. http://dx.doi.org/10.21931/RB/2024.09.01.4

ABSTRACT

Yellow pitahaya in the Ecuadorian Amazon has become one of the most important economic crops in the region. However, the presence of pests (nematodes) in the soil has caused up to 100% of the crop's growth stages to be affected. Faced with this problem, growers use various chemical nematicides that minimize this impact but cause contamination problems. For this reason, the objective of the research was to evaluate microorganisms that control or reduce the population of *Meloidogyne incognita* in the pitahaya crop at the greenhouse level. The design was DBCA, and the statistical analysis was performed with the statistical package Infostat 2017, using linear mixed models and Fisher's tests at 5%. The results show that root nodules decrease when P. lilacinum + T. asperellum is applied after nematode injection (261). In addition, the lowest number of nodulations (251) was obtained when microorganisms were applied after nematode inoculation (251 nodulations). Still, when microorganisms were used before, aerial biomass growth was stimulated (384.17 g) even when nematodes were present in the root system.

Keywords: microorganisms; nematodes; pitahaya.

INTRODUCTION

The pitahaya (*Selenicereus megalanthus* Haw.) is an exotic fruit cultivated in various Latin American countries such as Mexico, Central America, Venezuela, Ecuador, Colombia, and Peru [1]. Recently, countries such as Panama, Uruguay, Thailand, and Indonesia have also started cultivating this fruit due to its functional properties [2].

In Ecuador, it is estimated that there are around 2000 hectares dedicated to pitahaya cultivation, mainly in the provinces of Pichincha, Manabí, and in the Amazon region in Morona Santiago, Orellana, and Sucumbíos [3]. In the Amazon region, pitahaya cultivation is commercially a monoculture using conventional agronomic methods. This is mainly due to the vulnerability of pitahaya to various pests and diseases, such as fungi, bacteria, viruses, insects, and nematodes, which affect the plantations at all stages of growth. The most

common nematodes affecting pitahaya belong to the genera *Meloidogyne* sp. (50-81%), *Helicotylenchus dihystera* (82-100%), *Hemicycliophora* sp., *Tylenchorhynchus* sp., *Xiphinema* sp., *Trichodorus* sp., *Hoplotylus* sp., *Hemycicliophora* sp., *Dorylaimus* (27%), *Tylenchus* (23%), *Aphelenchus* (14%), and *Pratylenchus* (5%) [4-5]. In the Palora canton, which hosts the largest cultivated area of pitahaya, it has been observed that 97% of the plantations are affected by *Meloidogyne* sp. and *Helicotylenchus* spp.. In comparison, 3% are impacted by *Tylenchus* ssp. [6]. Nematode infestation, especially of the genus *Meloidogyne* sp., in the root system of pitahaya plants causes a decrease in crop yield. This is due to the formation of nodules in the roots, which hinders water absorption and nutrients from the soil [7-8]. Additionally, visible symptoms in the aboveground part of the plants include yellowing, thin and weak stems [9,6,5].

Currently, non-fumigant products, such as organophosphates and carbamates, chemical compounds with nematicidal activity, are used for nematode control in pitahaya cultivation. However, these products present environmental risks and can be toxic to humans [10]. Studies conducted in different crops, such as lettuce, tomato, cauliflower, celery, and broccoli, have found pesticide residues (organophosphates and carbamates) in 48% of the analyzed products [11-13]. Furthermore, it has been observed that 3% of agricultural workers exposed to pesticides suffer annually from chronic intoxication, neurological disorders, peripheral neuritis, male hormonal alterations, optic nerve problems, cataract formation, and respiratory effects [12].

Given that nematode control in pitahaya crops is mainly carried out with highly toxic nematicides, it is urgent to seek alternatives to the use of pesticides. In this regard, biological control through antagonistic organisms has been the research subject in recent years, and its potential for managing plant-parasitic nematodes has been recognized [14]. These beneficial organisms include *Pasteuria penetrans, Pasteuria hartismeri, Pochonia chlamydosporia, Bacillus firmus, Paecillomyces lilacinus,* and *Trichoderma* spp. These microorganisms act by adhering to the nematodes' cuticle or parasitizing the females' eggs, resulting in the death of the nematodes. Although variable results have been obtained in research on antagonistic organisms, their effectiveness in controlling plant-parasitic nematodes has been demonstrated. However, only a tiny group of antagonistic organisms has been studied in detail [15].
For this reason, this research aimed to evaluate microorganisms that control or reduce the population of Meloidogyne incognita in the pitahaya crop at the greenhouse level. For this study, strains of microorganisms from pitahaya plantations, which have been selected at the in vitro level, were used. In addition, a commercial product based on *P. lilacinum* + *T. asperellum* was employed because there are products that no longer have viable fungal spores when they do not receive a good storage process.

MATERIALS AND METHODS

Location of the Experiment

This study was conducted at the Central Experimental Station of the Amazon (EECA), National Institute of Agricultural Research (INIAP), in Orellana, La Joya de los Sachas canton province. The experimental site was situated at 0291649 latitude and 09962311 longitude, with an altitude of 282 meters above sea level. The climate in the area is warm and humid tropical, with an average annual temperature of 25°C, an average maximum temperature of 22°C, an average minimum temperature of 40°C, and an average relative humidity of 90%. In the greenhouse, the average relative humidity is 70%, and the average temperature is 35°C.

Treatments

The experiment was organized in a randomized complete block design with three replications. The experimental unit consisted of eight pots with yellow pitahaya cuttings. The treatments consisted of T1 (*Purpureocillium lilacinum*) Laboratory strains, T2 (*Trichoderma asperellum*) Laboratory strains, T3 (*Purpureocillium lilacinum* + *Trichoderma asperellum*) Laboratory strains, T4 (*Purpureocillium lilacinum* + *Trichoderma asperellum*) Comercial product, T5 (absolute control), and T6 (control + nematode). The microorganisms stored in the laboratory and used for this study already come from a previous research process; they arrive from pitahaya plantations.

Specific Management of the Experiment

The study was implemented under greenhouse conditions. Yellow pitahaya cuttings of 40 cm were planted in pots with 4500 g of sterilized soil at 2 to 3 cm depth. After 22 days, the cuttings began to emit their first roots [16].

M. incognita was extracted from the galled roots of yellow pitahaya. The roots were washed, cut into approximately 1 cm sections, and blended with 100 ml of water in a blender for 20 seconds in two intervals with five seconds of rest. Subsequently, the blender content was passed through a set of nested sieves with 250, 150, and 25 µm openings (mesh sizes of 60, 100, and 500, respectively). The content placed on the 250 and 150 µm sieve was rinsed with running water for 1 minute. The sediment on the No. 500 sieve was collected in a graduated cylinder and filled with 100 ml of water. It was then homogenized with an air pump, and a 4 ml aliquot was taken for nematode identification and counting using a trinocular inverted microscope with LWD IOS objectives, X-LED illumination, and EWF10X/22mm eyepieces [17].

Finally, *M. incognita* was inoculated into 15-day-old tomato plants (*Lycopersicum esculentum* Mill) from transplant. After 30 days, nematodes were extracted from the *L. esculentum* Mill plants and inoculated into pitahaya plants. Approximately 1200 J2 nematodes were applied. Four 5 cm deep holes were made in the soil near the base of the plant stem for injection, the nematode solution was poured, and then the holes were covered [18,19].

The biological control agents used were *T. asperellum* and *P. lilacinum*. Spore crystals were taken with sterile forceps and seeded on Petri dishes containing Potato Dextrose Agar (PDA) medium [20]. Sterilized rice substrates were used to mass produce the control agents and a conidial suspension of *T. asperellum* and *P. lilacinum*. The conidial suspension was prepared by adding 20 ml of sterile distilled water with 0.1% Tween 80 to each Petri dish containing *T. asperellum* and *P. lilacinum* with 6 days of growth. To this conidial suspension, 125 ppm of chloramphenicol was added. Subsequently, 3 ml of each suspension was taken using a sterile pipette and deposited in bags containing 150 g of the sterilized substrate (rice), which were then incubated for 15 days at a room temperature of 24 ± 2 °C [21]. To establish the inoculum concentration, 1 g of rice from each multiplied substrate was weighed, and a suspension was prepared in 10 ml of distilled water. The spore quantification was performed by performing 20 readings in a Neubauer chamber [22]. Once the concentration was determined, $1x10^{-9}$ spores were applied in 100 ml solutions per plant 7 days before and 7 days after the injection of M. incognita.

Evaluation Methods

At 30, 60, and 90 days after injection of *M. incognita*, a destructive evaluation was performed on 2 plants (treatment and replication). These plants were randomly selected, and the following parameters were assessed: incidence, severity, aboveground biomass weight, and final nematode population (PF).

a) **b)**

Figure 1. Nematode Sampling in *S. megalanthus* Plants. a) Extraction of the plant and sampling .b) Register agronomic variables (plant and roots).

The number of plants infected by M. incognita was recorded 30, 60 and 90 days after inoculation with the nematode to determine the incidence. The results were expressed as a percentage (%) [23]. To select the galling index (GI) in the root system of pitahaya plants, the number of galls formed in the root was counted and with the scale proposed by Taylor and Sasser [28] (0 to 6, where 0 = 0 galls; 1 = 1-2 galls; 2 = 3-10 galls; 3 = 11-30 galls; 4 = 31-100 galls; 5 = >100 galls) the severity was estimated [24].

All cladodes were collected per plant to determine aerial fresh weight (AFW). An analytical balance was initially used to define the fresh weight in grams (g). These procedures were carried out according to the study conducted by Gelpud et al. [25]. The multiplication rate of nematodes in soil and roots (MR) was also determined by dividing the final population (Pf) by the initial population (Pi) Berroterán et al. [26].

Statistical analysis was performed with the statistical package Infostat version 2017, and analysis of variance was conducted using Generalized Linear Mixed Models. The difference between the means of the treatments was estimated using the Least Significance Differences (LSD) Fisher with a significance level of 5% [27].

RESULTS

For the nematode incidence variable, it was determined that all plants in the different treatments were affected by nematode infestation (ranging from 89% to 100%) (Table 1), demonstrating that the applied inoculum concentration (1200 J2) caused an infection process. The presence of nematodes in the absolute control may be attributed to potential contamination of the experimental units during irrigation.

Treatment	Number of affected plants (before)	Incidence (%)	Number of affected plants (after)	Incidence (%)
*P. lilacinum**	8	89	16	89
*T. asperellum**	9	100	18	100
P. lilacinum + *T. asperellum**	9	100	18	100
P. lilacinum + *T. asperellum***	8	89	17	94
Absolute control	4	44	4	22
Control + nematodes	6	67	18	100

* Laboratory strains; ** Comercial product.

Table 1. Incidence of M. incognita in H. megalanthus plants.

A univariate analysis was performed for the variable "number of nodules" (Table 2). A highly significant difference was found for treatments ($p<0.0001$), a significant difference for the time of application "before and after," and the interaction (days*treatment) ($p=0.0026$; $p=0.0170$ respectively).

The main effect for treatments indicated that the lowest number of galls was formed when *T. asperellum* was applied. However, it was observed that the combination of the commercial product *P. lilacinum* + *T. asperellum* ($1x\ 10^{-11}$ cfu/g) resulted in a lower number of galls compared to the control + nematode. The treatments where laboratory-obtained strains were applied (*P. lilacinum* + *T. asperellum* and *P. lilacinum*) at concentrations of $1x10^{-9}$ spores yielded the highest number of galls (Table 3). According to the scale reported by Taylor and Sasser [28], the severity grades for the different treatments were 5, meaning that the number of galls in the experimental units was high (more than 100 galls) (Table 3).

Treatment	Number of gills
Treatment	**
Times of application	*
Times of application * treatment	*

** significant at $p \leq 0.01$, * significant at $p \leq 0.05$.

Table 2. The main effects and interaction effect for the number of galls on roots determined for each factor: Treatment and Time of application.

Treatments	Number of gills
P. lilacinum + *T. asperellum**	481 a
*P. lilacinum**	438 a
Control + nematodes	423 ab
P. lilacinum + *T. asperellum***	261 bc
*T. asperellum**	248 c
Absolute control	101 c

* Laboratory strains; ** Comercial product.

Table 3. Mean values of the number of galls in the root system of *H. megalathus.*

The analysis of the interaction treatment * season of application shows that the commercial product based on *P. lilacinum* + *T. asperellum* presents the least formation of nodulations at 60 and 90 days of evaluation. With *T. asperellum* the opposite happened, the lowest number of nodules was found at 30 days and as time passed the number of nodules increased (Table 4). On the other hand, the best time of application of the treatments was when the controllers were applied after the inoculation of the nematodes (251 nodulations) with respect to the 400 nodulations obtained when it was applied before (Table 4).

Treatments	Days	Number of gills
P. lilacinum + *T. asperellum**	30	522 abc
*P. lilacinum**		518 abc
P. lilacinum + *T. asperellum***		387 bcde
Control + nematodes		341 bcdef
*T. asperellum**		218 def
Absolute control		69 f
Control + nematodes	60	677 a
*P. lilacinum**		494 abcd
P. lilacinum + *T. asperellum**		377 bcde
*T. asperellum**		246 cdef
P. lilacinum + *T. asperellum***		214 def
Absolute control		122 ef
P. lilacinum + *T. asperellum**	90	542 ab
*P. lilacinum**		301 bcdef
*T. asperellum**		279 bcdef
Control + nematodes		251 cdef
P. lilacinum + *T. asperellum***		180 ef
Absolute control		111 ef

* Laboratory strains; ** Comercial product.

Table 4. Mean values of the number of galls by treatment and season of application.

The analysis in the air fresh weight (PFA) variable showed highly significant differences for the application time factor and treatments ($p<0.0001$) and not significant for the interaction ($p=0.4632$) (Table 5).

Treatment	Aerial biomass (g)
Time of application	**
Treatment	**
Time of application * treatment	NS

** significant at p ≤ 0.01; * significant at p ≤ 0.05; NS not significant.

Table 5. Main effects and interaction effect for aerial biomass determined for each factor: Treatment and Time of application.

It was determined that the amount of aerial biomass was higher when the biological controls were applied before the injection of nematodes (384.17 g) than when applied after (314.74 g). The main effect of the treatments showed that the amount of aerial biomass was higher when *P. lilacinu*m + *T. asperellum* (obtained at laboratory level) was applied. On the other hand, it was observed that when *T. asperellum* obtained at the laboratory level was involved, the amount of aerial biomass was the lowest (Table 6).

Treatments	Aerial biomass (g)
Absolute control	422.02 a
P. lilacinum + *T. asperellum**	365.40 b
*P. lilacinum**	352.17 bc
Control + nematodes	330.61 bc
P. lilacinum + *T. asperellum***	316,13 c
*T. asperellum**	310,40 c

* Laboratory strains; ** Comercial product.

Table 6. Aboveground biomass (g) of *H. megalanthus*.

The analysis of the variable number of nematodes in the soil showed significant differences for the application times factor (p=0.0011) and non-significant differences for treatments and interaction (p=0.6139, p=0.2152, respectively). (Table 7).

Treatments	Nematodes number
Time of application	*
Treatments	NS
Time of application x treatments	NS

* significant at p ≤ 0.05, NS not significant.

Table 7. Main effects and interaction effect for the number of nematodes in soil determined for each factor:

Treatment and time of application.

The lowest amount of nematodes in the soil was found when the inoculation with the biocontrol agents was carried out before the inoculation of *M. incognita* (Table 8). However, this did not help to control the damage suffered by the roots of the pitahaya plants.

Time of application	Soil nematodes number
Before	8857 b
After	22636 a

Table 8. Population of nematodes in the soil in two seasons of applications (before and after).

When analyzing the variable number of nematodes in the roots system of the pitahaya plants, significant differences were found for the time of application of the biocontrols (p=0.0198) and non-significant differences for the treatments and the interaction (p =0.5402, p=0.1429, respectively) (Table 9). That is, the biological controls, when applied before, did positively influence the population density of M. incognita (Table 10).

Treatments	Nematodes number
Time of application	*
Treatments	NS
Season x Treatments	NS

* significant at $p \leq 0.05$, NS not significant.

Table 9. The main effects and interaction effect for the number of nematodes in S. megalanthus root were determined for each factor: Treatment and time of application.

Time of application	Root nematodes number
Before	13199 b
After	21132 a

Table 10. Population of nematodes in the root system of S. megalanthus plants.

DISCUSSION

The number of galls in the root system of yellow pitahaya (*S. megalanthus*) indicates the plant's susceptibility to attack by *M. incognita*. In this study, the number of galls decreased by 62% and 70% when *T. asperellum* (laboratory strains) and *P. lilacinum* + *T. asperellum* (commercial) were applied, respectively. The excellent performance of *Asperellum* may be because it was collected in pitahaya plantations. It was also determined that applying *P. lilacinum* and *P. lilacinum* + *T. asperellum* strains obtained in the laboratory produced 4% and 13% more galls than the control + nematodes. This behavior could be attributed to certain micro-organisms possessing root growth-promoting properties, especially micro-organisms of the genus Trichoderma. This behavior could potentially be attributed to the root growth-promoting properties of the Trichoderma genus. This behavior is supported by Brotman et al. [29], who mentioned that Trichoderma activates auxins and several genes responsible for plant root development. However, Kariga et al. [30] mention that when placed, T. asperellum M2RT4 reduced the number of galls, egg mass, and nematode eggs. On the other hand, when both

microorganisms are applied together, they seem to exert more efficient control, as *T. asperellum* T203 colonizes the roots and *P. lilacinum* reduces root nodulation, mass and egg generation while favoring host growth. [30].

At 30 days, the presence of *T. asperellum* minimized nematode attack on the pitahaya root system, possibly because the concentration decreased by 26% at 60 days [31]. At 60 and 90 days, it was observed that *P. lilacinum* + *T. asperellum* (commercial) resulted in lower nodule formation compared to the control + nematode and the laboratory-obtained strains of *T. asperellum* and *P. lilacinum*. This may be attributed to the stable germination of the microorganisms [31]. The lowest amount of galling was observed when the organisms were applied after nematode inoculation, which differed from the reported behavior of reducing root galling, egg mass, and egg production when the microorganisms were applied ten days before (reference not provided).

Applying the microorganisms seven days earlier positively influenced plant growth (aboveground biomass). This is possible because the microorganisms stimulate the growth of the root system. Kariga et al. [30] noted that the application of *T. asperellum* M2RT4 and *P. lilacinum* (MR2 and KLF2) increased host growth and reduced nematode populations in soil and roots. Silva [32] also determined that *P. lilacinus* and several Trichoderma species promoted root development, growth and plant production when the microorganisms were applied before Meloidogyne inoculation. Also, it was resolved that plants had higher aerial biomass when inoculated with *P. lilacinum* + *T. asperellum* and laboratory-derived *T. asperellum*. This behavior may be attributed to these microorganisms being collected in pitahaya plantations in the Ecuadorian Amazon, which is why they performed better. Rodriguez-Kabana et al. [33] highlight the substantial divergence in the behavior of microorganisms, particularly concerning their efficacy in biocontrol and their proficiency in establishing themselves within the soil. This underscores the necessity of ensuring harmonious compatibility with distinct local conditions. For instance, Ortiz et al. [34] noted an illustrative case wherein the application of *P. lilacinum* on *Psidium guajava* to manage *Meloidogyne* spp. did not exhibit any detrimental impact on plant growth and development, even when nematodes were present within the root system. This finding is compelling in demonstrating that the behavior of microorganisms differs especially if they are used in other environments and are not native.

CONCLUSIONS

The application of the commercial dosage of *P. lilacinum* + *T. asperellum* led to a decrease in the number of galls present on the roots as compared to the untreated control. Nonetheless, no notable enhancement in plant growth was noted. Conversely, plant development was increased when employing a dosage of the laboratory-derived P. lilacinum + T. asperellum strain; however, the gall count did not decrease. These findings indicate that the strains under examination in this study possess constrained potential for nematode control.

This study established the importance of searching for new local strains and adjusting application rates since the behavior of microorganisms, especially in biocontrol and establishment capacity, can vary significantly from one place to another.

Author Contributions: Conceptualization, Y.V.-T., JP; methodology, Y.V.-T. and JP; statistical analysis, Y.V.-T., JP, writing—original draft preparation, Y.V.-T.; writing—review and editing, Y.V.-T., JP, NM, JS and AG All authors have read and agreed to the published version of the manuscript.

Funding:

This research was financed by the National Institute of Agricultural Research (INIAP) through the Central Experimental Station of the Amazon (EECA) and by the Research Fund for Agrobiodiversity, Seeds and Sustainable Agriculture (FIASA).

Institutional Review Board Statement:
Does not apply.
Informed Consent Statement:
Does not apply.

Data Availability Statement:

The data is contained in the article.

Acknowledgments:
This work was completed with the support of agronomists from the Fruit Programme of the Central Experimental Station of the Amazon.

Conflicts of Interest:

The authors declare no conflict of interest.

REFERENCES

1. Verona-Ruiz A, Urcia-Cerna J, Paucar-Menacho LM, Verona-Ruiz A, Urcia-Cerna J, Paucar-Menacho LM. Pitahaya (Hylocereus spp.): Cultivo, características fisicoquímicas, composición nutricional y compuestos bioactivos. Sci Agropecu 2020, 11(3):439-53.
2. Zúñiga Rizo CA. Biología floral y estructura vegetativa de la pitahaya (*Hylocereus undatus* Haworth) 2016.
3. Vargas Tierras YB, Pico JT, Díaz M. A, Sotomayor Akopyan DA, Burbano A, Caicedo V. C, et al. Manual del Cultivo de Pitahaya para la Amazonía Ecuatoriana 2020.
4. Castaño SP, Rincón A, Varón de Agudelo F. Identificación de nematodos asociados con pitaya Acanthocereus pitahaya Jaq. Dugand. Rev ICA 1991, Vol 26 Núm 1-2.
5. Guzmán-Piedrahita ÓA, Pérez L, Patiño A. reconocimiento de nematodos fitoparásitos en pitahaya amarilla (*Selenicereus megalanthus* HAW.). Bol Científico Cent Mus Mus Hist Nat 2012, 16(2):149-61.
6. Delgado A, Pico JT, Navia D, Suárez C. Memorias: Nemátodos fitoparásitos asociados al sistema radical del cultivo de pitahaya amarilla en el cantón Palora. EC: INIAP, Estación Experimental Central de la Amazonía 2019.
7. Cedeño Ronquillo AI. Ocurrencia de nematodos fitoparásitos en el cultivo de *Pitahaya Selenicereus megalanthus* en la zona de Las Naves, provincia de Bolívar. Facultad de Ciencias Agrarias Universidad de Guayaquil; 2021.

8. Osorno YCR, Hoyos LFP, Sánchez DAC. Efecto de los nematodos en la cantidad y calidad de raíces y métodos de evaluación. Rev Politécnica 2008.
9. Haro Altamirano JP, Zambrano Cárdenas GO, Cazorla Vinueza XR, Soplín Villacorta H, Garzón R. Evaluación de la sustentabilidad de fincas de la agricultura familiar, de dos eco tipos de Pitahaya amarilla (*Selenicereus megalanthus*), y su subproducto. Polo Conoc Rev Científico - Prof 2021.
10. Obando Vergara M, García Morera G, Araya M. Control químico de Globodera pallida (Stone) Behrens y la producción de papa (*Solanun tubersoum L.*), variedad Floresta. Rev Protección Veg 2017, 32(3):00-00.
11. Aguilar Calizaya VS, Heredia Araujo J. Determinación de la concentración de agroquímicos en productos hortícolas en la Localidad de Carapongo-Lima-Perú-2020. Univ Peru Unión 2020.
12. Ordoñez Beltrán V, Frías Moreno MN, Parra Acosta H, Martínez Tapia ME. Estudio sobre el uso de plaguicidas y su posible relación con daños a la salud. Rev Toxicol 2019, 36(2):148-53.
13. Karel, Zabala-Velin AA, Villarroel-Quijano KL, Sarduy-Pereira LB. Evaluación del impacto ambiental del cultivo de la pitahaya, Cantón Palora, Ecuador. TecnoLógicas 2020, 23(49):92-107.
14. Varela-Benavides I, Durán-Mora J, Guzmán-Hernández T. Evaluación in vitro de diez cepas de hongos nematófagos para el control de Meloidogyne exigua, *Meloidogyne incognita* y *Radopholus similis*. Rev Tecnol En Marcha 2017, 30(1):27-37.
15. Bishop AH, Gowen SR, Pembroke B, Trotter JR. Morphological and molecular characteristics of a new species of Pasteuria parasitic on *Meloidogyne ardenensis*. J Invertebr Pathol 2007, 96(1):28-33.
16. Rahad M, Islam M, Rahim M, Monira S. Effects of rooting media and varieties on rooting performance of dragon fruit cuttings (*Hylocereu sundatus* Haw.). ResearchGate 2016, 3(1):67-77.
17. Gilces CT, Santillan DN, Velasco L. Plant-Parasitic Nematodes Associated with rice in Ecuador. Nematropica 2016, 46(1):45-53.
18. Hussey R, Janssen G. Root-knot nematodes: Meloidogyne species. Plant Resist Parasit Nematodes 2022, 43-70.
19. Palacino JH, Leguizamon C, Jairo. Interaction between Glomus manihotis and Melidogyne incognita in yellow and red pitaya, under nursery conditions. Fitopatol Colomb 1991, 15(1):9-17.
20. Hoyos Carvajal LM, Jaramillo Villegas S, Orduz Peralta S. Evaluación de *Trichoderma asperellum* como biorregulador de Spongospora subterranea f. sp. subterranea. Rev Fac Nac Agron Medellín 2008, 61(2):4496-502.
21. Alcantara YML. Producción y formulación de trichoderma asperellum para el manejo de patógenos de la raíz de caña de azúcar 2019.
22. Ramírez HG, Granja AZ, Aguila E, Cantoral MT. Manual de producción y uso de hongos entomopatógenos. Lab Entomopatógenos SCB-SENASA 2014.
23. Álvarez S DE, Botina J JA, Ortiz C. AJ, Botina J LL. Nematicide evaluation of the essential oil from Tagetes zypaquirensis in the control of the nematode Meloidogyne spp. Rev Cienc Agríc 2016, 33(1):22-33.
24. Chaves CG, Marcillo EM, González CS, Garcia CB. Susceptibilidad de genotipos de Solanum spp. al nematodo causante del nudo radical Meloidogyne spp. (chitwood). Acta Agronómica 2011, 60(1):50-67.
25. Gelpud C, Mora E, Salazar C, Betancourth C. Susceptibilidad de genotipos de Solanum spp. al nematodo causante del nudo radical Meloidogyne spp. (chitwood). Acta Agronómica 2011, 60(1):50-67.
26. Berroterán G, Perichi G, Aguirre Y. Reacción de seis genotipos de caraota (Phaseolus vulgaris L.) al nematodo agallador Meloidogyne javanica (Treub) Chitwood. Bioagro 2020, 32(1):67-71.

27. Di Rienzo JA, Casanoves F, Balzarini MG, Gonzalez L, Tablada M, Robledo CW. Infostat versión 2018. 2015. Disponible en: http://www.infostat.com.ar/
28. Taylor A, Sasser J. Biología, identificación y control de los nematodos de nódulo de la raíz. Univ Carol Norte 1983;111.
29. Brotman Y, Landau U, Cuadros-Inostroza Á, Takayuki T, Fernie AR, Chet I, et al. Trichoderma-Plant Root Colonization: Escaping Early Plant Defense Responses and Activation of the Antioxidant Machinery for Saline Stress Tolerance. PLoS Pathog 2013, 9(3):e1003221.
30. Kiriga AW, Haukeland S, Kariuki GM, Coyne DL, Beek NV. Effect of Trichoderma spp. and Purpureocillium lilacinum on Meloidogyne javanica in commercial pineapple production in Kenya. Biol Control 2018.
31. Viera W, Noboa M, Bermeo J, Báez F, Jackson T, Viera W, et al. Parámetros de calidad de cuatro tipos de formulaciones a base de Trichoderma asperellum y Purpuricillium lilacinum. Enfoque UTE 2018, 9(4):145-53.
32. Silva Zegarra JA. Eficiencia de cinco especies de hongos nematófagos sobre el control de Meloidogyne spp. en pimiento del piquillo (Capsicum annuum L.) bajo condiciones de casa malla. Univ Priv Antenor Orrego 2021.
33. Rodriguez-Kabana R, Morgan-Jones G, Godoy G, Gintis BO. Effectiveness of species of Gliocladium, Paecilomyces and Verticillium for control of Meloidogyne arenaria in field soil. Nematropica. 1984, 14(2):155-70.
34. Ortiz Paz RA, Guzmán Piedrahita ÓA, Leguizamón Caycedo J. Manejo integrado del nematodo del nudo radical [Meloidogyne incognita (Kofoid & White) Chitwood Y Meloidogyne mayaguensis Rammh & Hirschmann] en almácigos de guayabo (Psidium guajava Linneo), variedad palmira ICA-1. Bol Científico Cent Mus Mus Hist Nat 2015, 19(2):104-38.

Received: 9 October 2023/ **Accepte**d: 15 January 2024 / **Published:**15 February 2024

Citation. Vargas Y, Pico J, Manobanda N, Garcia A, Sanmiguel J.Biological nematicides as an alternative for control of *Meloidogyne incognita* populations in yellow pitahaya (S*selenicereus megalanthus*). Revis Bionatura 2024; 9 (1) 4. http://dx.doi.org/10.21931/RB/2024.09.01.4

Additional information Correspondence should be addressed to *yadira.vargas@iniap.gob.ec*

Peer review information. Bionatura thanks anonymous reviewer(s) for their contribution to the peer review of this work using https://reviewerlocator.webofscience.com/

Bionatura
Ibero-American Journal of Biotechnology and Life Sciences

Article

Fighting moniliasis in Orellana with sensors and PWA for sustainable agriculture

Jessica Urquizo [1], Mirtha Jiménez [2], Pedro Aguilar [3], Wilson Chango [4]*

1 *University Escuela Superior Politécnica de Chimborazo sede-Orellana, Ecuador.*
2 *University Escuela Superior Politécnica de Chimborazo sede-Orellana, Ecuador. mirtha.jimenez@espoch.edu.ec:*
3 *University Escuela Superior Politécnica de Chimborazo sede-Orellana, Ecuador. pedro.aguilar@espoch.edu.ec:*
4 *University Escuela Superior Politécnica de Chimborazo sede-Orellana, Ecuador. wilson.chango@espoch.edu.ec,*
** Correspondence: jessica.urquizo@espoch.edu.ec*
Available from. http://dx.doi.org/10.21931/RB/2024.09.01.5

ABSTRACT

The primary objective of this research was to enhance cocoa production and quality in tropical countries, such as Latin America and Africa, where cocoa cultivation plays a pivotal role in the economy of rural communities. The primary challenge addressed in this study was moniliasis, a fungal disease that affects cocoa fruits and leads to a significant decline in crop production and quality. A multidisciplinary approach was employed to tackle this issue, combining sensors, MongoDB Compass databases, Progressive Web Applications (PWAs), and predictive models.

A research methodology incorporating predictive analysis techniques, particularly the logistic regression method, was utilized to achieve early detection and efficient management of moniliasis. Data collection instruments included sensors monitoring vital environmental factors like humidity and temperature alongside MongoDB Compass databases for storing and managing the gathered data. Furthermore, a PWA was developed for real-time data collection and analysis.

The results of implementing this sensor-based tool in cocoa cultivation were highly effective. Early detection of moniliasis allowed for more precise preventive and corrective measures, resulting in a significant improvement in cocoa production and quality. These results were substantiated with concrete data demonstrating the tool's efficacy.

Keywords: Data Prediction: Models and Applications; Efficient MongoDB Database Management; High-Quality Cocoa; Moniliasis: Treatment and Prevention; Progressive Web Apps (PWA): User Experience.

INTRODUCTION

Cocoa cultivation is of vital economic importance in many tropical countries and is an essential source of income in rural areas of Latin America and Africa. However, this valuable crop faces several problems that affect the quality and quantity of the harvest. One of the main problems confronting cocoa production is moniliasis, a fungal disease that affects cocoa beans and causes a drastic drop in yield and quality. [1]

Moniliasis is a severe threat to the cocoa industry, and early detection of the disease is essential to prevent its rapid spread and minimize its negative impact on production. Currently, many cocoa farmers resort to periodic visual inspections to detect the presence of moniliasis in their plantations. However, this manual method can be time-consuming and error-prone, costing growers much time and money. To effectively solve this problem and reduce the waste of time and money associated with candidiasis,[2]. We have developed a real-time monitoring system with sensors and an advanced web application (PWA). These sensors collect accurate real-time data on key environmental factors that affect cocoa growth, such as humidity and temperature. The accumulated information is transferred to a central database where predictive models are implemented to determine the crop's presence or probability of diseases.[3]

Implementing this monitoring and forecasting system is an essential advance in sustainable agriculture, as it allows farmers to quickly detect candidiasis in plantations and take preventive measures in time. Preventing further spread of the disease can reduce economic losses and optimize farming methods.[4]

As direct beneficiaries, we will have the farmers of the Province of Orellana and the people interested in taking care of their cocoa plantations since, through the respective analysis, we will obtain predictions about our plantation, and in this way, we will be able to intervene and avoid the loss of time and money of the farmers.[5]

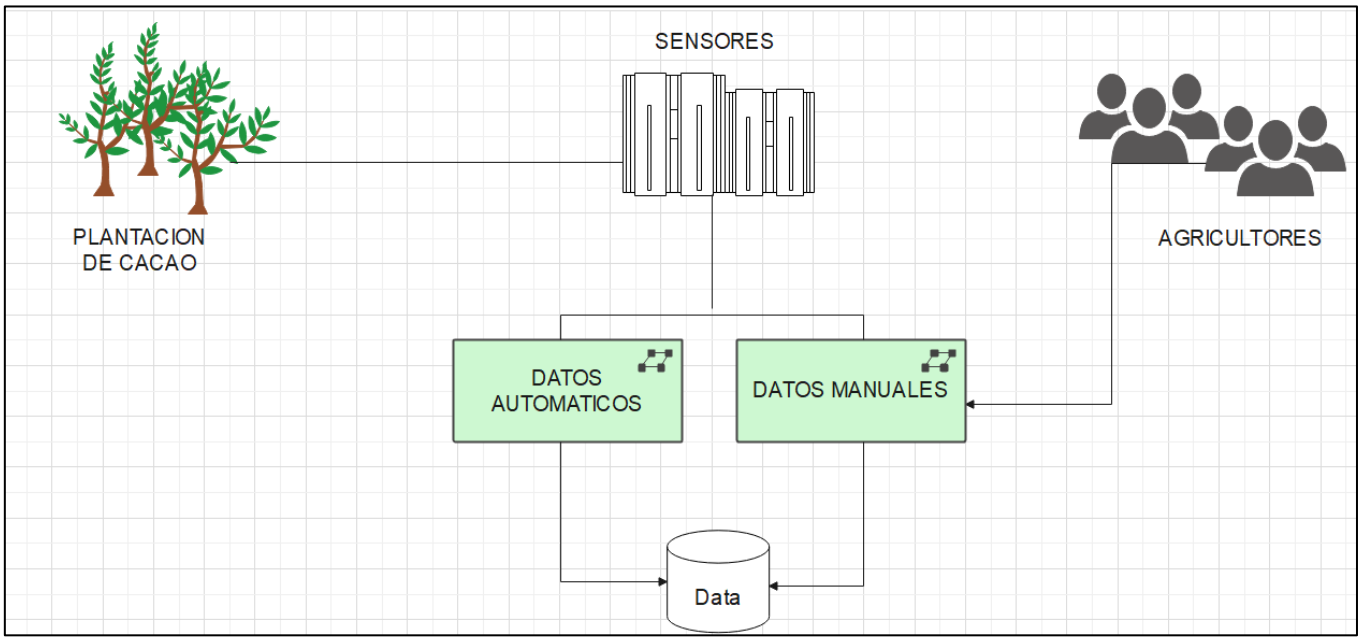

Figure 1. This figure shows the Project Model.

FUND

Cocoa quality is a crucial issue affecting chocolatiers and producers, and its improvement significantly impacts the entire supply chain.

As technology advances and the amount of available data grows, there is increasing interest in applying data analytics algorithms, especially machine learning, to solve complex problems such as forecasting and improving cocoa quality. These algorithms make it possible to analyze large amounts of data and discover patterns, trends and correlations that can be difficult to identify with traditional methods.

In this context, we developed an innovative cocoa quality prediction and monitoring system using advanced web applications (PWA) and advanced algorithms such as principal component analysis (PCA) and kernel PCA (KPCA). PWA provides an easy-to-use and accessible interface that allows farmers and producers to access valuable information in real-time and visualize relevant data on key environmental factors affecting cocoa quality.

A deeper insight into variables affecting cocoa quality is gained by integrating PWA's machine learning algorithms, such as PCA and KPCA. These algorithms can process complex data and discover subtle patterns that contribute to the quality of the final product. In this way, users can obtain accurate forecasts of cocoa quality to make informed and proactive decisions to improve production and processing. Implementing this monitoring and forecasting system should benefit farmers and chocolate producers. Farmers can optimize their growing and harvesting practices by adapting to environmental and cultural factors to improve cocoa quality at the origin. Manufacturers can use the predictive information to adjust their production processes and ensure high-quality cocoa beans for premium chocolate.

In addition, the system can potentially strengthen the global cocoa industry by increasing productivity and competitiveness. Sustainable growth and recognition of excellent cocoa produced in different parts of the world is facilitated by access to high-quality products that meet consumer demand.

Ultimately, combining advanced technologies such as PWA and machine learning algorithms with a focus on improving cocoa quality is a significant step forward in achieving sustainable agriculture and a more sustainable, efficient, and profitable chocolate industry. This monitoring and forecasting system opens a new era in cocoa farming and producing high-quality chocolate.

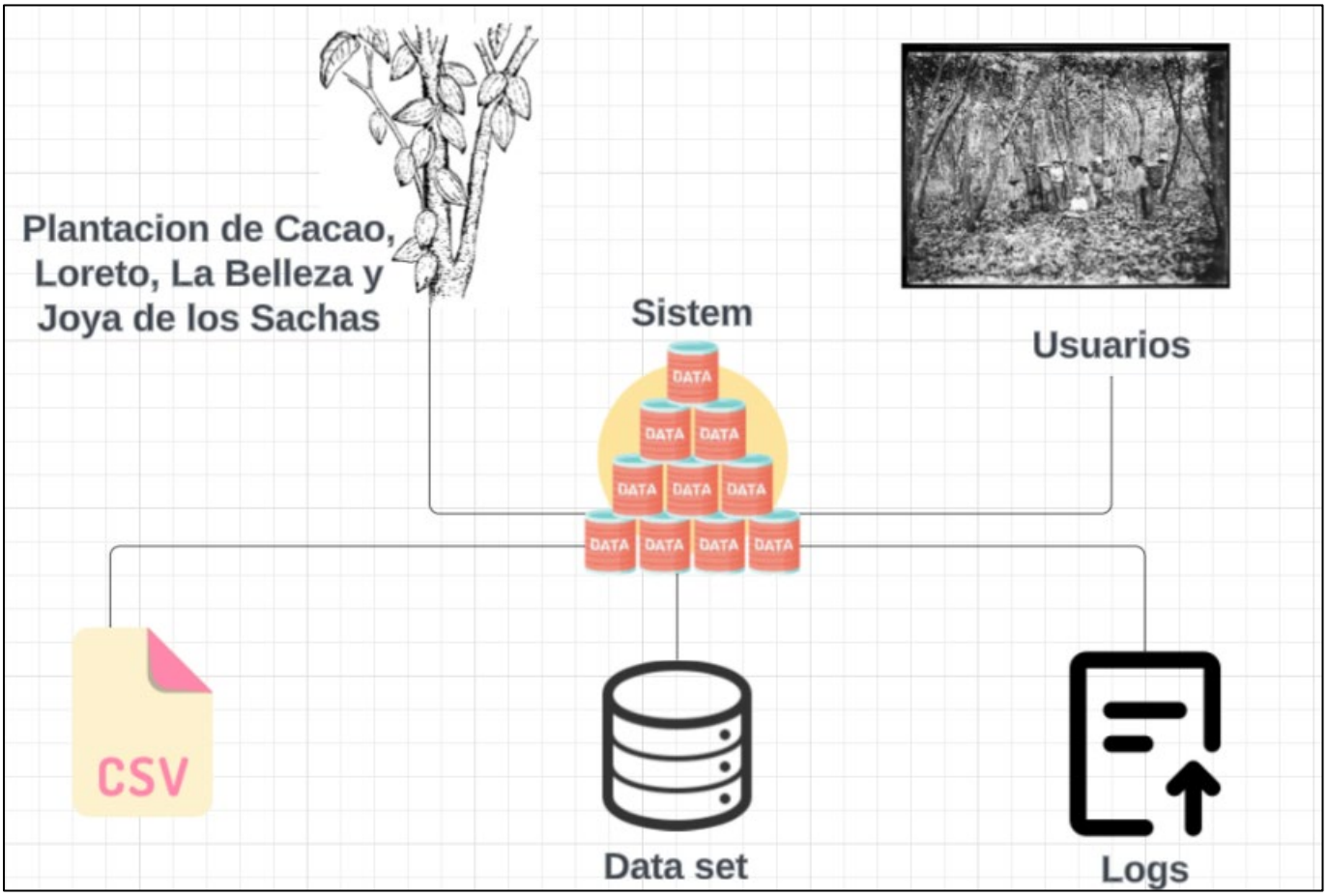

Figure 2. The figure represents data collection.

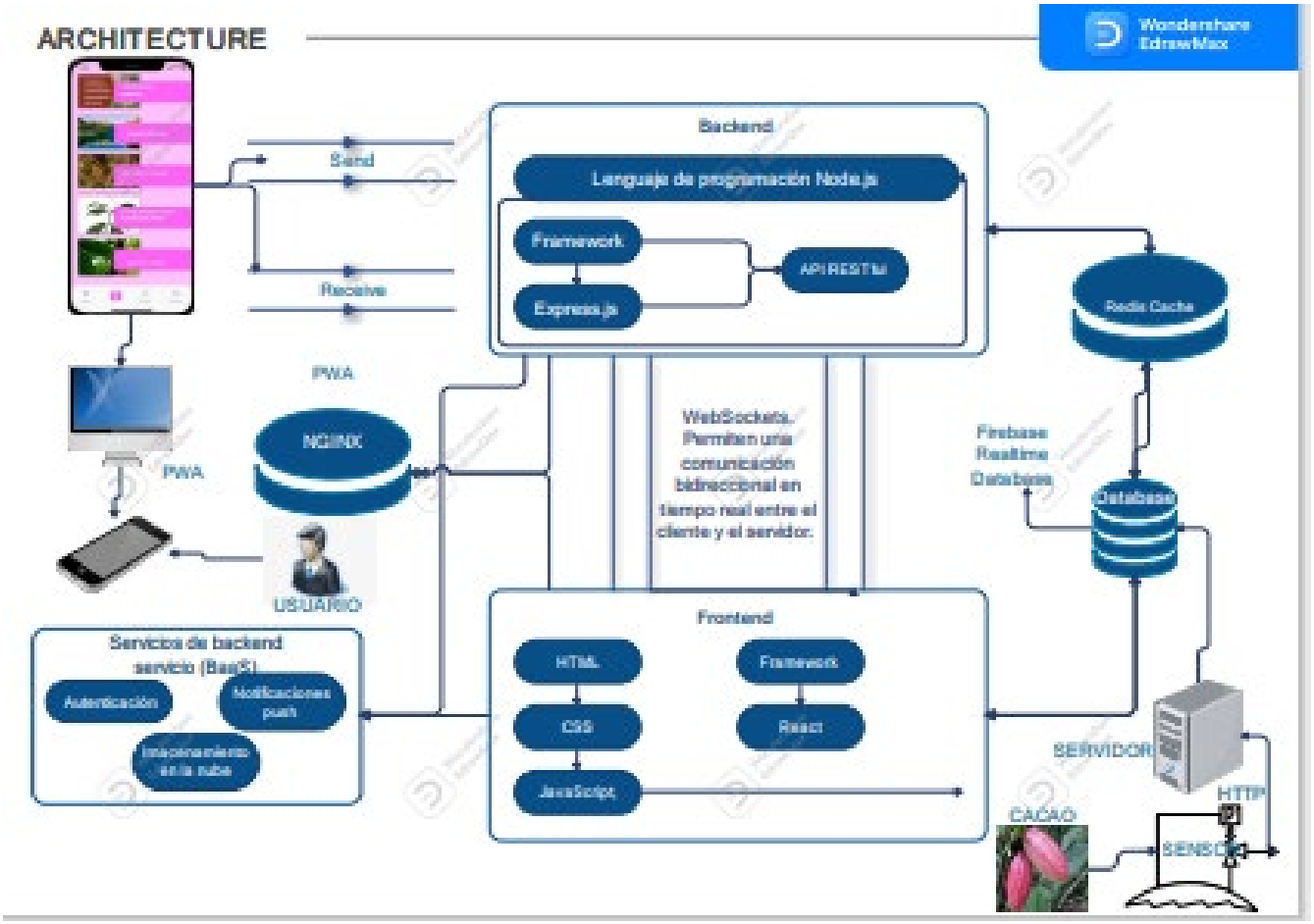

Figure 3. This figure represents the project architecture.

MATERIALS AND METHODS

This section describes the procedures and methodologies used to obtain the results and the resources employed in the study. The techniques and instruments utilized, the statistical methods applied and the criteria for selecting the population and the sample are detailed.

Definition of moniliasis

Monilia, also known as distemper, pasmo, tomato blight, or ice pod rot, is a fungal disease that affects various crops, including tomatoes, strawberries, pineapple, and potatoes. It is caused by the fungus *Moniliophthora roreri* and is spread through spores carried by wind or water. In addition, it is considered the central disease affecting cocoa crops in Colombia and other Central and South American countries,[6].

Python

According to Challenger-Pérez, [7], Python is a programming language recognized for being interpreted at a high level, standing out for its simplicity and ease of reading. In addition, it is considered a versatile language with a wide range of applications.

PWA

A PWA, or Progressive Web Application, is a technology based on the conventional web and uses browser resources and modern APIs to enhance the user experience. Some of its features include the ability to run offline, update automatically, access device resources, and be installable, among other advantages, [8].

MongoDBcompas
MongoDBcompas is a desktop application provided by MongoDB that is used as a graphical user interface (GUI) tool for interaction with MongoDB databases. Its primary purpose is facilitating the administration and exploration of data stored in a MongoDB database, [9.]

Definition of sensor
A sensor is an element or device that can detect or measure a specific physical or chemical phenomenon and transform that information into a signal or data that can be exploited practically. Sensors are essential components in electronic systems used in various industries, such as automotive, consumer electronics, medical industry, agriculture, and others, to cover a wide range of applications, [10.]

Variable
An investigation can quantify or measure a characteristic, quality or observed property known as a variable, which can acquire various values, [11.]

Methodology
This section describes in detail the procedure carried out to obtain the results and the resources used in the study. The procedures and methodologies followed are presented in chronological order of realization, and the techniques and instruments used are detailed to allow their reproduction.

In this way, it is shown that to prevent and control diseases such as cocoa moniliasis, several technologies have been developed, including sensors and mobile applications. The sensors measure environmental variables such as soil moisture, temperature, and luminosity. These data are transmitted through a wireless network to a Progressive Web App (PWA), which collects and analyzes the information in real-time.

Data description
Users (farmers) of cocoa from the canton Loreto, La Belleza and La Joya de los Sachas, province of Orellana, a database is generated from two sources of information; the data that we consider manual are those that the user (farmer) will add depending on the characteristics or data presented by his crop. The other automatic data are regarded as such because they are obtained by sensors that automatically capture accurate data.
We have collected the cocoa plantation data based on the above: manual data by the user (farmer) and automatic data by sensors that automatically capture data.
- Precipitation: Data obtained through a sensor, depending on the climate and the season in which the crop is located.
- Temperature: Data obtained daily from a sensor depending on the weather conditions.
- Relative Humidity (RH): The relative humidity data, a crucial environmental metric, requires further elucidation in the data description. RH is assessed through specialized sensors capable of gauging the humidity levels in the air.
- Dew point: Data obtained by the sensor from the measurement of the temperature at which the air becomes saturated with water vapor, meaning that the amount of water vapor in the air reaches its maximum and can begin to condense in the form of water droplets.
- Wind speed: Data obtained from sensors that measure the magnitude of the speed at which air moves in each direction. It is usually calculated in units of speed, such as meters per second (m/s), kilometers per hour (km/h) or miles per hour (mph).
- Gust speed: Obtained by the sensor, it is obtained when there is a sudden and temporary increase in wind speed compared to the average wind speed during a given period.
- Wind direction: Data obtained by the sensor based on the direction from which the wind is coming at a given place and time.
- Fruit: This data is considered manual since it is obtained by the farmer who will provide us with the data related to the production of his plantation.
- Incidence: This data is considered manual and relevant since the farmer provides us with approximate assessments of the incidence in the plantation through visual observation, where he compares the areas with different levels of shade and sun exposure and can provide us with an idea of the variations in the incidence of light in various parts of the plantation.
- Severity (%): This is considered manual, as the user uses a qualitative scaling technique to assess the severity of plant damage visually. A score or category is assigned to indicate the severity level, either in terms of

percentage of damage, area affected or symptom severity. For example, a scale of 1 to 5 may be used, with 1 indicating no damage and 5 indicating severe damage.

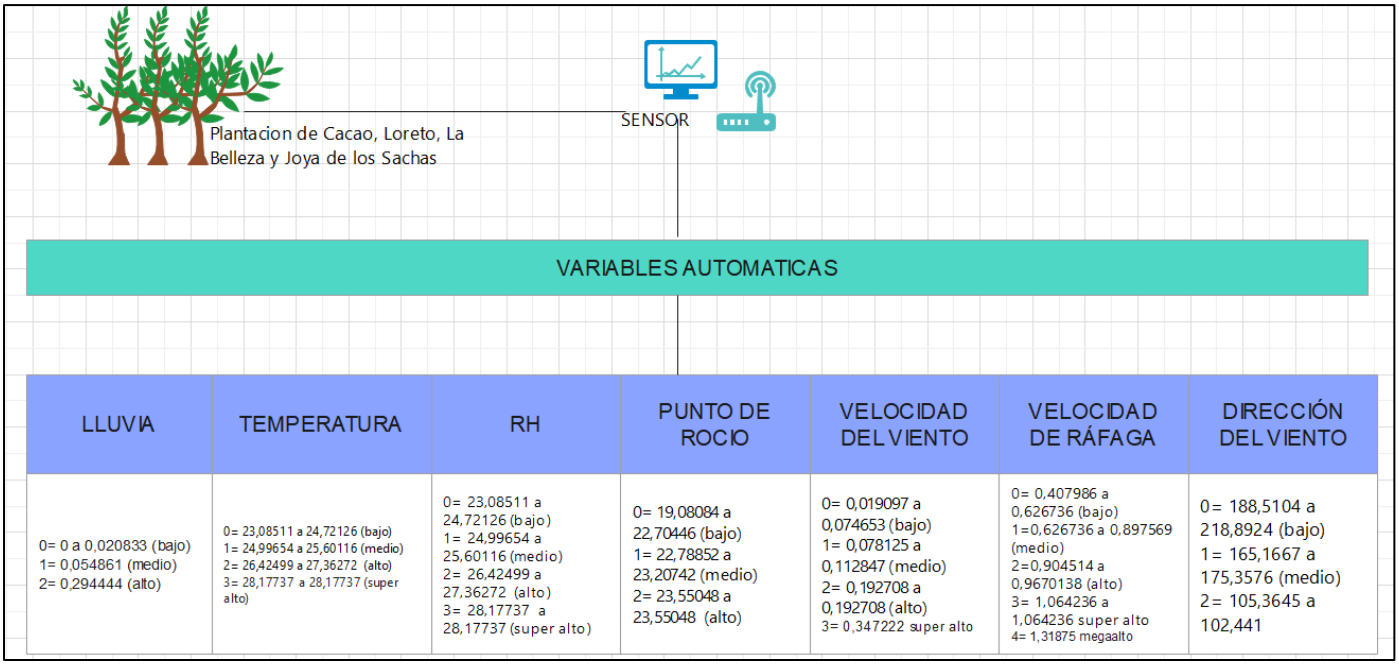

Figure 4. This figure shows the automatic variables to obtain the best prediction algorithm.

The data obtained automatically by the climatological measurement sensors are numerical values ranging from 0 to 102,441. The location of these values in the range depends on the specific variable being evaluated, which is assigned to one of seven automatic variables. Each of these seven variables has a designated ranking range, from "low" to "super high," this ranking is determined by the numerical value obtained for each variable.

Tests were performed with three different algorithms:

1. PCA (Principal Component Analysis):
   - It is used to reduce the dimensionality of a data set with numerical variables.
   - It is used to find the linear combinations of original variables that explain most of the variance of the data, [12].
   - It is suitable when it is desired to eliminate multicollinearity between variables or to reduce the complexity of the data.
2. KPCA (Kernelized Principal Component Analysis):
   - It is used when the data have a nonlinear structure and cannot be effectively separated by a linear transformation,[12].
   - It helps find nonlinear representations of the data.
   - Suitable for nonlinear classification and pattern recognition problems.
3. IPCA (Incremental Principal Component Analysis):
   - Used when performing principal component analysis on extensive data sets that do not fit in memory,[13].
   - It is helpful in the process and reduces the dimensionality of large volumes of data efficiently.
- It is suitable when working with massive or real-time data sets.

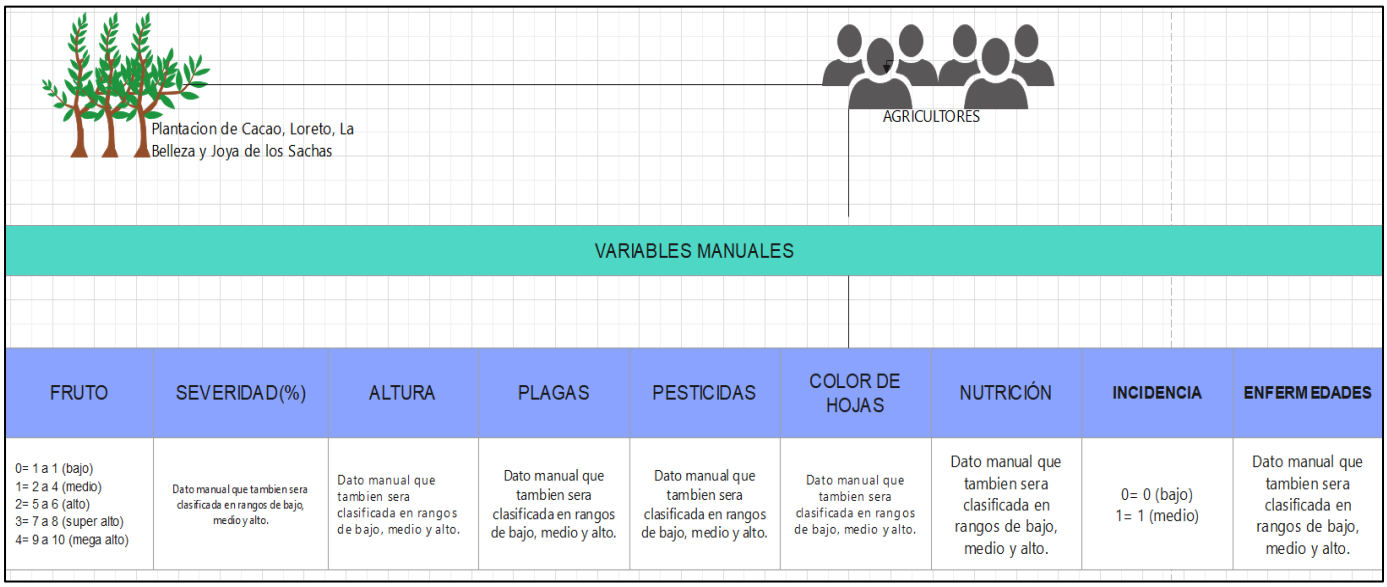

Figure 5. This figure shows the manual variables to obtain the best prediction algorithm.

Data obtained manually by digitization or records made by farmers are values obtained by visual evaluation. These values are classified in different ranges according to their specific variable. There are 9 variables in total, and each of them is assigned a range from "low," "medium," "high," and "medium-high" to "super high."

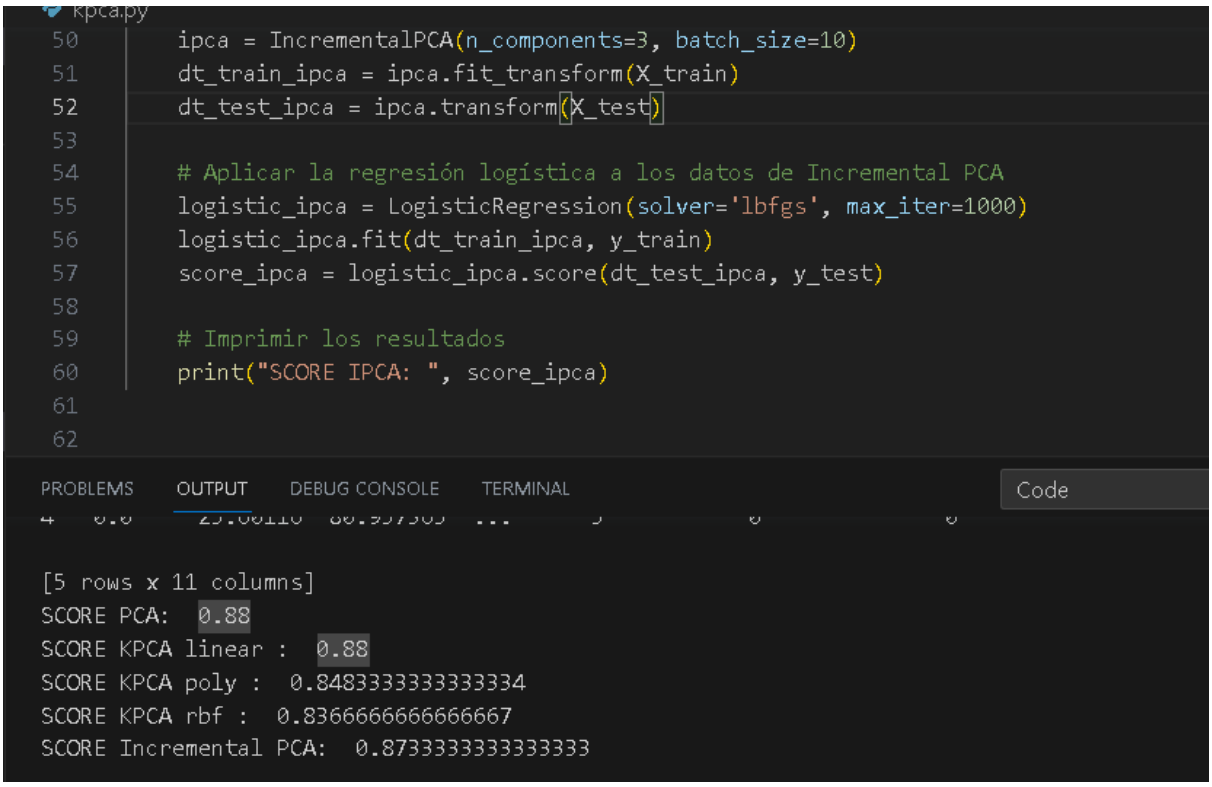

Figure 6. This figure represents the execution of the predictive models.

After applying logistic regression to the data transformed by PCA and IPCA, the following accuracy scores were obtained:

ALGORITHMS:	RESULTS	DEFINITION
- For the KPCA algorithm with the linear kernel: 0.88	88%	The KPCA algorithm with linear kernel achieved an accuracy of 0.88, meaning it correctly classified 88% of the test examples. This dimensionality reduction approach uses linear transformations to extract relevant features from the data.
- For the KPCA algorithm with polynomial kernel: 0.8483	84.83%	The KPCA algorithm with polynomial kernel obtained an accuracy of 0.8483, indicating that it correctly classified approximately 84.83% of the test examples. In this case, a polynomial kernel was used to map the data to a higher dimensional feature space, which allowed capturing nonlinear relationships between variables.
- For the KPCA algorithm with RBF kernel: 0.8367	83.67%	The KPCA algorithm with RBF (radial basis function) kernel obtained an accuracy of 0.8367. This means it correctly classified approximately 83.67% of the test examples. The RBF kernel helps capture nonlinear relationships and can be especially effective when the data have complex decision boundaries or nonlinear distributions. In this case, the KPCA algorithm with RBF kernel captured some underlying structure in the data, allowing accurate classification in most cases.
- For the PCA algorithm: 0.88	88%	The PCA (Principal Component Analysis) algorithm achieved an accuracy of 0.88%. This means that it was able to explain approximately 88% of the variability present in the data. PCA is a dimensionality reduction algorithm that searches for the principal components that best represent the original data. In this case, the PCA algorithm could effectively capture the data's underlying structure and reduce its dimensionality without significant loss of information, resulting in high classification accuracy for the test examples.
- For the IPCA algorithm 0.8733	87.33%	The IPCA (Incremental Principal Component Analysis) algorithm achieved an accuracy of 0.8733. IPCA is a variant of the PCA algorithm used when working with large data sets that do not fit in main memory. Unlike traditional PCA, which requires loading all the data into memory, IPCA divides the data into smaller blocks and performs the decomposition incrementally.

Table 1. This table contains a detailed comparison of the predictive models.

These results indicate that the PCA and IPCA algorithms demonstrated similar and superior performance to the various KPCA algorithms. However, the highest score was obtained using the PCA algorithm, with an accuracy score of 0.88. This suggests that PCA effectively captured the relevant information in the reduced data, which was reflected in a better predictive ability of the logistic regression model.

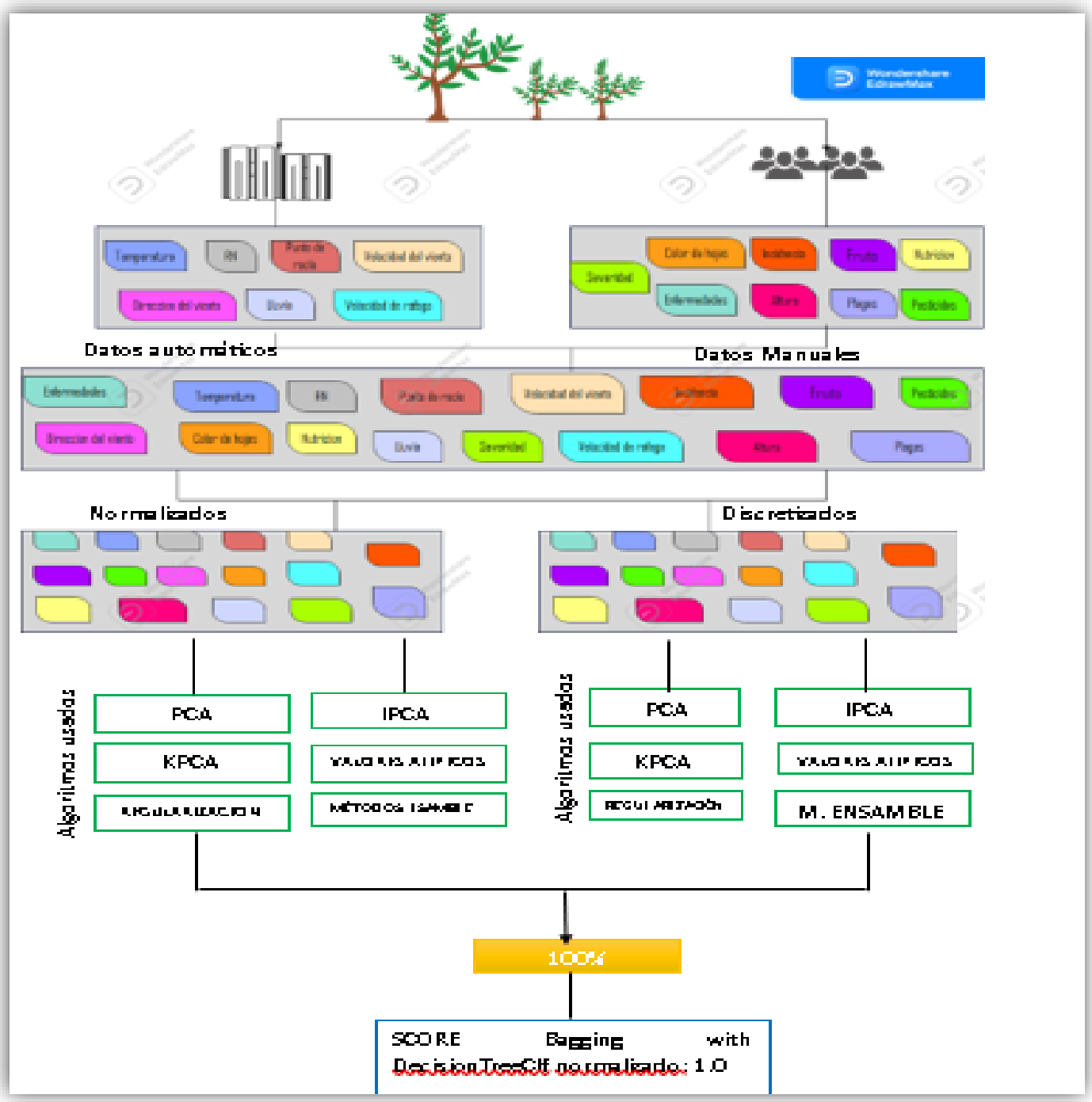

Figure 7. This figure is an Analysis of the algorithm.

In conclusion, from the results obtained, it is determined that the PCA algorithm is the most suitable for dimensionality reduction in this study. Its ability to preserve relevant information and its superior performance compared to the KPCA algorithms indicate that it is a valuable tool in analyzing and classifying the data used.

Statistical analysis

The logistic regression method was used as a classification and predictive analysis technique to evaluate the effectiveness of dimensionality reduction algorithms. The logistic regression implementation available in Scikit-learn was employed, with the 'lbfgs' solver and a maximum number of iterations of 1000.

The performance of the models was evaluated using the accuracy score as the evaluation measure. This score reflects the proportion of correct predictions made by the model.

Technologies used

REACT

React is a widely used JavaScript library for creating progressive web applications (PWA). Using React, you can make interactive and responsive user interfaces for your PWA applications. ,[14.]

Using React to create PWAs

Reusable components - React is based on the concept of components, allowing you to create reusable components that encapsulate the logic and UI of a specific application part. These components can be used in different application parts, facilitating a PWA's beginning and maintenance.
Virtual DOM: React uses a virtual DOM to perform efficient UI updates. Instead of directly manipulating the DOM, react compares the virtual DOM with the real DOM and applies only the necessary changes, which improves application performance.

Routing: React offers routers such as React Router that allow you to handle navigation and routing within a PWA. This is especially useful for creating dynamic routes and providing a smooth user experience.

Application state - React provides an easy way to manage the application state through its local state feature or state management libraries such as Redux. This allows for maintaining a consistent state in the application and makes it easy to manage data and changes in real-time.

PWA support: React supports a PWA's requirements, such as using Service Workers for caching and offline availability and the ability to install on the user's device. In addition, React-specific libraries and tools, such as Create React App, facilitate the initial setup of a PWA.

Connecting the PWA to MongoDB

Real-time queries and instant updates cement the link between PWAs and MongoDB. The interaction enables Progressive Web Applications to provide users instant updates, elevating their experience and interactivity.
Setting up MongoDB: first, we need a backend server that provides us with an API to interact with MongoDB. For this, we use the Python programming language and a framework.
Connecting to MongoDB from the backend server: We use a driver or client appropriate to the programming language we are employing. Each programming language has its own official MongoDB driver; for Node.js, we use the "Mongodb," which you can install through npm. To define the paths and drivers needed to manipulate the data in MongoDB.
This allows us to perform CRUD (create, read, update, delete) operations on the MongoDB database, such as making a new document, getting existing documents, revising documents, etc.
Integration of the PWA with the backend server: We use the Fetch API or an HTTP request management library to make requests from the PWA to the backend server. To create it secure. ,[15.]
Processing the responses from the backend server: When we receive the responses from the backend server in the PWA, we can process and display the data in our user interface as needed.

RESULTS

Figure 8. This figure represents the PWA design.

The monitoring and forecasting application results have exceeded our expectations, demonstrating its effectiveness in early and accurate detection of cocoa crop health. Integrating manual data provided by farmers and data collected by sensors has supplied a complete and precise picture of crop health in real-time.

Through detailed data analysis using machine learning algorithms, such as principal component analysis (PCA) and kernel PCA (KPCA), we identified key patterns and relationships between environmental variables and cocoa quality. These results are essential for developing effective predictive models that can accurately determine whether a crop is healthy or infected with Moniliasis. The application has proven to be a valuable tool for farmers and educational institutions. Farmers can use the application to constantly monitor their crops and obtain timely and accurate information on the health and performance of their plantings.

The ability to enter manual data, such as specific yield observations and environmental conditions, further enriches the forecasting models and allows for fine-tuning each planting.

Early and accurate detection of moniliasis is essential to avoid significant economic losses due to the spread of the disease. By receiving timely warnings of possible infections, growers can take targeted preventive and treatment measures in time. This reduces crop damage and maintains the quality of the cocoa beans, ensuring a high-quality end product.

Figure 9. This figure represents the result when the crop is healthy.

After all, good results were achieved by monitoring the application and predicting a positive impact on the cocoa industry. Farmers can gain higher productivity and competitiveness, increase yields, and deliver high-quality products that meet consumer expectations. In addition, the application contributes to strengthening the industry's sustainability by ensuring more efficient farming methods and reducing resource wastage.

Figure 10. This figure represents the result when the culture is infected.

DISCUSSION

Developing a cocoa crop monitoring and forecasting system represents a significant stride forward in both agricultural and educational sectors. Below, we present the primary outcomes and conclusions derived from this project.

To begin with, the real-time monitoring system has empowered farmers with access to precise and up-to-the-minute information regarding the condition of their crops. The sensors have meticulously measured pivotal environmental variables influencing cocoa growth, encompassing humidity, temperature, and wind speed. Augmenting these data with manual observations contributed by farmers has notably increased the predictive model. This synergy has facilitated the early and precise identification of moniliasis, a fungal ailment adversely impacting cocoa fruit. Consequently, farmers can shield their crops, preventing substantial losses and upholding the caliber of harvested cocoa by promptly implementing specific treatments and preventive measures.

The Progressive Web App (PWA) integration has conferred an intuitive and readily accessible experience upon users, mainly offering tangible benefits to farmers. Through the app, farmers can instantaneously scrutinize the state of their crops in real-time, both on their mobile devices and web platforms. The app's user-friendliness has emerged as a pivotal factor that has fostered its widespread adoption.

Nonetheless, it is imperative to acknowledge that the absence of robust antecedents within the research somewhat constrains the discussion. For a more comprehensive and substantiated debate, it would be advantageous to draw comparisons and contrasts between the findings of this study and those of prior research endeavors related to cocoa crop monitoring and disease detection. Such an approach would proffer a more precise context and facilitate a more adept assessment of this study's contribution and relevance to the field.

CONCLUSIONS

In conclusion, this study represents a significant achievement in the quest for innovative solutions to the challenges facing cocoa cultivation, particularly in critical regions of Latin America and Africa, where this crop plays a pivotal role in sustaining rural communities. Our research title, 'Fighting Moniliasis in Orellana with Sensors and PWA for Sustainable Agriculture,' encapsulates our endeavor and reflects the essence of our work.

We have conclusively demonstrated that integrating cutting-edge technologies, such as sensors, MongoDB database management, Progressive Web Apps (PWAs), and predictive models, is an effective strategy for addressing the menace of moniliasis. This fungal disease threatens cocoa production and quality and has encountered a formidable adversary in our monitoring and forecasting system.

Our approach has significantly enhanced moniliasis's early detection and management, resulting in a direct upsurge in cocoa production and quality. This achievement not only holds positive economic implications but also wields a transformative impact on the lives of rural communities reliant on cocoa cultivation.

The utilization of machine learning algorithms, notably Principal Component Analysis (PCA) and Kernel PCA (KPCA), has enabled us to dissect complex data and extract critical insights that bolster the efficacy of our forecasting system.

Furthermore, we have democratized access to this technology by creating a user-friendly interface as a Progressive Web App (PWA). This ensures that farmers and educational institutions can harness this invaluable tool, fostering informed decision-making and optimizing agricultural practices.

REFERENCES

1. Correa Álvarez, J., Castro Martínez, S., & Coy, J. (June 6, 2014). Status of cocoa moniliasis caused by *Moniliophthora roreri* in Colombia. SciELO, 63(4). doi:http://dx.doi.org/10.15446/acag.v63n4.42747

2. Mamani, M., Villalobos, M., & Herrera, R. (2017). Low-cost web system to monitor and control an agricultural greenhouse. SciELO, 25(4), 599-618. Retrieved from https://scielo.conicyt.cl/pdf/ingeniare/v25n4/0718-3305-ingeniare-25-04-00599.pdf

3. Edem Kongor, J., Hinneh, M., Van de Walle , D., Ohene Afoakwa, E., Boeckx, P., & Dewettinck, K. (April 2016). Factors influencing quality variation in cocoa (Theobroma cacao) bean flavour profile - A review. sciencedirect, 82, 44-52. doi:https://doi.org/10.1016/j.foodres.2016.01.012

4. Quintero R., M. L., & Díaz Morales, K. M. (January 2004). The world cocoa market. 9(18). Obtenido de http://ve.scielo.org/scielo.php?script=sci_arttext&pid=S1316-03542004000100004

5. Munirah Mohd, Y., Nur Fazliyana, R., Muhaini, O., R, M., Rozlini, M., & Mohd Hafizul Afifi, A. (June 19, 2018). M-DCocoa: M-Agriculture Expert System for Diagnosing Cocoa Plant Diseases. webofscience, 700, 363-371. doi:10.1007/978-3-3-319-72550-5_35.

6. Cubillos, G. (June 2017). Frosty Pod Rot, disease that affects the cocoa (Theobroma cacao) crops in Colombia. sciencedirect, 96, 77-82. doi:https://doi.org/10.1016/j.cropro.2017.01.011

7. Challenger-Pérez, I., Díaz-Ricardo, Y., & Becerra-García, A. R. (April-June 2014). The Python programming language. redalyc, XX(2), 1-13. Retrieved from https://www.redalyc.org/pdf/1815/181531232001.pdf

8. Llamuca-Quinaloa, J., Vera-Vincent, Y., & Tapia-Cerda, V. (May 2021). Comparative analysis to measure performance efficiency between a traditional web application and a progressive web application. SciELO, 24(51). doi:https://doi.org/10.22430/22565337.1892.

9. MongoDB. (June 16, 2023). MongoDB. Retrieved from MongoDB: https://www.mongodb.com/es/products/compass

10. Kovalska, E., Baldicheva, A., & Somov, A. (May 23, 2020). Wireless Graphene Temperature Sensor. webofscience. Retrieved from https://www.webofscience.com/wos/woscc/full-record/WOS:000646236300011

11.Oyola-Garcia, A. E. (2021). The variable. Retrieved from http://www.scielo.org.pe/scielo.php?script=sci_arttext&pid=S2227-47312021000100016

12. Marukatat, S. (2023). Tutorial on PCA and approximate PCA and approximate kernel PCA. REVIEW OF ARTIFICIAL INTELLIGENCE, 56, 5445-5477. doi:10.1007/s10462-022-10297-z. doi:10.1007/s10462-022-10297-z

13. Daga, y., & Nachar, R. (2006). Face recognition using IPCA-ICA algorithm. IEEE TRANSACTIONS ON PATTERN ANALYSIS AND ARTIFICIAL INTELLIGENCE, 28, 996-1000. doi:DOI10.1109/TPAMI.2006.118.

14. Boersma, S., & Lungu, M. (2021). React-bratus: Visualizing React Component Hierarchies. 2021 WORKING CONFERENCE ON SOFTWARE VISUALIZATION (VISSOFT 2021), 130-134. doi:10.1109/VISSOFT52517.2021.00025.

15. Sysel, M., & Dolezal, O. (2014). An Educational HTTP Proxy Server. MODERN TRENDS AND TECHNIQUES IN COMPUTATION SCIENCE (CSOC 2014), 285, 541-547. doi:10.1007/978-3-3-319-06740-7_46.

Received: 9 October 2023/ **Accepte**d: 15 January 2024 / **Published:**15 February 2024

Citation. Urquizo J, Jiménez M, Aguilar P, Chango W. Fighting moniliasis in Orellana with sensors and PWA for sustainable agriculture. Revis Bionatura 2024; 9 (1) 5. http://dx.doi.org/10.21931/RB/2024.09.01.5

Additional information Correspondence should be addressed to *jessica.urquizo@espoch.edu.ec*

Peer review information. Bionatura thanks anonymous reviewer(s) for their contribution to the peer review of this work using https://reviewerlocator.webofscience.com/

Bionatura
Ibero-American Journal of Biotechnology and Life Sciences

Article

In vitro evaluation of the inhibitory capacity of three *Trichoderma* isolates on *Ralstonia solanacearum*

Jimmy Pico Rosado[1]*, *Christopher Suárez Palacios*[1], *Jessenia Jiménez Cumbicus*[1], *Ernesto Paredes Puga*[1], *Gladys Sabando*[2], *Liliana Andrade Olalla*[1]

[1] *Instituto Nacional, de Investigaciones Agropecuarias, INIAP, Joya de los Sachas – Ecuador* jimmy.pico@iniap.gob.ec.
[1] *Instituto Nacional, de Investigaciones Agropecuarias, INIAP, Joya de los Sachas – Ecuador* christopher.suarez@iniap.gob.ec.
[1] *Instituto Nacional, de Investigaciones Agropecuarias, INIAP, Joya de los Sachas – Ecuador* jessenia.jimenez@iniap.gob.ec.
[1] *Instituto Nacional, de Investigaciones Agropecuarias, INIAP, Joya de los Sachas – Ecuador* ernesto.paredes@iniap.gob.ec.
[1] *Instituto Nacional, de Investigaciones Agropecuarias, INIAP, Joya de los Sachas – Ecuador* liliana.andrade@iniap.gob.ec.
[2] *Instituto Superior Tecnológico General Eloy Alfaro, Joya de los Sachas – Ecuador* gsabando@institutos.gob.ec.
* *Correspondence:* jimmy.pico@iniap.gob.ec
Available from. http://dx.doi.org/10.21931/RB/2024.09.01.6

ABSTRACT

Bacterial wilt in bananas, caused by *Ralstonia solanacearum* or Moko, limits crop production and threatens Ecuador. This study evaluated *Trichoderma* isolates in laboratory conditions as an innovative alternative to ensure sustainability in banana production. The four *R. solanacearum*. isolates were obtained from banana plants exhibiting disease symptoms and were characterized through morphological and biochemical tests. Four treatments were evaluated: three isolates of fungi from the genus *Trichoderma* (*Trichoderma viride*, T. *harzianum*, *T. asperellum*) and one consisting of a combination of the three isolates above. The inhibitory capacity of the *Trichoderma* isolates on *R. solanacearum* colonies was measured. A completely randomized design with three replicates was used, and general linear and mixed models were employed, with qq-plot graphs for normality and residual plots for variance homogeneity.

Furthermore, a Fisher's LSD test was conducted at a significance level of $\alpha = 0.05$. In the biochemical tests, the bacterial isolates exhibited specific characteristics of *R. solanacearum* in two bacterial isolates. In the inhibition tests, treatment four and treatment one (consortium of the three *Trichoderma* isolates and *Trichoderma viride*) showed the highest inhibitory potential, with 76.07% and 61.19%, respectively. The consortium of *Trichoderma* isolates demonstrated the highest inhibitory potential against *R. solanacearum*, with day 10 being the time with the highest percentage of inhibition (72.61%).

Keywords: Bacterial wilt, *Ralstonia solanacearum*, *Trichoderma*, inhibition

INTRODUCTION

In Ecuador, several species of Musaceae are cultivated, with bananas being the crop with the largest planted area, covering 165,080 hectares, followed by plantains with 145,501 hectares, and baby bananas or "oritos" with a cultivated area of 6,839 hectares [1–3]. Plantains are a prominent export crop and a fundamental staple for the country's food security and employment generation [4]. The central banana-producing provinces in

Ecuador are Manabí, Santo Domingo, Esmeraldas, Guayas, Los Ríos, Orellana, Morona Santiago, Napo, and Sucumbíos [1].

In the banana belt of Ecuador, where varieties such as Dominico and Barraganete are grown, banana producers, mostly small-scale farmers, face significant challenges caused by phytopathogenic fungi and pests such as the black weevil (*Cosmopolites sordidus*), nematodes of the genera *Pratylenchus* and *Helicotylenchus*, and Black Sigatoka (*Mycosphaerella fijiensis*). One of the most significant challenges is *Ralstonia solanacearum*, known as "Moko," a bacterium that colonizes and obstructs the plant's vascular system, leading to wilting and, eventually, plant death [5]. Despite being an essential crop for food security and the country's economy, this disease severely threatens plants.

Biological control has been adopted as part of integrated pest management to promote sustainable agriculture practices. In this context, fungi of the genus *Trichoderma* have shown effectiveness in controlling phytopathogenic fungi in different crops. *Trichoderma* spp., microscopic facultative anaerobic fungi, are naturally found in the soil and other environments with decomposing organic matter and plant residues [6,7].

This research aims to evaluate the potential of biological control using three *Trichoderma* isolates (*T. viride, T. harzianum, T. asperellum*) to inhibit the growth of *Ralstonia solanacearum* under laboratory conditions. The focus is reducing dependence on agrochemicals and minimizing negative environmental impacts. Additionally, using Trichoderma spp. as a biological control agent is expected to improve the plantain crop's productivity and mitigate problems caused by *R. solanacearum* in this critical sector. Through this research, we seek to provide scientific evidence of the effectiveness of biological control with *Trichoderma* spp. as a viable and sustainable alternative for managing *R. solanacearum* in the plantain crop. The results will strengthen integrated pest management strategies and promote more environmentally friendly agricultural practices, benefiting banana producers and food security in the country.

MATERIALS AND METHODS

The study was conducted at the Plant Protection Laboratory, Central Experimental Station of the Amazonia of the National Institute of Agricultural and Livestock Research (INIAP). This institution is located in San Carlos, La Joya de los Sachas Canton, Orellana Province, at 280 meters above sea level.

Obtaining *Trichoderma* isolates

The isolates identified as *Trichoderma Viride, Trichoderma Harzianum*, and *Trichoderma Asperellum* were provided by the Tropical Pichilingue Experimental Station and preserved in Eppendorf tubes with sterile distilled water, following the methodology described by [8]. The main objective of this methodology is to maintain the viability, authenticity, and purity of the microorganisms.

Activation of *Trichoderma* isolates

The following steps were carried out to activate the Trichoderma isolates preserved in sterile water: the microtubes containing the *Trichoderma* strains were shaken in an isolation chamber. Then, 0.5 ml of each isolate was taken using a micropipette with previously sterilized tips. These samples were poured into the center of a Petri dish containing PDA (Potato Dextrose Agar) culture medium supplemented with lactic acid. The Petri dishes were incubated at a temperature of 27°C for 10 days, allowing the *Trichoderma* isolates to develop and grow actively.

Obtaining the pathogenic bacterial isolate

The following steps were followed for bacterial isolation from plant tissues with disease symptoms: portions of affected tissue were taken and superficially disinfected with a 4% sodium hypochlorite and 70% (v/v) alcohol solution. Subsequently, they were washed with sterile distilled water. Approximately 5 mm² each, tissue fragments were cut and macerated in a mortar using sterile purified water. The resulting suspension was spread on Petri dishes containing nutrient agar using a previously sterilized Drigalski spatula. After 48 hours

of bacterial growth, a loopful of bacterial growth was transferred to a selective culture medium called "selective media from South Africa" (SMSA) modified. The Petri dishes were incubated at 30°C for 48 hours. During this time, typical colonies of slightly fluid reddish-purple color with a pink center were selected using criteria described by [9-10], and other relevant studies.

Characterization of pathogenic bacteria

Biochemical and physiological methods in plant microbiology studies were widely used to characterize the isolated bacteria based on the techniques described by Goszczynska and colleagues [11]. These methods included Gram staining to determine cell morphology, the use of 3% KOH to identify Gram-negative or Gram-positive bacteria, the oxidase test to verify the production of the oxidase enzyme, the catalase test to detect the presence of the catalase enzyme, the nitrate reduction test to evaluate the bacteria's ability to reduce nitrate, growth at 41°C to determine thermotolerance, and salt tolerance by growth in media with NaCl concentrations of 1%, 2%, and 3%. Additionally, the fluorescence test was performed to detect the production of fluorescence, an essential criterion for identifying *Ralstonia* strains. These biochemical and physiological tests are fundamental for determining and characterizing isolated bacteria, as they provide essential information about their metabolic characteristics and ability to survive in different environmental conditions.

Conservation of bacteria

The methodology for conserving bacterial isolates described by [8] was used to maintain the bacteria's viability, authenticity, and purity over time. Purified bacterial isolates were cultured on Petri dishes with a nutrient agar medium. Then, sterile test tubes with nutrient agar medium were prepared and inclined at a 45° angle to allow the medium to solidify. The bacteria were streaked onto the inclined tubes and left to rest for one day at room temperature. Finally, the test tubes were preserved through freezing, ensuring the preservation of the bacterial isolates for future use.

Experiment management

To perform the inhibition tests, the methodology described by Andrade [11], was used with some modifications. First, in a laminar flow cabinet, enriched potato-dextrose-agar and nutrient agar media were dispensed in 90 mm Petri dishes. For the dual confrontation, a 5 mm diameter disc of each *Trichoderma* isolate and the bacterial isolates were placed opposite each other on the surface of the culture medium. As for the consortium confrontation, using a sterile punch, a 5 mm disc was set at three points of the Trichoderma isolates, and one disc was set at the center of the bacterial isolate that tested positive for Ralstonia. The Petri dishes were incubated at room temperature, and the interaction between the antagonistic organism and the pathogen was recorded every 24 hours. This recording allowed the observation and evaluation of the effects of *Trichoderma* isolates on the bacterial isolates, both in the dual confrontation and the consortium.

Inhibition tests of bacterial isolates

Tests were conducted to measure the inhibitory effect of three *Trichoderma* isolates (*T. viride, T. harzianum*, and *T. asperellum*) on two bacterial isolates positive for *Ralstonia solanacearum*. Five treatments were established: T1 (*T. viride*), T2 (*T. harzianum*), T3 (*T. asperellum*), T4 corresponding to the consortium of the three *Trichoderma* isolates, and T5 as the control, consisting of the unrestricted growth of bacterial isolates. A completely randomized design with three replications was used, with a Petri dish as the experimental unit (Table 1). This allowed for a systematic and controlled evaluation of the effect of different *Trichoderma* treatments on the bacterial isolates, providing precise information about the inhibitory potential of the *Trichoderma* isolates against *R. solanacearum*.

Study parameters

In evaluating inhibitory potential, the percentage of colony growth inhibition (PCGI) was determined using a modified formula based on the work of Suárez and Cabrales [12]. This formula allowed for the precise calculation of the inhibition degree of bacterial colony growth in the presence of different *Trichoderma* treatments. In this way, the inhibitory effect of *Trichoderma* isolates on *R. solanacearum* isolates could be quantified objectively and comparatively.

$$\mathbf{PI}=\frac{(Mt-Ma)}{Mt}*100$$

Where:
Ma: Ralstonia solanacearum, inhibited.
Mt: Mycelium of free growth of Ralstonia solanacearum (control).

Data analysis

In the statistical analysis, the *Trichoderma* isolates and the number of evaluations over time were considered fixed effects, while repetitions were treated as random. The data obtained were analyzed using the statistical software InfoStat version 2015. General linear and mixed models [13], were employed, and model assumptions were verified through qq-plot graphs for normality and residual plots against predicted values for variance homogeneity. Additionally, a Fisher's LSD test with a significance level of $\alpha= 0.05$ was conducted to compare the means. To assess interactions between the antagonistic organism and the pathogen, the Image Tool program version 3.0, developed by Wilcox et al. (2002) in collaboration with the University of Texas, was used. Compatible with Windows 7, this program allowed for measurements using photographs as reference.

RESULTS

Characterization of *Ralstonia solanacearum* isolates

In the characterization of four bacterial isolates obtained from banana tissue exhibiting Moko symptoms, two bacteria (isolates 3 and 4) with distinctive morphological characteristics such as a reddish appearance, mucous texture, and positive biochemical tests for *Ralstonia solanacearum* were identified. These results are presented in Table 1, and the appearance of the bacteria can be observed in Figure 2.

Tests	Reaction
Gram Staining	Gram-negative
Potassium Hydroxide Test (3% KOH)	Positive
Catalase	Positive
Nitrate Test	Positive
Tolerance to 1% and 2% Salts	Positive
Tolerance to 3% Salts	Negative
Growth at 41 °C	Negative
Fluorescence Test	Negative

Table 1. Biochemical Test Results for Two Bacterial Isolates.

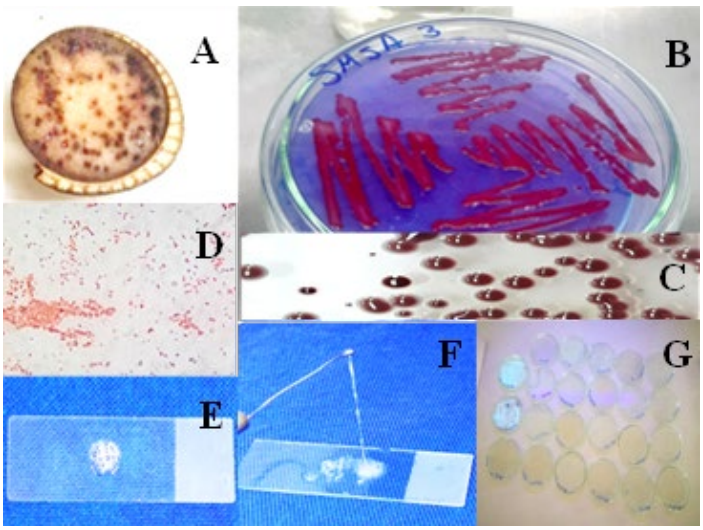

Figure 1. Response of the characterization of Ralstonia solanacearum. A; symptomatic tissue of the disease. B; Cultivation was performed in the SMSA culture medium. C; characteristics of the Ralstonia colony in SMSA medium. D; Gram stain (-). E; Catalase test (+). F; Potassium Hydroxide Test (+). G; Fluorescence test (-).

The results obtained in this research corroborate Torres's previous findings [14]. who also found similar characteristics in bacterial colonies' morphology and polysaccharide production. Furthermore, the results of this research are consistent with Mendoza's reports [15]. *they were* regarding the microscopic characteristics of Ralstonia solanacearum, such as its rod-shaped motile form and pink staining in the Gram stain using fuchsin. These results support the identification of the bacterium as Gram-negative, as determined by the 3% KOH test.

In summary, the results of the morphological and biochemical characterization of the bacterium in this research are consistent with previous findings and confirm the similarity of the isolated bacterium to Ralstonia. According to the study conducted by Pawaskar [16]. it aligns with the results of identifying Ralstonia solanacearum based on morphological and biochemical characteristics, including Gram staining, KOH test, colony coloration, starch hydrolysis, and cellulose decomposition.

Inhibition tests

In Figure 2, it can be observed that the evaluated *Trichoderma* isolates exhibited a remarkable ability to inhibit the growth of the studied bacterial colonies. These results are consistent with those previously obtained by other researchers [17–19]. It further supports the effectiveness of *Trichoderma* as a control agent. The treatments showed significant differences ($P < 0.0001$), indicating variability in the inhibitory potential of the different *Trichoderma* isolates. Specifically, treatment four, consisting of the consortium of the three *Trichoderma* isolates, and treatment one, showed the highest inhibitory potential with a percentage of colony growth inhibition of 76.07% and 61.19%, respectively. These values were statistically different from treatments two and three, which had inhibition percentages of 57.19% and 55.65%, respectively. The presented results demonstrate that the evaluated Trichoderma isolates can inhibit the growth of the studied bacterial colonies, with the consortium of the three isolates and an individual isolate being the most effective in this inhibition.

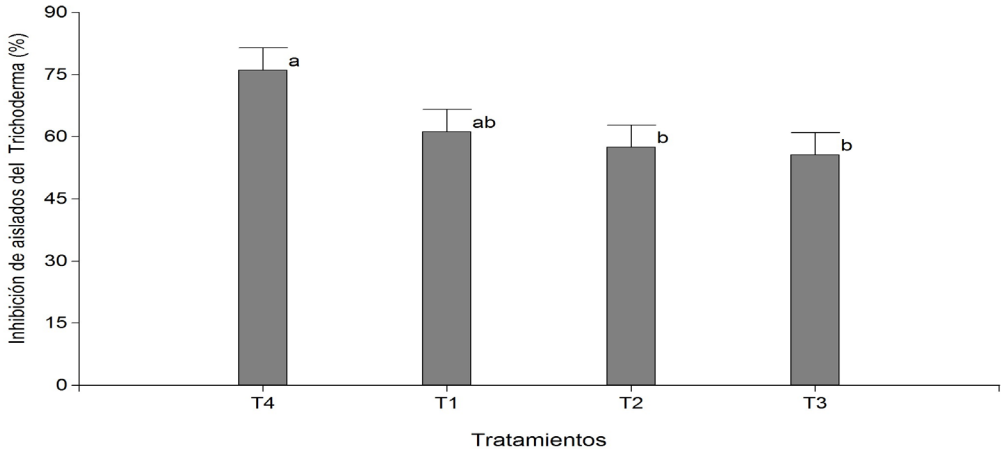

Means with a typical letter are not significantly different ($p > 0.05$)

Figure 2. Percentage of inhibition of Trichoderma isolates on Ralstonia sp. isolates (T1 *Trichoderma viride*, T2 *Trichoderma harzianum*, T3 *Trichoderma asperellum*, and T4 consortium of three Trichoderma isolates).

When analyzing the effect of days on inhibition, significant differences in days are observed ($P < 0.0118$), with day 10 achieving the highest percentage (72.61%), being statistically different from days six and two, which reached the lowest percentage (57.73% and 57.45%, respectively) (Figure 3).

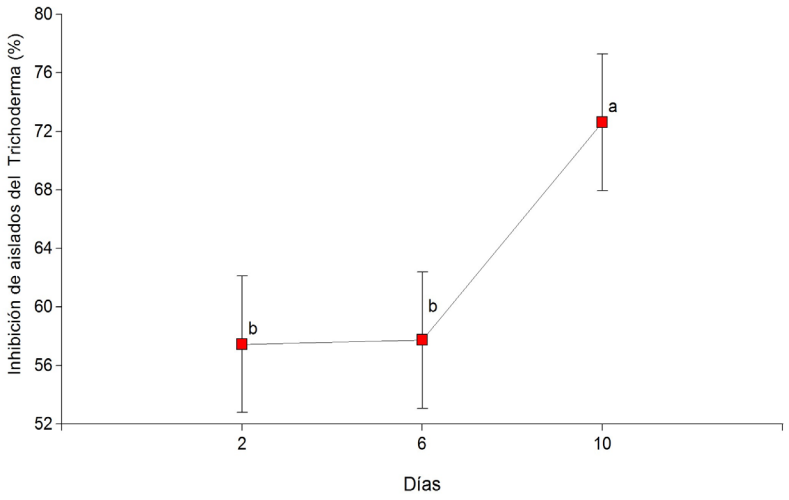

Means with a common letter are not significantly different (p > 0.05).

Figure 3. Percentage of inhibition of Trichoderma genus isolates on potential *Ralstonia solanacearum* isolates over time.

DISCUSSION

The in-depth analysis of the data presented, when compared to those of other authors, reveals that the results obtained in this research are consistent with previous studies conducted by Alvarez [20], Yendyo [21] and Goszczynska [22]. These studies have demonstrated that *Trichoderma* genus isolates possess a significant antibiotic effect due to the production of thermostatic metabolites. These metabolites have been associated with an increase in root collar height and diameter, which correlates with the results obtained in this research regarding the inhibitory capacity of the consortium of *Trichoderma* isolates.

Furthermore, a study by other researchers (23-24) (25) found that applying metabolites from *T. harzianum* resulted in maximum inhibition of the soil bacterial population and reduced disease severity. These findings are similar to the results obtained in this research, where bacterial inhibition was observed starting from the tenth day after the application of *Trichoderma* isolates.

On the other hand, the findings of Ceballos [7], Align [26] and Sutarman [27], support the results of this research by demonstrating that crude extracts of *Trichoderma* sp. have highly significant effects on the in vitro inhibition of colonies of different species of *R. solanacearum*. These results strengthen the evidence of *Trichoderma*'s antibacterial activity against the bacterium *R. solanacearum*.

According to the study by Khan [28], it aligns with the results obtained in this study, revealing that *Trichoderma* spp. Isolates significantly inhibited bacterial growth and cell damage by *R. solanacearum*.

CONCLUSIONS

This scientific study has significantly advanced our understanding of the interaction between Trichoderma isolates and Ralstonia solanacearum under laboratory conditions, as suggested in the article's title: "In vitro Evaluation of the Inhibitory Capacity of Three Trichoderma Isolates on Ralstonia solanacearum." Based on our results and concerning the objectives set forth, we have conclusively demonstrated that Trichoderma, especially the consortium of the three Trichoderma isolates and the T. viride isolate, possess a remarkable inhibitory potential against R. solanacearum. These findings strongly support using Trichoderma as an effective biological control agent in managing this phytopathogenic bacterium in banana crops. Furthermore, our

results pave the way for future research and applications in this field, potentially significantly benefiting farmers and promoting sustainable and safe agricultural practices for food production.

REFERENCES

.1. ESPAC. Encuesta de Superficie y Producción Agropecuaria Continua [Internet]. Instituto Nacional de Estadistica y Censos; 2020 [citado 3 de febrero de 2021] p. T34. Disponible en: https://www.ecuadorencifras.gob.ec/estadisticas-agropecuarias-2/
2. INEC IN de E y C. Superficie, según producción y ventas de orito (fruta fresca) por región y provincia en Ecuador. Instituto Nacional de Estadística y Censo; 2020.
3. SIPA S de IPA del E. CIFRAS AGROPRODUCTIVAS [Internet]. Ministerio de Agricultura y Ganadería; 2020. Disponible en: http://sipa.agricultura.gob.ec/index.php/cifras-agroproductivas
4. Ordoñez J, Cevallos HV, Barrezueta-Unda S. Análisis de rentabilidad económica del plátano (Musa balbisiana AAB Simmond) en el sitio Río Negro, provincia El Oro. Revista Metropolitana de Ciencias Aplicadas. 2019;2(2):160-70.
5. Ramírez M, Neuman BW, Ramírez CA. Bacteriophages as promising agents for the biological control of moko disease (Ralstonia solanacearum) of banana. Biological Control. 2020;149:104238.
6. Suárez C., Remache N., Pico J., Paredes E., Jiménez J, Andrade L., et al. Aislamiento y evaluación de cepas nativas de Trichoderma spp., como promotor de desarrollo radicular. CU [Internet]. 27 de mayo de 2023 [citado 31 de mayo de 2023];16(42). Disponible en: https://ojs.unemi.edu.ec/index.php/cienciaunemi/article/view/1719
7. Ceballos G, Álvarez E, Bolaños MM. Reducción de poblaciones de Ralstonia solanacearum raza 2 (Smith) en plátano (Musa AAB Simmonds) con aplicación de extractos de Trichoderma sp.(Alexopoulus y Mims) y bacterias antagonistas. Acta agrónomica. 2014;63(1):80-7.
8. Maridueña-Zavala MG, Quevedo A, Aguaguiña K, Serrano L, Sosa del Castillo D. Colección de cultivos microbianos CIBE (CCM-CIBE): Una colección para la investigación. Bionatura. 2021;6:1664-8.
9. Denny T. II. Gram negative bacteria, F. Ralstonia. Laboratory guide for identification of plant pathogenic bacteria. 2001;151-74.
10. Schaad NW, Jones JB, Chun W. Laboratory guide for the identification of plant pathogenic bacteria. American Phytopathological society (APS press); 2001.
11. Andrade-Hoyos P, Luna-Cruz A, Osorio-Hernández E, Molina-Gayosso E, Landero-Valenzuela N, Barrales-Cureño HJ. Antagonismo de Trichoderma spp. vs hongos asociados a la marchitez de chile. Revista mexicana de ciencias agrícolas. 2019;10(6):1259-72.
12. Suárez LY, Cabrales CP. Identificación de especies de cepas nativas de Trichoderma sp. y Bacillus sp. y evaluación de su potencial antagonista in vitro frente al hongo fitopatógeno nativo Moniliophthora roreri en el departamento de Norte de Santander. Respuestas. 2008;13(1):45-56.
13. Di Rienzo J, Casanoves F, Gonzales L, Tablada E, Díaz M, Robledo C, et al. Estadistica para las Ciencias Agropecuarias. Séptima Edición ed. Cordoba Argentina, Editorial Brujas p. 2008;
14. Torres-González C, Casas M, Díaz Ortiz JE. Manejo de Ralstonia Solanacearum raza 2 a través de productos químicos y biológicos. Iteckne. 2013;10(2):217-23.
15. Mendoza Andrade OA. Caracterización filogenética molecular de secuencias sobre genes de siete cepas de Ralstonia solanacearum. 2021;

16. Pawaskar J, Joshi M, Navathe S, Agale R, Sawant Konkan Krishi Vidyapeeth B. Physiological and biochemical characters of ralstonia solanacearum. International Journal of Research in Agricultural Sciences. 2014;1(6):2348-3997.
17. Narasimha Murthy K, Nirmala Devi D, Srinivas C. Efficacy of Trichoderma asperellum against Ralstonia solanacearum under greenhouse conditions. Annals of Plant Sciences. 2013;2(9):342-50.
18. Konappa N, Krishnamurthy S, Siddaiah CN, Ramachandrappa NS, Chowdappa S. Evaluation of biological efficacy of Trichoderma asperellum against tomato bacterial wilt caused by Ralstonia solanacearum. Egyptian Journal of Biological Pest Control. 2018;28:1-11.
19. Mohamed BF, Sallam NM, Alamri SA, Abo-Elyousr KA, Mostafa YS, Hashem M. Approving the biocontrol method of potato wilt caused by Ralstonia solanacearum (Smith) using Enterobacter cloacae PS14 and Trichoderma asperellum T34. Egyptian Journal of Biological Pest Control. 2020;30:1-13.
20. CIAT GCI, Álvarez E, D CIAT P, Llano G. Actividad antagónica de bacterias biocontroladoras y filtrados de Trichoderma spp. contra Ralstonia solanacearum en plátano.
21. Yendyo S, Ramesh G, Pandey BR. Evaluation of Trichoderma spp., Pseudomonas fluorescens and Bacillus subtilis for biological control of Ralstonia wilt of tomato. F1000Research. 2017;6.
22. Goszczynska T, Serfontein J, Serfontein S. Introduction to practical phytobacteriology: a manual for phytobacteriology by SAFRINET, SDC Switzerland. 83 p. Disponible en línea: https://www researchgate net/publication/237021880_Introduction_to_Practical _Phytobacteriology_A_manual_for_phytobacteriology. 2000;
23. Guo Y, Fan Z, Yi X, Zhang Y, Khan RAA, Zhou Z. Sustainable Management of Soil-Borne Bacterium Ralstonia solanacearum In Vitro and In Vivo through Fungal Metabolites of Different Trichoderma spp. Sustainability. 2021;13(3):1491.
24. Yan L, Khan RAA. Biological control of bacterial wilt in tomato through the metabolites produced by the biocontrol fungus, Trichoderma harzianum. Egyptian Journal of Biological Pest Control. 2021;31(1):1-9.
25. Rahman M, Borah SM, Borah PK, Bora P, Sarmah BK, Lal MK, et al. Deciphering the antimicrobial activity of multifaceted rhizospheric biocontrol agents of solanaceous crops viz., Trichoderma harzianum MC2, and Trichoderma harzianum NBG. Frontiers in Plant Science. 2023;14.
26. Alelign S. Evaluation of the efficacy of Trichoderma and Pseudomonas species against bacterial wilt (Ralstonia isolates) of tomato (Lycopersicum spp.). 2020;
27. Sutarman S, Jalaluddin AK, Li'aini AS, Prihatiningrum AE. Characterizations of Trichoderma sp. and its effect on Ralstonia solanacearum of tobacco seedlings. Jurnal Hama dan Penyakit Tumbuhan Tropika. 2021;21(1):8-19.
28. Khan RAA, Najeeb S, Mao Z, Ling J, Yang Y, Li Y, et al. Bioactive secondary metabolites from Trichoderma spp. against phytopathogenic bacteria and root-knot nematode. Microorganisms. 2020;8(3):401.

Received: 9 October 2023/ **Accepte**d: 15 January 2024 / **Published:**15 February 2024

Citation. Pico Rosado J, Suárez Palacios C, Jiménez Cumbicus J, Paredes Puga E, Sabando G, Andrade Olalla L. *In vitro* evaluation of the inhibitory capacity of three *Trichoderma* isolates on *Ralstonia solanacearum.* Revis Bionatura 2024; 9 (1) 6. http://dx.doi.org/10.21931/RB/2024.09.01.6

Additional information Correspondence should be addressed to *jimmy.pico@iniap.gob.ec*
Peer review information. Bionatura thanks anonymous reviewer(s) for their contribution to the peer review of this work using https://reviewerlocator.webofscience.com/

Bionatura ISSN. First 13909355 Ecuador. **Scopus coverage years**: from 2016 to the Present

Bionatura
Ibero-American Journal of Biotechnology and Life Sciences

Article

Description of the primary Loreto-coca river contamination through the measurement of physico-chemical parameters.

Jose Allauca P[1,2], *Carlos Lopez P*[1], *Jennyfer Daza*[1], *Joyce Chamba*[1]
[1] *Escuela Superior Politecnica de Chimborazo (ESPOCH), Sede Orellana, El Coca, 220101, Ecuador,*
[2] *Instituto Superior Tecnologico General Eloy Alfaro (ISTGEA), La Joya de los Sachas, 220101, Ecuador*
Escuela Superior Politecnica de Chimborazo (ESPOCH), Sede Orellana, El Coca, 220101, Ecuador
* *Correspondence: : j.luis_2010@yahoo.es / josel.allauca@espoch.edu.ec*
Available from. http://dx.doi.org/10.21931/RB/2024.09.01.7

ABSTRACT

The main objective of this article is to describe the pollution in the main Loreto-Coca rivers using physico-chemical parameters. Our analysis is focused on the Orellana province and examines the Suno, Napo, Coca, and Payamino rivers, which are adversely impacted by oil and mining activities. These activities result in toxic and chemical residues, such as heavy metals and other contaminants. Samples were collected following the INEN 2176 standard to do this. We could evaluate parameters such as pH, dissolved oxygen, conductivity, turbidity, nutrients (nitrates, phosphates), heavy metals, and COD using laboratory equipment and specific techniques and methods. The level of pollution was determined by comparing these results with permissible limits. Therefore, based on the comparative results obtained, environmental education is crucial for raising awareness about the importance of protecting and conserving water as a vital resource. Conducting these studies provides essential information for taking preventive and corrective measures and monitoring and addressing identified issues to safeguard public health and the environment.

Keywords: pollution, water, rivers, sample, standard, physicochemical parameters.

INTRODUCTION

Water has particular characteristics; it is fragile, scarce and essential for us living beings; it has been used as the primary issue of adaptation among the population to satisfy all its biological needs. The problem of this resource is due to the reproduction, circulation and generation of waste, including toxic-chemical waste or other particles found in the surroundings of our communities, when these pollutants enter the water, such as rivers, lakes, seas, etc. They dissolve in them, thus leaving suspended particles and even depositing at the bottom of rivers, thus causing degradation of water quality[1].

The extraction, refining or use of petroleum derivatives are still part of the world's economic activities. Petroleum is a mixture of paraffin, naphthenic and aromatic hydrocarbons, benzene, sulfur, nitrogen, oxygen and metallic compounds. However, its chemical components are detrimental to the health of the communities near the oil areas, which have shown carelessness in the traces left by their petrochemical activities, mainly the contamination of water resources. To this is added deficient government surveillance. River water is the primary source of consumption for the rural population, and being contaminated by chemical compounds, it is difficult to carry out water treatment[2].

The Latin American region is very rich in water resources, and people have the right to consume clean water. Drinking water is everyone's responsibility and must be ensured that it is acceptable, accessible and affordable for personal and domestic use. A safe, quality water supply is essential to prevent deaths from dehydration

and reduce the risk of waterborne diseases. Therefore, it is necessary to carry out physical parameters that indicate how polluted the rivers of the Coca and Loreto cantons are to know the water quality and if humans can consume them [3].

The factors most considered as potential pollutants in Ecuador are organic and inorganic products and heavy metals that are produced by industries, the agricultural sector and urban runoff surrounding the area; all these pollutants not only cause environmental damage but also cause severe diseases to the population, organophosphates and carbonates come into contact with humans, and there is a high percentage of probability that these are the cause of chronic diseases such as cancer and damage to internal organs. The human being needs at least 3 liters of drinking water a day for his existence and about 20 liters for daily activities; in our country, we have a significant advantage since Ecuador has a quantity of fresh water of 22,500 m3/inhab/year [4].

Environmental Education (EE) is so important due to the life we lead; focusing on EE, we know that it is essential to see the issue of water as a resource that must be cared for, conserved and enjoyed rationally. Therefore, in the last decade in our country. Due to this particular context, it should be logical to expect that the province in which this study will be carried out would present a relatively higher level of awareness than it may present for other topics. However, we have not even reached 50% awareness in our province; we are far from being able to affirm this approach [5].

It is time to focus on one of the most seen problems in the province of Orellana and the affectation caused by mining activity at the provincial level; we know that it is of great importance for the productive development of our country; however, the fact that heavy metals are used for their production implies a high risk of contaminating the environment and the communities where mining is practiced. We all make use of water; therefore, we want to find a way to propose a balanced design based on the narratives about the degree of contamination to go beyond the emotions and the humanistic side of man but rather through This can contribute to the commitment of societies with the environment [6].

When we talk about the detection and quantification of heavy metals in rivers, we cover techniques, methodologies, equipment and materials, all this with planning according to the situation; this has given way to the investigation of various methods to use, comparing time, cost and accuracy of the results, mentioning some we have Atomic Absorption Spectrometry, Inductively Coupled Plasma Spectrometry, Photometric Techniques, Electrochemical Techniques, among others, each technique has different advantages and disadvantages, some have derivations for specific metals which is essential for the results, others have low cost, all this allows us to decide the scope of the investigation and the price we want to reach [7].

For decades, there has been evidence that a high percentage of diseases come from poorly processed water, that is, it does not meet the standards of water suitable for human consumption; in turn, the rivers, precisely which the project focuses on, are not clean water, but contaminated with fecal matter that affects the decrease in water quality and therefore the life of living beings, bacterial and viral diseases caused by agents are present. Another factor is the excessive presence of chemical, organic and inorganic contaminants and heavy metals from industrial and agricultural sources and urban runoff, alterations in the nervous and immune systems, damage to the human genome and the product of reproduction [8].

With water quality evaluation, we refer to the substrate's chemical, physical and biological characteristics to be analyzed. Towards the tributaries of the Loreto-Coca rivers in the province of Orellana, we will require the widely known Water Quality Index (QWI). Still, first we will analyze the study of 5 physical-chemical parameters to determine the degree of contamination in the collection area. According to each river, all kinds of standardized norms will be carried out to collect the sample, transport it, and determine results; with this, we will have an adequate value to continue comparing the degree of contamination of the rivers mentioned above [9].

The contamination of rivers in the Orellana province in Ecuador is a matter of great concern for residents and government authorities. The province is located in the Amazon region of the country, which is one of the most biodiverse areas in the world and has significant ecological and economic importance. However, human activity, such as oil exploitation, agriculture and livestock, has caused a series of environmental problems, including the pollution of rivers.

According to a study [10], Orellana's rivers are contaminated with heavy metals, such as lead, mercury and cadmium, due to mining and oil activity. These metals can have toxic effects on human health and aquatic ecosystems. In addition, agriculture and livestock also contribute to the contamination of rivers with pesticides and fertilizers.

Another study carried out [11] found high levels of contamination in the Napo River, which runs through the province of Orellana. The contamination included high levels of fecal coliforms and other chemical contaminants, which can negatively affect human health and aquatic fauna.

Local and national authorities have implemented measures to address river pollution in Orellana, including regulating mining and oil activity and promoting sustainable agricultural practices. However, more decisive action is required to protect human health and the environment.

In the Unified Text of Secondary Environmental Legislation [12], Book VI Annex 1, we can find norms and regulatory standards for protecting and controlling water resources. The tables above contain water quality criteria for human consumption, aquatic and wildlife life preservation, agricultural irrigation, livestock use, and recreational use through contact and effluent discharge into the sewer, freshwater bodies and seawater.

Evaluating the physicochemical parameters of water is crucial to determining the level of contamination in water bodies. As indicated [13], these parameters make it possible to measure the presence of chemical substances and organic compounds that can harm human health and the environment. Early identification of contaminants helps to take preventive and corrective measures to avoid more significant problems. In addition, the periodic measurement of physicochemical parameters allows for monitoring the evolution of water quality and evaluating the effectiveness of environmental management policies and programs.

The detection of pH and electrical conductivity are vital parameters to determine the level of contamination in rivers, according to the authors [14] in their study on the monitoring of physicochemical parameters in the upper basin of the Bogotá River. The pH measurement allows us to know the water's acidity or alkalinity and detect the presence of acidic or basic substances that can affect the quality of the water and aquatic life. Electrical conductivity indicates the amount of dissolved salts in water and can indirectly infer the presence of organic and inorganic substances in water. Both parameters are essential to assess the impact of human activities on rivers.

The study carried out [15] on the physicochemical and microbiological evaluation of the water quality of the Machangara and Monjas rivers of the Quito metropolitan district (DMQ) water network is relevant due to its contribution to the identification of contamination levels in these rivers through the measurement of physicochemical and microbiological parameters. The information obtained through this study is helpful for decision-making regarding the management and conservation of the water of these rivers and, therefore, for the protection of the environment and public health.

Detecting heavy metals in river sediments is important to determine water quality and assess environmental impact. The digestion process is essential in this analysis since it allows the extraction of metals in the sediment and its subsequent quantification. The EPA Standard is a tool to establish allowable limits for metals in surface waters and sediments. The study carried out in [16] in the Puyango River basin, Ecuador, demonstrates the application of this methodology to assess the levels of heavy metals in river sediments.

Standard methods [17] for analyzing drinking water and wastewater are essential for determining water quality. Methods used include Method 2550-B for the determination of total solids, Method 2540-B for the determination of suspended solids, Method 2510-B for the determination of settleable solids, and Method 5220-D for the determination of dissolved oxygen. These methods provide detailed information on contaminants present in water and their concentration, allowing informed decisions to protect public health and the environment.

The advantage of using physicochemical water quality parameters is that the information obtained during monitoring can be easily transferred and interpreted. The indicator shows the level of contamination of the type of water tested, allowing the user to understand the water situation quickly. It can be excessive, moderate or non-existent, understandable and abstract; the studies of the characteristics of the water bodies quantify and simply present results that generate general or specific perceptions of the state of each case study so that measures can be taken to improve the general conditions of the bodies of water [18].

Most studies include physicochemical parameters, BOD variables, total coliform counts, and percent oxygen saturation. These first two variables reflect different sources of organic pollution, and the last variable represents the environmental response to varying types of pollution. The importance of using specific organisms as biological indicators is emphasized because these organisms occupy habitats that must meet specific environmental requirements. Therefore, when carrying out studies that involve physicochemical and biological parameters, conclusions can be drawn based on water quality [19].

The choice and use of these tools require a deep knowledge of various physical and chemical variables and their interactions with the biological communities that inhabit this type of ecosystem. Physicochemical parameters such as pH, temperature, conductivity and dissolved oxygen are measured, among others, in bodies

of water; it is probably the easiest way to define changes in their composition. These parameters also contain information on the evaluation of chemical and biological processes, which suggests that it can also help to identify geochemical processes such as self-purification [20].

Those studies that have served the scientific community to determine the level of contamination of natural water effluents are one of the main tools for remedying, purifying, and even preventing the contamination of this resource. Next, friendly options with the environment that can be implemented are disclosed.

Bioremediation: It is the application of microorganisms, plants and fungi that have the enzymatic capacity to degrade molecules that affect the natural composition of either water or soil [21].

We find specific applications within this field according to the species used.

- Phytoremediation: It uses plants to remove or degrade the contaminants in the place of interest [22].
- Mycoremediation: Use of fungal organisms due to their tolerance to contaminated systems; they also mineralize contaminants and spread quickly through their hyphae [23].

An important step is the implementation of treatment plants used by oil companies. It would not reduce pollution on a large scale, but control of the waste generated within the oil fields would be maintained. In turn, campaigns and contributions from the companies must be developed. They carry out oil extraction in extremely low-resource communities, the same ones that are affected; all this contamination goes hand in hand with the human being; the waste and detachment of crude oil generates diseases and causes damage to the skin, contributing to bioremediation a One step ahead of pollution, the damage to marine life is closer to becoming extinct [24].

Investigating different research areas, we found some alternatives for bioremediation in freshwater applied to heavy metals. The problem in the river is due to the high degree of contamination by heavy metals in these waters. The possibility of using microalgal biomass as a bioremediation agent for the purification of water contaminated with PM (Particulate matter) has demonstrated the effectiveness of four green microalgae species (*Chlamydomonas reinhardtii, Chlorella vulgaris, Scenedesmus almeriensis* and *Chlorophyceae sp*., isolated from the Loa River). These biological purification processes on the elements As, B, Cu, Mn and Zn, present in aqueous solutions, gave us good results by analyzing the operation factors and integration processes[25].

In the mineral extraction process, using large quantities of reagents such as cyanide and mercury is unavoidable and highly toxic to our environment. Today, the mining industry uses many methods to decontaminate cyanide effluents, such as The characterization of Cecropia peltata l. and Malva sylvestris; with both plants, a percentage of cyanide removal of 17% was obtained with Malva sylvestris and with Cecropia peltata l, 12%. On the other hand, when doing dosage tests, 14% and 11% removal percentages were obtained with the aqueous extracts. This treatment not only helps to decontaminate effluents, it also serves as a cost-reduction treatment since this type of plant is found in large numbers in our country [26].

Bioremediation is essential to act on the contamination of one or several rivers, for which microbial processes used for the recovery of soils contaminated by metals are employed so that the cleaning of degraded soils is an efficient process, optimal conditions must be biodegradation, taking into account the variables of humidity, pH and oxygen, through the inoculation process of bacteria of the genus Rhizopus, Penicillium and Phanerochaete, in addition, there is an extended field of bacteria capable of using hydrocarbons as a carbon source for their metabolic functions, being the most known genera, with biodegrading capacity: Achromobacter, Acinetobacter, Alcaligenes, Arthrobacter, Aspergillus, Bacillus, Brevibacterium, Candida, Corynebacterium, Flavobacterium, Fusarium, Micrococcus, Mucor, Mycobacterium, Nocardia, Penicillium, Pseudomonas, Rhodococcus, Rhodotorula, Sporobolomyces, Stenotrophomonas [27].

River pollution is a major environmental problem, and over the years, numerous scientific studies have contributed innovative ideas to remedy this situation. Among these studies is research that has explored the use of aquatic plants and bacteria to mitigate river pollution. Next, I will mention some relevant scientific articles in this field, along with the bacteria or plants mentioned:

1. They demonstrated that the aquatic plant Pistia stratiotes (water lettuce) can remove pollutants in the Tinto River [28].
2. They investigated the Lemna minor plant (duckweed) 's potential for removing heavy metals in a polluted river [29].

3. They evaluated the capacity of the bacterium Pseudomonas aeruginosa to degrade hydrocarbons in a polluted river [30].
4. They studied the ability of the bacterium Bacillus subtilis to degrade organic compounds in a polluted river [31].

These are just a few examples of the wide range of scientific research that has provided ideas for remediating river pollution using aquatic plants and bacteria. These studies demonstrate the potential of nature to deliver sustainable solutions to the environmental challenges we face.

Advances in the industrial sector have increased pollution by releasing toxic compounds such as chromium (VI) deposited in water and soil. Due to this problem, alternative methods of managing these resources have been developed to reduce their environmental impact. This algorithm identifies microbial communities based on their taxonomic and functional profiles, which can be used for bioremediation of polluted rivers to increase remediation efficiency by analyzing the practical characteristics of microbial communities.

The issues of awareness and care for the environment do not have as much value as they should be at present, and the threat to the planet will never cease to exist; technological advances and the lack of human motivation are factors that have generated concern at the time of seeking strategies for the conservation and preservation of life. Environmental education can be a beacon of salvation to reach communities, schools, colleges and universities and get current generations to commit to ecological care through methodological and didactic strategies that help the population see the causes and the effects caused by our pollution in rivers, forests and soils.

MATERIALS AND METHODS

Bibliographic searches were carried out, and several articles and theses with relevant information were selected, focused on the evaluation of water through the analysis of physicochemical parameters and the application practice was carried out for the determination of the measures of the matrices such as pH, conductivity, total solids, Chemical Oxygen Demand (COD) and turbidity, in the Basic Sciences and Specialization Laboratory (L-CB-E-1) of the North-Orellana Headquarters, as part of the investigative process.

Sample collection.

Water samples were collected in Loreto and Francisco Orellana, mainly from the Suno, Coca, Payamino, and Napo rivers, in compliance with INEN Standard 2176, to guarantee their quality.

Ecuadorian technical standard INEN 2176 establishes guidelines on the sampling techniques used to obtain the necessary data to analyze quality control of natural waters, contaminated waters, and wastewater for their respective characterization, which is for stagnant and flowing waters. Following this Standard, the point sampling technique was applied during the winter season for each river under study.

Standardization reflected in a legal and practical Standard is crucial to acquire concrete and acceptable results, such as the analysis and experimental study of freshwater. Therefore, the Ecuadorian Technical Standard, recognized by the Ecuadorian Institute of Normalization (INEN), was applied.

It helped obtain, transport, handle and preserve wastewater samples. According to NTE INEN 2 169:98, in 3.1, it emphasizes that wastewater is susceptible to changing the results in its concentration due to chemical, biological and physical reactions during sampling and analysis. Note that different results will be noticed in the period of the conservation of the samples in the laboratory and when determining the concentration.

Taking the sample in a container free of polyethylene and contaminants is essential. The new glass container must be washed with water and detergent, finishing with distilled water, for a subsequent chemical analysis. Sample collection should be immediate and sealed to avoid air ingress and variation of constituents such as pH. Mention that, when transporting the samples, each must be in a package and transported in a dry environment without the presence of light or external contamination concerning the refrigeration of the samples at 2 °C and 5 °C. It must be stored in a dark place for a short period, and in case of freezing, it is considered to be -20 °C.

Methods to determine physicochemical parameters.

pH measurement

Equipment provided by the chemical laboratory of the Orellana-ESPOCH campus was used for pH measurement.

Conductivity measurement

It is essential to know the conductivity of the water to see the degree of contamination. For this purpose, the conductivity meter present in the laboratory of the ESPOCH-ORELLANA Headquarters was used. The data obtained were recorded in a notebook and later tabulated in an Excel spreadsheet. For a correct technique, we rely on the NTE INEN 2 169:98 standard, which refers to the sampling, handling, and conservation of samples for an accurate determination of electrical conductivity, among other things.

Measurement of Chemical Oxygen Demand (COD).

The determination of the Chemical Oxygen Demand (COD) indicates the amount of oxidizable compounds in the water, which was carried out based on the Ecuadorian Technical Standard INEN 1203. For this purpose, a test tube was used with a solution available at the Chemical Laboratory - ESPOCH - Orellana, which contained potassium dichromate ($K_2Cr_2O_7$), sulfuric acid (H_2SO_4) and distilled water.

The different absorbances were taken to the calibration curve to calculate the COD of the sample, considering that these results are within the curve. Otherwise, the process was repeated. This calculation was made by measuring a blank, tearing it, and measuring the sample.

Since the CR25 reactor is used to heat 16 mm flasks safely and reliably, it becomes fundamental equipment to aid digestion for measurements of COD, total phosphorus, and nitrogen, among other parameters.

The calculations for obtaining COD were made based on the INEN 1 203 Standard, which establishes the following formula:

$$\frac{mg}{1DQO} = \frac{(a-b)N * 8000}{cm^3 muestra} \qquad (1)$$

Where:

COD = chemical oxygen demand.

a = cm^3 $Fe(NH_4)(SO_4)_2$ used for the blank.

b= cm^3 Fe (NH_4) $(SO_4)_2$ used for the sample.

N = normality of Fe (NH_4) $(SO_4)_2$

The difference between the results of a duplicate determination must not exceed 5% of the mean of the two values otherwise the determination must be repeated.

Total Solids Measurement

The determination of total solids using the gravimetric method is based on the evaporation of liquids and was carried out under adequate temperature conditions in the oven of 103-105ºC. Sufficient time for the determination of total solids is 24h. The application interval is 50 - 20,000 mg/L according to DEAM with code TP0436. Later it goes to the desiccator for 20 minutes, and with the help of tweezers, it is weighed on the analytical balance, allowing us to calculate results using the following formula:

$$ST = \frac{(A-B)100}{V} \qquad (2)$$

Where:

ST: Total Solids, in mg/L

A: Final weight of the capsule with the dry residue, in grams.

B: Initial weight of the tared capsule in grams.

V: Volume of dried sample, in liters.

The total solids are the sum of the suspended, dissolved, and settleable solids present in the freshwater matrix, determined in a single procedure in the digester in the chemistry laboratory of the ESPOCH - Orellana site. In addition, the results were calculated using the TICS tool in Microsoft Excel, as it allows us to load and save the data easily. We used the basic formula mentioned above to calculate the total solids.

Check the control standard; if the analytical result falls outside the normal control limits, the filtration procedure, analysis, or the control analyte should be reviewed (IDEAM TP0436, page 7). IDEAM also

mentions that coarse floating particles and submerged agglomerates, materials that are not homogeneous or foreign to the rest of the sample, must be removed since they require prolonged drying, proper drying and rapid weighing.

Turbidity Measurement

Turbidity determination is based on an optical measurement that indicates the presence of suspended particles in a sample. It is done by emitting light through the sample and quantifying the concentration of suspended particles. The greater the amount of particles present, the greater the turbidity recorded.

Ensuring that the turbidimeter is clean and in optimal working condition is essential. It should be verified that the batteries are charged or that the equipment is connected to a suitable power source.

Before starting the measurements, it is necessary to calibrate the turbidimeter following the instructions provided by the manufacturer. This process establishes a known reference point using a standard turbidity solution with 0 and 10 NTU values. It is recommended to wash the cell used in the process with distilled water and repeat this rinse three times. Then, the blank value is measured in the 10 mL cell using distilled water. It is essential to repeat the washing process before filling it with the sample avoiding forming bubbles. The washing procedure with distilled water and repetition must be done for each sample analyzed.

It is essential to record the turbidity values obtained for each sample in a laboratory notebook or other recording medium. Subsequently, these data must be analyzed, and the turbidity levels about the established water quality standards must be interpreted. Esto permitió evaluar la calidad del agua de los principales ríos Loreto-Coca, en términos de turbiedad, obtiendoses las respectivas conclusiones sobre su estado de contaminación.

It is necessary to follow the specific instructions provided by the turbidimeter manufacturer, as the steps may vary slightly depending on the model and brand of equipment used.

RESULTS

This section discloses the derivations obtained from each analysis mentioned above, which are based on the APHA norm according to the standard methods with the 2017 edition, Ed 232130 B, Ed 23 4500 H+ B, Ed 23 2510 B, Ed 23 5220 D and Ed 232540 B.

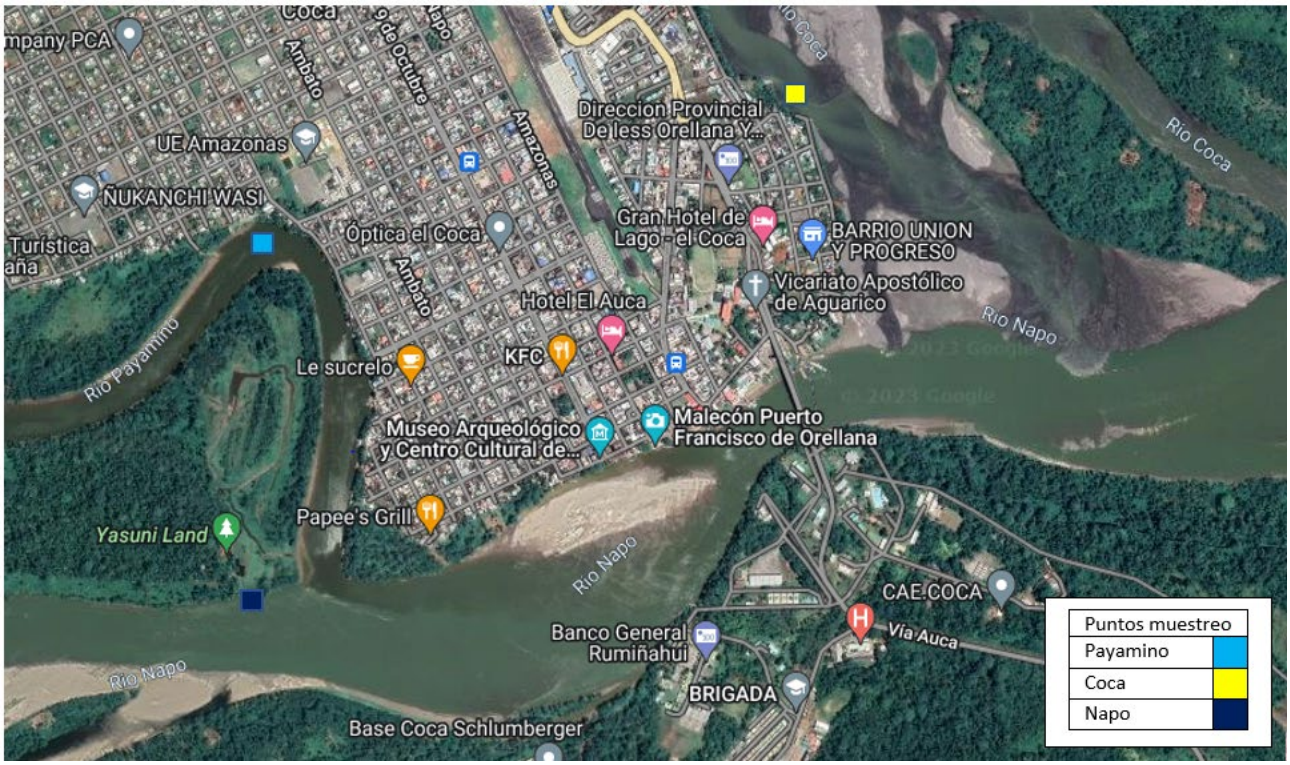

Figure 1. Geography of the surveyed area and sampling points (Google Maps).

				MATRIX			
ANALYSIS	**UNITS**	**TECHNIQUE**	**METHOD**	**COKE**	**NAPO**	**PAYAMINO**	**SUNO**
Conductivity	$\mu S/cm$	electrometry	Standard Methods 2017, Ed 23 2510 B	100.8	59	43	58
COD (Chemical Oxygen Demand)	mg/L	spectrophotometry A UV/Vis, HACH DR 1900	Standard Methods 2017, Ed 23 5220 D	---------- ----	8	fifteen	37
ST (Total Solids)	mg/L	gravimetry	Standard Methods 2017, Ed 23 2540 B	601.57	63.77	74.29	45.00
Duplicate (ST)				594.25	62.07	72.47	44.83
STD 500mg/L				492.81	492.81	492.81	492.81
Temperature	℃	electrometry	----------	22.2	23.8	24.4	23
turbidity	UNT	nephelometry	Standard Methods 2017, Ed 23 2130 B	92.9	1.94	4.48	2.46
pH	pH units	electrometry	Standard Methods 2017, Ed 23 4500 H+ B	6.85	6.81	6.88	6.87

Table 1. Results were obtained by measuring the physical-chemical parameters with the different matrices of the principal rivers of Orellana and Loreto.

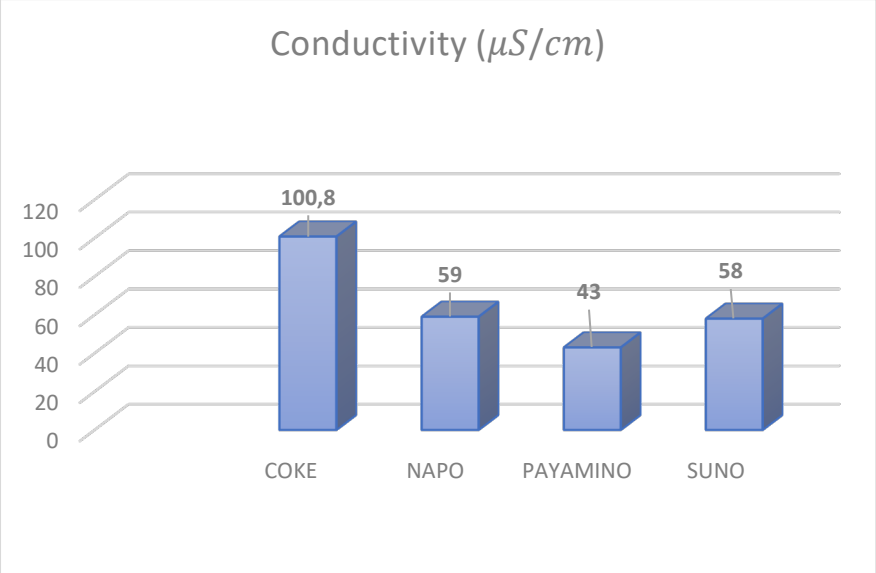

Figure 2. Conductivity results of the four water rivers.

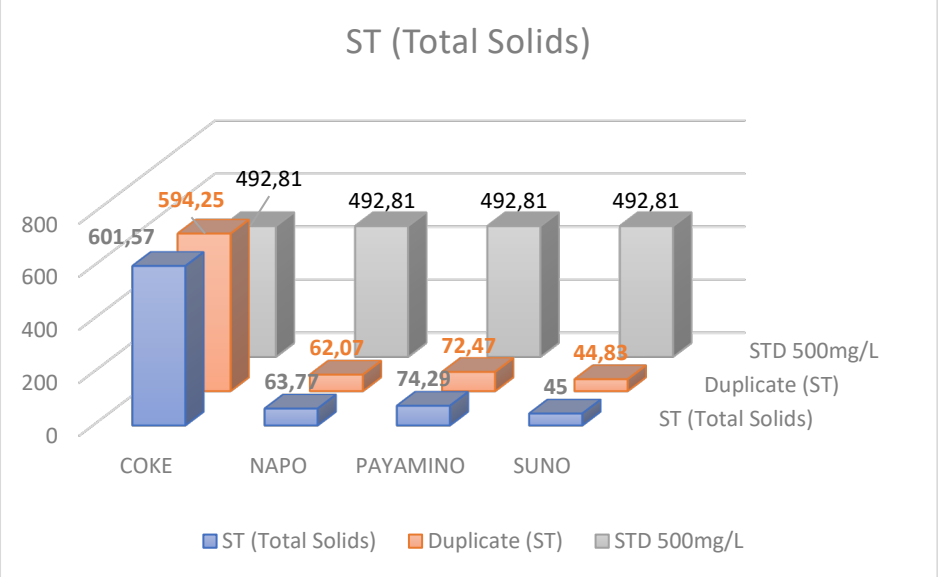

Figure 3. Total solids results.

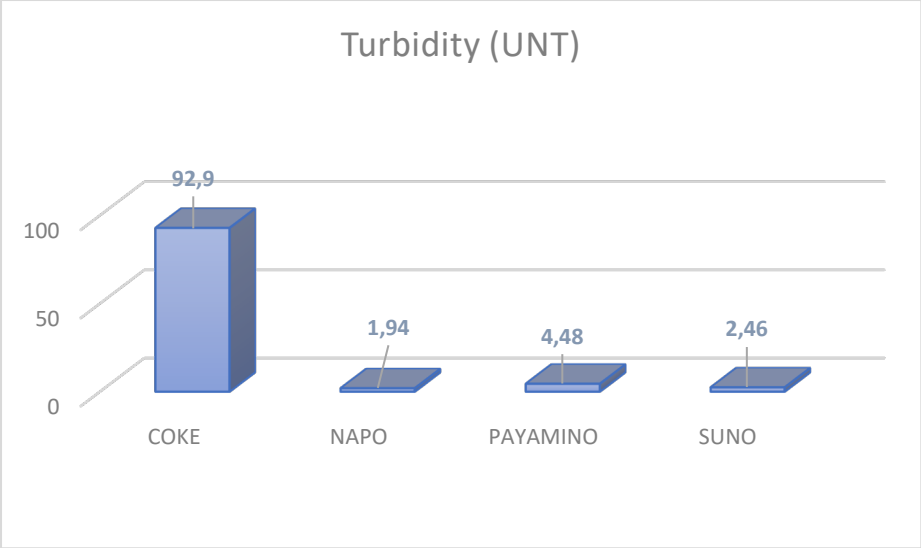

Figure 4. Turbidity results.

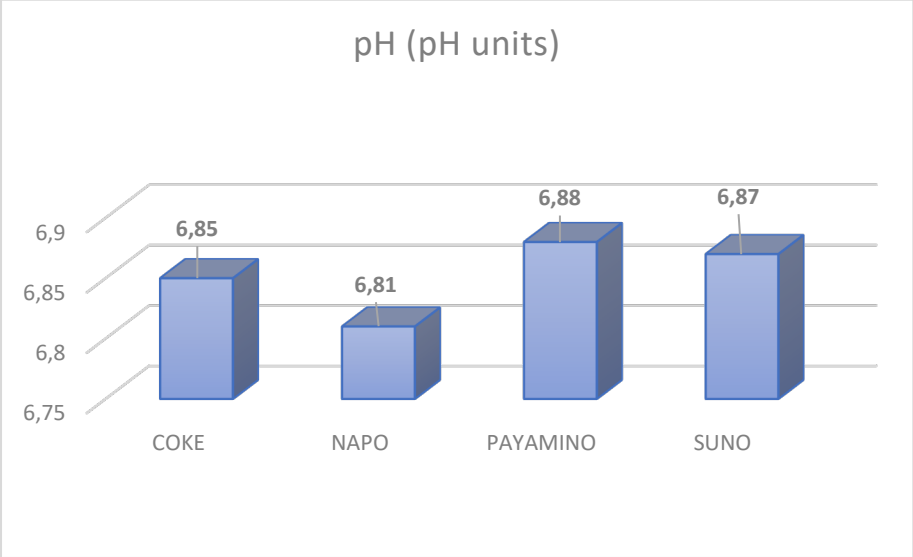

Figure 5. pH results.

ANALYSIS	UNITS	PERMISSIBLE LIMITS
Conductivity	$\mu S/cm$	----------
COD (Chemical Oxygen Demand)	mg/L	40
ST (Total Solids)	mg/L	max increase of 10% of the natural condition
Duplicate (ST)		
STD 500mg/L		
Temperature	℃	Natural conditions + 3
turbidity	UNT	5
pH	pH units	6, 5 - 9

Table 2. According to ANNEX 1 OF BOOK VI of TULSMA, there are permissible limits for quality control of river waters.

Within the framework of the present investigation, the analysis of physicochemical parameters was carried out. This was done in water samples from the rivers analyzed. Parameters evaluated included pH, temperature, COD, electrical conductivity, turbidity, and STD.

The results revealed that the pH of the water of the analyzed rivers varied between 6.81 and 6.88, indicating a slightly acid range. The recorded temperatures oscillated between 22°C and 24°C, reflecting conditions typical of the region's rivers during the sampling season. Regarding COD, values ranging between 8 and 37 mg/L were found, indicating adequate levels for the maintenance of aquatic life. The electrical conductivity ranged from 43 to 100 µS/cm, demonstrating a high presence of dissolved substances in the rivers analyzed. Regarding turbidity, values ranging between 1 and 92 NTU were observed, indicating that the Coca The river is outside the established ranges, compared with the other rivers analyzed, which are within the established ranges.

In general, the results obtained suggest that the water of the Payamino and Suno rivers presents physical-chemical characteristics within the ranges considered adequate for the maintenance of aquatic ecosystems and the supply of drinking water. However, the Coca and Napo rivers present analyses outside the permissible ranges; continuous monitoring and a more exhaustive evaluation are recommended to ensure the maintenance of water quality in the long term and detect possible changes or environmental impacts.

DISCUSSION

The Physicochemical results obtained cannot vary in comparison to the matrix with the duplicate. If the analytical result falls outside the standard control limits, the filtration procedure, analysis, or the control analyte should be reviewed. An important factor may be removing coarse floating particles and submerged agglomerates of materials that are not homogeneous or foreign to the rest of the sample.

Once the results without variations have been obtained, we can compare the quality obtained from the samples, with domestic uses, irrigation, recreational purposes and livestock use, with the standards established in Annexo I of book VI TULSAM "ENVIRONMENTAL QUALITY STANDARD AND DISCHARGE OF EFFLUENTS: WATER RESOURCE.

The results revealed variations in the electrical conductivity values, ranging between 43 µS/cm and 100.8 µS/cm. These findings show the presence of dissolved substances in the rivers analyzed, with the Coca River having the highest conductivity. These results point to the influence of minerals or other substances in the water, which could require further evaluation of its quality and origin.

The Chemical Oxygen Demand (COD) values in the Napo, Payamino and Suno rivers ranged from 8 mg/L to 37 mg/L. All were below the established permissible limit of 40 mg/L. These results indicate an organic load within acceptable limits in the analyzed rivers, crucial for maintaining aquatic life.

The total solids (TS) analyses revealed values ranging between 45.00 mg/L and 601.57 mg/L. The Coca River had the highest value, with the following values. Although these results exceeded the Standard of 500 mg/L, they were within the permissible limit, allowing an increase of up to 10% of the natural condition. Therefore, it is considered that the values obtained are within the acceptable limits regarding the presence of dissolved solids in the rivers analyzed.

The temperature measurements registered values that reflected the environmental conditions typical of the region during the sampling season, ranging between 22.2°Cand 24.4°C. These results indicate that the selected rivers present temperatures within the adequate limits for maintaining aquatic ecosystems.

Regarding turbidity, the values obtained varied between 1.94 and 92.9 UNT. These results indicate the presence of suspended particles in the water. The Coca River was the one with the highest turbidity. Although all the rivers analyzed remained within the permissible limit of 5 UNT, except the Coca River, the latter showed a higher load of sediments or suspended particles.

The pH of all the rivers analyzed showed slightly acid values, with results that oscillated around 6.81 pH units. This condition may have implications for certain aquatic species and highlights the importance of monitoring and regulating acidity levels in the water.

CONCLUSIONS

The results indicate that the Payamino and Suno rivers present physicochemical parameters within the ranges considered adequate for maintaining aquatic ecosystems and the drinking water supply. However, the Coca and Napo rivers show values outside the permissible ranges in some parameters analyzed. Therefore, continuous monitoring and thorough evaluation are recommended to ensure long-term water quality maintenance and to detect possible environmental changes or impacts. These conclusions support the need to implement appropriate management measures to preserve water quality in the analyzed rivers and ensure the sustainability of aquatic ecosystems.

For future researchers interested in determining the contamination of the main Loreto-Coca rivers through physicochemical parameters, a careful selection of parameters, establishment of strategic sampling points, adequate collection and preservation of samples, rigorous statistical analysis of the data and a contextualized interpretation of the results.

REFERENCES

1. Alcantara, M. G. The definition of health of the World Health Organization and interdisciplinarity. sapiens. University Research Journal. 2016, 93-107.
2. Gonzalez-Alonso, S. & Esteban-Hernandez J. Water contamination in sources near Bolivian oil fields. Panama Public Health Magazine. 2010, 235–43.
3. Silva, T.T., Santo K.S., Matsumoto, S.T. & Ribeiro, J. Monitoring of the water quality of the foz of Santa Maria da Vitória river and the Vitória Bayes, by systematic studies of physical-chemical and biological parameters. 2018, 1373-1392.
4. Baque-Mite, R., Simba-Ochoa, L., González-Osorio, B., Suatunce, P., Diaz-Ocampo, E. & Cadme-Arevalo, L. Quality of water intended for human consumption in a canton of Ecuador. Unemi Science Magazine. 2016, 109-117.
5. Morales, J. & Barroso, J. Construction of knowledge about the use, consumption and contamination of water. Conceptions of first-year high school students. 2012, 15.
6. Loayza, J. L. NarrativesTransmedia to raise awareness about the mining contamination of rivers in Ecuador: A review for environmental awareness.Visual Review International Visual Culture Review. 2022, 1–8.
7. Pabón, S. E., Benítez, R., Sarria, R. A., & Gallo, J. A. Water contamination by heavy metals, analysis methods and removal technologies. Between Science and Engineering. 2021, 1909.
8. Silva, R. F., Santos, J. V. & Pires, C. K. Analysisof the physical-chemical parameters of groundwater in the Enseada das Gaivotas neighborhood. 2021, 99-110.
9. April, J. & Weapons-Chugcho P. A. Water quality of the Puyo river and tributaries, Pastaza, Ecuador. Technology and water sciences. 2021, 379-417.

10. Jacoboski B. K. & Fachinetto, J. Quality water assessment of the Matadouro Stream, Ijuí, Rio Grande do Sul, by physicochemical parameters and the Allium cepa test. Eng Sanit Ambient. 2022, 489-497.
11. Sousa, A.M., Nunes, C. R., Santos L. F. & Araújo T.M. Multivariate Statistical Analysis Of Physico-chemical And Microbiological Parameters And Calculation Of The Water Quality Index Of "Lagoa De Cima". Geosciences. 2022, 689-702.
12. Castillo, Y. M., Fontalvo, J. A. & Borja, I. M. Bacteriological quality of the water of the manaure and casacara rivers, department of Cesar, Colombia. 2018, 46.
13. Prat, N., & Munne, A. Biomonitoring of water quality in Iberian rivers: Learned lessons.limnetics. 2014, 3.3
14. Sierra, J., Jaime, A. & Mora, A. Monitoring of physicochemical parameters in the upper basinof the Bogota river. New Granada Science and Engineering. 2002, 23-30.
15. Gutierrez-Fonseca, P. E. & Ramirez, A. Ecological evaluation of streams in Puerto Rico: Major threats and evaluation tools. Hydrobiology. 2016, 433-441.
16. Mora, A., Jumbo-Flores, D., Gonzalez-Merizalde, M. & Bermeo-Flores, S. A. Heavy metal levels in sediments from the Puyango river basin, Ecuador. Rev Int Contam Ambient. 2016, 385-397.
17. APHA, AWWA & WPCF. Standardized methods for the analysis of drinking and wastewater. (APHA,1992).
18. Caho-Rodriguez, C. & Lopez-Barrera, E. A. Determination of the Water Quality Index for the western sector of the Torca-Guaymaral wetland using the UWQI and CWQI methodologies. 2017, 35-49.
19. Tomas, P., & Moreno, J. L. Assessment of the ecological status of rivers of the Ebro Basin using the trophic macrophyte index IVAM-G (Macroscopic Aquatic Vegetation Index). 2016, 219-233.
20. Morell-Bayard, A.D., Bergues-Garrido, P. S. & Portuondo, F.. Assessment of the physicochemical parameters of the waters of the San Juan River in the wet and dry periods of 2014. 2015, 1-12.
21. Garzon, J. M., Rodríguez-Miranda, J. P. & Hernández-Gómez, C. Contribution of bioremediation to solve pollution problems and its relationship with sustainable development. 2017, 309-318.
22. Delgadillo, A. E., & Gonzalez, C. A. Phytoremediation: an alternative to eliminate contamination. 2011, 597-612.
23. Acosta, R., Rios, B., Rieradevall, M. & Prat N. Proposal for an evaluation protocol of the ecological quality of Andean rivers (CERA) and its use in two basins in Ecuador and Peru. 2009, 35-64.
24. Moreno, J. L., Navarro, C. & Heras, J. Generic index of aquatic vegetation (IVAM) for a rapid assessment of ecological quality of Spanish rivers: Taxonomic resolution and application to Castilla-La Mancha region. 2005, 48-53.
25. Meneses-Campo, Y., Castro-Rebolledo, M. I. & Jaramillo, A. M.. Comparison of water quality between two andean rivers by using the BMWP/COL. and ABI. 2019, 299-310.
26. Prat, N., & Munne, A. Biomonitoring of water quality in Iberian rivers: Learned lessons. Limnetica. 2014, 47-64.
27. Castillo, Y. M., Fontalvo, J. A. & Borja, I. M. Bacteriological quality of the water of the manaure and casacara rivers, department of Cesar, Colombia. 2018, 46.
28. Mendoza, Y. I., Perez, J. & Galindo, A. A. Evaluation of the contribution of the aquatic plants Pistia stratiotes and Eichhornia crassipes in the treatment of municipal wastewater. Technological information , 2018, 205-214.
29. Bres, P., Crespo, D., Rizzo, P., & Rossa, R. Ability of the macrophytes Lemna minor and Eichhornia crassipes to remove RIA nckel. Agricultural Research Journal. 2012, 153-157.
30. Mayz-Figueroa, J. & Manzi, L. Hydrocarbonlastic bacteria of the genus Pseudomonas in the rhizosphere of Samanea saman (Jacq.) 2017, 29-37.

31. Ferrera-Cerrato, R. Bioremediation processes for soil and water contaminated by petroleum hydrocarbons and other organic compounds. 2006, 179-187.

Received: 9 October 2023/ **Accepte**d: 15 January 2024 / **Published:**15 February 2024

Citation. Allauca P J, Lopez P C, Daza J, Chamba J. Description of the primary Loreto-coca river contamination through the measurement of physicochemical parameters. Revis Bionatura 2024; 9 (1) 7. http://dx.doi.org/10.21931/RB/2024.09.01.7

Additional information Correspondence should be addressed to *j.luis_2010@yahoo.es* / *josel.allauca@espoch.edu.ec*
Peer review information. Bionatura thanks anonymous reviewer(s) for their contribution to the peer review of this work using https://reviewerlocator.webofscience.com/

Bionatura ISSN. First 13909355 Ecuador. **Scopus coverage years**: from 2016 to the Present

Bionatura
Ibero-American Journal of Biotechnology and Life Sciences

Article

Detection of arsenic and lead ions in water through validation of the electrothermal atomic absorption method

*Tannia Vargas-Tierras [1], Vanessa Morales-León [2], Sharon Andi-Barrera [3], Rubén Toapanta-Topón [3], María Morales-León [4], Lissette Segovia-Tello [5], Viviana Lara-Villegas [6] **

[1] Research Group YASUNI-SDC, Sede Orellana, (Escuela Superior Politécnica de Chimborazo / El Coca 220001 / Ecuador); tannia.vargas@espoch.edu.ec;
[2] Research Group GIMA, Facultad de Recursos Naturales, (Escuela Superior Politécnica de Chimborazo / Riobamba 060106 / Ecuador); vanessa.moralesl@espoch.edu.ec;
[3] Tesista: Escuela Superior Politécnica de Chimborazo, Sede Orellana; sharo-nandi1999@gmail.com; https://orcid.org/0009-0003-8773-409X
[3] Tesista: Escuela Superior Politécnica de Chimborazo, Sede Orellana; rjtoapanta.28@gmail.com;
[4] Investigador independiente; m.augustamorales@gmail.com;
[5] Investigador independiente; lissegoviatello@hotmail.com;
[6] Investigador independiente; vivispaty2626@hotmail.com;
**Correspondence: tannia.vargas@espoch.edu.ec; +593 992708639.*

Available from. http://dx.doi.org/10.21931/RB/2024.09.01.8

ABSTRACT

The validation of the electrothermal spectrometry method for Arsenic and lead determination in water samples guarantees the quality of analytical data. The study was carried out at AQLAB. A theoretical and technical investigation was applied to ensure the reliability and accuracy of the analytical method. Parameters such as INEN standards, Eurachem international standards, AQLAB internal documents and environmental standards were used to validate the process. Several readings were performed on different samples to make calibration curves for As and Pb, evaluate the method's linearity, and obtain information on the slope, intercept and determination coefficient. Statistical calculations were used to determine the limit of detection and quantification, repeatability, reproducibility, trueness and uncertainty. The results show that the hypotheses were fulfilled, calibration curves with determination coefficient higher than 0.995, repeatability standard deviation lower than 16%, calculated F < critical F (4.96), calculated t student < theoretical (2.23), trueness was between 100.29-110.18 and 99.64-107.92%, uncertainty was 20% range 0.005 to 0.10 mg/L and 15% range 0.01-0.20mg/L, limit of detection was 0.001 and 0.005 mg/L and limit of quantification was 0.01 and 0.02mg/L, respectively. Therefore, the validation method was robust and accurate.

Keywords: water samples, analytical data, reliable results, Arsenic, Lead, validation.

INTRODUCTION

Atomic absorption spectroscopy (AAS) is a technique based on the measurement of the amount of light absorbed by free atoms in the sample, allowing the precise identification and quantification of the elements present; it has gained tremendous popularity in analytical chemistry due to its high sensitivity and a relative absence of interferences in the determination of most metals and metalloids[1].

One spectroscopy method is electrothermal atomic absorption (EAA), an analytical technique determining the concentration of metallic elements in liquid samples[2]. Electrothermal atomization using a graphite tube furnace as an atomizer is a powerful and advantageous technique in atomic absorption spectroscopy because it allows analysis of refractory and trace analyte elements[3], uses smaller samples, and provides higher sensitivity, making it a preferred choice in many analyses[4].

The advantages of AAE are that it offers much lower detection levels (20 to 1000 times better) than conventional flame techniques, can analyze the sample without additional treatment and requires a minimum amount of sample to perform the analysis[1]. On the other hand, it has limitations such as greater susceptibility to interferences (precision of the results), longer analysis time and sensitivity to contamination [5,6].

For this reason, atomic spectrometry is an analytical technique that makes it possible to detect and quantify the presence of Lead and Arsenic in different samples, essential for understanding their impact on human health and the environment[5]. Lead poisoning is a significant public health problem, and continued research is crucial to comprehend its effects better and to develop effective strategies to prevent and control lead exposure[7].

Lead contamination in surface, ground and drinking water is a global problem that has become more evident and problematic in the last decade due to increased public awareness, stricter regulations, scientific research and concerns about human health and the environment[8]. Lead exposure is linked to a variety of health problems. It is especially alarming for children, as no safe blood lead level and severe cognitive health effects have been found, which can adversely affect children's mental development and academic performance[9]. The US Environmental Protection Agency (EPA) has established an action level for Lead in drinking water of 15 µg/L; this action level is not designed to measure health risks but as a potential point at which additional measures should be taken[7,8].

On the other hand, Arsenic is a ubiquitous element that, in some geographical regions, arsenic concentrations can be significantly high[10] and, in such situations, represents a severe risk to human health because it can present genotoxic and carcinogenic effects[11]. The World Health Organization (WHO) considered a limit of 10 µg/L for Arsenic as a guideline for drinking water, while the standard in Iran is 50 µg/L[12,13].

For this reason, validating the electrothermal atomic absorption spectrometry method is essential to characterize the presence and concentration of Lead and Arsenic in water, especially within the province of Orellana, so that adequate measures can be taken to address contamination, reduce health risks and protect the most affected populations.

MATERIALS AND METHODS

The study was conducted at the Environmental Analysis and Evaluation Laboratory "AQLAB," located at 0279263 latitude and 9948509 longitude (UTM coordinates) in the Francisco de Orellana canton, Orellana Province. The average temperature inside the laboratory is 25°C, and the relative humidity is 85%.

A rigorous process of theoretical and technical research was carried out to ensure the reliability and accuracy of the analytical method. The theoretical research involved the study of relevant bibliographic sources, such as national standards of the Ecuadorian Accreditation Service, according to INEN NTE ISO/IEC 17025:2018[14], international standards, such as Eurachem, provides guidelines for method validation[15] and internal laboratory documents"AQLAB"[16], PG-AQLAB-07 for method validation (Table 1), PG-AQLAB-06 for uncertainty calculation, ITU-AQLAB-10 instructions for the use of graphite furnace and the ITE-AQLAB-96 for determination of metals in water by graphite furnace. The standard INEN 1108 the ministerial agreement 097A to establish the theoretical basis for the experiment design and the analytical need. For the technical part, validation of the metals (Arsenic and Lead), the electrothermal atomic absorption spectrometric method was used (Perkin Elmer-800-EFQ-086) (Table 2), preliminary filtration, preliminary metal digestion and nitric acid digestion, using Standard Methods for the Examination of Water and Wastewater APHA 3113 B, 3030 B, 3030 D, 3030 E, respectively.

Parameters	Established objective
Selectivity / Specificity	Determination of interference, AAS method (spectral and instrumental).
Linearity/Response function	Five Pb and As calibration curves were performed with a linear regression analysis, with a coefficient of determination $r^2 \geq 0.995$.
Detection limit	As y Pb ≤ 5 ug/L (0.005 mg/L)
Quantification limit	As y Pb ≤ 10 ug/L (0.01 mg/L)
Precision	Horwitz concentration levels. For a concentration of 10 ug/L, CV repeatability (16%) and reproducibility (21.3%). For a concentration of 100 ug/L, CV repeatability (11.3%) and reproducibility (15.1%).
Accuracy	With at least 85 to 115% at all levels.
Uncertainty	U ≤ 30% at all levels, 95.45% confidence interval.
Working Interval	As: 10 - 200 ug/L (0.01-0.2 mg/L) y Pb: 5 - 100 ug/L (0.005-0.1 mg/L)

Fuente: AQLAB[16].

Table 1. Parameters for evaluating methods for As y Pb con PG-AQLAB-06 y 07.

Element	Phases	Temperature (°C)	Ramp time (s)	Heating time (s)	Internal flow (ml/min)	Wavelength onda (λ)
Arsenic (As)	Heating	80	10	10	250	193.7
	Data	130	10	10	250	
	Incineration/ Pyrolysis	450	10	15	250	
	Atomization	2000	0	3	0	
	Cleaning	2100	1	3	250	
Lead (Pb)	Heating	80	10	10	250	287.3
	Data	130	10	10	250	
	Incineration/ Pyrolysis	400	10	15	250	
	Atomization	1900	0	3	0	
	Cleaning	2000	1	3	250	

Fuente: AQLAB[16].

Table 2. Optimal temperature and ramp time parameters for determining As y Pb con Perkin Elmer-800-EFQ-086.

The reagents used were As stock standard: 1 000 000 ug/L arsenic solution, Pb stock standard: 1 000 000 ug/L lead solution, inert gas: high purity argon ≥ 98%, distilled water: type I conductivity less than 2 uS/cm and pH 7.00, nitric acid: HNO_3 grade HPLC, HNO_3 2% solution: 2.9 of 70% concentrated HNO_3 was dissolved in 1 liter, As and Pb working standard: prepared from the respective stock standard of each metal. 0.125 mL of the stock solution was diluted in a 250 mL volumetric ball with 2% HNO_3 solution; the concentration of this solution was 500 ug/L. These standards and prepared solutions are crucial for accurate and reliable measurements of Arsenic and lead in water samples by electrothermal atomic absorption spectrometry.

Water samples for the determination of the presence of Arsenic (As) and Lead (Pb) were taken from the drinking water network (ACH) at the AQLAB Laboratory, the wastewater treatment plant (A.NYG) of the Autonomous Decentralized Municipal Government of Francisco de Orellana (GADMFO), and natural water (A.NAT) from the Payamino River. Fortified samples were also used (water sample + known concentration of the analyte): ACH + 10 ug/L solution of As or Pb, A.NAT + 20 ug/L As solution, A.NYG + 30 ug/L As solution, A. NAT + 30 ug/L Pb solution, A.NYG + 100 ug/L Pb solution. Control standard - STD CNTRL 25 ug/L As and 5 ug/L Pb, working standard-STD 200 ug/L As; reference material-MR-28 (121 ug/L ± 2 arsenic and 1 079 ± 10 ug/L lead). The methodology of technical standard INEN 2226: 2013 was followed13 for collecting water samples.

Standards were prepared according to ITE-AQLAB-96. Starting with the 1,000,000 ug/L standard for As and Pb, a working standard of 500 ug/L was organized, then a standard of 50 ug/L was prepared. Subsequently, the atomic absorption spectrophotometer was configured to schedule 4 more standards automatically with concentrations of 5, 10, 20, and 40 ug/L from the last standard prepared (50 ug/L).

For the readings of ACH, A.NYG, A.NAT, fortified samples, STD CNTRL, MR-28 and working STD. 2 analysts performed data, and 6 data were taken with a maximum of 6 levels.

Five readings (5 days) of the four concentration levels established in the working interval were taken, and statistical analysis was performed. To analyze the response function and linearity, the calibration curve standards (5, 10, 20 and 40 ug/L) were prepared, then the absorbance data of the different concentrations were recorded. Finally, the linear estimation of the slope (m), intercept (b), "y" type error (Sxy), "x" type error (Sxx), standard deviations of the slope (Sm) and intercept (Sb) and the confidence inter-values of the curves was performed.

The limits of detection and quantification were calculated with equations 10 and 11 (Table 3). For repeatability analysis, the readings of the fortified samples, control standards and reference material were used, and the average ($\bar{x}$), standard deviation (s^2) and coefficient of variation (CV%) were calculated by applying equation 14 (Table 3). For the determination of trueness, the fortified samples were used, obtaining from them the percentage recovery (%R) by applying equation 12 (Table 3); here, the value of the reading, standard addition value and multiplied by 100 was added. Subsequently, the $\bar{x}$ of recovery of the total of the readings performed by the 2 analysts was determined. For the calculation of reproducibility, the data of the fortified samples per analyst were used and $\bar{x}$ and variances (VAR) were selected. The t-calculated (t-c) was determined with equation 15 (Table 3) and was performed with the value of the t-theoretical (t-t) with 0.05 probability and 10 degrees of freedom and finally with the results the condition that t-calculated < t-theoretical was checked.

To determine the precision, the sums and quadratic differences were calculated, then with these results, the standard deviation of repeatability (Sr) was estimated with equation 16, intermediate precision (SL^2) with equation 17, and the standard deviation of reproducibility (SR) with equation 18. Then, repeatability limits (Lr) and reproducibility (LR) were calculated with equations 19 and 20, respectively. Finally, a comparison was made between the calculated Fisher's value (calculated F) equation 21 and the result of the analysis of variance (ANOVA) to observe similarity and to be able to continue validating the methods. The uncertainty calculations of the response function, trueness, volumetric material, mother standard, working standards and equipment calibration were performed with equations 22 to 35.

Formula	Description
$\boldsymbol{LOD = 3 * Sb'}$ **(10)**	$\bar{x}$: Average of measurements taken. Sb': Corrected standard deviation.
$\boldsymbol{LOC = 10 * Sb'}$ **(11)**	$\bar{x}$: Average of measurements taken. Sb': Corrected standard deviation.
$\boldsymbol{\%R = \frac{Value\ of\ reading}{Value\ addition} * 100}$ **(12)**	-
$\boldsymbol{CV(\%) = \frac{s^2}{\bar{X}} * 100}$ **(14)**	-
$\boldsymbol{Calculated\ T = \frac{(X1 - X2) - 0}{\sqrt{\frac{(n1-1)*V1 + (n2-1)*V2}{(n1+n2)-2}\left[\frac{1}{n1} + \frac{1}{n2}\right]}}}$ **(15)**	X1 y X2: Average of samples 1 y 2. n1 y n2: size of samples1 y 2. V1 y V2: sample unbiased variances.
$\boldsymbol{Sr = \sqrt{DCMw}}$ **(16)** $\boldsymbol{SL^2 = \frac{DCMb - DCMw}{n}}$ **(17)** $\boldsymbol{SR = \sqrt{Sr^2 + SL^2}}$ **(18)**	DCMw: Root mean square differences in within-group variance DCMb: Mean squared differences in variance between groups n: Number of readings
$\boldsymbol{Lr = (2,82 * Sr) * 100/\bar{X}level}$ **(19)**	$\bar{X}$ level: Average of analyst averages.
$\boldsymbol{R = (2,82 * SR) * 100/\bar{X}level}$ **(20)**	$\bar{X}$level: Average of analyst averages.
$\boldsymbol{Fcalculado = \frac{DCMb}{DCMw}}$ **(21)**	-
$\boldsymbol{Ucombined = \sqrt{Type\ A\ contributions + Type\ B\ contributions}}$ **(22)**	-

$$Uexpanded = Ucombined * k \quad (23)$$	-
$$u_{relative} = \frac{u_{(V)}}{V_f} \quad (24)$$	V*f:* volumen del material volumétrico uv: Incertidumbre del volumen
$$uFR = Sxy\ /m\sqrt{(1/p"" + 1/n" + "(C_0 - \overline{C})^2/\ Sxx"")} \quad (25)$$	uFR: Linearity uncertainty Sxy: Residual standard deviation m: Slope p: number of equipment readings to determine Co n: number of measurements for calibration. Co: curve value corresponding to the level. $\overline{C}$: mean value of different calibration standards. Sxx: residual sum.
$$(26)\quad uFR_{relative} = \frac{uFR}{\bar{x}STDcurve}$$	uFR: Uncertainty response function. $\bar{x}$STDDcurve: Standard average.
$$(27)\ uRec = (s^2/100)\sqrt{n}$$	uRec: Recovery uncertainty. s^2: Standard deviation n: Total number of analyst readings per level.
$$(28)\ uRec.relative = \frac{uRec}{\bar{x}\ recuperation}$$	$\bar{x}$ recovery: average percentage recovery.
$$(29)\ u(vf) = \sqrt{(u(cal))^2 + (u(v))^2 + (u(repet))^2}$$	u(vf): Volumetric material uncertainty. u(cal): Calibration uncertainty. u(v): Temperature uncertainty. u(repet): Repeatability uncertainty.
$$(30)\ u(cal) = \frac{u(vcal)}{k}$$	u(cal): calibration certificate. k: k factor coverage (generally k=2, 95% confidence level).
$$(31)\ u(v) = \frac{(Dif\ T)*Vf*\alpha}{\sqrt{3}}$$	u(v): Uncertainty of the temperature difference of the volumetric material. Vf: Volumetric material volume. Dif T: Temperature range 20 - 30°C: 10 α: Coefficient of expansion of borosilica glass (0.00025).
$$(32)\ u_{STDmother} = \frac{uMR}{k}$$	uSTD mother: Mother standard uncertainty. uMR: Calibration certificate. k: coverage factor (usually k=2, 95% confidence level).
$$uSTD = \sqrt{(u_{STD\ mother})^2 + (u_{Pipette})^2 + (u_{Matraz})^2} \quad (33)$$	uSTDmother: mother standard relative uncertainty. uPipette: Relative uncertainty of the pipette. uFlask: Relative uncertainty of the flask.
$$u_{equipo} = \sqrt{(uFR)^2 + (uSTD)^2 + (uResol)^2} \quad (34)$$	uSTD: Uncertainty standard preparation. u(FR): Response Function Uncertainty. u(Resol): Instrument resolution uncertainty.

$\boldsymbol{uResol = \frac{resolution\ \ del\ equipment}{\sqrt{12}}}$ **(35)**	u(resol): Resolution uncertainty.

Fuente: AQLAB[16].

Table 3. Equations for statistical analysis.

RESULTS

The validation of methods for the determination of heavy metals is fundamental because it allows us to obtain accurate results that serve to take corrective measures in the short, medium and long term. For the validation of the method for Arsenic in water, six readings were performed per analyst, using different concentrations of standards for water samples and reference material, resulting in a total of six concentration levels (Table 4).

Level	1	2	3	4	5	6
Conc.	**0,01**	**2**	**2,5**	**3**	**121**	**20**
Samples	**ACH + 10,00 ug/L**	**A.NAT +20,00 ug/L**	**STD CNTRL 25,00 ug/L**	**A.NYG +30,00 ug/L**	**MR-28 ug/L**	**STD 200 ug/L**
Dilution	**1**	**1**	**1**	**1**	**5**	**10**
Analyst 1	12.75	27.48	29.53	32.15	131.00	216.00
	11.66	25.45	28.47	30.10	137.25	195.70
	12.51	23.92	29.09	30.34	123.85	197.60
	13.11	26.47	25.71	30.17	139.85	197.80
	11.44	25.06	27.33	31.59	121.55	205.50
	12.75	26.02	28.57	28.22	141.95	209.80
Analyst 2	12.43	26.38	27.25	30.29	126.65	181.70
	11.72	26.45	30.37	33.60	141.85	200.00
	11.82	25.12	29.79	32.44	141.85	221.20
	11.45	26.80	27.29	32.70	135.75	195.50
	12.43	27.18	29.09	30.58	139.85	212.60
	12.58	24.38	27.76	30.23	137.5	219.30

Table 4. Initial data was used to validate the method for determining arsenic levels in water.

The results of the method validation for the determination of Arsenic show the five calibration curves in absorbance units for each of the concentrations from 5 to 40 ug/L. The coefficient of determination of 0.9983 represents the high correlation, therefore, the calibration curves are accepted (Figure 1).

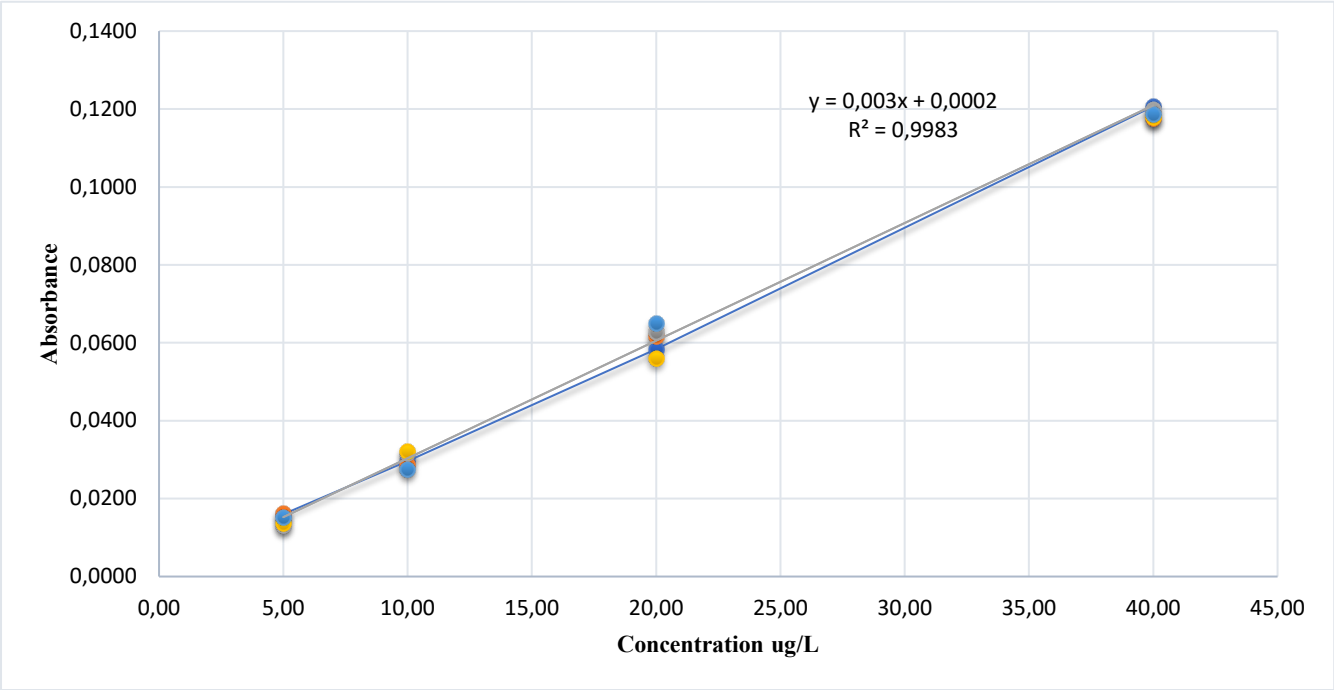

Figure 1. Linearity of the arsenic calibration curve.

Determining the maximum and minimum values of the five calibration curves allowed obtaining maximum values (0.00363 and 0.01532) and minimum values (0.00234 and -0.01464) as a control to control the curves during and after the process.

In the repeatability analysis (r) a CV of less than 7% was obtained in the six levels (ACH + 10.00 mg/L, A.NAT +20.00 ug/L STD CNTRL 25.00 ug/L, A.NYG +30.00 ug/L, MR-28 ug/L, STD 200 ug/L), analyst 1: 5.39, 4.76, 4.95, 4.94, 6.43 and 3.97 % and analyst 2: 3.87, 4.12, 4.70, 4.78, 4.17 and 7.50 %; these results are accepted because they comply with the validation objectives, being less than 16%. When performing the trueness analysis of the 12 readings, it was determined that the average maximum value was 113.42%, a value that is within the values established to accept the validation method. The reproducibility analysis (R) shows that the calculated t (0.90217, 0.48124, 0.60436, 0.60436, 0.60436, 1.11948 and 0.18649) was < t - theoretical (2.22814) in the six levels, therefore the validation of the method is accepted. The precision analyses at the six levels show that the calculated F (1.38792, 0.22927, 0.01784, 2.21193, 0.22004 and 0.37874) is < tabulated F (4.96460); therefore, the validation method is accepted. The values of response function uncertainty (u_{FR}) was 0.546, $u_{FR\ relative}$ (0.02910), u_{cal} (0.0028), $u_{(V)}$ (0.0721), $u_{relative}$ 50mL (0.0014), As 1 000 000 ug/L mother standard (0.0012), As mother standard relative U (0.000012), u_{std} 50 ug/L (0. 0014), u_{team} (0.02919), u_{resol} (0.000289) and in the six levels the values obtained in $u_{combined}$ (0.6772, 1.4560, 1.5984, 1.8366, 7.3397 and 12.3184) and u_{expa} (14, 15, 13, 12, 12, 12 and 12 %), these last values for being ≤ 30% the validation is accepted.

For the lead validation method, six readings were performed by each analyst with different concentrations of standards for water samples and reference material, resulting in a total of five concentration levels (Table 5).

Level	1	2	3	4	5
Conc.	5	10	30	100	1079
Samples	STD CNTRL 5,00 ug/L	ACH + 10,00 ug/L	A.NAT +30,00 ug/L	A.NYG +100,00 ug/L	MR-28 ug/L
Dilution	1	1	1	5	50
Analyst 1	4.75	11.20	29.90	103.00	1110
	5.38	10.40	29.60	103.50	1125
	5.15	11.90	29.20	100.50	1140
	5.38	10.90	29.80	106.00	1135
	5.34	10.20	30.00	103.00	1145
	5.27	11.30	29.90	99.00	1120
Analyst 2	5.12	10.40	29.10	105.50	1135
	5.84	11.30	29.90	110.00	1130
	5.17	10.30	30.70	104.00	1140
	5.39	10.50	30.60	106.00	1145
	5.15	10.60	29.20	99.50	1155
	5.77	10.50	30.80	99.50	1135

Table 5. Initial data was used to validate the method for determining Lead in water.

The validation of the method for determining Lead shows the five calibration curves in absorbance units for each concentration from 5 to 40 ug/L. The high correlation represented by the determination coefficient of 0.9999 indicates that the electrothermal atomic absorption spectrometry method is accurate and suitable for determining Lead in water for the range of concentrations evaluated (Figure 2).

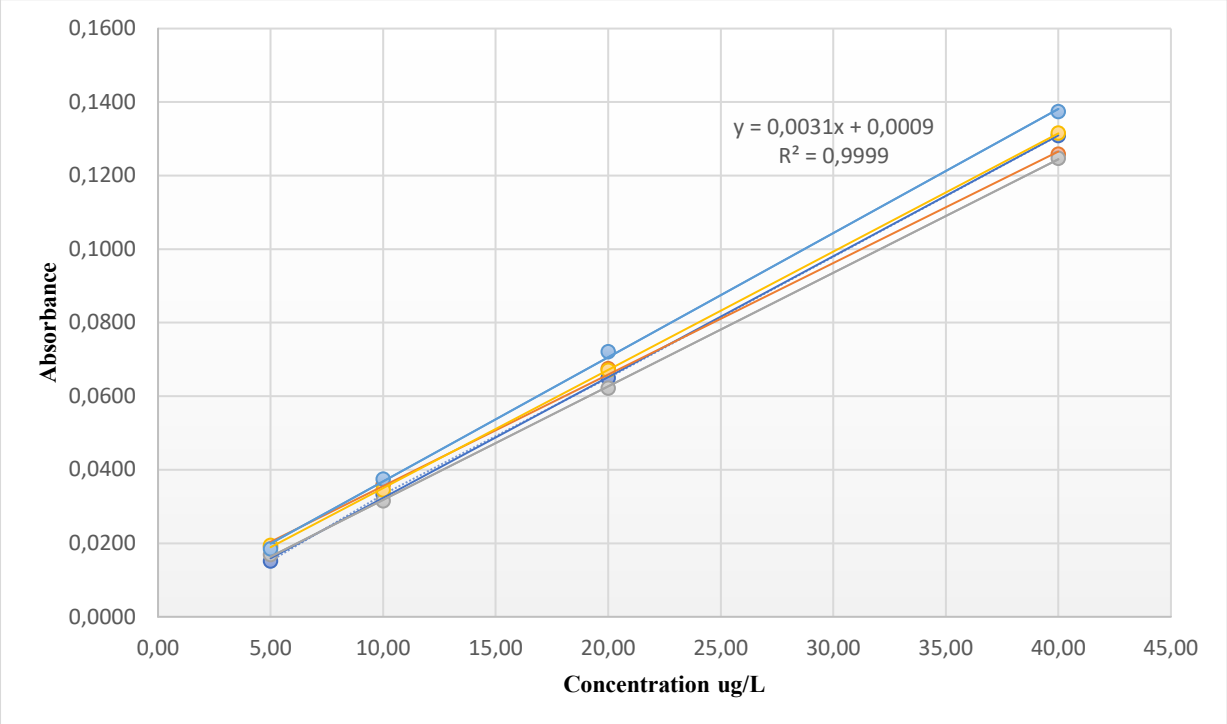

Figure 2. Linearity of the lead calibration curve.

Determining the maximum and minimum values of the five calibration curves allowed obtaining maximum values (0.00364 and 0.01109) and minimum values (0.00278 and -0.00370) as a control to control the curves during and after the process.

In the repeatability analysis (r) the CV was less than 6% at all five levels (STD CNTRL 5.00 ug/L ACH + 10.00 ug/L, A.NAT +30.00 ug/L, A.NYG +100.0 ug/L, MR-28 ug/L) (analyst 1: 4. 65, 5.68, 0.99, 2.39 and 1.17% and analyst 2: 5.99, 3.38, 2.55, 3.91 and 0.78 %); these results are accepted because they comply with the validation objectives, less than 16%. The trueness analysis of the 12 readings determined that the average maximum value was 107.92%, a value that is accepted in the validation. The reproducibility analysis (R) shows that the calculated t (1.18714, 1.31162, 0.94981, 0.82099 and 1.67286) was < t - theoretical (2.22814) in the five levels, therefore the validation of the method is accepted. The precision analyses at the five levels show that the calculated F (1.39521, 1.70316, 0.89312, 0.66728 and 2.77049) is < tabulated F (4.96460) therefore, the validation method is accepted. The values of the uncertainty of response function (u_{FR}) was 0.794, $u_{FR\ relative}$ (0.04235), u_{cal} (0.0042), $u_{(V)}$ of 250 ml (0.3608), $u_{relative}$ 250 ml (0.0014), U std mother lead (0.0012), mother standard relative U (0.000012); u_{std} (0.0014), u_{team} (0.08884), u_{resol} (0.000289) and in the five levels the values obtained in $u_{combined}$ (0.3677, 0.7145, 1,3789, 9.7710 and 12.8455), u_{expa} (15, 14, 9, 20 and 2 %) these last values for being ≤ 30% the validation is accepted.

DISCUSSION

It is evident that the research carried out in the "AQLAB" laboratory to validate the electrothermal atomic absorption spectrometry method for determining Arsenic and Lead in water was based on the review of literature and methodologies previously used by other researchers. Through these references, recommended practices were applied, and acceptable results were obtained to validate the method. Some critical aspects related to securing linearity, precision, trueness and uncertainty calculation are highlighted below:

Linearity: Obtaining linearity is essential to establish the relationship between the analyte concentration and the absorbance signal. In this case, standards prepared automatically by the equipment were used, which minimizes possible preparation errors by the analysts. The high correlation coefficients (r^2) of 0.998 for Arsenic and 0.999 for Lead indicate an excellent linear relationship between concentrations and absorbances, which supports the method's suitability. According to Perelonia[17], if the obtained R 2 value is higher than 0.995, the analytical response is linear in certain concentration ranges[13].

Analytical precision was calculated by evaluating the repeatability and reproducibility of the instrument response to the analyte. Repeatability refers to the precision under the same operating conditions (analysts and equipment) over a small time interval. Reproducibility expresses the accuracy of a method under different operational conditions. In addition, robustness was evaluated through reproducibility, as the technique was performed by different analysts[17]. The reproducibility analysis (R) shows that the calculated t (1.18714, 1.31162, 0.94981, 0.82099 and 1.67286) was < t - theoretical (2.22814) at all five levels, thus accepting the validation of the method. Y The precision analyses at the five levels show that the calculated F (1.39521, 1.70316, 0.89312, 0.66728 and 2.77049) is < tabulated F (4.96460), so the validation of the method is accepted. These values are below the values set by AOAC (2016)[18] where an appropriate maximum value should not exceed 15%. Therefore, it can be stated that the proposed method showed a good according to the values obtained.

Trueness: The trueness calculation is essential to evaluate the ability of the method to accurately recover the proper concentration of the analyte in the samples. Considering 6 fortified samples for validation and complying with the established acceptance ranges (85% to 115%) ensures that the method is accurate and provides results close to the actual values of Arsenic and Lead in the samples. These values are within those established within the AOAC 2015 method[19], where it is demonstrated that the recovery obtained during the validation of the method must be 100 ± 25%. Under this criterion, the elements analyzed showed a particularly good recovery[20].

Uncertainty: The research by Sanmiguel and Guerrero[21] provided the basis for calculating uncertainty using various statistical equations. These methodologies obtained uncertainty results within the acceptance range (u < 30%). This demonstrates that the "AQLAB" laboratory results are reliable and accurate, and a reasonable estimate of the uncertainty associated with the measurements is available.

CONCLUSIONS

The validation methods analyzed for the determination of metals (Lead and Arsenic) in water allowed the establishment that the ITE-AQLAB-96 method for the determination of Arsenic and lead in drinking, natural and wastewater with a range of 0.01 to 0.20 mg/L for As and 0.005 to 0.10 mg/L for Pb and an in-certainty of 15% As and 20% Pb.

Overall, the "AQLAB" laboratory work demonstrates a solid research and validation methodology for the electrothermal atomic absorption spectrometry method used to determine arsenic and lead levels in water. The results obtained and their comparison with the cited references support the quality and reliability of the data generated in the laboratory.

Author Contributions: Conceptualization, T.V-T., S.A-B., R.T-T.; methodology, TV-T., A.M-L S.A-B. and R.T-T.; statistical analysis, T.V.-T., S.A-B., R.T-T.; writing-original draft preparation, T.V.-T. V.M-L., writing-review and editing, T.V.-T., M.M-L, L.S-T. and V.L.-V. All authors have read and agreed to the published version of the manuscript.

Funding:

To the AQLAB Laboratory.

Institutional Review Board Statement:
Does not apply.

Informed Consent Statement:
Does not apply.

Data Availability Statement:

The data is contained in the article.

Acknowledgments:
Ing. Armando Meléndrez - Director of AQLAB, for allowing the students to conduct this study.

Conflicts of Interest:

The authors declare no conflict of interest.

REFERENCES

1. Hill SJ, Fisher AS. Atomic Absorption, Methods and Instrumentation. En: Lindon JC, Tranter GE, Koppenaal DW, editores. Encyclopedia of Spectroscopy and Spectrometry (Third Edition) [Internet]. Oxford: Academic Press; 2017 [citado 24 de julio de 2023]. p. 37-43. Disponible en: https://www.sciencedirect.com/science/article/pii/B9780128032244000996

2. Gallegos W, Vega M, Noriega P. Espectroscopía de absorción atómica con llama y su aplicación para la determinación de plomo y control de productos cosméticos. La Granja. 30 de junio de 2012;15(1):19.

3. Makarishcheva DD, Kolesnikova ON, Tregubova VE, Ustinnikova OB. Development of a Quantitative Determination Method for Aluminum Ions in Adsorbed Drugs Using Atomic Absorption Spectrometry with Electrothermal Atomization. Pharm Chem J. 2022;56(4):527-31.

4. Rada-Mendoza M del P, Villamiel-Guerra M del M, Hoyos-Saavedra OL, Alvira LF. Quantification of Lead using atomic absorption spectrometry in thermoformed and biodegradable flexible films made from cassava (Manihot esculenta crantz). DYNA. 2018;85(207):236-42.

5. Dias VMC, Cardoso ASB. The determination of Lead in sugar and sweets without digestion by electrothermal atomic absorption spectrometry (ETAAS) with a rhodium chemical modifier. Food Addit Contam. mayo de 2006;23(5):479-83.

6. Ohta K. Electrothermal atomic-absorption spectrometry of Arsenic and its application to environmental samples. Talanta. marzo de 1978;25(3):160-2.

7. Fawkes L, Sansom G. Preliminary Study of Lead-Contaminated Drinking Water in Public Parks—An Assessment of Equity and Exposure Risks in Two Texas Communities. Int J Environ Res Public Health. 14 de junio de 2021;18(12):6443.

8. Khaksar Fasaee MA, Pesantez J, Pieper KJ, Ling E, Benham B, Edwards M, et al. Developing early warning systems to predict water lead levels in tap water for private systems. Water Res. 1 de agosto de 2022;221:118787.

9. Lu W, Levin R, Schwartz J. Lead contamination of public drinking water and academic achievements among children in Massachusetts: a panel study. BMC Public Health. 15 de enero de 2022;22(1):107.

10. Aderibigbe AD, Stewart AG, Hursthouse AS. Seeking evidence of multidisciplinarity in environmental geochemistry and health: an analysis of Arsenic in drinking water research. Environ Geochem Health. 1 de febrero de 2018;40(1):395-413.

11. Stetson SJ, Lawrence C, Whitcomb S, Kanagy C. Determination of four arsenic species in environmental water samples by liquid chromatography- inductively coupled plasma - tandem mass spectrometry. MethodsX. 1 de enero de 2021;8:101183.

12. Alidadi H, Ramezani A, Davodi M, Peiravi R, Paydar M, Dolatabadi M, et al. Determination of Total Arsenic in Water Resources: A Case Study of Rivash in Kashmar City. Health Scope [Internet]. 2015 [citado 28 de julio de 2023];4(3). Disponible en: https://brieflands.com/articles/healthscope-20125.html#abstract

13. Komorowicz I, Barałkiewicz D. Determination of total Arsenic and arsenic species in drinking water, surface water, wastewater, and snow from Wielkopolska, Kujawy-Pomerania, and Lower Silesia provinces, Poland. Environ Monit Assess. 2016;188(9):504.

14. Servicio de Acreditación Ecuatoriano. Plan Institucional SAE – Servicio de Acreditación Ecuatoriano [Internet]. 2022 [citado 27 de julio de 2023]. Disponible en: https://www.acreditacion.gob.ec/plan-estrategico-institucional-sae/

15. Magnusson B, Örnemark U. Validacion Eurachem - Guía internacional de validación de métodos analíticos - Warning: TT: - Studocu [Internet]. 2014 [citado 27 de julio de 2023]. Disponible en: https://www.studocu.com/es-mx/document/universidad-de-celaya/quimica-analitica/validacion-eurachem-guia-internacional-de-validacion-de-metodos-analiticos/9164386

16. AQLAB. Blogs. 2020. Laboratorios de Análisis y Evaluación Ambiental. Disponible en: https://www.aqlabec.com/index.html

17. Perelonia KBS, Benitez KCD, Banicod RJS, Tadifa GC, Cambia FD, Montojo UM. Validation of an analytical method for the determination of cadmium, Lead and mercury in fish and fishery resources by graphite furnace and Cold Vapor Atomic Absorption Spectrometry. Food Control.2021;130:108363.

18. AOAC Official Method 2016.01: Heavy Metals in Food; AOAC: Arlington, USA, 2016.

19. AOAC Official Method 2015.01: Heavy Metals in Food; AOAC: Arlington, USA, 2015.

20. Garzón DA, Ahumada DA, Gamba JPA, Ágreda J, Castillo E. Quantification of Arsenic, Cadmium, Mercury and Lead in Pineapple: Method Development, Validation and Evaluation of In-House Reference Materials. J Braz Chem Soc.2020;31:1296-305.

21. Sanmiguel Torres JX, Guerrero Carrera SR. Validación del método para determinar Pb, Cd, Ni por espectrometría de absorción atómica de llama en agua y suelo. [Internet] [bachelorThesis]. Escuela Superior Politécnica de Chimborazo; 2017 [citado 28 de julio de 2023]. Disponible en: http://dspace.espoch.edu.ec/handle/123456789/7019

Received: 9 October 2023/ **Accepte**d: 15 January 2024 / **Published:**15 February 2024

Citation. Vargas-Tierras T, Morales-León V, Andi-Barrera S, Toapanta-Topón R, Morales-León M, Segovia-Tello L, Lara-Villegas V. Detection of arsenic and lead ions in water through validation of the electrothermal atomic absorption method. Revis Bionatura 2024; 9 (1) 8.
http://dx.doi.org/10.21931/RB/2024.09.01.8

Additional information Correspondence should be addressed to tannia.vargas@espoch.edu.ec
Peer review information. Bionatura thanks anonymous reviewer(s) for their contribution to the peer review of this work using https://reviewerlocator.webofscience.com/

Bionatura ISSN. First 13909355 Ecuador. **Scopus coverage years**: from 2016 to the Present

Bionatura
Ibero-American Journal of Biotechnology and Life Sciences

Article

Effect of Five Concentrations of Aqueous Extracts of *Pleurotus ostreatus* P. Kumm and *Tagetes minuta* L. on the Mortality of Two Nematodes in a Laboratory Setting.

Madison Chango[1], *Gabriela Rosero*[2,*], *Norma Erazo*[1,2], *Pablo Álvarez*[1,3]

[1] *Facultad de Recursos Naturales, Escuela Superior Politécnica de Chimborazo (ESPOCH) / Riobamba / Ecuador; madison.chango@espoch.edu.ec.*
[2] *Grupo de Investigación y Desarrollo para el Ambiente y el Cambio Climático GIDAC-ESPOCH / Riobamba / Chimborazo / Ecuador; nerazo@espoch.edu.ec.*
[3] *Grupo de Estudios Fitoentomológicos, Escuela Superior Politécnica de Chimborazo (ESPOCH) / Riobamba / Ecuador; pablo.alvarez@espoch.edu.ec.*
* *Correspondence: gabriela.rosero@espoch.edu.ec; Tel.: +593 999184660*
Available from. http://dx.doi.org/10.21931/RB/2024.09.01.9

ABSTRACT

The nematode attacks affect several plant species of Ecuadorian crops. There are fungi and plants with nematicide ability that have agricultural interest. This study assessed the effect of five concentrations of aqueous extracts of *Pleurotus ostreatus* and *Tagetes minuta* on the mortality of *Meloidogyne* spp. and *Panagrellus redivivus* nematodes in a laboratory setting. The aqueous extracts were obtained through hydro distillation where concentrations of 0%, 0.5%, 5%, 25%, 50% and 100% were prepared. A wholly randomized single-factor design was used for the *P. ostreatus* extract and a bifactorial for the *T. minuta* extract (leaves and flowers). The number of dead individuals was evaluated, and the efficacy and LC_{50} were determined. *T. minuta* leaf extract showcased higher nematicide activity against *P. redivivus* with an LC_{50} of 8.03 ppm; when applied to *Meloidogyne* sp., the extract showed nematicide activity with an LC_{50} of 0.01 ppm. For *P. ostreatus* extract, the greatest nematicide activity against *P. redivivus* was an LC_{50} of 1.22 ppm and nematicide activity against *Meloidogyne* sp., was an LC_{50} of 0.01 ppm. The aqueous extract of *T. minuta* flowers showed low nematicide activity and the aqueous extract of *T. minuta* leaf showed the best nematicide activity.

Keywords: nematicide; *Tagetes minuta*; *Pleurotus ostreatus*; *Panagrellus redivivus*; *Meloidogyne* sp.

INTRODUCTION

Nematodes are one of the phytopathogens that cause significant losses in global agricultural production, with estimated losses of up to one hundred billion dollars annually[1]. This group of phytoparasites is characterized by its diversity, complexity, and wide distribution across all productive agroecosystems worldwide[2]. These qualities and peculiarities enable them to induce other diseases[3], potentially causing annual losses between 11 and 14%, or even higher if another pathogen is introduced[4].

Ecuador has not been exempt from nematode attacks; reports from Ecuadorian fields indicate the presence of: *Meloidogyne incognita*, *Meloidogyne javanica*, *Meloidogyne arenaria*, *Meloidogyne hapla*, *Meloidogyne graminicola*, *Rotylenchulus reniformis*, and *Nacobbus aberrans*[5]. These nematodes affect plant species that are part of the daily diet of every Ecuadorian, as well as those destined for export, such as watermelon, melon, cucumber, sugarcane, corn, tomato, onion, pineapple, papaya, passion fruit, rice, summer flowers, etc.

Given this situation, one nematode control alternative has been synthetic chemical nematicides such as carbamates and organophosphates. However, these have shown alarming side effects, high toxicity, residue

persistence, and development of resistance[6]. Therefore, for several years now, there has been a search for more benign control methods for the environment and humans [7].

Various research projects are currently being conducted for the biological control of different phytopathogens[1,4,8]. One of these alternatives is the use of plant extracts[9,10,11], which are characterized by their biological origin, biodegradability, and minimal negative impact on human health and the environment. These extracts have shown the ability to act through their metabolites and exhibit nematicidal[12,13,14], insecticidal, acaricidal, or herbicidal activity. In this research, we worked with aqueous extracts of *Tagetes minuta* and *Pleurotus ostreatus*.

One of the extracts that have shown promising results as nematicide is garlic bulbil extract, which reduced galling index by 73%, egg and juvenile production by 80%, and female population by 94%[15]. A reality close to our area regarding integrating a biological control alternative has been the use of the Tagetes genus, which has pesticide characteristics related to its allelopathic function[13].

Pleurotus ostreatus is a fungus native to China but has been distributed worldwide except for the Arctic[11]. This fungus is known as oyster mushroom and is considered a health promoter and environmental restorer[16]. *Tagetes minuta* is an annual aromatic herb that grows in temperate grasslands and mountainous regions of South America[8]; it is known for being arthropod repellent and having herbicidal, nematicidal, insecticidal, fungicidal, antiviral properties, etc. According to research carried out, these particularities are due to its components: ocimenones (Z) and (E), piperitone, piperitenone, limonene, tagetone and caryophyllene[17]. Dihydrotagetone inhibits the hatching of *Meloidogyne incognita* eggs by 72 to 79% in 14 days; in the case of juveniles (Z)-β-ocimene is lethal in 72 hours[18].

Knowing the work with plant extracts in essential oils, which require complex processes to obtain, this research used the aqueous extract, which is the unstable liquid emulsion of saturated vapor and essential oil[10] of *Tagetes minuta* and *Pleurotus ostreatus* to evaluate the nematicide effect of the aqueous extracts of *Pleurotus ostreatus* and *Tagetes minuta* in the laboratory and to determine the best LC_{50} of *Pleurotus ostreatus* and *Tagetes minuta* on *Meloidogyne* spp. and *Panagrellus redivivus* in the laboratory.

Panagrellus redivivus is a free-living nematode that lives in humid environments in a state of fermentation and can feed on various cereals. Thanks to its qualities, tiny size, rapid growth, short life cycle, high fecundity, and easy handling, it is one of the most used nematodes in research work[19]. For its part, *Meloidogyne* spp. is an endoparasitic phytonematode that completely penetrates the root to feed, develop and reproduce through eggs[20], it is characterized by causing galls, damaging the root system and causing dwarfism, chlorosis, wilting, defoliation or premature senescencese[2].

MATERIALS AND METHODS

T. minuta was collected in the community San José de Cunduana, Licán Canton, Province of Chimborazo (Longitude 1°37'40 "S, Latitude 78°43'17"W, Altitude 3085 masl). 0.5 kg of leaves and 1 kg of fresh flowers were collected from native crops; they were cut into pieces of 1 cm long, placed in ziploc bags (17.7cm x 19.5cm) separately and transported in a flex-foam thermal cooler (Century-T40-3).

P. ostreatus and *P. redivivus* were cultured and provided by the store of the project "Study of the diversity of nematophagous fungi associated with the rhizosphere of tomato (*Solanum lycopersicum* L.) in three locations in the Province of Chimborazo", executed during 2018 and 2019 at the Biological Sciences Laboratory. *P. redivivus* was raised in a nutrient medium of oats in 250 g per 200 ml of sterile distilled water. After 15 days, an aliquot of the *P. redivivus* culture was taken with a flat-tip brush (0 Ø) and placed in a 100 ml glass bottle with sterile distilled water, this process was repeated until the suspension was opaque. Next, a 10 ml sample was placed in petri dishes (90 mm Ø) and 50 nematodes were fished for each of the experimental units with the help of round-tipped brushes (0 Ø - 4/0 Ø) (Figure 1).

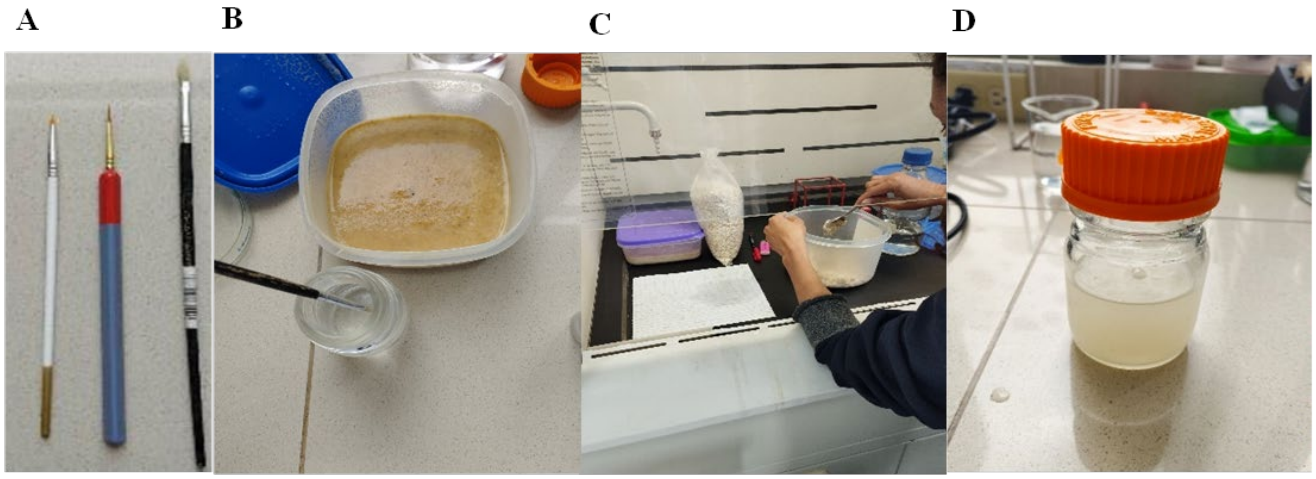

Figure 1. Nematode fishing brushes (A), Culture of *P. redivivus* (B), Inoculation of *P. redivivus* (C), Suspension of *P. redivivus* (D).

Both plant materials were processed in the Laboratory of Pharmaceutical Technology of the Faculty of Sciences at ESPOCH, Riobamba Canton, Chimborazo Province (01°38'51 "S, 78°40'59"W, altitude: 2850 masl)., the hydro-distillation method used by Silva[21] was applied: in a two 500 ml mouths, the chopped plant material was placed with hot water up to 3/4 parts of the funnel's capacity, in such a way that all the material was submerged, the heat was applied to start boiling and steam dragging, obtaining; as a result the aqueous extract. Once the aqueous extracts were received, the concentrations were prepared at 0%, 0.5%, 5%, 25%, 50% and 100% with sterile distilled water, each in 50 ml screw-top glass bottles containing. They were stored in a refrigerator (LG- Side by side of 615 l) at 5°C.

Meloidogyne sp. was obtained from infected root samples with nodules in greenhouse plantations of red bell pepper (*Capsicum annuum*) around 4 months old, located in the sector Quillan Loma Alto, Izamba Parish, Tungurahua Province (01°13'11"S, 78°33 '38"W, altitude 2672 masl). The root with nodules was placed in ziploc bags (17.7cm x 19.5cm) and transported in a flex-foam thermal cooler (Century-T40-3). The tray method for the extraction of Coyne and Claudios[22] nematodes was used as a principle with the following adaptations: The roots were washed to remove the adhering soil and cut into 1 cm long segments, 10 g of roots were placed on a napkin (23cm x 24cm) folded in 4 parts, later a tie was made, forming a kind of tea bags, which were suspended in a 500 ml glass jar with saline solution at 0.9% during 24 hours (Figure 2D).

After 24 hours, juvenile 2 (J2) was briefly identified using a stereoscope (Motic SMZ-171). The morphological characteristics detailed by Jaraba, Lozano and Suárez[23] and the illustrations by Carmona and Padilla[24] were utilized as a guide. It was also considered that when working with the females of *Meloidogyne* sp. the result was youth 2 (J2). Finally, 10 ml of the 0.9% saline solution was taken. The tea bag with nodules was suspended in glass petri dishes (90 mm Ø) and 20 nematodes were fished for each experimental unit with a traditional fishing instrument (Figure 2A).

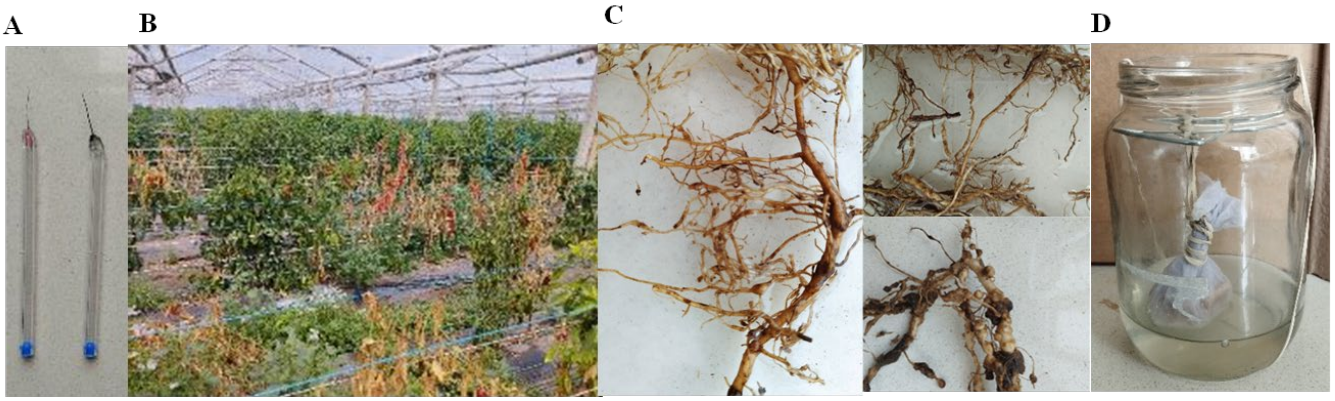

Figure 2. Nematodes fishers (A), Pepper crop with nodules. (B), Root nodules with *Meloidogyne* (C), Adapted method of Coyne and Claudius (D).

Bioassays were carried out in the Biological Sciences Laboratory of the Faculty of Natural Resources at ESPOCH. The number of juveniles 2 (J2) of the nematodes *P. redivivus* and *Meloidogyne* sp were obtained. For each of the experimental units, 6 ml of the different concentrations prepared (0%, 0.5%, 5%, 25%, 50% and 100%) of the aqueous extracts of *T. minuta* leaf-flower and *P. ostreatus*, was placed in each of the sections of the plastic tripetri boxes (90 mm Ø) according to the treatment. Each experimental unit counted the number of dead and alive J2 nematodes with the help of the stereoscope. Data were recorded every 4 h during the day, and the following efficacy equation of Abott[25] was applied.

$$Efficacy = \frac{IT-it}{IT}\ x\ 100 \quad (1)$$

Where:
IT= Live nematodes in the control
it= Live nematodes in the treatment

The Lethal Concentration 50 (LC_{50}) was estimated through a regression based on the efficacy of the different concentrations of the aqueous extracts of *T. minuta* and *P. ostreatus* on the mortality of the populations of *P. redivivus* and *Meloidogyne* sp. The LC_{50} was determined using the EC50 Estimator library of the R programming language of the RStudio version 2022.07.2 program.

The data analysis was performed for each exposure time, for which two types of experimental designs were used: A bifactorial complete randomized design for the aqueous extracts of *T. minuta* leaf and flowers and a completely randomized single factor for the aqueous extract of *P. ostreatus*, in both cases with five concentrations (0%, 0.5%, 5%, 25%, 50% and 100%) and two nematodes (*Panagrellus redivivus* and *Meloidogyne* sp.).

RESULTS

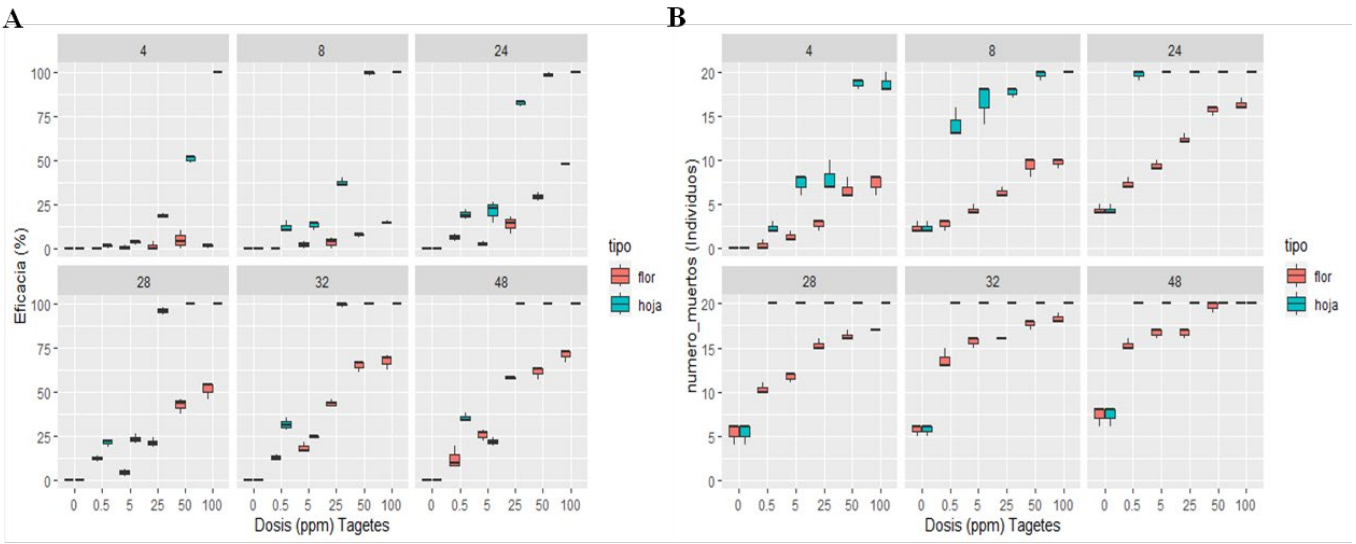

Figure 3. Aqueous extract of *Tagetes minuta* leaf and flower against *Panagrellus redivivus* (A), Aqueous extract of *Tagetes minuta* leaf and flower against *Meloidogyne* sp. (B).

Figure 3 (A) shows the efficacy of the aqueous extract of *T. minuta* leaf and flower on the mortality of the nematode *P. redivivus* during 48 h of exposure. The efficacy of the aqueous extract of *T. minuta* leaf was higher than that of flowers; this reached an efficacy in mortality more significant than 50% of the population of *P. redivivus* from the first 4 hours of exposure in concentrations of 50% and 100% whose efficacy was 50.57% and 100% respectively. Finally, after 48h of exposure, it reached an efficacy of 100% in the concentrations of 25%, 50% and 100%. On the other hand, the aqueous extract of *T. minuta* flower in none of the

concentrations managed to reach an efficacy of 100% in the mortality of *P. redivivus*; the maximum efficacy reached was 71% in the 100% concentration.

Figure 3 (B) shows the efficacy of the aqueous extract of *T. minuta* leaf and flower on the mortality of the nematode *Meloidogyne* sp. during 48 h of exposure, showing that the efficacy of the aqueous extract *T. minuta* leaf was superior to that of flowers, this reached an efficacy more significant than 50% in the mortality of the population of *Meloidogyne* sp. from the first 4h of exposure in the 50% and 100% concentrations with the efficacy of 93.33% in both cases and finally reached an efficacy of 100% after 48h of exposure in the concentrations of 0.5%, 5%, 25%, 50% and 100%. The aqueous extract of *T. minuta* flower reached an efficacy of 100% in the highest concentration at 100%.

The results of the mortality caused by *P. redivivus* and *Meloidogyne* sp. by the aqueous extracts of *T. minuta* leaf and flower showed through an analysis of variance at 48 h of exposure that in both cases the factors analyzed concentration (0%, 0.5%, 5%, 25%, 50%, 100%) and type (flower-leaf) were highly significant, therefore with the Tukey Test it was concluded that for the *P. redivivus* nematode the best concentrations were: 100%, 50% and 25%; and for the nematode *Meloidogyne* sp. the best concentrations were 100% and 50%; in both cases the best type of extract coincided with the aqueous extract of *T. minuta* leaf.

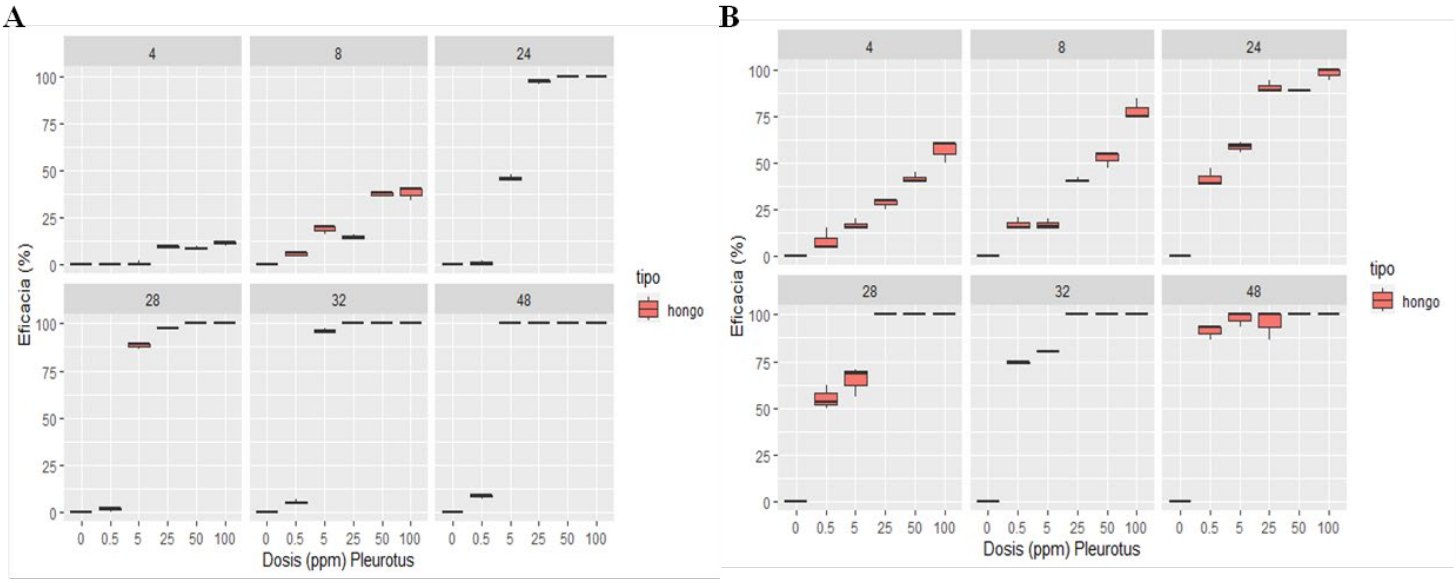

Figure 4. Aqueous extract of *Pleurotus ostreatus* against *Panagrellus redivivus* (A), Aqueous extract of *Pleurotus ostreatus* against *Meloidogyne* sp. (B).

Figure 4 (A) shows the efficacy of the aqueous extract of *P. ostreatus* on the mortality of the *P. redivivus* nematode during 48 h of exposure, showing that the effectiveness of said extract was greater than 50% at 24 h of exposure in concentrations at 25%, 50% and 100% with efficacy of 97.09%, 100%, 100% respectively and at 48h the efficacy of the aqueous extract on the mortality of *P. redivivus* was 100% in the concentrations at 5%, 25%, 50% and 100%.

Figure 4 (B) shows the efficacy of the aqueous extract of *P. ostreatus* on the mortality of the *Meloidogyne* sp. nematode during 48 h of exposure; this indicates that the extract presented an efficacy more significant than 50% at 4h of exposure in the 100% concentration with an efficacy value of 56.67% and at 48h the concentrations at 0.5%, 5%, 25%, 50% and 100% achieved an efficacy of 91.11%, 97.78%, 100% and 100% respectively.

The results of the mortality caused to *P. redivivus* and *Meloidogyne* sp. by the aqueous extract of *P. ostreatus* showed through an Analysis of Variance at 48 h of exposure that in both cases the factor analyzed concentration (0%, 0.5%, 5%, 25%, 50%, 100%) was highly Significant therefore with the Tukey test it was concluded that the best concentrations for both cases were: 100%, 50%, 25% and 5%.

Time	***T. minuta* leaf**		***T. minuta* flower**		***P. ostreatus***	
	P. redivivus	*Meloidogyne* sp.	*P. redivivus*	*Meloidogyne* sp.	*P. redivivus*	*Meloidogyne* sp.
4	132.15	306.74	15.66	40.10	14.21	481.06
8	26.58	7.42	830.58	67.39	217.24	607.09
24	13.04	0.01	246.32	251.81	5.39	20.47
28	8.03	-	35.01	115.59	2.40	11.97
32	13.20	-	95.16	11.76	1.48	3.30
48	19.22	-	37.38	50.59	0.89	0.07

Table 1. LC_{50} of the aqueous extract of *Tagetes minuta* and *Pleurotus ostreatus* against nematodes.

According to treatments against *P. redivivus*, Table 1 shows that the lowest aqueous extract of *T. minuta* leaf was 8.03 ppm at 28h of exposure with a minimum limit of - 4.03 ppm and a maximum of 20.10 ppm, while in the case of the aqueous flower extracts the lowest LC_{50} was 15.66 ppm after 4 hours of exposure with a minimum limit of -112.42 ppm and a maximum of 143.74ppm.

The highest LC_{50} in the aqueous extract of the leaf was 132.15 ppm in the first 4 hours of exposure with a minimum limit of -160.14 ppm and a maximum of 424.43 ppm; on the other hand, the aqueous extract flower was 830.58 ppm after 8 hours of exposure with a minimum limit of -5929.97 ppm and a maximum of 7591.14 ppm.

The lowest LC_{50} of *P. ostreatus* aqueous extract was 0.89 ppm at 48h of exposure, with a minimum limit of 0.84 ppm and a maximum of 0.95 ppm. In comparison, the highest LC_{50} was 217.24 ppm after 8 hours of exposure with a minimum limit of -2776.20 ppm and a maximum of 3210.68 ppm. In this case, the LC_{50} decreases as time passes.

According to *Meloidogyne* sp. results, the lowest aqueous extract of *T. minuta* leaf was 0.01 ppm at 24h of exposure with a minimum limit of 0.01 ppm and a maximum of 0.02 ppm. In contrast, in the aqueous flower extracts, the lowest LC_{50} was 11.76 ppm after 32h of exposure, with a minimum limit of -194.39 ppm and a maximum of 217.91 ppm.

The highest LC_{50} in the aqueous extract of the leaf was 306.74 ppm in the first 4h of exposure with a minimum limit of -4633.86 ppm and a maximum of 5247.33 ppm; on the other hand, the aqueous extract of flowers was 251.81 ppm after 24 hours of exposure with a minimum limit of -1972.92 ppm and a maximum of 2476.54 ppm. In the case of the aqueous extract of the leaf, it reaches its LC_{50} in just 24 hours of exposure.

The lowest LC_{50} of *P. ostreatus* aqueous extract was 0.07 ppm at 48h of exposure, with a minimum limit of 0.02 ppm and a maximum of 0.11 ppm. In comparison, the highest LC_{50} was 607.09 ppm after 8 hours of exposure with a minimum limit of -3935.96 ppm and a maximum of 5150.14 ppm; in this case, the LC_{50} decreases as time passes.

DISCUSSION

The aqueous extract of *T. minita* leaf presented an efficacy of more than 50% in 48 h of exposure in concentrations of 25%, 50% and 100% against *P. redivivus* (Figure 1) and in concentrations of 0.5%, 5%, 25%, 50% and 100% in the case of *Meloidogyne* sp. (Figure 1). This result is similar to that of Murga[26], where the aqueous extract of *T. minuta* was used to control *Meloidogyne incognita* in paprika pepper. They concluded that *T. minuta* leaf could limit root nodulation by eliminating infective J2 juveniles up to 50%. In the same way, Iannacone[27] was observed to it cause a mortality more significant than 50% in eggs and J2 juveniles.

The efficacy to a greater or lesser degree of the aqueous extracts of *Tagetes* is directly associated to the presence of secondary metabolites, according to the evaluations made by Zygadlo[28], the aqueous extract of *T. minuta* leaves present dihydroxyacetone, (E)-tagetone and limonene; instead, the extract of flowers only have

(E)-tagetone, a reason that could explain the low efficacy of the flowers aqueous extract. However, these metabolites are toxic to specific organisms and microorganisms[18]; therefore, toxicity depends on the percentage in which it is present, and this, in turn, relies on the geographical location and abiotic factors such as high and low temperatures, drought, alkalinity, salinity, UV light, etc[29].

Aqueous or oily extracts that have terpenes with phenolic, hydroxyl, or carboxylic groups have been characterized by having greater nematicide activity[14]; the genus *Tagetes* presents these groups and in the case of *T. minuta* it gives the group of terpenes. These same metabolites have a mechanism of action that increases lipid peroxidation rates, causing an induction of oxidative stress[30].

The aqueous extract of *T. minuta* leaf presented the best results with both *P. redivivus* and *Meloidogyne* sp. due to its secondary metabolites. Dihydrotagetone and (E)-tagetone have been the most found in investigations related to the nematicide action of the genus *Tagetes* towards nematodes. When comparing the nematicide action of the extract of *Tagetes zypaquirensis* with a nematicide of chemical origin (carbofuran), the extract showed a similar action, reducing the populations of *Meloidogyne* spp. Therefore, they highlighted that this extract can become an alternative for managing root nodules[13].

Limonene is a metabolite capable of reducing the hatching of *Meloidogyne incognita* eggs by 72 to 79% in 14 days[18]. In this case, the essential oil was used, so there was the presence of (Z)-β-ocimene, which was attributed to the mortality of J2 juveniles in 72 hours; possibly, this metabolite is also found in the aqueous extract used and is the explanation for the high mortality rate of nematodes since it contains a minimum percentage of essential oil[31]. Limonene is one of the metabolites present in the genus *Tagetes* and stands out for causing the mortality of the J2 of *Meloidogyne* sp. linked to the percentage in which it is present[9].

The best LC_{50} of the aqueous extract of *T. minuta* was that of the leaf; for *P. redivivus* it was 8.03 ppm (0.008 mg/ml) at 28h, and for *Meloidogyne* sp., it was 0.01 ppm (0.00001 mg/ml) after 24 hours of exposure (Table 1). The results of the LC_{50} are different from those found by Herrera and Sandoval[32], who determined that the best LC_{50} for *Meloidogyne* sp. of the ethanolic extract of *T. minuta* was 0.0017 mg/ml, possibly due to the type of extract handled, geographic location, and abiotic factors[29] since the data correspond to plant tissue collected in Peru. Zarate[33] determined the LC_{50} of the essential oil extract of *Tagetes lucida*, a species of the *Tagetes* family, which was 0.06 mg/ml, which reduced between 63 and 80% of tomato root galls.

Regarding the exposure time of the LC_{50}, this is related to the time required by the metabolism of the nematode to unfold the secondary metabolites or with the speed of action of the metabolites of the oil inside the nematode[34]. In this case, it is related to the secondary metabolites present in the aqueous extract. Despite the lack of research on aqueous extracts, the values found for the LC_{50} of the aqueous extract of *T. minuta* constitute a valuable reference for the management of plant substances.

The aqueous extract of *P. ostreatus* presented an efficacy more significant than 50% *against P. redivivus* (Figure 2) in concentrations of 5%, 25%, 50% and 100%, in the case of *Meloidogyne* sp. (Figure 2) in concentrations of 25%, 50% and 100% in both cases at 48h of exposure. Similar results show an efficacy in the mortality of 65.2% of *Globodera pallida*[12]. In addition, this aqueous extract of *P. ostreatus* was reported as having the ability to reduce the number of galls caused by *Meloidogyne incognita,* and they highlighted that this extract could be a promising measure for the control of this type of phytonematodes[35].

The efficacy of the aqueous extract of *P. ostreatus* on the mortality of both nematodes during 48 h of exposure it presented specific peaks of activity, in the case of *P. redivivus* the aqueous extract had a peak of efficacy at 24 h, while with *Meloidogyne* sp. it occurred in the first 4 h of exposure, in both cases the efficacy increased until reaching 100%, a similar investigation reported that *Pleurotus ostreatus* has a peak of activity during the first 4 h to 24 h of exposure[12].

P. ostreatus showed a high mortality rate of the nematodes, which is attributed to its toxic characteristics, which are typical of the genus *Pleurotus* sp. known to present several species with nematophagous activity, this activity is manifested through the system of production of immobilizing toxin reserves that they present in toxocysts that are produced laterally on the hyphae[36]. In the same way, Armas[37] identified these toxins,

finding in the case of *P. ostreatus* trans-2-decenedioic acid that corresponds to the nematotoxin called NRRL 3526[38].

The high mortality rate is due to the nematophagous activity that *P. ostreatus* presents, which begins when the nematotoxin present in the aqueous extract comes into contact with the nematode and immobilizes it, quickly digests it, producing hyphae that grow chemotropically and invade the oral cavity, the anus and the cuticle of the nematode[38,39]. The best LC_{50} of the aqueous extract of *P. ostreatus* for *P. redivivus* was 0.89 ppm and for *Meloidogyne* sp. 0.07 ppm in both cases after 48 hours of exposure (Table 1).

After the review of the research that has been carried out on this subject, all of them have aimed to determine the efficacy of the aqueous extract as a nematicide, but the CL_{50}[37,40,41] has not been defined. Despite this, each of the investigations emphasizes the particular mode of action and the efficacy of *P. ostreatus*, which is related to its ability to secrete trans-2-decenedioic acid and some proteases that have not yet been described[42]. The extract has a high nematicide efficacy, so it is advisable to take precautions when this type of extract is taken to the field since the effect of the metabolites can change once they interact with other molecules found in the soil[43].

CONCLUSIONS

The aqueous extracts of *Pleurotus ostreatus* and *Tagetes minuta* leaf and flower showed a nematicide effect on *Panagrellus redivivus* and *Meloidogyne* sp. The aqueous extract of *Tagetes minuta* leaf was better than that of flowers; an efficacy of 100% of the aqueous extract of *Tagetes minuta* leaf was achieved against *Panagrellus redivivus* in concentrations of 25%, 50% and 100% for *Meloidogyne* sp. in concentrations 0.5%, 5%, 25%, 50% and 100% after 48h of exposure. In the case of the aqueous extract *Pleurotus ostreatus*, an efficacy of 100% was achieved against *Panagrellus redivivus* in the concentrations 5%, 25%, 50% and 100%, for *Meloidogyne* sp. in concentrations 0.5%, 25%, 50% and 100% at 48h of exposure.

The best lethal Concentration 50 (LC_{50}) of the aqueous extract of *Tagetes minuta* leaf and flowers was that of leaves; for *Panagrellus redivivus,* the LC_{50} of 8.03 ppm in 28 h of exposure and for *Meloidogyne* sp., the LC_{50} of 0.01 ppm in 24 h of exposure. Regarding the aqueous extract of *Pleurotus ostreatus*, the best LC_{50} against *Panagrellus redivivus* was 1.22 ppm in 48 h of exposure and against *Meloidogyne* sp. 0.01 ppm in 48 h of exposure.

Author Contributions: Madison Chango: collection and analysis of data in the laboratory, presentation of results, discussion and writing of the draft article. Gabriela Rosero: laboratory data collection, review, editing and translation of the article. Norma Erazo: direction of the research project and laboratory methodology. Pablo Álvarez: approach to the experimental design and statistical analysis.

Funding: This research has received funding from Escuela Superior Politécnica de Chimborazo through project grant No. IDIPI-268.

Institutional Review Board Statement: This project has been approved by the Polytechnic Council's resolution No. 542. CP. 2021 and has written authorization from the Bioethics Committee head by Prof. María Viteri, dated on September 8th, 2021.

Acknowledgments: The authors of this research thank the engineer Juan Manzano and the biochemist Diego Vinueza for their collaboration in obtaining the aqueous extracts.

Conflicts of Interest: The authors declare no conflict of interest.

REFERENCES

1. Savary, S. *et al.* The global burden of pathogens and pests on major food crops. *Nat. Ecol. Evol.* 3, (2019).
2. Castillo, J. Identificación de especies de Meloidogyne spp. presentes en el municipio de Patzicía, Chimaltenango. (Universidad Rafael Landívar, 2014).
3. Sánchez-Moreno, S. & Talavera, M. Los nematodos como indicadores ambientales en agroecosistemas. *Ecosistemas* 22, (2013).
4. Pérez-Anzúrez, G. *et al.* Arthrobotrys musiformis (Orbiliales) Kills Haemonchus contortus Infective Larvae (Trichostronylidae) through Its Predatory Activity and Its Fungal Culture Filtrates. *Pathogens* 11, (2022).
5. Triviño Gilces, C., Navia Santillán, D. & Velasco Velasco, L. *Guía para reconocer daño en raíces y métodos de muestreo y extracción de nemátodos en raíces y suelo*. *INIAP Boletín Divulgativo No. 433* https://repositorio.iniap.gob.ec/bitstream/41000/3849/1/433.PDF (2013).
6. González Cardona, C. & Aristizabal Loaiza, M. Evaluación de un producto nematicida sobre nematodos fitoparásitos del plátano Dominico Hartón (Musa AAB). *Acta Agron.* 63, 71–79 (2014).
7. López-Alcántara, R. Nematodos, su implicación en la producción agrícola. *ECUADOR ES Calid. Rev. Científica Ecuatoriana* 2, 10–11 (2015).
8. Muthee Gakuubi, M., Wanzala, W., Wagacha, J. M. & Dossaji, S. F. Bioactive properties of Tagetes minuta L. (Asteraceae) essential oils: A review. *Am. J. Essent. Oils Nat. Prod.* 4, 27–36 (2016).
9. Ibrahim, S. K., Traboulsi, A. F. & El-Haj, S. View of Effects of Essential Oils and Plant Extracts on Hatching, Migration and Mortality of Meloidogyne incognita | Phytopathologia Mediterranea. *Phytopathol. Mediterr.* 45, 238–246 (2006).
10. Licet Mena Valdés, L. *et al.* Determinación de saponinas y otros metabolitos secundarios en extractos acuosos de Sapindus saponaria L. (jaboncillo). *Rev. Cuba. Plantas Med.* 20, 106–116 (2015).
11. Piska, K., Ziaja, K. & Muszynska, B. Edible mushroom pleurotus ostreatus (Oyster mushroom) – Its dietary significance and biological activity. *Acta Sci. Pol. Hortorum Cultus* 16, 151–161 (2017).
12. Arteaga, M. B., Soria, C. A. & Ordoñez, M. E. Determinación del potencial nematicida y nematostático in vitro de Pleurotus ostreatus (Jacq. ex Fr.) sobre larvas J2 de Globodera pallida (Stone). *Rev. Ecuat. Med. Cienc. Biol.* 41, 45–50 (2020).
13. Álvarez S., D. E., Botina J., J. A., Ortiz C., A. J. & Botina J., L. L. Evaluación nematicida del aceite esencial de Tagetes zypaquirensis en el manejo del nematodo Meloidogyne spp. *Rev. Ciencias Agrícolas* 33, 22–33 (2016).
14. Abdel-Rahman, F. H., Alaniz, N. M. & Saleh, M. A. Nematicidal activity of terpenoids. *http://dx.doi.org/10.1080/03601234.2012.716686* 48, 16–22 (2012).
15. Martinotti, M. D., Castellanos, S. J., González, R., Camargo, A. & Fanzone, M. Efecto nematicida de extractos vegetales sobre Meloidogyne incognita Nematicidal effects of extracts of garlic, grape pomace and olive mill waste, on Meloidogyne incognita, on grapevine cv Chardonnay. *Rev. la Fac. Ciencias Agrar.* 48, 211–224 (2016).
16. Naim, L. *et al.* Variation of Pleurotus ostreatus (Jacq. Ex Fr.) P. Kumm. (1871) performance subjected to differentdoses and timings of nano-urea. *Saudi J. Biol. Sci.* 27, 1573–1579 (2020).
17. Cornelius, W. W. & Wycliffe, W. Chapter 90 - Tagetes (Tagetes minuta) Oils. in *Essential Oils in Food Preservation, Flavor and Safety* (ed. Preedy, V. R.) 791–802 (Academic Press, 2016). doi:https://doi.org/10.1016/B978-0-12-416641-7.00090-0.

18. Singh, P. Management of Plant-parasitic Nematodes by the Use of Botanicals. *J. Plant Physiol. Pathol.* 02, (2014).
19. de Lara, on *et al.* La importancia de los nematodos de vida libre.
20. Guzmán-Piedrahita, O. A., Carolina, C. & López-Nicora, H. D. Physiological interactions of plants with plant-parasitic nematodes: A review. *Bol. Cient. del Cent. Museos* 24, 190–205 (2020).
21. Silva Olivo, J. C. "Evaluación de la actividad insecticida y/o repelente 'in vivo' de extracto acuoso de Artemisia absinthium y aceites esenciales de Tagetes minuta y Tagetes zipaquirensis sobre Lasius niger. (Escuela Superior Politécnica de Chimborazo, 2013).
22. Coyne, D. L., Nicol, J. M., Traducción, C.-C. & Verdejo-Lucas, S. *Nematología práctica: Una guía de campo y laboratorio*. (International Institute of Tropical Agriculture (IITA), 2007).
23. Jaraba, J. D., Lozano, Z. E. & Suárez Padrón, I. E. Meloidogyne incognita (Kofoid and White, 1919) Chitwood 1949 y Meloidogyne arenaria (Neal 1889) Chitwood 1949: Nematodos de las nudosidades radiculares en guayaba (psidium guajava l.) c.V. Manzana en Monteria, Cordoba. *Temas Agrar. ISSN-e 0122-7610, Vol. 8, Nº. 2, 2003, págs. 15-21* 8, 15–21 (2003).
24. Carmona, R. & Padilla, W. Morphological, morphometric and molecular identification of Meloidogyne exigua (Göeldi 1887) in coffee (Coffea arabica). *Agron. Mesoam.* 31, 531–545 (2020).
25. ICA. *Manual para la elaboración de protocolos para ensayos de eficacia con PQUA*. (Instituto Colombiano Agropecuario, 2020).
26. Murga-Gutiérrez, S. N., Alvarado-Ibáñez, J. C. & Vera-Obando, N. Y. Efecto del follaje de Tagetes minuta sobre la nodulación radicular de Meloidogyne incognita en Capsicum annuum, en invernadero. *Rev. peru. biol* 19, 257–260 (2012).
27. Iannacone, J. *et al.* Acute and chronic toxic effect of Tagetes minuta' Black mint' (Asteraceae) and carbaril on six important entomophages in biological control. *Biol.* 15, 85–97 (2017).
28. Zygadlo, J. A., Lamarque, A. L., Maestri, D. M., Guzman, C. A. & Grosso, N. R. Composition of the Inflorescence Oils of Some Tagetes Species from Argentina. *J. Essent. Oil Res.* 5, 679–681 (1993).
29. Peralta-Sánchez, M. G. *et al.* Metabolitos secundarios y clorofilas en cempasúchil en respuesta a estrés salino. *Rev. Mex. ciencias agrícolas* 5, 1589–1599 (2014).
30. Senatore, F. *et al.* Antibacterial activity of Tagetes minuta L. (Asteraceae) essential oil with different chemical composition. *Flavour Fragr. J.* 19, 574–578 (2004).
31. Alejandro Rojas, G. *et al.* Evaluación in vitro de la actividad nematicida de limoneno, isotiocianato de alilo, eucaliptol, β-citrolenol y azadiractina sobre Meloidogyne incognita (Nematoda, Meloidogynidae). *Trop. Subtrop. Agroecosystems* 22, (2019).
32. Herrera Moncada, W. L. & Sandoval Fuentes, M. G. Toxicidad del extracto etanólico de plantas de campo y callos in vitro de Tagetes minuta y Tagetes erecta sobre Meloidogyne spp. en Solanum lycopersicum L. *Universidad Nacional Pedro Ruiz Gallo* (Universidad Nacional Pedro Ruiz Gallo, 2019).
33. Zarate-Escobedo, J. *et al.* Concentrations and application intervals of the essential oil of Tagetes lucida Cav. against Nacobbus aberrans. *Rev. Mex. Ciencias Agrícolas* 9,.
34. Mendoza-García, E. *et al.* Efecto biológico del aceite de Tagetes coronopifolia (Asteraceae) contra Diaphorina citri (Hemiptera: Liviidae). *Rev. Colomb. Entomol.* 41, 157–162 (2015).
35. Erazo Sandoval, N. S. *et al.* Effect of Pleurotus ostreatus (Jacq.) and Trichoderma harzianum (Rifai) on Meloidogyne incognita (Kofoid & White) in tomato (Solanum lycopersicum Mill.). *Acta Sci. Biol. Sci.* 42, (2020).
36. Clémençon, H., Emmett, V. & Emmett, E. E. *Cytology and Plectology of the Hymenomycetes*. (2012).
37. Armas-Tizapantzi, A. *et al.* Estructuras tipo toxocistos en Pleurotus ostreatus y P. pulmonarius. *Sci.*

fungorum 49, e1250 (2019).
38. Ernesto, J., El, S., De La, C., Sur, F. & Royse, D. J. *La Biología, el cultivo y las propiedades nutricionales y medicinales de las setas Pleurotus spp. Edible mushroom cultivation View project oxidorreductases enzymes View project*. (2017).
39. Aguilar Marcelino, L. *et al.* Los hongos del género Pleurotus como agentes de biocontrol de parásitos de importancia pecuaria. 52, 1375 (2021).
40. Quevedo, A. *et al.* Interacciones ecológicas de los hongos nematófagos y su potencial uso en cultivos tropicales. *Sci. Agropecu.* 13, 97–108 (2022).
41. Jansson, H.-B. & Lopez-Llorca, L. V. Hongos nematófagos. 145–173 https://dcmba.ua.es/es/areas/botanica/hongos-nematofagos.html# (2001).
42. Leonardo, H. *et al.* Activity of the fungus Pleurotus ostreatus and of its proteases on Panagrellus sp. larvae. *African J. Biotechnol.* 14, 1496–1503 (2015).
43. Arteaga Paredes, M. B. Determinación del potencial nematicida y nematostático in vitro de Pleurotus ostreatus (Agaricales: Pleurotaceae) sobre larvas J2 de Globodera pallida (Tylenchida: Heteroderidae). (Pontificia Universidad Católica del Ecuador, 2018).

Received: October 9th 2023/ **Accepte**d: January 15th 2024 / **Published:**15 February 2024

Citation: Chango, M.; Rosero, G.; Erazo, N.; Álvarez, P. Effect of Five Concentrations of Aqueous Extracts of *Pleurotus ostreatus* P. Kumm and *Tagetes minuta* L. on the Mortality of Two Nematodes in a Laboratory Setting. Revis Bionatura 2024; 9 (1) **9**. http://dx.doi.org/10.21931/RB/2024.09.01.**9**

Additional information Correspondence should be addressed to gabriela.rosero@espoch.edu.ec

Peer review information. Bionatura thanks anonymous reviewer(s) for their contribution to the peer review of this work using https://reviewerlocator.webofscience.com/

Bionatura ISSN. First 13909355 Ecuador. **Scopus coverage years**: from 2016 to the present

Bionatura
Ibero-American Journal of Biotechnology and Life Sciences

Article

Evaluación de parámetros de calidad de naranja (*Citrus* × *sinensis*) en tres estados de madurez

Evaluation of orange (*Citrus* × *sinensis*) quality parameters at three maturity stages

Joselyn Villares[1], Mariela Cobos[1], Lesly Vásquez[1], Rocio Sarmiento[1], Fanny Maita[2], Cindy Freire[2], Lascano Alexis [2], Jermis Alvarado[2]*

[1] *Escuela Superior Politécnica de Chimborazo, El Coca / Ecuador*

[2] *Green Amazon, Research Center, Nueva Loja, Ecuador*

* *Correspondencia: joselyn.villares@espoch.edu.ec;*

Available from. http://dx.doi.org/10.21931/RB/2024.09.01.10

RESUMEN

En la Amazonía ecuatoriana los frutales son parte de la biodiversidad de la chakra y los cítricos es uno de los grupos relevantes dado que tienen un sin número de usos y cuyos excedentes son usados para la comercialización en las ferias locales, por lo que está investigación busca evaluar naranjas en tres estados de madurez mediante análisis físicos para la determinación del tiempo de cosecha. Se evaluaron los parámetros de calidad de la naranja *(Citrus × síntesis),* en tres estados de madurez *(inicial-medio-completo),* se determinó: peso, morfometría, color, firmeza y sólidos solubles. Las frutas se obtuvieron en el cantón Joya de los Sachas, se recolectaron frutas libres de defectos considerables. Como resultado se obtuvo que la naranja pierde peso a medida que transcurren los días. El diámetro se reduce desde el día 1 al 10 y a partir del día 7 la pérdida de longitud es igual en los tres estados de madurez. La luminosidad es el valor del color que sufre mayores cambios a lo largo del almacenamiento de la fruta. La firmeza disminuye más a partir del día 7. A medida que el estado de madurez avanza mayor será la cantidad de sólidos solubles. El estado de madurez perfecto es el medio, ya que ofrece un equilibrio entre alto contenido de azúcar y un peso y tamaño adecuados, beneficiando tanto al agricultor como al cliente debido a su dulzura.

Palabras clave: cítricos, Amazonía, Ecuador, calidad, frutas, postcosecha

ABSTRACT

In the Ecuadorian Amazon, fruit trees are part of the biodiversity of the chakra, and citrus is one of the relevant groups since they have many uses and their surpluses are used for marketing at local fairs. Hence, this research seeks to evaluate oranges at three stages of maturity through physical analysis to determine the optimal harvest time. The quality parameters of oranges *(Citrus × synthesis)* at three stages of maturity *(initial-medium-complete)* were evaluated, and the following were determined: weight, morpho-metrics, color, firmness, and soluble solids. The fruits were obtained from Joya de los Sachas and were harvested free of significant defects. As a result, it was found that the orange loses weight as the days go by. The diameter is reduced from day 1 to 10, and from day 7, the loss of length is equal in the three stages of maturity. Brightness is the color value with the most significant changes throughout fruit storage. Firmness decreases more from day 7 onwards. The higher the maturity stage, the higher the amount of soluble solids. The optimum maturity stage is medium, as it balances high sugar content and adequate weight and size, benefiting the farmer and the customer due to its sweetness.

Keywords: citrus, Amazon, Ecuador, quality, fruits, postharvest

INTRODUCCIÓN

El Ecuador cuenta con una superficie del cultivo de 55.953 hectáreas, de las cuales 10.639 hectáreas pertenecen a la provincia de Bolívar y 2.650 hectáreas al cantón Caluma. La naranja Blanca o Valencia ocupa la posición predominante en cuanto a producción en el país, mientras que las variedades más destacadas desde una perspectiva comercial son las siguientes: Valencia convencional, Washington, Naranja lima, Valencia tardía, Naranja agria, Valencia delta y Naranja pomelo [1]. La Producción de naranja se da en zonas cálidas y tropicales, en las provincias de Bolívar, Manabí, Tungurahua, Santo Domingo, Esmeraldas, Guayas y Los Ríos. En la región norte de la Amazonía, los árboles frutales diversifican el sistema productivo agroforestal utilizado por los agricultores llamado "chakra" al generar ingresos y satisfacer las necesidades alimenticias [2], además, tienen gran repercusión social y sostenible para el productor [3]. Los agricultores han establecido en sus lotes aproximadamente 41 especies de frutales, donde, el cultivo de naranja cuenta con un 76% de presencia en las fincas de la zona [4]. En la provincia de Orellana, según INEC [5], la superficie cosechada fue de 319 hectáreas con una producción de 1317 t y rendimiento 4,13 t/ha.

De acuerdo con [6] un fruto pasa por tres etapas fisiológicas importantes: crecimiento, maduración y senescencia, experimentando transformaciones metabólicas de acuerdo con el estado en el que se halle. El control de calidad concentra se centra en la fase de madurez, en la cual se efectúa una valoración sensorial y técnica a fin de reafirmar que las particularidades organolépticas y fisicoquímicas de los productos son las deseadas. Seguidamente, en [7] se menciona que los principales parámetros de calidad de las frutas son el peso seco, sólidos solubles, acidez, pH, color, firmeza, tamaño, forma, suavidad y calidad de sabor. Generalmente en la mayoría de las frutas el color es la cualidad externa más fundamental en la delimitación del punto de maduración y de la vida postcosecha, el cual es un factor importante en el momento de la adquisición por parte de los clientes. A su vez, es importante estudiar el comportamiento de los frutos cuando son sometidos a distintos ambientes de almacenaje, golpes provocados en los mismos, simulando el transcurso de la recolección, exportación y conducción en las plantas de empaquetado. Al igual que, la concentración de productos para el control de infecciones o inhibidores de etileno aplicados como 1-MCP *(1-metilciclopropeno)* para establecer las condiciones que permitan mayor vida en anaquel [8].

Los requisitos mínimos en todas las categorías, las naranjas deben estar: enteras, sanas, sin resequedad interna, sin presencia de plagas y enfermedades y sin excedentes de color y sabor. Los criterios de maduración se basan en la coloración y el contenido mínimo de zumo. Por otro lado, las naranjas se clasifican en: Categoría Extra deben ser de calidad superior y sus características deben ser igual a la variedad, Categoría I deben ser de calidad, se podrá permitir defectos leves sin que afecten a la calidad de la fruta, Categoría II estas no pueden clasificarse en superiores, pero satisfacen los requisitos mínimos de la naranja. Otro tipo de clasificación es por calibres, este se determina por el diámetro máximo de la sección ecuatorial del fruto siendo el máximo el 92-110 y el inferior de 53-60 mm [9]. Los índices de madurez de 8 o más se relacionan con el color amarillo anaranjado en al menos el 25 % de la superficie del fruto; y que el índice de madurez de 10 o más se relaciona con el color amarillo verdoso en el 25% o más de la superficie del fruto. Las temperaturas óptimas para almacenamiento oscilan entre 3-8°C por hasta 3 meses, dependiendo del cultivar, estado de maduración en la cosecha y área de producción, mientras que la humedad relativa varía entre 90-95%. Dentro de las tasas de respiración a 5°C es de 2-4 ml CO2 / kg·h y a 20°C es de 11-17 ml CO2 / kg·h. La tasa de producción de etileno es de < 0,1 µl/kg·h a 20 °C [10]. La firmeza se midió con un penetrometro, su ejecución consistió en penetrar una naranja, se midió la fuerza que opuso la fruta al ser perforada o comprimida a cierta profundidad de deformación. Los grados Brix son una medida de la concentración de azúcar en el jugo de la fruta, siendo

un indicador de su dulzura. En las naranjas Valencia, se busca un nivel de Brix específico; valores más bajos indican inmadurez, mientras que valores excesivamente altos sugieren sobremaduración. La firmeza se refiere a la resistencia de la pulpa al ser presionada y varía según el destino de las naranjas, generalmente entre 4 y 10 libras de fuerza en naranjas frescas. El espacio de color Lab* evalúa la tonalidad, con L* (luminosidad) más alta para naranjas más claras, a* positivo para tonos rojizos y b* positivo para tonalidades amarillas. Se buscó un equilibrio en estos valores para obtener un color naranja brillante y atractivo, aunque el color puede variar según la madurez y la variedad de las naranjas Valencia. Estos parámetros han sido críticos para determinar la calidad de la cosecha y seleccionar las naranjas en su punto óptimo de madurez.

Considerando la importancia de los cítricos en la producción de la chakra el objetivo general de esta investigación es evaluar la naranja en tres estados de madurez *(inicial, intermedia y máxima)* mediante los análisis físicos para la determinación del tiempo de cosecha óptimo.

MATERIALES Y MÉTODOS

El experimento se llevó a cabo en la ciudad de Francisco de Orellana en condiciones climáticas de 26 °C y HR DE 90 %, a una altitud de 255 m.s.n.m.
Las muestras se obtuvieron de una naranja de variedad Valencia que actualmente tiene 15 años de vida, ubicado en el Cantón Joya de los Sachas, parroquia Enokanqui, comunidad Unión Chimboracense. Luego de aplicar una técnica inspección visual en la que se examinó cuidadosamente las naranjas en el árbol antes de cosecharlas. Debían tener un color naranja brillante y uniforme. Evitando cosechar naranjas con manchas. Se sustrajeron las naranjas en tres estados de madurez: 12 en estado completo, 12 en intermedio y 12 en inicial para sus respectivos análisis.

Preparación de las frutas para el análisis

Una vez transcurrido las 24 horas desde su recolección, se inició con el análisis respectivo fueron seleccionadas las frutas que presentaron buen estado, se descartó las que presentaban daños por picaduras de insectos o golpeadas. Luego se lavaron en agua corriente para la remoción de la suciedad superficial, después fueron sumergidas en una solución de hipoclorito a una concentración del 1 % por 15 minutos, después del tiempo de inmersión, se drenó el agua y se colocó sobre papel absorbente y finalmente se las dejo secar al ambiente para sus respectivos análisis [11]. Los tratamientos permanecieron en cajas de cartón, divididas según su estado de madurez *(inicial, intermedia, completa),* en donde se tomó las respectivas medidas de temperatura y humedad relativa con el instrumento Elitech modelo RC – 4HC, obteniendo temperatura inicial de 20.2°C, intermedia 22.5°C y máxima 29.5°C, así mismo la Hr inicial 42.1%, intermedia 54.8% y máxima 63.9% los cuales fueron monitoreados en todo el proceso del experimento. El tiempo estimado para la recolección de datos en el experimento sobre la calidad de las naranjas Valencia, que incluyó parámetros como grados Brix, firmeza y espacio de color Lab*, dependió de la escala del experimento, la cantidad de muestras requeridas, la disponibilidad de personal y equipo especializado, la frecuencia de muestreo, las condiciones climáticas y el tiempo necesario para la preparación, el registro y el análisis de datos. En general, este proceso duró más de 10 días, ya que implicó la recolección y medición de múltiples muestras de naranjas en diferentes árboles, seguido de un procesamiento y análisis adecuados para obtener resultados precisos y confiables.

Figura 1. Cosecha de naranjas en distintos estados de madurez.

Variables evaluadas

En el contexto de este análisis, se establecen como factores independientes dos variables: el nivel de madurez *(inicial, medio y completo)* y el momento en el que se recopilan los datos, que incluye los días *(1, 3, 7 y 10)*.

Las variables dependientes evaluadas fueron diámetro, color, peso total y sólidos solubles totales establecidos como °Brix [12] . Además, otra variable, es la firmeza, es uno de los métodos físicos químicos que mejor se correlaciona con el estado de maduración de la fruta [13].

Peso. - El peso de la muestra fue tomado en la balanza BOECO BWL 51 con una precisión de 0,001.
Morfometría. - Se midió el diámetro y longitud de la fruta con un calibrador pie de rey RT005102. Los datos se tomaron, de la parte más ancha de la naranja el diámetro ecuatorial, y la longitud desde la extremidad del pedúnculo hasta el extremo inferior.

Color. Se determinaron los parámetros L*, a*, b* tanto de la cáscara *(en lados contrarios)* como de la pulpa, mediante el colorímetro KONICA MINOLTA SPECTRO PHOTO METER CM-700d. Mediante el sistema de visión artificial con medidas de color que indicaron el estado de madurez de las naranjas.

*Firmeza. S*e midió la firmeza de la cáscara con un penetrómetro LT Lutro FR-5120, punta número 6. Tomando en cuenta la penetración en el diámetro ecuatorial con una fuerza perpendicular en un punto y su lado opuesto, tanto de la cáscara como de la pulpa.

Sólidos solubles totales. Este parámetro se midió con refractómetro tipo ATAGO Pocket y los resultados se expresaron en °Brix.

Análisis estadístico

Para el análisis estadístico se utilizó el diseño factorial A*B, y el programa Infostat SPSS versión 26.0, se realizó un análisis de ANOVA simple de medias repetidas, seguido de una prueba de comparación de mediana según Tukey, con una significancia de 0,05.

RESULTADOS

La presente investigación tuvo como objetivo evaluar la naranja en tres estados de madurez *(inicial, intermedia y máxima)* mediante los análisis físicos para la determinación del tiempo de cosecha óptimo. Para ello, se han considerado dos factores principales: los estados de madurez de la naranja y el tiempo transcurrido desde

la recolección. Se evaluó variables morfométricas, como el peso, diámetro y longitud de las naranjas; variables físicas, como el color y la firmeza de la pulpa; y el contenido de sólidos solubles, que proporciona información sobre el sabor dulce de la fruta. En la Figura 2 se presentan las naranjas al final del tiempo en percha.

Figura 2. Naranjas en estados de madurez fisiológica después de 10 días en percha

Las naranjas en estados de maduración después de 10 días de almacenamiento se refieren al proceso específico del estudio en la que las naranjas fueron sometidas a un período de almacenamiento controlado en el periodo de tiempo mencionado, como parte de la metodología experimental. Durante este período, se monitoreó el proceso de maduración de las naranjas.

Variables morfométricas

Se realizo el análisis de variables morfométricas para proporcionar información sobre el tamaño y la forma de las naranjas en cada estado de madurez y día de análisis. En la Tabla 1 se muestra los resultados del análisis de varianza ejecutado.

Estado de madurez fisiológica	Día de almacenamiento	Peso (g)	Diámetro (mm)	Longitud (mm)
Inicial	1	280,94 ± 21,56 ^{f}	78,82 ± 5,56 ^{Bd}	82,32 ± 2,02 ^{d}
	3	199,63 ± 9,20 ^{de}	70,98 ± 1,47 ^{Bc}	68,54 ± 0,49 ^{c}
	7	149,19 ± 6,32 ^{abc}	64,57 ± 1,22 ^{Bb}	60,88 ± 1,85 ^{abc}
	10	134,58 ± 6,98 ^{abc}	64,57 ± 0,99 ^{Ba}	61,15 ± 1,25 ^{abc}
Medio	1	174,01 ± 22,53 ^{bcde}	68,83 ± 3,93 ^{Ad}	67,63 ± 1,98 ^{c}
	3	167,44 ± 7,44 ^{bcde}	67,49 ± 0,93 ^{Ac}	64,17 ± 1,32 ^{abc}
	7	139,4 ± 1,03 ^{bcd}	62,51 ± 0,00 ^{Ab}	62,44 ± 0,86 ^{abc}
	10	108,78 ± 20,56 ^{a}	55,24 ± 7,64 ^{Aa}	55,15 ± 5,20 ^{a}
Completo	1	216,09 ± 27,68 ^{e}	76,63 ± 2,46 ^{Bd}	68,1 ± 4,86 ^{c}
	3	180,79 ± 22,92 ^{de}	70,06 ± 3,78 ^{Bc}	65,7 ± 5,07 ^{bc}
	7	158,52 ± 16,08 ^{bcd}	66,82 ± 2,31 ^{Bb}	64,1 ± 3,02 ^{abc}
	10	125,1 ± 12,31 ^{ab}	60,98 ± 1,77 ^{Ba}	58,14 ± 3,68 ^{ab}

Los resultados se expresan como media ± desviación estándar (DE) (n = 3). La letra mayúscula muestra los grupos homogéneos para el estado de madurez mientras que las minúsculas para losdías de almacenamiento o los grupos homogéneos de la interacción de los factores cuando esta muestra diferencia significativa

Tabla 1. Análisis de variables morfométricas de la naranja

La firmeza de la cáscara de las naranjas se ve afectado significativamente por la interacción del estado de madurez y los días transcurridos después de la recolección. Las naranjas que se cosecharon en el estado inicial tuvieron una gran diferencia respecto a los días después de la cosecha debido a que existió un incremento del 5% de firmeza desde el día 1al 10, mientras que en los estados de madurez medio y completo no existió mayor variación durante los 10 días de almacenamiento. Esta variación de peso principalmente se debe a la deshidratación del producto debido a su condición higroscópica puesto que la humedad relativa en la que se conservaron fue del 54,8 % [14] . El grupo homogéneo abc corresponde a la interacción de los días 7 y 10 con los estados de madurez medio e inicial lo que sugiere que a partir del día 7 la pérdida de peso es similar para todos los estados de madurez.

El diámetro de las naranjas no presentó diferencias significativas para la interacción de los factores en estudio, pero si para cada uno de ellos. El estado de madurez medio muestra naranjas con diámetro menor a las del estado de madurez completo e inicial, sin embargo, esta es una característica que no se puede atribuir completamente al factor en estudio ya que bien podría ser homogenizada con un control de calibre más exhaustivo en el momento de la recolección. Respecto a los días después de la cosecha los resultados indican que las naranjas reducen su diámetro desde el día 1 al día 10, siendo significativo para su comercialización, este comportamiento se presentó para todos los estados de madurez.

La longitud de las naranjas se ve afectada de manera significativa por la combinación de su estado de madurez y los días transcurridos después de la recolección. En el décimo día después de la cosecha, las naranjas en un estado de madurez medio presentaron una longitud inferior, mientras que las naranjas en un estado de madurez inicial, al primer día después de la cosecha, presento una longitud mayor. El grupo homogéneo abc representa la interacción de los días 7 y 10 con los estados de madurez inicial, medio y completo, lo que sugiere que, a partir del séptimo día, la pérdida de longitud es similar en todos los estados de madurez.

Variables físicas

Se realizo un análisis de variables morfométricas para conocer el color *(Tabla 2)* y firmeza *(Tabla 3)* de cascara de la fruta a lo largo de 10 días de almacenamiento.

Estado de Madurez fisiológica	Día	Color de cascara		
		L*	a*	b*
Inicial	1	38,15 ± 1,88 ^{a}	-5,57 ± 1,34 ^{a}	21,18 ± 2,41 ^{a}
	3	41,16 ± 1,49 ^{a}	-8,09 ± 1,84 ^{a}	25,15 ± 3,96 ^{ab}
	7	43,6 ± 1,99 ^{ab}	-9,91 ± 0,32 ^{a}	29,52 ± 2,94 ^{ab}
	10	49,96 ± 1,82 ^{bc}	-4,95 ± 2,45 ^{a}	34,72 ± 6,76 ^{bc}
Medio	1	54,42 ± 3,53 ^{cde}	-2,16 ± 5,22 ^{ab}	47,49 ± 5,49 ^{de}
	3	53,55 ± 1,46 ^{cd}	-1,74 ± 1,28 ^{ab}	46,36 ± 1,72 ^{cde}
	7	61,89 ± 2,67 ^{fg}	4,94 ± 0,70 ^{bc}	46,36 ± 3,45 ^{ef}
	10	60,95 ± 2,62 ^{efg}	7,84 ± 3,50 ^{c}	55,75 ± 3,00 ^{def}
Completo	1	57,37 ± 0,60 ^{def}	12,76 ± 1,93 ^{cd}	52,26 ± 1,63 ^{def}
	3	58,41 ± 1,33 ^{defg}	11,05 ± 2,18 ^{cd}	53,01 ± 4,79 ^{def}
	7	52,28 ± 3,30 ^{cd}	10,78 ± 1,58 ^{cd}	44,83 ± 5,98 ^{cd}
	10	64,93 ± 3,82 g	18,2 ± 6,03 ^{d}	61,63 ± 2,24 ^{f}

Los resultados se expresan como media ± desviación estándar (DE) (n = 3). La letra mayúscula muestra los grupos homogéneos para el estado de madurez mientras que las minúsculas para los días de almacenamiento o los grupos homogéneos de la interacción de los factores cuando esta muestra diferencia significativa.

Tabla 2. Análisis color cascara

El valor L* (-blanco + negro) del color

El valor *L* del color de las naranjas se ve afectado significativamente por la interacción del estado de madurez y los días transcurridos después de la recolección. Los valores L* definen la luminosidad del color de la cascara, las naranjas en el estado de madurez inicial al día 1 tiene menor luminosidad, mientras que, las naranjas del estado de madurez completo del día 10 presentaron mayor luminosidad.

El valor a* (-verde + rojo) del color

El valor *a* del color a de las naranjas se ve afectado significativamente por la interacción del estado de madurez y los días transcurridos después de la recolección. Estos valores confirman que las naranjas seleccionadas como para el estado de madurez inicial tienen más color verde que aquellas cosechadas y categorizadas como estado de madurez completa que ya presenta presencia de color rojo. Demostrando que la variación de color en naranja definitivamente es un criterio de índice de madurez.

El valor b* (+amarillo, -azul) del color

El color b de las naranjas se ve afectado significativamente por la interacción del estado de madurez y los días transcurridos después de la recolección. Las naranjas en el estado de madurez inicial tienen los valores menores mientras que el estado de madurez medio y completo tiene valores mayores, lo que nos indica que el color amarillo es más predominante conforme el estado de madurez de la fruta es mayor.

Estado de madurez fisiológica	Día	Firmeza de cascara (Kg)
Inicial	1	6,95 ± 1,70 ^{bc}
	3	9,24 ± 2,04 ^{cd}
	7	12,77 ± 0,83 ^{e}
	10	12,65 ± 0,48 ^{e}
Medio	1	8,5 ± 0,30 ^{bcd}
	3	10,39 ± 1,76 ^{de}
	7	9,9 ± 1,19 ^{cde}
	10	7,98 ± 0,77 ^{bcd}
Completo	1	5,84 ± 0,57 ^{b}
	3	7,56 ± 0,69 ^{bcd}
	7	7,74 ± 0,46 ^{a}
	10	6,79 ± 0,80 ^{bc}

Los resultados se expresan como media ± desviación estándar (DE) (n = 3). Las letras minúsculas indican los grupos homogéneos generados para la interacción de los factores de estudio.

Tabla 3. Análisis firmeza cascara

La firmeza de la cáscara de las naranjas se ve afectado significativamente por la interacción del estado de madurez y los días transcurridos después de la recolección. Las naranjas que se cosecharon en el estado inicial tuvieron una gran diferencia respecto a los días después de la cosecha debido a que existió un incremento considerable de firmeza desde el día 1al 10, mientras que en los estados de madurez medio y completo no existió mayor variación durante el almacenamiento.

Color y firmeza de pulpa

El valor *a* del color de la pulpa de las naranjas *(Tabla 4)* se ve afectado significativamente por la interacción del estado de madurez y los días de almacenamiento. Las naranjas en el estado de madurez inicial en el día 10

presentaron valores de *a* bajos lo que indica que en esta predomina el color verde, mientras las naranjas en estado de madurez medio al día 7 presentaron una pulpa más bien de tonalidad rojiza. El valor *a* del color de la pulpa de naranja a lo largo del tiempo disminuye para los estados de madurez inicial e intermedio, sin embargo, para las naranjas en estado de madurez completo no mostró diferencia.

Estado de madurez fisiológica	**Día**	**Color a* de pulpa**
Inicial	1	1,92 ± 0,95 ^{abc}
	3	0,8 ± 0,34 ^{abc}
	7	-0,42 ± 0,68 ^{ab}
	10	-0,93 ± 0,89 ^{a}
Medio	1	2,16 ± 0,50 ^{bc}
	3	1,42 ± 0,19 ^{abc}
	7	3,47 ± 0,52 ^{c}
	10	-0,47 ± 1,30 ^{ab}
Completo	1	1,07 ± 1,25 ^{abc}
	3	0,77 ± 0,61 ^{abc}
	7	0,79 ± 2,56 ^{abc}
	10	1,25 ± 0,46 ^{abc}

Los resultados se expresan como media ± desviación estándar (DE) (n = 3). Las letras minúsculas indican los grupos homogéneos generados para la interacción de los factores de estudio

Tabla 4. Análisis de color pulpa

En cuanto a la firmeza de pulpa (Tabla 5) sus resultados no son variables, la pulpa de las naranjas en estado de madurez medio, inicial y completo del día 1 al 10 no presenta diferencias significativas, siendo el estado inicial qué presento menor firmeza de pulpa y el estado completo mayor firmeza de pulpa.

Estado de madurez fisiológica	**Día**	**Firmeza de pulpa (Kg)**
Inicial	1	0,26 ± 0,04 ^{a}
	3	0,25 ± 0,08 ^{a}
	7	0,36 ± 0,01 ^{ab}
	10	0,25 ± 0,04 ^{a}
Medio	1	0,35 ± 0,07 ^{ab}
	3	0,33 ± 0,16 ^{ab}
	7	0,25 ± 0,01 ^{a}
	10	0,3 ± 0,03 ^{ab}
Completo	1	0,48 ± 0,15 ^{abc}
	3	0,57 ± 0,10 ^{bc}
	7	0,75 ± 0,15 ^{c}
	10	0,44 ± 0,13 ^{ab}

Los resultados se expresan como media ± desviación estándar (DE) (n = 3). Las letras minúsculas indican los grupos homogéneos generados para la interacción de los factores de estudio

Tabla 5. Análisis firmeza de pulpa

Sólidos Solubles *(°Brix)*

Los datos presentados corresponden al contenido de sólidos solubles expresado en grados Brix en función del estado de madurez y el día de análisis de las naranjas.

Estado de madurez fisiológica	Día	Sólidos Solubles (°Brix)
Inicial	1	8,4 ± 0,95 [A]
	3	7,77 ± 0,06 [A]
	7	7,84 ± 1,04 [A]
	10	7,84 ± 0,25 [A]
Medio	1	11,57 ± 1,44 [B]
	3	11,17 ± 1,01 [B]
	7	9,5 ± 0,40 [B]
	10	9,7 ± 2,09 [B]
Completo	1	12,9 ± 2,17 [B]
	3	11,83 ± 1,58 [B]
	7	11,15 ± 0,75 [B]
	10	8,67 ± 2,85 [B]

Los resultados se expresan como media ± desviación estándar (DE) (n = 3). La letra mayúscula muestra los grupos homogéneos para el estado de madurez

Tabla 6. Análisis de Sólidos Solubles

En el análisis de Sólidos solubles (°Brix) se identificó diferencias significativas para el factor estado de madurez. Las naranjas en estado medio y completo de madurez presentaron mayor contenido de solidos solubles que el estado inicial, lo cual se ajusta a una característica de los frutos no climatéricos que una vez cosechados no incrementan su contenido de azúcares. Si las naranjas se cosechan en un estado de madurez más avanzado, tendrán un mayor contenido de azúcar, pero a medida que pasan los días después de la recolección, ese contenido de grados brix disminuye gradualmente.

DISCUSIÓN

En cuanto al peso las naranjas en estado de madurez inicial al día uno después de la cosecha presentó mayor peso mientras que las naranjas en estado de madurez medio al día 10 después de la cosecha fueron las que presentaron menor peso. La variación fue mayor en el estado de madurez inicial, ya que al día 1 pesa 280,94 g en relación al día 10 en el mismo estado de madurez que presenta un peso de 134,58 g. Según [15] manifiesta lo contrario, en la variable de peso, las naranjas presentaron una variación de 64,6 g en los de color cero hasta 365 g en frutos de color cinco, por lo que existe una mayor variación en su peso, obteniendo un promedio de 179,17 g, lo que posiciona a los frutos en un calibre entre C y D. A esto se suma [16] indicando que el peso promedio encontrado en el limón sutil fue de 25.65 g en estado verde; esto aumentó a 29.55 g en estado pintón y 33.48 g en estado maduro, con una desviación estándar de 0.88; 1.34 y 1.50 respectivamente, con esto se indicó que presenta una diferencia con los resultados del experimento, debido a que la variación del peso de la naranja es superior conforme a las escalas de los días en comparación al del limón sutil donde su variación es pequeña.

Las naranjas conforme van madurando, cambia su tonalidad piel de verde intenso, a verde claro naranja y amarillo. En la investigación de [17] se establece la correlación entre la tonalidad de la piel y la condición de calidad interna en naranjas de 'Sanguinelli', expresan resultados en cuanto a color de la cascara como en color de la pulpa mencionando que cuanto menor es la calidad interna de la fruta más intenso será la tonalidad rojiza de la cascara y pulpa de la naranja. Corrobora con su estudio, que, tanto para medir el color de la cáscara y de la pulpa, es oportuno calcular tal índice a*/b* como índice de color. Sin embargo, la coloración de las naranjas es diversa alrededor de su superficie, y según [18] la parte con más color es la parte del árbol que ve al norte.

Para [19] el ablandamiento en cítricos está relacionado con la degradación de la pared celular, dependiendo del tiempo transcurrido de la maduración del fruto, presentando una mayor firmeza el primer día de evaluación y por ende mayor resistencia a la penetrabilidad, capacidad que tiende a disminuir con la maduración, difiriendo con los resultados de nuestra investigación donde las naranjas que se cosecharon en el estado inicial a lo largo de los días después de su recolección incrementaron su firmeza, mientras que las de estado de madurez completa presentaron, al día 1 y 7, una menor firmeza. Esto ocurre a que la textura de las frutas cambia debido a la hidrólisis de los almidones y de las pectinas, por la reducción de su contenido de fibra y por los procesos degradativos de las paredes celulares.

En los sólidos solubles *(°Brix),* se presentó relación en cuanto al estado de madurez siendo homogéneo para el estado medio y completo presentando mayor contenido de solidos solubles que en estado inicial. Según [20] manifiesta que los grados Brix son un índice comercial aproximado ya que los sólidos no son solamente sacarosa. Asimismo, se realizó una prueba de grados Brix para determinar la cantidad de azucares, demostrando que las naranjas tienen una concentración mayor de azúcar en el jugo.

CONCLUSIONES

La disminución de peso y diámetro ecuatorial de las naranjas es influenciada por los días de almacena-miento más que por el estado de madurez en las que son cosechadas debido a la deshidratación. A partir del día 7 la pérdida de longitud es similar en los tres estados de madurez.

En el color de la fruta la luminosidad es el valor más afectado a lo largo del almacenamiento ya que en todos los estados de madurez conforme pasan los días aparece tonalidades más oscuras. En cuanto a la firmeza de la cáscara está influenciada principalmente por el estado de madurez puesto que las naranjas menos maduraz son más firmes.

Los sólidos solubles de la naranja al ser un fruto climatérico dependen exclusivamente del estado de madurez en el que fue cosechada ya que a lo largo del tiempo de almacenamiento este no muestra cambios significativos.

Según los hallazgos del experimento, el estado de madurez óptimo sería el estado medio, ya que ofrece un equilibrio en comparación con los otros estados. En este estado, se encuentra un nivel elevado de azúcar, junto con un peso y tamaño adecuados, lo que beneficia tanto al ingreso del agricultor por su peso de venta como a la satisfacción del cliente debido a su dulzura.

Contribución de los autores: En el caso de los artículos de investigación con varios autores, deberá incluirse un breve párrafo en el que se especifiquen sus contribuciones individuales. Deben utilizarse los siguientes enunciados "Conceptualización, J.V. y R.S.; metodología, F.M., C.F., investigación, L.V., J.V.; curación de datos, M.C. y L.V; redacción-revisión y edición, R.S. y J.V. Todos los autores han leído y aceptado la versión publicada del manuscrito.

Financiamiento: Esta investigación no ha recibido financiación externa

Declaración de consentimiento informado: No aplica

Agradecimientos: Los autores agradecen el apoyo brindado por la profesora Maritza Sánchez, considerando que la investigación corresponde a un trabajo de investigación formativa de la asignatura Poscosecha de la Carrera de Agronomía de la Escuela Superior Politécnica de Chimborazo, Sede Orellana.

Conflicto de intereses: Los autores declaran no tener ningún conflicto de intereses.

REFERENCIAS

1. Yances Astudillo S. Importancia de la producción de naranja en Caluma y el impacto que tiene en los festivales del cantón : análisis cultural turístico [Internet] [bachelorThesis]. Quito; 2018 [citado 1 de octubre de 2023]. Disponible en: http://repositorio.usfq.edu.ec/handle/23000/7935

2. Jadán Maza AO. Influence of land use with cocoa crops, chakras and primary forest on diversity, carbon storage and productivity in Sumaco Biosphere Reserve, Ecuador. Influencia del uso de la tierra con cultivos de cacao, chakras y bosque primario, sobre la diversidad, almacenamiento de carbono y productividad en la Reserva de la Biosfera Sumaco, Ecuador [Internet]. 2012 [citado 1 de octubre de 2023]; Disponible en: https://repositorio.catie.ac.cr/handle/11554/2395

3. Vega MEG. Revisión bibliográfica CHIRIMOYA (Annona cherimola Miller), FRUTAL TROPICAL Y SUB-TROPICAL DE VALORES PROMISORIOS. Cultivos Tropicales. 28 de marzo de 2013;34(3):52-63.

4. Tierras YBV, Prado-Beltrán JK, Nicolalde-Cruz JR, Casanoves F, Virginio-Filho E de M, Arroyo WFV. Caracterización y rol de los frutales amazónicos en fincas familiares en las provincias de Sucumbíos y Orellana (Ecuador). Ciencia y Tecnología Agropecuaria. 22 de agosto de 2018;19(3):485-99.

5. Cifras Agroproductivas [Internet]. [citado 1 de octubre de 2023]. Disponible en: http://sipa.agricultura.gob.ec/index.php/cifras-agroproductivas

6. Evolución de los parámetros de calidad en frutos de pepino dulce (Solanum muricatum Ait.) durante las fases de crecimiento, maduración y post-cosecha [Internet]. [citado 1 de octubre de 2023]. Disponible en: https://riunet.upv.es/handle/10251/61479

7. Torres R, Montes EJ, Pérez OA, Andrade RD. Relación del Color y del Estado de Madurez con las Propiedades Fisicoquímicas de Frutas Tropicales. Información tecnológica. 2013;24(3):51-6.

8. Metodologías de análisis de factores de calidad en frutas tropicales y suptropicales, implementadas por el laboratorio de postcosecha de la Universidad de California en Davis, Estados Unidos [Internet]. [citado 1 de octubre de 2023]. Disponible en: https://repositoriotec.tec.ac.cr/handle/2238/4000

9. Almache Almache MA, Villacres Escudero AE. Evaluación de los parámetros de calidad en dos variedades de naranja, valencia (Citrus x sinensis) y naranja agria (Citrus x aurantium) para la elaboración de jugo [Internet] [bachelorThesis]. Ecuador : Latacunga: Universidad Técnica de Cotopaxi (UTC); 2021 [citado 1 de octubre de 2023]. Disponible en: http://repositorio.utc.edu.ec/handle/27000/8160

10. Urraburu Bordón M. Comportamiento poscosecha y funcional de materiales genéticos de guayabo del país (Acca sellowiana (O. Berg.) Burret) y arazá (Psidium cattleianum Sab). 2017 [citado 1 de octubre de 2023]; Disponible en: https://www.colibri.udelar.edu.uy/jspui/bitstream/20.500.12008/24161/1/Urraburu-Bord%C3%B3nMariana.pdf

11. Bianchi M, Guarnaschelli A, Milisenda P. Dehidrocongelación de frutas: Estudio de los parámetros de calidad. Invenio. 2011;14(26):117-32.

12. Frutas frescas. naranja valenciana. especificaciones. [Internet]. [citado 1 de octubre de 2023]. Disponible en: https://tienda.icontec.org/gp-frutas-frescas-naranja-valenciana-especificaciones-ntc4086-1997.html

13. Brezmes Llecha J. Diseño de una nariz electrónica para la determinación no destructiva del grado de la maduración de la fruta [Internet]. Universitat Politècnica de Catalunya; 2001 [citado 1 de octubre de 2023]. Disponible en: https://upcommons.upc.edu/handle/2117/94188

14. Zhang J, Zhang J yi, Shan Y xia, Guo C, He L, Zhang L yan, et al. Effect of harvest time on the chemical composition and antioxidant capacity of Gannan navel orange (Citrus sinensis L. Osbeck 'Newhall') juice. Journal of Integrative Agriculture. 1 de enero de 2022;21(1):261-72.

15. Barón RD, Villa AL. Evolución de los parámetros de calidad de naranja valencia producida en el municipio de chimichagua, cesar - colombia. Temas Agrarios. 1 de enero de 2013;18(1):66-74.

16. Puente Huera CJ. Determinación de las Características Físicas y Químicas del Limón sutil (citrus aurantifolia swingle) [Internet] [bachelorThesis]. 2011 [citado 1 de octubre de 2023]. Disponible en: http://repositorio.utn.edu.ec/handle/123456789/352

17. Tarancón P, Cebrián B, Fernández-Serrano P, Besada C. Relación entre la coloración de la piel y la calidad interna de naranjas 'Sanguinelli'. Estudios físico-químicos y sensoriales. Levante Agrícola. 2020;(450):33-42.

18. Cruz MÁG, Tovar LG. La presente tesis titulada ECO-INTENSIFICACIÓN DE LA PRODUCCIÓN DE NARANJA (Citrus sinensis L. Osbeck), ESTUDIO DE CASO: EN PAPANTLA. [citado 1 de octubre de 2023]; Disponible en: http://ritaschwentesius.mx/tesis-profesionales/Eco-intensificacion_de_la_produccion_de_naranja.pdf

19. Muramatsu N, Takahara T, Kojima K, Ogata T. Relationship between texture and cell wall polysaccharides of fruit flesh in various species of citrus. HortScience. 1996;31(1):114-6.

20. Polo LB, Fernández LJ, Riesco AP, Tello DS, Fathallah O, Calvo RN, et al. CONTENIDO DE VITAMINA CY AZÚCAR EN ZUMO DE NARANJA Y DERIVADOS INDUSTRIALES. José Manuel Rivero

Martín Josefa Jaramillo Romero Fernando Alfonso Cervel Josefa Montero García Ma Elena Montejo González. 2019;22:33-8.

Received: October 9th 2023/ **Accepte**d: January 15th 2024 / **Published:**15 February 2024

Citation: Villares J, Cobos M, Vásquez L, Sarmiento R, Maita F, Freire C, Lascano A, Jermis A. Evaluación de parámetros de calidad de naranja (*Citrus* × *sinensis*) en tres estados de madurez. Revis Bionatura 2024; 9 (1) 10. http://dx.doi.org/10.21931/RB/2024.09.01.10

Additional information Correspondence should be addressed to gabriela.rosero@espoch.edu.ec
Peer review information. Bionatura thanks anonymous reviewer(s) for their contribution to the peer review of this work using https://reviewerlocator.webofscience.com/

Bionatura ISSN. First 13909355 Ecuador. **Scopus coverage years**: from 2016 to the present

Bionatura
Ibero-American Journal of Biotechnology and Life Sciences

Article

Evaluación del desempeño del cultivo de pepino (*Cucumis sativus*) frente a tres fertilizantes foliares en la parroquia Nuevo Paraíso, Orellana, Ecuador

Evaluation of cucumber (*Cucumis sativus*) crop performance against three foliar fertilizers in Nuevo Paraíso parish, Orellana, Ecuador.

Lourdes Aguirre-Cobeña[1,*] *Diego Salguero-Ramos*[2] *Amanda Bonilla-Bonilla*[3], *Rodrigo Salazar- López*[4]

[1] *Escuela Superior Politécnica de Chimborazo, Facultad de Recursos Naturales, Orellana, Ecuador; lourdes.aguirre@espoch.edu.ec.*
[2] *Unidad educativa "Capitán Giovanny Calles", Docente de Estudios Sociales, Orellana, Ecuador; disalgueiro@yahoo.com.*
[3] *Escuela Superior Politécnica de Chimborazo, Facultad de Recursos Naturales, Riobamba, Ecuador; amanda.bonilla@espoch.edu.ec.*
[4] *Escuela Superior Politécnica de Chimborazo, Facultad de Recursos Naturales, Riobamba, Ecuador; rodrigo.salazar@espoch.edu.ec.*
***** *Correspondencia: lourdes.aguirre@espoch.edu.ec; Tel.+593 960 134 396*
Available from. http://dx.doi.org/10.21931/RB/2024.09.01.11

RESUMEN

La producción de pepino en la región amazónica del Ecuador se ha intensificado en los últimos años, debido a las condiciones climáticas idóneas para este cultivo. En la parroquia Nuevo Paraíso, de la provincia de Orellana se siembra el pepino en pequeñas superficies (>1ha) destinado a consumo local. Los productores han visto la necesidad de aumentar sus rendimientos con la aplicación de fertilizantes foliares. El propósito de este estudio fue comparar el desempeño del cultivo de pepino utilizando tres tipos de fertilizantes foliares comerciales con su respectivo análisis económico. La prueba piloto se realizó en un terreno de 1200 m^2 donde se aplicaron los fertilizantes Evergreen (2.5 cm/2L), Metalasote (2.5 cm/2L), Agrostemin (1gr) evaluando la altura de planta, número de hojas y flores, diámetro del tallo y características del fruto a los 22, 37 y 49 días y comparándolo con el testigo. Los hallazgos mostraron que Evergreen es una opción rentable con un costo-beneficio de $1,27 y con mejores características de planta y fruto. Este estudio sugiere la aplicación del fertilizante Evergreen en la etapa de crecimiento y floración del cultivo de pepino dado que representa mejores ingresos por hectárea, un mejor costo-beneficio y mayor porcentaje de ganancia respecto a los demás fertilizantes foliares.

Palabras clave: Altura de planta; costo-beneficio; Fertilizantes; Pepino; análisis económico

ABSTRACT

Cucumber production in the Amazon region of Ecuador has intensified in recent years due to the ideal climatic conditions for this crop. In the Nuevo Paraíso parish in the province of Orellana, cucumber is grown in small areas (>1 ha) for local consumption. The producers have seen the need to increase their yields by applying foliar fertilizers. The purpose of this study was to compare the performance of the cucumber crop using three types of commercial foliar fertilizers with their respective economic analysis. The pilot test was carried out in a 1200 m2 field where Evergreen (2.5 cm/2L), Metalasote (2.5 cm/2L), and Agrostemin (1gr) fertilizers were

applied, evaluating plant height, number of leaves and flowers, stem diameter and fruit characteristics at 22, 37 and 49 days and comparing it with the control. The findings showed that Evergreen is a cost-effective option with a cost-benefit of $1.27 and better plant and fruit characteristics. This study suggests the application of Evergreen fertilizer in the growth and flowering stage of the cucumber crop since it represents better income per hectare, a better cost-benefit, and a higher profit percentage than other foliar fertilizers.
Keywords: Plant height; cost-benefit; fertilizer; cucumber; economic analysis.

INTRODUCCIÓN

La producción y cultivo de pepino (*Cucumis sativus* L.*)* es una actividad agrícola ampliamente practicada en muchos países del mundo. En el año 2021, se produjeron alrededor de 93.5 millones de toneladas, siendo este el año con la mayor producción registrada a nivel mundial. Se estima que alrededor de 198 países son productores de pepino, y entre los cinco principales productores se encuentran China en el primer lugar, con una producción de 75.548 millones de kilos, seguido por Turquía con 1.890 millones, Rusia con 1.649 millones, Ucrania con 1.079 millones y México con 1.039 millones de kilos [1].

El pepino es una hortaliza importante y uno de los miembros más populares de la familia Cucurbitaceae [2]. Se considera que es una de las hortalizas más antiguas cultivadas por el hombre, con registros históricos que se remontan a hace 5.000 años [3]. La necesidad de formas renovables de energía y la reducción de los costes de fertilización de los cultivos han reactivado el uso de abonos orgánicos en todo el mundo [4]. Los abonos orgánicos pueden sostener los sistemas de cultivo mediante un mejor reciclaje de nutrientes y la mejora de los atributos físicos del suelo [5]. Se ha recomendado el uso complementario de fertilizantes orgánicos con inorgánicos para mantener los cultivos a largo plazo en los trópicos [6]. Los nutrientes de los fertilizantes inorgánicos mejoran el establecimiento de los cultivos mientras que los de la mineralización de los abonos orgánicos mejoran el rendimiento cuando se combinan ambos fertilizantes [7].

La mayor producción de pepino en el Ecuador registrada ha sido de 4.512 toneladas y ocupan el puesto 92 a nivel mundial. Aunque se considera un producto no tradicional en los cultivos estacionales del país, la mayor producción de pepino se concentra en las regiones costeras del Ecuador, principalmente en las provincias de Manabí, Santa Elena y Guayas. Sin embargo, también se cultiva en pequeñas cantidades en los valles cálidos de la sierra y en algunas áreas de la región Amazónica, aunque su producción en esta última región es limitada [8]. En la Amazonía ecuatoriana, el cultivo de pepino es altamente demandado debido a su popularidad como hortaliza. Sin embargo, la producción de pepino en esta región es limitada debido a las condiciones climáticas principalmente (elevada humedad (94%) y temperatura (32°C). Estudios realizados en la provincia de Orellana han determinado que es posible cultivar pepino en estas condiciones, pudiendo haber mejoras en la producción [9].

Específicamente, en la provincia de Orellana, en la región amazónica de Ecuador, la producción de pepino ha experimentado un notable crecimiento en los últimos años, pero este cultivo es fundamental llevarlo a cabo mediante prácticas sostenibles que minimicen el impacto ambiental y promuevan la conservación de los recursos naturales en la región [10]. Concretamente, en la parroquia Nuevo Paraíso, no se lleva a cabo la siembra de pepino a gran escala, sino más bien en pequeñas parcelas para consumo local a base de fertilizantes orgánicos. Estudios de suelos de la zona han indicado condiciones edafológicas propicias para la producción de pepino debido a concentraciones adecuadas de nutrientes. Esto podría ofrecer una oportunidad económica para que los pequeños agricultores [11] de la parroquia mejoren el desempeño del cultivo de pepino incorporando fertilizantes inorgánicos en el proceso productivo del cultivo

El cultivo de pepino es atractivo para muchos agricultores debido a su capacidad de adaptación a diferentes tipos de suelos y climas, lo que permite su cultivo en diversas regiones. Sin embargo, es importante tener en cuenta que cada región puede requerir prácticas de cultivo y manejo específicas para maximizar su rendimiento. Según la FAO el 46,21% y 46,27% de los participantes de un estudio indicaron que la fertilización adecuada y periódica en pepino, en tiempos oportunos, solamente es necesario, siempre y cuando se cuente con una asesoría profesional para determinar la composición adecuada del fertilizante [12].

Los fertilizantes son sustancias que proporcionan nutrientes esenciales a las plantas para mejorar el crecimiento y rendimiento de los cultivos. Contienen diferentes macroelementos como nitrógeno, fósforo, potasios esenciales para el crecimiento de las plantas y microelementos que son absorbidos por las raíces y utilizados en la síntesis de proteínas y otros compuestos esenciales[13]. Los fertilizantes también pueden mejorar la calidad de los cultivos y aumentar su resistencia a enfermedades y estrés ambiental[14]. La fertilización es un factor crítico en la agricultura, ya que proporciona los nutrientes necesarios para el crecimiento y desarrollo óptimo de las plantas. Por lo tanto, llevar a cabo una evaluación de la aplicación de diferentes fertilizantes en el rendimiento del cultivo de pepino puede ser beneficioso para determinar la estrategia de fertilización más efectiva y obtener los mejores resultados en términos de productividad, calidad y retorno de inversión.

En base a lo anteriormente mencionado, el presente estudio hipotetiza que los fertilizantes inorgánicos aplicados mejoran no solamente a altura de la planta sino también incrementa el número de flores y hojas, así como el diámetro del fruto y las características de peso, largo y número de furtos por planta. El propósito de este estudio fue comparar tres tipos de fertilizantes ofertados en el mercado nacional sobre el desempeño del cultivo de pepino realizando el respectivo análisis económico a fin de determinar el mejor costo-beneficio. Lo anterior permite a los agricultores mejorar la calidad de sus cosechas y la rentabilidad del cultivo en la parroquia Nuevo Paraíso

MATERIALES Y MÉTODOS

La investigación se realizó en el terreno del señor Bequer Aguirre (Figura 1), ubicado en el Km 8 de la parroquia Nuevo paraíso del cantón Orellana posicionada en las coordenadas, latitud 0° 22’ 9,5” S y una longitud de 77° 1’ 26.6” E. El terreno posee una superficie de 1200 m^2 y se encuentra a una altitud de 282 msnm. La zona donde se encuentra el terreno presenta temperaturas entre 25 a 36°C con precipitaciones de 2650 mm/año entre marzo a junio y 4500 mm/año entre octubre a diciembre, una humedad relativa media del 81% y 1217 mm/año de evo transpiración.

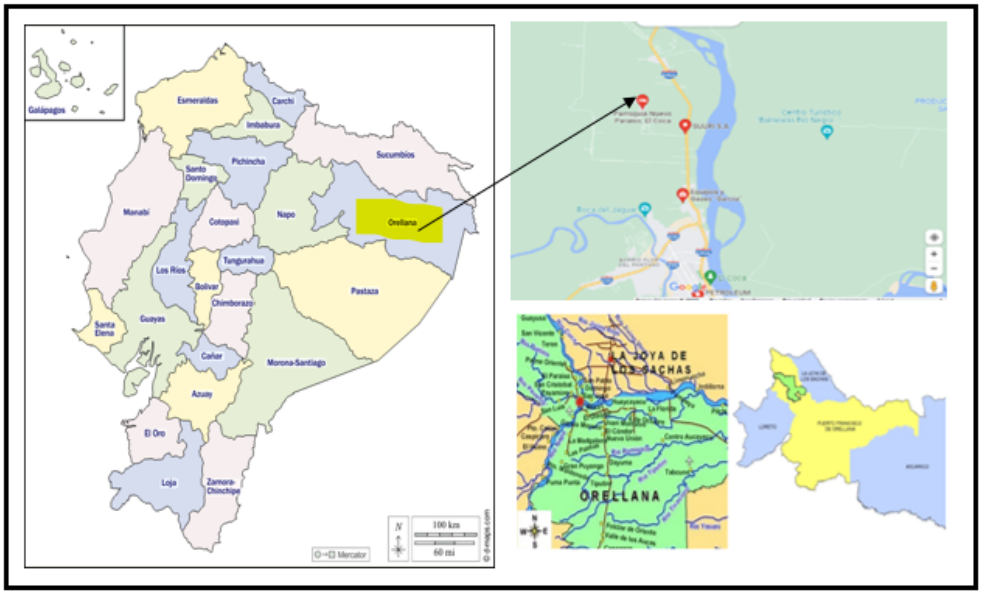

Figura 1. Localización del sitio de estudio

Se trabajó en 156 m^2 netos de los 1200 m^2 que tiene el terreno. Antes de iniciar la prueba piloto, se realizó una limpieza exhaustiva del terreno y se tomaron ocho muestras de suelo siguiendo una forma de zigzag por todo el terreno. Estas muestras fueron enviadas al Instituto Nacional de Investigaciones Agropecuarias (INIAP) de la ciudad de Quito para su evaluación. Se determinó que el suelo tuvo una textura “franca”, con un nivel de pH de 6.14 y con deficiencia de calcio. En base a ello, se decidió aplicar cal a todo el terreno a

manera de enmienda de esta deficiencia. Una vez preparado el suelo, se desinfectaron las bandejas de germinación y se colocaron semillas certificadas de la empresa AGROSAD. Las semillas se remojaron diariamente durante cuatro días hasta que germinaron y desarrollaron las tres primeras hojas donde alcanzaron una altura aproximada de 7 cm hasta ser trasplantadas al lugar definitivo. Una vez que cumplieron estas dos características, las plantas se sembraron en camas de dimensiones (4,20 m de largo por 1,6 m de ancho) con una separación de 1,6 m entre camas. La distancia de siembra fue de 20 m entre hileras y 1,5 m entre plantas. La siembra se realizó al inicio del periodo lluvioso (marzo-julio), aplicando un diseño completamente al azar. Dentro de cada cama se sembraron dos hileras de pepino y en cada hilera se ubicaron 9 plantas, teniendo un total de 18 plantas por cama. Las plantas se sembraron en un total de 12 camas. En la tabla 1, se visualiza las características de las unidades experimentales.

Características de las unidades experimentales	**unidades**
Unidades experimentales	10
Número de repeticiones	3
Número de tratamientos	4
Número de plantas por tratamiento	54
Número de plantas por repetición	10
Número de plantas en la investigación	216
Área total de ensayo	156 m2

Tabla 1. Características de las unidades experimentales

Durante la etapa de crecimiento y floración del cultivo se aplicaron tres tipos fertilizantes correspondientes a cada tratamiento (Tabla 2). Estas aplicaciones se realizaron cada ocho días, con un complemento de Yaramila para todas las plantas.

Tratamientos	**Nombre comercial**	**Dosis**	**Nombre**
L1	Evergreen	2.5 ml/2 litros	Evergreen
L2	Metalasote	2.5 ml/2 litros	Metalasote
L3	Agroestemin	1g	Ácidos húmicos
L4	Testigo	ninguna	Testigo

Tabla 2. Tratamientos aplicados en el sitio de estudio.

Una vez que las plantas alcanzaron una altura de 10 cm, se realizó la labor de tutorado para brindar soporte y favorecer el crecimiento vertical. Asimismo, se llevaron a cabo aplicaciones regulares de insecticidas para prevenir y controlar posibles plagas en el cultivo. La evaluación de los fertilizantes se los realizó a los 22, 37 y 49 días después del día de trasplante.

Para el conteo del número de hojas y flores se consideró los días fenológicos de la planta; es decir, al día cero (del trasplante), el día 22, día 37 y día 49. El conteo fue realizado manualmente eligiendo al azar el 60% de las plantas sembradas en cada cama durante días soleados en las primeras horas de la mañana (7 am) y registrando los datos en una libreta de campo. La altura de las plantas se midió con una regla matemática desde el día del trasplante, tomando en cuenta que la medida comenzó desde la base de la planta hasta el ápice de ésta. Se eligió el 60% de las plantas al azar sembradas en cada cama; estas plantas fueron otras, que las que se midió el número de hojas. Para el diámetro del tallo, se midió por medio de un calibrador de plástico de 1500 mm de modelo vernier obteniéndose la medida en cm^2. Estas mediciones fueron realizadas en otras plantas diferentes a la de las dos variables anteriores y realizadas a las primeras horas de la mañana (7am). En cuanto a la evaluación de los frutos, se tomaron medidas en cada cosecha, realizando un total de cuatro cosechas. Se

obtuvo un valor promedio para el número de frutos cosechados por planta, largo, diámetro y el peso de los frutos. Se seleccionó el 60% de plantas sembradas por cada cama. Toda la información recolectada en campo fue procesada en el programa IBM SPSS Statistics 26/libre 1989-2019 software estadístico.

RESULTADOS

Altura de planta

En la Tabla 3 se presentan las mediciones de la altura de las plantas de pepino en cuatro momentos distintos (al día 1, 22, 37 y 49), las cuales fueron medidas desde el ras del suelo hasta el ápice de la planta. En el día 1, se observó que el tratamiento L1 tuvo la mayor altura seguido por el tratamiento L4, L2 y L3. Al día 22, el tratamiento L1 se mantuvo con la mayor altura, seguido de los tratamientos L2, L3 y L4. A los 37 días y 49 días, los tratamientos se mantuvieron en este mismo orden, evidenciándose diferencias significativas en la altura de la planta, entre L1 y L2 con los tratamientos L3 y L4.

Tratamiento	Al día 1	A 22 días	A 37 días	A 49 días
L1	6,50 ± 0,09 **b**	12,83 ±0,17 **c**	111,83 ± 1,30 **c**	137,23 ± 2,80 **b**
L2	6,13 ± 0,10 **ab**	10,19 ±0,43 **b**	96,33 ± 1,92 **b**	129,17 ± 2,67 **b**
L3	5,87 ± 0,11 **a**	8,27 ± 0,14 **a**	86,83 ± 1,72 **a**	119,67 ± 2,42 **a**
L4	6,27 ± 0,12 **b**	8,10 ±0,14 **a**	81,83 ± 1,16 **a**	114,83 ±2,38 **a**

Las letras en minúscula (a,b) representan diferencia significativa de acuerdo con la prueba de Tukey (p<0,05).

Tabla 3. Altura de planta de pepino por tratamiento

Número de hojas

En la figura 2, se registraron los datos correspondientes al número de hojas para los diferentes tratamientos de fertilizantes. El número de hojas fue similar para todos los tratamientos en el día 22, sin embargo, al día 37, el número de hojas fue mayor con el tratamiento L1 (27 hojas), en relación con los demás tratamientos. Finalmente, al día 49, el número de hojas siguió siendo mayor para el tratamiento L1 (34 hojas), seguido de L2, L4 y L3, evidenciando diferencias significativas entre L1 y los otros tratamientos, así como entre L2 con L3 y L4.

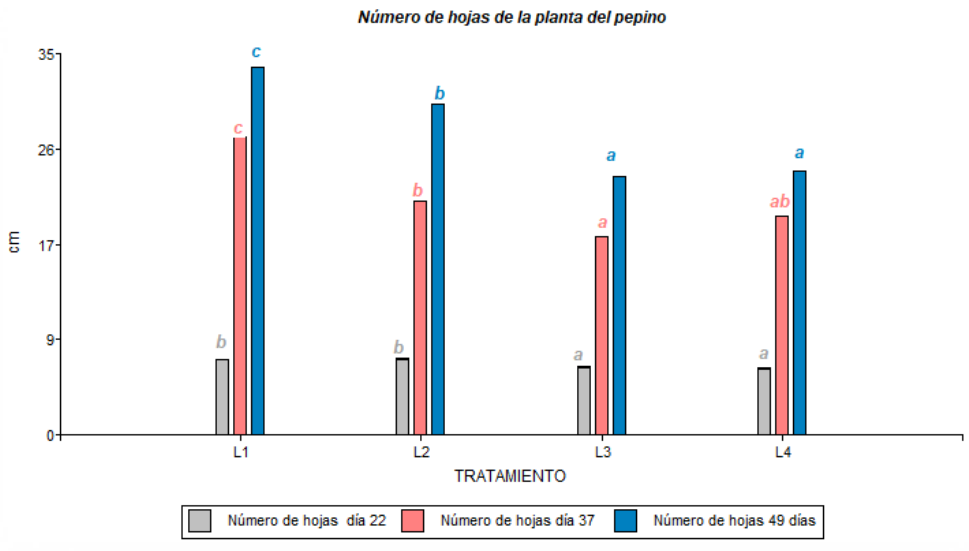

Figura 2. Número de hojas de pepino por cada tratamiento medidas en diferentes días

Diámetro del tallo

Según los resultados obtenidos después de 22 días, se observó una diferencia significativa en el diámetro del tallo entre los tratamientos. Específicamente, el tratamiento L2 mostró un mayor diámetro de tallo en esta etapa, seguido por el tratamiento L1, L3, y el tratamiento L4. Sin embargo, en los días 37 y 49, se produjeron cambios en el orden de los tratamientos, logrando el tratamiento L1 el mayor diámetro (11,17±0,20 cm) frente a los demás tratamientos. El tratamiento L2 registró un diámetro de 10,73 ± 0,14 cm, seguido de L3 (9,63 ±0,17) y L4 (9,40 ± 0,09 cm). Similarmente a las características anteriores, se evidenciaron diferencias significativas entre los dos primeros tratamientos (L1 y L2) frentes a los dos últimos (L3 y L4).

Tratamiento	A 22 días	A 37 días	A 49 días
L1	0,51 ± 0,01**b**	1,25 ± 0,03 **b**	11,17 ±0,20 **b**
L2	0,53 ± 0,01 b	1,14 ± 0,03 b	10,73 ± 0,14 b
L3	0,43 ± 0,01 a	0,89 ± 0,05 a	9,63 ±0,17 a
L4	0,41 ±0,02 a	0,90 ± 0,01 a	9,40 ± 0,09 a

Las letras (a,b) en minúscula representan las diferencias significativas de acuerdo con la prueba de Tukey ($p<0,05$).
Tabla 4. Diámetro del tallo de pepino por tratamiento

Número de flores

En la figura 3, se presentan los datos correspondientes al número de flores bajo la aplicación de los diferentes fertilizantes. Se pudo observar que os días 22 y 37, el tratamiento L1 mostró un mayor número de flores, seguido por el tratamiento L2, L3 y L4. Al día 37, se mantuvieron los tratamientos L1 y L2 con mayor número de flores, mientras que el tratamiento L4 superó al L3 en esta etapa. Finalmente, al día 49 el tratamiento L2 fue el que más flores se contabilizó (23) con respecto a los demás tratamientos, evidenciando diferencias significativas entre todos los fertilizantes.

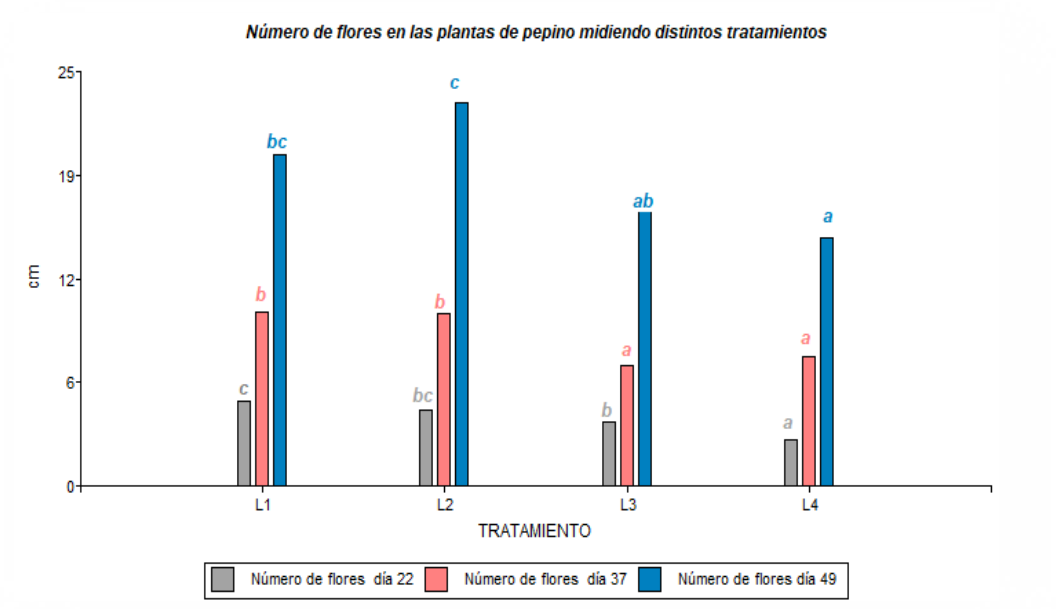

Figura 3. Número de flores de pepino por cada tratamiento

Medición del fruto

La tabla 5, evidenció que en todas las características con respecto al fruto (largo, diámetro, peso, número), el tratamiento L1 obtuvo los mejores resultados, seguido del tratamiento L2. El tratamiento L4 dio mejores resultados que el L3 en todas las características, exceptuando en el largo del fruto, sin embargo, esta diferencia no fue significativa.

Tratamiento	Números de frutos por planta	Largo (cm) promedio del fruto	Diámetro (cm) promedio del fruto	Peso (kg) promedio del fruto
L1	4,47± 0,20 b	21,71 ± 0,09 c	5,48 ± 0,07 b	0,50 ± 0,01 c
L2	3,67 ± 0,15 a	19,63 ± 0,15 b	5,00 ± 0,06 a	0,46 ± 0,01 a
L3	3,17 ± 0,15 a	19,39 ± 0,08 a	4,86 ± 0,11 a	0,43 ± 0,01 a
L4	3,50 ± 0,17 a	19,06± 0,13 a	5, 07 ± 0,05 a	0,45 ± 0,01 ab

Las letras en minúscula representan diferencia significativa de acuerdo con la prueba de Tukey ($p<0,05$).
Tabla 5. Medición del fruto del pepino por tratamiento

Finalmente, se realizó un análisis económico del cultivo de pepino para los diferentes tratamientos aplicados en campo, a fin de determinar el de mayor rentabilidad. Para el análisis económico se tomó en cuenta la inversión inicial del saco de fertilizante el cual tuvo un costo promedio de $38. En base a esta inversión y sumada al costo de producción ($15) se determinó el costo total por tratamiento. Los ingresos promedio por cada fertilizante estuvieron en el rango entre $USD 46,00 a $73,50 siendo el que obtuvo mayores ingresos el tratamiento L1 con una producción de 147 pepinos. Finalmente, se calculó el costo-beneficio de cada tratamiento para determinar cuál fue el más rentable.

Tratamiento	Ingresos/ha	Costo /ha	Costo beneficio	Porcentaje
Fertilizantes Evergreen (L1)	$ 73,50	$46,76	$ 1.57	27.50%
Fertilizante Agrostemin (L2)	$ 55,00	$35.93	$1,53	26,80%
Fertilizantes Metalosate (L3)	$ 47,50	$40,28	$1,18	20.67%
Testigo (L4)	$ 46	$32,38	$1.43	25.04%
Total	$222	$155,35	$5,71	100%

Tabla 6. Análisis económico de cada tratamiento

Se determinó que el fertilizante Evergreen (L1) tuvo una mayor rentabilidad, con un costo-beneficio de $1,57 y un porcentaje de ganancia del 27,50%, seguido del fertilizante Agrostemin (L2), con un ingreso de $1,53 y un porcentaje de ganancia del 26,80%. Como una tercera alternativa de uso, fue para el testigo (L4), con un ingreso de $1,43 y un porcentaje de ganancia del 25,04% y finalmente el fertilizante Metalosate el cual obtuvo el costo-beneficio más bajo ($1,18) con un porcentaje de ganancia inferior (20,67%) que los demás fertilizantes.

DISCUSIÓN

El estudio permite un reconocimiento amplio sobre los beneficios de los fertilizantes foliares en estudio, analizando cuales han obtenido mejores resultados que otros, así como contrastando con lo que se ha obtenido en otros estudios similares. En cuanto a la altura de la planta, en el día 49, fueron entre 114 y 137 cm que se asemejan con los resultados de un estudio llevado a cabo por Reyes et al.[15] en el cual reportaron la altura de la planta a los 45 días entre 113 y 129 cm. La medición de la altura es importante para monitorear el crecimiento y desarrollo de las plantas, así como para planificar el espacio en el cultivo y prevenir problemas como la densidad poblacional.

El número de hojas es otro aspecto relevante que se midió en los días 22, 37 y 49. El número de hojas contabilizadas entre el día 37 y 49 fueron entre 27 y 33 hojas, valores similares a las presentados por Marcano et al.[16], en donde a los 42 días registró un promedio de 29 hojas. Esto indica un patrón durante el desarrollo de las plantas de pepino durante la quinta y sexta semana. El registro y conteo preciso del número de hojas son fundamentales para evaluar el progreso vegetativo y la salud de las plantas, que a su vez sirve como una interfaz para controlar señales ambientales como la luz, temperatura, agua e insectos[17]. Una mayor cantidad de hojas indica un crecimiento vigoroso y saludable, mientras que un número reducido podría sugerir estrés por deficiencia de agua, deficiencias nutricionales o la presencia de plagas o enfermedades[18]. Por tanto, esta variable es esencial para tomar decisiones informadas en el manejo y cuidado de los cultivos.

El diámetro del tallo en el día 49 también mostró consistencia con los hallazgos de Erreyes-Jara et al. [8] quienes estudiaron el rendimiento del cultivo de pepino bajo condiciones de mulch plástico y reportaron diámetros similares en los días 30 y 65; lo que coincide con el día de medición número 49 para el presente estudio. Estudios han reportado que la aplicación de Evergreen en pepino a una dosis de 1 L/ha alcanzaron diámetros de 5 cm y una longitud de 23,9 cm[19]. Sin embargo, otras investigaciones encontraron que cuando se aplicó el fertilizante Evergreen a una dosis mayor de 1.5 L ha^{-1}, los frutos tuvieron mayores diámetros ecuatoriales y polares con respecto a fertilizantes de origen orgánico[20]. A una dosis de 1.5 L el diámetro obtenido del fruto fue de 5.52 cm, similar al valor obtenido en el presente estudio que fue de 5.48 cm a pesar de que se aplicó una dosis mayor (2.5 cm). Esto indica que no necesariamente una dosis mayor tendrá una relación directa y lineal con el aumento del diámetro del fruto.

El número de flores también fue evaluado en el día 49, revelando diferencias entre los tratamientos L1, L2, L3 y L4. Estos resultados contrastan con los hallazgos de Hidalgo et al[21]. donde el uso de biofertilizantes mostró los mejores resultados en cuanto al número de flores. Sin embargo, en el presente estudio, el tratamiento L2 destacó con un número más considerable de flores, lo que sugiere una mayor efectividad en la producción floral en comparación con los otros tratamientos. La medición precisa y detallada de las flores es esencial para comprender la salud de las plantas, la producción potencial y la eficacia de los tratamientos aplicados, lo que permite a los agricultores tomar decisiones más informadas para obtener un cultivo exitoso y rentable.

En cuanto a la evaluación de los frutos en cada cosecha, se observaron diferencias significativas en el diámetro promedio del fruto entre todos los tratamientos. Estas diferencias pueden influenciar la calidad final del fruto. La calidad final a su vez puede verse influenciado por las características propia de la hortaliza como el color sabor, defectos, textura, firmeza, estado de madurez, composición nutricional, entre otras[22]. A la luz de los resultados, el diámetro máximo del pepino registrado fue de 5.48 cm a los 49 días, valor que fue mayor al reportado por Marcano et al, donde registraron diámetros entre 2.08 y 3.78 cm[16]. Asimismo, el peso promedio del fruto que fue entre 430-500 g se encontró dentro del rango informado por Chacón & Monge[1]. En términos de número de frutos por planta, con Evergreen se contabilizaron en promedio 4 frutos al día 49, estos resultados son relativamente menor a los obtenidos por Solís [23] sin embargo, la longitud del fruto fue similar durante la última etapa de desarrollo (24.75 cm vs 21,71 cm). De igual manera el diámetro del fruto (5,65 cm) concuerda con lo medido en el presente estudio (5,48 cm). Estas concordancias con estudios previos validan y respaldan la precisión y consistencia de los datos experimentales obtenidos en este estudio.

En términos de costo-beneficio, se identifica que el tratamiento L1 ofrece la mayor rentabilidad, seguido por el L2, L4 y L3. Estos datos pueden ser valiosos para los agricultores al tomar decisiones informadas sobre qué

tratamiento es más eficiente en términos de ingresos y ganancias. Sin embargo, no se han reportado estudios que utilicen los mismos fertilizantes de prueba para poder contrastar los resultados de esta investigación, lo cual motiva a realizar más trabajos que impliquen este aspecto importante a considerarse dentro del cultivo de peino. Se enfatiza que para lograr una agricultura sustentable y amigable con el ambiente se recomienda no abusar del uso de fertilizantes comerciales foliares o de suelo, dado que su uso irracional y excesivo puede provocar contaminación ambiental, reducir la fertilidad de la tierra y afectar directa o indirectamente la salud humana[24]. Es por ello, que actualmente se esta dando paso a la nano fertilización como una alternativa a los fertilizantes químicos dada su capacidad para regular la liberación de nutrientes en función de la demanda del cultivo lo que aumenta la eficiencia de uso de nutrientes y reduce la contaminación ambiental [24,25].

CONCLUSIONES

En la parroquia Nuevo Paraíso de la provincia de Orellana, se llevó a cabo un estudio sobre el cultivo del pepino utilizando diferentes tratamientos de fertilizante. Se encontró que el tratamiento con la aplicación de Evergreen (L1) al 2.5 cm por cada 2 lt mostró el mejor desempeño del cultivo en relación con la altura de planta, número de hojas, diámetro del tallo, número de flores, número de frutos por planta, largo promedio del fruto, diámetro promedio del fruto y peso promedio del fruto. Con ello, se comprueba la hipótesis planteada inicialmente de que la aplicación de fertilizantes foliares no solamente mejora la altura de planta sino también otras características fenotípicas del cultivo de pepino. Este estudio sugiere la aplicación del fertilizante Evergreen en la etapa de crecimiento y floración del cultivo de pepino dado que representa mejores ingresos por hectárea, un mejor costo-beneficio y mayor porcentaje de ganancia respecto a los demás fertilizantes. Sin embargo, se sugiere no abusar del uso de fertilizantes de origen químico ya que su utilización excesiva puede generar contaminación ambiental y daño a la salud humana. Como futura línea de investigación, se enfatiza el estudio de los nano fertilizantes como una alternativa de agricultura verde para mejorar aun mas la eficiencia en el uso de nutrientes en cultivos.

Contribución de los autores: Conceptualización, Lourdes Aguirre-Cobeña.; Metodología, Lourdes Aguirre-Cobeña, Diego Salguero, Amanda Bonilla y Rodrigo Salazar.; Validación, Lourdes Aguirre-Cobeña y Rodrigo Salazar.; Análisis formal, Lourdes Aguirre-Cobeña y Diego Salguero.; Investigación, Lourdes Aguirre-Cobeña y Diego Salguero.; Análisis de datos Lourdes Aguirre-Cobeña, Amanda Bonilla y Rodrigo Salazar.; Escrito borrador del manuscrito, Lourdes Aguirre-Cobeña y Diego Salguero.; Revisión y edición, Lourdes Aguirre-Cobeña.; Supervisión, Rodrigo Salazar. Todos los autores han leído y aceptado la versión publicada del manuscrito.

Financiamiento: Esta investigación no recibió ninguna subvención específica de organismos de financiación de los sectores público, comercial o sin ánimo de lucro.

Agradecimientos: Los autores agradecen a los colegas de diversas disciplinas que aportaron con su conocimiento para la versión final del manuscrito.

Conflictos de interés: Los autores declaran no tener ningún conflicto de intereses.

REFERENCES

1. Chacón-Padilla K, Monge-Pérez J.E. Producción de pepino (Cucumis sativus L.) bajo invernadero: Comparación entre tipos de pepino. Tecnol. Marcha. 2020; 33:17-35.
2. Thoa, D.K. Cucumber seed multiplication and characterization. AVRDC/ARC Training Thailand. Research Report. 1998. Bangkok.
3. Wehner T.C, Guner N. Growth stage, flowering pattern, yield and harvest date prediction of four types of cucumber tested at 10 planting dates. Proc. xxvi IHC. Advances in Vegetable Breeding (Eds) J.D Mc.Creight and E. J Ryder Acta. Hort., 637, 2004. ISHS.

4. Ayoola O.T, Adeniran O.N. Influence of poultry manure and NPK fertilizer on yield and yield components of crops under different cropping systems in Southwest Nigeria. Afr. J. Biotechnol. 2006; 5:1336-1392.
5. El-Shakweer M.H.A, El-Sayad E.A, Ewees M.S. Soil and Plant analysis as a guide for interpretation of the improvement efficiency of organic conditioners added to different soils in Egypt. Commun. Soil Sci. Plant Anal. 1998; 29:2067-2088.
6. Ipimoroti R.R, Daniel M.A, Obatolu C.R. Effect of organic mineral fertilizer on tea growth at Kusuku Mabila Plateau Nigeria. Moor J. Agric. Res. 2002; 3:180-183.
7. Fuchs W, Rauch K, Wiche H.J. Effect of organic fertilizer and organo mineral fertilizing on development and yield of cereals. Abrecht- Thaer. Arch. 1970; 14:359-366.
8. Erreyes-Jara J.B, Montoya-Alejandro J, Luna-Romero Á.E. Rendimiento del cultivo de pepino (Cucumis sativus l.) bajo condiciones de mucho plástico, Ecuador. Rev. Cient Agroeco. 2023; 11: 44-51.
9. Ortiz K.M, Cachipuendo G.I. Evaluación de parámetros morfo-fisiológicos y productivos en el cultivo de pepino. Tesis de Grado, Universidad Estatal Amazónica, Lago Agrio, Ecuador.
10. Morán J.H, Pibaque M.S, Peñafiel J.F, Parrales J.E. Los recursos naturales y su incidencia en la responsabilidad social. Dominio de las Ciencias. 2021; 7: 1243-1261.
11. Olmedo P.J. Comportamiento agronómico del cultivo de pepino (Cucumis sativus) con diferentes dosis de biol en el cantón La Maná provincia de Cotopaxi. Tesis de grado, Universidad Técnica de Cotopaxi, Cotopaxi, Ecuador.
12. Adekiya A.O, Dahunsi S.O, Ayeni J.F, Aremu C, Aboyeji C.M, Okunlola F, Oyelami, A.E. Organic and in-organic fertilizers effects on the performance of tomato (Solanum lycopersicum) and cucumber (Cucumis sativus) grown on soilless medium. Sci. Rep. 2022; 12:12212.
13. Pahalvi H.N, Rafiya L, Rashid S, Nisar B, Kamili A.N. Chemical Fertilizers and Their Impact on Soil Health. En G. H. Dar, R. A. Bhat, M. A. Mehmood, K. R. Hakeem (Eds.), Microbiota and Biofertilizers, Vol 2: Ecofriendly Tools for Reclamation of Degraded Soil Environs (pp. 1-20). 2021. Springer International Publishing.
14. Diacono M, Persiani A, Testani E, Montemurro F, Ciaccia, C. Recycling Agricultural Wastes and Byproducts in Organic Farming: Biofertilizer Production, Yield Performance and Carbon Footprint Analysis. Sustainability. 2019; 11: 3824.
15. Reyes J, Luna R, Reyes M, Yépez A, Abasolo F, Espinosa K, López R, Vázquez V, Zambrano D, Cabrera D, Torres, J. Uso del humus de lombriz y jacinto de agua sobre el crecimiento y desarrollo del pepino (*Cucumis sativus, L*). Biotecnia. 2017; 2: 30-35.
16. Marcano C, Acevedo I, Contreras J, Jiménez O, Escalona A, Pérez P. Crecimiento y desarrollo del cultivo pepino (*Cucumis sativus L.*) en la zona hortícola de Humocaro bajo, estado Lara, Venezuela. Rev Mex Cienc Agríc. 2012; 3(8):1629-1636.
17. Li J, Cao J, Wang C, Hao N, Zhang X, Liu M, Wu, T. Research Progress on the Leaf Morphology, Fruit Development and Plant Architecture of the Cucumber. Plants. 2022; 11(16), 2128.
18. Jagadish S.V.K, Way D.A, Sharkey T.D. Plant heat stress: Concepts directing future research. Plant, Cell & Environment. 2021; 44(7): 1992-2005.
19. León J.A. Respuesta del cultivo de pepino (Cucumis sativus l.) al empleo de productos orgánicos en la zona de Quevedo. 2015. [Tesis de Grado, UTEQ].
20. Holguín R.V. Estudio de tres biorreguladores orgánicos en comparación con un fertilizante foliar comercial, en el cultivo de pepino (Cucumis sativus). 2021. [Tesis de Grado, UTEQ].
21. Hidalgo P, Sindoni M, Medina Y, Castellano G. Efecto de diferentes abonos químicos y orgánicos sobre el crecimiento y rendimiento del pepino (*Cucumis Sativus*). Geomina. 2014; 42(64): 139-141.
22. Gebretsadik K, Qiu X, Dong S, Miao H, Bo K. Molecular research progress and improvement approach of fruit quality traits in cucumber. Theoretical and Applied Genetics. 2021;134(11):3535-3552.
23. Solís, E. V. (2018). Estudio comparativo de la aplicación de varios bioestimulantes en el cultivo de Cucumis sativus (pepino) bajo riego por goteo. [Tesis de Grado, Universidad Estatal del Sur de Manabí].
24. Rahman Md. H, Haque K.M.S, Khan Md. Z.H. A review on application of controlled released fertilizers influencing the sustainable agricultural production: A Cleaner production process. Environ. Technol. Innov. 2021; 23: 101697.
25. Zulfiqar F, Navarro M, Ashraf M, Akram N.A, Munné-Bosch S. Nanofertilizer use for sustainable agriculture: Advantages and limitations. Plant Sci. 2019; 289: 110270.

Received: October 9th 2023/ **Accepte**d: January 15th 2024 / **Published:**15 February 2024

Citation: Aguirre-Cobeña L, Salguero-Ramos D, Bonilla-Bonilla A, Salazar- López R. Evaluación del desempeño del cultivo de pepino (*Cucumis sativus*) frente a tres fertilizantes foliares en la parroquia Nuevo Paraíso, Orellana, Ecuador. Revis Bionatura 2024; 9 (1) 11. http://dx.doi.org/10.21931/RB/2024.09.01.11

Additional information Correspondence should be addressed to *.aguirre@espoch.edu.ec*
Peer review information. Bionatura thanks anonymous reviewer(s) for their contribution to the peer review of this work using https://reviewerlocator.webofscience.com/

Bionatura ISSN. First 13909355 Ecuador. **Scopus coverage years**: from 2016 to the present

Bionatura
Ibero-American Journal of Biotechnology and Life Sciences

Article

Heart failure prognostic algorithm using Spectral Analysis and MATLAB software.

Siza Moposita Segundo Fabián [1], *Sáez Paguay Miguel Ángel* [2], *Fiallos Godoy Yesenia Maricela* [3] *Ricardo Fabián Siza Gualpa* [4],

[1] *Escuela Superior Politécnica de Chimborazo, Facultad de Ciencias. Orellana, Ecuador.*

[2] *Escuela Superior Politécnica de Chimborazo, Facultad de Recursos Naturales. Orellana, Ecuador.*

[3] *Hospital General Docente de Ambato. Ambato, Ecuador.*

[4] *Escuela Superior Politécnica de Chimborazo, Facultad de Ciencias. Riobamba, Ecuador.*

**Correspondence: fabian.siza@espoch.edu.ec; Tel.: +593 0984259193 SMSF*
Available from. http://dx.doi.org/10.21931/RB/2024.09.01.12

ABSTRACT

Fourier analysis for biological signals is based on the use of the infinite sum of sines and cosines that allows modeling: the periodic functioning of the heart, its amplitude, frequency, and phase period, transforming these signals into images called ECG, based on studies and programs that model the ideal functioning of the heart. In this work, a mathematical algorithm has been designed to predict the cardiac pathology called bradycardia, which relates the prolongation of the monthly QT interval in the order of 10-4 seconds/month in a time of 10 years with the ventricular alteration. MATLAB software and spectral analysis are used to contrast the spectrum without pathology, which contains harmonics of greater amplitude, with a spectrum already with pathology that reaches heart failure, where the most significant number of harmonics are grouped in the first values, and then the model with an exponential function the delay of the QT interval in the ECG, concluding that up to 40 months after the onset of the pathology, the patient can counteract the disease. In comparison, by 80 months, difficulties arise, even the disease becomes irreversible in the last months, and the blood-propelling organ ceases to function.

Keywords: Heart Failure Prognostic, Bradycardia, Fourier Series, Spectral Analysis.

INTRODUCTION

The increase in life expectancy brings more significant exposure to risk factors, which leads to greater exposure to adverse events; cardiovascular diseases affect the heart and blood vessels, being the leading cause of mortality worldwide, exceeding 200 deaths per 100 000 inhabitants, with 13.13 % corresponding to myocardial infarction, 2.24 % to arterial hypertension and 2.08 % to other ischemic pathology. In Latin America, they

are the leading cause of morbidity, mortality, and disability [1].
Heart failure is a prevalent syndrome indicating the terminal stage of several cardiovascular diseases; the heart does not adequately pump the blood volume to meet tissue requirements. In Western countries, it is the leading cause of hospitalization in older adults and is associated with high healthcare costs, with a hospital stay ranging from 4 to 11 days. This pathology has a poor prognosis, with a hospital mortality rate of 4-7%. The mortality rate after one year of hospitalization is 36% [2]

It is estimated that about 23.3 million people will die from cardiovascular disease in 2030. Due to the aging population in Latin America, mortality from cardiovascular disease will increase. However, there is little information on the assessment of cardiovascular disease risk, which is defined as "a person's probability of dying or suffering major cardiocirculatory events." [1,3]

Controlling cardiovascular disease is a public health priority, and predictive methods adequately designed to intervene in this pathology and guide the implementation of preventive measures and appropriate treatments are needed.

In this study, a basal ECG reading is considered, which complies with a sinus rhythm, its wave values, and the segments that compose them. To plot the ECG in MATLAB, all this information and basal measurements are considered to obtain an ECG without cardiac pathology and through a sequence of steps to observe what happens if there is an alteration in the cardiac muscle in a given time. Heart failure is the target pathology of the algorithm that will develop in a 10-year interval in people older than 45 years who do not have any treatment.

A mathematical algorithm for predicting heart disease by spectral analysis will provide the medical sector with a solution to the severe problems caused by heart diseases since it is currently impossible to predict the development of cardiovascular problems due to the lack of suitable equipment. In this study, a series of equations are considered to model the periodic behavior of the human anatomy, one of which accurately reproduces the heartbeat in an electrocardiogram.

The purpose of deriving a mathematical algorithm to predict cardiac pathology using spectral analysis and MATLAB software involves only the QT interval. It is considered that periodic beats govern healthy hearts, so ventricular changes are called bradycardia (prolonged bradycardia) of +1 QT interval and would be deemed to have a relatively slight monthly increase, on the order of 10-4 seconds/month. The average interval before heart failure (HF) is 10 years from the first changes in the regular cardiac function QT segment.

The proposed hypothesis is: "The study of spectral analysis and using MATLAB allows the derivation of predictive algorithms for cardiology," for which it is necessary to model the phenomenon from the beginning using numerical methods based on the interpolation of each segment, whether these: curves, straight lines, waves or triangles or strange curves, and in addition, one must use least squares, LaGrange interpolation, Newton interpolation among others to obtain the graph of the ideal electrocardiogram (ECG), then consider an exponential model of cardiac physiology to modify these equations.

MATERIALS AND METHODS

Signal processing is constantly evolving to facilitate the development of science and technology. The technique of Fourier analysis of biological signals is based on the use of periodic sine and cosine functions to model the function of different organs, including the ideal electrocardiogram. "Essentially, spectral methods decompose a stationary time series into a sum of a set of sequences of cyclic components with specific properties. In general, spectral analysis is called frequency domain analysis because frequency is a measure that expresses periodicity" [4]
The spectral analysis of a signal is not subject to a representation that generates results; instead, it is a sequence of analysis requiring a large amount of data. The periodic behavior of the body's heartbeat generates signals

that have their components, such as amplitude, frequency, phase period, and others, which have been transformed through the Fourier series to representations called Electrocardiogram ECG, which is an electrocardiograph that records the electrical activity of the heart [5]. This research procedure makes it possible to determine different forms of cardiovascular disease and supports the identification of the condition of the heart muscles. Consequently, spectral analysis can be used in the diagnostic stage of a seasonal adjustment procedure considering the following characteristics: Different spectrum representation models (frequency units, spectral density magnitude), where the powers associated with seasonality are located, the way the spectra of specific reactions are, how filters impact the spectrum and what differences are there between the spectral representation of stationary and integrated processes.

The instrument called an electrocardiograph is connected to the patient's skin through electrodes; the latter generates the electrocardiogram on a sheet of paper, which are distinguished: the P wave corresponding to atrial depolarization, the QRS wave corresponding to ventricular depolarization and the T wave corresponding to ventricular repolarization.

The usual electrocardiogram refers to an initial spectrum in the asymptomatic QT interval. These signals are not static due to age, gender, lifestyle, and hereditary characteristics. A time series can be understood as a set of real numbers represented by a combination of sines and cosine lines (or complex exponentials). Like time series, stochastic events can be exhibited by linear combinations (especially integrals) of trigonometric or complex exponential functions, albeit weighted by random coefficients. For the calculation of the coefficients of the Fourier series that allow modeling the physiological period of a normal heart, there are several studies, as well as the programming of its operation in software such as Scilab and MATLAB.

The calculation of the series that represents the ideal behavior of the heart has been developed in such a way that its calculated coefficients are then replaced in the general formula of the Fourier Series, which allows the use of an initial graph, which serves as a basis for comparison and diagnosis based on the alterations in the different wave segments that are forming the signal of the Electrocardiogram (ECG).

Given $f(t)$ as the general equation of the Fourier Series:

$$f(t) = \frac{1}{2}a_0 + \sum_{n=1}^{\infty}\left[a_n \operatorname{Cos}\left(\frac{2\pi nt}{T}\right) + b_n \operatorname{Sen}\left(\frac{2\pi nt}{T}\right)\right] \quad (1)$$

Where:

a_0, a_n, b_n They are Fourier coefficients, T is the period of the function, $\frac{1}{T}$ is the frequency of the function.

Integrating the equality in the interval $[-T/2, T/2]$, then we apply the orthogonality property to obtain the coefficients a_n, b_n

$$\begin{cases} a_n = \frac{2}{T}\int_{-T/2}^{T/2} f(t)\cdot \operatorname{Cos}\left(\frac{2\pi nt}{T}\right)dt \\ b_n = \frac{2}{T}\int_{-T/2}^{T/2} f(t)\cdot \operatorname{Sen}\left(\frac{2\pi nt}{T}\right)dt \end{cases} ; n \geq 1 \quad (2)$$

While the coefficient a_0 is as follows:

$$a_0 = \frac{2}{T}\int_{-T/2}^{T/2} f(t)dt \qquad (3)$$

"Indeed, it may happen that for certain functions the coefficients do not exist and therefore neither does the Fourier series nor the series exists and is divergent or that although it is convergent, it does not converge to the function." [6]

To analyze the signals of an electrocardiogram using the Fourier series, the spectrum analysis and the variation of its harmonics are used greatly, as well as the spectral analysis that allows the development of the present investigation.[7]. "Fourier series makes it possible to describe a signal, a function of time, as a superposition of simpler signals (sinusoids) of various frequencies multiples of the fundamental frequency. 1/T. The frequency spectrum measures the distribution of amplitudes or phases of each frequency. The process that quantifies the various intensities of each frequency is known as spectral analysis." [8]

Periodic signals are usually represented by a line graph parallel to the ordinate axis, which means the amplitude spectrum in the arrows of the signal.

ECG signal pre-processing technique

With the support of MATLAB software, a standard ECG signal is constructed and subjected to different alterations to draw some interesting conclusions about the effectiveness of the pathologies to be discussed in the next chapter. As a practical application, the standard values of the waves and pulses are counted to know the number of heartbeats in an ECG [9].

The ideal ECG signal is then compressed without losing critical information. Using segmentation and normalization, the most relevant characteristics of the waveform are detected, such as the QRS complex, P and T waves, and R wave peaks.

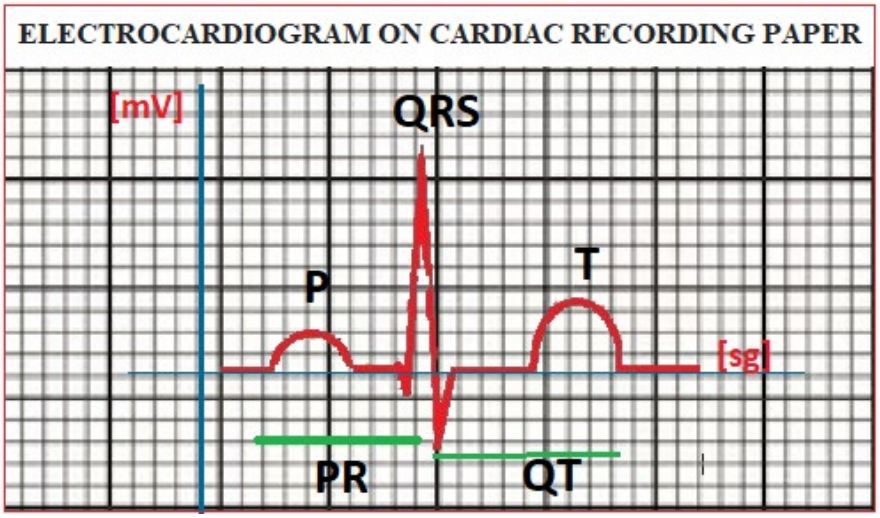

Figure 1. Code of an electrocardiogram signal using Matlab.

An electrocardiogram can be generated by the summation of triangular waves and half waves, which are visualized as an ideal electrocardiogram [10]

Applying the properties of the Fourier Series in the general equation, the coefficients for the triangular and half waves are derived.

Given the general equation:

$$f(x)=\left(\frac{a_0}{2}\right)+\sum_{n=1}^{\infty}a_n Cos\left(\frac{n\pi x}{T}\right)+\sum_{n=1}^{\infty}b_n Sen\left(\frac{n\pi x}{T}\right) \quad (4)$$

Where,

$$\begin{aligned} a_0 &= \left(\frac{1}{T}\right)\int_T f(x)dx \\ a_n &= \left(\frac{1}{T}\right)\int_T f(x)\text{Cos}\left(\frac{n\pi x}{T}\right)dx \rightarrow n = 1,2,3\ldots \\ b_n &= \left(\frac{1}{T}\right)\int_T f(x)\text{Sen}\left(\frac{n\pi x}{T}\right)dx \rightarrow n = 1,2,3\ldots \end{aligned} \quad (5)$$

Generation of periodic QRS complex portions of the ECG signal

It can be observed in an ECG period, the combination of 3 triangular waves and 2 half waves; each one of them represents the heart movement in different stages. 3 triangular waves form the QRS complex (Figure 2). [8]

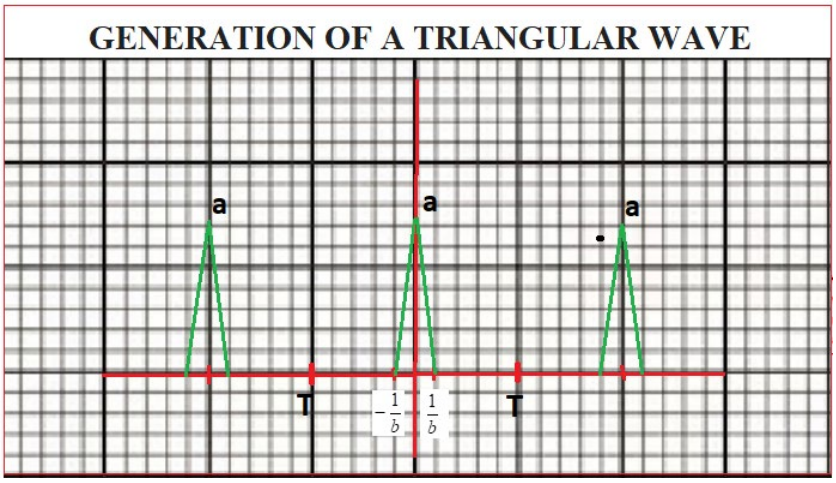

Figure 2. Data was generated to establish a triangle wave.

From equation (1), we have.

When x is between $0 < x < \left(\frac{1}{b}\right)$

Function is equal to $f(x) = \left(-\frac{bax}{T}\right) + a$

While if x is between $\left(-\frac{1}{b}\right) < x < 0$

Function is equal to $f(x) = \left(\frac{bax}{T}\right) + a$

$$a_0 = \left(\frac{1}{T}\right)\int_T f(x)$$
$$a_0 = \left(\frac{a}{b}\right) * (2 - b)$$
$$a_n = \left(\frac{1}{T}\right)\int_T f(x) \cdot \text{Cos}\left(\frac{n\pi x}{T}\right) dx$$
$$a_n = \left(\frac{2ab}{n^2\pi^2}\right) * \left(1 - \text{Cos}\left(\frac{n\pi x}{T}\right)\right)$$
$$b_n = \left(\frac{1}{T}\right)\int_T f(x) \cdot \text{Sen}\left(\frac{n\pi x}{T}\right) dx$$
$b_n = 0$ because it is an even function

$$f(x) = \left(\frac{a_0}{2}\right) + \sum_{n=1}^{\infty} a_n \text{Cos}\left(\frac{n\pi x}{T}\right) \quad (6)$$

Generation of periodic P waves of an ECG signal.

It can be observed that in an ECG period, in the combination of 2 half waves, each representing the heart movement in different stages. The QRS complex (Figure 1) is formed by 2 half waves known as P wave; and T wave; [8]

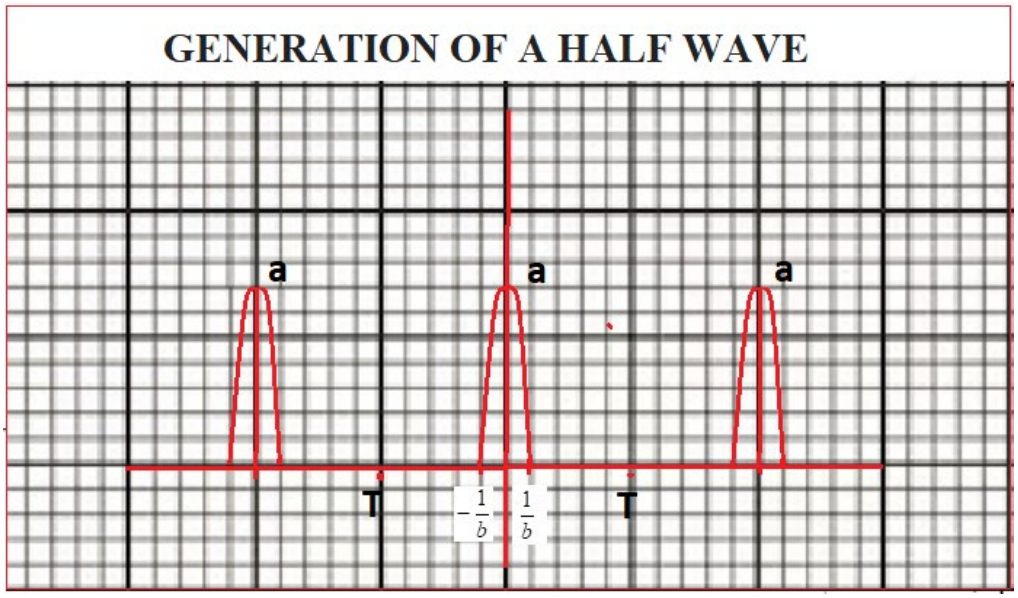

Figure 3. Data was generated to establish a half wave.

Starting from:

When x is between $-\frac{1}{b} < x < \frac{1}{b}$

$$f(x) = \text{Cos}\left(\frac{\pi bx}{2T}\right)$$

The coefficients of the series are analyzed:

$$a_0 = \frac{1}{T}\int_T \text{Cos}\left(\frac{\pi bx}{2T}\right)dx$$
$$a_0 = \frac{a}{2b}(2-b)$$
$$a_n = \frac{1}{T}\int_T \text{Cos}\left(\frac{\pi bx}{2T}\right)\text{Cos}\left(\frac{n\pi x}{T}\right)dx$$
$$a_n = \left(\frac{2ab}{i^2\pi^2}\right)\left(1-\text{Cos}\left(\frac{n\pi}{b}\right)\right)\text{Cos}\left(\frac{n\pi x}{T}\right)$$
$$b_n = \frac{1}{T}\int_T \text{Cos}\left(\frac{\pi bx}{2T}\right)\text{Sen}\left(\frac{n\pi x}{T}\right)dx$$
$b_n = 0$ because it is an even function

Therefore:

$$f(x) = \frac{a_0}{2} + \sum_{n=1}^{\infty} a_n \text{Cos}\left(\frac{n\pi x}{T}\right) \quad (7)$$

MATLAB and Signal Processing

Among the functions for signal processing, MATLAB has a wide variety of functions, such as ECG, convolution, matrix inversion, FFT, and DFT, among others [11].
Fourier states that "any continuous and periodic signal could be represented as the sum of a series of properly chosen sine waves". Sine waves are generated and summed.
The tools found in MATLAB allow the analysis and implementation of digital filters, including frequency response, group delay and phase delay [5]. In addition, filters can be implemented usingechniques in the frequency domain based on the FFT function [12].

ECG implementation in MATLAB

Heartbeat: 70	
- Breadth:	**- Duration:**
P-wave 25mV	P-R interval 0.12 – 0.20 s
R wave 1.60mV	S-T interval 0.12 - 0.18 s
Q-wave 0.025mV	Interval p 0.05 - 0.09 s
T-wave 0.35mV	QRS interval 0.07 - 0.11 s
Isoelectric QT interval	QT interval 0.35-0,45 s

Table 1. Standard data for ECG implementation in MATLAB.

RESULTS

Finally, the results indicate that the software can diagnose, track the progression, and predict heart diseases by analyzing the QT interval on ECG graphs. Furthermore, using the Fourier series has allowed us to identify alterations in harmonics related to QT lengthening. These findings represent a significant advance in early heart disease detection and understanding its distinguishing characteristics from pathological ECG.
The study was based on the equation that models cardiac output, relating this parameter to an exponential distribution. Through this approach, we developed an algorithm capable of predicting Heart Failure (HF) over a 10-year time horizon.

$$G_C = \frac{F}{\int_0^{t_0} A(t)dt} \quad (8)$$

Where:
G_c Cardiac output [beats/min].
F Arbitrary dose [mg] can be a drug or dye.

$\int_0^{t_0} A(t)dt$ Dose concentration as a function of time.

Suppose we develop the cardiac output formula that provides values within the range of 60-100 beats per minute, it is considered average in healthy individuals. Any deviation from these values, below 60 beats per minute or above 100 beats per minute, indicated cardiac pathology. We model the evolution of HF using an exponential function, the following is obtained:

$$r(t) = r_{MAX}\left(1 - e^{-t/B}\right) \quad (9)$$

Where:
$r(t)$ Final stage of pathology
r_{MAX} Initial stage of pathology
B Intrinsic speed of the pathological process
t Time elapsed since the onset of heart disease

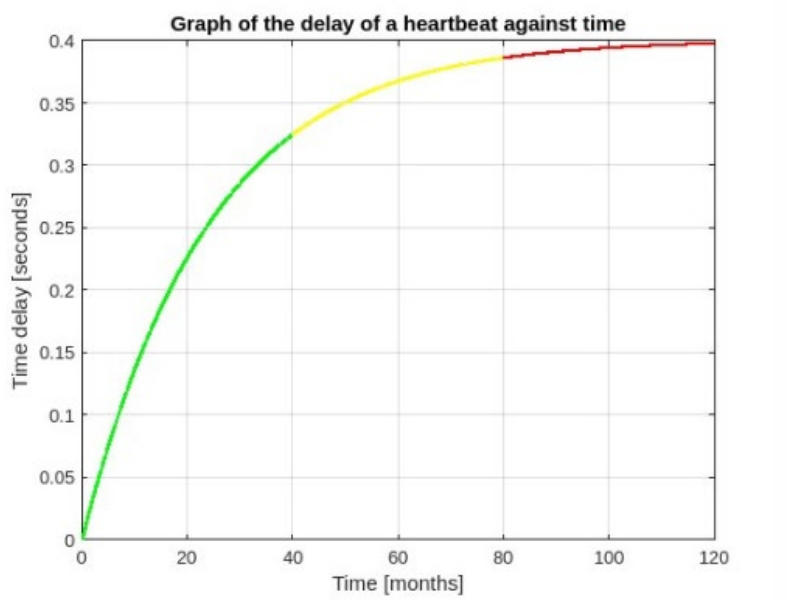

Figure 4. Stages according to the evolution of bradycardia until ending in heart failure.

The first interval, denoted in green, shows that the delay of the QT interval increases excessively, generating exponential bradycardia; it shows the exponential decay of the heartbeat (in seconds) as a function of time, evidencing the growth of the bradycardia from its onset to the first stage where the bradycardia can be reversible.

The second interval, denoted in yellow, can be observed that the QT interval delay decreases considerably, generating an onset of bradycardia close to Heart Failure; the third interval, denoted in red, can be observed that the QT interval, delay reaches its limit, generating an onset bradycardia and Heart Failure, which is entirely irreversible.

As shown in the figure, cardiac pathology tends to stabilize over 10 years, and this is because the heart begins to stop functioning, generating physiological cardiac arrest. The predictive algorithm also made it possible to generate two ECGs, one in the baseline state and the other in the pathological state.

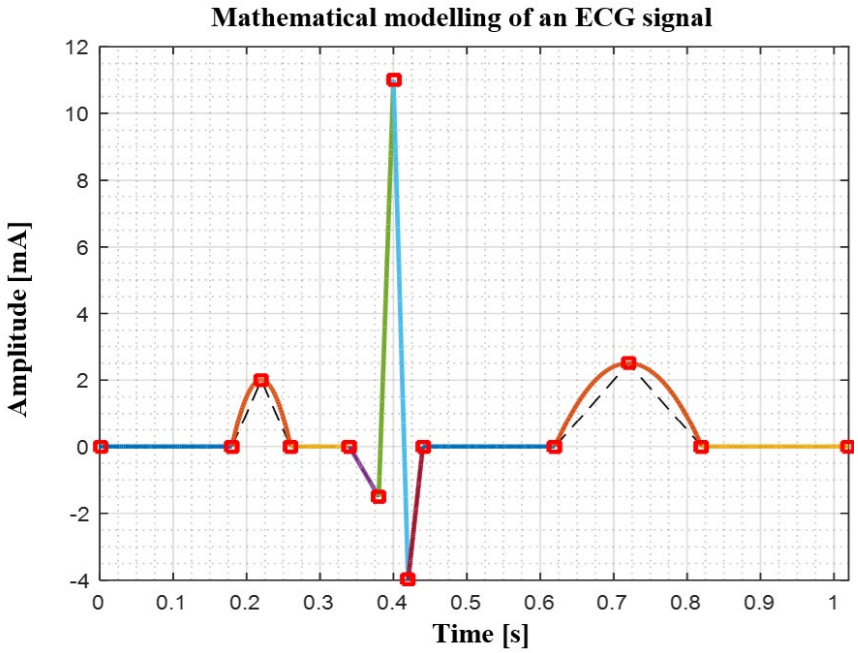

Figure 5. Normal ECG.

As can be seen, there is an ECG with its waveforms and complex with its basal characteristics.

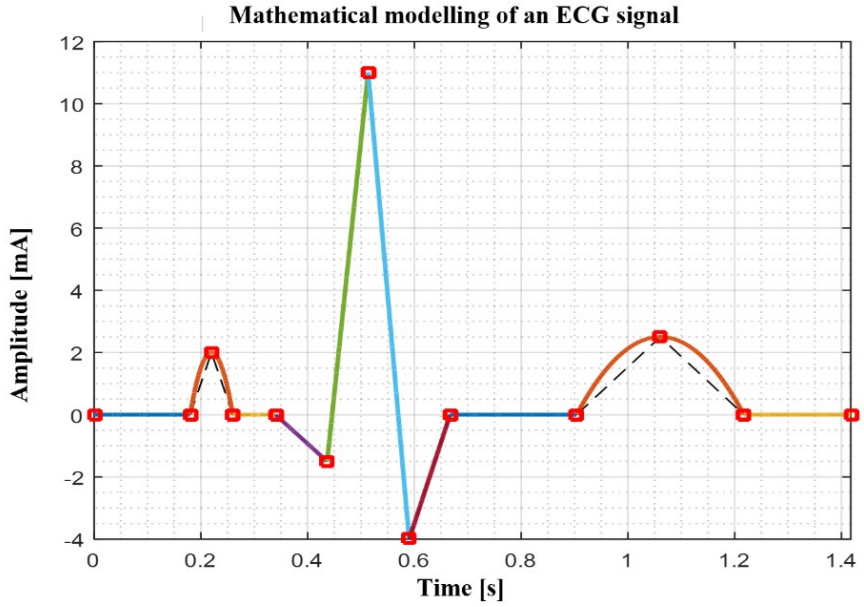

Figure 6. ECG with Heart Failure.

Although it is difficult to determine whether an ECG is normal or pathological, we can accurately observe the lengthening of the QT interval relative to the scale provided by the software. This phenomenon can be associated with pathologies such as cardiomegaly.

The analysis of the frequency spectra at months 40, 80 and 120 from different stages of the disease reveals that the variation in frequency amplitude is found in the fifth harmonic, suggesting a close relationship between this harmonic and the QT interval, as illustrated in Figures 7, 8 and 9.

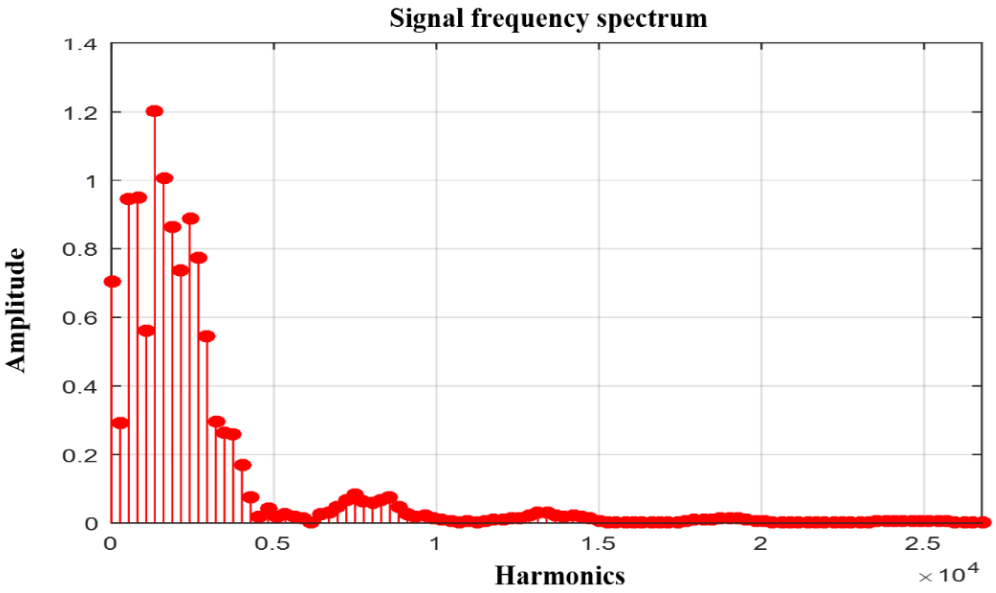

Figure 7. The frequency spectrum of the signal at month 40 using harmonics and its amplitude.

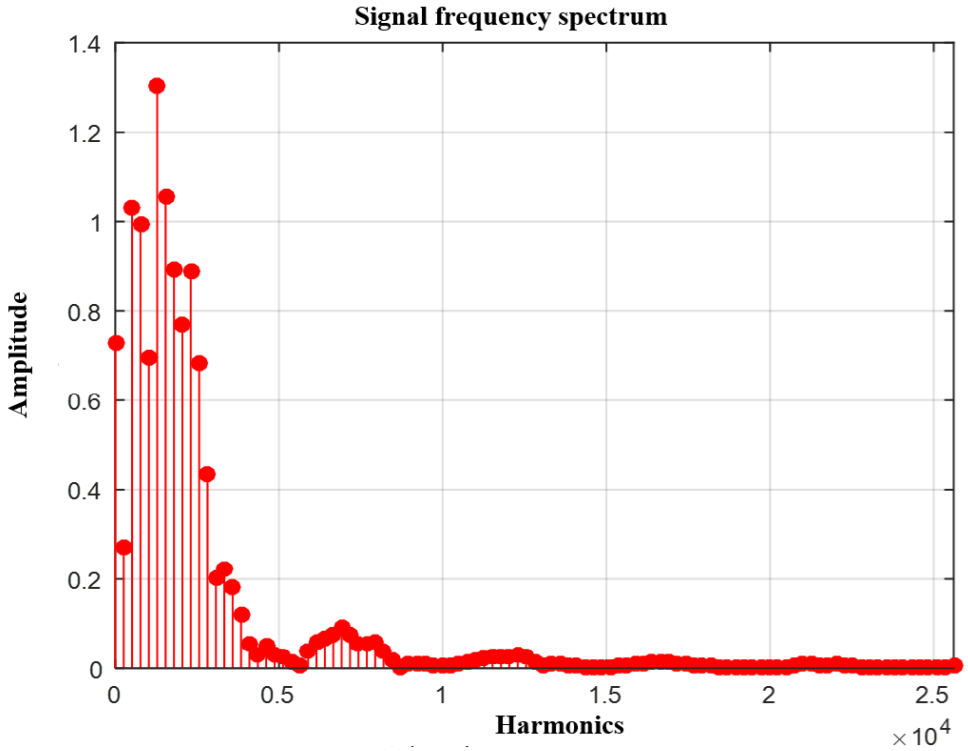

Figure 8. The frequency spectrum of the signal in month 80 using the harmonics and its amplitude.

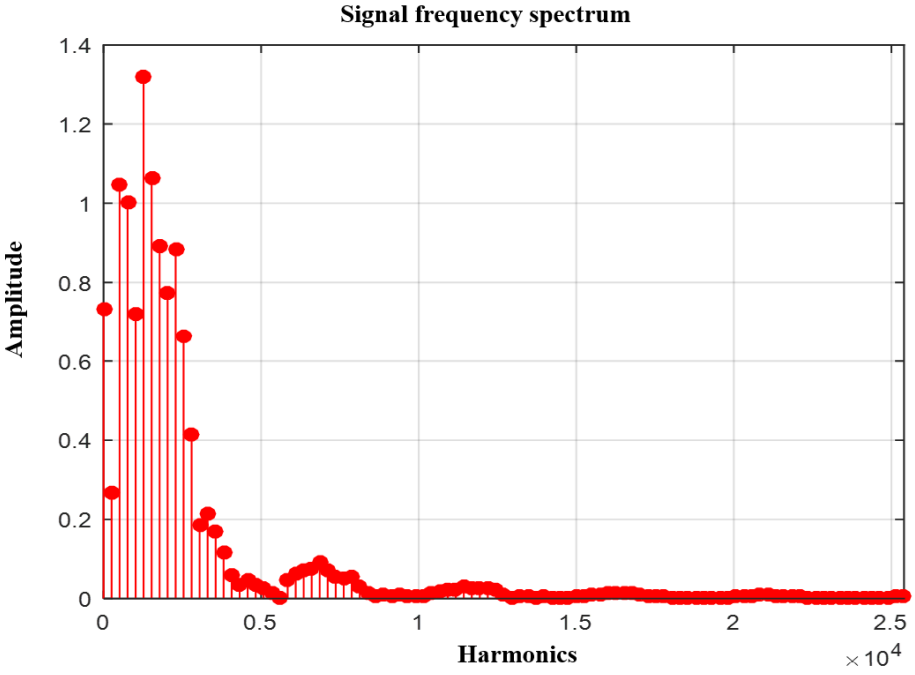

Figure 9. The frequency spectrum of the signal in month 120 using the harmonics and its amplitude.

Source: prepared by Fabián Siza.

These graphs show that the most significant variation in frequency amplitude occurs at harmonic 5, demonstrating that this harmonic is directly related to the QT interval.

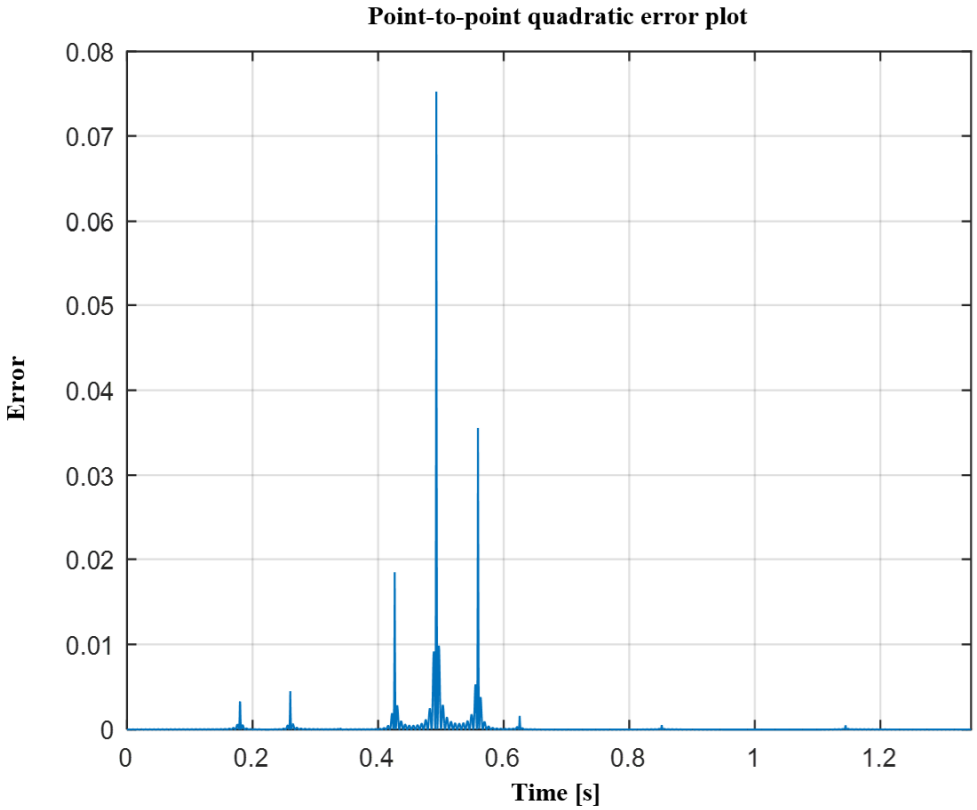

Figure 10. Quadratic error of the signal in month 40.

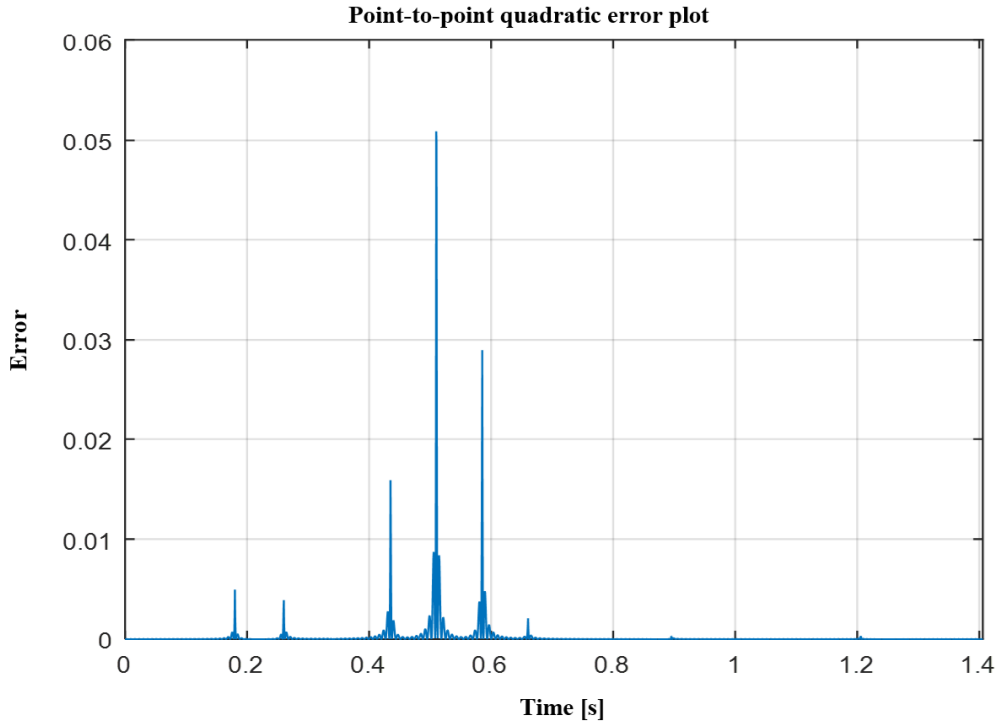

Figure 11. Quadratic error of the signal in month 80.

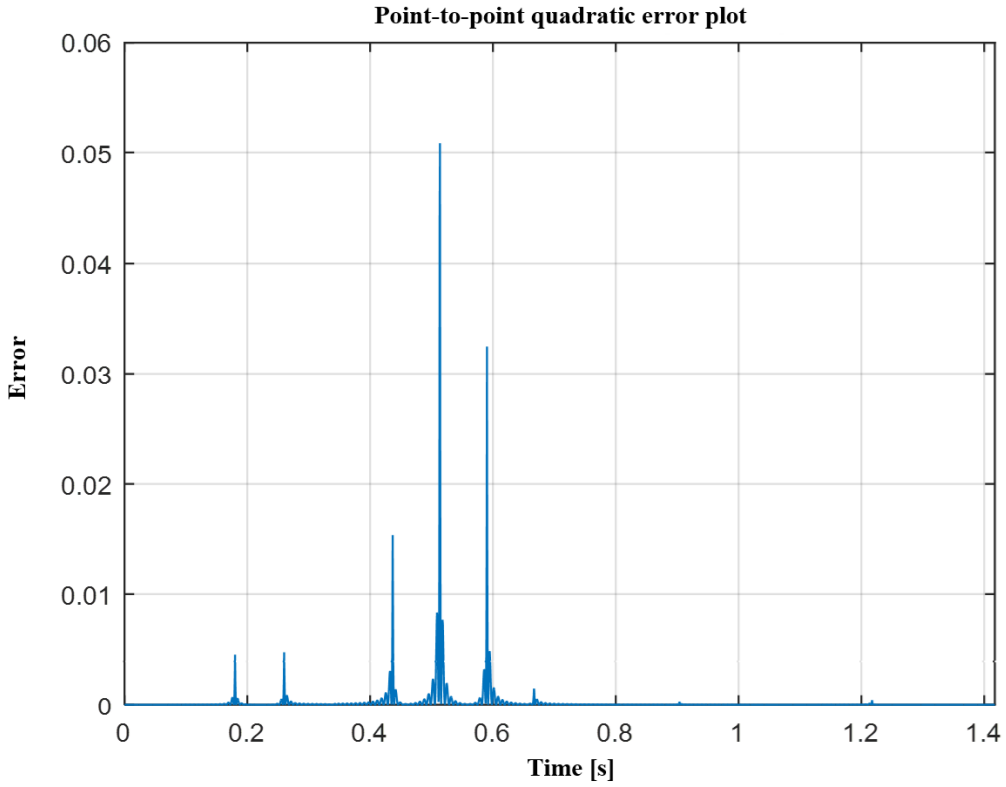

Figure 12. Quadratic error of the signal in month 120.

Subsequently, the mean square error between the original and the reconstructed signals was evaluated using the first 100 Fourier harmonics, as shown in Figures 10, 11 and 12. We observed that the most significant error peaks occur at the change points of intervals, specifically at 0.437, 0.514 and 0.591 seconds, corresponding to the beginning, middle and end of the QRS complex, modeled as a triangular signal.

It is important to note that, in this context, the Gibbs phenomenon is not observed. Since the 10 elements of the piecewise function do not present discontinuities. The most notable errors occur due to transitions between intervals, which are directly related to the change in the triangular signal that represents the QRS complex.

In summary, the research provides a solid basis for the prognosis of HF using a mathematical approach and Fourier series analysis in ECG. The results obtained suggest a clear relationship between the fifth harmonic and the QT interval, which may have significant implications in the early detection or diagnosis of this heart disease.

The software, designed to measure the QT interval on electrocardiograms (ECG), has proven to be a valuable tool for diagnosing, tracking the progression, and predicting heart disease. Through this software, we have created a graphic representation that identifies three heart disease stages of evolution: the health phase, the onset phase, and the advanced phase[13]. This program, therefore, provides an accurate view of the patient's health status based on the measured graphs of their ECG.

Using the Fourier series analysis, we carefully examined the harmonics in ECGs, comparing standard QT signals with those of patients with QT prolongation. Our approach has allowed us to identify which harmonics are related to QT segment prolongation and how they are altered in pathological conditions. Fourier series analysis and programming have provided a detailed understanding of these alterations, a result that is generated from the following algorithm:

Lines of code

GRAPH OF THE EXPONENTIAL FUNCTION
(Months Vs Abnormal QT Delay Time)

```
clc
clear
close all
% Declaración del máximo retraso en 10 años
rmax = 0.4;
tmax = 10*12;
ta = tmax/3;
t1 = linspace(0, ta, 3000);
B = tmax/5;
rt1 = rmax*(1-exp(-t1./B));
tb = 2*tmax/3;
t2 = linspace(ta, tb, 3000);
B = tmax/5;
rt2 = rmax*(1-exp(-t2./B));
tc = tmax;
t3 = linspace(tb, tc, 3000);
B = tmax/5;
rt3 = rmax*(1-exp(-t3./B));
% Grafica del retraso Vs el tiempo
plot(t1, rt1, 'g', 'Linewidth', 2)
hold on
plot(t2, rt2, 'y', 'Linewidth', 2)
grid on;
plot(t3, rt3, 'r', 'Linewidth', 2)
grid on;
xlabel('Tiempo [meses]');
ylabel('Retardo [segundos]');
title('Gráfica del retardo de un latido respecto al tiempo')
t = linspace(0, tmax, 3000);
B = tmax/5;
%_____________________________________________________________________
% Ingresar el valor del retraso del intervalo QT del electrocardiograma
                          rt = 0; % segundos
%_____________________________________________________________________

Mes =   (-B*log(1-rt/rmax));
% valor de tiempo de expandirse en el intervalo
dt = rt;
dti = (dt/7)/0.04;
```

```
hold on

plot(Mes, dt, '*r', 'Linewidth', 2);

fprintf('\nEl retraso de %f corresponde al mes %d. \n', dt, round(Mes));
```

BASIC ELECTROCARDIOGRAM SAMPLING

```
% Declaración de intervalos de puntos en "x" e "y"

x1 = [0 4.5];

y1 = [0 0];

x2 = [0 1 2] + x1(end);

y2 = [0 2 0];

x3 = [0 2]+x2(end);

y3 = [0 0];

% Declaración de los puntos donde se incluye el valor de tiempo a

% expandirse

x4 = [0 1+dti]+x3(end);

y4 = [0 -1.5];

x5 = [0 0.5+dti] + x4(end);

y5 = [-1.5 11];

x6 = [0 0.5+dti]+x5(end);

hold on

plot(Mes, dt, '*r', 'Linewidth', 2);

fprintf('\nEl retraso de %f corresponde al mes %d. \n', dt, round(Mes));
```

BASIC ELECTROCARDIOGRAM SAMPLING

```
% Declaración de intervalos de puntos en "x" e "y"

x1 = [0 4.5];

y1 = [0 0];

x2 = [0 1 2] + x1(end);

y2 = [0 2 0];

x3 = [0 2]+x2(end);

y3 = [0 0];

% Declaración de los puntos donde se incluye el valor de tiempo a

% expandirse

x4 = [0 1+dti]+x3(end);

y4 = [0 -1.5];

x5 = [0 0.5+dti] + x4(end);

y5 = [-1.5 11];

x6 = [0 0.5+dti]+x5(end);
```

```
y6 = [11 -4];
x7 = [0 0.5+dti] + x6(end);
y7 = [-4 0];
x8 = [0 4.5+dti] + x7(end);
y8 = [0 0];
x9 = [0 2.5+dti 5+2*dti] + x8(end);
y9 = [0 2.5 0];
x10 = [0 5] + x9(end);
y10 = [0 0];
% Acondicionamiento de los intervalos de x a variable de tiempo
x1 = x1*0.04;
x2 = x2*0.04;
x3 = x3*0.04;
x4 = x4*0.04;
x5 = x5*0.04;
x6 = x6*0.04;
x7 = x7*0.04;
x8 = x8*0.04;
x9 = x9*0.04;
x10 = x10*0.04;
% Grafica de los puntos tomados del ECG
figure
plot(x1, y1, '--k');       grid on; hold on
plot(x2, y2, '--k');
plot(x3, y3, '--k');
plot(x4, y4, '--k');
plot(x5, y5, '--k');
plot(x6, y6, '--k');
plot(x7, y7, '--k');
plot(x8, y8, '--k');
plot(x9, y9, '--k');
plot(x10, y10, '--k');
% Cálculo del periodo por muestra
T = x10(end);
fprintf('\n\nEl período de la señal es: %f s.con un alargamiento en QT de %f s.\n\n', T, dt);
xlim([0 T])
```

CALCULATION OF THE LAGRANGE INTERPOLATION FOR EACH INTERVAL

```
%% Calculo de la función del intervalo 1
% Asignación de variables auxiliares
vi = x1;
vd = y1;
```

```
% Declaración de la variable simbólica x
syms t
% Algoritmo de interpolación de Lagrange
n = length(vi)-1;
m = n+1;
for i = 1:m
    h = 0;
    for j = 1:m
        if j~=i
            h = h+1;
            L(h) = (t-vi(j))/(vi(i)-vi(j));
        end
    end
    P(i) = prod(L)*vd(i);
end
% Función de salida del intervalo
fx1 = expand(sum(P));

% Gráfica de la función interpolada
xa = linspace(min(vi), max(vi),3000);
plot(xa, subs(fx1, 't', xa), 'Linewidth', 2);
hold on;
plot(vi, vd, 'sr', 'Linewidth', 2);
grid on
disp('El polinomio encontrado por Lagrange es: ');
fprintf('y%d = %s\n\n', 1, char(fx1))
%% Calculo de la funcion del intervalo 2
vi = x2;
vd  = y2;
syms t
n = length(vi)-1;
m = n+1;
for i = 1:m
    h = 0;
    for j = 1:m
        if j~=i
            h = h+1;
            L(h) = (t-vi(j))/(vi(i)-vi(j));
        end
    end
    P(i) = prod(L)*vd(i);
end
```

```
fx2 = expand(sum(P));
xa = linspace(min(vi), max(vi),3000);
plot(xa, subs(fx2, 't', xa), 'Linewidth', 2);
hold on;
plot(vi, vd, 'sr', 'Linewidth', 2);
grid on
disp('El polinomio encontrado por Lagrange es: ');
fprintf('y%d = %s\n\n', 2, char(fx2))
%% Calculo de la función del intervalo 3
vi = x3;
vd  = y3;
syms t
n = length(vi)-1;
m = n+1;
for i = 1:m
   h = 0;
   for j = 1:m
      if j~=i
          h = h+1;
          L(h) = (t-vi(j))/(vi(i)-vi(j));
       end
    end
    P(i) = prod(L)*vd(i);
end
fx3 = expand(sum(P));
xa = linspace(min(vi), max(vi),3000);
plot(xa, subs(fx3, 't', xa), 'Linewidth', 2);
hold on;
plot(vi, vd, 'sr', 'Linewidth', 2);
grid on
disp('El polinomio encontrado por Lagrange es: ');
fprintf('y%d = %s\n\n', 2, char(fx3))
%% Calaulo de la funcion del intervalo 4
vi = x4;
vd  = y4;
syms t
n = length(vi)-1;
m = n+1;  clear P; clear L;
for i = 1:m
   h = 0;
```

```
    for j = 1:m
        if j~=i
            h = h+1;
            L(h) = (t-vi(j))/(vi(i)-vi(j));
        end
    end
    P(i) = prod(L)*vd(i);
end
fx4 = expand(sum(P));
xa = linspace(min(vi), max(vi),3000);
plot(xa, subs(fx4, 't', xa), 'Linewidth', 2);
hold on;
plot(vi, vd, 'sr', 'Linewidth', 2);
grid on
disp('El polinomio encontrado por Lagrange es: ');
fprintf('y%d = %s\n\n', 4, char(fx4))
%% Calaulo de la funcion del intervalo 5
vi = x5;
vd  = y5;
syms t
n = length(vi)-1;
m = n+1;  clear P; clear L;
for i = 1:m
   h = 0;
    for j = 1:m
        if j~=i
            h = h+1;
            L(h) = (t-vi(j))/(vi(i)-vi(j));
        end
    end
    P(i) = prod(L)*vd(i);
end
fx5 = expand(sum(P));
xa = linspace(min(vi), max(vi),3000);
plot(xa, subs(fx5, 't', xa), 'Linewidth', 2);
hold on;
plot(vi, vd, 'sr', 'Linewidth', 2);
grid on
disp('El polinomio encontrado por Lagrange es: ');
fprintf('y%d = %s\n\n', 5, char(fx5))
%% Calaulo de la funcion del intervalo 6
```

```
vi = x6;
vd  = y6;
syms t
n = length(vi)-1;
m = n+1;  clear P; clear L;
for i = 1:m
    h = 0;
    for j = 1:m
        if j~=i
            h = h+1;
            L(h) = (t-vi(j))/(vi(i)-vi(j));
        end
    end
    P(i) = prod(L)*vd(i);
end
fx6 = expand(sum(P));
xa = linspace(min(vi), max(vi),3000);
plot(xa, subs(fx6, 't', xa), 'Linewidth', 2);
hold on;
plot(vi, vd, 'sr', 'Linewidth', 2);
grid on
disp('El polinomio encontrado por Lagrange es: ');
fprintf('y%d = %s\n\n', 6, char(fx6))
%% Calaulo de la funcion del intervalo 7
vi = x7;
vd  = y7;
syms t
n = length(vi)-1;
m = n+1;  clear P; clear L;
for i = 1:m
    h = 0;
    for j = 1:m
        if j~=i
            h = h+1;
            L(h) = (t-vi(j))/(vi(i)-vi(j));
        end
    end
    P(i) = prod(L)*vd(i);
end
fx7 = expand(sum(P));
xa = linspace(min(vi), max(vi),3000);
```

```
plot(xa, subs(fx7, 't', xa), 'Linewidth', 2);
hold on;
plot(vi, vd, 'sr', 'Linewidth', 2);
grid on
disp('El polinomio encontrado por Lagrange es: ');
fprintf('y%d = %s\n\n', 7, char(fx7))
%% Cálculo de la funcion del intervalo 8
vi = x8;
vd  = y8;
syms t
n = length(vi)-1;
m = n+1;  clear P; clear L;
for i = 1:m
   h = 0;
   for j = 1:m
      if j~=i
         h = h+1;
          L(h) = (t-vi(j))/(vi(i)-vi(j));
      end
   end
   P(i) = prod(L)*vd(i);
end
fx8 = expand(sum(P));
xa = linspace(min(vi), max(vi),3000);
plot(xa, subs(fx8, 't', xa), 'Linewidth', 2);
hold on;
plot(vi, vd, 'sr', 'Linewidth', 2);
grid on
disp('El polinomio encontrado por Lagrange es: ');
fprintf('y%d = %s\n\n', 8, char(fx8))
%% Cálculo de la función del intervalo 9
vi = x9;
vd  = y9;
syms t
n = length(vi)-1;
m = n+1;  clear P; clear L;
for i = 1:m
   h = 0;
   for j = 1:m
```

```
        if j~=i
            h = h+1;
            L(h) = (t-vi(j))/(vi(i)-vi(j));
        end
    end
    P(i) = prod(L)*vd(i);
end
fx9 = expand(sum(P));
xa = linspace(min(vi), max(vi),3000);
plot(xa, subs(fx9, 't', xa), 'Linewidth', 2);
hold on;
plot(vi, vd, 'sr', 'Linewidth', 2);
grid on
disp('El polinomio encontrado por Lagrange es: ');
fprintf('y%d = %s\n\n', 9, char(fx9))
%% Cálculo de la función del intervalo 8
vi = x10;
vd  = y10;
syms t
n = length(vi)-1;
m = n+1;  clear P; clear L;
for i = 1:m
    h = 0;
    for j = 1:m
        if j~=i
            h = h+1;
            L(h) = (t-vi(j))/(vi(i)-vi(j));
        end
    end
    P(i) = prod(L)*vd(i);
end
fx10 = expand(sum(P));
xa = linspace(min(vi), max(vi),3000);
plot(xa, subs(fx10, 't', xa), 'Linewidth', 2);
hold on;
plot(vi, vd, 'sr', 'Linewidth', 2);
grid minor
disp('El polinomio encontrado por Lagrange es: ');
fprintf('y%d = %s\n\n', 10, char(fx10))
%% Etiquetas
```

```
xlabel('Tiempo [seg]')
ylabel('Amplitud [mA]');
title('Modelado matemático de una señal de ECG');
```

CALCULATION OF THE FOURIER SERIES COEFFICIENTS OF THE CARDIAC SIGNAL

```
syms t n
% Subintervalos de tiempo en los que se define la función a trozos
A = [x1 x2(end) x3(end) x4(end) x5(end) x6(end) x7(end) x8(end) x9(end) x10(end)];
% Funciones a trozos
f = [fx1 fx2 fx3 fx4 fx5 fx6 fx7 fx8 fx9 fx10];
% Declaración del número de armónicos
arm = 100;
% Cálculo del Periodo
T = max(A)-min(A);
% Cálculo de la frecuencia angular
wo = 2*pi/(T);
% cálculo de Ao
Ao = 0;
for i=1:length(f)
   Ao = Ao +int(f(i),'t', A(i), A(i+1));
end
Ao = eval(simplify(Ao/T));
% cálculo de An
An = 0;
wo = 2*pi/T;
for i=1:length(f)
   An = An +int(f(i)*cos(n*wo*t), A(i), A(i+1));
end
An = simplify(2*An/T);
% cálculo de Bn
Bn = 0;
for i=1:length(f)
   Bn = Bn +int(f(i)*sin(n*wo*t), A(i), A(i+1));
end
Bn = simplify(2*Bn/T);
```

RECONSTRUCTION OF THE GRAPH FROM OF A GIVEN NUMBER OF HARMONICS

```
% Gráfica de la señal reconstruida
n = [1:arm]';
Ane = sum(eval(An).*eval(cos(2*pi*n*t/T)));
Bne = sum(eval(Bn).*eval(sin(2*pi*n*t/T)));
% Calculo de la señal unificada
t = linspace(0, T, 3000);
```

```
ftu = eval(fx1).*(t>0 & t<x1(end))...
    + eval(fx2).*(t>x1(end) & t<x2(end))...
    + eval(fx3).*(t>x2(end) & t<x3(end))...
    + eval(fx4).*(t>x3(end) & t<x4(end))...
    + eval(fx5).*(t>x4(end) & t<x5(end))...
    + eval(fx6).*(t>x5(end) & t<x6(end))...
    + eval(fx7).*(t>x6(end) & t<x7(end))...
    + eval(fx8).*(t>x7(end) & t<x8(end))...
    + eval(fx9).*(t>x8(end) & t<x9(end))...
    + eval(fx10).*(t>x9(end) & t<x10(end));
figure
D(1) = subplot(2, 1, 1);
plot(t, ftu, 'Linewidth', 2)
grid on; box on
xlim([0 t(end)]);
xlabel('Tiempo [seg]')
ylabel('Amplitud [mA]');

title('Modelado matemático de una señal de ECG');
D(2) =  subplot(2, 1, 2);
t = linspace(0, T, 3000);
ftr = Ao + eval(Ane) + eval(Bne);
plot(t, ftr, 'r', 'Linewidth', 2);
grid on; box on
xlim([0 t(end)]);

xlabel('Tiempo [seg]')
ylabel('Amplitud [mA]');
title('Reconstrucción de la señal con un número finito de armónicos');
linkaxes(D, 'xy')
```

SIGNAL FREQUENCY SPECTRUM PLOT

```
figure
% Calculo del módulo de los coeficientes
Cne = sqrt(eval(An).^2 + eval(Bn).^2);
% Gráfica de los armónicos
% frec = [0:arm]*wo*180/pi;
frec = [0:arm];
stem(frec, [Ao; Cne], 'r', 'fill')
xlim([0 max(frec)])
grid on;
xlabel('Armónicos');
ylabel('Amplitud');
title('Espectro de Frecuencia de la señal');
```

CALCULATION AND GRAPHING OF THE MEAN SQUARE ERROR

```
figure

Ent = (ftu - ftr).^2;

plot(t, Ent); xlim([0 max(t)])

xlabel('Tiempo');

ylabel('Error');

grid on

title('Gráfica del error cuadrático punto a punto');

a = -T/2;

b = T/2;

n = length(t);

h = (b-a)/n;

i = 1:n;

xi = a:h:b;

fxi = Ent;

coef = rem(i(2:end-1), 3);
```

Finally, the results indicate that the software can diagnose, follow the progression of, and predict cardiac diseases by analyzing the QT interval in ECG graphs. In addition, using the Fourier series has also allowed us to identify alterations in the harmonics related to QT lengthening accurately. These findings represent a significant advance in the early detection of cardiac disease and understanding its distinguishing features from pathological ECG.

DISCUSSION

The research focuses on the prediction of heart failure through spectral analysis of ECG signals, which is of great relevance in Latin America, where cardiovascular diseases represent the leading cause of morbidity and mortality, as mentioned by [1]. Our contribution aligns with this concern for heart health and provides a specific tool to predict heart failure, a crucial step in preventive healthcare. This approach goes beyond observing alterations in the cardiac muscle in a given time, as suggested by 13, since we use spectral analysis to distinguish between normal ECGs and pathological ECGs, improving the accuracy of clinical diagnosis.

Theoretically, the concept of frequency domain analysis, introduced by [4], is fundamental in our research, as we share his focus on the spectral analysis of signals. This allows us to decompose ECG signals into cyclic components and to detect subtle differences in pathological ECGs. In addition, [5] points out the transformation of ECG signals through the Fourier series, a method related to our approach. However, our research focuses on heart failure prediction, which goes beyond simple signal transformation.

On the other hand, the study also validates the importance of spectral analysis, as highlighted by [7], by demonstrating that specific harmonics, such as harmonics 5 and 7, are particularly sensitive to differences between normal and pathological ECGs. Although we did not directly address the counting of standard values of waves and pulses in an ECG, as suggested by [9], we consider that this measure could be integrated into future research to improve the accuracy of our prediction of heart failure. Furthermore, the approach of Siza, Cazar, and Cortez (2013) [14] in generating an electrocardiogram from triangular and half-waves could enrich future studies in ECG signal modeling.

The basis in the equation that models cardiac output could provide a useful framework for understanding changes in cardiac function related to heart failure and should be considered in future research. Finally, the research brings additional value to the early detection of heart disease. It contributes to understanding the distinctive features of pathological ECGs, which could improve preventive healthcare and treatments for patients at risk of heart failure.

CONCLUSIONS

The study is based on mathematical models and equations to represent the behavior of the heart muscle over time, and its fundamental premise is the identification of an algorithm that uses QT interval widening in electrocardiograms to predict heart failure, which promises to be an innovative tool in cardiovascular medicine and biomedical engineering. In addition, spectral analysis has proven to be an effective tool for the study of electrocardiograms. It has enabled the development of an advanced algorithm for predicting heart failure, offering a new perspective in the early detection of this disease. The application of the Fourier series to biological models, such as the heartbeat, has been fundamental in understanding the evolution of heart failure, revealing significant changes in the coefficients of the Fourier series correlated with the progression of cardiac pathology; furthermore, it has been observed that harmonics 5 and 7 are particularly sensitive to the differences between a normal ECG and a pathological one, which makes them essential for the diagnosis and prognosis of heart failure. This study represents significant progress toward developing a predictor of heart failure in young adults. It focuses on analyzing electrocardiograms over 10 years, providing a potentially valuable tool for detecting this cardiovascular condition in its stages. Early. In addition to its relevance in the early detection of heart failure, the proposed predictor could be a valuable tool for public health by contributing to the diagnosis of alterations in the QT interval that often go unnoticed, which could lead to preventive medical care and more effective treatment for patients at risk. This research represents a significant step in improving preventive healthcare and treatment of patients at risk for heart failure, potentially substantially impacting public health and quality of life for people in Latin America as in other places of the world.

Funding: "This research did not receive external funding."
Conflicts of interest: "The authors declare no conflict of interest."

REFERENCES

1. Orellana R, Portillo I, Villarroel M. Calculadoras de riesgo cardiovascular como estrategia preventiva de eventos isquémicos en la población de Latinoamérica. ALERTA 2021;
2. Farmakis D, Parissis J, Lekakis J, Filippatos G. Insuficiencia cardiaca aguda: epidemiología, factores de riesgo y prevención. Rev Esp Cardiol [homepage on the Internet] 2015;68(3):245–248. Available from: https://www.sciencedirect.com/science/article/pii/S0300893214006563
3. Sisa I. Evaluación del riesgo cardiovascular en adultos mayores utilizando el modelo SCORE OP en una población latinoamericana: experiencia en Ecuador. Med Clin (Barc) [homepage on the Internet] 2018;150(3):92–98. Available from: https://www.sciencedirect.com/science/article/pii/S0025775317306498
4. Gonzales Gomez D. ANÁLISIS ESPECTRAL: CONSIDERACIONES TEÓRICAS Y APLICABILIDAD. Economía y Sociedad 2001;16(Economía y Sociedad):45–60.
5. Martínez I, Andrea P, Abaunza M. Procesamiento y análisis de señales electrocardiográficas (ECG). Publicaciones e Investigación [homepage on the Internet] 2022 [cited 2023 Sep 27];16(4). Available from: https://hemeroteca.unad.edu.co/index.php/publicaciones-e-investigacion/article/view/6496
6. Medina J. ANALISIS DE FOURIER PARA EL TRATAMIENTO DE SEÑALES. https://www.academia.edu/15454387/ANALISIS_DE_FOURIER_PARA_EL_TRATAMIENTO_DE_SE%C3%91ALES. 2010;1–39.
7. Tenorio ED, López PG, García JCS, Hernández MC, González LH. Generación de señales ECG con funciones de fourier en un microcontrolador de arquitectura ARM 32. Ciencia Latina Revista

Científica Multidisciplinar [homepage on the Internet] 2023 [cited 2023 Sep 27];7(2):10022–10035. Available from: https://ciencialatina.org/index.php/cienciala/article/view/6098/9260

8. Medina J. ANALISIS DE FOURIER PARA EL TRATAMIENTO DE SEÑALES. https://www.academia.edu/15454387/ANALISIS_DE_FOURIER_PARA_EL_TRATAMIENTO_DE_SE%C3%91ALES. 2010;1–39.
9. Araújo NM de, Oliveira EDS, Silva BVS da, Melo EBB de, Dantas RAN, Dantas DV. AUDIOVISUAL AIDS IN PREOPERATIVE CARDIAC SURGERY EDUCATION: A SCOPING REVIEW. Texto e Contexto Enfermagem 2022;31.
10. Siza R, Cazar D, Cortez M. ANÁLISIS DE SEÑALES CARDIOVASCULARES UTILIZANDO TÉCNICAS DE PROCESAMIENTO DIGITAL DE SEÑALES. PERFILES 2013;44–48.
11. Gonzalez R, Gianmarco V-L. Desarrollo de una interfaz gráfica para el cálculo de series de Fourier en Matlab. Revista Científica: BIOTECH AND ENGINEERING [homepage on the Internet] 2021 [cited 2023 Sep 27];1(02):41. Available from: https://revistas.untels.edu.pe/index.php/files/article/view/15
12. Casado M. MANUAL BÁSICO DE MATLAB. http://webs.ucm.es/centros/cont/descargas/documento11541.pdf. :1–62.
13. Sarmiento WCH, Mora G, Vanegas P. Prevención y manejo de la hipertrofia ventricular izquierda en pacientes adultos obesos. MQRInvestigar [homepage on the Internet] 2023 [cited 2023 Sep 27];7(2):342–357. Available from: https://www.investigarmqr.com/ojs/index.php/mqr/article/view/343
14. Siza R, Cazar D, Cortez M. ANÁLISIS DE SEÑALES CARDIOVASCULARES UTILIZANDO TÉCNICAS DE PROCESAMIENTO DIGITAL DE SEÑALES. PERFILES 2013;44–48.

Received: October 9th 2023/ **Accepte**d: January 15th 2024 / **Published:**15 February 2024

Citation: Siza Moposita S F, Sáez Paguay M Á, Fiallos Godoy Y M, Ricardo Fabián S G, Heart failure prognostic algorithm using Spectral Analysis and MATLAB software. Revis Bionatura 2024; 9 (1) 12. http://dx.doi.org/10.21931/RB/2024.09.01.12

Additional information Correspondence should be addressed to *fabian.siza@espoch.edu.ec*

Peer review information. Bionatura thanks anonymous reviewer(s) for their contribution to the peer review of this work using https://reviewerlocator.webofscience.com/

Bionatura ISSN. First 13909355 Ecuador. **Scopus coverage years**: from 2016 to the present

Bionatura
Ibero-American Journal of Biotechnology and Life Sciences

Article

Predictive Model in Production through Progressive Web Applications to Forecast Moniliasis in Cacao.

Aracely Miranda[1*], *Byron Bonifaz*[2], *Wilson Chango*[3], *Pedro Aguilar*[4].

[1] *Escuela Superior Politécnica de Chimborazo Orellana Campus, Coca, Ecuador..*
[2] *Escuela Superior Politécnica de Chimborazo Orellana Campus, Coca, Ecuador.*
[3] *Escuela Superior Politécnica de Chimborazo Orellana Campus, Coca, Ecuador.*
[4] *Escuela Superior Politécnica de Chimborazo Orellana Campus, Coca, Ecuador.*
* *Correspondence: aracely.miranda@espoch.edu.ec ; Tel.: 0987941316; country code: 593;*
Available from. http://dx.doi.org/10.21931/RB/2024.09.01.14

ABSTRACT

Cocoa is considered a significant crop in Ecuador, as it represents a favorable source of income for the country's economy, thanks to the remarkable quality of the product. However, it faces a significant issue in its crops: moniliasis, a fungal disease that attacks cocoa cultivation, is present in most Latin American countries. Consequently, this leads to decreased cocoa production and a lower final product quality. The study focuses on designing a predictive production model through a progressive web application to forecast moniliasis in cocoa. The objective is to create an application that anticipates the presence of this disease, thereby contributing to the improvement of the local economy for all farmers. Various methodologies were employed, including bibliographic methods, design science research methodology, and machine learning models. The results obtained from this research indicate that the Gradient Boosting Classifier is the algorithm that best fits the provided dataset. Once this algorithm was identified, a progressive web application was developed and made available for public use by farmers. Furthermore, the efficiency of the predictive model was verified using the statistical method of central tendency, demonstrating that the predictive model is beneficial, primarily by saving farmers a significant amount of time. Anticipating the disease enables timely preventive and corrective measures, which could reduce losses in cocoa production and enhance the quality of the final product.

Keywords: cacao, moniliasis, predictive model, progressive web apps, supervised learning.

INTRODUCTION

Ecuador is historically known as one of the leading producers of aromatic and delicious cocoa in the world, where the quality of the fruit depends on various aspects, such as proper ripeness, absence of insect infestation, diseases, and mechanical damage, among others. However, in recent years, cocoa seed imports have decreased mainly due to some diseases, with the most relevant being "Black Pod Rot," "Witch's Broom," and "Moniliasis," the latter being the most common disease in cocoa plantations. Therefore, there is a current desire to find a solution or method to prevent this disease from continuing to affect cocoa fruits and thereby mitigate damage to the plantations and benefit the farmers' economy[6 8].
This solution involves the development of a predictive model in cocoa production through a progressive web application aiming to predict moniliasis in the crop. We have come across research, such as that by Koysawat

et al.[10,] which emphasizes the importance of data collection in agriculture to obtain relevant information supporting decision-making. For this reason, they propose developing a progressive web application that replaces the traditional manual note-taking process, aiming to reduce errors in data recording and collection. This study was conducted to significantly reduce the time required to gather sugarcane sampling data, reducing 45.28%. Additionally, Ordoñez J.[15] points out that programming can be a powerful tool for generating algorithms from data, allowing for an approximation of the process that leads to conclusive results. This is what we know as Machine Learning, which involves creating a data model based on specific inputs and optimizing its parameters through programming. These optimized parameters are used to predict future outcomes. Machine Learning employs statistical theory principles to develop models, relying on inference from data samples. Furthermore, it utilizes computational programming and efficient algorithms to enhance and apply the model to predictions. This study demonstrated that this technology can be effectively used to predict total production, specifically in the case of cow lactation in the Northern Sierra of Ecuador.

Everything mentioned above significantly contributed to the development of this research, providing a clear understanding of concepts related to Progressive Web Applications, data collection, the use of Machine Learning, and predictive models. These technologies were combined to create a predictive model through a Progressive Web Application for forecasting moniliasis in cocoa. As a result, a novel and beneficial application for the agricultural sector has been developed, one that has not been seen before.

This research was conducted in the Canton of Joya de los Sachas because this location provided the relevant and necessary data obtained through a sensor in said Canton. Additionally, farmers provided some essential data manually regarding cocoa fruits, which helped make this prediction more accurate. Using machine learning techniques and developing a progressive web application will enable timely decision-making and contribute to developing a more efficient agricultural strategy to address moniliasis in cocoa.

The research problem is focused on the presence of moniliasis in cocoa crops, which negatively affects production and product quality, impacting the local economy and the livelihood of farmers.

That is why, in the present research, the following questions are posed, which are addressed throughout the development of this study:

1. Which algorithm among those developed provides the best predictive result?
2. Does the predictive model in production assist users in making timely decisions regarding the forecast of moniliasis?

This research aims to design a predictive model for cocoa production that allows forecasting moniliasis through a progressive web application, providing farmers with a tool to make timely decisions to address the disease and improve the local economy.

For the development of the predictive model in cocoa production, an expository bibliographic analysis was carried out to select and analyze relevant information about using predictive models for moniliasis in cocoa and the development of progressive web applications[2]. Supervised learning was used as the approach for machine learning, allowing for precise extraction of information about the expected outcome. Comparison and analysis tests of available algorithms were performed using Python and the Scikit-Learn library[12 17]. The NoSQL database management system, specifically MongoDB, was chosen due to its flexibility for data with significantly different structures. A progressive web application using JavaScript and React was also developed to offer an efficient and fast user experience[14 5].

The developed predictive model is expected to enable early detection of moniliasis in cocoa crops, allowing farmers to make timely decisions to address the disease and reduce damage to production and product quality. The progressive web application will provide a user-friendly tool for farmers, enhancing their capacity to address moniliasis and benefit the local economy[7].

The article is structured into different sections. It begins with an introduction that briefly places the study in a broad context and highlights its importance. Next, it defines the purpose of the work and its significance. The research problem is then presented, identifying the diseases affecting cocoa cultivation in Ecuador and the importance of addressing moniliasis. The methodology includes the expository bibliographic analysis and the selected machine learning approach. The tools and technologies used, such as Python, Scikit-Learn, MongoDB, and the progressive web application developed with JavaScript and React, are detailed[17 10]. Finally, the article's general structure is presented, including describing the materials and methods used, the results obtained, the discussion, and the study's conclusions.

MATERIALS AND METHODS

The study was based on a design science research methodology focused on creating a predictive model for cocoa production through a progressive web application to forecast moniliasis in the crop. Three cycles were carried out within the framework of the design science research methodology: the relevance cycle, rigor cycle, and design cycle. These cycles were centered on research and the search for helpful information to create an artifact within a specific context[16].

The variables considered in this study are related to aspects of cocoa cultivation and the presence of moniliasis. Various attributes of the crop were measured, such as proper ripeness, the presence of insect infestation, the occurrence of diseases, and mechanical damage, among others. This data was used to train the predictive model and forecast the probability of moniliasis in the crops[3].

The study procedure included conducting an expository bibliographic analysis to select and analyze relevant information about using predictive models for moniliasis in cocoa and developing progressive web applications. Supervised learning was used as the approach for machine learning, allowing for precise information extraction about the expected outcome[9]. Comparison and analysis tests of available algorithms were performed using Python and the Scikit-Learn library. A progressive web application using JavaScript and React was developed to provide an efficient and fast user experience[16].

Data analysis was performed using machine learning techniques and artificial intelligence models. Supervised learning algorithms, such as Support Vector Machines, Logistic Regression, Decision Trees, Linear Regression, Non-linear Regression, and Neural Networks, were applied to evaluate which one provided the best predictive result. Python and the Scikit-Learn library were used to implement and validate the predictive models[18 11].

Ethical considerations were considered in the study regarding the handling and privacy of the collected data. Confidentiality of the information provided by the farmers was ensured, and proper consent was obtained for the use of the data in the research.

The study may have faced limitations, such as the availability of complete and representative data to train the predictive models. Additionally, the model's performance could be affected by the quality of the data used and the variability of conditions in cocoa plantations.

To ensure the reproducibility of the results, widely used open-source tools and libraries, such as Python and Scikit-Learn, were employed. The procedure and methodology details were described clearly and concisely to enable other researchers to replicate the study and validate the findings.

RESULTS

Expository Bibliographic Analysis

In this bibliographic analysis, the search was conducted through physical and electronic books available on the Internet to design the predictive model to avoid any complexity. Additionally, it aimed to assist in developing the progressive web application and make it user-friendly, specifically for farmers, ensuring ease of use. After completing this review, it is possible to achieve an optimal level of learning to begin designing the predictive model and the web application.

Comparison of Algorithms

To obtain a predictive model that allows forecasting moniliasis in cocoa fruits with the highest level of reliability, a comparison of different types of Machine Learning algorithms was performed. Essentially, these

algorithms help reduce the complexity of possible issues that could arise in this predictive model by implementing specific models detailed in this report. The implemented methods include Dimensionality Reduction Techniques, Regularization trends, handling outliers with robust regressions, and ensemble methods. Furthermore, these algorithms were trained and compared using a data set to verify their correct or more accurate performance. For this reason, before implementing the algorithms, a general data set was created by combining the data obtained from the sensors and manually collected data reports from cocoa plants. Subsequently, data treatment was applied to create the data set with the .csv extension, as shown in **Figure *1***. The dataset created and used for the experiments has been uploaded to the Figshare repository. It can be found through the following private link https://figshare.com/s/4fb8bfd0ccbee4f4bcca or through the DOI provided when published in that repository 10.6084/m9.figshare.24112803.

	A	B	C	D	E	F	G	H	I	J	K
1	Rain	Temperature	RH	Dew Point	Wind Speed	Gust Speed	Wind Direction	Plant	Fruit	Severity	Incidence
2	0	25.6	80.96	21.54	0.04	0.63	188.51	1	1	0	0
3	0	25.6	80.96	21.54	0.04	0.63	188.51	1	2	0	0
4	0	25.6	80.96	21.54	0.04	0.63	188.51	1	3	0	0
5	0	25.6	80.96	21.54	0.04	0.63	188.51	1	4	0	0
6	0	25.6	80.96	21.54	0.04	0.63	188.51	1	5	0	0
7	0	25.6	80.96	21.54	0.04	0.63	188.51	1	6	0	0
8	0	25.6	80.96	21.54	0.04	0.63	188.51	1	7	0	0
9	0	25.6	80.96	21.54	0.04	0.63	188.51	1	8	0	0
10	0	25.6	80.96	21.54	0.04	0.63	188.51	1	9	0	0
11	0	25.6	80.96	21.54	0.04	0.63	188.51	1	10	0	0
12	0	25.6	80.96	21.54	0.04	0.63	188.51	2	1	0	0
13	0	25.6	80.96	21.54	0.04	0.63	188.51	2	2	0	0
14	0	25.6	80.96	21.54	0.04	0.63	188.51	2	3	0	0
15	0	25.6	80.96	21.54	0.04	0.63	188.51	2	4	0	0
16	0	25.6	80.96	21.54	0.04	0.63	188.51	2	5	0	0
17	0	25.6	80.96	21.54	0.04	0.63	188.51	2	6	0	0
18	0	25.6	80.96	21.54	0.04	0.63	188.51	2	7	0	0
19	0	25.6	80.96	21.54	0.04	0.63	188.51	2	8	0	0
20	0	25.6	80.96	21.54	0.04	0.63	188.51	2	9	0	0
21	0	25.6	80.96	21.54	0.04	0.63	188.51	2	10	0	0
22	0	25.6	80.96	21.54	0.04	0.63	188.51	3	1	0	0
23	0	25.6	80.96	21.54	0.04	0.63	188.51	3	2	0	0
24	0	25.6	80.96	21.54	0.04	0.63	188.51	3	3	0	0
25	0	25.6	80.96	21.54	0.04	0.63	188.51	3	4	0	0
26	0	25.6	80.96	21.54	0.04	0.63	188.51	3	5	0	0

Figure 1. Created dataset file with .csv extension

So, it was concluded that the techniques to be applied for the proper functioning of the model and to avoid falling into problems of complexity or simplicity are as follows:

Dimensionality Reduction Techniques

From the conducted data set, it is necessary to determine or identify which features affect the Machine Learning models or algorithms. It is not recommended to have too many features because variables might become irrelevant, leading to increased computational costs. There is also a risk of missing values, which can introduce significant biases and compromise the predictive capacity. To address this, dimensionality reduction techniques were applied using the following algorithms: PCA, IPCA, and KPCA. The latter has three standard kernels: linear, polynomial, and Gaussian. Part of the code is shown in **Table *1***:

Dimensionality reduction techniques
dt_data=pd.read_csv('./data/dataOT.csv') dt_features=dt_data.drop(['INCIDENCIA'],axis=1) dt_incidecia = dt_data['INCIDENCIA'] X_train,X_test,y_train,y_test =train_test_split(dt_features,dt_incidecia, test_size=0.30,random_state=42) print(X_train.shape) pca=PCA(n_components=4 pca.fit(X_train) ipca=IncrementalPCA(n_components=4, batch_size=10) ipca.fit(X_train) plt.plot(range(len(pca.explained_variance_)), pca.explained_variance_ratio_) logistic=LogisticRegression(solver='lbfgs') dt_train = pca.transform(X_train) dt_test = pca.transform(X_test) logistic.fit(dt_train, y_train) print("SCORE PCA: ", logistic.score(dt_test, y_test dt_train = ipca.transform(X_train) dt_test = ipca.transform(X_test) logistic.fit(dt_train, y_train) print("SCORE IPCA: ", logistic.score(dt_test, y_test)) kernel = ['linear','poly','rbf']

Table 1. Algorithms PCA, IPCA, and KPCA

If you wish to observe the developed algorithms in detail, you can access the following link: https://github.com/Abel272000/skict-01. This link leads to a repository created on GitHub. The results obtained with the three algorithms were as follows. They were implemented or conducted with normal, normalized, and discretized data. Surprisingly, the same results were obtained for each of them. These results are shown in **Table *2***:

Algorithms	Result	Analysis	Conclusion
PCA	0.9675376088677752	When running this algorithm with the selected dataset, a result of 0.9675 was obtained.	Upon analyzing these results, it can be concluded that both the PCA, IPCA, and KPCA Linear algorithms achieve the best and identical result of 0.9675.
IPCA	0.9675376088677752	This algorithm yields a result of 0.9675, identical to the PCA's value.	
KPCA LINEAR	0.9675376088677752	The result can be simplified to 0.9675, obtaining the same outcome as PCA and IPCA.	
KPCA POLY	0.9588281868566905	In this case, the observed result is 0.9588.	
KPCA RBF	0.6595407759303247	An outcome of 0.6595 is obtained, which is the lowest result.	

Table 2. Results with *standard* data, normalized data, and discretized data.

Based on all the tests conducted and the data analyzed through the presented table, it can be concluded that: We work with average, normalized, and discretized data to yield better PCA, IPCA, and KPCA Linear results. Therefore, these three algorithms can be chosen and used for training a predictive model.

Algorithms
dataset = pd.read_csv('./data/dataOT.csv') X = dataset[['Rain', 'Temperature', 'RH', 'WindSpeed', 'WindDirection', 'PLANTA', 'FRUTO', 'SEVERIDAD']] y = dataset[['INCIDENCIA']] X_train, X_test, y_train, y_test = train_test_split(X,y,test_size=0.25) modelLinear = LinearRegression().fit(X_train, y_train) y_predict_linear = modelLinear.predict(X_test) modelLasso = Lasso(alpha=0.2).fit(X_train, y_train) y_predict_lasso = modelLasso.predict(X_test) modelRidge = Ridge(alpha=1).fit(X_train, y_train) y_predict_ridge = modelRidge.predict(X_test) modelElasticNet = ElasticNet(random_state=0).fit(X_train,y_train) y_pred_elastic = modelElasticNet.predict(X_test) linear_loss = mean_squared_error(y_test, y_predict_linear) print("Linear Loss. "+"%.10f" % float(linear_loss)) lasso_loss = mean_squared_error(y_test, y_predict_lasso) print("Lasso Loss. "+"%.10f" % float(lasso_loss)) ridge_loss = mean_squared_error(y_test, y_predict_ridge) print("Ridge loss: "+"%.10f" % float(ridge_loss)) elastic_loss = mean_squared_error (y_test, y_pred_elastic) print ("ElasticNet Loss: "+"%.10f" % float(elastic_loss))

Table 3. Algorithms the regularization

Regularization Trend

Continuing with the methods to avoid complexity and simplicity issues, we have a regularization trend, which involves penalizing features that do not contribute or subtract relevant information to the predictive model. We find Linear, Lasso, Ridge, and ElasticNet in this technique. These are shown in **Table 3**.

The chosen results in this case are from the discretized data, as they yielded lower errors, as shown in **Table *4***:

Algorithms	Result	Analysis	Conclusion
Score Lineal	0.8168445746092333	With discretized data, we obtained a score of 0.8168.	The result of discretizing the data with the lowest errors is the Elastic Net score of 0.80.
Score Lasso	0.8086331011252863	This algorithm yields a result of 0.8086.	
Score Ridge	0.8167191749791375	The result can be simplified to 0.8167.	
Score Elastic Net	0.8076917959407464	In this case, the observed result is 0.8077.	

Table 4. Results with discretized data.

Algorithms

```
dataset = pd.read_csv ('./data/dataOT.csv')
print(dataset.head (4))
X = dataset.drop(['SEVERIDAD','INCIDENCIA'], axis=1)
y = dataset[['INCIDENCIA']]
X_train, X_test, y_train, y_test = train_test_split(X,y,test_size=0.3, random_state=42)
estimators = {
'SVR' : SVR (gamma= 'auto', C=1.0, epsilon=0.1),
'RANSAC' : RANSACRegressor(),
'HUBER' : HuberRegressor(epsilon=1.35)
}
warnings.simple filter("ignore")
for name, estimator in estimadores.items():
    estimator.fit(X_train, y_train)
    predictions = estimator.predict(X_test)
    print("="*64)
    print (name)
    print("MSE: "+"%.10f" % float(mean_squared_error(y_test,predictions)))
    plt. label('Predicted Score')
    plt. label('Real Score')
    plt.title('Predicted VS Real')
    plt.scatter(y_test, predictions)
    plt.plot(predictions, predictions,'r--')
    plt.show()
```

Table 5. Algorithms Outliers with Robust Regressions

This leads us to conclude that the regularization technique provides more favorable results when working with ElasticNet score, whether with average, normalized, or discretized data. This algorithm will yield results with the lowest possible errors. Examining which variable carries the most weight appears to be related to rainfall, temperature, and severity.

Outliers with Robust Regressions

We must consider outliers, as they may be present in our data set, which can introduce significant biases in our models. Robust regressions can help identify these outliers. In this context, Sci-kit learn provides RANSAC and Huber Regressor to address the presence of outliers in our data set. The model is presented in ***Table 5***.

In this model, tests were conducted with average, normalized, and discretized data, and the results in all three cases were the same, as shown in ***Table 6*** in general form:

Algorithms	Result	Analysis	Conclusion
SVR	0.1699674007	A result of 0.1699 is obtained.	The SVR algorithm indicates better performance in lower values, where a smaller result is considered better.
RANSAC	0.3404592241	This algorithm yields a result of 0.3405.	
HUBER	0.1952528881	The result can be simplified to 0.1953.	

Table 6. Results with normal data, normalized data, and discretized data.

Among the robust regression models, the SVR model performs better, where a lower value is considered better, with a score of 0.169.

Ensemble Methods

Next, ensemble methods, which combine different methods with various configurations and apply a consensus approach, are employed. There are two strategies:

Bagging Strategy

In this strategy, the variance of individual classifiers is reduced by combining them ***Table 7*** illustrates the strategy:

Algorithms

```
dt_heart = pd.read_csv('./data/dataOT.csv')
x = dt_heart.drop (['INCIDENCIA'], axis=1)
y = dt_heart ['INCIDENCIA']
X_train, X_test, y_train, y_test = train_test_split (x, y, test_size= 0.35, random_state=1)
knn_class = KNeighborsClassifier().fit (X_train, y_train)
knn_prediction = knn_class.predict(X_test)
print('='*64)
print('SCORE con KNN: ', accuracy_score (knn_prediction,y_test))
estimators = {
'LogisticRegression' : LogisticRegression(),
'SVC' : SVC(),
'LinearSVC' : LinearSVC(),
'SGD' : SGDClassifier (loss="hinge", penalty="l2",    max_iter=5),
'KNN' : KNeighborsClassifier(),
'DecisionTreeClf' : DecisionTreeClassifier(),
'RandomTreeForest' : RandomForestClassifier(random_state=0)
}
for name, estimator in estimators.items():
    bag_class = BaggingClassifier(base_estimator=estimator, n_estimators=50).fit(X_train, y_train)
    bag_predict = bag_class.predict(X_test)
    print ('='*64)
    print ('SCORE Bagging with {} : {}'.format(name,
    accuracy_score(bag_predict, y_test)))
```

Table 7. Algorithms Bagging

Working with normalized data was chosen in this strategy because it yields higher results than normal or discretized data. The results obtained are detailed in ***Table 8***:

Algorithms	Result	Analysis	Conclusion
SCORE con KNN	0.9776119402985075	The result of 0.9776 is obtained	When normalizing the data, there is a slight increase in each model's result, where RandomTreeForest continues to have the best result, this time with 0.9891.
SCORE Bagging with LogisticRegression	0.9687924016282226	This algorithm yields a result of 0.9688	
SCORE Bagging with SVC	0.9694708276797829	This algorithm with the selected data set obtains a result of 0.9695	
SCORE Bagging with LinearSVC	0.9606512890094979	This algorithm yields a result of 0.9607	
SCORE Bagging with SGD	0.9769335142469471	The result can be simplified to 0.9769	
SCORE Bagging with KNN	0.9776119402985075	In this case, it is observed that it has a result of 0.9776	
SCORE Bagging with DecisionTreeClf	0.9837177747625508	In this case, a result of 0.9837 is obtained	
SCORE Bagging with RandomTreeForest	0.989145183175034	And finally, this algorithm yields a result of 0.9891	

Table 8. Results with normalized data.

This result shows that more favorable results are obtained with the Bagging strategy when working with normalized data. RandomTreeForest consistently produces the best or highest results in all three cases.

Boosting Strategy

The other strategy is Boosting, a sequential method that gradually strengthens a learning model using the residual error from previous stages. The final result is also achieved through consensus among all the models. This strategy is presented in ***Table 9***:

Algorithms

```
    dt_heart = pd.read_csv ('./data/dataOT.csv')
    x = dt_heart.drop (['INCIDENCIA'], axis=1)
    y = dt_heart['INCIDENCIA']
        X_train, X_test, y_train, y_test = train_test_split (x, y,
test_size=0.35, random_state=1)
    estimators = range (1, 50, 1)
    total_accuracy = []
    best_result = {'result' : 0, 'n_estimator': 1}
    for i in estimators:
        boost = GradientBoostingClassifier(n_estimators=i).fit (X_train,
y_train)
        boost_pred = boost.predict (X_test)
        new_accuracy = accuracy_score(boost_pred, y_test)
        total_accuracy.append (new_accuracy)
        if new_accuracy > best_result['result']:
```

```
        best_result['result'] = new_accuracy
        best_result['n_estimator'] = i
        print(best_result)
```

Table 9. Algorithms Gradient Boosting Classifier

The best results were obtained with all three types of data, as shown in ***Table 10***:

Estimator	Result	Analysis	Conclusion
Normal data			When comparing the results of the three final estimators, it is observed that a result of 0.9905 is obtained in all three cases.
Estimator 4	0.9905020352781547	A result of 0.9905 is obtained.	
Normalized data			
Estimator 4	0.9905020352781547	This algorithm yields a result of 0.9905	
Discretized data			
Estimator 4	0.9905020352781547	This algorithm obtains a result of 0.9905	

Table 10. General Results

Based on these findings, it can be concluded that when working with Boosting using the Gradient Boosting Classifier algorithm, whether with average, normalized, or discretized data, the same results are obtained. However, compared to the previous models, Boosting presents the best possible result in this analysis.

Global analysis of all results obtained

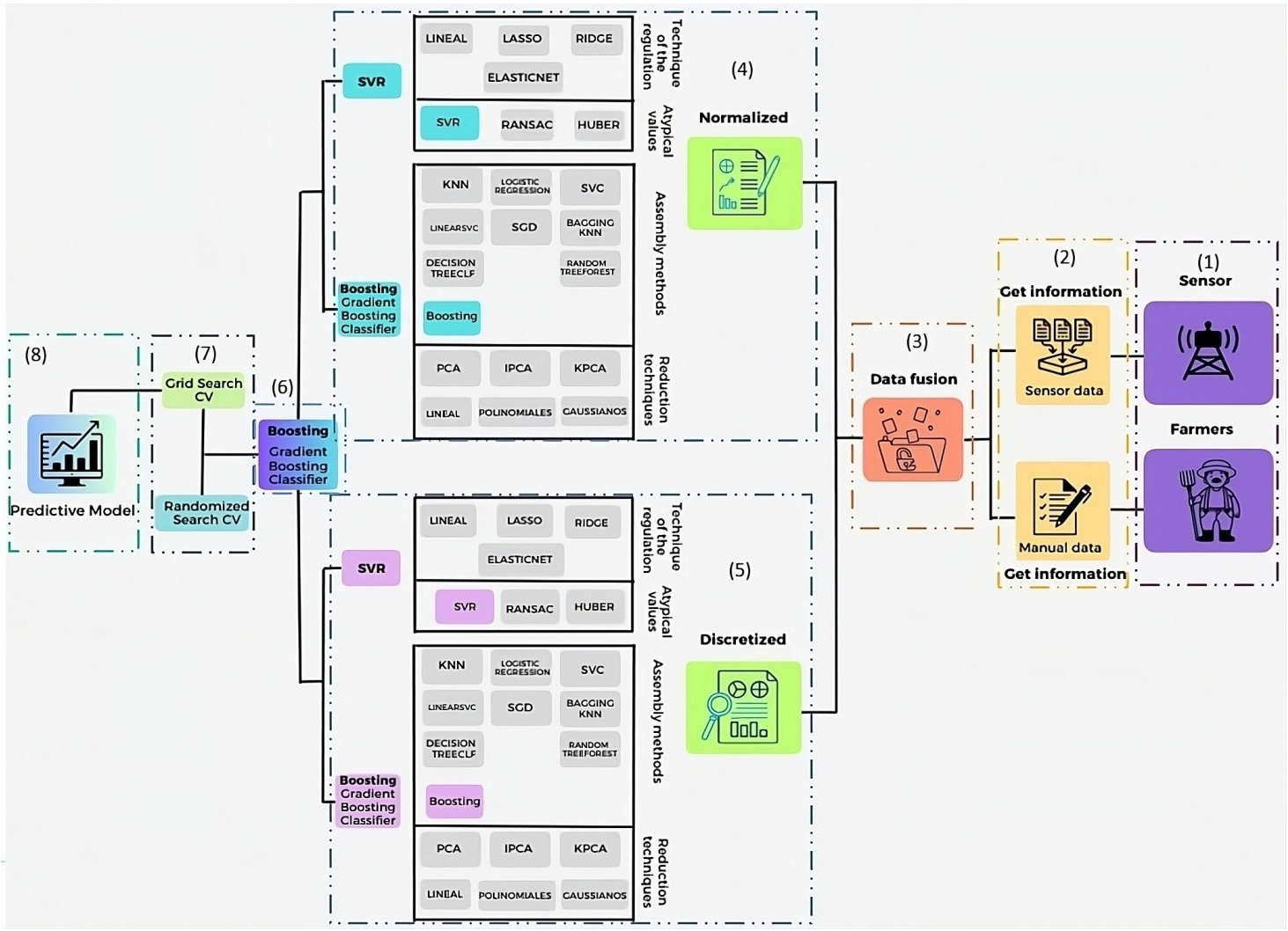

Figure 2. General analysis

According to the numbering in the previous graph:

1. To create this predictive model, data was needed from a sensor and data provided by farmers, which are represented in the purple-colored boxes in the previous graph.
2. The information from each source is stored in Excel documents. The sensor data includes key variables such as rainfall, temperature, and humidity. The information provided by farmers includes plant number, number of fruits, severity, and incidence, as shown in the yellow-colored box.
3. After gathering this data, it undergoes a process or treatment to create the final data set, represented by the orange-colored box.
4. Once the data is obtained, it is normalized, and each algorithm within each group (shown in the top-left box) is applied. The group includes algorithms for Trend regularization (Linear, Lasso, Ridge, and ElasticNet) and Outliers with Robust Regressions (RANSAC and Huber Regressor). In this case, the algorithm with the lowest result is SVR with a value of 0.1699. The bottom box includes techniques for Dimensionality Reduction (PCA, IPCA, and KPCA: linear, polynomial, and Gaussian) and Ensemble Methods (Bagging and Boosting), where the Gradient Boosting Classifier algorithm yields the best result with 0.99.
5. When discretizing the data, the same algorithms are applied in the groups for Trend regularization and Outliers with Robust Regressions, and the SVR algorithm still provides the lowest result with a value of

0.1699. In the bottom box, the Dimensionality Reduction and Ensemble Methods techniques still show that the Gradient Boosting Classifier algorithm yields the best result with 0.99.

6. The conclusion is reached that both normalized and discretized data can be used as they yield high results with the Gradient Boosting Classifier algorithm, obtaining 0.99.
7. Additionally, the implementation of the algorithm is analyzed with two parameter optimization techniques, Randomized Search CV and Grid Search CV, with the latter providing the highest result.
8. Finally, the trained predictive model is obtained after completing the entire process presented in this graph and can make accurate predictions.

Development of the Artifact

The development of the artifact follows the methodology of design science, which comprises three cycles: relevance cycle, rigor cycle, and design cycle[13].

a). Relevance Cycle

In the first cycle, a comprehensive investigation was conducted concerning moniliasis disease and the context of cocoa, which is considered a crucial crop in Ecuador. Cocoa represents a significant source of income for the country's economy due to its high-quality products. However, the presence of moniliasis, a fungal disease affecting cocoa crops, threatens the product's quality. Therefore, strategies were sought to manage and prevent this disease, aiming to propose possible alternatives for the predictive model. Additionally, it was crucial to analyze the real impact of this disease on cocoa crops to identify the farmers' urgent needs and how beneficial a predictive model would be for them.

b). Rigor Cycle

The previous analysis provided a better understanding of the requirements and needs for controlling or preventing the disease. The main goal here is to detect when the disease affects the product. This led to developing the predictive model and the subsequent creation and design of the progressive web application (PWA). The research involved investigating how to build the predictive model, which technologies to use, the utilization of sensors, data acquisition, system architecture, and more. All the findings from the literature review were incorporated into this phase.

c). Design Cycle

This study focuses on designing a predictive model in production by developing a progressive web application to forecast moniliasis in cocoa. The aim is to create an application that can predict the presence of this disease before it contaminates other plantations. With all the gathered information, the structure shown in ***Figure 3*** was established to provide a clear roadmap for the project's design process.

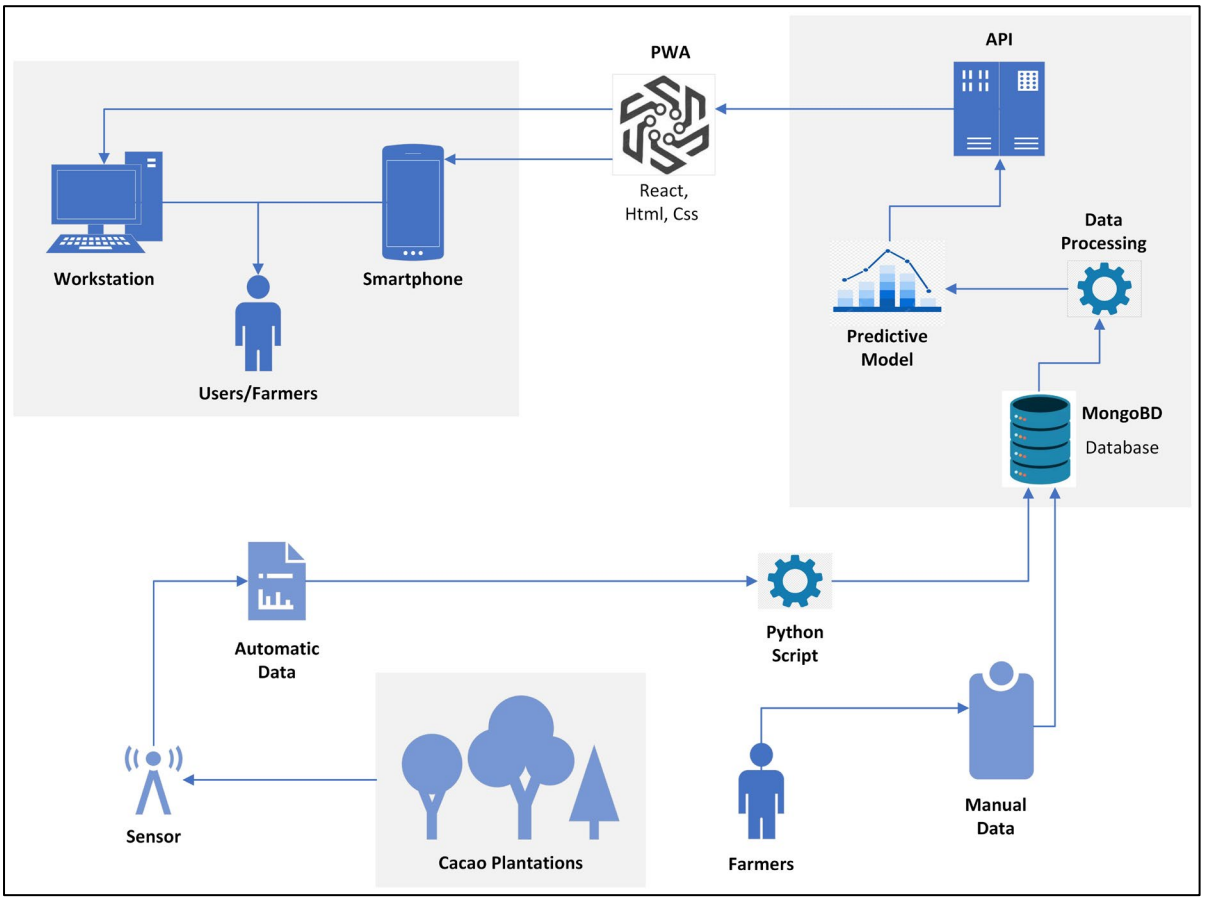

Figure 3. Architecture

Development

While developing the Progressive Web App (PWA), React, a JavaScript library, created the Frontend component. This library was chosen due to its capability to enable offline functionality, a characteristic that identifies a PWA. On the other hand, the Python programming language was selected for the Back-end component, utilizing the Flask framework. A simplified structure was designed, concentrating the business logic in a file called "app.py." This architectural decision was made to facilitate interaction and resource consumption by the Frontend component of the PWA. The predictive model is implemented within the back end, a fundamental element for the application's operation, as it can make real-time predictions. Its components and files can be seen in ***Figure 4***. To enable offline mode for the PWA, a "getdata" function sends a request to a predefined route in the back end, retrieving data from the database. This data is then stored in the browser's local storage for offline functionality.

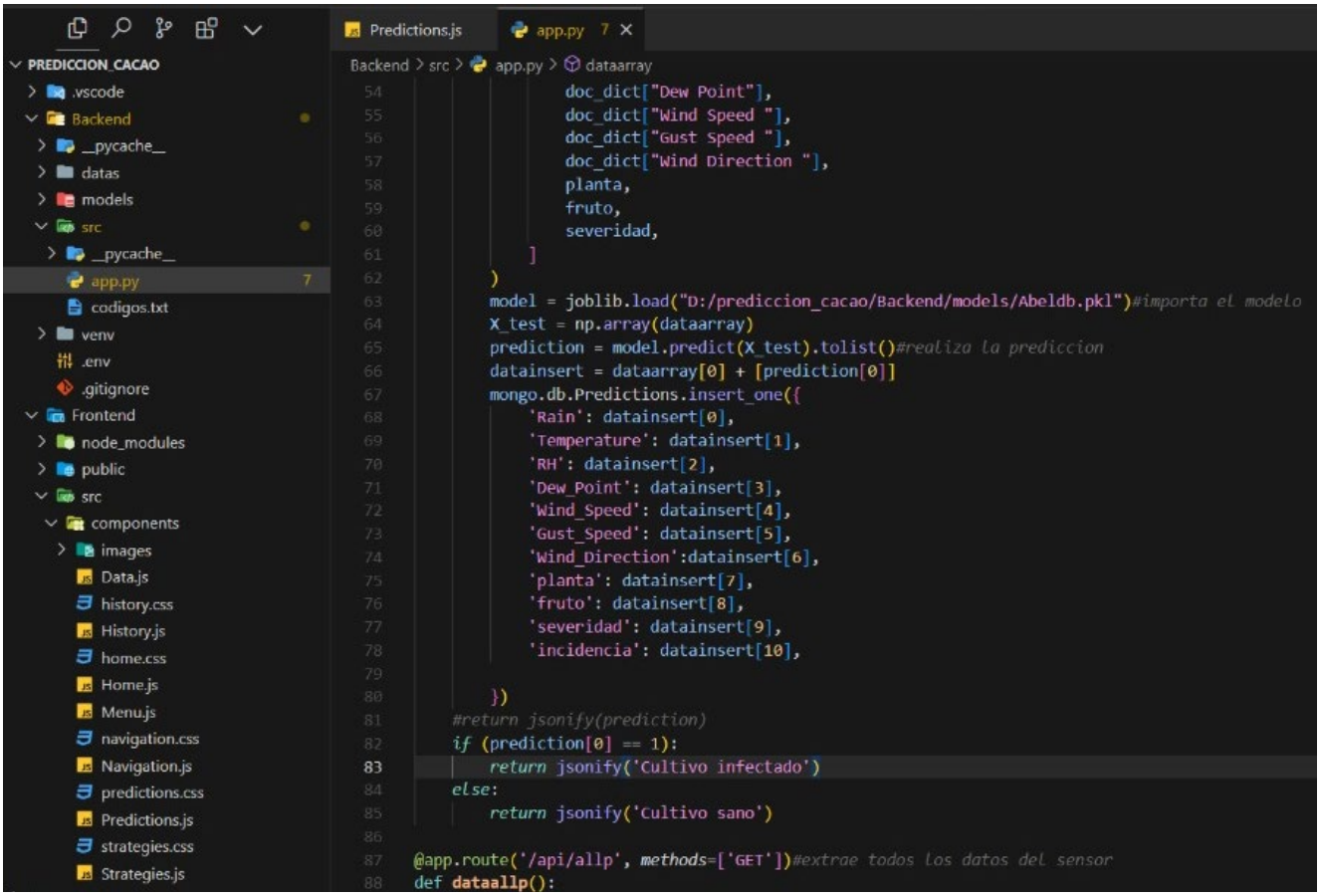

Figure 4. Back-end and frontend files

This predictive model represents a key component in the interface between the front end and back-end of the PWA, significantly contributing to achieving the research objectives. The PWA's interface can be observed in ***Figure 5,*** where data obtained from the sensor is extracted from the MongoDB database.

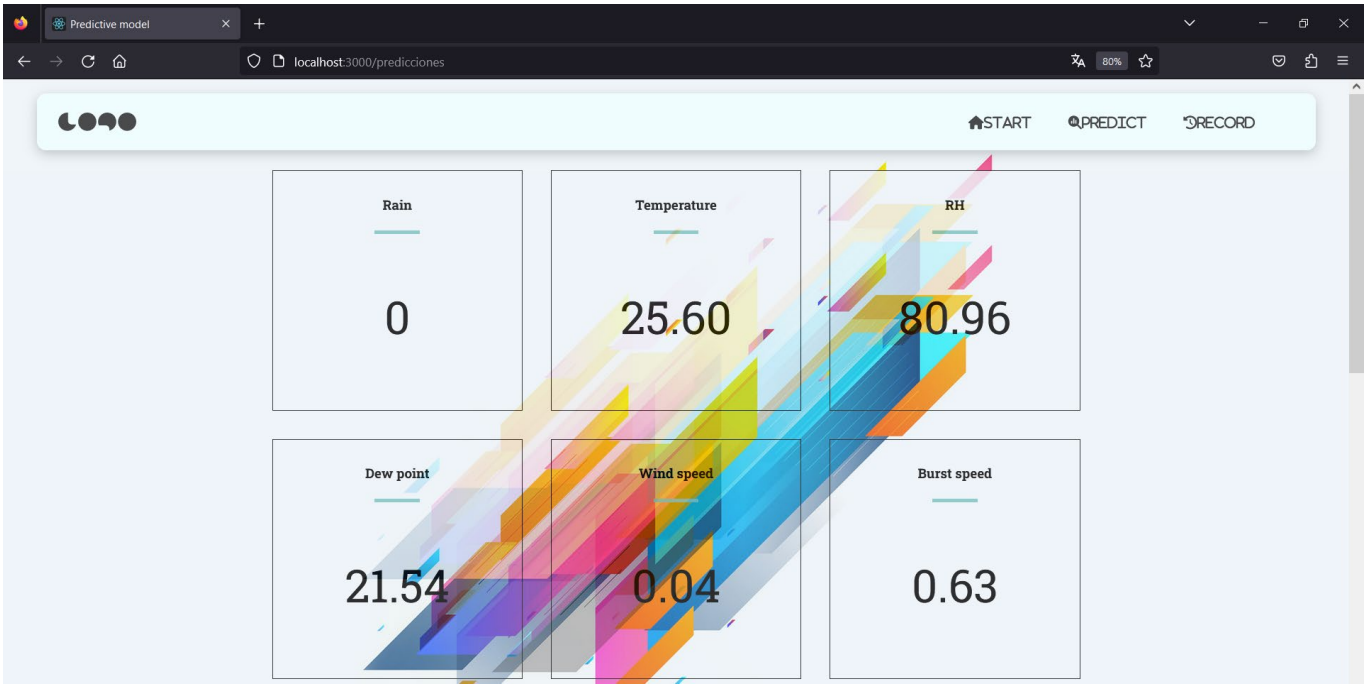

Figure 5. Data obtained from the sensor extracted from the database created in MongoDB

Next is the section where the farmer inputs manual data and clicks the "predict" button at the bottom. With this data entered by the farmer, it is sent to the back-end, which processes this data along with the latest data extracted from the database and sends it to the predictive model. The predictive model analyzes the data and provides a prediction of whether the fruit is contaminated or not, as seen in ***Figure 6***, with the result obtained, the farmer will have the opportunity to make timely decisions regarding whether their fruit has moniliasis, where they can apply control protocols or take precautions to prevent the contamination of their other fruits.

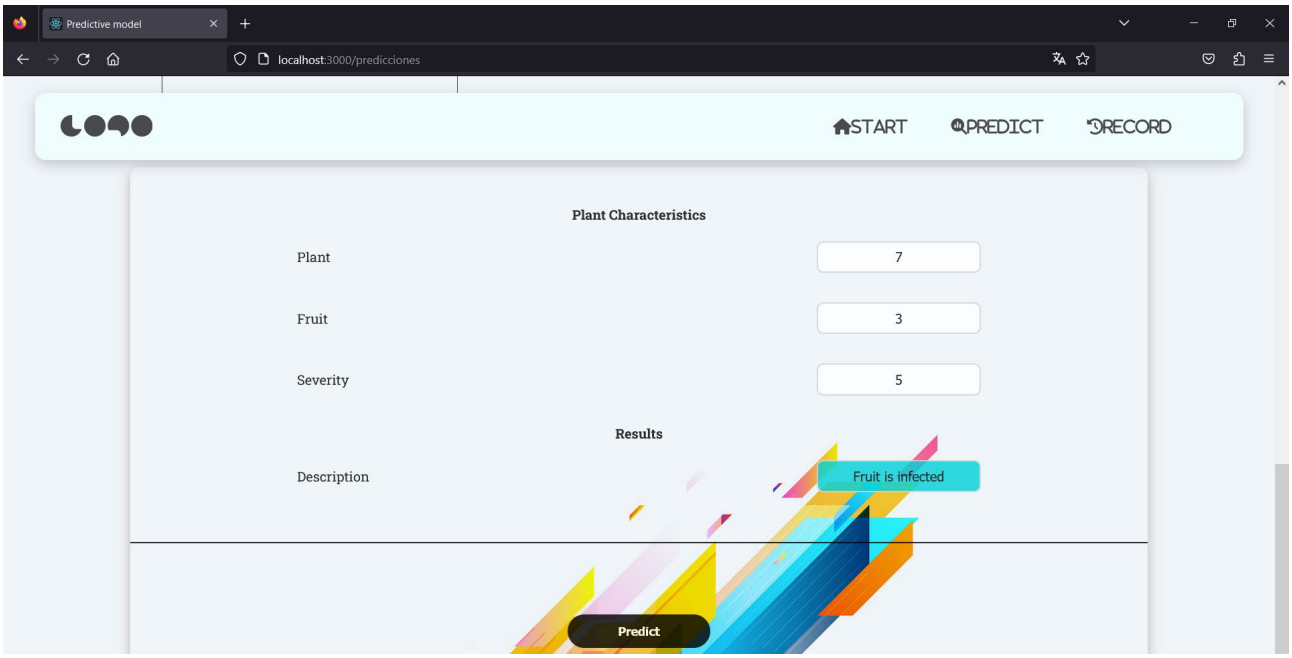

Figure 6. Data entered by the farmer and prediction made with all the data entered

Furthermore, the developed PWA has a section called "History," where all predictions made are stored, as seen in ***Figure 7***.

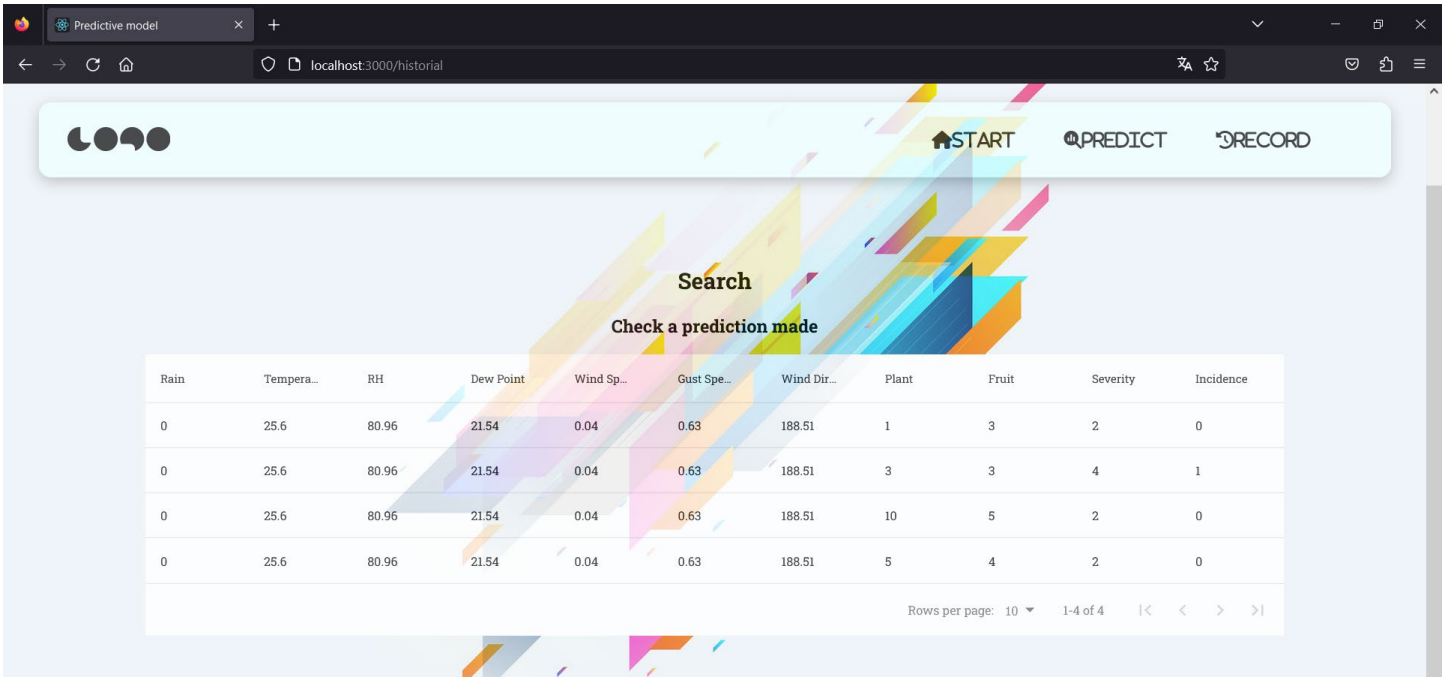

Figure 7. History of all predictions made

Data Analysis

Data analysis was performed to assess the efficiency of the predictive model using the statistical method of central tendency[4]. Two groups were established for data collection: a control group and an experimental group, from which quantitative data would be obtained. The authors of this research formed the experimental group, while the farmers in the Joya de los Sachas region constituted the control group. The data collection focused on assessing time efficiency, aiming to identify how long it takes for farmers to recognize the moniliasis disease in cocoa plantations and how long it would take them to identify the disease using the developed predictive model. To gather this information, interviews were conducted with some farmers to determine the time they take to identify the disease.

Additionally, a survey was conducted to collect data that would help the experimental group identify the time it takes to detect whether a fruit is infected. Around 25 farmers were interviewed, and 5 of them responded. The other farmers could not answer as they lacked the necessary tools to provide the required data for predicting in the predictive model.

The data obtained from the 5 farmers are presented in ***Table 11***.

N° Agri	Rain	Temp	Humid-ity	Dew Point	Wind Speed	Gust Speed	Wind Direc	Plan t	Fruit	Severity
1	0	25,6	80,96	21,54	0,04	0,63	188,51	2	5	3
2	0	26	94	23	1,3889	1,0289	324	5	1	0
3	0	24	83	22	1,667	1,0289	300	3	6	3
4	0	25	77	22	1,3889	0	293	8	1	1
5	0	24	68	23	19444	0,51444	305	7	3	0

Table 11. Data collection

With the data obtained, the control group (farmers) evaluates each fruit and records the time it takes to assess each one for infection, as presented in ***Table 12***.

Control Group Data												
N° Agri	**Rain**	**Temp**	**Hu-midity**	**Dew Point**	**Wind Speed**	**Gust Speed**	**Wind Direc**	**Plan t**	**Fruit**	**Se-ver ity**	**Inci-dence**	**Time (min)**
1	0	25,6	80,96	21,54	0,04	0,63	188,51	2	5	3	1	30
2	0	26	94	23	1,3889	1,0289	324	5	1	0	0	27
3	0	24	83	22	1,667	1,0289	300	3	6	3	1	26
4	0	25	77	22	1,3889	0	293	8	1	1	0	29
5	0	24	68	23	19444	0,5144	305	7	3	0	0	31

Table 12. Data collected from the control group

Similarly, the experimental group records the time it took them to identify whether a fruit is infected or not using the PWA, shown in ***Table 13***.

Experimental Group Data												
N° Agri	**Rain**	**Temp**	**Humidity**	**Dew Point**	**Wind Speed**	**Gust Speed**	**Wind Direc**	**Plant**	**Fruit**	**Severity**	**Incidence**	**Time (min)**
1	0	25,6	80,96	21,54	0,04	0,63	188,51	2	5	3	1	0.21
2	0	26	94	23	1,3889	1,0289	324	5	1	0	0	0.41
3	0	24	83	22	1,667	1,0289	300	3	6	3	1	0.25
4	0	25	77	22	1,3889	0	293	8	1	1	0	0.28
5	0	24	68	23	19444	0,5144	305	7	3	0	0	0.30

Table 13. Data collected from the experimental group

Upon comparing the data from these two groups and applying the mean as one of the measures of central tendency, the following results were obtained in ***Table 14*** and ***Figure 8***:

Time (min)	
Control Group	**Experimental Group**
30	0.21
27	0.41
26	0.25
29	0.28
31	0.3
Arithmetic average	
28.6	0.29

Table 14. Comparison of results obtained from both groups

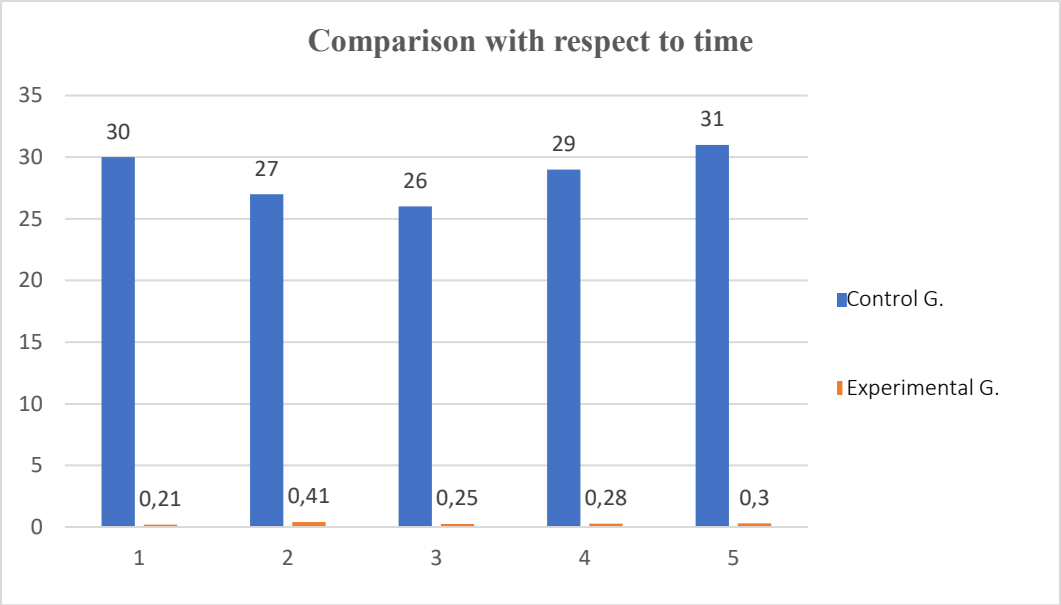

Figure 8. Comparison of the results obtained in verifying the efficiency regarding time

After the completion of data collection and processing, a stark difference was evident between the two groups. The control group took an average of 28.6 minutes per fruit to identify whether it was infected. In contrast, using the PWA with the implemented predictive model, the experimental group took an average of 0.29 minutes per fruit.

Threats to the Validity of the Study

External variables may affect or not provide validity to this study, for example, the lack of availability of complete data or new requirements needed to improve prediction. It can also happen that the pathogen causing moniliasis disease mutates or evolves with some antibodies or something similar, which can alter the prediction of this model. On the other hand, as it is known that every predictive model has a beginning and an end, the end may come when you want to update this model, that is, add relevant external features or factors such as the type of soil where cocoa plants are grown, or the type of climate, plant height, etc.

DISCUSSION

The discussion provides valuable insights into the various aspects of the study, such as the expository bibliographic analysis, comparison of different machine learning algorithms, the development of the artifact, data analysis, and the research presented by Koysawat et al.[10] and Ordoñez J.[15] greatly aided in the successful development of this research. Here are some key points from each section:

The study starts with a comprehensive literature review, which involves searching for relevant information through physical and electronic books available on the Internet. The objective was to design the predictive model and the progressive web application (PWA) in a user-friendly manner, specifically for farmers. This analysis aimed to achieve an optimal level of learning to begin designing the predictive model and the PWA.

The study compared different types of machine learning algorithms to build a reliable predictive model for forecasting moniliasis in cocoa fruits. These algorithms included Dimensionality Reduction Techniques (PCA, IPCA, and KPCA), Regularization Trends (Linear, Lasso, Ridge, Elastic Net), handling outliers with Robust Regressions (RANSAC, Huber Regressor), and Ensemble Methods (Bagging and Boosting).

The study conducted tests with different data sets (normal, normalized, and discretized data) to evaluate the performance of each algorithm. Results were recorded and analyzed for each algorithm, and conclusions were drawn based on the best-performing algorithms.

The development of the artifact (PWA) followed the methodology of design science, comprising three cycles: the relevance cycle, rigor cycle, and design cycle. In the relevance cycle, investigations were made concerning the moniliasis disease and cocoa cultivation. The rigor cycle involved understanding the requirements and needs for controlling or preventing the disease, leading to the development of the predictive model and PWA. The design cycle focused on designing the predictive model in production and creating the PWA.
This allowed for the integration of the PWA and the predictive model. With the data input and tests conducted, it was verified that the created Progressive Web Application functions perfectly, assisting in forecasting the disease more efficiently and quickly. This, in turn, helps farmers make early decisions regarding the salvation or treatment of fruits contaminated with this disease.
Data analysis was performed to assess the efficiency of the predictive model using the statistical method of central tendency. The study collected data from both a control group (farmers) and an experimental group (authors of the research) to evaluate the time efficiency of identifying moniliasis in cocoa fruits. The control group assessed each fruit manually, while the experimental group used the PWA with the predictive model to detect the disease.
The results showed a significant difference in time efficiency between the two groups. The experimental group using the PWA took an average of 0.29 minutes per fruit, while the control group took an average of 28.6 minutes per fruit. This highlights the effectiveness and potential time-saving benefits of using the predictive model and PWA for disease detection.
The study successfully achieved its objectives by designing a predictive model and a user-friendly progressive web application for forecasting moniliasis in cocoa cultivation. The comparison of different algorithms and the data analysis demonstrated the efficiency of the predictive model in significantly reducing the time required for disease detection.

CONCLUSIONS

The study's main objective was to develop a predictive model for cocoa production that would allow predicting the presence of moniliasis, a fungal disease that affects cocoa crops. To achieve this, a design science research methodology was used, and a Progressive Web Application (PWA) was implemented to facilitate farmers' access and use of the model. Specific objectives included conducting a bibliographic analysis to design the model, comparing different machine learning algorithms, performing data analysis using artificial intelligence techniques, and developing an efficient Progressive Web Application.
After conducting the data analysis and comparing different machine learning algorithms, the following key findings were obtained:
Dimensionality reduction algorithms (PCA, IPCA, and KPCA) and the Gradient Boosting Classifier algorithm showed the best predictive results. The SVR algorithm demonstrated the best performance in the Trend Regularization technique to reduce the complexity of the model. The Bagging technique with the Random Tree Forest algorithm yielded excellent results in the context of normalized data.
The Gradient Boosting Classifier is the algorithm developed and analyzed that provides the best predictive result and is placed in the predictive model.
Furthermore, a data analysis was performed, where the average time for the experimental group to identify the presence of moniliasis using the PWA with the predictive model was only 0.29 minutes per fruit, compared to the control group, which took an average of 28.6 minutes per fruit.
These findings indicate that the developed predictive model and the Progressive Web Application can effectively predict the presence of moniliasis in cocoa crops. Using machine learning algorithms and artificial intelligence techniques allowed for accurate and fast results, which can be highly useful for farmers in early disease detection and informed decision-making for control and prevention.
Furthermore, the study acknowledges some limitations, such as data's complete and representative availability to train the predictive models. Additionally, the model's performance may be affected by the quality of the data used and the variability of conditions in cocoa plantations. These limitations should be considered when interpreting the results and applying the model in practice.

The study's practical implications are significant, as the predictive model and Progressive Web Application can provide farmers with a valuable tool to improve the management and prevention of moniliasis in cocoa crops. It is recommended that the model be continuously improved and updated with new data to maintain its accuracy and effectiveness over time. Furthermore, exploring the integration of other variables and technologies is suggested to increase the predictive capability and user-friendliness of the tool.
The study successfully developed an effective predictive model to forecast the presence of moniliasis in cocoa crops and applied it through a Progressive Web Application. The results demonstrated the utility and potential of this tool in the agricultural context. The research reaffirms the importance of combining science and technology to address real problems and provide practical solutions to farmers. Hopefully, this initiative will contribute to improving the productivity and sustainability of cocoa crops and facing agricultural challenges with innovative and efficient approaches.

REFERENCES

1. de Andrade Cardieri G, Zaina LAM. PWA-EU: Extending PWA Approach for Promoting Customization based on User Preferences. Proc ACM Hum Comput Interact. 2019 Jun 13;3(EICS):1–28.
2. Andreina P, Ayala M. Bibliographic Research: Definition, Types, Techniques. 2018.
3. Arcentales Garcia. Estefania P. Variation in the potential distribution of cocoa cultivation in the coastal region of Ecuador by 2050, due to climate change. 2019.
4. Burgos-Martínez R, Argüelles-Pascual V, Palacios RH. Phases of the statistical method. Publicación semestral [Internet]. 2021; 9(17):35–6. Available from: https://repository.uaeh.edu.mx/revistas/index.php/huejutla/issue/archive
5. Castro Romero A, Sebastián González Sanabria J, Callejas Cuervo M. Utility and operation of databases NoSQL Databases NoSQL's Utility and Functioning. Vol. 21. 2012.
6. Correa Álvarez J, Castro Martínez S, Coy J. Biology stage of Moniliophthora roreri in Colombia. Acta Agron. 2014;4(63):388–99.
7. García-Briones AR, Pico-Pico BF, Jaimez RE. The Cocoa production chain in Ecuador: Resilience in the different production actors. NOVASINERGIA Digital Magazine of Science, Engineering and Technology. 2021 Dec 1;4(2):152–72.
8. James Quiroz V. Influence of agronomy and harvest on cocoa quality. 2012.
9. Judith Sandoval L. Machine learning algorithms for data analysis and prediction. ITCA-FEPADE. 2018;(11):36–40.
10. Koysawat P, Boonprakob C, Saengprachatanarug K, Chaosakul A, Wanjantuk P, Wongphati M, et al. Progressive Web App for Crop Field Data Collection. IOP Conf Ser Mater Sci Eng. 2021 Aug 1;1163(1):012018.
11. Majchrzak TA, Biørn-Hansen A, Grønli TM. Progressive Web Apps: the Definite Approach to Cross-Platform Development? [Internet]. Proceedings of the 51st Hawaii International Conference on System Sciences. 2018. 5735–5744 p. Available from: http://hdl.handle.net/10125/50607
12. Marcelino P, de Lurdes Antunes M, Fortunato E, Gomes MC. Machine learning for pavement friction prediction using scikit-learn. In: Lecture Notes in Computer Science (including subseries Lecture Notes in Artificial Intelligence and Lecture Notes in Bioinformatics). Springer Verlag; 2017. p. 331–42.
13. Norman Anuar N, Kamal Othman M. Integrating User-Centered Design with the Agile Software Development Methodology for a Cultural Heritage Information System. Interaction Design and Architecture(s) Journal - IxD&A. 2020;44:207–55.

14. de Oliveira DC, Barbosa UC, Bergland ACRO, Resende O, de Oliveira DEC. G-SOJA - website with prediction on soybean classification using machine learning. Engenharia Agricola. 2021;42(SpecialIssue).
15. Ordoñez Merino J. Predictive model applying machine learning algorithms for dairy production at the El Prado farm. 2023;
16. Robles S, Vásquez H, Naranjo L. Adapting Design Science Methodology in luminaires development. Revista de la Facultad de Ingenierías y Tecnologías de la Información y Comunicación. 2019;2(6).
17. Vadakkan AS, S SR, Khateeb A, Professor A. Cyberbullying Detection in Textual Modality. IJACSA) International Journal of Advanced Computer Science and Applications [Internet]. 2021;12(12):217–21. Available from: www.ijacsa.thesai.org
18. Zamorano Ruiz J. Comparison and analysis of machine learning algorithms for predicting the predominant type of tree cover. 2018.

Received: October 9th 2023/ **Accepte**d: January 15th 2024 / **Published:**15 February 2024

Citation: Miranda A, Bonifa B, Chango W, Aguilar P. Predictive Model in Production through Progressive Web Applications to Forecast Moniliasis in Cacao. Revis Bionatura 2024; 9 (1) **14**. http://dx.doi.org/10.21931/RB/2024.09.01.**14**

Additional information Correspondence should be addressed to *aracely.miranda@espoch.edu.ec*
Peer review information. Bionatura thanks anonymous reviewer(s) for their contribution to the peer review of this work using https://reviewerlocator.webofscience.com/

Bionatura ISSN. First 13909355 Ecuador. **Scopus coverage years**: from 2016 to the present

Bionatura
Ibero-American Journal of Biotechnology and Life Sciences

Article

Prevention of cocoa moniliasis using Progressive Web Applications and sensor data in the province of Francisco de Orellana

Darwin Romero [1]*, *Pilar Oña* [2]*, *Pedro Aguilar* [3], *Wilson Chango* [4]

[1] *Escuela Superior Politécnica de Chimborazo, Sede Orellana, Ecuador.*
[2] *Escuela Superior Politécnica de Chimborazo, Sede Orellana, Ecuador.*
[3] *Escuela Superior Politécnica de Chimborazo, Sede Orellana, Ecuador; pedro.aguilar@espoch.edu.e*
[4] *Escuela Superior Politécnica de Chimborazo, Sede Orellana, Ecuador; wilson.chango@espoch.edu.ec.*
* *Correspondence: darwin.romero@espoch.edu.ec , pilar.onia@espoch.edu.ec*
Available from. http://dx.doi.org/10.21931/RB/2024.09.01.15

ABSTRACT

Ecuador is an essential cocoa producer recognized for its quality and aroma. Additionally, it holds a prominent position among the country's traditional export products, making it the third-largest cocoa-producing country in the world. However, the cocoa industry faces challenges due to moniliasis, a fungal disease that affects cocoa trees and causes damage to the fruits, resulting in decreased production. This research aims to prevent cocoa moniliasis by conducting tests with different algorithms to select the best one for predicting moniliasis using sensor data in the progressive web application. Various supervised learning algorithms were applied, including PCA, IPCA, KPCA, Linear Regression, Sci-Kit Learning, and ensemble methods like Bagging and Boosting. Google's Lighthouse is utilized for artifact validation. It is concluded that the Boosting ensemble method with a value of 1.0 and 4 estimators is the algorithm that shows a good fit for prediction. In artifact validation, it yields favorable results with a score of over 90 in various Lighthouse parameters.

Keywords: Moniliasis 1; Progressive Web Application 2; PCA 3; IPCA 4; KPCA 5; Linear Regression 6; Bagging 7; Boosting 8; Lighthouse 9

INTRODUCTION

Thanks to its biodiversity and favorable geographical location, Ecuador is a significant cocoa producer.[1] For the authors[2], cocoa is scientifically known as Theobroma cacao and is prominent among the country's traditional export products. It is the third-largest cocoa producer in the world, earning international recognition and appreciation for its distinctive quality and aroma. As a result, cocoa cultivation extends across various regions of Ecuador, with an annual production of 212,249 tons in 491,221 hectares. Additionally, cocoa production is paramount, sustaining the country's economy and providing employment opportunities.

The province of Francisco de Orellana, located in Ecuador, is renowned for its significant cocoa production. It is cultivated in an environment of exceptional biodiversity and a favorable geographical location, providing ideal conditions for developing high-quality cocoa beans with a distinct flavor and aroma. However, moniliasis, a fungal disease severely affecting cocoa trees caused by the *Moniliophthora perniciosa* and *Moniliophthora roreri* fungi, poses a challenge. Moreover, the authors[3-2] mention that these fungi attack various plant tissues, such as fruits, floral cushions, and buds, leading to witch's broom formation and fruit loss. This disease

is favored by factors such as high temperatures, humidity, and the age of cocoa plants, resulting in economic losses and representing one of the main threats to this industry.
Francisco de Orellana has experienced significant climate changes characterized by highly high heatwaves and variations in humidity. The combination of high moisture and optimal temperatures creates a conducive environment for spore germination and the subsequent development of the disease. Notably, frequent rainfall and insufficient ventilation in cocoa plantations can contribute to maintaining high relative humidity levels, increasing the risk of moniliasis infection.
The most common method to control moniliasis is the use of chemical fungicides. However, prolonged use of these products can lead to resistance to pathogenic fungi, negatively impact the environment, and may not be suitable for organic production.[4] As a result, efforts have been made to implement innovative technological solutions to prevent and control cocoa moniliasis, including testing various supervised algorithms. This allows for identifying the best algorithm for the progressive web application.
The Progressive Web Application (PWA) is a revolutionary approach that transcends boundaries due to its adaptability to different technological devices.[4] It offers a pleasant user experience even with slow or no internet connectivity. As authors 4-5 mentioned, progressive web applications are responsive and independent of connectivity. They can be cached for offline use, providing enhanced security compared to native applications and reducing development costs by adapting to different platforms with a secure connection using the HTTP or HTTPS protocol.
To carry out predictions, it is necessary to use Supervised Machine Learning (ML), which, according to author[6], is a branch of artificial intelligence focused on learning from experience. It addresses problems such as classification, association, clustering, and feature selection based on large structured data sets. Supervised learning has proven to be helpful in decision-making and predicting potential outcomes. Hence, different supervised algorithms were tested using Python and various libraries. This comparison allowed the selection of the best algorithm for implementation in the progressive web application.
Furthermore, as the data generated by the sensors in cocoa plantations and manually collected data are required, a database is necessary. According to the author[7], NoSQL databases are recommended when handling large amounts of data thanks to their high availability, scalability, and Performance, as they are popular for storing and processing vast data quickly. As a result, one of the most recognized and open-source databases is MongoDB, which allows for dynamic changes in documents and flexible queries, thereby accelerating data retrieval.
This study employed four methods: literature review and documentary research, design science, and Google's Lighthouse.
The questions that have been raised for the development of this research are:

- Question 1: Which supervised machine learning algorithms produce the best predictive results?
- Question 2: What scores or percentages do the Performance, Accessibility, best practices, SEO, and Progressive Web App (PWA) compliance have when validating the artifact?

This study employed four methods: literature review and documentary research, design science, and Google's Lighthouse. The current state of the research field should be carefully reviewed, and key publications cited. Please highlight controversial and diverging hypotheses when necessary. Finally, briefly mention the main aim of the work and highlight the principal conclusions.

MATERIALS AND METHODS

The methodology to be used to develop this research involves a literature review using a documentary research method with a quantitative scope for analyzing supervised learning algorithms related to the issue of cocoa moniliasis. To address this problem, a progressive web application (PWA) will be developed to help farmers prevent this disease using data from sensors and manual inputs. The artifact will be assessed using the Lighthouse tool generated by Google for a more effective evaluation, which provides a scoring mechanism.

Procedure:

Phase I:
Literature Review and Documentary Research

According to the authors, combining both research methods (bibliographic and documentary) allows for a more in-depth investigation of the topic to determine the most suitable tools for developing the progressive web application for predicting cocoa moniliasis. The Design Science Research (DSR) method will also be employed, focusing on creating artifacts as innovative solutions to practical problems in a specific domain. These artifacts are constructed through an iterative design, construction, and evaluation cycle. The goal is to validate the artifact before its implementation, ensuring its utility and effectiveness in addressing the stated problem.[9]

Phase II:
Using the Design Science Research method, the design of the PWA application will be established in detail, including the selection of technologies used for building this application. The intention is to create an application that can be adopted by other applications for predicting cocoa moniliasis, as illustrated in Figure A.

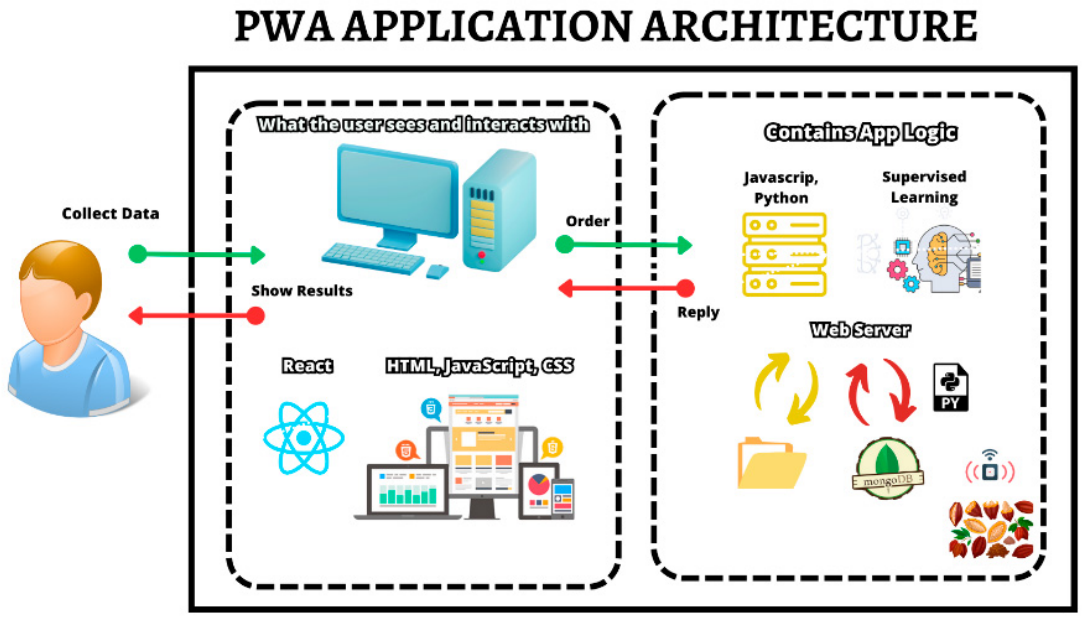

Figure 1. Architecture of the Predictive Progressive Web Application. Source: Conducted by authors, 2023.

Phase III
Data Collection
Data collection will be carried out in a cocoa plantation in the Francisco de Orellana canton for testing and training the cocoa moniliasis prediction algorithms. The data will include readings from sensors such as Rain, Relative Humidity (RH), Dew Point, Wind Speed, Gust Speed, and Wind Direction. Additionally, manual data will be collected, including essential characteristics related to cocoa moniliasis, such as plant name, plant age, fruiting months, humidity, disease severity, and incidence. These collected data will be used for training and validating the supervised learning algorithms. For implementing the algorithms, 10 data points will be selected for training and 1 for testing. In cases where data points are missing, they will be completed with a value of 0 to avoid errors during testing. Regularization and robustness algorithms will utilize the training data and one test data point within the coding.

Phase IV
Testing with Supervised Learning Algorithms
Seven supervised learning algorithms have been selected for testing, including dimensionality reduction techniques PCA, IPCA, and KPCA with standard kernels and ensemble Methods (Bagging and Boosting). These algorithms were used to determine the highest accuracy in predicting cocoa moniliasis. Additionally, Linear

Regression was implemented, focusing on data training regularization and Sci-Kit Learning, focusing on outliers with robust regressions. These tests are crucial for selecting the most effective algorithm before the final implementation of the prediction system.

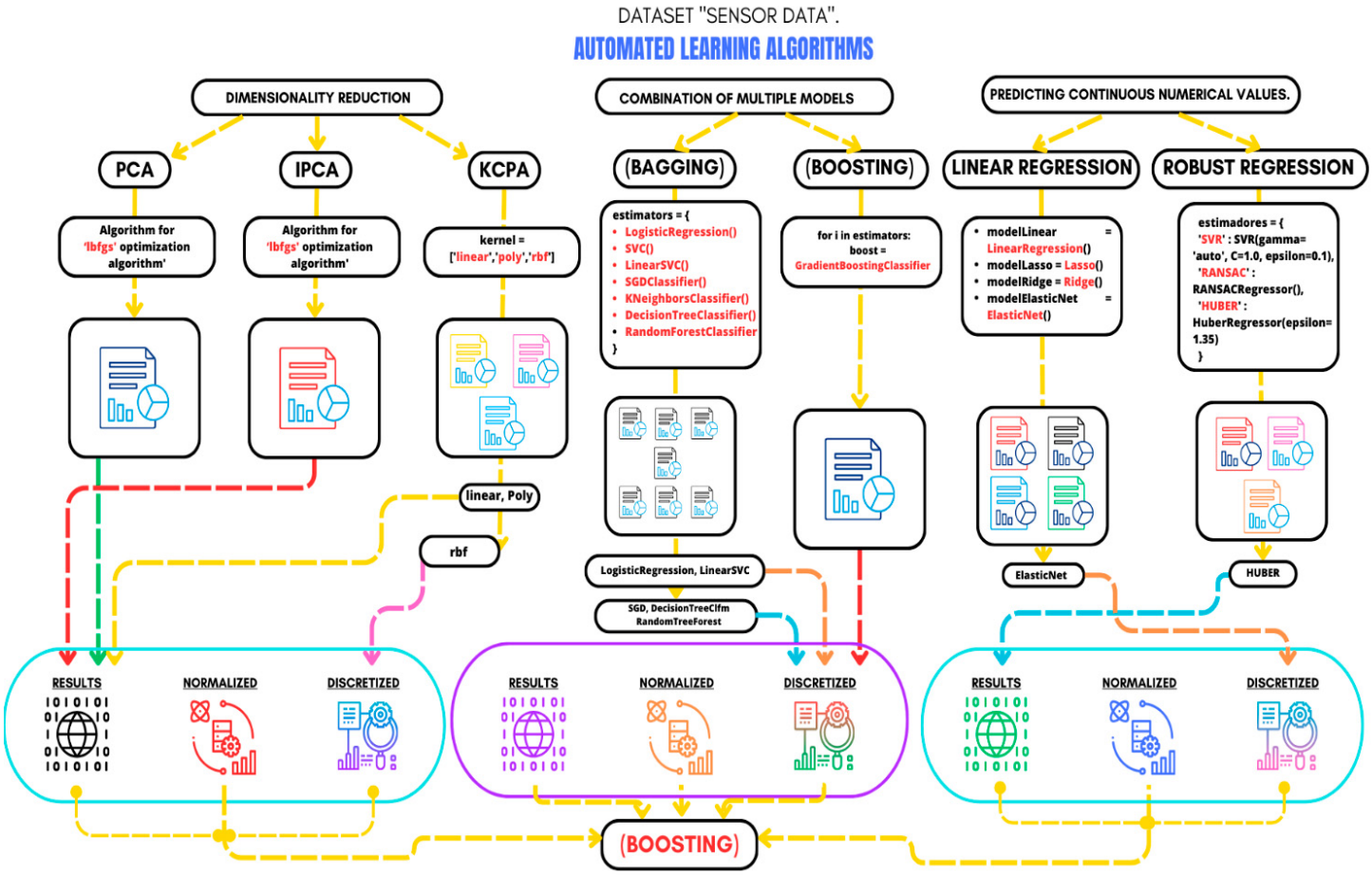

Figure 2 provides a detailed overview of the types of algorithms used and which one had the best fit during the data set testing. Source: Conducted by authors, 2023.

Phase VI

Artifact Validation

Lighthouse is an open-source tool that automates improving web applications' Performance, quality, and correctness. Analyzing a page, it performs a series of tests and generates a detailed report on its Performance. Identifying failed tests provides critical indicators to help developers improve their web applications.[4]

RESULTS

The extraction of sensor data and the collection of manual data took place at the La Belleza Experimental Station, which belonged to the Francisco de Orellana canton and was donated to the Escuela Superior Politécnica de Chimborazo Sede Orellana, covering an area of 37 hectares dedicated to Higher Education. Additionally, the artifact validation will be conducted using Google's tool.

Implementation of the Dimensionality Reduction Algorithm

PCA

According to authors[10], PCA is a method that uses principal components derived from the correlation matrix to simplify relationships between variables. Furthermore, the dataset contains many features, and not all of them are significant. The PCA algorithm was performed from three perspectives: average results, normalized

results, and discretized results, all of which showed a favorable fit with a score of 1 when using the dataset without normalization or discretization. This section may be divided into subheadings. It should provide a concise and precise description of the experimental results, their interpretation, and the experimental conclusions that can be drawn.

Algorithm Type	Types of results	Results
PCA	Normal result	1.0
	Resultado Normalizado	0.88
	Resultado Discretizado	0.9783333333333334

Table 1. Results with PCA Algorithms.Source: Conducted by authors, 2023.

The average results obtained a value of 1.0, indicating a good algorithm fit. The normalized results obtained a value of 0.88, suggesting the algorithm could not fit well. However, the discretized results showed an increased fit with a value of 0.9783333333333334.

IPCA

IPCA (Incremental PCA) is designed to use a memory-independent amount of memory when dealing with datasets that are too demanding[11]. A favorable outcome was achieved when using normal results, indicating a good algorithm fit. However, when implementing normalization and discretization, the algorithm's fit decreased, as shown below:

Algorithm Type	Types of results	Results
IPCA	Normal result	1.0
	Normalized Result	0.8733333333333333
	Discretized result	0.985

Table 2. Results with the IPCA Algorithms.Source: Conducted by authors, 2023.

Upon analyzing the results, it was found that the IPCA algorithm had an excellent fit to the data without any additional transformation, obtaining a value of 1.0. However, when normalization was applied, the algorithm's Performance decreased to 0.8733333333333333, indicating a negative impact. On the other hand, implementing discretization slightly improved the result to 0.985 compared to normalization, suggesting that discretization had a less negative impact on the algorithm's fit.

Implementation of Common Kernels Algorithm

KPCA

KPCA is a method that uses principal component analysis in a feature space to reduce the data's dimensionality when the data does not have a linearly separable structure, and a KERNEL is found[12]. The standard kernels

analyzed were linear, poly, and rbf, and when conducting training tests, the following results were obtained for average, normalized, and discretized data, as shown below:

Algorithm Type	Types of results	Results
KCPA	Normal result	Score KPCA linear: 0.9916666666666667 Score KPCA poly: 0.9916666666666667 Score KPCA rbf: 0.66
	Normalized Result	Score KPCA linear: 0.8883333333333333 Score KPCA poly: 0.85 Score KPCA rbf: 0.8433333333333334
	Discretized result	Score KPCA linear: 0.8733333333333333 Score KPCA poly: 0.8183333333333334 Score KPCA rbf: 0.8533333333333334

Table 3. Results with KPCA Algorithms.Source: Conducted by authors, 2023.

Upon analyzing the normal results, better fits were obtained in KPCA linear and poly with a value of 0.9916666666666667 compared to the normalized and discretized results, which improved the fit with KPCA rbf with a value of 0.8533333333333334. However, the normal KPCA linear result achieved the best fit.

Implementation of Linear Regression Algorithm

Linear Regression

The authors mention that this algorithm seeks to find the best straight line that fits the data by minimizing a loss function[13]. Regularization techniques include Linear, Lasso, Ridge, and ElasticNet, aiming to reduce model complexity and prevent overfitting by penalizing model coefficients. The following results were obtained for normal, normalized, and discretized data:

Algorithm Type	Types of results	Results
Linear Regression	Normal result	Score Lineal; 0.9337542850425272 Score Lasso; 0.9321976562616098 Score Ridge; 0.9337532615244014 Score ElasticNet; 0.9315081721345164
	Normalized Result	Score Lineal; 0.9144346008057538 Score Lasso; 0.9138052629638189 Score Ridge; 0.9144930223805792 Score ElasticNet; 0.9129496840895489
	Discretized result	Score Lineal; 0.901894410892162 Score Lasso; 0.9008801774658688 Score Ridge; 0.9018951542734359 Score ElasticNet; 0.9005362968682721

Table 4. Results with Linear Regression Algorithms.Source: Conducted by authors, 2023.

The Linear Regression algorithm did not yield favorable results, indicating that it did not fit the dataset well. However, a more favorable fit was achieved when discretizing the data, with ElasticNet obtaining a value of 0.9005362968682721.

Implementation of the Sci-Kit Learning Algorithm

Sci-Kit Learning

In Scikit-learn, a wide variety of robust regression estimators are provided to address problems related to outliers or noise in the data. SVR MSE, Ransac MSE, and Huber MSE are used with loss functions or fitting criteria that are less sensitive to outliers or noise in the data. These robust regression techniques have produced better results than linear regression[13], as shown below:

Algorithm Type	Types of results	Results
Sci-Kit Learning	Normal result	SVR MSE: 0.0212404219 RANSAC MSE: 0.0251234906 HUBER MSE: 0.0291127339
	Normalized Result	SVR MSE: 0.0212404219 RANSAC MSE: 0.3400000000 HUBER MSE: 0.0191127339
	Discretized result	SVR MSE: 0.0212404219 RANSAC MSE: 0.3400000000 HUBER MSE: 0.0291127339

Table 5. Results with Sci-Kit Learning Algorithms Source: Conducted by authors, 2023.

The best robust regression algorithm is SVR MSE, with a value of 0.0212404219. This value indicates a lower mean squared error than the other analyzed algorithms (Ransac MSE and Huber MSE). Therefore, SVR MSE demonstrated better Performance in model fitting to the data than the other mentioned robust regression algorithms.

Implementation of Ensemble Algorithm (Bagging and Boosting).

Bagging

Bagging combines predictions from multiple models trained on bootstrap samples, reducing variance and overfitting. It improves the accuracy and stability of the final model by averaging or voting the projections of the base models[14]. It also provides an estimation of uncertainty in forecasts. The predictive models used are KNN, LogisticRegression, SVC, LinearSVC, SGD, KNN, DecisionTreeClassifier, and RandomForestClassifier. The following results were obtained for average, normalized, and discretized data:

Algorithm Type	Types of results	Results
Ensemble Method (Bagging)	Normal result	Score con KNN: 0.99 Score Bagging with LogisticRegression: 1.0 Score Bagging with SVC: 0.99 Score Bagging with LinearSVC: 1.0 Score Bagging with SGD: 1.0 Score Bagging with KNN: 0.99 Score Bagging with DecisionTreeClf: 1.0 Score Bagging with RandomTreeForest: 1.0
	Normalized Result	Score con KNN: 0.99 Score Bagging with LogisticRegression: 1.0 Score Bagging with SVC: 0.99 Score Bagging with LinearSVC: 1.0 Score Bagging with SGD: 1.0 Score Bagging with KNN: 0.99 Score Bagging with DecisionTreeClf: 1.0 Score Bagging with RandomTreeForest: 1.0
	Discretized result	Score con KNN: 0.99 Score Bagging with LogisticRegression: 1.0 Score Bagging with SVC: 0.99 Score Bagging with LinearSVC: 1.0 Score Bagging with SGD: 1.0 Score Bagging with KNN: 0.99 Score Bagging with DecisionTreeClf**:** 1.0 Score Bagging with RandomTreeForest: 1.0

Table 6. Result of the Ensemble Method (Bagging) Algorithm.Source: Conducted by authors, 2023.

The results show a highly favorable fit, with values of 1.0 in most cases, indicating a perfect model fit to the data. This technique is beneficial in classification problems, reducing variance and overfitting.

Boosting

The Boosting algorithm trains weak models, such as simple decision trees, called "weak learners," in successive iterations, focusing on correcting errors[14]. Multiple GradientBoostingClassifier models were trained with different numbers of estimators, and the accuracy of each model was recorded. Then, the algorithm identified the best accuracy result along with the corresponding number of estimators. As shown below:

Algorithm Type	Types of results	Resultado
Ensemble Method (Boosting)	Normal result	{'result':0.6385714285714286, 'n_estimator': 2} {'result': 1.0, 'n_estimator': 4}
	Normalized Result	{'result':0.6385714285714286, 'n_estimator': 2} {'result': 1.0, 'n_estimator': 4}

	Discretized result	{'result':0.6385714285714286, 'n_estimator': 2} {'result': 1.0, 'n_estimator': 4}

Table 7. Result of the Ensemble Method (Boosting) Algorithm.Source: Conducted by authors, 2023.

Los resultados finales muestran que en los tres casos se dio el mismo resultado indicando un buen ajuste del algoritmo de predicción para cada modelo con un valor de 1.0 y con 4 estimadores representativos.
Para más detalle y verificación de las pruebas realizadas se pueden dirigir al siguiente link https://github.com/DarwinBRG/scikit-learn.git

Validación del artefacto

Metodo Lighthouse by Google

Se realizo la validación del artefacto con la herramienta de puntuación de Lighthouse que proporciona Google de código abierto para probar la progresividad de la aplicación web progresiva. Al realizar la el test, Lighthouse da una puntuación de Performance, Accessibility, Best Practices, SEO y PWA, se obtuvo la siguiente puntuación.[15-5]

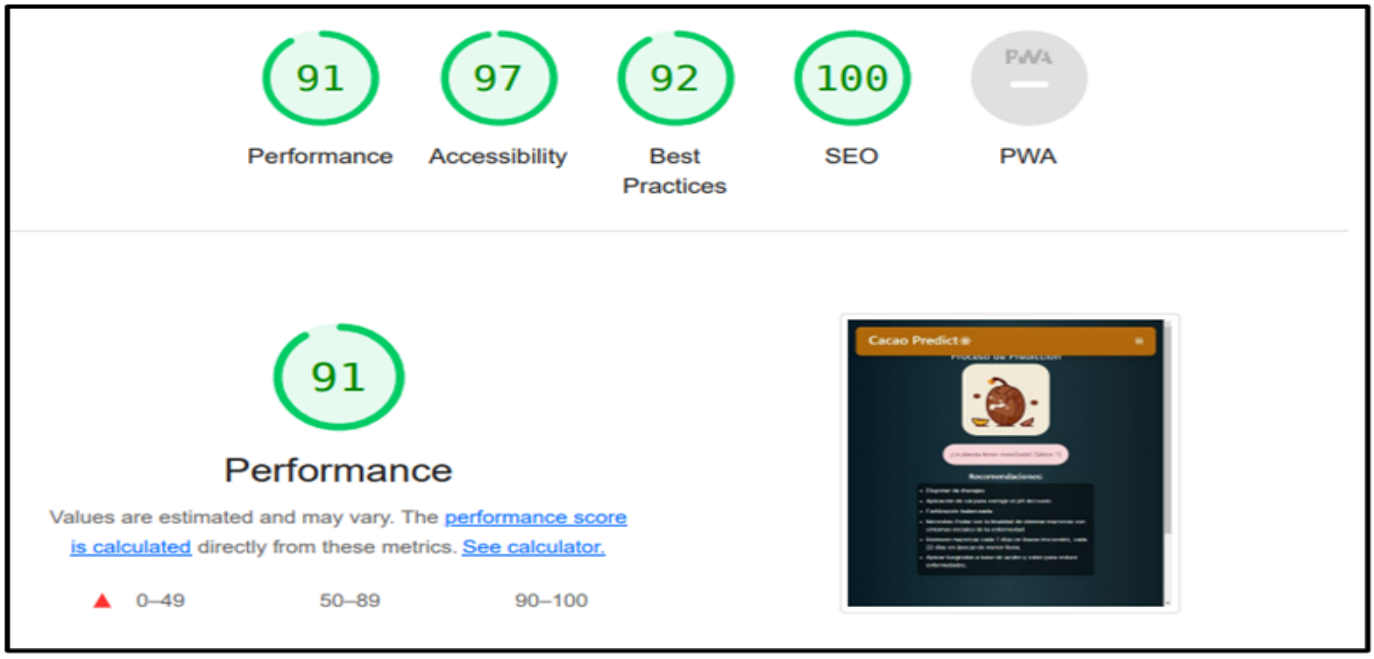

Figure 3. Artifact Validation.<Source: Conducted by authors, 2023.

Algorithm Type	Better result	Results
PCA	Normal result	1.0
IPCA	Normal result	1.0
KCPA	Normal result	Score KPCA linear: 0.9916666666666667
Linear Regression	Discretized result	Score ElasticNet 0.9005362968682721
Sci-Kit Learning	Normal result	SVR MSE: 0.0212404219

Ensemble Method (Bagging)	Discretized result	Score Bagging with LogisticRegression: 1.0 Score Bagging with LinearSVC: 1.0 Score Bagging with SGD: 1.0 Score Bagging with DecisionTreeClf: 1.0 Score Bagging with RandomTreeForest: 1.0
Ensemble Method (Boosting)	Discretized result	{'result': 1.0, 'n_estimator': 4}

Table 8. Analysis of relevant data.Source: Conducted by authors, 2023.

The application scored 91 in Performance, indicating good speed and efficiency. Regarding Accessibility, it scored 97, indicating that the application is accessible and usable for a broad audience, including people with disabilities. Regarding Best Practices, the application scored 92, signifying adherence to industry-recommended best practices for web development, contributing to its quality and security. The application received a perfect score of 100 for SEO, indicating that it is well-optimized for search engines and more likely to appear in relevant search results.

Additionally, an exact score is not provided in the PWA variable, but some noteworthy features are highlighted. The application is installable on any device and incorporates a service worker, allowing it to function offline by caching data. It can automatically update data and has a responsive design, ensuring adaptability to different devices. The application is also configured for a personalized presentation screen, and its content adjusts appropriately to the graphical window size. Furthermore, it establishes a theme color for the address bar and includes a "viewport" tag with the initial scale width. These features enhance the user experience and usability of the progressive web application across various environments and devices.

DISCUSSION

Analyzing the results obtained with the different supervised algorithms and considering the findings according to the authors[13], it can be mentioned that the best algorithm fit is achieved when it has a value greater than 0.80. Therefore, the following results are presented: The findings and their implications should be discussed in the broadest context possible.

It can be stated that favorable results have been obtained independently, indicating a good fit of the algorithms. However, the authors [14] mention that using decision trees helps achieve a better fit when making predictions. Therefore, it has been determined that the best algorithm is the Boosting ensemble method, and implementing this algorithm in the prediction process has yielded favorable outcomes.

CONCLUSIONS

The objective of this research was to prevent cocoa moniliasis by testing different algorithms, such as the dimensionality reduction techniques PCA, IPCA, and KPCA with standard kernels, Ensemble methods (Bagging and Boosting), Linear Regression focusing on data training regularization, and Sci-Kit Learning focusing on outliers with robust regressions. The aim was to compare these algorithms to select the one that fits the prediction well. PCA and IPCA algorithms showed an excellent fit during the tests, obtaining results of 1.0 in their tests with standard data. In contrast, the KPCA algorithm yielded favorable results, especially in its "linear" variant, with an adjustment of 0.9916666666666667. The Linear Regression algorithm demonstrated significant fit by discretizing the data, with the highest result obtained using ElasticNet (adjustment of

0.9005362968682721). The Sci-Kit Learning algorithm (SVR MSE) showed a favorable fit with a value of 0.0212404219. In the ensemble methods (Bagging and Boosting), excellent fit was demonstrated in their discretized tests. Bagging showed results of 1.0 with several estimators while Boosting achieved 1.0 with 4 estimators.

Therefore, when comparing the results with a value of 1.0, indicating a good fit, it was identified that the best algorithm for predicting cocoa moniliasis is Boosting, providing a valuable tool for disease prevention and control in cocoa cultivation. The developed progressive web application demonstrated good Performance in the artifact validation, scoring Performance (91), Accessibility (97), Best Practices (92), and SEO (100). Although the PWA parameter did not receive an exact score, it was highlighted for its ability to be installable on any device, to feature a service worker for offline operation, and to have a responsive design for adaptation to different devices. This showcases good Performance, Accessibility, compliance with best practices, and optimization for search engines, with scores over 90%. This makes it a valuable tool for cocoa producers and the agricultural sector. The relevance of this research lies in its contribution to the field of agriculture and the use of advanced technologies to improve crop production and sustainability.

REFERENCES

1. Venezuela J, Guevara F. Eco-Friendly Biocontrol of Moniliasis in Ecuadorian Cocoa Using Biplot Techniques. Sustainability. 2023;: p. 15. https://doi.org/10.3390/su15054223
2. Ceccarelli V, Lastra S, Loor R, Chacón W, Nolasco M, Conservation and use of genetic resources of cacao (Theobroma cacao L.) by gene banks and nurseries in six Latin American countries. Genet. Resour. Crop Evol. 2022; p. 1283-1302. https://doi.org/10.1007/s10722-021-01304-3
3. Almeida S, Silva S, Lima J, Fim Rosas J, Capelini V. Fuzzy modeling of the risk of cacao moniliasis occurrence in Bahia state, Brazil. SCIELO. 2020. https://doi.org/10.1590/1807-1929/agriambi.v24n4p225-230
4. Tandel S, Jamadar A. Impact of Progressive Web Apps on Web App Development. IJIRSET. 2018. http://dx.doi.org/10.15680/IJIRSET.2018.0709021
5. Adetunji O, Otuneme N, Iyasere E, Opiah O, Enaibe O. Enhanced online book store model: adopting the progressive. IJESRT. 2020. https://doi.org/10.29121/ijesrt.v9.i9.2020.1
6. Jiang T, Gradus J, Rosellini A. Supervised Machine Learning: A Brief Primer. Web of Science. 2020;: p. 675-687. https://doi.org/10.1016/j.beth.2020.05.002
7. Georgi G, Milko M. An approach to storing real-time sensor readings based on NoSQL database systems. 16ª Conferencia sobre Máquinas Eléctricas, Accionamientos y Sistemas de Potencia. 2019: p. https://doi.org/10.1109/ELMA.2019.8771666
8. Josep G, Angela O, Esperanza F. El artículo de revisión. Iberoamericana de Enfermeria. 2020.
9. Brendel A, Lembcke T, Muntermann J, Kolbe L. Toward replication study types for design science research. Journal of Information Technology.36(3). 2021: p. 198–215. https://doi.org/10.1177/02683962211006429
10. Vega J, Guzmán J. Regresión PLS y PCA como solución al problema de multicolinealidad en regresión múltiple. Revista de Matemática: Teoría y Aplicaciones, 18(1). 2021;: p. 9-20.
11. Donoso J, Guillaume G, Thomas A. Clasificación en imagenes hiperespectrales. Uchile.cl. 2017;: p. 1-4.
12. Hernández J. Dimensionality Reduction Methods: Comparative Analysis of methods PCA, PPCA and KPCA. UNICIENCIA Vol. 30, No. 1. 2016;: p. 115-122. https://doi.org/10.15359/ru.30-1.7
13. Sazzadur R, Javed S, Zarrin T, Joy R, Syed H. A Comparative Study On Liver Disease Prediction Using Supervised Machine Learning Algorithms. INTERNATIONAL JOURNAL OF SCIENTIFIC & TECHNOLOGY RESEARCH. 2020;: p. 419-422.
14. Aljamaan H, Alazba A. Software defect prediction using tree-based ensembles. Proceedings of the 16th ACM International Conference on Predictive Models and Data Analytics in Software Engineering. 2020;: p. 1-10. https://doi.org/10.1145/3416508.3417114
15. Cardieri GdA, Zaina LM. Analyzing User Experience in Mobile Web, Native, and Progressive Web Applications: Perspectives from Users and HCI Specialists. Proceedings of the 17th Brazilian Symposium on Human Factors in Computing Systems. 2018;(9): p. https://doi.org/10.1145/3274192.3274201

Received: October 9th 2023/ **Accepte**d: January 15th 2024 / **Published:**15 February 2024

Citation: Romero D, Oña P, Aguilar P, Chango W. Prevention of cocoa moniliasis using Progressive Web Applications and sensor data in the province of Francisco de Orellana. Revis Bionatura 2024; 9 (1) 15. http://dx.doi.org/10.21931/RB/2024.09.01.15

Additional information Correspondence should be addressed to *darwin.romero@espoch.edu.ec* , *pilar.onia@espoch.edu.ec*

Peer review information. Bionatura thanks anonymous reviewer(s) for their contribution to the peer review of this work using https://reviewerlocator.webofscience.com/

Bionatura ISSN. First 13909355 Ecuador. **Scopus coverage years**: from 2016 to the present

Bionatura
Ibero-American Journal of Biotechnology and Life Sciences

Article

Somatic Cell Count Evaluation in Early Lactation between Primiparous and Multiparous *Bos indicus* Cows

Santiago Alexander Guamán-Rivera[1,*], *Angela Edith Guerrero-Pincay*[1], *Nelson Rene Ortiz-Naveda*[2], *Raúl Lorenzo González-Marcillo*[1] *and Robinson J. Herrera-Feijoo*[3]

[1] *Escuela Superior Politécnica de Chimborazo (ESPOCH), Sede Orellana, El Coca 220150, Ecuador; a_guerrero@espoch.edu.ec ; raul.gonzales@espoch.edu.ec*

[2] *Facultad de Ciencias de la Tierra, Universidad Estatal Amazónica, Puyo, Pastaza, Ecuador nr.ortizn@uea.edu.ec*

[3] *Universidad Técnica Estatal de Quevedo, Quevedo 120550, Ecuador; rherreraf2@uteq.edu.ec*

** Correspondence: santiagoa.guaman@espoch.edu.ec*

Available from. http://dx.doi.org/10.21931/RB/2024.09.01.16

ABSTRACT

Using *Bos indicus* cows, a study examined the relationship between somatic cell count (SCC) and milk yield. For this study, one hundred fifty cows (Primiparous, PM, 75 and Multiparous, MP 75) in early lactation (days in milk, PM =134 ± 3; MP = 136 ± 5), milk production (9,88 kg/d, on average) of the creole breed Gyr lechers were enrolled. Before being assigned to each treatment, the SCC values were lower than 220,000 cells/mL, on average. All cows were maintained to graze daily on *Megathyrsus maximus* and supplemented with *Morus alba* ad libitum, being hand-milking at 0700 daily. Before analysis, the SCC was logarithmically transformed (log10). Then, PROC Mixed from SAS version 9.4 was used to evaluate all measurements. Regarding our results, the MP had greater milk yields than PM cows (10.83 vs. 9.18 ± 0.38 kg/d; $P = 0.003$). Similar results were observed for fat-corrected milk (8.26 vs. 6.80 ± 0.34; $P = 0.002$), although the fat values did not differ between both groups ($P = 0.86$) being lower than referential values for these breeds (2.46 ± 0.16, on average). No differences were observed in the other milk components (P = 0.65 to 0.85). Despite that, the somatic cell count (SCC) values showed a statistical tendency in PM than in MP (1.89 vs. 2.13 ± 0.05; $P = 0.07$). In conclusion, low-fat contents were observed in both groups, possibly due to the low quality of foods used in ruminant feeding. While that, the parity and advanced lactation conditioned the SCC contents. Therefore, other studies should be performed to identify more factors that could be determinants.

Keywords: Milk, Tropical livestock, Udder health

INTRODUCTION

According to Britt et al. [1], by 2067, the world's population is predicted to reach 10.4 billion, reducing the arable land available for food production. So, the sustainability of dairy farms will be vital to stopping the growing agricultural frontier. Compared to breeds from temperate regions, tropical bovine production is low regarding milk kilos, composition, or udder health. As a result, developing and tropical nations continue to face difficulties in increasing milk output[2,3]. Nevertheless, mastitis is among the costliest diseases affecting the dairy cattle industry[4]. Most of the immune cells in milk are lymphocytes, polymorphonuclear neutrophils (PMN), and macrophages, represented by the somatic cell count (SCC)[5]. This udder inflammation can be subclinical and chronic, but both forms have severe risks to obtaining milk of good hygienic quality and

farming profitability[6]. In addition, the resilience of high-yielding animals and poor efficacy of therapies and prevention (i.e., antibiotic resistance and dubious efficacy of vaccines) could be associated factors. In this sense, one of the most used indicators to assess milk quality and define milk prices is SCC[8]. According to Juárez et al.[6], the first and principal tool used by technicians and farmers to evaluate udder health in flocks is SCC, an essential tool with easy application. Although much scientific evidence has been reported from other continents[9–11] using breeds of *Bos taurus* at the Latin American level, few studies where the raising *Bos indicus* predominates have been informed. Data from MAGAP[12] have shown that in the Amazon region, cattle raising represents one of the more important activities to generate money resources for these families[2]. In fact, of 5236 agricultural productive units (UPA's) identified in Orellana province, approximately 46% are developed as small livestock farmers with low technological levels and bad management of their biotic resources[2,13–15]. Therefore, in this scenario, no studies have been conducted to explore the udder's health status and can recommend some mastitis control practices. Aimed this, this first study carried out in Orellana province aimed to explore the udder health in early lactation in *Bos indicus* cows.

MATERIALS AND METHODS

Dairy Farms

This study collected milk samples from one livestock farm in Joya de los Sachas, Orellana, Ecuador. According to González Marcillo et al.[13], the humid tropical rainforest conditions characterize this area's climate. Its altitude is 275 m above sea level, and the average annual rainfall is 2942 mm. The average yearly temperature is 29.7 °C. One hundred fifty cows (Primiparous, PM, 75 and Multiparous, MP 75) in early lactation (days in milk, PM =134 ± 3; MP = 136 ± 5), milk production (9,88 kg/d, on average) of the creole breed Gyr lechers were enrolled. The cows were maintained to graze daily on *(Megathyrsus maximus*, CP 12%) and supplemented with white mulberry *(Morus alba)* ad libitum, being all cows every day hand-milked at 0700. Before being assigned to each treatment, the SCC values were lower than 220,000 cells/mL, on average.

Milk samples

A complete design block with a randomized PM and MP was used to disperse the cows. The investigation lasted for 21 days. As a result, 50 mL samples of milk were aseptically collected, conserved with antimicrobial tablets (Bronopol, Broad Spectrum Micro-tabs II, D&F Control Systems Inc., San Ramon, CA), and maintained at 4°C until processing for milk composition and SCC analyses. Then, in the Uyunbicho at the Central University of Ecuador, milk composition was examined using infrared absorption, and SCC was calculated using an automatic somatic cell counter that had previously been calibrated for cow milk (Fossomatic 500, Foss-Electric, Hillerd, Denmark).

Statistic evaluation

PROC Mixed from SAS 9.4 (SAS Institute Inc., Cary, NC, USA) was used to analyze the data. The SCC was logarithmically converted ($\log_{10}$) prior to analysis. While residual error and cows were regarded as random variables, our fixed effects (PM and MP) were included in the model. With SAS's PDIFF option, differences between least squares means were calculated, and the Tukey test was used to compare them. Additionally, the PRO CORR of SAS was associated with the milk composition and SCC. Statistical differences and trends were announced at $P \leq 0.05$ and $P \leq 0.10$, respectively.

RESULTS

Table 1 shows the milk composition and SCC compared to primiparous (PM) and multiparous (MP). Days in milk were estimated to be 134 and 136 days for primiparous and multiparous does, respectively, at the start of the trial (P > 0.05). Comparing primiparous and multiparous women's milk yields revealed differences (P = 0.003); the MP showed a 15% higher milk yield than those in PM (10.83 vs. 9.18 ± 0.38 kg/d; Table 1). As for FCM values, although the fat contents did not change between treatments (2.46 ± 0.16%, on average; *P* = 0.68), the corrected milk by fat was greater in MP than those obtained for PM (8.26 vs. 6.80 ± 0.34%; Table 1)

Item	Treatments		SEM	*P* = value
	Primiparous	Multiparous		Treatment
Milk yield, kg/d	9.18	10.83	0.38	0.003
FCM, L/d[1]	6.80	8.26	0.34	0.002
Milk composition, %				
Total solids	11.10	11,17	0.17	0.76
Solids no fat	8.68	8.66	0.66	0.79
Fat	2.41	2.51	0.16	0.68
Protein	3.24	3.23	0.50	0.85
Lactose	4.71	4.69	0.02	0.60
Fat yield, g/d	208b	261a	16	0.02
Protein yield, g/d	299a	253b	14	0.01
Somatic cell count, log	1.89	2.13	0.05	0.07

[1]Fat corrected milk at 4%; FCM = kg of milk yield × [0.4+ 0.15 × (fat %)].

Table 1. Comparisons between the somatic cell counts (SCC) and milk yield features of 120 primiparous and multiparous Bos indicus cows.

In contrast, the other milk components did not differ between treatments (*P* = 0.60 to 0.85%; Table 1). Overall, the mean values were for total solids (11.14 ± 0.17%), solids non-fat (8.67 ± 0.66%), protein (3.24 ± 0.50%) and lactose (4.7 ± 0.02%). Nevertheless, when comparing the fat and protein contents expressed as g/d, the MP had greater fat contents than PM cows (261 vs. 208 ± 16; *P* 0.02) but with lower protein contents (253 vs. 299 ± 14; *P* 0.01; Table 1). On the other hand, statistical tendencies were observed for SCC (*P* = 0.07). In the current study, the overall averages of SCC were 153.703 × 103 mL-1 (log SCC 1.89) and 394.560 × 103 mL-1 (log SCC 2.13) for primiparous and multiparous cows, respectively. As shown in Figure 1, the regression analysis showed strong significant associations between total solids and fat (*P* < 0.001) and solids non-fat and CP (*P* < 0.001), as well as for SCC and lactose contents (*P* < 0.001).

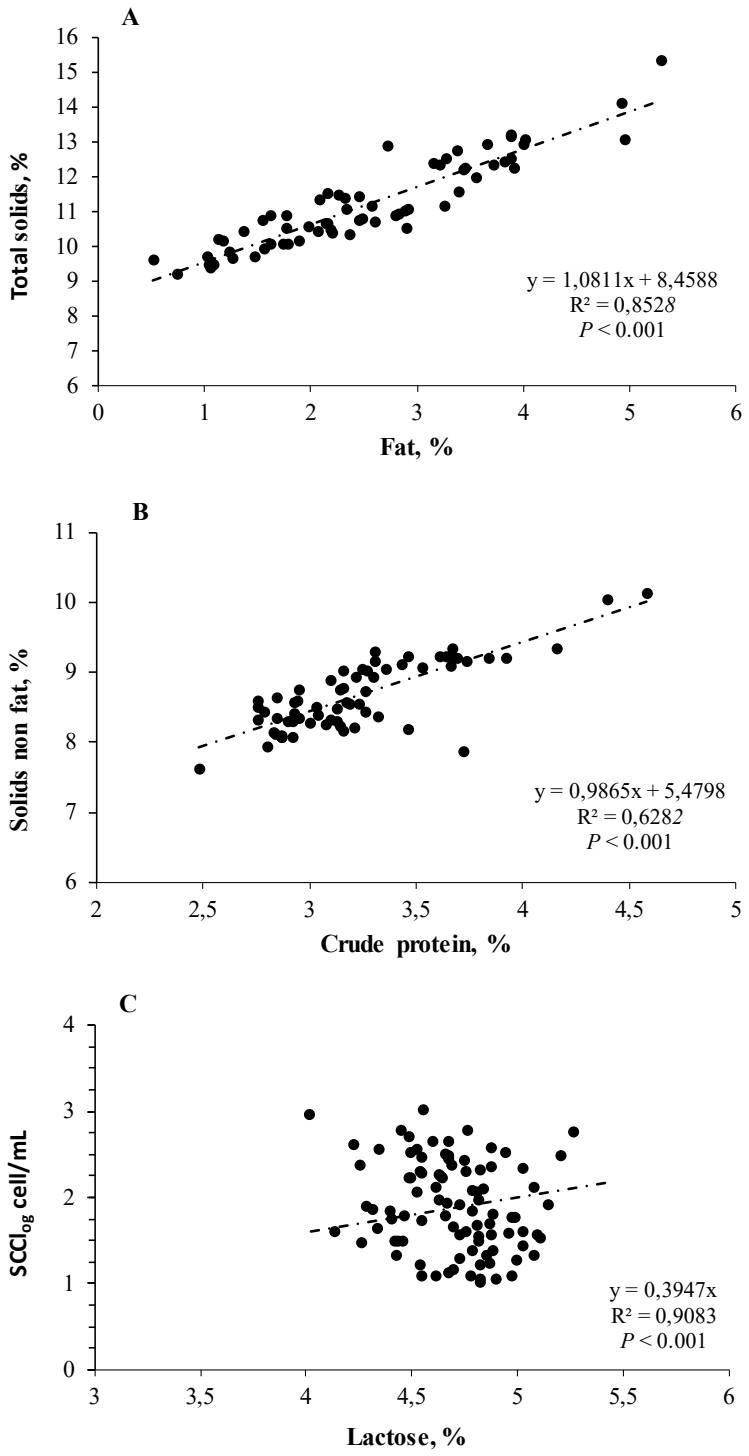

Figure 1. Regression analysis is linear for total solids and fat (A), solids non-fat and CP (B) and SCC and lactose (C).

Table 2 displays the simple correlation coefficients for milk yields, composition, and SCC. This study did not link Milk yield and SCC (-0.04 to 0.67; P = 0.50 to 0.64). Nevertheless, there were significant correlation coefficients for PM and MP between total solids and fat (r = 0.92 to 0.94; $P < 0.001$) and solids non-fat and CP (r = 0.79 to 0.90; $P < 0.001$: Table 2).

Variable	Milk, kg/d		Fat		CP		TS[1]		SNF[2]	
	PM	MP	PM	MP	PM	MP	PM	MP	PM	MP
Milk, kg/d			– 0.25 0.013	– 0.22 0.069	0.14 0.16	0.22 0.06	– 0.15 0.14	– 0.08 0.52	0.25 0.013	0.28 0.01
Fat	– 0.25 0.013	– 0.22 0.069							0.035 0.73	0.17 0.16
CP	0.14 0.16	0.22 0.06	0.000 0.99	0.27 0.02	0.000 0.99		0.30 0.003	0.54 0.001	0.90 0.001	0.79 0.001
TS	– 0.15 0.14	– 0.08 0.52	0.94 0.001	0.92 0.001	0.30 0.003	0.54 0.001			0.36 0.001	0.54 0.001
SNF	0.25 0.013	0.28 0.01	0.035 0.73	0.17 0.16	0.90 0.001	0.79 0.001	0.36 0.001	0.54 0.001		

[1] TS, total solids; [2]SNF, Solids non-fat; PM, primiparous cows and MP, multiparous cows.

Table 2. Somatic cell counts of primiparous (PM) and multiparous (MP) Bos indicus cows were correlated simply with milk yield attributes (n = 120).

DISCUSSION

Coulibaly and Nialibouly[16] observed that the evaluation of milk yield of lactating cows in tropical conditions is confounded by the fact that the calf must initiate milk letdown. Martínez-Velázquez et al.[17], using creole, Gujarat have reported at 210 DIM a higher milk yield (22 ± 1.7 kg/d) and fat (2.81 ± 0.1%) than those obtained in our study. Millogo et al.[3] in zebu dairy cattle at 41 ± 6 DIM observed lower milk yields than this study (1.3 vs. 10 kg/d, on average) but with more excellent fat contents (4.88 vs. 2.46 %). We hypothesized that our lower fat contents observer in this study could be related to poor forage quality for bad grazing management practices, as evidenced by Guaman-Rivera et al.[2,18] in Orellana province. According to Bonfoh et al.[19] and Farahani, Amanlou, and Kazemi-Bonchenari [20], the fat content in milk reflects supplementary feeding for the entire dry period, which in our conditions was not done.

However, it's crucial to remember that the variation in the amount of milk the calf suckled greatly impacted the daily variance in saleable milk yield. Additionally, since milk fat content rises during udder emptying, variation in the degree of udder evacuation and calf suckling may impact the fat content[3]. Another critical point to consider in this study is that the fat contents did not vary between PM and MP, but Bonfoh et al.[20] reported a higher fat content of Malian Zebu milk when the milk yield decreased. Based on the abovementioned evidence, estimating milk production in lactating zebu cows has always been difficult since using their calves to stimulate milk letdowns16 is necessary. Our research team decided to do this work at 134 DIM, avoiding the suckled effect.

As expected, the lactose contents did not differ between PM vs. MP (4.70 ± 0.02% on average), being their values like those reported by Millogo et al.[19] (4.84%), Martínez-Velázquez et al.[17] (4.71%), Sidibe-Anago, Ouedraogo, and Ledin[21] (4.6%). Despite weak correlations in PM and MP cows between SCC and lactose contents (r = 0.22 to 0.25), it was significant (P = 0.03 to 0.04).

According to Portnoy and Barbano[22], lactose is the main carbohydrate in milk at a concentration of around 4.6% on an anhydrous basis. Consequently, it is a key component in milk synthesis and secretion, regulating the osmotic equilibrium in the mammary cell. Decreased milk yield and compositional changes in milk, particularly concerning lactose concentration, have been reported in infected mammary glands in cows[23–25]. High-quality milk production is a primary factor for the safety and quality of dairy products[26]. Mastitis is a significant problem in dairy farming globally[5], occasioning also considerable economic losses. Besides this, Kirkeby et al.[5] stated that mastitis is a predominant reason for antibiotic use in dairy products and can impair animal welfare. The SCC in milk indicates the inflammatory response in the mammary gland[27]. In cattle breeds of

origin *Bos taurus*, ample scientific evidence stated that the optimal cut-off points to distinguish between infected and uninfected quarters should have less than 200,000 cells/mL[28,29]. However, in *Bos indicus* cattle breeds, information is scarce and confused on referential SCC values to consider as uninfected. At the level of Ecuador, legal normative declared by INEN[30] is regarded as an uninfected quarter when the SCC values are less than 500,00 cells/mL. Bonfoh et al.[19] reported that 9% of cows had a mean value of SCC greater than 654,000 cells/mL. Similar results have been observed by Juozaitiene, Juozaitis, and Micikeviciene[31] (SCC, 800,000 cells/mL). In this first study, in PM cows (n = 75), 57 and 43% had lower SCC values than 39,000 and 180,000 cells/mL, respectively.

Meanwhile, for MP cows (n = 75), the SCC values were 65% (> 81,000 cells/mL) and 35% (>979,000 cells/mL). Based on these findings, the MP cows showed to have more risk of obtaining subclinical mastitis, according to Juozaitiene et al.[31]. In SCC values of dairy ewes, Orman et al.[31] reported a negative correlation between milk yield and parity. This supported our results, in which the PM cows showed lower SCC values when compared to those of MP cows. In these tropical conditions, due to high ambient temperatures with high relative humidity. The cattle could face heat stress through physical, biochemical, and biological changes resulting in decreased production performance and poorer immunity (i.e., a high SCC), such as observed [32]. Although most milk parameters show substantial mastitis-related changes, no correlations were found between SCC and all milk components in this study. Nevertheless, we did not discard possible seasonal effects, stage of lactation, genetics (breed), productive systems and udder and teat morphology-like associated factors in *Bos indicus* cows[33].

CONCLUSIONS

Based on these findings, the lower fat contents observed in PM and MP cows could be related to forages of poor nutritional quality. In addition, the present investigation evidenced a progressive increase in SCC with parity and advanced lactation. So, this first study performed in Orellana Province might be a point to start formulating feeding strategies for achieving greater and lower milk composition and SCC, respectively.

Author Contributions: Conceptualization, SAGR and RJHF; methodology, AEGP, NRON and RLGM; software, SAGR and AEGP; validation, SAGR and RJHF; formal analysis, AEGP, NRON and RLGM; investigation, SAGR and RJHF; resources, AEGP, NRON, SAGR, RJHF and RLGM; data curation, SAGR and AEGP; writing—original draft preparation, AEGP, NRON, SAGR, RJHF and RLGM; writing—review and editing, SAGR and RJHF; visualization, AEGP and RLGM; supervision, SAGR and RJHF; project administration, RLGM; funding acquisition, AEGP, NRON, SAGR, RJHF and RLGM All authors have read and agreed to the published version of the manuscript.

Funding: This research received no external funding.

Acknowledgments: We thank the project Silvopastoral system in Orellana Province. In addition, we thank Theofilos Toulkeridis for the grammar check of this manuscript.

Conflicts of Interest: The authors declare no conflict of interest.

REFERENCES

1. Britt JH, Cushman RA, Dechow CD, Dobson H, Humblot P, Hutjens MF, et al. Invited review: Learning from the future—A vision for dairy farms and cows in 2067. J Dairy Sci. **2018**;101:3722-3741. http://dx.doi.org/10.3168/jds.2017-14025.
2. Guaman-Rivera S., Guerrero-Pincay A, Ortiz-Naveda N., González-Marcillo R. Prediction of the nutritional values by INRA (2018) feed evaluation system of *Megathyrsus maximus* subjected to different grazing strategies. J Agric Environ Int Dev. **2023**;117: 117-140.

3. Millogo V, Ouédraogo GA, Agenäs S, Svennersten-Sjaunja K. Day-to-day variation in yield, composition and somatic cell count of saleable milk in hand-milked zebu dairy cattle. African J Agric Res. **2009**;4:151-155.
4. Damm M, Holm C, Blaabjerg M, Bro-Novak M, Schwarz D. Differential somatic cell count—A novel method for routine mastitis screening in the frame of Dairy Herd Improvement testing programs. Minerva Med. **2017**;60:3922-3927. http://dx.doi.org/10.3168/jds.2016-12409.
5. Kirkeby C, Toft N, Schwarz D, Farre M, Nielsen SS, Zervens L, et al. Differential somatic cell count as an additional indicator for intramammary infections in dairy cows. J Dairy Sci. **2020**;103:1759-1775. http://dx.doi.org/10.3168/jds.2019-16523.
6. Juárez M., Blanco M., De La Fuente L., Beneitez E, Gonzalo C, Carriedo J., et al. Factors of Variation Influencing Bulk Tank Somatic Cell Count in Dairy Sheep. J Dairy Sci. **2010**;88(3):969–74.
7. Riva F, Latorre A., Moroni P. Ruminant mastitis: A 360° view. Vol. 9, Frontiers in Veterinary Science. **2022**.
8. Raynal-Ljutovac K, Pirisi A, de Crémoux R, Gonzalo C. Somatic cells of goat and sheep milk: Analytical, sanitary, productive and technological aspects. Small Rumin Res. **2007**;68: 126-144.
9. Shangraw EM, McFadden TB. Graduate Student Literature Review : Systemic mediators of inflammation during mastitis and the search for mechanisms underlying impaired lactation. J Dairy Sci. **2022**;105,20776. http://dx.doi.org/10.3168/jds.2021-20776.
10. Shangraw EM, Rodrigues RO, Mcfadden TB. Intramammary lipopolysaccharide infusion induces local and systemic effects on milk components in lactating bovine mammary glands. J Dairy Sci. **2020**; 103(8), 7487-7497. http://dx.doi.org/10.3168/jds.2019-18022.
11. Shangraw EM, Rodrigues RO, Witzke MC, Choudhary RK, Zhao F-Q, Mcfadden TB. Intramammary lipopolysaccharide infusion induces local and systemic effects on milk components in lactating bovine mammary glands. J Dairy Sci. **2019**;103:7487-7497. http://dx.doi.org/10.3168/jds.2019-18022.
12. MAGAP. Agricultural stadistic. Available online: www-magap.gob.ec. Accessed on 14 January 2022.
13. González Marcillo RL, Castro Guamàn WE, Guerrero Pincay AE, Vera Zambrano PA, Ortiz Naveda NR, Guamàn Rivera SA. Assessment of Guinea Grass Panicum maximum under Silvopastoral Systems in Combination with Two Management Systems in Orellana Province, Ecuador. Agriculture. **2021**;11(2):117.
14. Fuentes O., Guamán S., Zacarías F, Paredes V. Silvopastoral Systems as a Strategy for Reconversion of Livestock Farming in Ecuadorian Amazon. Adv Compos Bull. **2023**;1:135-138.
15. Guamán Rivera SA., Marcillo González RL, Carrasco R, Guamán Quinche F. Caracterización de los Sistemas Ganaderos de Aptitud Lechera en el Valle del Quijos, Provincia del Napo, Ecuador. Eur Sci J ESJ. **2019**;31;(15):279–792. http://eujournal.org/index.php/esj/article/view/12082/11516.
16. Coulibaly M, Nialibouly O. Effect of suckling regime on calf growth, milk production and offtake of zebu cattle in Mali. Trop Anim Health Prod.**1998**;30:179-189.
17. Martínez-Velázquez G, Palacios-Fránquez J., Bustamante-Guerrero J., Ríos- Utrerab A, Vega-Murillo V., Montańo-Bermúdez M. Composición de leche de vacas Criollo, Guzerat y sus cruzas F1 y su relación con el peso al destete de las crías. Rev Mex Ciencias Pecu. **2010**;1:311-324.
18. Guamán-Rivera S., Mira-Naranjo M., Peralta-Paredes VA, Aragón-vásquez E. Animal Diseases Reported by Livestock Farmers in Orellana Province , Ecuador : A Retrospective Observational Study from 2011 to 2019. Seybold Rep J. **2023**;18:7-24.
19. Bonfoh B, Zinsstag J, Farah Z, Simbé C., Alfaroukh I., Aebi R, et al. Raw milk composition of Malian Zebu cows (*Bos indicus)* raised under traditional system. J Food Compos Anal. **2005**;(1):18:29-38.
20. Farahani TA, Amanlou H, Kazemi-Bonchenari M. Effects of shortening the close-up period length coupled with increased supply of metabolizable protein on performance and metabolic status of multiparous Holstein cows. J Dairy Sci. **2017**;100:6199-6217. http://dx.doi.org/10.3168/jds.2016-12263.
21. Sidibe-Anago AG, Ouedraogo GA, Ledin I. Effect of partly replacing cottonseed cake with Mucuna spp. (var. Ghana) hay on feed intake and digestibility, milk yield and milk composition of zebu cows. Trop Anim Health Prod. **2006**;38:563-570.
22. Portnoy M, Barbano D. Lactose : Use , measurement , and expression of results. J Dairy Sci. **2021**;104:2020-18706. http://dx.doi.org/10.3168/jds.2020-18706.

23. Silanikove N, Rauch-Cohen A, Shapiro F, Blum S, Arieli A, Leitner G. Lipopolysaccharide challenge of the mammary gland in bovine induced a transient glandular shift to anaerobic metabolism. J Dairy Sci. 2011;94:4468-4475. http://dx.doi.org/10.3168/jds.2010-4092.
24. Kvidera SK, Horst EA, Abuajamieh M, Mayorga EJ, Fernandez MVS, Baumgard LH. Glucose requirements of an activated immune system in lactating Holstein cows. J Dairy Sci. **2017**;100:2360-2374. http://dx.doi.org/10.3168/jds.2016-12001.
25. Gross JJ, Grossen-Rösti L, Wall SK, Wellnitz O, Bruckmaier RM. Metabolic status is associated with the recovery of milk somatic cell count and milk secretion after lipopolysaccharide-induced mastitis in dairy cows. J Dairy Sci. 2020;103,5604-5615.
26. Albenzio M, Figliola L, Caroprese M, Marino R, Sevi A, Santillo A. Somatic cell count in sheep milk. Small Rumin Res. **2019**;176:24-30. https://doi.org/10.1016/j.smallrumres.2019.05.013.
27. Wall SK, Wellnitz O, Bruckmaier RM, Schwarz D. Differential somatic cell count in milk before, during, and after lipopolysaccharide- and lipoteichoic-acid-induced mastitis in dairy cows. J Dairy Sci. **2018**;101:5362-5373. http://linkinghub.elsevier.com/retrieve/pii/S0022030218302510.
28. Bradley A, Green M. Use and interpretation of somatic cell count data in dairy cows. In Pract. **2005**;27:310-315. http://inpractice.bmj.com/.
29. IDI. (International Dairy Federation). 2013. Guidelines for the use and interpretation of bovine milk somatic cell count. Bull. IDF. 466/2013. 2013;
30. INEN, Instituto Ecuatoriano Normalización. Raw milk. Requeriments.. 2012;1:2-7.https://www.gob.ec/sites/default/files/regulations/2018-10/Documento_BL NTE INEN 9 Leche cruda Requisitos.pdf.
31. Juozaitiene V, Juozaitis A, Micikeviciene R. Relationship between somatic cell count and milk production or morphological traits of udder in Black-and-White cows. Turkish J Vet Anim Sci. **2006**;30:47-51.
32. Rakib MRH, Zhou M, Xu S, Liu Y, Asfandyar Khan M, Han B, et al. Effect of heat stress on udder health of dairy cows. J Dairy Res. **2020**;87:315-321.
33. Collier RJ, Dahl GE, Vanbaale MJ. Major advances associated with environmental effects on dairy cattle. J Dairy Sci. **2006**;89:1244-1253. http://dx.doi.org/10.3168/jds.S0022-0302(06)72193-2.

Received: October 9th 2023/ **Accepte**d: January 15th 2024 / **Published:**15 February 2024

Citation: Guamán-Rivera S A, Guerrero-Pincay A E, Ortiz-Naveda N R, González-Marcillo R L and Herrera-Feijoo R J. Somatic Cell Count Evaluation in Early Lactation between Primiparous and Multiparous *Bos indicus* Cows. Revis Bionatura 2024; 9 (1) 16. http://dx.doi.org/10.21931/RB/2024.09.01.16

Additional information Correspondence should be addressed to *santiagoa.guaman@espoch.edu.ec*
Peer review information. Bionatura thanks anonymous reviewer(s) for their contribution to the peer review of this work using https://reviewerlocator.webofscience.com/

Bionatura ISSN. First 13909355 Ecuador. **Scopus coverage years**: from 2016 to the present

Bionatura
Ibero-American Journal of Biotechnology and Life Sciences

Article

Valoración de los servicios ecosistémicos del bosque primario de la comunidad Waorani Nampaweno, Orellana, Ecuador.

Jaime Larrea [1/], *Johana Rentería* [1]

1 *Instituto Tecnológico Superior Universitario Oriente ITSO, La Joya de los Sachas, Ecuador;;*
jmrenteria@itsoriente.edu.ec:
**Correponding autor. jlarrea@itsoriente.edu.ec.*
Available from. http://dx.doi.org/10.21931/RB/2024.09.01.17

ABSTRACT

The Yasuní National Park is the largest protected area in Ecuador; it houses excellent biodiversity of the Amazonian tropical humid forest; it is the home of the Waoranis, an indigenous people in voluntary isolation PIAV, who depend on the resources that the forest has, in this context, this article deals with the assessment of the ecosystem services provided by the tropical humid forest of the Ecuadorian Amazon, the main objective being to determine which of these services is the most important, in addition to showing the ancestral cultural manifestations of this ethnic group; therefore The ecosystem services of the Waorani Nampaweno community, located in the Dayuma parish, Orellana province, were analyzed. In the methodology used, interviews were carried out with the two elders of the community and the inventory sheets of the National Institute of Cultural Heritage INPC, later when applying the Likert scale, the results showed that the cultural ecosystem services obtained 34 points, the highest score, Cronbach's alpha of 0.87 validates the reliability of the research, with the food supply service being the one that allows survival, however, cultural services make visible the vast knowledge and ancestral wisdom that they have treasured. It is transmitted orally by the "pikenanis" (elders) throughout the generations. The highlights of the cards were preparation for the hunt, respect for animals such as eagle and tiger, and the use of annatto as facial ink. Hunting and abundant food are celebrated through dances. The crafts and clothing are made from fibers and seeds from the forest; however, threats such as the invasion of their territory due to colonization and oil exploitation are acculturating young people, ending their way of life, identity and loss. of its ancestral cultural wealth. The Waoranis are the forest's protectors, and their right to their way of life linked to the Amazon rainforest must be strengthened.

Keywords: Ecosystemic Services, waorani culture, Amazonian tropical forest, plants from Yasuní Park.

RESUMEN

El Parque Nacional Yasuní es el área protegida más grande del Ecuador, alberga una gran biodiversidad del bosque húmedo tropical amazónico, es el hogar de los waoranis, pueblo indígena en aislamiento voluntario PIAV, quienes dependen totalmente de los recursos que posee el bosque, en este contexto el presente artículo trata de la valoración de los servicios ecosistémicos que brinda el bosque húmedo tropical de la amazonía ecuatoriana, siendo el objetivo principal determinar cual de estos servicios es el mas importante, además de mostrar las manifestaciones culturales ancestrales de esta etnia, por tanto se analizaron los servicios ecosistémicos de la comunidad Waorani Nampaweno, ubicada en la parroquia Dayuma, provincia de Orellana. En la metodología utilizada se realizaron entrevistas a los dos ancianos de la comunidad y las fichas de inventario del Instituto Nacional de Patrimonio Cultural INPC, posteriormente al aplicar la escala de Likert, los resultados mostraron que los servicios ecosistémicos culturales obtuvieron 34 puntos, la puntuación mas alta, el alfa de Cronbach de 0,87 valida la confiabilidad de la investigación, siendo el servicio de suministro - alimento el que permite la supervivencia, sin embargo los servicios culturales visibilizan los vastos conocimientos y sabiduría ancestral, que han atesorado y transmitido de forma oral por los “pikenanis” (ancianos) a lo largo de las generaciones. Lo mas destacado de las fichas fueron: la preparación para la cacería y el respeto a los animales como águila y tigre, el uso del achiote como tinta facial. La caza y alimento abundante es celebrada mediante danzas. Las artesanías y vestimenta son hechas de fibras y semillas del bosque, sin embargo las amenazas como la invasión de su territorio por la colonización, asi como por la explotación

petrolera, están aculturando a los jóvenes acabando con su forma de vida, identidad y la pérdida de su riqueza cultural ancestral. Los waoranis son los protectores del bosque y se debe fortalecer su derecho a su forma de vida ligada a la selva tropical amazónica.

Palabras claves: Servicios Ecosistémicos, cultura waorani, bosque tropical amazónico, plantas del parque Yasuní.

INTRODUCCIÓN

El ser humano desde sus inicios ha tenido un contacto directo con la naturaleza y ha obtenido múltiples beneficios para sobrevivir y desarrollarse, como el alimento, medicina, vestido, entre otros, inclusive desde temprana edad se empieza a tener conciencia ecológica las cuales promueven valores y desarrollan creencias del entorno ecológico[1]. Sin embargo, con el paso del tiempo se incrementa la población y aumentan las necesidades, obligando a las sociedades a ampliar el consumo de los recursos que la naturaleza ofrece volviéndose insostenible, el ejemplo mas crucial es la deforestación de los bosques primarios, que trae consigo degradación del hábitat [2]. Además se debe considerar que la amazonía ecuatoriana constituye un referente de una basta biodiversidad, la cual incorpora a "pueblos y nacionalidades indígenas en aislamiento voluntario" PIAV, conformada por grupos humanos organizados por clanes, los cuales son cazadores-recolectores, manteniendo una alta movilidad dentro de su territorio, llegando a enfrentamientos con otros clanes y tribus, dentro de estos grupos étnicos, los mas destacados y conocidos son los Waoranis que significa "los seres humanos" [3].

En el Ecuador, la nacionalidad waorani es la última nacionalidad indígena amazónica que entró en contacto con la civilización en 1958 [13], en sus inicios el contacto por parte de misioneros fueron infructuosos e inclusive, acabaron en matanzas como lo menciona Cabodevilla, Smith [14] y aún continúan los enfrentamientos entre Waoranis y Taromenanis, la interacción con la comunidad se posibilitó a través del Instituto Lingüístico de Verano, organización evangelizadora estadounidense, que fue expulsada de Ecuador en 1980, en el gobierno del presidente Jaime Roldós Aguilera. acusada de ser cómplice de las compañías petroleras y demás trasnacionales extractivas para la obtención de territorios indígenas a través de métodos clientelares y turbios [15].

La población Waorani se encuentra en las provincias de Napo, Pastaza y Orellana, de acuerdo al último censo realizado por el Instituto Nacional de Estadísticas y Censos, INEC [16], existen aproximadamente 2.416 personas waorani en Ecuador. La mayoría distribuidas en más de 100 comunidades dentro de la Reserva de Biosfera y Parque Nacional Yasuní y su zona de influencia. Aunque el impacto cultural ha sido muy fuerte desvalorizando su identidad adoptando muchos elementos de la modernidad y cultura Occidental, aún mantienen muy vivos sus saberes y prácticas ancestrales. Sin embargo, es evidente que cada vez mas la colonización empuja al avance de la frontera agrícola y la explotación petrolera, lo cual ahonda mas su aislamiento, por tanto estos espacios vitales para su supervivencia están en dependencia directa del bosque y su ecosistema.

Actualmente el modelo extractivista del estado Ecuatoriano responde a una política de ingresos petroleros que financian en gran medida el presupuesto general del estado, lo cual ha llevado a una acelerada colonización, ampliación de la frontera agrícola, y todavía continua la exploración y asentamientos para instalar nuevos pozos petroleros, esto ha dado lugar a un verdadero cerco alrededor del territorio PIAV waorani, que cada vez más se encuentran en una situación crítica de supervivencia, llegando a considerarse un potencial exterminio o desaparición de este grupo étnico" [3] de no adoptarse medidas que garanticen su inexpugnabilidad de su territorio, sin embargo poco se ha realizado al respecto. Enclavados en lo que se ha denominado la "Reserva de Biósfera Yasuní" los waoranis obtienen sus alimentos, medicinas, combustible y otros insumos de la selva, aunque el Ecuador en el año de 1999, ubicó el bloque petrolero Ishpingo, Tambococha, Tiputini, ITT declarado zona "intangible" a esta área colindante del parque Nacional Yasuní para garantizar que estuviera alejada de la explotación petrolera lo que podría dar lugar a otro modelo de desarrollo, teniendo muy en cuenta a los grupos tagaeri y taromenanis, parientes de los huaorani, esta iniciativa fracaso en el año 2013, y mediante una consulta se decide sobre la incursión y expansión petrolera es esta zona [4].

Actualmente poco se ha investigado y valorado de lo que el bosque amazónico ecuatoriano posee, ligado a los PIAV waoranis, la inexistente medición de los servicios ecosistémicos que el bosque primario, conlleva a una perdida de conciencia del valor que podrá llegar a tener, redefine la revalorización en conjunto toda la riqueza que la dinámica del ecosistema provee, asi como la armónica interacción existente con estos grupos étnicos que inevitablemente están siendo amenazados dando lugar al fenómeno de "aculturación" de sus miembros mas jóvenes, ocasionando una paulatina pérdida de identidad cultural como en la comunidad Waorani de Nampaweno [5], la diversidad de servicios ecosistémicos sustentan formas de vida y cultura intangibles, lamentablemente solo se visibiliza la venta de madera, es indispensable la identificación de estos servicios para que permitirán la creación de planes de conservación y otros beneficios para la comunidad manteniendo su cultura

y conocimientos que aún siguen vigentes pero escondidos, el análisis de los servicios ecosistémicos visibilizará la estructura cultural formada por cientos de años, siendo una parte de la identidad y cultura ecuatoriana [6]. El objetivo de esta investigación fue la valoración de los servicios ecosistémicos del bosque primario amazónico ecuatoriano, describiendo las manifestaciones culturales ligadas al bosque húmedo tropical, lo cual debe contribuir a la concientización para la conservación de los recursos naturales y el patrimonio intangible procurando el aprovechamiento sostenible de los recursos del bosque, fortaleciendo su identidad cultural.
Los servicios ecosistémicos son sumamente importantes ya que proporcionan muchos productos y servicios que los bosques proveen. Se los ha considerado en 4 categorías: los de abastecimiento, aquellos que son de subsistencia y consumo para personas y animales por ejemplo los alimentos, medicinas, materias primas y agua dulce. Se tiene los servicios de regulación, que mantienen el equilibrio del ecosistema y la calidad de los factores ambientales, calidad de aire y agua, control de plagas, erosión del suelo. Los servicios de apoyo adecuan hábitats vitales para plantas y animales, además de la conservación genética. Los servicios culturales son aquellos denominados intangibles como "el paisaje", la estética, relacionados con la identidad cultural, experiencias espirituales sobre todo de los PIAV, y están estrechamente ligados con los servicios de abastecimiento y regulación. En el caso de las etnias y nacionalidades constan como los valores más importantes ya que sus miembros lo asocian con la naturaleza; sin embargo, a nivel mundial no se invierte lo necesario para su protección y adecuada gestión [7 - 8.]

MATERIALES AND METODOS

Para conocer la realidad del entorno de la comunidad indígena, se utilizó como metodología la entrevista, la cual se realizó a los miembros mas reconocidos de la comunidad, los ancianos o "Pikenanis" a los cuales se les realizaron 7 preguntas abiertas, cuyo enfoque esta centrado en la relación entre la provisión del bosque con las actividades y prácticas realizadas, determinando los beneficios a la comunidad, también se utilizó la matriz de observación directa, la cual proporciona información del entorno y como se observa en la tabla 1, evidencia con fotografías las plantas utilizadas y otros aspectos calificados, durante visitas de campo a la Comunidad Nampaweno, complementado con un análisis del entorno conociendo potenciales y debilidades del mismo [9] .
Para complementar la valoración de los servicios ecosistémicos identificados previamente en el ecosistema denominado Bosque Húmedo Tropical Lluvioso [20], de la comunidad waorani Nampaweno, se ha tomado en cuenta algunos criterios cualitativos de la Investigación Acción Participativa de Orlando Fals Borda [21]. La cual se centra en la parte social, realizando una participación mas integral con las personas de la comunidad involucrándose mas con ellos con una convivencia, lo que permite realizar un mejor acercamiento con la comunidad para obtener una percepción mas profunda de los servicios ecosistémicos que aporta el bosque primario, con énfasis en los servicios ecosistémicos culturales.

Para categorizar las respuestas se utilizó la escala de Escala de Likert, creada en 1932 por el psicométrico Rensis Likert, la cual "mide" opiniones, actitudes y las categoriza es una escala de evaluación, con respuestas cerradas, provistas de opciones numéricas agrupadas en un solo tema y sumando las respuestas, la puntuación final determina el total obtenido [10]. En este caso se encuentran en 3 categorías establecidas [11], las de Aprovisionamiento, Regulación y Culturales. Para la presente valoración, se tomó en cuenta un valor mínimo de 1 y un valor máximo de 5, con una escala de evaluación establecida de la siguiente manera:

1 = baja capacidad relevante
2 = capacidad relevante
3 = capacidad media relevante
4 = alta capacidad relevante
5 = muy alta capacidad relevante.

Nota: Renteria Johanna (2021).

La recopilación de información se centra en las actividades, rituales que realizan tanto diariamente, como en épocas especiales conviviendo con el entorno, las respuestas fueron los relatos de los dos líderes de la comunidad, para su sistematización y registro se utilizó las "fichas de inventario", del Instituto Nacional del Patrimonio Cultural (INPC), sistematizando los aspectos culturales mas importantes de la comunidad. Este patrimonio cultural esta basado en la recopilación de distintas manifestaciones que grupos de personas a través del tiempo han ido plasmando y se han repetido, siendo la herencia recibida de los ancestros, las cuales forman la "identidad" del grupo, incluye muchas obras intangibles conformando un conjunto de valores, plasmando diferentes expresiones y creatividad únicas de los pueblos, como el lenguaje, los rituales y sobretodo esos

aspectos inmateriales formalizados como creencias. Esta riqueza patrimonial que el Ecuador acuña es enorme, requiere de un proceso riguroso y sistémico desde su identificación y registro, pasando por su inventario y posterior difusión a través de catálogos [12].

El área del bosque esta detallada en el mapa de la figura 2, la cual presenta las coordenadas de los puntos de las localidades dentro del área de influencia de la comunidad Nampaweno, se muestra también el área de amortiguamiento cercana a la parroquia de Dayuma para lo cual se utilizó el programa QGIS 3.20.3 Odense.

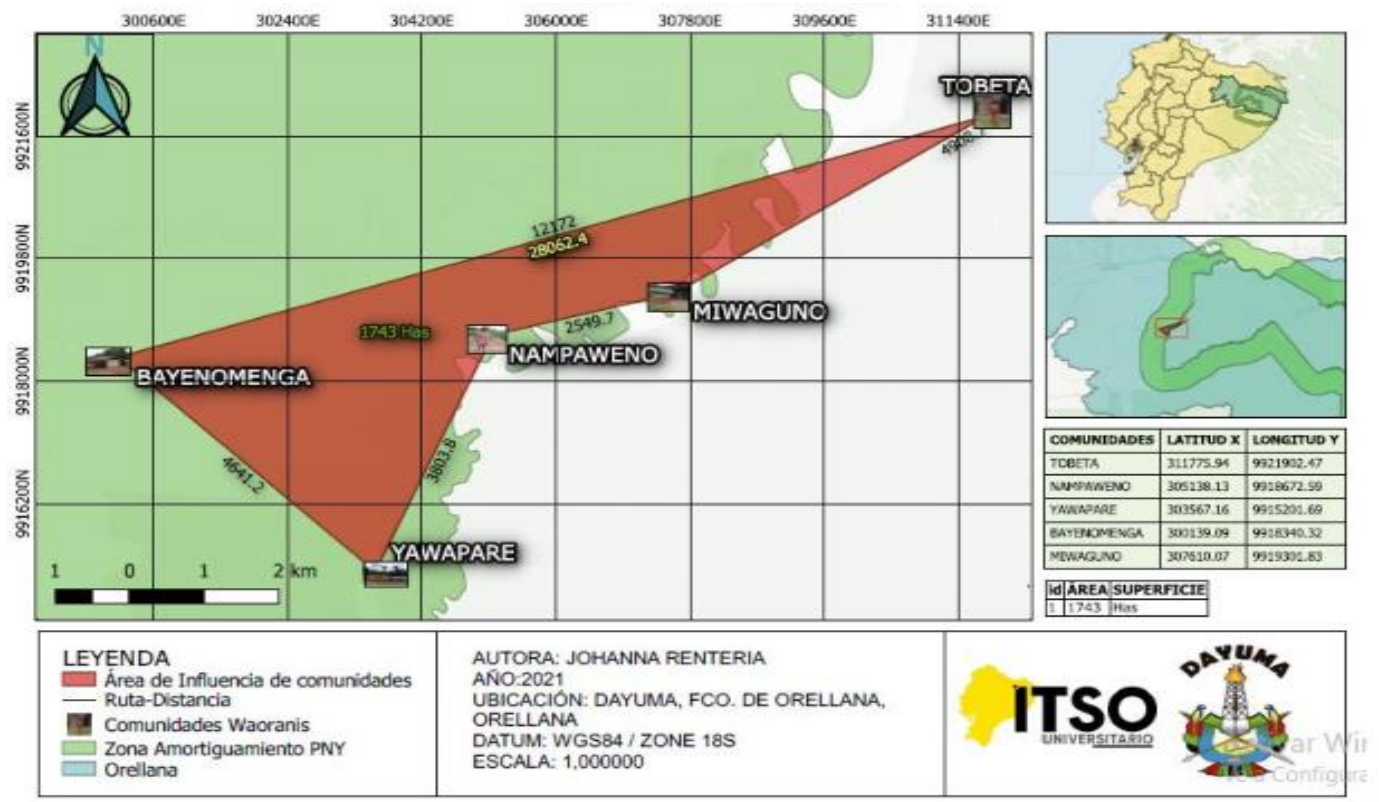

Figura 1. Mapa temático de la zona de amortiguamiento de la etnia Waorani del PNY, sector Dayuma

La ubicación de la comunidad esta referida a la parroquia Dayuma, cantón Francisco de Orellana, provincia de Orellana, en las cuales existen cinco comunidades de la nacionalidad Waorani: Tobeta, Miwaguno, Nampaweno, Yawepare, Bayenomenga. Como se observa en el mapa de la figura 1, el área total que ocupan las comunidades es de 1.743 has. En la zona o franja de amortiguamiento del parque nacional Yasuní.

RESULTS

La entrevista reveló que existe una dependencia total de los recursos que el bosque ofrece tanto es asi que, se puede considerar a los waorani como parte del hábitat del bosque húmedo tropical, de cual, obtienen todo para vivir dentro del bosque y han adquirido un especial conocimiento ancestral.

FICHA DE OBSERVACIÓN DIRECTA			
Lugar de la observación: **Comunidad Waorani Nampaweno**			
Nombre de la observadora: **Rentería Medina Johanna Maritza**			
Representantes de la Comunidad: Freddy Niwa , Elsa Niwa, Samuel Niwa			
ASPECTO	**DESCRIPCIÓN**	**IMAGEN**	**ESTADO**
Ubicación	La Comunidad Waorani de Nampaweno está localizada en la Parroquia Dayuma en el Parque Nacional Yasuní.	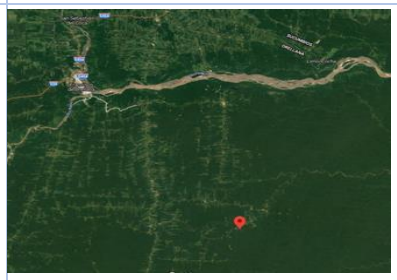	BUENO
Familias e integrantes de la comunidad Nampaweno	En la comunidad habitan 10 familias Nampaweno. Aproximadamente 44 personas entre hombres y mujeres.		BUENO
Plantas del bosque primario y sus usos	**Medicinales**: Sandi: utilizado como medicina exudado de la corteza color blanco, llamada leche de sandi (cura la gastritis), ajo, uña de gato, chuchuhuazo, sangre de drago, caoba, palo de yaguate, maticara, ortiga, achiote, cogollo de caimito, hoja de malaria, ayahuasca, ishpingo. **Frutales:** caimito, guaba, uvas, aguacate, chonta. **Materia prima:** Construcción de casas (pambil, capirona, hojas para el techo chapil). **Comestibles**: Palmito, hongo oreja de palo, hoja de yuca, papa silvestre, y fruto verde de tagua.		REGULAR
	Orquídea: Plantas epífitas adheridas al tronco de los árboles, diferentes especies, dentro de la selva desprenden un olor agradable.		BUENO
Plantas del bosque primario y sus usos	**Chapil:** Se utilizan sus hojas para construcción de viviendas, el fruto es comestible se hace jugo, una bebida local, exquisita color café caoba y sabor parecido al chocolate. **Helechos:** existen de esta especie diferentes subespecies.		BUENO

	Capulí de monte: fruto comestible, encontrado a las orillas de los ríos.		BUENO
	Maní de monte: fruto comestible, se lo encuentra en forma silvestre en la selva como también cultivado cerca de las chacras.	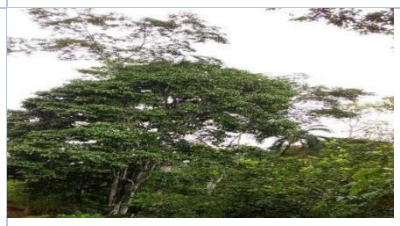	BUENO
	Chuncho: Árbol maderable del cual obtienen madera para la elaboración de sus viviendas y chacras.		BUENO
Suelo	Se observa en gran parte de los claros debajo de los árboles hojarasca, la cual crea un mulch, donde hay una alta biodiversidad microbiológica, destacando la lombriz de tierra que digiere los detritos, generando alta descomposición Materia orgánica		BUENO
Casa Tradicional	Desde antes y hasta ahora viven en casas en forma de "onko" (triangular) únicamente tapado con hojas de chapil en forma de cola de pescado forradas las paredes para prevenir el ingreso de insectos y depredadores.		BUENO
Artesanías	Hilos sacados de la planta chambira, pintados con colores naturales de otras plantas y que son utilizados para artesanías.		BUENO

Tabla 1. Matriz de Observación directa de los recursos que provee el bosque humedo tropical de la comunidad Nampaweno, Orellana

De los 11 aspectos presentados por los waoranis, el 91% esta en buen estado, estando solo una 9% en estado regular debido sobretodo a los árboles forestales que son escasos por la sobreexplotación de madera.
Se puede considerar dentro del análisis del entorno, que existe una gran biodiversidad de especies de flora y fauna, y el aprovechamiento de los recursos que ofrece el bosque no solamente para la supervivencia, si no que existe una conexión más profunda como los saberes ancestrales dentro de su cosmovisión y que se van transmitiendo de una generación a otra en función del tiempo, esto se ha denominado "servicios ecosistémicos culturales" [8].

Se describen a continuación la tabla 2 acerca de los servicios ecosistémicos encontrados en la comunidad Nampaweno en la cual se tiene servicios de aprovisionamiento, y culturales fundamentalmente.
Como se aprecia en la tabla 2 la base de vida tanto los servicios de aprovisionamiento en alimentación como en: medicina, artesanía, construcción de casas, y manifestaciones culturales son aprovechadas por especies de flora y fauna de la selva que son tanto nativas y algunas endémicas.

ACTIVIDAD / TIPO DE SERVICIO	FLORA o FAUNA	DESCRIPCIÓN	IMAGEN
Alimentación /Aprovisionamiento	Chonta (tewe) "*Bactris gasipaes"*	Se utiliza como alimento diario en los meses de enero – abril, hacen chicha y cocinada comparten a los visitantes.	
	Yuca (kene) *Manihot esculenta*	Es un tubérculo que los waoranis cultivan en sus charas, sirve para hacer chicha bebida ancestral y para comer junto a la carne de monte.	
	Chapil (tepe) *Euterpe oleracea L.* Chapil (tiwetapa)	Palma silvestre, sus frutos son de consistencia dura, se hace jugo y chicha. Con la misma palma del tallo de esta se elaboran minuciosamente las lanzas utilizadas para la caza.	
	Sahino *Dicotyles tajacu*	También conocido como puerco sahino se lo cocina ahumado, (proceso para que la carne no se dañe y concentre el sabor) junto a la yuca o verde.	
Medicinal / Aprovisionamiento	Chuchuhuazo *Maytenus macrocarpa (Ruiz y Pavon) Briq*	El chuchuhuazo, de su corteza es utilizada para curar enfermedades respiratorias [18]	

	Sangre de drago *"Croton lechleri"*	árbol maderable, de su corteza se extrae el líquido rojo oscuro, los waoranis lo utilizan para curar heridas	
	Raíz macho Pr. *Dysphania ambrosioides*	Raíz medicinal, sirve para curar el asma, bronquitis, tos, resfriados etc. Para la preparación de hierve la raíz triturada por una hora acompañado de otras plantas medicinales y se deja reposar para posteriormente beberla.	
	Aweini (sin NC)	Árbol medicinal de cual se extrae su corteza para curar enfermedades respiratorias y en conjunto con el chuchuhuazo la hierven y se hace una bebida medicinal	
Construcción casas / Aprovisionamiento	Bejuco *Callichlamys latifolia*	Planta trepadora como liana que sirve para amarrar postes y palos que van junto a las hojas en la construcción de la casa **onko**, también utilizado en la elaboración de artesanías	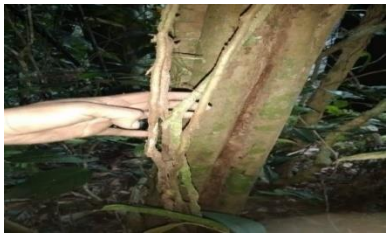
	Cola de Pescado *Caryota urens*	Es usada para la construcción de sus casas tradicionales y para impermeabilizar se usa el humo para que no ingresen polillas a dañar las hojas	
Artesanías / aprovisionamiento cultural	Chambira *Astrocaryum chambira*	Sus hojas tiernas son utilizadas para la elaboración de artesanías, como canastas, bolsas, pulseras, cadenas, aretes, etc.	
	Huayruro *Ormosia Coccinea*	Esta semilla de color rojo vivo es utilizada para realizar artesanías y se cultiva en la chacra o se extrae de la selva.	

	Palma de monte *Mauritia flexuosa*	Utilizado para realizar canastas que son amarradas con bejuco piquiwa (*Heteropsis ecuadorensis*), sirve para llevar chapil, carne de monte u otros frutos.	
Manifestaciones Culturales	Achiote *Bixa Orellana*	Usado para pintar el rostro en la parte de los ojos, también para pintar los pies de los niños recién nacidos como un repelente para que no ingresen enfermedades o maleficios, se cree que es un buen augurio el niño criará sano y fuerte.	
	Barbasco *Lonchocarpus utilis*	Se utiliza la raíz machada para la pesca en los ríos en época de verano, se obtiene una sustancia blanca vertida en los ríos y los peces mueran por asfixia [19]	
	Ortiga *Urera baccifera (L.) Gaudich.*	**Utilizada para castigar a los niños cuando tienen mal comportamiento son atados a un árbol y castigados con la ortiga.**	

Tabla 2. Plantas útiles que aportan servicios ecosistémicos en el bosque húmedo tropical amazónico en la comunidad Waorani Nampaweno, Orellana.

Se realizo la caracterización y evaluación de servicios ecosistémicos bosque primario perteneciente a la comunidad Waorani utilizando una escala LIKERT, de cinco puntos donde (1) sin importancia y (5) Muy importante, con valores intermedios. La calificación se realizó en base a rangos funcionales para la identificación de los servicios ecosistémicos presentes. Los resultados condensados se presentan en la tabla 3 donde se sumaron las calificaciones valoradas de los 14 servicios ecosistémicos identificados distribuidos en las 3 categorías (Abastecimiento, regulación y culturales).

VALORACIÓN DE SERVICIOS ECOSISTÉMICOS								
TIPO	SERVICIOS ECOSISTÉMICOS	Rangos Funcionales	VALORACIÓN					**subtotal**
			1	2	3	4	5	
Abastecimiento	Alimentos	Suelo agrícola (cultivo de yuca, chonta, maíz plátano, maní)					5	**33**
	Agua dulce	Fuentes de agua dulces (ríos)		2				

	Materias primas	Fibras textiles (lianas pikiwa, chambira, semi-llas)					5	
	Especies ve-getales(Sil-vestres)	Uso alimenticio (yuca, palmito, hojas de chilco, hongos)					5	
		Uso artesanía (pikiwa, chambira, achiote, bi-jao)				4		
	Medicinas naturales	Especies de plantas para uso medicina; achiote, ortiga,sierrilla, wanto, ayawaska, bar-basco				4		
	Especies animales (Sil-vestres)	Uso alimenticio (guanta, guatuso, venado, loros, culebras, peces)					5	
		Uso artesanía (piel de ti-gre, plumas de loros, colmillos de tigre, aguja de manta raya)			3			
Regulación	Regulación climática	Concentración de car-bono orgánico en el suelo				4		**28**
		Concentración de car-bono orgánico en la ve-getación				4		
	Purificación del aire	Concentración de car-bono orgánico en el suelo				4		
		Concentración de car-bono orgánico en la ve-getación				4		
	Control de la erosión	Cobertura vegetal				4		
		Concentración CO en el suelo				4		
	Polinización	Especies polinizadoras (abejas, polillas, etc.)				4		
Culturales	Educación ambiental	Programas de educación ambiental				4		**34**
	Conocimiento ecológ-gico local ancestral	Prácticas culturales					5	
		Costumbres ancestrales					5	
	Identidad cultural y sentido de pertenencia	Integrantes de la nacio-nalidad waorani ubica-das en el bosque primario de la comunidad Nampaweno					5	
	Disfrute espiritual y es-tético	Especies vegetales					5	
		Especies animales					5	
		Sitios (Atractivos tu-rísticos)					**5**	

Tabla 3. Identificación y calificación de los servicios ecosistémicos del bosque amazónico tropical, mediante una escala de Likert, en la comunidad Waorani Nampaweno, Orellana.

PUNTUACIÓN DE LOS SERVICIOS ECOSISTÉMICOS DE LA COMUNIDAD WAORANI NAMPAWENO			
Servicio Ecosistémico	**Puntuación**	**Puntuación de los sub-servicios de mayor utilidad**	
Aprovisionamiento o Abastecimiento	33	Servicio de Alimentación	15
Regulación	28	Servicio de control de erosión	8
Culturales	34	Servicio de conocimiento ancestral- Identidad Cultural	15

Tabla 4. Resumen de la valoración de los servicios ecosistémicos del bosque primario de la comunidad Nampaweno

Como se puede observar en la tabla 4, el servicio de abastecimiento obtuvo un total de 33 puntos, destacándose el servicio de alimentación con 15 puntos. Los Servicios de Regulación alcanzaron una puntuación de 28 puntos, siendo lo mas relevante el control de la erosión. En cuanto a los servicios culturales se obtuvo 34 puntos, y el mas importante el servicio de conocimiento ancestral con 15 puntos.

ESTADÍSTICAS DE FIABILIDAD		
Alfa de Cronbach	**Alfa de Cronbach de elementos estandarizados**	**N° de Elementos**
0,769	0,866	2

Tabla 5. Validación de la escala de Likert utilizada para la valoración de los servicios ecosistémicos

Para validar los resultados obtenidos de las encuestas y la escala de Likert para los servicios ecosistémicos de la comunidad Nampaweno - Huaorani, se aplicó la prueba del coeficiente del alfa de Cronbach, arrojando el resultado de 0,77 para todos los elementos, aumentando a 0,87 para elementos (variables) estandarizados. Por tanto, al ser mayor de 0,7 se puede afirmar que la escala aplicada para la valoración de los servicios de abastecimiento, regulación y culturales es confiable y sus resultados consistentes para afirmar que los servicios ecosistémicos que predominan en la comunidad son los culturales.

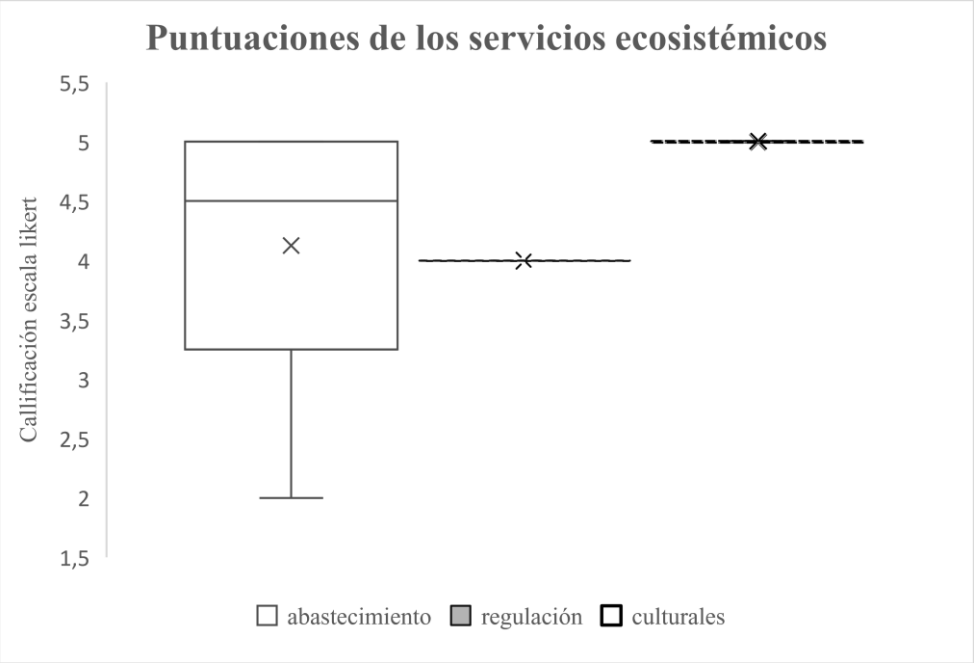

Figura 2. Gráfico de cajas de la valoración de los servicios ecosistémicos de la comunidad Nampaweno

El gráfico de cajas que se observa en la figura 2, compara los servicios ecosistémicos, siendo los servicios culturales los que obtienen una media mayor que los otros servicios (abastecimiento y regulación), ya que el

86% de todos los servicios culturales valorados son “muy importantes” (5). Con muy poca variabilidad estimada un coeficiente de variación de 8% a diferencia de los servicios de abastecimiento con el 27%. Los servicios de regulación tienen el 100% la misma valoración “importante” (4).

Por tanto, los servicios culturales ocupan el primer lugar en la valoración de los servicios que brinda el bosque, seguido por los servicios de abastecimiento y la alimentación que es imprescindible para la supervivencia, las manifestaciones culturales son importantes para la humanidad y se consideran parte de su patrimonio intangible y base de su identidad única como sociedad. Con estos resultados se sistematizó los aspectos mas importantes de los servicios ecosistémicos culturales basados en las fichas de Inventario del del INPC,

N°	Denominación	Ámbito	Subámbito	Detalle del subámbito
1	Cacería con Cerbatana Dayuma-Orellana	Conocimientos y Usos relacionados con la naturaleza y el universo	Técnicas y saberes Productivos Tradicionales.	Actividades de Sobrevivencia como la cacería.
2	Memorias de Conflicto entre Nacionalidades Indígenas waoranis Dayuma, orellana	Tradiciones y Expresiones Orales	Memoria local Vinculada a Acontecimientos históricos Comunidades.	Conflicto entre Nacionalidades por Venganza dentro de la selva
3	Dichos, leyendas de las comunidades Waoranis Dayuma-Orellana	Tradiciones y expresiones orales	Expresiones orales	Proverbios, dichos, supersticiones y creencias
4	El achiote usado como tinta facial por la etnia	Tradiciones y Expresiones	Memoria local Vinculada a Acontecimientos	Conflicto entre Nacionalidades por Territorios dentro

Tabla 6. Sistematización de las fichas del Inventario de los servicios ecosistémicos culturales en la Comunidad Waorani Nampaweno

Los resultados de la sistematización de las fichas se centraron en los siguientes ámbitos: Técnicas y saberes productivos tradicionales, memoria local vinculada a acontecimientos históricos reinterpretados por las comunidades, expresiones orales, memoria local vinculada a acontecimientos históricos reinterpretados por las comunidades, danza, técnicas artesanales tradicionales y gastronomía.

En la primera ficha se describe la “cacería” como una actividad fundamental, ya que significa llevar el sustento para su familia cotidianamente y también en días festivos, va acompañada de un ritual, en el cual se despiertan a las 4 am, beben chicha de yuca o chonta y salen solo 5 hombres acompañados de los pikenanis líderes, las mujeres cosechan yuca y verde. Para la caza utilizan tradicionalmente la “cerbatana” y lanzas, para ellos es importante mantener el equilibrio con la naturaleza y los animales que normalmente cazan son sahinos, guantas, venados, monos, y loros. Para la preparación de los alimentos lo hacen en grupos en cocinas de leña, al momento que ya están cocidos sus alimentos llaman a toda la comunidad e invitados a compartir sus alimentos acompañados de chicha. Esta costumbre es trasmitida de generación en generación y la consideran representativa en su cultura waorani. Con la influencia de la colonización se han adoptado algunas costumbres que no tenían sus ancestros como la cocción de la carne. La amenaza a esta costumbre es la extinción de la fauna silvestre por la excesiva caza ilegal y comercio de carne de monte por parte de los colonos.

La segunda ficha relata los conflictos entre nacionalidades indígenas por venganzas entre dos grupos waorani: los tagaeri y los taromenanis, este conflicto está dado por la invasión de territorios y un acontecimiento representativo fue el secuestro de dos niñas tagaeris, como consecuencia hubo decenas de personas muertas de ambos grupos y se remonta a 1993 que por el secuestro de una mujer waorani por parte de un grupo se motivo una división del grupo en dos. Los taromenanis, se consideran con atributos distintos al grupo de tagaeris, sin embargo, los tagaeris nunca aceptaron la imposición religiosa cristiana basada en el evangelio. La lideresa Tagaeri de Tigüino, “Babe Ima”, realizó acercamientos con el grupo de los taromenanis, en los límites entre las provincias de Pastaza y Orellana persuadiéndolos para que aceptaran el evangelio cristiano. Pero “Babe” secuestró a una chica menor de 20 años, ojos verdes, piel blanca y pelo negro lacio hasta la cintura, llamada “Omatuki”, rasgos muy diferentes a los waoranis y la retuvo por 24 días, los familiares presionaban para su

liberación, y temían un ataque, Babe accedió a devolver a Omatuki, en “Cuchiyacu”, acompañada de 6 hombres, la chica se despidió por su liberación sonriendo, sin embargo, aproximadamente a un kilómetro el otro grupo los atacaron con lanzas, dejando gravemente herido a “Carlos Ima”, hijo de Babe, el cual falleció, por tanto una década después, Babe ideo otro ataque para vengar las muertes de su clan e hijo, por tanto de este grupo 9 luchadores, se internaron en la selva el día 26 de mayo del año 2003, murieron otros 25 taromenanis, entre (mujeres y niños), luego prendieron fuego a la choza, tomaron sus lanzas y como trofeo llevaron la cabeza cortada de un guerrero. Declarándose “un acto de justicia propia”, sin remordimientos, ambientalistas y de dirigentes de otras etnias manifestaron: “estos enfrentamientos están influenciados por madereros y petroleros, pues los waoranis reciben sus beneficios”[22]. Históricamente los conflictos entre waoranis y los PIAV, son por disputas territoriales y venganzas antiguas que permanecen como vivos recuerdos en su tradición oral, no están abiertos al cambio, las personas de mayor de edad corren mayor riesgo de ataques, esto se ha incrementado ya que en la última década se dieron más de cinco ataques a madereros en "territorios Tagaeri". La constitución de Ecuador también les reconoce derechos a través del Art. 57, y es una deuda pendiente del Estado garantizar su integridad, autodeterminación y derecho al territorio sobre el cual estaría vedada toda actividad extractiva [23]

La tercera ficha relata los proverbios, dichos, supersticiones y creencias, el mas recordado, según cuentan ellos son hechos reales que hace 5 años atrás, 5 miembros de la comunidad se fueron de cacería de donde solo cuatro de ellos volvieron a la comunidad, el que se extravió dentro de la selva lo dieron por muerto y volvieron sin él, sin embargo en la montaña, estando vivo se adentraba más en la selva, después de días de caminar se le presentó un enorme tigre dispuesto a devorarlo, él se defendió para no dejarse devorar pero tuvo graves heridas por tanto cae inconsciente y en sus sueños se le presenta su padre ya fallecido (que era shamán) y en forma de tigre y se enfrenta al otro tigre para defender a su hijo, logrando su cometido después de pelear a muerte alejándose el otro tigre, se volvió otra vez humano y lo ayudó a salir de la selva después de días de estar perdido, salen a la vía al hormiguero donde se conecta con una plataforma que perteneció a la empresa “Andes Petroleum”. Su padre lo deja inconsciente con grandes heridas y un trabajador lo encontró lo subio al balde de la camioneta trasladándole hasta el subcentro de la comuna Río Tiputini, en donde le dieron los primeros auxilios y posteriormente ser trasladado hasta el hospital de la capital Francisco de Orellana. Dentro de su cosmovisión creen que cuando mueren se trasladan a otra vida y se convierten en algún animal salvaje de la selva. Los relatos generacionales son de vital importancia para mantener la cultura en los jóvenes del conocimiento de sus ancestros ya que en la actualidad quedan pocos pikenanis shamanes, la amenazando que estas historias que desaparezcan.

La cuarta ficha describe al achiote (*Bixa Orellana*), (kaka) en el idioma wao, es usado como tinta en el rostro para la buena suerte, siguiendo una tradición ancestral, en el cual los guerreros (llamados despectivamente Aucas por los kichwas), se pintaban la cara de rojo con la sangre de sus enemigos muertos, hoy en día mantienen la tradición usando la semilla de achiote para pintarse una gran franja en el rostro, ellos creen que les da buena suerte y les aleja de los malos espíritus. Sirve también el tinte para adornar los cuerpos, instrumentos de caza; lanzas y cerbatanas para tener buena cacería. Cuando llegan turistas a las comunidades las mujeres pintan el rostro de los visitantes con esta semilla como símbolo de bienvenida. En la cosmovisión de los waoranis este color rojo les proporciona “buena suerte” y ahuyenta los “malos espíritus” lejos de sus hogares y los niños de días de nacidos se les “pintan los pies”. Es un símbolo de cultura y tradición de la cultura waorani, su identidad esta construida y transmitida generacionalmente de padres a hijos y de abuelos a nietos garantizando que no pierda su cultura, y en eventos importantes manifiestan este comportamiento. Pero algunos de los jóvenes ya no se sienten tan cómodos al pintarse los rostros y solo se pintan puntos rojos.

La quinta ficha relata la danza de la comunidad waorani, que viene desde los pikenanis ellos cantan y bailan todos los días, este baile es simplemente a compás de la música entonada por ellos mismos y es repetitivo. Esto acontece cuando están felices, y hacen fiestas relacionadas con la abundancia de producción de sus chacras y caza en la selva, así como por los tiempos de paz y prosperidad entre ellos. Sus danzas les llevan a pasar toda la noche y dependiendo de que se trata la celebración que entonen los hombres se ubican en un mismo sitio en filas de tres o cuatro hacia atrás tomados de los hombros y las mujeres se colocan al frente. Bailan por lo general en grupo tomados de las manos, otras veces entrelazan los brazos y en algunas ocasiones bailan solamente juntos. En el caso específico de las bodas, danzan con pasos cortos acercándose y alejándose. Las personas que desean participar en la danza pueden ingresar cuando lo quieran, lo mismo ocurre si alguien decide retirarse. simplemente correr en circulo realizando ruidos en el idioma Huaorani como también imitando al águila y al tigre. Para este evento no se necesitan instrumentos musicales simplemente es necesaria la voz de cada uno de los integrantes de las personas que están realizando la danza bailable, ya que cada uno de ellos realizan un solo canto, en caso de que solo las mujeres cantan los hombres realizan unos gritos en simulación al águila y tigre, estas aves emblemas para esta nacionalidad. Esta manifestación enriquece su cultura

haciéndolos más fuerte y atrayendo abundancia y bendiciones para sus armas de caza. La amenaza es alta ya que los jóvenes ya no la practican por miedo y vergüenza de sus amistades colonas.
La sexta ficha esta relacionada con la elaboración de artesanías generalmente están tejidos con fibras naturales, antes de tener contacto con los colonos, vivían desnudos o semi desnudos. Es por ellos que se protegían con tapa rabo sus partes intimas y lianas hechas a base de chambira para proteger sus pechos. Hoy en día el traje típico son coronas llenas de plumas de aves de la selva amazónica, collares y pulseras hechos a base de semillas dientes de animales, materiales de la naturaleza a los que les atribuyen poderes protectores contra los malos espíritus y males externos, hamacas, faldas hechas de fibra de corteza de arboles y cestas. Todos estos productos son utilizados para celebraciones o presentaciones especiales y para la venta a los turistas, obteniendo una buena fuente de ingresos, creando fuentes de empleo para las señoras waoranis El arte de armar artesanías, mezclar los tintes, entorchar y convertir cada fibra de chambira en hilos con los que se elaboran las artesanías, viene de herencia desde sus abuelas, pues ellas han sido hábiles artesanas y ellas aprendieron de sus abuelas y éstas de las suyas, etc. Las artesanías waorani llevan impregnadas la sabiduría y la cosmovisión de sus mujeres, la lucha por tener un mejor futuro sin recurrir a la necesidad de destruir el territorio que ocupan. esta actividad tiene una influencia o alcance a nivel Internacional ya que vienen comerciantes extranjeros y adquieren este producto para vender en otros países. La amenaza recae en excesiva influencia externa que valora mas el dinero que la riqueza cultural por eso los jóvenes muestran desinterés en estas técnicas y procedimientos. Con la deforestación se extinguen las plantas proveedoras de semillas y fibras poniendo en peligro la artesanía waorani.
La séptima y última ficha describe acerca de la gastronomía en la elaboración de la chicha de yuca. Esta bebida ancestral viene desde los primeros “pikenanis” que consumían la chicha de yuca, chontaduro como su principal alimento. Es de vital importancia la práctica de la cacería porque es una costumbre ancestral y es fuente de alimentación para las familias Waoranis, aparte del consumo de la carne de monte y la preparación tradicional transmitido de generación en generación, ya que es su representación como cultura y consideran que la carne adquirida en el mercado tiene químicos que provocan cáncer, prefieren alejarse y consumir lo natural.

DISCUSSION

De los resultados presentados tanto de la valoración de los servicios ecosistémicos como de las manifestaciones culturales, se pueden corroborar algunos relatos presentando análisis sociales antropológicos y reportajes realizados por medios de comunicación. Se lo ha dividido en aspectos de su cotidianidad.

1. Se corrobora que del bosque obtienen madera para fabricar sus casas tradicionales y se menciona que: “ las casas son de gran tamaño amplias por dentro hechas a base de postes de árbol de chapil, bejuco “pikiwa” y hojas de “tawa” o cola de pescado”, por tanto es un servicio ecosistémico de aprovisionamiento del bosque , también se relata que el tiempo que duraba la casa donde habitaban “onko” en buen estado podía ser hasta de 15 años, porque el humo de los fogones que usaban permitía impermeabilizar las hojas del techo y aumentar con esto su vida útil, como lo registro el diario la “hora” [24], lo cual es parte de una manifestación cultural derivada del servicio de abastecimiento.
2. Relacionando los recursos que se obtienen del bosque húmedo tropical la vestimenta de los waorani, en función del clima imperante tradicionalmente se podría mencionar que están “desnudos”, sin embargo en la actualidad por la influencia externa muchos ya utilizan ropa, aunque en fiestas y rituales mantienen su vestimenta tradicional destacando los materiales que les provee el bosque como “pasacuerpos” de chambira, tobilleras con semillas, piola o “come” o “cumi”, para amarrar sus genitales los hombres, y facilitar sus movimientos también coronas de plumas de aves guacamayo y águila arpía, y coincide con la cartilla de saberes y conocimientos de la nacionalidad waorani[26].
3. En la mayoría de plantas presentadas se ha puesto de relevancia que la alimentación está basada en la chicha de yuca y otras especies, complementada por el ritual de la cacería, por tanto la selva es su casa y mercado, pues, les provee de variedad de carnes y plantas, nunca cazan venados, serpientes, jaguares ni otros depredadores carnívoros como el águila, una demostración del respeto a la dinámica del ecosistema, en cuanto a la pesca a los niños se les enseña a colaborar y aprender a pescar, hábito que mantiene la supervivencia Cada familia posee dos o tres chacras: en la primera, alrededor de la casa, cultivan básicamente yuca, como alimento principal, luego el plátano (verde y banano), también chonta, maíz y en menor cantidad papayas, piñas, limones, guayabas en los últimos años comercian maíz, uva de monte. Las plantas también tienen propiedades medicinales y rituales que utilizan los shamanes como balsaminas, el “yagé” “ayahuasca” y el bejuco, como lo menciona también en el boletín de plantas que usan los waoranis [27].
5. Lo mas llamativo y pintoresco en eventos culturales son las artesanías. Como se mencionó obtienen la materia prima directamente de la selva, como: “pepas de san pedro”, fibra de chambira, bejuco pikiwa, tallo

de cruz caspi que sirven de base para las canastas, y otras plantas que extraen gran variedad de colores para artesanías de llamativos colores, sus artesanías constan de utensillos como canastas, collares, aretes, tobilleras, pulseras, coronas, trajes típicos etc., siendo lo mas comercial que poseen para generar ingresos, se puede obtener mas información y otro tipo de artesanías en el libro los saberes de la artesanía [28].

6. Como las plantas están ligadas a sus manifestaciones culturales y costumbres como la celebración de "la fiesta de la chonta (kewe)" y "la fiesta de la yuca (kene)" realizada entre enero y abril, se aprovecha para celebrar matrimonios y los pikenanis elegían con quien casar a sus hijas adolescentes desde los 12 años, las tradiciones mencionan que: los niños son castigados con ají en los ojos para que no se enojen y obedezcan a los padres, para el castigo a niños mayores a un año, se les ata a un árbol y se les azota con ortiga, el color rojo es de buena suerte y mantiene a los malos espíritus alejados, razón por la cual se pintan los pies de los recién nacidos, el achiote también es insecticida y evita los hongos [26 29].
7. Expresiones culturales. La música es expresada para alejar los espíritus negativos dentro de la selva. Existen 3 tipos de expresiones musicales: para fiestas o celebración importante, guerras o muertes cuando se dan los enfrentamientos sanguinarios con los Tagaeri o Taromenanis, que hasta la fecha aún existen amenazas entre estas tribus y las ofrecidas a objetos como lanzas o seres vivos cuando van de cacería, esto lo hacen como un ritual cada que van de cacería para que les de la buena suerte de llevar muchos animales a casa [30]. Dentro de este contexto existen también algunos problemas que tienen los Waoranis, entre los que se destacan la tala, el tráfico tanto de madera como de especies nativas plantas y animales silvestres, el "lobby" de empresas petroleras que negocian con los jefes para ingresar a sus territorio, el fenómeno que se ha visto en estas últimas décadas es la migración de niños y jóvenes a los poblados llegando a constituir otras familias con otras etnias como las kichwas [17]. A pesar de otras amenazas como la colonización desordenada, contaminación petrolera, caza de animales por los colonos, inundaciones, incendios, existen algunas oportunidades para mantener su condición de vida en contacto con la naturaleza: como el turismo sostenible - ecológico, coordinación de esfuerzos gubernamentales y ONGs, difusión de su modo de vida como la demostración de la lengua nativa y costumbres y leyes que permitan su supervivencia.

CONCLUSIONS

- La comunidad Waorani Nampaweno, depende del bosque húmedo tropical y se valora mas los servicios ecosistémicos culturales logrando la puntuación mas alta con 34 puntos, de la escala de Likert que ha sido validada mediante el alfa de Cronbach con 0,87 de coeficiente para los elementos estandarizados, los waoranis del grupo Tagaeri, se encuentran en aislamiento voluntario y todas sus manifestaciones culturales están en función del Bosque manteniéndolas por varias generaciones conservando sus costumbres ancestrales.
- Se han descrito 16 especies de plantas amazónicas que proveen servicios de Alimentación, aprovisionamiento, medicina, construcción de casas, artesanías y manifestaciones culturales. Las creencias y conocimientos se mantienen por los pikenanis (adultos mayores con gran conocimiento ancestral), lamentablemente por influencia de la colonización sus saberes ancestrales están disminuyendo, por tanto los jóvenes y niños, están perdiendo su identidad cultural, en conclusión la presencia de los waoranis en el bosque húmedo tropical, ha permitido que se puedan mantener los servicios ecosistémicos en equilibrio, ya que la colonización a gran escala y la exploración petrolera han traído fragmentación de habitats, y desestabilizado los otros componentes como la fertilidad de los suelos, reciclaje de nutrientes, dinámica de organismos. Incluso la regulación del clima.
- Se han sistematizado 7 fichas de inventario de patrimonio cultural intangible de la etnia indígena waorani, donde se plasma su relación directa con el bosque y su identidad esta basada en este entorno natural. Cuando se reflexiona acerca de la apreciación del modo de vida de los waoranis, se amplia el conocimiento y valoración de todos los recursos y servicios que ofrece el bosque húmedo tropical.
- La influencia de colonos y empresas petroleras ha derivado en cambios de costumbres e intereses incrementando los enfrentamientos tanto por sus territorios ancestrales, asi como por mantener su autodeterminación libre y voluntaria de mantenerse aislados sin contacto con otros grupos étnicos, lo cual esta garantizado en la constitución ecuatoriana que defiende el derecho a su modo de vida.

Author Contributions: Las contribuciones realizadas por los autores se detallan a continuación en la siguiente declaración: la conceptualización, metodología, software, investigación, recursos, escritura original,

administración del proyecto, adquisición de fondos han sido realizado por la autora: Johanna Rentería. La validación, análisis formal, revisión de datos, escritura revisión y edición, supervisión han sido realizados por el autor Jaime Larrea. Todos los autores han leído y están de acuerdo con la versión publicada del manuscrito

Funding: "Esta investigación no recibió financiamiento externo"

Institutional Review Board Statement: "El estudio se realizó de acuerdo con las pautas de la Declaración de Helsinki y fue aprobado por la Junta de Revisión Institucional (o Comité de Ética) de NOMBRE DEL INSTITUTO (código de protocolo XXX y fecha de aprobación)".

Informed Consent Statement: Ya que se realizó el estudio con las personas de la comunidad Nampaweno, se declara: “"Se obtuvo el consentimiento informado de todos los sujetos involucrados en el estudio".

Data Availability Statement: La escala de likert detallada, asi como las fichas con el formato del INPC. Se encuentran en la tesis original del repositorio, e el siguiente link: Servicios ecosistémicos- Rentería Johanna.pdf

Acknowledgments: Es importante realizar algunos reconocimientos al trabajo realizado, empezando por la tecnóloga Johanna Rentería, la cual realizó el trabajo en la comunidad y evidenciando su modo de vida, también se reconoce el auspicio del Instituto superior Universitario Oriente ITSO, tanto en la parte estudiantil del documento de tesis, asi como este artículo. Y un reconocimiento especial para la comunidad Nampaweno por abrir su casa y narrar todas sus experiencias de vida en comunidad con sus pikenanis.

Conflicts of Interest: Cabe declarar que no existe ningún tipo de conflicto de intereses en la realización de este trabajo, mas que la confirmación de los testimonios de los habitantes de la comunidad, muchos de los cuales ya ha sido documentados en otros trabajos y reportajes.

REFERENCES

1. Corraliza JA, Collado S. Conciencia ecológica y experiencia ambiental en la infancia= Ecological awareness and children’s environmental experience. 2019.
2. Jean-Paul L. Los Factores de la Deforestación y de la Degradación de los Bosques. In: FAO, editor. XII Congreso Forestal Mundial Quebec - Canadá: FAO. 2003.
3. Montalvo PT. Identificación y dinámica de los pueblos indígenas en aislamiento voluntario (PIAV) en el Yasuní (Ecuador). Boletín de Antropología Universidad de Antioquia. 2018;33(55):271-96.
4. Quang ML. El proyecto ITT en Ecuador: dejar el crudo en tierra o el camino hacia otro modelo de desarrollo CIP-Ecosocial. 2009.
5. MAE. Plan de Manejo Comunitario Comunidad Waorani Nampaweno. In: Yasuní EtdMdAdE-PN, Equipo consultor hymidlcdN, editors. Francisco de Orellana GIZ. 2016. p. 121.
6. Renteria J. Valoración de los Servicios Ecosistémicos del Bosque Primario ubicado en la Comunidad Waorani Nampaweno, Cantón Francisco de Orellana, Provincia de Orellana. Joya de los Sachas: ITSO Instituto Tecnológico Superior Universitario Oriente. 2022.
7. FAO. Servicios ecosistémicos y biodiversidad. 2023. Disponible en:: https://www.fao.org/ecosystem-services-biodiversity/es/.
8. Leiva MLP, Arce CAV, Guzmán MCV, Gómez SPM, Ausique VFF, López CFV, et al. Los servicios ecosistémicos culturales. In: UNAD, editor. Desarrollo Rural. Bogotá - Colombia: UNAD. 2019. p. 237-50.
9. Talancón H. La matriz FODA: una alternativa para realizar diagnósticos y determinar estrategias de intervención en las organizaciones productivas y sociales Contribuciones a la Economía. 2006:16.
10. Wuensch KL. What is a Likert Scale? and How Do You Pronounce 'Likert?. 2005. [citado el 30 Abril de 2009]. Disponible en: https://core.ecu.edu/wuenschk/StatHelp/Likert.htm.
11. Assessment ME. Ecosystems and Human Well-being: Synthesis. . Island Press, Washington, DC.: ISLAND PRESS. 2005. 156 p.

12. INPC. Instructivo para fichas de registro e inventario Patrimonio Cultural Inmaterial. Quito - Ecuador: Instituto Nacional de Patrimonio cultural INPC. 2011. 188 p.
13. amazonfrontlines. editor. Estados Unidos. 2023. Disponible en: %20son%20los%20m%C3%A1s,dif%C3%ADcil%20en%20la%20sociedad%20moderna.
14. Cabodevilla MA, Smith R, Rivas A. Tiempos de Guerra Waorani contra Taromenanis. Quito - Ecuador: ABYA-YALA. 2004.
15. García PB. La Crónica del capuchino P. Manuel Labaka. Traducción de la cultura de la Amazonía ecuatoriana al español. 2016;3:183-99.
16. INEC. Población que se autoidentificó indígena, según provincia de empadronamiento, nacionalidad o pueblo indígena al que pertenece y sexo. In: WAORANIS, editor. Quito - Ecuador: ecuador en cifras. 2023.
17. Rivas A, Lara R. Conservación y Petróleo en la Amazonía Ecuatoriana Un acercamiento al caso huaorani. Quito - Ecuador: Abya-Yala. 2001.
18. Quiroga K. Evaluación del poder analgésico y antiinflamatorio de Maytenus macrocarpa (Ruiz & Pav.) Briq. (Chuchuhuasi).". Quito- Ecuador: Universidad Central del Ecuador. 2015.
19. Unimedios. Barbasco, aliado de los muinane en la pesca y en el control de plagas Colombia: Virtualpro. 2022. Disponible en:: https://www.virtualpro.co/noticias/barbasco-aliado-de-los-muinane-en-la-pesca-y-en-el-control-de-plagas.
20. UNESCO. Reserva de Biosfera Yasuní, Ecuador: UNESCO; 2021. Disponible en:: https://es.unesco.org/biosphere/lac/yasuncartiñi#:~:text=El%20ecosistema%20dominante%20es%20el,representada%20por%20vegetaci%C3%B3n%20natural%20original.
21. Figueiredo GdO. Investigación Acción Participativa: una alternativa para la epistemología social en Latinoamérica. Revista de Investigación 2015;39:20.
22. Universo E. Matanza de tagaeri fue por orden de madereros, dicen los huaorani. El Universo. 2003.
23. IGWIA. Dinamarca. 2003. Disponible en: https://iwgia.org/es/conocenos/contactanos.html.
24. Hora L. En las 'onko', el fogón y la hamaca son indispensables. Quito – Ecuador. 2015.
25. Velasco L. "Transferencia Lingüística del Huaorani Tededo en el Español Hablado Por Bilingües de Las Comunidades Konipare y Menipare": Estudio De Caso. Quito - Ecuador: Pontificia Universidad Católica del Ecuador. 2018.
26. MinEduc. Cartilla de saberes y conocimientos de la nacionalidad waorani. In: Educación Md, editor. Subsecretaría de educación intercultural bilingüe. 2019.
27. Zurita-Benavides MG. Cultivando las plantas y la sociedad waorani. Boletim do Museu Paraense Emílio Goeldi Ciências Humanas. 2017.12:495-516.
28. Alvarado AC. Los saberes de la artesanía waorani. 2016.
29. viajadox. Huaronanis. 2023. Disponible en:: https://ec.viajandox.com/orellana/huaorani-A1213#:~:text=Los%20Wao%20usan%20el%20achiote,semilla%20como%20s%C3%ADmbolo%20de%20bienvenida.
30. Hora L. Música waorani, expresión musical que evoca el tiempo sagrado. 2019.

Received: October 9th 2023/ **Accepte**d: January 15th 2024 / **Published:**15 February 2024

Citation: Larrea J, Rentería J. Valoración de los servicios ecosistémicos del bosque primario de la comunidad Waorani Nampaweno, Orellana, Ecuador.Revis Bionatura 2024; 9 (1) 7. http://dx.doi.org/10.21931/RB/2024.09.01.17

Additional information Correspondence should be addressed to *jlarrea@itsoriente.edu.ec.*

Peer review information. Bionatura thanks anonymous reviewer(s) for their contribution to the peer review of this work using https://reviewerlocator.webofscience.com/

Bionatura ISSN. First 13909355 Ecuador. **Scopus coverage years**: from 2016 to the present

Bionatura
Ibero-American Journal of Biotechnology and Life Sciences

Article

Análisis multitemporal de deforestación y cambio de la cobertura del suelo, en el cantón La Joya de los Sachas, período 1990-2018.

Multitemporal analysis of deforestation and land cover change in the canton La Joya de los Sachas, period 1990-2018.

Fernando Paredes-Arcos[1], *Leider Tinoco-Jaramillo*[1*], *Carlos Congo-Yépez*[1], *Yadira Vargas-Tierras*[1]

[1] *Instituto Nacional de Investigaciones Agropecuarias – Estación Experimental Central de la Amazonia /La Joya de los Sachas/Orellana/Ecuador; fernando.paredes@iniap.gob.ec* .
[1] *carlos.congo@iniap.gob.ec* .
[1] *yadira.vasgas@iniap.gob.ec* .
* *Correspondencia: leider.tinoco@iniap.gob.ec; Tel.: +(593)991495642*
Available from. http://dx.doi.org/10.21931/RB/2024.09.01.18

ABSTRACT

La Joya de los Sachas, es uno de los principales cantones productores de petróleo y productos agrícolas; sin embargo, el incremento de la frontera agrícola ha ocasionado cambios importantes en la cobertura y uso del suelo. Ante esta situación, el estudio tuvo la finalidad de conocer las causas y efectos que ha ocasionado el cambio de cobertura para obtener las tasas anuales e índices de cambio de cobertura. El análisis se realizó mediante el geoprocesamiento de información geográfica disponible en el portal del Ministerio de Ambiente Agua y Transición Ecológica (MAATE) y el Instituto Geográfico Militar (IGM), se utilizó el método de tablas de tabulación cruzada y sobreposición de capas para determinar el contraste de las coberturas entre las fechas establecidas. Los resultados muestran un incremento acumulado de 17.626,5 ha de tierra agrícola y 16.767,6 ha de pasto en los últimos 28 años; las actividades agropecuarias se han convertido en la principal causa de deforestación. Durante el período 1990-2018 se perdieron 36.413 ha de bosques, con una tasa anual de deforestación de 1.300 ha*año^{-1}. Este comportamiento permitió estimar si la tendencia persiste, en 30 años aproximadamente La Joya de los Sachas perderá completamente el bosque. Además, las políticas públicas, dolarización, apertura de caminos y cambios en la actividad agrícola causaron impactos en las coberturas y usos de suelo durante los tres periodos evaluados (1990-2000, 2000-2008 y 2008-2018).
Palabras Clave: Suelo, Uso de suelo, cobertura, tierra agrícola, pastizal, bosque, mapas.

ABSTRACT

La Joya de los Sachas is one of the leading oil and agricultural product-producing cantons; however, the increase of the agricultural frontier has caused significant changes in land cover and land use. Because of this situation, the study aimed to determine the causes and effects of land cover change to obtain annual rates and indices of land cover change. The analysis was carried out through the geoprocessing of geographic information available in the portal of the Ministry of Environment, Water and Ecological Transition (MAATE) and the Military Geographic Institute (IGM), using the method of cross-tabulation tables and overlapping layers to determine the contrast of coverages between the established dates. The results show a cumulative increase of 17,626.5 ha of agricultural land and 16,767.6 ha of pasture in the last 28 years; agricultural activities have become the leading cause of deforestation. During 1990-2018, 36,413 ha of forest were lost, with an annual rate of deforestation of 1,300 ha*year-1. This behavior allowed us to estimate that if the trend persists, in approximately 30 years, La Joya de los Sachas will ultimately lose its forest. In addition, public

policies, land development, road opening and changes in agricultural activity caused impacts on land cover and land use during the three periods evaluated (1990-2000, 2000-2008 and 2008-2018).
Keywords: Soil, Land use, cover, agriculture land, pastureland, forest, maps.

INTRODUCTION

El ser humano ha demostrado que puede adaptarse al entorno que lo rodea, superando todas las dificultades que le impidan subsistir[1,2]. Hace 10.000 años, los seres humanos se agruparon y permanecieron juntos por largos períodos de tiempo en el mismo sitio, con la finalidad de cultivar la tierra y domesticar animales[3,4]. Este comportamiento condujo al establecimiento de la agricultura como un pilar fundamental para satisfacer las crecientes necesidades alimentarias de una población en constante crecimiento[5,6].
En los años 1940 y 1970, la agricultura tuvo un punto de inflexión con la "Revolución Verde"[7], debido, al inicio del mejoramiento genético y la agricultura industrial (agricultura intensiva), donde se desarrollaron cultivos con mayor producción; también, se implementó la práctica de monocultivos (cultivos con una especie)[8,9]. Sin embargo, estas prácticas tuvieron graves consecuencias, como la pérdida de los recursos naturales, biodiversidad terrestre, acuática y especies forestales[10].
En Ecuador las especies que tomaron relevancia como monocultivos fueron Cacao (*Theobroma cacao*) en los años 1920 y 1930 y Banano (*Musa paradisiaca*) en el año 1950, consolidando al país como el mayor exportador de estas frutas[11]. Actualmente, en Ecuador el 50 % de la actividad agrícola se concentra en zonas rurales[12]. Durante el año 2020, se encontraban cultivadas en el país 5,2 millones de hectáreas, de las cuales, 1,5 millones se usan para cultivos permanentes de caña de azúcar, cacao, palma africana y banano, mientras que el resto de la superficie se dedica a cultivos de ciclo corto y flores[13].
Durante el año 1969, en Ecuador, se inició la explotación de pozos petroleros en la región amazónica. Como resultado de esta actividad, las compañías petroleras construyeron vías de comunicación para conectar la sierra central con la Amazonía. Aprovechando la accesibilidad proporcionada por estas nuevas vías, los primeros colonos llegaron al área conocida como La Joya de los Sachas, donde algunos se dedicaron a trabajar en compañías y el resto establecieron plantaciones de café, por los excelentes ingresos económicos. Sin embargo, desde 1998 al 2002 aproximadamente se da la denominada "Crisis cafetalera"[14] los precios se desplomaron y la mayoría de los habitantes se dedicaron a trabajar en las compañías petroleras y una mínima cantidad continúo en la agricultura, pero en otros rubros. En los últimos 4 años los habitantes del sector se han dedicado a cultivar cacao (34,5%), maíz (17%), palma africana (12,9%), plátano (10,4%), malanga (7,1%), frutales (3,2%), arroz (3,1%), palmito (1,7%) y caña de azúcar (0,4%)[14].
Las actividades que se desarrollaron desde el primer asentamiento de los colonos han desencadenado una serie de cambios en la cobertura y uso del suelo (CCUS), estos cambios se pueden estudiar y evidenciar con la ayuda de sensores remotos[16,17] que permiten conocer cuáles son las causas y efectos de los CCUS en áreas determinadas, por ejemplo: deforestación, erosión, perturbación, desertificación, pérdida de biodiversidad, entre otros[18,19]. La deforestación se define como la eliminación del componente arbóreo provocado principalmente por actividad antrópica[20]. Existen varios estudios que se han enfocado en identificar, describir, analizar e interpretar la dinámica del CCUS a nivel del mundo[11,18,19,21–27] y a nivel nacional[28–32]; sin embargo, no se encontró estudios realizados a nivel de Cantón, que permitan visualizar los cambios ocurridos en los últimos años[15].
Por esta razón, el presente estudio pretende determinar la deforestación y los cambios de cobertura y uso de suelo en los períodos 1990-2000, 2000-2008 y 2008-2018 en el Cantón La Joya de los Sachas, mediante la metodología, matriz de tabulación cruzada[19,33]; que permite evidenciar la dinámica de las coberturas, identificar las tasas de variación de cambios entre períodos y conocer si los CCUS se han mantenido inactivos y cuáles han sido los más activos.

MATERIALES Y MÉTODOS

Lugar de Estudio

El estudio se desarrolló en el cantón La Joya de los Sachas, que posee una superficie de 1.200 Km^2, ubicado al norte de la Región Amazónica Ecuatoriana (RAE) (Figura 1); limita al Norte y Este con la provincia de Sucumbíos, al Oeste y Sur con el cantón Francisco de Orellana. Cuenta con una población de 67.000 habitantes[15].

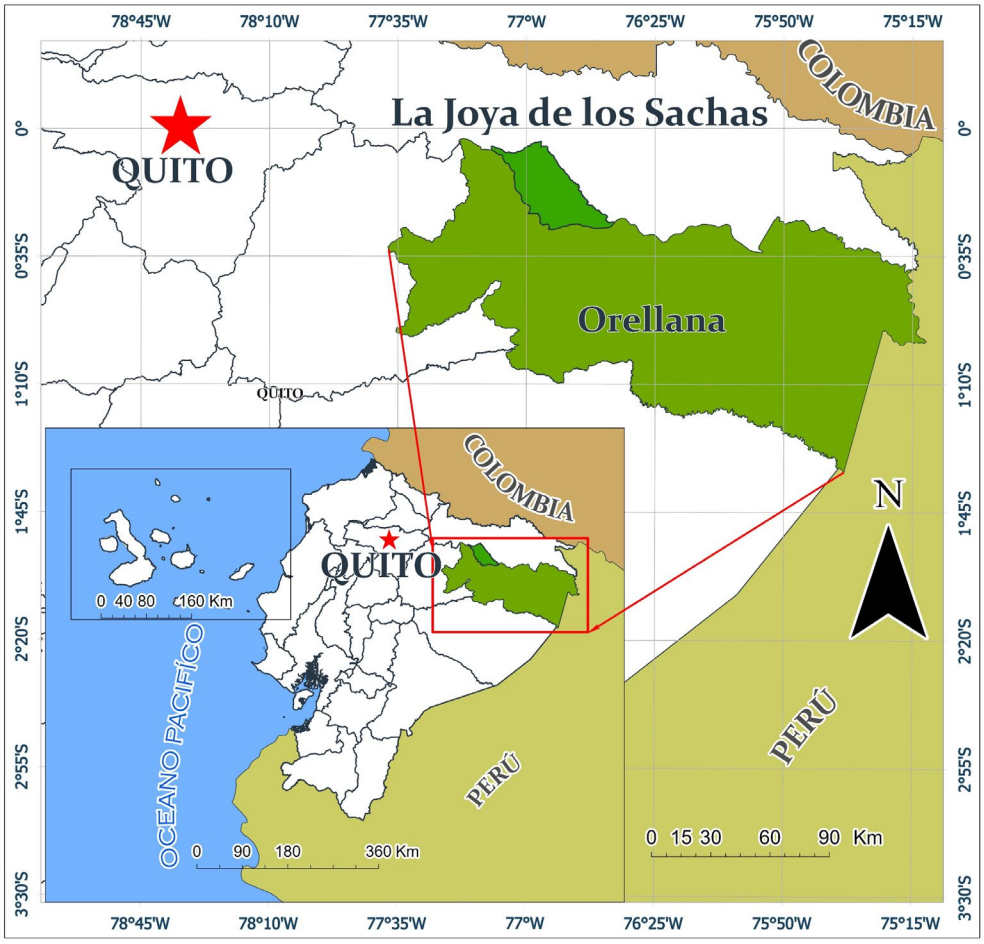

Figura 1. Ubicación geográfica del cantón La Joya de los Sachas[34].

Análisis de la dinámica del CCUS

Con la cartografía base del IGM[34] se extrajo el archivo en formato shapefile (.shp) del cantón La Joya de los Sachas, con la finalidad de realizar recortes de los años (1990, 2000, 2008 y 2018). Posteriormente para definir la interacción de las coberturas se realizó una sobreposición cartográfica y una tabulación cruzada, empleando dos fechas (fecha 1 y fecha 2). Para este estudio se consideró 3 períodos: período 1 (1990-2000), período 2 (2000-2008), período 3 (2008-2018)[19,37].

Cartografía Base

El área en estudio se delimitó con la cartografía base del geo portal del Instituto Geográfico Militar (IGM) [34] utilizando un Sistema de Información Geográfica (SIG). Para los CCUS se utilizó la información del geo portal del Sistema Único de Información Ambiental (SUIA)[31,35]. Los datos del SUIA fueron generados a partir de imágenes landsat 8 con resolución de píxel de 30 x 30 m, corrección atmosférica, clasificación supervisada y post procesamiento de acuerdo con la metodología propuesta por el MAATE, donde se establecen las categorías de las coberturas (Tabla 1)[36].

Nivel I	División para studio	Nivel II
Bosque	Bosque (BO)	Bosque Nativo
		Plantación Forestal
Tierra agropecuaria	Tierra agrícola (TA)	Cultivo anual
		Cultivo semipermanente
		Cultivo Permanente
		Mosaico Agropecuario
	Pastizal (PA)	Pastizal
Vegetación arbustiva y herbáce	Vegetación arbustiva y herbácea (VA)	Vegetación arbustiva
		Vegetación herbácea
		Páramo
Cuerpo de agua	Cuerpo de agua (CA)	Natural
		Artificial
Zonas antrópicas	Zonas antrópicas (ZA)	Área poblada
		Infraestructura
Otras Tierras	Otras tierras (OT)	Área sin cobertura
		Glaciar

Fuente: Ministerio de Ambiente [35].

Tabla 1. Capas de cobertura disponibles en el geo portal del Ministerio de Ambiente

Matriz de tabulación cruzada

A partir de la matriz de tabulación cruzada se estimó la tasa de cambio por año (S), el cambio total (Ct), el cambio neto (Cn), la ganancia (Gj), la pérdida (Li) y la estimación del intercambio (Int) entre coberturas. Al final de la matriz de tabulación cruzada se creó una columna donde se muestra la suma de las superficies de todas las categorías en la fecha 1 (Pi+) y en la parte inferior se crea una fila donde se encuentra la suma total para las categorías de la fecha 2 (P+j) (adaptada de[18,37]).

Fecha1	**Fecha2**				**∑ fecha 1(Pi+)**	**(S)**	**Pérdida (Li)**	**Cambio total (Ct)**	**Cambio neto (Cn)**	**Intercambio (Int)**
	Cat 1(j)	Cat 2	Cat 3	Catj						
Cat 1(i)	Pij	P12	P13	P1j	P1+		P1+-P11	L + G	Ct-Int	2*min(L,G)
Cat 2	P21	P22	P23	P2j	P2+		P2+-P22			
Cat 3	P31	P32	P33	P3	P3+		P3+-P33			
Cati	Pi1	Pi2	Pi3	Pij	Pi+					
∑ fecha 2 (P+j)	P+1	P+2	P+3	P+j						
Ganancia (Gj)	P+1-P11	P+2-P22	P+3-P33							

Nota: Categoría (Cat), Pij (Casilla donde el área se mantiene), fecha 1 (Fecha inicial), fecha 2 (Fecha final).

Tabla 2. Matriz de tabulación cruzada para estimar el cambio de cobertura por año.

Para conocer si la tasa de cambio anual (S)[39] es negativa o positiva se aplicó la ecuación 1. Si es positiva significa que la cobertura tuvo un crecimiento en área para ese período y si es negativa indica que se produce una pérdida de área en ese período.

$$s\ (\%) = \left(\left(\frac{S2}{S1}\right)^{\frac{1}{t2-t1}} - 1\right) * 100 \quad (1)$$

Donde; S1 y S2: superficies de CCUS en la fecha inicial y final; t1 y t2: fecha inicial y final del análisis.

En la ecuación 2, la ganancia (Gj) se calculó con la diferencia entre el área total de la categoría j en la fecha 2 (∑(P+j)) y el área que no tiene cambios en esa fecha (Pjj). Mientras que la ecuación 3, se utilizó para conocer la ganancia en porcentaje (Gj%) que se obtiene a partir de la división de (Gj) para el área total de todas las categorías en la fecha 2 (∑(P+j)).

$$Gj\ = \ (\sum(P + j) - \ (Pjj) \quad (2)$$

$$Gj\% = \left(\frac{Gj}{\sum(P+j)}\right) * 100 \quad (3)$$

Para determinar la pérdida (Li) se aplicó la ecuación 4 y 5, es la diferencia entre el área total de una categoría y la fecha 1 (∑Pi+) y la persistencia, (Pjj). Mientras que la pérdida en porcentaje (Li%) es la relación de la pérdida (Li) con la suma total de la pérdida (∑Pi+) y la para la fecha 2.

$$Li\ = \ (\sum Pi\ +) - \ (Pjj) \quad (4)$$

$$\text{Li}\% = \ (\frac{\text{Li}}{\sum(\text{Pi}+)}) \ * 100 \quad (5)$$

Para calcular el intercambio entre categorías (Int) se utilizó la fórmula 6 y 7, y se realizó dos veces el calculó del valor mínimo de las ganancias y las pérdidas de área en cada cobertura. Esta información ayuda a identificar el proceso de pérdida de una determinada cobertura en un lugar y la ganancia simultánea de otra cobertura.

$$Int\ \ 2\ \ MIN\ ((\sum Pi+) - \ (Pjj), (\sum P\ j) - \ (Pjj)) \quad (6)$$

$$Int\% = \ 2\ \times \ MIN\ (Li\%, Gj\%) \quad (7)$$

Para calcular el cambio total (CT) a nivel de categoría (Ct) se suma el cambio neto (Cn) y el intercambio (Int), o bien, se realiza la suma de las ganancias (Gj) y las pérdidas (Li).

$$Ct = Cn + \ Int \text{ ó } Ct = \ \sum Gl\ + \ \sum Li \quad (8)$$

$$Ct\% = Cn\% + \ Int\% \text{ ó } Ct\% = \ \sum Gl\% \ + \ \sum Li\%) \quad (9)$$

Serie de tiempo de coberturas

La serie de tiempo permitió describir los cambios que ha tenido las coberturas para los años evaluados. Para que las coberturas puedan ser comparables los datos fueron normalizados con (Log10); sin embargo, para visualizar los valores reales de las superficies para los CCUS se observó las etiquetas por año[40].

RESULTADOS

Mapas de Cobertura y Usos de Suelo

En la Figura 2. se puede observar que en La Joya de los Sachas en los años 1990, 2000, 2008 y 2018 se produjo un aumento en la superficie de tierra agrícola (TA), pastizales (PA) zonas antrópicas (ZA) y otras tierras (OT). Además, se puede observar los cuerpos de agua (CA), vegetación arbustiva (VA) y bosque (BO).

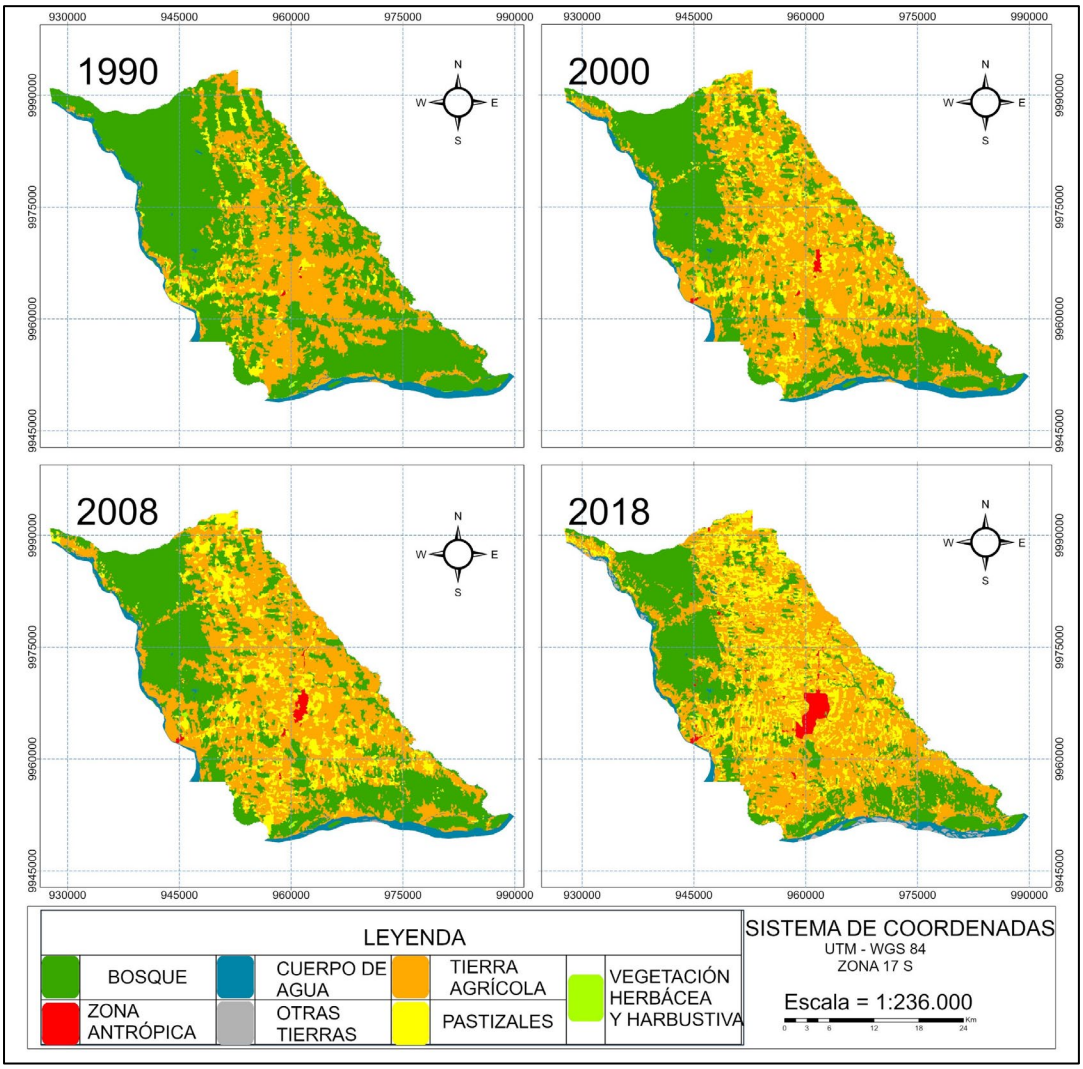

Figura 2. Mapas de cobertura y uso del suelo del Cantón La Joya de los Sachas

Tasas e índices de cambio

Durante el período de estudio de 28 años en La Joya de los Sachas, se observó un crecimiento positivo en la zona antrópica (ZA), con una tasa de cambio del 13% (70,9 ha*año^{-1}). Le siguió el grupo de otras tierras (OT), que abarcó el 11,5% (32,8 ha*año^{-1}) de crecimiento. Dentro de este grupo, se identificó que las categorías de pastizal (PA) y tierra agrícola (TA) presentaron las tasas de crecimiento más bajas, con un 4,9% (598,8 ha*año^{-1}) y 1,4% (629,5 ha*año^{-1}) respectivamente. Además, se encontraron pérdidas de cobertura en ciertas categorías, evidenciadas por tasas negativas. La vegetación arbustiva herbácea (VA) experimentó una tasa de cambio de -3,6% (5,1 ha*año^{-1}), seguida por el bosque (BO) con una tasa de -2,4% (1.300,4 ha*año^{-}

[1]) y los cuerpos de agua (CA) con una tasa de -0,7% (26,4 ha*año^{-1}). Por otro lado, la categoría que más superficie perdió desde 1990 hasta 2018 fue el bosque, con una disminución de 36.413,2 ha (Figura 3).

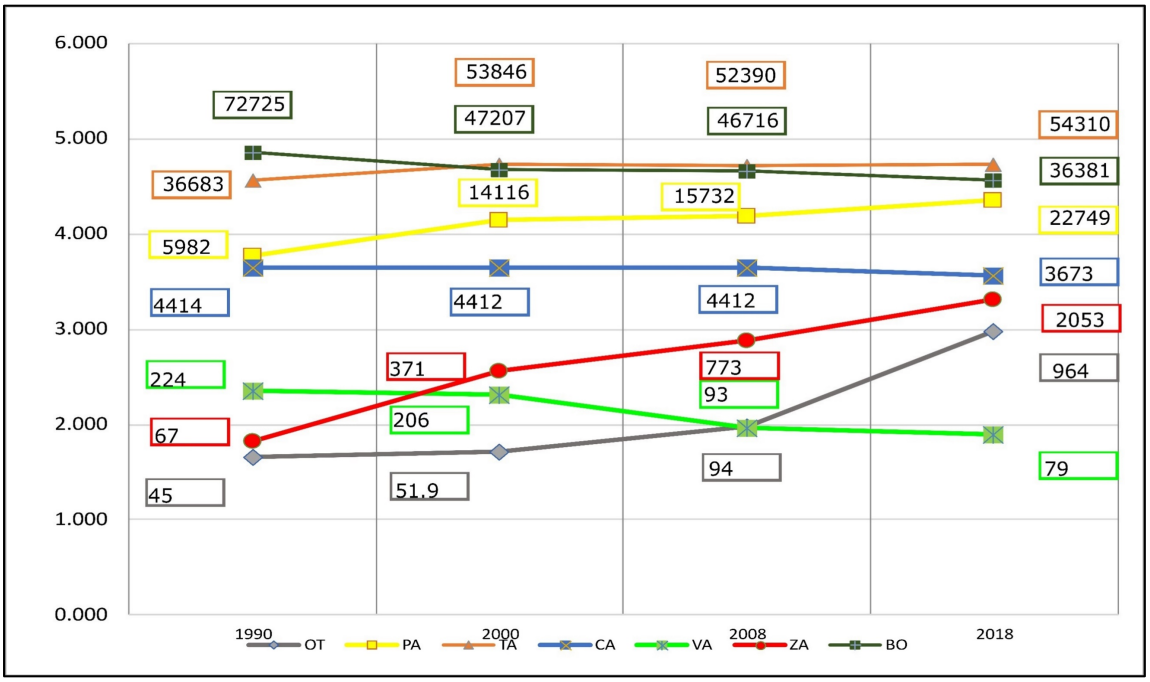

Figura 3. Cambio de las clases de cobertura y uso del suelo (ha) para los años 1990, 2000, 2008 y 2018 en el cantón La Joya de los Sachas.

Durante el primer período de análisis, se observó que la cobertura de bosque (BO) experimentó una pérdida significativa del 37,4% (27.236,8 ha). La mayor parte de esta pérdida se tradujo en la conversión de bosque a tierras agrícolas (TA) con una extensión de 22.632,1 ha, seguido de la transformación en pastizales (PA) con 4.594,1 ha. La cobertura de pastizales (PA) fue la que experimentó cambios más significativos durante este período de evaluación, con un aumento del 139,5%. Por otro lado, la cobertura tierra agrícola (TA) obtuvo la mayor ganancia en área, con un incremento de 26.508,3 ha. En cuanto a la cobertura vegetación arbustiva (VA), se observó un cambio neto del 7,2% y una pérdida del 14,5%. Por otro lado, la cobertura zonas antrópicas (ZA) no experimentaron pérdidas, pero si mostraron ganancias con un incremento de 371,3 ha.

1990	**2000 (ha)**							**∑ 1990 (ha)**	**Li (ha)**	**S**	**Li**	**Gj**	**Ct**	**Cn**	**Int**
	BO	**CA**	**OT**	**PA**	**TA**	**VA**	**ZA**			%					
BO	45558,3	0,0	10,5	4594,2	22632,1*	0,0	0,1	72795,1	27236,8	-4,2	37,4	3,5	40,9	33,9	7,0
CA	0,0	4412,8	0,0	0,0	0,0	0,0	1,7	4414,5	1,7	0,0	0,0	0,0	0,0	0,0	0,0
OT	0,0	0,0	28,6	0,0	15,2	1,8	0,0	45,6	17,0	1,3	37,3	45,0	82,3	7,7	74,6
PA	189,0	0,0	0,0	1809,0	3832,4	4,9	147,0	5982,2	4173,3	9,0	69,8	87,2	156,9	17,4	139,5
TA	1460,1*	0,0	11,7*	7710,2*	27338,1	8,3*	155,0*	36683,4	9345,3	3,9	25,5	49,2	74,7	23,8	51,0
VA	0,0	0,0	1,1	2,8	28,7	191,5	0,0	224,0	32,5	-0,8	14,5	7,2	21,8	7,3	14,5
ZA	0,0	0,0	0,0	0,0	0,0	0,0	67,6	67,6	0,0	18,6	0,0	81,8	100,4	100,4	0,0
∑2000 (ha)	47207,4	4412,8	51,9	14116,1	53846,5	206,4	371,3	**120201,4**							
Gj (ha)	1649,1	0,0	23,4	12307,2	26508,4	14,9	303,8								

Nota: *ganancias notables para las coberturas del 2008, subrayado pérdidas notables para coberturas de 2000, S: tasa de cambio, Li: pérdidas, Gj: ganancias, Ct: cambios totales, Cn: cambios netos, Int: Intercambio.

Tabla 3. Tasa de cambio anual e índices de cambios del período 1 (1990 – 2000).

En el análisis del período 2, se determinó que la cobertura BO tuvo una pérdida de 5.274 ha y la cobertura CA presentó una ganancia del BO de 0,04 ha. La cobertura OT, obtuvo una ganancia de cobertura del 37,9% y la cobertura TA presentó la ganancia más representativa de 44,7 ha, es decir la cobertura disminuyó porque tuvo un cambio neto del 2% y una tasa de cambio anual de -0,3%. La cobertura PA tuvo un cambio total de cobertura en este período del 121%, pero solo el 4,3% corresponde a un cambio neto de cobertura, porque las ganancias 62,6% y pérdidas 58,3% son similares. La cobertura VA presentó una tasa de cambio anual negativa de -9,5% en cambio, la cobertura ZA presentó una ganancia del 52% (Tabla 4).

2000	2008 (ha)							∑ 2000 (ha)	Li (ha)	S	Li	Gj	Ct	Cn	Int
	BO	CA	OT	PA	TA	VA	ZA			%					
BO	41933,1	0,0	1,5	694,1	4569,9	0,0	8,7	47207,4	5274,3	-0,1	11,2	10,2	21,4	0,9	20,5
CA	0,0	4412,8	0,0	0,0	0,0	0,0	0,0	4412,8	0,0	0,0	0,0	0,0	0,0	0,0	0,0
OT	2,6	0,0	44,0	0,0	5,3	0,0	0,0	51,9	7,9	7,7	15,3	53,2	68,5	37,9	30,6
PA	66,0	0,0	0,0	5880,5	7960,8*	0,0	208,8*	14116,1	8235,6	1,4	58,3	62,6	121,0	4,3	116,7
TA	4708,9*	0,0	44,7*	9154,1*	39753,6	0,5*	184,6	53846,5	14092,8	-0,3	26,2	24,1	50,3	2,1	48,2
VA	6,0	0,0	3,8	3,5	100,4	92,8	0,0	206,4	113,6	-9,5	55,1	0,5	55,5	54,6	1,0
ZA	0,0	0,0	0,0	0,0	0,0	0,0	371,3	371,3	0,0	9,6	0,0	52,0	52,0	52,0	0,0
∑ 2008 (ha)	46716,7	4412,8	94,1	15732,2	52390,0	93,2	773,5	**120212,5**							
Gj (ha)	4783,6	0,0	50,1	9851,7	12636,	0,5	402,1								

Nota: *ganancias notables para las coberturas del 2008, subrayado pérdidas notables para coberturas de 2000, S: tasa de cambio, Li: pérdidas, Gj: ganancias, Ct: cambios totales, Cn: cambios netos, Int: Intercambio.

Tabla 4. Tasa de cambio anual e índices de cambios del período 2 (2000-2008).

Durante el período 3, las coberturas que sufrieron mayores pérdidas fueron BO con el 27,2 %, la cobertura CA con 23,7% y la cobertura OT con 26,2%. La cobertura PA tuvo el mayor intercambio 114,8%, está tendencia se observó desde el primer período. La mayor pérdida (8.307,3 ha) y ganancia (14.025,2 ha) la obtuvo la cobertura TA, aunque en el segundo periodo esta cobertura presentó una tasa negativa; sin embargo, en este período se observa una tasa positiva de 0,4%, colocándola como la cobertura, con mayor superficie en el cantón con 54.310 ha. La cobertura VA continúa presentando una tasa de cambio anual negativa -1,6%. Finalmente, el análisis de la cobertura ZA, no muestra pérdidas, pero si presenta 62,3% de ganancia de otras coberturas (Tabla 5).

2008	2018 (ha)							∑ 2008 (ha)	Li (ha)	S	Li	Gj	Ct	Cn	Int
	BO	CA	OT	PA	TA	VA	ZA			%					
BO	33987,0	13,9	13,7	2012,1	10623,7*	1,4	65,0	46716,7	12729,7	-2,5	27,2	6,6	33,8	20,7	13,2
CA	6,2	3368,8	895,9*	12,1	129,4	0,0	0,4	4412,8	1044,0	-1,8	23,7	8,3	32,0	15,4	16,6
OT	0,0	43,9	42,8	0,0	7,3	0,0	0,0	94,1	51,2	26,2	54,5	95,6	150,0	41,1	108,9
PA	196,3	23,2	0,0	6700,3	8307,3	0,0	505,0	15732,2	9031,9	3,8	57,4	70,5	128,0	13,1	114,8
TA	2191,7*	224,0*	12,0	14025,2*	35224,7	2,7*	709,6*	52390,0	17165,3	0,4	32,8	35,1	67,9	2,4	65,5
VA	0,6	0,0	0,0	0,0	17,5	75,2	0,0	93,2	18,1	-1,6	19,4	5,1	24,5	14,3	10,2
ZA	0,0	0,0	0,0	0,0	0,0	0,0	773,5	773,5	0,0	10,3	0,0	62,3	62,3	62,3	0,0
∑ 2018 (ha)	36381,9	3673,9	964,4	22749,8	54310,0	79,2	2053,4	**120212,5**							
Gj (ha)	2394,9	305,1	921,5	16049,4	19085,2	4,1	1280,0								

Nota: *ganancias notables para las coberturas del 2018, subrayado pérdidas notables para coberturas de 2008, S: tasa de cambio, Li: pérdidas, Gj: ganancias, Ct: cambios totales, Cn: cambios netos, Int: Intercambio.

Tabla 5. Tasa de cambio anual e índices de cambios periodo 3 (2008-2018).

DISCUSIÓN

La Ley de Reforma Agraria creada en 1964, promovió el incremento de la productividad agropecuaria y la adjudicación de tierras[41] y, por otra parte, el ingreso de las empresas petroleras en el año 90 en la Amazonía Ecuatoriana[42] provocó una migración masiva de personas de otras regiones del país a esta región, desencadenando cambios profundos en la cobertura y uso de suelo. Una evidencia palpable de estos cambios es el incremento del 160% de la población desde el año 1990 (16.193 habitantes) [43] al año 2001 (26.363 habitantes)[44].

Durante el primer período de evaluación se determinó que las zonas antrópicas que comprende principalmente las vías de transporte e infraestructura muestran una tasa de crecimiento anual del 18,6%, debido al aumento de la población y la necesidad de movilización[45]. La deforestación de la cobertura boscosa fue negativa para este período, presentando la mayor tasa de cambio anual -4,24% que corresponde a una superficie de 22.632 ha y un incrementó en la superficie de tierras agrícolas de 53.846,5 ha. Este comportamiento fue corroborado por Mena [46] y Camacho-López et al.[23] quienes consideran que la cobertura más afectada en este período fue el bosque de la Amazonía ecuatoriana.

Para el periodo 2, se observó tasas de cambio anual menores en todas las coberturas. La cobertura de tierras agrícolas y bosque disminuyó (52.390,0 y 46.716,7 ha, respectivamente) con respecto al período 1 (53.846,48 y 47.207,4 ha, respectivamente). Aunque en este período se produjo esta ligera disminución de las tasas de cambio, la promoción de la ley de Desarrollo Agrario continuó fomentándose en el país[47], esto se evidenció con el III Censo Nacional Agropecuario del año 2002[48], donde se demostró que en el año 2000 el 40% de la población ecuatoriana se dedicaba a la agricultura; sin embargo, con el feriado bancario y la dolarización la mayoría de la población empezó a emigrar a otros países. Una de las consecuencias de la migración fue el abandono de los campos[49]. Otro fenómeno importante en este período es el comportamiento de las zonas antrópicas, debido a que presentaron una tasa positiva de cambio anual 9,61%, este comportamiento posiblemente se debió a la alta inversión de la filial de Petroecuador (Petro producción) en el área de explotación petrolera para mejorar la red vial e infraestructura[45].

Durante el periodo 3, el fenómeno que afecto la agricultura, el Cambio de cobertura y Uso del suelo (CCUS) fue la “Revolución Ciudadana”, que según Freidenberg[50] “La revolución Ciudadana era un proyecto social y político sin precedentes en la historia sociopolítica del Ecuador”. En este proyecto político se incluye en la constitución del Ecuador la creación de la Ley Orgánica del Régimen de Soberanía Alimentaria en la que incluye el Buen vivir y el derecho a la alimentación de los ecuatorianos. Este derecho plasmado en la constitución en este período promovió el cambio de la matriz productiva lo que se vio reflejado en el aumento de la superficie de las tierras cultivadas (54.310,0 ha) y pastizales (22.749,8 ha). Históricamente el cantón La Joya de los Sachas se ha formado por personas dedicadas al área agropecuaria y esto es visible en el cambio del paisaje de la actualidad[15].

CONCLUSIONES

El ritmo acelerado del proceso de deforestación transformó de manera drástica el paisaje del catón La Joya de los Sachas, disminuyendo el área de bosque del 60,6% a 30,2 % en un periodo de 28 años, con un ritmo de pérdida de masa boscosa de 1.300,5 ha*año^{-1}, situación que debería ser analiza por las autoridades locales tomadores de decisiones, debido a que si se continúa con esta tendencia en 30 años aproximadamente el cantón no contará con masa boscosa significativa.

Ante la pérdida de bosque, el crecimiento de la frontera agrícola sigue avanzando al mismo ritmo que el proceso de deforestación; en estos 28 años las actividades agrícolas y la ganadería muestran una ganancia acumulada de 17.626,5 ha y 16.767,6 ha respectivamente. En el año 2018 (período 3) el 45,17 % de la cobertura de uso de suelo se utilizó para la producción agrícola y el 18.97% para la ganadería. Por otra parte, las actividades relacionadas a infraestructura y vialidad tienen 2.053 ha, pero ha venido creciendo desde el primer periodo por el aumento demográfico del cantón y la necesidad de mejorar la red vial por cuestiones logísticas.

El uso de los SIG permitieron determinar, que las políticas públicas tuvieron un impacto directo e indirecto en los CCUS; por esta razón, se debería considerar estos hallazgos como un llamado de atención para utilizar herramientas que permitan tener una visión más holística de las causas y efectos que ocasiona la implementación de políticas públicas sobre la dinámica paisajística y socioeconómica de la localidad, con la finalidad de promover el uso de nuevos modelos de gestión agrícola, como el desarrollo de economías circulares, uso de tecnologías de producción sostenible que ayudarán a minimizar la ampliación de la frontera agrícola logrando así una adecuada planificación y gestión territorial.

Contribuciones de los autores: Conceptualización: FPA y LTJ; metodología: FPA; software: CCY; validación: FPA, YVT y CCY; análisis formal: FPA; investigación: LTJ y FPA; Depuración de datos: CCY; redacción-preparación del borrador original: FPA; revisión y edición, LTJ, CCY y YVT; visualización: YVT; supervisión: LTJ; administración del proyecto: LTJ; adquisición de fondos: FPA. Todos los autores han leído y aceptado la publicación de este manuscrito.

Financiamiento: Este manuscrito no recibió financiamiento externo.

Agradecimientos: Al Instituto Nacional de Investigaciones Agropecuarias (INIAP) y al Fondo de Investigación de la Agrobiodiversidad, Semillas y Agricultura Sustentable (FIASA) por el financiamiento y apoyo en la ejecución de este proyecto de investigación.

Conflictos e intereses: Los autores declaran no tener conflicto de intereses

REFERENCIAS

1. Little MA, Dyson-Hudson N, Dyson-Hudson R, Ellis JE, Swift DM. Human biology and the development of an ecosystem approach. En: The ecosystem concept in anthropology. *Routledge*; 2019. p. 103–31.
2. Romera CJ. La humanidad en su hábitat: técnicas de adaptación y de hegemonía. *Boletín CF+ S*. 2014;(37):11–8.
3. Merino MM. La Revolución Neolítica: ¿por qué adoptar la agricultura y una forma de vida sedentaria [Internet]. April; 2017 [citado el 26 de junio de 2023]. Disponible en: https://www.researchgate.net/publication/327837708_La_Revolucion_Neolitica_por_que_adoptar_la_agricultura_y_una_forma_de_vida_sedentaria
4. Wells JCK, Stock JT. Life History Transitions at the Origins of Agriculture: A Model for Understanding How Niche Construction Impacts Human Growth, Demography and Health. *J Frontiers in Endocrinology*. el 21 de mayo de 2020; 11:1–29.
5. Riechmann J. ¿Somos demasiados? Reflexiones sobre la cuestión demográfica. *Papeles de relaciones eco sociales y cambio global*. 2019;148:13–38.
6. García L. En los albores de la Humanidad: La revolución agrícola y sus consecuencias. Libro de Actas [Internet]. 2019 [citado el 24 de agosto de 2022];86. Disponible en: http://apfa.ugr.es/pages/_documentos/publicaciones/libroactasxxvaniversarioapfa/!#page=104
7. Martinez-Centeno AL, Sobalvarro KKH. La revolución verde. *R Iberoamericana de Bioeconomía y Cambio Climático.* 2018;4(8):1040–52.
8. Reyes-Palomino SE, Cano Ccoa DM, Reyes-Palomino SE, Cano Ccoa DM. Efectos de la agricultura intensiva y el cambio climático sobre la biodiversidad. *J of High Andean Research* [Internet]. el 21 de febrero de 2022 [citado el 24 de agosto de 2022];24(1):53–64. Disponible en: https://huajsapata.unap.edu.pe/index.php/ria/article/view/328
9. Sial A, Shankar T, Praharaj S, Sahoo U, Maitra S. Intensive Farming: It's Effect on the Environment. *Indian Journal of Natural Sciences* [Internet]. diciembre de 2021 [citado el 24 de agosto de 2022];12(69):37480–7. Disponible en: https://www.researchgate.net/publication/357423421_Intensive_Farming_It's_Effect_on_the_Environment
10. Ramankutty N, Evan AT, Monfreda C, Foley JA. Farming the planet: 1. Geographic distribution of global agricultural lands in the year 2000. *R Global Biogeochem Cycles*. 2008;22(1):1–19.
11. Marcillo JLM. Monocultures in the Vinces river basin (Ecuador) and their relationship between the supply of water for irrigation. RIAT: *R Interamericana de Medioambiente y Turismo*. 2021;17(2):113–23.

12. Lasso González G. La disputa de territorios en torno al sistema agroalimentario ecuatoriano. Estrategias de poder y resistencia, procesos de territorialización y desterritorialización [Internet] [Doctoral Thesys]. [Barcelona]: Universitat Autònoma de Barcelona; 2019 [citado el 28 de junio de 2023]. Disponible en: https://www.tdx.cat/bitstream/handle/10803/669517/glg1de1.pdf?sequence=1
13. Instituto Nacional de Estadísticas y Censos [INEC]. Encuesta de Superficie y Producción Agropecuaria Continua 2021 [Internet]. Unidad de Estadísticas Agropecuarias Quito; 2022 [citado el 29 de agosto de 2022]. p. 1–49. Disponible en: https://www.ecuadorencifras.gob.ec/documentos/web-inec/Estadisticas_agropecuarias/espac/espac-2020/Presentacion%20ESPAC%202020.pdf
14. Varangis P, Siegel P, Giovannucci, B y Lewin, B. La crisis cafetalera: Efectos y estrategias para hacerle frente. 2002.*BID*.
15. GAD Cantón la Joya de los Sachas. Plan de Desarrollo y Ordenamiento Territorial 2019 - 2023. 2019;10–543.
16. Fountas S, Wulfsohn D, Blackmore BS, Jacobsen HL, Pedersen SM. A model of decision-making and information flows for information-intensive agriculture. *R Agric Syst*. 2006;87(2):192–210.
17. Baeza S, Paruelo J. Land use/land cover change (2000–2014) in the Rio de la Plata grasslands: an analysis based on MODIS NDVI time series. *J Remote sensing*. 2020;12(3):1–22.
18. Sahagún-Sánchez FJ, Reyes-Hernández H, Sahagún-Sánchez FJ, Reyes-Hernández H. Impactos por cambio de uso de suelo en las áreas naturales protegidas de la región central de la Sierra Madre Oriental, México. CienciaUAT [Internet]. 2018 [citado el 22 de agosto de 2022];12(2):6–21. Disponible en: http://www.scielo.org.mx/scielo.php?script=sci_arttext&pid=S2007-78582018000100006&lng=es&nrm=iso&tlng=es
19. Gutiérrez MF, Rodríguez-Tapia G, Mas JF. Análisis jerárquico de la intensidad de cambio de cobertura/uso de suelo y deforestación (2000-2008) en la Reserva de la Biosfera Sierra de Manantlán, México. Investigaciones Geográficas, *Boletín del Instituto de Geografía*. 2016;2016(90):89–104.
20. García Marín M, La deforestación: una práctica que agota nuestra biodiversidad. *R Producción + Limpia.* 2016; 11(2):161–168
21. Aznar-Sanchez JA, Piquer-Rodriguez M, Velasco-Munoz JF, Manzano-Agugliaro F. Worldwide research trends on sustainable land use in agriculture. *J Land use policy*. 2019;87:1–15.
22. Briceño N, Castillo E, Quintana J, Cruz S, López R. Deforestación en la Amazonía peruana: Índices de cambios de cobertura y uso del suelo basado en SIG. Boletín de la Asociación de Geógrafos Españoles [Internet]. 2019 [citado el 28 de junio de 2023];(81):1–34. Disponible en: https://dialnet.unirioja.es/descarga/articulo/6985821.pdf
23. Camacho-López CO, Jara-Franco NE, González-Rivadeneira JL. Análisis multitemporal de la deforestación y cambio de la cobertura del suelo en Morona Santiago. *J Polo del Conocimiento*. 2022;7(1):797–807.
24. Comisión Nacional para el Conocimiento y Uso de la Biodiversidad [CONABIO]. Monitoreo de la cobertura de suelo. 2020 [citado el 23 de agosto de 2022]; Disponible en: https://www.biodiversidad.gob.mx/monitoreo/cobertura-suelo
25. Gallardo M, Martínez-Vega J. Cambios de usos del suelo en la Comunidad de Madrid: analizando el pasado y simulando el futuro. Congreso Tecnologías de la información geográfica en el contexto de Cambio Global. 2012;305–14.
26. Gutiérrez R, Romero E, Cunuhay P, Blanco G, Fonseca C. Análisis comparativo de las propiedades físico-mecánicas de la madera de Fernán Sánchez (triplaris cumingiana Fish. Mey.) de Quevedo y Balzar. *R Ciencia y Tecnología*. 2008;1(2):79–85.
27. Reyes Hernández H, Aguilar Robledo M, Aguirre Rivera JR, Trejo Vázquez I. Cambios en la cubierta vegetal y uso del suelo en el área del proyecto Pujal-Coy, San Luis Potosí, México, 1973-2000. *R Investigaciones geográficas*. 2006;(59):26–42.
28. Ati-Cutiupala GM, Muñoz-Jácome EA, Vistín-Guamantaqui DA, Cushquicullma-Colcha DF. Análisis de las actividades económicas de tres comunidades altoandinas y su relación con el cambio de uso de suelo y cobertura vegetal en la Reserva de Producción de Fauna Chimborazo. *R Polo del Conocimiento*. 2021;6(8):552–76.
29. Flores-Vaca A. Análisis multitemporal de cambio de uso del suelo y cobertura vegetal e influencia del programa Socio Bosque, en la Parroquia NONO, periodo 1990-2016 [Internet] [Tesis de pregrado]. [Quito]: PUCE; 2018 [citado el 29 de agosto de 2022]. Disponible en: http://repositorio.puce.edu.ec/handle/22000/15890

30. 28. Lasso G. Territorios en disputa: un análisis de la Soberanía alimentaria en el Ecuador. Vol. 40, El futuro de la alimentación y retos de la agricultura para el siglo XXI. Barcelona; 2017. p. 1–365.
31. Ministerio de Ambiente A y transición ecológica [MAATE]. Serie cartográfica de Cobertura y Uso de la Tierra (1990, 2000, 2008, 2014, 2016, 2018) [Internet]. 2020 [citado el 25 de agosto de 2022]. Disponible en: http://ide.ambiente.gob.ec/mapainteractivo/
32. Ministerio de Agricultura y Pesca [MAGAP]. Geoportal del Agro - Ecuatoriano. 2023 [citado el 16 de abril de 2023]; Disponible en: http://geoportal.agricultura.gob.ec/index.php/mapas-interactivos/2-uncategorised/37-mapa-cultivos
33. Pontius Jr RG, Shusas E, McEachern M. Detecting important categorical land changes while accounting for persistence. *R Agric Ecosyst Environ*. 2004;101(2–3):251–68.
34. Instituto Geográfico Militar. Descargas IGM[Internet]. 2012 [citado el 15 de mayo de 2022]. Disponible en: https://www.geoportaligm.gob.ec/downloads/public/login
35. Ministerio De Ambiente Agua y Transición Ecológica [MAATE]. Mapa Interactivo [Internet]. 2018 [citado el 21 de junio de 2021]. Disponible en: http://ide.ambiente.gob.ec/mapainteractivo/
36. Ministerio de Ambiente [MAE] y, Ministerio de Agricultura y Pesca [MAGAP]. Protocolo metodológico para la elaboración del mapa de cobertura y uso de la tierra del ecuador continental 2013 - 2014. Protocolo metodológico para la elaboración del mapa de cobertura y uso de la tierra del ecuador continental 2013 - 2014. 2015;1–49.
37. Bocco G, Mendoza M, Masera O. La dinámica del cambio del uso del suelo en Michoacán: Una propuesta metodológica para el estudio de los procesos de deforestación. *R Investigaciones geográficas*. 2001;(44):18–36.
38. Escobar D, Gutiérrez E, Montalvo F. Actividad del volcán Chaparrastique durante los años 2013 y 2014 Ministerio de Medio Ambiente y Recursos Naturales [MARN] Abril, 2016. 2016;1–39.
39. Food and Agriculture Organization [FAO]. Forest resources assessment 1990: survey of tropical forest cover and study of change processes. Food & Agriculture Org.; 1996. 1–152 p.
40. James G, Witten D, Hastie T, Tibshirani R. An introduction to statistical learning. Vol. 112. *R Springer*; 2013.
41. Madrid T. La política agraria en Ecuador 1965-2015. Propuestas para el Desarrollo. 2018;(II):47–8.
42. Jarrín Valladares PS, Tapia Carrillo L, Zamora G. La colonia interna vigente: transformación del territorio humano en la región amazónica del Ecuador. *Letras Verdes Revista Latinoamericana de Estudios Socioambientales*. el 17 de octubre de 2016;(20):22.
43. Instituto Nacional de Estadística y Censos [INEC]. VI Censo de población y V de vivienda, Resumen Nacional. Quito. 1991 [citado el 26 de junio de 2023]; Disponible en: https://www.ecuadorencifras.gob.ec/documentos/web-inec/Bibliotecas/Libros/Libros_Censos/19.%20V_Censo_de_Pobl_y_IV_de_Viv_1990_Resumen_Nac.pdf
44. Instituto Nacional de Estadística y Censos [INEC] y Fondo de Población de las Naciones Unida [UNFPA]s. Cantón Joya de los Sachas. Quito. 2002 [citado el 26 de junio de 2023]; Disponible en: https://www.ecuadorencifras.gob.ec/documentos/web-inec/Bibliotecas/Fasciculos_Censales/Fasc_Cantonales/Orellana/Fasciculo_La_Joya_de_los_Sachas.pdf
45. Petroecuador EP. El petróleo ecuador en el Ecuador: la nueva era petrolera. Quito: Alpallana; 2013.
46. Mena CF. Deforestación en el Norte de la Amazonía Ecuatoriana: Del patrón al proceso. *R Polémika*. 2010;2(5):58–65.
47. Peralta S, Aguilar H, Loayza A, Morejón L. Aporte del sector agropecuario a la economía del Ecuador. Análisis crítico de su evolución en el período de dolarización. Años 2000–2016. *R Espacios*. 2018;39(32):7.
48. Servicio de Información y Censo Agropecuario [SICA], Instituto Nacional de Estadísticas y Censos [INEC], Ministerio de Agricultura [MAG]. III Censo Nacional Agropecuario Ecuador: Resultados Nacionales y Provinciales. Volumen; 2002. p. 1–63.
49. Martín-Mayoral F. Estado y mercado en la historia de Ecuador: Desde los años 50 hasta el gobierno de Rafael Correa. *R Nueva Sociedad*. 2009;221:120.
50. Freidenberg F. Ecuador 2011: revolución ciudadana, estabilidad presidencial y personalismo político. *R de ciencia política* (Santiago). 2012;32(1):129–50.

Citación: Paredes-Arcos F, Tinoco-Jaramillo L, Congo-Yépez C, Vargas-Tierras Y. Análisis multitemporal de la deforestación y cambio de la cobertura del suelo, en el cantón La Joya de los Sachas, período 1990-2018.

Received: October 9th 2023/ **Accepte**d: January 15th 2024 / **Published:**15 February 2024

Citation: Paredes-Arcos F, Tinoco-Jaramillo L, Congo-Yépez C, Vargas-Tierras Y. Análisis multitemporal de deforestación y cambio de la cobertura del suelo, en el cantón La Joya de los Sachas, período 1990-2018. Revis Bionatura 2024; 9 (1) 18. http://dx.doi.org/10.21931/RB/2024.09.01.18

Additional information Correspondence should be addressed to leider.tinoco@iniap.gob.ec

Peer review information. Bionatura thanks anonymous reviewer(s) for their contribution to the peer review of this work using https://reviewerlocator.webofscience.com/

Bionatura ISSN. First 13909355 Ecuador. **Scopus coverage years**: from 2016 to the present

Bionatura
Ibero-American Journal of Biotechnology and Life Sciences

Article

Determination of the effectiveness of the electrocoagulation process in the treatment of leachate from the controlled landfill site in Francisco de Orellana canton

Cristian Cumbicus[1], Mayra Hurtado[1], Julio Coello[1], Pedro Peñafiel-Arcos[2], Jennifer Alexandra Orejuela-Romero[3], Marcos Barahona[2]

[1] *Independent researcher in environmental sciences, Ecuador*
[2] *Escuela Superior Politécnica de Chimborazo (ESPOCH), Sede Orellana, Coca 220150, Ecuador; pedro.penafiela@espoch.edu.ec.*
[3] *Grupo YASUNI-SDC, Escuela Superior Politécnica de Chimborazo (ESPOCH), Sede Orellana, Coca 220150, Ecuador; alexandra.orejuela@espoch.edu.ec.*
* *Correspondence: pedro.penafiela@espoch.edu.ec; Tel.: +593 995902280*
Available from. http://dx.doi.org/10.21931/RB/2024.09.01.19

ABSTRACT

The inadequate management of leachate produced in landfill sites, sanitary dumps, or its incomplete treatment generates significant environmental and public health impacts. These conditions are expected in developing countries and are a major concern, especially in sensitive areas like the Amazon. This study investigated the efficiency of electrocoagulation for removing BOD_5, COD, TSS, turbidity, and color using a laboratory-scale reactor. Samples of raw leachate from the controlled landfill site in Francisco de Orellana canton, located in the Ecuadorian Amazon, were used. First, the initial conditions of the leachate were determined through a physicochemical characterization, where a reduced presence of heavy metals and high biodegradability were identified, suggesting that it is old leachate. In turn, a reactor with 5 electrodes was installed, where aluminum was used as a cathode and iron as an anode. Finally, electrocoagulation was employed with various operational combinations, where a run using 2.5 V and 20 minutes showed the highest removal efficiency on average, with reductions of 85.23% of BOD_5, 98.20% of COD, 11.30% of TSS, 96.52% of turbidity, and 90.73% of color.

Keywords: Electrocoagulation; Leachate; Leachate treatment.

INTRODUCTION

The Amazon region, known for its exceptional biodiversity – and for being one of the wealthiest areas in the world in terms of natural resources – faces increasingly pressing challenges in terms of proper solid waste management [1–3]. As part of managing these wastes, fluids that seep through the waste are generated, leading to leachate formation. The production of leachate depends on many factors, such as the waste's degree of compaction and the organic matter's initial moisture content, the latter being the main factor contributing to an accelerated generation of leachate [4]. Other factors include the cell coating material, precipitation, atmospheric moisture, temperature, evapotranspiration, the field capacity of the landfill, and runoff [5].

Inadequate management of these fluids poses severe environmental problems for remediation due to the high content of organic matter (e.g., carboxylic acids and dissolved solids), toxic chemicals, inorganic salts, heavy metals, ammonia, minerals, and xenobiotic organic compounds [6]. In addition, inadequate leachate treatment poses a real threat to local ecosystems, public health, and the preservation of the natural environment [7,8].

Leachate from landfills is grouped into three categories according to its age: young (less than 5 years), intermediate (between 5 and 10 years), and old (more than 10 years), based on how long it has been in the landfill site [9,10]. Young leachate from landfills tends to have a BOD/COD ratio greater than 0.5, while old leachate tends to be less than 0.1 [11]. Because young leachate is highly biodegradable, conventional biological treatment (aerobic, anoxic, or anaerobic) is applied [12]. However, intermediate and older leachate requires chemical treatment due to the significant presence of recalcitrant substances [13]. The BOD/COD ratio decreases significantly with time, making applying biological treatments to older leachate more complicated. In this scenario, the challenge arises of developing adequate treatment processes for leachate due to variations in their composition and concentration [14].

To date, various techniques have been employed for leachate treatment; however, electrocoagulation has emerged as a promising alternative [15–17], which deserves further analysis in the context of the Ecuadorian Amazon. Electrocoagulation stands out for its ability to remove contaminants, such as heavy metals, organic matter, and other dissolved compounds, through coagulation, flocculation, and precipitation [18–20].

In the local context, there has been a controlled landfill site in operation in Francisco de Orellana canton since 1998, which is why old leachate mainly exists there. In the locality, the leachate is collected and stored in a tank and then transported by suction to a system of several pools, where it is first treated with aluminum sulfate. It subsequently undergoes a phytoremediation process and an oxidation process before being released into the environment.

The main objective of this article was to evaluate and determine the effectiveness of the electrocoagulation process as a viable and sustainable option for treating leachate from this canton's controlled landfill site. An experimental study was carried out to achieve this objective, in which several operational variables of the electrocoagulation process were analyzed. Moreover, the elimination efficiency of specific pollutants in the leachate was measured and quantified by considering both the removal of organic load and the reduced toxicity in the treated effluents.

This research seeks to contribute significantly to scientific knowledge in leachate treatment in the Amazon region, providing relevant information for decision-making in public policies and environmental management strategies. Likewise, the results obtained are expected to encourage the adoption of more responsible and environmentally friendly practices in solid waste management, thus contributing to the conservation and preservation of the Amazon region's invaluable biodiversity.

MATERIALS AND METHODS

Collection of leachate samples

The leachate samples were taken from the storage pool of the controlled landfill in Francisco de Orellana canton, located in the Ecuadorian Amazon. This leachate received no prior treatment apart from the partial sedimentation generated in the pool.

The collected samples were stored in a cooler with a refrigerant to preserve their original characteristics. They were transported to the AqLab and GADPO laboratories in the city of Coca for analysis. In addition, the containers were protected from direct light in a cool environment and sealed to prevent contamination during transport [21].

Analysis and characterization of the leachate

The leachate was characterized by analyzing physical and chemical parameters presented in Tables 1 and 2.

Parameter	Unit	Method	Instrument
Temperature	C	IN SITU	Multi-thermometer
Turbidity	NTU	SM 2130 B, 23rd Ed.	Turbidity meter
Hydrogen potential	~	SM 4500-H + B, 23rd Ed./PT-01	Electrometer
Total solids	mg/L	SM 2540 D, 23rd Ed.	Gravimeter

Table 1. Characterization of physical parameters

Parameter	Unit	Method	Instrument(s)
Zinc	mg/L	SM 3030 B, SM 3111 B, 23rd Ed./PT-05	Atomic absorption spectrophotometry
Cadmium	mg/L	SM 3030 B, SM 3111B, 23rd Ed./PT-05.	Atomic absorption spectrophotometry
Copper	mg/L	SM 3030 B, SM 3111 B, 23rd Ed./PT-0	Atomic absorption spectrophotometry
Chromium	mg/L	SM 3030 B, SM 3111 B, 23rd Ed./PT-05	Atomic absorption spectrophotometry
Lead	mg/L	SM 3030 B, SM 3111 B, 23rd Ed./PT-05	Atomic absorption spectrophotometry
Chemical oxygen demand	mg/L	SM 3030 B, SM 3111 B, 23rd Ed./PT-05	Spectrophotometry

Chemical oxygen demand	mg/L	SM 5210 D / 08	Oxygen meter and incubator
Actual color	U Pt-Co	SM 2120 C / 23	Photometer

Table 2. Characterization of chemical parameters

Process of design and construction of a laboratory-scale reactor for the electrocoagulation process

Both [22] and [23] indicated in their studies that acrylic glass is an effective electrical insulator in the application of electrocoagulation processes; it is also necessary to consider that this material is low-cost and is available in the market. For this reason, the prototype for the electrocoagulation process with an acrylic glass reactor was designed and constructed.

To determine the volume of the reactor, as recommended by [24], the following Equation 1 was used:

$$V_{reactor} = x * y * z * (0.001\ L/cm^3)$$ **(Equation 1)**

Where:

$V_{reactor}$: reactor volume (L)

x = reactor height (cm)

y = reactor length (cm)

z = reactor width (cm)

To determine the number of electrodes, we took what was stated by [23] as a reference. They used a reactor length of 28 cm and a separation distance of 4 cm between the plates, using Equation 2:

$$\text{Number of electrodes} = \frac{(\text{cell length}) - 2 * (\text{distance between electrodes and side face})}{(\text{maximum electrode distance} + \text{plate thickness})}$$ **(Equation 2)**

Determination of the optimal conditions for the electrocoagulation treatment of leachate

Voltage, time, and amperage were considered to determine the optimum conditions for the electrocoagulation treatment. The operating variables obtained for the electrocoagulation reactor were voltages of 2.5V and 3.0V, with a current intensity of 5 amperes and a reaction time of 15 and 20 minutes. These variables are comparable to the study by Yagual and Revelo [24], who analyzed types of water from leachate using the same variables.

Time (min)	Voltage (V)	Amperage (A)
15	2.5	5
	3	
20	2.5	
	3	

Table 3. Operational variables of the leachate electrocoagulation process

Efficiency of the electrocoagulation process

To determine the efficiency of the electrocoagulation process, the values obtained for the parameters at the beginning of the characterization and after the application of the electrocoagulation process were compared by applying Equation 3:

$$n = \frac{C_i - C_f}{C_i} * 100 \quad \textbf{(Equation 3)}$$

where:

n: Removal percentage of the parameter analyzed (%)

C_i: Initial concentration of the parameter (mg/L)

C_f: Final concentration of the parameter (mg/L)

RESULTS

Characterization of leachate from the controlled landfill site in Francisco de Orellana canton

Table 4 shows the results characterizing the raw leachate from the landfill above the site.

Parameter	Expressed as	Unit	Maximum permissible limit	Initial conditions
Cadmium	Cd	mg/L	0.02	< 0.03
Zinc	Zn	mg/L	5.0	< 0.10
Copper	Cu	mg/L	1.0	< 0.30
Actual color	Actual color	Units of color	Inappreciable in dilution: 1/20	133
Hexavalent chromium	Cr+6	mg/L	0.5	< 0.30
Chemical oxygen demand	BOD_5	mg/L	100	5,700
Chemical oxygen demand	COD	mg/L	200	113,715.45
Lead	Pb	mg/L	0.2	< 0.30
Hydrogen potential	pH		6–9	6.73
Total suspended solids	TSS	mg/L	130	295.00
Temperature	°C	°C	Natural condition +-3	28
Turbidity	Turbidity	NTU		7,372.804

Table 4. Leachate Characterization Results

The results show a high concentration of biochemical oxygen demand, chemical oxygen demand, total suspended solids, turbidity, and actual color. All listed parameters are outside the maximum permissible limits established in current regulations. These values are attributed to the high presence of decomposing, including organic matter, detergent dregs, and other liquids, which mix to form leachate (Torres-Lozada et al., 2014). On the other hand, the presence of heavy metals is deficient.

Design and construction of the prototype for the electrocoagulation process

Reactor dimensions and volume

The acrylic glass reactor was constructed with the following dimensions: 21cm wide, 28cm long, 11cm tall, and a thickness of 2mm, as shown in Figure 1. These measurements were taken from the research by Reyes and Bermeo [23].

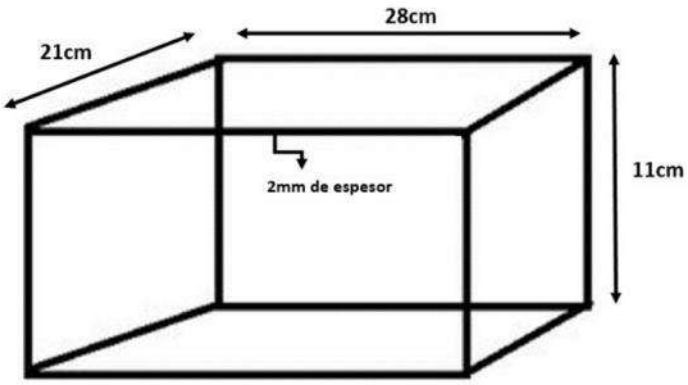

Figure 1. Reactor dimensions

Furthermore, considering the dimensions above, the reactor's volume was 6.5 liters.

Number of electrodes

Similarly, the number of electrodes calculated was 5, where 3 serve as cathodes (aluminum) and 2 as anodes (iron), as shown in Figure 2.

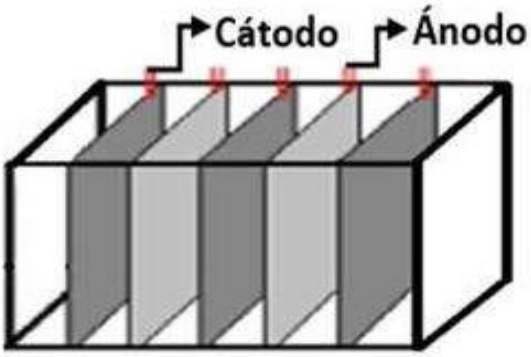

Figure 2. Number of electrodes

Finally, the laboratory-scale reactor was installed in the primary and specialized science laboratory of the Escuela Superior Politécnica de Chimborazo (ESOCH), Orellana campus, as shown in Figure 3.

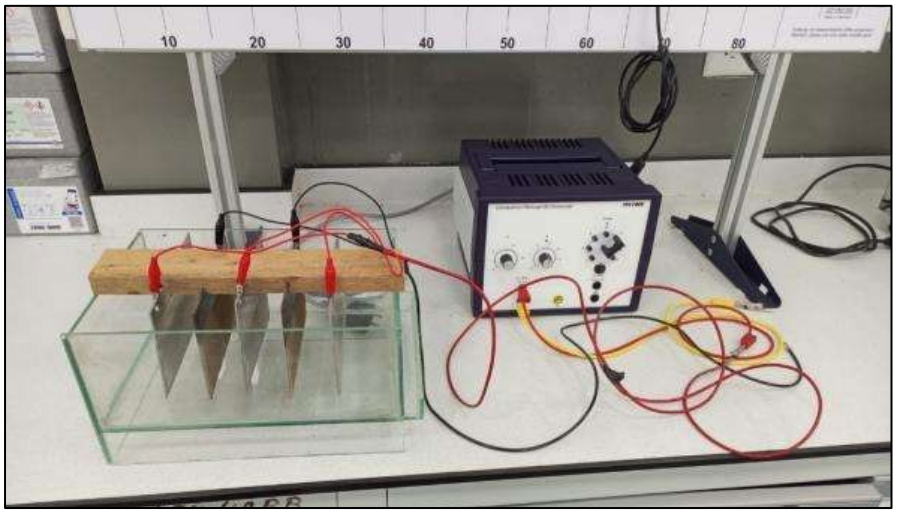

Figure 4. Final reactor prototype.

The installation had a power source of 5 amperes and 15 volts, 5 plates or electrodes (3 aluminum and 2 iron), an acrylic glass reactor, and a black wire for the positive charge and red wire for the negative charge, designed to achieve a better conductivity of electricity.

Effectiveness of the electrocoagulation process

Below is the behavior of the parameters examined in the electrocoagulation process by considering the times and voltages used in the experimental tests.

PARAMETER	UNIT	MAXIMUM PERMISSIBLE LIMIT	INITIAL CONDITIONS	TIME (MIN) 15 MIN						TIME (MIN) 20 MIN					
				Voltage: 2.5			Voltage: 3.0			Voltage 2.5			Voltage 3.0		
				Test 1	Test 2	Test 3	Test 1	Test 2	Test 3	Test 1	Test 2	Test 3	Test 1	Test 2	Test 3
BOD	mg/L	100	5,700	1,175	925	1,250	1,075	1,225	1,050	950	750	825	1,025	1,000	975
COD	mg/L	200	113,715.45	2,752.6	2,839.51	2,887.61	3,061.43	2,697.75	2,381.33	2,280.92	1,814.3	2,056.43	2,532.37	2,620.12	2,564.43
TSS	mg/L	130	295.00	150	265	260	200	250	240	285	280	220	245	115	295
Turbidity	NTU	NR	7,372.804	377.14	396.54	289.0	218.8	258.13	226.39	233.2	288.73	248.62	136.58	97.91	100.2
pH		6–9	6.73	6.95	6.93	6.93	6	7.07	6.94	7	6.78	7.1	6.97	6.94	7
Actual color	Color units	Inappreciable in dilution: 1/20	133	10	10	10	10	10	10	17	10	10	10	10	10

Table 5. Detailed results after electrocoagulation

PARAMETER	UNIT	MAXIMUM PERMISSIBLE LIMIT	INITIAL CONDITIONS	AVERAGES			
				TIME: 15 MIN		TIME: 20 MIN	
				VOLTAGE: 2.5 V	VOLTAGE: 3.0 V	VOLTAGE: 2.5 V	VOLTAGE: 3.0 V
BOD	mg/L	100	5,700	1116.67	1116.67	841.67	1000.00
COD	mg/L	200	113,715.45	2826.57	2713.50	2050.55	2572.31
TSS	mg/L	130	295.00	225.00	230.00	261.67	218.33
Turbidity	NTU	NR	7,372.804	354.23	234.46	256.85	111.57
pH		6–9	6.73	6.94	6.67	6.96	6.97
Actual color	Units of color	Inappreciable in dilution: 1/20	133	10.00	10.00	12.33	10.00

Table 6 shows the average performance of the elimination process for each parameter.

Efficiency of the electrocoagulation process for the treatment of leachate

The efficiency of the electrocoagulation process developed at a laboratory scale is shown in Table 7.

PARAMETER	UNIT	MAXIMUM PERMISSIBLE LIMIT	INITIAL CONDITIONS	REMOVAL EFFICIENCY			
				TIME: 15 MIN		TIME: 20 MIN	
				VOLTAGE: 2.5	VOLTAGE: 3.0	VOLTAGE: 2.5	VOLTAGE: 3.0
BOD	mg/L	100	5,700	80.41%	80.41%	85.23%	82.46%
COD	mg/L	200	113,715.45	97.51%	97.61%	98.20%	97.74%
TSS	mg/L	130	295.00	23.73%	22.03%	11.30%	25.99%
Turbidity	NTU	NR	7,372.804	95.20%	96.82%	96.52%	98.49%
pH		6 – 9	6.73	0.62%	4.44%	0.29%	0.14%
Actual color	Color units	Inappreciable in dilution: 1/20	133	92.50%	92.48%	90.73%	92.48%

Table 7. Removal efficiency of the electrocoagulation process

DISCUSSION

During the initial diagnosis of the contaminant load of the leachate analyzed, it was determined that the concentrations of heavy metals were low, falling below the maximum permissible limits established by Ecuadorian regulations. Heavy metal concentration levels are influenced by the composition of the buried waste and by the age of the leachate [28–30], the latter being the primary condition in this study.

The results obtained for BOD_5 and COD show a non-biodegradable fluid since the BOD_5/COD biodegradability index is less than 0.3. This suggests that it is an old leachate [31,32], as aforementioned. Similarly, TSS and turbidity show high values – 295 mg/L and 7,372.8 NTU, respectively – which agrees with other studies in the country [33].

Regarding treatment efficiency, high reductions of both BOD and COD were obtained, reaching removal percentages of 85.23% and 98.20%, respectively. This high efficiency has also been found in several other laboratory-scale studies [9,20].

Currently, electrocoagulation is combined with various advanced oxidation processes such as peroxide-coagulation [34], sulfate radical-based advanced oxidation process (SR-AOP) and electro-Fenton (EF) [35], and electrooxidation (EO) and peroxymonosulfate (PMS)/UV/CuFe2O4 [20]. Equally, the change in polarity from anode to cathode presents significant results [36]. This presents a valuable opportunity for further research into the most efficient option for each operating condition.

The operating variables obtained for the electrocoagulation reactor with voltages of 2.5V and 3.0V, a current intensity of 5 amperes, and a reaction time of 20 minutes are in line with previous studies, such as the analysis of water types from leachate by Yagual and Revelo [24], where high removal efficiencies were also obtained.

CONCLUSIONS

The physicochemical properties of the leachate from the controlled landfill site in Francisco de Orellana canton showed concentrations of color of 133 Pt/Co, biological oxygen demand of 5,700 mg/L, chemical oxygen demand of 113,715.45 mg/L, total suspended solids of 295 mg/L, and turbidity of 7,372.804. These are outside the maximum permissible limits set down by current TULSMA (Ecuadorian Environment Ministry's Unified Text of Secondary Legislation or Texto Unificado de Legislación Secundaria del Ministerio del Ambiente) regulations in Book VI, Table 9. Heavy metals were found within the maximum permissible limits due to the nature of the waste in the study area and the age of the leachate.

For the design and construction of the prototype, calculations were made to establish reactor dimensions, reactor volume, number of electrodes, and electrode dimensions for the electrocoagulation process of the leachate. The optimum conditions in the electrocoagulation treatment for leachate were a voltage of 2.5 and 3.0 V and a time of 20 minutes for the reduction of 5 parameters: biochemical oxygen demand, chemical oxygen demand, total suspended solids, turbidity, and actual color.

The efficiency of the applied method is evidenced in the percentages of pollutant removal obtained. Specifically, with a voltage of 2.5 V and a time of 20 minutes, these were 85.23% for biochemical oxygen demand and 98.20% for chemical oxygen demand. Meanwhile, a higher voltage (3.0 V) and the same period resulted in removals of 98.49% for turbidity, 92.48% for actual color, 25.99% for total suspended solids, and 13.21% for temperature.

REFERENCES

1. de Oliveira, B. O. S., de Medeiros, G. A., Mancini, S. D., Paes, M. X. & Gianelli, B. F. Eco-efficiency transition applied to municipal solid waste management in the Amazon. *J. Clean. Prod.* **373**, 133807 (2022).
2. Bernardes, C. & Günther, W. M. R. Generation of domestic solid waste in rural areas: case study of remote communities in the Brazilian Amazon. *Hum. Ecol.* **42**, 617–623 (2014).
3. Diéguez-Santana, K., Sarduy-Pereira, L. B. & De Decker, M. Characterization and Quantification of Municipal Solid Waste in Fátima, Ecuadorian Amazon Parish. *J. Environ. Treat. Tech.* **9**, 392–401 (2021).
4. Caiza, D., Chimbo, A., Sarduy Pereira, L. B., Pisco, W. & Diéguez Santana, K. Propuesta de producción más limpia en el proceso de elaboración de abonos orgánicos con desechos del camal, realizado en el relleno sanitario del cantón Baños de Agua Santa, provincia de Tungurahua. (2018).
5. Brennan, R. B. *et al.* Management of landfill leachate: The legacy of European Union Directives. *Waste Manag.* **55**, 355–363 (2016).
6. Nanda, S. & Berruti, F. Municipal solid waste management and landfilling technologies: a review. *Environ. Chem. Lett.* **19**, 1433–1456 (2021).
7. Flores, C. A. R., da Cunha, A. C. & Cunha, H. F. A. Solid waste generation indicators, per capita, in Amazonian countries. *Environ. Sci. Pollut. Res.* **29**, 33138–33151 (2022).
8. Arenhardt, V., Pedro Filho, F. de S., Schalch, V., Manthey Benevides, S. L. & de Souza, S. B. Waste Management In The Amazon And The Conceptual Innovation Of Sustainability. *J. Solid Waste Technol. Manag.* **45**, 329–339 (2019).
9. Nidheesh, P. V, Murshid, A. & Chanikya, P. Combination of electrochemically activated persulfate process and electrocoagulation for the treatment of municipal landfill leachate with low biodegradability. *Chemosphere* **338**, 139449 (2023).
10. Kow, S., Fahmi, M. R., Abidin, C. Z. A. & Soon-An, O. Advanced oxidation processes: process mechanisms, affecting parameters and landfill leachate treatment. *Water Environ. Res.* **88**, 2047–2058 (2016).
11. Wu, R., Li, Y.-Y. & Liu, J. Refractory dissolved organic matter as carbon source for advanced nitrogen removal from mature landfill leachate: A review and prospective application. *J. Clean. Prod.* 134962 (2022).
12. Tałałaj, I. A., Biedka, P. & Bartkowska, I. Treatment of landfill leachate with biological pretreatments and reverse osmosis. *Environ. Chem. Lett.* **17**, 1177–1193 (2019).
13. Da Costa, F. M., Daflon, S. D. A., Bila, D. M., da Fonseca, F. V. & Campos, J. C. Evaluation of the biodegradability and toxicity of landfill leachate after pretreatment using advanced oxidative processes. *Waste Manag.* **76**, 606–613 (2018).
14. Brennan, R. B., Clifford, E., Devroedt, C., Morrison, L. & Healy, M. G. Treatment of landfill leachate in municipal wastewater treatment plants and impacts on effluent ammonium concentrations. *J. Environ. Manage.* **188**, 64–72 (2017).
15. Othmani, A. *et al.* A comprehensive review on green perspectives of electrocoagulation integrated with advanced processes for effective pollutants removal from water environment. *Environ. Res.* 114294 (2022).
16. Amusa, A. A., Taib, M. R. & Xian, W. Z. Continuous Flow Electrochemical Process for Sanitary Landfill Leachate Treatment: Role of Inlet Flow Rate and Current Density. *Water, Air, Soil Pollut.* **234**, 488 (2023).

17. Gautam, P., Kumar, S. & Lokhandwala, S. Advanced oxidation processes for treatment of leachate from hazardous waste landfill: A critical review. *J. Clean. Prod.* **237**, 117639 (2019).
18. Guo, Z. *et al.* Electrochemical methods for landfill leachate treatment: A review on electrocoagulation and electrooxidation. *Sci. Total Environ.* **806**, 150529 (2022).
19. Núñez, J. *et al.* Operational variable effect on the COD removal efficiency using electrocoagulation in landfill leachate treatment. *Environ. Sci. Water Res. Technol.* **9**, 781–793 (2023).
20. Ghanbari, F., Wu, J., Khatebasreh, M., Ding, D. & Lin, K.-Y. A. Efficient treatment for landfill leachate through sequential electrocoagulation, electrooxidation and PMS/UV/CuFe2O4 process. *Sep. Purif. Technol.* **242**, 116828 (2020).
21. Norma Técnica Ecuatoriana NTE INEN 2687. Mercados saludables. Requisitos. *Serv. ecuatoriano Norm.* **1**, 21 (2013).
22. Reyes Ávila, D. & Mercado Martínez, I. D. Estudio de tratabilidad por electrocoagulación de los lixiviados del relleno sanitario La Esmeralda. *Ing. Química* (2003).
23. Callejas Herández, J., Prieto García, F., Reyes Cruz, V., Marmolejo Santillán, Y. & Bustos, B. Optimización del proceso de electrocoagulación de un lactosuero ácido con recuperación de fósforo. *VI Encuentro Investig. del Área Académica Ciencias la Tierra y Mater.* 77–92 (2013).
24. Revelo Anaguano, D. A. Diseño de un sistema de electrocoagulación para tratar aguas residuales de una industria de insumos médicos. at (2021).
25. Torres-Lozada, P., Barba-Ho, L. E., Ojeda, C. & Martínez, J. Influencia de la edad de lixiviados sobre su composición físico-química y su potencial de toxicidad. *Rev. UDCA Actual. Divulg. Científica* **17**, 245–255 (2014).
26. Guanoluisa Acero, L. J. Diseño de un sistema de tratamiento de lixiviados del relleno sanitario El Inga mediante electrocoagulación y fitorremediación. at (2012).
27. Guevara, A., Guanoluisa, L. & de la Torre, E. Diseño de Sistemas de Tratamiento de Lixiviados del Relleno Sanitario. *Rev. Politécnica* **34**, 1 (2014).
28. Pasalari, H., Farzadkia, M., Gholami, M. & Emamjomeh, M. M. Management of landfill leachate in Iran: valorization, characteristics, and environmental approaches. *Environ. Chem. Lett.* **17**, 335–348 (2019).
29. Hussein, M., Yoneda, K., Mohd-Zaki, Z., Amir, A. & Othman, N. Heavy metals in leachate, impacted soils and natural soils of different landfills in Malaysia: An alarming threat. *Chemosphere* **267**, 128874 (2021).
30. Kjeldsen, P. *et al.* Present and long-term composition of MSW landfill leachate: a review. *Crit. Rev. Environ. Sci. Technol.* **32**, 297–336 (2002).
31. Santin-Gusman, M., Moreno-Andrés, J., Cisneros-Abad, M. & Aguilar-Ramírez, S. Optimization for fenton process in removal of COD for landfill leachate treatment. *Int. J. Environ. Sci. Dev.* **6**, 920 (2015).
32. Banchon, C., Cañas, R., Baldeón, H. & Córdova, A. Coagulation and oxidation strategies for landfill leachate wastewater. (2022).
33. Vallejo, M. V. P. & Cahueñas, N. P. P. Treatment of mixed leachate type I and type III by filtration and chemical oxidation. *Rev. Investig. Talent.* **10**, 79–89 (2023).
34. Simon, S., Suresh, B. K. & Anantha-Singh, T. S. A sequential aerated electrocoagulation and peroxicoagulation process for the treatment of municipal stabilized landfill leachate by iron and graphite electrodes. *Chemosphere* 139692 (2023).
35. Kashani, M. R. K. *et al.* Sequential treatment of landfill leachate by electrocoagulation/aeration, PMS/ZVI/UV and electro-Fenton: Performance, biodegradability and toxicity studies. *J. Environ. Manage.* **338**, 117781 (2023).

36. Sanei, E. & Mokhtarani, N. Leachate post-treatment by electrocoagulation process: Effect of polarity switching and anode-to-cathode surface area. *J. Environ. Manage.* **319**, 115733 (2022).

Received: October 9th 2023/ **Accepte**d: January 15th 2024 / **Published:**15 February 2024

Citation: Cumbicus C, Hurtado M, Coello J, Peñafiel-Arcos P, Alexandra Orejuela-Romero J, Barahona M. Determination of the effectiveness of the electrocoagulation process in the treatment of leachate from the controlled landfill site in Francisco de Orellana canton. Revis Bionatura 2024; 9 (1) 19. http://dx.doi.org/10.21931/RB/2024.09.01.19

Additional information Correspondence should be addressed to pedro.penafiela@espoch.edu.ec

Peer review information. Bionatura thanks anonymous reviewer(s) for their contribution to the peer review of this work using https://reviewerlocator.webofscience.com/

Bionatura ISSN. First 13909355 Ecuador. **Scopus coverage years**: from 2016 to the present

Bionatura
Ibero-American Journal of Biotechnology and Life Sciences

Article

Determination of water quality through using bioindicators, physical-chemical and microbiological analysis of the lagoon Santo Domingo of the national park Cotopaxi, province of Pichincha, period 2018

Karen Nathali Ceballos Peñafiel *[1], *Moisés Alejandro Quishpe Guanoluisa* [2].

[1] *Instituto Superior Tecnológico General Eloy Alfaro (ISTGEA), La Joya de los Sachas, 220101,*
[2] *Instituto Superior Tecnológico General Eloy Alfaro (ISTGEA), La Joya de los Sachas, 220101*
alejoquishpe@hotmail.es..
* *Correspondence:natthi.ceballos@gmail.com ; Tel.: KC: 0988096244*
Available from. http://dx.doi.org/10.21931/RB/2024.09.01.20

ABSTRACT

The current research project carried out in the Santo Domingo Lagoon of the Cotopaxi National Park, a Protected Area that is located in the canton of Mejia, province of Pichincha, and retains their transcendental goal to determine the water quality from the application of bioindicators and physical-chemical and microbiological laboratory analysis.

They obtained results about the quality of water using bioindicators according to the methodology used (scientific induction, inductive, deductive, measurement, quantitative), where samples were taken at five specific points of entry and exit of the lake body in April, May and June, making use of water quality identification techniques for tolerance; Biological Monitoring Working Part (BMWP/Col.), Ephemeroptera, Plecoptera, Tricoptera (EPT), Andean Biotic Index (ABI), and Biotic Index of Families (IBF). Meanwhile, the environmental quality indices were used for the physical, chemical and microbiological analysis: DINUS - Fundación Nacional de Saneamiento (NFS), defining that the water conditions are wrong or contaminated. By contrast, from the application of the BMWP/Col. and ABI indices, the water quality pertains to waters of questionable and critical condition.

However, with the application of the BMWP/Col. and ABI indices, it was defined that the water quality corresponds to waters of doubtful and critical condition, which are, in conclusion, very contaminated waters. On the other hand, one of the techniques for using bioindicators from the IBF index yielded a different result in areas of apparent organic contamination, determining that the Santo Domingo Lagoon demonstrates an "excellent" indicator.

Keywords: water, analysis, bioindicators, quality, indices, lagoon.

INTRODUCTION

Ecuador, recognized as one of the megadiverse countries on the planet due to its varied geography and geographic location, hosts a wide range of climates and ecosystems. Promoting the preservation of these valuable natural resources at our disposal is imperative.

The Ecuadorian Environment Ministry, in their commitment to promoting the conservation of ecosystems and their valuable goods and services, manages the National System of Protected Areas (SNAP), intending to ensure their care, preservation and sustainable management.

In this context, the Santo Domingo lagoon, located within the System of Protected Areas of Ecuador, specifically in the Cotopaxi National Park (PNC), has been identified as the object of the present investigation. Surprisingly, up to this point, no previous research has been conducted in this environment, which lends significant value to the present study in its efforts to promote the conservation of the water resource it houses. In addition, the findings of this investigation will be of great use in making decisions regarding the use and exploitation of this resource, taking into account aspects such as environmental care and protection, preservation, human health, a guide for sustainable management, ecological condition indicators, contribution to scientific knowledge and awareness and education[1].

The main objective of this investigation is to collect precise information on water quality in Laguna Santo Domingo. For this purpose, various tools were employed, using macroinvertebrates and physical-chemical and microbiological analysis, which provided an accurate diagnosis of the conditions of the lake environment. The methodology used included indices such as BMWP/Col, ICA - NFS, ICA-DINIUS, I. ABI and I. IBF, which facilitated obtaining data on the water quality of Laguna Santo Domingo. The results indicated that the waters of this lake can be used for recreational purposes, which is supported by their membership in the National System of Protected Areas (SNAP)[2].

It is essential to mention that the execution of this research faced various difficulties and challenges, including the remote location, adverse weather conditions, and the problematic access routes to the lake, which is situated at an altitude of 4005 meters above sea level.

MATERIALS AND METHODS

Inductive Method

The observation was strategically planned to draw universal conclusions from the specific data gathered within the study area, namely the Santo Domingo Lagoon in Cotopaxi National Park.

Deductive Method

With this method, the data from water samples collected at Santo Domingo Lagoon during fieldwork were analyzed to generalize to other fields, based on logical reasoning or conjecture, and propose conclusions.

Method of scientific induction

It was carried out from the study of the Santo Domingo Lagoon of the Cotopaxi National Park through this scientific induction that facilitated the support of empirical methods such as the observation of biodiversity in the surroundings of the study area.

It was carried out from the species register to determine the abundance and sensitivity, from the degree of tolerance to pollution, through the scientific study of the collected species.

Measurement method

A precise observation was made of the presence of a specific property and quality of each species observed in each of the sampling points that were carried out in the Santo Domingo lagoon, attributing numerical values, levels of tolerance and relationships to evaluate them, which allowed represent them adequately, in the results of the present investigation.

Quantitative method

This method was carried out in the count of each individual identified in the study area, the classification into categories according to the taxonomic characteristics found and the valuation of the water quality index, elaborating calculations by recording data from figures.

Descriptive research

The results of the water samples obtained in April and June 2018 from Laguna Santo Domingo were interpreted correctly, and the following types of studies were included: investigative and laboratory analysis. The quantitative and qualitative indicators obtained through the collection of species were classified. The information was organized in distribution tables, that is, the description, record, analysis and interpretation of the actual nature, the relevant, characteristic, specific and distinctive aspects of each species found to determine their classification.

Explanatory research

By conducting this type of study focused on the application of different indicators (I. ICA-NSF, I. EPT, I. ABI, I. BMWP/Col, ICA-DINIUS and I. IBF), applied and identified methods to obtain accurate information on water quality of Laguna Santo Domingo in the period of evaluation April (rainy), May (transition) and June (dry - summer).

An explanatory investigation was developed because the Santo Domingo Lagoon is poorly studied and has little information; primordial in the study of macroinvertebrates allowed us to obtain data that facilitates determining their water quality.

Bibliographic research

This type of research allowed us to obtain necessary information about the water quality of Santo Domingo Lagoon since it provided the knowledge for the development of the research project, including the formulation of hypotheses and comparison of results obtained. Information about macroinvertebrate species was sought through various means such as book reviews, bibliographic references, the internet, etc., [3].

Field Investigation

The study was conducted directly in the natural environment where the phenomenon under investigation occurs. This involved the collection of water samples and macroinvertebrates.

According to the objectives of the investigation, the established was executed to be able to perform the determination of the sampling points in the work area, using programs like GPS, Google Earth Pro, SAS Planet, and ArcGIS; this enabled the monitoring of macroinvertebrate species and the collection of water samples from both the main inlet and outlet of the tail.

Observation

Direct observation was conducted in the study area (Santo Domingo Lagoon), where macroinvertebrates and water samples were collected, respectively, to obtain the most effective data for the research.

Structured observation was carried out with the help of appropriate technical elements such as forms, charts, and tables.

Field observation: Field observation was performed during the collection of species and in-situ water sampling at Santo Domingo Lagoon.

Water Sampling (physical-chemical and microbiological analysis): A representative portion of a water mass was extracted to examine various characteristics. The Ecuadorian technical standard INEN 20169:98 specifies that sample containers for physical-chemical and microbiological analysis should be wide-mouthed containers, jars, or bottles made of either plastic or glass.

Protocol for taking water samples for physical-chemical and microbiological analysis

Field phase

The following protocol was applied with the sampling points identified for taking water samples in the main inlet and outlet of the lake of Santo Domingo immersed in the Cotopaxi National Park on April 9 and June 20, 2018.

Filling the container.

The water sampling was carried out in compliance with the Ecuadorian Technical Standard INEN 20169:98. To achieve this, the bottles from Laguna Santo Domingo were sterilized with water three times. Afterward, the bottles were filled and sealed underwater to eliminate air, preventing interaction with the gaseous phase and agitation during transportation to the laboratory.

Identification sample.

The water samples were identified and labeled with their respective date, time, point and place of sampling from which they were taken, allowing no margin of error in the laboratory.

Conservation technique

The samples obtained on the different sampling days were kept at 2 ºC and 5 ºC, kept in a cooler with a certain amount of ice that allowed them to reach said temperature; in contrast, the samples were transported to the laboratory.

Transportation sample

The containers with the water samples were protected and sealed to prevent them from deteriorating or losing any part of them during transport from the Santo Domingo Lagoon to the cities of Ambato (April) and Sangolqui (June), where they were found in the laboratory. During transportation, the samples were placed in a safe place to protect them from light and kept in a cool environment, separating each sample in a different impermeable container.

Laboratory stage

Reception sample to the laboratory.

The samples were transported to the laboratory in the cities of Ambato and Sangolqui. The samples obtained from the monitors in April -09 and June -20, 2018 were preserved and deposited in refrigerators under conditions established in the Ecuadorian Technical Standard INEN 20169:98, preventing any external contamination and change in their content.

PHYSICS	CHEMICALS	MICROBIOLOGICAL
Color	total alkalinity	Fecal coliforms
electrical conductivity	Chlorides	Total coliforms
pH	DBO5	
Solids in suspension	DQO	
Temperature	tough	
Turbidity	Phosphate total	
	Nitrogen (N)	
	Nitrites (NO2)	
	Nitrate (NO3)	
	dissolved oxygen	
	potassium (K)	
	Sales dissolves	

Table 1. Physical parameters, chemical and microbiological.

Collection of samples for the analysis of macroinvertebrates.

Field phase

The field phase was carried out in April - 09, May - 10 and June - 20 of 2018. At each sampling point, a transect of 30 to 50 meters was established, from which various specimens were collected for the respective samples. The collection technique with red Surber used a 250 μm aperture mesh with an area of 0.1 m2. This involves capturing the individuals, the same ones who were identified in the laboratory; if they used multiple bottles, each one was labeled with the date, time and point of sampling; therefore, in all the bottles in the monitoring and, or control area, the individuals of each group were identified and counted to obtain the total number of individuals (abundance) and do the same with all the bottles in the sampled area.

The technique involves introducing the net into the lake at a determined sampling point. He removed to remove and hit the substrate dynamically with his feet for approximately one minute. This was repeated in the five monitoring points in the Santo Domingo Lagoon, where the established climatic seasons (precipitation, transition and dry season) were monitored.

To obtain more precise information about the water quality conditions of the Santo Domingo Lagoon, the presence of macroinvertebrates, they will be collected in the Surber network if the macroinvertebrates are separated from the other animals with the help of Entomological forceps. The separated specimens were placed in bottles previously labeled with 96% alcohol for each sample. During the water body sampling, information was recorded in a notebook: geographic coordinates, date, time of sampling, climate, habitat, and description of the water body, among others.

With the help of the identification sheet, they grouped similar individuals, if they resembled which group they belonged to, and counted how many specimens each group had. This process was repeated with the macroinvertebrates collected in the other bottles from the different points.

The plates for identifying macro specimens will facilitate the identification of the most common groups found in rivers, estuaries and lagoons.

The Figure of each species of macroinvertebrate identified in the Santo Domingo lagoon allowed for obtaining the following information:

- Scientific classification.
- Local numbers.
- Figures or drawings that indicate the type of food and the place where you live.
- Furthermore, a number indicating the sensitivity of each macroinvertebrate to pollution

Laboratory stage

Once the samples of macroinvertebrates were transported to the laboratory, they used materials such as: a stereo microscope, Petri dishes and entomological tweezers to analyze the samples of aquatic macroinvertebrates obtained from the water body of Laguna Santo Domingo.

The specimens were identified in terms of order, family and gender with the help of field guides and relevant photographic guides [4]. The samples allowed quantitative and qualitative analysis of each of the sampling points.

Sampling frequency

The field trips for the different samplings were carried out during the wet (April), transition (May) and dry (June) seasons of 2018, whose frequency of sampling was carried out once for me during a previously established period, where they have collected the samples for subsequent analysis.

Water quality indices

ICA

The ICA applied for the evaluation of the constituents that affect the water quality for their different uses and to summarize this evaluation in a simple value that served as a way to communicate and represent the water quality of the Santo Domingo lagoon. An Index of water quality (ICA) indicates the degree of water contamination in a specific sampling date and is expressed as a percentage of pure water; being so, highly contaminated water presents an ICA close to or equal to 0%, in contrast, water in excellent conditions will have an index close to 100% [2].

The NSF index (1978) is fundamental in the equation:

$$NSF = \sum_{i=1}^{9} SI_i * W_i \quad \text{Formula 1}$$

why,

- SI is from the subscript of the variable i, y;
- Wi is from the weighted weight of subindex i (Otto, 1978).

Variables	Valor WI-NSF (1978)	units
Dissolved oxygen	0.17	mg/l
Fecal coliforms	0.16	NMP/100 ml
pH	0.11	a. pH

DBO5	0.11	mg/l
nitrates	0.10	mg/l
Total phosphorus	0.10	mg/l
Δt °C of equilibrium	0.10	ºC
Turbidity	0.08	UNT
Total solids	0.07	mg/l

Table 2. ICA NSF established pesos and units.

Index of NSF (1978)		Color
quality	**Rank**	
Excellent	91-100	blue
Suitable	71-90	green
Environmental	51-70	yellow
Wrong	26-50	orange
Evil	0-25	a stream

Table 3. Characterization of results based on the NSF Index.

ICA - DINIUS

The study was carried out with the application of this index for the extensive use of physical, chemical and microbiological parameters, which allowed a detailed analysis of the water quality of the Santo Domingo Lagoon, concerning the tourist advantage, as it is found inside a protected area.

From the quality index of Dinius (1987), it is determined as:

$$ICA = \prod_{i=1}^{n} [Q_i^{W_i}] \quad \text{Formula 2}$$

why,

- W_i, represents the specific weights established for each parameter (i) And weighing between 0 y 1, of such a manner that it fulfills a summation that corresponds to one;
- Q_i, means the quality of the parameter (i) taking into account the concentration between $(1 - 100)$;
- PI, symbolizes the multiplication of the variables Q elevated to the W_i^5.

Index of Dinius (1987)			
Color	In detail	Recreational Use	
		Rank	In detail
blue	excellent quality	70 – 100	Any sport aquatic
green	Quality acceptable	50 - 70	Restrict immersion sports; caution ingests dad the possibility of bacteria
yellow	Contamination high	40 - 50	Doubtful for water contact
orange	Contaminated	30 - 40	Avoid contact

golden	Heavy contamination	20 - 30	Visible contamination, avoid proximity
a stream	Contaminated excess	00 – 20	Unacceptable for recreation

Table 4. Characterization of results based on the Dinius Index.

Analysis EPT

It was used to identify the presence of Ephemeroptera, Plecoptera, and Trichoptera in the Santo Domingo Lagoon, to determine the water quality of the said lake, Table of macroinvertebrate assessment and the following formula.

The calculation consists of dividing the corresponding Number of EPT present in the sample according to the total number of organisms:

$$\textbf{I. EPT}= (\frac{NEPT}{N})100 \quad \text{Formula 3}$$

why,

- $I. EPT = EPT\ Index$;
- $NEPT = Total\ Number\ of\ EPT\ individuals\ in\ the\ sample;$
- $N = Total\ number\ of\ individuals\ in\ the\ sample.$

Continuing with the research, it was removed to evaluate the results obtained with the detailed values according to this Table of Sensibility.

CLASS	ETP RATE (%)	WATER QUALITY	COLOR
1	75 - 100	very suitable	blue
2	50 - 74	suitable	green
3	25 - 49	fair	orange
4	0 - 24	wrong	a stream

Table 5. Sensitivity of the macroinvertebrates.

Index BMWP/COL.

The BMWP/Col Index (Biological Monitoring Working Party) was used, from which values from 1 to 10 were assigned to macroinvertebrates identified at the family level. Those who do not tolerate the loss of water quality will be given high scores; in contrast, those who endure the loss of quality have low scores.

The total scores of all those found in a site were proportional to the value of the water property of Laguna Santo Domingo.

FAMILY	SCORE
Lampyridae, Lymnessiidae (Hydracarina), Psephenidae, Ptilodactylidae, Blepharoceridae, Perlidae, Polythoridae, Polymitarcidae, Oligoneuriidae, Euthyplociidae, Anomalopsychidae, Unionidae, Hydroptilidae, Hydridae, Calamoceratidae, Odontoceridae, Glossossmatidae, Atriplectididae, Rhyacophilidae.	10
Chordodidae, Gordiidae, Ampullariidae, Xiphocentronidae, Philopotamidae, Hydrobiosidae, Megapodagrionidae, Gomphidae, Coenagrionidae, Pyralidae, Leptophlebiidae, Ephemeridae, Simuliidae, Scirtidae, Hirudinae, Gyrinidae.	9
Chilinnidae, Leptoceridae, Helicopsychidae, Hidropsychidae (Leptonema y Smicridea), Lestidae, Calopterygidae, Veliidae, Saldidae, Pleidae, Hebridae, Geriidae, Caenidae, Baetidae, Dixidae, Dytiscidae, Dryopidae, Pseudothelphusidae, Alaemonidae.	8
Planariidae, Dugessidae, Melaniidae, Hydrobiidae, Planorbidae, Ancylidae, Neritidae, Polycentropodidae, Naucoridae, Aeshnidae, Notonectidae, Mesoveliidae, Corixidae, Tricorythidae, Leptohyphidae, Dixidae, Psychodidae (Maruina), Staphylinidae, Imidae.	7
Nepidae, Corydalidae, Hydrometridae, Gelastocoridae, Belostomatidae, Dolichopodidae, Lutrochidae, Limnichidae, Atyidae, Hyalellidae, Sialidae, Libellulidae.	6
Thiaridae, Tabanidae, Stratiomydae, Empididae, Haliplidae (Haliplus), Curculionioidea: Brachyceridae (Neochetin; Neohydronomus).	5
Chrysomelidae, Hydraenidae, Hydrophilidae, Noteridae, Sphaeridae, Ceratopogonidae, Tipulidae, Sphaeridae, Lymnaeidae	4
Cylicobdellidae (Blanchardiella), Culicidae, Muscidae, Sciomyzidae, Physidae	3
All families except Tubificidae: Tubifex, Chironomiidae (Chironomus ROJO) Ephydridae, Syrphidae	2
Tubificidae (Tubifex)	1

Table 6. System for Determining Biological Monitoring Index - BMWP (Biological Monitoring Working Party Score System) - Adaptation for Colombia.

CLASS	QUALITY	BMWP/Col	SIGNIFICANCE	COLOR
I	SUITABLE	>150 101-120	Wáter spotless cleans	blue
II	ACCEPTABLE	61-100	Wáter slightly contaminated	green
III	DOUBTFUL	6-60	Wáter moderately contaminated	yellow
IV0	CRITICAL	16-35	Highly contaminated waters	orange
IV	VERY CRITICAL	<15	Wáter strongly contaminated	a stream

Table 7. Biological Quality of Water – Index BMWP/Col.

Index ABI

The Andean Biological Index made it possible to determine the quality of the water, which was determined through the use and identification of macroinvertebrates as natural aquatic bioindicators, assigning values from 1 to 10 to each family and the total sum of these values given in the identification stage of the macroinvertebrates from a specific value of the ABI index.

Understanding that this value should be divided by the resulting Figure of rates found at the monitoring site where the investigation is being conducted [6].

FAMILY	SCORE
Athericidae, Blepharoceridae, Leptophlebiidae, Oligoneuriidae,Polythoridae, Gripopterygiidae, Perlidae, Anomalopsychidae, Calamoceratidae, Helicopsychidae, Odontoceridae.	10
Calopterygidae, Gomphidae, Hydrobiosidae, Leptoceridae,Philopotamidae, Polycentropodidae, Xiphocentronidae.	8
Leptohyphidae, Glossosomatidae, Limnephilidae	7
Hyalellidae, Aeshnidae, Coenagrionidae, Libellulidae, Hydroptilidae, Ancylidae.	6
Dryopidae, Elmidae, Hydraenidae, Lampyridae, Psephenidae, Ptilodactylidae, Scirtidae, Simuliidae, Tipulidae, Corixidae, Gerridae, Naucoridae, Notonectidae, Veliidae,Hydropsychidae (Leptonema y Smicridea), Dugesiidae.	5
Arrenuridae (Arrenurus), Hydrachnidae (Hidrachna), Limnocharidae (Limnochares*American*), Ceratopogonidae, Dixidae, Dolichopodidae, Empididae, Limoniidae, Stratiomyidae, Tabanidae, Baetidae, Belostomatidae, Pyralidae.	4

Glossiphoniidae, Cipprididae (Strandesia), Cipprididae (Plesiocypridopsis), Dytiscidae, Gyrinidae, Hydrophilidae, Staphylinidae, Psychodidae (Maruina), Sphaeridae, Mytilidae, Lymnaeidae, Planorbidae, Hydrobiidae.	3
Chironomiidae (Chironomus ROJO), Culicidae, Ephydridae, Muscidae	2
Tubificidae (Tubifex), Athericidae	1

Table 8. Valorization of macroinvertebrates according to the ABI index.

A score that allowed determining the water quality according to the Andean Biotic Index (ABI).

CLASS	QUALITY FROM WATER	SCORE	**SIGNIFICANCE**	COLOR
I	very suitable	>96	Spotless water, which has not been altered	blue
II	well	59 – 96	Water slightly contaminated	green
III	fair	35 – 58	Contaminated waters, the source of contamination is unknown	yellow
IV	opposite	14 – 34	Highly contaminated waters	orange
V	terrible	<14	Hardly contaminated waters	a stream

Table 9. Score for the determination of water quality according to the ABI index.

Índice IBF (Biotic Index of Families)

The IBF index made it possible to evaluate the water quality of the Santo Domingo Lagoon, so this family biotic index was calculated as a weighted average of the abundance of different species of benthic macroinvertebrates. The weighting value measures the tolerance that each group presents to organic pollution. For each family, the tolerance score is multiplied by the number of individuals, and then the results of all families are added together [7].

To be able to use the IBF index, the following formula is used:

$$\boldsymbol{IBF} = \left(\frac{\sum \boldsymbol{n_i} * \boldsymbol{T_i}}{\boldsymbol{N}}\right) \qquad \text{Formula 4}$$

where:

- $N =$ *The total number of individuals in the sample*;
- $n_i =$ *number of individuals per taxa*;
- $T_i =$ Weighting value assigned to each taxa.

FAMILY	**TOLERANT**
Athericidae, Blepharoceridae, Leptophlebiidae, Oligoneuriidae, Corydalidae, Gripopterygiidae,	10

FAMILY	TOLERANT
Perlidae, Anomalopsychidae, Leptoceridae	
Aeshnidae, Calopterygidae, Cordulidae, Gomphidae, Lestidae, Libellulidae, Glossosomatidae, Philopotamidae	8
Ecnomidae, Hydrobiosidae, Limnephilidae, Polycentropodidae	7
Hyalellidae, Hydroptilidae, Ancylidae	6
Dryopidae, Elmidae, Simuliidae, Hydropsychidae (Leptonema y Smicridea), Dugesiidae	5
Arrenuridae (Arrenurus), Hydrachnidae (Hidrachna), Limnocharidae (Limnochares americana), Curculionioidea: Brachyceridae (Neochetina; Neohydronomus), Haliplidae (Haliplus), Psephenidae, Ceratopogonidae, Dixidae, Empididae, Limoniidae, Psychodidae (Maruina), Stratiomyidae, Tabanidae, Baetidae, Caenidae, Belostomatidae, Sialidae	4
Glossiphoniidae, Dytiscidae, Gyrinidae, Hydrophilidae, Corixidae, Gerridae, Notonectidae, Sphaeridae, Mytilidae, Lymnaeidae, Physidae, Planorbidae	**3**
Chironomiidae (Chironomus ROJO), Culicidae, Ephydridae	**2**
Tubificidae (Tubifex), Syrphidae	**1**

Table 10. Tolerance values of macroinvertebrates from the Biotic Index of Families.

CLASS	IBF	ENVIRONMENTAL CHARACTERISTICS	COLOR
I	0.00-3.75	Very suitable, undisturbed	blue
II	3.76-4.63	Well, moderately disturbing	green
III	4.64-6.12	Regular, disturbing	yellow
IV	6.13-7.25	On the contrary, perturbed	orange
V	7.26-10.00	Evil heavily disturbed	a stream

Table 11. Quality classes for the Biotic Index of Families.

Instruments and materials

INSTRUMENTS TO BE USED	MATERIALS TO USE
Field notebooks Data sheet Sampling card Photo camera Laboratory analysis GPS (System of Terrestrial Positioning) Microscope	Sterilized containers for samples 100ml and 1000ml wolf Seals and labels Pinch Red Surber Industrial alcohol 96% gloves Permanent markers Mask Rubber boots Nylon sieve Dropper Microscope Petri dishes Camera

Table 12. Instruments and materials that were used in the research project.

RESULTS

Analysis ICA – INSF - April

SAMPLE WATER (1): MAIN ENTRANCE SANTO DOMINGO LAGOON – APRIL 2018

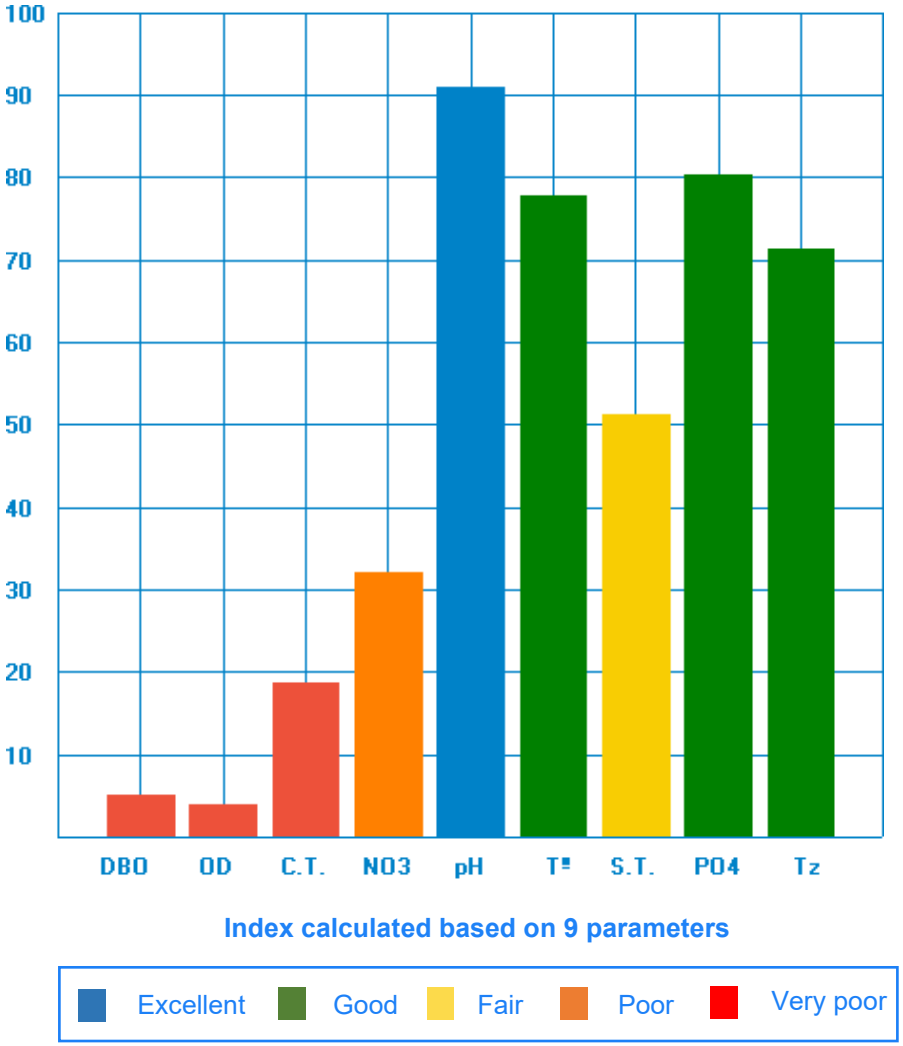

Figure 1. NFS Analysis - April - Q Values – Entrance.

The results obtained according to the analyzed parameters, the following values were obtained: (DBO – 52mg/L), (OD – 3.7 mg/L), (CF – 1800 NMP/100mL), (NO3 – 25 mg /L), (pH – 7.7 UnpH), (Tº - 3.8 ºC), (ST – 364 mg/L), (PO4 – 0.31 mg/L), (Tz – 12.3 NTU), and according to ICA Test - INSF we have that the quality of the water of Laguna Santo Domingo has an index value of 42.52 giving as a result a wrong qualification, each one of this qualification and, or weighting corresponding to each one of the parameters: DBO evil, OD evil, CF evil, NO3 wrong, pH excellent, T° suitable, ST average, PO4 suitable, and Tz suitable.

SAMPLE WATER (2): EXIT SANTO DOMINGO LAGOON – APRIL 2018

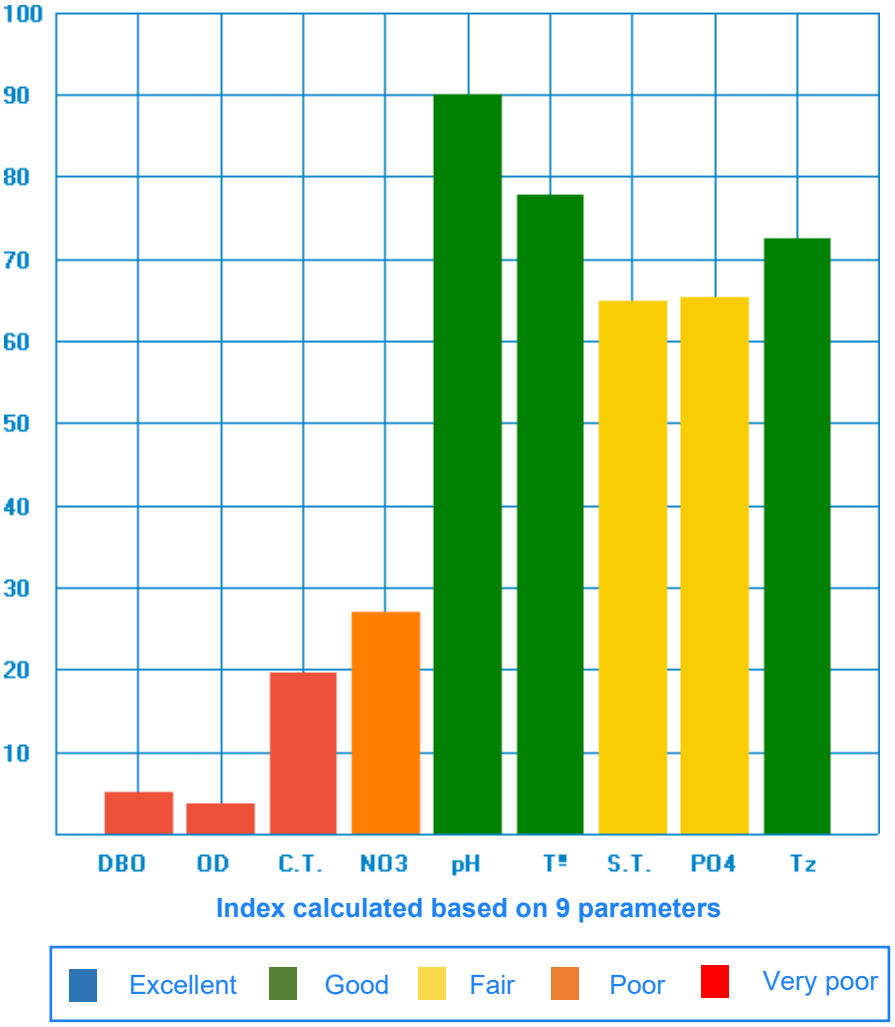

Figure 2. NFS Analysis - April - Q Values - Exit.

The results obtained according to the analyzed parameters, the following values were obtained: (DBO – 67mg/L), (OD – 3.2 mg/L), (CF – 1620 NMP/100mL), (NO3 – 30 mg /L), (pH – 7.8 UnpH), (Tº - 3.8 ºC), (ST – 258 mg/L), (PO4 – 0.45 mg/L), (Tz – 11.8 NTU) , according to the ICA Test - INSF we have that the quality of the water of the Santo Domingo Lagoon has an index value of 41.53 giving as a result a wrong qualification, each one of this qualification and, or weighting corresponding to each of them parameters: DBO evil, OD evil, CF evil, NO3 wrong, pH suitable, T° suitable, ST medium, PO4 medium, and Tz suitable.

- **Analysis ICA – DINIUS - April**

SAMPLE WATER (1): MAIN ENTRANCE SANTO DOMINGO LAGOON – APRIL 2018

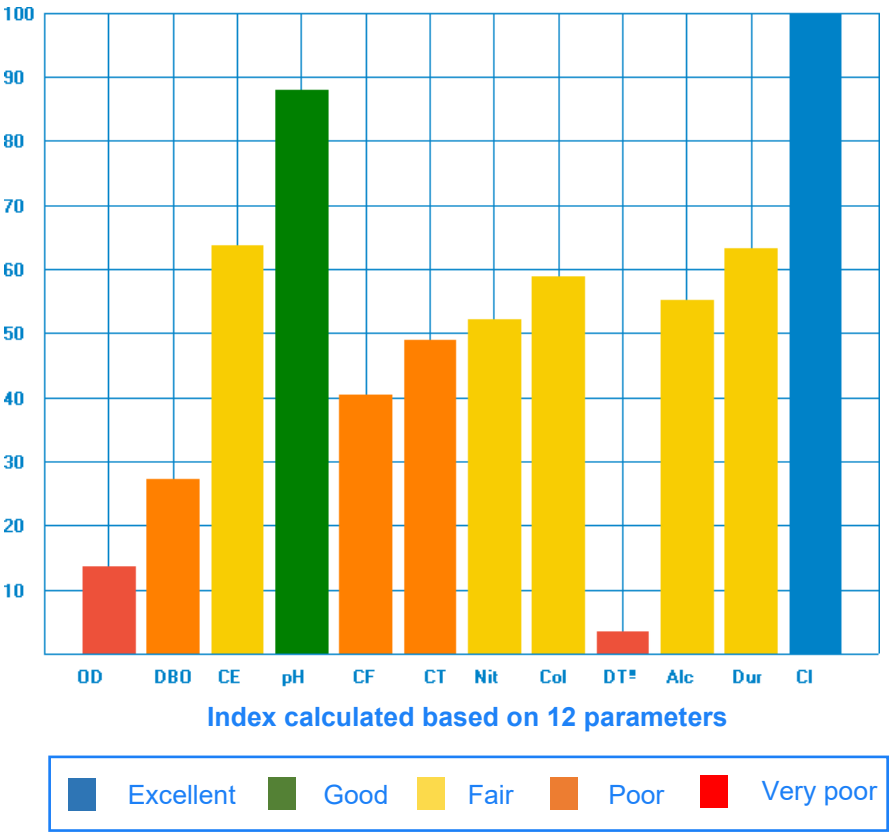

Figure 3. DINIUS Analysis, April - Q Values - Entrance.

The results obtained according to the analyzed parameters, the following values were obtained: (DBO – 52mg/L), (OD – 3.7 mg/L), (CE – 518.88 µΩ/cm), (CF – 1800 NMP/100mL), (CT – 2400 NMP/100mL), (NO3 – 25 mg/L), (Col – 25 Unid.), (Tº - 3.8 ºC), (Alc – 174 mg/L), (Dur. – 125mg/L), (Cl – 28 mg/L), and according to ICA Test – Indice DINIUS the water quality of Laguna Santo Domingo is 37.66, resulting in classification as contaminated, since it is evaluated for recreational use, for which each qualification and, or weighting of each parameter is: OD evil, DBO wrong, CE average, pH suitable, CF wrong, CT wrong, NO3 average, Col average, T° evil, Alc medium, Dur medium y Cl excellent.

SAMPLE WATER (2): EXIT SANTO DOMINGO LAGOON - APRIL 2018.

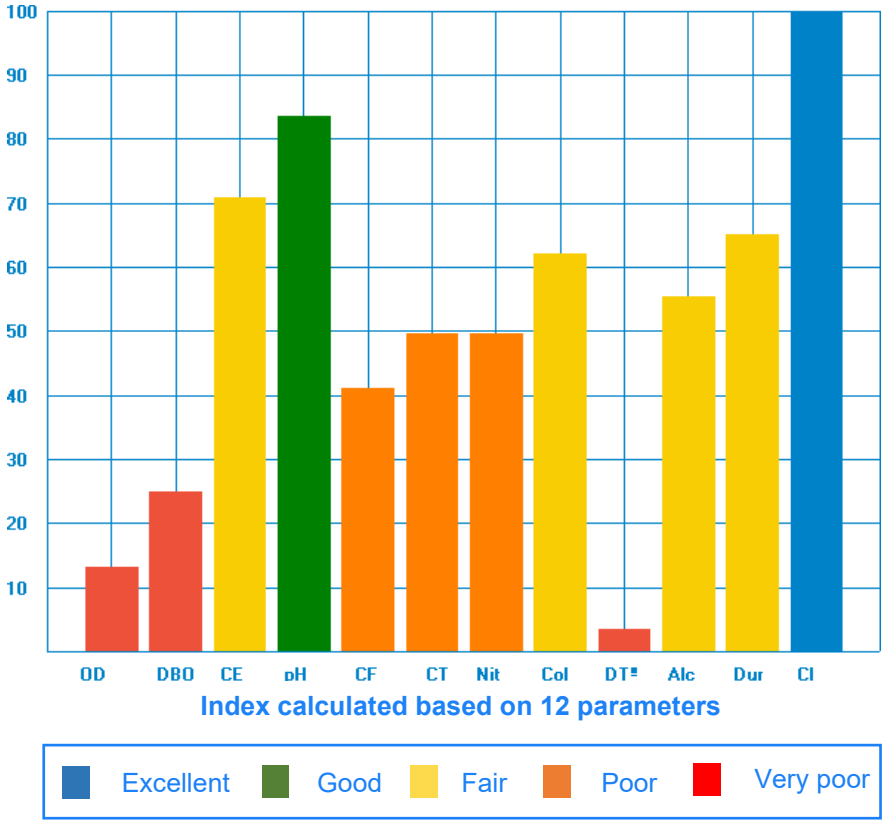

Figure 4. DINIUS Analysis, April - Q Values - Exit.

The results obtained according to the analyzed parameters, the following values were obtained: (DBO – 67mg/L), (OD – 3.2 mg/L), (CE – 376.6 µΩ/cm), (pH – 7 ,8 UnpH), (CF – 1620 NMP/100mL), (CT – 2150 NMP/100mL), (NO3 – 30 mg/L), (Col – 20 Unid.), (Tº - 3.8 ºC), (Alc – 165 mg/L), (Dur. – 117mg/L), (Cl – 24 mg/L), and according to ICA Test – DINIUS Index the water quality of Laguna Santo Domingo is 37.61, resulting in classification as contaminated, since it is evaluated for recreational use, for which each qualification and, or weighting of each parameter is: OD evil, DBO evil, CE medium, pH suitable, CF wrong, CT wrong, NO3 wrong, Col medium, T° evil, Alc medium, Dur medium and Cl excellent.

Analysis ICA – INSF - June

SAMPLE WATER (3): MAIN ENTRANCE LAGUNA SANTO DOMINGO - JUNE 2018.

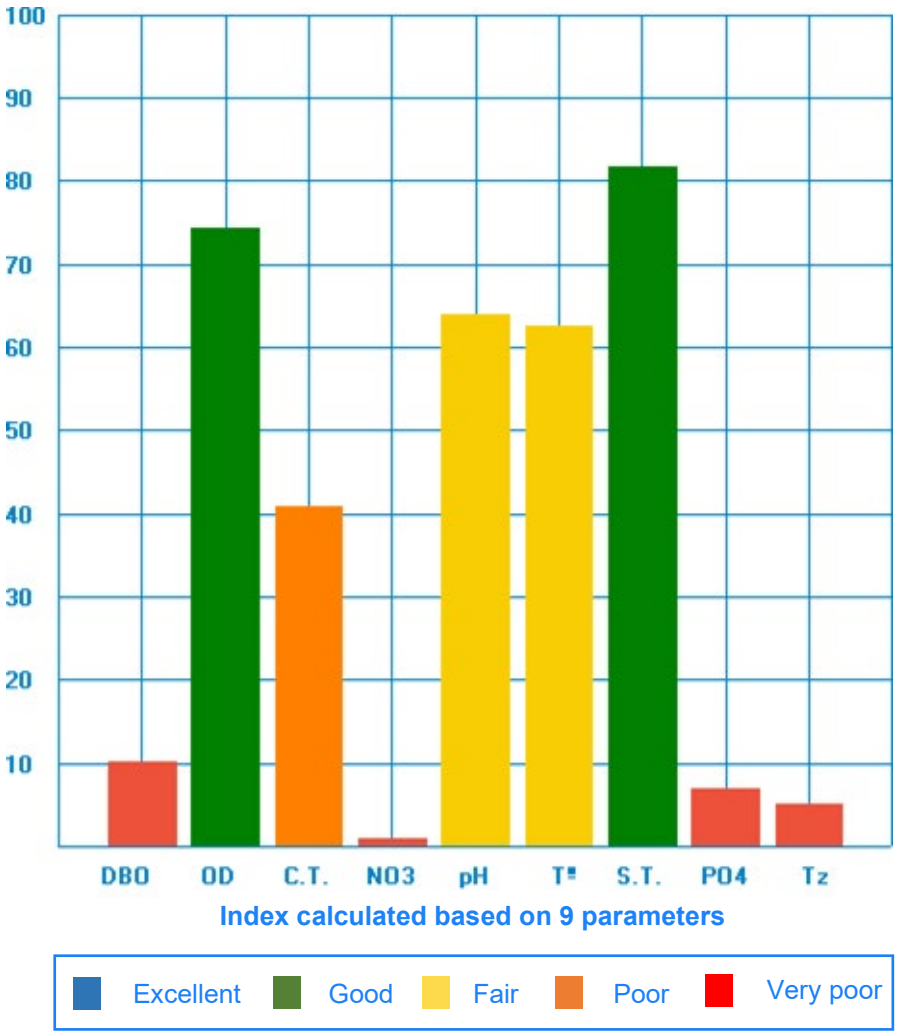

Figure 5. NFS Analysis - June - Q Values - Entrance.

The results obtained according to the analyzed parameters, the following values were obtained: (DBO – 21mg/L), (OD – 69.58 mg/L), (CF – 140 NMP/100mL), (NO3 – 115 mg /L), (pH – 6.3 UnpH), (Tº - 6.8 ºC), (ST – 9 mg/L), (PO4 – 10 mg/L), (Tz – 121 NTU), and according to ICA Test - INSF the water quality of Laguna Santo Domingo is wrong has an index value of 40.47, being each one of this rating and, or weighting corresponding to each of the parameters: DBO evil, OD suitable, CF wrong, NO3 evil, pH average, T° average, ST suitable, PO4 evil, and Tz evil.

SAMPLE WATER (4): EXIT SANTO DOMINGO LAGOON - APRIL 2018

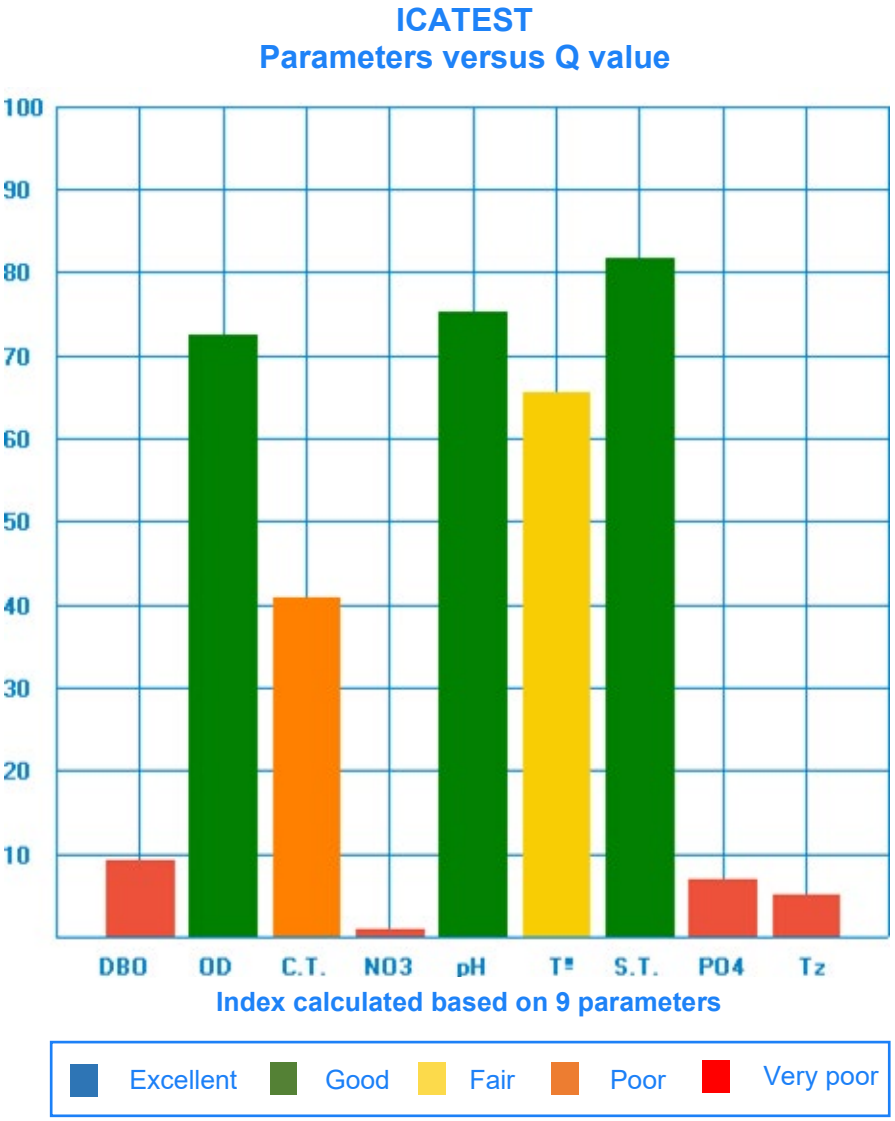

Figure 6. NFS Analysis - June - Q Values – Exit.

The results obtained according to the analyzed parameters, the following values were obtained: (DBO – 22.32 mg/L), (OD – 68.53 mg/L), (CF – 140 NMP/100mL), (NO3 – 116 mg/L), (pH – 6.6 UnpH), (Tº - 6.3 ºC), (ST – 9 mg/L), (PO4 – 10 mg/L), (Tz – 119 NTU), and according to ICA Test - INSF we have that the quality of the water of Laguna Santo Domingo has an index value of 41.64 giving as a result a rating of wrong, each one of this rating and, or weighting corresponding to each of them parameters: DBO evil, OD suitable, CF wrong, NO3 evil, pH suitable, T° medium, ST suitable, PO4 evil, and Tz evil.

Analysis ICA – DINIUS – June

SAMPLE WATER (3): MAIN ENTRANCE SANTO DOMINGO LAGOON - JUNE 2018

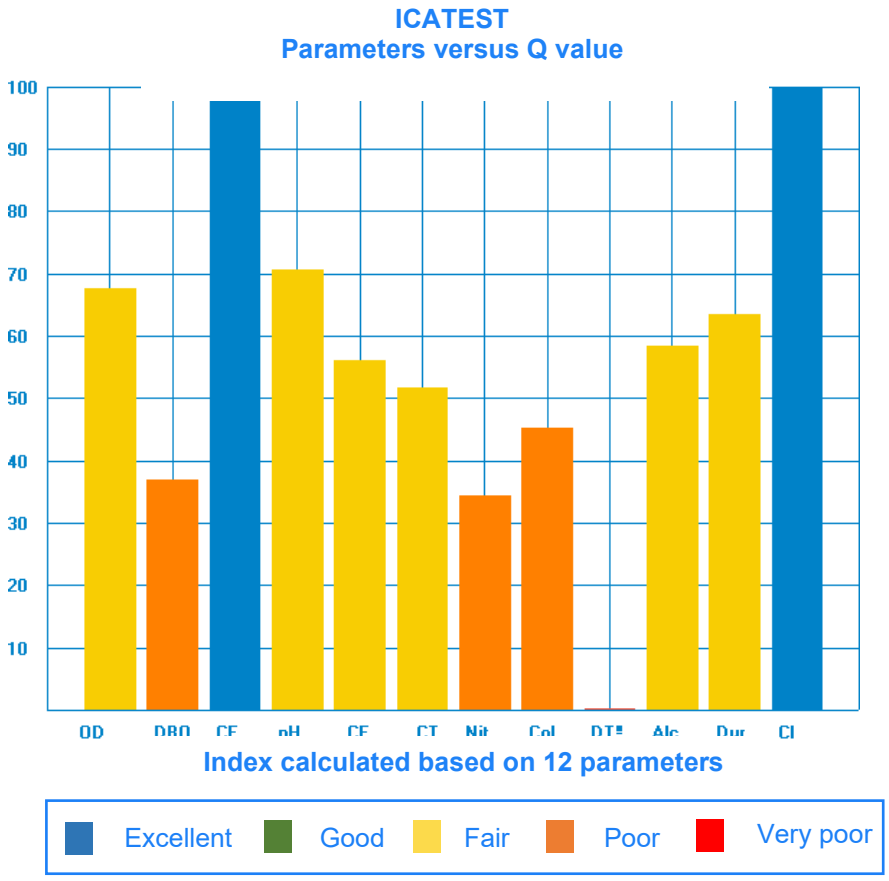

Figure 7. DINIUS Analysis, June - Q Values – Entrance.

The results obtained according to the analyzed parameters, the following values were obtained: (DBO – 21.42 mg/L), (OD – 69.58 mg/L), (CE – 19 µΩ/cm), (pH – 6.3 UnpH), (CF – 140 NMP/100mL), (CT – 1600 NMP/100mL), (NO3 – 115 mg/L), (Col – 75 Unid.), (Tº - 6.8 ºC), (Alc – 112 mg/L), (Dur. – 124 mg/L), (Cl – 19.74 mg/L), in where, according to the result of the ICA Test – DINIUS Index, the water quality of Laguna Santo Domingo is contaminated has an index value of 38.20, since it is evaluated for recreational use, for which each qualification and, or weighting of each parameter is: OD average, DBO wrong, CE excellent, pH medium, CF medium, CT medium, NO3 wrong, Col wrong, T° evil, Alc medium, Dur medium y Cl excellent.

SAMPLE WATER (4): EXIT SANTO DOMINGO LAGOON - JUNE 2018

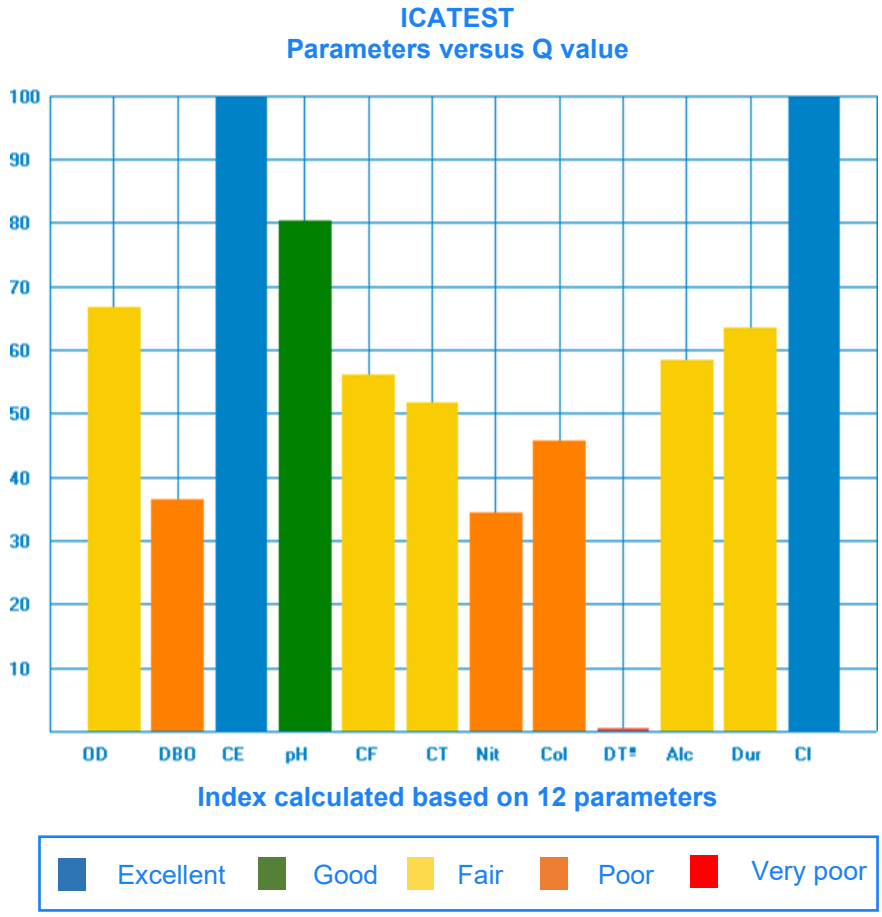

Figure 8. DINIUS Analysis, June - Q Values – Exit.

The results obtained according to the analyzed parameters, the following values were obtained: (DBO – 22.32mg/L), (OD – 68.53mg/L), (CE – 19 µΩ/cm), (pH – 6, 6 UnpH), (CF – 140 NMP/100mL), (CT – 1585 NMP/100mL), (NO3 – 116 mg/L), (Col –71 Unid.), (Tº - 6.3 ºC), (Alc – 112mg/L), (Dur. – 124mg/L), (Cl – 18.40 mg/L), and according to ICA Test – Index DINIUS we have that the quality of the water of Santo Domingo Lagoon has a value of an index of 39.93 result a qualification of contaminate, since it is evaluated for recreational use, for which each qualification and, or weighting of each parameter is: OD average, DBO wrong, CE excellent, pH well, CF average, CT medium, NO3 wrong, Col wrong, T° evil, Alc medium, Dur medium and Cl excellent.

Comparison of results between the ICA DINIUS and NFS in the Santo Domingo Lagoon

Main Water Inlet, April and June

	APRIL	JUNE	QUALIFICATION
ICA-NFS	42,52	40,47	Wrong (26 - 50)
ICA- DINIUS	37.66	38.2	Contaminated (30-40)

Table 13. Results, ICA DINIUS and ICA NFS.

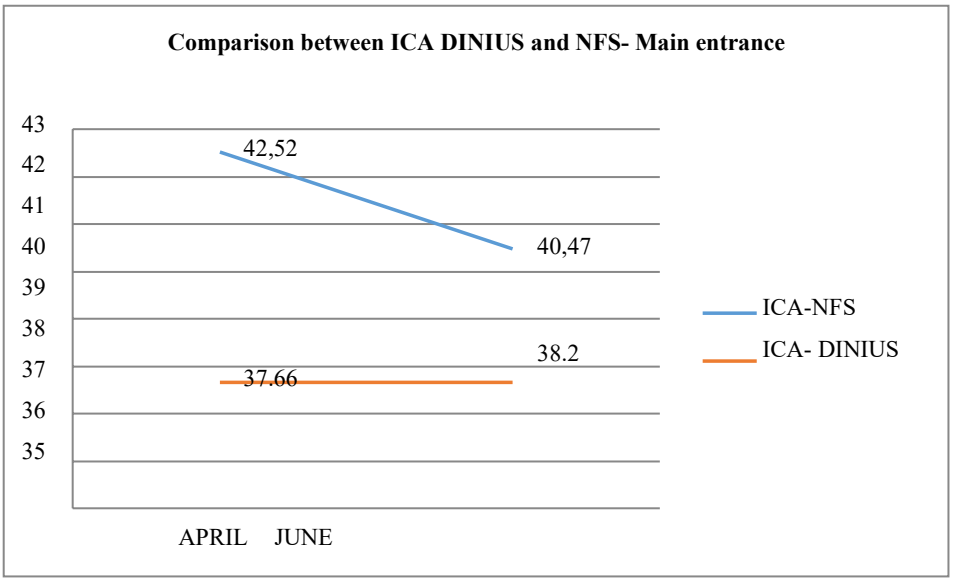

Figure 9. Comparison between ICA DINIUS and ICA NFS.

In Figure Nº9, it is expressed that in the months that water samples were taken for subsequent analysis (April and June), from the main entrance of the Santo Domingo lagoon, the results obtained were similar with ranks of between 37 and 42, justifying that the two indices determine that the water quality is wrong and, or contaminated.

Main Water Outlet, April and June.

	APRIL	JUNE	QUALIFICATION
ICA-NFS	41,53	41.64	Wrong (26 - 50)
ICA- DINIUS	37,61	39.93	Contaminated (30-40)

Table 14. Results, ICA DINIUS and ICA NFS.

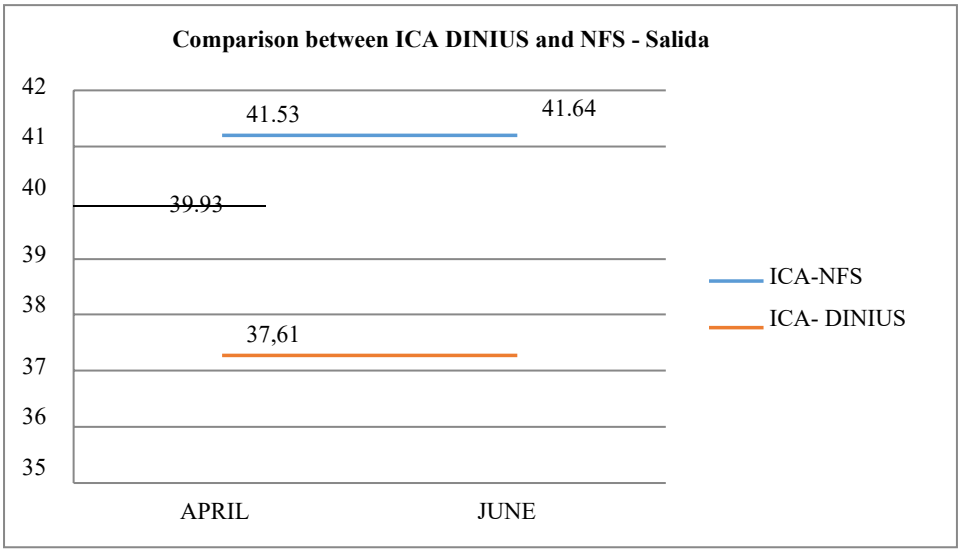

Figure 10. Comparison between ICA DINIUS and ICA NFS - Exit.

In Figure Nº 10, it is determined that in April and June, when the water samples were obtained from the main outlet of the lake, the results obtained were of a rank between 37 and 41, being similar to the results obtained from the analysis of the main entrance of the river, arguing that the two indices determine that the quality of the water is poor and, or contaminated.

Analysis of macroinvertebrates index EPT

In the monitored months (April, May and June), no families belonging to the EPT group (Ephemeroptera, Plecoptera and Trichoptera) were identified, so this index cannot be applied to determine the water quality index.

BMWP/Col index analysis:

In Table Nº 15, the water quality values are observed through the BMWP index with their respective class for each month of sampling (April, May and June).

	APRIL	MAY	JUNE
BMWP	24	30	37
CLASS	IV	IV	III
QUALITY	Critique	Critique	Doubtful

Table 15. Water quality through the BMWP index.

In Table No. 15, it is stated that in the months of April and May, values were obtained with a similarity range of 24 and 30, which determine a class IV, indicating that the water is in a state of critical quality. In June, the index value was 37, resulting in the water quality being considered doubtful, corresponding to moderately contaminated waters.

According to the BMWP index, for April, 424 species were registered, among which 6 tolerant and sensitive families were identified, among them the sensitive families with values of 6 the Hyalellidae family, followed by the tolerant families with values of between 5 y 1: Notonectidae, Lymnaeidae, Cylicobdellidae, Glossiphoniidae and Tubificidae.

In the middle of May, the BMWP index was determined for 309 species of 7 families identified, tolerant and sensitive, among them the sensitive families with values of 6, such as the Hyalellidae family and increasing the Libellulidae family, followed by the tolerant families with values from between 5 and 1: Notonectidae, Tipulidae, Cylicobdellidae, Glossiphoniida and Oligochaeta.

The result obtained from the BMWP index for June was determined based on 338 species from 8 identified families, both tolerant and sensitive. The sensitive families to pollution, such as Hyalellidae, Notonectidae, Libellulidae, and Planariidae, had values of 7 and 6, respectively. This was followed by pollution-tolerant families with values ranging from 4 to 1: Cylicobdellidae, Glossiphoniidae, Tubificidae, and Lymnaeidae. This result differs from previous months, as an additional family sensitive to pollution was identified.

ABI Index Analysis:

In Table Nº 16, the water quality values are observed through the ABI index with their respective class for each month of sampling (April, May and June).

	APRIL	**MAY**	**JUNE**
ABI	21	29	32
CLASS	IV	IV	IV
QUALITY	Opposite	Opposite	Opposite

Table 16. Water quality through the biological index ABI.

Table Nº. 16 shows that similar values were obtained in April, May, and June, ranging between 21 and 32, categorizing it as Class IV, indicating poor water quality.

In April, according to the tolerance values of the ABI index, tolerant and sensitive families were identified, among them the family with a value of 6 such as Hyalellidae, followed by the tolerant families with values of between 5 y 1: Notonectidae, Lymnaeidae, Cylicobdellidae, Glossiphoniida and Tubificidae.

In May, two sensitive families with values of 6 were identified: Hyalellidae and Libellulidae, followed by five families tolerant to pollution with values of between 5 and 1, those Notonectidae, Tipulidae, Cylicobdellidae, Glossiphoniida and Tubificidae.

For June, eight families have been collected, of which two are sensitive to contamination, registered with values of six, those Hyalellidae and Libellulidae, continuing with the tolerant families which are primarily with values of between 5 and 1: Cylicobdellidae, Notonectidae, Glossiphoniidae, Tubificidae, Lymnaeidae, Planariidae.

Comparison between BMWP Index and ABI Index

Table Nº 17 shows the water quality values between the BMWP and ABI indexes observed in the three months of study (April, May and June).

	APRIL	MAY	JUNE
BMWP	24	30	37
ABI	21	29	32

Table 17. Index BMWP and Index ABI.

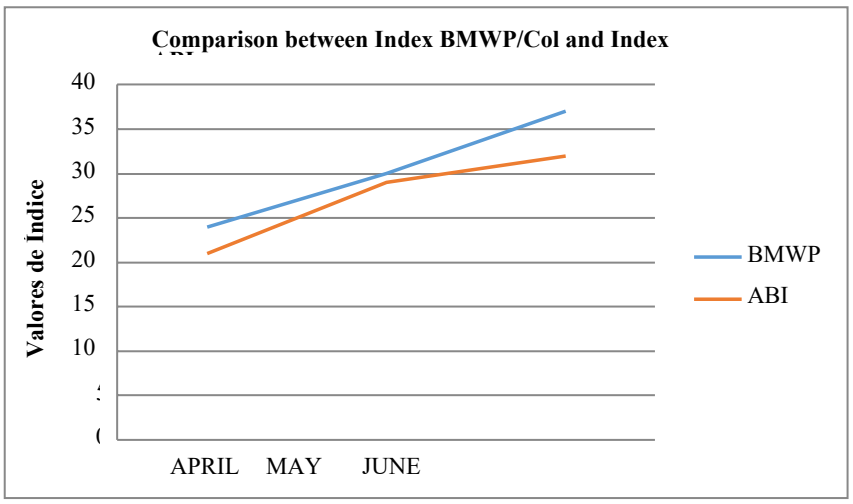

Figure 11. Comparison between BMWP and ABI indexes.

In Figure Nº11, it is shown that, in April, May and June, similar results were obtained between 21 and 37, proving that the two indices determine that the water quality is critical and, or doubtful.

IBF Index Analysis

In Table No. 18, the water quality values are displayed using the IBF index along with their respective classifications for each month of sampling (April, May, and June).

	APRIL	MAY	JUNE
IBF	3,033	2,974	3,021
CLASS	I	I	I
QUALITY	excellent	excellent	excellent

Table 18. Water quality through the IBF biological index.

In Table Nº 18, it is shown that in April, May, and June, similar values ranging from 3.021 to 3.033 were obtained, indicating a Class I rating. This means the water is of excellent quality, with no apparent organic contamination.

According to the application of the IBF index, in April, tolerant and sensitive families were identified, recording a sensitive family with a value of 6, the Hyalellidae family, followed by the tolerant families with values of between 3 and 1 those Notonectidae, Lymnaeidae, Cylicobdellidae, Glossiphoniida and Tubificidae.

In May, the most sensitive family recorded with a value of 8, the Libellulidae family and the least sensitive with a value of 6, the Hyalellidae family, and the pollution-tolerant families with values of between 3 and 1: Notonectidae, Tipulidae, Cylicobdellidae, Glossiphoniida and Tubificidae.

In the last monitoring carried out in June, 8 families were recorded, according to the tolerance value of the IBF index; a family with high sensitivity to pollution with a value of 8 was recorded, the Libellulidae family, with a value of 6, the family Hyalellidae that is less sensitive and the tolerant families with values of between 4 and 1: Cylicobdellidae, Notonectidae, Glossiphoniidae, Tubificidae, Lymnaeidae, Planariidae.

DISCUSSION

This research demonstrates the application of physical-chemical and microbiological analyses to calculate the Water Quality Index (WQI), specifically the National Foundation for Sanitation (NFS) Index and the DINIUS Index. These indices were applied to Santo Domingo Lagoon in Cotopaxi National Park, classifying water conditions during both rainy (April) and dry seasons (June) as poor and contaminated. These assessments were compared with current Ecuadorian legislation. It is worth noting that certain parameters analyzed are not specified in the bill (NE), making it challenging to determine compliance. For instance, dissolved oxygen levels fluctuate with seasonal changes.

It is recommended not to utilize the IBF index, as it is unsuitable for this type of lacustrine system studied in the research. Climatic factors such as precipitation and altitude contribute to the absence of the Ephemeroptera, Plecoptera, and Trichoptera (EPT) groups, which are considered water quality indicators. The substantial variations in flow during the studied months (April, May, and June) significantly reduced the number of

species compared to months with lower water flow. It is essential to note that many organisms develop depending on the climatic conditions of the environment.

The most common and abundant species detected at the sampling points are Notonectidae, Cylicobdellidae, and Hyalellidae. Families found in lower abundance include Lymnaeidae, Glossiphoniidae, Tubificidae, Libellulidae, Tipulidae, and Planariidae. In total, 1071 aquatic macroinvertebrates have been collected and classified into 9 families. According to the BMWP, ABI, and IBF methods, which indicate the degree of pollution tolerance, the application of the BMWP index defined the conditions of the lagoon, evaluating each of the identified families based on the ecology of each order and family of macroinvertebrates with the guidance of [8], taking into account the matrix of sensitivity of aquatic macroinvertebrates BMWP/Col. (2008), SENAGUA-Ecuador, the result showed that the lagoon belongs to class III and IV, indicating critical water conditions, meaning heavily polluted waters, and class III in June, indicating questionable water quality, or moderately polluted waters.

Using the ABI index, adapted from the BMWP index for high mountain ranges due to similar values (Jacobsen, 2008), tolerance levels were assigned based on the morphological characteristics and habitat of each family of macroinvertebrates, about [8]. Additionally, the matrix of sensitivity of aquatic macroinvertebrates ABI was complemented with the standardization project of tolerance levels of aquatic macroinvertebrates by SENAGUA - Ecuador, yielding similar results. It was demonstrated that the lagoon is in class IV, signifying poor water quality, i.e., highly polluted or critical waters. On the other hand, the IBF index was applied to determine organic pollution without needing specific organism identification [7].

Tolerance values for each identified family were also estimated with the help of [8]. The sensitivity matrix of aquatic macroinvertebrates IBF and the standardization project of tolerance levels of aquatic macroinvertebrates by SENAGUA - Ecuador resulted in a class I rating, signifying excellent water conditions. Therefore, Santo Domingo Lagoon shows no apparent organic pollution.

The pollution tolerance values estimated through the applied techniques, utilizing four biotic indices (two quantitative - ETP and IBF, and two qualitative - BMWP and ABI), will serve as a basis for creating a guide to aquatic macroinvertebrates applicable in Ecuador. In contrast, less demanding organisms may be abundant but do not indicate a healthy environment, resulting in lower qualitative indices [9].

Research employing bioindicators and physical, chemical, and microbiological analyses has proven highly relevant in the research field. These tools aim to ensure the conservation of ecosystems and optimize economic resources for future investigations. Similar studies have been conducted, such as "Assessment of the

Ecological Health of High-Altitude Lakes in Latin America" [10] which applied bioindicators and physical-chemical analyses, providing valuable information on the health of these ecosystems, and "Assessment of Biodiversity and Water Quality in Volcanic Lakes" [11] which focused on assessing water quality using bioindicators and physical-chemical analyses.

CONCLUSIONS

Through the application of the indexes NFS and DINIUS, it was determined that the water quality ranges from poor to contaminated. On the other hand, according to the BMWP/Col and ABI indexes, the water quality of Laguna Santo Domingo falls within Class III and IV, indicating critical, questionable, poor, and contaminated waters. However, the IBF Index established that the body of water falls into Class I, corresponding to water in excellent condition. Therefore, organic contamination is not apparent.

During the research period, 1071 aquatic macroinvertebrate individuals were collected and grouped into 9 families. The most representative groups were Notonectidae, Cylicobdellidae, and Hyalellidae. Environmental disturbances, such as the high altitude location and downstream position, directly and negatively affect the abundance of EPT families, one of the most sensitive groups to pollution. These environmental factors also contribute to the recent increase in abundance of those Lymnaeidae, Glossiphoniidae, Tubificidae, Libellulidae, Tipulidae, and Planariidae.

The application of indices and the physical-chemical and microbiological analyses will determine the water quality of Santo Domingo Lagoon, which is considered critical, poor, and contaminated. The results will enable the relevant authorities to propose strategies for improving the quality and conservation of water resources.

Through the application of the IBF index and based on the results obtained, the conclusion was reached that it contradicts the other water quality indices. Therefore, this index does not apply to this type of lake system.

REFERENCES

1. Segnini S. The use of benthic macroinvertebrates as indicators of the ecological condition of flowing water bodies. Ecotropics. In.: Universidad de LAF de CD de BL de E. de ILHMV; 2003. p. 16(2), 45 – 63.
2. Romero H. Contamination of water, soil and air. In. Barcelona: Herder; 2015.
3. (SIT) SIoT. Biological Question of Oxygen.. In.; 2006.
4. Carrera C, Fierro K. The aquatic macroinvertebrates as indicators of water quality: Monitoring manual.. In EcoScience. ; 2001; Quito - Ecuador. p. 67.
5. Brown, R., McCleland, N. Water Quality Index. Application in the Kansas River Ba-sin. In ; 1973.
6. Ríos Touma B., et Al. The Andean Biotic Index (ABI): revised tolerance to pollution values for macroinvertebrate families and index performance evaluation. In. España; 2014.
7. Resh VH, Myers MJ and Hannaford MJ. Macroinvertebrates as biotic indicators of environmental quality. In Methods in Stream Ecology. San Diego: In FR Hauer. y GA Lamberti; 1996. p. 647-668.
8. Roldán G. Bioindication of water quality in Colombia: Use of the BMWP/Col method. In. Colombia: University of Antioquia; 2003. p. 164.
9. SH D. Design of an Index of Water Quality., Water Resources Bulletin. In ; 1987. p. 833, 843.
10. Mandaville S. Benthic Macroinvertebrates in Taxa Tolerance Values, Metrics, and Protocols Soil & Water Conservation Society of Metro Halifax. In.; 2002.
11. Rosenberg, DM and Resh VH. Freshwater biomonitoring and benthic macroinvertebrates. In. New York: Chapman and Hall; 1993. p. 488.
12. Abdel Raouf, Homaidan, IBM Ibraheem. Microalgae and wastewater treatment. In.: Saudi Journal of Biological Sciences 19; 2012. p. 257-275.
13. American society for testing and materials. ABS (Annual book of Standards). 1994.
14. Determination of pH in water.. In Method ASTM D.; 1990. p. 1293-84.
15. Acosta R, Rieradevall M, Ríos B, Prat, N. Proposal of a protocol for evaluating the ecological quality of andean rivers (CERA) and its application to two watersheds in Ecuador and Peru. In.: Limnetica; 2009. p. 35-64.
16. Tercedor A. Aquatic macroinvertebrates and river water quality. In.; 1996.
17. Water Symposium in Andalucía (SIAGA). In Memorias IV. Almeria Nº2 p. 203-213.
18. Alba Tercedor, Sanchez O. A quick and simple method to evaluate the biological quality of running water based on Hellawell. In.; 1988.

19. Arocena R, Conde D. Methods in Ecology of Continental Waters, with Examples of Limnology in Uruguay. In. Montevideo: DIRAC/FC/UDELAR; 1999. p. 233.
20. 512-89 A. Standard Test Methods for Chloride Ion in Water. In. Hiladelphia PA: American Society for Testing and Materials, USA, ASTM Committee on Standards; 1989. p. 481-484.
21. Brenes R RL. The water: its properties and its biological importance. In ; 2015.
22. Chapman D. Water Quality Assessments: A Guide to the Use of Biota, Sediments and Water in Environmental Monitoring.. In ; Chapman, D; London. p. 626.
23. I C. Development of a biotic index to evaluate the ecological quality of water. In ; 2000.
24. I C. Development of a biotic index to evaluate the ecological quality of water. In ; 2000.
25. Sh D. Social Accounting System for Evaluating Water Resources. In ; 1972; Water 2. , vol 8, no. 5, October 1972, pp. : Resources Research. p. 1159 – 1177.
26. Domínguez L., Goethals P. and De Pauw N. Aspects of the physicochemical environment of the Chaguana river: a first step in the use of benthic macroinvertebrates in the evaluation of water quality.. In ; 2005: ESPOL Technological Journal. p. 127-134.
27. W H. Rapid Field Assessments of Organic Pollution With A Family Level. In ; 1988.
28. Biotic Index. In Journal Of The North American Benthological Society. ; USA.
29. INEC. Population by sex, according to province, parish and registration district. [Online].; 2010 [cited 2023 10 15. Available from: http://www.ecuadorencifras.gob.ec/documentos/web- inec/Tabulados_CPV_2010.
30. INEN. In Standard Ecuadorian NTE INEN 2.; 1998. p. 169, 98.
31. A J. Macroinvertebrates: composition, life histories and production. In Tropical stream ecology, chapter 4.; 2008.
32. MAE. [Online].; 2017. Available from: http://suia.ambiente.gob.ec/documents/10179/1232803/Reporte+Registro+Visitas+2017+%28 hasta+septiembre%29.pdf/2d336694-0d3e-4d1b-8698-d5628fe03b37.
33. R M. Ecology. In.; 1991. p. 951.
34. ORGANIZATION PH. Guide lines for Drinking Water Quality, criteria relative to the health and other information base. In World Health Organization. Washington DC: Scientific Publication N° 506; 1987.
35. W O. Environmental indices, theory and practice, AA science, Ann Arbor. In. Michigan; 1978.
36. Ryding, S & Rast, W. The Control of Eutrophication in Lakes and Marshes. In.; 1992.
37. Madrid and UNESCO. In. Paris: Pirámide p. 375.
38. Shuval, IH et al.. Health effects of nitrates in water.. In.: EPA; 1977. p. 600/1-1-77-030.
39. Simboni Ruiz, N., Carvajal, Y. & Escobar, J. Revision of physicochemical parameters as indicators of water quality and contamination. In Engineering and Research.: National University of Colombia; 2007. p. 172-181.

40. SNET. Proposals for the decontamination of the rivers Acelhuate, Sucio and Suquiapa. In.; 2002.
41. National Service of Territorial Studies. In.
42. Valenzuela J. Exploration of possibilities to propose a train of treatments for hardness removal that achieves technical and economic optimization of the process. In. Mexico: Universidad de las Americas Puebla; 2004. p. 12-20.
43. Vázquez G., Castro G., González I., Pérez R. & Castro T.. Bioindicators as tools to determine water quality. In.; 2006. p. 7.

Received: October 9th 2023/ **Accepte**d: January 15th 2024 / **Published:**15 February 2024

Citation: Ceballos Peñafiel K N, Quishpe Guanoluisa M A. Determination of water quality through using bioindicators, physical-chemical and microbiological analysis of the lagoon Santo Domingo of the national park Cotopaxi, province of Pichincha, period 2018. Revis Bionatura 2024; 9 (1) 20. http://dx.doi.org/10.21931/RB/2024.09.01.20

Additional information Correspondence should be addressed to *natthi.ceballos@gmail.com*
Peer review information. Bionatura thanks anonymous reviewer(s) for their contribution to the peer review of this work using https://reviewerlocator.webofscience.com/

Bionatura ISSN. First 13909355 Ecuador. **Scopus coverage years**: from 2016 to the present
Publisher's Note: Bionatura stays neutral concerning jurisdictional claims in published maps and institutional affiliations.

Bionatura
Ibero-American Journal of Biotechnology and Life Sciences

Article

Salud mental en reclusos del centro de Privación de Libertad de Bolívar. 2022

Mental health in inmates of the Bolívar Deprivation of Liberty Center. 2022

Silvana Ximena López Paredes[1*]; *María Rosa Mas Camacho*[2]; *Vanessa Katherin Erazo Guzmán*[3]; *Shirley Estefanía López Zapata*[4]

[1]*Universidad Estatal de Bolívar. Campus Académico "Alpachaca" Av. Ernesto Che Guevara s/n y Av. Gabriel Secaira, Guaranda, Ecuador,*

[2]*Universidad Estatal de Bolívar. Campus Académico "Alpachaca" Av. Ernesto Che Guevara s/n y Av. Gabriel Secaira, Guaranda, Ecuador, mmas@ueb.edu.ec*

[3]*Universidad Estatal de Bolívar. Campus Académico "Alpachaca" Av. Ernesto Che Guevara s/n y Av. Gabriel Secaira, Guaranda, Ecuador, kerazo@mailes.ueb.edu.ec*

[4]*Universidad Estatal de Bolívar. Campus Académico "Alpachaca" Av. Ernesto Che Guevara s/n y Av. Gabriel Secaira, Guaranda, Ecuador, shlopez@mailes.ueb.edu.ec*

** Correspondence: slopez@ueb.edu.ec*

Available from. http://dx.doi.org/10.21931/RB/2024.09.01.23

RESUMEN

El trabajo que se expone describe un estudio realizado en el Centro de privación de libertad Bolívar N.1, con el personal recluso en sus instalaciones. Dada la importancia social y el derecho de todos los seres humanos a una condición de salud satisfactoria, el objetivo fue evaluar la condición física y mental de los reclusos, así como promover actividades de promoción en salud. Se realizó una investigación descriptiva transversal cuantitativa a 230 personas del género masculino, internas en la institución, mediante el uso del inventario de Beck, para evaluar la condición física y mental; el desarrollo de un programa educativo, con la aplicación del método IKIGAI, la técnica de lluvia de ideas y el método de árbol de causa y efecto; que facilitaron la expresión de sentimientos, emociones y la identificación de sus propósitos de vida, con el apoyo de talleres de lectura, pintura y bailoterapia. Los resultados arrojaron estados de depresión en porcentajes similares de leve y moderado, que suman un 68% de afectados, y signos emocionales predominantes de somnolencia, ganas de llorar y cansancio; y en porcentajes significativos, la irritabilidad, insomnio, desconcentración, tristeza, pérdida de interés, ansiedad y culpabilidad. El programa educativo permitió a los prisioneros visualizar su futuro, descubrir sus pasiones en la vida y adquirir confianza para un correcto y armonioso estilo de vida.

Palabras clave: Depresión, prisioneros, programa, reclusos, salud mental

ABSTRACT

The work presented describes a study conducted at the Bolívar N.1 Detention Center with detained personnel in its facilities. Given all human beings' social importance and right to a satisfactory health condition, the objective was to assess prisoners' physical and mental condition and promote health promotion activities. A quantitative transversal descriptive research was carried out on 230 men internally in the institution using the

Beck inventory to evaluate their physical and mental condition; the development of an educational program with the application of the IKIGAI method, the technique of the rain of ideas, and the tree of cause and effect method, which facilitated the expression of feelings and emotions and the identification of their life purposes, supported by workshops of reading, painting, and dance therapy. The results cast states of depression in similar percentages of mild and moderate, summing up 68% of affected and predominant emotional signs of drowsiness, cravings for crying, and fatigue, and in significant percentages, irritability, insomnia, discontent, sadness, loss of interest, anxiety, and guilt. The educational program enabled prisoners to visualize their future, discover their passions in life, and gain confidence for a proper and harmonious lifestyle.

Keywords: Depression, prisoners, program, inmates, mental health

INTRODUCCIÓN

La depresión, según la Organización Mundial de la Salud[1], es una enfermedad mental que se presenta de forma común a nivel mundial, estimándose que cerca del 5% de los adultos la padecen, siendo esto cerca de 280 millones de personas. Esta enfermedad afecta directamente la carga mundial en los sistemas de salud, siendo una de las principales causas de discapacidad. Explica la Organización Mundial de la Salud que la depresión es un trastorno mental que puede presentarse en diferentes formas, dependiendo los contextos y se clasifican en episodios leves, moderados o graves, según la intensidad de los síntomas. Esta enfermedad es causada por la conjunción de diversos factores de riesgo, tales como los sociales, psicológicos o biológicos, siendo aquellos que se encuentran expuestos a eventos traumáticos los más expuestos a padecerla.

En el caso de las personas que se encuentran privadas de libertad, existen diversas situaciones que hacen que estas sean más propensas a sufrir de enfermedades de salud mental, según un estudio realizado por Jiménez-Puid[2] en Cuba, se identifica que en las poblaciones de reclusos se identifican manifestaciones psicológicas displacenteras, con una incidencia de enfermedades mentales de hasta 7 veces mayor que en la población general, debido principalmente a los cambios del entorno, aislamiento afectivo, escasa intimidad, rutina, frustración y cambios en las escalas de valores.

Por su parte, Valle Vega[3] en elestudio realizado con las personas privadas de libertad del Centro de Rehabilitación Social Cotopaxi encontró un 48% a que ocurriera algo, palpitaciones o aceleración cardíaca en el 38%, sensación de terror en el 48,5%, agitación en el 35,8%, con miedo a morir el 37%, y asustados el 40% de los que formaron oarte del estudio.

En este mismo orden de ideas en Colombia, Acosta et al.[4] pudieron establecer que de 4997 hombres privados de libertad en un centro penitenciario de Antioquia, un porcentaje importante de ellos presentaban cuadros depresivos asociados a su condición de estar en un centro penitenciario, al sufrimiento, la angustia, la separación de sus familiares y la imagen negativa que tienen de ellos mismos.

En un estudio realizado por Rodas[5], en Ecuador se identificó la prevalencia de depresión en nivel leve y moderado, específicamente en una población de adultos mayores que se encuentran privados de libertad en el "Centro de Rehabilitación Social Regional Sierra Centro Norte Cotopaxi", los cuales repercuten en la calidad de vida de los reclusos e interfieren en la realización de las actividades diarias, por lo que se propone una intervención valorar continuamente la situación de la salud mental de los reclusos y aplicar una serie de actividades terapéuticas a fin de mejorar la calidad de vida y aminorar la incidencia o agravamiento de la depresión.

Igualmente, en Ecuador, en otro estudio realizado en el "Centro de detención provisional El Inca, Masculino Pichincha N.1" con 261 hombres privados de libertad, Chacaiza[6] estableció que casi en su totalidad presentaba algún trastorno de salud mental, como ansiedad generalizada, depresión mayor y riesgo de suicidio, condición que se ve más generalizada en aquellos reclusos con mayor tiempo de permanencia en el centro.

Aunque el trabajo realizado por Abedrabbo[7] en Guaranda no es de fecha reciente, se incluye puesto que pudo establecer al encuestar a 96 hombres y 3 mujeres recluidas en el "Centro de Rehabilitación Social Guaranda" en el primer semestre del 2011, que a mayor tiempo de reclusión el riesgo de desarrollar síntomas somáticos, disfunción social, depresión severa, ansiedad e insomnio, aumentaba, encontrando además que el 85% de los privados de libertad presentaba depresión y ansiedad.

La promoción y el cuidado de la salud mental en las personas privadas de la libertad son temas de gran importancia en la sociedad actual, ya que estas personas tienen un mayor riesgo de desarrollar problemas de salud mental debido a las condiciones de encierro y a la naturaleza de sus delitos. La promoción de la salud mental en las personas privadas de la libertad incluye medidas preventivas para ayudar a estas personas a mantener un buen estado mental y evitar la aparición de problemas de salud mental. Estas medidas incluyen la promoción de un ambiente seguro y estable, la educación sobre la salud mental y la prevención de la violencia, así como la promoción de actividades recreativas y programas de rehabilitación[8].

Por otro lado, el cuidado de la salud mental en las personas privadas de la libertad incluye el tratamiento y la atención de los problemas de salud mental existentes. Esto puede incluir terapia, medicación y programas de rehabilitación específicos. Es importante que los tratamientos y programas sean personalizados y adaptados a las necesidades individuales de cada persona, ya que los problemas de salud mental pueden variar ampliamente. Además, es importante que estos tratamientos estén disponibles de manera continua y sostenible, para garantizar la mejoría y la recuperación de las personas privadas de libertad[9].

Se hace fundamental que los profesionales que trabajan en estos entornos estén especialmente capacitados para atender a personas privadas de libertad y estén familiarizados con las necesidades y desafíos únicos que enfrentan estas personas. La colaboración interdisciplinaria entre profesionales de la salud mental, el sistema penal y otros servicios de apoyo es esencial para garantizar un enfoque integral y efectivo en la promoción y el cuidado de la salud mental de las personas privadas de la libertad.

En Ecuador, para el año 2022, se contaba con una población carcelaria de 36.599 reclusos, con 36 centros de rehabilitación de los cuales 93.46% son hombres y 6.54% mujeres. Actualmente se promueve la implementación de terapia conductual y ocupacional en todos los centros de rehabilitación social a nivel nacional, a través del Ministerio de Justicia. Sin embargo, es un proceso que aún está lejos de ser completado. En el país no existen unidades criminológicas dentro de las unidades penitenciarias (centros de privación de la libertad) ni asistencia médica psiquiátrica disponible para sus residentes, por lo que no existe un sistema que pueda prevenir o tratar los trastornos del estado de ánimo y tampoco tratar ni evitar complicaciones que deriven de los mismos[10].

Ahora bien, desde el punto de vista legal y normativo, la Constitución del Ecuador[11] establece en el artículo 203 que el sistema de centros de rehabilitación social y detención provisional debe promover y ejecutar planes educativos, de capacitación laboral, de producción agrícola, artesanal, industrial, salud mental y física, y de cultura y recreación. Además, se indica que se deben tomar medidas de acción afirmativa para proteger los derechos de las personas, incluyendo la salud, que es un derecho garantizado sin discriminación alguna. El artículo 51 de la Constitución también reconoce los derechos de las personas privadas de libertad, incluyendo el derecho a contar con los recursos humanos y materiales necesarios para garantizar su salud integral en los centros de privación de libertad.

La salud física y la salud mental son fundamentales para los privados de libertad, ya que estos individuos se encuentran en una situación especialmente vulnerable. El derecho a la salud integral, gratuita y de calidad es un derecho fundamental que debe ser garantizado por el Estado, tanto en la Constitución como en leyes específicas como el Plan Creación de Oportunidades[12] y la Ley Orgánica de Salud[13]. Estas leyes reconocen que la salud no solo se refiere a la ausencia de enfermedades, sino al completo estado de bienestar físico, mental y social, y que es un derecho humano inalienable e indivisible, responsabilidad primordial del Estado. Además, es importante destacar que la salud mental también es un derecho fundamental y necesario para garantizar el bienestar integral de las personas privadas de libertad.

En el caso de las acciones de salud dentro del sistema penitenciario del Ecuador, se destacan en el Reglamento del Sistema Nacional de Rehabilitación Social[14] en el artículo 92 que se debe realizar una evaluación de salud inicial, donde entre otros se debe identificar los problemas de salud mental, con énfasis en la ansiedad, depresión, riesgo suicida, entre otros. Así mismo, en el artículo 222 de la atención de salud mental se establece que el ente encargado de la salud pública implementará servicios de salud mental para personas con problemas de uso y consumo de alcohol y otras drogas, así como trastornos mentales, en los centros de privación de libertad mediante programas especializados para la gestión, intervención y tratamiento de las personas privadas de libertad. Estos servicios se brindarán a través de modalidades ambulatorias e intensivas ambulatorias, según el modelo de gestión que sea adecuado para el contexto de privación de libertad.

El artículo antes referido del Reglamento del Sistema Nacional de Rehabilitación Social[15] destaca la importancia de brindar servicios de salud mental a las personas en los centros de detención, quienes pueden tener tasas más altas de abuso de sustancias y problemas de salud mental en comparación con la población general. También señala que los servicios serán adaptados a las necesidades específicas de los centros de detención, lo que sugiere un enfoque en la personalización y adaptabilidad en la prestación de servicios de salud mental a las personas privadas de libertad.

En el contexto del presente estudio, se abordó la problemática de la gestión de la salud mental en el Centro de Privación de Libertad Bolívar N.1 ubicado en el cantón Guaranda, donde se atienden a 217 personas privadas de libertad. Según el Informe de Visita al Centro de Rehabilitación Social de Varones Guaranda, realizado por la Defensoría del Pueblo (2018) con relación al acceso de los sujetos privados de libertad a la atención de salud mental, se identifica que el Centro de Privación cuenta con un profesional de psicología del Ministerio de Salud Pública, atendiéndose entre cuatro o cinco reclusos diarios, sin embargo en las entrevistas directas a los sujetos privados de libertad estos manifestaron no recibir atención psicológica y desconocer a las profesionales encargados del área.

En una visita preliminar realizada se logró identificar, según información suministrada por la administración del Centro de Privación de Libertad Bolívar N.1, que, de las 217 personas privadas de libertad, al menos 200 padece de algún nivel de depresión. Con relación a su situación, se describe por parte de las autoridades en materia sanitaria, que dentro de las principales causas de la depresión se encuentra que las visitas familiares son cada 15 días.

El proyecto que se describe tuvo por objetivo aportar en el ámbito de la prevención de salud de los sujetos privados de libertad en el Centro De Privación De Libertad Bolívar N.1., enfocado en la reducción del riesgo de eventos de depresión o aumento del nivel de depresión para lo que se desarrolló un plan educativo en conjunto con los profesionales que laboran en el área junto a estudiantes de la carrera de enfermería de la Universidad Estatal de Bolívar en la institución mencionada enfocado en brindar cuidados en salud mental en las líneas de acción expuestas.

MATERIALES Y MÉTODOS

El proyecto desarrollado es una investigación cuantitativa de corte transversal que tuvo como población 241 personas privadas de libertad en el Centro De Privación De Libertad Bolívar Número 1, a quienes se les consultó sobre la aceptación para su participación en el proyecto, accediendo 230 personas del género masculino que conformaron la muestra del estudio.

Se aplicó el inventario de Beck[16] como instrumento para evaluar la condición física y mental de los reclusos participantes. Se establecieron las medidas antropométricas mediante una ficha de registro y se estableció el nivel de depresión de los PPL mediante el inventario de depresión de BECK, la cual es un cuestionario auto aplicado diseñado para evaluar los síntomas de depresión en adultos, el mismo fue desarrollado por el Dr. Aaron T. Beck y su equipo en la década de 1960. La escala consta de 21 preguntas, cada una relacionada con un síntoma específico de la depresión, como el estado de ánimo triste, la falta de interés o placer en actividades, la falta de energía, la dificultad para conciliar el sueño, la autoevaluación negativa, entre otros[17].

Las preguntas se responden en una escala de 0 a 3, donde 0 indica que el síntoma no está presente, 1 indica que el síntoma es leve, 2 indica que el síntoma es moderado y 3 indica que el síntoma es grave. Los puntos obtenidos en las preguntas se suman para obtener un puntaje total. El puntaje total se utiliza para determinar el nivel de depresión del paciente, siendo un puntaje de 0-13 considerado como un rango normal, de 14-19 considerado como un rango leve de depresión, de 20-28 considerado como un rango moderado de depresión y un puntaje de 29 o más considerado como un rango grave de depresión.

Para este proceso se hacen visitas al centro de privación en tres ocasiones por parte de los investigadores y estudiantes colaboradores, logrando completar así el registro de los datos de cada persona.

El Inventario de Beck es considerado una herramienta útil y confiable para evaluar los síntomas de depresión en adultos y se ha utilizado ampliamente en investigaciones clínicas y en la práctica clínica. Sin embargo, es importante tener en cuenta que los resultados de la escala de Beck deben ser interpretados por un profesional de la salud capacitado ya que no es una herramienta diagnóstica y debe ser utilizada en conjunto con otras evaluaciones[17].

El uso de una escala de esta naturaleza permitió a los investigadores recolectar datos objetivos y medibles sobre el nivel de depresión de los privados de libertad. Los resultados de la investigación fueron utilizados para desarrollar un programa educativo para abordar el problema de la depresión entre los privados de libertad, y para la promoción de cuidados de salud mental en las personas privadas de libertad en el Centro de Privación de Libertad Bolívar número 1.

Durante el proceso de abordaje de la depresión, se realizaron diversas actividades para mejorar el conocimiento y la comprensión de los participantes, lo que se realizó por grupos acorde a la clasificación previamente realizada de depresión: mínima, leve, moderada y grave. Inicialmente se llevaron a cabo dos charlas en cada grupo referido, donde se abordó la definición de la depresión, sus síntomas y los factores de riesgo, así como los principales detonantes. Posteriormente se realizó, también por grupos de clasificación, una actividad de retroalimentación donde se construyó un árbol de causa y efecto que les ayudaría a reconocer los signos de la depresión. Además, se efectuaron conversatorios con preguntas abiertas referentes a las causas de su condición de privación de libertad, narrando anécdotas personales que permitieron recopilar información de los PPL sobre el desarrollo y avance de las actividades.

Por otra parte, se planificaron y desarrollaron tres talleres iniciales con enfoques diferentes (por grupos de clasificación de ansiedad), un primer taller para la identificación de factores estresantes y las causas y consecuencias de la depresión, y los dos siguientes constituyeron actividades interactivas que permitieron a los participantes generar opiniones sobre las consecuencias de la depresión y reconocer sus propias emociones.

Una cuarta actividad interactiva se centró en definir el propósito de vida con la aplicación del método IKIGAI, enfocado a que manifestaran sobre su pasión, misión, profesión y vocación, lo que se hizo con la entrega de material impreso donde graficaron y completaron espacios respecto a lo que ama, lo que le hace falta y en lo que se destaca y hace bien y es por lo que gana dinero.

A posteriori, de igual forma por grupos de clasificación de la ansiedad, se aplicó la técnica de lluvia de ideas en una quinta actividad interactiva donde realizaron propuestas de proyectos productivos según su visión de futuro de vida. Por su parte, el sexto taller se centró en el reconocimiento de los síntomas físicos de la depresión con actividades interactivas enfocadas en el manejo del estrés y la prevención de la depresión a través de la bailoterapia y un concurso de pintura. Finalmente, los grupos de lectura se establecieron como una actividad interactiva orientada a fomentar la participación y el aprendizaje continuo de los reclusos.

La bailoterapia se desarrolló de manera conjunta con la participación de todos los PPL, apoyados por equipos de sonido con música dinámica, bailes tradicionales y populares. Por otra parte, el concurso de pintura se trabajó solo con los adultos mayores a los que se les entregó un lienzo, temperas, acuarelas, pinceles, pegatinas, con lo que conformaron imágenes expresivas con creatividad.

Es importante destacar que la psicóloga del Centro de Privación de Libertad acompañó en todas las actividades efectuadas como parte del proyecto, quien recibió al concluir el mismo, un listado con la caracterización de cada recluso, su evaluación y las necesidades y requerimientos que cada quien manifestó, y que se sugiere deberían tenerse en consideración para mejorar sus calidades de vida.

Se llevó un registro de asistencia de los participantes y una bitácora como evidencia de cada actividad o sesión de trabajo efectuada con firmas e imágenes que avalan la veracidad del proceso desarrollado.

El proyecto fue desarrollado en un período de dos meses con la participación de 14 estudiantes y dos docentes de la carrera, alcanzando a beneficiar al 95,44% de las personas privadas de libertad de la institución. Durante este periodo se identificaron limitaciones como incongruencias del tiempo y horario del centro de privación de libertad, las que fueron solventadas de manera satisfactoria, y las limitaciones asociadas al sistema de seguridad y acomodamiento del equipo de trabajo para garantizar la seguridad del equipo en todo momento.

RESULTADOS Y DISCUSIÓN

Resultados de la clasificación de la depresión en privados de libertad

Los resultados obtenidos a partir del análisis de las respuestas a los 21 ítems del Inventario de Depresión de Beck muestran la distribución de la clasificación de depresión en personas privadas de libertad (Tabla 1). Del total de 230 que respondieron a la encuesta, el 35% de las personas presentaron síntomas de depresión leve, seguido por el 33% que afirma tener síntomas de depresión moderada, y solo el 3% de las personas presentaron síntomas de depresión grave, que si bien es un bajo porcentaje no por ello desprecia la necesidad de requerimiento de atención médica o psicológica a lo que debe sumarse con mayor inmediatez los de depresión moderada. El 12% de los casos se clasificaron como depresión mínima, lo que sugiere que una minoría de las personas no presentó síntomas significativos de depresión.

	Frecuencia	Porcentaje
Mínimo	27	12
Leve	80	35
Moderado	75	33
Grave	7	3
No participante	41	18
TOTAL	230	100

Tabla 1. Clasificación de depresión en PPL

Resultados de los grupos de apoyo conformados

Con el diagnóstico del examen preliminar se conformaron tres grupos de apoyo, en donde se clasificaron los reclusos en grupos de apoyo según la identificación de consumidoras de sustancias ilícitas, personas consumidoras de narcóticos anónimos y personas que cumplen un rango de edad avanzado. Las personas que formaron parte de estos grupos recibieron charlas educativas y de aprendizaje en donde se realizaron actividades motrices y audiovisuales.

Resultados del reconocimiento de los signos emocionales de la depresión en PPL

Se identificaron 12 signos emocionales (Tabla 2) en los que es absoluta la manifestación de somnolencia (100%), seguido de los deseos de llorar (91,66%) y el cansancio (75%). Son coincidentes los porcentajes de

las personas en reclusión que experimentan insomnio y desconcentración (66,66%), mientras que la mitad de ellos presentan irritabilidad (50,26%). Así mismo, en un porcentaje significativo se aprecian tristeza (41,66%), pérdida de interés (33,33%), ansiedad (41,66%), problemas físicos (41,66%) y culpabilidad (41,66%). Respecto a tener pensamientos suicidas, si bien no es un alto porcentaje, sí se considera de atención por su trascendencia (16,66%). Los resultados aseveran que es la depresión un problema común en privados de libertad y de la importancia de su identificación en estas poblaciones para actuar en consecuencia en el mejoramiento de la calidad de vida y la salud mental de estas poblaciones.

Signos emocionales		
	Frecuencia	**%**
Ganas de llorar	173	91,53
Irritabilidad	95	50,26
Tristeza	79	41,80
Pérdida de interés	63	33,33
Insomnio	126	66,67
Cansancio	142	75,13
Falta de apetito	47	24,87
Ansiedad	79	41,80
Desconcentración	126	66,67
Pensamientos de Suicidio	31	16,40
Problemas físicos	79	41,80
Somnolencia	189	100,0
Culpabilidad	79	41,80

Nota: Se corresponde a las respuestas de la encuesta aplicada en el estudio.

Tabla 2. Signos emocionales identificados en los reclusos.

Resultados de aplicación del método IKIGAI

El método IKIGAI se aplicó a las personas privadas de libertad en el Centro de Rehabilitación Social de Guaranda con el objetivo de ayudarlas a identificar sus fortalezas y debilidades, descubrir qué les da placer y cómo pueden aportar al mundo. Este ejercicio resultó ser muy valioso, ya que permitió a cada persona analizar el propósito de su existencia y dar sentido a sus acciones, motivándoles a mejorar día a día.

Los resultados obtenidos tras aplicar el método IKIGAI a personas con depresión leve, moderada y grave fueron positivos. Todos respondieron a los ítems sobre sus gustos, irritaciones, fuentes de felicidad y objetivos a futuro, lo cual ayudó a encontrar el equilibrio entre lo que hacen en el presente y lo que desean hacer en el futuro. Además, esto les permitió manejar situaciones difíciles sin alterarse y mantener una vida más saludable, incluyendo una alimentación sana, actividad física y cambios positivos en su vida diaria.

Resultados de la construcción del árbol de causa y efecto (Causas de la depresión, efecto de la depresión)

El método realizado con las personas privadas de libertad (PPL) buscó identificar los factores que influyen en la depresión. Se consideraron factores genéticos, físicos y ambientales apoyados en presentaciones y elementos dinámicos de participación individual. El resultado del método del árbol de causa y efecto fue un éxito, permitiendo que las PPL expresen sus sentimientos y emociones.

Árbol de problemas de la depresión en personas privadas de libertad respecto a la problemática de la depresión

I. Problema Central: Depresión en personas privadas de libertad

II. Causas:

A. Factores individuales:

- Trauma pasado.
- Historial de abuso de sustancias.
- Condiciones médicas preexistentes.
- Historia de problemas de salud mental.
- Falta de habilidades para manejar el estrés y las emociones.
- Falta de apoyo social.
- Dificultades para adaptarse a la vida en prisión.

B. Factores ambientales:

- Condiciones de vida en prisión.
- Aislamiento social.
- Estigma asociado con la prisión.
- Acceso limitado a servicios de atención médica y de salud mental.
- Falta de actividades y programas de rehabilitación.
- Problemas en las relaciones familiares y personales.

III. Efectos:

A. En el individuo:

- Sentimientos de tristeza y desesperanza.
- Pérdida de interés en actividades y relaciones previas.
- Problemas de sueño y apetito.
- Aislamiento social y problemas de relaciones interpersonales.
- Problemas de autoestima.
- Pensamientos y comportamientos suicidas.

B. En la sociedad:

- Mayor tasa de reincidencia.
- Mayor carga económica en el sistema de justicia penal.
- Efectos negativos en la familia y la comunidad.

IV. Soluciones:

- Mejora de las condiciones de vida en prisión.
- Aumento de las oportunidades de educación y trabajo en prisión.
- Programas de rehabilitación y tratamiento para abuso de sustancias.
- Mayor acceso a servicios de atención médica y de salud mental.
- Mejora de las relaciones familiares y personales a través de visitas y apoyo externo.

Resultados de la retroalimentación sobre la consecuencia de la depresión

La depresión es un trastorno que puede tener consecuencias en tres áreas principales: psicológica, física y social. La tristeza, falta de interés y aislamiento social son algunos de los síntomas más comunes, así como dolores, alteraciones del sueño y problemas cognitivos. La depresión no tratada puede limitar la vida de la persona y empeorar con el tiempo.

Para reducir las consecuencias de la depresión en personas privadas de libertad, es importante buscar un tratamiento adecuado lo antes posible. Investigaciones muestran que la duración sin tratamiento es un factor clave en la gravedad y las consecuencias de la depresión. A partir de las encuestas aplicadas se identificaron los estados anímicos, referidos con anterioridad en el presente trabajo, y se desarrollaron charlas y actividades de entretenimiento como formas de ayuda para superar la depresión.

Resultados del concurso de lectura

Se ejecutó un concurso de lecturas con las Personas Privadas de Libertad (PPL) que ayudó a desarrollar capacidades como la comprensión y concentración, y se usaron libros como Los Siete Hábitos de la Gente Exitosa[18], El Poder del Ahora[19], La Sabiduría de las Emociones[20] y El Camino del Guerrero[21]. Al tener una mayor comprensión de esta, los participantes disfrutaron de la lectura y fue también un elemento que favoreció la relajación individual, el desarrollo de la imaginación y el fomento del interés por aprender. Además, el desarrollo de la resiliencia y la sensación de valor y alegría tuvieron un impacto positivo en su salud y bienestar.

En resumen, el concurso de pintura y el curso de lectura fueron herramientas efectivas para mejorar la vida de los participantes en términos de comprensión, relajación y desarrollo personal.

Resultado del proceso y resultado de Bailoterapia

La bailoterapia consiste en una combinación de gimnasia aeróbica con pasos de diferentes ritmos latinoamericanos. Su objetivo fue bailar bajo la dirección de un instructor para adaptarse al ritmo de la música y hacer ejercicio de una manera divertida. La actividad requirió que los PPL usaran ropa cómoda y contaran con hidratación. Se seleccionaron canciones adecuadas de canciones conocidas y la preparación de una coreografía. Inició con un calentamiento previo, y luego se realizó la jornada durante 30 minutos de tiempo mínimo. La bailoterapia fue implementada en el cronograma de actividades de un grupo de personas (PPL) como forma de liberar estrés y salir de la rutina. Se obtuvieron resultados positivos, ya que los PPL se sintieron relajados y liberados del estrés, no se evidenció preferencia por algún tipo de música o ritmo, y solo experimentaban.

Resultados de tormentas de ideas de proyectos productivos

La realización de la actividad de tormenta de ideas se desarrolló de manera satisfactoria por la colaboración de las PPL quienes aportaron de forma entusiasta con ideas de proyectos productivos que pueden ser aprovechados a futuro por ellos mismos, expusieron ideas tales como taller de carpintería, huertos y jardines, programas de reciclaje, producción de textiles y artesanías, todo con el fin de comercializar de la mejor manera y que este sea productivo.

DISCUSIÓN

Acorde a lo mencionado por Revelo[22], es necesario asegurar el acceso a programas y tratamientos de alta calidad que estén disponibles, sean accesibles y aceptables para garantizar el derecho a la salud. Esto debe ser impulsado con la ética médica y con políticas públicas que sean inclusivas y restauren los derechos de las personas privadas de libertad. De esta manera, se contribuye a la construcción de una cárcel justa y respetuosa de los derechos humanos, lo cual es una obligación del Estado.

De forma similar, el estudio de Gómez-Figueroa y Camino-Proaño[23], identificaron que tras la revisión de distintos artículos se determina que hay necesidad de implementar un programa que contemple la evaluación diagnóstica de los presos al ingresar y la implementación de intervenciones terapéuticas para contrarrestar los efectos en la salud mental al estar privados de libertad. Para ello, se deben considerar factores como el tipo de trastorno detectado, los antecedentes del interno, el riesgo de padecer otras patologías o las características específicas de la cárcel. Entre las terapias que se recomiendan para tratar los trastornos mentales en las cárceles se encuentran la terapia cognitivo-conductual y el tratamiento farmacológico en casos específicos.

Algunos estudios se han realizado en el área, los cuales persiguen el objetivo de mejorar la salud mental de las personas privadas de libertad, tal como el realizado por Sierra, et al.[24] en Colombia, el cual se enfocó en desarrollar un programa de actividad física, la cual tuvo una duración de 15 semanas, donde se ejecutaron 45 sesiones 3 veces a la semana, lo cual generó mejoras en el estado de ansiedad. Otra experiencia similar fue la presentada en la investigación de Serrano[25] la cual se centró en la recuperación emocional de un grupo de privadas de libertas en el centro de rehabilitación de la provincia El Oro, donde por medio de un programa estructurado por talleres y actividades para la recuperación de la autoestima, mejoramiento del autoconcepto, de la autoimagen, control y autorregulación de impulsos.

Por otra parte, en otra investigación de orden similar fue la realizada por Illiana y Currás[26], donde se plantearon crear una intervención para tratar conductualmente los factores de riesgo relacionados con el suicidio en la cárcel, dicho programa se enfocó en técnicas cognitivas, empleando la psicoeducación con temáticas sobre la explicación de la conducta suicida, emociones y su impacto en la vida, habilidades de inteligencia emocional, y el impacto de la depresión en la conducta.

Finalmente, en un estudio realizado por Zamora[27], desarrollo una intervención psicoterapéutica llevada en 6 fases: la adquisición de conocimientos teóricos sólidos, la evaluación de la institución en cuestión, la revisión minuciosa de los registros, la implementación de terapia grupal para mejorar las habilidades sociales, la terapia individual y el monitoreo sistemático del progreso. Los talleres grupales fueron utilizados para fomentar la comprensión de los conceptos, las presentaciones audiovisuales se utilizaron para analizar situaciones de la vida real relacionadas con los temas discutidos, y los grupos de discusión se emplearon para examinar el discurso de los participantes. Como resultado de este trabajo, se observaron mejoras positivas en la población y se demostró la capacidad de cambio en las personas privadas de libertad.

CONCLUSIONES

Existe un predominio de estados de depresión en las personas privadas de libertad de la institución de consideración moderada y leve como sobresaliente, siendo la clasificación de grave en un porcentaje mínimo. Se identifican como signos emocionales predominantes la somnolencia, las ganas de llorar y el cansancio, así como con presencia en porcentajes significativos los signos de tener irritabilidad, insomnio, desconcentración, tristeza, pérdida de interés, ansiedad y culpabilidad.

Las actividades desarrolladas como parte del programa educativo permitieron a los prisioneros visualizar su futuro, descubrir pasiones en la vida y adquirir confianza para un correcto y armonioso estilo de vida, lo que acompañado por el apoyo de la familia les impulsó a mejorar, comprender y reconocer el valor de sus actos.

Se puede resumir que la promoción y el cuidado de la salud mental en las personas privadas de la libertad constituye un tema que debe ser abordado de manera proactiva y sistemática mediante servicios de salud mental de calidad que brinden un enfoque integral y personalizado, y así mejorar la calidad de vida de las personas en condición de reclusión social, lo que contribuirá a la seguridad y estabilidad de la sociedad en general.

Conflicto de interés: Los autores declaran no tener conflicto de interés.

REFERENCIAS

1. Organización Mundial de la Salud. (Marzo de 2021). Depresión. [Internet].OMS; 202 Disponibe en: Disponibe en: https://www.who.int/es/news-room/fact-sheets/detail/depression Publicado 31 de marzo de 2023. Accedido el 17 de noviembre de 2023.

2. Jiménez-Puig Elizabeth, Martínez Rodríguez Lesnay, Alzola Suárez Claritza. Ansiedad, depresión, bienestar subjetivo y salud mental general en reclusos. Rev Cub Med Mil [Internet]. 2021 Sep [citado 2023 Nov 17] ; 50(3): e1292. Disponible en: http://scielo.sld.cu/scielo.php?script=sci_arttext&pid=S0138-65572021000300005&lng=es. Epub 01-Sep-2021.

3. Valle Vega, EP. "Salud mental de las personas privadas de libertad en el contexto de la pandemia covid 19" [tesis de grado]. Pontificia UniversidadCatóloca del Ecuador. Sede Ambato: 2022

4. Acosta Tobón SA, Mosquera Perea KM, Córdoba Moreno LM, Murillo Urrego LD, Galeano Bonilla AK. Síntomas depresivos en hombres privados de libertad en el establecimiento carcelario Bellavista. Forenses [Internet]. 15 de enero de 2023 [citado 18 de noviembre de 2023];(6):107-30. Disponible en: https://ojs.tdea.edu.co/index.php/mforenses/article/view/1138

5. Rodas Castillo, M. "La depresión y su influencia en el deterioro cognitivo de los adultos mayores privados de la libertad del Centro de Rehabilitación Social Regional Sierra Centro Norte Cotopaxi". [Tesis de grado]. Universidad Tecnológica Indoamérica. Ambato: 2020.

6. Chacaiza Casco, NS. "Problemas de salud mental presentes en las personas privadas de libertad del : Centro de detención provisional El Inca, Pichincha Masculino N. 1". [tesis de grado]. Universidad Central del Ecuador. Quito: 2022.

7. Abedrabbo F. "Factores de riesgo para depresión y ansiedad en internos privados de su libertad del Centro de Rehabilitación Social Guaranda". [tesis de grado]. Ecuador: Universidad San Francisco de Quito. Quito: 2015.

8. Cuenca Gómez P. El tratamiento de las personas con problemas de salud mental en la normativa penal y penitenciaria. Reflexiones y propuestas. Revista de la Asociación Española de Neuropsiquiatría. [Internet]. [citado 2023 Nov 17] ; 2022; 42(141): p. 141-158.

9. Servicio Nacional de Atención Integral a personas adultas privadas de la libertad y a adolescentes infractores. (2020). Reglamento del sistema nacional de rehabilitación social. 86. Ecuador. Disponible en: https://atencionintegral.gob.ec/wp-content/uploads/2020/08/Reglamento-del-SIstema-de-Rehabilitacio%CC%81n-Social-SNAI-2020_compressed.pdf

10. Comisión Interamericana de Derechos Humanos. (2022). Personas Privadas de Libertad en Ecuador. 102. Ecuador: OEA. Disponible en. https://www.oas.org/es/cidh/informes/pdfs/Informe-PPL-Ecuador_VF.pdf

11. Asamblea Nacional Constituyente. (2008). Constitución de la República del Ecuador. Ultima modificación: 25-ene.-2021, 219. Ecuador. Disponible en: https://jprf.gob.ec/wp-content/uploads/2022/06/1.-Constitucion-de-la-Republica-del-Ecuador_MAYO2022.pdf

12. Secretaría Nacional de Planificación. (2021). Plan de Creación de Oportunidades 2021-2025. 122. Ecuador. Disponible en: https://www.planificacion.gob.ec/wp-content/uploads/2021/09/Plan-de-Creacio%CC%81n-de-Oportunidades-2021-2025-Aprobado.pdf

13. Congreso Nacional. Ley Orgánica de la Salud. Ley 07 (Registro Oficial Suplemento 423), Ultima modificación: 18-dic.-2015, 1-46. Ecuador. Disponible en: https://www.salud.gob.ec/wp-content/uploads/2017/03/LEY-ORG%C3%81NICA-DE-SALUD4.pdf

14. Servicio Nacional de Atención Integral a personas adultas privadas de la libertad y a adolescentes infractores. Resolución Nro. SNAI-SNAI-2020-0031-R. Reglamento del sistema nacional de rehabilitación social. 2020.

15. Defensoría del Pueblo. Defensoría del Pueblo Ecuador. Informe No. DPE- MNPT-2018-004-I. Informe de visita al centro de rehabilitación social de varones Guaranda. 2018.

16. Beck Aaron T. Inventario de Depresión de Beck (BDI-2). Consejo General de la Psicología. 2013. Disponible en: https://www.psi.uba.ar/academica/carrerasdegrado/psicologia/sitios_catedras/obligatorias/070_psicoterapias1/material/inventario_beck.pdf

17. Sanz J, Gutiérrez S, Gesteira C, García M. Criterios y baremos para interpretar el "Inventario de Depresión de Beck-II" (BDI-II). Behavioral Psychology [Internet]. 2014; 22(1): p. 37-59. Disponible en: https://www.behavioralpsycho.com/producto/criterios-y-baremos-para-interpretar-el-inventario-de-depresion-de-beck-ii-bdi-ii-pp-37-59/

18. Covey, S. Los Siete Hábitos de la Gente Exitosa. Argentina: Simón and Schuster, Nueva York. 2003. Disponible en: https://www.colomos.ceti.mx/documentos/goe/los7HabitosGenteAltamenteEfectiva.pdf

19. **Tolle E. El Poder del Ahora. Digital ed. México: Random House Mondadori, S. A; 2013.** Disponible en: https://www.colomos.ceti.mx/documentos/goe/los7HabitosGenteAltamenteEfectiva.pdf

20. Levy, N. La Sabiduría de las Emociones. España: Plaza& Janes Editores. S.A; 2000. Disponible en: https://www.studocu.com/es-ar/document/universidad-nacional-de-san-martin-argentina/psicologia-social/norberto-la-sabiduria-de-las-emociones-levy-doc-pdf-free/30312397

21. Long, J. El Camino del Guerrero. Japón. (s.f). Disponibe en: https://doi.org/https://pluckyvacancy40navarro.files.wordpress.com/2018/10/el-camino-del-guerrero-pa.pdf

22. Revelo, A. Salud mental y tratamiento penitenciario en las personas privadas de la libertad de los centros carcelarios en Colombia: una revisión sistemática. [tesis de grado]. Colombia. Universidad Cooperativa de Colombia. 2021. Disponible en: https://repository.ucc.edu.co/server/api/core/bitstreams/22c26205-afd4-4db5-9ec0-b8c0f6fb38c5/content

23. Gómez Figueroa, H., y Camino Proaño, A. Trastornos mentales y del comportamiento en el contexto carcelario y penitenciario. Rev. Esp Sanid Penit, [Internet]. 2022 [citado 18 de noviembre de 2023] 24(2), 70-80. Disponible en: https://scielo.isciii.es/pdf/sanipe/v24n2/es_2013-6463-sanipe-24-02-66.pdf

24. Sierra, M., Rodríguez, L., y López, N. Programa de actividad física sobre los niveles de ansiedad en adultos mayores privados de libertad. EFDeportes.com, Revista Digital, [Internet]. 2012 [citado 18 de noviembre de 2023] 17(173). Disponible en: https://www.efdeportes.com/efd173/actividad-fisica-en-adultos-privados-de-la-libertad.htm

25. Serrano, M. (2019). Programa de autoestima y habilidades sociales para ayudar a la recuperación de las internas del Centro de Rehabilitación Social Femenino del cantón Zaruma, en la provincia de El Oro, Reública del Ecuador. [tesis de grado]. Ecuador: Universidad Internacional de la Rioja. 2019. Disponible en:

https://reunir.unir.net/bitstream/handle/123456789/9571/Serrano%20Jaramillo%2C%20Maria%20Fernanda.pdf?sequence=1&isAllowed=y

26. Illana, I., y Currás, H. Propuesta de un programa de prevención del suicidio en la cárcel. Behavior & Law Journal, [Internet]. 2021 [citado 18 de noviembre de 2023] 7(1), 23-34. Disponible en: https://doi.org/10.47442/blj.v7.i1.85

27. Zamora, J. (2019). Intervención psicoterapéutica en promoción de habilidades sociales en personas privadas de libertad. Humanitas , [Internet]. 2019 [citado 18 de noviembre de 2023] 16(16), 1-21. Disponible en: http://74.208.91.144/uccr/index.php/humanitas/issue/view/17

Received: January 15th, 2023/ **Accepte**d: March 1st, 2024 / **Published:** March 15th, 2024

Citation: López Paredes S X; Mas Camacho M R; Erazo Guzmán V K; López Zapata S E. Salud mental en reclusos del centro de Privación de Libertad de Bolívar. 2022. Revis Bionatura 2024; 9 (1) 23. http://dx.doi.org/10.21931/RB/2024.09.01.23

Additional information Correspondence should be addressed to gabriela.rosero@espoch.edu.ec

Peer review information. Bionatura thanks anonymous reviewer(s) for their contribution to the peer review of this work using https://reviewerlocator.webofscience.com/

Bionatura ISSN. First 13909355 Ecuador. **Scopus coverage years**: from 2016 to the present

Bionatura
Ibero-American Journal of Biotechnology and Life Sciences

Article

Microorganisms associated with bacterial wilt disease in *Dendrocalamus asper* (Giant Bamboo) from Ecuador

Jaime Morante-Carriel[1,2], Marlon Vera-Carranza[1], Carlos Belezaca-Pinargote[1], Mercedes Carranza-Patiño[1], Robinson J. Herrera-Feijoo[1]**

[1]Faculty of Agricultural and Forestry Sciences, Quevedo State Technical University, Av. Quito Km 1/2, vía a Santo Domingo de Los Tsáchilas. 120302, Quevedo, Ecuador
[2]Plant Proteomics and Functional Genomics Group, University of Alicante, C/ San Vicente del Raspeig, s/n. 03690, San Vicente del Raspeig, Alicante, Spain
** Correspondencia: rherreraf2@uteq.edu.ec; jmorante@uteq.edu.ec*
Available from. http://dx.doi.org/10.21931/RB/2024.09.01.32

ABSTRACT

Dendrocalamus asper (Bamboo) is an essential component of forest ecosystems, whose health and survival are intrinsically linked to complex interactions with its microbiome. This study focuses on the pathogenic dynamics between the fungi *Arthrinium spp*. and *Erwinia spp*. Bacteria and their impact in the shoots wilting and culm rot in bamboo. Through humid chamber induction methods and selective cultivation techniques, pathogenic strains that significantly affect the regeneration and propagation of bamboo were identified and isolated. The investigation revealed a pathogenic synergy resulting in a high prevalence of diseases, 97% of the shoots evaluated showed signs of deterioration. Morphological identification challenged conventional techniques due to the variability of *Arthrinium spp*—conidia, suggesting the need for more specific identification methods. The findings suggest that regulating soil pH and using beneficial biofilms could be promising strategies to mitigate bacterial infection. This study highlights the importance of sustainable management and in-depth knowledge of microbial ecology for integrated disease management in bamboo ecosystems. Understanding these microbial interactions is crucial for developing effective control strategies and long-term conservation of these vital ecosystems.

Keywords: *Dendrocalamus asper*, *Arthrinium spp*., *Erwinia spp*., bacterial wilt, disease management.

INTRODUCTION

Bamboo is vital in forest ecosystems, providing critical structure and support for microorganisms. Microorganisms, in particular, significantly influence the nutrition and health of bamboo. Studies have shown that bacteria such as *Flavobacterium, Bacillus*, and *Stenotrophomonas* are essential in absorbing nitrogen elements in moso bamboo, which could influence its flowering time [1]. Bamboo planting can enrich soil fertility and increase tree species diversity in coastal ecosystems. In the bamboo forests of southeastern China, it has been observed that soil enzymatic and microbial activity is significantly altered [2]. Microorganisms not only improve nutrient availability [3]. Microbial communities also protect against pathogens [4], underscoring the importance of understanding microbial dynamics to sustain bamboo ecosystems.

Bamboo faces various diseases that can vary in prevalence and distribution worldwide, and microorganisms play a central role in these pathologies. Research has revealed that bamboo is an extensive reservoir of microorganisms, including fungi and bacteria, that should be investigated extensively, given its potential role in

plant growth and ecosystem functioning [5]. The invasion of native bamboo in subtropical forests can alter soil microbial communities. Disturbance affects litter decomposition and nutrient cycling. The threat of local forest ecosystems is affected due to microbial disturbance [6]. The findings highlight the need to carefully monitor bamboo planting and expansion to prevent adverse impacts on biodiversity and ecosystem health.

Adverse effects negatively correlate with soil pH and the abundance of stress, virulence, and sulfur-cycling genes [7]. Furthermore, specific genera such as *Arthrobacter*, *Pseudomonas*, *Acidobacteria* GP6, and *Pasteuria* may be potential biological control agents for bacterial wilt [8]. The findings underline the importance of understanding soil bacterial community structure for effectively managing bacterial wilt in bamboo.

The interaction between microorganisms and the plant response allows activating the defense mechanisms of *the Dendrocalamus asper* against microbial attacks crucial for survival. Research has shown that biofilm formation in the rhizosphere, observed in organic hydroponic systems, may be responsible for suppressing bacterial wilt [9]. Soil acidification aggravates the occurrence of bacterial wilt, suggesting that the regulation of soil acidification is a prerequisite and fundamental condition for disease control [10]. Previous findings are critical to developing management strategies that improve the physiological and biochemical responses of bamboo to bacterial infection, which could include modulation of soil pH and utilization of beneficial biofilms as part of an integrated approach to control diseases.

Microorganisms, including specific bacteria, play a crucial role in bacterial wilt that affects various plants, including *D. asper*. Studies have identified that strains of bacteria such as *Ralstonia solanacearum* vary considerably in Brazil, suggesting that host resistance to control bacterial wilt should be targeted primarily by region [11]. Researchers have reported relevant findings on endophytic bacteria. Bacteria isolated from live oak trees in Texas showed the ability to inhibit the pathogen that causes oak wilt in vitro. Preinoculation with the bacteria Pseudomonas denitrificans 1-15 resulted in a 50% reduction in the incidence of diseased trees. Preinoculation decreased crown loss in affected trees by 17% [12]. The findings highlight the importance of accurately identifying and classifying wilt-associated bacteria to develop effective control strategies.

D. asper possesses intrinsic defense mechanisms against microbial attacks, which include complex physiological and biochemical responses. Induction of resistance against diseases such as wilt caused by *Bursaphelenchus xylophilus* using selected pine endophytic bacteria is an example of how microorganisms can manage diseases by inducing systemic resistance in plants [13]. It has been observed that soil acidification can lead to outbreaks of bacterial wilt, underscoring the dynamic interaction between soil conditions and plant susceptibility to diseases [14]. The studies underscore the need to understand better plant responses to bacterial infection to improve disease management strategies.

The Bamboo *Dendrocalamus giganteus* is found in an environment where synergy between microorganisms can play a crucial role in its health and survival. Studies have shown that different species of tree-dwelling insects carry a variety of microorganisms, including pathogens, indicating their potential as vectors of plant diseases [15]. It has been observed that interactions between plant pathogens can lead to disease complexes that are more common than expected. Understanding these mechanisms can have essential implications in the epidemiology and management of plant diseases [16]. Therefore, it is plausible that a synergistic action between microorganisms could be present in pathogenic attacks on *D. giganteus* Munro. However, direct evidence specific to this bamboo species has yet to be established in the scientific literature.

The hypothesis that there is a synergy between different pathogenic microorganisms that contribute to bacterial wilt in *D. asper* in Ecuador is supported by the observation that interactions between plant attackers can be asymmetric, time-dependent and species-specific [17]. These complex interactions can influence the susceptibility of plants to diseases and their ability to resist or succumb to pathogen attacks. It has been reported that

plant pathogenic microorganisms can colonize insect tissues, revealing a network of interactions that affects substantial invaders [18]. The findings highlight the need to investigate further the possibility of microbial synergies in bacterial wilt of bamboo, particularly in regions such as Ecuador, where this disease can negatively impact bamboo production. This research aimed to identify and characterize the microorganisms associated with bacterial wilt diseases in *D. asper* (giant bamboo) from Ecuador.

MATERIALS AND METHODS

Plant material

The plant material was collected on the premises of the Special Forces Group (SFG) No. 26 CENEPA in Quevedo (Ecuador), which was subjected to a humid chamber to induce the manifestation of the causal agent(s) of the disease. This study area was selected based on the prevalence of disease symptoms in bamboo, which provides a relevant context for pathogen induction for the exact location of the study area (Figure 1). The experimental research was conducted in the "La María" Campus laboratories at the State Technical University of Quevedo, Ecuador.

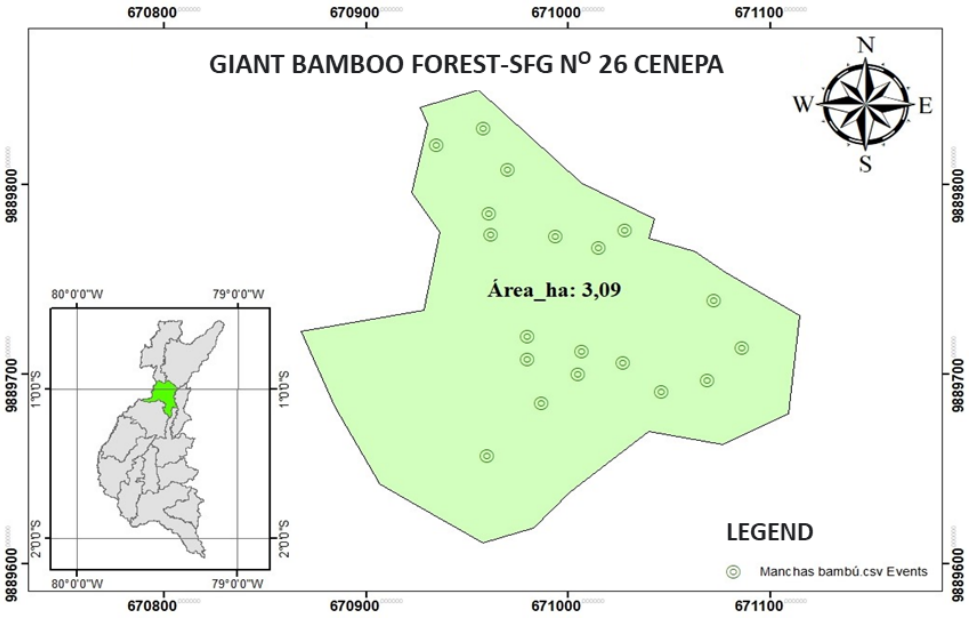

Figure 1: Location of plant material.

Induction in a wet chamber

Plant material with signs of necrosis was placed in 14" x 20" polypropylene covers to induce the manifestation of disease-causing agents in bamboo. A controlled relative humidity was maintained for 72 to 96 hours. The effectiveness of this method was evaluated by observing morphological changes in the bamboo tissue, which were documented photographically. This technique is common in plant pathology to promote the manifestation of pathogens [14].

Preparation of culture medium

Two modified culture media were prepared to promote the selective growth of fungi and bacteria. The PDA medium was enriched with Streptomycin (1mg L^{-1}) to inhibit unwanted bacterial growth, while nutrient agar was used for bacterial cultivation. Both media were diluted in distilled water and autoclaved at 121°C for 25 minutes. These media were selected based on previous literature indicating their effectiveness in isolating pathogens from bamboo [19].

Sowing in Petri plates

Aseptic samples of the induced plant material were seeded in Petri plates containing the prepared culture media [20]. Pieces of bamboo culm were cut with a length and width of 2.5 cm and a thickness of 0.5 to 1 mm and incubated at 28 ± 2 °C for 8 days. Incubation was performed in a calibrated incubator to ensure consistency of growth conditions.

Sowing in carrot sandwiches

The carrot sandwich technique was used as a complementary method for pathogen induction. Carrots were washed, peeled, and disinfected with 80% ethanol before exposure to UV light for 15 minutes. The culm pieces were placed between two slices of carrot and secured with paper tape. This method allows a detailed observation of the pathogen-host interaction.

Isolation of microbial strains

Colonies developed in the Petri dishes were isolated using a sterile seed loop. They were transferred to new Petri containing the modified culture media [PDA (Streptomycin, 1mg L^{-1}) and nutrient agar (1mg L^{-1})] to obtain pure cultures [21]. This step was critical for the subsequent identification of the pathogens through biochemical and molecular tests

RESULTS

Description of the symptoms of the disease

The disease was observed to affect shoots in the early stages of development, with symptoms of internal rot evident in roots and young tissues at growth sections. This condition seriously compromises the production of new shoots, resulting in diminished natural regeneration, stunted growth and, ultimately, plant death. Affected shoots present dark brown to black exudates in the apical area, and the leaves are dark brown with black spots (Figure 2).

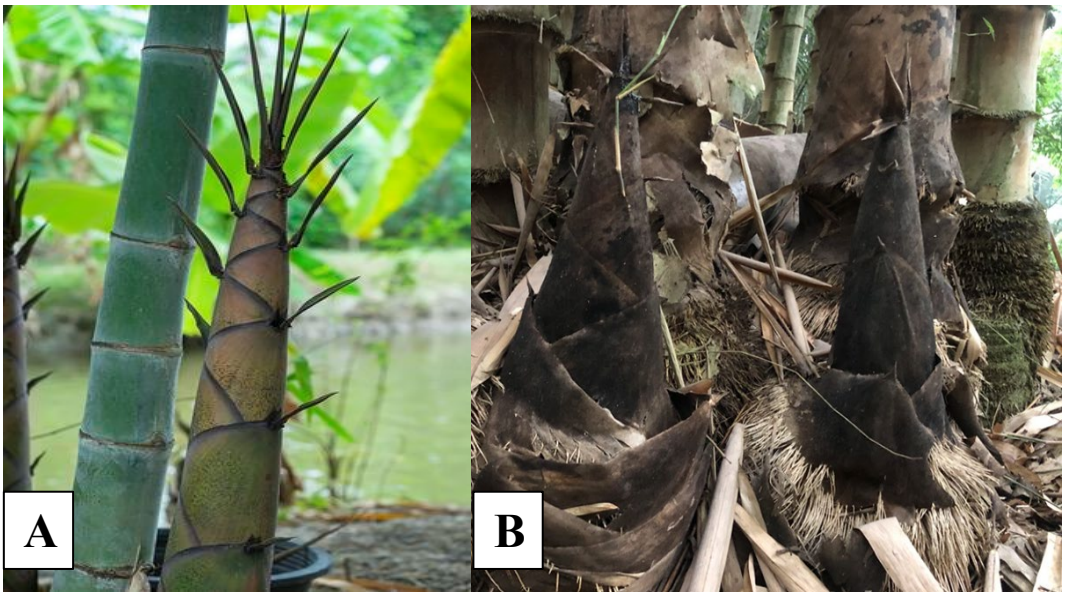

Figure 2: Comparison of healthy shoots and those affected by the disease. A) Healthy shoots from *D. asper*; B) *D. asper* shoots with exudations in the apical area.

The enzymatic action of *E. sinocalami* and *Arthrinium spp*. It resulted in spraying the internal part of the shoots, stopping the disease when reaching the culm area, which presents resistance due to its high cellulose content (Figure 3).

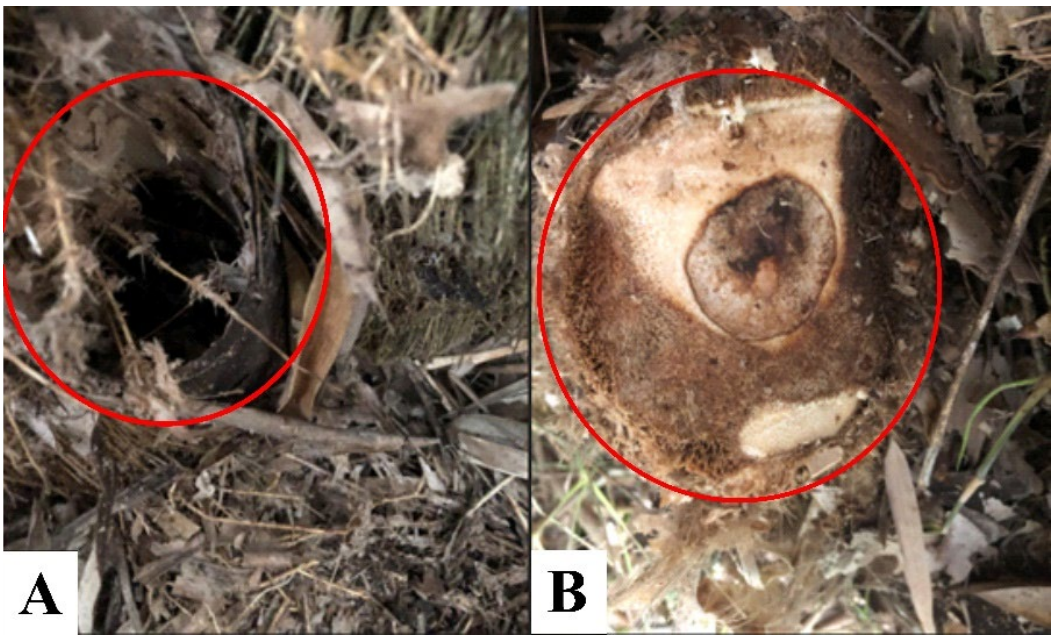

Figure 3: Evidence of enzymatic action on shoots and culm. The enzymatic action of *E. sinocalami* and *Arthrinium spp*. A) Internal part of the shoot pulverized by bacterial action; B) Attack by *E. sinocalami* and *Arthrinium spp*. in the culm internode.

Disease severity

The severity of the pathogen attack was reflected in a meager natural regeneration rate. The phenological evaluation showed that 97% of the shoots were affected and showed signs of spraying by phytopathogens (Table 1).

ITEM	Cane average	DCH	Live shoots (%)	Dead shoots (%)
Scale 1	0,2	8,80	3%	97%
Scale 2	10,0	12,50		
Scale 3	45,0	10,68		
Scale 4	3,0	14,16		
Scale 5	6,0	17,46		

Note: The phenological scale was arbitrarily based on vigor, diameter and hue.

Table 1. Phenological scale and percentage of affected shoots

Morphological recognition of microorganisms associated with bacterial wilt in D. asper

A strain of filamentous fungi and a bacterial strain of the genus Erwinia, closely related to bacterial wilt, were isolated and identified. Bacterial strains grew optimally on modified nutrient agar at room temperature, while fungal colonies preferred a PDA culture at 28°C. Identification was based on Gram staining and trypan blue pigmentation techniques, using microscopy with close-ups of 10, 40 and 100x and taxonomic keys to determine the genus of the strains.

Arthrinium species can produce varied fruiting bodies depending on growing conditions. It was observed that the aerial hyphae took on a white tone in the incubator and brown at room temperature. The identification of Arthrinium was confirmed by the observation of conidiogenous structures and spores with a germinal cleft (Figure 4).

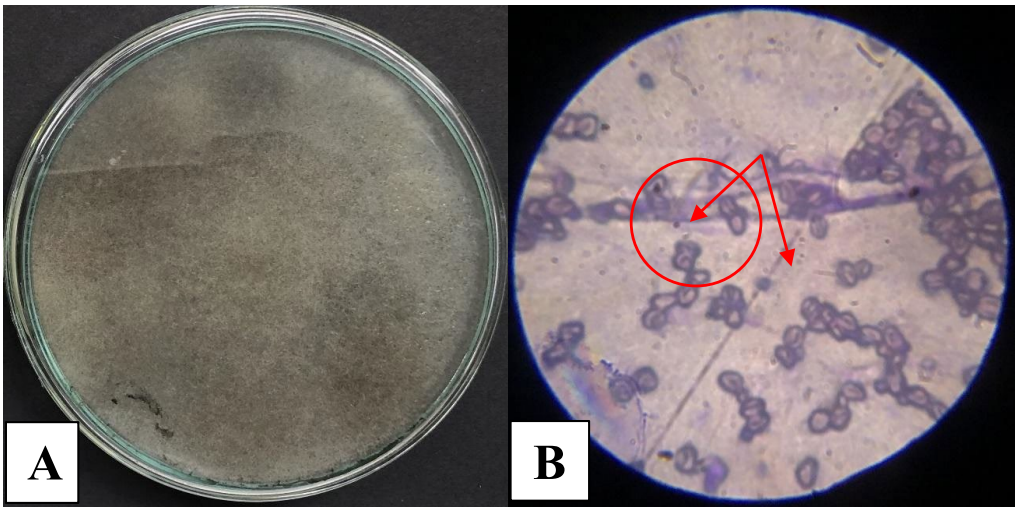

Figure 4: Morphology of *Arthrinium spp*. Observed in culture. A) Macroscopic view of *Arthrinium spp*.; B) Spores with germinal cleft.

DISCUSSION

This study provides a detailed insight into the complex interaction between pathogenic microorganisms and *D. asper*, revealing the synergy between *E. sinocalami* and *Arthrinium spp*. in the induction of bacterial wilt and culm degradation The complex interplay between microorganisms and bamboo, particularly in the context of disease management and control strategies, is a critical area of focus. Recent studies have shed light on various aspects of this interaction, offering insights that could be instrumental in developing more effective disease management strategies for *D. asper*. Darma et al. [22] explored the potential of *Bacillus subtilis* BMB26, a bacterium isolated from bamboo powder, as a biocontrol agent against phytopathogenic fungi. This finding is particularly relevant to our study as it suggests the possibility of utilizing bamboo-associated microorganisms for biologically controlling pathogens in *D. asper*. The use of such biocontrol agents could provide a sustainable alternative to chemical control methods, aligning with the need for eco-friendly disease management practices in bamboo ecosystems [22]. The impact of forest management practices on the soil microbial community was highlighted by Yang et al. [23]. Their study indicated that converting secondary broadleaf forests to Moso bamboo plantations alters the soil bacterial community structure. This alteration could have significant implications for disease dynamics in bamboo plantations, underscoring the importance of considering forest management practices in disease management strategies.

Zhang et al. [24] found that chicken farming under Moso bamboo forests significantly increased bacterial and fungal diversity. This increase in microbial diversity could influence the prevalence and severity of diseases such as bacterial wilt in bamboo, suggesting that agricultural practices in bamboo forests must be carefully managed to maintain ecological balance and prevent disease outbreaks [24].

Fuke et al. 25 emphasized rhizospheric microbial communities' role in bamboo health. These communities play a significant role in nutrient immobilization and phytoremediation, which could enhance the overall health and disease resistance of *the Dendrocalamus asper*. Understanding and harnessing these microbial interactions could improve bamboo resilience against pathogens. The study by Shen et al.[26] on endophytic fungi isolated from Moso bamboo seeds revealed their broad-spectrum antimicrobial activity. These fungi could be a valuable source of bioactive compounds for developing plant defense activators, offering a novel approach to disease management in bamboo.

The interaction of fungi of the genus *Arthrinium* and bacteria *Erwinia spp*. with bamboo is complex and multifaceted. These microorganisms can exist in symbiosis with bamboo or become disease-causing pathogens [27]. In particular, *E. sinocalami* and *Arthrinium spp*. have been identified as causing bacterial wilt and rot. of

shoots and culms, respectively [28]. This study reveals a coordinated attack of these pathogens on bamboo shoots, suggesting more complex disease dynamics than previously recognized. The persistence of bacterial wilt in bamboo, associated with *E. sinocalami*, has been documented for over two decades [29]. The limitation of this bacteria to attack only young shoots has significant implications for the regeneration and propagation of bamboo, as observed in the bamboo patches evaluated, where most shoots were affected or destroyed by pathogens. Identifying species of the genus *Arthrinium* is challenging due to the similarity of their conidia between different species and the morphological variability depending on the incubation environment [30,31]. In this study, identification was achieved by observing conidiogenous structures and spores with a germinal cleft, which aligns with the existing literature's descriptions. Furthermore, it is essential to consider the role of natural products in crop protection, as discussed in the work of Dayan et al. [32], which highlights the need to discover and develop new pesticides based on natural products to replace compounds lost due to stricter regulations. This could be relevant for the development of biological control strategies against pathogens in bamboo.

The diversity of microorganisms in fermented foods and beverages globally, as reviewed in the study by Tamang et al. [33], also provides a context for understanding the complexity of microbial communities and their potential in biological control applications. Finally, the review by Bhardwaj et al. [34] on xylanases highlights the importance of these enzymes in the cleavage of complex polysaccharides and their application in various industrial and biotechnological sectors. Since *Arthrinium spp*. and *Erwinia spp*. are involved in the revision of plant tissues, understanding the enzymes involved could offer ways to mitigate their pathogenic impact.

These findings and comparisons with existing literature underscore the need for a deeper understanding of interactions between pathogens and host plants. They could inform the development of integrated disease management strategies for the conservation and sustainable use of bamboo ecosystems.

CONCLUSIONS

This study provides a detailed insight into the complex interaction between pathogenic microorganisms and *D. asper*, revealing the synergy between *E. sinocalami* and *Arthrinium spp*. in the induction of bacterial wilt and culm degradation in bamboo. The findings demonstrate that *E. sinocalami* targets young shoots, while Arthrinium spp. is associated with the degradation of culm structure, suggesting a coordinated attack mechanism that could have significant implications on the health and viability of bamboo plantations. Identifying *Arthrinium spp*. was particularly challenging due to the morphological similarity of its conidia to other fungal species. However, accurate identification was achieved through detailed analysis of hyphae, conidiogenous structures and spores, highlighting the importance of meticulous diagnostic techniques in plant pathology.

The results of this study emphasize the need to develop integrated disease management strategies that consider the interaction between different pathogens. Furthermore, it is crucial to continue research to understand better the epidemiology of bacterial wilt and pathogen-host interactions in bamboo to develop effective and sustainable control measures that ensure the protection of this important plant species in ecosystems: forestry and agricultural production. Collaboration between plant pathologists, microbiologists and agronomists will be essential to address the challenges presented by bacterial wilt in *D. asper* and other bamboo genera, ensuring the sustainability of these valuable resources worldwide. Finally, these studies collectively highlight the need for a holistic approach to disease management in bamboo ecosystems. By considering both beneficial and pathogenic microorganisms and the impact of environmental and management practices, we can develop more effective and sustainable strategies for the conservation and health of *D. asper*.

Author Contributions: Conceptualization, MV, JM; methodology, CB, MV, JM and MC; validation, JM, CB and RH; formal analysis JM, MV and CB; investigation, MV; CB and JM; writing-original draft

preparation, MV, JM, MC and RH; writing-review and edition, JM, MC, RH and MV; visualization, JM, MC, RH and MV; project administration, CB, MV and JM; funding acquisition, MV, CB and JM All authors have read and agreed to the published version of the manuscript.

Acknowledgments: The authors are grateful for the support of the Universidad Técnica Estatal de Quevedo (UTEQ).

Conflicts of Interest: There is no conflict of interest.

REFERENCES

1. Yuan, Z.-S. *et al.* Structural variability and differentiation of niches in the rhizosphere and endosphere bacterial microbiome of moso bamboo (Phyllostachys edulis). *Sci. Rep.* **11**, 1574 (2021).
2. Tu, Z., Chen, L., Yu, X. & Zheng, Y. Rhizosphere soil enzymatic and microbial activities in bamboo forests in southeastern China. *Soil Sci. plant Nutr.* **60**, 134–144 (2014).
3. Caycedo Lozano, L., Ramírez, L. C. C. & Suárez, D. M. T. Las bacterias, su nutrición y crecimiento: una mirada desde la química. *Nova* **19**, 49–94 (2021).
4. Cano, M. A. Interacción de microorganismos benéficos en plantas: Micorrizas, Trichoderma spp. y Pseudomonas spp. Una revisión. *Rev. UDCA Actual. Divulg. Científica* **14**, 15–31 (2011).
5. Morakotkarn, D., Kawasaki, H. & Seki, T. Molecular diversityof bamboo-associated fungi isolated from Japan. *FEMS Microbiol. Lett.* **266**, 10–19 (2007).
6. Tian, X.-K. *et al.* Native bamboo invasions into subtropical forests alter microbial communities in litter and soil. *Forests* **11**, 314 (2020).
7. Zhang, H. *et al.* Microbial taxa and functional genes shift in degraded soil with bacterial wilt. *Sci. Rep.* **7**, 39911 (2017).
8. Li, C., Zong, Z., Qie, H., Fang, Y. & Liu, Q. CiteSpace and Bibliometric Analysis of Published Research on Forest Ecosystem Services for the Period 2018–2022. *Land* **12**, 845 (2023).
9. Fujiwara, K., Aoyama, C., Takano, M. & Shinohara, M. Suppression of Ralstonia solanacearum bacterial wilt disease by an organic hydroponic system. *J. Gen. plant Pathol.* **78**, 217–220 (2012).
10. Li, S. *et al.* Soil acidification aggravates the occurrence of bacterial wilt in South China. *Front. Microbiol.* **8**, 703 (2017).
11. Santiago, T. R., Lopes, C. A., Caetano-Anollés, G. & Mizubuti, E. S. G. Phylotype and sequevar variability of Ralstonia solanacearum in Brazil, an ancient centre of diversity of the pathogen. *Plant Pathol.* **66**, 383–392 (2017).
12. BRooks, Da. S., Gonzalez, C. F., Appel, D. N. & Filer, T. H. Evaluation of endophytic bacteria as potential biological-control agents for Oak Wilt. *Biol. Control* **4**, 373–381 (1994).
13. Kim, N. *et al.* Induction of resistance against pine wilt disease caused by Bursaphelenchus xylophilus using selected pine endophytic bacteria. *Plant Pathol.* **68**, 434–444 (2019).
14. Li, S.-J. *et al.* Purification of protein AP-Toxin from Arthrinium phaeospermum causing blight in Bambusa pervariabilis× Dendrocalamopisis grandis and its metabolic effects on four bamboo varieties. *Phytopathology* **103**, 135–145 (2013).
15. Dohet, L., Gregoire, J.-C., Berasategui, A., Kaltenpoth, M. & Biedermann, P. H. W. Bacterial and fungal symbionts of parasitic Dendroctonus bark beetles. *FEMS Microbiol. Ecol.* **92**, fiw129 (2016).
16. Lamichhane, J. R. & Venturi, V. Synergisms between microbial pathogens in plant disease complexes:

a growing trend. *Front. Plant Sci.* **6**, 385 (2015).
17. van Dijk, L. J. A., Ehrlén, J. & Tack, A. J. M. The timing and asymmetry of plant–pathogen–insect interactions. *Proc. R. Soc. B* **287**, 20201303 (2020).
18. Graziosi, I. & Rieske, L. K. A plant pathogen causes extensive mortality in an invasive insect herbivore. *Agric. For. Entomol.* **17**, 366–374 (2015).
19. Mishra, R. K., Pandey, B. K., Muthukumar, M., Pathak, N. & Zeeshan, M. Detection of Fusarium wilt pathogens of Psidium guajava L. in soil using culture independent PCR (ciPCR). *Saudi J. Biol. Sci.* **20**, 51–56 (2013).
20. Cheng, S.-F. *et al.* Identification of differentially expressed genes induced by bamboo mosaic virus infection in nicotiana benthamianaby cdna-amplified fragment length polymorphism. *BMC Plant Biol.* **10**, 1–12 (2010).
21. Wang, H. *et al.* Dominance of zoonotic genotype D of Enterocytozoon bieneusi in bamboo rats (Rhizomys sinensis). *Infect. Genet. Evol.* **73**, 113–118 (2019).
22. Darma, R. *et al.* A strong antifungal-producing bacteria from bamboo powder for biocontrol of Sclerotium rolfsii in melon (Cucumis melo var. amanta). *J. Plant Pathol. Microbiol* **7**, 334 (2016).
23. Yang, C., Zhong, Z., Zhang, X., Bian, F. & Du, X. Responses of soil organic carbon sequestration potential and bacterial community structure in moso bamboo plantations to different management strategies in subtropical China. *Forests* **9**, 657 (2018).
24. Zhang, X. *et al.* Leaf-associated shifts in bacterial and fungal communities in response to chicken rearing under moso bamboo forests in subtropical China. *Forests* **10**, 216 (2019).
25. Fuke, P., Kumar, M., Sawarkar, A. D., Pandey, A. & Singh, L. Role of microbial diversity to influence the growth and environmental remediation capacity of bamboo: a review. *Ind. Crops Prod.* **167**, 113567 (2021).
26. Shen, X.-Y. *et al.* Diversity and antimicrobial activity of culturable endophytic fungi isolated from moso bamboo seeds. *PLoS One* **9**, e95838 (2014).
27. Hyde, K. D., Zhou, D., McKenzie, E. H. C., Ho, W. H. & Dalisay, T. Vertical distribution of saprobic fungi on bamboo culms. *Fungal Divers.* (2002).
28. Wang, S. *et al.* Electron transport chains in organohalide-respiring bacteria and bioremediation implications. *Biotechnol. Adv.* **36**, 1194–1206 (2018).
29. Fonseca, W. & Rojas, M. Acumulación y predicción de biomasa y carbono en plantaciones de bambú en Costa Rica. *Ambient. y Desarro.* **20**, 85–98 (2016).
30. Crous, P. W. & Groenewald, J. Z. A phylogenetic re-evaluation of Arthrinium. IMA Fungus 4 (1): 133–154. at (2013).
31. Dai, D. Q. *et al.* Bambusicolous fungi. *Fungal Divers.* **82**, 1–105 (2017).
32. Dayan, F. E., Cantrell, C. L. & Duke, S. O. Natural products in crop protection. *Bioorg. Med. Chem.* **17**, 4022–4034 (2009).
33. Tamang, J. P., Watanabe, K. & Holzapfel, W. H. Diversity of microorganisms in global fermented foods and beverages. *Front. Microbiol.* **7**, 377 (2016).
34. Bhardwaj, N., Kumar, B. & Verma, P. A detailed overview of xylanases: an emerging biomolecule for current and future prospective. *Bioresour. Bioprocess.* **6**, 1–36 (2019).

Received: October 9th 2023/ **Accepte**d: January 15th 2024 / **Published:**15 February 2024

Citation: Morante-Carriel J., Vera-Carranza M., Belezaca-Pinargote C., Carranza-Patiño M., Herrera-Feijoo R.J.. Microorganisms associated with bacterial wilt disease in *Dendrocalamus asper* (Giant Bamboo) from Ecuador. Revis Bionatura 2024; 9 (1) **32**. http://dx.doi.org/10.21931/RB/2024.09.01.**32**

Additional information Correspondence should be addressed to jmorante@uteq.edu.ec

Peer review information. Bionatura thanks anonymous reviewer(s) for their contribution to the peer review of this work using https://reviewerlocator.webofscience.com/

Bionatura ISSN. First 13909355 Ecuador. **Scopus coverage years**: from 2016 to the present

Bionatura
Ibero-American Journal of Biotechnology and Life Sciences

Article

Tools and computational resources for the design of CRISPR/Cas9 sgRNA for *NPR3* gene knockout in sour orange (*Citrus aurantium* L.)

Mao Yupanqui-Celestino[1], Lizet Karina Azañero-Huaynacari[1], Carlos Roberto Pesantes-Rojas[2], Miguel Angel Aguilar-Luna-Victoria[3], Desiderio Elías Cotos-Durán[1], Linder Ramírez-Viena[4]*

[1]Escuela Profesional de Biología con mención en Biotecnología, Facultad de Ciencias, Universidad Nacional José Faustino Sánchez Carrión, Huacho, Perú.
[2]Escuela Profesional de Matemática Aplicada, Facultad de Ciencias, Universidad Nacional José Faustino Sánchez Carrión, Huacho, Perú.
[3]Escuela Profesional de Estadística e Informática, Facultad de Ciencias, Universidad Nacional José Faustino Sánchez Carrión, Huacho, Perú.
[4]Departamento de Ciencias Naturales, Facultad de Educación, Universidad Nacional José Faustino Sánchez Carrión, Huacho, Perú.
**Correspondence: Mao Yupanqui-Celestino (Cusy2000@gmail.com)*
Available from. http://dx.doi.org/10.21931/RB/2024.09.01.33

ABSTRACT

Citrus fruits are the most nutritious foods widely used in flavoring, beverages, and medicines due to their outstanding curative effects. Sour orange (*Citrus aurantium* L.) is the predominant rootstock in most citrus growing areas due to its good agronomic attributes such as high quality, yield and tolerance to various pathogens. However, the citrus tristeza virus (CTV) is the leading epidemic agent of sour and sweet orange. This study aimed to design *in silico* guide RNA (sgRNA) for CRISPR/Cas9-mediated inactivation of the Non-expression of Pathogenesis-Related genes 3 (*NPR3*) in sour orange (*CaNPR3*). The protein sequence of the *CaNPR3* gene is 584 amino acid residues long. The amino acid sequence of the *CaNPR3* gene was compared with the homologous sequences of other nearby vegetative species, showing a close similarity with *Citrus sinensis* and *Citrus Clementina* with 100% and 97.27%, respectively. CRISPR RGEN Tools provided 61 results for exon two of the *CaNPR3* gene, filtering to 19 sequences and selecting four sgRNA sequences for genetic editing, which were: sgRNA 1 (5'-CATCAGGAAAAGACTTGAGT-3'), sgRNA 2 (5'-AGAACCTCAGACAACACACCTT-3'), sgRNA 3 (5'-CATCAGATTTGACCCTGGAT-3') and sgR-NA 4 (5'-TTCTGGAGGGAGGGAGAGAAATGAGGAGG -3'). The predicted secondary structures of the four selected sgRNAs present efficient structures for gene editing of the target gene, allowing it to recognize, interact with Cas9 protein and edit the target region.

Keywords: Gene editing, guide RNA, *CaNPR3*, *in silico*.

INTRODUCTION

Citrus is one of the most abundant fruit crops and the essential economic mainstay for many domestic and foreign farmers[1,2]. In the previous cycle, sour orange (*Citrus aurantium* L.) was the predominant rootstock in most citrus growing areas due to its good agronomic attributes such as high quality, yield, tolerance to various

pathogens and resistance to abiotic stresses[3-5]. Sour oranges belong to the Rutaceae family, which are medium-sized cosmopolitan angiosperms. Recently, the fruit industry has faced unavoidable problems due to climate change and global warming, causing an increase in epidemics of new and invasive pathogens in agricultural fields[6-9].

Citrus tristeza virus (CTV) is the main epidemic agent causing the worldwide loss of nearly 100 million trees of sweet orange (*Citrus sinensis* (L.) Osb.), grapefruit (*C. paradis*e Macf.), mandarin (*C. reticulata* Blanco), and lime (*C. aurantifolia* (Christ.) Swing.) propagated on sour orange (*C. aurantium* L.)[10]. CTV causes collapse, obliteration, and necrosis of the crypt tubes and accompanying cells near the bud junction and induces the appearance and excessive development of non-functional phloem, which decreases water and mineral transport in the plant[10,11]. It has been shown that silencing of the Non-expression of Pathogenesis-Related genes 3/4 gene, associated with these defense pathways, improved virus propagation and accumulation in sour orange plants compared to non-silenced controls[12].

The non-expression of pathogenesis-related genes (*NPR*) is a genuine transcription cofactor in the salicylic acid (SA) signal transduction pathway and plays critical regulatory roles in plant immunity[13]. Within the NPR family, the most representative gene is *NPR1*, containing a BTB/POZ domain and an anchor protein repeat domain. The genome of *Arabidopsis thaliana* contains six genes related to the NPR gene family[14], *NPR3* and NPR4 have been identified as homologous genes of *NPR1*[15]. The *NPR3* gene is involved in the transduction of the SA signal transduction pathway and also functions as a negative regulator of the basal defense response[16]. In sour grapes, it has been shown that gene silencing decreases CTV accumulation and increases growth concerning control.

The CRISPR/Cas (Clustered Regularly Interspaced Short Palindromic Repeats-CRISPR-associated) system has become one of the most widely used systems due to its low cost, easy adaptation and high efficiency during gene editing in plants[17,18]. The CRISPR Cas9 nuclease is directed by a short single guide RNA (sgRNA) that recognizes the target DNA within the genome. The sgRNA combines CRISPR RNA (crRNA) and the crRNA transactivator (tracrRNA). The CRISPR/Cas system requires a well-defined adjacent short protospacer motif (PAM) located immediately downstream of the protospacer on the non-target DNA strand[19-23]. In addition, Double-Strand Breaks (DSBs) of target DNA occur three nucleotides upstream of the PAM motif by incorporation of the HNH and RuvC domains belonging to the Cas9 endonuclease[24,25], DSB is repaired by homology-directed repair (HDR) pathway or non-homologous end joining (NHEJ) pathways in the genome[26]. This repair pathway has been exploited as NHEJ causes indel mutation-producing Knockout (KO) genes. HDR causes point mutation accompanied by an exogenous gene of interest, producing a Knock-In (KI) gene. Therefore, in recent years, in silico designs have been performed because they do not require time-consuming experimental procedures, which are based on practical and optimized molecular biology tools adapted to the issue of the organism that has been previously developed, with the ability to clone, predict protein structure, analyze gene expression, predict mutagenesis sites directed by CRISPR/Cas. The design of sgRNA is determinant in the specificity of targeting and the efficiency of excision or insertion because if off-target Cas9 activity is present (off-target), it can lead to unexpected effects[26-28]; cases of off-target occur because similar sgRNA sequences exist in other parts of the genome, this type of designs in computational machines is called *in silico*[29]. As a result, current researchers are forced to develop new tolerant varieties and rootstocks with the support of genetic engineering, allowing industries to gain experience to face these and similar future problems[30].

The present study aims to design in silico sgRNA editing sgRNAs for *NPR3* gene knockout for positive regulation against CTV in sour orange (*Citrus aurantium* L.) mediated by CRISPR/Cas9, being a previous step in the genetic improvement of orange against these pathogens, using computational tools (bioinformatics).

MATERIALS AND METHODS

Identification of amino acid sequences of CaNPR3

The amino acid sequence of the *Citrus aurantium NPR3* gene (*CaNPR3*) was based on the reference sequence GCF_022201045.2. It was compared with other NPR amino acid sequences in plant species with a higher similarity percentage than 77%. The sequences were obtained from NCBI (http://www.ncbi.nlm.nih.gov/). The sequences were aligned using the Bioedit program, and a phylogenetic tree was formed using the Neighbor-Joining method with 1000 Bootstrap analysis repeats with the MEGA 11 program. The determination of

the motifs and conserved regions of the aligned amino acid sequences was performed using the virtual platforms The MEME Suite (https://meme-suite.org/meme/) and WebLoGo (https://weblogo.berkeley.edu/logo.cgi).

In silico design of sgRNA for CaNPR3 gene

The design of the sgRNAs for the target region of the CaNPR3 gene was performed using the online CRISPR RGEN Tools (http://www.rgenome.net/) on the sour orange genome with the Cas-Designer function in order to perform frameshift recognition and mutation on the target sequence. In addition, the LOC102621158 gene was selected with the accession XM_006468378.4 mRNA, which is located NC_023047.1 (8114278.8117323) furthermore the gene is referenced by Gómez-Muñoz et al.[12]. The mRNA has 4 exons, in this work we will work with exon 2 of CsNPR3 from accession XM_006468378.4 exons. The RGEN-eligible target sequences (5' to 3') obtained were evaluated with the criteria of GC content between 40% to 60% and out-of-frame score greater than 70.

In silico prediction of sgRNA structure

The selected sgRNA structure was predicted using the online tool The Vienna RNA Web Services (http://rna.tbi.univie.ac.at/#webservices) in the RNAfold web server function. The prediction focused on the selected mRNA secondary structures complemented by an RNA scaffold set up for CRISPR/Cas9-mediated gene editing methodology. The selection of sgRNAs based on their secondary structures was established by forming two hairpins at the upper ends and a RAR stem-loop. Further microhomology prediction of the selected gRNAs with the Microhomology function (CRISPR RGEN Tools) allows prediction of mutation patterns caused by the NHEJ or MMEJ pathway and assessment of in- or out-of-frame target deletion.

RESULTS AND DISCUSSION

Identification of amino acid sequences of the CaNPR3 gene

The sequence of *CaNPR3* shows 100% similarity to *Citrus sinensis*, followed by *Citrus Clementina* with 97.27% (Table 1). Lengths of 584 to 590 amino acid residues were found in the compared sequences. All *CaNPR3*-like sequences contain an ankyrin repeat domain and a BTB/POZ dominium (Figure 1), indicating high levels of functional conservation in the *NPR*-like family[31,32]. However, as the list of *NPR*-like proteins in different plant species increases, so does the complexity and variability of their function [33,34]. Phylogenetic tree construction is a crucial method to analyze the functionality of CaNPR3-like genes; in this study, based on the results of phylogenetic tree classification, *NPR3* protein sequences from various species were classified into two clades. Among these, clade II exhibited the most significant number of members, with 9, and clade I consisted of 5 members (Figure 1). From this, it can be observed that *Citrus sinensis* and *Citrus clementina* were assigned to clade I, of which their proteins are reported to function as positive and negative regulators of systemic acquired resistance (SAR) for each species, respectively [35]. In addition, conserved motifs were identified in *CaNPR3*-like proteins (Figure 2). The protein sequences of the species analyzed share most of the motifs. However, all the sequences had ten motifs, except *Citrus Clementina*, which had motif 8 exclusively. The presence of shared conserved motifs within the *CaNPR3*-like gene family supports the classification of these genes as a multigene family[35]. The conserved structural do-mini analysis reveals that all *CaNPR3*-like proteins (Figure 2) contain an N-terminal BTB/POZ structural domain and a central ankyrin repeat domain (Figure 3). In addition, genes on both the first and second branches of the evolutionary tree exhibit the C-terminal *CaNPR3*-like region, which is known to be a crucial component of the *NPR*-like gene family and assumes a key role[36,37].

N°	Accession	Scientific name	Cover page of the query (%)	Percentage of identity (%)
1	XP_006468441.2	*Citrus sinensis*	100%	100.00
2	XP_024047266.1	*Citrus clementina*	100%	97.27
3	KAJ6294437.1	*Salix suchowensis*	100%	78.88
4	KAJ6761117.1	*Salix purpurea*	100%	78.53
5	KAJ6410587.1	*Salix udensis*	100%	78.53
6	XP_034887663.1	*Populus alba*	100%	79.90
7	XP_031280798.1	*Pistacia vera*	100%	82.00
8	KAJ0081498.1	*Pistacia atlantica*	100%	82.00
9	XP_015575545.1	*Ricinus communis*	98%	77.72
10	KAB1222144.1	*Morella rubra*	99%	77.00
11	NP_001238674.1	*Glycine max*	95%	77.30
12	KHN14362.1	*Glycine soja*	95%	77.13
13	XP_007024872.1	*Theobroma cacao*	96%	77.66
14	XP_044496684.1	*Mangifera indica*	100%	80.27

Table 1: Accessions of plant species with the highest sequence similarity to *CaNPR3*.

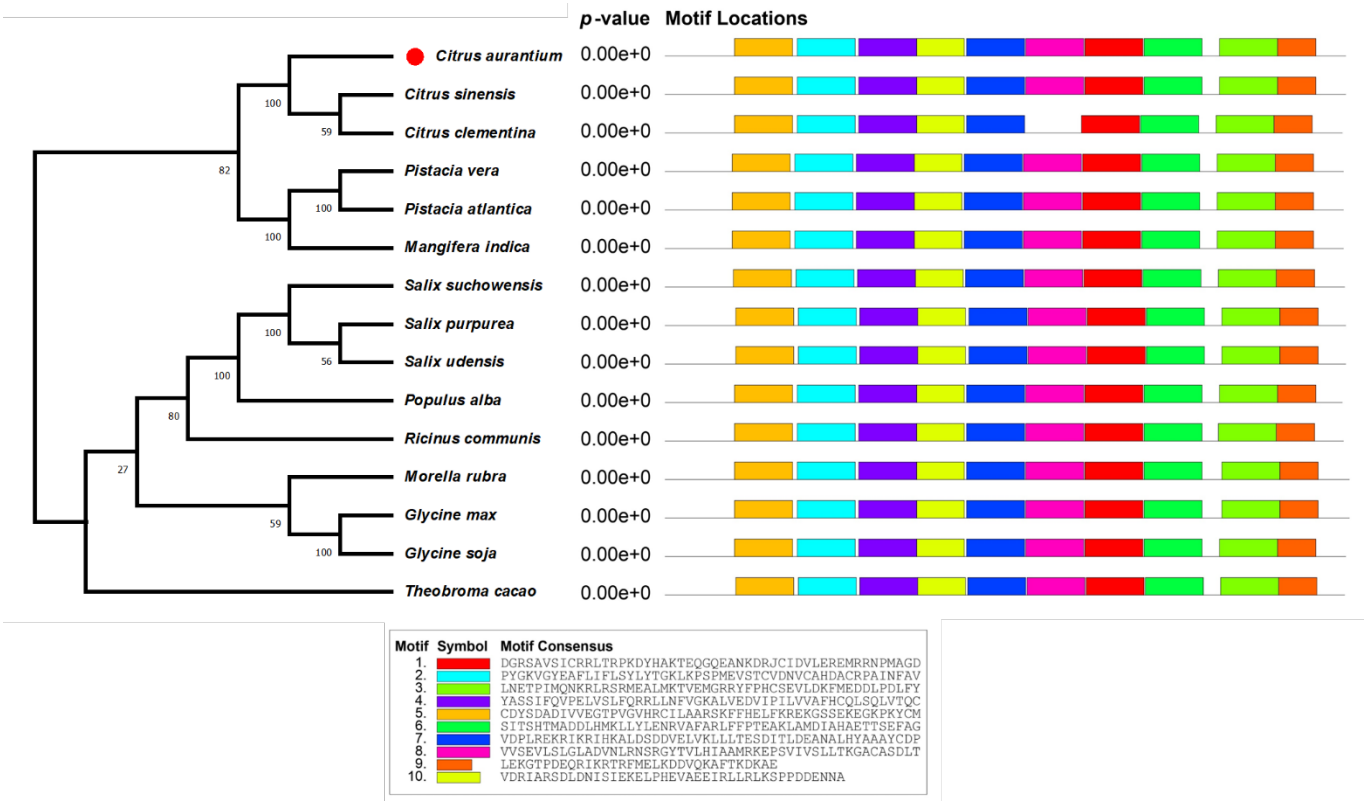

Figure 1: Phylogenetic tree analysis of neighbor-joining and conserved motifs of the *NPR3* protein from sour orange and nearby species.

Figure 2: Sequence comparison of conserved *NRP3* motif sequences of sour orange and nearby species.

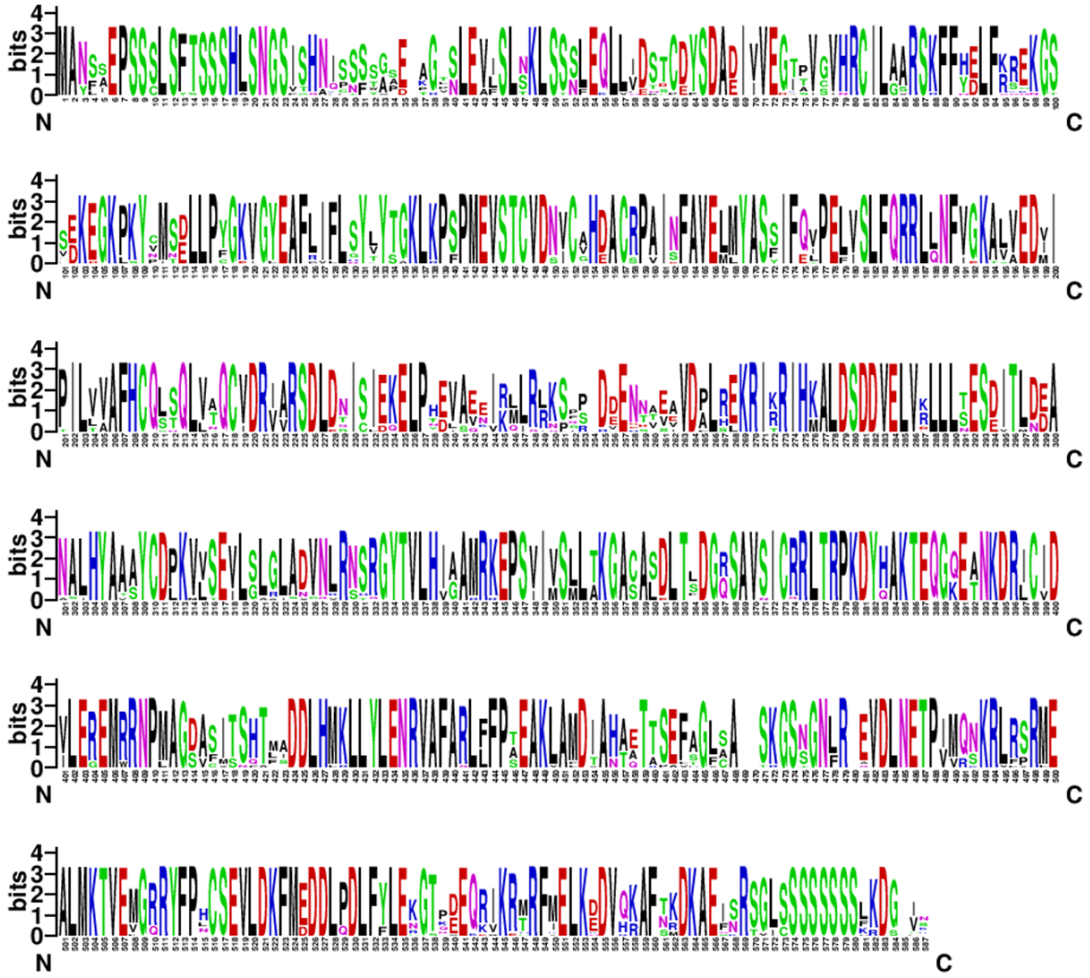

Figure 3: Conserved regions of the *NPR3* protein sequence of sour orange and related species.

In silico design of sgRNA for CaNPR3 gene

In silico design, they identified 61 candidate sgRNA sequences for Citrus aurantium gene editing in the *CaNPR3* exon 2 region. By filtering, 19 candidate sgRNA sequences or RGENs are decreased (Table 2), finally reduced to 16 sgRNA sequences by employing additional evaluations on Mismatch "1" values in Mismatch 0, which confirms the target locus within the target region and proceeds by adding filter "0" in Mismatch 1 and 2 number of targets found outside or inside the target region.

The guanine (G) and cytosine (C) content of sgRNA was based on Liu et al.[38], who mentions that sgRNA efficacy is positively influenced by increasing GC content, but at the same time, increasing GC content decreases cleavage activity significantly. We established that the GC content of gRNA for this work should present a 40-60% range. It was estimated that the 16 sgRNA for the second exon of the *CaNPR3* gene has a high reliability because the GC values are between 30 to 80%, evidenced in the selection of highly efficient sgRNA for plant genome editing me-died by CRISPR/Cas9[39]. However, if exon 2 *CaNPR3* is an inefficient region, sgRNAs are found to be between 41 and 55% tested in evaluating the efficacy of CRISPR/Cas9 sgRNAs targeting inefficient regions in Arabidopsis thaliana[40].

Out-of-frame scores are essential because choosing high-scoring sites increases the probability of obtaining permanent mutant clones. In addition, the out-of-frame score mentioned by Bae et al.[41] correlates with the probability that sgRNA-induced mutations disrupt the open reading frame (ORF). All 16 sgRNAs for exon 2 CaNPR3 possess an out-of-frame score ≥ 70.2, and the gRNA scores are above the minimum score recommended (Out-of-frame≥ 66) to create knockouts.

RGEN Target (5' to 3')	Position	Cleavage Position	Direction	GC Contents	Out-of-frame Score	Mismatches		
						0	1	2
TGGAAGGCAGCCAAAAGGATTGG	49	7.2	-	50	68.4	1	0	3
GACAATGGAAGGCAGCCAAAAGG	54	7.8	-	50	71.2	1	0	0
CATCAGGAAAAGACTTGAGTCGG	189	25.8	-	40	83.9	1	0	0
TGCAGCGTACTGTGATCCCAAGG	363	50.3	+	55	80.5	1	0	0
TGATCCCAAGGTGTTGTCTGAGG	375	51.9	+	50	72.4	1	0	0
AGAACCTCAGACAACACCTTGGG	379	51	-	45	76.7	1	0	0
GAGAACCTCAGACAACACCTTGG	380	51.1	-	50	73.5	1	0	0
TTGTCTGAGGTTCTCAGCCTCGG	388	53.7	+	50	66.6	1	0	0
TATAACCCCGAGAACTTCTAAGG	426	57.2	-	40	71.5	1	0	0
ACATATTGGTGCAATGCGCAAGG	456	62.7	+	45	66.7	1	0	0
TTGTGCATCAGATTTGACCCTGG	516	70.7	+	45	74.3	1	0	0
GCATCAGATTTGACCCTGGATGG	520	71.2	+	50	74.9	1	0	0
CATCAGATTTGACCCTGGATGGG	521	71.3	+	45	77.6	1	0	0
GCATCTGTAGAAGATTGACAAGG	557	76.1	+	40	76.5	1	0	0
GACAAGGCCGAAAGATTATCAGG	573	78.2	+	45	72.6	1	0	0

ATGTTCTGGAGGGAGAAATGAGG	644	87.6	+	45	79.6	1	0	0
TTCTGGAGGGAGAAATGAGGAGG	647	88	+	50	79.5	1	0	0
ATGAGGAGGAATCCGATGGCTGG	661	89.9	+	55	81.5	1	0	0
ATAAAGGCATCACCAGCCATCGG	673	90	-	45	86.7	1	0	0

Table 2: Accessions of plant species with the highest sequence similarity to *CaNPR3*.

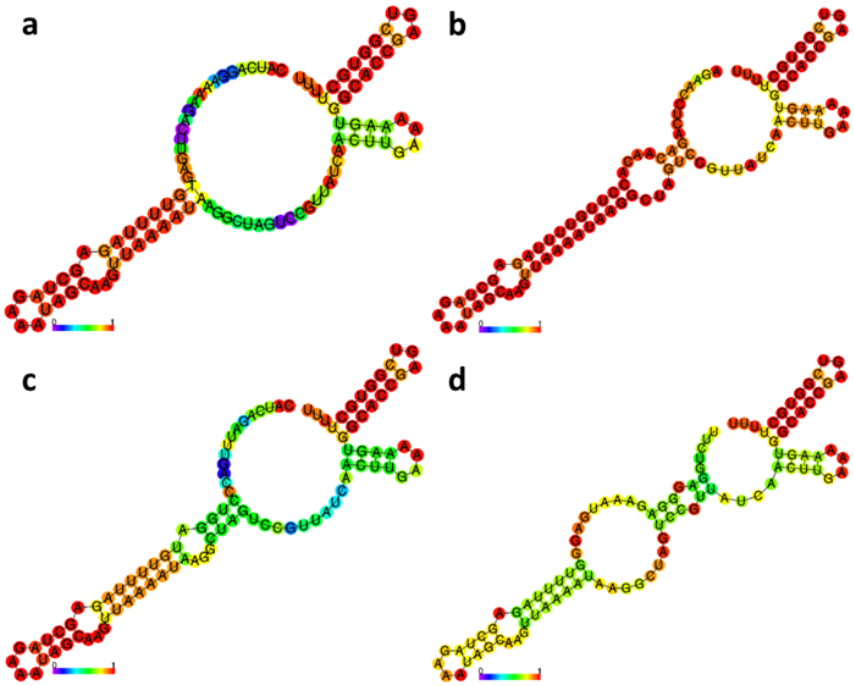

Figure 4: Secondary structures of sgRNAs for CaNPR3 gene editing: (a) sgRNA 1, (b) sgRNA 2, (c) sgRNA 3 and (d) sgRNA 4.

Objective sequence	Position	Genome location	Microhomology Score	Out-of-frame Score	Deletion Length
sgRNA 1(-): CATCAGGAAAAGACTT-GAGT	188	NC_023047.1	3908.5	83.86849175	16
Predicted Patterns				Microhomo-logy	Pattern Score
WT: AGTTGCGGAGGAAATT-AGAATGCTCCGACTCAAGTCTTTTCCTGATGATGAGAACACTGC Mutation 1: AGTTGCGGAGGAAATTAGAATGCTCC----------TGATGATGA-GAACACTGC				TCC	224.5
sgRNA 2(-): AGAACCTCAGACAACA-CCTT	378	NC_023047.1	4009.2	76.71106455	11
Predicted Patterns				Microhomo-logy	Pattern Score
WT: CATTATGCTGCAGCGTACTGTGATCCCAAGGTGTT-GTCTGAGGTTCTCAGCCTCGGATTA Mutation 2: CATTATGCTGCAGCGTACTGTG----------TTGTCTGAGGTTCTCAGCCTCGGATTA				GTG	288.5

sgRNA 3(+): CATCAGATTTGAC-CCTGGAT	520	NC_023047.1	4095.3	77.57429248	4
Predicted Patterns				Microhomo-logy	Pattern Score
WT: AAAGGAGCTTGTGCATCAGATTTGACCCTGGATGGGCGAAGTGCCGTCAG-CATCTGTAGA Mutation 3: AAAGGAGCTTGTGCATCAGATTTGACCCTG----GGCGAAGTGCCGTCAGCATCTGTAGA				TG	245.7
sgRNA 4(+): TTCTGGAGGGAGAA-ATGAGG	646	NC_023047.1	5677.3	79.47439804	14
Predicted Patterns				Microhomo-logy	Pattern Score
ATATGCATTGATGTTCTGGAGGGAGAAATGAGGAGGAA-TCCGATGGCTGGTGATGCCTTT Mutation 4: ATATGCATTGATGTTCTGGAGG----------AATCCGATGGCTGGTGATGCCTTT				GGAGG	447.3

Table 3: Calculation of microhomology-associated scores for 4 sgRNA for *CaNPR3*.

The 16 selected sgRNAs pose as a 1-0-0 filter in the Mismatches. This indicates that each sgRNA only has a single target site within the sour orange genome, in addition to not possessing off-target hits that differ by several nucleotides from the on-target sites, evidencing that the 16 designed sgRNAs are site-specific and probably efficiently in gene editing. Cho et al.[27] mention that RNA-guided endonucleases (RGENs) can distinguish on-target from off-target sites with mismatches starting from two bases but not those with a single-base mismatch.

In silico secondary sgRNA structures for CaNPR3

The secondary structures of the four selected sgRNAs stably present stem loops 2 and 3 at the upper end and stem-loop RAR stably possessing between 1 to 3 bubbles (Figure 4). From the structural evaluation, four sgRNA sequences were selected, the sequences sgRNA 1 (5'-CATCAGGAAAAGACTTGAGT-3'), sgRNA 2 (5'-AGAACCTCAGACAACAACACCTT-3'), sgRNA 3 (5'-CATCAGATTTGACCCTGGAT-3') and sgRNA 4 (5'-TTCTCTGGAGGGAGGGAGGGAGAAATGAGGAGG -3'). Thus, even the evaluation of mutation patterns produced by the 4 sgRNAs identified that the four predicted patterns of mutations produced in target sites P1x, Px2, Px3 and Px4 were caused by the MMEJ repair pathway and located in NC_023047.1 (Table 3). The predicted target site patterns were selected by their pattern score and microhomology score, which are related to silico-predicted deletion patterns resulting from microhomology-associated DNA repair and deletion length[41].

Determining secondary structures is important because it allows the identification of sgRNA sequences that may present structural variations that impair the ability to recognize and edit the target region[42,43]. It is known that a sgRNA functions by interacting its secondary structure with the Cas9 protein[44]. Ma et al.[45] mentioned that the secondary structure of sgRNAs can hinder the efficiency of gene editing. The secondary structure of the four sgRNAs (Figure 4) presents the RAR stem-loop region, which triggers the processing of the pre-crRNA precursor by the RNase III enzyme and subsequently activates the cleavage of crRNA-directed DNA by Cas9, as the four sgRNAs present second and third stem-loops which promote the formation of stable complexes and improve in vivo activity[44,46]. However, the structures of the 4 sgRNAs do not present stem loop 1, but Liang et al.[39] have shown that it is not related to editing efficiency in plants.

CONCLUSIONS

Four sgRNAs were designed in silico for CRISPR/Cas9-mediated inactivation of the *CaPRN3* gene susceptible to the citrus tristeza virus. The design was achieved by comparing the *CaPRN3* gene to the *CsPRN3* gene. The amino acid sequence of PRN3 from sweet orange was compared with sour orange and more plant species and showed close similarity with *Citrus sinensis* and *Citrus Clementina* with 100% and 97.27%, respectively. The sgRNAs found have excellent GC and out-of-frame content values and provide high efficiency in gene editing. The predicted secondary structures of the four selected sgRNAs show reliable structures in gene editing with CRISPR/Cas9. The sgRNAs were designed using silico computational tools, which are crucial in predicting the accuracy and exhibiting the success of gene editing on the target target.

Author Contributions: Conceptualization, MYC; methodology, MYC, LKAH; software, MYC and LKAH; validation, DCD, CRPR and LRV; formal analysis, DCD, CRPR, MAALV and LRV; research, MYC and LKAH; data curation, MYC; writing the original draft, MYC and LKAH; writing, revising and editing, DCD, CRPR, MAALV and LRV; supervision, LRV; All authors have read and accepted the published version of the manuscript.

Conflicts of interest: The authors declare no conflicts of interest.

REFERENCES

1. Dala-Paula, B.M.; Plotto, A.; Bai, J.; Manthey, J.A.; Baldwin, E. A.; Ferrarezi, R. S.; Gloria, M.B. Effect of Huanglongbing or Greening Disease on Orange Juice Quality, a Review. *Frontiers in Plant Science* **2019**.
2. Jia, X.; Jiang, X.; Li, Z.; Mu, J.; Wang, Y.; Niu, Y. Application of Deep Learning in Image Recognition of Citrus Pests. *Agriculture* **2023**, 13(5).
3. Acosta-Pérez, J.A.; Ortiz-García, C.F.; Zaldívar-Cruz, J.M.; Rodríguez-Cuevas, M.; Bautista-Muñoz, C.C.; Cruz Castillo-Aguilar, C. de la. Identificación del agente causal e importancia de la gomosis en la zona citricola de Huimanguillo, Tabasco, México. *Universidad y ciencia* **2012**, 28(3), 245-258.
4. Ghorbel, R.; Domínguez, A.; Navarro, L.; Penña, L. High-efficiency genetic transformation of sour orange (*Citrus aurantium*) and production of transgenic trees containing the coat protein gene of citrus tristeza virus. *Tree Physiology* **2000**, 20(17), 1183-1189.
5. Hernández-Amasifuen, A.D.; Pineda-Lázaro, A.J.; Díaz-Pillasca, H. B. *In vitro* micropropagation of sour orange (*Citrus aurantium* L.) from nodal segments. *Bionatura* **2021**, 6(4), 2216-2221.
6. Teixeira, D.C.; Saillard, C.; Couture, C.; Martins, E.C.; Wulff, N.A.; Eveillard-Jagoueix, S.; Yamamoto, P.T.; Ayres, A.J.; Bové, J.M. Distribution and quantification of *Candidatus Liberibacter* americanus, agent of huanglongbing disease of citrus in São Paulo State, Brazil, in leaves of an affected sweet orange tree as determined by PCR. *Molecular and Cellular Probes* **2008**, 22(3), 139-150.
7. Bassanezi, R.B.; Montesino, L. H.; Stuchi, E.S. Effects of huanglongbing on fruit quality of sweet orange cultivars in Brazil. *European Journal of Plant Pathology* **2009**, 125(4), 565-572.
8. Endo, T.; Fujii, H.; Omura, M.; Shimada, T. Fast-track breeding system to introduce CTV resistance of trifoliate orange into citrus germplasm, by integrating early flowering transgenic plants with marker-assisted selection. *BMC Plant Biology* **2020**, 20, 224.
9. Díaz-Pillasca, H.B.; Hernández-Amasifuen, A.D.; Machahua, M.; Pineda-Lázaro, A.J.; Argüelles-Curaca, A., & Lugo, B. (2021. Código de barras de ADN de tres especies de árboles frutales con potencial económico del valle de Huaura, Lima, Perú. *Bionatura* **2021**, 6(3), 1992-2000.
10. Moreno, P.; Ambrós, S.; Albiach-Martí, M.R.; Guerri, J.; Peña, L. Citrus tristeza virus: A pathogen that changed the course of the citrus industry. Molecular Plant Pathology **2008**, 9(2), 251-268.
11. Da-Silva, M.; Germano, S.; Duarte, A.; Pinto, P.; Marques, N.T. Callose synthase and xyloglucan endotransglucosylase gene expression over time in *Citrus* × *clementina* and *Citrus* × *sinensis* infected with citrus tristeza virus. *Phytoparasitica* **2023**.
12. Gómez-Muñoz, N.; Velázquez, K.; Vives, M.C.; Ruiz-Ruiz, S.; Pina, J.A.; Flores, R.; Moreno, P.; Guerri, J. The resistance of sour orange to the Citrus tristeza virus is mediated by the salicylic acid and RNA silencing defense pathways. *Molecular Plant Pathology* **2016**, 18(9), 1253-1266.

13. Wang, P.; Zhao, Z.; Zhang, Z.; Cai, Z.; Liao, J.; Tan, Q.; Xiang, M.; Chang, L.; Xu, D.; Tian, Q.; Wang, D. Genome-wide identification and analysis of NPR family genes in *Brassica juncea* var. *Tumida*. *Gene* **2021**, 769, 145210.
14. Fu, Z.Q.; Yan, S.; Saleh, A.; Wang, W.; Ruble, J.; Oka, N.; Mohan, R.; Spoel, S.H.; Tada, Y.; Zheng, N.; Dong, X. NPR3 and NPR4 are receptors for the immune signal salicylic acid in plants. *Nature* **2012**, 486(7402).
15. Canet, J.V.; Dobón, A.; Roig, A.; Tornero, P. Structure-function analysis of npr1 alleles in *Arabidopsis* reveals a role for its paralogs in the perception of salicylic acid. Plant, *Cell & Environment* **2010**, 33(11), 1911-1922.
16. Shi, Z.; Maximova, S.; Liu, Y.; Verica, J.; Guiltinan, M.J. The Salicylic Acid Receptor NPR3 Is a Negative Regulator of the Transcriptional Defense Response during Early Flower Development in *Arabidopsis*. *Molecular Plant* **2013**, 6(3), 802-816.
17. Yin, K.; Gao, C.; Qiu, J.L. Progress and prospects in plant genome editing. *Nature Plants* **2017**, 3(8).
18. Jung, C.; Capistrano-Gossmann, G.; Braatz, J.; Sashidhar, N.; Melzer, S. Recent developments in genome editing and applications in plant breeding. *Plant Breeding* **2018**, 137(1), 1-9.
19. Deveau, H.; Barrangou, R.; Garneau, J.E.; Labonté, J.; Fremaux, C.; Boyaval, P.; Romero, D.A.; Horvath, P.; Moineau, S. Phage response to CRISPR-encoded resistance in *Streptococcus thermophilus*. *Journal of Bacteriology* **2008**, 190(4), 1390-1400.
20. Chylinski, K.; Makarova, KS; Charpentier, E.; Koonin, E.V. Classification and evolution of type II CRISPR-Cas systems. *Nucleic Acids Research* **2014**, 42(10), 6091-6105.
21. Hsu, P.D., Lander, E.S., Zhang, F. Development and Applications of CRISPR-Cas9 for Genome Engineering. *Cell* **2014**, 157(6), 1262-1278.
22. Wu, Y.; Battalapalli, D.; Hakeem, M.J.; Selamneni, V.; Zhang, P.; Draz, M.S.; Ruan, Z. (2021). Engineered CRISPR-Cas systems for the detection and control of antibiotic-resistant infections. *Journal of Nanobiotechnology* **2021**, 19(1), 401.
23. Sharma, V.K.; Marla, S.; Zheng, W.; Mishra, D.; Huang, J.; Zhang, W.; Morris, G.P.; Cook, D.E. CRISPR guides induce gene silencing in plants in the absence of Cas. *Genome Biology* **2022**, 23(1), 6.
24. Zhang, X.H.; Tee, LY; Wang, X.G.; Huang, Q.S.; Yang, S.H. Off-target Effects in CRISPR/Cas9-mediated Genome Engineering. *Molecular Therapy - Nucleic Acids* **2015**, 4, e264.
25. Miri, S.M.; Tafsiri, E.; Cho-Shing, W. C.; Ghaemi, A. CRISPR-Cas, a robust gene-editing technology in the era of modern cancer immunotherapy. *Cancer Cell International* **2022**, 20(1), 456.
26. He, X.; Tan, C.; Wang, F.; Wang, Y.; Zhou, R.; Cui, D.; You, W.; Zhao, H.; Ren, J.; Feng, B. *Knock-in* of significant reporter genes in human cells via CRISPR/Cas9-induced homology-dependent and independent DNA repair. *Nucleic Acids Research* **2016**, 44(9), e85.
27. Cho, S.W.; Kim, S.; Kim, Y.; Kweon, J.; Kim, H.S.; Bae, S.; Kim, J.S. Analysis of off-target effects of CRISPR/Cas-derived RNA-guided endonucleases and nickases. *Genome Research* **2014**, 24(1), 132-141.
28. Leenay, R. T.; Beisel, C. L. Deciphering, communicating, and engineering the CRISPR PAM. *Journal of Molecular Biology* **2017**, 429(2), 177-191.
29. Biswas, A.; Gagnon, J.N.; Brouns, S.J.J.; Fineran, P. C.; & Brown, C.M. (2013). CRISPRTarget: Bioinformatic prediction and analysis of crRNA targets. *RNA Biology* **2013**, 10(5), 817-827.
30. Hernández-Amasifuen, A.D.; Argüelles-Curaca, A.; Cortez-Lázaro, A.A.; Díaz-Pillasca, H.B. In vitro induction of callus from foliar explants in rocoto (*Capsicum pubescens* Ruiz & Pav.). *Granja* **2021**, 34(2), 127-135.
31. Li, J.; Mahajan A.; Tsai, M.D. Ankyrin repeat: a unique motif mediating protein-protein interactions. *Biochemistry* **2006**, 45 15168–15178.
32. Spoel, S.H., Mou, Z.; Tada, Y.; Spivey, N.W.; Genschik, P.; Dong, X. Proteasome-mediated turnover of the transcription coactivator NPR1 plays dual roles in regulating plant immunity. *Cell* **2009**, 137 860–872.
33. Backer, R.; Naidoo, S.; Van-Den, B.N. The NONEXPRESSOR OF PATHOGENESIS-RELATED GENES 1 (NPR1) and Related Family: Mechanistic Insights in Plant Disease Resistance. *Plant Sci* **2019**; 10:102.
34. Zhang, Y.; Cheng, Y.T.; Qu, N.; Zhao, Q.; Bi, D.; Li, X. Negative regulation of defense responses in Arabidopsis by two NPR1 paralogs. *The Plant Journal* **2006**. 48 647–656.

35. Jiang, D.; Yang, G.; Chen, K.; Yu, P.; Chen, J.; Luo, Y.; Li, N.; Huang, L.J. Identification and Functional Characteri-zation of the Nonexpressor of Pathogenesis-Related Genes 1 (NPR1) Gene in the Tea Plant (*Camellia sinensis*). *Forests* **2023**; 14(8):1578.
36. Rochon, A.; Boyle, P.; Wignes, T.; Fobert, P.R.; Després, C. The Coactivator Function of Arabidopsis NPR1 Requires the Core of Its BTB/POZ Domain and the Oxidation of C-Terminal Cysteines. *Plant Cell* **2006**, 18, 3670–3685.
37. Boyle, P.; Le Su, E.; Rochon, A.; Shearer, H.L.; Murmu, J.; Chu, J.Y.; Fobert, P.R.; Després, C. The BTB/POZ Domain of the Arabidopsis Disease Resistance Protein NPR1 Interacts with the Repression Do-main of TGA2 to Negate Its Function. *Plant Cell* **2009**, 21, 3700–3713.
38. Liu, X.; Homma, A.; Sayadi, J.; Yang, S.; Ohashi, J.; Takumi, T. Sequence features associated with the cleavage efficiency of CRISPR/Cas9 system. *Scientific Reports* **2016**, 6, 19675.
39. Liang, G.; Zhang, H.; Lou, D.; Yu, D. Selection of highly efficient sgRNAs for CRISPR/Cas9-based plant genome editing. *Scientific Reports* **2016**, 6, 21451.
40. Malik, A.; Gul, A.; Munir, F.; Amir, R.; Alipour, H.; Babar, M.M.; Bakhtiar, S.M.; Paracha, R.Z.; Khalid, Z.; Hayat, M.Q. (2021). Evaluating the cleavage efficacy of CRISPR-Cas9 sgRNAs targeting ineffective regions of Arabidopsis thaliana genome. *PeerJ* **2021**, 9, e11409.
41. Bae, S.; Kweon, J.; Kim, H.S.; & Kim, J.S. Microhomology-based choice of Cas9 nuclease target sites. *Nature Methods* **2014**, 11(7).
42. Robins, H.; Li, Y.; Padgett, R.W. Incorporating structure to predict microRNA targets. *Proc Natl Acad Sci USA* **2005**, 102(11), 4006-4009.
43. Konstantakos, V.; Nentidis, A.; Krithara, A.; Paliouras, G. CRISPR-Cas9 gRNA efficiency prediction: an overview of predictive tools and the role of deep learning. *Nucleic Acids Res* **2022**, 50(7), 3616-3637.
44. Nishimasu, H.; Ran, F.A.; Hsu, P.D.; Konermann, S.; Shehata, S.I.; Dohmae, N.; Ishitani, R.; Zhang, F.; Nureki, O. Crystal structure of Cas9 in complex with guide RNA and target DNA. *Cell* **2014**, 156(5), 935-949.
45. Ma, X.; Zhang, Q.; Zhu, Q.; Liu, W.; Chen, Y.; Qiu, R.; Wang, B.; Yang, Z.; Li, H.; Lin, Y.; Xie, Y.; Shen, R.; Chen, S.; Wang, Z.; Chen, Y.; Guo, J.; Chen, L.; Zhao, X.; Dong, Z.; Liu, Y.G. A Robust CRISPR/Cas9 System for Convenient, High-Efficiency Multiplex Genome Editing in Monocot and Dicot Plants. *Molecular Plant* **2015**, 8(8), 1274-1284.
46. Jinek, M.; Chylinski, K.; Fonfara, I.; Hauer, M.; Doudna, J.A.; Charpentier, E. A programmable dual-RNA-guided DNA endonuclease in adaptive bacterial immunity. *Science* **2012**, 337(6096), 816-821.

Received: October 9th 2023/ **Accepte**d: January 15th 2024 / **Published:**15 February 2024

Citation: Yupanqui-Celestino M., Azañero-Huaynacari L. K., Pesantes-Rojas C. R., Aguilar-Luna-Victoria M. A., Cotos-Durán D. E., Ramírez-Viena L. Tools and computational resources for the design of CRISPR/Cas9 sgRNA for *NPR3* gene knockout in sour orange (*Citrus aurantium* L.). Revis Bionatura 2024; 9 (1) **33**. http://dx.doi.org/10.21931/RB/2024.09.01.**33**

Additional information Correspondence should be addressed to *Cusy2000@gmail.com*

Peer review information. Bionatura thanks anonymous reviewer(s) for their contribution to the peer review of this work using https://reviewerlocator.webofscience.com/

Bionatura ISSN. First 13909355 Ecuador. **Scopus coverage years**: from 2016 to the present

Bionatura
Ibero-American Journal of Biotechnology and Life Sciences

Article

Chronic Kidney Disease affects Thyroid Hormones

Tiba Mohammed Jadaan[1], Haitham L. Al-Hayali[2]

[1]Department of Biology, College of Science, Mosul University, Mosul, Iraq; E-mail: tiba.20scp138@student.uomosul.edu.iq. ORCID 0009-0008-4933-7671
[2]Department of Biology, College of Science, Mosul University, Mosul, Iraq; E-mail: haysbio68@uomosul.edu.iq. ORCID 0000-0002-8937-9285
** Correspondence: haysbio68@uomosul.edu.iq.*
Available from. http://dx.doi.org/10.21931/RB/2024.09.01.34

ABSTRACT

Kidney disease is one of the causes of death in many countries around the world. This study found that chronic kidney disease affects thyroid hormone formation, release, and storage. The results show a decrease in T3 and T4 thyroid hormones and an increase in TSH hormone in both sexes and people of different ages. The research aims to study the effect of chronic kidney disease on the thyroid gland's activity and its deficiency's effect on health ailments. Results showed a significant decrease in T3 concentration in patients at the probability level ($p \leq 0.05$) (0.8±0.1) compared with the control group (1.0±0.1).

Additionally, a significant decrease in T4 concentration at the probability level ($p \leq 0.05$), (6.8±1.5) compared with the control group (8.7±0.9) and a significant increase in TSH concentration at the probability level ($p \leq 0.05$), (4.8±0.6) compared with the control group (1.2±0.5). The CDK affects thyroid hormones; low T3 and T4 are the most common thyroid dysfunction. High TSH, enlarged thyroid gland, hypothyroidism, thyroid dysfunction.

Keywords: CKD, Thyroid Hormones, Thyroid dysfunction.

INTRODUCTION

It has been found that there is an increase in the prevalence of chronic kidney disease in all parts of the world it used to be. Today, the disease affects about 10-15% of the adult population with different age stages. Furthermore, the percentage of people over 60 years was higher than the rest of the ages, as the infection rate reached about 39%, compared to ages between 40-50 years, when the infection rate reached about 13%.

The kidney disease family history is a risk factor for chronic kidney disease. Some sources illustrate that 24% of patients who suffer from it in its final stages have at least a first-degree relative, as well as a previous history of urinary tract problems, urinary tract obstruction, stones, decrease in kidney mass (single kidney), nephrotoxins, polyuria analgesic abuse, low birth weight[1].

Kidney damage is defined as a chronic disease that affects the kidneys and leads to a defect in its structure or function, causing kidney weakness, which ranges from mild damage to kidney failure, as the kidneys cannot get rid of excess nitrogenous waste, salts, and excess water from the body's need. The disease begins without a decrease in the glomerular filtration rate (GFR), but a decrease occurs over time and delayed treatment[2].

CKD affects about 8-16% all over the world. Diabetes and high blood pressure are among the leading causes of the disease in developed countries. The rate of early detection of it is at most 5% [3].

The thyroid gland produces three hormones, which play a role in the development and functioning of the kidneys and the state of salt and water balance in the blood and the body. Low thyroid activity decreases the amount of water absorbed by the kidneys. Subclinical hypothyroidism is the most common disorder of the gland in CKD patients[4].

The growing body of evidence shows that thyroid dysfunctions such as low circulating levels of triiodothyronine and hypothyroidism are related to a higher risk of CVD and death in hemodialysis patients.

MATERIALS AND METHODS

Study samples

The study included 54 males and females randomly ill cases, with ages ranging from 48 -76 years, who attended private kidney and urology clinics and private medical laboratories in the city of Mosul, and who were diagnosed with chronic kidney disease by specialized doctors for the period from September 2020 to June 2022. It included 30 males and 24 females. In addition, 30 healthy 15 males and 15 females were in the control group .

Collect Blood Samples

5.0 ml of venous blood was drawn after fasting for a period ranging between 10-12 hours, then blood samples were placed in a gel tube and left for 15 minutes until clot formation using centrifugation at 3000 rpm for 10 minutes to separate Serum while excluding decomposed specimens. The blood serum was divided into 1.5 ml Eppendorf tubes and then kept at a temperature of -80 °C using a deep freezer for later.use

Hormonal measurements

The hormones measured are the thyroid-stimulating hormone (TSH), the triiodothyronine (T3) and the tetra iodothyronine (T4), using the technique of the Automated Immunoassay Analyser (AIA-360) equipped by the Japanese company TOOSOH (The research is extracted from a master's thesis and contains the part, not all the information, just hormones)

Statistical Analysis

The data were analyzed according to the system of simple and universal experiments using a completely randomized design. The different information was significantly distinguished by different alphabet letters under the probability level of 1% and performed by Duncan's test at SPSS version 26[6].

RESULTS

The results of the effect of CKD on thyroid hormones are shown in Tables (1) and (2). There is a significant decrease in T4 and T3 compared with the control group; the differences were at different ages and for both sexes, directly proportional to the progression of chronic kidney disease. As the patient gets older, the impact of CKD becomes more severe and may lead to death. Conversely, there is a significant increase in TSH compared to the control group due to a deficiency of thyroid hormones. The differences were at different ages and for both sexes.

Parameters	45-55		56-65		66-75	
	Control	Patients	Control	Patients	Control	Patients
	Mean± SD	Mean± SD	Mean± SD	Mean± SD	Mean± SD	Mean± SD
T3	1.0 ± 0.1^{ab}	0.8 ± 0.1^{bc}	1.0 ± 0.3^{a}	0.7 ± 0.1^{d}	1.1 ± 0.1^{a}	0.7 ± 0.1^{cd}
T4	8.7 ± 0.9^{a}	6.8 ± 1.5^{b}	8.8 ± 0.6^{a}	5.0 ± 1.4^{c}	8.6 ± 0.8^{a}	4.9 ± 1.1^{c}
TSH	1.2 ± 0.5^{c}	4.8 ± 0.6^{bc}	1.8 ± 0.2^{c}	12.0 ± 9.3^{a}	1.3 ± 0.08^{c}	8.3 ± 8.1^{ab}

*According to the Duncan test, the different numbers horizontally indicate significant differences at the probability level $p \leq 0.05$.

Table1: Effect of kidney disease on male petition at different ages.

The results showed a significant decrease in T3 concentration in patients at the probability level $p \leq 0.05$ compared to the control group. Additionally, there was a significant decrease in T4 concentration at the probability level $p \leq 0.05$ compared with the control group.

The results also showed a significant increase in TSH concentration at the probability level $p \leq 0.05$ compared with the control group.

Parameters	45-55		56-65		66-75	
	Control	Patients	Control	Patients	Control	Patients
	Mean± SD	Mean± SD	Mean± SD	Mean± SD	Mean± SD	Mean± SD
T3	2.8 ± 2.0^{a}	1.0 ± 0.1^{a}	1.1 ± 0.1^{a}	0.7 ± 0.1^{a}	1.1 ± 0.1^{a}	0.8 ± 0.1^{a}
T4	9.3 ± 1.0^{a}	6.0 ± 15^{b}	9.9 ± 0.8^{a}	5.6 ± 1.7^{a}	9.3 ± 0.3^{a}	6.6 ± 1.6^{b}
TSH	1.0 ± 0.1^{b}	8.2 ± 5.4^{b}	1.0 ± 0.1^{a}	13.0 ± 11.0^{a}	1.6 ± 0.4^{b}	5.2 ± 3.6^{b}

*** According to the Duncan test, The different numbers horizontally indicate significant differences at the probability level $p \leqslant 0.05$.**

Table 2: Effect of kidney disease on female patients at different ages.

Table 2 (A physician diagnosed the samples taken as having chronic kidney disease and the effect only on hormones) illustrates the effect of CKD on thyroid hormones in females of different ages between 45 and 75. The results showed a significant decrease in T3 and T4 concentration compared with the control group. The results also indicate a significant increase in TSH concentration compared with the control group.

DISCUSSION

The result showed a high prevalence of thyroid dysfunction. These are consistent with that illustrat[ion7]. Chronic kidney disease can alter thyroid hormone secretion, metabolism, synthesis and degradation, presenting different clinical syndromes of thyroid dysfunction. Multiple mechanisms could explain these syndromes: alteration of peripheral hormone metabolism, Decreased concentration of T.H., disturbed binding to carrier proteins, increased iodine stores in thyroid glands and possible reduction in tissue thyroid content[8].

Triiodothyronine is the most metabolically active thyroid hormone, for instance, could be dropped in CKD patients even with an average TSH level. This is termed as 'Low T3 Syndrome'. Thyroid dysfunction might appear as one of the subsequent: Thyroid enlargement, thyroid hormone deficiency or excess (hyperthyroidism or hypothyroidism); asymptomatic or symptomatic (the subclinical state or overt)[9]. The thyroid gland affects

metabolic processes in the body, and the research supports a link between thyroid and kidney function. Patients with end-stage kidney disease and chronic kidney disease are at risk of developing hypothyroidism[10].
Thyroid function can also affect kidney function, the development of chronic kidney disease, and increase the risk of cardiovascular disease. CKD patients have the highest risk of cardiovascular disease, and impaired thyroid function may lead to increased CVD risks as well as mortality, as shown for patients with ESKD[11].
Reports indicate that CDK development is linked with complications such as hypothyroidism, dyslipidemia, and cardiovascular disease. Usually, the kidneys play an essential role in the degradation, metabolism and secretion of thyroid gland hormones. Chronic kidney disease affects the hypothalamic-pituitary-thyroid axis. Chronic kidney disease affects thyroid function in several ways, including altered iodine storage in the thyroid gland, altered metabolism of peripheral hormone, decreased tissue thyroid hormone content, insufficient binding to carrier proteins and decreased thyroid hormone levels. Thus, in chronic kidney disease, thyroid hormone metabolism is impaired, and chronic kidney disease is associated with primary hypothyroidism[12].
On the other hand[13], we reported that 10.6% of CDK cases in the community, in the presence of diabetes and advanced age, are one of the factors that predict the disease. We found a higher prevalence of thyroid gland dysfunction in CKD patients. A hemodialysis patients in western Nepal study indicates a prevalence of clinical and subclinical hypothyroidism of 26.6% of patients[14].
Thyroid-stimulating hormone (TSH) is produced from the anterior pituitary gland and promotes the inhibition and stimulation of thyroid hormone secretion from the gland. TSH production is controlled by a hypothalamic hormone called thyrotropin, depending on developmental, environmental, and circadian stimuli[15].
Chronic kidney disease affects the hypothalamic-pituitary-thyroid axis, the central control axis for thyroid hormones and metabolism. Primary hypothyroidism is common in
CKD patients who have a low estimated (GFR). Low T3 syndrome is the most common disorder in patients with CKD. T4 levels are also affected because of impaired protein binding of T4[16]. Several factors are associated with T3 reduction in patients with CKD, such as systemic acidosis, markers of endothelial damage and inflammation. The 1,5′-deiodinase enzyme is responsible for converting T4 into T3 during inflammation. Specific cytokines inhibit the enzyme expression, like interleukin (IL)-1 and tumor necrosis factor[17].
The decrease in T3 level is expected in CKD patients due to decreased conversion of peripheral deiodinase from T4 to T3. This effect is caused by metabolic acidosis and protein malnutrition, both present in CKD[18].
In response to the feedback inhibition of T3 and T4, the pituitary gland produces TSH, levels of which are decreased in CKD patients due to poor responsiveness to TSH, decreased renal clearance of TSH, poor responses to thyrotropin-releasing hormone, and decreased responsiveness of TRH. This can be caused by non-thyroid disease, which returns to normal after resolution of CKD[19].
Thyroid hormones are significant determinants of health; according to the confidence interval (CI) 95% criterion for the disease-free residents, normal thyroid function is defined. These standard laboratory reference intervals are widely applied in research and clinical practice regardless of age. Thyroid hormones vary with age, and current reference intervals may not be appropriate for all age groups. Age is significant because age-related symptoms such as fatigue and tiredness are potential but not strongly predictive features of hypothyroidism[20].

CONCLUSIONS

This study confirms a high prevalence of thyroid dysfunction in chronic kidney disease (CKD) patients due to disrupted hormone metabolism and function. The findings highlight mechanisms like decreased T3 levels and impaired protein binding, leading to different presentations of thyroid dysfunction. CKD patients are at

increased risk of hypothyroidism and potentially worse cardiovascular outcomes, underlining the importance of thyroid function evaluation and management in this population.

Funding: "This research received no external funding,"

Acknowledgments: The author would like to thank the Dean of the College of Science and the Head of the Department of Biology at the College of the Science / University of Mosul for providing all the facilities to complete this research.

Conflicts of Interest: "The authors declare no conflict of interest."

REFERENCES

1. Babić Leko, M., Gunjača, I., Pleić, N., & Zemunik, T. Environmental factors affecting thyroid-stimulating and thyroid hormone levels. *Int. J.Mol. Sci.*,2021: 22(12), 6521.
2. Delles, C., & Vanholder, R. Chronic kidney disease. *Cli. Sci.*,2017: 131(3), 225-226.
3. Pinho, N. A. D., Silva, G. V. D., & Pierin, A. M. G. Prevalence and factors associated with chronic kidney disease among hospitalized patients in a university hospital in the city of São Paulo, SP, Brazil. *Braz. J. Neph.,2015:* 37, 91-97.
4. Narasaki, Y., Sohn, P., & Rhee, C. M. The interplay between thyroid dysfunction and kidney disease. In Seminars in nephrology.,2021:(Vol. 41, No. 2, pp. 133-143). WB Saunders.
5. Rhee, C. M., & Kalim, S.Thyroid Status in Chronic Renal Failure Patients. In Textbook of Nephro-Endocrinology.,2018: (pp.477-492). Academic Press.
6. George, D., & Mallery, P. IBM SPSS statistics 27 step by step: A Simple Guide and reference..,2021:Routledge.
7. Keunmoe, P., Halle, M. P., Nguedia, J. C., Njounendou, A. J., Tengen, J., & Ngowe, M. The spectrum of thyroid function abnormalities and associated biochemical factors in patients with chronic kidney disease in Cameroon. *Am J Biomed Sci Res*.,2020:8(5), 387-396.
8. Iglesias, P., Bajo, M. A., Selgas, R., & Díez, J. J. Thyroid dysfunction and kidney disease: an update. *Revi. Endocr. and Metabol. Diso*.,2017: 18, 131-144.
9. Pan, B., Du, X., Zhang, H., Hua, X., Wan, X., & Cao, C. Relationships of chronic kidney disease and thyroid dysfunction in non-dialysis patients: A pilot study. *Kidney and Blood Pre. Res*.,2019: 44(2), 170-178.
10. Schultheiss, U. T., Daya, N., Grams, M. E., Seufert, J., Steffes, M., Coresh, J., ... & Köttgen, A. Thyroid function, reduced kidney function and incident chronic kidney disease in a community-based population: the Atherosclerosis Risk in Communities study. *Nephrology Dialysis Transplantation*.,2017:32(11), 1874-1881.
11. Moon, S., Kim, M. J., Yu, J. M., Yoo, H. J., & Park, Y. J. Subclinical hypothyroidism and the risk of cardiovascular disease and all-cause mortality: a meta-analysis of prospective cohort studies. Thyroid,2018:28(9), 1101-1110.
12. Khatiwada, S., Kc, R., Gautam, S., Lamsal, M., & Baral, N. Thyroid dysfunction and dyslipidemia in chronic kidney disease patients. *BMC endocrine disorders*,2015:15(1), 1-7.

13. Sharma, S. K., Dhakal, S., Thapa, L., Ghimire, A., Tamrakar, R., Chaudhary, S., ... & Lamsal, M. Community-based screening for chronic kidney disease, hypertension and diabetes in Dharan. *J. Nep. Med. Assoc*.,2013:52(189), 205-212.
14. Paudel, K.Prevalence and clinical characteristics of hypothyroidism in a population undergoing maintenance hemodialysis. *JCDR,2014:* 8(4), MC01.
15. Salih, S. S., & Yenzeel, J. H. Evaluation of Thyroid Hormones and Some Biochemical Variables in Patients with Chronic Kidney Disease. IRQ. J. Sci.,2020:985-992.
16. Bajaj, S., Purwar, N., Gupta, A., Gupta, P., & Srivastava, A.Prevalence of hypothyroidism in nondiabetic chronic kidney disease and effect of thyroxine replacement on estimated glomerular filtration rate. *Ind. J. nephron.,2017:* 27(2), 104.
17. Fan, J., Yan, P., Wang, Y., Shen, B., Ding, F., & Liu, Y.Prevalence and clinical significance of low T3 syndrome in non-dialysis patients with chronic kidney disease. Medical science monitor*: Int. Med.J. exper. And clin.Res.2016:*22,1171.
18. Rhee, C. M. The interaction between thyroid and kidney disease: an overview of the evidence. Current opinion in endocrinology, diabetes, and obesity,2016: 23(5), 407.
19. Praw, S. S., Way, J. S. A., & Weiss, R. Evaluating Thyroid Function Tests in Patients with Kidney Disease. Endocrine Disorders in Kidney Disease: Diagnosis and Treatment,2019:85-96.
20. Taylor, P. N., Lansdown, A., Witczak, J., Khan, R., Rees, A., Dayan, C. M., & Okosieme, O.Age-related variation in thyroid function–a narrative review highlighting essential implications for research and clinical practice. Thyroid Research,2023:16(1),1-12.

Received: October 9th 2023/ **Accepte**d: January 15th 2024 / **Published:**15 February 2024

Citation: Jadaan T. M., Al-Hayali H. L. Chronic Kidney Disease Effect Thyroid Hormones. Revis Bionatura 2024; 9 (1) **34**. http://dx.doi.org/10.21931/RB/2024.09.01.**34**

Additional information Correspondence should be addressed to haysbio68@uomosul.edu.iq

Peer review information. Bionatura thanks anonymous reviewer(s) for their contribution to the peer review of this work using https://reviewerlocator.webofscience.com/

All articles published by Bionatura Journal are made freely and permanently accessible online immediately upon publication, without subscription charges or registration barriers.
Bionatura ISSN. First 13909355 Ecuador. **Scopus coverage years**: from 2016 to the present
Publisher's Note: Bionatura stays neutral concerning jurisdictional claims in published maps and institutional affiliations.

Bionatura
Ibero-American Journal of Biotechnology and Life Sciences

Article

Isophreatic curves of groundwater wells in the upper zone of Cerro de Hula, Santa Ana, Francisco Morazán

Kelly Almendares-Rivera [1,2] *, *Tania Peña-Paz* [3]

[1] *Master's in Water Resources with a Focus on Hydrogeology/ Universidad Nacional Autónoma de Honduras/Tegucigalpa/Honduras.*
[2] *Water Resources Unit, Honduran Institute of Earth Sciences (IHCIT in Spanish) / Universidad Nacional Autónoma de Honduras/Tegucigalpa/Honduras*
[3] *Experimental and Innovation Center for Water Resources (CEIRH-IHCIT in Spanish), Master's in Water Resources Coordination - Universidad Nacional Autónoma de Honduras; tania.pena@unah.edu.hn;*
* *Correspondence: kelly.almendares@unah.edu.hn; Tel.: (Almendares-Rivera, K.)*
Available from. http://dx.doi.org/10.21931/RB/2024.09.01.39

ABSTRACT

The research is part of a master's research thesis, the aim of which is the generation of groundwater well curves in Cerro de Hula, located south of the capital of Honduras, which serves as a baseline to understand the movement of groundwater flow in the area preliminarily. To achieve this, groundwater level surveys were carried out in the field in April 2022 (dry season), which were analyzed, processed, and interpolated using the Kriging method in ArcGis software. The main findings show the survey of 21 groundwater extraction points, belonging to shallow and deep wells that supply around 2900 people in the area, and that the preliminary water movement according to the isophreatic curves corresponds to a radial flow, with curves ranging from 5 m deep of the water table remaining in the western part of the area (highest part), and moving downwards to the 100 m deep curves (eastern region). It is conclusive to mention that this is a preliminary tool for managing the area's underground water resources.

Keywords: groundwater, water table, isophreatic curves, radial flow.

INTRODUCTION

The study area is located south of the capital of Honduras, the city of Tegucigalpa, specifically in Cerro de Hula, between the municipalities of Santa Ana, San Buenaventura, and Ojojona, belonging to the department of Francisco Morazán, with an area of 18.7 km2.

Within the study area are two of the main villages of the municipality of Santa Ana, El Limón and La Bodega (see Figure 1), identifying around 11 communities (between villages and hamlets) with an approximate population of 3,287 people, living in 727 homes[1].

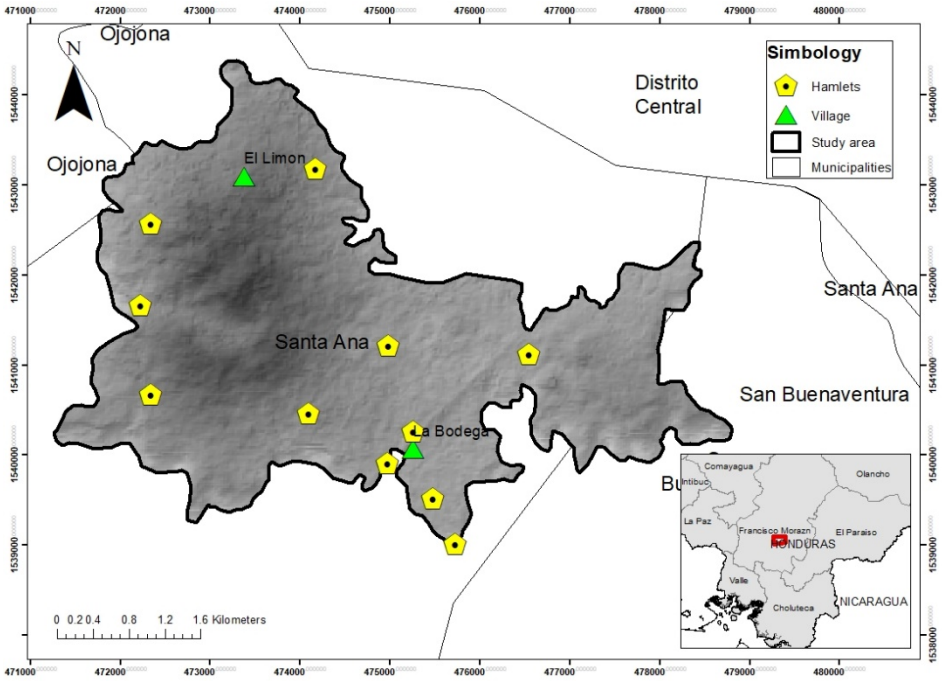

Figure 1: Location map of the study area and main villages and hamlets.

Land use in the study area is dominated by pastures and crops, broadleaf forest and deciduous secondary vegetation, with 35.4%, 35.3%, and 23%, respectively (see Figure 2 and Table 1). It is essential to highlight that the abundance of pastures and crops is consistent with the area's predominant economic activities (agriculture and livestock) and that, between the urban area and bare land, they add up to 1.2%[2].

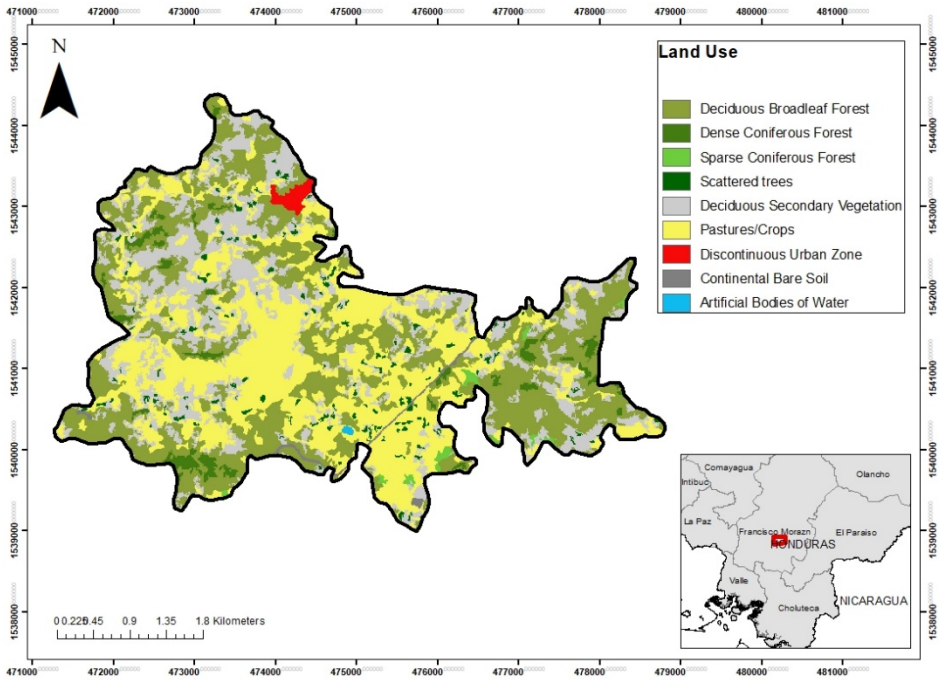

Figure 2: Land use map in the study area

The distribution of land use by percentage is shown in the following table:

Land Use	Area (Ha)	%
Scattered trees	33.8	1.8%
Dense Coniferous Forest	47.2	2.5%
Sparse Coniferous Forest	12.6	0.7%
Deciduous Broadleaf Forest	658.5	35.3%
Artificial Bodies of Water	1.2	0.1%
Pastures/Crops	661.6	35.4%
Continental Bare Soil	11.5	0.6%
Deciduous Secondary Vegetation	429.3	23.0%
Discontinuous Urban Zone	11.7	0.6%

Table 1. Land uses study area

The climate is characterized by relatively high rainfall, with average annual precipitation ranging between 1197 mm and minimum values of 1126 mm, and average annual temperatures between 22.6°C, the maximum value, and 21.5°C, the lowest value[3].

Morphologically, this study area has elevations exceeding 1460 meters above sea level (masl), reaching its highest part in Cerro de Hula with approximately 1700 masl (see Figure 3), considered one of the central hills in the area's municipalities. This hill has been considered in geological studies as a water shield volcano, where the activity has now ceased, and according to the presence of rocks, it is regarded as a fractured basaltic dome located in the western part of the work area, where the basaltic lava flows that have given it this table-like morphology[4] originated. Therefore, it has a rugged relief due to fractures, faults, and other geological structures. Moreover, as Ruiz (2015) indicates, prior to the volcanic event, rocks' high erosion and sedimentation rates led to numerous fluvial terraces evident today[4].

Among the geological formations present in the study area are the Quaternary basalts, a series of lava flows of basalt-to-basalt andesite type; the Padre Miguel basalts are dark gray to black basalts[5], and in some areas of red color, this is a product of iron alteration. These basalts present a porphyritic to aphanitic texture, with some plagioclase minerals and a little augite and olivine visible, and Quaternary alluvium (see Table 2), which presents unconsolidated materials of gravels, coarse to fine sands and clays, a product of the alteration of the pyroclastic rocks and basalts.[4, 5, 6, 7].

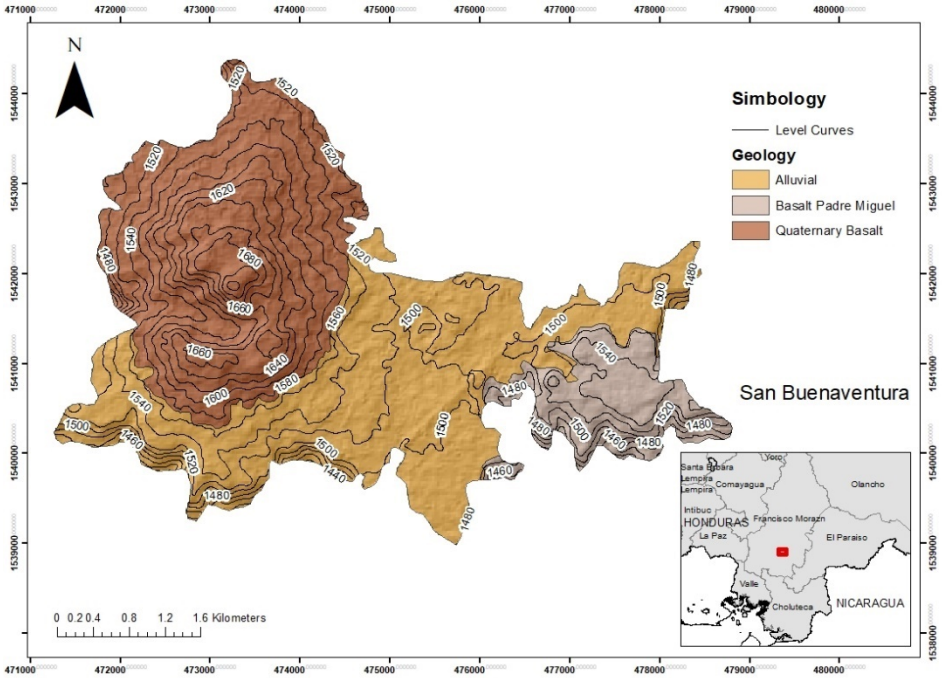

Figure 3: Geological map of the study area

The proposed lithological column is as follows:

Period		Unit	Litology
Quaternary		Qal	Unconsolidated alluvial sediments: sandy, clayey and sandy clayey, with an approximate thickness of 20 m.
		Qvc	Quaternary basalts: lava flows of the basalt to andesitic basalt type, approximately 100 m thick.
Terciario		Tpb	Basalt Padre Miguel: black to dark gray basalt, approximately 120 m thick.

Table 2. Lithological column of the area

Therefore, the hydrogeology of the place is primarily conditioned by the area's geology, with two types of aquifers: fractured and porous (see Figure 7). The fractured aquifer is dominated by the geological structures present, the basalts found as a product of lava flows, generating outcrops of igneous rocks in some places, and this set of structures is called a fractured aquifer. Due to its high degree of fracturing, this type of aquifer suggests high permeabilities, which could indicate that it is a potential groundwater recharge zone conditioned by other elements such as land use, slope, and soil type[4].

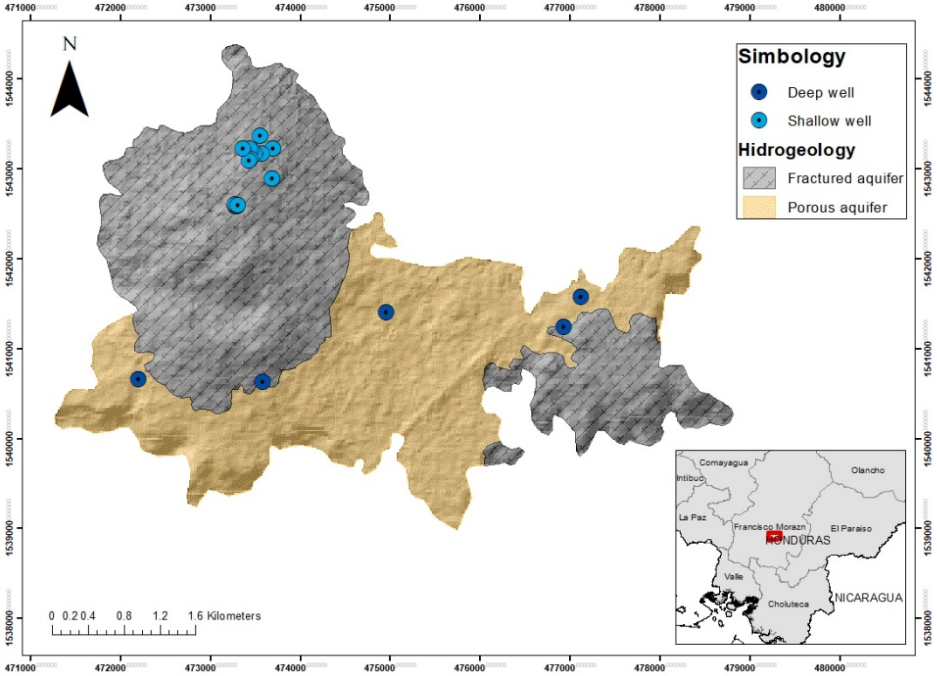

Figure 4: Hydrogeological map of the area under study and distribution of water sources identified and analyzed.

According to Simmons (1969)[8], the study area features valley soils, characterized as alluvial soils that cover much of the country's surface and are suitable for intensive cultivation. These are mainly found in valley and terrace elements.

In line with the morphological and geological description, the study area is suggested to be a basaltic dome structure that has undergone erosion processes to form the terraces. Therefore, the present hydrography is of ephemeral drains that feed water bodies around the lower parts, mainly Qda. El Trapiche, Río Ojojona, Qda. El Sauce, Qda. Agua Fría, and Qda. Sicacatare, part of the surface water sub-basins Verdugo, Grande, and Texiguat, belong to the Choluteca River Basin.[9].

Due to its great height, Cerro de Hula's primary water supply source is groundwater. This area has recently become an area of importance for the capital of Honduras since a large percentage of its population commutes to the city of Tegucigalpa for work[10]. Approximately 90% of the population of the municipality of Santa Ana is employed by companies that engage in different economic activities in Tegucigalpa[11]. Moreover, there are opportunities to obtain housing in new developments at a lower cost [12], supplied mainly by groundwater sources. Therefore, it becomes essential to conduct studies of the area's underground water resources, which can serve as management tools for underground water resources to stop or reverse these processes of ground-water depletion.

Among the main findings is identifying 21 groundwater supply sources in the area, of which 8 were surveyed in a study of the Adaptation Fund Project in 2014, and the remaining 13 points have been analyzed during this research. Out of the total wells, 5 are deep wells exceeding 150 m in depth, and 16 are shallow wells whose depths do not exceed 15 m. From these points, it was possible to measure the water table levels in April 2022, from which the isophreatic curves of the water in the study area have been constructed.

MATERIALS AND METHODS

The methodology used has been, first, data collection in the field. For this, field trips were carried out in April 2022 to update the healthy inventory in the area, where data collection forms were created and completed together with the local population and representatives of the entities managing the registered water source. This form collects the following aspects: general data, georeferencing of the source, data from the underground source, and physical data of the well. The physical information of the well includes depth, diameter, extraction

pump, extraction flow rate (when it could be measured), and groundwater level, the data of which was the main one used to achieve the study's objective. All this information was recorded and adjusted in Excel for subsequent analysis.

For the construction of the isophreatic curves, the measured values for all the obtained points, whether from shallow or deep wells, were taken, understanding from its geology that there is a layer of fractured basalt with a depth exceeding 100m. This information created a grid of points with the spatial location and one of its properties, the measured water table level. With this information, the interpolation was carried out using the Kriging method, defined as a method for geostatistical analysis of data variation. This means that it analyzes the behavior of data in space by studying variograms[13, 14].

This method has been applied in mining, geology, and hydrology, as it is a flexible spatial interpolation method. For example, one practical application is for the design of sampling networks, as Kriging is a method that can be used for data analysis in geohydrology[15, 16, 17, 18].

During the geostatistical analysis, the geostatistical analyst tool available in the ArcGIS software was used[19, 20]. With this tool, an initial exploratory analysis was first performed, in which it was possible to visualize how the data are distributed, spatial trends, and outlier values. Subsequently, a random sample of the data was taken to generate the interpolation model, and another sample was used to validate this model. Next, the interpolation model was made using the Kriging method with the generated random sample. Finally, this generated model was validated with the data that were not included in the previously mentioned random sample, meeting the statistical quality standards and which best fit the behavior of the data. Once the interpolation model was created, the isophreatic curves were generated every 5 meters.

The materials and equipment used for this update, verification, and well census were GPS and Solinst 101 metric probes.[21], plastic bucket, tape measure, stopwatch, camera, clipboard, field forms, and pencils. Excel and ArcGIS software were used for the analysis.

RESULTS

Among the main results is the census of new groundwater sources in the study area, of which 13 of 21 were analyzed for constructing the isophreatic curves. Of the total number of water wells used for the analysis, 5 belong to deep wells, and the rest belong to shallow wells (see Table 3).

Code	Registration Status	Community	X	Y	Z	Type of water source	Population supplied
CEA-01	New	Cerrito de Ayastas	476937	1541249	1523	Deep well	325
LB-01	Registered	La Bodega	474958	1541413	1511	Deep well	1440
LE-01	New	Los Encinos	473298	1542594	1657	Shallow well	5
LE-02	New	Los Encinos	473555	1543371	1580	Shallow well	5
LE-03	New	Los Encinos	473690	1542897	1612	Shallow well	4
LE-04	Registered	Los Encinos	473704	1543229	1595	Shallow well	5
LE-05	New	Los Encinos	473580	1543178	1605	Shallow well	8
LE-06	Registered	Los Encinos	473503	1543178	1619	Shallow well	10
LE-07	Registered	Los Encinos	473462	1543223	1608	Shallow well	6
LE-08	Registered	Los Encinos	473448	1543231	1606	Shallow well	2

LE-09	New	Los Encinos	473453	1543120	1610	Shallow well	15
LE-10	New	Los Encinos	473433	1543100	1605	Shallow well	15
LE-11	New	Los Encinos	473372	1543237	1597	Shallow well	5
LE-12	New	Los Encinos	473456	1543226	1600	Shallow well	6
LE-13	New	Los Encinos	473280	1542597	1649	Shallow well	520
LE-14	New	Los Encinos	473292	1542590	1661	Shallow well	
LE-15	New	Los Encinos	473282	1542609	1649	Shallow well	
LE-16	New	Los Encinos	473312	1542599	1652	Shallow well	
LP-01	Registered	Los Patios	472203	1540666	1551	Deep well	80
LQB-01	Registered	Las Quebradi-tas	473588	1540641	1583	Deep well	325
YPC-01	Registered	Yastepec	477125	1541584	1510	Deep well	150

Table 3. Data from groundwater wells analyzed

The depths of the wells under study, for the case of shallow wells, do not exceed 15 m, while deep wells range from 70 m to 153 m (see Figure 5).

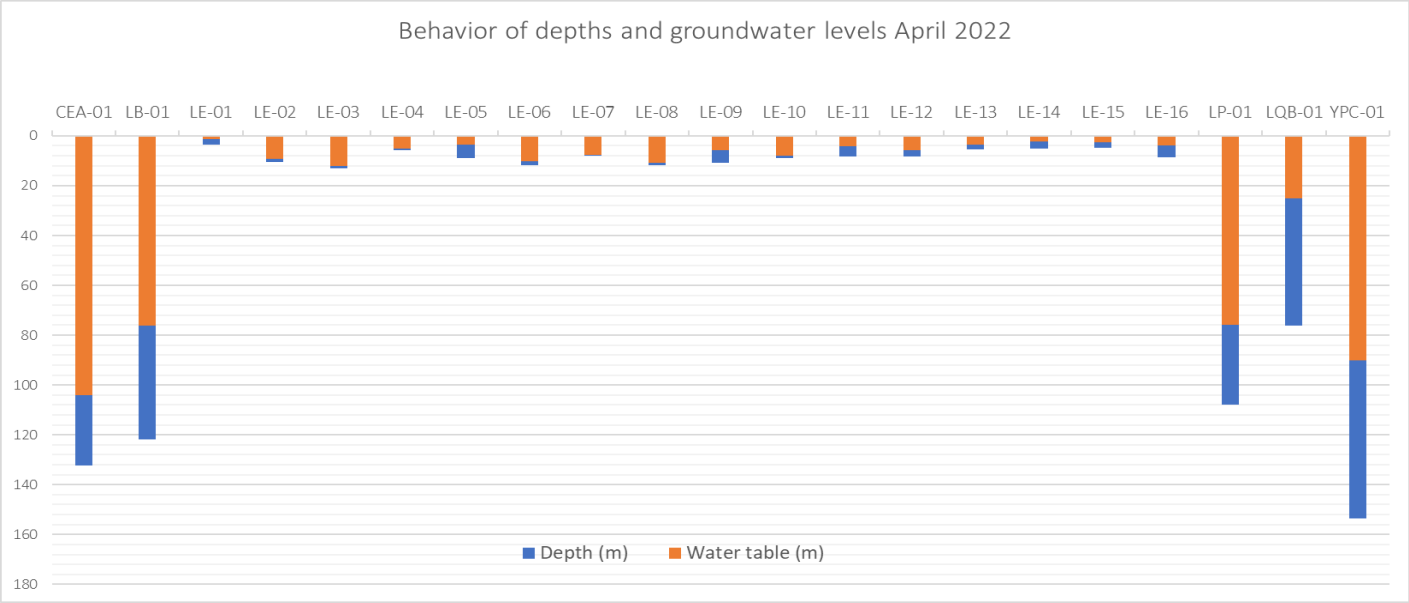

Figure 5: Graph of the behavior of the depths and groundwater levels of the wells under study.

It is essential to highlight that the population supplied by these wells is around 2900 people, which are distributed, as can be seen in Figure 6 and Table 3.

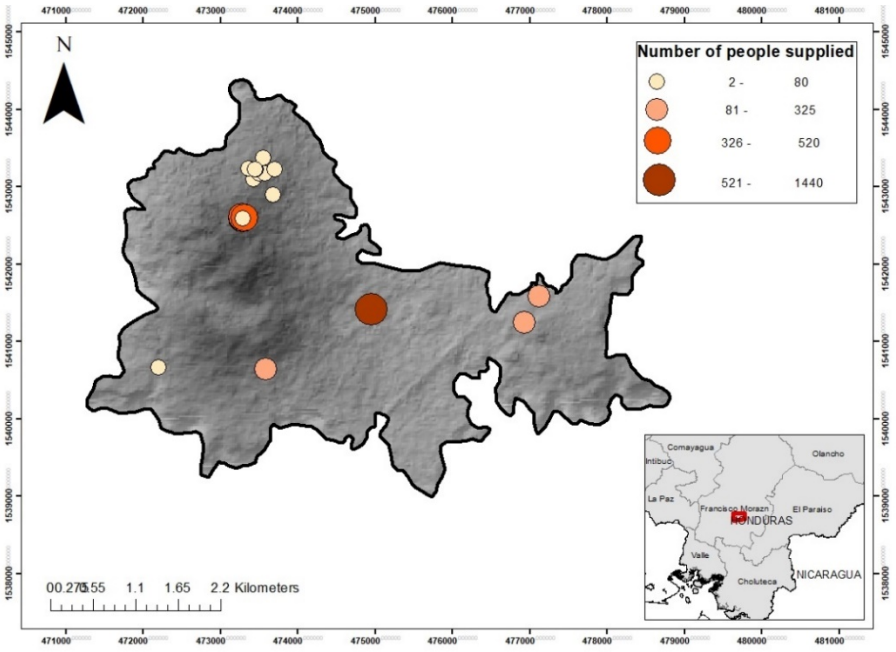

Figure 6: Population-supplied map

Upon analyzing groundwater wells, the isophreatic curves were constructed. These curves range from the 5m contour located at the highest point of Cerro de Hula, situated to the west of the study area, and the lowest curve presents at over 100m, found in the deepest part of the well belonging to the community of Cerrito de Ayasta on the eastern side of the study area. (see Figure 7).

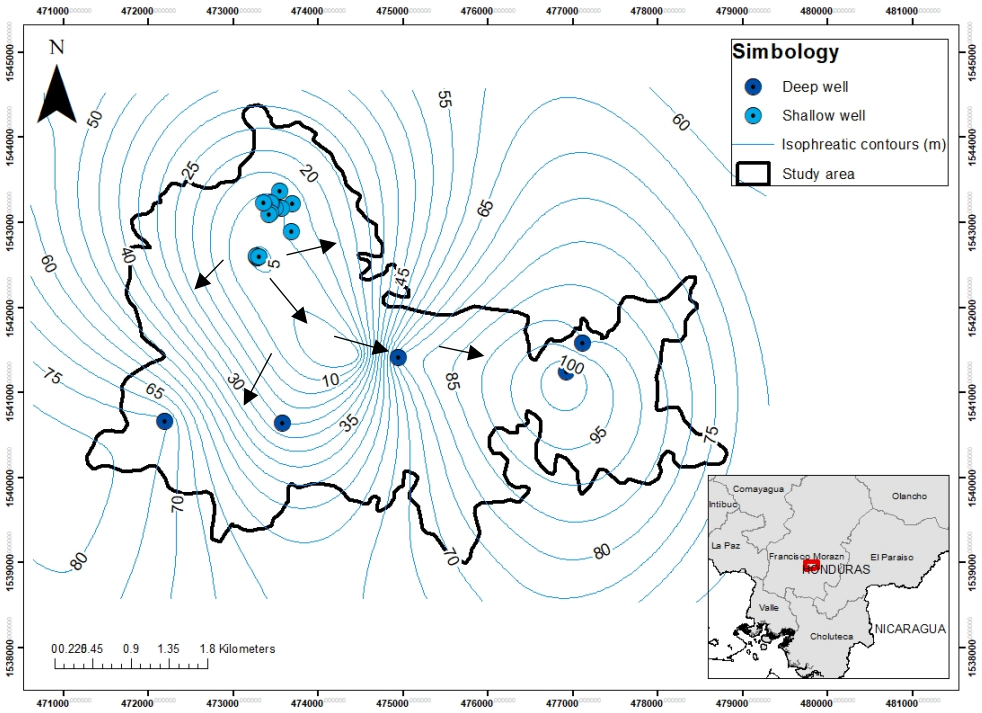

Figure 7: Isophreatic curves map of the study area

DISCUSSION

The analysis of the isophreatic curves provides a preliminary view of the behavior of the underground flow[22] in the area, which is dominated by its topography, as it is an area with a basalt dome structure at the highest part of Cerro de Hula [23], that over time has undergone erosion, which is why a shallow porous hydrogeological medium is located in the center of the area (see Figures 4 and 7)

This isophreatic behavior observed in the curves of Figure 7 shows that they have a radial flow[24, 25] from the highest point of Cerro de Hula with curves ranging from 5 m deep at the water table level in the western part of the area and moving downwards to the 100 m curves in the eastern region, corresponding to the well of the communities of Cerrito de Ayasta.

This radial behavior converges in the central part of the study area, from the 10 m contour to the 100 m water depth contour, potentially representing a groundwater discharge behavior. In contrast, from the highest part, the 5 m contour to the south shows a potential recharge zone[26].

Analyzing the isophreatic curves is a management tool for underground water resources in the study area, as it preliminarily shows us how the water moves there. This sets a baseline for future initiatives around groundwater study in the region and the country.

This study is just the beginning, mainly in building conceptual and numerical models whose elements aim to describe groundwater[27]. Understanding that a groundwater flow model becomes a fundamental tool to help understand how the system works and what volumes of the mass balance components are available to manage the underground water resource28 properly.

CONCLUSIONS

Within the study area, 21 underground sources were identified, of which 13 were surveyed during the research, and 8 sources had their information updated but had already been identified in previous studies. Of the total water wells used for this study, 5 are deep wells, and 16 are shallow wells, with depths ranging between 70 m to 153 m and 15 m, respectively.

The obtained isophreatic behavior shows a divergent radial flow from the highest part to the 10 m curve, representing a recharge zone in the study area. Also, a divergent flow is shown between the 15 m and 85 m curves, thus being a potential discharge area for groundwater.

The obtained isophreatic curves are a preliminary water management tool to understand the behavior of the underground flow in the study area, as it is essential for supplying approximately 2900 people.

Author Contributions: Research, analysis, and original writing, Kelly Almendares-Rivera; Review and supervision, Tania Peña-Paz.

Funding: This research received no external funding.

Acknowledgments: Special thanks to the Coordination of the Master's Degree in Water Resources with a focus on Hydrogeology at the Universidad Nacional Autónoma de Honduras for their support in providing equipment for field data collection, which belongs to the Honduran Institute of Earth Sciences (IHCIT in Spanish) of UNAH. Also, we acknowledge the support from the Project of the Adaptation Fund to Climate Change, known as "Ecosystem-Based Adaptation in the Central Forest Corridor of Tegucigalpa," carried out by the Secretariat of Natural Resources and Environment (SERNA in Spanish) and the United Nations

Development Programme (UNDP), as this project funded the preliminary information. Additionally, we extend our gratitude to Dr.-Ing. Carlos R. Guevara from Bundesanstalt für Geowissenschaften und Rohstoffe (the Federal Institute for Geosciences and Natural Resources (BGR)) in Hanover, Germany, for his thematic expertise and Research translated by Andrea José Rosales Tamashiro.

Conflicts of Interest: The authors declare no conflict of interest.

REFERENCES

1. INE. Instituto Nacional de Estadistica Honduras . Obtenido de INE: http://181.115.7.199/binhnd/RpWebEngine.exe/Portal?BASE=MUNDEP08&lang=ESP (2022).
2. ICF. Geoportal del Sector Forestal de Honduras. Obtenido de http://www.geoportal.icf.gob.hn/geoportal/main (2022).
3. IHCIT-UNAH. *Evaluación de los Recursos Hídricos en su Régimen Natural.* Tegucigalpa. (2014).
4. Ruiz, M.. *Geología del área de influencia de los municipios de: Santa Ana, Ojojona y San Buenaventura.* UNAH, Instituto Hondureño de Ciencias de la Tierra, Tegucigalpa. (2015).
5. Harwood, R. *Geology of Ojojona Quadrangle.* Instituto Geográfico Nacional y Dirección General de Minas e Hidrocarburos, Tegucigalpa, Honduras. (1991).
6. Anderson, M.. *Geology of Lepaterique Quadrangle.* Instituto Cartografico Nacional, Tegucigalpa, Honduras. (1985).
7. Rogers, R. O.. *Geología del Cuadrangulo de Tegucigalpa, Francisco Morazán.* Instituto Cartográfico Nacional, Tegucigalpa, Honduras. (1993).
8. Simmons, C. S.. *Los Suelos de Honduras.* Organizacion de las Naciones Unidas para la Agricultura y la Alimentación (FAO), Roma. (1969).
9. SINIT. *Sistema Nacional de Información Territorial de Honduras*. Obtenido de http://www.sinit.hn/ (2022).
10. Cruz, V. H., Galindo, K., Vásquez, C., & Edwar.. *Plan de Desarrollo Municipal - Municipio de Santa Ana Francisco Morazán.* Municipalidad de Santa Ana, Unidad Técnica Municipal, Santa Ana, Francisco Morazán. (2020). Obtenido de https://www.sgjd.gob.hn/biblioteca-virtual/docspdm/pdm-certificados/fco-morazan-pdm-certificados/1207-pdm-santa-ana-francisco-morazan/file
11. Municipalidad de Santa Ana.. *Informe Levantamiento Línea Base Municipio de Santa Ana, Francisco Morazán.* Santa Ana, Francisco Morazán. (2018). Obtenido de https://www.sgjd.gob.hn/biblioteca-virtual/docspdm/linea-base/08-francisco-morazan/1475-linea-base-santa-ana-francisco-morazan/file
12. Heraldo, E.. La zona sur de la capital se perfila como el nuevo polo de desarrollo. *El Heraldo*. Obtenido de https://www.elheraldo.hn/tegucigalpa/zona-sur-tegucigalpa-desarrollo-honduras-LXEH1465097#image-1. (2021).
13. Villatoro, M., Henríquez, C., & Sancho, F.. Comparación de los interpoladores idw y kriging en la variación espacial de ph, ca, cice y p del suelo. *Agronomía Costarricense,* **2008**. *32*(1), 95-105. Obtenido de https://revistas.ucr.ac.cr/index.php/agrocost/article/view/6773
14. Zucarelli, A., Paris, M., & Macor, J.. *Utilización de kriging para la elaboración de curvas isohietas de precipitación mensual en la Provincia de Santa Fe, Argentina.* Universidad Nacional del Litoral, Facultad de Ingeniería en Ciencias Hídricas, Santa Fé, Argentina. (2014). Obtenido de http://www.tvdigitalargen.ina.gov.ar/ifrh-2014/Eje3/3.39.pdf
15. Hughes, J., & Lettenmaier, D.. Data Requirements for Kriging: Estimation and Network Design. *Water Resources Research,* **1981**. *17*(6), 1641-1650. doi: https://doi.org/10.1029/WR017i006p01641

16. Rouhani, S., & Hall, T. J.. Geostatistical Schemes for Groundwater Sampling. *Journal of Hydrology,* **1988**. *103*, 85-102. doi: https://doi.org/10.1016/0022-1694(88)90007-8
17. Rouhani, S.. Geostatistics in Water Resources. *Georgia Water Resources Conference.* Georgia. (1989). Obtenido de https://repository.gatech.edu/server/api/core/bitstreams/e66fc3cd-6b12-4e20-af07-69a98da79499/content
18. Kitanidis, P. K.. *Introduction to Geostatistics: : Applications in Hydrogeology.* Stanford, California, EUA. 1997. Obtenido de https://books.google.es/books?hl=es&lr=&id=ZvoibTTS9QwC&oi=fnd&pg=PR19&dq=Introduction+to+Geostatistics+P.+K.+KITANIDIS&ots=q7BwBHFQqV&sig=9Fy-vSPhmDW_-OHUMROL40RMyNE#v=onepage&q=Introduction%20to%20Geostatistics%20P.%20K.%20KITANIDIS&f=false
19. Mejía Rivera, O., Betancur Vargas, T., & Londoño Ciro, L.. Aplicación de técnicas geoestadisticas en la hidrogeología del bajo Cauca Antioqueño. *SciELO Analytics,* **2007**. *74*(152), 137-149. Obtenido de http://www.scielo.org.co/scielo.php?script=sci_arttext&pid=S0012-73532007000200012
20. Gaspari, F. J., & Delgado, M. I.. Caracterización morfométrica geoespacial. Estudio de caso: Arroyo Belisario, Argentina. *Tecnociencia Chichuahua,* **2010**. *4*(3), 154-163. doi: https://doi.org/10.54167/tch.v4i3.711
21. Solinst, C.. *Solinst Canada Ltd*. Obtenido de Solinst Canada Ltd: https://www.solinst.com/espanol/productos/instrumentos-de-medicion-de-nivel/101-medidor-de-niveles-de-agua/ficha-tecnica/?utm_source=GA-&utm_medium=Search-&utm_campaign=101-GA-101-search-sa&utm_term=LM-SA-&utm_content=responsivetextad-spanish1&gad=1&gclid. (2023).
22. Barrera-de-Calderón, M., Garfias, J., Martel, R., & Salas-García, J.. Controles geológicos en el flujo de agua subterránea y distribución de volúmenes de extracción asociados a una estructura volcánica compleja. *Boletín de la Sociedad Geológica Mexicana,* **2021**. *73*(1), A170820 doi: https://doi.org/10.18268/BSGM2021v73n1a170820
23. Ruffo, A. G., Albouy, R., Giorgi, J., & Bastianelli, N.. El agua subterránea para abastecimiento humano en las dunas costeras del suroeste bonaerense. *I Jornadas del agua en el Sudoeste Bonaerense*, (págs. 293-296). Bahía Blanca, Argentina. (2019). Obtenido de https://www.researchgate.net/publication/338047277_El_agua_subterranea_para_abastecimiento_humano_en_las_dunas_costeras_del_suroeste_bonaerense
24. Gastmans, D., Veroslavsky, G., Kiang Chang, H., Caetano-Chang, M. R., & Nogueira Pressinotti, M. M.. Modelo hidrogeológico conceptual del Sistema Acuífero Guaraní (SAG): una herramienta para la gestión. *Boletín Geológico y Minero,* **2012**. *123*(3), 249-265. Obtenido de https://www.igme.es/boletin/2012/123_3/8_ARTICULO%204.pdf
25. Barrera de Calderón, M. L., Garfias, J., Martel, R., & Salas Garcia, J.. Influencia potencial de las fallas en el flujo de agua subterránea de un acuífero volcánico conformado por materiales porosos y fracturados. (T. y. agua, Ed.) *Repositorio Institucional Universidad Autónoma del Estado de México*. (2020). Obtenido de http://ri.uaemex.mx/handle/20.500.11799/106013
26. Auge, M.. *Hydrogeology of Plains.* Buenos Aires, Argentina: Springer. (2016). Obtenido de https://www.bfa.fcnym.unlp.edu.ar/id/42552
27. Enemark, T., Peeters, L., Mallants, D., & Batelaan, O.. Hydrogeological conceptual model building and testing: A review. *Journal of Hydrology*, **2018**. *569*, 310-329. https://doi.org/10.1016/j.jhydrol.2018.12.007
28. Mira, A., Vives, L., Rodríguez, L., & Veroslavsky, G.. Modelo hidrogeológico conceptual y numérico del Sistema Acuífero Guaraní (Argentina, Brasil, Paraguay y Uruguay). *Sociedad Geológica de*

España-Geogaceta, **2018**. 64, 67-70. Obtenido de https://sge.usal.es/archivos/geogacetas/geo64/geo64_17.pdf

Received: October 9th 2023/ **Accepte**d: January 15th 2024 / **Published:**15 February 2024

Citation: Almendares-Rivera, K.; Peña-Paz. Isophreatic curves of groundwater wells in the upper zone of Cerro de Hula, Santa Ana, Francisco Morazán. Revis Bionatura 2024; 9 (1)3**9**. http://dx.doi.org/10.21931/RB/2024.09.01.3**9**

Additional information Correspondence should be addressed to *kelly.almendares@unah.edu.hn*
Peer review information. Bionatura thanks anonymous reviewer(s) for their contribution to the peer review of this work using https://reviewerlocator.webofscience.com/

All articles published by Bionatura Journal are made freely and permanently accessible online immediately upon publication, without subscription charges or registration barriers.

Bionatura ISSN. First 13909355 Ecuador. **Scopus coverage years**: from 2016 to the present
Publisher's Note: Bionatura stays neutral concerning jurisdictional claims in published maps and institutional affiliations.

Bionatura
Ibero-American Journal of Biotechnology and Life Sciences

Article

Estimation of the shelf life of sweetened soft drinks based on microbiological and sensory analysis

Enrique Salazar Llorente[1*], *María Cabanilla*[1], *Daniel Arias-Toro*[1], *Gabriela Medina*[1]

[1]*Facultad de Ciencias Agropecuarias, Universidad Técnica de Babahoyo, Km 7.5 Vía Babahoyo – Montalvo, Ecuador*
** Correspondence: ejsalazar@utb.edu.ec*
Available from. http://dx.doi.org/10.21931/RB/2024.09.01.40

ABSTRACT

In the present investigation, the shelf life of sweetened beverages was investigated through microbiological and sensory analyses. An experimental design was employed, which included the variable of storage time. This allowed for the identification of significant differences in the organoleptic and microbiological characteristics of the beverages.

Samples of the beverages were taken during their processing and evaluated over time, especially during the pasteurization process at 85°C for 120 seconds. Laboratory analyses focused on microbiological tests, sensory studies, and assessments of the processed product's quality.

The microbiological results remained within the limits established by INEN standards, with counts of mesophilic aerobes < 100 CFU/cm3, yeasts and molds < 50 CFU/cm3, total coliforms < 3 MPN/cm3, and fecal coliforms < 3 MPN/cm3. Regarding sensory analysis, it was found that the beverages had a characteristic aroma, a slightly yellow color, and a characteristic citrus flavor, making them highly acceptable to consumers. Furthermore, the shelf life of the beverages was determined through accelerated aging at 32°C, resulting in a shelf life of 2 months. These findings supported the conclusion that the beverages could be stored for 6 months at room temperature, as indicated in another study that employed a similar methodology and evaluated properties such as color, aroma, and flavor.

Keywords: Analysis, mesophilic aerobes, fecal coliforms, yeasts and fungi[4], shelf life.

INTRODUCTION

Current lifestyles are causing changes in eating habits, which lead to more and more products with high nutritional characteristics that are easy to prepare and consume. In these processed products, the nutritional properties and some sensory ones are of great importance as quality attributes that encourage consumer interest and contribute to product acceptance. [1]

In the beverage market, there is also a high level of competition. Companies constantly try to win consumers' preferences by selling their product ideas through significant advertising campaigns. This point is also related to the many substitute products that significantly affect the demand for beverages. [2]

The production of drinks based on natural emulsions is the second most crucial operation in the technology of these drinks. High-purity sucrose syrups, glucose syrups or granulated sugar are often used. It begins with the

mixture of water and the different ingredients intended for each brand, and pasteurization is carried out at around 80ºC. The syrup, once pasteurized, is passed through a filter to remove possible solid impurities. Then, it is introduced into a Brix degree concentration unit, which regulates the amount of water to be added until the desired concentration is obtained for each soft drink. Once the exact preparation of the syrup is finished, flavorings, colorings, sweeteners, emulsifiers and, depending on each case, a small portion of natural juices are added. [3]

Sweeteners are chemical substances synthesized in a laboratory that impart a sweet taste to food and have sensory properties most people appreciate. [4]

Sweetened products, when in their chemical composition, sugar (sucrose), have been replaced by a sweetening additive that considerably reduces the amount of calories we consume. [5]

The food industry has in the sensory evaluation an instrument that allows it to assess the consumer's perception of a product as a whole or of a specific aspect of it. In this type of testing, the information provided by a panel is perceived by the sensory organs of sight, smell, hearing, taste, and touch, and the results make it possible to determine how the processing and formulation of a product affect the acceptability of a food. [6]

Sensory evaluations demand careful organization. It begins with selecting the attributes to be categorized in the sample, the design of the instruments for the collection of information, the type of test to be carried out and the determination of the type and number of panelists who will participate in the evaluation. [7]

The selection of attributes depends on the type of food and the product recipient. On the other hand, the instrument's design relies on the kind of test to be carried out, and, ultimately, the number of inspectors necessary for a valid sensory test depends on the type of auditors used.[8]

Microbiological analysis is the detection, identification or enumeration of microorganisms in materials using biological, biochemical, molecular or chemical methods. This generally applies to microorganisms that cause disease and food spoilage. [9]

Coliforms are indicators of water and food contamination; the determination and concentration of these bacteria in the condensed water for technological uses in juice-producing plants, and their means of transmission or contamination is through feces. [10]

Fecal coliforms are microorganisms with a structure similar to the bacteria known as *E. coli*. Their means of transmission is through excrement in food; it can occur due to the misapplication of BPM in processes and poor personal hygiene. [11]

They are mesophilic, psychrophilic, aerobic, or facultative anaerobic bacteria that can grow in the nutrient agar culture medium. However, high counts of mesophilic anaerobes are not considered inadequate since the process these beverages go through allows the development of microorganisms called fermenters (lactic acid bacteria, yeast molds) since their presence is naturally present and they are the main reasons for fermentation to take place, in addition to giving the drinks new physical-chemical and organoleptic properties. [12]

Molds and yeasts that cause spoilage in products with high water activity tolerate high osmotic pressure and low pH and tend to grow at refrigeration temperatures. However, the minimum inhibitory concentration of sodium benzoate and potassium sorbate decreases when water activity, pH and incubation temperature decrease. Some yeasts are extraordinarily resistant to preservatives. [13]

MATERIALS AND METHODS

The evaluation method chosen was the intervals (Category & Scaling Test), which allows for establishing the level of liking between several samples, having as indicators the color, smell and flavor, and making the respective evaluations against the flavor in general. (balance, touches of naturalness or artificiality). This method is easy to understand and apply, and it does not require the training or experience of the participants.

A scale from 1 to 5 was used, where 1 is very unpleasant, and 5 is very pleasant.
The evaluations were conducted in a beverage manufacturing company with previously selected administrative personnel.
The products (soft drinks to be evaluated) were offered individually in the afternoon, giving the judges a neutralizing agent (purified water) to alternate between the samples.
In all sessions, the samples were presented at refrigerated temperature (8°C) in disposable containers coded with three-digit random numbers containing 25 ml. of product.

Microbiological Testing of Soft Drinks

The microbiological tests for soft drinks are based on the following INEN standards that are detailed below, specific for each microorganism evaluated: Coliforms- INEN 1529-6 Standard, Fecal coliforms- INEN 1529-8 Standard, Mesophilic aerobic-Standard INEN 1529-5, Count of fungi and yeasts-Standard INEN 1529-10.

INEN 1529-6 Standard

The method is based on determining coliforms using the Most Probable Number (MPN) technique by tube dilution, using the selective liquid medium bile-lactose brilliant green broth or similar for the presumptive test and the tubes that present gas are confirmed. On eosin methylene blue (EMB) agar. The presumptive and confirmatory assay incubation temperature is 30+1°C for refrigerated products and 35+1°C for products kept at room temperature. [14]

INEN 1529-8 Standard

It is used in the determination of fecal coliforms and *E. Coli*. The method is based on the modified Eijkman test to detect lactose fermentation, with gas production at 44 - 45.5 + 0.2°C and complemented with the indole test at this temperature. These assays are carried out in brilliance-lactose bile broth and tryptone broth, starting with an inoculum taken from each gas-positive tube of the culture for total coliforms and incubated at 45.5 + 0.2°C. The confirmation of *E. Coli* and the differentiation of the species and varieties of the fecal coliform group are carried out using the tests for indole, methyl red, Voges-Proskauer and sodium citrate. [15]

INEN 1529-5 Standard

Determining the amount of mesophilic aerobic microorganisms is based on the certainty that a vital microorganism present in a food sample, when inoculated in a solid nutrient medium, will reproduce, forming a visible individual colony. So that the count of the colonies is possible, decimal dilutions of the initial suspension of the sample are made, and the nutrient culture medium is inoculated. The inoculum is incubated at 30°C for 72 hours, and then the number of colonies formed is counted. The count calculates the number of microorganisms per gram or cubic centimeter of food. [16]

INEN 1529-10 Standard

To determine fungi and yeasts, the method is based on the cultivation between 22°C and 25°C of the propagating units of fungi and yeasts, using the plate count technique by deep seeding and in a medium containing extract yeast, glucose and mineral salts. Table 1 presents the microbiological requirements for soft drinks. [17]

Microorganisms	No	m	M	C.	Testing method
Coliforms MPN/cm ^{3}	3	<3	-	0	NTE INEN 1529-6
Fecal coliforms MPN/cm ^{3}	3	<3		0	NTE INEN 1529-8
Standard count in REP CFU/cm ^{3} plates	3	1.0 x 10 ^{2}	1.0 x 10 ^{3}	1	NTE INEN 1529-5
Count of fungi and yeasts UP/cm ^{3}	3	5.0 x 10 ^{1}			NTE INEN 1529-10
Where: **MPN: Most Probable Number** **CFU: Colony Forming Units** **UP: Propagation Units** **n: Number of units** **M: Rejection level** **C: Number of units allowed between m and M**					

Source: INEN 2304 Standard. [18]

Table 1. Microbiological requirements for soft drinks.

Evaluation of the Sensory Table of Soft Drinks

The descriptive sensory analysis consisted of analyzing and evaluating the organoleptic characteristics of the product and the most relevant aspects of it, such as color, flavor and texture.

The organoleptic analysis will consist of 3 differentiated phases:

Appearance and visual presentation of the product, which encompasses two parameters

Clarity: The degree of transparency and brightness the liquid offers to the eye is measured; color: both the hue and intensity of the color of the sample presented are valued, which varies depending on the type of soft drink valued and its typicality.

Olfactory phase, in which three aspects are taken into account

Intensity: Power or olfactory magnitude of the valued sample. Openness: Aromatic limpidity of the analyzed reference. Absence of defective memories and the presence of natural memories outside of all artificiality. Quality: The soft drink has complexity and elegance in this olfactory phase. Positive sensations are all those that offer nuances of the aromatic range of the "raw material" from which its preparation starts (in this case, lemon emulsion), as well as the specification that the product can offer in its denomination.

The gustatory phase, in which five parameters are assessed. Intensity: Degree of strength of the soft drink in its taste phase; Openness: The non-appearance of unpleasant and typical flavors of the soft drink in question, free of defects, according to its composition, will be valued positively, Quality: A set of taste sensations that refer to the soft drink's character, complexity and personality, which can come from its raw materials and the additives used in its preparation. It represents the parameter with the highest valuation of those included. Balance: The balance of the different taste sensations as it pass through the mouth is studied, with particular attention to the fundamental flavors of sweetness and acidity. The "freshness" of the product will be considered positive, given the type of soft drink.

Persistence: Sensations similar to those perceived when the soft drink is in the mouth. Taste the length of the sample.[19]

Evaluation to Predict the Shelf Life of Soft Drinks.

Shelf life or stability studies of soft drinks were carried out in the quality control laboratory to determine when a food product will maintain its "fit for consumption" characteristic and its acceptance by the consumer.

Essentially, the shelf life of a food is defined as the time in which it will retain its physicochemical, organoleptic and nutritional properties.

Shelf life encompasses several facets of nutritional value, including safety, feeding value, and sensory characteristics. When this nutritional value is affected, it significantly influences consumer purchasing decisions.[20]

The fundamental factors that influence the shelf life of a product are Formulation, Prosecution, Packing, and Storage conditions.

To predict the product's shelf life under study, a refreshing drink based on the lemon emulsion, an oven programmed at 40°C and with a humidity of 70%, the parameters with which the products are transported, were used. They are stored in trolleys for distribution under such conditions.

The forms of deterioration affecting the product, subject to physiological and biochemical processes determining its quality, were identified during the study. These systems are complex due to their chemical, physical and biological composition; consequently, knowledge and control of these processes are essential to preserve quality characteristics, that is, acceptability and safety.[20]

The order of reactions, temperature, activation energy, and organoleptic and microbiological analyses must be considered to analyze the speed of deterioration reactions. Each sample was evaluated over time (independent variable at 10 levels).

The samples will be evaluated with the parameters detailed below:

Microbiologic analysis: Total count of mesophilic aerobic, Fungus and Yeast Count, Presence of total and fecal coliforms, Sensory evaluation: Acceptance Tests, Comparison tests (Triangular, Duo-Trio).

Once the evaluation time (4 months) has concluded, the data measured over time will be collected, and the product's shelf life will be established, which must comply with the optimal organoleptic characteristics and safety required according to the INEN 2304 standard. [20] Figure 1 shows the stove used.

Figure 1. Measuring oven to predict shelf life in beverages. Source: [21]

RESULTS

Results and Statistical Analysis of Microbiological Tests

The tests were carried out in triplicate for each microbiological parameter indicated in the Ecuadorian standard. In the case of total and fecal coliforms, the mere presence in the drink led to the rejection of the sample. According to the INEN 2304 standard, the results of coliforms are expressed <3 UFC/ cm^3, which indicates the absence of the bacteria above in the sample evaluated. The counts of total aerobics, fungi and yeasts were taken to analyze the behavior concerning time.

Aerobes				
Days	C.F.O.	CF1	SFO	SF1
0	43	35	41	36
1	1	0	0	0
15	3	1	4	2
30	5	1	5	3
5	6	3	5	3
60	8	4	7	4
75	10	5	7	6
90	10	7	9	6
105	11	7	9	7
120	14	8	10	7

Table 2. Microbiological count in soft drink (UFC/cm3)

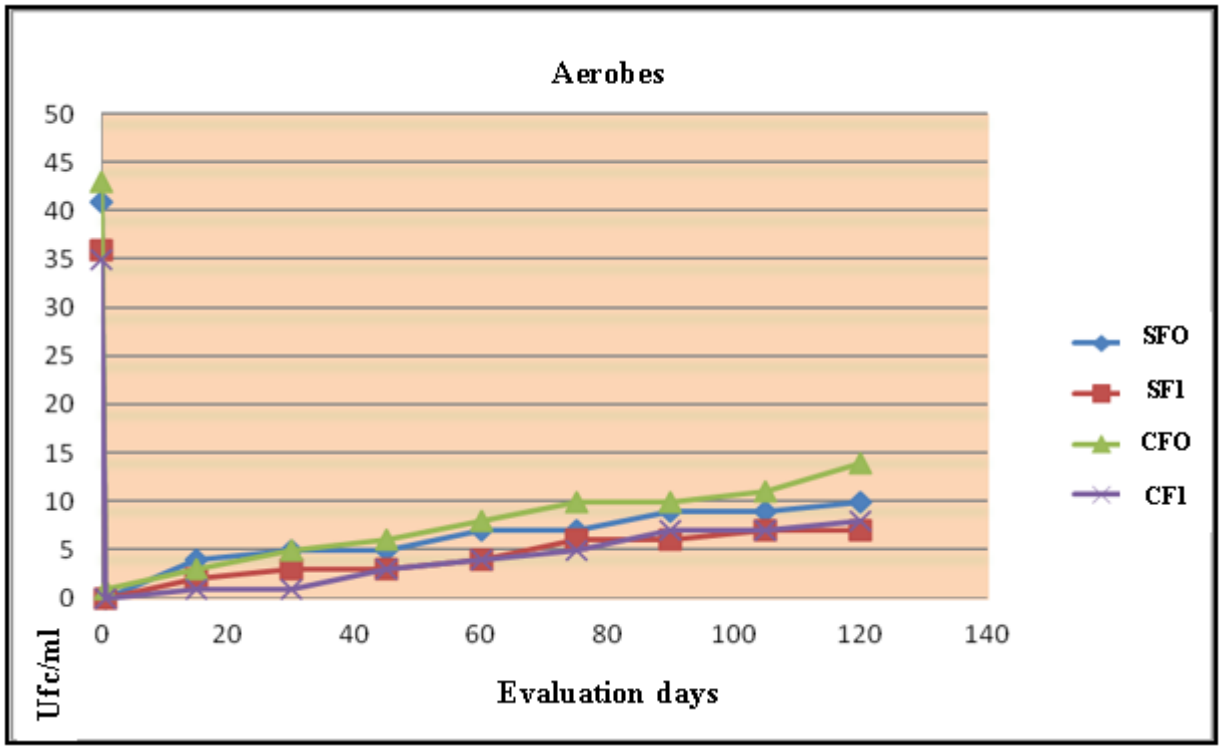

Figure 2. Behavior of aerobic soft drink evaluated for 4 months.

Variance analysis					
Fountain	Sum of squares	G1	middle square	Coefficient - F	P-value
between groups	109.475	3	364,917	0.3	0.8225
Intra Groups	4326.3	36	120,175		
Total (corr.)	4435.77	39			

Table 3. Analysis of variance for the aerobic count.

Table 3 shows the ANOVA table and that the coefficient F equals 0.303654. Since the p-value of the F test is greater than 0.05, there is no statistically significant difference between the means of the four variables at 95.0%. These means are represented in Figure 3.

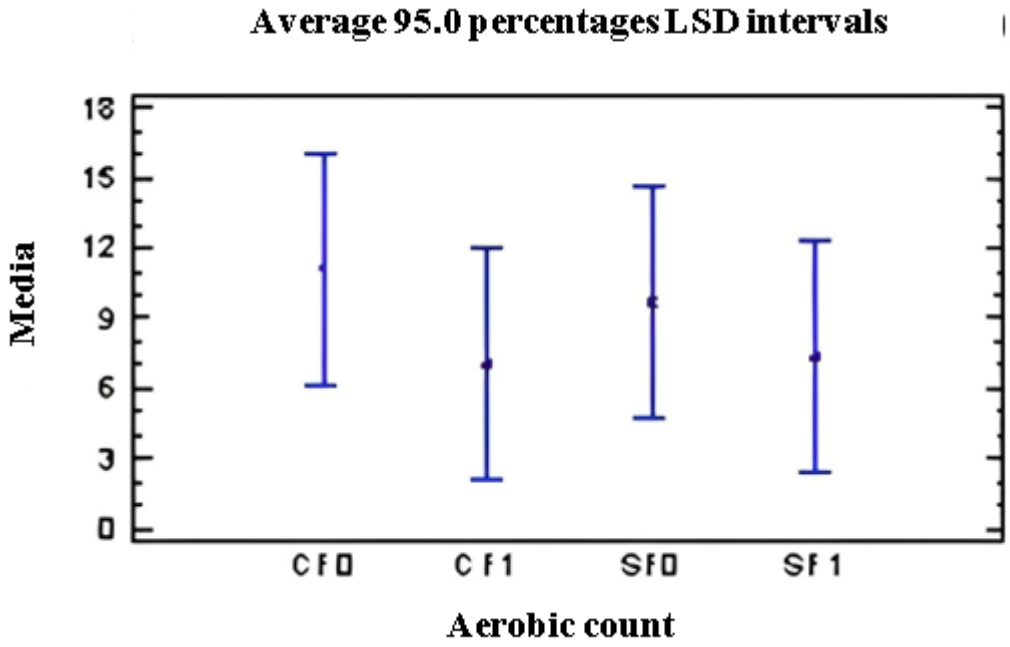

Figure 3. Graph of means (aerobic count)

Suppose only the values of the counts are considered after carrying out the pasteurization in Figure 3. In that case, a ratio F = 2.49 results are obtained for a p-value = 0.0784, which, being more significant than 0.05, would indicate no significant differences for 95% confidence. When the means are analyzed (Figure 4), it can be seen that the CF0 sample presents a slightly higher mean than the rest, so a multiple-range test was applied. This test shows a statistically significant difference between CF0 and CF1 and CF0 and SF1. When sucrose has been partially substituted by sweetener, the average aerobic count is lower than when working with fiber and only with sucrose. This is because there is less substrate in the beverages, which contributes to reducing the growth of microorganisms over time. However, the product is within the standard, indicating a maximum of 100 UFC/cm^3.

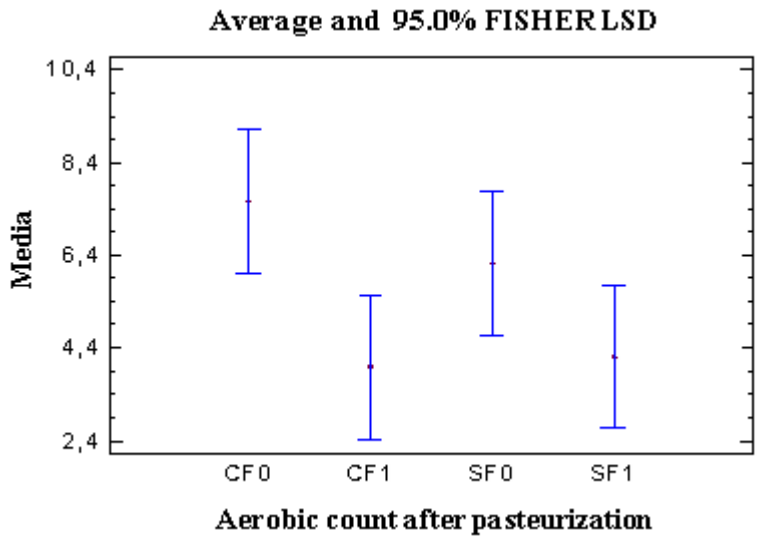

Figure 4. Aerobic count after pasteurization

Fungi and yeast				
Days	C.F.O.	CF1	SFO	SF1
0	22	11	24	15
0.5	3	2	4	0
15	5	2	5	3
30	5	3	5	3
4.5	6	5	6	5
60	6	5	6	5
75	7	5	7	5
90	7	6	9	7
105	8	7	10	7
120	10	7	12	7

Table 4. Microbiological count of fungi and yeasts in the soft drink cfu/ cm^3

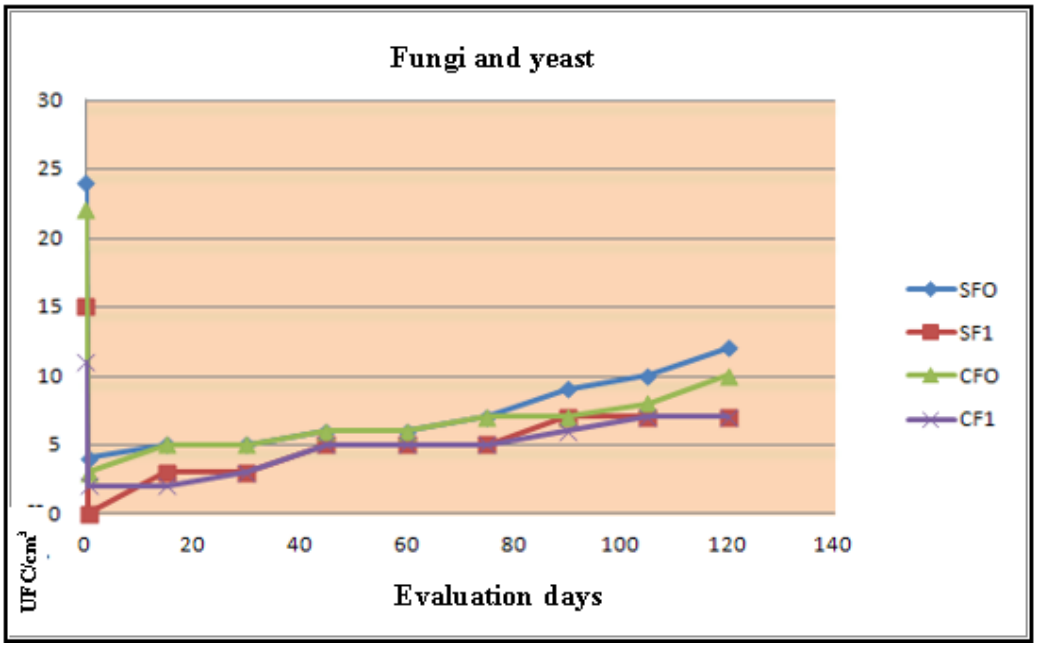

Figure 5. Behavior of fungi and yeasts in soft drinks.

Variance analysis					
Fountain	Sum of squares	G1	middle square	Coefficient - F	P-value
between groups	86.075	3	28.6917	1.34	0.2777
Intra Groups	772.7	36	21.4639		
Total (corr.)	858.775	39			

Table 5. Analysis of variance for fungi and yeast count

The ANOVA in Table 5 presents an F ratio of 1.33674, with a p-value greater than 0.05, where there is no statistically significant difference between the means of the 4 variables at 95.0% confidence.
Figure 6 presents the means for the samples and their confidence intervals.

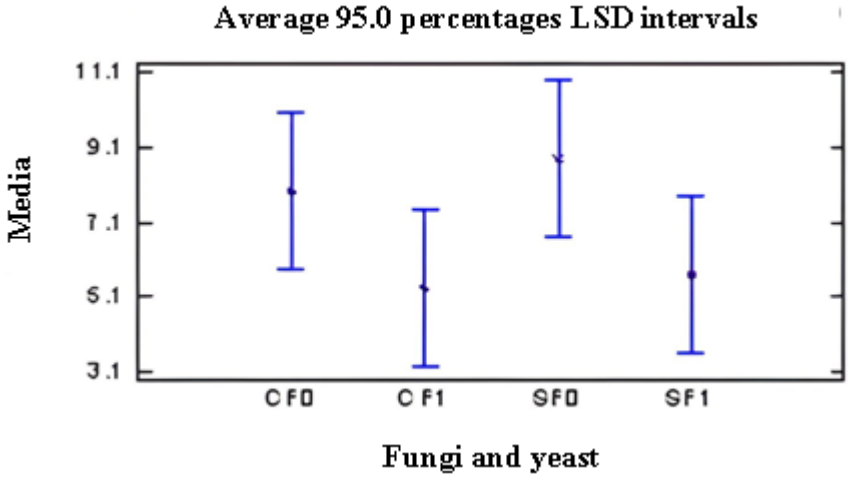

Figure 6. Graph of means (fungi and yeast)

The analysis of variance in Figure 6for the counts from 0.5 days after the pasteurization shows a ratio F=2.53 with p-value = 0.0744, where there are no statistically significant differences for the four samples. with 95% confidence. However, from the graph of the means (Figure 7), a slightly higher mean can be seen for the sample without fiber with 100% sucrose; this is the initial sample. This was verified with a multiple-range test finding two homogeneous groups.

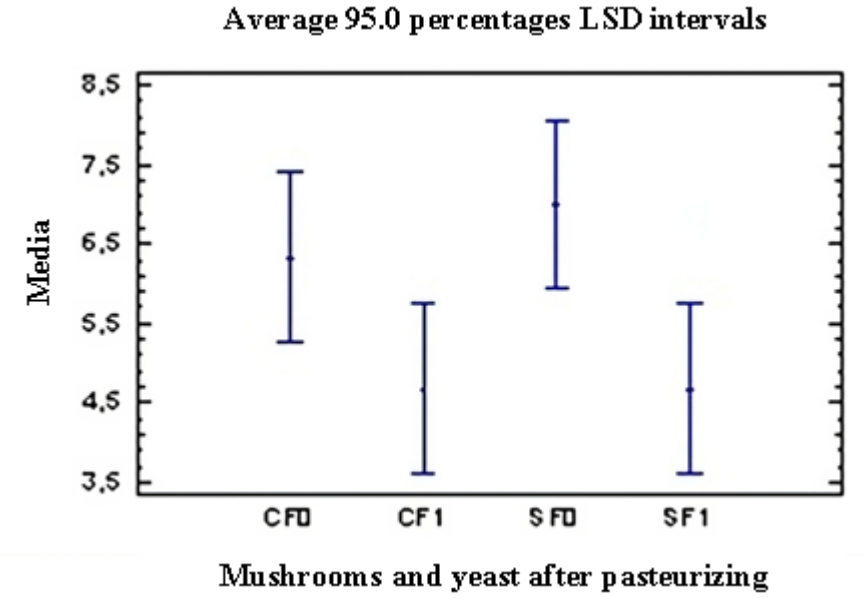

Figure 7. Graph of means (mushrooms and yeasts after pasteurizing)

Results and Analysis of Sensory Evaluation of Soft Drinks

It was explained to the sensory panel that the objective is to choose the formula with the taste threshold of best acceptance towards them. The method used is the hedonic scale test, based on a scale of liking and disliking the samples.

The scale comprises seven alternatives (table 6) divided into three for the level of liking, three for the level of dislike and one that specifies indifference to the sample.

The coding used was indicated in the Chapter on Materials and Methods. Four different formulas would be obtained according to the established formulation as specified.

Attributes to evaluate-Taste	Qualification
I like it extremely	7
Very nice	6
slightly nice	5
Neither nice nor unpleasant	4
slightly unpleasant	3
Very unpleasant	2
I dislike it extremely	1

Table 6. Hedonic taste acceptance scale.

The evaluation results were tabulated based on the rating each judge attributed according to the coded samples. It should be noted that each sample was identified based on the processing time. To obtain the results, the average of each of them was determined. The evaluations were issued by the judges (Table 7).

Attributes to evaluate - Flavor

Days	C.F.O.	CF1	SFO	SF1
0	6	7	7	6
0.5	7	6	7	6
15	7	6	6	7
30	6	7	6	6
4.5	7	6	5	6
60	5	5	6	5
75	5	5	5	5
90	4	5	4	4
105	4	4	4	4
120	4	4	4	4

Table 7. Tabulation of results

Variance analysis					
Fountain	**Sum of squares**	**G1**	**middle square**	**Coefficient - F**	**P-value**
Between groups	0.275	3	0.0916667	0.07	0.9758
Intra Groups	47.5	36	1.31944		
Total (corr.)	47.775	39			

Table 8. Analysis of variance for flavor

The ANOVA in Table 8 shows an F coefficient equal to 0.0695, with a p-value greater than 0.05, where there is no statistically significant difference between the means of the 4 variables at 95.0% confidence. Figure 8 shows this behavior.

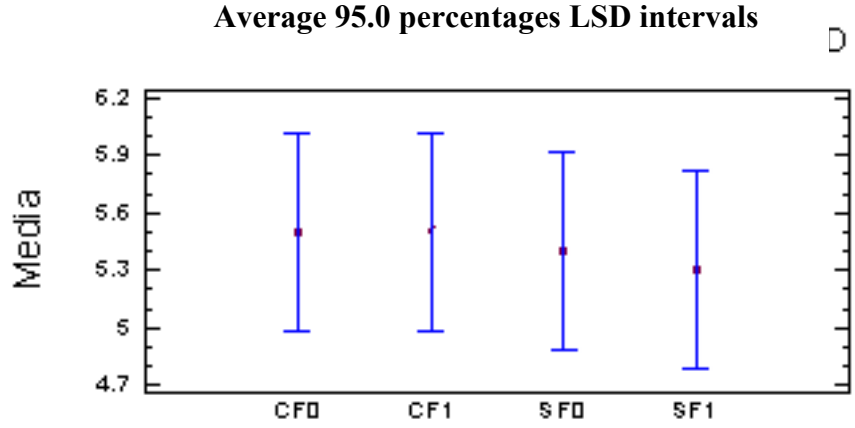

Figure 8. Graph of means

However, there is a tendency to decrease the attribute's value as time increases, reaching values from three months after the drink is produced, framed in the criterion "neither pleasant nor unpleasant".

Formulation

The integrated analysis of the variables studied in the previous sections shows no significant differences between the samples. Therefore, for the formulation of the soft drink, it was decided to choose the sample coded as CF1, the soft drink sweetened with 60% sugar and 40% sucralose, where an evaluated fiber concentration of 1.60% by weight was obtained. According to the panel's result, sixty days is the time that was chosen as the product's useful life. The product enriched with dietary fiber and partially substituted with 40% sucralose presents the following formulation (Table 9).

Ingredients	Percentage
Water	90.949
Saccharose	6.888
Sweetener	0.008
Sodium benzoate	0.012
Potassium sorbate	0.012
Sodium citrate	0.027
Ascorbic acid	0.007
EDTA	0.003
Citric acid	0.310
Colorant	0.014
lemon emulsion	0.170
Dietary fiber	1.600
Total	100

Table 9. Sweetened soft drink formula

Characterization of the Final Product

Sweetened lemon-flavored refreshing drink

Storage and Handling

Store in a cool, dry place, free of odors and protected from the sun. Preferably drink cold.

Useful lifetime

2 months at 32ºC

Organoleptic parameters

Characteristic odor

Color Slightly yellow

Characteristic citrus flavor

Microbiological parameters

Mesophilic aerobes < 100 CFU /cm3

Yeasts and fungi < 50 UFC/cm3

Total Coliforms < 3 MPN/cm3

Fecal Coliforms < 3 MPN/cm3

DISCUSSION

The study by Machín mentions that yeasts tolerate pH between 3 and 4, but pH between 4.5 and 6.5 is more favorable for their growth. Therefore, the sweetened beverage is a medium for its growth as it is in the above-mentioned pH ranges. [22]

According to the results of other studies, it is agreed that pasteurization has positive effects on sweetened beverages, reducing the microbial load and guaranteeing food safety due to heat treatment.[23]

Coliforms are a family of bacteria commonly found on plants, soil, and animals, including humans. Coliform bacteria are generally found in greater abundance in the surface layer of water or bottom sediments. Fecal

contamination has been, and continues to be, the leading health risk in water since it involves the incorporation of pathogenic microorganisms from patients and carriers and water transmission to the susceptible population. For this reason, sanitary control of microbiological risks is so important and constitutes an essential sanitary measure to maintain an adequate level of health in the population. [10]

As for the study's results, it was found that the evaluated sweetened beverage met the INEN 2304 standard in terms of microbiological aspects, indicating a low microbial load and good microbiological stability. Furthermore, it was determined that the beverage had a shelf life of 6 months at room temperature, which is valuable information for the beverage industry.

Regarding the implications of these findings, it is essential to note that the results can be helpful in the formulation and production of sweetened beverages and in implementing quality control and food safety measures. For example, these results can be employed to establish an appropriate shelf life for the product and ensure its microbiological and sensory quality. Additionally, the findings can benefit food product regulation, as they provide valuable insights into product quality and consumer safety.

However, it is essential to consider the study's limitations and potential sources of error. For instance, the study focused on a single sweetened beverage, so the results may not be generalizable to other similar products. Furthermore, the specific microbiological analysis techniques used are not specified in the text, which could impact the accuracy of the results. Finally, the study did not include an analysis of the physical stability of the product, which could be a significant limitation in terms of product quality.

In summary, the study's findings hold significant implications for the beverage industry and food product regulation. Nevertheless, it's crucial to consider the study's limitations and potential sources of error when interpreting the results. In the future, conducting additional studies to assess the quality and safety of other food products and enhancing the accuracy of the microbiological and sensory analyses used in this study would be significant.

CONCLUSIONS

The sensory analysis reveals that the sweetened beverage does not significantly alter the beverage's flavor profile. However, the impact of adding these sweeteners over time becomes evident through the increase in the beverage's solid content. This increase can be attributed to water evaporation during the stability test, driven by differences in partial pressures, resulting in a higher concentration of soluble solids in the beverage.

Regarding microbiological behavior, it can be concluded that sweetened beverages comply with the INEN 2304 standard. This compliance is linked to the reduced substrate content in the beverages, contributing to a decline in microbial growth over time. As a result, extending the product's shelf life from two to three months is possible, based on the findings of the sweetened beverage study.

The study's key findings indicate that the evaluated sweetened beverage possesses suitable organoleptic and microbiological characteristics while enjoying favorable consumer acceptability. Furthermore, it has been determined that the beverage has a shelf life of 6 months at room temperature, as inferred from the study's results. These findings hold significant implications for the beverage industry, as they enable the establishment of an appropriate product shelf life and assurance of its microbiological and sensory quality. Moreover, the results obtained can guide decisions related to the formulation and production of sweetened beverages and the implementation of quality control and food safety measures. In summary, the study furnishes valuable insights into the beverage industry, contributing to enhancing product quality and safety for consumers.

REFERENCES

1. Acevedo L, Mendoza C, Oyón Rafael. Total and fecal coliforms, some enterobacteria staphylococcus sp. and moulds in salads for hot dogs sold in Maracay, Venezuela. Latin America Nutrition Archives [Internet]. 2001 [cited 2024 Feb 23];51(4):366–70. Available from: https://pubmed.ncbi.nlm.nih.gov/12012562/
2. Ancasi EG, Carrillo L, Benítez Ahrendts M. Moulds and yeasts in bottled water and soft drinks. Argentine Journal of Microbiology [Internet]. 2006 [cited 2024 Feb 23];38(2). Available from: https://www.researchgate.net/publication/6758660_Moulds_and_yeasts_in_bottled_water_and_soft_drinks
3. Anzaldua-Morales Antonio. La evaluación sensorial de los alimentos en la teoría y la práctica. 1994 [cited 2024 Feb 23]; Available from: https://www.editorialacribia.com/libro/la-evaluacion-sensorial-de-los-alimentos-en-la-teoria-y-la-practica_53649/
4. Fernández-Santisteban MT. Determination of total and fecal coliforms in water for technological use for centrifuges. ICIDCA About Sugar Cane Products [Internet]. 2017 [cited 2024 Feb 23];51(2):70–3. Available from: http://www.redalyc.org/articulo.oa?id=223154251011
5. García-Flores C, López-Espinoza A, Gabriela Martínez Moreno A, Patricia Beltrán Miranda C, Patricia Zepeda-Salvador A. Estrategias para la disminución del consumo de bebidas endulzadas. Revista Española de Nutrición Humana y Dietética [Internet]. 2018 Jul 12 [cited 2024 Feb 23];22(2):169–79. Available from: https://www.renhyd.org/renhyd/article/view/426
6. Gómez R. Sensient Food Colors. 2017 [cited 2024 Feb 23]. Totally natural opacifying emulsions for beverages. Available from: https://sensientfoodcolors.com/es-la/id/emulsiones-opacificantes-totalmente-naturales-para-bebidas/
7. Corrales LC, Antolinez Romero DM, Bohórquez Macías JA, Corredor Vargas AM. Anaerobic bacteria: processes they perform and their contribution to life sustainability on the planet. Nova [Internet]. 2015 [cited 2024 Feb 23];13(24). Available from: http://www.scielo.org.co/scielo.php?script=sci_arttext&pid=S1794-24702015000200007
8. Álvarez Munárriz L, Álvarez de Luis A. Estilos de vida y alimentación. Gazeta de Antropología [Internet]. 2009 Dec 3 [cited 2024 Feb 23]; Available from: https://digibug.ugr.es/handle/10481/6858
9. Huezo M. AN. Evaluación física y sensorial de un prototipo de bebida de maracuyá con semillas de chía (Salvia hispanica L.) y análisis químico de la semilla de chía [Internet]. 2008 [cited 2024 Feb 23]. Available from: https://bdigital.zamorano.edu/handle/11036/164
10. Ávila Pineda GT, Fonseca Moreno MM. Microbiological quality of juices prepared in family welfare homes in the northern area of Cundinamarca. 2008.
11. Quitral R V, Pinheiro F AC, Carrera P C, Gallo U G, Moyano S P, Salinas V J, et al. Effect of non caloric sweeteners in sensory quality of orange juice. Revista chilena de nutrición [Internet]. 2015 Mar [cited 2024 Feb 23];42(1):77–82. Available from: http://www.scielo.cl/scielo.php?script=sci_arttext&pid=S0717-75182015000100010&lng=es&nrm=iso&tlng=es
12. Zavaleta Mercado R. Preparation of sucrose syrups by volumetric measurements. Acta Nova [Internet]. 2011 [cited 2024 Feb 23];5(1):110–37. Available from: http://www.scielo.org.bo/scielo.php?script=sci_arttext&pid=S1683-07892011000100006&lng=es&nrm=iso&tlng=es
13. Seijas Noya I, Jaurena G, Wawrzkiewicz M, Gaggiotti M, Romero LA, Méndez M. Quality evaluation of soybean by-products. J Agric Res [Internet]. 2020 [cited 2024 Feb 23];46(2):258–66. Available from: https://www.redalyc.org/journal/864/86464924014/html/

14. Ponce Chauca JL, Torres Beltrán LM. Estudio de factibilidad para la creación de una empresa dedicada a la producción y comercialización de jugos naturales en el Distrito Metropolitano de Quito. 2011 [cited 2024 Feb 23]; Available from: http://dspace.ups.edu.ec/handle/123456789/4474
15. Vito Villa JJ. Determinación de la vida útil mediante pruebas aceleradas (ASLT) de un producto extruido enriquecido con concentrado proteico de pota (Dosidicus gigas). Universidad Nacional Agraria La Molina [Internet]. 2019 [cited 2024 Feb 23]; Available from: http://repositorio.lamolina.edu.pe/handle/20.500.12996/4195
16. León P ÁM, Montoya C OI, Motato KE, Granda DM, Acaro C, Restrepo JM, et al. Colombian Wild Lactic Acid Bacteria (Lab) Show Good Properties in Sourdough Manufacture. Vitae, Journal of the Faculty of Pharmaceutical Chemistry. 2006;13(2):26–35.
17. Noguera F, Gigante S. Principios de la preparación de alimentos. 2018;
18. Instituto Ecuatoriano de Normalización I. NTE INEN 1529-7: Control microbiológico de los alimentos. Determinación de microorganismos coliformes por la técnica de recuento de colonias. 1990;2.
19. Instituto Ecuatoriano de Normalización I. NTE INEN 1529-10-1: Control microbiológico de los alimentos. Mohos y levaduras viables. Recuentos en placa por siembra en profundidad. [Internet]. 2013 [cited 2024 Feb 23]. Available from: https://es.scribd.com/document/488093112/1529-10-1R-MOHOS-Y-LEVADURAS-VIABLES-pdf
20. Instituto Ecuatoriano de Normalización I. NTE INEN 2304: Refrescos o bebidas no carbonatadas requisitos [Internet]. 2017 [cited 2024 Feb 23]. Available from: https://es.scribd.com/document/537817176/nte-inen-2304-1
21. López MF. Temperatures and pasteurization times of Guarapo on the microbiological, physicochemical and organoleptic characteristics for a refreshing drink. 2022;
22. Suárez-Machín C, Garrido-Carralero NA, Guevara-Rodríguez CA. Yeast Saccharomyces cerevisiae and alcohol production - Review. ICIDCA About Sugar Cane Products [Internet]. 2016 [cited 2024 Feb 23];50(1):20–8. Available from: http://www.redalyc.org/articulo.oa?id=223148420004
23. Bermeo Pin ML, Chiadó Loor GD. Temperatures and pasteurization times of guarapo on microbiological, physicochemical and organoleptic characteristics for a refreshing drink. 2022 [cited 2024 Feb 23]; Available from: http://repositorio.espam.edu.ec/handle/42000/1689

Received: October 9th 2023/ **Accepte**d: January 15th 2024 / **Published:**15 February 2024

Citation: Salazar Llorente E, Cabanilla M, Arias-Toro D, Medina G. Estimation of the shelf life of sweetened soft drinks based on microbiological and sensory analysis.Revis Bionatura 2024; 9 (1) 40. http://dx.doi.org/10.21931/RB/2024.09.01.40

Additional information Correspondence should be addressed to
Peer review information. Bionatura thanks anonymous reviewer(s) for their contribution to the peer review of this work using https://reviewerlocator.webofscience.com/

Bionatura ISSN. First 13909355 Ecuador. **Scopus coverage years**: from 2016 to the present

Bionatura
Ibero American Journal of Biotechnology and Life Sciences

Article

Diseño de un sistema de agitación para un biorreactor de 1m^3 de capacidad para la producción de ácido glicérico a partir de glicerol por fermentación microbiana de *Acetobacter tropicalis*

Design an agitation system for a 1m3 capacity bioreactor to produce glyceric acid from glycerol by microbial fermentation of *Acetobacter tropicalis*.

Daniel Cabrera-Valle [1]*, *Henry Pérez* [1]

[1]*Universidad Técnica de Ambato/Facultad de Ciencia e Ingeniería en Alimentos y Biotecnología/ Ambato/Ecuador*
HP: hperez0889@gmail.com;
** Correspondence: da.cabrera@uta.edu.ec*
Available from. http://dx.doi.org/10.21931/RB/2024.09.01.42

ABSTRACT

This work presents the design of an agitation system for a 1m3 capacity bioreactor intended to produce glyceric acid (GA) through microbial fermentation of *A. tropicalis* using 20% v/v glycerol as the primary substrate. Building on previous studies that evaluated ideal conditions for glyceric acid production, initial data were utilized to identify the impeller type and perform subsequent calculations, including impeller Reynolds number, power consumption, and mixing time. Once the agitator type was specified, standard geometric relationships were employed to size components of the agitation system, such as tank size, baffle plates, and agitator dimensions. Power consumption calculations were compared with results from other studies on fermentation media with similar rheological characteristics. The agitator's power consumption for mixing 1m3 of medium was determined to be 8.35 kW, achieving 95% homogenization in 5.14 seconds, with a mixing time error of approximately 10%, operating at an agitation speed of 500 rpm.

Keywords: agitation system; glyceryc acid; bioreactor

RESUMEN

Este trabajo presenta el diseño de un sistema de agitación para un biorreactor con capacidad de 1m^3, destinado al uso en la producción de ácido glicérico (AG) mediante la fermentación microbiana de *A. tropicalis* utilizando glicerol al 20% v/v como sustrato principal. Basándose en estudios previos que evaluaron las condiciones ideales para la producción de ácido glicérico, se utilizaron datos iniciales para identificar el tipo de impulsor y realizar cálculos subsiguientes, incluyendo el número de Reynolds del impulsor, el consumo de potencia y el tiempo de mezclado. Una vez identificado el tipo de agitador, se emplearon relaciones geométricas estándar para dimensionar componentes del sistema de agitación, como el tamaño del tanque, las placas deflectoras y las dimensiones del agitador. Los cálculos de consumo de potencia se compararon con resultados de otros estudios sobre medios de fermentación con características reológicas similares. Se determinó que el consumo de potencia del agitador para mezclar 1m^3 de medio es de 8.35 kW, logrando una homogeneización del 95%

en 5.14 segundos, con un error en el tiempo de mezclado de aproximadamente el 10%, operando a una velocidad de agitación de 500 rpm.

Palabras Calve: Sistema de agitación; ácido glicérico; biorreactor

INTRODUCCIÓN

El agotamiento futuro de los combustibles fósiles y del petróleo ha suscitado la necesidad imperante de explorar y emplear nuevas fuentes de energía renovable, destacando los bio-combustibles[1]. En la actualidad, el etanol y el biodiésel figuran como los biocombustibles más prevalentes. Sin embargo, en el proceso de producción de biodiésel, al igual que en cualquier proceso industrial, se generan residuos y subproductos que con frecuencia son subestimados debido a la presencia de impurezas o a sus limitadas aplicaciones industriales. Este fenómeno resulta en una acumulación excesiva y devaluación de subproductos, ejemplificado por el glicerol, un subproducto común en la producción de biodiésel [2].

A nivel global, la producción anual de glicerol asciende a aproximadamente 900,000 toneladas (2,000 millones de libras). Las fuentes preeminentes de su generación incluyen la producción de biodiésel, los ácidos grasos, los alcoholes grasos, la saponificación y rutas sintéticas [3].

La principal fuente de obtención de glicerol se encuentra en el proceso de producción de biodiésel, como se documenta en un estudio previo. La Unión Europea, al ser uno de los principales productores mundiales de biodiésel, lideró también en la producción de glicerol, alcanzando 170,000 barriles por día en 2011. Le siguen Centro y Sur América, aproximándose a una producción diaria de 100,000 barriles [4].

En el presente, la producción y el consumo de biocombustibles han experimentado un potencial incremento en comparación con años anteriores, fenómeno evidenciado tanto en los mercados consolidados como en la generación de nuevos mercados que buscan mitigar las emisiones de gases de efecto invernadero. El crecimiento en la producción de biocombustibles, particularmente de biodiésel, y las perspectivas para los años venideros [4].

Según la Agencia Internacional de Energía [4], la producción mundial de biocombustibles experimentó un notable incremento hasta el año 2018, alcanzando un récord de 154 mil mi-llones de litros, lo que representa un aumento del doble en comparación con el año 2017, con una tasa de crecimiento anual del 7%. Se proyecta un aumento adicional del 25% para el año 2024, especialmente en mercados clave como China, Brasil y Estados Unidos.

Este crecimiento global en la industria de biocombustibles ha generado una sobreproducción de glicerol, con la consiguiente disminución de su precio, lo que ha impulsado la búsqueda de alternativas para procesar y utilizar eficientemente los subproductos y residuos generados por este mercado en expansión [5].

En Ecuador, desde 2007 se ha trabajado en la formulación de combustibles, como la gasolina extra con bioetanol anhidro y diésel con biodiésel en una proporción del 5%, con el objetivo de generar empleo y promover el desarrollo sustentable del sector agrícola [6]. Empresas como La Fabril han destacado como uno de los principales productores de biodiésel en el país, aprovechando excedentes en la producción de palma para agregar valor mediante la fabricación de biocombustibles. La producción de palma ha mostrado una tendencia al alza, con un excedente de 270,000 toneladas en 2012, 100,000 toneladas más que en 2010 [7].

La expansión de la industria del biodiésel ha llevado a una sobreproducción de glicerol a nivel mundial, resultando en una disminución de su precio. Ante esta situación, se ha explorado la posibilidad de transformar el glicerol en productos de alto valor agregado, como los bioplásticos [5]. La producción de bioplásticos a partir

de glicerol ha adquirido relevancia debido a preocupaciones medioambientales y de disposición final asociadas con los plásticos petroquímicos.

Otras aplicaciones del glicerol incluyen la producción de ácido glicérico (GA) mediante la oxidación biológica de bacterias acéticas. El GA tiene diversas aplicaciones, como la producción de polímeros biodegradables utilizados en bioplásticos. Sin embargo, a pesar de su potencial, el GA es costoso como reactivo para investigaciones y procesos industriales [8].

Para transformar materias primas de bajo costo, como el glicerol, en productos de alto valor, se requiere el empleo de biorreactores que mantengan condiciones óptimas de operación para garantizar la rentabilidad del bioproceso. Estos biorreactores deben controlar parámetros como pH, temperatura, humedad, agitación de la mezcla y presencia de oxígeno [9]. El biorreactor de tanque agitado es comúnmente empleado en la industria y puede operar según métodos como discontinuo (batch), semicontinuo (Fed-Batch) y continuo [10].

El éxito de un bioproceso depende de la comprensión de la cinética de las reacciones biológicas, los balances de materia y energía, así como de mantener condiciones ideales para la formación del producto [10,11]. Los biorreactores suelen incluir un agitador, fuentes de alimentación y salida de sustrato y producto, y en procesos aeróbicos, también se requieren fuentes de entrada y salida de gas, deflectores, aireadores y un recubrimiento térmico [11].

El glicerol, también conocido como 1,2,3-trihidroxipropano o glicerina, es un subproducto derivado de la transesterificación de grasas animales y vegetales durante la producción de biodiésel, con una relación molar de 1/10 (glicerol/biodiésel) [12]. Este polialcohol se presenta como un líquido viscoso, incoloro y ligeramente dulce a temperatura ambiente. Su presencia en diversos compuestos lo hace parte integral de aceites y grasas, tanto de origen animal como vegetal, en forma de mono-, di- o triacilglicéridos, que consisten en glicerol y una, dos o tres moléculas de ácidos grasos. Asimismo, se encuentra incorporado en fosfolípidos que forman parte de las membranas celulares [4]. La naturaleza de sus grupos hidroxilo confiere al glicerol solubilidad en agua y alcoholes, con una solubilidad ligeramente menor en disolventes orgánicos y una insolubilidad en hidrocarburos.

Un derivado del glicerol de alto valor es el ácido glicérico (GA), obtenido mediante la oxidación catalítica metálica de los grupos hidroxilo presentes en el glicerol. A pesar de que el mercado del ácido glicérico se ve limitado por los costos asociados con su síntesis química, posee un significativo potencial de aplicación en diversos compuestos químicos, particularmente en las industrias cosmética y farmacéutica. La síntesis química del ácido glicérico conlleva la obtención de una mezcla racémica de GA (D–L), siendo el D-GA el isómero requerido en la industria. Este último se obtiene principalmente mediante la descomposición de fructosa en procesos biotecnológicos [8].

En la producción de ácido acético, las bacterias acéticas desempeñan un papel crucial. La acción de la enzima alcohol deshidrogenasa convierte el alcohol en acetaldehído, que, a su vez, se transforma en ácido acético mediante la enzima acetaldehído deshidrogenasa. En paralelo, la oxidación de los grupos hidroxilo del glicerol, facilitada por las enzimas alcohol y aldehído deshidrogenas dependientes de NAD, puede generar D-GA al oxidar el alcohol primario. Por otro lado, la oxidación del alcohol secundario resulta en la formación de DHA [13].

En este trabajo, se presenta el diseño de uno de los componentes esenciales de los biorreactores, el sistema de agitación, para la producción de ácido glicérico mediante fermentación bacteriana de glicerol. Este enfoque se basa en investigaciones previas que han identificado condiciones óptimas para la producción de ácido glicérico.

MATERIALES AND METODOS

El sistema de agitación se diseñó para operar bajo un conjunto de parámetros específicos para optimizar la producción. La tasa de aereación se estableció en 2.5 volúmenes de aire por volumen de medio por minuto (vvm), lo que proporciona una oxigenación adecuada para el proceso. Se utilizó una concentración de glicerol del 20 % v/v como sustrato principal. La densidad del medio de fermentación fue de 1048,17 kg/m³, una medida que es crucial para calcular la transferencia de masa y la dinámica del fluido en el biorreactor. La temperatura de fermentación se mantuvo constante a 30 °C para favorecer la actividad metabólica óptima de los microorganismos. La velocidad de agitación se fijó en 500 revoluciones por minuto (rpm), lo que asegura una mezcla homogénea y una distribución uniforme de los nutrientes. Finalmente, el volumen del biorreactor se diseñó para una capacidad de 1m³, lo que permite escalabilidad y viabilidad económica para aplicaciones industriales [8].

Identificación del tipo de rodete que se ajusta a las necesidades de agitación de A. tropicalis para la producción de GA

Existen distintos tipos de rodetes que pueden aplicarse según el uso y las características reológicas de una amplia variedad de medios de cultivo. Según Doran en 1998 [14] la viscosidad, al ser uno de los factores que más afecta al comportamiento y flujo de los fluidos, ejerce un impacto significativo en las operaciones de bombeo, mezcla, transferencia de energía y materia en los biorreactores. Con base en estas características y tras estudiar diversos tipos de rodetes en un amplio rango de viscosidades, Doran en 1998 [14], recomienda la selección del tipo de rodete de acuerdo con los intervalos de viscosidad de los medios de fermentación, ofreciendo una guía visual en la Figura 1.

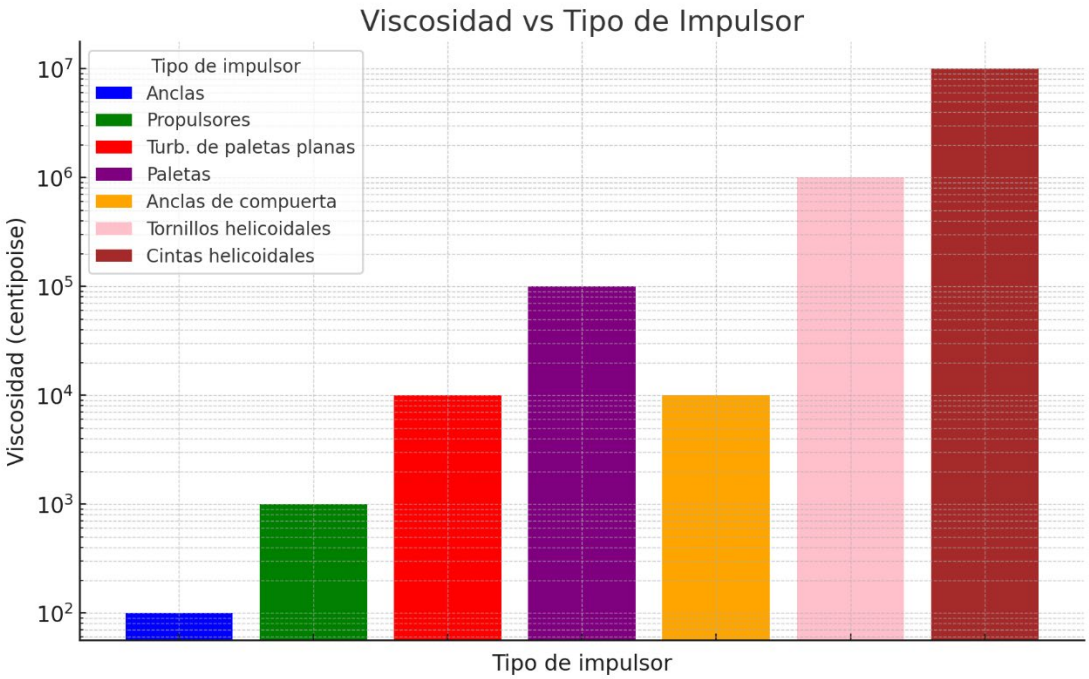

Figura 1. Intervalos de viscosidad para diferentes impulsores

Dimensionamiento geométrico de los componentes del sistema de agitación

Conforme a lo señalado por Rojas en 2019 [9], las características del flujo generadas en un tanque agitado están intrínsecamente vinculadas al tipo de rodete utilizado para movilizar la mezcla, así como a sus dimensiones, las propiedades del fluido y las proporciones geométricas tanto del tanque como de las placas deflectoras. Cada una de estas consideraciones ejerce un impacto significativo en el tipo de flujo, la velocidad y el consumo de potencia asociados al sistema de agitación. No obstante, es posible recurrir a las proporciones geométricas establecidas en la literatura científica como punto de partida para el diseño de los componentes del sistema de agitación.

En el proceso de dimensionamiento del tanque y el rodete, se tomarán en cuenta las relaciones geométricas estándar aplicables a una turbina tipo Rushton con paletas planas, siguiendo las Ecuaciones (1, 2, 3, 4, 5, 6, 7, 8, 9, 10 y 11) [15,16]:

$$\frac{H_t}{D_t} = \frac{3}{2} \quad (1)$$

$$\frac{E}{D_t} = \frac{1}{3} \quad (2)$$

$$\frac{D_a}{D_t} = \frac{1}{3} \quad (3)$$

$$\frac{L}{D_a} = \frac{1}{4} \quad (4)$$

$$\frac{W}{D_a} = \frac{1}{5} \quad (5)$$

$$\frac{j}{D_t} = \frac{1}{10} \quad (6)$$

$$\frac{D_d}{D_a} = \frac{2}{3} \quad (7)$$

$$\frac{D_h}{D_d} = \frac{1}{4} \quad (8)$$

$$\frac{E_d}{D_d} = \frac{1}{30} \quad (9)$$

$$\frac{E_p}{D_d} = \frac{1}{40} \quad (10)$$

$$\frac{H_L}{D_t} = 1 \quad (11)$$

Cálculo del consumo de potencia requerida para la agitación

Una vez establecidas las dimensiones del sistema de agitación, es imperativo determinar la potencia necesaria para mantener la velocidad de giro del impulsor en 500 rpm. Para llevar a cabo este análisis, se considerarán las dimensiones del tanque y del rodete, así como la viscosidad y densidad del líquido, la velocidad del agitador y, dado que parte del líquido asciende durante la agitación y debe vencer la fuerza de gravedad, también se tomará en cuenta este factor [15]

En consonancia con Katoh en 2012 [17], es importante destacar que la potencia no puede estimarse de manera teórica incluso en sistemas agitados simples. En cambio, su determinación debería basarse en análisis dimensionales y mecánica de fluidos, respaldados por estudios experimentales. Se han desarrollado, a través de estudios de mecánica de fluidos en tanques agitados, curvas y ecuaciones empíricas que relacionan el número de potencia con el número de Reynolds para diversos tipos de rodetes, permitiendo así la estimación del consumo de potencia en tanques agitados.

De acuerdo con Doran en 1998 [14], las relaciones entre las variables que influyen en el cálculo de la potencia se expresan típicamente en forma de números adimensionales, como el número de Reynolds del rodete Rei (Ecuación 12) y el número de potencia Np (Ecuación 13), como se presenta a continuación.

$$Re_i = \frac{N_i D_i^2 \rho}{\mu} \quad (12)$$

Donde:
$N_i = Velocidad\ del\ agitador$
$D_i = Diámetro\ del\ rodete$
$\rho = Densidad\ del\ fluido$
$\mu = Viscosidad\ del\ fluido$

Utilizando la relación que existe entre el número de Reynolds del rodete Rei y el Número de Potencia (Np), se calculó la potencia requerida mediante la Ecuación (13) [17],

$$N_p = \frac{P}{\rho N_i^3 D_i^5} \quad (13)$$

Donde:
$P = Potencia$

$\rho = Dendidad\ del\ fluido.$
$N_i = Velocidad\ de\ agtacion.$
$D_i = Diámetro\ del\ rodet$

Cálculo del tiempo de mezcla

El tiempo de mezcla permite conocer la efectividad de mezclado, se puede calcular mediante varios métodos experimentales, los más comunes son mediante el empleo de un trazador, simulación o ecuaciones empíricas [18]. Según Doran en 1998 [14], el tiempo de mezcla dependerá de variables como la viscosidad del fluido, tipo de rodete, el tamaño y la velocidad de agitación. Gracias a la determinación experimental del tiempo de mezcla y su relación con varias de estas variables para un determinado tipo de rodete, se puede emplear ecuaciones que relacionan estos factores con el comportamiento del fluido según el número de Reynolds rodete y la velocidad de agitación.

Conociendo el número de Reynolds rodete se aplica la Ecuación 14, que representa el producto adimensional $N_i t_m$ en función del número de Reynolds rodete, el producto adimensional $N_i t_m$ representa los giros que debe dar el agitador para homogenizar la mezcla con una desviación del t_m de 10% [14].

$$\boldsymbol{N_i t_m = \frac{1.54\ V}{D_i^3}} \qquad (14)$$

Donde:
$V = Volumen\ del\ líquido$
$D_i = Diámetro\ del\ rodete$
$N_i = Velocidad\ de\ agitación$

RESULTADOS Y DISCUSIÓN

Identificación del tipo de rodete que se ajusta a las necesidades de agitación de A. tropicalis para la producción de GA

Para una viscosidad de 1,35 cP se presenta la opción de elegir entre un rodete tipo hélice o uno tipo turbina de palas planas. No obstante, los rodetes tipo hélice se caracterizan como agitadores de flujo axial, siendo utilizados principalmente en fluidos agitados que contienen sólidos. Su fuerte flujo axial evita que los sólidos se sedimenten en el fondo del tanque, y su rango de velocidad típico oscila entre 400 y 800 rpm, siendo empleados en tanques de dimensiones extremadamente grandes con múltiples agitadores. En contraste, los agitadores tipo turbina son eficaces en un amplio intervalo de viscosidades y generan corrientes principalmente radiales y tangenciales, evitando la formación de zonas muertas. Estas corrientes resultan particularmente útiles para la dispersión o disolución eficiente de gases en el fluido [15].

Considerando estas consideraciones, y para un medio de baja viscosidad que requiere aireación, se selecciona como la mejor alternativa un rodete tipo turbina, específicamente un agitador tipo turbina Rushton. Este tipo de agitador ofrece una agitación uniforme y una adecuada dispersión de gases en sistemas aireados. Como señala [19], los agitadores más comúnmente utilizados en procesos fermentativos son aquellos de flujo radial, como la turbina Rushton. Esto se debe a su facilidad de montaje tanto en la parte inferior como en la superior del tanque, su capacidad de drenaje sencillo y su baja capacidad de cizallamiento en las paredes celulares.

Según Rushton en 1950 [20], la turbina Rushton, un agitador tipo turbina con palas planas ampliamente adoptado en aplicaciones industriales, es capaz de generar flujos tanto radiales como tangenciales cuando se utiliza con deflectores adecuados. Este diseño se caracteriza por inducir altos niveles de cizallamiento y turbulencia,

siendo notablemente eficiente en términos de bombeo. La eficacia de este agitador se manifiesta especialmente en procesos de dispersión de fases líquido-líquido y gas-líquido. Esta capacidad para promover una mezcla intensiva lo hace particularmente útil en diversas aplicaciones industriales.

Dimensionamiento de los componentes del sistema de agitación

Para la producción de ácido glicérico a partir de glicerol por fermentación de A. tropicalis, se ha diseñado un sistema de agitación para un biorreactor de 1m^3 de capacidad que consta de un tanque cilíndrico provisto de 4 deflectores adecuadamente separados y un agitador tipo Turbina Rushton de paletas planas cuyas dimensiones se presenta en la Tabla 2.

Factor	Dimensiones (mm)
Altura del Tanque $(\boldsymbol{H_t})$	1500
Altura del líquido $(\boldsymbol{H_L})$	1000
Diámetro del Tanque $(\boldsymbol{D_t})$	1000
Altura entre el fondo y la paleta $(\boldsymbol{E})$	330
Diámetro del rodete $(\boldsymbol{D_a})$	330
Largo de la paleta $(\boldsymbol{L})$	83
Numero de palas	6 unidades
Alto de la paleta $(\boldsymbol{W})$	66
Diámetro del disco $(\boldsymbol{D_d})$	220
Diámetro del eje del disco $(\boldsymbol{D_h})$	55
Ancho de la placa deflectora $(\boldsymbol{j})$	100
Número de placas deflectoras	4 unidades

Tabla 1. Dimensiones del sistema de agitación

La Tabla 1 muestra el resumen de las dimensiones geométricas del sistema de agitación para 1 m^3 de capacidad, el cual consta de un tanque de agitación de 1000 mm de diámetro por 1500 mm de altura, con 4 deflectores de 100 mm de ancho, acompañado de un rodete tipo turbina de disco con hojas planas de 330 mm de diámetro cuyas dimensiones son: diámetro del disco $(D_d) = 220\ mm$, alto de la paleta $(W) = 66\ mm$ y largo de la paleta $(L) = 83\ mm$. Las dimensiones y configuración del sistema de agitación (Tabla 2) se muestran en la Figura 2.

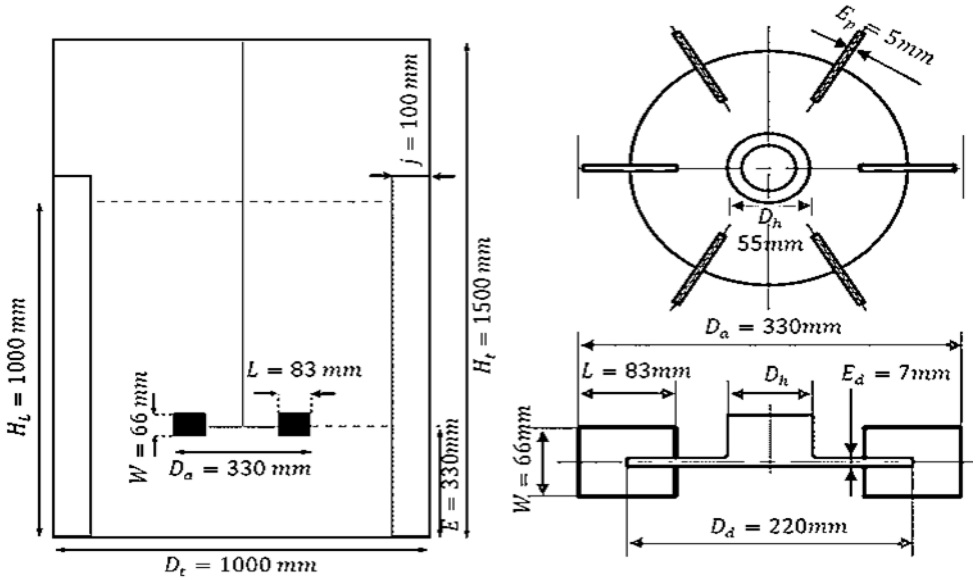

Figura 2. Configuración y dimensionamiento geométrico del sistema de agitación con turbina Rushton.

La Figura 2 muestra la configuración estándar del sistema de agitación y sus dimensiones desde la vista superior y lateral del agitador. [15], durante los últimos años la forma física de los biorreactores más utilizados no ha sufrido cambios significativos, sin embargo, para cubrir las necesidades de producción de ciertos procesos específicos se han desarrollado nuevas formas de biorreactores, pero en general se mantienen las relaciones geométricas estándar. Lázaro en 2013 [19], menciona que para mantener un bioproceso adecuadamente agitado y reducir el consumo energético es importante considerar las relaciones geométricas estándar HL/Dt = (1 - 1,5) y Di/Dt = (0,3 – 0,5). Según Katoh en 2015 [17], en biorreactores en los que la altura del líquido es mayor al diámetro del tanque, el flujo generado por un solo agitador no es suficiente para mantener la mezcla homogénea y se corrige con la colocación de otro rodete en el mismo eje rotor a una altura superior.

En este caso se han respetado los criterios geométricos de diseño de biorreactores propuestos por McCabe [15] y Li [16] con relaciones Ht/Dt =1,5, HL/Dt =1 y Di/Dt = 0,33, recalcando que las relaciones Di/Dt pueden variar dependiendo del tipo de rodete especifico que se emplee debido a las características del flujo que estos generan.

Los efectos en la velocidad de agitación y el consumo de potencia causado por diferentes relaciones Di/Dt con turbinas Rushton se muestra en los estudios realizados por Cortés en 2009 [21], el autor emplea relaciones Di/Dt de 0,33 – 0,36 y 0,39, mostrando que el aumento de estas relaciones para un mismo volumen de medio genera una disminución en la velocidad de agitación de 460, 385 y 345rpm respectivamente.

Además, Cortés [21], destaca la importancia de adherirse a los criterios de diseño geométrico específicos para un tipo determinado de rodete. Incluso pequeñas variaciones en las dimensiones pueden resultar en que el sistema no alcance la eficiencia para la cual fue diseñado. En el caso analizado, si el objetivo fuera alcanzar una velocidad de agitación de 480 rpm empleando la relación Di/Dt = 0,39, se requeriría un mayor consumo de potencia, lo cual tendría un impacto negativo en la economía del proyecto.

Finalmente, las dimensiones y la disposición de los deflectores son factores críticos que influyen en las características del flujo y la homogeneización de la mezcla. La presencia de cuatro deflectores, espaciados adecuadamente, previene la formación de vórtices y flujo circular. Estos deflectores pueden ubicarse a diferentes distancias y disposiciones con respecto a la pared del tanque, dependiendo de la viscosidad del fluido [14]. Trabajando con una viscosidad baja de 1,35 *10-3 kg·m-1·s-1, los deflectores se encuentran unidos a la pared del tanque y miden 100 mm de ancho. Es ideal emplear relaciones de 1/10 a 1/12 del diámetro del tanque [14], y la distancia entre los deflectores y el agitador en relación a 0,2 D_t, correspondiente a 200 mm para este estudio.

Consumo de potencia

En el proceso de producción de ácido glicérico a partir de glicerol en un biorreactor con una capacidad de $1m^3$, se hace necesario emplear un agitador tipo turbina Rushton. El consumo de potencia estimado para este agitador es de 8,35 kW. Se considera prudente utilizar aproximadamente 9 kW para compensar posibles pérdidas de potencia en el sistema, proporcionando un margen adicional para mantener la velocidad de agitación en 500 rpm. Estos resultados, junto con otros parámetros relacionados con el consumo de potencia, como el número de Reynolds, el número de potencia y la velocidad de agitación, se comparan en la Tabla 3 con los obtenidos en otros estudios que involucran medios de características reológicas similares.

Sistema de producción	Densidad $Kg.m^{-3}$	Viscosidad $kg.m^{-1}s^{-1}$	Velocidad de agitación (rpm)	Re_i	Np	Consumo de Potencia ($kW.m^{-3}$)	Fuente
Acido glicérico	1050	$1{,}35*10^{-3}$	500	$7 * 10^5$	7,5	8,35	Propia
Etanol	1100	$1{,}00*10^{-3}$	250	$4 * 10^4$	5	3,98	(22)
Cerveza	1040	-	600	$1{,}0 * 10^5$	10	11,60	(23)
Aminoácidos esenciales	980	$2{,}63 * 10^{-3}$	150	$1{,}1 * 10^5$	6,3	2,1	(24)

Tabla 2. Resultados y comparación con estudios similares.

La Tabla 2 exhibe la influencia de los parámetros de operación en el consumo de potencia de los agitadores. El consumo de potencia se presenta como la cantidad de energía requerida para agitar 1 m^3 de medio para cada sistema de producción. Aunque no todos los sistemas están diseñados para una capacidad de 1 m^3, se estima esta cifra aplicando el criterio de escalado conocido como consumo de potencia por unidad de volumen.

La densidad y viscosidad de los medios son factores clave en muchos cálculos y son comparables en cada sistema de producción de la Tabla 3. El número de Reynolds del rodete en estos sistemas varía entre 10^4 y 10^5, un parámetro crucial que indica el comportamiento del fluido en tanques agitados. Según Katoh en 2015 [17], para lograr una mezcla efectiva, es conveniente mantener el régimen turbulento, y en tanques agitados, se alcanza el régimen turbulento completamente desarrollado a $Re_i \geq 10^4$.

La velocidad de agitación difiere en la mayoría de los sistemas y guarda una relación directamente proporcional con el consumo de potencia. Dado que las características del medio son similares entre los estudios de la Tabla 3, es posible comparar el consumo de potencia según las condiciones de operación. En la producción de etanol descrita por Abuámer en 2005 [25], se emplea una velocidad de agitación de 250 rpm, mientras que, en este estudio, la velocidad de agitación es de 500 rpm, resultando en consumos de potencia de 3,98 y 8,35 kW respectivamente. Esto revela un consumo de potencia proporcional al aumento en la velocidad de agitación, siendo en este estudio el consumo de potencia aproximadamente el doble al duplicarse la velocidad de agitación. Este mismo comportamiento se observa en el trabajo descrito por Argemí en 2016 [26] para la producción de cerveza y Roja en 2019 [9], en la producción de aminoácidos esenciales. La utilización de turbinas Rushton en estos sistemas de agitación demuestra su aplicabilidad en procesos fermentativos aireados, y si estos sistemas hubieran sido diseñados para una misma velocidad de agitación (500 rpm), los consumos de potencia serían comparables al obtenido en este estudio

Tiempo de mezcla

En los biorreactores, una de las funciones fundamentales de los sistemas de agitación es asegurar una mezcla eficiente que permita la transferencia adecuada de energía y masa en el sistema [27]. El tiempo de mezclado es un parámetro crucial que caracte-riza la eficiencia del sistema de agitación al medir la rapidez con la que la mezcla alcanza un estado de homogeneización determinado, generalmente establecido en un 95% [28]. En este estudio, se empleó el modelo descrito por Doran en 1998 [14], utilizando ecuaciones empíricas que describen el comportamiento hidrodinámico del fluido en función de las con-diciones de operación para una turbina tipo Rushton de 6 palas planas con 4 deflectores, considerando el número de Reynolds del rodete y la velocidad de agitación. El resultado obtenido fue un tiempo de mezcla de 5,14 segundos.

Según Katoh en 2015 [17], en reactores industriales con capacidad inferior a 10 m^3, los tiempos de mezclado suelen ser menores a 100 segundos. El tiempo de mezcla obtenido en este estudio se sitúa dentro de este rango, con una desviación aproximada del 10%. Un valor más bajo indica una mejor agitación, ya que significa que el flujo generado por el impulsor es turbulento y la mezcla es efectiva.

CONCLUSIONES

En este estudio, se ha desarrollado un diseño efectivo para un sistema de agitación en un biorreactor de 1 m^3 destinado a la producción de ácido glicérico mediante la fermentación microbiana de *A. tropicalis*. El uso de un agitador tipo turbina Rushton de 6 palas planas, con dimensiones cuidadosamente calculadas, ha demostrado ser eficiente en la generación de corrientes de flujo para asegurar una homogeneización del 95% en un tiempo de mezcla de 5,14 segundos. Con un consumo de potencia calculado de 8,35 kW y una recomendación de 9 kW para compensar posibles pérdidas, se garantiza un rendimiento óptimo del sistema. Este diseño, aplicable a medios de baja viscosidad como el compuesto por un 20% (v/v) de glicerol con viscosidad de 1,35 cP, ofrece un enfoque práctico y prometedor para la producción eficiente de ácido glicérico en procesos fermentativos aireados, subrayando la viabilidad del agitador tipo turbina Rushton en este contexto.

Conflicts of Interest: "The authors declare no conflict of interest."

REFERENCES

1. Callejas Edmar. Biocombustibles. https://www.redalyc.org/pdf/325/32512739009.pdf. 2008;
2. Plaza A. GLICERINA Y GLICEROL, investigan nuevos usos para transformar subproductos del biodiesel - BIODIESEL ARGENTINA-NOTICIAS SOBRE BIODIÉSEL BIOCOMBUSTIBLES Y ENERGIAS RENOVABLES. 2010. Available from: https://biodiesel.com.ar/2435/glicerina-y-glicerol-investigan-nuevos-usos-para-transformar-subproductos-del-biodiesel
3. Lafuente G. Glicerol : Síntesis Y Aplicaciones. Universidad Nacional De Educación a Distancia. 2017;
4. Agencia Internacional De Energia (IEA). https://www.iea.org/fuels-and-technologies/bioenergy. 2019. Bioenergía - Combustibles y tecnologías.
5. Bautista C. Subproductos Generados en el Proceso De Producción de Biodiesel a Partir De Aceite De Tempate. 2009; Available from: www.ufg.edu.sv
6. La Hora. Canchimalero, alternativa gastronómica : Noticias Esmeraldas : La Hora Noticias de Ecuador, sus provincias y el mundo. https://lahora.com.ec/noticia/574954/produccic3b3n-de-biodic3a9sel. 2011;
7. Revista-Líderes. La Fabril llena más tanques con biodiésel | Revista Líderes. 2013. Available from: https://www.revistalideres.ec/lideres/fabril-llena-tanques-biodiesel.html
8. Habe H, Shimada Y, Yakushi T, Hattori H, Ano Y, Fukuoka T, et al. Microbial production of glyceric acid, an organic acid that can be mass produced from glycerol. Appl Environ Microbiol. 2009;75(24).
9. Rojas E. Diseño y cálculo de un biorreactor de una planta piloto de producción de aminoácidos esenciales en la ciudad de Arequipa. [Arequipa]: Universidad Nacional San Agustin de Arequipa; 2019. Available from: http://repositorio.unsa.edu.pe/handle/UNSA/9894
10. Rovira JG. Diseño de un biorreactor para la obtención de Ácido Glicérico por fermentación bacteriana de Glicerol. [Barcelona]: Escuela Técnica Superior de Ingeniería Industrial de Barcelona (ETSEIB); 2013.
11. Dondé Castro MJ. Transporte de momentum y calor : teoría y aplicaciones a la ingeniería de proceso. 2005;316.
12. Martínez Guadalupe. Producción de plásticos biodegradables en bacterias. UDELAR; 2013. Available from: file:///C:/Users/DANIEL%20CABRERA/Downloads/uy24-17152.pdf
13. Habe H, Fukuoka T, Kitamoto D, Sakaki K. Biotransformation of glycerol to D-glyceric acid by Acetobacter tropicalis. Appl Microbiol Biotechnol. 2009;81(6).
14. Doran Pauline. Principios de ingeniería de los bioprocesos. Editorial Acribia SA; 1998. 133–158 p.
15. L. McCabe, Julian C. Smith. Operaciones básicas de ingeniería química - Google Libros. Available from: https://books.google.com.ec/books?id=YBXZz82jwksC&pg=PA275&lpg=PA275&dq=rodetes+recomendados+segun+la+viscosidad&source=bl&ots=IZaRviRSAu&sig=ACfU3U07wLFVufzSeJb9rz1J_fBs44vi9A&hl=es&sa=X&ved=2ahUKEwjZ0qHD0afqAhXIGM0KHYbwAGsQ6AEwAnoECAgQAQ#v=onepage&q=rod&f=false
16. Li Z, Bao Y, Gao Z. PIV experiments and large eddy simulations of single-loop flow fields in Rushton turbine stirred tanks. Chem Eng Sci. 2011;66(6).

17. Katoh S. Ingeniería bioquímica: un libro de texto para ingenieros, químicos y biólogos. 2015. Available from:https://ebookcentral.proquest.com/lib/uta-ebooks/reader.action?docID=1896078&query=bioprocess
18. Ramirez A, RR, AA, & ME. AGITACION Y MEZCLADO. RE VISTA E NLACE QUÍMICO, UNIVE RSIDAD DE GUANAJUATO. 2012;4.
19. Lázaro Ana. Tecnología de los bioprocesos – Diseño de biorreactores y fermentadores. Tecnologías Críticas para la Industria. 2013;
20. Rushton JH, Costich EW, Everett HJ. Power characteristics of mixing impellers, Parts 1 and 2. Chem Eng Prog. 1950;46(8).
21. Cortés L. Diseño de una planta piloto multiuso. Instituto Politécnico Nacional; 2009. Available from: https://tesis.ipn.mx/jspui/bitstream/123456789/19585/1/TOLALPA.pdf
22. Abuámer Y. Diseño Básico De Una Planta Piloto De Producción De Etanol. 2005. p. 1–17.
23. Argemí M. Diseño de un biorreactor para la fabricación de la cerveza. Etseib. 2016;1–84.
24. Rojas E. Diseño y cálculo de un biorreactor de una planta piloto de producción de aminoácidos esenciales en la ciudad de Arequipa. 2019. Available from: http://repositorio.unsa.edu.pe/handle/UNSA/9894
25. Abuámer Y. Diseño Básico De Una Planta Piloto De Producción De Etanol. 2005. Available from: https://biblus.us.es/bibing/proyectos/abreproy/20046/fichero/Cap%C3%ADtulos%252FCap%C3%ADtulo+3.pdf
26. Argemí M. Diseño de un biorreactor para la fabricación de la cerveza. ETSEIB. 2016;
27. Manuel C, Díaz S, Abelardo L, Méndez Hernández A. Construcción y Validación Experimental de un Biorreactor Artesanal Tipo Tanque Agitado para Fermentaciones Sumergidas a Escala de Laboratorio.
28. Ruffo Durán J, FCA, & DMJC. Características de la hidrodinámica de un biorreactor industrial tipo tanque agitado. Rev Mex Ing Quim. 2014;3.

Received: October 9th 2023/ **Accepte**d: January 15th 2024 / **Published:**15 February 2024

Citation: Cabrera-Vall, D**,** Pérez H**.** Diseño de un sistema de agitación para un biorreactor de 1m^3 de capacidad para la producción de ácido glicérico a partir de glicerol por fermentación microbiana de *Acetobacter tropicalis* Revis Bionatura 2024; 9 (1) **42**. http://dx.doi.org/10.21931/RB/2024.09.01.**42**

Additional information Correspondence should be addressed to *da.cabrera@uta.edu.ec*

Peer review information. Bionatura thanks anonymous reviewer(s) for their contribution to the peer review of this work using https://reviewerlocator.webofscience.com/

Bionatura ISSN. First 13909355 Ecuador. **Scopus coverage years**: from 2016 to the present

Bionatura
Ibero American Journal of Biotechnology and Life Sciences

Article

Niveles de Vitamina D en pacientes con y sin Enfermedad Renal Crónica, perfil clínico y epidemiológico: un análisis preeliminiar en un hospital de segundo nivel en Quito, Ecuador.

Vitamin D levels in patients with and without Chronic Kidney Disease, clinical and epidemiological profile: preliminary analysis in a second level hospital in Quito, Ecuador

André Benítez-Baldassari [1*], *Estefanía León-Hernández* [2], *Andrea Banegas-Sarmiento* [3], *Santiago Aguayo-Moscoso* [4], *Jorge Luis Vélez-Paéz* [3,5]

1. *Universidad Central del Ecuador, Facultad de Ciencias Médicas, Escuela de Medicina, Quito, Ecuador, Rabenitezb@uce.edu.ec ,*
2 *Hospital Pablo Arturo Suárez, Departamento de Nefrología y Unidad de Hemodiálisis, Quito, Ecuador; tefyleonh@gmail.com .*
3 *Hospital de Especialidades De las Fuerzas Armadas numero 1 Quito, Servicio de Medicina Interna , andreabanegassarmiento@gmail.com*
4 *Hospital Pablo Arturo Suárez, Unidad de Terapia Intensiva, Centro de Investigación Clínica, Quito, Ecuador, drsaguayo@gmail.com*
5 *Universidad Central del Ecuador, Facultad de Ciencias Médicas, Escuela de Medicina, Quito, Ecuador, jlvelez@uce.edu.ec .*
** Correspondence: baar_ebola@outlook.com*
Available from. http://dx.doi.org/10.21931/RB/2024.09.01.43

ABSTRACT

Vitamin D has been associated with different effects unrelated to bone-mineral metabolism, such as its association with arterial hypertension. This study determines the prevalence profile of vitamin D deficiency and insufficiency in Ecuadorian patients, its epidemiological profile, and its relationship with other diseases such as arterial hypertension, diabetes mellitus, and chronic kidney disease. This is a pioneering study in Ecuador of a retrospective type, carried out at the Pablo Arturo Suarez Hospital over 6 months, in which it was found that the prevalence of vitamin D insufficiency was 28.5% (levels between 21 to 30 ng/ml) and deficiency was 57% (levels less than 20 ng/ml); Likewise, we ratify the inverse relationship between vitamin D levels and age, as well as finding a certain association between vitamin D levels and the presence of arterial hypertension; while no significant differences were found in its relationship with diabetes mellitus, chronic kidney disease without the use of renal replacement therapy and the general population.
Keywords: vitamin D, chronic kidney disease, metabolism.

INTRODUCCIÓN

La vitamina D es un secoesteroide que interactúa con un receptor nuclear específico similar a otras hormonas esteroides y desempeña un papel fundamental en la homeostasis del calcio y el fosforo [1].
La deficiencia de vitamina D se define como una concentración sérica baja de 25-hidroxivitamina D (25[OH]D) total, está relacionada con una mayor mortalidad y se relaciona con diferentes entidades patológicas: cardiovasculares, diabetes, infecciosas, neoplasias, autoinmunes y renales [2].

No existe un consenso sobre la definición de suficiencia de Vitamina D, pero la mayoría de expertos, han sugerido que el nivel sérico de 25(OH)-VD debe ser igual o superior a 30 ng/mL y se define como insuficiencia de vitamina D a un nivel sérico de 25(OH)-VD entre 20–29 ng/mL, mientras que deficiencia de Vitamina D a niveles de 25 (OH) -VD menores de 20 ng /ml. En diálisis no hay un límite establecido para la deficiencia de vitamina D[3–5].

Los pacientes con ERC están en el grupo de alto riesgo de déficit de vitamina D, debido a las restricciones dietéticas, la pérdida progresiva de megalina, la pérdida de proteína transportadora de vitamina D a través del dializador y a los valores elevados de FGF23 (factor de crecimiento fibroblástico) en la enfermedad renal crónica, promoviendo el catabolismo de calcitriol y calcidiol [4,6].

La uremia, también puede atenuar la respuesta de la Vitamina D plasmática a la irradiación UVB [7]. Los pacientes crónicos en hemodiálisis en algunos estudios exhibieron un menor respuesta a la Vitamina D que los individuos normales cuando se exponen a una dosis fisiológicamente equivalente de UVB [8]. Además, la hiperpigmentación cutáneo en pacientes de hemodiálisis, puede desempeñar un papel adicional en la síntesis endógena alterada de VD [9].

Hay pocos datos epidemiológicos regionales y de lo que conocemos, ninguno local, sobre la prevalencia de la deficiencia de ésta vitamina en población con y sin patología renal.

En este trabajo, buscamos determinar la prevalencia de la deficiencia de vitamina D en una corte monocéntrica de pacientes ecuatorianos con y sin fallo renal y su asociación con variables clínicas, analíticas y epidemiológicas.

MATERIALES Y METODOS

Diseño del estudio y criterios de inclusión

Realizamos un estudio observacional retrospectivo que incluyó pacientes con falla renal crónica en diferentes estadios y sin patología renal, atendidos en un hospital de segundo nivel perteneciente a la salud pública en Quito, Ecuador, desde el Enero del 2022 hasta Junio de 2022. Se definió falla renal a tasas de filtrado glomerular menor de 60 ml/min/1.73 m2 (estadios 3,4 y 5) ya que según bibliografía se espera alteraciones del metabolismo fosfocalcico en estos estadios. Los criterios de inclusión fueron los siguientes: (1) edad mayor de 18 años; (2) ingreso hospitalario con reporte de valores de vitamina D. Los participantes del estudio fueron clasificados retrospectivamente como deficientes o no deficientes (la deficiencia de vitamina D se definió como valores iguales o menores de 20 ng/ml). Se renunció al consentimiento informado debido a la naturaleza retrospectiva de este estudio de acuerdo con las regulaciones locales. El objetivo del estudio fue determinar un perfil clínico epidemiológico con base a la deficiencia o no de vitamina D en pacientes con falla renal avanzada y con función renal normal.

Recopilación de datos

Se recolectó información de las historias clínicas electrónicas sobre variables clínico-epidemiológicas como edad, género, comorbilidades (diabetes mellitus (DM), hipertensión arterial) y valores de variables analíticas como, creatinina, albúmina, paratohormona, calcio total, hemoglobina. Estas variables se obtuvieron al ingreso hospitalario. Los recuentos sanguíneos de rutina (hemograma) se midieron utilizando un analizador de hematología automatizado (Advia 2120i, Tarrytown, NY, EE. UU.), mientras que la albúmina, el calcio, la urea se

evaluaron mediante fotometría (COBAS 503). La paratohormona se midió mediante quimioluminiscencia (COBAS 503). La vitamina D se cuantificó por electroquimioluminiscencia

Análisis estadístico

No se realizó un cálculo formal del tamaño de la muestra debido a la naturaleza exploratoria, descriptiva y retrospectiva del estudio ya que se analizo todo el universo de los pacientes que cumplieron los criterios de inclusión y que fueron atendidos en el Hospital Pablo Arturo Suarez en el lapso de 6 meses.Se escogió el test de Kolmogorov para determinar la distribución normal de las variables sobre Shapiro Wilk ya que hay mas de 50 pacientes en el estudio. Los análisis se realizaron con los paquetes estadísticos RStudio e IBM SPSS versión 28, para lo cual se empleó estadísticas descriptivas, utilizando tablas representando los valores absolutos y relativos de las variables cualitativas, así como medidas de tendencia central y dispersión para las cuantitativas.

Se verificó el supuesto de normalidad de las variables cuantitativas mediante la Prueba de Kolmogorov-Smirnov, donde se empleó la prueba de Mann Whitney para la variable sin normalidad. Para las variables cualitativas se utilizó la prueba Chi-cuadrado o el estadístico exacto de Fisher. La significancia estadística se estableció para p-valor <0,05.

RESULTADOS

Se analizaron 193 pacientes con edad promedio de 64,4 años, 53.4% mujeres y 46.6 % hombres. Entre los antecedentes personales se observó con mayor frecuencia Hipertensión arterial con un 56.5%, Enfermedad Renal Crónica estadio 3, 4 y 5 con 62.7% y la presencia de Diabetes Mellitus con un 32.6%; la media de vitamina D fue de 18,71 ng/ml. Con relación a los niveles de vitamina D apenas el 14.5% de la población tenia niveles de vitamina D mayores a 30 ng/dl, mientras que el 28.5% tuvieron niveles entre 20 y 30 ng/ml (correspondiente a insuficiencia) y el 57% correspondieron a niveles menores de 20 ng/ml (correspondiente a deficiencia).

Características clínicas	**Frecuencia**
Edad	
Media *(DE)*	64,4 *(19,76)*
Mayores de 65 años	108 (56%)
Sexo	
Mujer	103 (53,4%)
Hombre	90 (46,6%)
Comorbilidades	
Diabetes mellitus	63 (32.6%)
Hipertensión arterial	109 (56.5%)
Enfermedad Renal Crónica estadio 3,4 o 5	121(62.7%)
Enfermedad Renal Crónica en hemodiálisis	36 (18.7%)
Niveles de Vitamina D	

Media de Vitamina D en ng/ml *(DE)*	18,71 *(9,15)*
Vitamina D >30ng/ml	28 (14.5%)
Insuficiencia de Vitamina D	55 (28.5%)
Deficiencia de vitamina D	110 (57%)
Fuente: Elaboración propia	

*Valores presentados de frecuencia con sus %

Tabla 1. Características de los pacientes: edad, sexo, comorbilidades, niveles de Vitamina D

Al relacionar las características clínicas de los pacientes según los niveles de vitamina D se observó que la edad presentó diferencias significativas con p-valor 0,002, siendo las medianas de 70 años para pacientes con niveles menores de 20 ng/ml de vitamina D vs 58,37 años para pacientes con niveles mayores de 20 ng/ml. De igual forma el grupo de pacientes mayores de 65 años, es decir el de adultos mayores presentó mayor porcentaje de deficiencia en un 63,8% en relación al 36.1% que presentó niveles mayores de 20 ng/ml de vitamina D, siendo estadísticamente significativo con valor de p de 0.029.

La presencia de Hipertensión Arterial presentó diferencias significativas con p-valor 0.004, donde los pacientes con valores de vitamina D menores a 20 ng/ml correspondían al 66.1% en tanto que el 33.9% tenían niveles mayores a 20 ng/ml.

En cuanto al género, la presencia de Diabetes Mellitus y Enfermedad Renal crónica no hubo diferencias estadísticamente significativas en cuanto a los niveles de vitamina D.

CARACTERISTICAS	**NIVELES DE VITAMINA D**		**p-valor**
	MENORES DE 20ng/ml	MAYORES DE 20ng/ml	
Género masculino	46 (51%)	44 (49%)	0.123
Mediana de edad	70 (54 - 82)	58,37 (42 - 67)	0,002*
Mayores de 65a	69 (63.8%)	39 (36.1 %)	0.029*
Diabetes Mellitus	35 (55%)	28 (44%)	0.779
Hipertensión Arterial	72 (66.1%)	37 (33,9%)	0.004*
Enfermedad Renal Crónica	74 (61.1%)	47 (38.9%)	0.130
Fuente: Elaboración propia			

* p<0.05 significancia estadística

Tabla 2. Características de los pacientes y niveles de vitamina D

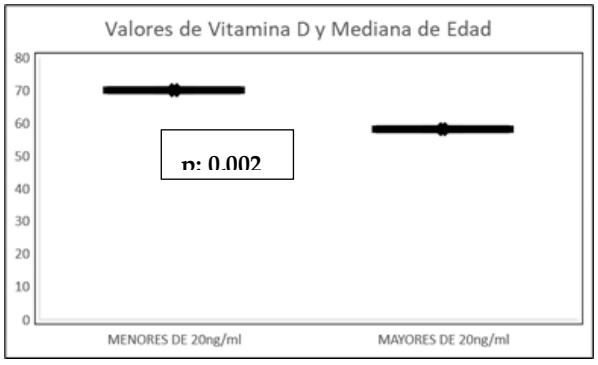

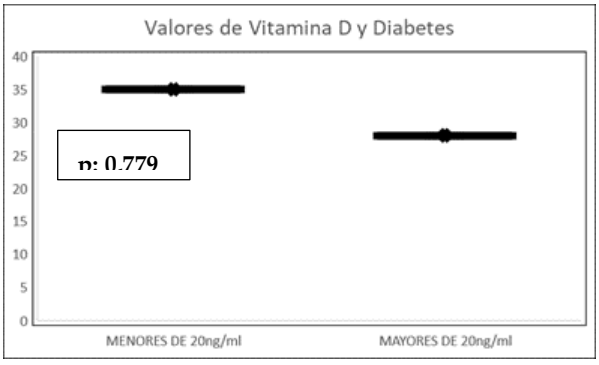

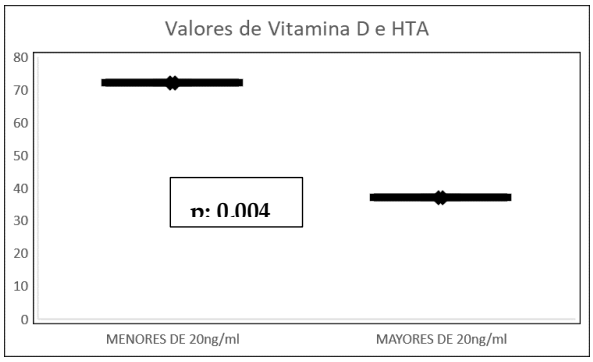

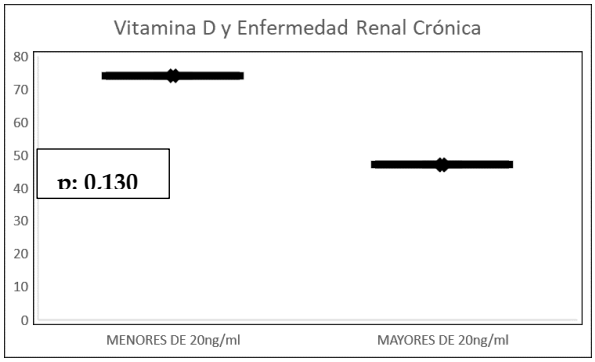

Figura 1. Valores dicotomizados de vitamina D (mayor o menor de 20 ng/ml) comparados con mediana de edad, diabetes, HTA y enfermedad renal crónica. p<0.05 significancia estadística

Al valorar los niveles de vitamina D no se evidencio diferencia estadísticamente significativa entre hombres y mujeres (p =0.16), sin embargo si se evidenció diferencia en cuanto a la edad en relación a pacientes menores de 65 años y los mayores de 65 años (p=0.02).

Con respecto a diabetes y los niveles de vitamina D no se evidencio diferencia estadísticamente significativa (p=0.9), mientras que en caso de hipertensión si se evidencia diferencia estadísticamente significativa con respecto a los niveles de vitamina D (p=0.01).

Con respecto a la presencia de disminución de tasa de filtrado glomerular menor de 60 ml/min (correspondiente a estadios de enfermedad renal crónica estadios 3,4 y 5) no hubo diferencias estadísticamente significativas frente a pacientes sin enfermedad renal crónica (p=0.55).

CARACTERISTICAS	NIVELES DE VITAMINA D	p-valor	t
Género			
Masculino	20.77 (9.99)	0.160	-1.40
Femenino	18.63 (10.94)		
Edad			
Mayores de 65a	18.11 (10.47)	0.024	-2.77
Menores de 65a	21.56 (10.37)		
Diabetes Mellitus			
Con historia de Diabetes Mellitus	19.5 (11.67)	0.90	-0.11
Sin Diabetes Mellitus	19.69 (9.99)		
Hipertensión arterial			
Con historia de Hipertensión Arterial	17.53 (10.46)	0.001	-3.22
Sin hipertensión Arterial	22.35 (10.15)		
Enfermedad Renal Crónica			

TFG más de 60 ml/min	19.28 (11.15)	0.55	-0.59
TFG menos de 60ml/mi	20.21 (9.47)		

* p<0.05 significancia estadística y valores t.

Fuente: Elaboración propia

Tabla 3. Relación niveles de vitamina D y comorbilidades

En el grupo de pacientes con antecedentes de enfermedad renal crónica se pudo obtener datos de calcio, fósforo, albúmina y PTH, demostrando que los pacientes sin y con deficiencia de vitamina D, existe diferencia significativa, excepto para la PTH, como lo indicado en la Tabla 4.

Características clínicas	**Deficiencia de Vitamina D <20ng/mL**		**p-valor**
	No	Si	
Albumina (mediana (IQR)) g/dL[1/]	4,36 (3,98 - 4,57)	4,06 (3,17 - 4,39)	0,004*
Calcio (mediana (IQR)) mg/dL[1/]	9,37 (8,82 - 9,82)	8,96 (8,2 - 9,54)	0,006*
Fosforo (mediana (IQR)) mg/dL[1/]	4,07 (3,55 - 4,85)	3,65 (1,97 - 4,33)	0,040*
PTH (mediana (IQR)) pg/mL[1/]	69,5 (57,28 - 131,25)	80,6 (52,9 - 128)	0,845
Nota: IQR=Rango Intercuartílico; * diferencias significativas, 1/ prueba Mann Whitney, 2/ prueba Chi-cuadrado			

Tabla 4. Relación características clínicas y presencia de deficiencia vitamina D

DISCUSION

En Latinoamérica existe escasa información sobre el déficit de vitamina D en la población general, lo cual dificulta evaluar con precisión el estado de la vitamina D a nivel regional, la mayoría de los estudios realizados han evaluado la asociación entre la deficiencia de vitamina D y la salud mineral ósea en niños, adolescentes, adultos, mujeres posmenopáusicas y ancianos[10–13]. Los datos encontrados en nuestro estudio demuestran niveles bajos de vitamina D en la población de estudio, así como lo reportado por Restrepo et al. en Colombia, a 2,200 metros de altura. En pacientes con enfermedad renal crónica sin diálisis, se reportó niveles bajos de vitamina D, lo que constituye un factor para el desarrollo de hiperparatiroidismo secundario [14].

Los datos del déficit de vitamina D en subgrupos son aún más limitados, por lo que en este estudio se realizó un análisis en el subgrupo de Enfermedad Renal Crónica estadios 3 al 5, siendo el primer estudio de este tipo en Ecuador, se eligió estos estadíos ya que son aquellos en los que son más frecuentes las alteraciones a nivel del metabolismo mineral óseo, dentro de los cuales se incluye las alteraciones de la vitamina D [3,15].

La prevalencia de deficiencia de vitamina D a nivel mundial oscila entre 2 al 90% dependiendo del punto de corte utilizado y la población seleccionada [16], en nuestro estudio la prevalencia de insuficiencia de vitamina D es del 28.5 % y la deficiencia es de 57%, lo cual constituye un importante problema de salud.

Encontramos que la edad presentó diferencias significativas en cuanto a los niveles de vitamina D, siendo mayor el déficit en la población de los adultos mayores con una media de edad de 70 años y el déficit de

vitamina D se presentó en el 63.8% de este grupo. En otro estudio realizado en Ecuador la prevalencia de vitamina d menor a 40 nmol/L (16 ng/ml) entre los ancianos oscilan entre el 9 al 19% [17].Entre los factores que determinan menores niveles séricos de vitamina D en ancianos se encuentran la menor ingesta en la dieta y la capacidad disminuida de la piel de producir vitamina D disminuyendo un 25% en los 75 años, adicionalmente en un metanálisis se observó mayores niveles de deficiencia en los ancianos que viven solos o están institucionalizados [18,19].

En cuanto al sexo no se encontraron diferencias significativas en relación a los niveles de vitamina D en la población estudiada, al igual que en el metaanálisis realizado por Hilger et al. [20], quien reportó que no se observaron diferencias relacionadas con el sexo en ninguna región, con excepción de Asia y Medio Oriente/África, probablemente debido a la heterogeneidad de los estudios.

Con respecto a las comorbilidades, destacamos a la población de pacientes con hipertensión arterial quienes presentaron niveles inferiores a 20 ng/ml de vitamina D. En varios estudios se ha observado una asociación inversa entre los niveles de vitamina D y presión arterial [21] , entre los mecanismos sugeridos está que la vitamina D inhibe el sistema renina angiotensina aldosterona, favorece la protección de los vasos sanguíneos, contribuye a la homeostasis del calcio, disminuye el estrés oxidativo y favorece la síntesis de prostaglandinas [5]. Recientemente se reportó que las personas presentan el polimorfismo FokI en el gen que codifica para el receptor de la vitamina D tienen un riesgo incrementado de desarrollar hipertensión arterial [22]. En el estudio realizado por Zhou et al., realizado en ratones de laboratorio demostraron que la hipertensión pudo ser revertida con la administración de 1,25-dihidroxicolecalciferol [23].

En el tercer análisis NHANES [24] realizado en 12.644 pacientes permitió demostrar que aquellas personas con valores de 25-hidroxicolecalciferol ≥ 30 ng/mL, mantienen cifras de presión arterial sistólica de 3,0mmHg (p=0,0004) y presión arterial diastólica de 1,6mmHg (p=0,011) menores, en comparación con los que presentan valores plasmáticos de 25-hidroxicolecalciferol ≤ 16 ng/ml. Las diferencias entre los valores de 25-hidroxicolecalciferol y las cifras de la Presión arterial fue mayor en los participantes ≥ 50 años de edad, en comparación con los jóvenes (p=0,021). Estos resultados apoyan la hipótesis que plantea una relación entre la capacidad de producción y/o absorción de la vitamina D en las personas de la tercera edad y el riesgo de presentar HTA [21,25].

La prevalencia del déficit de vitamina D en pacientes con enfermedad renal crónica varía desde el 78% para insuficiencia y 18% para deficiencia severa, en pacientes en diálisis se estima que oscila entre el 50 y el 100% [5]; contrastando las diferencias obtenidas en la población de nuestro estudio, en que se evidencio que un 24% de pacientes con enfermedad renal crónica estadios 3, 4 y 5 presentaban insuficiencia y 61,2% presentaban deficiencia. Así mismo se evidenció que en la población sin enfermedad renal crónica la prevalencia de insuficiencia de vitamina D fue 36.1% y la de deficiencia fue 50%, los cuales no tuvieron significancia estadística para los estadios 3 y 4 en comparación a la población sin enfermedad renal crónica.

La deficiencia de vitamina D está presente en todas las etapas de la ERC, y su prevalencia aumenta a medida que se reduce la función renal. A su vez, otros estudios han reportado una asociación entre la deficiencia de vitamina D y la reducción en la tasa de filtrado glomerular en pacientes con enfermedad renal crónica [15,26]. González et al. informaron que el 86% de los pacientes en prediálisis y el 97% de los pacientes en hemodiálisis

presentaron niveles inadecuados de 25(OH)-VD [27]. Un estudio de cohorte que incluyó 1056 pacientes en diálisis en Estados Unidos reportó que el 79% y 57% de 908 individuos en hemodiálisis crónica respectivamente, tenían niveles de 25(OH)-VD de <30 y <20 ng/mL, respectivamente [28].

Son factores de riesgo para la deficiencia de vitamina D en la población con Enfermedad Renal Crónica, la hipoalbuminemia, la raza negra y el sexo femenino [28,29]; en concordancia con los resultados obtenidos en nuestro estudio, dónde, la mediana de albumina en los pacientes sin deficiencia de vitamina D fue superior a la de los pacientes con deficiencia de vitamina D. Las pérdidas de vitamina D aumentan cuando la proteína fijadora de vitamina D, la albúmina y los metabolitos de la vitamina D unidos a estas proteínas se eliminan por medio de la proteinuria [(34)].

En el estudio realizado por Yonemura et al. se evidenció una correlación positiva entre los niveles de albumina y vitamina D, se observó que al suplementar vitamina D se elevaron las concentraciones de albumina sérica en pacientes con ERC. La hipoalbuminemia quizá está relacionada con la desnutrición y la ingesta deficiente de vitamina D[30].

Así mismo es relevante la presencia de diferencia estadísticamente significativa entre los niveles más bajos de calcio y fosforo en el grupo de deficiencia de vitamina D y el grupo de no deficiencia de vitamina D lo que concuerda con el efecto fisiológico de la vitamina D [31].

De destacar, que la intervención para mejorar los niveles de este sustrato puede prevenir eventos cardiovasculares, equilibrar la conexión hueso-grasa, corregir los trastornos del recambio óseo, mejorar la función endotelial, aliviar la proteinuria y, en última instancia, reducir la morbilidad y la mortalidad en pacientes con ERC [16,32,33].

Para los pacientes con ERC, las directrices de la NKF recomiendan una concentración objetivo de vitamina D más alta (> 30 ng/ml) que para la población general [35]. No existen pautas bien establecidas en base al manejo del déficit de vitamina D y las alteraciones del metabolismo mineral óseo en la ERC ya que los rangos de concentración óptimos de vitamina D y PTH no están bien determinados en cada una de las etapas de esta enfermedad. El número limitado de ensayos que han informado efectos sobre el tratamiento con vitamina D y sus análogos en este grupo de pacientes han dado resultados contradictorios [1,34].

La vitamina d es el precursor inactivo de la 1,25 (OH)2 D y es la más utilizada para la prevención de la deficiencia de la misma. Existe en dos formas, vitamina D3 (colecalciferol) y D2 (ergocalciferol), la única diferencia entre ambas es que la vitamina D3 genera un aumento más prolongado de 25 (OH)D. En un metanálisis realizado en pacientes con enfermedad renal crónica estadios 3 y 4, en el que se incluyó 9 estudios mostró resultados inconsistentes; las dosis variaron de 2000 a 4000 UI diarias o de 40000 a 50000 UI semanales y la duración fue entre 1 y 12 meses, en todos los estudios se observó un aumento en las concentraciones sanguíneas de 25 (OH) D, en 4 de 9 estudios se observaron reducción en valores de PTH y 5 estudios se mostró una reducción no significativa de PTH de 18 pm/ml, no se observó efectos sobre las concentraciones de calcio y fósforo [33,37].

El calcifediol o 25 (OH) D es otra forma de presentación, su absorción intestinal es más eficiente, ya que no depende de la absorción de grasas, el aumento de su concentración en el plasma es más rápido y la relación dosis respuesta es mayor que la del original. Hay 3 formas de 25 (OH) D: calcifediol, formula de liberación prolongada y la fórmula de liberación inmediata (retirado del mercado de Estados Unidos en el 2022) [34]. En los pocos estudios realizados en pacientes con enfermedad renal crónica, en un ensayo realizado en el 2016 la dosis empleada fue de calcifediol de liberación prolongada de 30 o 60 µg administrada una vez al día por 26 semanas, se logró la normalización de las concentraciones séricas totales de 25-hidroxivitamina D (>30 ng/ml) en >95% de la población estudiada y redujo hormona paratiroidea intacta en plasma (PTHi) en al menos un 10% en el 72%, sin evidenciar cambios en valores de calcio y fósforo [38].

La forma activa de vitamina D y sus análogos utilizados en el tratamiento de pacientes con ERC incluyen el calcitriol y los análogos de la vitamina D paricalcitol (19-nor-1,25$(OH)_2$ D_2) y el precursor del 1,25 $(OH)_2$ D_3 alfacacidiol (1a$(OH)D_3$) [39,40]. El paricalcitol y el alfacalcidol son análogos sintéticos de la vitamina D, también se conocen como activadores del receptor de vitamina d, estos medicamentos se indican para el manejo del Hiperparatiroidismo secundario, se ha visto que el Paricalcitol presentan efectos renoprotectores, reduce los eventos cardiovasculares y suprime la secreción de PTH [41]. En los estudios realizados la duración de la administración varió de 2 a 48 semanas y las dosis utilizadas en estos estudios de 0,25 a 2 µg. Como efecto adverso presentaron hipercalcemia e hiperfosfatemia [33].

Los análogos de la vitamina D se recomiendan sólo para pacientes con un aumento progresivo de la PTH y para el tratamiento del Hiperparatiroidismo secundario, el uso de calcifediol para suprimir la PTH en pacientes con ERC es prometedor, ya que el riesgo de sobresupresión de PTH e hipercalcemia parece menos probable en comparación con el calcitriol y el paricalcitol, hay pocos estudios que respaldan esta postura por lo que se requiere más investigación.

Limitaciones

Nuestro estudio tiene importantes limitaciones, es monocéntrico, con una muestra pequeña y el diseño retrospectivo con sus sesgos inherentes.

CONCLUSIONES

Hemos determinado de manera pionera, los primeros datos de niveles de vitamina D en poblaciones específicas (sin falla renal y con falla renal estadios 3,4 y 5); determinando que los niveles de esta vitamina son inferior en pacientes de tercera edad, pacientes hipertensos, sin embargo no se evidencio diferencias significativas entre estadio 3,4 y 5 .Es relevante que la diferencia significativa se dio en pacientes con enfermedad renal crónica estadio 5 en hemodiálisis.

El conocer estos datos debe promever más estudios sobre el tema y ajustar las política de salud pública que promueven el control de los valores de ésta vitamina en poblaciones de enfermos renales.

Author Contributions. Conceptualization, André Benítez-Baldassari, Estefanía León-Hernández Methodology. André Benítez-Baldassari, software, Andrea Banegas-Sarmiento, Jorge Luis Vélez-Paéz, validation, , Andrea Banegas-Sarmiento Jorge Luis Vélez-Paéz.; Santiago Aguayo-Moscoso, visualization; Andrea Banegas-Sarmiento, formal analysis. André Benítez-Baldassar, investigation; André Benítez-Baldassari*;* Estefanía León-Hernández, resources, André Benítez-Baldassari [1], Estefanía León-Hernández; Andrea Banegas-Sarmiento, data curation,.; Andrea Banegas-Sarmiento, Jorge Luis Vélez-Paéz, writing—original draft preparation, André Benítez-Baldassari, Estefanía León-Hernández, writing—review and editing, Jorge Luis Vélez-Paéz.; Santiago Aguayo-Moscoso, visualization, Andrea Banegas-Sarmiento, supervision; Jorge Luis Vélez-Paéz, project administration, André Benítez-Baldassari, Jorge Luis Vélez-Paéz.

Agradecimiento: Agradecimiento al personal del Laboratorio del Hospital Pablo Arturo Suarez y a los estudiantes de la Universidad Central del Ecuador

Conflictos de interes: no conflicto de interés por declarar

REFERENCIAS

1. Rochel N. Vitamin D and Its Receptor from a Structural Perspective. Nutrients. 12 de julio de 2022;14(14):2847.

2. Wang H, Chen W, Li D, Yin X, Zhang X, Olsen N, et al. Vitamin D and Chronic Diseases. Aging Dis. 2 de mayo de 2017;8(3):346-53.

3. Bover J, Massó E, Gifre L, Alfieri C, Soler-Majoral J, Fusaro M, et al. Vitamin D and Chronic Kidney Disease Association with Mineral and Bone Disorder: An Appraisal of Tangled Guidelines. Nutrients. 24 de marzo de 2023;15(7):1576.

4. Zhang Y, Darssan D, Pascoe EM, Johnson DW, Pi H, Dong J. Vitamin D status and mortality risk among patients on dialysis: a systematic review and meta-analysis of observational studies. Nephrol Dial Transplant. 1 de octubre de 2018;33(10):1742-51.

5. Martin-Romero A, Perelló-Martínez J, Hidalgo-Santiago JC, Michan-Doña A, Bosco López Sáez J, Gómez-Fernández P. Efecto de la administración de diferentes formas de vitamina D en la presión arterial y rigidez aórticas, y su implicación en la reducción de la albuminuria en la enfermedad renal crónica. Clínica e Investigación en Arteriosclerosis. 1 de noviembre de 2022;34(6):311-21.

6. Barreto DV, Barreto FC, Liabeuf S, Temmar M, Boitte F, Choukroun G, et al. Vitamin D affects survival independently of vascular calcification in chronic kidney disease. Clin J Am Soc Nephrol. junio de 2009;4(6):1128-35.

7. Jacob AI, Sallman A, Santiz Z, Hollis BW. Defective photoproduction of cholecalciferol in normal and uremic humans. J Nutr. julio de 1984;114(7):1313-9.

8. Fournier A, Fardellone P, Achard JM, Ghazali A, Pruna A, El Esper N, et al. Importance of vitamin D repletion in uraemia. Nephrology Dialysis Transplantation. 1 de abril de 1999;14(4):819-23.

9. Pilz S, Iodice S, Zittermann A, Grant WB, Gandini S. Vitamin D Status and Mortality Risk in CKD: A Meta-analysis of Prospective Studies. American Journal of Kidney Diseases. 1 de septiembre de 2011;58(3):374-82.

10. Coccia P, Blazquez J, Contreras M, Ferraris V, Raddavero C, Ghezzi L, et al. Alta prevalencia de deficiencia de vitamina D en niños con enfermedad renal crónica y trasplante renal. Arch argent pediatr. 2017;220-6.

11. Palacios C, González L. La deficiencia de vitamina D es un problema global de salud pública. Anales Venezolanos de Nutrición. junio de 2014;27(1):57-72.

12. Martínez-Torres J, Barajas-Lizarazo MA, Cárdenas-Malpica PA, Escobar-Velásquez KD, Carvajal-Suárez LS, Moreno-Bayona JA, et al. Prevalencia de la deficiencia e insuficiencia de vitamina D y factores asociados en mujeres colombianas en 2015. Nutrición Hospitalaria. agosto de 2022;39(4):843-51.

13. Herrera-Vázquez A, Avendaño-Vázquez E, Torres-Alarcón CG, Herrera-Vázquez A, Avendaño-Vázquez E, Torres-Alarcón CG. Deficiencia de vitamina D en adultos mayores con fractura de cadera. Medicina interna de México. octubre de 2019;35(5):669-75.

14. Restrepo Valencia CA, Aguirre Arango JV, Restrepo Valencia CA, Aguirre Arango JV. Niveles de vitamina D (25(OH)D) en pacientes con enfermedad renal crónica estadios 2 a 5. Colombia Médica. septiembre de 2016;47(3):160-6.

15. Ureña-Torres P, Metzger M, Haymann JP, Karras A, Boffa JJ, Flamant M, et al. Association of kidney function, vitamin D deficiency, and circulating markers of mineral and bone disorders in CKD. Am J Kidney Dis. octubre de 2011;58(4):544-53.

16. Amrein K, Scherkl M, Hoffmann M, Neuwersch-Sommeregger S, Köstenberger M, Tmava Berisha A, et al. Vitamin D deficiency 2.0: an update on the current status worldwide. Eur J Clin Nutr. noviembre de 2020;74(11):1498-513.

17. López Gavilanez E, Orces CH, Guerrero Franco K, Segale Bajaña A, Veliz Ortega J, Bajaña Granja W, et al. Insuficiencia de vitamina D en mujeres postmenopáusicas ecuatorianas con diabetes mellitus tipo 2. Revista de Osteoporosis y Metabolismo Mineral. marzo de 2018;10(1):7-14.

18. Castellote Varona FJ, Buttazzo M, López Azorín F, Ruiz Espejo F. Niveles de vitamina D en el anciano. Revista española de geriatría y gerontología: Órgano oficial de la Sociedad Española de Geriatría y Gerontología. 2010;45(5 (Septiembre / Octubre)):301-2.

19. Fernández del Buey RM, Castro Barrio M, Martínez Gordillo N, Ruiz Sanz E. Hipovitaminosis D en la población anciana institucionalizada: variables asociadas y valoración geriátrica. Gerokomos. diciembre de 2016;27(4):153-6.

20. Hilger J, Friedel A, Herr R, Rausch T, Roos F, Wahl DA, et al. A systematic review of vitamin D status in populations worldwide. Br J Nutr. 14 de enero de 2014;111(1):23-45.

21. Castro Torres Y, Fleites Pérez A, Carmona Puerta R, Vega Valdez M, Santiestebán Castillo I. Déficit de la vitamina D e hipertensión arterial. Evidencias a favor. Revista Colombiana de Cardiología. 1 de enero de 2016;23(1):42-8.

22. Swapna N, Vamsi UM, Usha G, Padma T. Risk conferred by FokI polymorphism of vitamin D receptor (VDR) gene for essential hypertension. Indian J Hum Genet. 2011;17(3):201-6.

23. Zhou C, Lu F, Cao K, Xu D, Goltzman D, Miao D. Calcium-independent and 1,25(OH)2D3-dependent regulation of the renin-angiotensin system in 1alpha-hydroxylase knockout mice. Kidney Int. julio de 2008;74(2):170-9.

24. Hintzpeter B, Mensink GBM, Thierfelder W, Müller MJ, Scheidt-Nave C. Vitamin D status and health correlates among German adults. Eur J Clin Nutr. septiembre de 2008;62(9):1079-89.

25. Scragg R, Sowers M, Bell C. Serum 25-hydroxyvitamin D, ethnicity, and blood pressure in the Third National Health and Nutrition Examination Survey. Am J Hypertens. julio de 2007;20(7):713-9.

26. Franca Gois PH, Wolley M, Ranganathan D, Seguro AC. Vitamin D Deficiency in Chronic Kidney Disease: Recent Evidence and Controversies. Int J Environ Res Public Health. 17 de agosto de 2018;15(8):1773.

27. González EA, Sachdeva A, Oliver DA, Martin KJ. Vitamin D insufficiency and deficiency in chronic kidney disease. A single center observational study. Am J Nephrol. 2004;24(5):503-10.

28. Bhan I, Burnett-Bowie SAM, Ye J, Tonelli M, Thadhani R. Clinical Measures Identify Vitamin D Deficiency in Dialysis. Clin J Am Soc Nephrol. marzo de 2010;5(3):460-7.

29. Wolf M, Shah A, Gutierrez O, Ankers E, Monroy M, Tamez H, et al. Vitamin D levels and early mortality among incident hemodialysis patients. Kidney Int. octubre de 2007;72(8):1004-13.

30. Yonemura K, Fujimoto T, Fujigaki Y, Hishida A. Vitamin D deficiency is implicated in reduced serum albumin concentrations in patients with end-stage renal disease. Am J Kidney Dis. agosto de 2000;36(2):337-44.

31. Akimbekov NS, Digel I, Sherelkhan DK, Razzaque MS. Vitamin D and Phosphate Interactions in Health and Disease. Adv Exp Med Biol. 2022;1362:37-46.

32. Cianciolo G, Cappuccilli M, Tondolo F, Gasperoni L, Zappulo F, Barbuto S, et al. Vitamin D Effects on Bone Homeostasis and Cardiovascular System in Patients with Chronic Kidney Disease and Renal Transplant Recipients. Nutrients. 25 de abril de 2021;13(5):1453.

33. Al-Ishaq RK, Kubatka P, Brozmanova M, Gazdikova K, Caprnda M, Büsselberg D. Health implication of vitamin D on the cardiovascular and the renal system. Archives of Physiology and Biochemistry. 4 de mayo de 2021;127(3):195-209.

34 Christodoulou M, Aspray TJ, Schoenmakers · Inez. Vitamin D Supplementation for Patients with Chronic Kidney Disease: A Systematic Review and Meta-analyses of Trials Investigating the Response

to Supplementation and an Overview of Guidelines. 2021 [cited 2023 Dec 16];109:157–78. Available from: https://doi.org/10.1007/s00223-021-00844-1

35 A Clinical Update on Vitamin D Deficiency and Secondary Hyperparathyroidism: Vitamin D Testing and Supplementation in CKD Stages 3-4 Part 2 References. 2016 [cited 2023 Dec 16]; Available from: www.opko.com/products/point-of-care-diagnostics/.

36 Koizumi M, Komaba H, Fukagawa M. Parathyroid function in chronic kidney disease: role of FGF23-Klotho axis. Contrib Nephrol [Internet]. 2013 [cited 2023 Dec 16];180:110–23. Available from: https://pubmed.ncbi.nlm.nih.gov/23652554/

37 Dogan E, Erkoc R, Sayarlioglu H, Soyoral Y, Dulger H. Effect of depot oral cholecalciferol treatment on secondary hyperparathyroidism in stage 3 and stage 4 chronic kidney diseases patients. Ren Fail [Internet]. 2008 May [cited 2023 Dec 16];30(4):407–10. Available from: https://www.tandfonline.com/action/journalInformation?journalCode=irnf20

38 Sprague SM, Crawford PW, Melnick JZ, Strugnell SA, Ali S, Mangoo-Karim R, et al. Use of Extended-Release Calcifediol to Treat Secondary Hyperparathyroidism in Stages 3 and 4 Chronic Kidney Disease. Am J Nephrol [Internet]. 2016 Oct 18 [cited 2023 Dec 16];44(4):316–25. Available from: https://dx.doi.org/10.1159/000450766

39 Larsen T, Mose FH, Bech JN, Pedersen EB. Effect of paricalcitol on renin and albuminuria in non-diabetic stage III-IV chronic kidney disease: A randomized placebo-controlled trial. BMC Nephrol [Internet]. 2013 Jul 26 [cited 2023 Dec 16];14(1):1–11. Available from: https://bmcnephrol.biomedcentral.com/articles/10.1186/1471-2369-14-163

40 Alborzi P, Patel NA, Peterson C, Bills JE, Bekele DM, Bunaye Z, et al. Paricalcitol Reduces Albuminuria and Inflammation in Chronic Kidney Disease. Hypertension [Internet]. 2008 Aug 1 [cited 2023 Dec 16];52(2):249–55. Available from: https://www.ahajournals.org/doi/abs/10.1161/HYPERTENSIONAHA.108.113159

41 Thadhani R, Appelbaum E, Pritchett Y, Chang Y, Wenger J, Tamez H, et al. Vitamin D Therapy and Cardiac Structure and Function in Patients With Chronic Kidney Disease: The PRIMO Randomized Controlled Trial. JAMA [Internet]. 2012 Feb 15 [cited 2023 Dec 16];307(7):674–84. Available from: https://jamanetwork.com/journals/jama/fullarticle/1104984

Received: October 9 2023/ **Accepte**d: January 15 2024 / **Published:**15 February 2024

Citation: Niveles de Vitamina D en pacientes con y sin Enfermedad Renal Crónica, perfil clínico y epidemiológico: un análisis preeliminiar en un hospital de segundo nivel en Quito, Ecuador. Benítez-Baldassari A, León-Hernández E, Banegas-Sarmiento A, S Aguayo-Moscoso, Vélez-Paéz J L. Revis Bionatura 2024; 9 (1) 43. http://dx.doi.org/10.21931/RB/2024.09.01.43

Additional information. Correspondence should be addressed to *baar_ebola@outlook.com*

Peer review information. Bionatura thanks anonymous reviewer(s) for their contribution to the peer review of this work using https://reviewerlocator.webofscience.com/

Bionatura ISSN. First 13909355 Ecuador. **Scopus coverage years**: from 2016 to the present

Bionatura
Ibero-American Journal of Biotechnology and Life Sciences

Article

HIV knowledge and preventive Standards Precautions Among Healthcare Workers in Blood Transfusion Centers

Nasir Muwfaq Younis[1], Mahmoud Mohammed Ahmed[2], Alaa Yousif Ayed[3]

[1]Assist. Prof, PhD. Nursing of CH, College of Nursing / University of Mosul/ IRAQ
ORCID: 0000-0002-7987-0484
[2]Assist. Prof. PhD. CH. N, College of Nursing / University of Mosul /IRAQ
ORCID: 0000-0002-7059-7119
[3]Assist. Lecture, College of Nursing / University of Mosul/ IRAQ
ORCID:0000-0003-1935-8128
Corresponding Author: E-mail: nasir.mufaq@uomosul.edu.iq
Available from. http://dx.doi.org/10.21931/RB/2024.09.01.44

ABSTRACT

The number of instances of HIV has climbed considerably in the previous ten years, which is cause for alarm. Because healthcare workers are future healthcare professionals, they must have proper knowledge and preventive standards and precautions about HIV because they will play a vital role in the prevention of HIV transmission and treatment of HIV patients. The article aims to identify HIV knowledge and preventive standard precautions among healthcare workers in blood transfusion Centers**.** Cross-sectional descriptive research to characterize and provide information about the knowledge and preventive standards precautions among healthcare workers in blood transfusion Centers from March 25 to April 15, 2022. Participants from the described Studies (N = 34) provided data for these analyses. This result revealed that the participants' knowledge ranged between acceptable and good (47.05 and 52.95). Also, participants' knowledge of prevention strategies was similar, but the hand hygiene strategy was the most valuable (M: 3.62 and SD: 0.45). The instrument consists of 3 parts: part 1: demographical variables. Part two: healthcare workers' knowledge of HIV, Part 3: preventive standards precautions among healthcare workers. The current study of healthcare personnel shows that they have a decent understanding of HIV based on the precise results and adhere to the preventive measures during the blood transfusion.

Keywords: HIV, knowledge, preventive Standards precautions, Healthcare Workers, Blood Transfusion Centers.

INTRODUCTION

Of its high rates of morbidity and mortality, as well as its high treatment costs around the world, HIV has been seen as a severe health issue in past years. At the end of 2017, the World Health Organization and the Joint (UNAIDS) projected that 40 million individuals worldwide had HIV. In addition, according to WHO (2017) estimates, HIV prevalence increased in 2017, with 1.8 million new infections and 1.0 million deaths worldwide due to HIV-related causes[1]. Nurses who are exposed to blood on the job are more likely to contract blood-borne illnesses. The amount of danger is determined by the number of patients in the healthcare facility

who have that virus, as well as the precautions used by healthcare workers while dealing with HIV[2]. In most countries, nurses comprise most of the various cadres of healthcare workers. Working with clients' blood or body fluids necessitates them to be on the front lines of care.

As a consequence, they risk getting HIV and other blood diseases at work. Workers exposed among healthcare employees are accountable for 2.3 percent of global HIV cases, according to the World Health Organization. In order to provide high-quality HIV care, preventive measures are critical[4]. The World Health Organization (WHO) has been a global leader in implementing preventative measures for healthcare personnel[5]. The WHO defines preventive precautions as "the absence of preventable harm to a patient during healthcare, as well as the reduction of the risk of unnecessary harm connected with healthcare to an acceptable minimum." We need strong laws and skilled healthcare personnel to successfully incorporate patient safety science into world educational institutions' training programs to create significant and effective changes in healthcare safety[6]. All governments should have measures in place to address HIV-related stigma and prejudice, as well as to protect people from acquisition, provide medication, and provide assistance to people living with the disease[7]. Iraq's Ministry of Health and Environment offers HIV/AIDS patients both prevention and treatment services, and they have the same rights as other patients. So, according to the British HIV Association (BHIVA), nurses working in blood banks should prescribe qualifications[8,9]. Several studies have found that blood bank nurses are afraid of HIV/AIDS patients and have negative opinions toward them. These have been connected to a lack of understanding of the condition; as a result, they may be hesitant to treat HIV/AIDS patients[10]. The findings of this study are hoped to raise nurses' knowledge and safeguards when caring for HIV-positive patients. Nursing that focuses on Aids and other infectious disease skills and information is regarded as effective for improving patient care and resulting in better healthcare[11]. The focus of this research was to assess the knowledge of nurses who may be exposed to HIV and to assess the preventive actions for nurses working in blood banks who may be responsible for Aids patient care in the future.

MATERIALS AND METHODS

Cross-sectional descriptive research to characterize and provide information about the awareness and preventive standards precautions among healthcare workers in blood transfusion Centers without trying to influence or manipulate the participants. Participants from the described Studies (N = 34) provided data for these analyses. This study was applied to the correct workers in the blood transfusion center in the state of Nineveh for 20 days, during which the knowledge of the correct workers was assessed. I monitored the right workers' preventive measures from March 25 to April 15, 2022. After evaluating previously published material, The questionnaire method was constructed by the researchers participating in the research. The questionnaire focused on three main aspects: demographic information (age, gender, level of education, experience, type of work and previous exposure to infection). The second aspect is the knowledge of the correct workers about HIV, which was evaluated using the 3_likert scale: Yes, no, and I do not know. The instrument categories, according to the researcher, Poor (0 of 20), acceptance (21–40 of 14), and sound (41 of 60) knowledge were the three categories. The third aspect is the measurement of the preventive measures used by the correct workers inside the blood transfusion centers, which were evaluated using the 4_likert scale, including (Always, often, rarely, never). The mean, standard deviation, frequency, percentage regression, and percentages were used by the SPSS Ver:26 program to analyze [12,13]. The knowledge of the right workers, as well as in the analysis of the paragraphs of preventive measures, which included (personal hygiene, use of gloves, prevention of needle prick injuries, environmental hygiene, waste disposal, and finally, sick care equipment).

RESULTS

Table 1 In describing the demographic variables of the study sample, most participants were between 20 and 29 years old, and most had a bachelor's degree. Women were slightly more than males. The majority of the participants had experience between 1 to 10 years, and the majority of them had been exposed to infection previously. The researchers looked at a total of 34 healthcare personnel, 16 of whom were male and 18 of whom were female. The Internet and television were the primary sources of HIV knowledge for most students (65.0%) in this study, followed by school or university and friends/relatives (26.0 percent). Table 3 The results showed that the participants' knowledge ranged between acceptable and good (47.05 and 52.95), respectively. Table 4 The results showed that most participants' knowledge of prevention strategies was similar, but the hand hygiene strategy was the most valuable (M: 3.62 and SD: 0.45). Finally, The results showed no effect of demographic data on the level of knowledge except for (exposure to communicable diseases in the workplace) which had a positive effect of 0.034.

Variables	No.	%
Age		
20-29 Years	17	50
30-39 Years	9	26.5
40-49 Years	6	17.6
50 Or More	2	5.9
Level of education	No.	%
Secondary	10	29.4
Diploma	10	29.4
Bachelors	13	38.2
Master degree	1	2.9
Gender	No.	%
Male	16	47.1
Female	18	52.9
Experience	No.	%
Less 1 year	12	35.3
(1-5 Y)	12	35.3
(6-10 Y)	6	17.6
(11-15 Y)	3	8.8
More than 15Y	1	2.9
Type of work	No.	%
Physician	3	8.8

Nurse	26	76.5
Others	5	14.7
Previous exposure to infection	No.	%
Yes	29	85.3
No	5	14.7

Table (1): The study sample was divided into groups based on demographic characteristics.

In describing the demographic variables of the study sample, it appears that most participants were between 20 and 29 years old, and most had a bachelor's degree. Women were slightly more than males. Most participants had experience between 1 and 10 years, and most had been exposed to infection previously.

Source of information	Number	Percent.
Internet	**15**	**44.11%**
Television	**7**	**20.58%**
Friends/relatives	**4**	**11.76%**
Newspaper	**2**	**5.88%**
School or university	**5**	**14.7%**
Continuing education	**1**	**2.94%**
Non-governmental organizations	**1**	**2.94%**

Table (2): Source of information about HIV.

The researchers looked at a total of 34 healthcare personnel, 16 of whom were male and 18 of whom were female.
The Internet and television were the primary sources of HIV knowledge for the majority of students (65.0%) this study, followed by school or university and friends/relatives (26.0 percent).

Knowledge	Score Knowledge	No	%	Mean	SD
Poor	(0-20)	0	0	0	0
Acceptance	(21_40)	16	47.05	35.43	3.75
Good	(41_60)	18	52.95	44.11	2.51
Total		34	100	40.02	5.38

Table (3): Knowledge of blood bank workers towards infection control.

The results showed that the participants' knowledge ranged between acceptable and sound (47.05 and 52.95).

Prevention Strategies	Mean	SD	Rank
Hands hygiene	3.62	0.45	1
Gloves	3.58	0.51	2
Equipment care	3.57	0.44	3

Tingling prevention	3.53	0.48	4
Clean the environment	3.47	0.58	5
Waste management	3.26	0.59	6

Table (4): Distribution of the participant's knowledge rank regarding prevention strategies against HIV.

The results showed that most of the participants' knowledge of prevention strategies was similar, but the hand hygiene strategy was the most valuable (M: 3.62, and SD: 0.45)

Model	Unstandardized_ Coefficients		Standardized_ Coefficients	t	Sig.
	B	Std. Error	Beta		
(Constant)	36.25	8.888		4.079	0.000
Age	-1.22	1.488	-0.216	-0.825	0.417
Educational level	-0.03	1.288	-0.006	-0.028	0.978
Experience	-.039	1.364	-0.008	-0.029	0.977
Gender	-1.71	2.182	-0.161	-0.78	0.439
Specialty	0.72	1.976	0.066	0.36	0.716
Exposure to communicable diseases	**6.58**	**2.93**	**0.44**	**2.24**	**0.034**
Training	0.31	2.25	0.02	0.140	0.890

Table (5): Linear regression analysis to predict the knowledge among staff of blood bank
a. Dependent Variable: Knowledge

The results showed that there was no effect of demographic data on the level of knowledge except for (exposure to communicable diseases in the workplace) had a positive effect of 0.034.

DISCUSSION

The current study's findings show that respondents had a strong understanding of HIV. Nevertheless, given that the current study's target demographic was healthcare workers, their HIV knowledge was good and sufficient for future healthcare professionals. In describing the demographic variables of the study sample, it appears that most participants were between 20 and 29 years old, and most had a bachelor's degree. Women were slightly more than males. The majority of the participants had experienced between (1 to 10 years), and the majority of them had been exposed to infection previously. The main reason that the right workers who were less served by them have the least knowledge and experience in adhering to the correct preventive measures during blood transfusion is that they did not have any courses or workshops for HIV/AIDS. Knowledge and precautionary measures are essential factors in lowering the risk of HIV transmission in the workplace. Health workers encounter patients with known and unknown HIV status. As a result, there is a genuine need for healthcare staff to be aware of preventive measures. The majority of those polled had prior knowledge of HIV, according to the findings. In terms of knowledge, 52.95 percent of respondents were aware of HIV. This finding is consistent with the findings of another Ethiopian study, which found that 72.0 percent

of respondents believe PEP minimizes the risk of HIV infection following exposure [14]. Similar findings were found in previous studies, which revealed that nurses had a high degree of understanding regarding HIV and AIDS[15]. For responders, the Internet was the most popular source of HIV-related information. This demonstrates that the respondents are concerned about the risk of contracting HIV. This can be explained by the fact that the current society in general and the society of the correct workers are the most use of social media. Therefore, the results of more than half of the correct workers have appeared in taking information from the Internet.

The current study's findings were satisfactory and aligned with previous research findings. In this research, the most popular source of HIV knowledge was the Internet (85.0 percent), followed by the newspaper, friends, and relatives (40 percent). Likewise, in a study, India mentioned that the Internet was the source of information for 90% of women of reproductive age (7). As a result, it may be stated that both nurses and healthcare workers have similar sources of HIV/AIDS information. The results showed that most participants' knowledge of prevention strategies was similar, but the hand hygiene strategy was the most valuable (M: 3.62 and SD: 0.45). Waste management was a lower precaution between preventive measures used in bank transfusion (M=3.26 & SD=0.59). This study is similar to those (Singh & Paudel 2015) in Nepal, who found that nurses had the maximum number of needle stick injuries at approximately (76.7%)[16].

The results showed no effect of demographic data on the level of knowledge except that (exposure to communicable diseases in the workplace) had a positive effect of (0.034). This makes the right workers in the future. All preventive measures must be followed in dealing with infectious diseases, as they pose a threat to the lives of nurses, doctors, and the rest of the workers inside the blood transfusion centers17,18. We only included one blood Transfusion Center in this study because it was conducted for only 20 days. The study's drawback was this. The sample size was insufficient to detect a substantial difference in knowledge between male and female participants. Despite these restrictions, we were able to determine the level of awareness among healthcare personnel concerning HIV transmission and treatment, as well as preventive standards.

CONCLUSIONS

The current study of healthcare personnel shows that they have a decent understanding of HIV based on the precise results and adhere to the preventive measures during the blood transfusion**.**

Author Contributions:

Design and collection data: Nasir M. Younis

Statistical expertise and analysis and interpretation of data: Mahmoud M. Ahmed

Drafting of the article and Final approval: Alaa Y. Ayed

Funding: There was no external support for this study.

Acknowledgments: This work is supported by the director of health in Nineveh (4240211) from the University of Mosul, Iraq.

Conflict of Interest: There are no declared conflicts of interest.

REFERENCES

1. World Health Organization. Young people and HIV/AIDS: Opportunity in crisis. The Stationery Office; 2017.

2. Alam M. Knowledge, attitude and practices among health care workers on needle-stick injuries. Annals of Saudi Medicine. 2002 Sep;22(5-6):396-9.
3. Hamidi O, Tapak L, Poorolajal J, Amini P. Identifying risk factors for progression to AIDS and mortality post-HIV infection using illness-death multistate model. Clinical Epidemiology and Global Health. 2017 Dec 1;5(4):163-8.
4.Al-Rashidi RR, Naeem W, Alsadoon Z, Al-Shaikhli H, Alsaray RA, Kadhim MM. Knowledge, awareness and attitude of an Iraqi college undergraduate students towards patient safety Particularly HIV. HIV Nursing. 2021 Jul 1;21(01).
5. Organization WH. Patient safety: making health care safer, 2017.
6. Abbas AS, Younis NM. Efficacy of Pender's Health Promotion-based Model on Intervention for Enhancing University of Mosul Hypertensive Employees' Eating Behaviors: A randomized Controlled Trial. Revis Bionatura. 2022;7(3):35.
7. Stangl AL, Lloyd JK, Brady LM, Holland CE, Baral S. A systematic review of interventions to reduce HIV-related stigma and discrimination from 2002 to 2013: how far have we come?. Journal of the International AIDS Society. 2013 Nov;16:18734.
8. Bura'a LN, Younis NM. Nurses' knowledge regarding to phototherapy at neonatal care units in Mosul City, Iraq. Rawal Medical Journal: 2023 Apr. Vol. 48,(2):379-.
9.Younis NM, Ibrahim RM, Idrees NH.Prevalence of snake bite among children in Nineveh Governorate/Iraq: A retrospective study. International Journal of Medical Toxicology & Legal Medicine. 2022;25(3and4):169-172.
10. Ibrahim MS, Fatal GA, Rasheed MN. Polymorphism within the 5'UTR genomic region of hepatitis G virus (HGV) isolated from beta-thalassemia population in Iraq. Biomedicine. 2023 Apr 8;43(01):477-81.
11. Suominen T, Laakkonen L, Lioznov D, Polukova M, Nikolaenko S, Lipiäinen L, Välimäki M, Kylmä J. Russian nursing students' knowledge level and attitudes in the context of human immunodeficiency virus (HIV)–a descriptive study. BMC nursing. 2015 Dec;14(1):1-8.
12. Ibrahim RM, Idrees NH, Younis NM. Epidemiology of leukemia among children in Nineveh Province, Iraq. Rawal Medical Journal: 2023 Jan. Vol. 48, (1):137-.
13. Ahmed MM, Younis NM, Abdulsalam RR. Assessment of changes in sleep habits in elementary students during covid_19 lockdown. International Journal of Medical Toxicology & Legal Medicine. 2022;25(1and2):76-80.
14. Tebeje B, Hailu C. Assessment of HIV post-exposure prophylaxis use among health workers of governmental health institutions in Jimma Zone, Oromiya Region, Southwest Ethiopia. Ethiopian journal of health sciences. 2010;20(1).
15.Adea MK, Lefta RM, Younis NM. Impact of psychosocial aspect parameters on psoriasis patients' quality of life at outpatient clinic in Al-Dewania City, Iraq. Rawal Medical Journal. 2022 Dec 11;47(4):892-.
16. Singh B, Paudel B, Kc S. Knowledge and practice of health care workers regarding needle stick injuries in a tertiary care center of Nepal. Kathmandu University Medical Journal. 2015;13(3):230-3.
17.Ali HA, Abbas FF, Younis NM. Mothers' knowledge and attitudes towards breastfeeding in Thi-Qar City, Iraq. Rawal Medical Journal: 2023 Apr. Vol. 48,(2):514-.
18. Khadilkar NP, Mamatha BV, Bhat BM, Crasta PS. Knowledge, attitudes and practices among medical students on blood donation. Biomedicine. 2022 Dec 31;42(6):1228-32.

Received: October 9th 2023/ **Accepte**d: January 15th 2024 / **Published:**15 February 2024

Citation: Younis N. M., Ahmed M. M., Ayed A. Y. HIV knowledge and preventive Standards Precautions Among Healthcare Workers in Blood Transfusion Centers. Revis Bionatura 2024; 9 (1) 44. http://dx.doi.org/10.21931/RB/2024.09.01.44

Additional information Correspondence should be addressed to nasir.mufaq@uomosul.edu.iq

Peer review information. Bionatura thanks anonymous reviewer(s) for their contribution to the peer review of this work using https://reviewerlocator.webofscience.com/

Bionatura ISSN. First 13909355 Ecuador. **Scopus coverage years**: from 2016 to the present

Bionatura
Ibero-American Journal of Biotechnology and Life Sciences

Article

Cytogenotoxic effect of trichothecene T2 toxin on Allium sativum root tip meristematic cells

*Nasreen Jalal Hussein[1] and Asia A. M. Saadullah[2]**

[1]Department of Biology/ College of Science/ University of Zakho, Zakho, Kurdistan region/Iraq; nasreen.hussein@uoz.edu.krd . https://orcid.org/0000-0002-2221-1330.
[2]Department of Biology/ College of Science/ University of Duhok, Duhok, Kurdistan region/ Iraq; asia.saadullah@uod.ac . ORCID: https://orcid.org/0000-0001-6166-4394
** Correspondence: asia.saadullah@uod.ac*
Available from. http://dx.doi.org/10.21931/RB/2024.09.01.45

ABSTRACT

Trichothecene T2 is a mycotoxin from the Fusarium species. This research aims to test the effect of the Trichothecene T2 toxin on mitotic index% (M.I.%) and induction of mitotic aberrations by using the Allium sativum (garlic) test system. The toxin concentrations in ppm were: 0.00, 0.30, 0.60, 0.90, and 1.20 for 12 hours. The garlic roots were then cut and mitotic slides were prepared by the squash method and examined under a light microscope. The results revealed that the mycotoxin has a significant mitodepressive effect at all concentrations compared to the control and the MI% reduction was proportional to increasing toxin concentration. The highest reduction in mitotic index was observed in the 1.2 ppm treatment. Moreover, this mycotoxin induced and increased the rate of mitotic abnormalities% (MA%) with increasing the mycotoxin concentration. The observed mitotic abnormalities were star-shaped anaphase, sticky metaphase, C-mitosis, sticky anaphase, depolarization, micronuclei, laggard chromosomes, anaphase bridges, and chromosome loss. The least frequently observed abnormality was micronuclei compared to the most frequent aberration, laggard chromosomes. The total mitotic abnormalities significantly increased with increasing the toxin dose concentration. These results suggest that this mycotoxin can inhibit the mitotic activity of the meristematic cells, it is mutagenic and can disrupt the spindle fibers activity of the dividing cells at all concentrations, especially at its higher doses in food. Therefore, the foods must be tested for fungi producing this mycotoxin.

Keywords: Mycotoxin; mitodepressive; root tip; spindle fibers; mutagenic

INTRODUCTION

Mycotoxins are natural chemicals produced by fungus that infect cereals and other agricultural foods. They have a detrimental impact on Animal and human health. They are also thermally stable and easily transmitted to humans through animal products, sophisticated food preparation, and food chains[1.] toxic compounds are produce in foods and feeds by several strains of toxigenic fungi[2] , which ultimately cause health problems in humans and animals[3]. Trichothecenes (TCTs) are a family of chemically related mycotoxins produced most commonly by filamentous fungi such as Fusarium, Myrothecium, Stachybotrys, Trichoderma, and Trichothecium, Verticimonosporium, Cylindrocarpon, threatening the health of both animals and human[4,5]. The fungi that produce TCT are found all over the world. Their ability to grow under a variety of environmental conditions, including nutrient content, moisture content, temperature, and oxygen level in growth medium, results in successful colonization[6,7]. T-2 toxin can be found in diverse regions worldwide and affects negatively on

both human and animal health. It affects many organs and organ systems in the various ways: neurotoxicity, immunotoxicity, hepatotoxicity, dermal toxicity, nephrotoxicity, as well as the reproductive system disruption, maternotoxic and embryo lethal[8]. T-2 toxin is thought to be a primary contributor in human alimentary toxic aleukia. TCT are non-volatile sesquiterpenoids with low molecular weight (usually 200-500 Da) produced by the terpenoid biosynthesis pathway[9,10]. They are somewhat soluble in water but very soluble in polar organic solvents such ethyl acetate, chloroform, ethanol, methanol, and propylene glycol[1]. TCTs share a three-ring molecule called 12,13-epoxytrichothec-9-ene (EPT) [11,12]. The A-ring cyclohexene is fused to the B-ring tetrahydropyran, which is bridged by a two-carbon chain at C-2 and C-5, generating a cyclopentyl moiety (C-ring)[13]. TCT are classified into four kinds (A-D) based on the substitution pattern of EPT[14]. A hydroxyl (OH) group distinguishes type A TCT.

Define C-8 as having a group, an ester function, or no oxygen substitution[15]. Trichothecenes are quickly absorbed and suppress protein synthesis in growing tissues. Mycotoxins are natural chemicals generated by fungus that infect grains and other agricultural goods. Trichothecenes mycotoxin produced by the species Fusarium and Trichoderma is becoming increasingly important in agriculture globally because to the potential health implications. The most dangerous type A trichothecene mycotoxin is T-2 toxin, an unavoidable environmental hazard. T-2 toxin has a considerable detrimental effect on reproduction. Plant systems like onion, garlic and bean are widely used to determine the cytotoxic and genotoxic effects of various chemicals like food additives, and various pesticides, and different toxins[16,17,18]. Trichothecenes are important foodborne mycotoxins implicated in human health and have immune cytotoxic effects. Toxicity data on HT-2 toxin are very limited. To the best of the authors' knowledge, there is no published data that tests the cytogeneotoxic effects of this mycotoxin on A sativum root tip meristematic cells. Therefore, the aim of this study is to test the Cytogenotoxic effect of T-2 mycotoxin on mitotic index and T-2 toxin-induced mitotic aberrations in A. sativum dividing cells at the root apical meristem.

MATERIALS AND METHODS

Garlic heads (Allium sativum, 2n=16) were purchased from a local store in Zakho, free from fertilizers.

Source of the mycotoxin T2 toxin:

Mycotoxin used in the current study is the 8230 Veratox for T-2/HT-2 (NEOGEN company /USA), Cross Reactivity T-2 toxin 100%, HT-2 toxin B 100%. The product details is Veratox® for T-2/HT-2 is a competitive direct ELISA that provides a quantitative analysis of T-2 toxin and HT-2 toxin in commodities such as wheat, rye, barley, oats, and corn. The different concentrations were diluted by using distilled water.

The garlics were placed on tubes filled with distilled water for a few days until the roots were emerged and reached the length of about 1 cm then they were removed from those tubes and placed on another set of tubes with different concentrations of the mycotoxin T2 for about 12 hours. Then the roots were harvested and prepared microscopic slides for the root tip by squash method and stained with Feulgen Giemsa stain and visualized under light microscopy[19].

The mitotic index calculation:

The MI% calculation was done according to the following formula as published by Fiskesjö, (1985).

M.I.%= DC/TC *100 (1)

Where, M.I.= Mitotic Index, DC=Dividing Cells, TC=Total counted Cells.

Mitotic abnormalities percentage:

The mitotic abnormalities percentage was calculated by the following formula (Palsikowski et al., 2017)

MA%= ADC/TC*100 (2)

Where, MA=Mitotic Abnormalities, ADC=Abnormal dividing cells, TC=Total counted cells.

Statistical analysis:

Most of the statistics were done using SPSS (Statistical Package for the Social Sciences) software version 14, by One way ANOVA, and differences between all the treatments were determined by Duncan's multiple-range test [20]. The data were calculated as mean ± standard error. Each experiment was repeated at least three times. The significance was measured at P<0.05. The bar graphs were generated using GraphPad Prism version 9.0.

RESULTS

Trichothecenes are a class of structurally related mycotoxins that have different degrees of cytotoxicity. Because of the potential health risks, trichothecene (TCT) mycotoxin is becoming increasingly important in agriculture around the globe. It is primarily metabolized and eliminated after consumption, producing more than 20 metabolites, the most important of which is the hydroxy trichothecenes-2 toxin. (A12). The effect of T2 toxin on mitotic index% is shown in Table 1 and figure, 1.

Treatments (ppm)	Time (hours)	Total no. of cells	interphase	Dividing cells	Mitotic index%
0.00	12	1127.000 ± 23.643	1009.400 ±19.954 a, b	117.600 ± 4.345 a	10.4300 ± 0.222 a
0.30	12	990.000 ±45.655	915.928 ±42.771 b	74.072 ± 2.942 b	7.4867 ± 0.075 b
0.60	12	1102.000 ± 56.580	1049.593 ±53.323 a	52.407 ± 3.311 c	4.75 ± 0.078 c
0.90	12	1052.333 ±26.194	1013.816 ±25.189 a, b	38.518 ± 1.073 d	3.68 ± 0.036 d
1.20	12	996.667 ±3.844	978.223 ±4.019 a, b	18.444 ± 0.939 e	1.851 ± 0.095 e
Significance			n.s.	***	***

[1] Note: n.s. means non-significant, *** means significant at p<0.001. Different superscript letters were produced by DMRT.

Table 1: The effect of T2 toxin on the mitotic index% of *A. sativum* root tip cells.

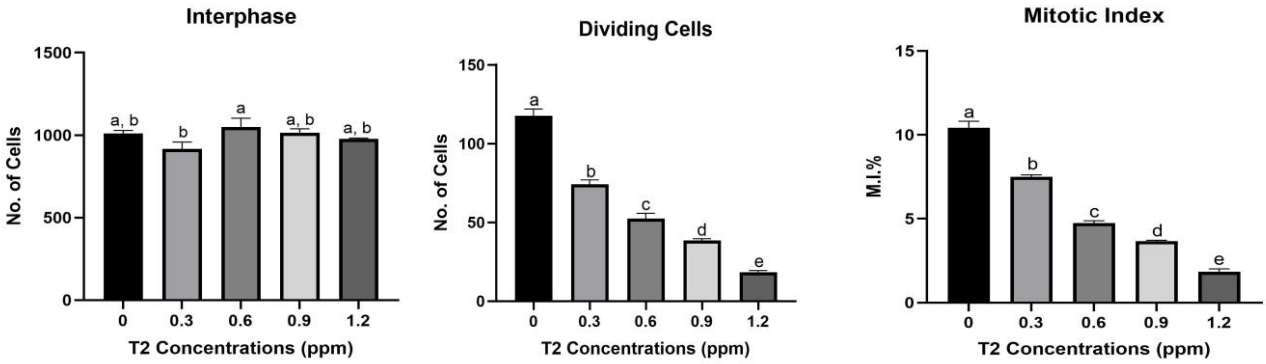

Figure 1: The effect of T2 toxin on no. of cells in interphase and dividing cells, and mitotic index% of *A. sativum* root tip cells.

The highest concentration, 1.5 ppm which caused it to decrease from 10.53 in the control to 0.7633 at 1.5 ppm. The mitodepressive effect was significant at P<0.001.

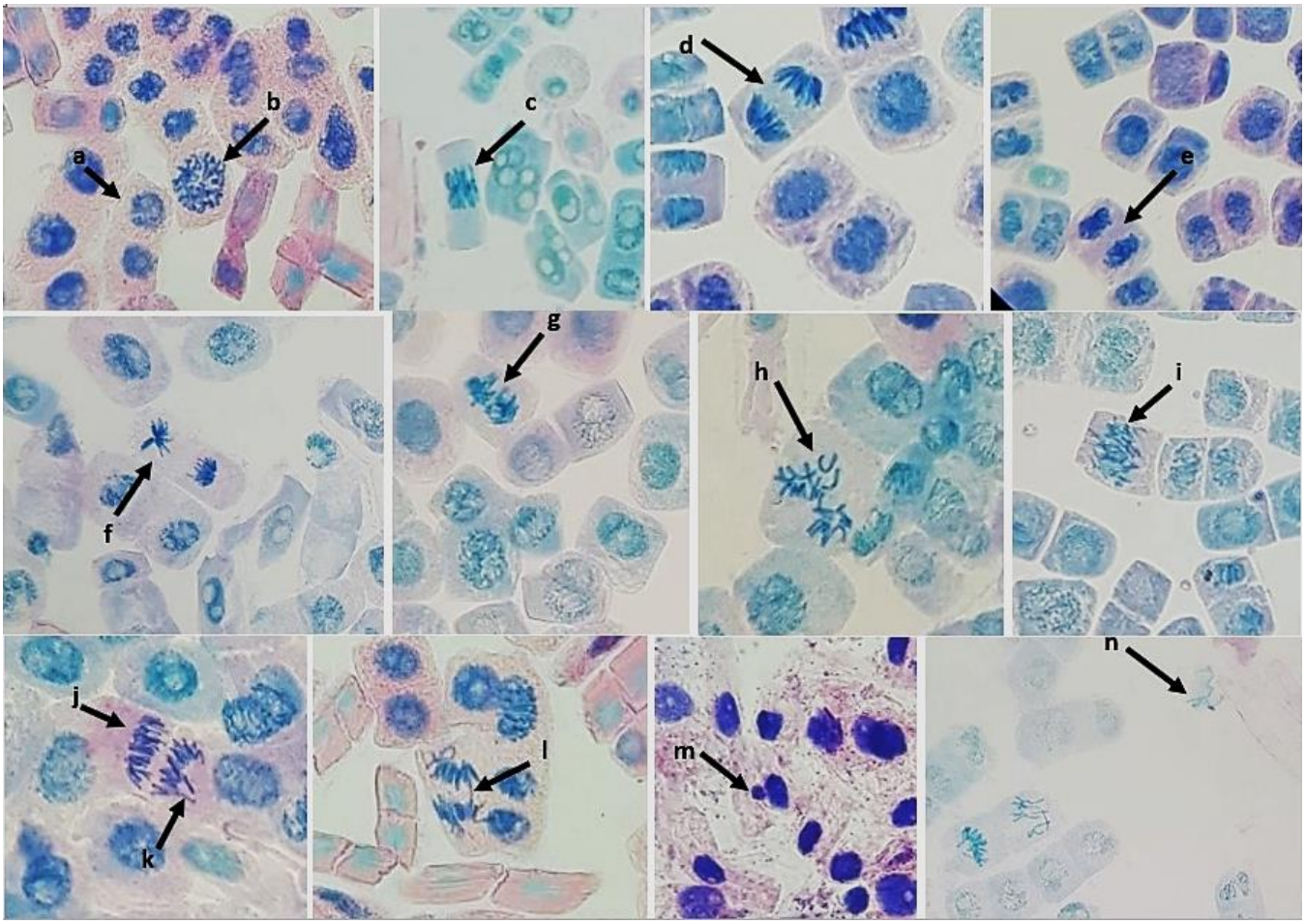

Figure 2: Normal mitosis and different abnormalities in A sativum root apical meristematic cells: a-normal interphase, b- normal prophase, c- normal metaphase, d- normal anaphase, e- normal telophase, f- Star-shaped anaphase, g- Sticky Metaphase, h- C-Mitosis, i- Sticky anaphase, j- Depolarization, k- Laggard Chromosomes, l- Anaphase Bridge, m- Micronucleus, n- Chromosome Loss.

The effect of the T2 toxin on chromosomal aberrations% is shown in table, 2 and figure, 3. According to the table, the aberrations increased proportionally with increasing mycotoxin concentration. Total mitotic abnormalities increased proportionally with increasing the concentration of the mycotoxin. The observed mitotic abnormalities were star-shaped anaphase, sticky metaphase, C-mitosis, sticky anaphase, depolarization, micronuclei, laggard chromosomes anaphase bridges, and chromosome loss. The least frequently observed abnormality was micronuclei at 0.00 in the control and increased to 0.1672 in the 1.2 ppm of T2. As compared to the most frequent aberration, laggard chromosomes were 0.0536% in the control and increased to 1.1341% in 1.2 ppm of the tested mycotoxin. The total CAI% were 0.1106 in the control group, which increased to about 5.2168% at the highest concentration of the mycotoxin. There were significant differences between treatments at $p<0.001$ for all mitotic aberrations.

T2 Concentration (ppm)	Star shaped anaphase%	Sticky metaphase%	C-Mitosis%	Sticky anaphase%	Depolarization%	Laggard Chromosomes%	Anaphase bridges%	Micronuclei%	Chromosome loss%	Total CA%

0.0	0.000 ± 0.000 d	0.0000 ± 0.000 d	0.0571 ± 0.022 c	0.0000 ± 0.000 e	0.000 ± 0.000 d	0.0536 ± 0.0192 5 e	0.000 ± 0.000 c	0.000 ± 0.000 c	0.000 ± 0.000 e	0.1106 ± 0.03676 d
0.3	0.0761 ± 0.011 c	0.1175 ± 0.008 c	0.5833 ± 0.039 b	0.1910 ± 0.027 d	0.245 ± 0.030 c	0.2406 ±0.035 18 d	0.004 ± 0.004 c	0.000 ± 0.000 c	0.108 ± 0.003 d	1.5644 ±0.0815 8 c
0.6	0.100 ± 0.005 c	0.4700 ± 0.041 a	1.0310 ± 0.058 a	0.3741 ± 0.012 c	0.287 ± 0.025 b, c	0.4142 ± 0.0029 0 c	0.079 ± 0.008 b	0.0000 ± 0.000 c	0.174 ± 0.0120 c	2.9284 ±0.1397 5 b
0.9	0.1869 ± 0.008 b	0.2466 ± 0.027 b	0.6432 ± 0.005 b	0.5285 ± 0.019 b	0.358 ± 0.016 b	0.6268 ± 0.0201 9 b	0.085 ± 0.0074 2 b	0.1112 ± 0.013 b	0.387 ± 0.004 b	3.1728 ±0.0207 7 b
1.2	0.2802 ± 0.010 a	0.4619 ± 0.031 a	0.9601 ± 0.033 a	0.8026 ± 0.015 a	0.532 ± 0.034 a	1.1341 ± 0.0397 2 a	0.197 ± 0.010 a	0.1672 ± 0.016 a	0.682 ± 0.039 a	5.2168 ±0.0526 3 a
F value	192.205	62.803	116.06 4	329.04 3	63.116	240.15 3	142.99 0	70.784	212.055	591.802
Significance	***	***	***	***	***	***	***	***	***	***

*** means significant at p<0.001. superscript letters are produced by DMRT

Table 2: the effect of T2 toxin on mitotic abnormalities% of A. sativum root tip meristematic cells after 12 hours.

The abnormalities caused by this mycotoxin in A. sativum root tip meristematic cells were: star-shaped anaphase, sticky metaphase, C-Mitosis, sticky anaphase, depolarization, micronuclei, and laggard Chromosomes. The most frequent abnormality was C-mitosis and sticky anaphase. According to Table, 2, the total abnormalities were increasing with increasing the toxin concen-tration. The highest number was observed with the 1.5 ppm treatment. The different abnormalities along with normal mitosis are shown in Figure, 2. The mycotoxin T2 induces the distortion and inhibition of mitotic spindle formation which causes the C-mitotic cells and stickiness in metaphase and anaphase. Moreover, the induction of chromosome loss and micronuclei.

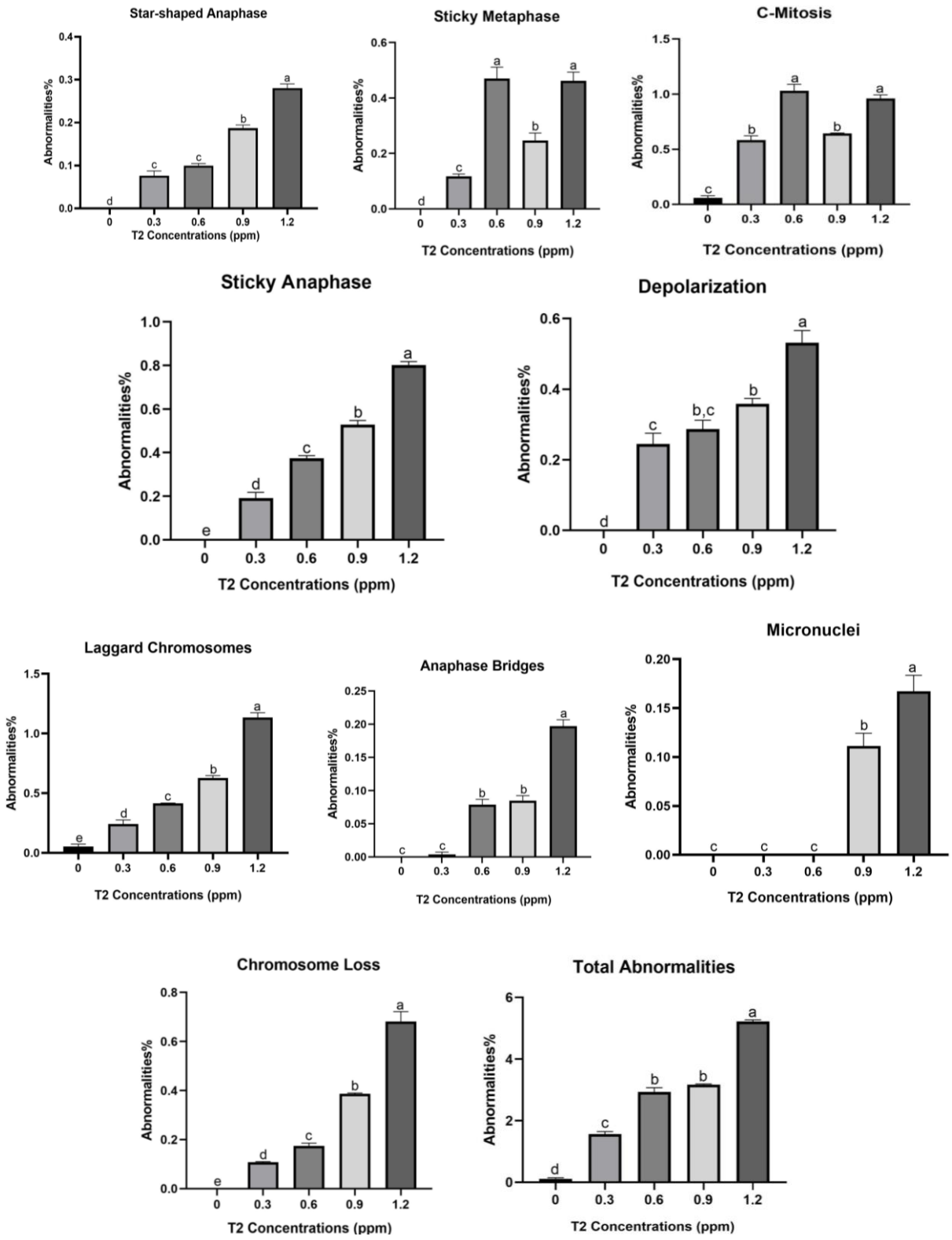

Figure 3: The effect of T2 toxin on mitotic abnormalities in A. sativum root tip meristematic cells.

About 1000 cells were counted for each slide and each experiment was repeated at least three times. According to table 1, the different concentrations of the mycotoxin caused a significant reduction in the mitotic index at all treatments along with reduction in the dividing cells number. However, the greatest effect on the mitotic index was observed at the highest concentration of the mycotoxin treatment (1.2 ppm) which caused the

mitotic index% to decrease from (10.4300 ± 0.222) in the control group to (1.851 ± 0.095) at 1.2 ppm treatment. The mitodepressive effect was significant at P<0.001. Moreover, there were significant differences among the treatments as detected by DMRT.
The effect of the T2 toxin on chromosomal aberrations% is shown in table, 2 and figure, 3. The abnormalities caused by this mycotoxin in A. sativum root tip meristematic cells were: star-shaped anaphase, sticky metaphase, C-Mitosis, sticky anaphase, depolarization, micronuclei, and laggard chromosomes. The most frequent abnormalities were C-mitosis and sticky anaphase. According to Table, 2, the total abnormalities were proportionally increasing with increasing toxin concentration. The highest number was observed with the 1.2 ppm treatment. The different abnormalities along with normal mitosis are shown in Figure, 2.
The total MA% was (0.1106 ± 0.03676) in the control group, which increased to about (5.2168 ±0.05263) at the highest concentration of the mycotoxin used. There were significant differences between treatments at p<0.001 for all mitotic aberrations. The ability to induce different abnormalities in the A. sativum cells at the root apical meristem indicates its mutagenic activity.

DISCUSSION

According to table, 1 the different concentrations of mycotoxin caused a significant reduction in the mitotic index at all treatments. However, the greatest reduction in the mitotic index was observed at. other research which tested tested the effect of Aflatoxin B1 induces reactive oxygen species-dependent caspase-mediated apoptosis in normal human cells, inhibits Allium cepa root cell division [21], and another research tested the toxic activity of citrinin, a fungal phytotoxin, and its mode of action in onion cells [22].
The abnormalities caused by this mycotoxin in A. sativum root tip meristematic cells were: star-shaped anaphase, sticky metaphase, C-Mitosis, sticky anaphase, depolarization, micronuclei, and laggard Chromosomes. The most frequent abnormality was C-mitosis and sticky anaphase. According to Table, 2, the total abnormalities were increasing with increasing the toxin concentration. The highest number was observed with the 1.5 ppm treatment. The different abnormalities along with normal mitosis are shown in Figure, 2. The mycotoxin T2 induces the distortion and inhibition of mitotic spindle formation which causes the C-mitotic cells and stickiness in metaphase and anaphase. Moreover, the induction of chromosome loss and micronuclei.
The ability to induce different abnormalities in the A. sativum cells at the root apical meristem indicates its mutagenic activity. The induction of both Micronuclei and stickiness are the most obvious indicators of cytotoxicity. According to Table 2, the increase in the frequency of micronuclei was dose-dependent. These results are in agreement with results obtained by [23]. The total abnormality percentage increase was also dose-dependent. This increase is in agreement with previous results of testing various substances on onion root tips [24,25].
These results are in agreement with other researches which tested the effect of Aflatoxin B1 on reactive oxygen species-dependent caspase-mediated apoptosis in normal human cells, and on inhibition of Allium cepa root cell division [26], and another research tested the toxic activity of citrinin, a fungal phytotoxin, and its mode of action in onion cells [27]. The mycotoxin T2 induces the distortion and inhibition of mitotic spindle formation which causes the C-mitotic cells and stickiness in metaphase and anaphase. Moreover, the induction of chromosome loss and micronuclei. The least frequently observed abnormality was micronuclei at (0.000 ± 0.000) in the control and increased to (0.1672 ± 0.016) in the 1.2 ppm of T2. On the other hand, the most frequent aberration observed was laggard chromosomes were (0.0536 ± 0.01925) in the control and increased to (1.1341 ± 0.03972) in 1.2 ppm of the tested mycotoxin. A laggard chromosome is defined as the chromosome that did not overlap along the long axis of the spindle with any of the properly segregating chromosomes [28].
The induction of both Micronuclei and stickiness are the most obvious indicators of cytotoxicity , Micronuclei are small membrane bounded compartments with a DNA content encapsulated by a nuclear envelope and spatially separated from the primary nucleus (Krupina et al., 2021). Chromosome stickiness may result from chromatin fibers' sticking to each other or breaking due to erroneous or inadequate condensation of these fibers, as a consequence of this, movement of mitotic spindle fibers together with inner-chromosome stickiness when the chromosome is drawn to the pole causes secondary anomalies (bridge and fragment occurrence) , Stickiness in chromosomes is an indication of the high toxicity of the chemical substance and usually this may kill the cells with the irreversible damages [25]

CONCLUSIONS

The mycotoxin T2 is a mutagen and it inhibits cell division and induce a wide range of abnormalities in A sativum root apical meristematic cells at lower doses and is very strong mutagen. Therefore, the food grains that contain this mycotoxin should be tested carefully to ensure that they are not contaminated with the T2 toxin producing fungi to avoid its hazardous health risks.

REFERENCES

1. Polak-Śliwińska, M.; Paszczyk, B. 2021. Trichothecenes in Food and Feed, Relevance to Human and Animal Health and Methods of Detection: A Systematic Review. Molecules. 26, 454.
2. Bryden, W. L. 2007. Mycotoxins in the food chain: Human health implications. Asia Pacific journal of clinical nutrition. 16:95–101.
3. Bennett, J. W., and Klich, M. 2003. Mycotoxins. Clinical Microbiology Reviews. 16:497–516.
4. Chen, P.; Xiang, B.; Shi, H.; Yu, P.; Song, Y.; Li, S. Recent advances on type A trichothecenes in food and feed: Analysis, prevalence, toxicity, and decontamination techniques. Food Control. 2020, 118, 107371.
5. Milićević, D.R.; Škrinjar, M.; Baltić, T. 2010. Real and Perceived Risks for Mycotoxin Contamination in Foods and Feeds: Challenges for Food Safety Control. Toxins. 2, 572.
6. McCormick, S.P.; Stanley, A.M.; Stover, N.A.; Alexander, N.J. 2011. Trichothecenes: From simple to complex mycotoxins. Toxins. 3, 802–814.
7. Foroud, N.A.; Baines, D.; Gagkaeva, T.Y.; Thakor, N.; Badea, A.; Steiner, B.; Bürstmayr, M.; Bürstmayr, H. 2019. Trichothecenes in Cereal Grains—An Update. Toxins. 11, 634.
8. S K Kudury, I A Abed and B A Mahdi . The Effect of Local Bio Fertilizer and Their Enzymatic Activity on Growth of Maize Plant and some Biological Therites in the Soil. IOP Conf Ser Earth Environ Sci 2023, 1252 (1), 012050. https://doi.org/10.1088/1755-1315/1252/1/012050.
9. Arunachalam, C., and Doohan, F.M. 2013. Trichothecene toxicity in eukaryotes: Cellular and molecular mechanisms in plants and animals. Toxicology Letters. 217, 149–158.
10. Bottalico, A., & Perrone, G. (2002). Toxigenic Fusarium species and mycotoxins associated with head blight in small-grain cereals in Europe. Mycotoxins in Plant Disease: Under the aegis of COST Action 835 'Agriculturally Important Toxigenic Fungi 1998-2003', EU project (QLK 1-CT-1998-01380), and ISPP 'Fusarium Committee', 611-624.
11. Çavuşoğlu, D. 2022. Powerful toxic activity of citrinin, a fungal phytotoxin, and its mode of action in onion cells. Environmental Science and Pollution Research, 29(4): 6205-6218.
12. A A Al-Azzami , Th T Mohammed . Effect of Adding Dry Leaves of Lemongrass (Cymbopogon Citratus) To the Diet on Some Biochemical Tests of Blood in Broiler (Ross 308). IOP Conf Ser Earth Environ Sci 2023, 1252 (1), 12125. https://doi.org/10.1088/1755-1315/1252/1/012125.
13. Das, T., S. Hazra, S. Sengupta, P. Hazra, and D. Chattopadhyay. 2021. Genotoxic effect of saccharin on Allium cepa root tips. Biologia. 76: 3191-3199.
14. R S Obaid, S H S Al-Warshan and I A Abed . Efficiency of Some Clays and Organic Materials on the Reduction of Aflatoxin B1 Produced from Isolates of the Fungus Aspergillus flavus Contaminating Corn Grains. IOP Conf Ser Earth Environ Sci 2023, 1252 (1), 012003. https://doi.org/10.1088/1755-1315/1252/1/012003.
15. Duncan, D. B. 1955. Multiple range and multiple F tests. Biometrics. 11: 1-42.
16. EFSA (European Food Safety Authority) Scientific Opinion on the risks for animal and public health related to the presence of T-2 and HT-2 toxin in food and feed. EFSA Journal. 2011:2481–2668. doi: 10.2903/j.efsa.2011.2481.
17. A A Al-Azzami , Th T Mohammed . The Effect of Adding Lemongrass Leaf Powder (Cymbopogon Citratus) to the Diet as a Natural Supplement on Some Productive Traits and Oxidation Indicators in Broiler (Ross 308). IOP Conf Ser Earth Environ Sci 2023, 1252 (1), 12123. https://doi.org/10.1088/1755-1315/1252/1/012123.

18. Foroud, N.A.; Shank, R.A.; Kiss, D.; Eudes, F.; Hazendonk, P. 2016. Solvent and Water Mediated Structural Variations in Deoxynivalenol and Their Potential Implications on the Disruption of Ribosomal Function. Frontiers in Microbiology. 7, 1239.
19. Garvey, G.S.; McCormick, S.P.; Rayment, I. Structural and Functional Characterization of the TRI101 Trichothecene 3-O-Acetyltransferase from Fusarium sporotrichioides and Fusarium graminearum: Kinetic insights to combating fusarium head blight. Journal of Biological Chemistry, 283(3), 1660-1669.
20. Hussein, N. J. 2023. "Evaluation of Cytogenotoxic Effect of Potassium Acetate on Allium Cepa L. Root Tips". Emirates Journal of Food and Agriculture. 35(8):708-714. doi:10.9755/ejfa.2023.3129.
21. Ameen M. Shaman , Th. T. Mohammed. Effect Using Feed Additives Instead of Imported Premixes Affects the Physiology of Broiler Chickens. IOP Conf Ser Earth Environ Sci 2023, 1262 (7), 72080. https://doi.org/10.1088/1755-1315/1262/7/072080.
22. Jebur, S. F.; Abdulateef, S. M. Effect of The Critical Period and Gene Silencing on Blood Cellular Traits in Local Chicken and Level of Welfare. IOP Conf Ser Earth Environ Sci 2023, 1252 (1), 12141. https://doi.org/10.1088/1755-1315/1252/1/012141 .
23. Nielsen, C.; Casteel, M.; Didier, A.; Dietrich, R.; Märtlbauer, E. 2009. Trichothecene-induced cytotoxicity on human cell lines. Mycotoxin Research. 25, 77–84.
24. Palsikowski, P. A., Roberto, M. M., Sommaggio, L. R., Souza, P. M., Morales, A. R., & Marin-Morales, M. A. (2018). Ecotoxicity evaluation of the biodegradable polymers PLA, PBAT and its blends using Allium cepa as test organism. Journal of Polymers and the Environment. 26: 938-945.
25. Pestka, J. J. 2007. Deoxynivalenol: Toxicity, mechanisms and animal health risks. Animal Feed Science and technology. 137: 283–298.
26. Elkhateeb, S. Z.; Ebraheem, M. O.; Abdulateef, S. M.; Ahmed, I. A. Constraints Affecting the Welfare of Domestic Sheep Grazing in the Natural Pasture. IOP Conf Ser Earth Environ Sci 2023, 1252 (1), 12144. https://doi.org/10.1088/1755-1315/1252/1/012144.
27. Saadullah, A. A. M. (2022). Studies on teratogenic and maternal effects of Trichothecene (TCT) extracted from Fusarium and Trichoderma culture on pregnant Albino Mice. Revis Bionatura. 2023; 8 (2) 58.
28. Sharma, A. and A. Sharma. 1999. Chromosome Techniques. 3rd ed. Buterworths, London.

Received: October 9th 2023/ **Accepte**d: January 15th 2024 / **Published:**15 February 2024

Citation: Hussein N. J. and Saadullah A. A. M. Cytogenotoxic effect of trichothecene T2 toxin on Allium sativum root tip meristematic cells. Revis Bionatura 2024; 9 (1) 45. http://dx.doi.org/10.21931/RB/2024.09.01.45

Additional information Correspondence should be addressed to *asia.saadullah@uod.ac*

Peer review information. Bionatura thanks anonymous reviewer(s) for their contribution to the peer review of this work using https://reviewerlocator.webofscience.com/

Bionatura ISSN. First 13909355 Ecuador. **Scopus coverage years**: from 2016 to the present

Bionatura
Ibero-American Journal of Biotechnology and Life Sciences

Article

The effect of locally extracted and imported aloe vera oil on some productive traits of broilers

Nuha Talib Shareef Al Salman[1], and Jassim Kassim Menati Al-Gharawi[2]*

[1]Animal Production Department, Agriculture College, Al-Muthanna University, Iraq.
[2]Animal Production Department, Agriculture College, Al-Muthanna University, Iraq.
** Correspondence: nuha.alsalman88@gmail.com*
Available from. http://dx.doi.org/10.21931/RB/2024.09.01.46

ABSTRACT

The study was conducted at a poultry field, Agricultural Research and Experiment Station at the College of Agriculture, Al-Muthanna University, to determine the effect of locally extracted and imported aloe vera oil on some productive traits of broilers, different levels of oil extracted from the leaves of the aloe vera plant were used, from 22/2/2022 to 29/3/2022. A total of 405 unsexed, one-day-old chicks of Ross 308 broiler were used; chicks were randomly distributed to nine treatments with three replicates for each, 45 chicks per treatment (15 chicks for each replicate), the treatments were followed; T1: without any addition, as for the treatments T2, T3, T4 and T5, they were local aloe vera oil and the treatments T7, T6, T8 and T9, they were imported aloe vera oil, the addition of oil was at the levels 0.3 and 0.4 per kg feed. The results of the experiment indicated a significant improvement in some productive traits, including Body Weight (BW), Weight Gain (WG), Feed Intake (FI) and Feed Conversion (FC), with a significant decrease in mortality for all treatments of locally extracted and imported oil compared to the control treatment, the treatments of the oil extracted locally showed the best results in a significant way compared to the rest of the treatments of the imported oil of the aloe vera plant.

Keywords: Locally extracted, imported, aloe vera oil, productive traits, broilers.

INTRODUCTION

Aloe vera (Aloe barbadensis Miller) is a perennial plant belonging to the family Aloaceae, distinguished by its green leaves [1]. Aloe vera is a drought-tolerant herbaceous succulent plant and a perennial tropical plant with green leaves that ripens after 7-8 months of planting. It has a large base. Leaves are approximately 25-30 cm long and 10 cm wide. The number of sheets varies between 12 and 16 leaves. Thorns surround the sides of the leaves, and at the base of the leaves are short stems; the plant is a little branched, and the lifespan of the total plant is approximately 12 years [2].

Aloe vera is an ancient medicinal plant used in many fields and contains many active compounds, more than 200; numerous studies have shown that the aloe vera plant contains compounds that significantly impact humans and animals through its physiological impact [3]. Aloe vera leaves contain many antioxidants, including phenols, vitamin C, tannins, flavonoids, and soaps; Aloe vera leaves also contain antioxidant enzymes. [4]. It contains olein at a concentration of 1499.1 µg/ g. The gel and peels of Aloe vera leaves contain chemical ingredients (Tanine, saponins, flavonoids, carbohydrates, anthraquinones, phenolics, triterpenes, sterols, and alkaloids), and different concentrations of phenolic compounds; the aloe vera plant improves the immune response and increases cellular and humoral immunity (Sinha et al., 2017).

Adding aqueous extract of aloe vera leaves at a level of (50, 100) mg/liter of drinking water for 30 days for broilers increases the immune response to viruses. Bacteria in the intestines play an important role in poultry, leading to the utilization of food and thus improving growth and immunity [5,6].

MATERIALS AND METHODS

The study was conducted at the poultry field, Agricultural Research and Experiment Station, Agriculture College, Al-Muthanna University, to determine the effect of aloe vera oil extracted locally and imported on some productive traits of broilers, different levels of oil extracted from the leaves of the aloe vera plant, from 22/2/2022 to 29/3/2022.

405 unsexed, one-day-old chicks of Ross 308 broilers were used. Chicks were randomly distributed to nine treatments with three replicates for each, 45 chicks per treatment (15 chicks for each replicate). The treatments were followed: T1: without any addition, as for the treatments T2, T3, T4 and T5, they were local aloe vera oil and the treatments T7, T6, T8 and T9, they were imported aloe vera oil, the addition of oil was at the levels 0.3 and 0.4 per kg feed. The birds were reared on four-story batteries; each floor containing a cage with dimensions of 1×1.5 m. The Aloe vera leaves were brought from the Aloe vera farm in Anbar Governorate, and the oil was extracted locally in two ways:

Extraction by water bath

Cut the leaves of the plant into tiny pieces, then put it in a glass container with a quantity of corn oil, close it tightly, place it in a water bath, and leave it on the fire for an hour. Then we notice the oil separation from the water, leave it for a few minutes to cool, place it in the cooling to facilitate the separation of oil from water, then separate it and place it in cans and keep it in a cool and dry place. [7]

Extraction by saturation method with fats or oils

Aloe vera leaves are placed in the electric mixer to get an amount of aloe vera juice. After getting an amount of aloe vera juice, put an equal amount of corn oil on the fire. Leave it on the fire for about 45 minutes, where all the water is evaporated, and only the olive oil remains with the remains of the plant, then the oil is filtered to obtain pure oil, left to cool, and then packed in special containers, store in a cool, dry place. [7].

Productive traits

Body Weight (BW), Weight Gain (WG), Feed Intake (FI) and Feed Conversion (FC).

Statistical analysis

A Complete Randomized Design (CRD) was used to study the effect of different treatments on the studied traits; significant differences between means were compared with [8] multiple-range tests under significance levels of 0.05 and 0.01. The program [9] was used in the statistical analysis.

RESULTS

Table (1) shows the effect of using the oil extract of aloe vera leaves on average body weight, weight gain, feed intake and feed conversion at 21 days of broilers. Significant differences were among all the experimental treatments at 21 days of the chick's age. In contrast, treatment T3 (0.4 ml oil extract of aloe vera leaves / kg of feed) was significantly superior ($P \leq 0.05$) compared to the other treatments concerning body weight, weight gain, feed intake and feed conversion, continued superiority of treatment T3 significantly ($P \leq 0.05$) compare with T2, T4, T5 and T6 treatments, there were no significant differences between the treatments T2, T4 and T5, and these treatments, outperformed compare with T7, T8, T9 and T1, as for the weight gain, T3 (0.4ml oily extract of aloe vera leaves/kg feed) significantly increase ($P \leq 0.05$) compare with other the treatments (T2, T4, T5, T6, T7 and T8) which outperformed treatment T1. As for the feed intake, a significant improvement ($P \leq 0.05$) was observed for all the treatments of the local oil extract (T2, T3, T4, and T5) compared with T6, T7, T8, and T9, which in turn outperformed compare with T1. As for the feed conversion, a significant

superiority (P≤0.05) continued for T3 compared with other the treatments, where treatment T3 outperformed treatment T4 and T5, which in turn outperformed T2, T6, T8, T9, T7 and T1

Table 2 shows a significant increase in the relative weight of the main cuts (breast, thigh and drumstick) with a significant decrease in the relative weight of the secondary cuts (neck, wings and back) for all treatments of locally extracted aloe vera oil compared to the imported Aloe vera oil treatments and the control treatment. Tables 3, 4 and 5 show that the relative weight of meat in the main cuts (chest, thigh and atta drum) significantly increased in treatments (T2, T3, T4 and T5) compared to treatments T6, T7, T8 and T9, which in turn were significantly superior compared to the control treatment for meat In all the studied significant cuts, as for the bone and skin of all the studied major cuts, there was a significant decrease in treatments (T2, T3, T4 and T5) compared to treatments (T6, T7, T8 and T9), which decreased significantly compared to the control treatment.

Table 3 shows the effect of using the oil extract of the leaves of the aloe vera plant on the dressing percentage, where the significant superiority (P≤0.05) of the treatment T3 (0.4 ml aloe vera leaves oil extract / kg of feed) compared to the treatment T2, T4 and T5, which significantly outperformed compared to the treatments T6 and T7, which significantly outperformed compared to treatments T8 and T9, which excelled compared to the control treatment, where we note the continued superiority of treatment T3 significantly (P≤0.05) compare with the other treatments with respect to the percentage of purification without giblet, as there were no significant differences among the treatments with respect to the relative weight of the heart, as for the relative weight of the liver, we note the continued superiority of T3 significantly compare with the treatments T2 and T4, which was significantly superior (P≤0.05) compared to treatments T6 and T7, which was significantly superior compared to treatments T8 and T9, they outperformed the control treatment. The continued superiority of the T3 treatment was significant concerning the relative weight of the gizzard and the dressing percentage with the giblet compared with the other treatments.

Treatments	Body weight (g)	Weight Gain (g)	Feed Intake (g)	Feed Conversion (g diet/ g weight gain)
T_1	4.40±668.33c	5.13± 302.00e	9.75±498.33c	.01±1.65f0
T_2	3.75±684.55ab	3.57±311.69abc	2.87±443.56a	.01±1.42ab0
T_3	0.84± 690.00a	.62±317.26a0	2.35±440.98a	0.01±1.39a
T_4	1.36±683.55ab	0.77±311.04abc	2.21±448.94a	0.00±1.44b
T5	ab0.61±685.11	.75±314.84ab0	4.98±449.18a	0.01±1.42b
T6	±679.06b1.74	.71±309.48bcd0	2.30±470.40b	0.01±1.52cd
T7	±680.89b1.05	.58±312.22ab0	.80±467.29b0	0.003±1.49c
T8	c0.58±669.89	1.25±302.55cd	1.20±471.96b	0.01±1.56e
T9	±672.11c1.34	2.39±304.37cde	6.12±468.70b	0.02±1.54de
Sig.	*	*	*	*

Table 1: Effect of locally extracted and imported aloe vera oil on some productive traits of broiler broilers at the age of 21 days (mean ± standard error).

Treatments	Body weight (g)	Weight Gain (g)	Feed Intake (g)	Feed Conversion (g diet/ g weight gain)
T_1	17.32± 1650.00d	18.90±568.66d	32.11±1072.64a	.006±1.88g0
T_2	2.08±1851.00a	4.09±728.66ab	7.54±1204.73b	0.003±1.65b
T_3	2.60± 1865.66a	2.72±731.33a	7.54±1196.96b	0.006±1.63a
T_4	3.21± 1849.00a	2.84±728.66ab	8.13±1236.32b	0.006±1.69c
T5	±1850.33a2.96	.88±728.33ab0	3.86±1226.03b	0.003±1.68c
T6	±1818.33b2.72	4.58±702.00c	12.67±1237.92b	0.006±1.76d
T7	±1824.66b3.28	2.02±706.66bc	4.41±1239.02b	0.003±1.75d
T8	±1776.66c3.28	5.68±688.00c	8.05±1284.21c	0.006±1.86f
T9	±1780.00c6.35	6.08±694.00c	9.18±1281.55c	0.003±1.84e
Sig.	*	*	*	*

Table 2: Effect of locally extracted and imported aloe vera oil on some productive traits of broilers aged 35 days (mean ± standard error).

Treatments	Weight Gain (g)	Feed Intake (g)	Feed Conversion (g diet/ g weight gain)
T_1	17.32±1610.00d	28.13±2761.04a	.003±1.71g0
T_2	2.08±1811.00a	2.22±2813.76b	0.003±1.55b
T_3	2.60±1825.66a	9.37±2794.73ab	0.005±1.53a
T_4	3.21±1809.00a	8.82±2860.36c	0.005±1.58c
T5	2.96±1810.33a	11.85±2836.12bc	0.003±1.56b
T6	2.72±1778.33b	15.05±2898.28def	0.005±1.63d
T7	3.28±1784.66b	9.63±2889.61de	0.006±1.61d
T8	3.28±1736.66c	8.69±2938.54f	0.003±1.69f
T9	6.35±1740.00c	9.89±2914.72ef	0.003±1.61e
Sig.	*	*	*

Table 3: Effect of locally extracted and imported Aloe vera oil on some of the total productive characteristics of broilers (mean ± standard error).

DISCUSSION

Regarding body weight gain, this increase is due to the aloe vera plant containing the active compounds found in aloe vera gel to reduce the growth of pathogenic bacteria [10]. The aloe vera plant also contains the active compound saponins, which has an influential role in increasing the permeability of the intestinal cell wall, thus increasing the absorption of nutrients [11]. Also, aloe vera gel increases the growth of beneficial bacteria (Lactobacillus), which produces lactic acid, organic and fatty acids, and hydrogen peroxide, increasing beneficial bacteria's growth [12]. The aloe vera plant contains many antioxidant vitamins (A, C and E) [13]. The significant improvement that occurred in the weight of the carcass and the weight of the main cuts due to the presence of a large number of active compounds in the leaves of the aloe vera plant, which has a significant role in improving feed consumption and absorption, then increase growth and build tissues and muscles, as the active compound saponins have a significant role in increasing the utilization of nutrients by increasing the permeability of cell wall amino acids (Kim, 14) and fatty acids [15], which play an essential role in increasing feed consumption, then weight gain, and thus improving the characteristics of the carcass. Also, the aloe vera plant increases the growth of beneficial bacteria (Lactobacillus), which produces lactic acid and many other compounds, proving harmful bacteria's growth and thus improving growth and weight gain [16].

CONCLUSIONS

The results of the experiment indicated a significant improvement in carcass traits for broilers (carcass weight, dressing percentage without giblet, the relative weight of liver, heart and gizzard, the dressing percentage with giblet, the main cut and secondary cuts) and deboning percentage. The oil extracted locally showed the best results significantly compared to the rest of the treatments of the imported oil of the aloe vera plant. The current concluded is to determine the effect of locally extracted and imported aloe vera oil on some productive characteristics of broilers.

REFERENCES

1. Srujana, P., Kishore, V. S., Srikanth, K., and Shanmukha, P. Y. *Aloe vera*-A Review. *Research journal of pharmacognosy and phytochemistry*,**2012**. *4(2)*, 119-123.
2. Ahlawat, K.S., and Khatkar, B.S. Processing, food applications and safety *of Aloe vera* products: A review. *Journal of Food Science and Technology*, **2011**, *48(5)*, 525-533.
3. Sánchez, I., R. Machado, Z.Ledesma and M. Martínez. Inversiones eficientes: papel del proceso inversionista en las condiciones de Cuba. *Economía y Desarrollo*,**2017**. *158(1)*, 127-139.
4. Ahmed, M., and F. Hussain. "Chemical Composition and Biochemical Activity of Aloe Vera (*Aloe Barbadensis* Miller) Leaves." *International Journal of Chemical and Biochemical Science.* **2013**. *3*: 29-33.
5. Ojiezeh, T. I., and N. Eghafona. "Humoral Responses of Broiler Chickens Challenged with NDV following Supplemental Treatment with Extracts of Aloe Vera, Alma Millsoni, Ganoderma Lucidum and Archachatina Marginata." *Central European Journal of Immunology*, **2015**; *3 (3)*: 300–306.
6. Ameen M. Shaman, Th. T. Mohammed. Effect Using Feed Additives Instead of Imported Premixes Affects the Physiology of Broiler Chickens. IOP Conf Ser Earth Environ Sci 2023, 1262 (7), 72080. https://doi.org/10.1088/1755-1315/1262/7/072080.
7. An A Al-Azzami, Th T Mohammed . The Effect of Adding Lemongrass Leaf Powder (Cymbopogon Citratus) to the Diet as a Natural Supplement on Some Productive Traits and Oxidation Indicators in Broiler (Ross 308). IOP Conf Ser Earth Environ Sci 2023, 1252 (1), 12123. https://doi.org/10.1088/1755-1315/1252/1/012123.
8. Al Salman, N.T.Sh. and J.K.M. Al-Gharawi. Effect of Eucalyptus leaves water extract on some productive traits of broilers. *Plant Archives.* **2019**,*Vol. 19,* Supplement 1, 2019 pp. 920-923.
9. Swami, S., H. Suman, P. Singh, K. Gennaro, L. Dev and D. Rakesh. Extraction Technologies for Medicinal and Aromatic Plants. United Nations Industrial Development Organization and the International Centre for Science and High Technology. **2008**.
10. Duncan, D.B. Multiple ranges test and Multiple F – test. Biometrics. 11: 1-42. **1955**.
11. SPSS. SPSS users guide. Statistics version 20. Statistical Package Solution Service. **2012**.
12. Irshad S., Butt M., Younus H. In-vitro antibacterial activity of *Aloe barbadensis* Miller (*Aloe vera*) *International Research Journal of Pharmaceuticals,* **2011**. *1*:60–65.
13. A A Al-Azzami , Th T Mohammed . Effect of Adding Dry Leaves of Lemongrass (Cymbopogon Citratus) To the Diet on Some Biochemical Tests of Blood in Broiler (Ross 308). IOP Conf Ser Earth Environ Sci 2023, 1252 (1), 12125. https://doi.org/10.1088/1755-1315/1252/1/012125.
14. Jebur, S. F.; Abdulateef, S. M. Effect of The Critical Period and Gene Silencing on Blood Cellular Traits in Local Chicken and Level of Welfare. IOP Conf Ser Earth Environ Sci 2023, 1252 (1), 12141. https://doi.org/10.1088/1755-1315/1252/1/012141.
15. Spoorthy N., S. Babu and A. Noor. Bioactive constituents of the genus Aloe and their potential therapeutic and pharmacological applications: A review. *Journal of Applied Pharmaceutical Science,* **2020**. *Vol. 10(11),* pp 133-145.
16. Wijesundara, W. M. A. S. and Adikari, A. M. J. B. 'Development of aloe vera (*Aloe barbadensis* Miller) incorporated drinking yoghurt. .**2017**.*7(11),* pp. 334– 342.

Received: October 9th 2023/ **Accepte**d: January 15th 2024 / **Published:**15 February 2024

Citation: Al Salman, N.T.S.; Al-Gharawi, J.K.M. The effect of locally extracted and im-ported aloe vera oil on some productive traits of broilers. Revis Bionatura 2024; 9 (1) 46. http://dx.doi.org/10.21931/RB/2024.09.01.46

Additional information Correspondence should be addressed to *nuha.alsalman88@gmail.com*

Peer review information. Bionatura thanks anonymous reviewer(s) for their contribution to the peer review of this work using https://reviewerlocator.webofscience.com/

All articles published by Bionatura Journal are made freely and permanently accessible online immediately upon publication, without subscription charges or registration barriers.

Bionatura ISSN. First 13909355 Ecuador. **Scopus coverage years**: from 2016 to the present

Publisher's Note: Bionatura stays neutral concerning jurisdictional claims in published maps and institutional affiliations.

Bionatura
Ibero-American Journal of Biotechnology and Life Sciences

Article

Effect of *Solanum aculeastrum* on hematological parameters of Al-bino mice infected with *Aspergillus fumigatus*

*Sara Ghalib Allwi Al-Saffy[1] and Dalia Abdalkareem Abdulshaheed[2]**

[1]Department of Microbiology, College of Veterinary Medicine, University of Baghdad, Baghdad, Iraq; saragh199577@gmail.com. https://orcid.org/0000-0002-6658-1237
[2]Department of Microbiology, College of Veterinary Medicine, University of Baghdad, Baghdad, Iraq; dalia@covm. uobaghdad. Edu. Iq. https://orcid.org/0000-0003-1369-8826
** Correspondence: dalia@covm. uobaghdad. Edu. I.Q.*
Available from. http://dx.doi.org/10.21931/RB/2024.09.01.48

ABSTRACT

The goal of the current study was to research the changes in hematological parameters: WBC count, RBCs count, Hb, PCV, neutrophil, lymphocyte, and monocyte in albino mice infected with *Aspergillus fumigatus* by intraperitoneal injection after induced immunosuppression by intraperitoneal injection of cortisone. The current research also examined an attempt to reduce the infection load by treating with *Solanum aculeastrum*. The result shows higher decreased significance (P≤0. 05) in RBCs, Hb, and PCV after being infected with *A. fumigatus* 7. 1 ± 0. 8, 11. 3 ± 0. 5 and 41. 5 ± 2. 4, respectively, while the total WBC count, neutrophil, lymphocyte, and monocytes were increased significantly (P≤0. 05) after treatment with *S. aculeastrum* in groups infected with *A. fumigatus*, compared to other groups. According to these results, we conclude that the alcoholic extract of *S. Astrum* has significant therapeutic and antifungal characteristics that lead to an increase in the total WBC count and, therefore, is considered a necessary alternative therapy for increasing immunity.

Keywords: Cortisone, Hematology, Fungi, Iraq.

INTRODUCTION

Fungi are a major, diverse, ubiquitous group of heterotrophic organisms that live as saprophytes or parasites or are related to many other organisms as symbiotes [1]. According to estimates of global richness, it constitutes the second largest group of organisms, with about 3 million species expected. Also, it ranks third among the eukaryotic kingdoms regarding the wealth of known species [2, 3]. The most prevalent pathogenic species in the animal kingdom is *Aspergillus fumigatus*, a saprotrophic fungus that lives vegetatively on decaying organic matter in the soil and spreads by asexual sporulation [4, 5]. This fungus can survive high temperatures above (50°C) and may happen in piles of decomposing plant matter. The fungus releases a significant amount of asexual airborne spores [6]. These fungi have a broad clinical spectrum, ranging from allergy to chronic infections and acute invasive aspergillosis (I.A.) in humans and animals [7]. Aspergilli are known for their capacity to secrete different types of biologically active chemical compounds, including antibiotics, mycotoxins, immune-suppressant substances, and cholesterol-lowering factors [8]. According to the host's underlying immunological state, these fungi can cause overlapping chronic, noninvasive types of infection that range from the formation of a fungal ball (Aspergilloma) to a long-lasting inflammatory and fibrotic process that is presently categorized as chronic lung infection similar to invasive pulmonary aspergillosis (IPA) [4, 9].

Solanum aculeastrum, "goat bitter-apple" Hnzal (Arabic), is extensively dispersed in a native of Africa and South Africa. *S. aculeastrum* is a spiny perennial that grew to 3 m tall with white blooms and bears berries resembling lemons and turning yellow-green when ripe. For both people and domestic animals, the tart fruits of this plant are utilized medicinally in various techniques for the treatment of cancer, indigestion, and stomach disruption; the boiling extract of the fruits and leaves is administered orally route. Both fresh and cooked fruit are used as a therapy for acne, gonorrhea, and jigger wounds [10], according to the presence of bioavailable

phyto-constituents including steroidal saponins, steroidal alkaloids, terpenes, flavonoids, lignans, sterols, phenolic compounds, and coumarins. *Solanum* spp. is essential in the nutraceutical and pharmaceutical industries. Both steroidal alkaloids and glycoalkaloids serve as important chemical indicators of this genus. Both ancient and modern systems of medicine place special importance on steroid alkaloids and glycoalkaloids since they exhibit a variety of bioactivities, including antibacterial, analgesic, immunomodulatory, hepatoprotective, neurogenetic, anticancer, etc. [11]. Considering the above facts and minimal studies, this study was designed to study the effects of *S. aculeastrum* on hematological parameters in albino mice infected with *A. fumigatus*.

MATERIALS AND METHODS

Fungal isolation

The fungus was isolated from different veterinary clinics and stray cats in Baghdad province, identified on Sabouraud Dextrose Agar and malt extract agar, and diagnosed by traditional morphological examination laboratory methods.

Preparation of A. fumigatus fungal suspension

The suspension of A. fumigatus was prepared according to a previously carried out study [12].

Solanum aculeastrum fruit extraction

Solanum aculeastrum (Hanzal) was purchased from local Baghdad markets, and the extraction was performed previously [13].

Induction of immunosuppression

Immunosuppression was induced by treatment of the mice with cortisone intraperitoneal administration at a single dose one day before conidial administration. Each mouse receives 2mg of Dexamethasone per mouse (14).

Animal and design experiments

Fifty-six albino mice were used in the study at 10-12 weeks and weighing 25. 3 ± 0. 9 g, maintained on a standard laboratory diet, water and temperature-controlled at the animal house laboratory at the College of Veterinary Medicine (University of Baghdad, Baghdad, Iraq), were randomly assigned to different groups: 8 mice per group as following:

- G1: Negative control mice (untreated).
- G2: Infected mice with a single dose *of A. fumigatus* at 2×10^7 cells/ml per mouse intraperitoneally (I/P).
- G3: Treated mice with cortisone at 2 mg/mice I/P.
- G4: Treated mice orally with a single dose of *S. aculeastrum* at 10 mg/kg B. W.
- G5: In which mice were treated with a single dose of cortisone at 2mg/mice I/P for one day prior to fungal spore infection and then infected with a single dose of *A. fumigates* 2×10^7 cells/ml per mouse I/P.
- G6: In which mice were treated with a single dose of *S. aculestrum* at 10 mg/kg B. W orally, one week after infection with a single dose *of A. fumigates* 2×10^7 cells/ml per mouse I/P.
- G7: Mice were treated orally with a single dose of *S. aculestrum* at 10 mg/kg B. W simultaneously with the fungal infection.

Blood samples collection

According to (16), the blood samples from all groups were taken at the end of the experiment.

Statistical analysis

SPSS calculated data for Windows TM version 23. 0 by using one-way ANOVA. All experimental data are presented as Mean ± S.E. and significant differences at P≤ 0. 05 [17].

RESULTS

Hematological study

Hematological parameters: total WBC counts, neutrophils, lymphocytes, monocytes, RBC count, Hb level, and PCV. The blood samples were taken from all the groups to analyze by employment tubes containing an anticoagulant agent in the laboratory. In the current study, the results showed that the control positive group of *A. fumigatus* infection, cortisone and group infected with *A. fumigatus* plus cortisone treated caused significant (p≤ 0. 05) decrease in RBCs count, Hb and PCV, whereas, no significant (p≤ 0. 05) differences were noticed in groups of mice treated with Solanumaculeastrum alone or plus cortisone and *A. fumigatus* in both G6 and G7 when compare with G1 (Table 1).

Parameter	G1	G2	G3	G4	G5	G6	G7
RBCs 10^6/mm^3	9. 9 ± 0. 4 a	7. 1 ± 0. 8 b	7. 8 ± 0. 3 b	9. 7 ± 1. 3 a	7. 9 ± 0. 1 b	9. 9 ± 0. 3 a	9. 7 ± 0. 5 a
Hb mg/dl	14. 2 ± 0. 1a	11. 3 ± 0. 5 b	11. 4 ± 0. 3 b	14. 4 ± 1. 5 a	12. 4 ± 0. 6 b	13. 7 ± 0. 9 a	13. 4 ± 0. 3 a
PCV %	46. 8 ± 0. 2a	41. 5 ± 2. 4 b	39. 9 ± 0. 4 b	44. 7 ± 6. 3 a	43. 6 ± 1. 5 b	43. 5 ± 1. 8 a	47. 4 ± 2. 4 a

Variation in horizontal small letters refers to significant differences (P<0. 05).

Table 1: Effects of *A. fumigatus* infection, cortisone, and *S. aculeastrum* treated after two weeks on parameters of RBC count, Hb, and PCV (mean ± S.E.).

Total WBCs, neutrophils, lymphocytes, and monocyte count were found to be decreased significantly (p≤ 0. 05) in both groups infected with *A. fumigates* and *S. aculeastrum* alone. Also, mice representing control-positive cortisone decreased significantly (p≤ 0. 05) in neutrophils and monocytes. At the same time, total WBCs and lymphocytes were not affected significantly (p≤0. 05). The results also showed no significant differences (p≤0. 05) in a group of mice treated with cortisone plus infection of *A. fumigatus*. Total WBCs and lymphocytes were increased significantly (p≤0. 05), and neutrophils and monocytes were not affected significantly (p≤0. 05) in G6 treated with *S. aculeastrum* after one week of infection. Total WBCs, neutrophils, and lymphocytes were increased significantly (p≤0. 05), and monocytes were not affected significantly (p≤0. 05) in the group treated with *S. aculeastrum* at the same time of infection comparable with the controls regarding the WBCs (Table 2).

Parameter	G1	G2	G3	G4	G5	G6	G7
WBCs 10^9/L	5. 3 ± 0. 5 a	3. 7 ± 0. 8 b	5. 0 ± 0. 5 a	2. 5 ± 0. 4 b	5. 8 ± 1. 9 a	6. 6 ± 0. 9 a	7. 6 ± 3. 0 b
Neutrophil %	3. 2 ± 0. 8 a	1. 8 ± 0. 7 b	1. 8 ± 0. 1 b	1. 6 ± 0. 5 b	2. 4 ± 0. 9 a	3. 4 ± 1. 1 a	4. 2 ± 1. 0 b
Lymphocyte %	2. 1 ± 0. 4 a	1. 4 ± 0. 2 b	2. 6 ± 0. 4 a	1. 1 ± 0. 5b	2. 5 ± 0. 8 a	1. 5 ± 0. 2 b	4. 0 ± 0. 3 b
Monocyte %	1. 2 ± 0. 1 a	0. 1 ± 0 b	0. 1 ± 0 b	0. 1 ± 0. 5 b	0. 2 ± 0 a	0. 6 ± 0. 1 a	0. 7 ± 0. 04 a

Variation in horizontal small letters refers to significant differences (P<0. 05).

Table 2: Effects of *Aspergillus fumigatus* infection, cortisone, and *Solanumaculeastrum* treated after two weeks on parameters of (WBCs, neutrophils, lymphocytes, and monocytes) (mean ± S.E.).

DISCUSSION

The present results indicated that the hematological picture of *A. fumigatus*-infected mice is similar to that of another study [18]. The mycotoxin from pathogenic fungi caused anemia, observed as decreases in PCV Hb% and RBC count. Also, the phospholipase enzyme in *Aspergillu*s spp. is the essential virulence factor that can cause destabilization and penetration, break down membrane phospholipids surrounding the red blood cell, and generate arachidonic acid [19]. Additionally, phospholipase hydrolyzes RBCs to release phosphatidylserine and produce lysophosphatidic acid (LPA), the latter of which results in the flow of substances through a blood cell membrane and causes swilling before exploding [20].

Previous studies also found decreased hematological parameters because of cortisone treatment [21, 22]. Exposure to Dexamethasone demonstrates a significant change in red blood cells, such as anemia, destruction of cells, or inhibition of hematopoiesis. All these reasons affect RBC, Hb, and PCV levels, and these changes led to observing the result compared with a control group and explaining the result that Dexamethasone may cause suppression of the bone marrow. Such decreases could also be attributed to hemodilution. However, they could also result from RBC reaction or inhibition of RBC synthesis, which limits the capacity of these cells to absorb oxygen in conjunction with increased hemolysis brought on by excessive physical stress and results in severe anemia. The WBC decrease results in the lysis of neutrophils affected by phospholipase enzymes, the elimination of lipid phosphorus, and hydrolysis of membrane phospholipids occurred after exposure to this enzyme. This led to decreased cell size, sphering, and increased susceptibility to osmotic stress, which altered the cell's functional properties and caused cell lysis [23]. Another reason represented that phospholipase enzyme and *Aspergillus* spp. The infection effect on hormones responsible for the production of blood cells is represented by the erythropoietin hormone from the kidney, which is the primary catalyst for the production of blood cells; this finding agrees with other researchers [24].

The reduction in neutrophil and monocyte counts after cortisone-treated mice indicated immunosuppression. This finding agrees with another study [25]. Steroids impair alveolar macrophage activity, lowering the primary defense against lung infection. Additionally, they affect T and B cell lymphocytes and reduce cytokine production, which impairs the adaptive immune response to invasive aspergillosis [26].

Solanum aculeastrum affects hematological parameters; the results indicated that plants cause a decrease in total WBC count and differential cells. WBC count is an indicator of an organism's capacity to eradicate infection. A reduction in WBC count in the group of mice treated with Solanumaculeastrum agrees with another study [27]. The animal's capacity to fight infection, attack, and destroy infectious agents in the blood may be adversely impacted by the decline in WBC levels. Additionally, the immune system's effector cells may have a severe effect. Also, the WBC count decreases, as observed by other results [28]. The decrease in WBC count suggests that the extract ingredients may have damaged or prevented the maturation of these blood cells. The committed stem cells that produce these blood cells are regulated by proliferation, differentiation, and maturation by granulocyte-macrophage colony-stimulating factors, interleukins IL-2, IL-4, and IL-5. Therefore, the extract might have interfered with the sensitivity of the committed stem cells responsible for generating these white blood cells and differential cells, or it might have decreased the synthesis of these regulatory factors [29-32].

Mice in both G6 and G7 showed an increase in total WBC count and its differential cells compared with other treated groups; best results were obtained when mice treated at the same time of infection compared with mice received the plant extract after one week of fungal spores infected, the stress factor of infection on the immune system and weakness of mice body can interfere with immune responses. Also, lymphocyte counts may be decreased with handling or other stressors and with age. Increased neutrophil counts (neutrophilia) are commonly seen in conditions of infection and acute inflammation and are related to immune system reactions to stress or excitement and infectious diseases [33].

Previous research proved that *S. aculeastrum* has a chemical and pharmaceutical component that acts as an antifungal against a number of fungal species [34, 35.]. Other researchers have investigated the effect of ethanolic extract using the diffusion method, and the findings showed that the strongest antifungal activity was by *A. fumigates* [13,36, 37]. At the same time, other authors found that alcohol extracts from fruit ultimately impeded the growth of *A. flavus* (100%) [28, 35-37]. The results of the present study agree with all the research above; the hematological findings showed improvements in white blood cells, neutrophils, lymphocytes and monocytes when given the ethanolic extract orally at the same time as infected with *A. fumigatus*, indicating the treatment power of the plant at the applied dose of 10 mg/kg B. W was elevated the immune status by increasing of immune cells that fight infection comparing with other groups.

CONCLUSIONS

This study concluded that using the alcoholic extract of *S. aculeasttrum* could provide an effective therapeutic tool in the treatment of fungal infections as well as in the correction of abnormalities in hematological and immunological markers due to exposure to different infections. Furthermore, studies are of great importance to detect the efficacy of this extract on body organs and other infections.

Author Contributions: Conceptualization, S. G. A. A. and D. A. A.; methodology, S. G. A. A. and D. A. A.; software, S. G. A. A.; validation, S. G. A. A. and D. A. A.; formal analysis, S. G. A. A. and D. A. A.; investigation, S. G. A. A.; resources, S. G. A. A.; data curation, D. A. A.; writing-original draft preparation, S. G. A. A.; writing-eview and editing, S. G. A. A. and D. A. A.; visualization, D. A. A.; supervision, D. A. A.; project administration, S. G. A. A. All authors have read and agreed to the published version of the manuscript.

Funding: This research received no external funding.

Institutional Review Board Statement: The study was conducted according to the guidelines of the Declaration of Helsinki and approved by the Scientific Ethics Committee of the Department of Microbiology at the College of Veterinary Medicine (University of Baghdad, Baghdad, Iraq).

Acknowledgments: The authors dramatically acknowledge the Head Department and the staff of the Department of Microbiology at the College of Veterinary Medicine for their valuable support.

Conflicts of Interest: The authors declare no conflict of interest.

REFERENCES

1. McCoy, C.W; Samson, R.A; Boucias, D.G. Entomogenous fungi.Handbook of natural pesticides, *CRC Press*, **2019**, pp.151-236.
2. Barkai-Golan, R.; Paster, N. Mycotoxins in fruits and vegetables.*Elsevier*, **2011**, pp. 74.
3. Lücking, R.; Aime, M.C.; Robbertse, B.; Miller, A.N.; Ariyawansa, H.A.; Aoki, T.; Latgé, J.P.; Chamilos, G. Aspergillus fumigatus and Aspergillosis in 2019. *Clin Microbiol Rev* **2019**, 33(1), 140-148.
4. Tell, L.A.; Burco, J.D.; Woods, L.; Clemons, K.V. Aspergillosis in birds and mammals: considerations for veterinary medicine. In Recent Developments in Fungal Diseases of Laboratory Animals. Springer, Cham. **2019**. pp.49-72.
5. Schoustra, S.E.; Debets, A.J.; Rijs, A.J.; Zhang, J.; Snelders, E.; Leendertse, P.C.; Verweij, P.E. Environmental hotspots for azole resistance selection of Aspergillus fumigatus, the Netherlands. *Emerg Infect Dis* **2019**, 25 (7), 1347-1353.
6. Resendiz Sharpe, A.; Lagrou, K.; Meis, J.F.; Chowdhary, A.; Lockhart, S.R.; Verweij, P.E.; ISHAM/ECMM Aspergillus Resistance Surveillance Working Group. Triazole resistance surveillance in Aspergillus fumigatus. *Med Mycol* **2018**, 56(suppl_1), S83-S92.
7. May, G.S. Mitogen-activated protein kinase pathways in Aspergilli.In *The aspergilli*.*CRC Press*. **2007**, pp.141-148.
8. Dewi, I.M.; Janssen, N.A.; Rosati, D.; Bruno, M.; Netea, M.G.; Brüggemann, R.J.; van de Veerdonk, F.L. Invasive pulmonary aspergillosis associated with viral pneumonitis.*Curr Opin Microbiol* **2021**, *62*, 21-27.
9. Koduru, S.; Grierson, D.S.; Afolayan, A.J. Antimicrobial Activity of Solanumaculeastrum. *Pharm Biol* **2006**, 44(4), 283-286.
10. Patel, P.; Prasad, A.; Srivastava, K.; Singh, S.S.; Chakrabarty, D.; Misra, P. Updates on steroidal alkaloids and glycoalkaloids in Solanum spp.: Biosynthesis, in vitro production and pharmacological values. *Stud Nat Prod Chem* **2021**, 69, 99-127.
11. Su, H.; Li, C.; Wang, Y.; Li, Y.; Dong, L.; Li, L.; Zhu, M. Kinetic host defense of the mice infected with *Aspergillus Fumigatus*. *Future Microbiol* **2019**, 14(8), 705-716.

12. Eidi, S.; Azadi, H.G.; Rahbar, N.; Mehmannavaz, H.R. Evaluation of antifungal activity of hydroalcoholic extracts of Citrulluscolocynthis fruit. *J Herb Med* **2015**, 5 (1), 36-40.
13. Marina A.Shevchenko, Andrey O.Bogorodskiy, Natalia I.Troyanova, Ekaterina A.Servuli, Elena L.Bolkhovitina, Georg Büldt, ChristophFahlke, Valentin I. Gordeliy, Thomas Gensch, Valentin I. Borshchevskiy, Alexander M. Sapozhnikov, "*Aspergillus fumigatus* Infection-Induced Neutrophil Recruitment and Location in the Conducting Airway of Immunocompetent, Neutropenic, and Immunosuppressed Mice. *J Immunol Res* **2018**, 12, 20-28.
14. Gargiulo, S.; Greco, A.; Gramanzini, M.; Esposito, S.; Affuso, A.; Brunetti, A.; Vesce, G. Mice anesthesia, analgesia, and care, Part I: anesthetic considerations in preclinical research. *ILAR J* **2012**, 53(1), E55-E69.
15. Coles, E.H. Veterinary clinical Pathology 4th ed WB Saunders company Philadelphia.London, Toronto, Mexico, Riodejenario, Sydney, Tokyo Hong Kong, **1986**, 136-170.
16. Gharban, H.A. Cumulative Effect of Subclinical Mastitis on Immunological and Biochemical Parameters in Cow Milk.*Arch Razi Instit*, **2021**, 76 (6), 1599-1608.
17. Mohamad, S.H.; Thalij, K.M.; AL-Bander, K.; Dheeb, B.I. Effects of Allergic fungi on hematological and immunological parameters of human patients and rabbits. *Egypt Acad J Biol Sci GMicrobiol* **2014**, 6(2), 41-48.
18. Mansoor, S. S.; Al-Esawi, J. S. . .; Al-Falahi, M. N. Assessing The Efficiency Of Cement Kiln Dust For Heavy Metals Removal From Simulated Polluted Water. *JLSAR* **2023**, 4, 45-52.
19. Neidlinger, N.A.; Larkin, S.K.; Bhagat, A.; Victorino, G.P.; Kuypers, F.A. Hydrolysis of phosphatidylserine-exposing red blood cells by secretory phospholipase A2 generates lysophosphatidic acid and results in vascular dysfunction. *J Biol Chem* **2006**, 281 (2), 775-781.
20. Razzaq, S.A.; Jaber, I.J.; Kadhim, S.A.; Abbas, A.A. Pharmacological Effects of Dexamethasone in Rats. *Indian J Forensic Med Toxicol* **2020**,14 (3), 1003.
21. Ribas, J.L.C.; Zampronio, A.R.; Silva De Assis, H.C. Effects of trophic exposure to diclofenac and Dexamethasone on hematological parameters and immune response in freshwater fish. *Environ Toxicol Chem* **2016**, 35(4), 975-982.
22. Ghannoum, M.A. Potential role of phospholipases in virulence and fungal pathogenesis. *Clin Microbiol Rev* **2000**,13 (1), 122-143.
23. Auda, M.A. Effect of phospholipase and the fungus which it produced (Aspergillusniger) on the some of blood parameters of male mice (Musmusculus). *Al-Qadisiyah J Pure Sci* **2009**, 14 (1). 22-39.
24. Al-Maliki, S.J.; Al-Ali, A.A.; Kathim, A.S. Effect of corticosteroids cortisol hormone [hydrocortisone] on the of the blood parameter in pregnant and non-pregnant laboratory females mice. *J Histol Cell Biol* **2018**, 1 (1): 16-22.
25. S. Hameed, T., Sawicka, B. Role Of Agricultural Extension In Adoption Of Sustainable Agriculture Practices. *Anbar Journal Of Agricultural Sciences*, **2023**; 21(1): 250-260. doi: 10.32649/ajas.2023.179947.
26. A A Al-Azzami , Th T Mohammed . Effect of Adding Dry Leaves of Lemongrass (Cymbopogon Citratus) To the Diet on Some Biochemical Tests of Blood in Broiler (Ross 308). IOP Conf Ser Earth Environ Sci 2023, 1252 (1), 12125. https://doi.org/10.1088/1755-1315/1252/1/012125.
27. Aboyade, O.M.; Yakubu, M.T.; Grierson, D.S.; Afolayan, A.J. Studies on the toxicological effect of the aqueous extract of the fresh, dried and boiled berries of SolanumaculeastrumDunal in male Wistar rats.*Hum Exp Toxicol* **2009**, 28 (12), 765-775.
28. Aboyade, O.M.; Yakubu, M.T.; Grierson, D.S.; Afolayan, A.J. Safety evaluation of aqueous extract of unripe berries of Solanumaculeastrum in male wistar rats. *Afr J Pharm Pharmacol* **2010**, 4(3), 90-97.
29. Al-gharban, H.A.; Dhahir, S.H. Serological diagnosis of persistent infection with Anaplasma marginale bacteria in cattle. *Iraqi J Vet Med* **2015**, 39 (1), 33-39
30. Gharban, H.A.; Yousif, A.A. Serological and Molecular Phylogenetic Detection of Coxiella burnetii in Lactating Cows, Iraq. *Iraqi J Vet Med* **2020**, 44(E0), 42-50
31. Gharban, H.A.; Yousif, A.A. Serological, Clinical and Hematological prevalence of Coxiella burnetii in Adult Cows, Iraq. *Biochem Cell Arch* **2020**, *20*(1), 67-74.
32. Ameen M. Shaman , Th. T. Mohammed. Effect Using Feed Additives Instead of Imported Premixes Affects the Physiology of Broiler Chickens. IOP Conf Ser Earth Environ Sci 2023, 1262 (7), 72080. https://doi.org/10.1088/1755-1315/1262/7/072080.

33. A A Al-Azzami , Th T Mohammed . The Effect of Adding Lemongrass Leaf Powder (Cymbopogon Citratus) to the Diet as a Natural Supplement on Some Productive Traits and Oxidation Indicators in Broiler (Ross 308). IOP Conf Ser Earth Environ Sci 2023, 1252 (1), 12123. https://doi.org/10.1088/1755-1315/1252/1/012123.
34. O'Connell, K.E.; Mikkola, A.M.; Stepanek, A.M.; Vernet, A.; Hall, C.D.; Sun, C.C.; Brown, D.E. Practical murine hematopathology: a comparative review and implications for research. *Comp Med* **2015**, 65(2), 96-113. .
35. Gurudeeban, S.; Ramanathan, T.; Satyavani, K.; Dhinesh, T. Antimicrobial effect of coastal medicinal plant â€“Citrulluscolocynthis against pathogenic microorganisms. *Afr J Pure Appl Chem* **2011**, 5(5), 119-122.
36. Hameed, B.; Ali, Q.; Hafeez, M.M.; Malik, A. Antibacterial and antifungal activity of fruit, seed and root extracts of Citrulluscolocynthis plant. *Biol Clin Sci Res J* **2020**, 19 (1), 1-15.
37. Mohammad, H.A.; Ajaj, E.A.; Gharban, H.A. The first study on confirmation and risk factors of acute and chronic canine distemper in stray dogs in Wasit Province, Iraq, using enzyme-linked immunosorbent assay and reverse transcription-polymerase chain reaction. *Vet World* **2022**, 15 (4), 968-974
38. Koduru, S.; Grierson, D.S.; Afolayan, A.J. Antimicrobial Activity of Solanumaculeastrum.*Pharm Biol* **2006**, 44(4), 283-286.

Received: October 9th 2023/ **Accepte**d: January 15th 2024 / **Published:**15 February 2024

Citation: Chango, M.; Rosero, G.; Erazo, N.; Álvarez, P. Effect of *Solanum aculeastrum* on hematological parameters of Albino mice infected with *Aspergillus fumigatus*. Revis Bionatura 2024; 9 (1) 48. http://dx.doi.org/10.21931/RB/2024.09.01.48

Additional information Correspondence should be addressed to dalia@covm.

Peer review information. Bionatura thanks anonymous reviewer(s) for their contribution to the peer review of this work using https://reviewerlocator.webofscience.com/

Bionatura ISSN. First 13909355 Ecuador. **Scopus coverage years**: from 2016 to the present

Bionatura
Ibero-American Journal of Biotechnology and Life Sciences

Article

Histopathological effects of *Cryptococcus neoformans* on liver and kidney in mice

*Sara Saad Hussamaldeen Al-Bakir[1] and Dalia Abdalkareem Abdalshaheed[2]**

[1]Department of Microbiology, College of Veterinary Medicine, University of Baghdad, Baghdad, Iraq; saadsara434@gmail.com. https://orcid.org/0000-0003-0633-6616
[2]Department of Microbiology, College of Veterinary Medicine, University of Baghdad, Baghdad, Iraq; da-lia@covm.uobaghdad.edu.iq. https://orcid.org/0000-0003-1369-8826
** Correspondence: dalia@covm.uobaghdad.edu.iq.*
Available from. http://dx.doi.org/10.21931/RB/2024.09.01.49

ABSTRACT

This study provides a brief review of approaches for the detection of histopathological effects of *Cryptococcus neoformans* on the liver and kidney in mice that were injected I/P with 10^5 yeast cells of *C. neoformans* suspended in 1 ml phosphate-buffered saline at a single dose. After 14 days, the mice were sacrificed, and histopathological sections from the liver and kidney were prepared and stained with Haematoxylin and Eosin by the P.A.S. method. The results show that the liver was infiltrated with inflammatory cells, primarily mononuclear cells, in the portal. In addition to the activation of Kupffer cells and vacillation of hepatocytes, most blood vessels were congested. The section of the kidney shows sluffing of epithelia lining tubules and complete destruction of glomeruli, in addition to infiltration of mononuclear cells. These results suggested that the fungus invasiveness of mice has substantial effects on vital organs and may lead to death.

Keywords: *Cryptococcus neoformans*, Hepatic cryptococcal infection, Cryptococcuria.

INTRODUCTION

A fungal illness known as cryptococcosis is brought on by the pathogens *Cryptococcus neoformans* and *C. gattii*, which resemble yeast [1]. *Cryptococcus neoformans* serotype A accounts for around 95% of reported cryptococcal infections; the remaining 5% are caused by other serotypes or *Cryptococcus gattii* [2]. It is an illness contracted by inhaling spores or yeast cells that have been dried from environmental sources such as plant matter, soil, and bird excrement [3].

Cryptococcus spp. is widespread and the most significant species concerning medicine [4]. When seen under a microscope, the fungus appears as an oval or globular yeast with a diameter of 3mm to 8 mm. It is often encased in a mucopolysaccharidal capsule. The phenoloxidase enzyme causes the capsule to create a significant amount of melanin. The abundance of substrates for phenoloxidase activity in brain tissue may help to partially explain *Cryptococcus's* preference for the central nervous system [5]. As an encapsulated yeast known as Torulahistolytica or European blastomycosis, *Cryptococcus* spp. may avoid the immune system's defense mechanisms and spread primarily from the lungs and central nervous system to the blood, skin, eyes, skeletal system, and urinary tract [7]. Cryptococcosis is brought on by inhaling spores or dried yeast cells, and it results in approximately 180,000 fatalities globally each year, including nearly 15% of all AIDS-related deaths [8]. Although a population of *C. neoformans* may remain dormant for long periods in immunocompetent persons, this often results in an asymptomatic lung infection managed by the host immune response [9]. The disease progression results in a highly lethal form of meningoencephalitis [8]. Cryptococcosis in animals is a systemic fungal infection of worldwide significance that usually initially infects the nasal cavity, paranasal tissues, or

lungs. It can then disseminate to the skin, eyes, or central nervous system. Nasal cryptococcosis is frequently seen in clinical signs including sneezing, snoring or snorting, dyspnea, nasal deformities, or a mucopurulent, serous, or sero-sanguineous nasal discharge [10,11]. *Cryptococcus* infections have been reported in many animals, including cats, dogs, horses, birds, and koala bears [12]. The most common symptom of hepatic cryptococcal infection is cholestatic jaundice, which can quickly proceed to liver failure and death in cases of widespread illness [13]. Cryptococcosis is a relatively uncommon presentation in human patients in urinary tract infections or a diffused illness manifestation (U.T.I.). Patients frequently have an underlying, immune-compromising illness when cryptococcosis is diagnosed in individuals [14]. Renal involvement with cryptococcosis in animals is rare, and it has only sporadically been demonstrated in cats with systemic cryptococcosis by detecting fungi during necropsy or urine sediment analysis [15]. Therefore, this research aimed to study the histopathological effects of *C. neoformanson* on the liver and kidney.

MATERIALS AND METHODS

Animals utilized in the experiment

Twenty albino BALB/C female mice weighing an average of 22–25g were used. Animals were housed in cages in pairs and were fed water. A total of 10 mice from the first group (G1) were utilized as the control group and not given any treatment, whereas 10 mice were injected intraperitoneally with a single dose of *Cryptococcus neoformans* suspension that contained 10^5 yeast cells into each 1 ml of PBS.

Histopathological sections

Samples of liver and kidney were collected after scarification of mice at 14 days of a single administration of *C. neoformans* and kept in 10% formaldehyde solution for fixation in order to preserve the figures, size, and tissue for specimens, then processed routinely using the stockinette [16]. The specimens were washed with distilled water several times in order to remove a large proportion of fixative and dehydration by passing the specimens through ascending gradual of ethanol (50,70,80,95 and 100) % in each run of the treatment with methyl benzoate 24 hrs. Then, they were rehydrated by gradual ethanol (100, 95, 80, 70, and 50) % in each run. The samples were cleared by xylol, embedded in paraffin wax at 70ºC, and sectioned by microtome at 5-6 microns of thickness. The slides were mounted and covered with a coverslip using albumin at 56ºC, stained with Eosin and Hematoxylin, and examined under a light microscope at 400X [17, 18].

RESULTS

Microscopic examination of liver sections for the control group revealed the typical architecture of hepatic lobules and sinusoids lined by thin capillaries and surrounded by a portal area composed of a portal vein, portal artery, and bile ductules in the interstitium (Figure 1a). While the liver of mice infected with *C. neoformans* showed liver with infiltrated of inflammatory cells, primarily mononuclear cells in the portal area, in addition to activation of Kupffer cells and vacillation of hepatocytes, most blood vessels were congested (Figure 1b & c).

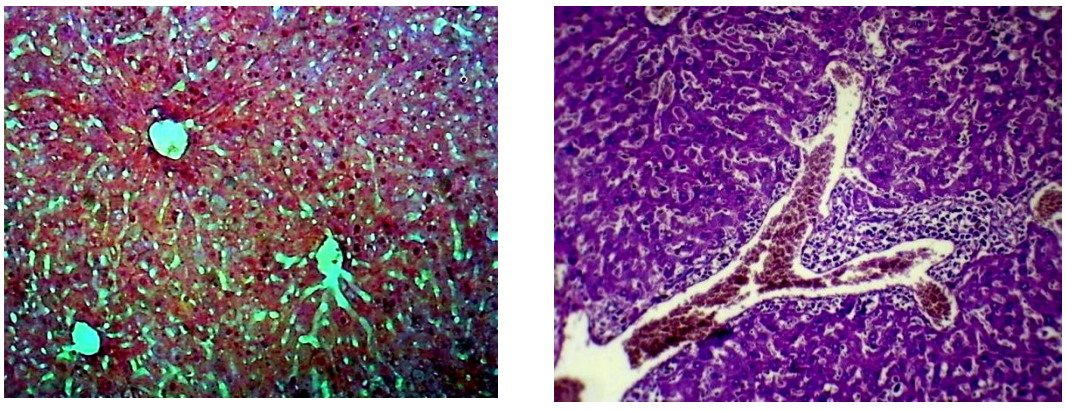

(**a**) (**b**)

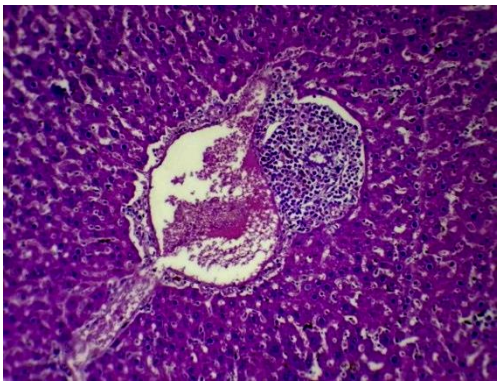

(**c**)

Figure 1: Histopathological section of liver of (a) Control group showing many lobules each lobule contains central vein surrounded by hepatic cord and separated by sinusoid; (b & c) Infected mice with *C. neoformans* showing infiltration of inflammatory cells, primarily mononuclear cells in the portal area in addition to activation of Kupffer cells and vacillation of hepatocytes, most blood vessels were congested, (H & E stain, 400X).

For the kidney, a microscopic examination of a histological section of control mice showed normal renal tubules. The cortex and normal glomerular tufts were also covered by a thin, dense connective tissue capsule with adipose tissue (Figure 2a). Meanwhile, the kidney section of infected mice with *C. neoformans*showsga kidney with sluffing of epithelia lining tubule and complete destruction of glomeruli, in addition to infiltration of mononuclear cells (Figure 2b, c).

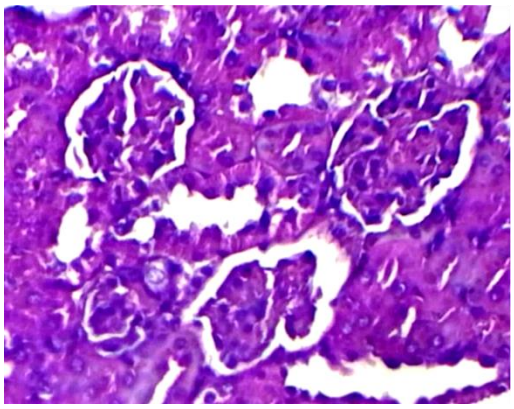

(**a**)

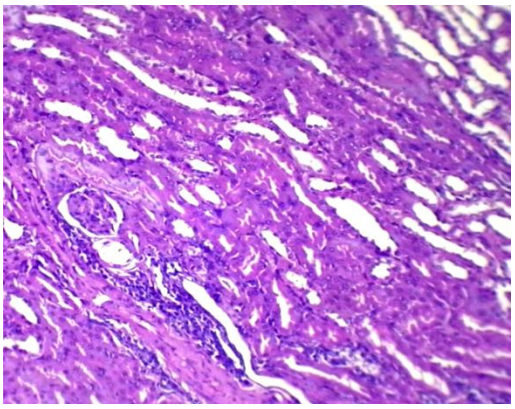

(**b**)

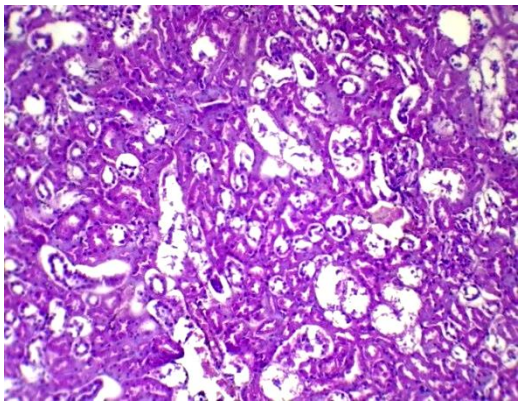

(**c**)

Figure 2: Histopathological section of kidney of (a) Control group showing normal glomeruli and tubules; (b) Infected mice with *C. neoformans* showing kidney with sluffing of epithelia lining tubules, and destruction of glomeruli with infiltration of mononuclear cells, (H & E stain, 400X).

DISCUSSION

The results showed the hepatic tissue section of mice infected with *C. neoformans* with vacuolation of hepatocytes, dilation of sinusoids and central veins as well as portal veins that containing the fibrinous network trapped few P.M.N.s, fibrilles of fibrin precipitated on the endothelial layer of blood vessel cause thickening of vascular wall and congestion of blood vessels which agreement with Al Kaaby (2009) [19]. Additionally, inflammatory cells were infiltrated, especially mononuclear cells, and activation of Kupffer cells in hepatic lobules; fungi can enter the liver or even the whole body through the damaged mucosal membrane, causing aggravated liver damage [20]. As observed in figure (2), the renal section of mice treated with *C. neoformans* revealed destruction of glomerular tuft, sluffing, and convoluted tubules proximal and distal epithelial linings, which are deteriorating with infiltration mononuclear cells. These defects are also seen in another study [21-23]. These findings might be due to the dissemination of cryptococcosis. Fungal infection is associated with animals losing weight, their blood cell and leukocyte counts dropping, their plasma glucose levels dropping, and their stomach, liver, and kidneys developing pathological abnormalities [24].

CONCLUSIONS

Cryptococcus neoformans causes severe damage to the liver and kidneys, suggesting it impacts public health. Furthermore, studies are of great importance to estimate the effect of this bacterium on other tissues and organs and to invent active methods for preventing or reducing their severe effects.

Author Contributions, Conceptualization, S.S.H.A. and D.A.A.; methodology, S.S.H.A.; software, S.S.H.A.; validation, S.S.H.A.; and D.A.A.; formal analysis, S.S.H.A.; investigation, S.S.H.A.; resources, S.S.H.A.; writing-original draft preparation, S.S.H.A.; writing-review and editing, S.S.H.A.; and D.A.A.; visualization, D.A.A.; supervision, D.A.A.; project administration, S.S.H.A.. All authors have read and agreed to the published version of the manuscript.

Funding: This research received no external funding.

Institutional Review Board Statement: The study was conducted according to the guidelines of the Declaration of Helsinki and approved by the Ethics of the Scientific Committee of the Department of Microbiology in the College of Veterinary Medicine, University of Baghdad (Baghdad, Iraq).

Acknowledgments: In this section, you can acknowledge any support given that is not covered by the author's contribution or funding sections. This may include administrative and technical support or donations in kind (e.g., materials used for experiments).

Conflicts of Interest: The authors declare no conflict of interest.

REFERENCES

1. Kwon-Chung, K.J.; Varma, A. Do major species concepts support one, two or more species within Cryptococcus neoformans? *FEMS Yeast Res* **2006**, 6 (4), 574–587.
2. Maziarz, E.K.; Perfect, J.R. Cryptococcosis. *Infect Dis Clin* **2016**, 30 (1), 179-206.
3. Kwon-Chung, K.J.; Fraser, J.A.; Doering, T.L.; Wang, Z.A.; Janbon, G.; Idnurm, A.; Bahn, Y.S. *Cryptococcus neoformans* and *Cryptococcus gattii*, the etiologic agents of cryptococcosis. *Cold Spring Harb Perspect Med* **2014**, 4 (7), 197-216.
4. Zain, H.; Tatar , A.; Alabi, O. M. .; Samiei Zafarghandi, M. . The Effect Of Using Different Vitamin E Levels On The Antioxidants Status Of Broiler Chickens. JLSAR 2023, 4, 37-44.
5. Moretti, M.L.; Resende, M.R.; Lazéra, M.S.; Colombo, A.L.; Shikanai-Yasuda, M.A. Guidelines in cryptococcosis. *Rev Soc Bras Med Trop* **2008**; 41, 524–544.
6. Setianingrum, F.; Rautemaa-Richardson, R.; Denning, D.W. Pulmonary cryptococcosis, a review of pathobiology and clinical aspects. *Med Mycol* **2019**, 57(2),133–150.

7. Kwon-Chung, K.J.; Boekhout, T.; Fell, J.W.; and Diaz, M. Proposal to conserve the name *Cryptococcus gattii* against *C. hondurianus* and *C. bacillisporus* (Basidiomycota, Hymenomycetes, Tremellomycetidae). *Taxon* **2002**, 51(4), 804-806.
8. Rajasingham, R.; Smith, R.M.; Park, B.J.; Jarvis, J.N.; Govender, N.P.; Chiller, T.M.; Denning, D.W.; Loyse, A.; Boulware, D.R. Global burden of disease of HIV-associated cryptococcal meningitis, an updated analysis. *Lancet Infect Dis* **2017**, 17,873–881.
9. A. Al-Badawi, S., T. Al-Wasity, R. AN .Economic Analysis Of The Most Important Variables Affecting Agricultural Employment In Iraq For The Period (1998 - 2019). Anbar Journal Of Agricultural Sciences, 2023; 21(1): 224-249. doi: 10.32649/ajas.2023.179764.
10. Meng, H.C.; Lu, C.H.; Wang, H.C.; Chen, H.L.; Tsai, N.W.; Li, S.H.; Hsu, N.W.; Lin, W.M.; Kung, C.T.; and Lin, W.C. Long-Term Neuropsychological Sequelae in HIVSeronegativeCryptococcal Meningoencephalitis Patients with and without Ventriculoperitoneal Shunts, A Cine M.R.I. Study. *Behav Neurol* **2015**, 1-10.
11. Pimenta, P.; Sofia, A.; João, B.; Maria, J.; Pereira, L.; Paula Maduro, A.; LuísCardoso, C.C. Blepharitis due to *Cryptococcus neoformans* in a cat from northern Portugal. *J Feline Med Surg* **2015**, 1, 20-25.
12. Malik, R.; Krockenberger, M.B.; Brien, C.R.O.; Carter, D.E.E.A.; Meyer, W.; Canfield, P.J. Veterinary insights into cryptococcosis caused by *Cryptococcus neoformans* and *Cryptococcus gattii*. In, Heitman J, Kozel T, Kwon-ChungKJ, Perfect JR, Casadevall A, eds. Cryptococcus, From Human Pathogen to Model Yeast. Washington, DC, A.S.M. Press, **2011**, 489–502.
13. A A Al-Azzami , Th T Mohammed . Effect of Adding Dry Leaves of Lemongrass (Cymbopogon Citratus) To the Diet on Some Biochemical Tests of Blood in Broiler (Ross 308). I.O.P. Conf Ser Earth Environ Sci 2023, 1252 (1), 12125. https://doi.org/10.1088/1755-1315/1252/1/012125.
14. Kiertiburanakul, S.; Sungkanuparph, S.; Buabut, B. Cryptococcuria as a manifestation of disseminated cryptococcosis and isolated urinary tract infection. *Jpn J Infect Dis* **2004**, 57, 203-205.
15. Malik, R.; Krockenberger, M.; O'Brien, C. Cryptococcosis. In, Greene CE, ed. Infectious Disease of the Dog and Cat. 3rd ed. Missouri, Saunders, *Elsevier* **2006**,584-598.
16. Luna, L.E. Vegetalismo, shamanism among the mestizo population of the Peruvian Amazon. Vol. 27, Stockholm, Almqvist&Wiksell International, 1986. Pp,429.
17. Ameen M. Shaman , Th. T. Mohammed. Effect Using Feed Additives Instead of Imported Premixes Affects the Physiology of Broiler Chickens. I.O.P. Conf Ser Earth Environ Sci 2023, 1262 (7), 72080. https://doi.org/10.1088/1755-1315/1262/7/072080.
18. Elkhateeb, S. Z.; Ebraheem, M. O.; Abdulateef, S. M.; Ahmed, I. A. Constraints Affecting the Welfare of Domestic Sheep Grazing in the Natural Pasture. I.O.P. Conf Ser Earth Environ Sci 2023, 1252 (1), 12144. https://doi.org/10.1088/1755-1315/1252/1/012144.
19. Al-Shaeli, S.J.; Ethaeb, A.M.; Gharban, H.A. Molecular and histopathological identification of ovine neosporosis (Neospora caninum) in aborted ewes in Iraq. *Vet World* **2020**, 13(3), 597-603.
20. Al Kaaby, H.T. Isolation of Cryptococcus neofrmans from pigeon dropping and study of some pathogenesis aspects. *J Kerbala Univer* **2009**, 7 (2), 316-321
21. A A Al-Azzami , Th T Mohammed . The Effect of Adding Lemongrass Leaf Powder (Cymbopogon Citratus) to the Diet as a Natural Supplement on Some Productive Traits and Oxidation Indicators in Broiler (Ross 308). I.O.P. Conf Ser Earth Environ Sci 2023, 1252 (1), 12123. https://doi.org/10.1088/1755-1315/1252/1/012123.
22. Ramdial, P.K.; Sing Y.; Deonarain, J.; Bhimma, R.; Chotey, N.; Sewram, V. Pediatric renal cryptococcosis, novel manifestations in the acquired immunodeficiency syndrome era. *Int J Surg Pathol* **2011**, 19, 386–392.
23. Pongmekin, P.; Chongtrakool, P.; Santanirand, P.; Kiertiburanakul, S. Clinical characteristics and mortality risk factors of cryptococcal infection among HIV-negative patients. *J Med Assoc Thai* **2014**, 97,36-43.
24. Abbas, O.S.; Abdualshahed, D.A. Effect of Grape Seed Extract on the T-2 Toxicity in mice. *Iraqi J Cancer Med Gene* **2013**, 6(2), 120-125.

Received: October 9th 2023/ **Accepte**d: January 15th 2024 / **Published:**15 February 2024

Citation: Al-Bakir, S.S.H.; Abdalshaheed, D.A. Histopathological effects of *Cryptococcus neoformans* on liver and kidney in mice. Revis Bionatura 2024; 9 (1) 49. http://dx.doi.org/10.21931/RB/2024.09.01.49

Additional information Correspondence should be addressed to dalia@covm.uobaghdad.edu.iq.

Peer review information. Bionatura thanks anonymous reviewer(s) for their contribution to the peer review of this work using https://reviewerlocator.webofscience.com/

Bionatura ISSN. First 13909355 Ecuador. **Scopus coverage years**: from 2016 to the present

Bionatura
Ibero-American Journal of Biotechnology and Life Sciences

Article

Identification of Diagnosis Fungi that Cause Potato Root Rot

Saja W. A´shour[1] and Theyab A. Farhan[2]

[1]Department of Plant Protection, College of Agriculture, University of Anbar, Iraq.
saj20g7013@uoanbar.edu.iq.
[2]Department of Plant Protection, College of Agriculture, University of Anbar, Iraq.
deab.frahen@uoanbar.edu.iq
** Correspondence: saj20g7013@uoanbar.edu.iq.*
Available from. http://dx.doi.org/10.21931/RB/2024.09.01.51

ABSTRACT

Results of collecting samples from different regions of Anbar Governorate (Al-Amiriyah, Al-Khalidya, Fallujah, Heet and Ramadi) showed that potato root rot disease is widespread in all regions collected. The results of isolation and phenotypic and molecular diagnosis using the polymerase chain reaction (PCR) technique indicated showed the presence of fungus *Rhizoctonia* spp., and Fungus *Fusarium* spp. Accompanying potato root rot disease and the pathogenicity test using radish seeds on water Agar (W.R.) culture media, all tested isolates achieved a significant reduction in radish seed plants compared with control treatment uncontaminated by any of the isolates of fungi, which recorded infection rate 0%.

Keywords: Potato Root Rot, Diagnosis, Fungi, *Rhizoctonia solani* , *Fusarium solani*.

INTRODUCTION

Potato, *Solanum tuberosum* L., is considered a strategic vegetable crop and comes in fourth place after wheat, corn and rice. It is from the family *Solanaceae*, of strategic importance in most countries of the world in general and Iraq in particular, as it is considered one of the easiest crops to manage when compared to other vegetable crops as well as Most of its varieties, especially the early ones, complete their life cycle less than 100 days [1]. Due to the ease of management of this crop and its high productivity and short life cycle, its cultivation has expanded significantly [2]. As a result of the expansion in the cultivation of this crop, many problems appeared, foremost of which are fungal causes, especially root rot pathogens, leg ulcers and black crust, which cause economic losses. It increases farmers' production [3], [4] . Root rot disease is one of the most essential plant diseases worldwide that affects many crops [5]. Root rot disease of potato plants caused by the fungi *Rhizoctonia solani* and *Fusarium solani* is among the most common diseases due to its highly destructive effects that may reach chronic effects in every potato growing area. Each of them can have an economic impact on the season and does not cause Economic losses are only on an annual basis and therefore considered a problem for producers who often suffer economic losses from this disease. Mold was first described as a potato tuber disease in Ireland in 1913, has been known to occur in North America since then, and has become a significant soil-borne disease. Statistics show that this species is becoming increasingly common, which poses a significant threat to potato production, especially in warm regions [6]. Root rot symptoms represent a

significant threat because the damage begins underground, where the first symptoms cannot be distinguished—the appearance of pathological symptoms on infected plants [7], [8]. Because of the importance of the potato crop and the danger of root rot disease, the study aimed to isolate and characterize the phenotypic and molecular diagnosis of the fungi accompanying the samples infected with root rot disease.

MATERIALS AND METHODS

Sample collection

Samples were collected from potato plants that showed symptoms of disease (yellow, plant wilt, plant death, burn edges of leaves) [9] from some fields of Anbar Governorate (Al-Khalidiya, Al-Amiriya, Sadat Al-Fallujah, Nuaimiya, Heet and Saqlawiyah) for the agricultural season Two thousand twenty-one for the spring loop, and the affected plant parts were placed in sterile polyethylene bags, with the place and date of sample collection recorded, and the samples were kept in the refrigerator at a temperature of 4 C° until the isolation process**.**

Isolation of fungi associated with potato root rot

Parts of roots that showed symptoms of rot were taken and washed with water to get rid of dust and cut into small pieces with a length of 0.5-1 cm. and superficially sterilized with sodium hypochlorite solution Nacl (chlorine 6% active substance) for 3 minutes after which the plant pieces were washed with distilled water Sterilized 3 times to get rid of the effects of the sterile material, dried with sterile filter paper and transferred by sterile forceps, and 4 plant pieces were planted in each Petri dish with a diameter of 9 cm containing the sterilized culture medium (PDA) Potato Dextrose Agar with an Autoclaved at 121 °C and a pressure of 5.1 bar/cm^3 for 20 minutes and the antibiotic (Amoxicillin) was added to it at a concentration of 200 mg. L^{-1}, after sterilizing medium. The dishes were incubated at 25 ± 2 °C for 3 days, after which a microscopic examination was conducted to investigate the presence of pathogenic fungi**.**

Phenotypic diagnosis

Fungi isolates were diagnosed after the growth of fungal colonies on the PDA medium was prepared, as microscopic slides were examined using a light microscope, and depending on the cultural characteristics and using the taxonomic key specific to the species, the fungi were morphologically diagnosed [10].

Molecular diagnosis

DNA was isolated and extracted in the Scientific Progress Laboratory / Baghdad - Al-Harithiya according to the ABIOpure protocol. Prepared by the Korean company Macrogen ITS13 -5'- TCCGTAGGTGAACCTGCGG, ITS43 - 5'-TCCTCCGCTTATTGATATGC**.** The Korean company Macrogen prepared the primers in lyophilized form in nuclease-free water to give a final concentration of 100 µl.$µl^{-1}$. A working solution of these primers was prepared by adding 10 µl of the starting primer (stored at -20 °C) to 90 µl of distilled water to obtain an effective starting solution of 10 µl. mol-1 After PCR, gel electrophoresis to confirm the presence of amplification using polymerase chain reaction (PCR) was fully approved on the parameters of the extracted DNA. After completing the DNA amplification and migration steps on Agarose Gel, the samples were sent to the Korean Macrogen Company to obtain the sequence of nitrogenous bases (Sequencing). Several studies have relied on this technique in the diagnosis of fungi, as [11] showed that the PCR technique is used to diagnose *R. solani* fungi and relied in its diagnosis on the transcribed spacer internal region between (ITS4-ITS1) to distinguish between types of fungi. specialized. [12] also used PCR technique to diagnose species of the genus *Rhizoctonia* such as *R. solani*, isolated from different families of plants.

Pathogenicity tests of isolated fungi on radish seeds

The pathogenicity of seven isolates of *R.solani* spp. (Al-Amiriya - Rs1, Al-Amiriya 2 - Rs2, Al-Khalidiya - Rs3, Sadat Al-fallujah - Rs4, Al-Nuaimiya - Rs5, Heet - Rs6 and Al-Saqlawiyah- Rs7) And seven isolates of *Fusarium* spp. (Al-Amiriya - Fu1, Al-Amiriya 2 - Fu2, Al-Khalidiya - Fu3, Al-Khalidiya - Fu4, Al-Nuaimiya - Fu5, Heet - Fu6Furthermore, Al-Saqlawiyah - Fu7) was tested. In the Department of Plant Protection at the College of Agriculture / University of Anbar, the test was carried out according to the method of [13] according to a Randomized completely design (CRD) sterile nutrient medium (Water Ager) was prepared and distributed in Petri dishes with a diameter of 9 cm containing15-20 mm. From the more significant culture medium and water (W.A.) (20 g acre, liter of distilled water), sterilized by an autoclaved 121 °C and a pressure of 5.1 bar/cm3 for 20 minutes, added to the antibiotic Amoxicillin at a concentration of 200 mg/L^{-1}, the dishes were inoculated by taking a 5 mm diameter disc using A sterile cork piercing was placed in the middle of the dish. 3 dishes were used for each isolate of the tested fungi, and 3 were used as a comparison treatment (without adding a tablet from the mushroom colony). Then the dishes were transferred to the incubator and left at a temperature of 25 ± 2 for three days, after which the sterilized radish seeds were sown superficially with a solution of Sodium hypo chlori; 100%, 10 seeds were used for each plate. The seeds were sown in a circular motion around the fungal perennial disc so that the seeds were separated by 1 cm from the edge of the plate. Then, the plates were incubated for 14 days, after which the percentage of infection was calculated for each isolate according to the following equation:

$$\text{Germination \%} = \frac{\text{Number of Infected Plants}}{\text{Total Number of Plants}} \text{ x } 100.$$

RESULTS AND DISCUSSION

The results of sampling. in Fig. (1) and Fishow g. (1) Potato root rot disease is widespread in most potato growing areas in the world, and that is consistent with findings found by [14, 15].

Figure 1: Potato plants infected with root rot disease.

No.	Sample Code	Location	Collection Date 2021
1	A1	Al-Amiriya	**25 /10**
2	A2	Al-Amiriya2	**27 /10**

3	A3	Al-Khalidiya	**3 /11**
4	A4	Sadat Al-Fallujah	**5 /11**
5	A5	Al-Nuaimiya	**11 /11**
6	A6	Heet	**12 /11**
7	A7	Al-Saqlawiyah	**14 /12**

Table 1: Areas from which samples were collected from Potato root rot disease.

Phenotypic diagnosis

The results of the phenotypic diagnosis shown in Table (2) showed the presence of the fungus *R.solani* spp. and *Fusarium* spp., which were associated with potato root rot disease, which is the main cause of the disease, and this is consistent with what was indicated by [16, 17].

No.	Sample Code	Fungi	Location	Collection Date 2021
1	A1	*Rhizoctoina spp.* and *Fusarium spp.*	Al-Amiriya	**25 /10**
2	A2	*Rhizoctoina spp.* and *Fusarium spp.*	Al-Amiriya 2	**27 /10**
3	A3	*Rhizoctoina spp.* and *Fusarium spp.*	Al-Khalidiya	**3 /11**
4	A4	*Rhizoctoina spp.* and *Fusarium spp.*	Sadat Al-Fallujah	**5 /11**
5	A5	*Rhizoctoina spp..*and *Fusarium spp.*	Al-Nuaimiya	**11 /11**
6	A6	*Rhizoctoina spp* and *Fusarium spp.*	Heet	**12 /11**
7	A7	*Rhizoctoina spp.* and *Fusarium spp.*	Al-Saqlawiyah	**14 /12**

Table 2: The most important fungi related to potato root rot were isolated and diagnosed phenotypically to the genus level.

Molecular Diagnostics

Table (3) shows the results of the molecular diagnosis that the fungi that cause potato root rot disease are of the genus *Rhizoctonia* spp. and *Fusarium* spp., according to the arrangement of nitrogenous bases in the single DNA strand. These results are consistent with what was mentioned by [16, 18], and 19, and these fungi are the leading cause of potato root rot disease.

No.	Location	Code	Fungi	Accession
1	Al-Amiriya	**A1**	*Fusarium Falciforme*	**MN545530.1**
2	Al-Khalidiya	**K**	*Fusarium Oxysporum*	**OL691079.1**
3	Al-Saqlawiyah	**B**	*Rhizoctoina solani*	**LC507904.1**
4	Sadat Al-fallu-jah	**C**	*Rhizoctoina solani*	**MG654436.1**
5	Al-Nuaimiya	**D**	*Rhizoctoina solani*	**KY965394.1**
6	Heet	**E**	*Rhizoctoina solani*	**KY965394.1**
7	Al-Khalidiya	**F**	*Rhizoctoina solani*	**AJ318420.1**
8	Al-Amiriya 2	**A2**	*Fusarium Kerato-plasticum*	**KY965394.1**
9	Heet	**A3**	*Rhizoctoina solani*	**MF440630.1**

Table 3: Fungi associated with potato root rot diagnosed by PCR technique.

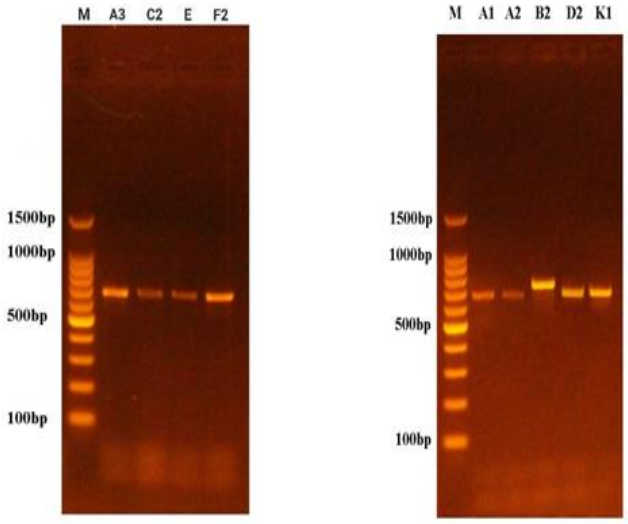

Figure 2: Results of ITS gene amplification of fungal species on Agarose Gel.

The pathogenicity test of some fungi isolates and their effect on the germination of radish seeds on the culture medium Water agar (W.A.)

Results showed in Table (4) that all tested fungi isolates tested on radish seeds were isolates of *Rhizoctonia* spp. and isolates of *Fusarium* spp. It significantly reduced the germination of radish seeds on water agar (W.A.) culture media compared to the control treatment that was not contaminated with any of the tested isolates *Rhizoctonia*, in which the infection rate was 0%. The test also showed the variation of the isolates in their effect on the germination of radish seeds, and the most influential of them was the isolate *Rhizoctonia* taken from Al-Anbar, Heet region, in which the infection rate was 90%. In contrast, *Fusarium* isolate is the strongest in the Al-Saqlawiya region, which achieved a 90% infection rate. Results agreed with that mentioned, and y [20, 21].

Location	**Isolation code *Rhizoctonia***	**Infection ratio %**	**Isolation code *Fusarium***	**Infection ratio %**
Amiriyah	*Rhizoctonia* Rs1	83.334	*Fusarium* Fu1	**83.334**
Amiriyah 2	*Rhizoctonia* Rs2	80	*Fusarium* Fu2	**86.667**
Khalidiya	*Rhizoctonia* Rs3	80	*Fusarium* Fu3	**80**
Sadat Al-Fallujah	*Rhizoctonia* Rs4	76.667	*Fusarium* Fu4	**83.334**
Nuaimiya	*Rhizoctonia* Rs5	90	*Fusarium* Fu5	**83.334**
Heet	*Rhizoctonia* Rs6	76.667	*Fusarium* Fu6	**86.667**
Saqlawiyah	*Rhizoctonia* Rs7	83.334	*Fusarium* Fu7	**90**
	Control	0.00	Control	**0.00**

	LSD 0.817		**LSD 1.236**

Table 4: Effects of different isolates of *Rhizoctonia* spp. and *Fusarium* spp. in germination of Radish seeds on water agar medium.

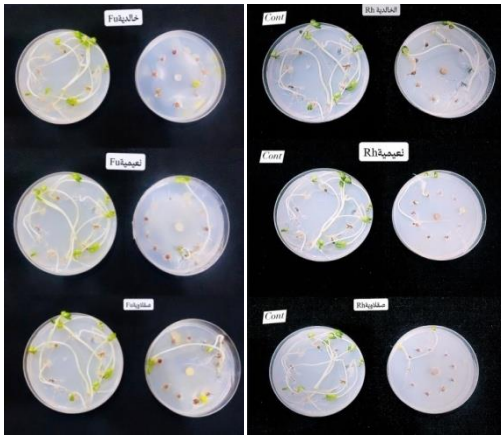

Figure 3: Fungus Rhizoctonia spp. and *Fusarium* spp. in germination of radish seeds on Water Agar media.

CONCLUSIONS

Potato root rot was observed as a disease in all sample collections. Two fungi, Rhizoctonia spp, mainly caused and *Fusarium* spp. according to the results of phenotypic and molecular diagnosis.

REFERENCES

1. Tunio M.H., Jianmin G., Sher A. S., Imran A. L., Waqar A. Q., Kashif A. S., and F. A. Chandio. 2020. Potato production in aeroponics: An emerging food growing system in sustainable agriculture for food security. Chilean Journal of Agricultural Research. 80: (1).
2. Nasir, M.W. and Toth, Z.2022. Effect of Drought Stress on Potato Production: A Review. Agronomy, 12, 635. https://doi.org/ 10.3390/ agronomy 12030635.
3. Kamar U. , Sami u., Shafi M. , Shakil A. P. , Razia S. , Amit H. , Chao W. and C. H. Jian. 2021. In vitro and silico approach of fungal growth inhibition by Trichoderma asperellum HbGT6-07 derived volatile organic compounds. Arabian Journal of Chemistry. Volume 14, Issue 9.
4. Vilvert E., Stridh L. , Andersson B., Olson K., Aldén L. and A. Berlin. 2022. Evidence-based disease control methods in potato production: a systematic map protocol. Environmental Evidence .11:6. https://doi.org /10.1186/ s13750-022-00259-x .
5. Bodah E.T. 2017. Root Rot Diseases in Plants: A Review of Common Causal Agents and Management Strategies. Agri Res & Tech: Open Access J 5(3): ARTOAJ.MS.ID.555661.
6. Nguyen, N. H., Song, Z., Bates, S. T., Branco, S., Tedersoo, L., Menke, J. 2016. FUN Guild is an open annotation tool for parsing fungal community datasets by ecological guild. Fungal Ecol. 20, 241–248. doi: 10.1016/ j. funeco. 2015.06.006.
7. Jiang, J., Yu, M., Hou, R., Li, L., Ren, X., Jiao, C. 2019. Changes in the soil microbial community are associated with Panaxquin quefolius L. root rot diseases. Plant Soil 438, 143–156. doi: 10.1007/s11104-018-03928-4.

8. Giachero, M. L.; Declerck, S.; Marquez, N. 2022. Phytophthora Root Rot: Importance of the Disease, Current and Novel Methods of Control. Agronomy, 12, 610. https:// doi.org/ 10.3390/ agronomy 12030610.
9. Agrios , G. N. 2005. Plant Pathology . 5th Ed. Elsevier Inc. USA. 998 pp.
10. Barnett, H. L., and B. B.Hunter. 1998. Illustrated genera of imperfect fungi. The American Phytopathological Society. U.S. Department of Agriculture, Agricultural Research Service, Washington State University, Pullman. APS Press. USA. St. Paul, Minnesota USA. 218p.
11. Lee, Y.M., Y.K. Choi and B.R. Min. 2000. Molecular characterization of Fusarium solani and its form aespeciales based on sequences analysis of the internal transcribed spacer (ITS) region of ribosomal DNA. Mycobiology. 28(2): 82-88.
12. Alhussaini M.S , Moslem M.A , Alghonaim M.I., Al-Ghanayem A.A. , Al-Yahya A.A.I ,HefnyH.M. and A. M. Saadabi. 2016. Characterization of Cladosporium Species by Internal Transcribed Spacer - PCR and Microsatellites-PCR.Pak. J. Biol Sci.; 19(4): 143-157. doi: 10.3923 /pjbs . 143.157.
13. Bolkan, H.H. and Butler, E.E. 1974. Studies on Hetero karyosis Virulence of Rhizoctonia solani. Phytopathology, 64: 513-522.
14. Vatankhah M. , Saberi -Riseh R. , Eskandari M. M. and H. A. fzali. 2019. Evaluation of some fungicides for the control of Fusarium dry rot of potato. J. Crop Prot. 2019, 8 (3): 275 -285 .
15. El-kazzaz, M.K.; Ghoneim, K.E.; Agha, M.K.M.; Helmy, A.; Behiry, S.I.; Abdelkhalek, A.; Saleem, M.H.; Al-Askar, A.A.; Arishi, A.A.; Elsharkawy, M.M. 2022. Suppression of Pepper Root Rot and-Wilt Diseases Caused by Rhizoctonia solani and Fusarium oxysporum. Life, 12, 587. https://doi.org/10.3390/ life12040587 .
16. Errampalli, D. and Johnston, H. W. 2001. Control of tuber -born black scurf (Rhizoctonia solani) and common scab (Streptomyces scabies) of potato with a combination of sodium hypochlorite and thiophanate -methyl preplanting seed tuber treatment. Canadian Journal of Plant Pathology, 23: 68 -77.
17. Sandipan, P. B., Solanki, B. P., Patel, N. N., Patel, R. L., Verma, P. D. and Desai, H. R. 2016. Effect of different fungicides against dry rot pathogens of potato caused by Fusarium spp. under in vitro condition. Cercetari Agronomic in Moldova, 4 (168): 69 -74.
18. Cullen D.W. , I. K. Toth, Y. Pitkin, N. Boonham, K. Walsh, I. Barker, and A. K. Lees. 2005. Use of Quantitative Molecular Diagnostic Assays to Investigate Fusarium Dry Rot in Potato Stocks and Soil. Phytopathology. DOI: 10.1094/ 95-1462·
19. Ghosh R. , Tarafdar A. and Sharma M. 2017. Rapid and sensitive diagnoses of dry root rot pathogen of chickpea (Rhizoctonia bataticola (Taub.) Butler using loop-mediated isothermal amplification assay. SCIenTIfICREPOrTS | 7:42737 | DOI: 10.1038/ srep42737 .
20. Majumdar, R.; Strausbaugh, C.A.; Galewski, P.J.; Minocha, R.; Rogers, C.W.2022. Cell-Wall-Degrading Enzymes-Related Genes Originating from Rhizoctonia solani Increase Sugar Beet Root Damage in the Presence of Leuconostocmes enteroides. Int. J. Mol. Sci. 2022, 23, 1366. https://doi.org/ 10.3390/ijms23031366.
21. Abo-Elyousr, K.A.M.; Ali, E.F.; Sallam, N.M.A.2022. Alternative Control of Tomato Wilt Using the Aqueous Extract of Calotropisprocera. Horticulturae , 8, 197. https:// doi.org/ 10.3390/ horticulturae. 8030197
22. Cullen, D.W., Toth, I.K., Pitkin, Y., Boonham, N., Walsh, K., Barker, I. and Lees, A.K.,. Use of quantitative molecular diagnostic assays to investigate Fusarium dry rot in potato stocks and soil. *Phytopathology*, **2005**, *95*(12), pp.1462-1471·

23. Ghosh, R., Tarafdar, A. and Sharma, M., Rapid and sensitive diagnoses of dry root rot pathogen of chickpea (Rhizoctonia bataticola (Taub.) Butler) using loop-mediated isothermal amplification assay. *Scientific reports*, **2017**, *7*(1), pp.1-12.
24. Ameen M. Shaman , Th. T. Mohammed. Effect Using Feed Additives Instead of Imported Premixes Affects the Physiology of Broiler Chickens. IOP Conference Series: Earth and Environmental Science.2023, 1262, 072080. https://doi.org/10.1088/1755-1315/1262/7/072080.
25. A. Jassim, A., I. Al-Jugifi, W. Gradually Increasing In Lighting Intensity On Characteristics Of Ross 308 Broiler Carcass And Some Internal Organs. Anbar Journal Of Agricultural Sciences, 2023; 21(1): 205-213. doi: 10.32649/ajas.2023.179730.
26. Abo-Elyousr, K.A., Ali, E.F. and Sallam, N.M., Alternative Control of Tomato Wilt Using the Aqueous Extract of Calotropis procera. *Horticulturae*, **2022**., *8*(3), p.197..

Received: October 9th 2023/ **Accepte**d: January 15th 2024 / **Published:**15 February 2024

Citation: A'shour, S.; Farhan, T. Identification or Diagnosis of Fungi that Cause Potato Root Rot. Revis Bionatura 2024; 9 (1) 51. http://dx.doi.org/10.21931/RB/2024.09.01.51

Additional information Correspondence should be addressed to saj20g7013@uoanbar.edu.iq.
Peer review information. Bionatura thanks anonymous reviewer(s) for their contribution to the peer review of this work using https://reviewerlocator.webofscience.com/

Bionatura ISSN. First 13909355 Ecuador. **Scopus coverage years**: from 2016 to the present

Bionatura
Ibero-American Journal of Biotechnology and Life Sciences

Article

Root-shoot ratio and its relationships with physiological characteristics, growth and biomass yield of *Gynura procumbens* under different shade levels and plant density

Omar Ali Ahmed[1,2], Martini Mohammad Yusoff[1], Azizah Misran[1], Puteri Edaroyati Megat Wahab[1] and Qusay Abdualhamza Muttaleb[1,3]**

[1]Department of Crop Science, Faculty of Agriculture, Universiti Putra Malaysia, 43400 Serdang, Selangor, Malaysia.
[2]Department of Crop Science, Faculty of Agriculture, University of Diyala, Iraq. ORCID
[3]Technical Institute of Babylon, Al-Furat Al-Awsat Technical University (ATU), Iraq. ORCID
** Correspondence: omerahmed@uodiyala.edu.iq*
Available from. http://dx.doi.org/10.21931/RB/2024.09.01.52

ABSTRACT

Gynura procumbens is one of the most common medicinal plants in the Asteraceae family, with extensive pharmacological properties. The experiment was conducted to evaluate the effects of different shade levels (0 and 30% shade) and plant density (9, 15, and 25 plants m-2) on root-shoot ratio and it is a relationship with physiology, growth, and biomass yield using split-plot design with three replications. Increasing shade level to 30% shade significantly decreased root-shoot ratio (RSR) by22.54%, while total leaf dry weight per plant (TLDW) and total leaf dry weight per square meter (TLDW m-2) increased by 35.64, 11.58, and 32.18%, respectively due to negative correlation with RSR. Increasing plant density from 9 to 25 plants m-2 significantly increased RSR and TLDW m-2 by 67.71 and 18.54%, respectively, while TLDW decreased by 57.31%. There was a negative correlation between RSR and biomass yield per plant. Under stressed conditions (full sunlight and high plant density), G. procumbent plants appeared to change strategy to absorb limited resources, allocate more biomass to the root system, and reduce above-ground parts' size to survive, resulting in high RSR.

Keywords: *Gynura procumbens*, shade, plant density, root-shoot ratio, physiology, growth, biomass.

INTRODUCTION

The *Gynura procumbens* is an evergreen medicinal shrub belonging to the Asteraceae family. It is widely distributed in Africa [1,2] and tropical regions of Southeast Asia and China [3,4]. It is non-toxic leaves have extensive pharmacological properties, including anti-diabetic, anti-hypertensive, antioxidant, and vasorelaxant activity [5]. The medicinal benefits of *G. procumbens* are related to its bioactive compounds, such as saponins, flavonoids, and terpenoids[4,6].

The root-shoot ratio (RSR) is the ratio of the below-ground biomass to the biomass of the aerial part reflected in plant biomass allocation. The differences in biomass allocation between the shoot and root systems would result in variations in the RSR ratio. The decrease in biomass under biotic and abiotic stress conditions is associated with the availability of resources above and below-ground, thereby resulting in trade-offs in biomass allocation between above-ground and below-ground biomasses, suggesting that plants allocate biomass to acquire the most limiting resources [7,8,9,10]. Many plants would change their RSR to respond to shading and low nutrient availability [11,12]. Therefore, RSR is vital in studying competitive interactions between different growth conditions [13].

Biomass allocation between above and below-ground parts results from long-term environmental modification, which significantly affects plant growth and reproduction plants [14,15,16]. The root biomass was less

affected by biomass allocation under stress conditions than shoot biomass, reflected in the plant RSR ratio [17]. The differences in RSR due to the differences in above and below-ground biomass indicate that different biomass exhibits various biomass allocation strategies. RSR for grass (4.23) was significantly higher than that of shrubs (1.68) and trees (0.40), and evergreen plants had higher RSR than deciduous plants in tropical rainforests [17].

Generally, the response of plants to light intensity depends on the type of plant, resulting in different concentrations of plant secondary metabolites [18]. Consequently, the medicinal properties of the target plants are affected, which also brings about changes in the morphology and physiology of the plants in question [19,20]. Changes in microclimate and light intensity due to shading of the canopy resulting from different plant densities also affected above and below-ground biomass [21].

Plant density or plant canopy is also a critical agronomic practice for effectively capturing environmental resources such as solar radiation, water, and nutrients [22], which can enhance optimum plant population [23] and influence the physiological and phytochemical characteristics of the plants. An increasing number of plants per unit area led to increased interplant competition for resources, resulting in the depletion of some limited resources. Plants allocated more biomass to roots in order to absorb more water and nutrients for survival and acclimatization under high competition or stress conditions [24,13]. Moreover, the competition for resources led to a change in biomass allocation in the plant, which resulted in a variation in RSR [25,26].

Therefore, understanding the effects of different environmental conditions on the above- and below-ground biomass of *G. procumben*t plants through RSR helps improve the quality and quantity of medicinal plants to meet the high demand. Therefore, the present study was conducted to determine the RSR and its relationship to growth, physiological attributes, and biomass yield under different shade levels and plant densities of *G. procumbens.*

MATERIALS AND METHODS

Experimental design and treatments

The experiment was conducted in November 2017 in a split-plot design (main plots presented by shade levels; subplots presented by plant densities) with three replicates using wooden planting boxes (2 m × 1 m × 0.5 m). The two levels of shade used were 0 and 30% using custom-made polyethylene shade netting with three plant densities (9, 15 and 25 plants m^{-2}) using 9 plants m^{-2} = 33.3 × 33.3 cm, 15 plants m^{-2} = 20 × 33.3 cm and 25 plants m^{-2} = 20 × 20 cm, respectively were implemented.

Root: Shoot Ratio (RSR)

Root: shoot ratio (below-ground biomass to above-ground biomass) for each treatment was determined according to the following formula:

RSR = Total root dry weight / Total shoot dry weight

Net Photosynthesis Rate and Total Chlorophyll Content.

A portable photosynthesis system (LICOR-64001 LI-COR Inc., USA) measured the net photosynthesis rate between 0900 and 1100 hours.

Total leaf chlorophyl1 content was also measured using a modified method of Lichtentaler and Wellburn (1983). Leaf weighing 0.2 g were collected from plant samples and stored in small plastic vials containing 20 mL of 80% (v/v) acetone. Absorbance was measured using a scanning spectrometer Model UV 3101 PC, and the total chlorophyll was calculated as the sum of chlorophyll *a* and chlorophyll *b* using the following.

Chlorophyll *a* = 11.75 (Absorbance 662) − 2.350 (Absorbance 645)

Chlorophyll b = 18.61 (Absorbance 645) − 3.960 (Absorbance 662)

Leaf area and Leaf area index.

A leaf area meter (LI-3100 Area Meter, USA) measured the total leaf area of all harvested leaves (TLA, cm2). The leaf area index (LAI) for each sample was computed after measuring the TLA and area of each plant using the following formula:

LAI = TLA (cm^2) / Soil area (cm^2)

Biomass dry weight.

The plants were harvested to measure the biomass yield of leaves per plant and square meter. Three plants per treatment were harvested. Fresh samples were oven-dried at 45 °C until a constant weight of dry samples was achieved. An electronic balance (BP 2100, Sartorius, Germany) was used to determine the total dry leaf weight per plant and the dry leaf weight per square meter.

Crop growth rate (CGR)

Was measured using the formula, CGR = (W2 – W1) / (t2 – t1), where W1= total dry weight of plant at time 1 (t1) and W2= total dry weight of plant at time 2 (t2).

Statistical data analysis

Data collected were subjected to statistical analysis of variance (ANOVA) for split-plot design using the SAS program (SAS version 9.4, Car, NC) to determine the statistical significance of main and interaction effects. Significant main effects means were separated using Least Significant Differences (LSD) ($P \leq 0.05$). Only the main effect comparisons were performed if an interaction between shade levels and plant density was insignificant. The relationship between parameters was determined using correlation analysis.

RESULTS

Root-shoot ratio (RSR)

Shade and plant density significantly affected the root-shoot ratio (RSR). The RSR of *G. procumbens* decreased by 30.09% with increasing shade levels from 0 to 30% (Figures 1-A). The percentage of increment of RSR at high plant density was 67.71 and 33.33 % compared with 9 and 15 plant m^{-2}, respectively (Figures 1-B).

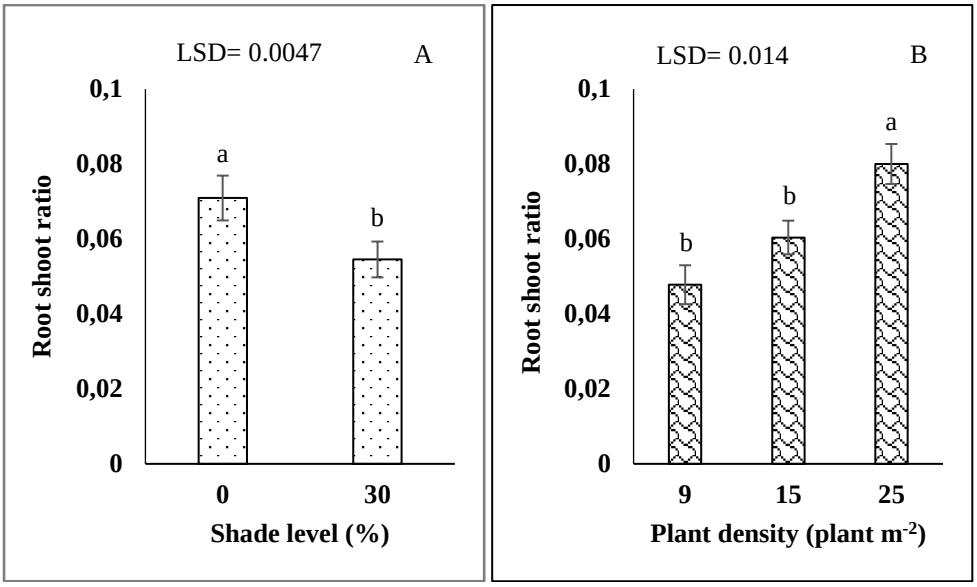

Figure 6.1: Effects of shade levels (A) and plant density (B) on *G. procumbens* root-shoot ratio.

There were significant interaction effects of plant density and plant age on the RSR of *G. procumben*t plants (Figure 6.2). The high value of RSR was 0.134 under all plant densities at 0 DAT. Regardless of plant density, the RSR decreased to 72.38% with increasing plant age from 0 to 30 days after transplanting. At 30 days after transplanting, the RSR increased by 27.4% at low plant density (9 plants m^{-2}) than at high plant density (25 plants m^{-2}). On the other hand, at 60 DAT, the high plant density (25 plants m^{-2}) increases RSR by (42.45 and 33.34%) more than both 9 and 15 plants m^{-2}. The percentage of increment in RSR at high plant density (25 plants m^{-2}) at 60 DAT was 52.0% as compared with 30. In addition, the RSR increased with increased plant density and plan age from 60 to 90 DAT. At 90 DAT, the RSR increased by 67.39% at high plant density (25 plants m^{-2}) compared with low plant density (9 plants m^{-2}). The result demonstrated no significant differences between 30, 60 and 90 DAT on RSR under low plant density. At the same time, the result showed that the RSR, after 30 days of transplanting, started to increase with increasing plant age under both 15 and 25 plants m^{-2} (Figure 6.2).

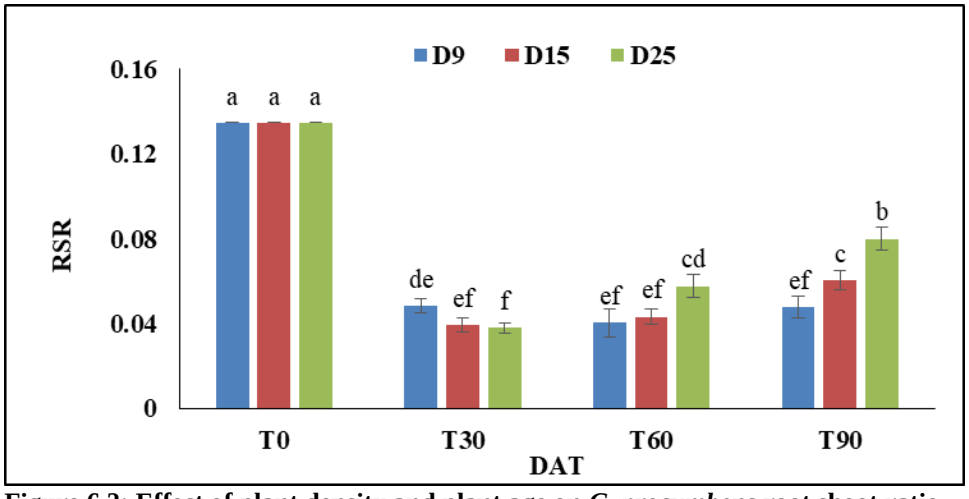

Figure 6.2: Effect of plant density and plant age on *G. procumbens* root shoot ratio.

Net photosynthesis rate (PN)

Different shade levels and plant densities had significant effects on net photosynthesis rate (P*N*) ($P \leq 0.05$) (Table 1). Thirty percent shade level increased net photosynthesis rate by 12.16% in comparison with zero level of shade. In contrast, *G. procumbens*' net photosynthesis rate decreased markedly to 20.12% when planted at 25 plants m^{-2}, whereas a density of 9 plants m^{-2} resulted in the highest net photosynthesis rate.

According to the correlation result, the net photosynthesis rate response to the studying factors was the opposite of the RSR response (Table 4).

*Total chlorophyll (a+b)***)**
Shade and plant density had significant effects (P≤0.05) on total chlorophyll content *Chl (a+b)* (Table.1). High shade level of 30% showed higher total chlorophyll *Chl (a+b)* (19.30 mg g^{-1} FW). In contrast, lower shade levels recorded the lowest total chlorophyll (16.85 mg g^{-1} FW). Higher plant density of 25 plants m^{-2} displayed lower total chlorophyll content *Chl (a+b)* (16.61 mg g^{-1} FW) in comparison with control (19.81 mg g^{-1} FW) of 9 plants m^{-2}. The increase in total chlorophyll content in the *G. procumbens* plant was accompanied by a decrease in RSR due to the result of the coefficient of variation analysis (Table 4).

Shade level (S) (%)	**P*N***	**Chl**	**LA**	**LAI**
0	12.38 b	16.85 b	4554.74 b	6.94 b
30	13.89 a	19.31 a	6336.86 a	9.45 a
Density (D) (plant m^{-2})				
9	14.56 a	19.81a	6851.62 a	6.17 c
15	13.21 a	17.81 b	5297.56 b	7.95 b
25	11.63 c	16.62 c	4188.22 c	10.47 a
S×D	ns	ns	ns	ns

Means with the same letters in the same columns are not significantly different at p < 0.05 (LSD); ns = insignificant.
Table 1: Effects of shade levels and plant density on *G. procumbens* net photosynthesis rate (P*N*), total chlorophyll content (Chl), leaf area (LA) and leaf area index (LAI).

Leaf area (LA)
Shade levels and plant density had significant effects (P≤0.05) on the leaf area of G. procumbens plants (Table 1). The result showed shade effects were more visible on leaf area (6336.86 cm2) when plants were grown under 30% shade level. However, under full sunlight (0% shade), plants had leaf area at the lowest level (4554.71 cm2). The leaf area increased by 39.12% under 30% shade compared to 0%. On the other hand, low plant density (9 plants m-2) had higher leaf area (6851.62 cm2) than 15 plants m-2 (5297.56 cm2) and 25 plants m-2 (4188.23 cm2) densities, as shown in Table 2. There was an inverse relation between leaf area and RSR in G. procumbens due to their strong negative correlation (Table .4).

Leaf area index (LAI)
Shade level and plant density significantly affected the leaf index of G. procumbens (Table 1). There was an increase in leaf area index under 30% shade level by 36.16% compared with the control 0% shade. The results showed a linear increase in leaf area index with an increase in the number of plants grown per unit area. It increased around 28.85 and 69.69% for 15 and 25 plants grown per square meter, respectively, in comparison with 9 plants m-2. There was no correlation between LAI and RSR in G. procumbens (Table 6.4).

Fresh and dry weight
Total leaf fresh weight per plant (TLFW)

Total leaf fresh weight per plant was significantly affected by different levels of shade and total number of plants growing per unit area (plant density) (P≤0.05) as presented in (Table.2). Higher level of shade (30%) linearly increased leaf fresh weight of G. procumbens by 32.39% plant-1 in relation to control (0% shade). On the contrary, plant density decreased total leaf fresh weight from 26.54 to 40.75% as plant density increased from 15 to 25 plants m-2 compared to 9 plants m-2. A strong negative correlation existed between total leaf fresh weight per plant and RSR in G. procumbens (Table 6.4).

Total leaf fresh weight per square meter (TLFW m-2)

Shade levels and plant density had significant effects on leaf fresh weight per unit area (P≤0.05) (Table 2). The results revealed that the total leaf fresh weight of G. procumbens per square meter increased as shade level and plant density increased. The corresponding increase values were 26.8% for a 30% level of shade compared to 0% shade and 22.44 and 64.55% for a plant density of 15 and 25 plants m-2 compared to 9 plants m-2, respectively.

Total fresh weight per plant (TFW)

Shading and plant density had significant effects (P≤0.05) on total fresh weight per plant (Table 2). There was an increase of 37.64% with an increase in shade level from 0 to 30%. Results showed that total fresh weight per plant considerably decreased with the increase of plant density from 9 to 15 and 25 plants m-2 densities. The total fresh weight of plants decreased by 26.47 and 41.95% at 15 and 25 plants m-2 than 9 plants m-2, respectively. The total fresh weight per plant inversely responded to shade level and plant density more than RSR due to their strong negative correlation (Table 4).

Total fresh weight per square meter (TFW m-2)

Total fresh weight per square meter was significantly affected by different levels of shading and plant density (Table 2). Total fresh weight increased by 33.71% when G. procumbens plants were subjected to 30% shade than complete sun treatment. Consequently, the same parameter increased by 22.55 and 61.25% at 15 and 25 plants m-2, respectively, as compared with low plant density (9 plants m-2).

Shade level (S) (%)	**TLFW**	**TLFW/m^2**	**TFW**	**TFW/m^2**
0	278.99 b	4279.21 b	454.21 b	6888.71 b
30	369.37 a	5425.13 a	625.20 a	9211.43 a
Density (D) (plant m^{-2})				
9	417.93 a	3761.39 b	699.16 a	6292.44 c
15	307.03 b	4605.43 b	514.08 b	7711.22 b
25	247.59 b	6189.70 a	405.86 c	10146.56 a
S×D	ns	ns	ns	ns

Means with the same letters in the same columns are not significantly different at p < 0.05 (LSD); ns = not significant

Table 2: Effects of shade levels and plant density on G. procumbens total leaf fresh weight (TLFW), total leaf fresh weight per square meter (TLFW/m2), total fresh weight (TFW), and total fresh weight per square meter (TLW/m2).

Total leaf dry weight per plant (TLDW)

Total leaf dry weight per plant were significantly affected by different levels of shading and plant density (Table.3). level of 30% shade resulted in higher total leaf dry weight per plant than under control, with a percentage increase of 35.63%. In contrast, the total leaf dry weight per plant decreased with an increase in plant density. The reductions were 29.28 and 57.31% when G. procumbens plants were grown at 15 and 25

plants m-2 densities compared with 9 plants m-2. There was an inverse relationship between total leaf dry weight per plant and RSR in G. procumbens due to their strong negative correlation (Table .4).

Total leaf dry weight per square meter (TLDW m-2)
Different shade levels and plant density significantly affected total leaf dry weight per square meter (Table 3). Total leaf dry weight per square meter increased by 32.17% under 30% shade than under control. In contrast, the total leaf dry weight of G. procumbent plant per square meter increased by 18.54% with an increase in plant density from 9 to 25 plants m-2, without any differences between 25 and 15 plant m-2.

Total dry weight per plant (TDW)
Different shade levels and plant densities significantly affected the total dry weight per plant for G. procumbens (Table 3). The result shows an increase in total dry weight per plant by 34.92% under 30% shade compared to 0%. Conversely to the above results, higher plant densities of 15 and 25 plants m-2 reduced total dry weight by 29.82 and 52.92% compared with low plant densities of 9 plants per square meter. The total dry weight per plant in G. procumbens was inversely related to studying factors other than RSR due to their strong negative correlation (Table 4).

Shade level (S) (%)	**TLDW**	**TLDW/ m^2**	**TShDW**	**TRDW**	**TDW**	**TDW/m^2**	**CGR**
0	26.21 b	377.41 b	50.08 b	3.28 a	53.36 b	775.53 b	0.59 b
30	35.55 a	498.85 a	68.54 a	3.45 a	71.99 a	1030.04 a	0.80 a
Density (D) (plant m^{-2})							
9	43.41 a	390.69 b	82.80 a	3.75 a	86.54 a	778.89 b	0.96 a
15	30.70 b	460.55 a	57.34 b	3.40 a	60.73 b	911.00 ab	0.67 b
25	18.53 c	463.14 a	37.79 c	2.95 a	40.74 c	1018.46 a	0.45 c
S×D	ns	ns	ns	ns	ns	ns	ns

Means with the same letters in the same columns are not significantly different at $p < 0.05$ (LSD); ns = not significant
Table 3: Effects of shade levels and plant density on G. procumbens total leaf dry weight (TLDW), total leaf dry weight per square meter (TLDW/m2), total shoot dry weight (TShDW), total root dry weight (TRDW), total dry weight (TDW), total dry weight per square meter (TDW/m2), and crop growth rate (CGR).

Total dry weight per square meter (TDW m-2)
Shading and plant density significantly affected the total dry weight per square meter (TDW) of G, procumbens (Table 3). Shading of 30% recorded higher total dry weight per square meter compared to 0% shade when it increased by 32.81% compared to full sunlight (0% shade). Total dry weight per square meter rose with the increase in plant density. The higher plant density of 25 plants m-2 recorded a higher total dry weight per square meter of 30.75% compared with 9 plants m-2. No correlation existed between total dry weight per square meter of G, procumbens and RSR (Table .4).

Crop growth rate (CGR)
Crop growth rate (CGR) showed high effects by both shading and the number of plants per unit area (Table 3). The crop growth rate increased by 35.06% under a 30% level of shade. Density at 9 plants m-2 reported a

higher CGR value (0.959 g day-1) in comparison with (0.67 and 0.45 g day-1) at density levels of 15 and 25 plants m-2, respectively. There was an inverse relationship between crop growth rate and RSR (Table .4).

	RSR	***PN***	Chl	LA	LAI	TFW	LDW	LDW m^2	RDW	TDW	TDW m^{-2}	CGR
RSR	-	-0.83 ***	-0.77 **	-0.84 ***	0.26 ns	-0.83 ***	-0.86 ***	-0.18 ns	-0.33 ns	-0.88 ***	-0.06 ns	-0.88 ***
PN		-	0.73 **	0.80 ***	-0.25 ns	0.80 ***	0.84 ***	0.24 ns	0.32 ns	0.84 ***	0.05 ns	0.84 ***
Chl			-	0.81 ***	-0.23 ns	0.78 **	0.80 ***	0.19 ns	0.51 *	0.81 ***	0.03 ns	0.81 ***
LA				-	-0.06 ns	0.96 ***	0.91 ***	0.31 ns	0.54 *	0.93 ***	0.18 ns	0.94 ***
LAI					-	-0.13 ns	-0.36 ns	0.67 **	-0.37 ns	-0.31 ns	0.86 ***	-0.32 ns
TFW						-	0.96 ***	0.33 ns	0.58 *	0.97 ***	0.16 ns	0.97 ***
LDW							-	0.23 ns	0.63 *	0.99 ***	-0.001 ns	0.99 ***
LDW m^2								-	0.06 ns	0.22 ns	0.92 ***	0.22 ns
RDW									-	0.60 *	-0.16 ns	0.60 *
TDW										-	0.04 ns	0.99 ***
TDW m^{-2}											-	0.03 ns
CGR												-

Table 4: Correlation coefficient (r) between photosynthesis rate (PN), chlorophyll content a+b (Chl), leaf area (LA), leaf area index (LAI), total fresh weight (TFW), total leaf dry weight (TLDW), total leaf dry weight per square meter (TLDW m^{-2}), total root dry weight (TRDW), total dry weight (TDW), total dry weight per square meter (TDW m^{-2}), and crop growth rate (CGR) of G. procumbens under different shade levels and plant density. Ns, insignificant. *, significant at P<0.05, **, P<0.01. ***, P<0.001

DISCUSSION

The root-shoot ratio reflects the differences in biomass allocation between above-ground and below-ground associated with climatic conditions, resulting in root/shoot competition and cooperation about resources for adaptation and survival in variable and complex conditions[27,28]. The shoot-root system plays an essential role in plant development and productivity as well as the photosynthetic process and, finally, the growth and maintenance of roots[29-33].

The reduction in total root dry weight TRDW by 21.33% with increasing plant density from (9 to 25 plants m^{-2}) (Table. 3), while total shoot dry weight TShDW was reduced by 54.35%, which proved that roots (below-ground part) were less affected by study factors than shoot (above-ground part) which resulted in increased RSR due to inverse relationship between RSR and TShDW (above-ground part). On the other hand, increasing the shade level from full sunlight (0% shade) to 30% shade increased the above-ground part (TShDW) by 36.86%; however, the below-ground part (root system) increased by 5.18% only, which demonstrated that under optimum light condition, *G. procumbens* plants allocated more biomass to aerial part than root. Improvement of wheat grain yield was associated with the dry matter distribution ratio between aerial parts and the root system under drought conditions[34]. Root systems consume double assimilation products than aerial

parts[36]. The results demonstrated that the root (below-ground part) of *G. procumbent* plants was less affected by shade level and plant density.

The high values of RSR of *G. procumbens* under high plant density are in agreement with Ericsson[36], who reported that high competition of resources between plants under high plant density resulted in high RSR due to differences in dry matter allocation when the low nutrient resource inhibits plant growth. Similarly, the results of 37 and 38 demonstrated that the root-shoot ratio of plants growing in variable patchy soil nutrient conditions was smaller than those in stable soil nutrient conditions, which promoted more fine root growth than a variable one. Dolt[39] *et al*. elucidated that the increase in biomass of *B. erectus* under high density was superior in exploiting surplus light and the increase in available below-ground resources.

Similar findings were reported by Martins[40], who illustrated the shoot contribution to root growth even when shoot growth is inhibited due to a severe reduction in shoot development without any effect on root growth on tomato plants. Under limited exogenous resources, plants allocate more biomass to those organs that absorb the scarcest resources[28]. Biomass allocation between above- and below-ground parts depends on adjusting C allocation[43], which results from long-term modification to the environmental conditions, which has critical effects on plant growth and reproduction[14-16].

Accordingly, increasing allocation to underground organs such as fine roots in place of above-ground parts indicates the growing relative importance of limiting soil resources, i.e., nutrients and/or water[42]. The root-shoot ratio increased with increasing plant density and decreased with increasing aerial biomass, stand age, and volume[34].

Higher reduction in TShDW than TRDW of *G. procumbens* plants, which resulted in high RSR, supported the optimal partitioning theory that referred to trade-offs in biomass allocation between above-ground and below-ground parts in order to acquire the most limiting resources[7-10]. According to Qi *et al.*[13], the various environmental conditions proved the optimal partitioning theory that the more significant growth and photosynthetic rates for deciduous plants than evergreen plants, RSR of evergreen plants (angiosperms) was significantly higher than deciduous plants (gymnosperms).

As plants grow larger and higher, they allocate more biomass to the above-ground components. However, more biomass yield would be needed in the root systems to acquire more water and nutrients for survival and acclimatization under different stress conditions. The differences in RSR of G. procumbent plants at different plant ages illustrated that in the first stage, the roots grew faster, and the plants allocated more biomass to the roots, resulting in the high value of RSR to stabilize the plants and absorb water and elements. Meanwhile, RSR, after 30 days of transplanting, started to grow slowly. This result parallels Qi *et al.*[13]'s findings, which reported that plants allocated more biomass to roots in the seedling stage or due to climatic conditions, soil fertility, and management practices[5,43,44].

Results of the present experiments showed that the highest net photosynthetic rate of G. procumbens was 13.89 µmol m^{-2} s^{-1} at 30% shade than 12.38 µmol m^{-2} s^{-1} at 0% shade (full sunlight) (Table 1). Net photosynthetic was negatively affected by excessive light under an open field due to photoinhibition[45].

Increasing plant density from 9 to 25 plants m^{-2} decreased the net photosynthetic rate by 20.12% (Table 1). Competition among plants increases with an increasing number of plants per unit area. These results agree with 47, which reported that a reduction in the photosynthetic rate of blessed thistle was associated with nitrogen reduction under high plant density. Hence, the net photosynthetic rate of *G. procumbent* plants decreased under full sunlight but at higher plant density.

The present study revealed a significant negative correlation (r = -0.83) between RSR and PN (Table 4). Under high light intensity (full sunlight) and high plant density, the net photosynthetic rate of *G. procumbens* is reduced as the plant responds to excessive light. Meanwhile, RSR increased under the same conditions because the root system was less affected by stress conditions than above-ground parts or plants, which allocated more biomass to the root than the shoot. For survival and multiplication, plants have to modify their distribution of photosynthetic to different organs for adaptation as it could impair other plants' functions such as photosynthesis, nutrient uptake, and growth[48]. A similar observation was also reported on wheat[34]. The findings align with 33,49, who reported that crops with higher grain yields due to partitioning more dry matter to above-ground parts have lower RSR. A high photosynthetic rate offsets the low RSR under low plant density. Low photosynthetic rate recorded under high plant density yielded high RSR as revealed in Compositae plants[50].

Increase chlorophyll content Chl (a+b) by increasing shade levels from full sunlight to 30%. It significantly decreased with increasing plant density from 9 to 25 plants m^{-2}. The percentage of increments of Chl a+b was 14.54%, with increasing shade levels from 0 to 30% shade. It decreased by 16.15% with increasing plant density from 9 to 25 plants m^{-2}. The decrease in total chlorophyll content under full sunlight compared to 30% shade may be related to chlorophyll pigment impairment due to absorbing excessive light energy[51].

On the other hand, shade and low light conditions caused chlorophyll content to increase as a physiological response to low light environment. This maximized available light utilization by channeling more resources into chlorophyll synthesis[51,52]. The plants regulated their chlorophyll synthesis to absorb more solar radiation for photosynthesis, and changes in irradiance level may elicit physiological responses at the level of leaf and chloroplast[53]. In addition, the low total chlorophyll content of *G. procumbens* under high plant density may be due to interplant competition for resources under high plant density. In the present study, an increase in plant density resulted in decreased chlorophyll content of high plant density, which led to the depletion of some resources and nutrients, especially nitrogen[47,54]. The results of the present experiment agree with those of other researchers[47,55,56].

There was a significant negative correlation (r = - 0.77) between RSR and total chlorophyll content (Table .4). The inverse relationship between them means that under stress conditions (high light intensity and plant density), *G. procumbent* plants allocated more biomass to root despite the low chlorophyll content. Decreased chlorophyll pigments as a response to full sunlight and a high number of plants per square meter to survive was offset by adverse response in the root system to water and nutrient supply. The findings in the present experiment align with results reported[61], which explained that decreased RSR was associated with high yield due to high photosynthetic rate and chlorophyll content, which accelerated the growth and development of above-ground parts.

Leaf area (LA) and leaf area index (LAI) were highly affected by shade levels and plant density. The treatment of 30% shade resulted in higher LA (6336.86 cm^2) and LAI (9.45) than the lowest under full sunlight. *G. procumbens* plants recorded the highest LA (6851.62 cm2) at low plant density than (4188.23 cm^2) recorded at high plant density (25 plants m^{-2}). At the same time, the highest LAI was (10.47) at high plant density than (6.17) at 9 plants m^{-2}. The results suggested that in order to absorb a high amount of light under low light conditions, *G. procumbent* plants increased leaf size as a physiological response. The results agree with those of other studies 58,59,60 which reported that plants under low light conditions maximize available leaf surface area by producing bigger and thinner leaves for interception of limited light incident. Also, wider intra-row spacing (45 cm) resulted in higher LA than (15 cm) in Thymus vulgaris L[61]. The increasing plant density from 20 to 25 plants m^{-2} led to higher LAI of soybean[66]. *G. procumbens* plants responded to low irradiance by increasing LAI to increase light penetration within the canopy to absorb more light resulting in higher biomass per unit area.

There was a significant negative correlation (r = -0.84) between LA and RSR, while there was no significant correlation (r = 0.26) between LAI and RSR (Table .4). The results showed that plants under stressed conditions modified size and biomass allocated between shoot and root system in order to survive. Leaf area decreased under full sunlight and high plant density, resulting in increased RSR due to a reduction in plant size compared to the root system. This reduction in LA was probably due to decreased leaf growth and expansion under stress conditions with nutrient deficiency[42,63,64].

The *G. procumbens* total leaf dry weight (TLDW), and total dry weight (TDW) per plant increased by 35.63 and 34.92% as the shade level increased from full sunlight to 30% shade. Also, total leaf dry weight per square meter (TLDW m^{-2}) and total dry weight per square meter (TDW m^{-2}) increased by 32.17 and 32.81% under 30% shade compared to 0% shade. At the same time, the low number of plants per square meter (9 plants m-2) resulted in higher TLDW and TDW g per plant, which were 43.41 and 86.54 g $plant^{-1}$, respectively. However, the higher TLDW m^{-2} and TDW m^{-2} were 463.14 and 1018.46 g m^{-2} at low plant density (25 plants m-2).

The present experiments showed a significant positive correlation between TLDW per plant and PN and LA (r = 0.84 and 0.92), respectively (Table 4). The results indicated higher biomass yield in individual plant under 30% shade and low plant density (9 plants m^{-2}) related to high photosynthesis rate and leaf area which resulted in high CGR due to the significant positive correlation between both CGR with PN and LA (r = 0.84 and 0.94)

(Table.4). When there were no stress conditions, the high LA and PN of *G. procumbens* resulted in high biomass per plant; however, under stress condition (high plant density) high biomass per square meter associated with high LAI. These results are in agreement with the finding of 24,65,66, which reported that optimal plant density enhances using of resources (radiation, water, and nutrients) due to optimal LAI, but decreased biomass in individual plants under high plant density was related to high competition for resources which result in low LA and low photosynthetic capacity.

The higher dry biomass yield per square meter under 30% shade and high plant density (25 plants m^{-2}) was associated with a significant positive correlation with LAI only (r = 0.86) (Table 4). This result indicated that the high biomass yield per square meter under 30% shade and high plant density was associated with high LAI. Shading conditions resulting from net shade or canopy under high-density produce higher biomass than open field conditions. The increasing water evaporation, canopy senescence, and increase in maintenance respiration in open fields than shade due to warmer temperatures led to a decrease in final biomass[67]. High plant density was a sustainable strategy to improve rice yield than low plant density, under full sunlight and 30% shade[67]. The condition that results from an increasing number of plants per unit area is favorable for producing a high biomass of *G. procumbens*.

The present results agree with a number of other previous studies[57,59,68]. There was a significant negative correlation (r = -0.83, - 0.89, and – 0.88) between (TFW, TShDW, and TDW) with RSR, respectively (Table 4). The increase in shade level from 0 to 30% shade resulted in an increase of TFW, TShDW, and TDW by 37.64, 36.86, and 34.92%, while RSR decreased by 23.13%. On the other hand, an increasing the number of plants per unit area from 9 to 25 plants m^{-2} resulted in decreased TFW, TShDW, and TDW by 41.95, 54.35, and 52.92%, but RSR increased by 67.71%. Under 30% shade and low plant density (9 plants m^{-2}), *G. procumbens* plants allocated more biomass to the aerial part than root. In contrast, with increasing light intensity (no shade) and the high number of plants per square meter, plants allocated more biomass to root as a physiological response to stress conditions to survive. The contrast between biomass yield and RSR is associated with a negative relationship between RSR and (photosynthetic rate, LA, and number of branches).

CONCLUSIONS

The current study has demonstrated that the higher *G. procumbens* biomass per plant, which had a negative correlation with RSR, was under 30% shade and 9 plants per square meter due to more biomass allocated to the above-ground part at 30% shade and low plant density. Meanwhile, under full sunlight and high plant density, *G. procumbens* plants allocated more biomass to below-ground parts, which resulted in low biomass and high RSR value. Low biomass yield, high RSR under full sunlight (0 % shade), and high plant density are associated with low photosynthesis rate, chlorophyll content, and leaf area—higher biomass per unit area under 25 plants per square meter is associated with high LAI. Under stress conditions, *G. procumbent* plants change their biomass allocation strategy to absorb limited resources due to surviving by the reduced size of above-ground parts rather than root, which resulted in high RSR.

REFERENCES

1. Rahman, A., & Al Asad, M. S. (2013). Chemical and biological investigations of the leaves of Gynura procumbens. International Journal of Biosciences, 3(4), 36–43.
2. Sukadeetad, K., Nakbanpote, W., Heinrich, M., & Nuengchamnong, N. (2018). Effect of drying methods and solvent extraction on the phenolic compounds of Gynura pseudochina (L.) DC. Leaf extracts and their anti-psoriatic property. Industrial Crops and Products, 120, 34–46.
3. Li, X., Schmid, B., Wang, F., & Paine, C. E. T. (2016). Net assimilation rate determines the growth rates of 14 species of subtropical forest trees. PloS One, 11(3), e0150644.
4. Mou, P., Jones, R. H., Tan, Z., Bao, Z., & Chen, H. (2013). Morphological and physiological plasticity of plant roots when nutrients are both spatially and temporally heterogeneous. Plant and Soil, 364(1–2), 373–384.

5. Rohin, M. A. K., Jumli, M. N., Ridzwan, N., Baig, A. A., Latif, A. Z. A., & Hadi, N. A. (2018). Effect of Gynura procumbens extracts on anti-proliferative activity and its associated morphological changes of human Glioblastoma multiforme cell line (U-87). Pharmacognosy Journal, 10(3), 492-496.
6. Tan, H. L., Chan, K.-G., Pusparajah, P., Lee, L.H., & Goh, B.H. (2016). Gynura procumbens: an overview of the biological activities. Frontiers in Pharmacology, 7, 52
7. Hertel, D., Strecker, T., Müller-Haubold, H., & Leuschner, C. (2013). Fine root biomass and dynamics in beech forests across a precipitation gradient–is optimal resource partitioning theory applicable to water-limited mature trees?. Journal of Ecology, 101(5), 1183-1200.
8. Kobe, R. K., Iyer, M., & Walters, M. B. (2010). Optimal partitioning theory revisited: nonstructural carbohydrates dominate root mass responses to nitrogen. Ecology, 91(1), 166–179.
9. Tredennick, A. T., Adler, P. B., Grace, J. B., Harpole, W. S., Borer, E. T., Seabloom, E. W., Anderson, T.M., Bakker, J. D., Biederman, L. A., Brown, C. S., & Brown, C. S. (2016). Comment on Worldwide evidence of a unimodal relationship between productivity and plant species richness. Science, 351(6272), 457.
10. Ledo, A., Paul, K. I., Burslem, D. F. R. P., Ewel, J. J., Barton, C., Battaglia, M., Brookshank, K., Carter, J., Eid, T. H., England, J. R., & Fitzgerald, A. (2018). Tree size and climatic water deficit control root to shoot ratio in individual trees globally. New Phytologist, 217(1), 8–11.
11. Aphalo, P. J., Ballare, C. L., & Scopel, A. L. (1999). Plant-plant signalling, the shade-avoidance response and competition. Journal of Experimental Botany, 50(340), 1629–1634.
12. Reynolds, H. L., & D'antonio, C. (1996). The ecological significance of plasticity in root weight ratio in response to nitrogen: opinion. Plant and Soil, 185(1), 75–97.
13. Qi, Y., Wei, W., Chen, C., & Chen, L. (2019). Plant root-shoot biomass allocation over diverse biomes: A global synthesis. Global Ecology and Conservation, 18, e00606.
14. Brown, S. (2002). Measuring carbon in forests: current status and future challenges. Environmental Pollution, 116(3), 363–372.
15. Houghton, R. A. (2005). Aboveground forest biomass and the global carbon balance. Global Change Biology, 11(6), 945–958.
16. Kang, M., Ji, W., & Jiang, Y. (2012). Responses of belowground biomass and biomass allocation to environmental factors in central grassland of Inner Mongolia. Acta Agrestia Sinica, 20(2), 268–274.
17. Wang, X., Fang, J., & Zhu, B. (2008). Forest biomass and root–shoot allocation in northeast China. Forest Ecology and Management, 255(12), 4007–4020.
18. Gu, X.-D., Sun, M.-Y., Zhang, L., Fu, H.-W., Cui, L., Chen, R. Z., Zhang, D. W., & Tian, J. K. (2010). UV-B induced changes in the secondary metabolites of Morus alba L. leaves. Molecules, 15(5), 2980–2993.
19. Briskin, D. P., & Gawienowski, M. C. (2001). Differential effects of light and nitrogen on production of hypericins and leaf glands in Hypericum perforatum. Plant Physiology and Biochemistry, 39(12), 1075–1081.
20. Kurata, H., Matsumura, S., & Furusaki, S. (1997). Light irradiation causes physiological and metabolic changes for purine alkaloid production by a Coffea arabica cell suspension culture. Plant Science, 123(1–2), 197–203.
21. Dolt, C., Goverde, M., & Baur, B. (2005). Effects of experimental small-scale habitat fragmentation on above-and below-ground plant biomass in calcareous grasslands. Acta Oecologica, 27(1), 49–56.
22. Singh, R. D., Meena, R. L., Singh, M. K., Kaul, V. K., Lal, B., Acharya, R., & Prasad, R. (2006). Effect of manure and plant spacing on crop growth, yield and oil-quality of Curcuma aromatica Salisb. in mid hill of western Himalaya. Industrial Crops and Products, 24(2), 105–112.
23. Rossini, M. A., Maddonni, G. A., & Otegui, M. E. (2011). Inter-plant competition for resources in maize crops grown under contrasting nitrogen supply and density: Variability in plant and ear growth. Field Crops Research, 121(3), 373–380.
24. Wang, R., Cheng, T., & Hu, L. (2015). Effect of wide–narrow row arrangement and plant density on yield and radiation use efficiency of mechanized direct-seeded canola in Central China. Field Crops Research, 172, 42-52.

25. Gersani, M., Brown, J. S., O'Brien, E. E., Maina, G. M., & Abramsky, Z. (2001). Tragedy of the commons as a result of root competition. Journal of Ecology, 89(4), 660–669.
26. Brien, E. E., Gersani, M., & Brown, J. S. (2005). Root proliferation and seed yield in response to spatial heterogeneity of below-ground competition. New Phytologist, 168(2), 401–412.
27. Hermans, C., Hammond, J. P., White, P. J., & Verbruggen, N. (2006). How do plants respond to nutrient shortage by biomass allocation? Trends in Plant Science, 11(12), 610–617.
28. Marschner, H. (1995). Mineral Nutrition of Higher Plants. Second Edition Academic Press Edition London.
29. Araya, T., von Wirén, N., & Takahashi, H. (2016). CLE peptide signaling and nitrogen interactions in plant root development. Plant Molecular Biology, 91(6), 607–615.
30. Manschadi, A. M., Hammer, G. L., Christopher, J. T., & Devoil, P. (2008). Genotypic variation in seedling root architectural traits and implications for drought adaptation in wheat (Triticum aestivum L.). Plant and Soil, 303(1–2), 115–129.
31. Osaki, M., Shinano, T., Matsumoto, M., Zheng, T., & Tadano, T. (1997). A root-shoot interaction hypothesis for high productivity of field crops. In Plant Nutrition for Sustainable Food Production and Environment (pp. 669–674). Chap, Springer.
32. Yang, C., Yang, L., Yang, Y., & Ouyang, Z. (2004). Rice root growth and nutrient uptake as influenced by organic manure in continuously and alternately flooded paddy soils. Agricultural Water Management, 70(1), 67–81.
33. Zhang, H., Xue, Y., Wang, Z., Yang, J., & Zhang, J. (2009). Morphological and physiological traits of roots and their relationships with shoot growth in "super" rice. Field Crops Research, 113(1), 31–40.
34. Zhang, X., Chen, S., Sun, H., Pei, D., & Wang, Y. (2008). Dry matter, harvest index, grain yield and water use efficiency as affected by water supply in winter wheat. Irrigation Science, 27(1), 1–10.
35. Passioura, J. B. (1983). Roots and drought resistance. In Developments in Agricultural and Water Management, 7(1-3), 265-280.
36. Ericsson, T. (1995). Growth and shoot: root ratio of seedlings in relation to nutrient availability. In Nutrient uptake and cycling in forest ecosystems (pp. 205–214). Chap, Springer.
37. Maskova, T., & Herben, T. (2018). Root: shoot ratio in developing seedlings: How seedlings change their allocation in response to seed mass and ambient nutrient supply. Ecology and Evolution, 8(14), 7143–7150.
38. Mou, K. M., & Dash, P. R. (2016). A Comprehensive Review on Gynura Procumbens Leaves. International Journal of Pharmacognosy, 3(4), 167–174.
39. Martins, A. O., Omena-Garcia, R. P., Oliveira, F. S., Silva, W. A., Hajirezaei, M.-R., Vallarino, J. G., Ribeiro, D. M., Fernie, A. R., Nunes-Nesi, A. & Araújo, W. L. (2019). Differential root and shoot responses in the metabolism of tomato plants exhibiting reduced levels of gibberellin. Environmental and Experimental Botany, 157, 331–343.
40. Leuschner, C., Moser, G., Bertsch, C., Röderstein, M., & Hertel, D. (2007). Large altitudinal increase in tree root/shoot ratio in tropical mountain forests of Ecuador. Basic and Applied Ecology, 8(3), 219–230.
41. Bolinder, M. A., Angers, D. A., Bélanger, G., Michaud, R., & Laverdière, M. R. (2002). Root biomass and shoot to root ratios of perennial forage crops in eastern Canada. Canadian Journal of Plant Science, 82(4), 731–737.
42. Bloom, A. J., Chapin, F. S., & Mooney, H. A. (1985). Resource limitation in plants--an economic analogy. Annual review of Ecology and Systematics, 363-392.
43. Sainju, U. M., Allen, B. L., Lenssen, A. W., & Ghimire, R. P. (2017). Root biomass, root/shoot ratio, and soil water content under perennial grasses with different nitrogen rates. Field Crops Research, 210, 183–191.
44. DaMatta, F. M., Ronchi, C. P., Maestri, M., & Barros, R. S. (2007). Ecophysiology of coffee growth and production. Brazilian Journal of Plant Physiology, 19(4), 485–510.
45. Geromel, C., Ferreira, L. P., Davrieux, F., Guyot, B., Ribeyre, F., dos Santos Scholz, M. B., Pereira, L. F. P., Vaast, P., Pot, D., Leroy, T., & Androcioli, F. A. (2008). Effects of shade on the development

and sugar metabolism of coffee (Coffea arabica L.) fruits. Plant Physiology and Biochemistry, 46(5–6), 569–579.
46. Oskoee, M., AghaAlikhani, M., Sefidkon, F., Mokhtassi-Bidgoli, A., & Ayyari, M. (2018). Blessed thistle agronomic and phytochemical response to nitrogen and plant density. Industrial Crops and Products, 122, 566–573.
47. Lambers, H., Chapin III, F. S., & Pons, T. L. (2008). Plant Physiological Ecology. Springer Science & Business Media. University of Western Australia.
48. Ma, S.-C., Li, F.-M., Xu, B.-C., & Huang, Z.-B. (2010). Effect of lowering the root/shoot ratio by pruning roots on water use efficiency and grain yield of winter wheat. Field Crops Research, 115(2), 158–164.
49. Yang, Y., Dou, Y., & An, S. (2017). Environmental driving factors affecting plant biomass in natural grassland in the Loess Plateau, China. Ecological Indicators, 82, 250–259.
50. Bertamini, M., Muthuchelian, K., Rubinigg, M., Zorer, R., Velasco, R., and Nedunchezhian, N (2006). Low-night temperature increased the photoinhibition of photosynthesis in grapevine (Vitis vinifera L. cv. Riesling) leaves. Environ. Exp. Bot., 57(1-2): 25-31.
51. Wittmann, C., Aschan, G., & Pfanz, H. (2001). Leaf and twig photosynthesis of young beech (Fagus sylvatica) and aspen (Populus tremula) trees grown under different light regime. Basic and Applied Ecology, 2(2), 145–154.
52. Bailey, S., Walters, R. G., Jansson, S., & Horton, P. (2001). Acclimation of Arabidopsis thaliana to the light environment: the existence of separate low light and high light responses. Planta, 213(5), 794–801.
53. Jiang, W., Wang, K., Wu, Q., Dong, S., Liu, P., & Zhang, J. (2013). Effects of narrow plant spacing on root distribution and physiological nitrogen use efficiency in summer maize. The Crop Journal, 1(1), 77–83.
54. Labrooy, C. D., Abdullah, T. L., Abdullah, N. A. P., & Stanslas, J. (2016). Optimum shade enhances growth and 5,7-Dimethoxyflavone ac-cumulation in Kaempferia parviflora Wall. ex Baker cultivars. Scientia Horticulturae, 213, 346–353.
55. Omar, N. F. (2018). Growth and phytochemical composition of Andrographis paniculata (Burm.F.) Wall. ex Nees in relation to different light intensities, photoperiod, and pruning. Universiti Putra Malaysia, Serdang, Malaysia.
56. Wang, C., Liu, W., Li, Q., Ma, D., Lu, H., Feng, W., Xie, Y., Zhu, Y., & Guo, T. (2014). Effects of different irrigation and nitrogen regimes on root growth and its correlation with above-ground plant parts in high-yielding wheat under field conditions. Field Crops Research, 165, 138–149.
57. Casey, C. A., Mangan, F. X., Herbert, S. J., Barker, A. V, & Carter, A. K. (2002). The effect of light intensity and nitrogen fertilization on plant growth and leaf quality of ngo gai (Eryngium foetidum L.) in Massachusetts. In XXVI International Horticultural Congress: The Future for Medicinal and Aromatic Plants 629, 215–229.
58. Kumar, R., Sharma, S., & Pathania, V. (2013). Effect of shading and plant density on growth, yield and oil composition of clary sage (Salvia sclarea L.) in north western Himalaya. Journal of Essential Oil Research, 25(1), 23–32.
59. Urbas, P., & Zobel, K. (2000). Adaptive and inevitable morphological plasticity of three herbaceous species in a multi-species community: field experiment with manipulated nutrients and light. Acta Oecologica, 21(2), 139–147.
60. Ezz, A. L. (2009). Plant growth strategies of Thymus vulgaris L. in response to population density. Industrial Crops and Products, 30(3), 389-394.
61. ZHANG, M. C., SUN, W. X., LIU, Y. Y., LUO, S. G., Jing, Z., Qiong, W. U., ... & Jiang, Y. (2014). Timing of N application affects net primary production of soybean with different planting densities. Journal of Integrative Agriculture, 13(12), 2778-2787.
62. Deng, J., Wang, G., Morris, E. C., Wei, X., Li, D., Chen, B. M., Zhao, B. M., Liu. J., & Wang, Y. (2006). Plant mass–density relationship along a moisture gradient in north-west China. Journal of Ecology, 94(5), 953–958.

63. Schachtman, D. P., & Goodger, J. Q. D. (2008). Chemical root to shoot signalling under drought. Trends in Plant Science, 13(6), 281–287.
64. Liu, T., Gu, L., Dong, S., Zhang, J., Liu, P., & Zhao, B. (2015). Optimum leaf removal increases canopy apparent photosynthesis, 13C-photosynthate distribution and grain yield of maize crops grown at high density. Field Crops Research, 170, 32–39.
65. Fang, X., Li, Y., Nie, J., Wang, C., Huang, K., Zhang, Y., Zhang, Y., She, H., Liu, X., Ruan, R., &Yuan, X. (2018). Effects of nitrogen fertilizer and planting density on the leaf photosynthetic characteristics, agronomic traits and grain yield in common buckwheat (Fagopyrum esculentum M.). Field Crops Research, 219, 160–168.
66. Derks, H., Mitchell, R. A. C., Mitchell, V. J., & Lawlor, D. W. (1998). Response of sugar beet (Beta vulgaris L.) yield and biochemical composition to elevated CO2 and temperature at two nitrogen applications. Plant, Cell & Environment, 21(8), 829–836.
67. Xie, X., Shan, S., Wang, Y., Cao, F., Chen, J., Huang, M., & Zou, Y. (2019). Dense planting with reducing nitrogen rate increased grain yield and nitrogen use efficiency in two hybrid rice varieties across two light conditions. Field Crops Research, 236, 24–32.
68. Ali, A., Ahmad, A., Khaliq, T., & Akhtar, J. (2012). Planting density and nitrogen rates optimization for growth and yield of sunflower (He-lianthus annuus L.) hybrids. The Journal of Animal and Plant Sciences, 22(4), 1070–1075.

Received: October 9th 2023/ **Accepte**d: January 15th 2024 / **Published:**15 February 2024

Citation: Ahmed, O.; Yusoff1, M.; Wahab, A. M., Muttaleb, Q. Root-shoot ratio and its relationships with physiological characteristics, growth and biomass yield of *Gynura procumbens* under different shade levels and plant density. Revis Bionatura 2024; 9 (1) 52. http://dx.doi.org/10.21931/RB/2024.09.01.52

Additional information Correspondence should be addressed to omerahmed@uodiyala.edu.iq

Peer review information. Bionatura thanks anonymous reviewer(s) for their contribution to the peer review of this work using https://reviewerlocator.webofscience.com/

All articles published by Bionatura Journal are made freely and permanently accessible online immediately upon publication, without subscription charges or registration barriers.

Bionatura ISSN. First 13909355 Ecuador. **Scopus coverage years**: from 2016 to the present

Publisher's Note: Bionatura stays neutral concerning jurisdictional claims in published maps and institutional affiliations.

Bionatura
Ibero-American Journal of Biotechnology and Life Sciences

Article

Effect of injection with microelements, jasmonic and citric acid on some date palm c.v Khastawi yield traits

*W. Taha[1], Kh.A.S. Al-Hamdani[2] and KH. N. AL-Assal[2]**

[1]Tikrit University, College of Agriculture; ammarwaleedtaha@gmail.com.
[2]Samarra University, College of Agriculture; khaild_sa@tu.edu.iq.
** Correspondence: ammarwaleedtaha@gmail.com.*
Available from. http://dx.doi.org/10.21931/RB/2024.09.01.53

ABSTRACT

The study was conducted at the Ishaqi palm plant affiliated with the Department of Horticulture/Ministry of Agriculture during the growing season of 2021 on date palm trees of the Khastawi variety to study the response of the yield traits of the Khastawi date palm trees to the injection of microelements, jasmonic and citric acid. The study included three factors: The first factor is the injection of microelements with three treatments: injection with water only, symbolized by D_0, iron injection at a concentration of 300 mg, and iron sulfate. Palm^{-1}, symbolized by D_1, and boron injection through boric acid at a concentration of 40 mg Palm^{-1}, symbolized by D_2. The second factor is the treatment of injections with the Jasmonic growth regulator, which was injected three days after the injection with the microelements and with the same number of additions (0, 50, 100) micrograms. L^{-1} is symbolized by G0, G_1, and G_2 sequentially. The trees were injected with the microelements and the Jasmonic growth regulator before Immunization, after vaccination in 20 days, and after 40 days. The third factor was injection with citric acid and included three levels (0, 500, 1000) mg l^{-1} symbolized by S_0, S_1, and S_2 sequentially. The results showed that the D_2 treatment was significantly superior in the average diameter, length, size and weight of the fruit and the total yield, as it reached 24.86 mm, 3.46 cm, 11.10 cm, 10.07 g, 36.00 kg.palm^{-1} sequentially, while the comparison treatment gave the lowest average for the traits. As for the effect of jasmonic acid, the injection treatment was superior to (100 µg L^{-1}). (G_2) gave the highest average for the diameter, length, size, weight of the fruit, and the total yield, which reached 25.90 mm, 3.63 cm, 12.09 cm, 10.93 g, and 35.96 kg. Palm-1, respectively, while the comparison treatment gave the lowest average for the traits above as for the effect of citric acid. The treatment exceeded 1000 mg.L^{-1} (S_2) gave the highest rate in the diameter, length, size, and weight of the fruit, and the total yield, reaching 24.84 mm, 3.49 cm, 11.13 cm, 9.04 g, and 36.30 kg. Palm-1, respectively, while the comparison treatment gave the lowest average for the traits above, as the two- and three-interactions showed. The research factors have significant differences for all the studied traits.

Keywords: Trace elements, jasmonic acid, citric acid, Khastawi variety.

INTRODUCTION

The date palm (*Phoenix dactylifera* L.) belongs to the order Palmae and the family Palmaceae. This includes different types of palms, the most important of which is the date palm, which is widely cultivated in tropical, semi-tropical and subtropical regions, and some of them can live in temperate regions. Iraq is one of the oldest palm plantations in the world, with more than 600 varieties grown in it; God Almighty has singled him out with many virtues, as they are a source of goodness and blessings and was mentioned in 22 verses in the Holy Qur'an [1]. The number of date palm trees in Iraq is 16,492,121 palm trees, while the total production is 676,111 tons, with an average production per palm of 68 kg Tree^{-1}, [2].

The method of injecting elements into tree trunks is directly and immediately available to the tree, especially one that lacks these elements. Therefore, it works to reduce the symptoms of deficiency of these elements

and improve the growth of the tree through its reflection on the health status of the leaves within days of conducting the treatment [3].

This technique of fertilization is of little use. However, it is more practiced in the control of pests and diseases, and it is recommended to use it when fertilization methods on the soil or the leaves do not yield sufficient results. Therefore, its use on olive trees is limited to treating the deficiency of some nutrients, and the injection of the tree trunk prevents contamination of Air and water as the substance remains inside the tree and thus contributes to the effectiveness of the treatment [4]. Stipes (1999) showed that the tree injection method includes two parts. The first is called microinjection, and the injection process is carried out under pressure and with a high concentration of fertilizers inside the hole in the tree. The second method is called normal macro injection. It is either by pressure or diffusion (without pressure), and a diluted solution is used in larger quantities than the first method and is achieved by making a hole in the stem or base of the tree. [5] stated that the fertilizer injected into the tree moves through the outer ring of the wood, where the majority of the water run-off is, and that 90% of the water run-off is located in the outer ring of the wood.

[6] found significant differences in injecting Musa trees and Grand Naine with different concentrations of organic fertilizers. The two concentrations gave 75% and 100% on the highest results in each of the areas of one leaf, the total area of the leaves, number of leaves, specific weight, plant height and stem diameter, [7] that inject some nutrients into the trunks of Valencia orange trees at a concentration of 2.5 ml. L^{-1} led to significant differences, as the treatment Ca=0.7% was significantly superior to the total yield, acidity and K concentration, While the treatment N=0.8% was significantly superior to the percentage of juice and the concentration of Ca, Mg, Cu. [8] found that the Khastawi date palm cultivar was superior to the cucumber in the percentage of carbohydrates and total sugars when the stem was injected with Nutreeno nutrient solution at a concentration of 40 mlL^{-1}. [9] when treating Al-Sayer date palm trees with citric acid at a concentration of 200 gm $Palm^{-1}$, The treatment led to a significant increase in the length of the fruit and the content of the fruits from soluble solids and quantitative sugars, a decrease in the percentage of sucrose in the fruit, and an increase in the ratio of potassium to sodium in the leaves. And an increase in the weight of the weight and the quantitative yield of a tree.

Ten explained that when spraying date palm offshoots of Al-Barhi and Al-Sayer cultivars with citric acid in order to reduce soil salinity at a concentration of 500 and 1000 mg L^{-1}, the concentration gave 500 mgL^{-1} significant increase in the leaves content of chlorophyll, potassium element and plant hormone IAA, While the spraying treatment with citric acid at a concentration of 1000 mgL^{-1} recorded a significant increase in the leaf area and number of leaves, and the same treatment also recorded a significant increase in the leaves content of the amino acid proline and carbohydrates.

[11] showed that injecting FeSO4 solution into the trunks of date palm trees at a concentration of 2.5 g L^{-1} gave the highest fruit yield, weight and size.

Plant growth regulators are influential in stimulating the physiological processes necessary for plant growth and development, including jasmonic acid. This stress hormone consists of linolenic fatty acid and plays a key role in stress resistance.

MATERIALS AND METHODS

The study was conducted at the Ishaqi date palm plant belonging to the Horticultural Department/Ministry of Agriculture during the 2021 growing season on date palm trees, Khastawi variety, aged 10 Years. The trees were chosen as homogeneous as possible in their vegetative growth and planted in the quadruple method 5 * 5 m. Soil samples were taken from the orchard before the treatments were conducted at a depth of 60 cm to conduct physical and chemical tests (Table 1).

Analysis	The unit of measurement used	analysis' results
Degree PH	……	7.71
electrical conductivity	$ds.m^{-1}$	2.72
Gypsum	$Mg.kg\ Soil^{-1}$	13.1
Calcium carbonate	Mg.kg Soil1-	41
Mud	Mg.kg Soil1-	10

the sand	Mg.kg Soil1-	830
Silt	Mg.kg Soil1-	125
Ca +2 Calcium	Meq .L-1	20.60
Mg+2 Magnesium	Meq .L-1	1.45
Na+ Sodium	Meq .L-1	2.15
K+ Potassium	Meq .L-1	1.55
HCO3 -	Meq .L-1	1.13
soil texture	Clay	Mud
total nitrogen	g.kg-1	24.3
total phosphorous	g.kg-1	3
total potassium	g.kg-1	60.01

Table 1: Some physical and chemical properties of the study soil.

RESULTS

Average diameter, length and size of the fruit:

The results of Tables (2, 3 and 4) showed significant differences in the diameter, length and size of the fruit as a result of the trees being injected with microelements, as treatment D_2 gave the highest average for the diameter, length and size of the fruit, as it reached 24.86 mm, 3.46 cm and 11.10 cm 3 in sequence. D1 followed it by giving it an average Measured at 24.45 mm, 3.40 cm, and 10.66 cm^3, respectively, While the comparison treatment D0 gave the lowest average, as it reached 23.90 mm, 3.26 cm, and 10.46 cm 3, respectively.

The results of the same tables indicate that there are significant differences as a result of the injection with jasmonic acid, as treatment G_2 gave the highest rate for the diameter, length and size of the fruit, as it reached 25.90 mm, 3.63 cm, 12.09 cm^3 sequentially, followed by treatment G_1 by giving it an average of 24.29 mm, 3.38 cm, 10.41 cm^3 sequentially, While the comparison treatment G_0 gave the lowest average for the diameter, length and size of the fruit, as it reached 23.02 mm, 3.12 cm, 9.70 cm 3 sequentially. It was found that the injection with citric acid achieved a significant increase in the diameter, length and size of the fruit, as the treatment S_2 gave the highest rate of 24.84 mm, 3.49 cm, 11.13 cm^3 sequentially, Then followed by treatment S_1 at a rate of 24.54 mm, 3.38 cm and 10.77 cm^3 respectively, while treatment S_0 gave the lowest average of 23.83 mm, 3.26 cm and 10.31 cm 3 respectively.

The bilateral interaction between boron and jasmonic had a significant effect, as the results of Tables (2, 3 and 4) showed significant differences, as the D_2G_2 treatment gave the highest average fruit diameter, length and size of 25.3 mm, 3.74 cm, 12.51 cm^3, respectively, Whereas, treatment D_0S_0 gave the lowest average fruit size diameter and length, which were 22.45 mm, 3.14 cm, and 9.20 cm^3 sequentially.

The results of the same tables showed a significant effect on the average diameter, length, and size of the fruit due to the interaction of boron and citric. The D_2S_2 treatment gave the highest rate of 25.31 mm, 3.58 cm, and 12.51 cm^3 sequentially. Meanwhile, treatment D_0S_0 sequentially gave the lowest average fruit diameter, 23.26 mm, 3.14 cm, and 9.94 cm^3.

The results of the tables also showed a significant increase when jasmonic and citric acid were overlapped, as treatment G_2S_2 was unique in giving it the highest rate of diameter, length and size of the fruit as it reached 26.14 mm, 3.73 cm, 12.54 cm^3 sequentially, while treatment G_0S_0 gave the lowest rate of diameter, length and size of the fruit amounting to 21.99 mm. 2.96 cm and 8.93 cm^3 sequentially.

As for the tripartite interaction of the search treatments, the results of Tables (2, 3 and 4) indicate significant differences, as the treatment $D_2G_2S_2$ gave the highest average for the diameter, length and size of the fruit amounted to 26.41 mm, 3.89 cm, 12.98 cm^3, compared to the comparison treatment $D_0G_0S_0$, which gave the lowest rate of 21.10 mm, 2.76 cm, 8.01 cm^3 sequentially.

micro-elements (D)	jasmonic acid (G)	citric acid			D×G
		S_0	S_1	S_2	
D_0	G0	21.10	22.95	23.29	22.45
	G1	23.32	23.79	23.84	23.65
	G2	25.35	25.65	25.79	25.60
D_1	G_0	22.20	23.35	23.80	23.12
	G_1	23.84	24.40	24.70	24.58
	G_2	25.58	25.99	26.22	24.91
D_2	G_0	22.69	23.62	24.20	24.36
	G_1	24.46	24.91	25.32	24.91
	G_2	25.93	26.20	26.41	25.31
The effect of microelements					
S×D	D_0	23.26	24.13	24.31	23.90
	D_1	23.87	24.58	24.91	24.45
	D_2	24.36	24.91	25.31	24.86
The effect of jasmonic acid					
S×G	G_0	21.99	23.31	23.76	23.02
	G_1	23.87	24.37	24.62	24.29
	G_2	25.62	25.95	26.14	25.90
Citric Acid Effect(S)		23.83	24.54	24.84	

LSD 5%

D×G×S	G×S	D×S	D×G	S	G	D
0.51	0.30	0.30	0.30	0.17	0.17	0.17

Table 2: Effect of microelements, jasmonic growth regulator and citric acid and the interaction between them on the average fruit diameter (mm).

micro-elements (D)	jasmonic acid (G)	citric acid			D×G
		S_0	S_1	S_2	
D_0	G0	2.76	3.14	3.20	3.03
	G1	3.21	3.24	3.26	3.24
	G2	3.46	3.50	3.60	3.52
D_1	G_0	3.07	3.16	3.22	3.15
	G_1	3.23	3.33	3.71	3.42
	G_2	3.58	3.64	3.69	3.64
D_2	G_0	3.05	3.21	3.28	3.18
	G_1	3.37	3.49	3.57	3.48
	G_2	3.64	3.68	3.89	3.74
The effect of microelements					
S×D	D_0	3.14	3.29	3.35	3.26
	D_1	3.29	3.38	3.54	3.40
	D_2	3.35	3.46	3.58	3.46
The effect of jasmonic acid					

S×G	G_0	2.96	3.17	3.23	3.12
	G_1	3.27	3.35	3.51	3.38
	G_2	3.56	3.61	3.73	3.63
Citric Acid Effect(S)		3.26	3.38	3.49	

LSD 5 %

D×G×S	G×S	D×S	D×G	S	G	D
0.17	**0.09**	**0.09**	**0.09**	**0.06**	**0.06**	**0.06**

Table 3: Effect of microelements, jasmonic growth regulator and citric acid and the interaction between them on the average fruit length (cm).

microelements (D)	jasmonic acid (G)	citric acid			D×G
		S_0	S_1	S_2	
D_0	G0	8.01	9.75	9.84	9.20
	G1	9.92	10.13	10.15	10.07
	G2	11.90	12.07	12.24	12.07
D_1	G_0	9.44	9.96	10.14	9.85
	G_1	10.00	10.40	10.90	10.43
	G_2	11.30	11.37	12.40	11.69
D_2	G_0	9.33	10.30	10.52	10.05
	G_1	10.58	10.64	11.00	10.74
	G_2	12.28	12.27	12.98	12.51
					The effect of microelements
S×D	D_0	9.94	10.65	10.74	10.45
	D_1	10.25	10.58	11.15	10.66
	D_2	10.73	11.07	11.50	11.10
					The effect of jasmonic acid
S×G	G_0	8.93	10.00	10.17	9.70
	G_1	10.17	10.39	10.68	10.41
	G_2	11.83	11.90	12.54	12.09
Citric Acid Effect(S)		10.31	10.77	11.13	

LSD 5 %

D×G×S	G×S	D×S	D×G	S	G	D
0.77	**0.45**	**0.45**	**0.45**	**0.26**	**0.26**	**0.26**

Table 4: Effect of microelements, jasmonic growth regulator and citric acid and the interaction between them on the average fruit size (cm).

Fruit Weight (gm): -

The results of Table (5) showed significant differences in the weight characteristic of the fruit as a result of the trees being injected with microelements. The effect increased when treatment D_2 gave the highest average fruit weight of 10.07 g, followed by treatment D_1, giving it an average of 9.81 g, while the comparison treatment D_0 gave the lowest average weight. The fruit reached 9.14 g.

The results of the same Table also indicate significant differences as a result of jasmonic acid injection, as treatment G_2 gave the highest fruit weight rate of 10.93 g, followed by treatment G_1, giving it an average of 9.36 g. The comparison treatment G_0 gave the lowest fruit weight rate of 8.73 g.

It was also found that the injection of citric acid achieved a significant increase in the average fruit weight, as treatment S_2 gave the highest percentage of 9.04 g, followed by treatment S_1 with a percentage of 9.82 g, while

treatment S_0 gave the least significant difference of 10.16 g. As for the effect of the injection, we note from the results of the same Table that the characteristic weight of the fruit is significantly affected by the injection of jasmonic acid and boron.

The interaction between boron and jasmonic had a significant effect, as the results of Table (5) showed significant differences, as the treatment D_2G_2 gave the highest average fruit weight of 28.67 g, whereas treatment D_0G_0 gave the lowest average fruit weight, which was 7.89 g. The same Table showed the significant effect on the average fruit weight due to the interaction of boron and citric. The D_2S_2 treatment gave the highest rate of 27.67 g, while the D_0S_0 treatment gave the lowest fruit weight rate of 11.78 g. The results of the same Table also showed a significant increase when jasmonic and citric acid were overlapped, as treatment G_2S_2 was unique in giving it the highest average fruit weight, which amounted to 11.68 g. In comparison, treatment G_0S_0 gave the lowest average fruit weight of 7.94 g. As for the tripartite interaction of the search treatments, the results of Table (5) indicate significant differences, as treatment $D_2G_2S_2$ gave the highest average fruit weight of 30.00 g, compared to the comparison treatment $D_0G_0S_0$, which gave the lowest fruit weight rate of 7.00 g.

microelements (D)	**jasmonic acid (G)**	**citric acid**			**D×G**
		S_0	S_1	S_2	
D_0	G0	7.00	8.33	8.33	7.89
	G1	15.67	14.00	15.67	13.78
	G2	21.33	17.67	21.33	18.56
D_1	G_0	14.00	15.67	14.00	15.22
	G_1	18.00	18.00	18.00	17.00
	G_2	23.67	19.67	23.67	21.78
D_2	G_0	24.00	18.00	24.00	20.00
	G_1	29.00	26.00	29.00	26.89
	G_2	30.00	28.00	30.00	28.67
The effect of microelements					
S×D	D_0	11.78	13.33	15.11	9.14
	D_1	17.67	17.78	18.56	9.81
	D_2	23.89	24.00	27.67	10.07
The effect of jasmonic acid					
S×G	G_0	7.94	9.05	9.18	8.73
	G_1	9.07	9.40	9.61	9.36
	G_2	10.10	10.99	11.68	10.93
Citric Acid Effect(S)		10.16	9.82	9.04	

LSD 5 %

S×G×D	**S×G**	**S×D**	**G×D**	**S**	**G**	**D**
1.73	**1.00**	**1.00**	**1.00**	**0.58**	**0.58**	**0.58**

Table 5: Effect of microelements, jasmonic growth regulator and citric acid and the interaction between them on the average fruit weight (gm).

Total Yield (kgpalm^{-1}**): -**

The results of Table (6) indicated that the percentage of the total yield was significantly affected as a result of the injection with microelements, as treatment D_2 gave the highest content of 36.00 kg palm^{-1}, followed by treatment D_1 with a significant difference of 34.70 kg. palm^{-1}, while it gave Treatment D_0 is the lowest in the total yield of 30.30 kg. palm^{-1}. It was also found from the results of the same Table that there were significant differences in the rate of the total yield as a result of the injection of jasmonic acid, as treatment G_2 gave the

highest rate of 35.96 kg. palm^{-1}, followed by treatment G_1 at a rate of 34.74 kg palm^{-1}, Whereas, treatment G_0 gave the least significant difference, which was 30.30 kgpalm^{-1}.

It was also found that the injection of citric acid achieved a significant increase in the total yield rate, as treatment S_2 gave the highest rate of 36.30 kg palm^{-1}. Then, treatment S_1 followed with a rate of 34.67 kg. palm^{-1}, while treatment S_0 gave the lowest rate of 30.04 kg. palm^{-1}. The binary interaction between boron and jasmonic acid positively affected the overall yield; the D_2G_2 treatment showed the highest rate of 40.44 kg palm^{-1}, compared to the control treatment, which showed the lowest rate of 26.22 kg palm^{-1}.

The results of Table (6) showed that the interaction of boron acid with citric acid caused a significant increase in the rate of the total yield, as the treatment D_1S_2 gave the highest rate of 35.44 kg palm^{-1}, While the comparison treatment D_0S_0 gave the lowest rate of 24.56 kg palm^{-1}. We also note from the results of Table (6) that the dual interaction of jasmonic acid with citric acid made a significant difference, as the treatment G_2S_2 gave the highest total yield of 41.67 kg. palm^{-1}, Whereas treatment G_0S_0 gave the least significant difference for the total yield, which was 26.56 kg palm-1. As for the tripartite interaction of the search treatments, the results of Table (6) found significant differences, as the treatment $D_2G_2S_2$ gave a higher total yield of 50.33 kgpalm^{-1}, compared to the comparison treatment $D_0G_0S_0$, which gave the lowest yield rate of 18.00 kgpalm^{-1}.

microelements (D)	**jasmonic acid (G)**	**citric acid**			**D×G**
		S_0	S_1	S_2	
D_0	G0	18.00	34.67	26.00	26.22
	G1	31.00	31.67	37.00	33.22
	G2	24.67	35.00	34.67	31.44
D_1	G_0	31.33	35.00	30.00	32.11
	G_1	35.67	36.00	36.33	36.00
	G_2	33.33	34.67	40.00	36.00
D_2	G_0	30.33	31.00	36.33	32.56
	G_1	33.00	36.00	36.00	35.00
	G_2	33.00	38.00	50.33	40.44
					The effect of microelements
S×D	D_0	24.56	33.78	32.56	30.30
	D_1	33.44	35.22	35.44	34.70
	D_2	32.11	35.00	32.11	36.00
					The effect of jasmonic acid
S×G	G_0	26.56	33.56	30.78	30.30
	G_1	33.22	34.56	36.44	34.74
	G_2	30.33	35.89	41.67	35.96
Citric Acid Effect(S)		30.04	34.67	36.30	

LSD 5 %

D×G×S	**G×S**	**D×S**	**D×G**	**S**	**G**	**D**
7.48	**4.31**	**4.31**	**4.31**	**2.49**	**2.49**	**2.49**

Table 6: Effect of injections with microelements, jasmonic growth regulator and citric acid and the interaction between them on the total yield (kg).

DISCUSSION

The moral superiority in yield characteristics (diameter, size, weight of the fruit, total yield) of palm fruits shown in tables (2, 3, 4, 5) is only a result of the role played by the chemical fertilizer consisting of zinc and boron in maintaining plant growth and activity through its effect On the physiological functions of trees,

especially the photosynthesis process, which stimulates the plant to absorb water , And the nutrients that the plant needs in performing its vital processes and giving direct signals to build specific hormones to perform certain functions of the plant, such as the hormone fluorogen, which is specific to flowers, which accelerates the maturation of tissues and internal cells and thus pushes trees to form flowers and build different compounds and proteins and activate the cofactors of enzymes and hormones in building cell walls and transporting Sugars, absorption of major and minor minerals, gathering of various amino acids within plant tissues, and an increase in the rate of fruit setting, thus increasing the yield of trees [12], [13]. The positive superiority in the weight, size, diameter and length of the fruit was due to the elements zinc and boron in creating a state of balance in regulating vital processes and increasing the absorption of mineral elements such as nitrogen, phosphorous, potassium, zinc and boron in the leaf, which in turn stimulated cell division and doubling, which led to an increase in the size of the fruit and the thickness of the pulp And its weight, it may also be due to the role of the two elements in increasing the ratio of carbohydrates to nitrogen C/N, which positively reflected on the accumulation of various elements and nutrients in plant tissues [14, 15]. At the same time, the moral superiority in yield traits may be due to the effect of citric acid, which increases the ability of the plant to carry out the process of photosynthesis, which helps the plant absorb food. It also has a role in improving the qualities of fruits [16].

CONCLUSIONS

1 - The injection of micro-elements (iron and boron) showed a positive response in all vegetative growth characteristics, as well as the percentage of knots and fruit yield in palm trees, especially when treated with D2 at a level of (40 mg. L-1) under the conditions of the current experiment.

2- Jasmonic acid has a significant role in giving the best growth of trees and increasing the formation of chemical compounds and mineral elements in the leaves, as well as the other studied characteristics. These results were achieved when the treatment G2 level (100 µg.l-1).

3- The injection of citric acid led to a significant increase in the vegetative growth and production of trees, as the treatment (S2) outperformed (1000 mg.L-1).

4 - There is an apparent significant effect on the leaf content of citric jasmonic acid with increased jasmonic acid injections, as shown by GC-MS Chromatography Mass Spectrometry (Gas).

5- Injection of micro-elements, citric acid, and jasmonic acid together led to a clear increase in all studied traits, such as vegetative and fruit growth, average of (the diameter, length, size, weight of the fruit, and the total yield).

REFERENCES

1. Al-Hamdani, Kh. A. S., M. M. Hassan, M. N.Hussein. 2022. Date palm. Tikrit University Press. Ministry of Higher Education and Scientific Research, Iraq.
2. Central Statistical Organization. 2017. Annual Statistical Group - Ministry of Planning - Department of Publication and Public Relations - Baghdad - Iraq.
3. Hill Road. 2011. Iron chlorosis. www.arborjet.com .
4. Darwish, Monem Abed. The olive tree, techniques of cultivation and processing of its fruits. Baghdad, Iraq, Ministry of Agriculture - Department of Horticulture - Project for developing and disseminating cultivation in Iraq. 2015. Joy Press.
5. Harrell, M . Tree injections and implants. 2011. Tactics and Tools for IPM, Chapter 5, pp 3234.
6. Felipe, G. R.; U.V. Andres; C.S. Gerardo; S. Magnitskiy, and J. S. Henao . Effect of fertilizer insertion in the harvested mother banana plant pseudostem (Musa AAA Simmonds). Agronomía Colombiana. 2013. 31(1), 103-111.

7. Paula, A. L. ; M. Maria and Y. Elvira . Effects of nutritional trunk injections on Valencia late orange production. Cultivon Tropicales , . 2015 vol.36 , no.2 , pp. 142 – 147 .
8. Al-Dulaimi, R. M. H. and I. N. S. Al-Jumaili. Effect of injecting Nutreeno Nutrient solution on Khastawi and Cucumber date palm cultivars yield traits.Anbar Journal of Agricultural Sciences. 2015. Volume 13, Issue 1.
9. Toaimo, Mohamed Hadi. Effect of sulfur, calcium and ,citric acid in improving salt tolerance, specific fruit characteristics and ,productivity of date palm (L dactylifera Phoenix Al-Sayer). Master Thesis - Agricultural College - University of Basra - Iraq . 2015. - 97 p.
10. Shareef, H.J. Role of antioxidants in stress tolerant of date Palm offshoots (Phoenix dactylifera L.) femal and male cultiver . International Journal of Current Agricultural Research. 2015. , 3 (12).
11. Jahanshah S. ; Y. Hosseini, and M. Ghoreishi . Is Trunk Injection More Efficient Than Other Iron Fertilization Methods in Date Palms Grown in Calcareous Soils. Journal of Advanced Agricultural Technologies. 2016 . Vol. 3, No. 3, September .
12. Makhoul. G , Mouhammad .N , Abu Alshamlat A. Z. R. Influence of Foliar Application of Boron , Zinc and Humic acid on Tree Growth and Flowering of Olive tree (khodeiry variety). Tishreen University Journal for Research and Scientific Studies - Biological Sciences Series .2020. Vol. (14) No. (5) 9142.
13. Genaidy, A. E., N. Abd-Alhamid, S. A. Hassan, A. M. Hassan and L.63 F. Hagagg Effect of foliar application of boron trioxide and zinc oxide nanoparticles on leaves chemical composition, yield and fruit quality of Olea europaea L. cv. Picual, Genaidy et al. Bulletin of the National Research Centre 2020. 44:106.
14. Jasrotia. A, P. Bokshi and V.K.Wall Influence of girdling and zinc and boron application on growth ,quality and leaf nutrient status of olive Cv.Frantoio.Afr.J .Agric. . 2014 .9 (8):1354-1361.
15. Haluk, B., Gurel, S The influence of Zn, Fe and B applications on leaf and fruit absorption of table olive "Gem-like" based on phonological stages. Scientia Horticulturae. 2016. 198. 336–343..

Received: October 9th 2023/ **Accepte**d: January 15th 2024 / **Published:**15 February 2024

Citation: Taha, A..; Al-Hamdani, Kh.A.; AL-Assal, KH. Effect of injection with microelements, jasmonic and citric acid on some date palm c.v Khastawi yield traits. Revis Bionatura 2024; 9 (1) 53. http://dx.doi.org/10.21931/RB/2024.09.01.53

Additional information Correspondence should be addressed to ammarwaleedtaha@gmail.com.

Peer review information. Bionatura thanks anonymous reviewer(s) for their contribution to the peer review of this work using https://reviewerlocator.webofscience.com/

Bionatura ISSN. First 13909355 Ecuador. **Scopus coverage years**: from 2016 to the present

Bionatura
Ibero-American Journal of Biotechnology and Life Sciences

Article

The Application of Wheat Farmers to Modern Agriculture Technology Related to Improve Crop Production in Thi-Qar

Hakeem, S. Abd. AL.Rekibe

Department of Field Crops, College of Agriculture, Wasit University, Iraqabdulmutalib.raafat@garmian.edu.krd
**Correspondence: hsultan@uowasit.edu.iq*
Available from. http://dx.doi.org/10.21931/RB/2024.09.01.56

ABSTRACT

The research aim is to determine the level of application farmers of Modern Agricultural Technology have in improving wheat crop production in Thi-Qar Province. A multistage sample probability proportionates of size (P.P.S.) was used to conduct this study. The sample number was (75 farmers from the Qalat Sukkar district, 105 farmers from the AL-Rifai district, 45 farmers from the AL-Shatrah district, and 29 farmers from the AL-Nasr district) (15% of the total number of farmers) it was 254 farmers. Questionnaire techniques and interviews with the farmers were adopted to collect the data (March to May 2019). The study has revealed that the highest percentage (62.6 %) belonged to the medium category in applying modern agricultural technology to improve wheat crop production. The application level of modern agricultural technology was significant and positive at a 1% probability level under six variables. Multiple regression analyses have been studied with ten variables: social class, age, Education, Occupation, Farm power, Size of land holding, Family type, Family size, social participation, and Source of information utilized. This research has contributed nine independent variables with significant levels of variation to the extent of the application level of modern agricultural technology in improving wheat crop production (R2= 0.759). The importance of farmers using modern agricultural technology with the parts (Soil preparation, Planting and crop service, harvesting processes and marketing) was high according to (72.12, 70.72, and 68.41) respectively. The data were used for analysis: Frequency, percentage, mean, Standard deviation, and multiple regression analysis. According to the result, farmers' application of modern technology in improving wheat crop production was good. Modern agricultural technology will reduce costs, increase productivity, and save soil quality. The importance of farmers with the parts (Soil preparation, planting, crop service, harvesting processes, and marketing) was high according to (72.12, 70.72, and 68.41) respectively. Because of this, it is necessary to improve the cultivation of wheat crops to achieve high productivity and reduce the problems that happen during agricultural production.

Keywords: Technology, Independent variables, Farmers, Harvesting, Size of land holding

INTRODUCTION

Wheat crop is a key staple cereal for many people worldwide. Wheat is expected to increase strongly soon due to global population growth and dietary changes. So, the major challenge of wheat production is increasing this crop. In the threatening global food security, there has been a global decline in wheat yield growth since the mid-1990s[1]. Wheat is grown on more land areas than any other commercial crops. It is the most important grain food source for human consumption[2]. Wheat occupies the largest cultivated area compared with other

food crops, as well as the entry of wheat crops in many trade and economic transactions among the countries in the world. Many countries produce this crop, and many countries import it. Also, many countries are interested in ongoing research to improve the productivity of this crop by improving high-yield genotypes suitable for diverse environmental conditions; some of these countries have become the primary source of this crop, which has a competitive ability to produce it. Iraq ranked 31st by production in 2013, 3.3 million tons, while China, India, United States, and Russia ranked first, second, third, and fourth globally for the same year with 121.7, 93.5, 60, and 52 million tons, respectively[3]. As a staple food for half of the world's population, this plant is very important and, therefore, shall be considered a strategic crop[4] In Iraq, most wheat production relies on irrigation water. It is only 39.7% of the in Iraq, and most wheat production relies on irrigation water. Only 39.7% of the wheat cultivation area is rain-fed.

The areas of rain-fed wheat production have been located in the north of Iraq. Climatic conditions favor such requirements because Iraqi wheat is cultivated during November and harvested on May 5. The introduction of suitable wheat varieties and improved cultivation techniques such as fertilizing, pest control, and harvesting are necessary to fill the role. Furthermore, supplemental irrigation techniques need to be introduced so that the limited water resources can be utilized to maximize crop productivity[6]. New technologies developed by researchers are disseminated among the farmers by the agricultural extension department. In addition, agricultural extension provides farmers with management, decision-making, and organizational skills. It provides feedback and keeps agricultural research abreast of real problems faced by the farmers[7].

Agricultural extension programs have been one of the primary conduits of addressing rural poverty and food insecurity. This is because it has the means to transfer technology, support rural adult learning, assist farmers in problem-solving, and get farmers actively involved in the agricultural knowledge and information system [8] Agricultural extension programs should provide opportunities for agricultural subject matter knowledge and skill development through a variety of methods, including early field experiences[9]. To adopt a new Production technology correctly, the farmers should know how to learn and use these techniques correctly in farming systems. The major job of an effective extension worker is to educate the farmers on how to improve their skills, motivate them to use improved agricultural implements, prepare a cropping plan, and adopt the practices evolved through recent scientific research. To apply a new technology successfully, they must be aware of how to learn to incorporate it into their farming systems[10]. The demand for all foodstuffs grows. At the same time, the supply of natural resources should be expanded or increased gradually. For this result, we are studying the application of modern agricultural technology to improve wheat production to face many problems that may lead to low productivity in the future.

The study is trying to answer these questions:

1. what is the level of application of farmers to modern agricultural technology in improving wheat crop production in Thi-Qar province?
2. what is the relationship between the application farmers' level of Modern Agricultural Technology and the independent variables?
3. What is farmers' satisfaction level about applying modern agricultural technology to improve wheat crop production?

To answer these research questions, a study entitled "The application level of Modern agricultural technology in the improved wheat crop production in Thi-Qar Province" was undertaken with the following objectives:

1. To determine the application level of Modern Agricultural Technology in improving wheat crop Production in Thi-Qar Province.
2. To study the relationship between the application farmers' level of Modern Agricultural Technology with the independent variables in improving wheat crop production.
3. To study farmers' satisfaction level with the application of modern agricultural technology for improving wheat crop production.

MATERIALS AND METHODS

1. Research Methodology:

To achieve the research objectives, the descriptive approach is used, which is one of the methods to obtain adequate and accurate information from social reality and contribute to the analysis of its phenomena.

2. Research area:

The research has been done in Thi-Qar province in southern Iraq. The Thi-Qar province has been selected based on maximum area and production among other provinces in Iraq for wheat production in the national program for wheat development[11].

3. The research population:

The research population included the total number of farmers in the year 2019 was 1692 farmers (**500** farmers in the Qalat Sukkar district,700 farmers in the AL-Rifai district, 300 farmers in the AL-Shatrah district, and 192 farmers in the AL-Nasr district). The respondents' samples of this study for collecting data have been selected based on probability proportionate to size (P.P.S.). (15% of the total number of farmers was 254). Number of respondents samples for the study were (75 farmers in the Qalat Sukkar district, 105 farmers in the AL-Rifai district, 45 farmers in the AL-Shatrah district, and 29 farmers in the AL-Nasr district). A questionnaire was developed, pre-tested, revised, and used to collect necessary information from the farmers. The data were collected through personal interviews and questionnaires (during two months in 2019).

4. Data collection

The data have been collected through the questionnaire method and personal interviews. The number of questions in the test was 20 items to measure the application level of modern agricultural technology in improving wheat crop production. The questionnaire is divided into three parts (soil preparation, planting, crop service and harvesting processes). It is given a weight (1.0). The role of modern agricultural technology was divided into three categories: high, medium, and low, respectively.

5. Statistical analysis:

In this research, descriptive statistical measures (mean, averages, frequency, percentages, standard deviation, and multiple regressions) have been used for analyzing the data were analyzed by using a statistical analysis program (S.P.S.S.).

6. Face validity

The form has been presented to experts in plant production and agricultural extension areas to ensure the appropriateness of the paragraphs; all observations were recorded and reformulated, and adjustments were made according to their suggestions to improve the study. Seven in agricultural extension exports have been recording the apparent validity of the instrument, such as the type of expressions, the style of writing, the

extent of clarity, the accuracy of their measurement, and the way to answer the paragraphs, as some paragraphs were removed from the form according to their suggestion.

7. Reliability

The reliability content means " The degree of representation of the test of the content of the behavior and objectives," the content has validated this name because it relates to the behavior content to be measured[12]. Furthermore, whenever the value approaches (100%), this indicates a degree of stability. The result of the Cronbach alpha test for the study scale was (0.95), so the tool can be described as stable, and the data obtained were suitable for measuring varieties and were within a high degree of reliability. On 3/2/2019, a test was recorded for outside the sample in the research.

RESULTS

1. To determine the level of application farmers of Modern Agricultural Technology to Improve wheat crop Production in Thi-Qar Province.

The application of modern agricultural technology in improving wheat crop production was divided into three categories (low, medium, and high) and standard deviation. The result showed that in Table (2), the majority of respondents (62.6 %) are in the second category (medium), followed by high and low categories (20.86% and 16.54 %), respectively. The findings in Table reveal that most farmers belong to the middle category (62.6%). The farmers in Thi-Qar province had a good level of application of modern agricultural technology to improve wheat production. Modern agricultural technology will reduce costs, increase productivity, and save soil quality.

Furthermore, modern agricultural technology can be used in different aspects of agriculture, like applying herbicides, pesticides, fertilizers, and improved seeds. Technology has proved to be extremely useful in the agricultural sector. Farmers can grow crops in areas where they thought they could not grow. Furthermore, extension services create the platform for the acquisition of relevant information that promotes the adoption of technology. The findings are in tune with the findings of [13,14,15,16].

2. To study the relationship between the application farmers' level of Modern Agricultural Technology with the independent variables.

An effort has been made to analyze the relationship between the application of modern agricultural technology and independent variables to Improve wheat crop production. As shown in Table (3), the nine variables studied are significantly related to the application of Modern Agricultural Technology in improving Wheat Crop Production**.** Table (3) shows that only nine variables are significantly related to the application of modern agricultural technology in improving Wheat Crop Production**.** According to Table 3, the results showed that younger farmers were likely to use modern agricultural technology more than older ones. Some operations need to increase education levels and independent variables that influence the adoption of modern agricultural technology to improve wheat crop production.

Multiple regressions:

The technique of multiple regression was used to predict critical, independent variables. The technique has been used to determine the impact of the independent variables on the dependent variable, namely the application level of modern agricultural technology in improving wheat crop production. Only nine independent variables have been fitted with the farmers' application in the multiple regression equation. The findings have been combined in Table 4.

Table (4) showed that nine variables explained the variation in application to the extent of 0.759 percent of the use of modern agricultural technology. The respective "F" value (significant at 0.01 percent) at (13.80) degrees of freedom given in parenthesis was 6.77. Therefore, the results showed that only nine independent variables would account for highly significant variation in farmers' application levels. From the coefficients of regression (b-value), nine variables are significant with the application level of farmers. Therefore, these variables have a definite role in affecting the application of modern agricultural technology in improving Wheat Crop Production. The finding is in line with findings[17 18,]

To study farmers' satisfaction level with the application of modern agricultural technology to improve wheat crop production.

An effort has been made to determine respondents' satisfaction with the application level of improved wheat crop production. The result is presented in Table 4.

The above Table (5) depicts that (30.71 percent), of the respondents were fully satisfied with Land leveling in the soil preparation. The farmers think this process is very important in order to create good conditions for plants. (28.74 percent) of the respondents were having just satisfied with the fertilization process in the planting and crop service. Because so many farmers think this is a very important process to save the plant from other conditions. (27.95 percent) of the respondents were not satisfied with harvesting processes in the harvesting processes and marketing.

Arranging the study aspects according to importance for the respondents

It was divided into three main aspects, in descending order, according to the level of importance that each aspect obtained.

Table 6 depicts (72.12%) of the high percentage with soil preparation axis because they think this process is very important to prepare the field for wheat crop planting and for solving many problems facing the crop during the first growth stages. The planting and crop service was taking (70.72%) because they thought this was a process to help them control the production conditions.

DISCUSSION

According to the result, farmers' level of application of modern technology in improving wheat crop production was found to be good. Most of them think that using modern agricultural technology will reduce costs, increase productivity, and save soil quality. The importance of farmers with the parts (Soil preparation, planting, crop service, harvesting processes, and marketing) was high according to (72.12, 70.72, and 68.41) respectively. Because of this, it is very necessary to improve the cultivation of wheat crops to achieve high productivity and reduce the problems that may happen during agricultural production. The agricultural extension is the basis for the development of the agricultural sector, and with agricultural extension, it has benefited from modern agricultural techniques and information. Agricultural Extension is responsible for the transfer of agricultural technologies to farmers. According to this result, the level of application of modern agricultural technology in improving wheat crop production is that most farmers belong to the middle category (62.6%). The farmers in Thi-Qar province had a good level of application of modern agricultural technology to improve wheat production.

CONCLUSIONS

Accordingly, the researcher recommended that the competent authorities (directorates of agriculture in the Thi-Qar province, the Department of Agricultural Extension and Training) should adopt the proposal of the

requirements of developing the farmer's capacities in the field of application of modern technology in the improvement of wheat crop Production. Supporting the farmers in getting modern agricultural technology

No.	District	No. of farmers	P.P.S.
1	Qalat Sukkar	500	75
2	Al.Rifai	700	105
3	Al.Shatrah	300	45
4	Nasr	192	29
		1692	254

Table 1: The studied physicochemical parameters.

NO.	Classes	Freq.	%	Mean	S.D.
1	Low (less than (Mean – S.D.)	42	16.54	12.88	3.15
2	Middle boundary = Mean + S.D	159	62.6		
3	High above the minimum middle = class Mean + S.D.	53	20.86		
		254	100		

Table 2: Distribution of respondents as per their level of applying technology in improving wheat crop production (N= 254).

SI.NO	Variables	r -value	t -value
X1	Ages	0.1559*	2.665
X2	Social classes	0.3872**	4.786
X3	Occupation	0.488**	4.377
X4	Education	0.2785**	3,487
X5	Size of land holding	0.2855*	2.966
X6	Farm power	0.386**	4.467
X7	Family size	0.297*	2.775
X8	Family type	0.384**	3.758
X9	Social participation	-0.083 Ns	-0.776
X10	Source of information utilized	0.287**	2.789

*Means significant at a 5% probability level ** means significant at a 1% probability Ns= means non-significant.

Table 3: Relationship between the application level of respondents and the selected socio-personal.

SI.NO	Variables	“b” value	Std.	“ t”
X1	Ages	0.02574	0.0976	0.2733ns
X2	Social classes	0.36885	0.0198	25.566**
X3	Occupation	0.084976	0.0144	6.5654**
X4	Education	0.37625	0.0152	22.64**
X5	Size of land holding	0.35608	0.0157	31.460**
X6	Farm power	0.90163	0.0757	12.710**
X7	Family size	0.3674	0.427	25.199**
X8	Family type	1.48148	0.0737	30.370**
X9	Social participation	0.08917	0.0708	7.2540**
X10	Sources of information utilized	0.089285	0.0224	6.2034**

*significant at 5% level of probability ** significant at 1% level of probability Ns=non-significant R^2= 0.759 F value=6.77 ** d.f (13, 80) Intercept constant (a)=25.22

Table 4: Distribution of multiple regression analysis is independent variables with application level of Modern Agricultural Technology in the Improve of Wheat Crop Production.

	Statements of satisfaction		**Fully satisfied**		**Just satisfied**		**Satisfied only to some extent**		**Not Satisfied**		**Total**
	parts	Process	f	%	F	%	f	%	f	%	
1	Soil preparation soil preparation	Tilling	76	29.92	58	22.83	70	27.55	50	19.68	254
		Land leveling	78	30.71	63	24.80	60	23.62	53	20.87	254
2	Planting and crop service	Planting process	58	22.83	70	27.55	66	25.98	60	23.62	254
		Fertilization process	59	23.23	73	28.74	55	21.65	67	26.37	254
		Control process	57	22.44	62	25.98	69	27.16	66	25.98	254
3	Harvesting processes and marketing	Harvesting processes	67	26.37	61	24.01	55	21.65	71	27.95	254

Table 5: Distribution of respondents according to satisfactory application of improved wheat production technology.

No.	**Aspects**	**%**
1	Soil preparation	72.12
2	Planting and crop service	70.72
3	Harvesting processes and marketing	68.41

Table 6: arrangement of aspects according to importance of farmers.

REFERENCES

1. Savary, S. *et al.* The global burden of pathogens and pests on major food crops. *Nat. Ecol. Evol.* 3, (2019).
2. Castillo, J. Identificación de especies de Meloidogyne spp. presentes en el municipio de Patzicía, Chimaltenango. (Universidad Rafael Landívar, 2014).
3. Sánchez-Moreno, S. & Talavera, M. Los nematodos como indicadores ambientales en agroecosistemas. *Ecosistemas* 22, (2013).

4. Pérez-Anzúrez, G. *et al.* Arthrobotrys musiformis (Orbiliales) Kills Haemonchus contortus Infective Larvae (Trichostronylidae) through Its Predatory Activity and Its Fungal Culture Filtrates. *Pathogens* 11, (2022).
5. Triviño Gilces, C., Navia Santillán, D. & Velasco Velasco, L. *Guía para reconocer daño en raíces y métodos de muestreo y extracción de nemátodos en raíces y suelo*. *INIAP Boletín Divulgativo No. 433* https://repositorio.iniap.gob.ec/bitstream/41000/3849/1/433.PDF (2013).
6. González Cardona, C. & Aristizabal Loaiza, M. Evaluación de un producto nematicida sobre nematodos fitoparásitos del plátano Dominico Hartón (Musa AAB). *Acta Agron.* 63, 71–79 (2014).
7. López-Alcántara, R. Nematodos, su implicación en la producción agrícola. *ECUADOR ES Calid. Rev. Científica Ecuatoriana* 2, 10–11 (2015).
8. Muthee Gakuubi, M., Wanzala, W., Wagacha, J. M. & Dossaji, S. F. Bioactive properties of Tagetes minuta L. (Asteraceae) essential oils: A review. *Am. J. Essent. Oils Nat. Prod.* 4, 27–36 (2016).
9. Ibrahim, S. K., Traboulsi, A. F. & El-Haj, S. View of Effects of Essential Oils and Plant Extracts on Hatching, Migration and Mortality of Meloidogyne incognita | Phytopathologia Mediterranea. *Phytopathol. Mediterr.* 45, 238–246 (2006).
10. Licet Mena Valdés, L. *et al.* Determinación de saponinas y otros metabolitos secundarios en extractos acuosos de Sapindus saponaria L. (jaboncillo). *Rev. Cuba. Plantas Med.* 20, 106–116 (2015).
11. Piska, K., Ziaja, K. & Muszynska, B. Edible mushroom pleurotus ostreatus (Oyster mushroom) – Its dietary significance and biological activity. *Acta Sci. Pol. Hortorum Cultus* 16, 151–161 (2017).
12. Arteaga, M. B., Soria, C. A. & Ordoñez, M. E. Determinación del potencial nematicida y nematostático in vitro de Pleurotus ostreatus (Jacq. ex Fr.) sobre larvas J2 de Globodera pallida (Stone). *Rev. Ecuat. Med. Cienc. Biol.* 41, 45–50 (2020).
13. Álvarez S., D. E., Botina J., J. A., Ortiz C., A. J. & Botina J., L. L. Evaluación nematicida del aceite esencial de Tagetes zypaquirensis en el manejo del nematodo Meloidogyne spp. *Rev. Ciencias Agrícolas* 33, 22–33 (2016).
14. Abdel-Rahman, F. H., Alaniz, N. M. & Saleh, M. A. Nematicidal activity of terpenoids. *http://dx.doi.org/10.1080/03601234.2012.716686* 48, 16–22 (2012).
15. Martinotti, M. D., Castellanos, S. J., González, R., Camargo, A. & Fanzone, M. Efecto nematicida de extractos vegetales sobre Meloidogyne incognita Nematicidal effects of extracts of garlic, grape pomace and olive mill waste, on Meloidogyne incognita, on grapevine cv Chardonnay. *Rev. la Fac. Ciencias Agrar.* 48, 211–224 (2016).
16. Naim, L. *et al.* Variation of Pleurotus ostreatus (Jacq. Ex Fr.) P. Kumm. (1871) performance subjected to differentdoses and timings of nano-urea. *Saudi J. Biol. Sci.* 27, 1573–1579 (2020).
17. Cornelius, W. W. & Wycliffe, W. Chapter 90 - Tagetes (Tagetes minuta) Oils. in *Essential Oils in Food Preservation, Flavor and Safety* (ed. Preedy, V. R.) 791–802 (Academic Press, 2016). doi:https://doi.org/10.1016/B978-0-12-416641-7.00090-0.
18. Singh, P. Management of Plant-parasitic Nematodes by the Use of Botanicals. *J. Plant Physiol. Pathol.* 02, (2014).
19. de Lara, on *et al.* La importancia de los nematodos de vida libre.
20. Guzmán-Piedrahita, O. A., Carolina, C. & López-Nicora, H. D. Physiological interactions of plants with plant-parasitic nematodes: A review. *Bol. Cient. del Cent. Museos* 24, 190–205 (2020).
21. Silva Olivo, J. C. "Evaluación de la actividad insecticida y/o repelente 'in vivo' de extracto acuoso de Artemisia absinthium y aceites esenciales de Tagetes minuta y Tagetes zipaquirensis sobre Lasius niger.

(Escuela Superior Politécnica de Chimborazo, 2013).
22. Coyne, D. L., Nicol, J. M., Traducción, C.-C. & Verdejo-Lucas, S. *Nematología práctica: Una guía de campo y laboratorio*. (International Institute of Tropical Agriculture (IITA), 2007).
23. Jaraba, J. D., Lozano, Z. E. & Suárez Padrón, I. E. Meloidogyne incognita (Kofoid and White, 1919) Chitwood 1949 y Meloidogyne arenaria (Neal 1889) Chitwood 1949: Nematodos de las nudosidades radiculares en guayaba (psidium guajava l.) c.V. Manzana en Monteria, Cordoba. *Temas Agrar. ISSN-e 0122-7610, Vol. 8, Nº. 2, 2003, págs. 15-21* 8, 15–21 (2003).
24. Carmona, R. & Padilla, W. Morphological, morphometric and molecular identification of Meloidogyne exigua (Göeldi 1887) in coffee (Coffea arabica). *Agron. Mesoam.* 31, 531–545 (2020).
25. ICA. *Manual para la elaboración de protocolos para ensayos de eficacia con PQUA*. (Instituto Colombiano Agropecuario, 2020).
26. Murga-Gutiérrez, S. N., Alvarado-Ibáñez, J. C. & Vera-Obando, N. Y. Efecto del follaje de Tagetes minuta sobre la nodulación radicular de Meloidogyne incognita en Capsicum annuum, en invernadero. *Rev. peru. biol* 19, 257–260 (2012).
27. Iannacone, J. *et al.* Acute and chronic toxic effect of Tagetes minuta' Black mint' (Asteraceae) and carbaril on six important entomophages in biological control. *Biol.* 15, 85–97 (2017).
28. Zygadlo, J. A., Lamarque, A. L., Maestri, D. M., Guzman, C. A. & Grosso, N. R. Composition of the Inflorescence Oils of Some Tagetes Species from Argentina. *J. Essent. Oil Res.* 5, 679–681 (1993).
29. Peralta-Sánchez, M. G. *et al.* Metabolitos secundarios y clorofilas en cempasúchil en respuesta a estrés salino. *Rev. Mex. ciencias agrícolas* 5, 1589–1599 (2014).
30. Senatore, F. *et al.* Antibacterial activity of Tagetes minuta L. (Asteraceae) essential oil with different chemical composition. *Flavour Fragr. J.* 19, 574–578 (2004).
31. Alejandro Rojas, G. *et al.* Evaluación in vitro de la actividad nematicida de limoneno, isotiocianato de alilo, eucaliptol, β-citrolenol y azadiractina sobre Meloidogyne incognita (Nematoda, Meloidogynidae). *Trop. Subtrop. Agroecosystems* 22, (2019).
32. Herrera Moncada, W. L. & Sandoval Fuentes, M. G. Toxicidad del extracto etanólico de plantas de campo y callos in vitro de Tagetes minuta y Tagetes erecta sobre Meloidogyne spp. en Solanum lycopersicum L. *Universidad Nacional Pedro Ruiz Gallo* (Universidad Nacional Pedro Ruiz Gallo, 2019).
33. Zarate-Escobedo, J. *et al.* Concentrations and application intervals of the essential oil of Tagetes lucida Cav. against Nacobbus aberrans. *Rev. Mex. Ciencias Agrícolas* 9,.
34. Mendoza-García, E. *et al.* Efecto biológico del aceite de Tagetes coronopifolia (Asteraceae) contra Diaphorina citri (Hemiptera: Liviidae). *Rev. Colomb. Entomol.* 41, 157–162 (2015).
35. Erazo Sandoval, N. S. *et al.* Effect of Pleurotus ostreatus (Jacq.) and Trichoderma harzianum (Rifai) on Meloidogyne incognita (Kofoid & White) in tomato (Solanum lycopersicum Mill.). *Acta Sci. Biol. Sci.* 42, (2020).
36. Clémençon, H., Emmett, V. & Emmett, E. E. *Cytology and Plectology of the Hymenomycetes*. (2012).
37. Armas-Tizapantzi, A. *et al.* Estructuras tipo toxocistos en Pleurotus ostreatus y P. pulmonarius. *Sci. fungorum* 49, e1250 (2019).
38. Ernesto, J., El, S., De La, C., Sur, F. & Royse, D. J. *La Biología, el cultivo y las propiedades nutricionales y medicinales de las setas Pleurotus spp. Edible mushroom cultivation View project oxidorreductases enzymes View project*. (2017).
39. Aguilar Marcelino, L. *et al.* Los hongos del género Pleurotus como agentes de biocontrol de parásitos

de importancia pecuaria. 52, 1375 (2021).
40. Quevedo, A. *et al.* Interacciones ecológicas de los hongos nematófagos y su potencial uso en cultivos tropicales. *Sci. Agropecu.* 13, 97–108 (2022).
41. Jansson, H.-B. & Lopez-Llorca, L. V. Hongos nematófagos. 145–173 https://dcmba.ua.es/es/areas/botanica/hongos-nematofagos.html# (2001).
42. Leonardo, H. *et al.* Activity of the fungus Pleurotus ostreatus and of its proteases on Panagrellus sp. larvae. *African J. Biotechnol.* 14, 1496–1503 (2015).
43. Arteaga Paredes, M. B. Determinación del potencial nematicida y nematostático in vitro de Pleurotus ostreatus (Agaricales: Pleurotaceae) sobre larvas J2 de Globodera pallida (Tylenchida: Heteroderidae). (Pontificia Universidad Católica del Ecuador, 2018).

Received: October 9th 2023/ **Accepte**d: January 15th 2024 / **Published:**15 February 2024

Citation: Hakeem, S. A. A. The Application of Wheat Farmers to Modern Agriculture Technology Related to Improve Crop Production in Thi-Qar. Revis Bionatura 2024; 9 (1) 56. http://dx.doi.org/10.21931/RB/2024.09.01.56

Additional information Correspondence should be addressed to hsultan@uowasit.edu.iq

Peer review information. Bionatura thanks anonymous reviewer(s) for their contribution to the peer review of this work using https://reviewerlocator.webofscience.com/

Bionatura ISSN. First 13909355 Ecuador. **Scopus coverage years**: from 2016 to the present

Bionatura
Ibero-American Journal of Biotechnology and Life Sciences

Article

Relationship Polymorphism of STAT5A Gene in Performance Production of Local Goats

Bashar Adham Ahmed[1], Hamza Sajid Khudair[2]

[1]Assi. Prof. - Department of Animal Production - College of Agriculture - University of Diyala – Iraq
[2]Master student https://orcid.scopusfeedback.com/#/start
**Correspondence: basharadham@uodiyala.edu.iq*
Available from. http://dx.doi.org/10.21931/RB/2024.09.01.57

ABSTRACT

The study was conducted on a sample of 30 local goats in Diyala governorate / Canaan district in one of the goat breeders' fields in the region for the period from 13/11/2022 to 1/5/2022 to determine the genotype of the gene STAT5A EXON-7 and Its relationship to milk production (daily milk production-DMP and total milk production-TMP) and growth traits (birth weight-BWT, weaning weight-WWT and total weight gain-TWG). The analysis showed three-point mutations (CC=18 CT=12 C47064T AA=17 AT=13 A47088T and GG=15 GA=15 G47162A). There was no significant effect of the genotypes of the three mutations on all studied traits DMP, TMP, BWT, WWT, TWG, and body dimensions of the newborn at birth and weaning, body dimensions of the newborn at birth and weaning.

Keywords: Local goats, milk production, gene STAT5A EXON-7.

INTRODUCTION

Interest in raising and improving goats to benefit from milk and meat has recently begun, and goat milk is considered distinctive and healthy, especially for people who suffer from severe allergies [1, 2]. Because of the increasing population numbers around the world, the demand for animal products has increased, which prompted researchers to find ways to improve the productivity of farm animals, including goats, and this was evident in many different studies [3]. use of molecular genetics techniques has recently led to the discovery of genes that affect mainly and directly in many important productive and economic traits, as well as recognizing the effect of those genes by knowing the quantitative trait loci [4]. Therefore, genetic markers were relied upon. In selection programs because they are more accurate than phenotypic and biochemical markers [5]. Many transcription factor binding sites in the region close to the catalytic regions (promoter) have an essential effect on the transcription process, such as Nf1, CIEBP, STAT5A, and GR [6], and the STAT5A gene plays a critical role in many physiological processes. , as it is related to multiple traits such as the viability of fetuses and milk production traits [7], and the STAT5A gene is considered a mammary gland factor (Mammary Gland Factor-MGF), so it participates in the development of the mammary gland and is key in signaling the hormone prolactin (PRL) in addition to the activity of reproducing milk protein genes [8]. This gene is a transcription factor for the milk protein gene (K-casin) due to its relationship to milk production and mammary gland traits [9].

Because of the relationship of the STAT5A gene in milk production and growth traits in goats, as well as its sizeable genetic morphology, the study highlighted:

1. Determination of the genotypes of the local goats bred in Iraq based on the frequency and ratios of the genotypes of the STAT5A EXON-7 gene under study.

2. Studying the relationship of genetic polymorphism of STAT5A EXON-7 gene to animal performance in growth traits, milk production traits and its components.

MATERIALS AND METHODS

30 local Iraqi goats were used in the experiment. Molecular genetic analyses were carried out in the Biotechnology Laboratory of the Department of Animal Production / College of Agriculture / University of Diyala for the period from 2/1/2022 to 1/3/2022 to separate the genetic material (DNA) and conduct electrophoresis Polymerase chain reaction (PCR) analysis of STAT5A EXON-7 gene. The data on milk production were collected weekly for the morning circuit, and the newborn's birth weight was taken 12 hours after birth. The weaning weight was weighed after three months of birth, and the total weight gain was calculated through the weaning weight minus the birth weight, while the body dimensions of the newborns were measured. At birth and weaning according to method [10], blood samples were drawn from the jugular vein 2.5 ml using 5 ml test tubes containing Diamine Tetra acidic acid Ethylene (EDTA). After withdrawal, the blood samples were frozen at frozen temperature (-18).) It is used in the extraction of genetic material (DNA). Kit FAVORGEN is of Taiwanese origin.

Primer Seq	Primer Name	Amplicon size (pb)	name gene	Annealing temp Cº
F- CTGCAGGGCTGTTCTGAGAG	Primer–F	215 pb	STAT5A EXON 7	64º
R-TGGTACCAGGACTGTAGCACAT	Primer-R			

Table 1: Primer used with a length of 215 N bases of STAT5A EXON-7 gene in local goats.

After that, the studied segment of the STAT5A EXON-7 gene was detected using the polymerase chain reaction (PCR) technology. After the reaction was completed, the product of the polymerase reaction was migrated to ensure the presence of PCR products using the same method of preparing the agarose gel in the DNA migration, as DNA with a known molecular weight was loaded. (100-1500 nitrogen bases) in the first hole of the gel template and then loading the PCR product by 5 microliters into the pits of the gel template at (70V for 90 minutes) to be seen by the UV Light Transilluminator and photographing these beams. With a special camera, the packages appear colored orange ethidium bromide.

After electrophoresis, the PCR product, in a volume of 20 microliters, was sent to the Korean company Micro Gene Corporation. After obtaining the results by e-mail, Genious Software was used to analyze the results on Genebank's global website, www.ncbi.nlm.nih.go. The nucleotide sequence profile was used to determine the presence or absence of the mutation, and the curve profile was used to determine the phenotypic polymorphism of the three-point mutations of the STAT5A EXON-7 gene. The data were statistically analyzed using the statistical program SAS (Statistical Analysis System) [11] to study the relationship between the genetic structures of the STAT5A EXON-7 gene in milk production and growth traits for newborns. The test for significant differences between the means was carried out using Duncan's polynomial test [12].

$Yijklm = \mu + Tj + Sk + Ml + eijklm$

Since:

Yijklm: watch value m.

μ: the general average of the adjective.

Gi = the effect of the polymorphism of the STST5A gene on the studied traits.

Tj: the effect of birth type j (single, twin).
Sk: the effect of the gender of the newborn k (male, female).
Ml: The effect of the month of birth (November, December, January, February).
Eikon: the random error that is usually and independently distributed with a mean of zero and a variance of $\sigma^2 e$

RESULTS AND DISCUSSION

The current research detected point mutations in the studied sample of Region of STAT5A EXON-7 gene consisting of 215 bp. When analyzing the sequencing, three point mutations, C47064T A47088T and G47162A, were detected with two genotypes(CC, CT)(AA.AT) and (GG, AG), respectively.

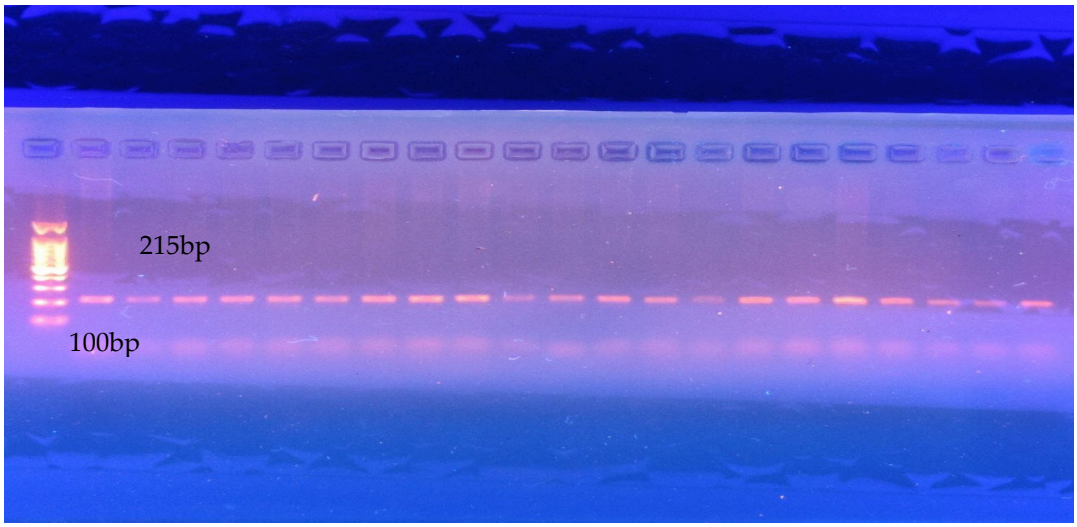

Figure 1: Shows the electrophoresis of the studied segment of the STAT5A EXON7 gene.

Were detected with two genotypes: the dominant wild CC and the hybrid CT. The frequency of the wild allele C is 0.80, While the mutant allele T is 0.20 (A47088T) with two genotypes, dominant wild AA and hybrid AT, the repeat of the wild allele A is 0.78 while the mutant allele T of 0.22, (G47162A) with two genotypes dominant wild GG and hybrid GA, the frequency of the wild allele G is 0.75 While the mutant allele C was 0.25 as shown in Table (1). A significant superiority of the chi-square value ($P \leq 0.01$) is observed for all mutations (C47064T) = 0.022 (A47088T) = 0.09 (G47162A) = 0.048.

Mutations	Genotypes	No.	Percentage	Observed	Expected	Chi-square value	Allelic frequency
C47064T	CC	18	60	0.60	P^2=0.64	Total(observed-expected)^2/expected 0.022= p≤0.01	C=0.80 T=0.20
	CT	12	40	0.40	2pq=0.32		
A47088T	AA	17	56.7	0.56	P^2=0.604	Total(observed-expected)^2/expected 0.09= p≤0.01	A=0.78 T=0.22
	AT	13	43.3	0.43	2pq=0.343		
G47162A	GG	15	50	0.50	P^2=0.562	Total(observed-expected)^2/expected 0.048= p≤0.01	G=0.75 C=0.25
	GC	15	50	0.50	2pq=0.375		

Table 2: Number, percentages of genotypes and allelic frequency of the studied mutations in the STAT5A EXON-7 gene.

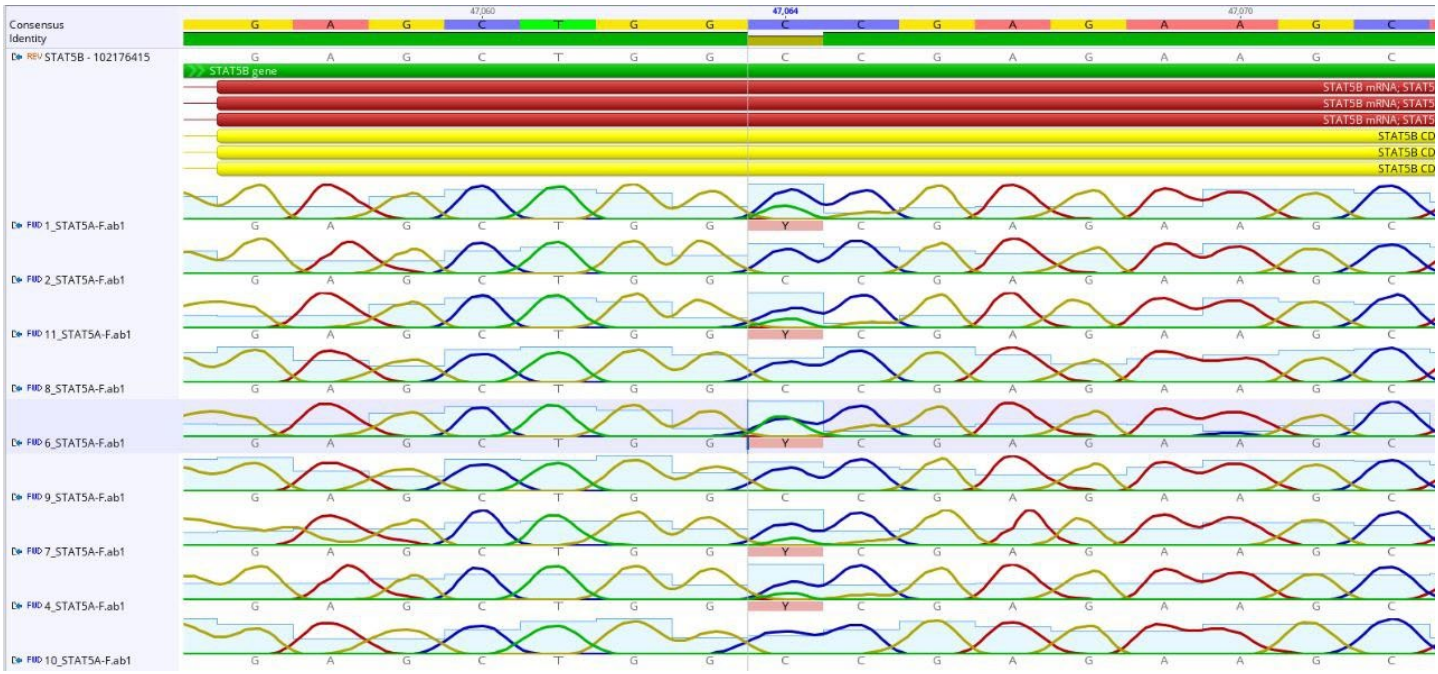

Figure 2: Shows the location of the mutation (C47064T) in the STAT5A gene EXON-7.

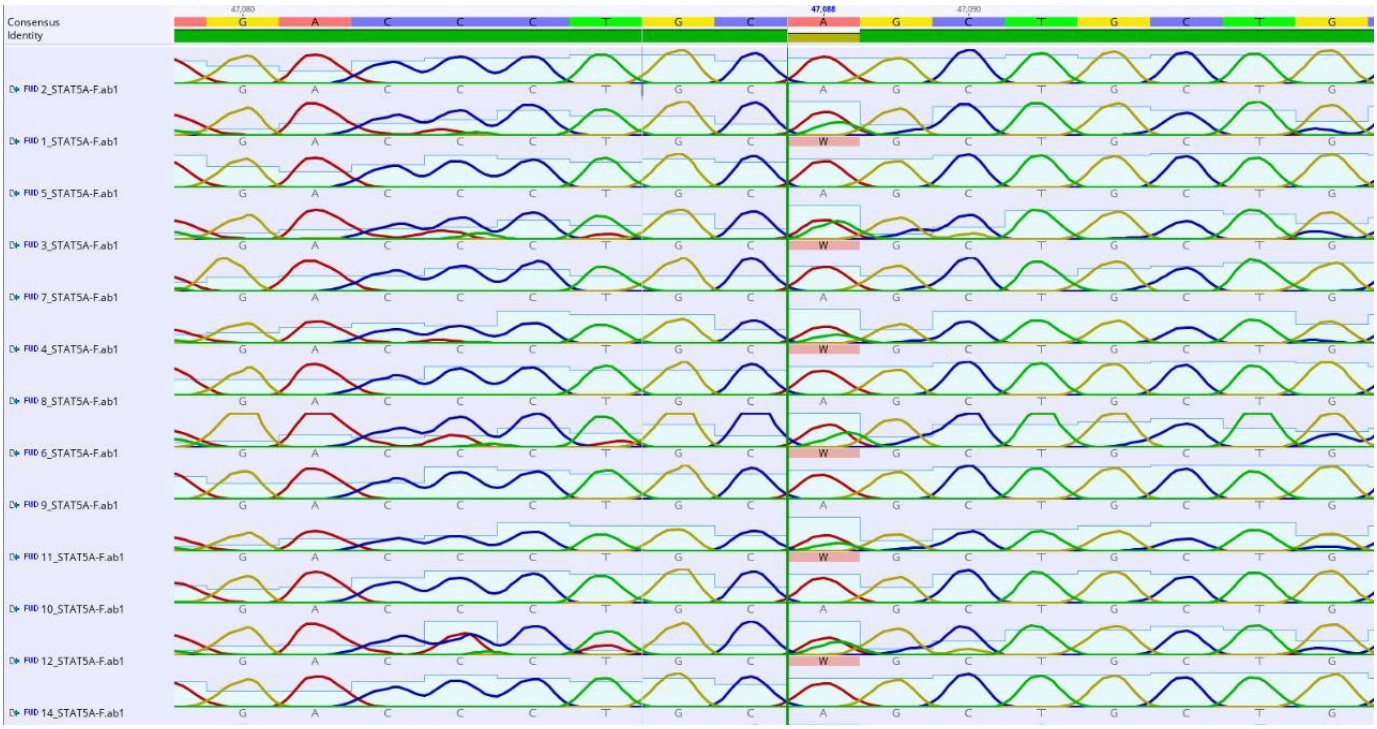

Figure 3: Shows the location of the mutation (C47088T) in the STAT5A gene EXON-7.

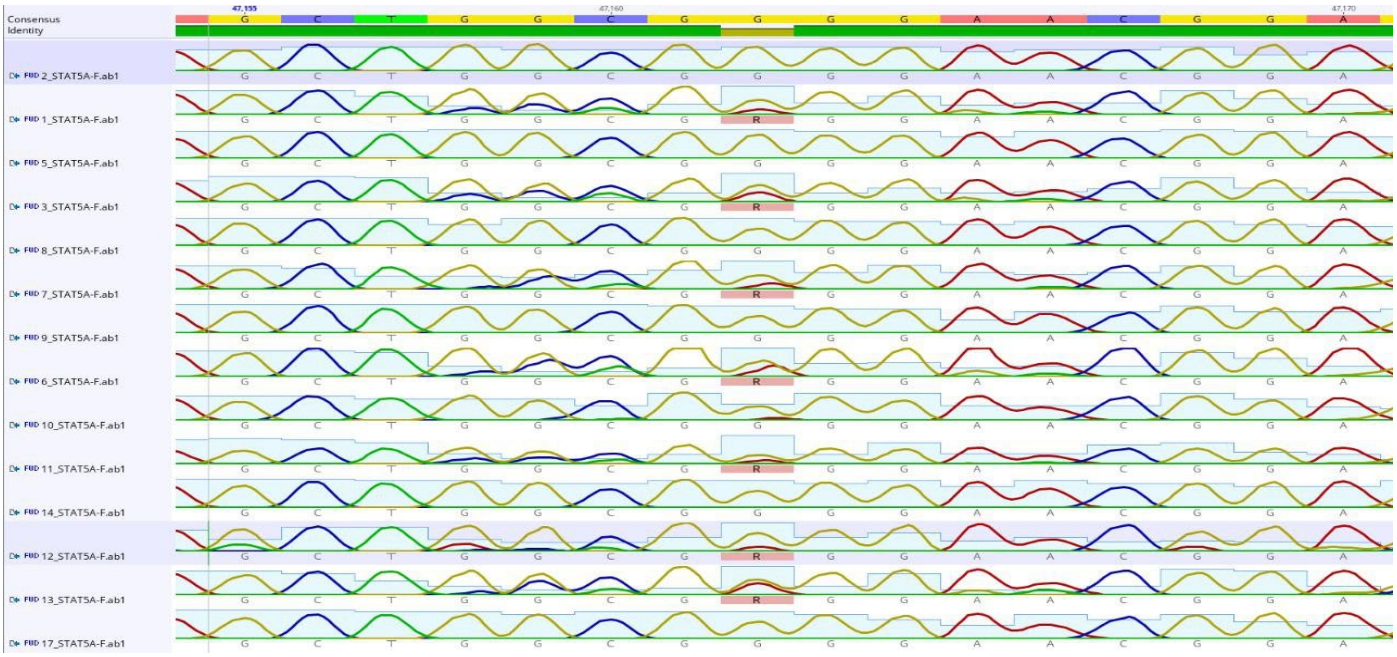

Figure 4: Shows the location of the mutation (C47062T) in the STAT5A gene EXON-7.

The results of the statistical analysis in Tables 2,3,4,5 and 6 showed that there was no significant effect of the point mutation (C47064T), (A47088T) and (G47162A) on Daily and total milk production, growth traits (birth weight, weaning weight and total weight gain) and dimensions at birth and weaning.

Total milk production kg/season	Daily milk production g/day	No. 30	Trait
C47064T			
2.61 ± 28.06	33.55 ± 359.80	18	CC
2.64 ± 26.15	33.93 ± 335.30	12	CT
A47088T			
2.65 ± 26.43	34.03 ± 338.86	17	AA
2.65 ± 28.43	34.06 ± 364.56	13	AT
G47162A			
2.96 ± 27.17	37.97 ± 348.39	15	GG
2.39 ± 27.42	30.70 ± 351.61	15	GA
NS	NS		level significant

Table 3: Shows the effect of genotypes in milk production for the studied point mutants.

Total weight gain kg	Weaning weight kg	Birth weight kg	No. 30	Trait
C47064T				
1.11±11.54	1.12±14.43	0.17±2.89	18	CC
1.51±10.96	1.45±13.91	0.16±2.95	12	CT
A47088T				
1.10±10.72	1.10±13.66	0.18±2.94	17	AA
1.27±12.08	1.43±14.95	0.13±2.87	13	AT
G47162A				
1.23±10.90	1.24±13.89	0.18±2.98	15	GG
1.30±11.71	1.26±14.56	0.16±2.84	15	GA
NS	NS	NS		level significant

Table 4: Shows the effect of genotypes on birth weight, weaning weight and total weight gain.

Body length cm	Back height cm	Front height cm	Chest circumference	Abdominal circumference	No. 30	Trait
C47064T						
0.57±24.27	0.97±36.61	0.79±35.22	0.80±33.83	0.94±35.0	18	CC
0.45±23.08	0.80±36.08	0.79±34.33	0.54±33.58	0.74±35.0	12	CT
A47088T						
0.61±24.17	1.03±36.58	0.83±35.17	0.83±33.64	1.00±35.05	17	AA
0.41±23.30	0.74±36.15	0.73±34.46	0.55±33.84	0.69±34.92	13	AT
G47162A						
0.68±24.40	1.10±36.86	0.93±35.33	0.89±33.86	1.06±35.20	15	GG
0.36±23.20	0.73±35.93	0.64±34.40	0.58±33.60	0.71±34.80	15	GA
NS	NS	NS	NS	NS		level significant

Table 5: Shows the effect of genotypes on the body dimensions of lambs at birth.

Body length cm	Back height cm	Front height cm	Chest circumference cm	Abdominal circumference	No. 30	Trait
C47064T						
0.69±35.38	1.20±55.66	1.59±53.88	1.16±57.38	1.90±61.66	18	CC
0.98±36.08	1.64±56.16	2.30±53.08	1.40±56.75	1.96±62.41	12	CT
A47088T						
0.60±34.82	1.26±55.17	1.56±52.82	1.17±56.94	1.86±60.64	17	AA
0.99±36.76	1.49±56.76	2.25±45.53	1.38±57.38	1.96±63.69	13	AT
G47162A						
0.67±34.93	1.41±55.46	1.76±52.93	1.31±57.06	2.12±60.66	15	GG
0.89±36.40	1.33±56.26	1.96±45.20	1.21±57.20	1.71±36.26	15	GA
NS	NS	NS	NS	NS		level significant

Table 6. Shows the effect of genotypes on the body dimensions of lambs when weaning.

Table (3) shows no significant effect of the point mutations C47064T, A47088T, and G47162A on daily and total milk production characteristics. The result of this study is consistent with what was reached by [13] in their study on sheep, as they did not find any significant effect of the genotypes. STAT5A gene in total milk production, while the result of the current study differs from what [14] found in their research on breeds of goats, as they found superiority of the CC genotype at the 6852C>T mutation site in total milk production.

The current study showed that there were no significant differences for the studied point mutations C47064T, A47088T, and G47162A in birth weight, weaning weight, and total weight gain, as shown in Table (4), and the result of this study agreed with what was reached by [13] in their study on sheep, as no A significant effect of the genotypes of the STAT5A gene was found on birth weight, weaning, and daily weight gain, while the results of this study agreed with part of what was reached by [15] in their study on male goats, as they did not find a significant effect of the genotypes at the mutation site (T11289C) in... Body weight: As for the location of the mutation A14320G, the genotype (GG) is significantly superior to the two combinations (AG, AA) in this trait, 6852C>T.

The current study showed in Table (5) that there were no significant differences for the studied point mutations C47064T, A47088T, and G47162A in the body dimensions of the lambs at birth. This study is partially consistent with what [15] reached in their study on male goats, as they did not find a significant effect of the genotypes. Site The mutation (T11289C) and (A14320G) in both body length, body height and shoulder width, and they found the superiority of the two genotypes CC (mutation site (T11289C)) and GG mutation site (A14320G) in the depth of the chest, and it partly agreed with what [16] found in their study on females. Goats aged 2-3 years found superiority of the mutant genotype (TT) in body height, chest circumference, and shoulder width.

It is clear from Table (6) that there are no significant differences for the studied point mutations in body dimensions at weaning. This result contradicts what [16] reached in his study on 2-3-year-old females of Chinese goats, the HNBG breed, for meat production. They found a significant superiority of the mutant genotype (TT) compared to the two genotypes (CC and TC) in chest circumference, body height, and butt width. They also found no significant effect of the genotypes of this gene in both body weight and chest depth.

CONCLUSIONS

The results of this study showed the presence of three mutations within the studied region of the seventh exon: the first mutation at the C47064T site resulting from the transformation of the base C to T, the second at the A47088T site resulting from the transformation of the base A to T, and the third mutation G47162A resulting from the transformation of the G base to A. The studied mutations had no significant effect on milk production and growth characteristics.

REFERENCES

1. Gipson, A. Terry. Recent advances in breeding and genetics for dairy Goats **2019**. Asian-Australas J Anim Sci. 32(8): 1275–1283.
2. Raziye, I. and Güldehen, B. Associations between genetic variants of the POU1F1 gene and production traits in Saanen goats. **2019**. Arch. Anim. Breed., 62, 249–255.
3. Oget, C., Servin, B. and Palhière, I. Genetic diversity analysis of French goat populations reveals selective sweeps involved in their differentiation. Anim Genet. **2019**.; 50:54–63.
4. Alakilli, S. Y. M., Karima, F. Mahrous, Lamiaa, M. S. and Ekram, S A. Genetic polymorphism of five genes associated with growth traits in goat. **2012**. African Journal of Biotechnology Vol. 11(82), pp. 14738- 14748.
5. Williams, J. L. The use of marker-assisted selection in animal breeding and biotechnology. **2005**. Rev. Sci. Tech. 24(1): 379-91.
6. Chughtar N, Schimchowitsch S, Lebrun JJ, Ali S. Prolactin induces SHP-2 association with Stat5, nuclear translocation, and binding to the beta-casein gene promoter in mammary cells. **2012**. J Biol Chem. 277:31107.
7. Brym, S. Kamiński, and Ruść A. New SSCP polymorphism within bovine STAT5A gene and its associations with milk per-formance traits in Black-and-White and Jersey cattle. **2004**. Journal of Applied Genetics, vol. 45, pp. 445-452.
8. Wakao H, Gouilleux F and Groner. B . Mammary gland factor (MGF) is a novel member of the cytokine regulated transcription factor gene family and confers the prolactin response. **1994**. EMBO J 13:2182–2191.
9. Aaronson, D. S. and Horvath, C. M. A road map for those who don't Know JAK-STAT. **2002**. Science, 296(5573):1653-1655.
10. Cam, M. A.; M. Olfaz and E. Soydan. Body Measurements Reflect Body Weight and Carcass Yields in Kara Yaka Sheep. **2010**. Asian J. Anim .Vet.Adv,(5):120-127.
11. SAS . SAS/STAT User's Guide for Personal Computers . **2012**. Release 9.1 SAS Institute Inc. , Cary , N. C. , USA .
12. Duncan, D.D. Multiple range and multiple F-test Biometrics **1955** , 11: 1-42.
13. Abousoliman, I., Reyer, H., Oster, M., Muráni, E., Mourad, M., Abdel-Salam Rashed, M., & Wimmers, K. Analysis of candidate genes for growth and milk performance traits in the Egyptian Barki sheep. *Animals*, **2020.** *10*(2), 197.
14. An, X. P., Hou, J. X., Zhao, H. B., Bai, L., Peng, J. Y., Zhu, C. M., ... & Cao, B. Y. Polymorphism identification in goat DGAT1 and STAT5A genes and association with milk production traits. *Czech J. Anim. Sci*, **2013.** *58*(7), 321-327.

15. Xie, H. Q., Sun, Y. Y., Pan, D. X., Yang, Y. Q., Jiao, R. G., Gong, Y., ... & Liu, R. Y. Association analysis between polymorphism of STAT5a gene and growth traits in Chinese guizhou black goats. *Pak. J. Agri. Sci***2015.**, *52*(4), 1119-1123.
16. Wu, X., Jia, W., Zhang, J., Li, X., Pan, C., Lei, C., & Lan, X. Determination of the novel genetic variants of goat STAT5A gene and their effects on body measurement traits in two Chinese native breeds. *Small Ruminant Research*, **2014.** *121*(2-3), 232-243.

Received: October 9th 2023/ **Accepte**d: January 15th 2024 / **Published:**15 February 2024

Citation: Bashar A.; Hamza K. Relationship Polymorphism of STAT5A Gene in Performance Production of Local Goats. Revis Bionatura 2024; 9 (1) 57. http://dx.doi.org/10.21931/RB/2024.09.01.57

Additional information Correspondence should be addressed to gabriela.rosero@espoch.edu.ec
Peer review information. Bionatura thanks anonymous reviewer(s) for their contribution to the peer review of this work using https://reviewerlocator.webofscience.com/

All articles published by Bionatura Journal are made freely and permanently accessible online immediately upon publication, without subscription charges or registration barriers.
Bionatura ISSN. First 13909355 Ecuador. **Scopus coverage years**: from 2016 to the present
Publisher's Note: Bionatura stays neutral concerning jurisdictional claims in published maps and institutional affiliations.

Bionatura
Ibero-American Journal of Biotechnology and Life Sciences

Article

Ameliorative Effect of Cinnamon and Rosemary Oils in Acrylamide–Induced Hepatic Injury in Rats

Hala Elsayed[1], Ashraf Abd El-Hakim El komy[2], Elham Abd-El Moneim El-Shewy[3], Faten Ebrahim Elsayed Abdallah[4]*

[1]Department of Pharmacology, Faculty of Veterinary Medicine, Benha University, Toukh 13736, Egypt.; haladiab1986@yahoo.com.
[2]Department of Pharmacology, Faculty of Veterinary Medicine, Benha University, Toukh 13736, Egypt.; ashraf.komy@hotmail.com.
[3]Department of Forensic Medicine Faculty of Veterinary Medicine, Benha University, Toukh 13736, Egypt.; Elhamshewy@yahoo.com.
[4]Department of Pharmacology, Faculty of Veterinary Medicine, Benha University, Toukh 13736, Egypt.; Faten.Abdalla@fvtm.bu.edu.eg.
** Correspondence: haladiab1986@yahoo.com.; Tel.: +20 102 608 7482.*
Available from. http://dx.doi.org/10.21931/RB/2024.09.01.58

ABSTRACT

Liver diseases can result from various causes, such as viruses, bacteria, autoimmune disorders, or certain medications and toxic substances. While modern medicine offers treatments for these conditions, there needs to be more effective drugs that can protect and regenerate liver cells. Therefore, it is crucial to identify new treatment options and liver-protective agents that are both highly efficient and safe. This study is assigned to investigate the adverse effects of acrylamide on the liver in rats and explore whether these effects can be mitigated by co-administration of cinnamon oil (C.O.), rosemary oil (R.O.), or a combination of both oils during acrylamide exposure. A total of 70 male albino rats were divided randomly into 7 groups, each group of 10 rats, that received different treatments: control group, acrylamide-treated group (20 mg/kg b.wt), cinnamon oil-treated group (200 mg/kg b.wt), rosemary oil-treated group (250 mg/kg b.wt), acrylamide and cinnamon oil-treated group, acrylamide and rosemary oil-treated group, and acrylamide, cinnamon oil, and rosemary oil-treated group. These treatments were administered orally for 28 consecutive days. Blood and liver tissue samples were gathered at the end of the study to assess the outcomes. The results revealed that cinnamon oil and rosemary oils exhibited hepatoprotective effects, as evidenced by normalized liver function parameters (alanine transaminase, Aspartate transaminase, and Alkaline phosphatase), as well as improvements in non-enzymatic parameters (total protein, albumin, cholesterol, triglyceride, low-density lipoprotein, and high-density lipoprotein). The observed hepatoprotection of cinnamon oil and rosemary oils was attributed to their ability to reduce oxidative stress caused by acrylamide, as demonstrated by lower levels of liver cell lipid peroxidation product (malondialdehyde) and enhanced activity of antioxidative enzymes (glutathione and catalase) in liver tissue.

Keywords: Cinnamon, Rosemary, Acrylamide, Liver, Rats, Antioxidants.

INTRODUCTION

Acrylamide is a compound that dissolves in water and is extensively utilized in various fields, including dye production, soil coagulation, wastewater treatment, paper packaging, and laboratory applications [1]. This compound is not naturally present. Research has revealed that foods with high carbohydrate content, when exposed to high temperatures during heating or frying processes, tend to contain significant levels of acrylamide [2]. Acrylamide forms when carbohydrate-rich foods like crackers, potatoes, crisps, cereals, bread, and French

fries are grilled, fried, baked, or roasted at temperatures exceeding 120°C. This process involves the reaction between the amino acid asparagine and a reducing sugar such as glucose [3].

Acrylamide has been associated with several harmful effects in rodents, including genotoxicity, neurotoxicity, hepatotoxicity, nephrotoxicity, carcinogenicity, and reproductive toxicity [4]. The International Agency for Research on Cancer has classified acrylamide as a 2A substance [5]. From the *Lauraceae* family, Cinnamon is a widely used spice in the food industry, often added to baked goods and chili sauce for flavoring purposes [6]. It contains various constituents that act as food additives, providing antioxidant, anti-inflammatory, anti-cancer, antimicrobial, and antidiabetic properties [7]. From the *Lamiaceae* family, Rosemary is a well-known aromatic plant used for flavoring in food processing and medicinal purposes [8]. Rosemary is recognized for its potent antioxidant properties, which help eliminate free radicals, strengthen the antioxidant system, and prevent oxidative stress [9].

Rosemary extracts have been reported to possess hepatoprotective activity in a rat model of azathioprine-induced toxicity and acetaminophen-induced liver damage. When administered to rats with hepatotoxicity, cinnamon and rosemary or their combination resulted in a notable reduction in the average level of MDA and a significant increase in hepatic GSH.[9] Currently, the toxic effects of acrylamide on liver tissue in animals have been examined, along with the evaluation of the beneficial effects of cinnamon and rosemary in relieving acrylamide-induced hepatotoxicity in adult albino rats.

MATERIALS AND METHODS

Acrylamide, a white crystalline powder obtained from Fine–Chem Limited Company with a purity of approximately 98.5%, was dissolved in distilled water just before administration at a dose of 20 mg/kg body weight [10].

Cinnamon and rosemary oils, sourced from El-captain Company for extracting natural oils, herbs, and cosmetics in Cairo, Egypt, were used at 200 mg/kg body weight [11] and 250 mg/kg body weight 12, respectively.

Various diagnostic kits were used for measuring levels of aspartate aminotransferase (AST), alanine aminotransferase (ALT), alkaline phosphatase (ALP), total protein, albumin, triglycerides, cholesterol, HDL, LDL, as well as oxidative stress markers including malondialdehyde (MDA), glutathione peroxidase (GSH), and catalase (CAT) in plasma and liver tissue homogenate. These kits were obtained from BioDiagnostic Company in Giza, Egypt.

The study utilized 70 male white albino Wistar rats of about 180-200 grams. These rats were brought from the Center of Laboratory Animals at the Faculty of Veterinary Medicine, Benha University, Egypt. Prior to the experiment, the rats were given one week to acclimatize. During this period, they were provided with a standard laboratory-balanced commercial diet and had access to water ad libitum. The research adhered to the guidelines for animal care and procedures set by the Faculty of Veterinary Medicine, Benha University, Benha, Egypt, under number (03-03-23). The basal diet provided to the rats met their nutritional requirements for maintenance as specified by the National Research Council and Reeves.

The acclimatized rats were divided into seven groups, each consisting of 10 rats. The groups were treated differently according to the objective of the study [10]. The treatments were as follows:

- Group 1: Control group, where rats were given distilled water orally once a day for 28 consecutive days.
- Group 2: Rats given acrylamide orally at a dose of 20 mg/kg body weight once daily for 28 consecutive days to induce hepatic injury **[9].**
- Group 3: Rats given cinnamon oil orally at 200 mg/kg body weight once daily for 28 consecutive days **[10].**
- Group 4: Rats given rosemary oil orally at a dose of 250 mg/kg body weight once a day for 28 consecutive days **[11].**
- Group 5: Rats were given acrylamide (20 mg/kg body weight) and cinnamon oil (200 mg/kg) daily for 28 consecutive days.
- Group 6: Rats were given acrylamide (20 mg/kg body weight) and rosemary oil (250 mg/kg) daily for 28 consecutive days.
- Group 7: Rats that were given acrylamide (20 mg/kg body weight) followed by cinnamon oil (200 mg/kg body weight) and then rosemary oil (250 mg/kg body weight) once a day for 28 consecutive days.

Sampling:
At the end of the 28-day treatment period, all rats were euthanized. Blood and liver samples were collected to conduct biochemical and histopathological examinations.
Blood samples were obtained from 10 rats in each group after 28 days of treatment by puncturing the retro-orbital plexus, which is located at the inner corner of the eye. Capillary tubes were used to collect the blood samples and immediately placed in plain sampling tubes. The samples were then centrifuged at 1200 g for 10 minutes to separate the clear plasma, which was transferred into Eppendorf tubes using automatic pipettes. The plasma samples were stored at -20 °C for further analysis.

Tissue specimens:
The liver underwent an examination and rinsing process using a standard saline solution to remove traces of blood, fat, and connective tissue. Liver samples of approximately 1 gram were carefully collected from each group of 10 rats and placed into secure and labeled Eppendorf tubes. These samples were blended with a pH 7.4 phosphate buffer solution and then centrifuged at a speed of 1200 g for 10 minutes. The resulting clear liquid was carefully preserved at -20°C for further analysis of the oxidative markers in the tissues. Moreover, additional liver tissue samples were obtained and preserved in a 10% formalin solution for histopathological examinations following a 28-day treatment period.

Biochemical and antioxidant effects:
In order to evaluate the safety of the drug, the levels of certain enzymes in blood and liver tissue homogenates were determined. The plasma activities of AST, ALT, and ALP were measured using specialized kits and the methods outlined by Reitman & Frankel [12] for ALT and ALT and by Haussament [13] for ALP, following the instructions provided by the manufacturer. Other biochemical parameters such as total protein, albumin, T.G.s, HDL cholesterol, and LDL were also measured using specific spectrophotometric methods [13]. Furthermore, the oxidative and antioxidative parameters in liver homogenate were determined using specific kits for measuring MDA, GSH, and Catalase through spectrophotometry [14].
Histopathological examination was conducted according to Bancroft [15].

Data management and statistical analysis:
The collected data were analyzed using one-way analysis of variance (ANOVA), and post hoc testing was performed using Duncan's test. The analysis was conducted using the Windows version of SPSS 25. The results were presented as mean±standard error (SEM), and statistical significance was considered at P values ≤ 0.05.

RESULTS

The results of the biochemical parameters analysis revealed that rats treated with acrylamide exhibited a significant rise in AST, ALT, ALP, cholesterol, triglycerides, and LDL-cholesterol levels and a significant decrease in total protein, albumin, and HDL cholesterol levels compared to the control groups. However, the administration of cinnamon and rosemary led to a notable improvement in these parameters, as depicted in Tables 1 and 2. Regarding oxidative stress results (Figures 1, 2, and 3), acrylamide-treated rats demonstrated a marked increase in MDA levels and a significant reduction in CAT and GSH levels in their liver tissues compared to the control groups. However, the administration of cinnamon and rosemary resulted in a considerable improvement in these parameters. Furthermore, a histopathological examination of the liver tissues from the acrylamide-treated group showed changes in their structural appearance. Nevertheless, an enhancement in histopathology was observed after the administration of cinnamon and rosemary, as shown in Figure 4.

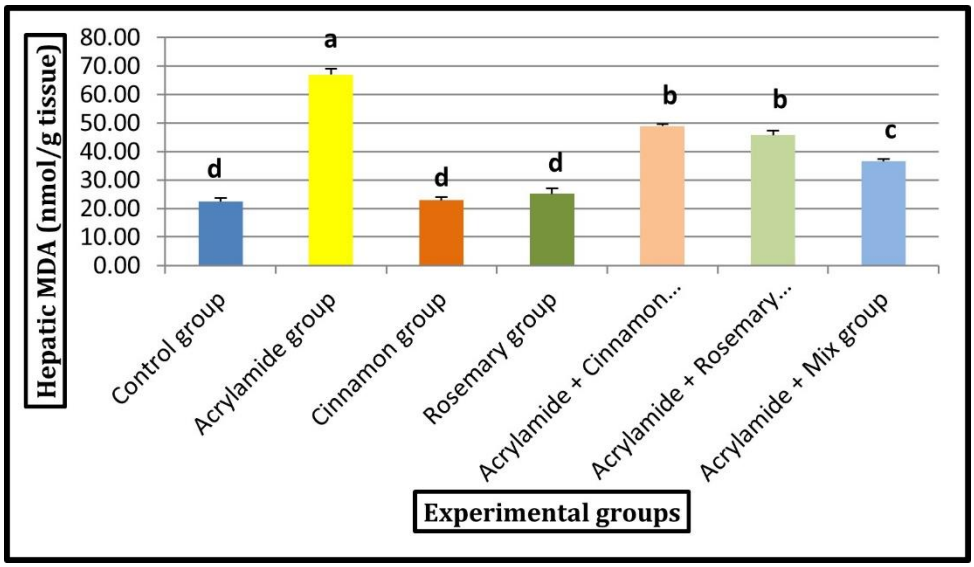

Figure 1: Effect of acrylamide, cinnamon oil and rosemary oil on hepatic MDA.

Experimental Group	ALT (U/L)	AST (U/L)	ALP (U/L)	Albumin (g/dL)	T.P. (g/dL)
Control group	23.91±1.00^{d}	81.15±3.27^{d}	250.87±3.25^{e}	3.80±0.11^{a}	7.46±0.12^{a}
Acrylamide group	89.23±2.65^{a}	161.03±4.27^{a}	389.97±4.13^{a}	1.53±0.11^{d}	3.61±0.16^{e}
Cinnamon group	22.30±1.22^{d}	81.33±3.17^{d}	258.06±2.48^{e}	3.72±0.11^{a}	7.78±0.16^{a}
Rosemary group	24.23±1.38^{d}	78.63±1.97^{d}	258.14±6.21^{e}	3.60±0.09^{a}	7.62±0.09^{a}
Acrylamide + Cinnamon group	58.57±1.99^{b}	130.16±2.42^{b}	356.45±3.96^{b}	1.78±0.10^{d}	5.15±0.07^{d}
Acrylamide + Rosemary group	54.44±1.60^{b}	123.94±1.73^{b}	326.02±4.88^{c}	2.33±0.07^{c}	6.08±0.13^{c}
Acrylamide + Mix group	38.97±1.26^{c}	104.52±2.06^{c}	289.90±4.37^{d}	3.00±0.03^{b}	6.70±0.10^{b}

Data are presented as (Mean ± S.E.). S.E. = Standard error.
Mean values with different superscript letters in the same column significantly differ at (P<0.05).
Table 1: Effect of acrylamide, cinnamon, and rosemary oil on serum ALT, AST, ALP, Albumin, and T.P.

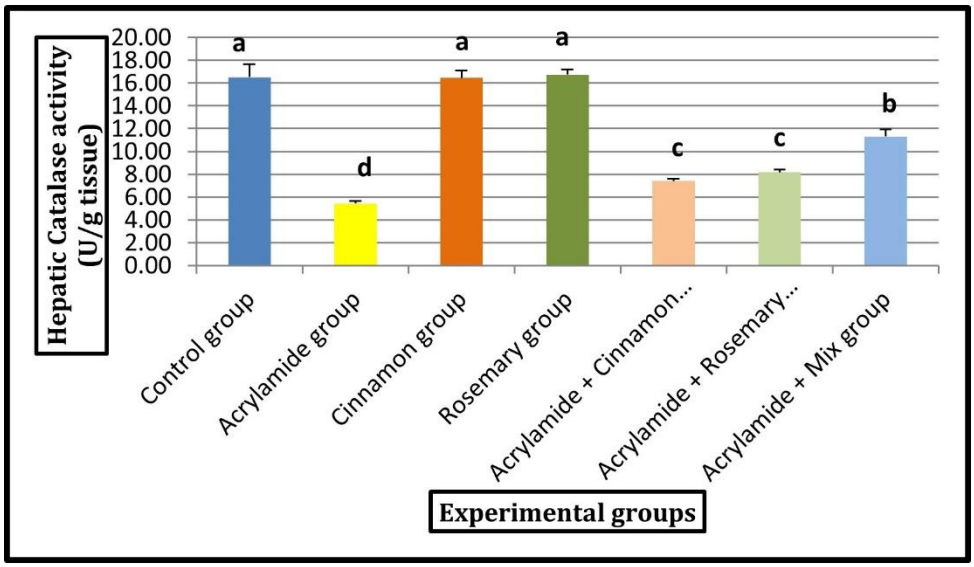

Figure 2: Effect of acrylamide, cinnamon oil and rosemary oil on Hepatic catalase activity.

Experimental Group	Cholesterol (mg/dL)	Triglycerides (mg/dL)	HDL (mg/dL)	LDL (mg/dL)
Control group	97.69±1.06^{e}	157.23±2.56^{e}	36.07±1.77^{a}	30.18±1.15^{e}
Acrylamide group	162.11±1.61^{a}	209.72±3.13^{a}	23.29±1.40^{c}	96.87±2.38^{a}
Cinnamon group	94.58±1.65^{e}	156.53±1.46^{e}	36.18±1.23^{a}	27.09±1.64^{e}
Rosemary group	94.55±1.40^{e}	155.69±1.87^{e}	37.68±1.48^{a}	25.73±1.96^{e}
Acrylamide + Cinnamon group	144.91±1.94^{b}	190.94±1.68^{b}	27.71±1.06^{b}	79.01±2.15^{b}
Acrylamide + Rosemary group	137.54±1.49^{c}	183.21±2.93^{c}	31.57±1.27^{b}	69.32±2.08^{c}
Acrylamide + Mix group	115.99±1.69^{d}	174.96±1.85^{d}	37.51±1.12^{a}	43.48±1.54^{d}

Table (2) displays the data as Mean ± S.E., where S.E. represents the standard error. The mean values in the same column with distinct superscript letters indicate significant differences below 0.05 ($P<0.05$).

Table 2: Effect of acrylamide, cinnamon oil and rosemary oil on lipid profile.

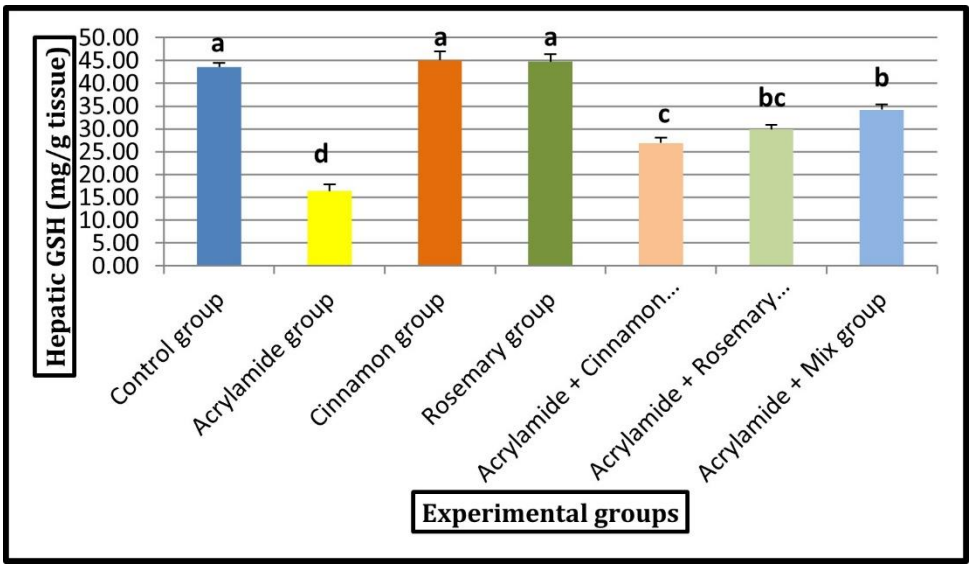

Figure 3: Effect of acrylamide, cinnamon oil and rosemary oil on Hepatic GSH.

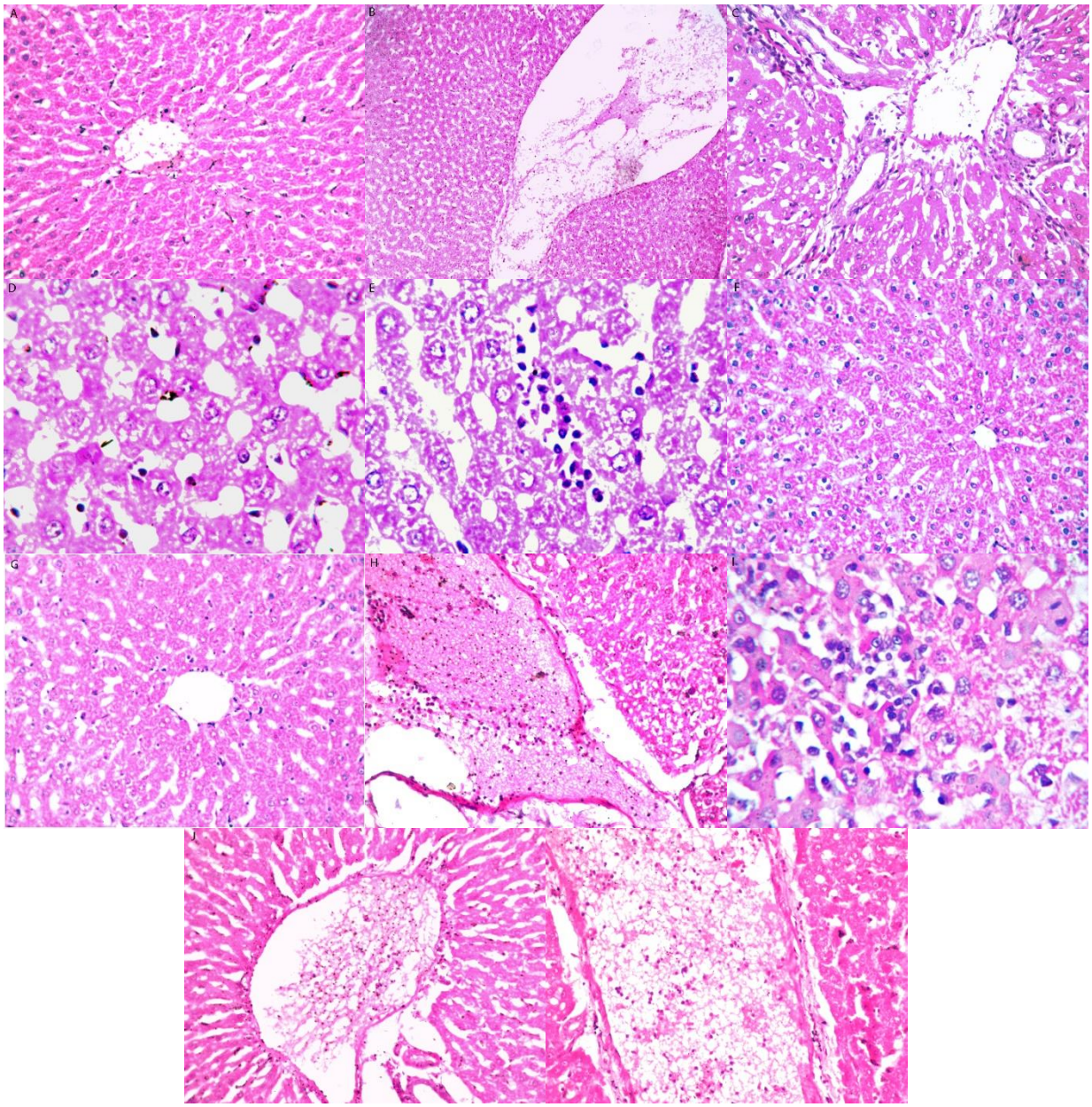

Figure 4: Histopathological examination findings of the hepatic tissue.

The histopathological examination of the hepatic tissue in the control group (A) revealed no histopathological changes. The histological structure of the central vein and the hepatocytes around it within the lobules of the parenchyma appeared normal. The acrylamide group showed (B) thrombosis in the lumen of the dilated central vein and (C) associated with edema and a few inflammatory cell infiltrations in the portal area, as well as dilatation in the portal vein as well as in the bile ducts. (D) There was focal inflammatory cell infiltration and (E) diffuse Kupffer cell proliferation between the degenerated hepatocytes. The cinnamon group showed (F) no histopathological alteration. The rosemary group showed (G) no histopathological alteration. The ACR+Cin group showed (H) thrombosis in the lumen of the dilated portal vein (I) associated with focal inflammatory cell infiltration between the hepatocytes. The ACR+ Ros group showed (J) thrombosis in the lumen of the dilated portal vein. ACR+Cin+Ros showed (K) thrombosis in the lumen of the dilated portal vein.

DISCUSSION

The liver's crucial role in metabolism makes it prone to damage caused by exposure to chemicals. Chemical-induced liver injury poses a significant health risk, often leading to acute liver failure [16]. The primary reason behind this specific liver damage is the generation of reactive oxygen species. These reactive compounds cause oxidative stress, subsequently damaging cellular molecules. Consequently, oxidative stress is a well-established contributor to the onset of diverse liver diseases [17].

Oxidative stress plays a significant role in the process of tissue damage. It occurs due to an imbalance between the production of reactive oxygen species and the body's ability to neutralize or counteract their harmful effects [18].

The use of natural antioxidant products has been rapidly growing globally, owing to their proven efficacy and safety. These products are increasingly employed in treating various liver ailments, reflecting their rising popularity in the medical field [3].

Acrylamide is a byproduct formed when starchy foods like potatoes and bread are cooked at high temperatures above 120°C, such as frying or baking. Acrylamide harms living organisms, including genotoxic, neurotoxic, carcinogenic, nephrotoxic, and hepatotoxic [19].

The production of free radicals by acrylamide leads to liver damage. Free radicals are highly reactive and can severely damage cell membranes, nucleic acid, and proteins [20].

Abdel-Daim found that acrylamide has dangerous effects on liver and kidney tissues by increasing the occurrence of lipid peroxidation and altering antioxidant enzyme systems. The significant increase in lipid peroxidation in the liver and kidney can affect the oxidative stress levels in an organism [21].

In this study, we provided evidence that co-treatment with cinnamon and rosemary can improve liver function, histology, and oxidative stress caused by acrylamide exposure. This study showed that oral administration of acrylamide at a dose of 20 mg/kg body weight for four weeks led to a significant increase in liver enzymes and cholesterol, triglycerides, and hepatic MDA levels. There was also a significant decrease in albumin, T.P., HDL, and hepatic CAT and GSH levels compared to other groups.

These findings align with a previous study by Erfan [22], who reported elevated levels of liver enzymes ALT and AST and evident histopathological liver injury in the group treated with acrylamide.

The current study showed that the acrylamide-treated group had significantly higher levels of MDA in liver tissue, indicating severe oxidative damage. These findings are consistent with previous studies [5, 23] that also observed increased levels of AST and ALT due to acrylamide administration.

A study conducted by Elhelaly [23] found that oral administration of acrylamide significantly increased levels of ALT and AST, damaging tissue membranes. Acrylamide impaired the viability of hepatic tissue and caused acute toxic damage over time. They also indicated that acrylamide oral administration significantly increased MDA levels and decreased GPX and SOD levels. [23]

The present study demonstrated a significant increase in total cholesterol (T.C.) and triglycerides (T.G.); this comes in agreement with Akram[24,] who reported that low doses of acrylamide caused elevated T.C. and T.G. levels compared to the control group due to lipid peroxidation.

On the other hand, co-treatment with rosemary extract reduced elevated levels of ALT, AST, and ALP in the serum and improved the oxidant-antioxidant status, as seen by decreased MDA levels and increased GSH levels [23, 25].

These results align with the findings of Samaha [26], who reported that carnosic acid prevented liver damage and disturbances in lipid metabolism, leading to decreased levels of ALT, AST, and ALP in the serum.

In another study conducted by Raskovic et al. [27], it was observed that liver injury led to increased levels of AST and ALT enzymes due to hepatocyte damage and leakage. However, treatment with rosemary was found to mitigate these effects, as indicated by the reduction in elevated MDA levels, which signify oxidative damage to cell membranes. The researchers concluded that adding rosemary supplements partially restored the altered biochemical parameters and significantly reversed markers associated with oxidative stress in experimental models of liver injury.

A study done by Zhao et al. [28] discovered that adding Rosemary to the diet of mice fed a high-fat diet resulted in significant reductions in body weight gain, fat percentage, plasma ALT, triglycerides, free fatty acids, and levels of MDA in the liver and plasma. Furthermore, Rosemary improved liver histology and function, as indicated by a significant decrease in serum levels of ALT and AST, which are markers of liver injury.

Oxidative stress is countered by the complex antioxidant system in mammals. MDA, a byproduct of lipid peroxidation, indicates the level of oxidative damage in the liver tissue.

Cinnamon, a perennial tropical herb from the *Lauraceae* family, contains essential oil, cinnamaldehyde, cinnamic acid, and cinnamate. Its medicinal properties, including antioxidant, antidiabetic, anti-inflammatory, cardiovascular, anti-cancer, and lipid-lowering effects, make it helpful in treating inflammatory conditions. Cinnamon can reduce organ damage by alleviating oxidative stress [29]. Moreover, cinnamon has protective properties that guard against liver abnormalities in rats.

The current study showed a significant decrease in average ALT and AST levels and a slight reduction in T.C. and T.G. in the liver of rats treated with cinnamon, rosemary, or both. These findings align with Ismail et al. [30], who observed significant decreases in ALT and AST, triglycerides, and cholesterol levels in rats with liver damage upon cinnamon administration.

Shalaby and Saifan [31] discovered that the use of cinnamon aqueous extract in diabetic obese rats resulted in a reduction in lipid levels, and it induced liver protection owing to its antioxidant properties. The hepatoprotective effect of cinnamon extract aids in accelerating the recovery and growth of liver cells by promoting the synthesis of proteins. It stimulates the enzyme RNA polymerase 1, which increases ribosomal protein production and facilitates the regeneration of damaged hepatocytes [32].

The consumption of cinnamon in the diet inhibits the activity of hydroxy-3-methylglutaryl-coenzyme A [HMG Co-A] reductase in the liver, which leads to a decrease in lipids and improved lipid peroxidation. This is achieved by enhancing the functioning of lipid antioxidant enzymes. Additionally, cinnamon helps in the expression of the LDL-R gene, which contributes to its lipid-lowering effects [33].

Pre-treatment with 200mg/kg/day of cinnamon aqueous extract for 14 days before administering a single toxic dose of acetaminophen significantly reduced the elevated level of ALT and AST levels [34]. This provides evidence for the hepatoprotective nature of cinnamon and its capability to repair liver damage. The positive effects of cinnamon on liver damage may be attributed to its ability to enhance the antioxidant defense system, scavenge reactive oxygen species, and inhibit lipid peroxidation.

Studies have revealed that cinnamon oil benefits liver toxicity, lipid oxidation, inflammation (specifically IL-1β, IL-6), DNA fragmentation, and histopathological alterations caused by acetaminophen [35]. The potential protective effects of cinnamon can be attributed to its polyphenols and flavonoids, which act as scavengers for reactive oxygen and nitrogen species, chelators for redox-active transition metals, and modulators of enzymes.

Shatwan et al. [36] observed that cinnamon and ginger decreased the high levels of total cholesterol (T.C.) and triglycerides (T.G.) in men and rats.

The demonstrations by Hindawy and Hendawy [37] were biochemical and histopathological alterations caused by acrylamide on rat livers, and the administration of the potent antioxidant lycopene effectively treated the oxidative damage.

The research by Gawesh et al. [38] discovered that cinnamon administration to rats with liver toxicity significantly reduced the levels of alanine transaminase (ALT), aspartate transaminase (AST), malondialdehyde (MDA), and tumor necrosis factor (TNF), while simultaneously increasing the levels of superoxide dismutase, glutathione peroxidase, and total antioxidant capacity. They also concluded that cinnamon and ginger are protective against abnormalities in rats with liver toxicity.

In this study, administering cinnamon and rosemary, individually or in combination, to rats with liver toxicity resulted in a significant reduction in MDA levels and a significant elevation in hepatic glutathione (GSH). These findings align with Qin et al. [39], who reported that cinnamon extract supplementation decreased tumor necrosis factor Alpha (TNF-α) and MDA. Dehghan et al. [40] asserted that cinnamon administration led to a significant reduction in MDA and TNF levels, along with increased TAC and SOD, attributed to its ability to scavenge free radicals and its high phenol content.

CONCLUSIONS

Our findings provide clear biochemical and histopathological evidence that the administration of cinnamon and/or rosemary oils to acrylamide-treated rats significantly decreased serum levels of AST and ALT and efficiently reduced hepatic MDA levels; they also increased GSH and CAT activity in liver tissue. Cinnamon and/or rosemary oils treatment mitigated liver damage associated with acrylamide treatment, attributed to their potent antioxidant activities. We highly recommend using cinnamon and rosemary oils with people with high frequency of exposure to acrylamide.

Author Contributions: Conceptualization, H.E. and F.E.; methodology, H.E.; investigation, H.E.; resources, E.A.; data curation, H.E.; writing—original draft preparation, H.E.; writing—review and editing, F.E.; visualization, H.E.; supervision, A.E.; project administration, A.E. All authors have read and agreed to the published version of the manuscript.

Funding: This research received no external funding.

Institutional Review Board Statement: The study followed the guidelines in the 8th edition of the National Institutes of Health's Guide for the Care and Use of Laboratory Animals. Additionally, it adhered to the principles set forth by the International Council for Laboratory Animal Science (ICLAS) and those of the Benha University Animal Care and Use Committee, assigned with the identification number (03-03-23).

Informed Consent Statement: Not applicable.

Data Availability Statement: Data is available on request.

Acknowledgments: No acknowledgment to be mentioned.

Conflicts of Interest: The authors declare no conflict of interest.

REFERENCES

1. Savary, S. *et al.* The global burden of pathogens and pests on major food crops. *Nat. Ecol. Evol.* 3, (2019).
2. Castillo, J. Identificación de especies de Meloidogyne spp. presentes en el municipio de Patzicía, Chimaltenango. (Universidad Rafael Landívar, 2014).
3. Sánchez-Moreno, S. & Talavera, M. Los nematodos como indicadores ambientales en agroecosistemas. *Ecosistemas* 22, (2013).
4. Pérez-Anzúrez, G. *et al.* Arthrobotrys musiformis (Orbiliales) Kills Haemonchus contortus Infective

Larvae (Trichostronylidae) through Its Predatory Activity and Its Fungal Culture Filtrates. *Pathogens* 11, (2022).

5. Triviño Gilces, C., Navia Santillán, D. & Velasco Velasco, L. *Guía para reconocer daño en raíces y métodos de muestreo y extracción de nemátodos en raíces y suelo*. *INIAP Boletín Divulgativo No. 433* https://repositorio.iniap.gob.ec/bitstream/41000/3849/1/433.PDF (2013).
6. González Cardona, C. & Aristizabal Loaiza, M. Evaluación de un producto nematicida sobre nematodos fitoparásitos del plátano Dominico Hartón (Musa AAB). *Acta Agron.* 63, 71–79 (2014).
7. López-Alcántara, R. Nematodos, su implicación en la producción agrícola. *ECUADOR ES Calid. Rev. Científica Ecuatoriana* 2, 10–11 (2015).
8. Muthee Gakuubi, M., Wanzala, W., Wagacha, J. M. & Dossaji, S. F. Bioactive properties of Tagetes minuta L. (Asteraceae) essential oils: A review. *Am. J. Essent. Oils Nat. Prod.* 4, 27–36 (2016).
9. Ibrahim, S. K., Traboulsi, A. F. & El-Haj, S. View of Effects of Essential Oils and Plant Extracts on Hatching, Migration and Mortality of Meloidogyne incognita | Phytopathologia Mediterranea. *Phytopathol. Mediterr.* 45, 238–246 (2006).
10. Licet Mena Valdés, L. *et al.* Determinación de saponinas y otros metabolitos secundarios en extractos acuosos de Sapindus saponaria L. (jaboncillo). *Rev. Cuba. Plantas Med.* 20, 106–116 (2015).
11. Piska, K., Ziaja, K. & Muszynska, B. Edible mushroom pleurotus ostreatus (Oyster mushroom) – Its dietary significance and biological activity. *Acta Sci. Pol. Hortorum Cultus* 16, 151–161 (2017).
12. Arteaga, M. B., Soria, C. A. & Ordoñez, M. E. Determinación del potencial nematicida y nematostático in vitro de Pleurotus ostreatus (Jacq. ex Fr.) sobre larvas J2 de Globodera pallida (Stone). *Rev. Ecuat. Med. Cienc. Biol.* 41, 45–50 (2020).
13. Álvarez S., D. E., Botina J., J. A., Ortiz C., A. J. & Botina J., L. L. Evaluación nematicida del aceite esencial de Tagetes zypaquirensis en el manejo del nematodo Meloidogyne spp. *Rev. Ciencias Agrícolas* 33, 22–33 (2016).
14. Abdel-Rahman, F. H., Alaniz, N. M. & Saleh, M. A. Nematicidal activity of terpenoids. *http://dx.doi.org/10.1080/03601234.2012.716686* 48, 16–22 (2012).
15. Martinotti, M. D., Castellanos, S. J., González, R., Camargo, A. & Fanzone, M. Efecto nematicida de extractos vegetales sobre Meloidogyne incognita Nematicidal effects of extracts of garlic, grape pomace and olive mill waste, on Meloidogyne incognita, on grapevine cv Chardonnay. *Rev. la Fac. Ciencias Agrar.* 48, 211–224 (2016).
16. Naim, L. *et al.* Variation of Pleurotus ostreatus (Jacq. Ex Fr.) P. Kumm. (1871) performance subjected to differentdoses and timings of nano-urea. *Saudi J. Biol. Sci.* 27, 1573–1579 (2020).
17. Cornelius, W. W. & Wycliffe, W. Chapter 90 - Tagetes (Tagetes minuta) Oils. in *Essential Oils in Food Preservation, Flavor and Safety* (ed. Preedy, V. R.) 791–802 (Academic Press, 2016). doi:https://doi.org/10.1016/B978-0-12-416641-7.00090-0.
18. Singh, P. Management of Plant-parasitic Nematodes by the Use of Botanicals. *J. Plant Physiol. Pathol.* 02, (2014).
19. de Lara, on *et al.* La importancia de los nematodos de vida libre.
20. Guzmán-Piedrahita, O. A., Carolina, C. & López-Nicora, H. D. Physiological interactions of plants with plant-parasitic nematodes: A review. *Bol. Cient. del Cent. Museos* 24, 190–205 (2020).
21. Silva Olivo, J. C. "Evaluación de la actividad insecticida y/o repelente 'in vivo' de extracto acuoso de Artemisia absinthium y aceites esenciales de Tagetes minuta y Tagetes zipaquirensis sobre Lasius niger. (Escuela Superior Politécnica de Chimborazo, 2013).

22. Coyne, D. L., Nicol, J. M., Traducción, C.-C. & Verdejo-Lucas, S. *Nematología práctica: Una guía de campo y laboratorio*. (International Institute of Tropical Agriculture (IITA), 2007).
23. Jaraba, J. D., Lozano, Z. E. & Suárez Padrón, I. E. Meloidogyne incognita (Kofoid and White, 1919) Chitwood 1949 y Meloidogyne arenaria (Neal 1889) Chitwood 1949: Nematodos de las nudosidades radiculares en guayaba (psidium guajava l.) c.V. Manzana en Monteria, Cordoba. *Temas Agrar. ISSN-e 0122-7610, Vol. 8, Nº. 2, 2003, págs. 15-21* 8, 15–21 (2003).
24. Carmona, R. & Padilla, W. Morphological, morphometric and molecular identification of Meloidogyne exigua (Göeldi 1887) in coffee (Coffea arabica). *Agron. Mesoam.* 31, 531–545 (2020).
25. ICA. *Manual para la elaboración de protocolos para ensayos de eficacia con PQUA*. (Instituto Colombiano Agropecuario, 2020).
26. Murga-Gutiérrez, S. N., Alvarado-Ibáñez, J. C. & Vera-Obando, N. Y. Efecto del follaje de Tagetes minuta sobre la nodulación radicular de Meloidogyne incognita en Capsicum annuum, en invernadero. *Rev. peru. biol* 19, 257–260 (2012).
27. Iannacone, J. *et al.* Acute and chronic toxic effect of Tagetes minuta' Black mint' (Asteraceae) and carbaril on six important entomophages in biological control. *Biol.* 15, 85–97 (2017).
28. Zygadlo, J. A., Lamarque, A. L., Maestri, D. M., Guzman, C. A. & Grosso, N. R. Composition of the Inflorescence Oils of Some Tagetes Species from Argentina. *J. Essent. Oil Res.* 5, 679–681 (1993).
29. Peralta-Sánchez, M. G. *et al.* Metabolitos secundarios y clorofilas en cempasúchil en respuesta a estrés salino. *Rev. Mex. ciencias agrícolas* 5, 1589–1599 (2014).
30. Senatore, F. *et al.* Antibacterial activity of Tagetes minuta L. (Asteraceae) essential oil with different chemical composition. *Flavour Fragr. J.* 19, 574–578 (2004).
31. Alejandro Rojas, G. *et al.* Evaluación in vitro de la actividad nematicida de limoneno, isotiocianato de alilo, eucaliptol, β-citrolenol y azadiractina sobre Meloidogyne incognita (Nematoda, Meloidogynidae). *Trop. Subtrop. Agroecosystems* 22, (2019).
32. Herrera Moncada, W. L. & Sandoval Fuentes, M. G. Toxicidad del extracto etanólico de plantas de campo y callos in vitro de Tagetes minuta y Tagetes erecta sobre Meloidogyne spp. en Solanum lycopersicum L. *Universidad Nacional Pedro Ruiz Gallo* (Universidad Nacional Pedro Ruiz Gallo, 2019).
33. Zarate-Escobedo, J. *et al.* Concentrations and application intervals of the essential oil of Tagetes lucida Cav. against Nacobbus aberrans. *Rev. Mex. Ciencias Agrícolas* 9,.
34. Mendoza-García, E. *et al.* Efecto biológico del aceite de Tagetes coronopifolia (Asteraceae) contra Diaphorina citri (Hemiptera: Liviidae). *Rev. Colomb. Entomol.* 41, 157–162 (2015).
35. Erazo Sandoval, N. S. *et al.* Effect of Pleurotus ostreatus (Jacq.) and Trichoderma harzianum (Rifai) on Meloidogyne incognita (Kofoid & White) in tomato (Solanum lycopersicum Mill.). *Acta Sci. Biol. Sci.* 42, (2020).
36. Clémençon, H., Emmett, V. & Emmett, E. E. *Cytology and Plectology of the Hymenomycetes*. (2012).
37. Armas-Tizapantzi, A. *et al.* Estructuras tipo toxocistos en Pleurotus ostreatus y P. pulmonarius. *Sci. fungorum* 49, e1250 (2019).
38. Ernesto, J., El, S., De La, C., Sur, F. & Royse, D. J. *La Biología, el cultivo y las propiedades nutricionales y medicinales de las setas Pleurotus spp. Edible mushroom cultivation View project oxidorreductases enzymes View project*. (2017).
39. Aguilar Marcelino, L. *et al.* Los hongos del género Pleurotus como agentes de biocontrol de parásitos de importancia pecuaria. 52, 1375 (2021).

40. Quevedo, A. *et al.* Interacciones ecológicas de los hongos nematófagos y su potencial uso en cultivos tropicales. *Sci. Agropecu.* 13, 97–108 (2022).
41. Jansson, H.-B. & Lopez-Llorca, L. V. Hongos nematófagos. 145–173 https://dcmba.ua.es/es/areas/botanica/hongos-nematofagos.html# (2001).
42. Leonardo, H. *et al.* Activity of the fungus Pleurotus ostreatus and of its proteases on Panagrellus sp. larvae. *African J. Biotechnol.* 14, 1496–1503 (2015).
43. Arteaga Paredes, M. B. Determinación del potencial nematicida y nematostático in vitro de Pleurotus ostreatus (Agaricales: Pleurotaceae) sobre larvas J2 de Globodera pallida (Tylenchida: Heteroderidae). (Pontificia Universidad Católica del Ecuador, 2018).

Received: October 9th 2023/ **Accepte**d: January 15th 2024 / **Published:**15 February 2024

Citation: Elsayed H., El komy A. A. E., El-Shewy E. A., Abdallah F. E. E. Ameliorative Effect of Cinnamon and Rosemary Oils in Acrylamide–Induced Hepatic Injury in Rats. Revis Bionatura 2024; 9 (1) 58. http://dx.doi.org/10.21931/RB/2024.09.01.58

Additional information Correspondence should be addressed to haladiab1986@yahoo.com.

Peer review information. Bionatura thanks anonymous reviewer(s) for their contribution to the peer review of this work using https://reviewerlocator.webofscience.com/

Bionatura ISSN. First 13909355 Ecuador. **Scopus coverage years**: from 2016 to the present

Bionatura
Ibero-American Journal of Biotechnology and Life Sciences

Article

Influence of a natural colorant powder from *Syzygium cumini* L. (skeels) on sensorial and physico-chemical properties during storage of a heat-treated flavored fermented milk

Fabián M. Gaibor[1], Daliannis Rodríguez[2], Mario A. García[3], Alicia Casariego[4]*

[1]Yachay University for Experimental Technology and Research, Imbabura, Ecuador; mauricio-gaibor@gmail.com. https://orcid.org/0000-0003-0304-0799
[2]Dept. of Food, Pharmacy and Food Institute, University of Havana, Cuba; rcdaly92@gmail.com. https://orcid.org/0000-0003-0389-740X
[3]La Maná Extension, Faculty of Agricultural Sciences and Natural Resources, Technical University of Cotopaxi, Ecuador; marioifal@gmail.com. https://orcid.org/0000-0002-0304-9665
[4]Dept. of Food, Pharmacy and Food Institute, University of Havana, Cuba; alicia@ifal.uh.cu. https://orcid.org/0000-0002-7687-5984
** Correspondence: marioifal@gmail.com; Tel.: +593 995537689*
Available from. http://dx.doi.org/10.21931/RB/2024.09.01.59

ABSTRACT

This study aimed to evaluate the influence of a powder colorant obtained from a hydroalcoholic extract of jambolan (*Syzygium cumini*) on the chemical, microbiological, and sensory characteristics of heat-treated flavored fermented milk. The extraction of anthocyanins from the pulp was carried out by maceration with 90% (v/v) ethanol acidified with citric acid. This extract was concentrated (14 to 15% w/v of total solids). Maltodextrin DE 12 was added to obtain 25% (w/v) total solids. Guar gum (0.06% w/w) was added as a stabilizer to whole milk reconstituted with sterilized distilled water (11% w/v total solids). The colorant powder was homogenized at a rate of 1.5 and 2 g per 100 mL of powdered whole milk dissolved in the corresponding amount of water, and sucrose and concentrated strawberry flavoring were added. The natural colorant addition allowed us to obtain a product with pH (4.23-4.75), titratable acidity (1.28-1.47% w/w lactic acid), and color stability, similar to those of yogurt with synthetic colorants. No microbial growth or color changes were detected. The judges did not notice any strange odor, taste, or color. Natural colorants can be a beneficial option for developing healthy and sustainable foods.

Keywords: *Syzygium cumini*; anthocyanins; spray-dried; natural colorant; heat-treated fermented milk.

INTRODUCTION

Consumer trends focus on consuming fresh foods or processed foods that offer some health benefits.[1] To meet these demands, many native or little-explored fruits have been evaluated as raw materials for the food industry.[2]

Syzygium cumini (L.) Skeels is one of these fruits, known in various places as jambolan. When ripe, it has an intense purple color that is very attractive for industrial processing. Its ripe fruits, with a high anthocyanin content,[2] is used to produce juices, nectars, and jams.[3] Interest in anthocyanin pigments in scientific research has increased in recent years due to the color they impart to products that contain them and their possible health benefits.[4] Therefore, besides their functional role, anthocyanins as natural pigments constitute potential agents for obtaining value-added products for human consumption.

Anthocyanins are phenolic compounds from the flavonoid family, widely distributed in nature.[5] They are water-soluble, facilitating their incorporation into many aqueous food systems. This quality makes these pigments attractive natural colorants[6] for preparing foods such as heat-treated flavored fermented milk.

Milk and dairy products are important foods for people of any age. Along with milk, fermented milk has reached a higher proportion in the daily diet of modern society due to its nutritional value and sensory characteristics. In the United States of America, between 2000 and 2023, per capita yogurt consumption experienced growth of more than 50%.[7] Of all dairy products, fermented milk is well known and the most popular around the world[6].

Some researchers have examined the elements that impact the stability of anthocyanins in fruit products. However, information on the factors influencing the stability of anthocyanins during storage of fruit yogurts is limited.[8] Furthermore, in most cases, fruit pulps or extracts rich in anthocyanins are added, but not natural powdered colorants. This work evaluated the influence of adding a colorant powder obtained by spray drying from a hydroalcoholic extract of jambolan (*S. cumini*) on some physical, chemical, and sensory characteristics of heat-treated flavored fermented milk. The novelty of this work lies in the incorporation of a powdered colorant explicitly obtained from the jambolan, which expands the sources of anthocyanins studied as alternatives to synthetic colorants in flavored fermented milks, demonstrating their effectiveness for color without altering the physical, chemical and sensory properties, opening new possibilities of industrial application that take advantage of the nutraceutical potential of this natural pigment.

MATERIALS AND METHODS

Raw material

Ripe jambolan fruits were harvested between September and November 2022 in Havana, Cuba, considering similarities in size, color, uniform ripeness, and absence of visible defects. The pulp and skin were ground in an IKA T25 digital Ultra-Turrax (model T25 D S25).

Chemical reagents and other materials

For the extraction of anthocyanins and their evaluation, absolute ethanol (Sigma-Aldrich, St. Louis, MO, USA), citric acid food grade (Solvesa, Ecuador), Folin-Ciocalteu reagent (Sigma-Aldrich, St. Louis, MO, USA), and potassium chloride and sodium acetate (Merck KGaA, Darmstadt, Germany) as buffers were used. Maltodextrin DE 12 (Glucidex®, Roquette America, Inc., USA) was used as a spray drying aid. In the production of fermented milks whole milk powder (La Vaquita, Ecuador), guar gum (Merck KGaA, Darmstadt, Germany) as a stabilizer, sucrose (Sigma-Aldrich, St. Louis, MO, USA), strawberry flavor concentrate (Esencias Levapan® Fresa, Ecuador), yogurt starter culture (YC280, Ferlact Biotech, Ecuador), commercial colorant (Colorantes Levapan® Rojo, Ecuador) were used. Sabouraud dextrose agar (Sigma-Aldrich, St. Louis, MO, USA) was used as the culture medium, and in the determinations of titratable acidity, sodium hydroxide solution (1.0 N, Sigma-Aldrich, St. Louis, MO, USA) and phenolphthalein (Sigma-Aldrich, St. Louis, MO, USA). In addition, distilled water was needed.

Preparation of anthocyanin extract

The extraction of anthocyanins from the pulp was carried out by maceration with a pulp/ethanol dissolution ratio of 1 g per 5 mL of 90% (v/v) ethanol acidified with 0.03% (w/v) citric acid. The mixture was kept at room temperature for 6 h on a sieve (Retomed, Mizard. 2001) at 285 rpm. After that time, the solid residue was filtered and discarded.[9] The polyphenolic compounds, expressed as gallic acid in mg/100 g, were quantified with the Folin-Ciocalteu reagent,[10] and the anthocyanin content was determined by the pH differential

method[11] and was expressed as cyanidin-3- glucose with a molar extinction coefficient of 26900 L/cm mol and molar mass of 449.2 g/mol.[9] In this determination, buffer potassium chloride solutions were used at 0.025 M (pH 1.0, adjusted with HCl) and sodium acetate at 0.4 M (pH 4.5). This diluted hydroalcoholic extract determined the extraction yields of total polyphenols and anthocyanins and pH (Mod. Basic 20, Crison, España)[12]. Both yields (%) were calculated as the ratio between the contents of the extract and the pulp.[9]

Spray drying

The diluted hydroalcoholic extract was concentrated to a total solids content between 14 and 15 % in a rotary evaporator (IKA, Germany) at 40 °C with a rotation of 85 rpm, vacuum pump (ULVAC DTC-21). In addition, the concentrated extract was determined by its density using a capillary tube pycnometer,[13] soluble solids in an Abbe refractometer with temperature correction, and total solids with a thermogravimetric balance (Sartorius, Göttingen, Germany) until constant mass at 105 ºC.[12]

Maltodextrin DE 12 was added to 50 mL of the concentrated extract for a final total solids content of 25% (w/v). Drying was carried out in a spray dryer, Mod. B-191 (BÜCHI, Switzerland) has a 0.7 mm diameter nozzle and 60 m^3h^{-1} of airflow when the aspirator is 100 %. The inlet air temperature was guaranteed by preheating the equipment for 15 min. The outlet temperature was kept constant at 70 ºC. The feed rate was 65 % (963 mL/h) for 165 ºC.[14]

Preparation of the heat-treated flavored fermented milk

The milk was prepared by reconstitution of whole milk powder with sterilized distilled water to obtain a product with 11% (w/v) of total solids, and guar gum (0.06% w/w) was added. The mixture was pasteurized at 90 ºC for 15 min. Once this process was finished, samples were cooled until 42 ºC and the powdered colorant was added and homogenized under hygienic conditions at a rate of 1.5 and 2 g per 100 mL of whole milk powder dissolved in the amount of water followed by sucrose and 0.016% (v/v) strawberry flavor concentrate (Esencias Levapan® Fresa, Ecuador). They were then inoculated with 2% (w/v) yogurt starter culture (YC280, $2x10^{12}$ CFU/mL). During fermentation (42 ºC), the pH was measured at 30-minute intervals until reaching values around 4.5 to 4.7. Once the fermentation was finished, the product was pasteurized. The samples were then cooled to 5 ºC and packed in 150 mL amber glass bottles.

The maximum concentration of powdered natural colorant to be added to flavored fermented milk (1.5 and 2 g of powder per 100 mL) was determined through an acceptance/rejection test in focus group sessions where 10 semi-trained judges participated.[15] The judges visually indicated that the coloration was similar to commercial strawberry fermented milk.

To compare the changes in microbiological, chemical, and sensory indicators during storage, a control heat-treated fermented milk was prepared with the addition of a commercial colorant (Colorantes Levapan® Rojo, Ecuador). All samples were stored between 4 and 5 ºC for 23 days.

Microbiological and chemical determinations

As part of the microbiological control, counting molds and yeasts[16] was carried out on Sabouraud agar. These cultures were incubated at a controlled temperature of 25 °C for a standard incubation period of 5 days, allowing the formation and development of microbial colonies. Counting was performed using serial dilution techniques to ensure the accuracy of the results.

In addition, the pH (Mod. Basic 20, Crison, España) and titrable acidity[17] in the yogurt were evaluated. The pH was measured using a calibrated electrode immersed directly in the yogurt samples at 25°C. The

determination of acidity, expressed as a percentage of lactic acid, was measured using neutralization titration. All measurements were performed in triplicate to ensure reproducibility of the results.

Sensory evaluation

The sensory evaluation was done using a balanced block design through the Quantitative Descriptive Analysis. The sensory descriptors (characteristic color, strange color, smell of fermented product, fruity smell, strange smell, characteristic flavor, strange flavor, sweetness, acidity, fruity flavor, viscosity, and overall quality), obtained by the controlled association method,[18] were evaluated on a structured scale, bounded at both ends with increasing intensity of the descriptor, from left to right. Ten semi-trained judges evaluated the samples.

Statistical analysis

Variance analysis was performed, and in the event of significant differences, Duncan's multiple range test was applied to determine the differences with a confidence level of 5%. The STATISTICA program (version 7, 2004, StatSoft. Inc., Tulsa, USA) was used.

RESULTS AND DISCUSSION

Characterization of diluted hydroalcoholic extract and concentrated extract

The extraction process presented yields of total polyphenols and anthocyanins of 73 and 31%, respectively, with a density of 0.8824 g/mL, pH of 4.2, and 2.7% (w/v) of total solids. The jambolan extract concentrated by rotary evaporation was evaluated before the addition of maltodextrin DE 12. The anthocyanin content was 66.91 mg/100 g, and the total polyphenol content was 1781.32 mg/100 g. The percentage values of total solids, density, and soluble solids corresponded to 14.64%, 1.1033 g/mL, and 20.73 ºBrix, respectively. Similar results of 60.57 mg/100 g of anthocyanins, 82.59 % humidity, 17.41 % total solids, and 20 ºBrix were reported for jabuticaba extracts.[19]

The behavior of the pH values of heat-treated flavored fermented milk during storage

Table 1 presents the behavior of the pH values of flavored fermented milk during storage between 4 and 5 ºC. At the beginning of storage, the fermented milk with the natural powdered colorant showed significant differences from the control fermented milk. However, the pH values ranged between 4.23 and 4.75, corresponding with this product type.[20] The products with the addition of the natural powdered colorant had a lower pH value ($p \leq 0.05$) than that of the control fermented milk, which could be due to the acidity provided by the powder (~4.5).

Time (d)	Treatment		
	Control heat-treated fermented milk	Heat-treated fermented milk with 1.5% (w/v) of natural colorant powder	Heat-treated fermented milk with 2% (w/v) of natural colorant powder
0	4,75 ± 0,01 a	4,26 ± 0,01 e	4,23 ± 0,03 of
5	4,63 ± 0,02 b	4,17 ± 0,04 g	4,18 ± 0,03 fg
9	4,56 ± 0,01 c	4,13 ± 0,03 gh	4,11 ± 0,02 hi
13	4,47 ± 0,01 d	4,06 ± 0,04 ij	4,06 ± 0,02 ij
16	4,41 ± 0,02 d	4,08 ± 0,01 hij	4,08 ± 0,01 hij
19	4,44 ± 0,05 d	3,91 ± 0,01 m	4,05 ± 0,02 ij
21	4,41 ± 0,06 d	3,98 ± 0,05 kl	4,02 ± 0,04 jk
23	4,44 ± 0,02 d	3,93 ± 0,02 lm	3,93 ± 0,06 lm

Mean ± standard deviation; n= 3.

Different letters indicate significant differences ($p \leq 0.05$).

Table 1: The behavior of the pH of heat-treated flavored fermented milk during refrigerated storage.

At the end of storage, all the formulations presented pH values in the recommended range (3.6 to 4.5) in the Brazilian technical regulation of identity and quality of fermented milk of normative instruction No. 46 that establishes pH values for identity and quality.[21]

In a study [22] about the effect of *Hibiscus sabdariffa* (Calyce) extract on the chemical and organoleptic properties of yogurt, a pH of 4.3 was obtained. In contrast, in another work,[23], a pH of 4.6 was reported for yogurt with natural colorant rich in anthocyanins extracted from strawberries (*Fragaria* × *ananassa*).

The behavior of the acidity values of heat-treated flavored fermented milk during storage

The behavior of the acidity corresponded, in a general way, with the variation of the pH during storage (Figure 1). In the beginning, the acidity of the control-fermented milk was 0.97%, while for the fermented milk with 1.5 and 2% (w/v) of powdered natural colorant, the values were 1.28 and 1.47, respectively. These last values were similar to those reported for yogurt with microencapsulated anthocyanins extracted from *Solanum melongena* L. Bark.[24]

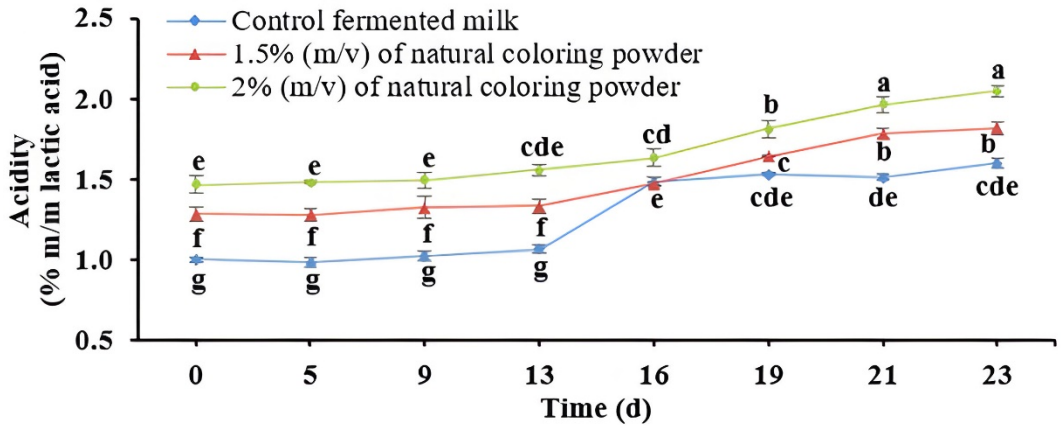

Figure 1: Acidity behavior of heat-treated flavored fermented milk during refrigerated storage. Error bars indicate the standard deviation. Different letters indicate significant differences ($p \leq 0.05$).

In the beginning, in the control product and in the fermented milk flavored with natural colorant, the acidity was by the quality specifications, which established a minimum ideal acidity expressed as lactic acid, 0.3% for yogurt.[25] The titratable acidity for all the flavored fermented milk increased as the powdered colorant content increased during storage. This behavior of acidity during storage corresponded to what was reported.[24]

Microbiological indicators

The products of the three treatments met the sanitary requirements in correspondence with the limits specified in the NTE-INEN 2395[20] for fermented milk. During storage, mold and yeast growth was detected in 19 days in all cases, with counts between 2 and 3 CFU/mL maintained until 23 days of storage. According to these results, the microbiological quality for the three formulations during the 23 days of storage was satisfactory, complying with what is established for this type of product.

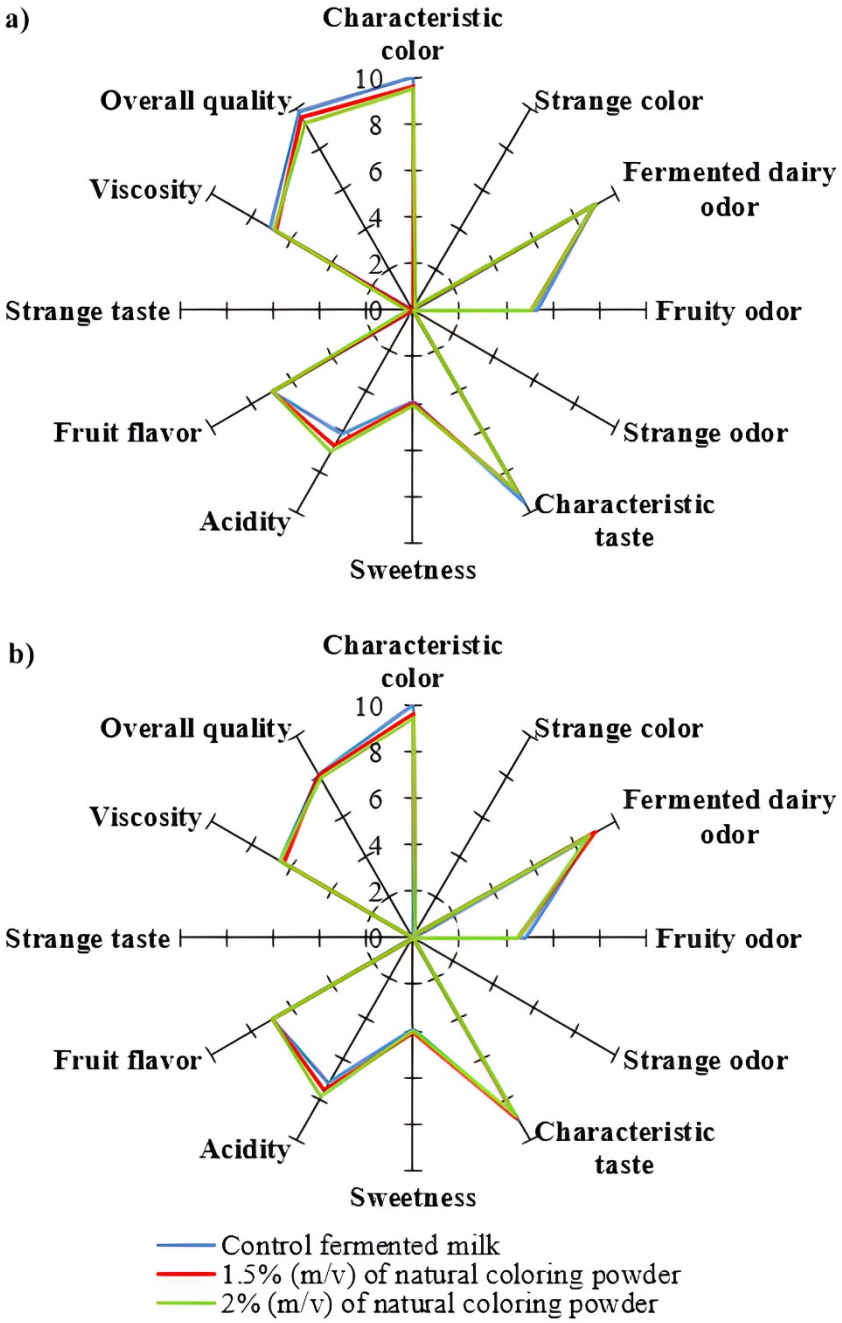

Figure 2: Sensory descriptors evaluated in the heat-treated flavored fermented milk (a) at the beginning of the storage; (b) at 23 days of storage between 4 and 5 ºC.

Sensory evaluation

Figure 2 shows some of the sensory descriptors evaluated during storage. For all the treatments, the tasters thought that products with an odor, acidity, and viscosity characteristic of this fermented product were obtained. The color appeared uniformly and homogeneously. As can be seen in the figure, the order of addition of the natural colorant did not influence the perception of the color of the product. However, there is evidence suggesting that the timing of placing the natural colorant from fruits can influence the stability of anthocyanins during fermentation. Studies, such as the one on fruit yogurt, indicate that adding anthocyanin extract before the fermentation of milk could impact the pigment content in yogurt, affecting its color stability during storage.[8] Additionally, research on fermented plant-based products, like potato blueberry yogurt, points out that

adding fruit preparations before fermentation can cause color changes, impacting sensory properties and physicochemical parameters.[26]

No lumps were observed, indicating that the lactic acid bacteria acidified the medium quickly and correctly, so there were no defects in the microstructure; therefore, adding the colorant to the flavored fermented milk did not affect its development. Lactic acid bacteria significantly contribute to the effective acidification of the matrix and rapidly consume sugars during fermentation.[27]

They also reported positive criteria regarding flavor-related descriptors, typical of a fermented milk product and characteristic of fruit. The sweetness was adequate. The tasters did not detect the presence of strange color, odor, or flavor in the recently prepared products.

At the end of storage, the tasters scored with a higher value for the acidity of all the treatments, corresponding with the variation of the titratable acidity (Figure 1) and pH (Table 1). In general, the scores given to the sensory descriptors decreased due to the loss of characteristics of a fresh fermented product. Although the overall quality rating of the three treatments could be considered `very good,' the increase in acidity caused an increase in the flavor of coagulated sour milk and the smell of the fermented product, related to the occurrence of the fermentation process during storage.

A result of interest for the study was related to the fact that the tasters did not detect changes in the color of the products during their storage, even in treatments with the addition of natural powdered colorant. The increase in acidity during storage could favor the development and stability of a characteristic color expected for these strawberry-flavored fermented milk. Anthocyanins have more excellent stability in aqueous solutions at acid pH.[28] It has been suggested that a high pH accelerates the degradation of pigments during storage. In contrast, slight variations in the pH of the medium did not affect the stability of the anthocyanins.[29]

CONCLUSIONS

The addition of natural colorant allowed fermented milk with a flavor and a pH (4.23-4.75), titratable acidity (1.28-1.47% w/w lactic acid), and color stability similar to those of fermented milk with synthetic colorants. No microbial growth or color changes were detected. The judges did not notice any strange odors, flavors, or colors. The use of natural colorants in the food industry is a beneficial option for both human health and the environment, and its use can contribute to the development of healthier, more attractive, and sustainable food products.

Author Contributions: Conceptualization, F.G. and D.R.; methodology, F.G.; software, M.G.; validation, M.G. and A.C.; formal analysis, F.G. and D.R.; investigation, F.G. and D.R.; data curation, M.G.; writing—original draft preparation, F.G. and D.R.; writing—review and editing, M.G.; visualization, A.C.; supervision, A.C.

Funding: This research received no external funding.

Institutional Review Board Statement: Not applicable.

Informed Consent Statement: Not applicable.

Conflicts of Interest: The authors declare no conflict of interest.

REFERENCES

1. Rodrigues, N.R.; Pinheiro, R.; Flávio, F. Jambolan (*Syzygium cumini* (L.) Skeels): A review on its nutrients, bioactive compounds and health benefits. *J. Food Compos. Anal.* **2022**, 109, 104491. https://doi.org/10.1016/j.jfca.2022.104491
2. Qamar, M.; Akhtar, S.; Ismail, T.; Wahid, M.; Abbas, M.W.; Mubarak, M.S.; Yuan, Y.; Barnard, R.T.; Ziora, Z.M.; Esatbeyoglu, T. Phytochemical profile, biological properties, and food applications of the medicinal plant *Syzygium cumini*. *Foods* **2022**, 11(3), 378. https://doi.org/10.3390/foods11030378
3. Ayyanar, M.; Subash-Babu, P. *Syzygium cumini* (L.) Skeels: a review of its phytochemical constituents and traditional uses. *Asian Pac. J. Trop. Biomed.* **2012**, 2(3), 240-6. https://doi.org/10.1016/S2221-1691(12)60050-1
4. Khoo, H.E.; Azlan, A.; Tang, S.T.; Lim, S.M. Anthocyanidins and anthocyanins: colored pigments as food, pharmaceutical ingredients, and the potential health benefits. *Food Nutr. Res.* **2017**, 61(1), 1361779. https://doi.org/10.1080/16546628.2017.1361779
5. Tonon, V.; Brabet, C.; Pallet, D.; Brat, P.; Hubinger, D. Physicochemical and morphological characterization of açai powder produced with different carrier agents. *Int. J. Food Sci. Technol.* **2009**, 44(10), 1950-58. https://doi.org/10.1111/j.1365-2621.2009.02012.x
6. Gangwar, R.; Hai, H.A.; Kumar, P.; Sharma, N.K. Development and quality evaluation of yoghurt fortified with pineapple, apple and sweet lemon juice (Fruit Yoghurt). *Int. J. Eng. Res. Technol.* **2016**, 5(3), 621-9. https://doi.org/10.17577/IJERTV5IS030484
7. USDA-ERS. Dairy Data. Available online: https://www.ers.usda.gov/data-products/dairy-data.aspx (accessed on 15 January 2024).
8. Ścibisz, I.; Ziarno, M. Effect of fermented matrix on the color and stability of strawberry and blueberry anthocyanins during the storage of fruit yogurts and soy-based and bean-based fruit yogurt alternatives. *Molecules* **2023**; 28(17), 6222. https://doi.org/10.3390/molecules28176222
9. Gaibor, F.M.; Cuba, A.; Rodríguez, D.; García, M.A.; Casariego, A. Optimización del proceso de extracción hidroalcohólica a partir de pulpa de cerezo negro (*Syzygium cumini* L. Skeels). *Cienc. Tecnol. Aliment.* **2017**, 27(2), 51-9.
10. Singleton, V.L.; Orthofer, R.; Lamuela-Raventos, R.M. Analysis of total phenols and other oxidation substrates and antioxidants by means of Folin-Ciocalteau reagent. *Method. Enzymol.* **1999**, 299, 152-78. https://doi.org/10.1016/S0076-6879(99)99017-1
11. Lee, J.; Durst, R.W.; Wrolstad, R.E. Determination of total monomeric anthocyanin pigment content of fruit juices, beverages, natural colorants, and wines by the pH differential method: collaborative study. *J. AOAC Int.* 2005, 88(5), 1269-78. PMID: 16385975.
12. Gaibor, F.M.; Rodríguez, D.; Fundora, L.; Salas, E.; Rodríguez, J.L.; Falco, A.S.; Casariego, A.; García, M.A. Evaluación de las características físicas, químicas, toxicológicas, antibacterianas y sensoriales del cerezo negro (*Syzygium cumini* L.). *Cienc. Tecnol. Aliment.* **2016**, 26(2), 62-8.
13. Mercali, G.D.; Ribeiro, J.; Pez, D.; Tessaro, I.C.; Ferreira, L.D. Physical properties of acerola and blueberry pulps. *J. Food Eng.* **2011**, 106(4), 283-289. https://doi.org/10.1016/j.jfoodeng.2011.05.010
14. Gaibor, F.M.; Rodríguez, D.; García, M.A.; Peraza, C.M.; Vidal, D.; Nogueira, A.; Casariego, A. Development of a food colorant from *Syzygium cumini* L. (Skeels) by spray drying. *J. Food Sci. Technol.* **2022**, 59, 4045-55. https://doi.org/10.1007/s13197-022-05454-9

15. Powell, R.A.; Single, H.M.; Lloyd, K.R. Focus groups in mental health research: enhancing the validity of user and provider questionnaires. *Int. J. Soc. Psychiatry* **1996**, 42(3), 193-206. https://doi.org/10.1177/002076409604200303
16. NTE-INEN 1529-10. Control microbiológico de los alimentos. Mohos y levaduras viables. Recuentos en placa por siembra en profundidad. Ecuador; 1998.
17. AOAC. Official Methods of Analysis. 21rst Edition. Association of Official Analytical Chemists, Gaithersburg, Maryland, USA; 2019.
18. Damasio, M.H.; Costell, E. Análisis Sensorial Descriptivo. Generación de descriptores y selección de catadores. *Rev. Agroquim. Tecnol. Alim.* **1991**, 2, 165-78.
19. Silva, P.; Stringheta, P.; Teófilo, R.; Nolasco, I. Parameter optimization for spray-drying microencapsulation of jaboticaba (*Myrciaria jaboticaba*) peel extracts using simultaneous analysis of responses. *J. Food Eng.* **2013**, 117(4), 538-44. http://dx.doi.org/10.1016/j.jfoodeng.2012.08.039
20. NTE-INEN 2395. Leches fermentadas. Requisitos. Ecuador; 2011.
21. Ministério da Pecuária, Agricultura e Abastecimento. Instrução Normativa n° 46, de 23 de outubro de 2007, Regulamento Técnico de Identidade e Qualidade de Leites Fermentados. Brasil. Available online: http://www.cidasc.sc.gov.br/inspecao/files/2012/08/instru%C3%87%C3%83o-normativa-n%C2%BA-46-de-23-de-outubro-de-2007.pdf (accessed on 15 January 2024).
22. Iwalokun, B.A.; Shittu, M.O. Effect of *Hibiscus sabdariffa* (Calyce) extract on biochemical and organoleptic properties of yogurt. *Pak. J. Nutr.* **2007**, 6(2), 172-82. https://doi.org/10.3923/pjn.2007.172.182
23. Benchikh, Y.; Aissaoui, A.; Allouch, R.; Mohellebi, N. Optimising anthocyanin extraction from strawberry fruits using response surface methodology and application in yoghurt as natural colorants and antioxidants. *J. Food Sci. Technol.* **2021**, 58(5), 1987-95. https://doi.org/10.1007%2Fs13197-020-04710-0
24. Barretto, F.J.F.P.; Clemente, H.A.; Santana, A.L.B.D.; Vasconcelo, M.A.S. Stability of encapsulated and non-encapsulated anthocyanin in yogurt produced with natural dye obtained from *Solanum melongena* L. Bark. *Rev. Bras. Frutic.* **2020**, 42(3), e-137. http://dx.doi.org/10.1590/0100-29452020137
25. CXS 243. Norma para leches fermentadas. *Codex Alimentarius*. Food and Agriculture-United Nations Organization. World Health Organization; 2003.
26. Li, M.; He, Z.; He, L.; Li, C.; Tao, H.; Ye, C.; Liu, L.; Zeng, X.; Ran, G. Effect of fermentation parameters on the anthocyanin content, sensory properties, and physicochemical parameters of potato blueberry yogurt. *Fermentation* **2022**, 8, 489. https://doi.org/10.3390/fermentation8100489
27. Faria-Oliveira, F.; Diniz, R.H.S.; Godoy-Santos, F.; Piló, F.B.; Mezadri, H.; Castro, I.M.; Brandão, R.L. The role of yeast and lactic acid bacteria in the production of fermented beverages in South America. In *Food Production and Industry*; Amer, A.H., Ed.; IntechOpen: London, 2015; pp. 107-35. http://dx.doi.org/10.5772/60877
28. Dangles, O.; Fenger, J.A. The chemical reactivity of anthocyanins and its consequences in Food Science and Nutrition. *Molecules* **2018**, 7, 23(8), 1970. https://doi.org/10.3390/molecules23081970
29. Duan, C.; Xiao, X.; Yu, Y.; Xu, M.; Zhang, Y.; Liu, X.; Dai, H.; Pi, F.; Wang, J. In situ Raman characterization of the stability of blueberry anthocyanins in aqueous solutions under perturbations in temperature, UV, pH. *Food Chem.* **2024**, 431, 137155. https://doi.org/10.1016/j.foodchem.2023.137155

Received: October 9th 2023/ **Accepte**d: January 15th 2024 / **Published:**15 February 2024

Citation: Gaibor, F.M.; Rodríguez, D.; García, M.A.; Casariego, A. Influence of a natural colorant powder from *Syzygium cumini* L. (Skeels) on sensorial and physi-co-chemical properties during storage of a heat-treated flavored fermented milk. Revis Bionatura 2024; 9 (1) 59. http://dx.doi.org/10.21931/RB/2024.09.01.59

Additional information Correspondence should be addressed to marioifal@gmail.com;

Peer review information. Bionatura thanks anonymous reviewer(s) for their contribution to the peer review of this work using https://reviewerlocator.webofscience.com/

Bionatura ISSN. First 13909355 Ecuador. **Scopus coverage years**: from 2016 to the present

Bionatura
Ibero-American Journal of Biotechnology and Life Sciences

Article

Genotypic Detection of Carbapenems Resistance Genes in Acinetobacter baumannii Isolated from Urinary Tract Infection Patients

*Thualfakar Hayder Hasan[1], Ameer Sadeq Yasir AL-Ethari[2], Sddiq Ghani Al-Muhanna[3], Israa Abdul Ameer Al-Kraety[4]**

[1]jabir ibn Hayyan Medical University, Iraq, Najaf, thualfakar.h.hasan@jmu.edu.iq https://orcid.org/0000-0003-2294-2771,
[2,3,4]Department of Medical Laboratory Techniques, College of Health and Medical Techniques, University of Alkafeel. Najaf, Iraq
Sddiq.g@gmail.com, https://orcid.org/0000-0002-0589-2939
**Correspondence: israa.ameer@alkafeel.edu.iq, https://orcid.org/0000-0001-6739-1948*
Available from. http://dx.doi.org/10.21931/RB/2024.09.01.60

ABSTRACT

Acinetobacter baumannii is a Gram-negative bacterium characterized by its short, round, rod-shaped morphology. It is an opportunistic pathogen that poses a significant threat, particularly to immunocompromised patients, often those with hospital stays lasting less than 90 days. Between June 2022 and July 2023, 214 urine samples were collected from individuals suspected of having urinary tract infections (UTIs). These samples were subjected to antibiotic resistance testing, focusing on detecting specific genes related to carbapenem resistance, namely blaNDM, blaKPC, and blaVIM.The study's results revealed a notable trend in antibiotic resistance among the bacterial isolates. Ceftazidime, cefotaxime, and ceftriaxone, commonly used antibiotics for UTIs, showed a high resistance rate among the tested isolates. This resistance highlights the challenges healthcare professionals face when treating UTIs caused by Acinetobacter baumannii. On the other hand, the isolates displayed a comparatively lower resistance rate to imipenem and meropenem, two necessary carbapenem antibiotics. This lower resistance to carbapenems is encouraging as these drugs are often considered the last line of defense against multidrug-resistant bacterial infections. The presence of carbapenem resistance genes, such as blaNDM, blaKPC, and blaVIM, in the Acinetobacter baumannii isolates is of particular concern. These genes confer resistance to carbapenem antibiotics, crucial for treating severe infections caused by multidrug-resistant bacteria. In conclusion, the study aims to study the growth of antibiotic resistance in Acinetobacter baumannii, especially in urinary tract infections in immunocompromised patients with more extended hospital stays. It also highlights the need for Surveys and periodic examinations to detect the spread of bacteria and their resistance.

Keywords: Carbapenems, UTI, genes, blaNDM, blaKPC, and blaVIM.

INTRODUCTION

Acinetobacter baumannii is a Gram-negative bacterium that is small, spherical, and rod-shaped. An opportunistic bacterium [1]. Regularly, it has been shown to colonize the skin, oropharynx, and respiratory tract. Recently, it has been shown that *A. baumannii* determines a “red alert” in hospital settings due to the emergence of antibiotic resistance [2]. The phenomenon of multi-drug resistance (MDR) organism’s phenomenon has progressively become a cause of severe nosocomial and community-acquired infections [3]. Over time, antibiotics became less effective due to the emergence of many resistance mechanisms, such as secretion of beta-lactamase enzymes, receptor modulation, and others [4]. Carbapenem antibiotics are considered one of the most effective antibiotics today and the least affected by bacterial resistance; the resistant-isotype testing showed that the isolates were effective against a wide range of bacterial illnesses [5]. Carbapenems are the most potent

beta-lactam antibiotics, exhibiting broad-spectrum antibacterial action against Gram-positive and Gram-negative bacteria. Combining a carbapenem and beta-lactam rings gives this compound its peculiar molecular structure[6]. Most beta-lactamases are immune to this mix (ESBLs) of antibiotics, including ampicillin, carbenicillin, and the extended-spectrum beta-lactamases [7]. Gram-negative bacteria resistance to carbapenem is a global public health issue. Such resistance, especially when mediated by genes expressing carbapenemase, rapidly develops and generates significant outbreaks, significantly reducing the treatment options available [8]. Resistance to β-lactams, notable carbapenems, is mainly caused by enzymatic breakdown by -lactamases in the Enterobacteriaceae. The NDM-1, KPC, was first identified in 2008, although NDM-1 was found in water samples from New Delhi since 2006. [9]. The majority of NDM-1 infections are from the Indian subcontinent [10]. Horizontal gene transfer across bacteria promotes the transmission of antibiotic-resistance genes [11]. These plasmids have populations with identical structures but distinct antibiotic drug-resistance cassette compositions [12]. This mechanism has allowed antibiotic resistance genes to spread quickly among Enterobacteriaceae and other pathogens like *Acinetobacter baumanii* [13]. Antibiotic resistance genes [14], such as the extended-spectrum -lactamase CTX-M-15 in *Escherichia coli* ST131 and KPC in *Klebsiella pneumoniae* sequence type (ST) 258, may clonally propagate in successfully pathogenic strains [15,16]. Due to HGT and clonal growth [17], KPC and NDM-1 quickly spread after their first appearance. Comparable mobile elements will likely make KPC and NDM-1 accessible in comparable pathogen populations [18]. This is because KPC and NDM-1 have similar distributions and resistance spectra (both give resistance to practically all B-lactam antimicrobials). Clinical Enterobacteriaceae isolates from Pakistan and the United States [18] tested negative for carbapenemase, NDM-1, and KPC. This research aimed to phenotypically and genetically evaluate the antibacterial efficacy of imipenem and meropenem. The study aimed to investigate antibiotic resistance in Acinetobacter baumannii isolated from urinary tract infections (UTIs). Specific objectives included assessing resistance to common UTI antibiotics, detecting carbapenem resistance genes, and evaluating resistance to carbapenem drugs. The research focused on immunocompromised patients with shorter hospital stays. The findings provide insights into the antibiotic resistance landscape of Acinetobacter baumannii, informing strategies for UTI management.

MATERIALS AND METHODS

Isolation and identification of *Acinetobacter baumanii*

Urine samples were randomly collected from 214 outpatients with suspected UTIs from June 2022 to July 2023. The urine inoculates onto blood agar plates and MacConkey agar. The colony-formed unit method grows a singular, refined bacterial colony. The urine specimens that contain lower than 10^5 CFU / ml are eliminated. All bacteria secluded are resembled according to colony morphologic and criterion microbiological experience as colony morphologic, gram lines, oxidase experience, catalase, IMVIC tests, coagulation trial, and outgrowth in Maconkey agar (OxoidTM). The *Acinetobacter baumanii* suspected colonies were diagnosed depending on the vitec2 system.

Antimicrobial sensitivity test

Disk diffusion method on Muller-Hinton agar medium (Oxoid, UK) was carried out to determine the susceptibility of Acinetobacter baumannii isolates against five standard antibiotic disks including Cefotaxime (30µg), Ceftriaxone (30µg), Ceftazidime (30µg), Imipenem (10 µg), and Meropenem (10µg). MacFarland microbial suspension was used as an inoculum of approximately 1×10^8 CFU/ml. The cultures were incubated at 37 degrees Celsius for 18h under aerobic conditions, according to Kirby-Baur[19]. Zones of inhibition were calculated and interpreted as recommended by the National Committee for Clinical Laboratories Standard guidelines (Clinical and Laboratory Standards Institute,2023).

PCR for detecting genes

The DNA extraction by extraction DNA kit. The primers used in this study and the PCR thermocycling conditions are described in Tables 1 and 2 for detecting three resistance genes associated with carbapenems.

gene	sequence	bp	Reference
blaNDM	**F- GGTTT-GGCGATCTGGTTTTC**	**699**	**20**
	R- CGGAATGGCTCATCAC-GATC		
blaKPC	**F- CGTCTAG-TTCTGCTGTCTTG**	**798**	**21**
	R- CTTGTCATCCTT-GTTAGGCG		
blaVIM	**F-AGTGGTGAG-TATCCGACAG**	**261**	**22**
	R- ATGAAAGTGCGTGGA-GAC		

Table 1: The primer sequence used in PCR for *Acinetobacter baumannii.*

Gene		Temperature (°C) / Time				Cycles Number
	premier Denature	Denature	Anneal	Extension	last Extension	
blaNDM	**95°C -5m**	**94°C - 1min**	**55°C-1min**	**72°C-2min**	**72°C-5min**	**30**
blaKPC	**95°C -5m**	**95°C - 1min**	**55°C-1min**	**72°C-1min**	**72°C-5min**	**30**
blaVIM	**95°C -5m**	**94°C - 1min**	**58°C-40sec**	**72°C-50sec**	**72°C-6min**	**34**

Table 2: PCR thermal cycling conditions for *Acinetobacter baumannii* resistance gene.

RESULTS AND DISCUSSION

Total bacterial isolates

Out of (214) collected urine samples, the result showed that 184 samples (85.98%) were G- bacterial isolates and 28 samples (13.08%) were G+ bacterial isolates. In contrast, the results showed 2 samples (0.93 %) with no growth, as shown in Figure 1.

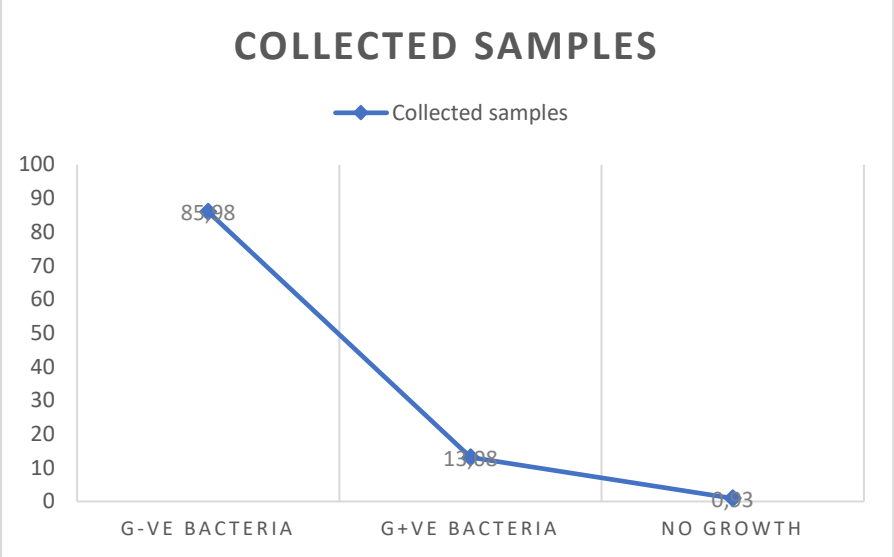

Figure 1: Percentage of total samples isolated from unhealthy with UTI.

The study results proved that the gram-negative bacterial isolates were 89 isolates (48.36%) for *E. coli*, 62 isolates (33.69%) for *K. pneumonia*, 19 isolates (10.32%) for *A. bumanni*, 8 isolates (0.43%) for *Pseudomonas aeruginosa*, and 6 isolates (0.32%) for *Proteus spp*.). Gram-positive bacterial isolates were 21 isolates (75%) for *S. aureus* and 7 isolates (25%) for *E. faecalis*, as shown in figure-2.

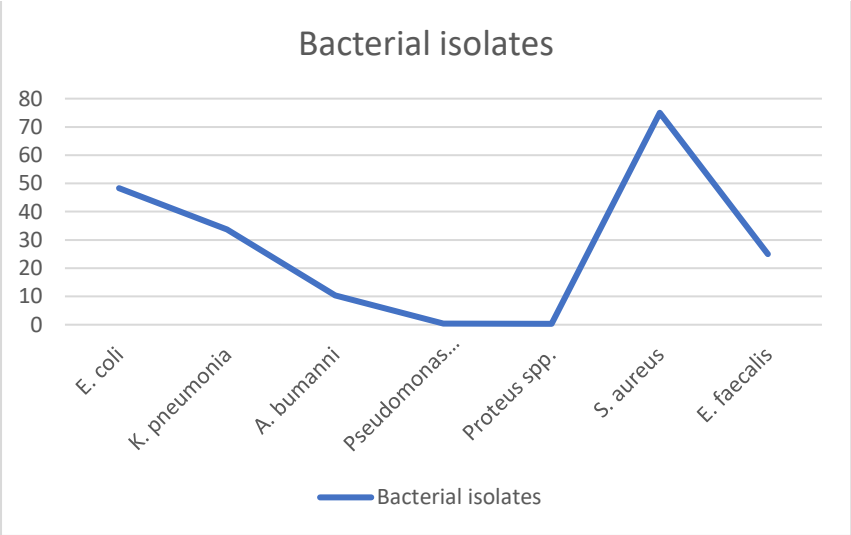

Figure 2: Bacterial isolates according to collected samples.

Antimicrobial sensitivity testing

In this study, there are 5 different antimicrobials were used. The results showed that 17 (89.47%) isolates exhibited a high resistance rate to ceftazidime, followed by cefotaxime and ceftriaxone in 15 (78.94%) isolates. On the other hand, the *A. Baumann* showed notably lowest resistance to imipenem and meropenem 13(68.42%) isolates and 12(63.15%), respectively, as shown in Figure 3.

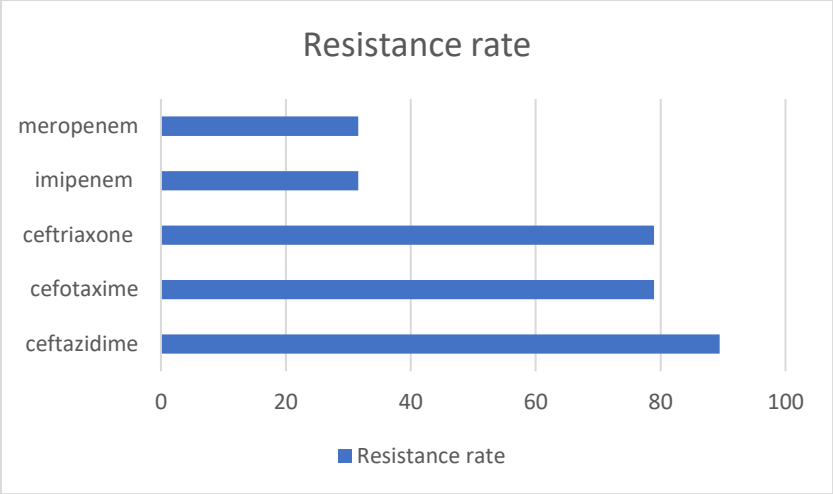

Figure 3: Antimicrobial susceptibility patterns for *A. baumannii.*

Carbapenem's resistance-associated genes:

Carbapenemase-producing bacteria due to the acquisition of various antimicrobial resistance. *A. baumannii* causes a variety of infections, such as UTI, bacteremia, septicemia, catheter-associated infections, and wound infections. In the present study, most of the *A. baumannii* were recovered from urine (n=19). Similarly, a study conducted in Hong Kong also reported that 20.4% and 13% of *A. baumannii* were recovered from urine culture in Iran. Antimicrobial resistance has been seen from the initial use of these drugs and is a growing global concern. *Acinetobacter baumannii* treatment of these infections is often tricky, and carbapenems are currently the antibiotics of choice. In this study, there is an emergence of remarkable resistance to carbapenem antibiotics (imipenem and meropenem 31.58% and 36.85%, respectively); in Iran, it has been proved that the *A. baumannii* was isolated from UTI and showed resistance to imipenem and meropenem (78% and 44%) respectively. Also, another study in Iran by Alavi-Moghadam et al. in 2014 showed that 100% of isolates were resistant to imipenem. Carbapenemases belong to the B-lactamases classes (A, B, and D), enzymes that play the main role in B-lactam resistance. In *A. baumannii* bla (KPC, VIM, and NDM), genes are encoded for carbapenemases the class A (i.e., blaKPC) exhibiting a minor role in phenotypic resistance. The results indicated that 5 isolates (26.31%) were carrying the *blaNDM* gene, as shown in (Figure-4); this result agrees with [1, 9], and [10.] Twenty percent of *A. baumannii* PCR results employing gene-specific primers included the blaNDM-1 gene. Furthermore, forty percent of *A. baumannii* isolates were found to be blaNDM-2 gene-positive when their DNA was amplified using blaNDM-2 primers. Carbapenems are a kind of -lactam antibiotic that has strong antibacterial action against *Acinetobacter baumannii*. However, the emergence and dissemination of acquired carbapenem resistance in these species have questioned the efficacy of treatment and control measures. In bla (NDM-1) genes, they are responsible for carbapenem resistance by encoding enzymes that partly hydrolyze carbapenems and other B-lactams [2.] Only two bactericidal drugs, colistin and fosfomycin, and one bacteriostatic drug are effective against bla NDM-1 producers (tigecycline). According to the study, One of the most distinguishing features of NDM producers is that they are not only nosocomial pathogens but also Gram-negative community members, such as *Acinetobacter baumannii*, which can operate as a natural reservoir for bla (NDM) genes in Enterobacteriaceae [3.] Thus, screening and detecting NDM-1 *A. baumannii* producers is necessary to aid inappropriate treatment. On the other hand, three isolates (18.75%) were carrying the *blaVIM* gene. The discovery of MBL-producing organisms has been difficult using phenotypic approaches

such as the double-disc synergy test, MBL E-test, and combination disk test; however, molecular technologies, particularly next-generation sequencing, will throw some light on their detection [7]. Phenotypic techniques only find some MBL-producing strains since they are not sensitive enough. As a result of the discovery of blaVIM-1 using PCR in 14.3% of *A. baumannii* isolates that had been determined to be MBL negative by E-test, it is clear how important it is to use molecular methods in everyday practice to find these concealed MBLs. Due to the lack of fitness cost and NDM lactamases being favored over other MBLs, they do not hinder bacterial development and have spread worldwide among Gram-negative bacteria. This finding conflicts with [4]. Carbapenemase genes from class A, blaKPC, even though the bacterial isolates had not possessed the blaKPC gene. According to reports, Kuwait and America 5 had a 75% and 18% prevalence of bla GES, respectively. The prevalence of blaKPC in *A. baumannii* is rarely observed. *A.baumannii* clinical As this gene is found on the transportable elements, which may be passed from one bacterium to another and across the community, isolates containing the blakpc gene are disseminated in Iran. The blakpc gene's presence in These mechanisms is necessary for the formation of *A.baumannii* strains that are resistant to a variety of innate and acquired antimicrobials (carbapenems are the selective antibiotic for treating the infections caused by multiple-drug resistant *A.baumannii* strains). Therefore, the judicious use of antibiotics for infection control in hospitals, particularly in ICU departments, can significantly delay the emergence of these resistant strains and the diseases they are associated with. This amplifies the significance of prudent antibiotic use in hospitals for managing infections, especially in the intensive care unit, and lowers the risk of nosocomial transmission and potential outbreaks [6].

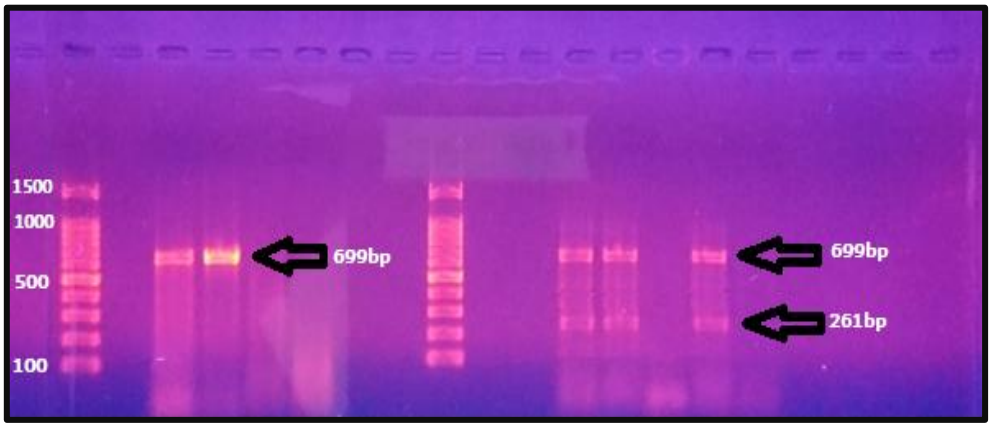

Figure 4: Gel electrophoresis of PCR products of *blaNDM* (699bp) and *blaVIM* (261bp).

CONCLUSIONS

Numerous Acinetobacter baumannii isolates were found to harbor the carbapenem resistance genes, namely blaNDM and blaVIM, indicating their genetic predisposition for carbapenem resistance. Notably, the blaKPC gene was conspicuously absent in these isolates. These findings indicate a multifaceted resistance profile, as these isolates also displayed phenotypic resistance to a broad spectrum of commonly prescribed antibiotics. This highlights the complexity of antibiotic resistance mechanisms employed by Acinetobacter baumannii and raises concerns about the efficacy of conventional treatment approaches. The presence of carbapenem resistance genes underscores the clinical challenge posed by this pathogen, necessitating ongoing vigilance and Non-payment of antibiotics without laboratory tests in order to limit the spreading of bacteria resistance, especially in hospitals and create units or specialized teams in each hospital or medical center interested in developing high-definition programs for the use of antibiotics.

Author Contributions: "Conceptualization, T.H.H. and I.A.A.; methodology, T.H.H. and S.G.A.; software,A.Y.S.A.; valida-tion, S.G.A., I.A.A and A.S.Y.A.; formal analysis, I.A.A.; investigation, T.H.H..; resources, S.G.A.; data curation, I.A.A and S.G.A.; writing—original draft preparation, A.S.Y.A.; writ-ing—review and editing, I.A.A.; visualization, I.A.A.; supervision, T.H.H.; project administration, I.A.A.; funding acquisition, S.G.A., I.A.A and A.S.Y.A. All authors have read and agreed to the published version of the manuscript."

Funding: "This research received no external funding".

Informed Consent Statement: Not applicable

Acknowledgments: The authors would like to express their thanks and appreciation to the presidency of the University of Alkafeel for its support in completing this research.

Conflicts of Interest: "The authors declare no conflict of interest."

REFERENCES

1- Hasan TH, Alasedi KK, Aljanaby AA. A comparative study of prevalence antimicrobials resistance Klebsiella pneumonia among different pathogenic bacteria isolated from patients with urinary tract infection in Al-Najaf City, Iraq. Latin American journal of pharmacy. 2021 Apr 1;40:174-8

2- Al-Ethari AS, Hasan TH, Tikki KA, Bustani GS. Genotypic Detection of qnrA and qnrC Genes in Citrobacter koseri Isolated from Patients with Urinary Tract Infection. Institut Razi. Archives. 2022 Mar 1;77(2).

3-Hasan, T.H., Kadhum, H.A., Al-Khilkhali, H.J.B. Epidemiology of VZV virus in Najaf Government, Iraq. Latin American Journal of Pharmacy, 2023, 42(Special Issue), pp. 188–190.

4-Safari M, Mozaffari Nejad AS, Bahador A, Jafari R, Alikhani MY. Prevalence of ESBL and MBL encoding genes in Acinetobacter baumannii strains isolated from patients of intensive care units (ICU). Saudi J Biol Sci,2015 22: 424-29.

5-El-Shazly S, Dashti A, Vali L, Bolaris M, Ibrahim AS.Molecular epidemiology and characterization of multiple drug-resistant (MDR) clinical isolates of Acinetobacter baumannii. Int J Infect Dis,2015, 41: 42-49.

6-Hassan, L.A., Darweesh, M.F., Hasan, T.H. The Immune-modulator Activity of Pseudomonas aeruginosa Extracted Protein: Azurin Charming Protein. Latin American Journal of Pharmacy, 2023, 42(Special Issue), pp. 245–251.

7-Moulana, Z.; Babazadeh, A.; Eslamdost, Z.; Shokri, M.; Ebrahimpour, S. Phenotypic and genotypic detection of Metallo-beta-lactamases in Carbapenem-resistant Acinetobacter baumannii. Casp. J. Intern. Med,2020, 11, 171–176.

8-López, C.; Ayala, J.A.; Bonomo, R.A.; González, L.J.; Vila, A.J. Protein determinants of dissemination and host specificity of metallo-β-lactamases. Nat. Commun,2019, 10, 3617.

9-Al-Muhanna, S. G., Banoon, S. R., & Al-Kraety, I. A. A. Molecular Detection Of Integron Class 1 Gene In Proteus Mirabilis Isolated From Diabetic Foot Infections. Plant Archives, 2020, Volume 20 No.1 Pp. 3101-3107.

10-Al-Kraety, I. A.A, Al-Muhanna, S. G.& Banoon, S. R. .Molecular Exploring of Plasmid-mediated Ampc beta Lactamase Gene in Clinical Isolates of Proteus mirabilis. Revistabionatura,2021, Volume 6 No. 3 .

11-Wyres, K. L., & Holt, K. E. Klebsiella pneumoniae as a key trafficker of drug resistance genes from environmental to clinically significant bacteria. *Current opinion in microbiology*, 2018, *45*, 131-139.

12- Aljanaby AA, Al-Faham QM, Aljanaby IA, Hasan TH. Epidemiological study of mycobacterium tuberculosis in Baghdad governorate, Iraq. Gene Reports. 2022 Mar 1;26:101467.

13-Hayder T and Aljanaby AAJ. Antibiotics susceptibility patterns of *Citrobacter freundii* isolated from patients with urinary tract infection in Al-Najaf governorate – Iraq. Int.J.Pharm.Sci. 2019a, 10(2): 1481-1488.

14-Hayder T and Aljanaby AAJ. Genotypic characterization of antimicrobial resistance-associated genes in *Citrobacter freundii* isolated from patients with urinary tract infection in Al-Najaf Governorate-Iraq. OnLine Journal of Biological Sciences,2019 b, 19 (2): 132.145.
15-Majeed, H.T., Hasan, T.H. and Aljanaby, A.A.J. Epidemiological study in women infected with toxoplasma gondii, rubella virus, and cytomegalovirus in Al-Najaf Governorate-Iraq. *International Journal of Pharmaceutical Research*, 2020;*12*, pp.1442-1447.
16-Kadhum HA, Hasan TH. The Study of Bacillus Subtils Antimicrobial Activity on Some of the Pathological Isolates. International Journal of Drug Delivery Technology,2019 21;9(02):193-6.
17-Hasan TH, Al-Harmoosh RA. Mechanisms of Antibiotics Resistance in Bacteria. Sys Rev Pharm. 2020,11(6):817-23.
18-Hasan TH. Extended Spectrum Beta Lactamase E. Coli isolated from UTI Patients in Najaf Province, Iraq. International Journal of Pharmaceutical Research.2020,12(4).
19- Bauer, R. A., & Wortzel, L. H. Doctor's choice: The physician and his sources of information about drugs. *Journal of Marketing Research*,1996, *3*(1), 40-47.
20-Firoozeh F, Mahluji Z, Shams E, Khorshidi A, Zibaei M. New Delhi metallo-β-lactamase-1-producing Klebsiella pneumoniae isolates in hospitalized patients in Kashan, Iran. Iranian journal of microbiology. 2017 Oct;9(5):283.
21- Bina M, Pournajaf A, Mirkalantari S, Talebi M, Irajian G. Detection of the Klebsiella pneumoniae carbapenemase (KPC) in K. pneumoniae Isolated from the Clinical Samples by the Phenotypic and Genotypic Methods. Iranian journal of pathology. 2015;10(3):199.
22-Abdulla, Y.N., Aljanaby, A.J.I., Hasan, H.T., Aljanaby, A.J.A. Assessment of ß-lactams and Carbapenems Antimicrobials Resistance in Klebsiella Oxytoca Isolated from Patients with Urinary Tract Infections in Najaf, Iraq.Archives of Razi Institute, 2022, 77(2), pp. 669–673

Received: October 9th 2023/ **Accepte**d: January 15th 2024 / **Published:**15 February 2024

Citation: Hasan T. H., AL-Ethari A. S. Y., Al-Muhanna S.G., Al-Kraety I. A. A. Genotypic Detection of Carbapenems Resistance Genes in *Acinetobacter baumannii* Isolated from Urinary Tract Infection Patients. Revis Bionatura 2024; 9 (1) 60. http://dx.doi.org/10.21931/RB/2024.09.01.60

Additional information Correspondence should be addressed to israa.ameer@alkafeel.edu.iq
Peer review information. Bionatura thanks anonymous reviewer(s) for their contribution to the peer review of this work using https://reviewerlocator.webofscience.com/

Bionatura ISSN. First 13909355 Ecuador. **Scopus coverage years**: from 2016 to the present

Bionatura
Ibero-American Journal of Biotechnology and Life Sciences

Article

Detection of *bla-AIM* Metallo Beta Lactamase Gene among *Stenotrophomonas Maltophilia* and Carbapenem Resistant *Pseudomonas Aeruginosa* Isolated from Various Infections in AL- Najaf Province

Enas Jalil Baqer AL-Mayali[1], Sddiq Ghani Al-Muhanna[2], Israa Abdul Ameer Al-Kraety[3]

[1]Jabir Ibn Hayyan Medical University, Iraq, Najaf, enas.j.baqir@jmu.edu.iq, https://orcid.org/0000-0002-5302-911X.
[2,3]Department of Medical Laboratory Technique, College of Health and Medical Techniques, University of Alkafeel Najaf, Iraq
** Correspondence: enas.j.baqir@jmu.edu.iq, Sddiq.g@gmail.com, https://orcid.org/0000-0002-0589-2939*
israa.ameer@alkafeel.edu.iq, https://orcid.org/0000-0001-6739-1948
Available from. http://dx.doi.org/10.21931/RB/2024.09.01.61

ABSTRACT

Stenotrophomonas maltophilia is a "rapidly evolving pathogen of concern" that is increasingly being identified. The World Health Organization also recognizes it as one of the hospitals' most significant multi-drug-resistant pathogens. Also, *Pseudomonas aeruginosa* is an opportunistic human pathogen that causes most healthcare-associated infections, and it is considered a paradigm of antibiotic resistance development. In many hospitals across the globe, carbapenem-resistant *Pseudomonas aeruginosa* has emerged as a significant source of infection. The present study aimed to study the isolation and diagnosis of *S. maltophilia* and *P. aeruginosa* from different clinical samples, Evaluate the occurrence of carbapenem resistance *of P. aeruginosa* isolated from clinical samples and investigate the dissemination of the bla-AIM genes between these isolates. A total of 850 specimens were collected from various clinical samples between 2022 and 2023. The specimens included 220 swabs (burn), 200 (urine), 140 (stool), and 130(wound). 90 (ear),50 (throat), 10 (Cerebrospinal fluid), and 10 (blood). Represented by 680 specimens contained bacterial growth, and 170 specimens had no bacterial growth. Out of the 680 bacterial growth isolates, 410 revealed growths of Gram-negative bacteria, and 270 were Gram-positive bacteria. On MacConkey ag, ar 180/410 bacteria were lactose ferment; other isolates, es 230/410 of the isolates were lactose non-fermented bacteria. In a cross-sectional manner, *Stenotrophomonas maltophilia* and *Pseudomonas aeruginosa* isolates during this period were isolated and identified depending on the primary methods of diagnosis, then the use of the VITEK-2 compact system. The results showed 42 isolates of *S. maltophilia* and 80 isolates of *P. aeruginosa* from total Gram-negative bacteria. The results show that only five isolates contained the *AIM* gene, with a percentage of (10.4 %) of the 48 Carbapenem Resistant *Pseudomonas aeruginosa* isolates, five isolates from 42 *S. maltophilia* contain the *AIM* gene with a percentage (11.9%), based on the Polymerase chain reactions assay.

Keywords: *Stenotrophomonas maltophilia*, Carbapenem Resistance, *Pseudomonas aerginosa.*

INTRODUCTION

The opportunistic pathogen *Stenotrophomonas maltophilia* is becoming more critical. It has emerged as a hospital-acquired infection because of the widespread use of broad-spectrum antibiotics and the increasing number of invasive operations and immunocompromised patients. *S. maltophilia* exhibits a variety of antimicrobial resistance mechanisms, including the production of enzymes that hydrolyze or modify antibiotics, changes in membrane permeability, and a multi-drug efflux mechanism [1]. Infections caused by *P. aeruginosa*, an opportunistic bacterium, include pneumonia, urinary tract infection, soft-tissue infection, and septicemia [2]. Multidrug-resistant (MDR) *P. aeruginosa* infections have been linked to high rates of illness and death.

Antibiotic treatment options are limited by the high degree of inherent and acquired resistance shown by *P. aeruginosa*. Carbapenems have been generally acknowledged as the most effective -lactams and extensively employed as the cornerstone and empirical therapy of severe infections caused by MDR *P. aeruginosa*; as a last-resort antibiotic, the discovery of carbapenem resistance is concerning, Carbapenem-resistant *P. aeruginosa* has now been discovered and is spreading across the globe [3]. When it comes to the hydrolysis of carbapenem and other beta-lactamases (excluding monobactam), metallo beta-lactamases have a high degree of efficacy and are unaffected by any of the currently known clinically available beta lactamases-inhibitors, all but a few MBL genes are found in integron gene cassettes coupled to mobile elements, which makes it easier for them to be transferred across different bacterial genera and species through horizontal gene transfer [4]. In the early 1990s, the Impeneme and Vancomycin-type enzymes, the most prominent of the acquired Metalobeta-lactamase, were discovered, and since then, several more kinds of acquired Metalobeta-lactamase enzymes [5]. This study aims to determine the occurrence of *the bla-AIM* gene among multi-resistance *S. maltophilia* and *P. aeruginosa* isolated from hospitals in Najaf.

MATERIALS AND METHODS

Patients Demography

Between 2022 and 2023, 850 clinical samples were taken from patients at the Al-Sadder Medical City, Al-Hakeem General Hospital, Al-Forat General Hospital, Al-Zahra Maternity and Children, Al-Sajad Hospital, and Burn Center in the province of Al-Najaf who were af-flicted with various infections. Al-Sadder Medical City 190 (22.3%) and Burn Center 220 (25.8%) produced the majority of the isolates, respectively, as shown in Table (1).

Table (1): Distribution of the number of clinical samples in different Najaf hospitals

Hospitals	Samples No.	Percentage
Burn Center	220	25.8%
Al-Sadder Medical City	190	22.3%
Al-Hakeem General Hospital	160	18.8%
Al-Forat General Hospital	150	17.6%
Al-Zahra for Maternity and Children	100	11.7%
Al-Sajaad Hospital	30	3.5 %
Total	850	100%

All samples were cultured on MacConkey medium and blood agar. After a 24-hour incubation period, the results showed 680 samples containing only bacterial growth. Two hundred two isolates represented the bacterial growth isolates were recovered from burn infections, 178 from urinary tract infections, 100 were from gastroenteritis, 103 bacterial isolates recovered from wounds, and 60, 30, and 3,4 were obtained from ear, throat, cerebrospinal fluid, blood respectively as show Table (2).

Table (2): Distribution of bacterial growth with infection site

Results

Specimens	Bacterial Growth	No Growth	Total
Burn	202	18	220
Urine	178	22	200
Stool	100	40	140
Wound	103	27	130
Ear	60	30	90
Throat	30	20	50
CSF	3	7	10
Blood	4	6	10
Total	680	170	850

Isolation and Identification of Stenotrophomonas maltophilia and Pseudomonas aerginosa Isolates.
The colony appearance, microscopic inspection, and biochemical characteristics were used to identify bacterial isolates. 410 of the 680 bacterial growth isolates showed Gram-negative bacteria growth, while the remaining 270 could not grow on the differential medium (Mac-Conkey Agar) utilized in this investigation. On MacConkey agar, 180/410 of the bacteria produced pink colonies since the bacteria lactose fermented grew on MaCconkey agar and produced pink colonies; other isolates 230/410 isolates produced yellow or colorless colonies since they were lactose non-fermented bacteria. In microscopic examination (Gram film), the organism appeared as a Gram-negative bacillus with a slightly smaller size. These are 230 samples, on which many of the biochemical tests available were conducted, including catalase, oxidase, motility, IMVICs, urease and TSI test to approximate the results for the diagnosis of Stenotrophomonas maltophilia and Pseudomonas aeruginosa using VITEK2 system. The re-sults showed the presence of 230 Gram-negative bacterial isolates that did not ferment to lactose after growing on MacConkey, including 42 isolates of S. maltophilia and 80 isolates of P. aeruginosa.
As a result of S. maltophilia having polar flagella, it became mobile and grew effectively on MacConkey, in addition to producing a distinctive pigment on the medium. The catalase test was positive, and the oxidase test was negative, distinguishing it from other members of the genus. In addition, the IMVC test was negative, except for the citrate test, the result of which was different between the isolat, es, but P. aeruginosa produces pyocyanin and gives off a strong oxidase positive7.
Antibiotic susceptibility test to detect carbapenem resistance P. aeruginosa.
The Eighty clinical isolates of P. aeruginosa were examined for their ability to develop in the presence of carbapenem drugs, Using the Kirby-Bauer disk diffusion technique and an-ti-pseudomonal drugs (imipenem and meropenem) from one antimicrobial category (be-ta-lactam medication), recommendations were followed to conduct preliminary susceptibility screening on the isolates. The findings of drug susceptibility testing include 48 isolate re-sistance to imipenem and 44 isolate resistances to meropenem 8.
DNA extraction
Based on the commercial kits used to extract the genome, the kit (Favorgen, Taiwan) was used in this study.
Molecular identification
The bla-AIM gene for S. maltophilia and P. aeruginosa was detected by PCR using a specific primer with the sequence mentioned in Table 3. Amplification conditions were performed as previously described by (Reference) and summarized in Table 4

Gene	Name of gene	Primer sequence (5 -3)	Bp	References
AIM	Adelaide imipenemase	CTGAAGGTGTACGGAAACAC		
		GTTCGGCCACCTCGAATTG	322	9

Table (3) primer used in this study

Gene	Initial Denaturation	Denaturation	Annealing	Extension	Final Extension	Cycle
AIM	95˚C / 5 min	95˚C/ 30 sec	58˚C/30sec	72˚C/40sec	72˚C/7min	35

Table (4) PCR program to (bla-AIM gene).

RESULTS AND DISCUSSION

Molecular screening of *blah-AIM* producers to *Stenotrophomonas maltophilia* and Molecular screening of *AIM* producers to carbapenem resistance *Pseudomonas aeruginosa*

Molecular screening of *bla-AIM* producers *S. maltophilia*.

Using specialized Ambler class B MB (AIM) primers, all *S. maltophilia* isolates underwent conventional PCR screening for possible MBL gene determinants. With only five isolated positive findings and a proportion of (11.9%) %) as shown in Figure (1).

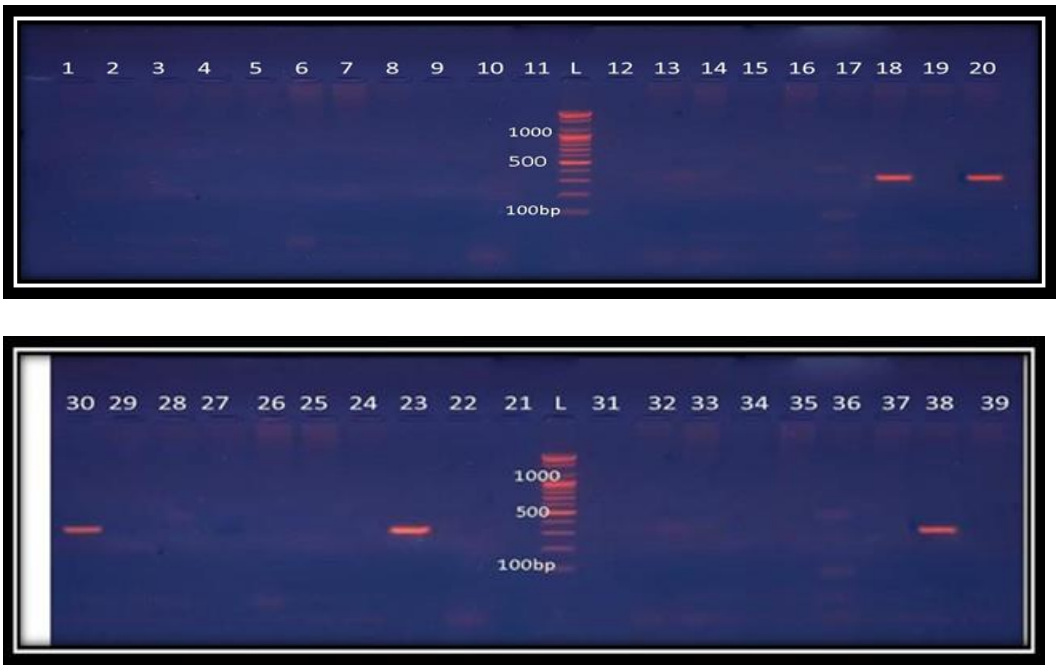

Figure 1: Amplification of *bla-AIM* gene by PCR from *S. maltophilia* isolates. Lane (18, 20, 23, 30, 38) shows positive results of *the bla-AIM* gene with 322 bp.

Even though multiple stable medications and inhibitor combinations are in different phases of development, they elude all recently approved -lactam—lactamase inhibitor combinations.[9] in Iraq reported that *S. maltophilia* is an emerging opportunistic nosocomial pathogen causing various infections. Ceftazidime and chloramphenicol did not affect any of the specimens. Moreover, 100 percent and 43 percent of them developed extended spectrum β-lactamases (ESBLs) and carbapenemases, respectively.

Molecular screening of *bla-AIM* producers to carbapenem resistance *Pseudomonas aeruginosa.*

All 48 carbapenem-resistant *P. aeruginosa* isolates were screened by conventional PCR for potential gene determinants encoding MBL using specific Ambler class B MBL(*AIM*) primers. Only five isolates had positive results for this gene with a percentage (10.4%), as shown in Figure (2).

Figure 2. Amplification of *bla-AIM* gene by PCR from *Pseudomonas aeruginosa* isolates. lanes (4, 9, 24, 38, 39) show positive results of the *bla-AIM* gene with 322 bp.

S. maltophilia has shown high resistance to many antibiotics, including beta-lactams, aminoglycosides, and chloramphenicol because it contains genes carried on the chromosome such as *blaL1* metallo β-lactamase and *blaL2* β-lactamase genes, this was consistent with the isolate's resistance profile[10]. This result agrees with another study in Iraq showing that *S. maltophilia* possesses many resistance genes, the most important of which is the metallo beta-lactamase gene[11].

Contrary to the other B3 MBLs (such as *Stenotrophomonas maltophilia L1 and Janthina bacteria lividum THIN-B, Chryseobacterium meningosepticum GOB, Legionella gormanii FEZ-1, and Caulobacter crescentus CAU-1*), this one can survive in the presence of antibiotics. Despite having the same MBL fold, B3 enzymes have a significantly different active site architecture than other subclasses [12].

An earlier investigation found that Carbapenemase synthesis in *P. aeruginosa* is particularly critical because of the fast spread of CRPA due to the acquisition of carbapenemase genes through mobile genetic elements. *P. aeruginosa* has been shown to generate carbapenemases of classes A, B, and D so far, with the most common being the Verona Integron-encoded Metallo—lactamase (*VIM*), imipenemases (*IMP*), and New Delhi Metallo—lactamase (*NDM*) all belonging to class B Metallo—lactamase (MBL) enzymes [13]

This result also agrees with another research *study, P. aeruginosa*, a prominent human pathogen, which produced *AIM-1*. This subclass B3 enzyme was the first to be discovered on a mobile genetic element; *AIM-1* hydrolyzes most lactams, except aztreonam and ceftazidime, to a lesser extent. However, it has much higher activity for cefepime and carbapenems than most other MBLs[14].

CONCLUSIONS

The presence of isolates of *S. maltophilia*, causing several infections, containing a gene (*bla-AIM*) with a percentage (11.9%). Also, the presence of Carbapenem Resistant *Pseudomonas aeruginosa* isolates caused several infections, containing a gene (*bla-AIM*) with a percentage (10.4%).

Author Contributions: "Conceptualization, E.J.B.A. and I.A.A.; methodology, E.J.B.A. and S.G.A.; software,E.J.B.A..; validation, S.G.A., I.A.A and E.J.B.A.; formal analysis, I.A.A.; investigation, E.J.B.A..; resources, S.G.A.; data curation, I.A.A and S.G.A.; writing—original draft preparation, E.J.B.A.; writ-ing—review and editing, I.A.A.; visualization, I.A.A.; supervision, E.J.B.A.; project administration, I.A.A.; funding acquisition, S.G.A., I.A.A and E.J.B.A. All authors have read and agreed to the published version of the manuscript."

Funding: "This research received no external funding".

Informed Consent Statement: Not applicable

Acknowledgments: The authors would like to express thanks and appreciation to the presidency of the University of Alkafeel for the support in completing this research.

Conflicts of Interest: "The authors declare no conflict of interest."

REFERENCES

1. Huang Y.-W., Liou R.-S., Lin Y.-T., Huang H.-H., and Yang T.-C.A linkage between SmeIJK efflux pump, cell envelope integrity, and σEmediated envelope stress response in Stenotrophomonas maltophilia.2014.
2. Rosenthal V.D., Bijie H. Maki D.G., Mehta, Y. Apisarnthanarak A. and Medeiros E.A. International Nosocomial Infection Control Consortium (INICC) report, data summary of 36 countries, for2004–2009. Am J Infect Control .2012;40:396–407.
3. Vural E., Delialioglu N., Ulger S. T., Emekdas G. and Serin M. S. Phenotypic and molecular detection of the metallo-beta-lactamases in carbapenem-resistant Pseudomonas aeruginosa isolates from clinical samples. Jundishapur, J. Microbiol. 2020 e90034: 1-8. 10.5812/jjm.90034.
4. Edelstein M.V., Skleenova E.N., Shevchenko O.V., D'Souza J.W., Tapalski D.V., Azizov I.S., Sukhorukova M.V., Pavlukov R.A., Kozlov R.S., Toleman M.A. and Walsh T.R. Spread of extensively resistant VIM-2-positive ST235 Pseudomonas aeruginosa in Belarus, Kazakhstan, and Russia: a longitudinal epidemiological and clinical study. Lancet Infect Dis. 2013; 13:867-76.
5. Wachino J., Yoshida H., Yamane K., Suzuki S., Matsui M., Yamagishi T., Tsutsui A., Konda T., Shibayama K. and Arakawa Y. SMB-1, a novel subclass B3 metallo-beta-lactamase, associated with ISCR1 and a class 1 integron, from a carbapenem- resistant Serratia marcescens clinical isolate. Antimicrob Agents Chemother.2011 ;55:5143-9.
6. Miller, R. D., Iinishi, A., Modaresi, S. M., Yoo, B. K., Curtis, T. D., Lariviere, P. J., ... & Lewis, K. (2022). Computational identification of a systemic antibiotic for gram-negative bacteria. *Nature Microbiology*, *7*(10), 1661-1672.
7. Koneman E. W., Allen S. D., Janda W.M., Winn W.C., Procop G.W., Schreckenberger P.C. and Woods,G.L.The non fermentive gram negative bacilli, Color Atlas And Textbook of Diagnostic Microbiology, 6 th edition, (J.B.Lippincott Co., Philadelphia,).2006;316-328.
8. Bassetti M, Vena A, Croxatto A, Righi E, Guery B. How to manage Pseudomonas aeruginosa infections. Drugs in context. 2018;7.
9. Poirel L., Walsh T. R., Cuvillier V. and Nordmann P. Multiplex PCR for detection of acquired carbapenemase genes. Diagnostic microbiology and infectious disease.2011; 70(1), 119-123.
10. Kumwenda, G. P.; Kasambara, W.; Phiri, A.; Chizani, K.; Banda, A.; Choonara, F. and Lichapa, B. (2021). A multidrug-resistant Stenotrophomonas maltophilia clinical isolate from Kamuzu Central Hospital, Malawi. Malawi Medical Journal, 33(2), 82-84.
11. Saleh, R. O.; Hussen, B. M.; Mubarak, S. M. and Mostafavi, S. K. (2021). High diversity of virulent and multidrug-resistant Stenotrophomonas maltophilia in Iraq. Gene Reports, 23.
12. Khorvash F., Yazdani M., Shabani S. and Soudi A. Pseudomonas aeruginosa-producing metallo-β-lactamases (VIM, IMP, SME, and AIM) in the clinical isolates of intensive care units, a university hospital in Isfahan, Iran. Advanced biomedical research.2017;6.
13. Bording-Jorgensen M., Tyrrell H., Lloyd C., & Chui, L. Comparison of Common Enrichment Broths Used in Diagnostic Laboratories for Shiga Toxin—Producing Escherichia coli. Microorganisms.2021; 9(3), 503.
14. Yong, D.; Toleman, M. A.; Bell, J.; Ritchie, B.; Pratt, R.; Ryley, H. and Walsh, T. R. (2012). Genetic and biochemical characterization of an acquired subgroup B3 metallo-β-lactamase gene, bla AIM-1, and its unique genetic context in Pseudomonas aeruginosa from Australia. Antimicrobial agents and chemotherapy, 56(12), 6154-6159.

Received: October 9th 2023/ **Accepte**d: January 15th 2024 / **Published:**15 February 2024

Citation: AL-Mayali E. J. B., Al-Muhanna S. G., Al-Kraety I. A. A. Detection of *bla-AIM* Metallo Beta Lactamase Gene among *Stenotrophomonas maltophilia* and Carbapenem Resistant *Pseudomonas*

Aeruginosa Isolated from Various Infections in AL- Najaf Province. Revis Bionatura 2024; 9 (1) 61. http://dx.doi.org/10.21931/RB/2024.09.01.61

Additional information Correspondence should be addressed to enas.j.baqir@jmu.edu.iq

Peer review information. Bionatura thanks anonymous reviewer(s) for their contribution to the peer review of this work using https://reviewerlocator.webofscience.com/

Bionatura ISSN. First 13909355 Ecuador. **Scopus coverage years**: from 2016 to the present

Bionatura
Ibero-American Journal of Biotechnology and Life Sciences

Review

The Role of Quorum Quenching in Medical Application

Ghada A. Mohammad[1], *Huda Waleed Hadi*[2]*

[1]*University of Mosul / Mosul City / Iraq. kadsbio32@uomosul.edu.iq*
[2]*University of Mosul / Mosul City / Iraq. hudsbio114@uomosul.edu.iq.*
* *Correspondence: hudsbio114@uomosul.edu.iq Tel.: 0750216632 Iraq code: +964*
Available from. http://dx.doi.org/10.21931/RB/2024.09.01.62

ABSTRACT

The attempts are continuing in the various fields of life sciences to resolve a big problem, which is the ability of bacteria to cause pathogenicity for humans, animals, and plants, whether by chemical or biological methods and in ways that are hoped to be safe. Among these attempts, the control of the Quorum Sensing (QS) mechanism that occurs naturally in bacteria under certain conditions helps to increase the virulence of bacteria, starting from its ability to adhere and form a biofilm. Then, the tissues are invaded with various enzymes according to the tissue type, increasing antibiotic resistance. Therefore, the idea came to solve these problems through a mechanism opposite to the Quorum Quenching (QQ), which lies in the investigation of substances that can disrupt the QS pathway, whether at the molecular level or the physiological level, as well as benefiting from different organisms (Prokaryotes or Eukaryotes) that live in the same environment and produce substances that inhibit bacterial signaling molecules. Lastly, the discovery of varying novel QQ agents from extreme environmental bacteria will be most interesting in the future.

Keywords: Quorum sensing, quorum quenching, acyl homoserine lactones, medical application.

INTRODUCTION

The population density and bacterial behavior in different environments are regulated by a specific mechanism known as Quorum Sensing (QS). Small molecules responsible for QS are called signaling molecules or Autoinducers (AIs), sensed by intracellular or membrane-bound receptors in the producer cell or other bacterial cells in the population [1, 2].

There are different types of AIs according to their chemical structure and mechanism of action. The main types of AIs are (i) Acyl Homoserine Lactones (AHLs) that are used by gram harmful bacteria, (ii) Auto-Inducing Peptides (AIPs) in gram-positive bacteria [3]. Other references add a third type of AI: furanosyl diester borate (AI-2) [4]. Meanwhile, others divide AI-1 into two types: AHLs that carry out intraspecies communications and AI-2 that involve furanosyl borate interspecies communications. [5]. Furthermore, studies can provide additional AI types, such as fatty acids (FA), quinolone in *Pseudomonas* spp., and butrylactone in *Streptomyces* spp. [1].

Various AI types have the same function as QS molecules when their concentration increases to a certain level. At this concentration level, AIs bind with their receptors (Figure 1). This binding stimulates the regulation of specific genes [6, 3].

AHL molecules may perform other functions as antibacterial agents, mainly when composed of long carbon chains [7], such as N-3-oxo-dodecanoyl-L-homoserine Lactone (OC12-HSL), which are named bacteriocin when they act as antibiotics [8].

Cascades of QS enhance virulence factors such as biofilm production, plasmid transfer, enzymes, and motility. Also, QS gives additional bacterial adaption properties to harsh environmental conditions and activation of bioluminescence in *Vibrio fisheri* bacteria [9, 6].

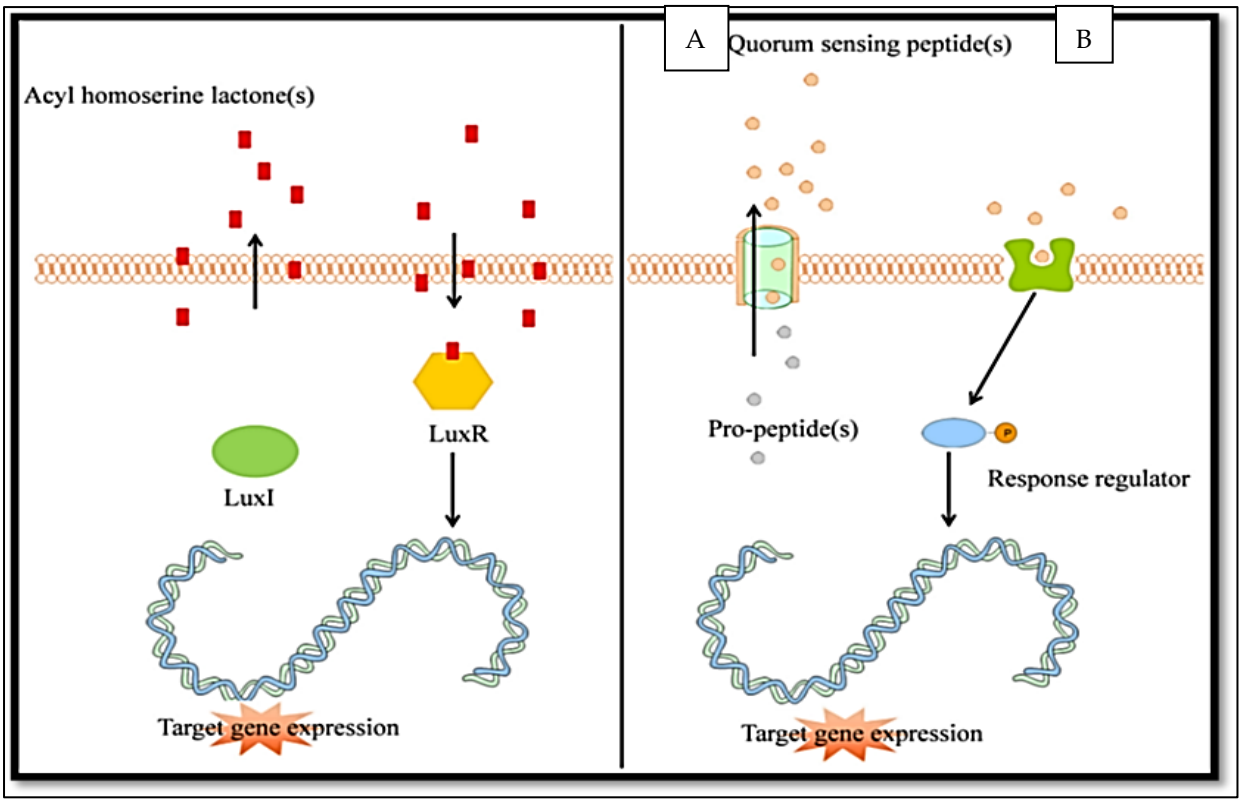

Figure 1: The quorum sensing mechanism. A: in Gram-negative. B: in Gram-positive bacteria [3].

QUORUM QUENCHING (QQ)

The Quorum Quenching (QQ) is a molecular mechanism of processes that interrupt bacterial communication; it is achieved by several modes of action [10- 12]. QQ was first discovered in *Erwinia carotovora,* which produces AHL-degrading enzymes that cause QS blocking [12, 13]. QS Pathway consists of multiple steps. Each step can be interfered with by specific QQ molecules, also called QS inhibitors (QSIs). Biological molecules and other physical factors such as pH and temperature can act as QSIs. [6].

The competitive inhibitors for AI molecules can be biosynthesized from microorganisms such as bacteria or eukaryotic organisms like algae, marine animals, plants, and fungi. These inhibitors block AIs-receptors binding, leading to QS disrupting [14]. Extracellular QQ enzymes can degrade or modify AIs. These enzymes produce bacteria with competitive advantages to get nutrients in their environments [15, 16].

There is no pathogenic commensal flora present in healthy skin. When the skin is exposed to wounds, lesions, and burns, this flora colonizes damaged skin, multiplying and forming biofilm. Signaling molecules AIs produce a biofilm that enables bacteria to become more virulent and resistant to antibiotics, phage therapy, and antibody goals. However, the QQ molecules that are used against biofilm bacteria remain not harmful and without defenses (Figure 2). Therefore, QQ helps cure unhealthy skin and helps it stay in a noninfectious state [17].

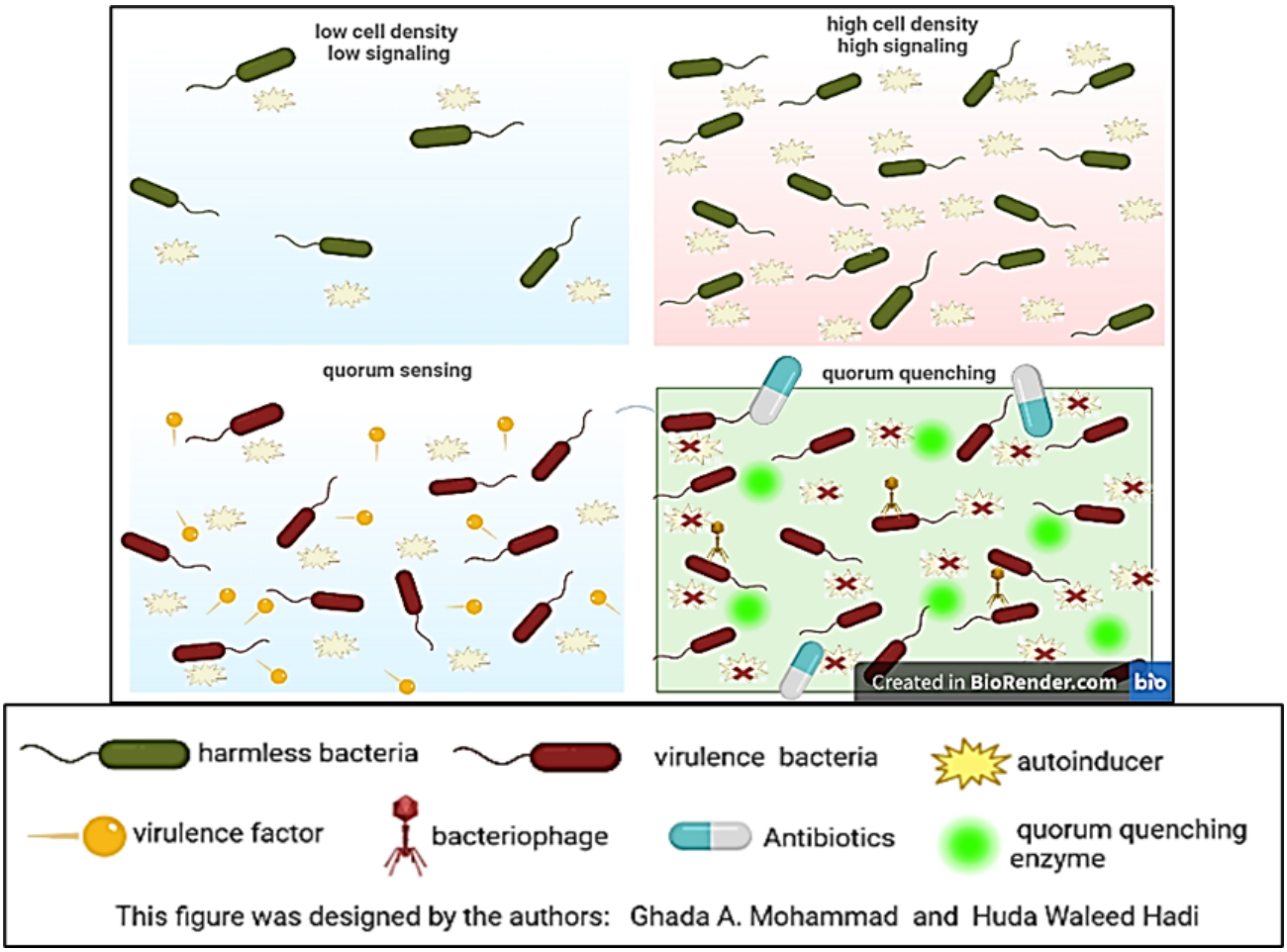

Figure 2: Quorum sensing vs. quorum quenching in this review.

FIRST: NATURAL COMPOUNDS

Natural compounds have important antibacterial features and anti-virulence characteristics. QQ molecules from natural compounds, either eukaryotic or prokaryotic sources, are efficient and safe. They are readily biodegradable and can interrupt bacterial infection in a very active manner [18, 19].

A- Bacterial QSIs

Bacterial QQ molecules are isolated from different bacterial taxa such as Firmicutes, Actinobacteria, Proteobacteria, Bacteroides, and Cyanobacteria. These bacterial QQs are very active against *Pseudomonas aeroginosa* biofilm producers and also have an essential role in biofilm removal in the wastewater treatment plant. The bacteria produce three types of enzymes: AHL lactonase, AHL acylase, and AHL oxide reductase [13, 11]. Other references add a fourth class to these enzymes to become four classes by separating oxidase enzymes such as cytochrome from reductase enzymes [20, 1].

AHL-Lactonase Enzymes

This type of enzyme belongs to the Metallo-β-Lactamase (MBL) family [11]. Some references further divided the lactonase enzymes in addition to the previous class according to their protein folding and active motif, such as the Phosphodiesterase- Lactonase (PLLs), the α/β hydrolase fold lactonase, and the paraoxonase. Classes of lactonase have been observed evolutionary convergence with low specificity to the substrate level except PLLs that show high specificity to the long chains AHL [16, 21]. Lactonase enzymes can degrade or modify the lactone ring (Figure 3) in different molecules of AHL, therefore blocking swarming motility in *P. aeroginosa* by lactonase produced by *Pectobacterium carotovora*[22]. Hence, they are efficient in interfering with QS. AHL-lactonase enzymes have been isolated from various prokaryotic, archaea, and eukaryotic

organisms. They have been assessed in their controlling of different diseases. Therefore, increasing their effectiveness activity by engineering studies leads to the rise of their catalytic activity and stability [23].
Lactonase enzymes do not interfere with QS only; they can interfere with other biological processes, such as the bacterium *Agrobacterium tumefacien*t, which is controlled by Ti plasmid [24, 1].

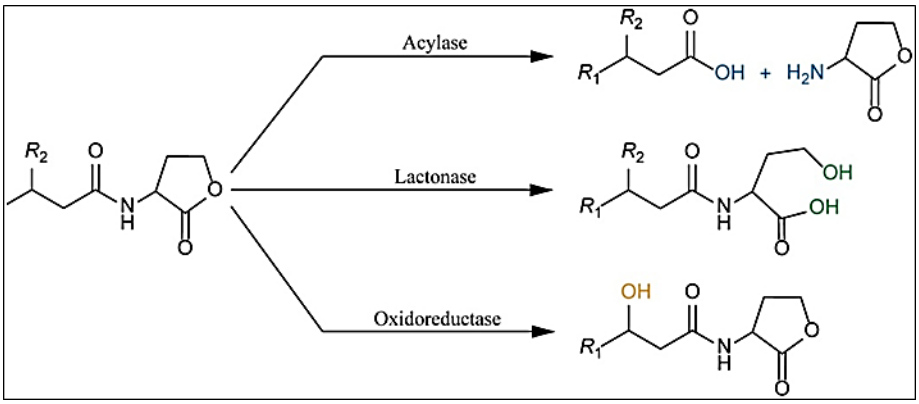

Figure 3: Prokaryotic Enzymes Action on AHL molecoule [25].

AHL-Acylase Enzymes

Acylase enzymes separate acyl chains from lactone rings (Figure 3). Amidase enzymes (or acylase) are considered from this type of enzyme. *P. aeroginosa* can degrade the AHL molecules by its amidase enzymes [1].
It has been proved that treatment of wastewater biofilms by AHLs degrading enzymes (Aculeacin A Acylase (AuAAC) which is obtained from Actinoplanes utahensis) can prevent the four systems of QS in *P. aeroginosa* [13].
AHL-acylase enzymes belong to the family of N-terminal nucleophilic hydrolases (Ntn- hydrolases). PvdQ is an example of these enzymes that can split an acyl chain with more than 10 carbon atoms [16].

AHL-Oxidoreductase Enzymes

These enzymes can modify the AHL molecules without degrading them (Figure 3). They can reduce or oxidize AHL molecules [26]. Oxidoreductase enzymes spread in the bacteria that used AHL molecules as nitrogen or carbon sources [11]. also include oxidoreductase and esterase enzymes [26].

B- Eukaryotic QSI

Varieties of QQ eukaryotic molecules have been isolated from different taxa of the eukaryotic cells. These molecules are very active as QQ; therefore, they have essential roles in medical fields[20,27]. Eukaryotic enzymes have been extracted and purified from different animals, which can disrupt QS signals, such as the acylase 1 enzyme of porcine kidney [28]. paraxonases 1, 2, 3, and QQ enzymes are found in epithelial cells and mammalian sera [29].
However, the plant extracts represent valuable and safe compounds for disrupting the bacterial QS (Table 1). Because of the ability of these compounds to disrupt bacterial infection without causing antibacterial resistance, QQ phytocompounds are very important in fighting bacterial virulence and antibiotic resistance, especially in *P. aeruginosa* [19].
Isolated substances from fungi also have a role in the QS blocking, such as ethyl acetate extracts from *Plectosphaerella cucumerina* fungus against *P. aeroginosa* PAO1 strain; the treatments by the fungal compounds lead to a high potential in blocking the biofilm formation without killing the producing bacteria[30].
The marine red algae *Halemenia durvilleican* produces metabolites that disrupt the AHL in gram-negative bacteria such as *Klebsiella pneumonia* and *P. aeroginosa* [31]. Complex reactions can occur in the relationships between algae and QS-associated bacteria, which may affect their ecology system [32].

Quorum Sensing Inhibitor Compounds	Quorum Sensing Efficacy
Curcumin	Motility phenotypes and production of biofilm
Flavonoids (naturally-produced plant Metabolites)	LasR and RhlR receptors
Ajoene, a Sulfur-Rich Molecule from Garlic	Pathogenic factors production
Salicylic acid	Secretion of protease, elastase, pyocyanin and production of biofilm and the expressions of lasI, lasR, rhlI, rhlR genes
Clove oil	Protease, chitinase and pyocyanin secretion, swimming motility and production of biofilm
Caffeine	Motility phenotypes
Allium sativum (Garlic) extract	Production of biofilm, elastase secretion

Table 1: The Herbal Extracts as Quorum Sensing Inhibitors [11]

SECOND: SYNTHETIC QSI

The use of nanoparticles (NPs) and engineering nanoparticles as antimicrobial agents gained importance in previous years because of the increased bacterial resistance to ward antimicrobial agents. NPs have little or no toxicity and have pharmaceutical properties as antibiotics [33, 34, 35]. Other studies suggested that NPs can be used as anti-QS signals. Because of its ability to penetrate the biofilm, genes cascade and stop cell-to-cell signaling, which leads to the cessation of biofilm formation [33, 36].

Cationic polysaccharides chitosan NPs have many clinical properties, but the important one is anti-QS signals. It has a positive charge that reacts with the negative charge of the lipopolysaccharides in *the P. aeroginosa* cell wall. This reaction causes membrane permeability changes, leading to bacterial killing; furthermore, the NPs can affect the virulence factors such as pyocyanin and protease gene expression of biofilm formation [37].

The zinc oxide NPs can combat *P. aeroginosa* signals such as rhamnolipid, pyocyanin, pyoverdin, hemolysin, elastase, and protease in addition to the inhibition of QS genes, which leads to a decrease in the pathogenicity and virulence of *P. aeroginosa* in vivo [38].

Quorum Quenchers Application

The QQ has an essential role in the medical field, health care, aquaculture, agriculture purposes, phytochemicals, antibiotics, and water engineering [39].

Quorum Quenching in Medical Application

The QQ controls various virulence factors such as sporulation, biofilm formation, enzyme production, motility, pigment production, flagella, and pili[40]. Also, biofilm formation is the main problem that makes most diseases, such as oral cavities and cystic fibrosis, hardly curing[41].

There are several mechanisms in the medical application of QQ, such as:

1- Using synthetic analogs of AHL molecules, which disrupt the binding of AHLs with their receptors, can also alter the chemical function of the acyl chain tail or the head of AHL molecules [42].
2- Using engineering QQ enzymes such as lactonase and acylase isolated from various organisms may become more efficient in the degradation of AHL molecules [23].
3- Down-regulation of the bacterial virulence genes by Qs inhibitors using trans-cinnamaldehyde and salicylic acid in QS inhibition of *P. aeroginosa* PAO1 strain [43].
4- Blocking the signaling cascades [44].
5- Inhibition of the signal molecules' biosynthesis [45].

In the field of Medical Devices

Most Hospital Acquired Infections (HAIs) are associated with using various contaminated medical devices [46]. The emergence of QQ molecules in synthesizing various medical devices is a very useful method to avoid

HAIs (Table 2). The recent generation of catheters, trauma, dressing, aerosols, contact lenses, and implantable devices are involved in QQ molecules [17]. For example, device surfaces coated with pro and anti-QS peptides show high antibacterial potential against *Staphylococcus aureus* strains [47].
Medical devices containing QQ require further testing with more pathogenic and virulent bacterial strains. Therefore, researchers seek to use highly resistant QQ enzymes or compounds isolated from microorganisms of extreme environments, such as *Solfolobus solfataricus* [17].

QQ strategy	QQ agent	Application
QSI	5-fluorouracil	Catheters
	Thiazolidinedione-8	Urinary catheters
	Furanone and DHP	derivatives Implanted medical devices
Peptides	Macrocyclic peptides	Nanofiber coatings
	RNAIII-inhibiting peptide	Dacron graft
QQ Enzymes	Acylase from A malleus.	Catheters and other coated devices
	Lactonase from *Bacillus* sp. ZA12	Topical treatments
	AI-2 processing kinase LsrK	Capsules
Natural compounds	Polyphenols of honey	Nanovectors

Table 2: Quorum quenching-based medical devices [17].

QQ-Based Antibacterial Treatments in Medicine

Conventional antibiotics cannot penetrate the extracellular matrix of bacterial biofilm, which leads to the loss of 80% of their efficiency. The infections caused by biofilm production in oral cavities and cystic fibrosis occur directly via this biofilm, and most infections associated with HAIs result from biofilm contamination of medical devices[48 41].

Antibody-based QQ efforts

The blocking of bacterial cell communication via the use of monoclonal antibodies (mAbs) is a beautiful strategy to prevent infections. These mAbs can also detect homoserine lactones (HSLs), which control QS system-dependent LuxI/LuxR in *P. aeroginosa.* The groups of mice treated with the QQ mAbs are found to be protected and cured from pneumonia caused by *P. aeroginosa* compared with control groups [49].
The mAbs-based QQ have acquired importance in recent years because of their high specificity and little toxicity; they also can degrade the signaling molecules by inhibiting the pyocyanin production in *P. aeroginosa*[50].

Antibiotics as QSI

Antibiotics cannot inhibit the growth, metabolic activities, or cell wall synthesis of bacteria only. Still, they also interfere with the QS pathways as macrolides and β -lactam antibiotics, inhibiting the several appearances of QS[51].
Azithromycin, imipenem, cefepime, tazobactam, and piperacillin were examined as antivirulence factors of wild and mutant *P. aeroginosa* strains. Virulence factors include pyocyanin, biofilm, hemolysin, protease, and DNAse, all of which depend on QS signals. Antibiotics in their sub-inhibitory concentration (SIC) can interfere with QS better than the highest concentrations and do not cause the appearance of antibacterial resistance and side effects[52].

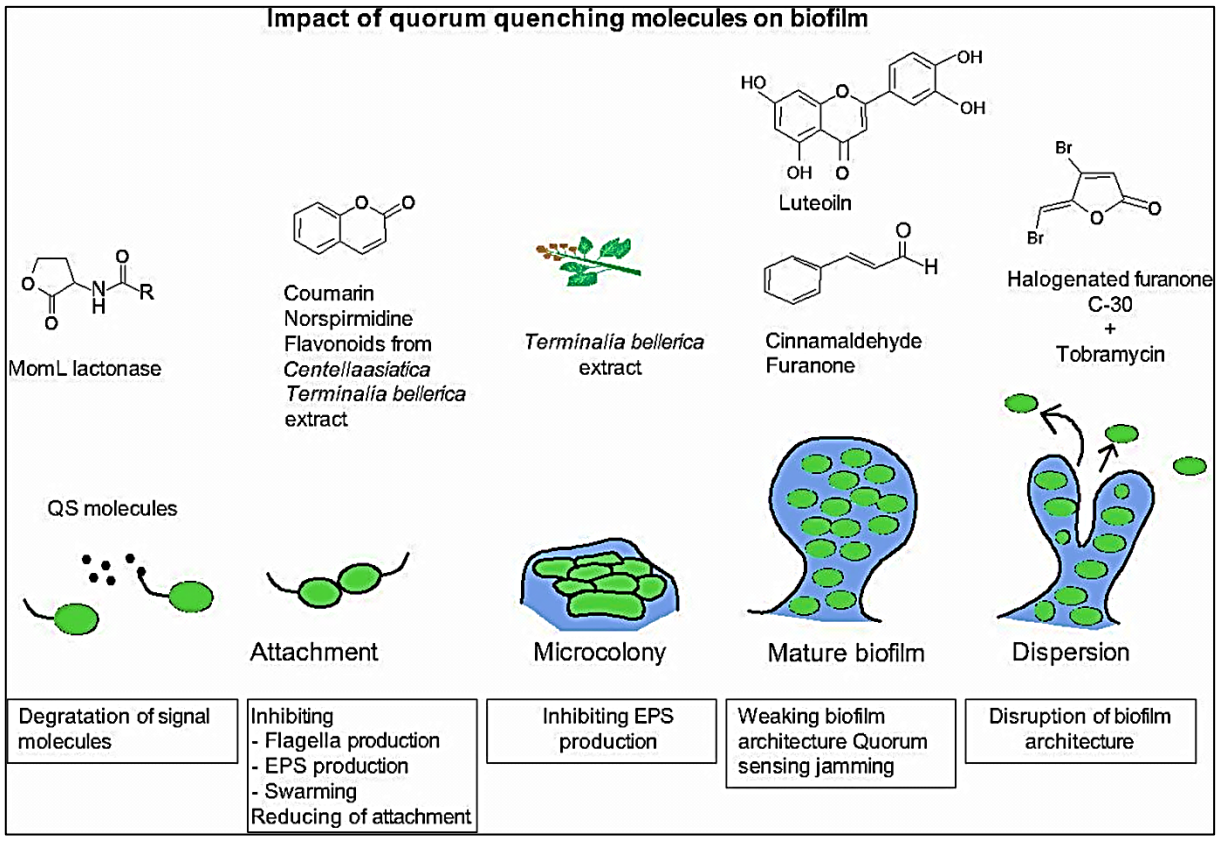

Figure 4: The impact of quorum quenching molecules on biofilm formation [6].

Similar results with *P. aeroginosa* and *Acinetobacter baumannii*, which are considered from MDR bacteria, were obtained by the study of Saleem and co-workers, who mentioned that the Erythromycin, chloroquine, and propranolol antibiotics were able to inhibit (in SIC) virulence based on QS such as biofilm, enzymes, resistance to oxidative stress, swarming and twitching [53].

CONCLUSIONS

As bacterial response mechanisms are regulated by what is known as Quorum Sensing QS, other mechanisms meet it and work to stop it, and they are called Quorum Quenching QQ. Both QS and QQ mechanisms are diverse and vary with a wide range of chemical compositions. So, scientists compete to reach the most efficient means of QQ by various means to eliminate the bacterial pathogenicity and virulence factors, especially in resistant pathogenic bacteria. Nowadays, the QQ methods represent a global goal to eliminate antibiotic resistance mechanisms that have recently spread comprehensively. Therefore, this article highlights the most important and latest applications based on QQ, especially medical equipment and devices in direct contact with the patient's life, to eliminate hospital nosocomial infections and the widespread bacterial resistance to the latest choice of antibiotics.

Conflicts of Interest: "The authors declare no conflict of interest." "The funders had no role in the study's design; in the collection, analyses, or interpretation of data; in the writing of the manuscript, or in the decision to publish the results."

REFERENCES

1. Grandclément, C., Tannières, M., Moréra, S., Dessaux, Y., Faure, D. Quorum quenching: role in nature and applied developments. *FEMS microbiology reviews* **2016**, 40:86-116.
2. Xiao, Y., Zou, H., Li, J., Song, T., Lv, W., Wang, W., ... Tao, S. Impact of quorum sensing signaling molecules in gram-negative bacteria on host cells: current understanding and future perspectives. *Gut Microbes* **2022**; 14: 2039048.
3. Verbeke, F., De Craemer, S., Debunne, N., Janssens, Y., Wynendaele, E., Van de Wiele, C., De Spiegeleer, B. Peptides as quorum sensing molecules: measurement techniques and obtained levels in vitro and in vivo. *Frontiers in neuroscience* **2017**, 11, 183.
4. Huang, J., Shi, Y., Zeng, G., Gu, Y., Chen, G., Shi, L., ... Zhou, J. Acyl-homoserine lactone-based quorum sensing and quorum quenching hold promise to determine the performance of biological wastewater treatments: an overview. *Chemosphere* **2016**, 157, 137-151.
5. Hmelo, L. R. Quorum sensing in marine microbial environments. *Annual review of marine science* **2017**, 9, 257-281.
6. Paluch, E., Rewak-Soroczyńska, J., Jędrusik, I., Mazurkiewicz, E., Jermakow, K. Prevention of biofilm formation by quorum quenching. *Applied microbiology and biotechnology* **2020**, 104, 1871-1881.
7. Daniels, R., Reynaert S.,HoekstraH, et al. Quorum signal molecules as biosurfactants affect swarming in *Rhizobium etli*. *P NatlAcad Sci USA* **2006**,103:14965–70.
8. Lowery, C.A., Park, J., Gloeckner, C., et al. We are defining the mode of action of tetramic acid antibacterials derived from *Pseudomonas aeruginosa* quorum sensing signals. *J Am Chem Soc* **2009**;131:14473–9.
9. Nazzaro, F., Fratianni, F., Coppola, R. Quorum sensing and phytochemicals. International journal of molecular sciences **2013**, 14(6), 12607-12619.
10. Natrah, F. M. I., Kenmegne, M. M., Wiyoto, W., Sorgeloos, P., Bossier, P., Defoirdt, T. Effects of micro-algae commonly used in aquaculture on acyl-homoserine lactone quorum sensing. *Aquaculture* **2011**, 317(1-4), 53-57.
11. Hemmati, F., Salehi, R., Ghotaslou, R., Kafil, H. S., Hasani, A., Gholizadeh, P., Nouri, R. Rezaee, M. A. Quorum quenching: A potential target for antipseudomonal therapy. *Infection and Drug Resistance* **2020**, 13, 2989.
12. Dong, Y. H., Xu, J. L., Li, X. Z., Zhang, L. H. AiiA, an enzyme that inactivates the acylhomoserine lactone quorum-sensing signal and attenuates the virulence of *Erwinia carotovora*. *Proceedings of the National Academy of Sciences* **2000**, 97(7), 3526-3531.
13. De Celis, M., Serrano-Aguirre, L., Belda, I., Liébana-García, R., Arroyo, M., Marquina, D., ... Santos, A. Acylase enzymes disrupting quorum sensing alter the transcriptome and phenotype of *Pseudomonas aeruginosa*, and the composition of bacterial biofilms from wastewater treatment plants—*science of the Total Environment* **2021**, 799, 149401.
14. Surpeta, B., Grulich, M., Palyzová, A., Marešová, H., Brezovsky, J. Common Dynamic Determinants Govern Quorum Quenching Activity in N-Terminal Serine Hydrolases. *ACS Catalysis* **2022**, 12, 6359-6374.
15. Sikdar, R., Elias, M. Quorum quenching enzymes and their effects on virulence, biofilm, and microbiomes: a review of recent advances. *Expert review of anti-infective therapy* **2020**, 18(12), 1221-1233.
16. Rehman, Z. U., Leiknes, T. Quorum-quenching bacteria isolated from Red Sea sediments reduce biofilm formation by *Pseudomonas aeruginosa—frontiers in microbiology* **2018**, 9, 1354.
17. Rémy, B., Mion, S., Plener, L., Elias, M., Chabrière, E., Daudé, D. Interference in bacterial quorum sensing: a biopharmaceutical perspective. *Frontiers in pharmacology* **2018**, 9, 203.
18. Asfour, HZ. Anti-quorum sensing natural compounds. *Journal of microscopy and ultrastructure* **2018**, 6(1), 1.
19. Moradi, F., Hadi, N. Quorum-quenching activity of some Iranian medicinal plants. *New Microbes and New Infections* **2021**, 42, 100882.

20. Chowdhary, P. K., Keshavan, N., Nguyen, H. Q., Peterson, J. A., González, J. E., Haines, D. C. *Bacillus megaterium* CYP102A1 oxidation of acyl homoserine lactones and acyl homoserines. *Biochemistry* **2007**, 46(50), 14429-14437.
21. Hiblot, J., Bzdrenga, J., Champion, C., Chabriere, E., Elias, M. Crystal structure of VmoLac, a tentative quorum quenching lactonase from the extremophilic crenarchaeon *Vulcanisaeta moutnovskia*. *Scientific Reports* **2015**, 5(1), 1-11.
22. Dong, W., Zhu, J., Guo, X., Kong, D., Zhang, Q., Zhou, Y., Liu, X., Zhao, S. Ruan, Z. Characterization of AiiK, an AHL lactonase, from Kurthia huakui LAM0618T and its application in quorum quenching on *Pseudomonas aeruginosa* PAO1. *Scientific reports* **2018**, 8(1), 1-11.
23. Billot, R., Plener, L., Jacquet, P., Elias, M., Chabrière, E., Daudé, D. Engineering acyl-homoserine lactone-interfering enzymes toward bacterial control. *Journal of Biological Chemistry* **2020**, 295(37), 12993-13007.
24. Haudecoeur, E., Tannières, M., Cirou, A., Raffoux, A., Dessaux, Y., Faure, D. Different regulation and roles of lactonases AiiB and AttM in *Agrobacterium tumefaciens* C58. *Molecular plant-microbe interactions* **2009**, 22(5), 529-537.
25. Chen, F., Gao, Y., Chen, X, Yu, Z., Li, X. Quorum Quenching Enzymes and Their Application in Degrading Signal Molecules to Block Quorum Sensing-Dependent Infection. *International Journal of Molecular Sciences* **2013**, 14:17477 - 17500.
26. Utari, P. D., Vogel, J., Quax, W. J. Deciphering physiological functions of AHL quorum quenching acylases. *Frontiers in microbiology* **2017**, 8, 1123.
27. AL-Sabagh, F. S. H., Ghaima, K. K., Sh.AL-Dabbagh, A. H. The antibacterial activity of LL-37 peptide against multidrug-resistant *Pseudomonas aeruginosa* isolated from burn infections. *Revis Bionatura* **2023**, 8 (1), 69.
28. Dong, Y. H., Zhang, L. H. Quorum sensing and quorum-quenching enzymes. *Journal of Microbiology* **2005**, 43(spc1), 101-109.
29. LaSarre, B., Federle, M. J. Exploiting quorum sensing to confuse bacterial pathogens. *Microbiology and molecular biology reviews* **2013**, 77(1), 73-111.
30. Zhou, J.W., Chen, T.T., Tan, X.J., Sheng, J.Y., Jia, A.Q. Can the quorum sensing inhibitor resveratrol function as an aminoglycoside antibiotic accelerant against *Pseudomonas aeruginosa*?. International journal of antimicrobial agents **2018**, 52: 35-41.
31. Boominathan, R., Devanesan, S., AlSalhi, M.S., Balasubramanian, A., Alkhalid, I.Z., Paul, P., Singh, AR. Quorum quenching action of marine red alga Halemenia durvillei on biofilm forming Gram negative bacterial isolates from contact lens. *Algal Research* **2022**, 64, 102693.
32. Zhang, Y., Zheng, L., Wang, S., Zhao, Y., Xu, X., Han, B., Hu, T. Quorum sensing bacteria in the phycosphere of hab microalgae and their ecological functions related to cross-kingdom interactions. *International Journal of Environmental Research and Public Health* **2022**, 19(1), 163.
33. Pelgrift, R.Y., Friedman, A.J. Nanotechnology as a therapeutic tool to combat microbial resistance. *Advanced drug delivery reviews* **2013**, 65, 1803-1815.
34. Selah, M. T., Mohammad, G. A. Ability of three species of *Enterobacter* bacteria to synthesize iron nanoparticles and detection of the efficacy to inhibitory effect on other pathogenic bacteria. *Biochemical and Cellular Archives* **2021**, 21, 2085-2090.
35. Ahmed, A.M., Al Marjani, M.F., Rheimah, A.M. Antibacterial and anti-biofilm action of cobalt oxide nanoparticles beside persister *Pseudomonas aeruginosa* isolates. *Revis Bionatura* **2023**,8 (2), 78.
36. DAS, Bhaskar; PATRA, Sanjukta. Antimicrobials: Meeting the challenges of antibiotic resistance through nanotechnology. En Nanostructures for antimicrobial therapy. Elsevier, 2017. p. 1-22.
37. Qais, F.A., Khan, M.S., Ahmad, I. Nanoparticles as quorum sensing inhibitor: Prospects and limitations. Springer, Singapore. *In Biotechnological applications of quorum sensing inhibitors* **2018**. 227-244.
38. Ma, Z., Garrido-Maestu, A., Jeong, K. C. Application, mode of action, and in vivo activity of chitosan and its micro-and nanoparticles as antimicrobial agents: A review. *Carbohydrate polymers* **2017**, 176, 257-265.
39. Saleh, M. M., Refa't A, S., Latif, H. K. A., Abbas, H. A., Askoura, M. Zinc oxide nanoparticles inhibits quorum sensing and virulence in *Pseudomonas aeruginosa*. *African health sciences* **2019**, 19(2), 2043-2055.

40. Maddela, N. R., García Cruzatty, L. C., Leal-Alvarado, D. A., Olaya, J. C., Chakraborty, S., Mukherjee, A. Quorum Quenching for Sustainable Environment: Biology, Mechanisms, and Applications. Springer, Singapore.*In Microbial Technology for Health and Environment* **2020** (pp. 73-112).
41. Krzyżek, P. Challenges and limitations of anti-quorum sensing therapies. *Frontiers in microbiology* **2019**, 10, 2473.
42. Pawlaczyk-Kamieńska, T., Borysewicz-Lewicka, M., Batura-Gabryel, H., Cofta, S. Oral Care Recommendation for Cystic Fibrosis Patients–Recommendation for Dentists. *Journal of Clinical Medicine* **2022**, 11(10), 2756.
43. Palmer, A. G., Senechal, A. C., Haire, T. C., Mehta, N. P., Valiquette, S. D., Blackwell, H. E. Selection of appropriate autoinducer analogues for the modulation of quorum sensing at the host–bacterium interface. *ACS chemical biology* **2018**, 13(11), 3115-3122.
44. Ahmed, S.A., Rudden, M., Smyth, T. J., Dooley, J. S., Marchant, R., Banat, I. M. Natural quorum sensing inhibitors effectively downregulate gene expression of *Pseudomonas aeruginosa* virulence factors. *Applied microbiology and biotechnology* **2019**, 103(8), 3521-3535.
45. Oh, M. H., Choi, C. H. Role of LuxIR homologue AnoIR in *Acinetobacter* nosocomialis and the effect of virstatin on the expression of anoR gene. *Journal of Microbiology and Biotechnology* **2015**, 25(8), 1390-1400.
46. Lade, H., Paul, D., Kweon, J. H. Quorum quenching mediated approaches for control of membrane biofouling. *International journal of biological sciences* **2014**, 10(5), 550.
47. Neoh, K. G., Li, M., Kang, E. T., Chiong, E., Tambyah, P. A. Surface modification strategies for combating catheter-related complications: recent advances and challenges. *Journal of Materials Chemistry B* **2017**, 5(11), 2045-2067.
48. Kim, M. K., Zhao, A., Wang, A., Brown, Z. Z., Muir, T. W., Stone, H. A., Bassler, B. L. Surface-attached molecules control *Staphylococcus aureus* quorum sensing and biofilm development. *Nature Microbiology* **2017**, 2(8), 1-12.
49. Lebeaux, D., Chauhan, A., Rendueles, O., Beloin, C. From in vitro to in vivo models of bacterial biofilm-related infections. *Pathogens* **2013**, 2(2), 288-356.
50. Palliyil, S. Quorum Quenching Monoclonal Antibodies for the Detection and Treatment of Gram-Negative Bacterial Infections. *Trends in Quorum Sensing and Quorum Quenching* **2020**, 285-290.
51. Jiang, Q., Chen, J., Yang, C., Yin, Y., Yao, K. Quorum sensing: a prospective therapeutic target for bacterial diseases. *BioMed Research International* **2019**, 2019.
52. El-Mowafy, SA., Abd El Galil, KH., Habib, ES. E., Shaaban, MI. Quorum sensing inhibitory activity of sub-inhibitory concentrations of β-lactams. *African Health Sciences* **2017**, 17(1), 199-207.
53. Aleanizy, FS., Alqahtani, FY., Eltayb, EK., Alrumikan, N., Almebki, R., Alhossan, A., ... AlQahtani, H. Evaluating the effect of antibiotics sub-inhibitory dose on *Pseudomonas aeruginosa* quorum sensing dependent virulence and its phenotypes. *Saudi Journal of Biological Sciences* **2021**, 28(1), 550-559.
54. Seleem, N. M., Abd El Latif, H. K., Shaldam, M. A., & El-Ganiny, A. Drugs with new lease of life as quorum sensing inhibitors: For combating MDR *Acinetobacter baumannii* infections. European *Journal of Clinical Microbiology & Infectious Diseases* **2020**, 39(9), 1687-1702.

Received: October 9th 2023/ **Accepte**d: January 15th 2024 / **Published:**15 February 2024

Citation: Mohammad G. A., Hadi H. W. The Role of Quorum Quenching in Medical Application. on the Mortality of Two Nematodes in a Laboratory Setting. Revis Bionatura 2024; 9 (1) 62. http://dx.doi.org/10.21931/RB/2024.09.01.62

Additional information Correspondence should be addressed to hudsbio114@uomosul.edu.iq

Peer review information. Bionatura thanks anonymous reviewer(s) for their contribution to the peer review of this work using https://reviewerlocator.webofscience.com/

Bionatura ISSN. First 13909355 Ecuador. **Scopus coverage years**: from 2016 to the present

Bionatura
Ibero-American Journal of Biotechnology and Life Sciences

Article

Composición química y evaluación del sinergismo de la actividad antioxidante de mezclas de los aceites esenciales de *Luma chequen* (Arrayan) y *Citrus maxima* (Pomelo).

Chemical composition and evaluation of the synergism of the antioxidant activity of blends of the essential oils of *Luma chequen* (Arrayan) and *Citrus maxima* (Grapefruit)

*Carla del Carpio-Jiménez[1,2], R. Giancarlo Gutierrez-Chavez[2], H. Angelica Quispe-Dávila[3], Ciro Tomaylla-Cruz[4] and Mario J. Urrunaga-Ormachea[2]**

[1]Laboratorio de Tecnología Farmacéutica, Universidad Nacional de San Antonio Abad del Cusco
delcarpiojc_daqf@unsaac.edu.pe. ORCID: https://orcid.org/0000-0001-7487-354X
[2]Departamento Académico de Farmacia, Universidad Nacional de San Antonio Abad del Cusco
roger.gutierrezch@unsaac.edu.pe. ORCID: https://orcid.org/0000-0002-1672-9117
mario.urrunaga@unsaac.edu.pe. ORCID: https://orcid.org/0000-0002-3451-8890
[3]Escuela Profesional de Farmacia y Bioquímica, Universidad Nacional de San Antonio Abad del Cusco
161156@unsaac.edu.pe
[4]Departamento Académico de Química, Universidad Nacional de San Antonio Abad del Cusco
ciro.tomaylla@unsaac.edu.pe. ORCID: https://orcid.org/0000-0001-6921-1250
**Correspondence: mario.urrunaga@unsaac.edu.pe; Tel.: +51-984225514*
Available from. http://dx.doi.org/10.21931/RB/2024.09.01.63

RESUMEN

Los aceites esenciales son componentes bioactivos usados en áreas como la medicina, la farmacia, la cosmética y la industria alimentaria, se emplean como conservantes por sus propiedades antioxidantes. El objetivo de la presente investigación fue extraer, determinar las propiedades fisicoquímicas y cuantificar por cromatografía de gases/espectrometría de masas los principales componentes de los aceites esenciales de *Luma chequen* y *Citrus maxima*, así como evaluar la actividad antioxidante de la mezcla de ambos aceites usando el método de inhibición del radical ácido 2,2'-azino-bis-3-etilbenzotiazolina-6-sulfónico (ABTS•+). El rendimiento de extracción fue de 0,82% y de 0,95% para *Luma chequen* y *Citrus maxima* respectivamente. El pH fue de 4,5 y 5,5; la densidad fue de 0,877 g/ml y 0,844 g/ml y el índice de refracción fue de 1,4688 y 1,4741 respectivamente. Ambos aceites esenciales presentan alto contenido de monoterpenos siendo el α-pineno (57,6%) el más abundante para *Luma chequen* y el limoneno (30,3%) para *Citrus maxima*. Respecto a la actividad antioxidante; la inhibición del radical ABTS•+ fue de 49,1% y 93,4% respectivamente, sin embargo, la mezcla constituida por 50% de aceite esencial de *Luma chequen* y 50% de aceite esencial de *Citrus maxima* presentó un porcentaje de inhibición de 102.8%, evidenciándose sinergismo.

Keywords: *Luma chequen, Citrus maxima*, antioxidante, monoterpenos, sinergismo

ABSTRACT

Essential oils are bioactive compounds used in areas such as medicine, pharmacy, cosmetics, and the food industry, and are used as preservatives due to their antioxidant properties. The aim of the present investigation was to extract, determine the physicochemical properties and quantify by gas chromatography/mass spectrometry the main components of the essential oils of *Luma chequen* and *Citrus maxima*, as well as to evaluate the antioxidant activity of the mixture of both oils using the 2,2'-azino-bis-3-ethylbenzothiazoline-6-sulphonic acid radical (ABTS•+) inhibition method. The extraction yield was 0.82% and 0.95% for *Luma chequen* and

Citrus maxima respectively. The pH was 4.5 and 5.5; specific gravity was 0.877 g/ml and 0.844 g/ml, and refractive index was 1.4688 and 1.4741 respectively. Both essential oils have a high content of monoterpenes, α-pinene (57.6%) is the most abundant for *Luma chequen* and limonene (30.3%) for *Citrus maxima*. Regarding the antioxidative activity, the inhibition of the ABTS•+ radical was 49.1% and 93.4% respectively, however, the mixture consisting of 50% essential oil of *Luma chequen* and 50% essential oil of *Citrus maxima* presented an inhibition percentage of 102.8%, showing synergism.

Keywords: *Luma chequen*, *Citrus maxima*, antioxidant, monoterpenes, synergism

INTRODUCCIÓN

En la actualidad existe un gran interés por el uso de componentes bioactivos provenientes de plantas como una alternativa al uso de compuestos químicos en diferentes áreas como la medicina, agronomía, perfumería y la industria alimentaria, lo que ha incrementado las investigaciones en este campo[1-3].

Los aceites esenciales (AE) se utilizan ampliamente como componentes de medicamentos, aditivos biológicamente activos y suplementos dietéticos, así como en aromaterapia, industria alimentaria y cosmética. Su uso está muy extendido debido a su olor agradable o picante[4].

Los AE son reconocidos por sus propiedades antioxidantes, y se emplean ampliamente como conservantes para proteger componentes susceptibles de oxidación y para otorgar determinadas características organolépticas deseables por los consumidores[5].

Los AE son compuestos aromáticos volátiles generados por el metabolismo secundario de las plantas. Cada AE está compuesto por varios componentes, principalmente terpenos y terpenoides, incluidos derivados oxigenados, como aldehídos, cetonas, alcoholes, éteres, ésteres y epóxidos[6]. También se sabe que algunos AE contienen átomos de nitrógeno, azufre o cloro en su estructura[7,8]. Además, los AE contienen dobles enlaces conjugados y grupos funcionales fenólicos. En los últimos años se han estudiado en profundidad sus importantes propiedades para la eliminación de radicales libres[9-11].

El pequeño tamaño de las moléculas de los AE les permite penetrar fácilmente las paredes celulares y afectar a diversos procesos bioquímicos. La actividad biológica de los aceites esenciales depende de su composición. El timol, el carvacrol y el eugenol son los antioxidantes más potentes contenidos en los AE[12-14].

Los efectos adversos producidos por varios conservantes sintéticos entre los que destacan el hidroxitolueno, el ácido etilendiaminotetraacetico disódico (EDTA disodico), el ácido cítrico y los polifosfatos incluyen dolor de cabeza, náuseas, debilidad, retraso mental, convulsiones, anorexia y efectos cancerígenos que han sido evidenciados en investigaciones previas[15,16], lo que hace evidente la necesidad de buscar alternativas naturales. La actividad antioxidante de los aceites esenciales cobra mayor relevancia en alimentos con alto contenido lipídico ya que son más susceptibles de sufrir oxidaciones[17].

Se conoce que los principales componentes antioxidantes de los AE son los compuestos fenólicos y los terpenos. Los compuestos fenólicos pueden ejercer su acción ya sea actuando como agentes quelantes de iones metálicos, favoreciendo la eliminación de radicales libres ya existentes y eliminando carbonilos provenientes de lípidos ya que estos podrían reaccionar con otras moléculas como proteínas, monosacáridos y otros[17].

Se han realizado diversos estudios sobre la actividad antioxidante de diferentes tipos de aceites esenciales, pero son escasos los estudios que evalúan el efecto antioxidante de la mezcla de 2 o más aceites esenciales provenientes de diferentes especies. Este efecto sinérgico entre aceites esenciales podría mejorar el efecto antioxidante por la complejidad de los componentes en cada uno de los aceites esenciales donde los componentes de uno pueden ayudar a potenciar los efectos del otro, permitiendo el uso de concentraciones mucho más bajas y efectivas, además esta interacción sinérgica puede reducir los efectos secundarios adversos, así como los efectos organolépticos negativos y, así mejorar la aceptación del producto por parte del consumidor[17,18].

Luma chequen (Arrayan) es una especie que pertenece al género Luma y a la familia Myrtaceae crece entre los 2 500 y 4 000 msnm en diferentes regiones del Perú, Bolivia y Chile y es capaz de adaptarse a zonas húmedas y suelos arenosos, su aceite esencial tiene propiedades antibacterianas, fungicidas, ansiolíticas y antioxidantes[19-21].

Citrus maxima (Pomelo) pertenece al género Citrus y familia Rutaceae, los cítricos de esta familia se encuentran entre los cultivos más comerciales de regiones de clima tropical y subtropical, la cáscara de los cítricos son una valiosa materia prima para la producción de aceites esenciales con amplios usos en la cosmética, agricultura, medicina y otros, los terpenoides presentes poseen actividades insecticidas, repelentes, ansiolíticas y antioxidantes[22,23].

En el presente estudio se propone evaluar el efecto antioxidante de la mezcla de los aceites esenciales de *Luma chequen* y *Citrus maxima*, como una alternativa al uso de antioxidantes sintéticos, aprovechando la eficacia a concentraciones mucho más bajas que si se evaluaran por separado, reduciendo efectos secundarios y tóxicos, disminuyendo las alteraciones organolépticas negativas y logrando estabilizar alimentos, cosméticos y productos farmacéuticos. Se conoce que las alternativas de origen natural como los aceites esenciales resultan más económicas, poseen amplia disponibilidad y mejor biodegradabilidad, pudiendo convertirse en una alternativa más inocua frente a las sustancias sintéticas[15,16].

MATERIALES Y MÉTODOS

Material vegetal

Las especies vegetales *Luma chequen* (Arrayan) y *Citrus maxima* (Pomelo) fueron recolectadas en la localidad de Huertawayq'o en la provincia de Calca, Cusco, Perú. La identificación taxonómica fue realizada por el botánico adscrito al Herbario Vargas CUZ en la Universidad Nacional de San Antonio Abad del Cusco.

Extracción de los aceites esenciales

La extracción de los aceites esenciales se realizó por separado en un destilador usando el método por arrastre de vapor de agua. En el caso de *Luma chequen* se usaron las hojas frescas y en *Citrus maxima* las cáscaras frescas. Los aceites obtenidos se secaron usando sulfato de sodio anhidro. Los aceites esenciales obtenidos fueron almacenados a una temperatura de 4 °C al abrigo de la luz usando frascos de color ámbar hasta su análisis y caracterización.

Características organolépticas y propiedades fisicoquímicas de los aceites esenciales

Las características organolépticas evaluadas de ambos aceites esenciales fueron olor, color, textura y sabor. Las propiedades fisicoquímicas evaluadas fueron densidad a 20°C, pH y el índice de refracción usando los métodos oficiales de la AOAC (2006)[24].

Cuantificación de los componentes químicos de los aceites esenciales

Los componentes químicos de cada uno de los aceites esenciales fueron determinados usando una columna Agilent HP-5 de 30 m x 0,32 mm x 0,25 µm en un cromatógrafo de gases (Agilent 7820 A) acoplado a un espectrómetro de masas (CG-EM). Las condiciones establecidas para el método fueron: Temperatura de la columna 50 °C durante el primer minuto incrementándose 3°C/min gradualmente hasta 200 °C. El flujo de helio fue de 1 mL/min. El volumen de inyección fue de 1µL. La detección se realizó a 220 °C. La inyección Split tuvo la proporción 50:1.

Sinergismo de la actividad antioxidante de las mezclas binarias de los aceites esenciales de *Luma chequen* y *Citrus maxima*

La actividad antioxidante se determinó mediante el método ABTS[25]. El catión radical ABTS•+ se preparó mediante la reacción de 7 mM de ABTS y 2,45 mM de persulfato de potasio, se incubó a 25°C en la oscuridad durante 16 horas. La solución de catión radical ABTS se diluyó con metanol al 80% (disuelto con agua pura) para obtener una absorbancia de 0,700 ± 0,005 a 734 nm ($A_{control}$). 3,9 ml de la solución anterior se añadió a 0,1 ml de la muestra problema (AE a diferentes concentraciones como se muestra en la Tabla 5) y se mezcló enérgicamente y se dejó en reposo por 6 minutos y la absorbancia a 734 nm ($A_{muestra}$) se registró inmediatamente en el espectrofotómetro UV-Vis Thermo Scientific Evolution™ 201/220. Como control positivo se usó Trolox. El porcentaje de inhibición fue calculado con la siguiente ecuación:

$$\% \, inhibición = \frac{Acontrol - Amuestra}{Acontrol} \, X \, 100$$

RESULTADOS Y DISCUSIÓN

Extracción del aceite esencial

El métoto utilizado para la extracción de los aceites esenciales fue la destilación por arrastre de vapor de agua. El resultado obtenido para cada una de las especies vegetales se muestran en la Tabla 1.

Fuente vegetal	Porcentaje de extracción
Luma chequen	0,82%
Citrus maxima	0,95%

Tabla 1: Porcentaje de rendimiento del aceite esencial de las hojas de *Luma chequen* y de las cáscaras de *Citrus maxima*.

Los resultados muestran porcentajes diferentes para las dos especies en estudio, en este punto es necesario tener en cuenta las diferencias en la taxonomía pues las plantas pertenecen a familias biológicas distintas, y por ello responden diferente al medio ambiente, biosintetizando metabolitos o grupos fitoquímicos diferentes tanto en proporciones como en componentes[26]. En el estudio desarrollado por Borja et al.[19] se reportó un porcentaje de extracción de 0,52% para la especie *Luma chequen*, porcentaje inferior al encontrado en el presente trabajo de investigación. Por otro lado, Visakh et al.[27], reportaron un porcentaje de extracción de 0,58% para las cáscaras de *Citrus maxima* usando el método de hidrodestilación, este porcentaje se encuentra por debajo del encontrado en nuestra investigación. Es importante destacar que la composición química y la cantidad de componentes de los aceites esenciales varía en función de la geografía, la genética, el origen botánico, los endofitos bacterianos y las técnicas de extracción[14].

Características organolépticas y propiedades fisicoquímicas de los aceites

La Tabla 2, muestra las características organolépticas y fisicoquímicas de los aceites esenciales de *Luma chequen* y *Citrus maxima*, debiendo resaltarse que los resultados están dentro de los parámetros establecidos para cada una de las especies en investigaciones previas.

Características organolépticas	***Luma chequen***	***Citrus maxima***
Color	Amarillo pálido	Amarillo pálido a incoloro
Olor	Herbáceo, alcanforado, amaderado, balsámico	Característico, citrico potente, dulce
Sabor	Menta fuerte alcanforado	Cítrico potente
Aspecto	oleoso	oleoso
Características fisicoquímicas		
pH	4,5	5,5
Densidad (20°)	0,877g/ml	0,844 g/ml
Índice de refracción (20°)	1,4688	1,4741

Tabla 2: Características organolépticas y propiedades fisicoquímicas del aceite esencial de *Luma chequen* y *Citrus maxima*.

Composición química de los aceites esenciales de Luma chequen y Citrus maxima

En la Tabla 3, se detallan los componentes mayoritarios del aceite esencial de las hojas de *Luma chequen*, destacando el α-pineno con un 57,6% como el principal componente, seguido del 1,8-cineol con un 9,4%, β-pineno con 5,6%, linalool con 3,8% y limoneno con 2,7%.

Pico	IR Calc	Componente	Estructura Química	Peso Molecular (g/mol)	Tipo	Porcentaje %
1	983	α-Tujeno	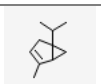	136,23	MH	1,4
2	990	**α-Pineno**	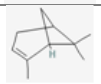	136,24	MH	**57,6**
3	1010	**β -Pineno**	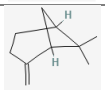	136,24	MH	**5,6**
4	1037	Isobutirato metil butilo	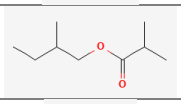	158,24	--	1,5
5	1042	**Limoneno**	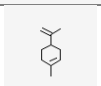	136,24	MH	**2,7**
6	1044	**1,8-Cineol**		154,25	MO	**9,4**
7	1064	Oxido de linalool	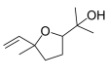	170,25	MO	0,7
8	1101	**Linalool**	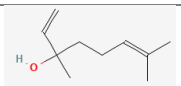	154,25	MO	**3,8**
9	1183	α -Terpineol	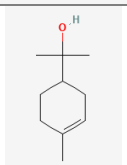	154.25	MO	1,9
10	1407	**β -Cariofileno**	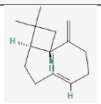	204,35	SH	**1,3**
11	1475	Germacreno d		204,35	SH	2,1
12	1485	**β-Selineno**	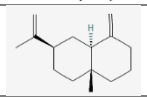	204,35	SH	2,5
		Otros				9,5

MH: Monoterpenos hidrocarbonados (67,3%); MO: Monoterpenos oxigenados (15,8%); SH: Sesquiterpenos hidrocarbonados (5,9%).

Tabla 3: Composición química del aceite esencial de las hojas de *Luma chequen*.

El análisis de CG-MS realizado por Borja et al.[19], reportó un 44% de α-pineno, seguido de un 9,4% de 1,8-Cineol, resultados similares a los hallados en la presente investigación, asimismo es interesante mencionar la presencia del sesquiterpeno β-Selineno en ambas investigaciones, siendo los porcentajes 4,7% y 2,5% respectivamente.

En cuanto a la proporción de monoterpenos en el trabajo de Borja et al[19]., se llegó a un 70,8%, siendo los componentes mayoritarios el α-pineno, 1,8-cineol, limoneno, β-pineno y linalol, los sesquiterpenos

constituyeron 18,1% destacando los selinenos: α-Selina, β-Selina y δ-Selinen en un 10,9%. En nuestro caso como se muestra en la Tabla 3, los monoterpenos llegan a un 83,1% (MH= 67,3% + MO=15,8%) mientras que los sesquiterpenos alcanzaron sólo 5,9%. Este último porcentaje de los sesquiterpenos es más parecido al encontrado por Gonçalves et al[28]. quienes reportaron 3,1% de sesquiterpenos en el aceite esencial de *Luma chequen*.

En la Figura 1, se aprecia el cromatograma en el que destacan los picos de los componentes identificados por cromatografía de gases – espectrometría de masas en el aceite esencial de *Luma chequen*.

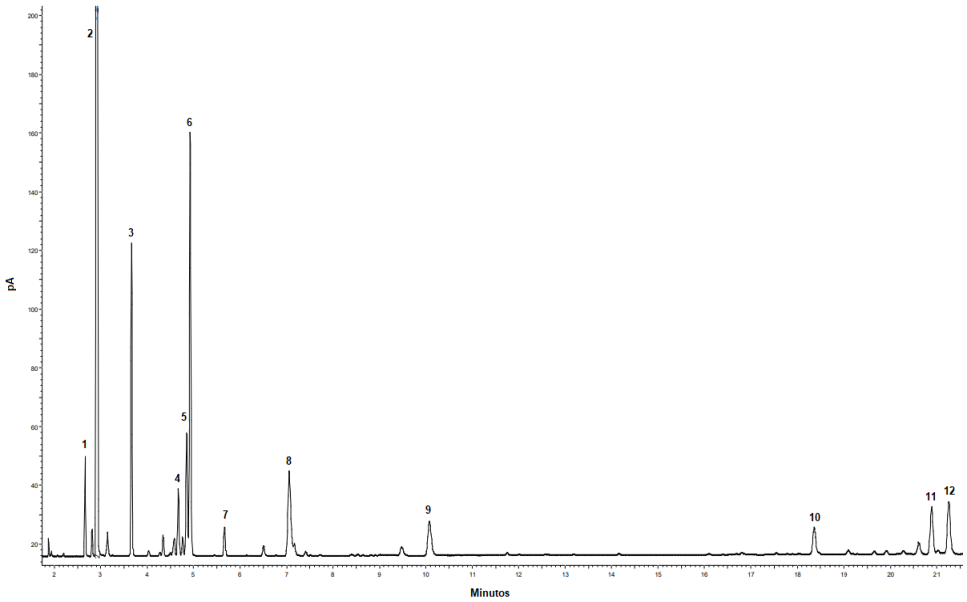

Figura 1: Cromatograma GC-MS de los componentes del aceite esencial de *Luma chequen*. (1) α-Tujeno; (2) α-Pineno; (3) β -Pineno; (4) Isobutirato metil butilo; (5) Limoneno; (6) 1,8-Cineol; (7) Oxido de linalool; (8) Linalool; (9) α -Terpineol; (10) β-Cariofileno; (11) Germacreno d; (12) β-Selineno

En la Tabla 4, se detallan los componentes mayoritarios del aceite esencial de las cáscaras de *Citrus maxima*, destacando el limoneno con 30,3% como el principal componente, seguido del β-pineno con 29,6,1%, E-β-ocimeno con 10,0%, citronelal con 3,3% y mirceno con 3,2%.

Pico	IR Calc	Compo-nente	Estructura Química	Peso Molecu-lar (g/mol)	Tipo	Por-centaje %
1	989	α-pineno		136,24	MH	1,7
2	1009	β-pineno		136,24	MH	**29,6**
3	1020	Mirceno	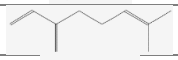	136,24	MH	3,2
4	1034	α-terpineno	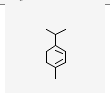	136,24	MH	1,1
5	1042	**Limoneno**	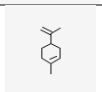	136,24	MH	**30,3**
6	1051	Z-β-ocimeno	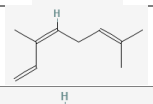	136,24	MH	0,5
7	1058	**E-β-ocimeno**	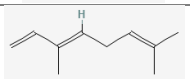	136,24	MH	**10,0**

8	1064	γ-Terpineno	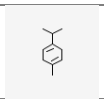	136,24	MH	2,0
9	1086	Terpinoleno	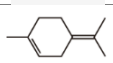	136,23	MH	**0,6**
10	1101	Linalool	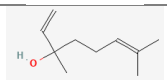	154,25	MO	**0,8**
11	1148	**Citronelal**	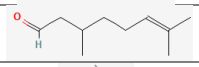	154,25	MO	**3,3**
12	1167	Terpinen-4-ol	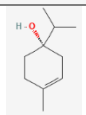	154,25	MO	1,7
13	1234	Neral	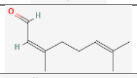	152,23	MO	0,5
14	1267	Geranial	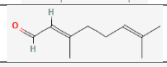	152,23	MO	0,6
15	1356	Acetato citronelila	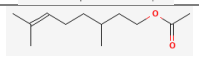	198,30	MO	0,7
16	1385	Eugenol	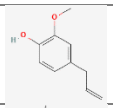	164,20	MO	2,4
17	1407	β-cariofileno	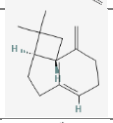	204,35	SH	2,7
18	1494	Aromadendreno	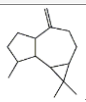	204,35	SH	1,7
19	1693	Farnesol		222,37	SO	0,9
20	2256	Nootkatona	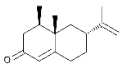	218,33	SO	0,1
		Otros				5,5

MH: Monoterpenos hidrocarbonados (79%); MO: Monoterpenos oxigenados (10%); SH: Sesquiterpenos hidrocarbonados (4,4%); SO: Sesquiterpenos oxigenados (1%).

Tabla 4: Composición química del aceite esencial de las cáscaras de *Citrus maxima.*

De acuerdo a los resultados evidenciados por Visakh et al.[27], los componentes predominantes en el aceite de *C. maxima* fueron limoneno (33,61%), β-sitosterol (17,99%), α-sitosterol (12,19%), estigmasterol (5,22%) y α-pineno (4,32%). En el estudio realizado por Hardjono et al[29], se obtuvo un contenido de limoneno de 90,43%, porcentaje elevado comparado con el obtenido en el presente trabajo de investigación, que a pesar de que también es el componente mayoritario sólo alcanzó un 30,3%. El limoneno es el principal componente de los aceites esenciales de las cáscaras de *Citrus sp*., se utiliza mucho como aditivo de sabor y fragancia en perfumes, bebidas, detergentes y jabones[30]. Últimamente se está estudiando el limoneno como un disolvente de la espuma de poliestireno porque se ha demostrado que puede ser utilizado como agente destructor de los residuos de espuma de poliestireno procedentes de los envases de alimentos, electrónicos, planchas de espuma de vidrio y vasos, siendo importante destacar que es un disolvente respetuoso con el medio ambiente[29].

En la Figura 2, se aprecia el cromatograma en el que destacan los picos de los componentes identificados por cromatografía de gases – espectrometría de masas en el aceite esencial de *Citrus maxima.*

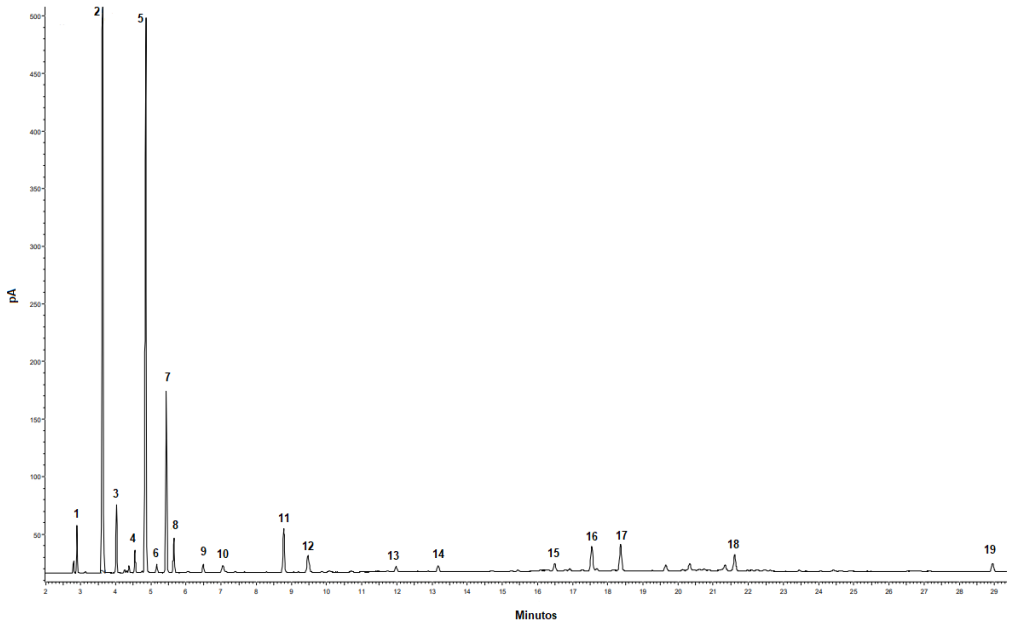

Figura 2: Cromatograma GC-MS de los componentes del aceite esencial de *Citrus maxima*. (1) α-pineno; (2) β-Pineno; (3) Mirceno; (4) α-terpineno; (5) Limoneno; (6) Z-β-ocimeno; (7) γ-Terpineno; (8) Terpinoleno; (9) Linalool; (10) Citronelal; (11) Terpinen-4-ol; (12) Neral; (13) Geranial; (14) Acetato citronelila; (15) Eugenol; (16) β-cariofileno; (17) Aromadendreno; (18) Farnesol; (19) Nootkatona.

La composición de los aceites esenciales producidos por las plantas se ve influida por muchos factores tales como la estacionalidad, la temperatura, luminosidad, agua y la disponibilidad de nutrientes, ataque de plagas, enfermedades y la genética[31]. La variación en la composición química de los aceites esenciales puede afectar a su actividad biológica[32].

Sinergismo de la actividad antioxidante de la mezcla binaria de los aceites esenciales de Luma chequen y Citrus maxima

El sinergismo de la actividad antioxidante fue evaluada usando el ensayo de ABTS, se realizaron las mezclas binarias de los aceites esenciales de *Luma chequen* y *Citrus maxima* en diferentes proporciones como se detalla en la Tabla 5. Los resultados del procentaje de inhibición del catión *ABTS*•+ se muestan en la siguiente Tabla:

Mezcla	*Luma chequen*	*Citrus maxima*	% de inhibición
1	0	100	93.4
2	6	94	98.9
3	13	87	96.9
4	25	75	101.9
5	50	50	102.8
6	75	25	99.2
7	87	13	97.8
8	94	6	100.3
9	100	0	49.1

Tabla 5: Porcentaje de inhibición del radical ABTS•+ de las mezclas binarias de los aceites de *Luma chequen* y *Citrus maxima*.

La Tabla 5 nos muestra los resultados obtenidos para el porcentaje de inhibición del radical ABTS•+ de los aceites esenciales de *L. chequen* y *C. maxima* por separado, destaca el aceite esencial de *Citrus maxima* que obtuvo un 93,4% de inhibición, en tanto que el aceite esencial de *Luma chequen* obtuvo solamente 49,1%, siendo casi la mitad de lo obtenido por *C. maxima*. Los resultados experimentales ponen de manifiesto que la mezcla 5 constituida por 50% de aceite esencial de *Luma chequen* y 50% de aceite esencial de *Citrus maxima*

que logró un porcentaje de inhibición de 102.8%. La mezcla 4 que contiene 25% de aceite esencial de *L. chequen* y 75% de aceite esencial de *C. maxima* logró un porcentaje de inhibición de 101.9% siendo la segunda mezcla con mejores resultados de inhibición. Estos resultados ponen de manifiesto que las mezclas en las que el aceite esencial de *C. maxima* se encuentra en mayor proporción tienen mejores resultados.

La investigación sobre las combinaciones de los aceites esenciales en diferentes porcentajes permite establecer información sobre la interacción de los componentes mayoritarios y minoritarios presentes. En nuestro estudio los componentes mayoritarios son el α-pineno y limoneno respectivamente. Las diferentes interacciones entre los componentes mayotritarios pueden dar lugar a los efectos sinérgicos[33] . La actividad resultante de estas combinaciones puede ser mayor/menor o igual que la observada para el aceite puro.

En estudios anteriores como el desarrollado por de Araujo et al[34] se ha demostrado que, en las mezclas binarias de aceites esenciales, la mayor actividad antioxidante exhibida por los aceites esenciales en comparación con sus simulaciones (constituidas únicamente por los compuestos mayores) evidencia que esta actividad no está relacionada únicamente con la presencia de los compuestos mayores, es decir, estaría relacionada con el sinergismo tanto de los componentes mayoritarios y minoritarios encontrados en los aceites esenciales.

Los aceites de cítricos han atraído la atención de los investigadores en los últimos años porque pueden obtenerse como principios activos a partir de subproductos de la industria del zumo. Los aceites de naranja o bergamota se extraen mediante hidrodestilación de las cáscaras tras la extracción del zumo, siendo una materia prima secundaria que puede utilizarse eficientemente en el contexto de la economía circular[35].

Actualmente el estudio de las mezclas de aceites esenciales (AE) ha despertado el interés de los investigadores en la búsqueda de nuevos antioxidantes naturales debido a la disponibilidad del recurso vegetal, la menor presencia de efectos secundarios o toxicidad, y la mejor biodegradabilidad en comparación con los conservantes sintéticos disponibles[36,37].

CONCLUSIONES

El uso de antioxidantes sintéticos ha dado lugar a carcinogenicidad, por lo que ha surgido el interés de sustituir estos productos químicos por aditivos naturales con capacidad antioxidante, como los aceites esenciales. La demanda por antioxidantes naturales ha aumentado debido a la preocupación por la salud y la tendencia a llevar un estilo de vida saludable. Por ello, los aceites esenciales que han demostrado tener componentes con buena actividad antioxidante se consideran una alternativa de interés científico debido a sus diversas aplicaciones.

En la presente investigación se obtuvo un porcentaje de rendimiento de 0,82% y 0,95% para el aceite de *Luma chequen* y *Citrus maxima* respectivamente. Dentro de las propiedades fisicoquímicas se determinó un pH de 4,5 y 5,5; una densidad de 0,877 g/ml y 0,844 g/ml, un índice de refracción de 1,4688 y 1,4741 para *Luma chequen* y *Citrus maxima* respectivamente. En la composición química del aceite de *Luma chequen* destacan los monoterpenos hidrocarbonados en un 67,3%, siendo el α-Pineno el más abundante (57,6%), seguido del 1,8-Cineol (9,4%), en el aceite de *Citrus maxima* destacan también los monoterpenos en un 79%, siendo limoneno el más abundante (30,3%) seguido del β-pineno (29,6%). Respecto a la actividad antioxidante; se obtuvo como resultado de inhibición del radical ABTS•+ para el aceite esencial de *Citrus maxima* un 93,4% de inhibición, mientras que para el aceite esencial de *Luma chequen* solamente un 49,1% de inhibición, en tanto que, los resultados experimentales mostraron que la mezcla constituida por un 50% de aceite esencial de *Luma chequen* y 50% de aceite esencial de *Citrus maxima* presentó el porcentaje de inhibición más alto con un 102.8%, demostrándose que existe un sinergismo.

Contribuciones de los autores: Conceptualización, C.D.C-J., M.U.O., A.Q.; metodología, C.D.C-J., R.G.G.C., C.T.C., A.Q. y M.U.O., redacción—preparación del borrador original, C.D.C-J., R.G.G.C., y M.U.O.; redacción—revisión y edición, C.D.C-J. y M.U.O Todos los autores han leído y aceptado la versión publicada del manuscrito.

Financiamiento: Este articulo ha sido financiado por los autores.

Conflictos de intereses: Los autores declaramos no tener ningún conflicto de intereses.

REFERENCIAS

1. Castro-Alayo, E.M.; Chávez, S.G.; Auquiñivin EA, Fernandez AB, Acha O, Rodríguez N… & Sepúlveda, D.R. Essential oils of native plants from Peru: Effect of the place of cultivation on the physicochemical characteristics and antioxidant activity. *Sci Agropecu*. **2019**,10(4):479-87. http://dx.doi.org/10.17268/sci.agropecu.2019.04.04
2. Van Haute, S.; Raes K.; Van der Meeren, P.; Sampers, I. The effect of cinnamon, oregano and thyme essential oils in marinade on the microbial shelf life of fish and meat products. *Food Control*. **2016**,68:30-9. https://doi.org/10.1016/j.foodcont.2016.03.025
3. Alarcon, A.I.; Mora, J.L.; Cabrera, D.O.; Garcia, F.S. Estudio Comparativo de la Composición Química, Fenoles Totales y Actividad Antioxidante de *Citrus sinensis*, *Citrus reticulata* y *Citrus maxima*. RECIA-MUC. **2022**,6(3):535-45. https://doi.org/10.26820/reciamuc/6.(3).julio.2022.535-545
4. Misharina, T.A. & Samusenko, A.L. Antioxidant properties of essential oils from lemon, grapefruit, coriander, clove, and their mixtures. *Applied Biochemistry and Microbiology*.**2008**, 44, 438-442. https://doi.org/10.1134/S0003683808040182
5. Crespo, Y.A.; Sánchez, L.R.B.; Quintana, Y.G.; Cabrera, A.S.T.; Del Sol, A.B.; Mayancha, D.M.G. Evaluation of the synergistic effects of antioxidant activity on mixtures of the essential oil from Apium graveolens L., Thymus vulgaris L. and Coriandrum sativum L. using simplex-lattice design. *Heliyon.* **2019**, 5(6), e01942. https://doi.org/10.1016/j.heliyon.2019.e01942
6. Bajpai, V.K.; Baek, K.H. Biological efficacy and application of essential oils in foods-A review. *Essent. Oil-Bear. Plants*. **2016**, 19, 1–19.
7. Bakkali, F.; Averbeck, S.; Averbeck, D.; Idaomar, M. Biological effects of essential oils – a review. *Food Chem. Toxicol*. **2008**,46, 446–475. https://doi.org/10.1080/0972060X.2014.935033
8. Nagella, P.; Ahmad, A.; Kim, S.J.; Chung, I.M. Chemical composition, antioxidant activity and larvicidal effects of essential oil from leaves of *Apium graveolens*. *Immunopharmacol. Immunotoxicol*. **2012**,34, 205–209. https://doi.org/10.3109/08923973.2011.592534
9. Aruoma, O.I. Free radicals, oxidative stress, and antioxidants in human health and disease. *J. Am. Oil Chem. Soc*. **1998**,75, 199–212. https://doi.org/10.1007/s11746-998-0032-9
10. Baj, T.; Baryluk, A.; Sieniawska, E. Application of mixture design for optimum antioxidant activity of mixtures of essential oils from *Ocimum basilicum* L., *Origanum majorana* L. and *Rosmarinus officinalis* L. *Ind. Crops Prod*. **2018**,115, 52–61. https://doi.org/10.1016/j.indcrop.2018.02.006
11. Kamatou, G.P.P.; Viljoen, A.M. A review of the application and pharmacological properties of α-bisabolol and α-bisabolol-rich oils. *J. Am. Oil Chem. Soc*. **2010**,87, 1–7. https://doi.org/10.1007/s11746-009-1483-3
12. Amerah, A.M.; Ouwehand, A.C. Use of essential oils in poultry production. In: Essential Oils in Food Preservation, Flavor and Safety. Victor R. Preedy; Elsevier:London, UK. **2016**,101–110. https://doi.org/10.1016/B978-0-12-416641-7.00010-9
13. Elgndi, M.A.; Filip, S.; Pavlić, B.; Vladić, J.; Stanojković, T;, Žižak, Ž.; Zeković, Z. Antioxidative and cytotoxic activity of essential oils and extracts of Satureja montana L., Coriandrum sativum L. and Ocimum basilicum L. obtained by supercritical fluid extraction. *The Journal of Supercritical Fluids*. **2017**,128, 128-137. https://doi.org/10.1016/j.supflu.2017.05.025
14. Firenzuoli, F.; Jaitak, V.; Horvath, G.; Bassolé, I.H.N.; Setzer, W.N.; Gori, L. Essential oils: new perspectives in human health and wellness. J. Evid Based Complement. Altern. Med. **2014,** 2014. https://doi.org/10.1155/2014/467363.
15. Basavegowda, N.; Baek, K.H. Synergistic Antioxidant and Antibacterial Advantages of Essential Oils for Food Packaging Applications. *Biomolecules*. **2021**;11(9):1267. https://doi.org/10.3390/biom11091267
16. Bag, A.; Chattopadhyay, R.R. Evaluation of Synergistic Antibacterial and Antioxidant Efficacy of Essential Oils of Spices and Herbs in Combination. Galdiero M, editor. PLOS ONE. **2015**,10(7): e0131321. https://doi.org/10.1371/journal.pone.0131321
17. Juncos, N.S.; Cravero, C.F.; Olmedo, R.H.; Grosso, N.R. El sinergismo de aceites esenciales como modelo para prevenir el deterioro oxidativo y microbiano de los alimentos. Nexo agropecuario CONICET, **2021**, 9(1).

18. Sharma, K.; Guleria, S.; Razdan, V.K.; Babu, V. Synergistic antioxidant and antimicrobial activities of essential oils of some selected medicinal plants in combination and with synthetic compounds. *Ind Crops Prod*. **2020,**154:112569. https://doi.org/10.1016/j.indcrop.2020.112569
19. Borja, M.E.; Jiménez, A.; Miranda, E.M.; Escobedo, F.A. Effect of drying on the extraction yield of *Luma chequen* (Molina) A. Gray essential oil. *Rev Mex Ing Quím*. **2022,**21(2): Proc2623-Proc2623.
20. Cadillo, K. Polifenoles, flavonoides y actividad antioxidante del extracto hidroalcohólico de las hojas de *Luma chequen* (Molina) A. Gray "Arrayan". Tesis para optar al título profesional. Facultad de Farmacia y Bioquímica.UNMSM. Lima Perú **2020**.
21. Alvarado, P.A.A.; Soto, M.R.; Rosales, L.E.; Jara, D.R.; Benites, S. Anxiolytic-like Effect of *Luma chequen* Essential Oil: A Pilot Study. *Pharmacogn J*. **2021,**13(6s):1607-13. http://dx.doi.org/10.5530/pj.2021.13.207
22. Dao, P.T.; Tran, N.Y.T.; Tran, Q.N.; Bach, G.L.; Lam, T.V. Kinetics of pilot-scale essential oil extraction from pomelo (*Citrus maxima*) peels: Comparison between linear and nonlinear models. *Alex Eng J*. **2022**,61(3):2564-72. https://doi.org/10.1016/j.aej.2021.07.002
23. Bhandari, D.P.; Poudel, D.K.; Satyal, P.; Khadayat, K.; Dhami, S.; Aryal, D.; Chaudhary, P.; Ghimire, A.; Parajuli, N. Volatile Compounds and Antioxidant and Antimicrobial Activities of Selected Citrus Essential Oils Originated from Nepal. *Molecules*. **2021**,26(21):6683. https://doi.org/10.3390/molecules26216683
24. AOAC. Official Methods of Analysis. 18th Edition. Gaithersburg, MD.: Association of Official Analytical Chemists; **2006**.
25. Re, R.; Pellegrini, N.; Proteggente, A.; Pannala, A.; Yang, M.; Rice-Evans, C. Antioxidant activity applying an improved ABTS radical cation decolorization assay. *Free radical biology and medicine*. **1999**,26(9-10), 1231-1237. https://doi.org/10.1016/S0891-5849(98)00315-3
26. Gros, E.; Pomilio, A.; Seldes, A.; Burton G. Introducción al estudio de los productos naturales. Monografía Nº 30. Secretaría General de la Organización de los Estados Americanos. Programa Regional de Desarrollo Científico y Tecnológico, Washington, D.C., EEUU. **1985**.
27. Visakh, N.U.; Pathrose, B.; Narayanankutty, A.; Alfarhan, A.; Ramesh, V. Utilization of Pomelo (*Citrus maxima*) Peel Waste into Bioactive Essential Oils: Chemical Composition and Insecticidal Properties. *Insects*. **2022**, 13, 480. https://doi.org/10.3390/ insects13050480
28. Gonçalves, M. J.; Cavaleiro, C.; da Cunha, A. P.; Salgueiro, L. R. Chemical Composition and Antimicrobial Activity of the Commercially Available Oil of *Luma chequen* (Molina) A. Gray. Journal of Essential Oil Research, **2006**, 18(1), 108–110. doi:10.1080/10412905.2006.9699402
29. Hardjono, H.; Dewi, E.N.; Lusiani, C.E.; Febriansyah, I.; Bachtiar, R.I. D-limonene from orange (*Citrus maxima*) peel extraction as destructive agent of styrofoam waste. In IOP Conference Series: Materials Science and Engineering. **2021**, 1073(1), 012013. DOI 10.1088/1757-899X/1073/1/012013
30. Erasto, P.; Viljoen, A.M. Limonene-a review: biosynthetic, ecological and pharmacological relevance. Natural Product Communications. **2008**, 3(7). http://dx.doi.org/10.1177/1934578X0800300728
31. Gobbo-Neto, L.; Lopes, N. P. Plantas medicinais: fatores de influência no conteúdo de metabólitos secundários. Química Nova. **2007**, 30(2), 374–381. doi:10.1590/s0100-40422007000200026
32. de Morais, L. A. S. (2009). Influência dos fatores abióticos na composição química dos óleos essenciais. Horticultura Brasileira. 2009, 27(2), S3299-S3302.
33. Katiki, L.M.; Barbieri, A.M.E.; Araujo, R.C.; Veríssimo, C.J.; Louvandini, H.; Ferreira, J.F.S. Synergistic interaction of ten essential oils against Haemonchus contortus in vitro. Veterinary Parasitology. **2017**, 243, 47-51. https://doi.org/10.1016/j.vetpar.2017.06.008
34. De Araújo Couto, H.G.S.; Blank, A.F.; de Oliveira e Silva, A.M.; de Lima Nogueira, P.C.; de Fátima Arrigoni-Blank, M.; de Castro Nizio, D.A.; de Oliveira Pinto, J.A. Essential oils of basil chemotypes: major compounds, binary mixtures, and antioxidant activity. Food Chemistry. **2019**, 293, 446-454. doi:10.1016/j.foodchem.2019.04.07
35. Alexa, V.T.; Szuhanek, C.; Cozma, A.; Galuscan, A.; Borcan, F.; Obistioiu, D.; Dehelean, C.A.; Jumanca, D. Natural Preparations Based on Orange, Bergamot and Clove Essential Oils and Their Chemical Compounds as Antimicrobial Agents. *Molecules* **2020**, 25, 5502. https://doi.org/10.3390/molecules25235502
36. Auddy, B.; Ferreira, M.; Blasina, F.; Lafon, L.; Arredondo, F.; Dajas, F.; Tripathi, P.C.; Seal, T.; Mukherjee, B. Screening of antioxidant activity of three Indian medicinal plants, traditionally used for the

management of neuro-degenerative diseases. *J. Ethnopharmacol*. **2003**, 84, 131–138. https://doi.org/10.1016/S0378-8741(02)00322-7
37. Cho, T.J.; Park, S.M.; Yu, H.; Seo, G.H.; Kim, H.W.; Kim, S.A.; Rhee, M.S. Recent Advances in the Application of Antibacterial Complexes Using Essential Oils. *Molecules*. **2020**, 25, 1752. https://doi.org/10.3390/molecules25071752

Received: October 9th 2023/ **Accepte**d: January 15th 2024 / **Published:**15 February 2024

Citation: del Carpio-Jiménez, R. C. Gutierrez-Chavez G., Quispe-Dávila H. A., Tomaylla-Cruz C. and Urrunaga-Ormachea M. J. Chemical composition and evaluation of the synergism of the antioxidant activity of blends of the essential oils of *Luma chequen* (Arrayan) and *Citrus maxima* (Grapefruit). on the Mortality of Two Nematodes in a Laboratory Setting. Revis Bionatura 2024; 9 (1) 63. http://dx.doi.org/10.21931/RB/2024.09.01.63

Additional information Correspondence should be addressed to mario.urrunaga@unsaac.edu.pe

Peer review information. Bionatura thanks anonymous reviewer(s) for their contribution to the peer review of this work using https://reviewerlocator.webofscience.com/

Bionatura ISSN. First 13909355 Ecuador. **Scopus coverage years**: from 2016 to the present

Bionatura
Ibero-American Journal of Biotechnology and Life Sciences

Article

Comparative Analysis of Threshold Cycle Results for RNA Extraction in SARS-CoV-2 RT-qPCR Using Magnetic Beads and Spin Column Methods

Fardiah Tilawati Sitanggang[1], *James Perdinan Simanjuntak*[2]*, *Nasrah Nasrah*[3], *Arvida Bar*[5] *Ridwansyah Ridwansyah*[4],

[1]*Department of Medical Laboratory Technology, Health Polytechnic of Ministry of Health Jambi, Jambi, Indonesia, fardiahtilawati@gmail.com,*
[2]*Department of Medical Laboratory Technology, Health Polytechnic of Ministry of Health Jambi, Jambi, Indonesia, jamesperdinansimanjuntak@gmail.com,*
[3]*Department of Medical Laboratory Technology, Health Polytechnic of Ministry of Health Jambi, Jambi, Indonesia, nasraz@gmail.com,*
[4]*Nursing Department, Health Polytechnic of Ministry of Health Jambi, Jambi, Indonesia, avrida.jambi@gmail.com,*
[5]*Department of Medical Laboratory Technology, Health Polytechnic of Ministry of Health Jambi, Jambi, Indonesia, ridwansyahxanda@yahoo.co.id,*
**Correspondence: jamesperdinansimanjuntak@gmail.com; Tel.: +62 853-6600-3099*
Available from. http://dx.doi.org/10.21931/RB/2024.09.01.64

ABSTRACT

Coronavirus Disease-2019 (COVID-19) belongs to the large family of SARS-CoV viruses, initially emerging in 2002-2003. In humans, this virus triggers respiratory infectious diseases. COVID-19, a new variant of SARS-CoV, was identified in humans following an unprecedented incident in Wuhan, China, in December 2019. This virus typically manifests mild symptoms, including a runny nose, sore throat, cough, and fever. The Nucleic Acid Amplification Test (NAAT), specifically the realtime Reverse Transcription Polymerase Chain Reaction (rRT-PCR) examination, is recommended by the World Health Organization (WHO) for diagnosing COVID-19. This study assessed potential differences in Threshold Cycle results during RNA extraction using magnetic beads compared to spin columns in the SARS-CoV-2 rRT-PCR method. The population for this study was selected through accidental sampling from nasopharyngeal and oropharyngeal swabs of COVID-19 patients obtained between December 2022 and April 2023, with Threshold Cycle values <30,000. The samples were stored at -80°C. The findings revealed that the average N (VIC) was 23.359, and RdRP (FAM) was 25.558 in the Magnetic Beads method, indicating a lower value compared to the average N (VIC) of 29.200 and RdRP (FAM) of 29.661 in the Spin Column method. This suggests that the Magnetic Beads method exhibited greater sensitivity than the Spin Column method. The statistical analysis confirmed these differences, with a P value of 0.003 in N (VIC) and the P value of 0.000 in RdRP (FAM). Consequently, it can be concluded that there is a significant 19.5% difference in the Threshold Cycle during RNA extraction using Magnetic Beads and Spin Column in the examination of the SARS-CoV-2 rRT-PCR method.

Keywords: Sars-CoV-2; rRT-PCR; Magnetic Beads; Spin Column; Threshold Cycle.

INTRODUCTION

Coronavirus Disease-2019 (COVID-19) is part of the large family of SARS-CoV viruses that initially emerged between 2002 and 2003. In humans, this virus leads to respiratory infectious diseases [1,2]. This virus causes mild symptoms such as a runny nose, sore throat, cough, and fever. About 80% of cases can be recovered without specialized treatment. Patients with comorbidities and the elderly are at a higher risk of developing severe, potentially fatal diseases [3].

The Nucleic Acid Amplification Test (NAAT), specifically the realtime Reverse Transcription Polymerase Chain Reaction (rRT-PCR) examination, is recommended by the World Health Organization (WHO) for diagnosing COVID-19. The PCR technique amplifies the genetic material of the virus, SARS-CoV-2, making it a susceptible, specific, and rapid method [4,5]. Before entering the PCR stage, specimen preparation is necessary, involving the extraction of nucleic acids from clinical specimens obtained from nasopharyngeal and oropharyngeal swabs [6,7].

The process of extracting DNA and RNA genetic material follows the principle of breaking cells and separating the genetic material within the cells—DNA and RNA—from other cellular components like fats, proteins, carbohydrates, and other substances. These additional components can affect the purity and integrity of the extracted genetic material. After extraction, storing the RNA base in the appropriate medium is essential to preserve its integrity and quality [8–11].

The spin column extraction method employs a silica membrane to capture DNA released from the cell. DNA-containing samples are introduced into a column containing silica gel or silica beads, along with chaotropic salts. These salts disrupt the hydrogen bonds between strands, facilitating DNA binding to silica by rendering the nucleic acid hydrophobic [12,13]. The DNA binds to the silica, while the remaining solution undergoes ethanol wash to remove chaotropic salts and other extraneous elements. One limitation of this approach is its relatively extended timeframe, spanning approximately 2 to 24 hours from the initiation of cell lysis to the completion of DNA extraction [14,15].

The Magnetic Beads method employs magnet-assisted separation in nucleic acid purification. It is based on the modified alkaline lysis principle, with subsequent binding of nucleic acids to magnetic particles [16–18]. A magnetic instrument captures nucleic acids bound to magnetic particles, and impurity contaminants are removed through a wash with the provided buffer. The nucleic acid is then eluted from the magnetic particles using a designated elution buffer. Despite its high effectiveness and efficiency, it may pose a challenge for small to medium-sized laboratories due to the associated costs of reagent kits and instruments [19–21].

RT-PCR serves as a technique for the amplification (multiplication) of viral nucleic acids. This amplification process is initiated by binding specific primers and probes to the target segment of the gene [22–24]. The polymerase enzyme facilitates the multiplication process. In rRT-PCR, the detection of amplification products can be directly observed, eliminating the need for post-amplification stages such as gel reading or electrophoresis [7,25,26].

In 2021, the number of COVID-19 cases continued to increase [by 27]. This surge in cases overwhelmed the UPTD Jambi City Regional Health Laboratory due to the substantial volume of samples, reaching up to 450 per day. Currently, the Spin Column and Magnetic Beads Extraction methods are employed to examine SARS-CoV-2 at the UPTD Jambi City Regional Health Laboratory. A laboratory assistant performs The Spin Column method manually, while the Magnetic Beads method is conducted using an Automated DNA and RNA Extraction System tool. However, it remains to be seen whether there is a difference in the extraction results between these two methods [16,28,29].

Cecilia Ambrosi et al. [30] research demonstrated that nasopharyngeal and oropharyngeal swab samples, when extracted using the Spin Column method with the Qiamp DSP Virus Spin kit, exhibited higher sensitivity and maintained RNA purity. Similarly, the research by Zhen Zhao et al. [31] indicated that extraction using the Magnetic Nano Particle method, whether done manually or with automatic machines, proved more time-efficient. This method eliminated the need for toxic reagents and allowed for manual or automated (robotic) execution, ensuring high purity and productivity.

The literature review findings indicate a scarcity of studies comparing the two methods. Notably, more research must be applied to both methods to examine the SARS-CoV-2 rRT-PCR method.

Based on the findings of several studies highlighting the advantages of each RNA extraction method, the author is interested in conducting a study to determine which RNA extraction method is more effective and efficient by comparing the Threshold Cycle results of the two extraction methods.

MATERIALS AND METHODS

Study design

The type of research used in this study is analytical experimental by comparing the results of 2 types of Sars-CoV-2 RNA extraction methods by looking at the Threshold Cycle results from reading the rRT-PCR tool. The research design employs a post-test-only control group design, a specific experimental design designed to assess and compare the effectiveness of two interventions [32].

Samples

This study was conducted from March to May 2023 at the Molecular Biology Laboratory of the UPTD Health Laboratory of Jambi City. Samples were collected from nasopharyngeal and oropharyngeal swabs of COVID-19 patients from December 2022 to April 2023, with a Threshold Cycle value < 30,000. The samples were stored in a refrigerator at -80°C. The study included a sample size of 30 individuals meeting the criteria of having Acute Respiratory Infection (ARI) and, in the 14 days preceding symptom onset, having been in contact with confirmed COVID-19 patients, selected through simple randomization.

Data collection

Data were obtained from the results of the Magnetic Beads Method and the Spin Column Method by analyzing the same 30 samples with 2 different extraction methods and continued with the reading of RNA Amplification on the rRT-PCR tool.

Variables

The dependent variable is the Threshold Cycle of RNA Extraction using the Spin Column Method, measured through the realtime PCR method with the rRT-PCR measuring instrument. The independent variable is the Threshold Cycle of RNA Extraction using the Magnetic Beads Column Method, measured through the realtime PCR method with the rRT-PCR measuring instrument.

Realtime Reverse Transcription Polymerase Chain Reaction (rRT-PCR) propagates DNA templates or Complementary DNA (cDNA) using the Taq Polymerase enzyme in vitro [6].

Manual Extraction Procedure (Spin Column Method)

First, dilute the Reagent Kit, prepare the Micro Tube, VNE Column, and Elution Tube and Label the microtube to avoid swapping samples. Vortex the sample until it is homogeneous. Pipette 560 ul VNE Buffer into the

Microtube, add 140 ul sample, then vortex until homogeneous, then Incubate for 10 minutes. Add 560 ul Absolute Ethanol, then vortex again; transfer into the spin column, then centrifuge for 10 seconds at 5000 X.g; prepare a vacuum Manifold, then attach the spin column to the vacuum manifold hole. Add wash buffer 1 as much as 500 ul, then suck until the liquid is wasted into the vacuum manifold, then add wash buffer 2 as much as 1000 ul, then suck until the liquid is wasted into the vacuum manifold, put it back into the Elution Tube. Centrifuge the spin column for 1 minute at 10,000 X.g to remove residual liquid. Discard the elution tube and replace it with the microtube. Add 50 ul of RNase - Freewater and incubate for 1 minute. Centrifuge again at 10,000 X.g for 1 minute. Finally, discard the spin column and store the Microtube that contains RNA, then hand it over to the clerk in the Template room.

Automated Extraction Procedure (Magnetic Beads Method)

Turn on the Automated DNA & RNA Extraction System tool. Before use, use UV first for 15 minutes. Prepare the Plate/Cartridge Extraction Kit and the Automated DNA and RNA Extraction System sample map. Homogenize the Cartridge Extraction Kit and sample using a Vortex Mixer. Add 200µ sample to each well in the 1st and 7th column series according to the sample map, and work inside the BSC. Open the glass front cover of the device. Place the plate/Cartridge in the device. Put the mixing sleeve in place. Select the desired type of examination, here selected for Sars-CoV-2 (Covid-19) examination, then press OK. After the extraction, open the Automated DNA & RNA Extraction System, then discard the Mixing Sleeve into the infectious waste container. Take the plate/cartridge and place it on the BSC. Pipette the extraction results in as much as 45µ in column 6 and column 12, and save the RNA into a microtube. Hand over the RNA to the clerk in the template room. Notes: The sample pipetting and extraction process is carried out in the biosafety cabinet

Buffer Mix Preparation Procedure (Master Mix Room)

Prepare the MasterMix Kit. Prepare plate, aluminum foil, tips, waste container, ice pack, and alcohol tissue. Put Pipette Universal Probes Reaction Mix as much as 10 ul into Microtube. Pipette Reverse Transcriptase as much as 0.2 ul into the microtube. Pipette RNase Inhibitor as much as 0.4 ul into the microtube. Pipette Primer-Probes Mix of 1.5 ul into the microtube. Pipette 2.9 ul of nuclease-free water into the microtube. Vortex the microtube until the reagents are homogeneous at 1700 RPM. Pipette 15 ul into each healthy plate (depending on the number of samples examined). Submit to the Template Note clerk: The above volume is for 1 sample, and the above process is done in Laminar flow.

Mixing Procedure of Buffer Mix and RNA (Template Chamber)

Prepare the extracted RNA. Vortex the microtube containing RNA. Pipette 5 ul of RNA into the well containing MasterMix reagent. Pipette positive control into column (12 H). Close the plate using Optical Seal, then hand it over to the PCR Application room clerk. Note: The above process is carried out in the BSC.

PCR Amplification Procedure

Turn on RT-PCR Quant Studio 5 and connect to the PC. Open the DA1 Application and input data from the MasterMix Reagent Kit into the application. Input target channels FAM (Helicase), HEX (RdRP), and Cy5 (RPP30) in the application for each well to be read. Insert the plate from the template room into the QuantStudio 5 RT-PCR tool and then run from the PC with the input data. After running is complete, open the DA2 application to read the results.

Statistical Data

Analysis of this research data to determine the comparison of CT Value results on RNA Extraction using Magnetic beads and Spin Column on Sars-CoV-2 Examination RT-PCR Method. Statistical unpaired T-tests were calculated using the SPSS version 16.0 application program. The unpaired t-test compares means between two independent groups, utilizing interval or ratio data scales.

RESULTS

The disparity in results between the Magnetic Beads method and the Spin Column method is depicted in Figure 1. Notably, the average Threshold Cycle values differ for each target, with 5.841 for target N (VIC) and 4.102 for target RdRP (FAM).

Figure

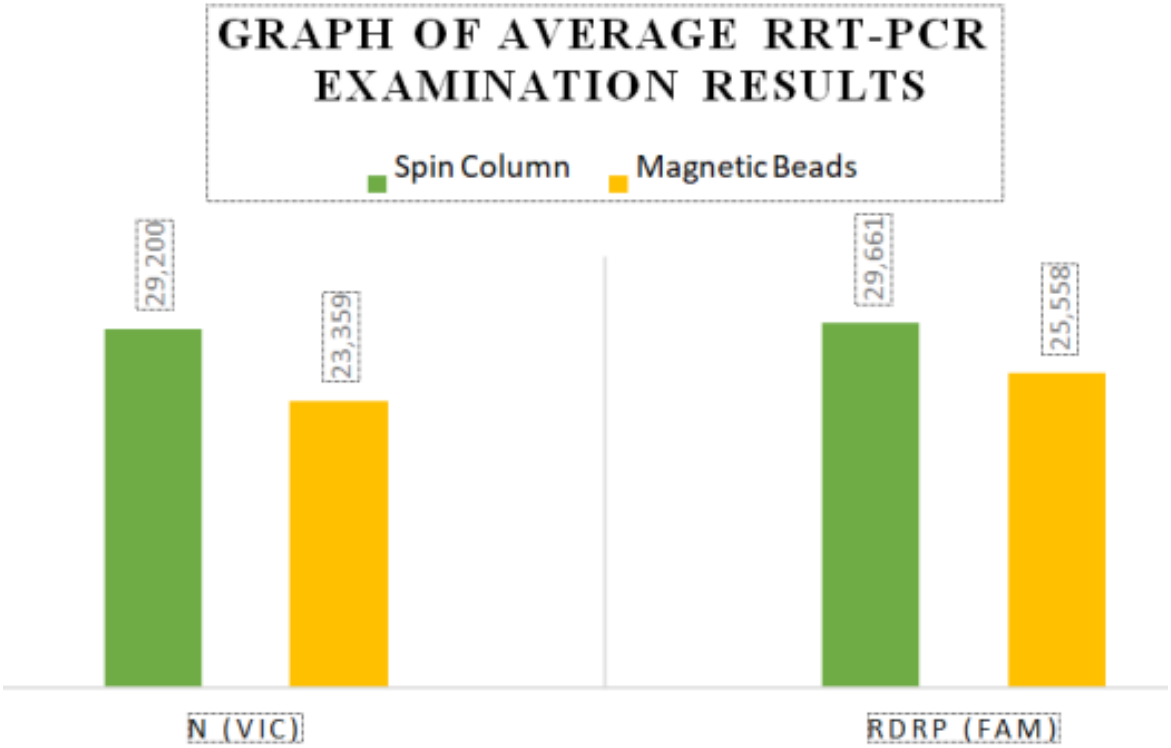

Figure 1. Average RRT-PCR examination results

Target	Method	Mean±SD	Min	Max	p
N (VIC)	Magnetic Beads	23.36±5.66	14,863	36,862	0.003
	Spin Column	29.20±6.19	14,613	36,465	
RdRP (FAM)	Magnetic Beads	25.59±5.59	16,473	37,215	0.000
	Spin Column	29.66±6.20	16,757	38,234	

Table 1: Threshold Cycle Differences in RNA Extraction using Magnetic Beads and Spin Column in the Examination of Sars-CoV-2 rRT-PCR Method.

Table 1 shows that the average N (VIC) 23.359 and RdRP (FAM) 25.558 in the Magnetic Beads method has a lower value than the average N (VIC) 29.200 and RdRP (FAM) 29.661 in the Spin Column method, which value indicates the Magnetic Beads method is more sensitive than the Spin Column method. The results of the paired t-test showed a p-value <0.05 in N (VIC) and RdRP (FAM), so it can be concluded that there is a

significant difference from the Threshold Cycle in RNA extraction using Magnetic Beads and Spin Column in the examination of Sars-CoV-2 rRT-PCR method.

DISCUSSION

This study involved 30 nasopharyngeal and oropharyngeal swab samples using Magnetic Beads and Spin Column in the examination of the rRT-PCR method for Sars-CoV-2 at the UPTD Regional Health Laboratory of Jambi City. The results of the Magnetic Beads and Spin Column extraction methods showed different Threshold Cycle values. The average Threshold Cycle for the Magnetic Beads method on the N (VIC) target was 23.359, and on the RdRP (FAM) target was 25.558, while the average Threshold Cycle for the Spin Column method on the N (VIC) target was 29.200, and on the RdRP (FAM) target was 29.660. According to the interpretation of the results using the Tianlong bufferMix Reagent kit used in this study, higher Threshold Cycle values indicate lower patient infection rates. Samples with Threshold Cycle values above 40,000 were declared as Negative.

Instruments such as micropipettes and rRT-PCR tools must be calibrated yearly [t]o ensure testing quality [33]. Based on the results of this study, the Magnetic Beads method is more efficient and effective, as it maintains RNA purity and minimizes contamination. This aligns with the findings of Zhen Z [31], which pointed out one of the drawbacks of column-based extraction: the difficulty in automation. In contrast, the Magnetic Nano Particle (MNP) method allows comprehensive nucleic acid purification, which is crucial for SARS-CoV-2 diagnosis. Overall, the improved Magnetic Beads-based extraction method exhibits high extraction efficiency and PCR amplification compatibility across various patterns, simplifying sample processing quickly and making it highly suitable for SARS-CoV-2 rRT-PCR testing.

Instruments such as micropipettes and rRT-PCR tools should undergo annual calibration to ensure the accuracy of testing[33]. The study's results conclude that the Magnetic Beads method is more efficient and effective, maintaining RNA purity while minimizing contamination. This finding aligns with the observations of Zhen Z [31], who highlighted a limitation of column-based extraction—precisely, the automation challenge. In contrast, the Magnetic Nano Particle (MNP) method enables comprehensive nucleic acid purification, crucial for SARS-CoV-2 diagnosis. Overall, the enhanced Magnetic Beads-based extraction method demonstrates high efficiency in extraction and compatibility with PCR amplification across various patterns. This simplification of sample processing makes it highly suitable for SARS-CoV-2 rRT-PCR testing.

According to research by Ni'mah D [34], the filter-based kit (FBK) was developed from the silica-gel approach, evolving into the silica membrane spin column method. However, a drawback of the silica membrane is its inability to effectively purify DNA in the presence of phenolic compounds and humic substances, which can bind to the membrane intended for DNA binding. Moreover, the potential for RNA contamination arises due to suboptimal RNAse handling. The Spin Column method entails numerous steps, such as replacing 4-6 microcentrifuge tubes, multiple stages of incubation, precipitation, elution, washing, and drying. This often requires specialized equipment and results in suboptimal purity. Additionally, the Spin Column method can be wasteful, necessitating changing microtubes and transferring supernatant to glass containers multiple times during extraction. In contrast, the Magnetic Beads method eliminates the need to change microtubes, contributing to its overall efficiency [17].

Sodium polyanethole sulfonate (SPS) is an anti-coagulant and an inhibitor in the PCR process. DNA, a polyanion molecule, can readily bind to the silica column. During the DNA extraction process, SPS binds to silica owing to the presence of chaotropic molecules, leading to the entrapment of both DNA and SPS in the silica column. Unfortunately, the centrifugation process proves ineffective in removing SPS from the column since the molecule is too large to pass through the membrane.

SPS, co-trapped with DNA on the column, hinders DNA escape during the elution step. SPS's large molecules effectively clog the silica membrane, impeding DNA release in the final extraction stage. Consequently, the DNA extraction results obtained through the spin column method lack DNA. Subsequent steps involving PCR and electrophoresis proved unsuccessful since the extraction results did not contain the necessary DNA.

CONCLUSIONS

The results of RNA extraction using the Magnetic Beads and Spin Column methods exhibit a notable disparity. Through statistical and average calculations, we have determined that the Magnetic Beads method is 19.5% more sensitive than the Spin Column method when extracting SARS-CoV-2 virus RNA.

Author Contributions: "Conceptualization, AV and JPS; methodology, software, validation, FTS and JPS; formal analysis, JPS; investigation, resources, data curation, NAS and RID; writing—original draft preparation, FTS; writing—review and editing, JPS.

Funding: This research received no external funding.

Institutional Review Board Statement: The study was conducted according to the guidelines of the Declaration of Helsinki and approved by the Health Research Ethics Commission, Polytechnic Health Ministry of Jambi, Indonesia, number: LB 02.06/2/531/2023

Informed Consent Statement: Patients who will undergo swabbing or potential respondents are provided with an explanation of informed consent by the researcher. The consent to participate as a respondent is conveyed by signing a statement expressing willingness.

Acknowledgments: The authors wish to extend their gratitude to the director of the Health Polytechnic, Ministry of Health, Jambi, Indonesia, for providing support during the execution of this research. Additionally, the authors would like to thank all those who contributed to this study, including the participants and the laboratory where the samples were examined.

Conflicts of Interest: The authors declare no conflict of interest.

REFERENCES

1. Hu B, Guo H, Zhou P, Shi Z-L. Characteristics of SARS-CoV-2 and COVID-19. Nature Reviews Microbiology. 2021;19(3):141–54.
2. Kumar S, Nyodu R, Maurya VK, Saxena SK. Host immune response and immunobiology of human SARS-CoV-2 infection. Coronavirus Disease 2019 (COVID-19) Epidemiology, Pathogenesis, Diagnosis, and Therapeutics. 2020;43–53.
3. WHO U, UNDP FAO. COVID-19 UPDATE. WHO Switzerland; 2022.
4. Zhang WS, Pan J, Li F, Zhu M, Xu M, and H et al. Reverse transcription recombinase polymerase amplification coupled with CRISPR-Cas12a for facile and highly sensitive colorimetric SARS-CoV-2 detection. Analytical chemistry. 2021;93(8):4126–33.
5. Li C, Debruyne DN, Spencer J, Kapoor V, Liu LY, Zhou B, et al. High sensitivity detection of coronavirus SARS-CoV-2 using multiplex PCR and a multiplex-PCR-based metagenomic method. BioRxiv. 2020;2020:988246.
6. Agustianingsih S, Reorita R, Renny R. Optimal control for SIR Model with The Influence of Vaccination, Quarantine and Immigration factor. Jurnal Matematika, Statistika dan Komputasi. 2020;16(3):311–24.

7. Agustianingsih DP, Shaw R. Community disaster resilience using multi-hazard assessment during Covid-19: The case of Denpasar, Indonesia. Natural Hazards Research. 2023;
8. Volpato F, Lima-Morales D, Wink PL, Willig J, de-Paris F, Ashton-Prolla P, et al. Pooling of samples to optimize SARS-CoV-2 diagnosis by RT-qPCR: comparative analysis of two protocols. European Journal of Clinical Microbiology & Infectious Diseases. 2021;40:889–92.
9. Alcoba-Florez J, González-Montelongo R, Íñigo-Campos A, de Artola DG-M, Gil-Campesino H, Team TMTS, et al. Fast SARS-CoV-2 detection by RT-qPCR in preheated nasopharyngeal swab samples. International Journal of Infectious Diseases. 2020;97:66–8.
10. Miller M, Jansen M, Bisignano A, Mahoney S, Wechsberg C, Albanese N, et al. Validation of a self-administrable, saliva-based RT-qPCR test detecting SARS-CoV-2. MedRxiv. 2020;2006–20.
11. Alcoba-Florez J, Gil-Campesino H, de Artola DG-M, Díez-Gil O, Valenzuela-Fernández A, González-Montelongo R, et al. Increasing SARS-CoV-2 RT-qPCR testing capacity by sample pooling. International Journal of Infectious Diseases. 2021;103:19–22.
12. Bruce EA, Huang M-L, Perchetti GA, Tighe S, Laaguiby P, Hoffman JJ, et al. Direct RT-qPCR detection of SARS-CoV-2 RNA from patient nasopharyngeal swabs without an RNA extraction step. PLoS Biology. 2020;18(10):e3000896.
13. Borghei Y-S, Samadikhah HR, Hosseinkhani S. Exploitation of N-gene of SARS-CoV-2 to develop a new rapid assay by ASOs@ AuNPs. Analytical Chemistry. 2022;94(39):13616–22.
14. Graham TGW, Dugast-Darzacq C, Dailey GM, Nguyenla XH, Van Dis E, Esbin MN, et al. Open-source RNA extraction and RT-qPCR methods for SARS-CoV-2 detection. PloS one. 2021;16(2):e0246647.
15. Hirotsu Y, Maejima M, Shibusawa M, Nagakubo Y, Hosaka K, Amemiya K, et al. Pooling RT-qPCR testing for SARS-CoV-2 in 1000 individuals of healthy and infection-suspected patients. Scientific reports. 2020;10(1):18899.
16. Klein S, Müller TG, Khalid D, Sonntag-Buck V, Heuser A-M, Glass B, et al. SARS-CoV-2 RNA extraction using magnetic beads for rapid large-scale testing by RT-qPCR and RT-LAMP. Viruses. 2020;12(8):863.
17. Babler KM, Amirali A, Sharkey ME, Williams SL, Boone MM, Cosculluela GA, et al. Comparison of electronegative filtration to magnetic bead-based concentration and V2G-qPCR to RT-qPCR for quantifying viral SARS-CoV-2 RNA from wastewater. ACS ES&T Water. 2022;2(11):2004–13.
18. Parra-Guardado AL, Sweeney CL, Hayes EK, Trueman BF, Huang Y, Jamieson RC, et al. Development of a rapid pre-concentration protocol and a magnetic beads-based RNA extraction method for SARS-CoV-2 detection in raw municipal wastewater. Environmental Science: Water Research & Technology. 2022;8(1):47–61.
19. Tohari TR, Anshori I, Baroroh U, Nugroho AE, Gumilar G, Kusumawardani S, et al. Development of a Single-Chain Variable Fragment of CR3022 for a Plasmonic-Based Biosensor Targeting the SARS-CoV-2 Spike Protein. Biosensors. 2022;12(12):1133.
20. Litanto V, Kim Y, Sungono V, Siswadi Y, Nugroho EH, Jo J. Assessment on COVID-19 Antibody and Antigen Rapid Test Devices as Screening Tools for SARS-CoV-2 Infection at the Academic Premises. GCISTEM Proceeding. 2022;1:152–9.
21. Koentjoro MP, Shamsudin SB, Bermawi B, Prayekti E, Prasetyo EN. RNA Internal Control (IC) for Routine Clinical Diagnostic Realtime Reverse Transcription-PCR SARS-CoV-2. In: First International Conference on Medical Technology (ICoMTech 2021). Atlantis Press; 2022. p. 86–92.

22. Sakai J, Tarumoto N, Orihara Y, Kawamura R, Kodana M, Matsuzaki N, et al. Evaluation of a high-speed but low-throughput RT-qPCR system for detection of SARS-CoV-2. Journal of Hospital Infection. 2020;105(4):615–8.
23. Kudo E, Israelow B, Vogels CBF, Lu P, Wyllie AL, Tokuyama M, et al. Detection of SARS-CoV-2 RNA by multiplex RT-qPCR. PLoS Biology. 2020;18(10):e3000867.
24. Minami K, Masutani R, Suzuki Y, Kubota M, Osaka N, Nakanishi T, et al. Evaluation of SARS-CoV-2 RNA quantification by RT-LAMP compared to RT-qPCR. Journal of Infection and Chemotherapy. 2021;27(7):1068–71.
25. Boni MF, Lemey P, Jiang X, Lam TT-Y, Perry BW, Castoe TA, et al. Evolutionary origins of the SARS-CoV-2 sarbecovirus lineage responsible for the COVID-19 pandemic. Nature microbiology. 2020;5(11):1408–17.
26. Pavan M, Bassani D, Sturlese M, Moro S. From the Wuhan-Hu-1 strain to the XD and XE variants: is targeting the SARS-CoV-2 spike protein still a pharmaceutically relevant option against COVID-19? Journal of Enzyme Inhibition and Medicinal Chemistry. 2022;37(1):1704–14.
27. Skevaki C, Karsonova A, Karaulov A, Xie M, Renz H. Asthma-associated risk for COVID-19 development. Journal of Allergy and Clinical Immunology. 2020;146(6):1295–301.
28. Li S, Han B, Zhou D, Gu Y, Li B, Ma J, et al. One-Stop Extraction and In Situ RT-qPCR for Ultrasensitive Detection of Highly Diluted SARS-CoV-2 in Large-Volume Samples from Aquatic Environments. Analytical Chemistry. 2023;95(4):2339–47.
29. Pérez-Cataluña A, Cuevas-Ferrando E, Randazzo W, Falco I, Allende A, Sanchez G. Comparing analytical methods to detect SARS-CoV-2 in wastewater. Science of the Total Environment. 2021;758:143870.
30. Ambrosi C, Prezioso C, Checconi P, Scribano D, Sarshar M, Capannari M, et al. SARS-CoV-2: Comparative analysis of different RNA extraction methods. Journal of virological methods. 2021;287:114008.
31. Zhao Z, Cui H, Song W, Ru X, Zhou W, Yu X. A simple magnetic nanoparticles-based viral RNA extraction method for efficient detection of SARS-CoV-2. BioRxiv. 2020;2002–20.
32. Arifin Z. Metodologi penelitian pendidikan. Vol. 1, Jurnal Al-Hikmah. 2020.
33. Gogoi S, Bora I, Debnath E, Sarkar S, Jais MB, Sharma A. Perplexity vs Clarity in choosing the right molecular diagnostic techniques for SARS-COV2 detection in Indian setup. Journal of Family Medicine and Primary Care. 2021;10(2):615.
34. Sinaga LP, Kartika D, Ni'mah N, Monalisa C. Stability and optimal control of the coronavirus (SARS-CoV-2) SEIR model in Indonesia. In: AIP Conference Proceedings. AIP Publishing; 2022.

Received: October 9th 2023/ **Accepte**d: January 15th 2024 / **Published:**15 February 2024

Citation: F. T. Sitanggang, Simanjuntak J. P., Nasrazuhdy, Ridwansyah, Bar A. Comparative Analysis of Threshold Cycle Results for RNA Extraction in SARS-CoV-2 RT-qPCR Using Magnetic Beads and Spin Column Methods. Revis Bionatura 2024; 9 (1) 64. http://dx.doi.org/10.21931/RB/2024.09.01.64

Additional information Correspondence should be addressed to jamesperdinansimanjuntak@gmail.com
Peer review information. Bionatura thanks anonymous reviewer(s) for their contribution to the peer review of this work using https://reviewerlocator.webofscience.com/

Bionatura ISSN. First 13909355 Ecuador. **Scopus coverage years**: from 2016 to the present

Bionatura
Ibero-American Journal of Biotechnology and Life Sciences

Article

Incidence of Vibrio parahaemolyticus *Coryphaena hippurus* (dorado fish) and *Thunnus alalunga* (albacore fish) sold in high-demand markets in Guayaquil City

Aura Hidalgo[1], Melissa León[1], Enrique Salazar Llorente[2], María Gabriela Maridueña- Zavala[3] and Juan Cevallos Cevallos[3,4]*

[1]Facultad de Ingeniería Mecánica y Ciencias de la Producción, Escuela Superior Politécnica del Litoral, Guayaquil, Ecuador.
[2]Facultad de Ciencias Agropecuarias, Universidad Técnica de Babahoyo, Km 7.5 Vía Babahoyo – Montalvo, Ecuador.
[3]Centro de Investigaciones Biotecnológicas del Ecuador, Escuela Superior Politécnica del Litoral, Guayaquil, Ecuador.
[4]Facultad Ciencias de la Vidas, Escuela Superior Politécnica del Litoral, Km 30.5 Vía Perimetral, P.O. Box 09-01-5863, Guayaquil, Ecuador
**Correspondence: adhidalg@espol.edu.ec*
Available from. http://dx.doi.org/10.21931/RB/2024.09.01.65

ABSTRACT

Foodborne diseases affect around 600 million people in the world. In Ecuador, the Ministry of Public Health (MSP) reported 12,203 cases of food poisoning caused mainly by Salmonella species, hepatitis virus or other pathogenic microorganisms in 2019. However, there are no reports of diseases caused by Vibrio species in Ecuador. The present study assessed the presence of V. parahaemolyticus, mesophilic aerobics, total coliforms and E. coli. Samples of *Coryphaena hippurus* (dorado fish) and *Thunnus alalunga* (albacore fish) in 3 different markets in the city of Guayaquil, Ecuador. As a result, Vibrio parahaemolyticus was not found in any of the 60 samples analyzed. In contrast, the E. coli levels met the requirements established in the INEN 183 - 2013 Standard norm. All samples from Market 1 were within the acceptance range regarding mesophilic aerobic levels. However, high mesophilic aerobic levels were obtained in 60% of the albacore samples and 50% of the dorado samples from this market. In the same way, 40% of the albacore and 100% of Dorado samples from market 3 were high in mesophilic microorganisms. However, the mesophilic aerobic analyses revealed safer levels in samples from market 1 than in markets 2 and 3, according to the NTE INEN. 183:2013.

Keywords: Foodborne diseases[1], fish[2], Albacore[3], E coli[4], mesophilic aerobics[5], Dorado[6].

INTRODUCTION

According to the WHO, one thousand five hundred million cases of diarrheal diseases are reported every year and three million children under the age of five die in the world due to the intake of contaminated food [1]. It is currently known that in products from the sea, the presence of the *Vibrio parahaemolyticus bacterium* has been identified worldwide as an essential cause of disease outbreaks and transmitted by food or ETAs [2]. This pathogen is the leading cause of gastroenteritis transmitted by seafood [3]. They have not had inadequate cooking or suffered contamination during preparation or non-compliance with the cold chain during transport that favors the proliferation7 of the bacteria [4]. *Vibrio parahaemolyticus* is a Gram-negative bacterium that is spread

through food and can cause mild illness with a medium-high probability of mortality in individuals with weak immune systems [5]. Different strains are known to cause cases of acute gastroenteritis in humans, with food-borne transmission being one of the most common forms. Seafood is considered one of the primary sources of these bacteria [6]. According to recent information, *Vibrio parahaemolyticus* is one of the most critical emerging pathogenic microorganisms in food and is currently a significant concern in the food industry [7].

In 1950, 20 people died, and 270 were hospitalized in Japan from eating contaminated sardines. Between 1973 and 2006, 45 outbreaks of ATS caused by seafood were recorded, with 1,393 cases and 24 hospitalizations in the United States [8]. Likewise, four outbreaks were reported by the European Food Safety Authority (EFSA) in 2015 in France. In two outbreaks, the consumption of crustaceans, mollusks and their products was suspected [9]. Because of the high number of hospitalized and deceased patients (20-30%), various regulatory agencies, such as the U.S. Food and Drug Administration (FDA), have adopted a zero-tolerance policy for the presence of L. monocytogenes in foods prepared for direct consumption (RTE) [10]. In addition, it has been possible to identify that inadequate post-capture handling of shellfish increases the risk of incorporation of other pathogenic microorganisms such as *Salmonella spp*, *Listeria monocytogenes*, *Aeromonas hydrophyla*, *Shigella ssp,* among others. Quantifying indicator microorganisms such as mesophilic aerobics, coliforms, and *E. coli* provides an idea of the level of post-harvest contamination of shellfish [11]. These categories are used as a precautionary measure before harvesting to detect when to limit harvesting and to decide whether post-harvest treatments are required [12]. An evaluation of three different commercialized fish species (boquichico, pomfret and catfish) in the port of Pucallpa, Ucayali, Peru, identified contamination in food by *E. coli* and *V. parahaemolyticus* [13]. The Escherichia coli tests were not compliant and are used to monitor how antimicrobial resistance and sensitivity trends evolve [14]. In this way, the importance of studies on the prevalence of pathogens in food is demonstrated as an initial step to determine the risks associated with their consumption.

Ecuador has a high demand for shellfish, which can bring gastrointestinal diseases when eaten raw or undercooked. Currently, no known pathogenic microorganisms in Ecuador are associated with *Coryphaena hippurus* (dorado) and *Thunnus alalunga (albacore)* fish, which are the most consumed nationwide. Recent investigations of the microbiological quality of 450 samples of foods in high demand in Guayaquil, Quito, and Cuenca, such as bolón, onion, sauces, ceviche, fruit, fruit juice, fruit salad, cheese, raw chicken, and ground beef. The country's popular street markets identified levels of total mesophilic aerobic, total coliform, fecal coliform, and bacteria such as *Escherichia coli, Salmonella enterica,* and *Listeria monocytogenes* in food. The result of the study was a high prevalence of *Salmonella, L. monocytogenes*, and various opportunistic pathogens, which indicates a risk of microbiological contamination of foods sold in mass markets [15 16]. However, the study did not contemplate a microbial evaluation of the fish sold in the markets. In foods such as fish, the high content of water and nutrients such as proteins, fats, vitamins and minerals, together with a pH close to neutral and warm temperatures, create an ideal environment for the rapid growth of bacteria [17]. The absence of this information prevents knowing the biological risks associated with shellfish consumption in Ecuador and makes it difficult to develop training strategies on post-harvest shellfish handling. Although microbiological tests are carried out to identify whether dangerous microorganisms are present in seafood products, they are not always carried out [18].

The purpose of this study was to determine the presence of *Vibrio parahaemolyticus* and safety indicator microorganisms in *Coryphaena hippurus* (dorado) and *Thunnus alalunga* (albacore) fish samples through traditional microbiological analysis (total mesophilic aerobes, total coliforms and *E. coli*) at to evaluate the risk of microbial contamination of these seafood products in three high-demand markets in the city of Guayaquil.

MATERIALS AND METHODS

Sample collection

Samples of each fish species were obtained from three crowded markets in Guayaquil (markets 1, 2 and 3). The sample size was estimated following the classification of "sampling plans with the type of concern and danger" according to the Codex Alimentarius [19], which indicates many samples (n) of 10 and a maximum number allowed for the presence of the pathogen. (c) from 0 [20]. Thus, 60 random samples were taken, divided into 10 albacore samples and 10 dorado samples for each market. The sampling was carried out during May and June 2021 using polyethylene bags. The temperature was obtained using an AMPROBE IR-712 12:1 digital thermometer when obtaining the samples. After this, the samples were placed in a cooler (polyurethane container) with ice and transported to the laboratory.

Microbiologic analysis

To quantify indicator microorganisms, 25 grams of each sample were taken aseptically, and 225 ml of phosphate buffer was added. Subsequently, serial dilutions were made before inoculation in PCA medium (Plate count Agar), and Petrifilm Total Coliforms/ *E. coli slides.* Subsequently, the Petri dishes and the petrifilm sheets were incubated for 48 hours at 35°C. All PCA and petrifilm colonies were enumerated, while gas-blue colonies on petrifilm were counted as *E. coli* [21]. To determine *V. parahaemolyticus,* the sample was homogenized, and a 25-gram aliquot was suspended in 225 ml of alkaline peptone water (APA). Subsequently, the suspension was incubated at 35 ± 2°C for 18 to 24 hours. After the incubation, seeding was carried out by spreading on TCBS agar (thiosulfate-citrate-bile salts-sucrose) followed by incubation at 35°± 2°C for 18 to 24 hours. After the mentioned time, typical *Vibrio colonies were searched for. parahaemolyticus*, considering the morphological characteristics such as turquoise green, shiny, smooth, and flattened strains with a green or blue center. After incubation, the oxidase test was performed to inoculate an aliquot of the previous culture with AP 0%, 3%, 6%, 8%, and 10% [22 23].

Statistical analysis

This study defined the counts of *V. parahaemolyticus,* mesophilic aerobics, total coliforms, and *E. coli* as the response or dependent variables. At the same time, the type of fish and market were considered independent variables. For the statistical analysis, the Minitab version 17 statistical software was used [24], with the two-way ANOVA statistical tool to measure the effect of the fish species, the market, and the species-market interaction on the response variables. For individual comparisons, Tukey's pairwise comparison test was applied [25]. Given the selected sample size, 95% confidence level and normality assumptions were used for the analyses.

RESULTS

Sample temperature

The fish samples showed bright eyes, shiny scales, red gills, firm meat, and a characteristic smell of the sea, indicating that the products were fresh and without signs of decomposition [26]. The temperatures recorded in degrees Celsius (°C) obtained during the sampling are those detailed in Table 1. A higher product storage temperature is observed, which varies between 6 to 7°C in Markets 2 and 3 and temperatures ranging from 1°C to 3°C for Market 1.

	Market: 1		**Market: 2**		**Market: 3**	
	Albacore	Golden	Albacore	Golden	Albacore	Golden
Sample 1	1.2°C	2.1°C	6.5°C	5.9°C	4.5°C	4.1°C
sample 2	2.1°C	1.5°C	7.2°C	5.2°C	4.1°C	7.9°C
sample 3	1.8°C	2.3°C	6.7°C	6.1°C	4.9°C	6.7°C
sample 4	2.3°C	1.8°C	6.8°C	5.5°C	5.8°C	5.6°C
sample 5	3.1°C	2.1°C	7.1°C	6.3°C	6.5°C	5.4°C
sample 6	1.8°C	1.7°C	5.8°C	6.8°C	5.2°C	4.6°C
sample 7	2.2°C	3.2°C	6.0°C	5.4°C	4.7°C	4.2°C
sample 8	1.1°C	2.5°C	5.9°C	5.7°C	5.8°C	6.5°C
sample 9	2.5°C	1.7°C	6.0°C	6.5°C	5.6°C	5.1°C
sample 10	2.2°C	2.1°C	5.7°C	5.7°C	4.5°C	5.6°C

Table 1: Temperatures of the fish samples were taken in the three different markets of the city of Guayaquil.

In this investigation, 60 samples of albacore and mahi-mahi fish were analyzed in order to identify the presence of microorganisms that cause illnesses due to food intake, such as total aerobic, total coliforms and Vibrio parahaemolyticus. Initially, regarding the temperatures of the samples, we observed that in market 1, they were the lowest at the time of sampling with an average of 2.06 °C, unlike markets 2 and 3, where their average temperatures were 6.14 and 5.37 °C, respectively. However, this factor did not influence the greater or lesser presence of microorganisms, especially in Vibrio, evidence that agrees with what has been reported in other studies where it was shown that temperature fluctuations during transportation and storage of shellfish may be less critical. for fish than for raw oysters, mainly because V. parahaemolyticus did not show significant growth in fish samples until after four hours at 25°C [27].

Microorganism count

Vibrio parahaemolyticus

Regarding the presence of the pathogen, the presence of *V. parahaemolyticus was detected in none of the samples analyzed*. These results were also observed in Peru in the port of Pucallpa, Ucayali, in which this pathogen was not detected in shellfish samples [28]. In the same way, other studies suggest that the flora of microorganisms present in fish samples can make it difficult to isolate the pathogen [29], so it is always recommended to update the isolation protocols [30]. Based on this and the data obtained, the research results suggest that the dorado and albacore species are not essential reservoirs of this pathogen, which has been confirmed using PCR techniques (Polymerase Chain Reaction) for the detection of Vibrio in samples of golden fish in Mercados de La Libertad, in which the absence of the pathogen for this type of fish was confirmed, corroborating the results of the investigation and suggesting that its appearance may be limited to species such as Jurel, Lisa [31]and Silverside like those found in Peru [32] or species like Picudo reported in Ecuador.

Aerobic mesophiles

^{6} CFU/g was counted and compared to the Albacore samples with 45 x 10 ^{4} CFU/g. In general, mahi-mahi samples had significantly higher mesophilic aerobic levels than albacore samples. Likewise, the amount of aerobes on average differed significantly between markets 1 (45 x 10 4 ^{CFU} /g) and markets 3 (45 x 10 5 ^{CFU} /g) and 2 (80 x 10 ^{4} CFU/g). In markets 1 and 2, it was observed that there are no significant differences in the levels of mesophilic aerobics, and it was observed that the lowest average levels of aerobics occur in market 1.

Figure 1 shows the means and standard error of mesophilic aerobics obtained by market and species.

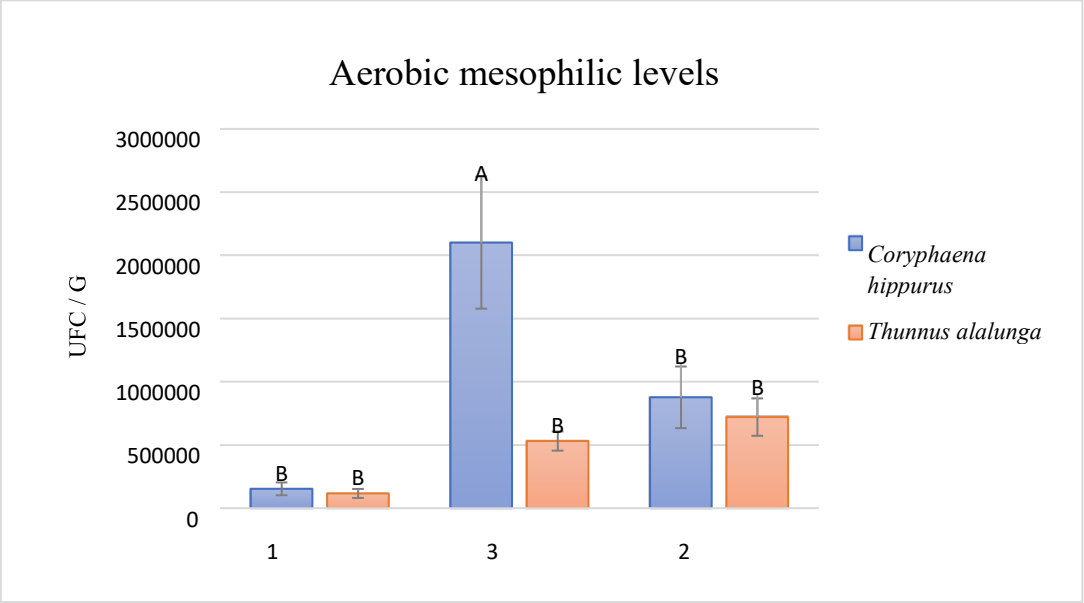

Figure 1: Values of aerobic mesophiles found in Coryphaena hippurus (dorado) and Thunnus alalunga (albacore) in three markets in Guayaquil. Different letters represent significant differences (p ≤ 0.05).

Tukey's comparison between the response variable, quantity of aerobics, and the interaction between the qualitative factors of species-market type showed that the levels of mesophilic aerobics in dorado fish from market 3 were significantly higher (21 x 10^5 CFU/g) than those found in the other samples analyzed. Likewise, the two-way ANOVA showed that the number of aerobes did not differ statistically between the interactions of Dorado-market 2, Albacora-market 2, Albacora-market 3, Dorado-market 1, and Albacora-market 1 (Table 2).

Species-Market	Amount	Mean (CFU/g)	Grouping
Gold - 3	10	2'100,500	TO
Gold - 2	10	877,000	B.
Albacore - 2	10	720,500	B.
Albacore - 3	10	531,000	B.
Gold - 1	10	152,820	B.
Albacore - 1	10	116,560	B.

Table 2: Mesophilic aerobes observed in the different species-market interactions. Different letters represent significant differences (p ≤ 0.05).

Total coliforms

With the results obtained, it can be seen that the amount of total coliforms on average differs significantly between market 2 (8.26 x 10^2 CFU/g) and markets 3 (2.4 x 10^3 CFU/g) and 1 (4 x 10^2 CFU/g). There were no significant differences in these last two markets. The highest average amount of total coliforms was observed in market 2. Figure 2 shows the averages and standard error of the total coliforms found in each sample.

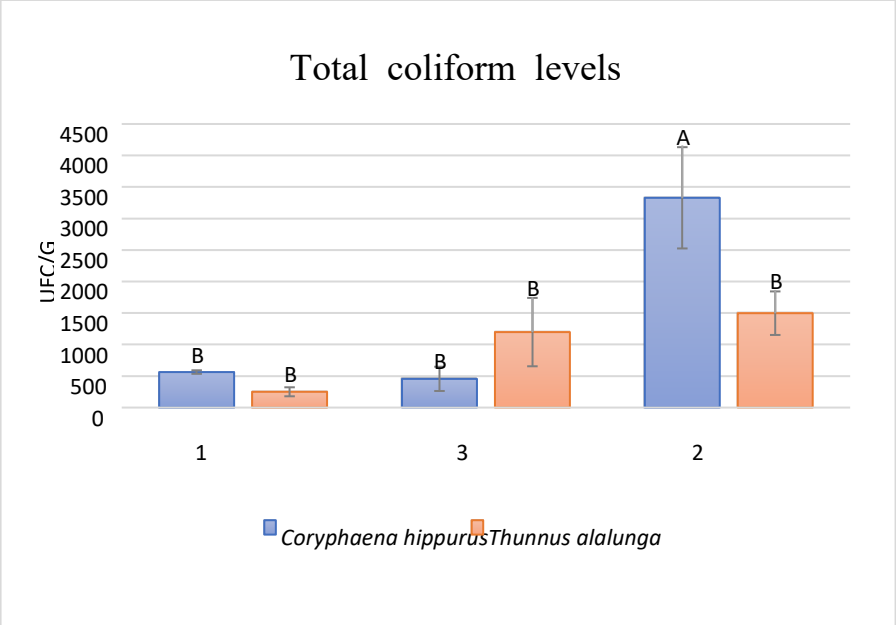

Figure 2: Values of total coliforms found in Coryphaena hippurus (dorado) and Thunnus alalunga (albacore) in three markets in Guayaquil. Different letters represent significant differences ($p \leq 0.05$).

Additionally, Tukey's pairwise comparison test was used to statistically determine which factor or factors have a significant effect on coliform levels. Applying ANOVA of two factors, it was determined that there are significant differences ($p \leq 0.05$) in the total coliforms of the market factor and the species-market interaction. For the factor corresponding to the species, no significant effect was found on total coliform levels.
Likewise, it was observed that the Dorado fish from Market 2 presented significantly higher levels of total coliforms than the other fish analyzed. Likewise, it can be concluded that the number of total coliforms did not differ statistically between the interaction of Albacora-market 2, Albacora-market 3, Dorado-market 1, Dorado-market 3, and Albacora-market 1, as shown in Table 3.

Species-Market	Amount	Mean (CFU/g)	Grouping
Gold -2	10	3,328.5	TO
Albacore- 2	10	1,497.5	B.
Albacore -3	10	1,197.5	B.
Gold -1	10	563.0	B.
Gold- 3	10	455.0	B.
Albacore- 1	10	250.0	B.

Table 3: In comparing the Tukey test of total coliforms between the species-market response variable in the evaluated markets of Guayaquil, different letters represent significant differences ($p \leq 0.05$).

E. coli

Figure 3 shows the averages and standard error of the E. coli levels found in each sample; a higher amount of CFU/g is observed in the Coryphaena samples—hippurus (golden).

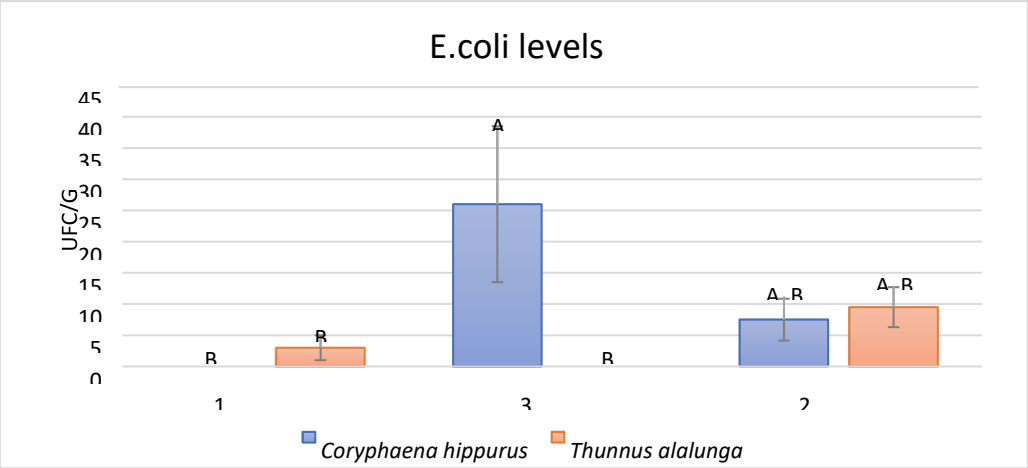

Figure 3: Values of Escherichia coli found in Coryphaena hippurus (dorado) and Thunnus alalunga (albacore) in three markets in Guayaquil. Different letters represent significant differences ($p \leq 0.05$).

Applying ANOVA of the general linear model with two factors, it was observed that only the interaction of the type of species and market showed a significant effect ($p \leq 0.05$) on the levels of E. coli.
The E. coli levels of the interaction of the type of Dorado species from Market 3 were significantly higher than the levels of this microorganism in all the fish species from Market 1. Likewise, it was observed that the levels of E coli in the fish of both species from market 2 did not differ significantly from those observed in the fish of both species from the other markets, as shown in Table 4.

Species-market	Amount	Mean (cfu/g)	Grouping
Gold – 3	10	26.0	TO
Albacore – 2	10	9.5	AB
Gold – 2	10	7.5	AB
Albacore – 1	10	3.0	B.
Gold – 1	10	0.0	B.
Albacore – 3	10	0.0	B.

Table 4: In comparing the E. Coli Tukey test between the species-market response variable in the evaluated markets of Guayaquil, different letters represent significant differences ($p \leq 0.05$).

DISCUSSION

In this investigation, the levels of aerobic mesophiles in gold-type fish from market 3 had an average count of 21.0×10^5 CFU/g, with a 95% confidence interval between 9.18×10^5 and 32.8×10^5 CFU/g. Therefore, according to the BAM 2001 reference method, they are outside the requirement established by the Ecuadorian Technical Standard NTE INEN 183:2013, which is between 5×10^5 and 10×10^5 CFU/g. These results are comparable with the study carried out in Peru in which the total aerobic samples were higher than those specified in the SANIPES (2016a) standard. Likewise, the values coincide with those reported [33] in samples of golden fish in a study in Mercado municipality of Cantón Chone for microbiological identification, reporting high levels of mesophilic aerobics [34]. The results suggest foods handled in poor conditions and not stored at the proper temperatures. Additionally, the levels of *E. coli* and coliforms were within what was allowed, according to the

reference method AOAC 21, 991 -14, in all the samples analyzed. These results suggest the absence of fecal contamination while handling the different fish species.

The samples of both species from market 1 had the lowest levels of aerobes. The average aerobic count was $13.0x10^{4}$ CFU/g, with a 95% confidence interval between $7.09x10^{4}$ CFU/g and $19.8x10^{4}$ CFU/g. Therefore, according to the BAM 2001 reference method, there are within the established norm for both species studied. In the case of total coliforms, the average of both species in market 1 was 40.6×10^{1} CFU/g, and the albacore species in this market had the lowest levels of coliforms, possibly due to better control of the supply chain—cold and high demand for this species.

CONCLUSIONS

The present study to detect *V. parahaemolyticus* in albacore and mahi-mahi fish species sold in three of the busiest markets in Guayaquil represents an essential step to knowing the state of food safety in the country. The results showed no presence of this bacterium in the samples analyzed, so these fish species would not be important reservoirs of the pathogen. Regarding the study of detection of indicator microorganisms, such as total aerobic, total coliform and *E. coli*, significant effects were observed between market factors and fish species.

For total aerobes, there was no significant difference between markets 1 and 2 for both fish species. The dorado species from market 3 presented a higher average amount of mesophilic aerobics than both species from the other markets. No significant differences were observed in the aerobic levels of the albacore species in all markets.

For total coliforms, it can be concluded that there were no significant differences in total coliform levels between the albacore and dorado species from markets 1 and 3. The Dorado species from Market 2 presented significantly higher coliform levels than the other markets. And species. No significant differences were observed in the coliform levels of the albacore species in all markets.

For *E. coli*, it can be concluded that the Dorado species from market 3 had a significantly higher amount of *E. coli* than the albacore species from the same market and that both species from market 1. No significant differences were observed in the levels of *E. coli* of the albacore species from all markets. No significant differences were observed when comparing the levels of *E. coli* between markets 3 and 2 or 1 and 2 in both species. Generally, the lowest levels of the microorganisms analyzed were observed in market 1 in both species.

REFERENCES

1. Soto Varela, Z., Pérez Lavalle, L. and Estrada Alvarado, D. (2016) 'Bacteria that cause foodborne diseases: a look at Colombia*, 'Salud Uni3* , 32(1), pp. 105–122
2. Scott, B. (2015) *Analysis of the Ecuadorian Fishing Sector after Dollarization*. San Francisco de Quito University.
3. Franco- Monsreal, J., Lara-Zaragoza, EB, Villa-Ruano, N., Mota-Magaña, L., Del, LE, Serralta-Peraza, S., Cuevas-Albarrán, V., Sosa-Castilla, F. and Monsreal, JF (2014) *Clinically essential species of the genus Vibrio in seafood of animal origin from establishments in Puerto Ángel, Oaxaca, Mexico*.
4. Soto Varela, Z., Pérez Lavalle, L. and Estrada Alvarado, D. (2016) 'Bacteria that cause foodborne diseases: a look at Colombia*, 'Salud Uni3* , 32(1), pp. 105–122
5. Ryser ET. Chapter 11 - Listeria. En: Morris JG, Vugia DJ, editores. Foodborne Infections and Intoxications (Fifth Edition) [Internet]. Academic Press; 2021 [citado 2 de abril de 2023]. p. 201-20. Disponible en: https://www.sciencedirect.com/science/article/pii/B9780128195192000281

6. Mashak Z, Banisharif F, Banisharif G, Reza Pourian M, Eskandari S, Seif A, et al. Prevalence of Listeria Species and Serotyping of Listeria monocytogenes Bacteria Isolated from Seafood Samples—Egyptian Journal of Veterinary Sciences. 1 de abril de 2021;52(1):1-9.
7. Bolívar A, Garrote Achou C, Tarlak F, Cantalejo MJ, Costa JCCP, Pérez-Rodríguez F. Modeling the Growth of Six Listeria monocytogenes Strains in Smoked Salmon Pâté. Foods. enero de 2023;12(6):1123.
8. Achipia. Risk Analysis Support Area (2017) *Vibrio parahaemolyticus* .
9. European Food Safety Authority (2016) *The European Union summary report on trends and sources of zoonoses, zoonotic agents and foodborne outbreaks in 2015* , *EFSA Journal* . John Wiley and Sons Inc. Available at: https://doi.org/10.2903/J.EFSA.2016.4634 .
10. Basha KA, Kumar NR, Das V, Reshmi K, Rao BM, Lalitha KV, et al. Prevalence, molecular characterization, genetic heterogeneity and antimicrobial resistance of Listeria monocytogenes associated with fish and fishery environment in Kerala, India. Letters in Applied Microbiology. 1 de octubre de 2019;69(4):286-93.
11. Alejandra González (2017) *Consuming raw fish and shellfish. Is it safe for health?* , *http://www.ideafoodsafetyinnovation.com/news/2017/09/index.html* .
12. Gyawali P, Fletcher GC, McCoubrey DJ, Hewitt J. Norovirus in shellfish: An overview of post-harvest treatments and their challenges. Food Control. 1 de mayo de 2019;99:171-9.
13. Rondón , JE, Ramos, DD, Vilca , ML, Salazar, ES, Mendoza, YQ and González, R. v. (2020) 'Sanitary characterization and identification of microbial contamination points in the fishing marketing chain in the port of Pucallpa, Ucayali, Peru', *Revista de Investigaciones Veterinarians of Peru* , 31(1). Available at: https://doi.org/10.15381/rivep.v31i1.17539 .
14. Hidalgo-Sindoni M. Seasonal trends and sampling time of day on overall microbial population and indicator organisms in catfish parts and catfish processing environment. Theses and Dissertations [Internet]. 9 de diciembre de 2022; Disponible en: https://scholarsjunction.msstate.edu/td/5651
15. Cevallos, JM, Ruales , J., Ortiz, J. and Maldonado, P. (2019) 'Advances in biosciences and food safety in Ecuador', pp. 1–127.
16. Salazar- Llorente , E., Morales, M., Sornoza , I., Mariduena-Zavala, MG, Gu, G., Nou , X., Ortiz, J., Maldonado-Alvarado, P. and Cevallos-Cevallos, JM (2021) 'Microbiological quality of high-demand food from three major cities in Ecuador ', *Journal of Food Protection* , 84(1), pp. 128–138. Available at: https://doi.org/10.4315/JFP-20-271 .
17. Cortés-Sánchez ADJ, Espinosa-Chaurand LD, Díaz-Ramirez M, Torres-Ochoa E. Plesiomonas: A Review on Food Safety, Fish-Borne Diseases, and Tilapia. Romalde JL, editor. The Scientific World Journal. 21 de septiembre de 2021;2021:1-10.
18. Spaur M, Davis BJK, Kivitz S, DePaola A, Bowers JC, Curriero FC, et al. A systematic review of post-harvest interventions for Vibrio parahaemolyticus in raw oysters. Science of The Total Environment. 25 de noviembre de 2020;745:140795
19. FAO. Revision of the code of practice for fish and fishery products (cxc 52-2003) and Revisions of the section on sampling, examination and analysis related to Histamine food safety [Internet]. Panama City, Panama: Codex Alimentarius Commission; 2018 nov p. 28. (Codex committee on food hygiene). Report No.: Agenda Item 6. Disponible en: https://www.fao.org/fao-who-codexalimentarius/sh-proxy/fr/?lnk=1&url=https%253A%252F%252Fworkspace.fao.org%252Fsites%252Fcodex%252FMeetings%252FCX-712-50%252FWD%252Ffh50_06_add1s.pdf
20. Ecuadorian Institute for Standardization (2014) *GENERAL GUIDELINES ON SAMPLING (CAC/GL 50-2004, IDT)* . quit.
21. Maturrin , L. and Peeler, JT (2001) *Laboratory Methods (Food)* . Available at: https://www.fda.gov/food/laboratory-methods-food/bam-chapter-3-aerobic-plate-count#conventional (Accessed: 22 January 2023).

22. Kaysner , CA, DePaola , A. and Jones, J. (2004) *Bacteriological Analytical Manual (BAM)* . Available at: https://www.fda.gov/food/laboratory-methods-food/bam-chapter-9-vibrio (Accessed: 22 January 2023).
23. Kaysner , CA, DePaola , A. and Jones, J. (2019) *Bacteriological Analytical Manual (BAM)* . FDA.
24. Arend , D.N. (2010) 'Minitab 17 Statistical Software'. State College .
25. Montgomery, DC (2003) *Design and analysis of experiments* . Limousa Wiley. World Health Organization (2001) *Joint FAO/WHO Expert Consultation on Risk Assessment Associated with Microbiological Hazards in Foods* .
26. Ecuadorian Institute for Standardization (2014) *GENERAL GUIDELINES ON SAMPLING (CAC/GL 50-2004, IDT)* . quit.
27. López Hernández, KM, Pardío Sedas, V. trinidad, Flores Primo, A., Martínez Herrera, D. and Uscanda Serrano, R. (2022) 'Estimation of the microbiological risk associated with the consumption of raw oysters contaminated with Vibrio cholerae and Vibrio parahaemolyticus ', *Journal of Biological and Health Sciences* , XXV(1), pp. 14–23. Available at: https://doi.org/10.18633/biotecnia.v25i1.1701 .
28. Rondón , JE, Ramos, DD, Vilca , ML, Salazar, ES, Mendoza, YQ and González, R. v. (2020) 'Sanitary characterization and identification of microbial contamination points in the fishing marketing chain in the port of Pucallpa, Ucayali, Peru', *Revista de Investigaciones Veterinarians of Peru* , 31(1). Available at: https://doi.org/10.15381/rivep.v31i1.17539
29. Váradi L, Lin Luo J, E. Hibbs D, D. Perry J, J. Anderson R, Orenga S, et al. Methods for the detection and identification of pathogenic bacteria: past, present, and future. Chem Soc Rev. 2017;46(16):4818-32.
30. Fernández Rendon, E., Nava Fernández, LM and Mota de la Garza, N. (1988) 'Absence of vibrio parahaemolyticus in raw fish / Abscence of vibrio parahemolyticus in raw fish ', *Rev. latinoam . microbiol* , 30(2)
31. Santistevan Magallán, AS (2020) *Identification of Vibrio parahaemolyticus by PCR in dry-salted fishery products sold in the municipal market of La Libertad canton* . Agrarian University of Ecuador.
32. Aliaga, R., Miranda, J. and Zevallos, J. (2010) 'Isolation and identification of Vibrioparahaemolyticus O3:K6 in fish and bivalve molluscs from a fish market in Lima , Peru.', *Rev mid Inherited* , 139.
33. Rondón , JE, Ramos, DD, Vilca , ML, Salazar, ES, Mendoza, YQ and González, R. v. (2020) 'Sanitary characterization and identification of microbial contamination points in the fishing marketing chain in the port of Pucallpa, Ucayali, Peru', *Revista de Investigaciones Veterinarians of Peru* , 31(1). Available at: https://doi.org/10.15381/rivep.v31i1.17539
34. Cedeño Mendoza, AL, Vargas Zambrano, PA, Talledo Solórzano, MV and Cuenca Nevárez, GJ (2021) 'The microbiological evaluation of fresh Albacore fish (Thunnus alalunga) in the Central Market of Cantón Chone', *Revista de las Agrociencias* , pp. 1–13.

Received: October 9th 2023/ **Accepte**d: January 15th 2024 / **Published:**15 February 2024

Citation: Hidalgo A., León M., Salazar-Llorente E., Maridueña- Zavala M. G. and Cevallos-Cevallos J. Incidence of Vibrio parahaemolyticus *Coryphaena hippurus (*dorado fish) and *Thunnus alalunga* (albacore fish) sold in high-demand markets in Guayaquil City. Revis Bionatura 2024; 9 (1) 65. http://dx.doi.org/10.21931/RB/2024.09.01.65

Additional information Correspondence should be addressed to adhidalg@espol.edu.ec

Peer review information. Bionatura thanks anonymous reviewer(s) for their contribution to the peer review of this work using https://reviewerlocator.webofscience.com/

Bionatura ISSN. First 13909355 Ecuador. **Scopus coverage years**: from 2016 to the present

Publisher's Note: Bionatura stays neutral concerning jurisdictional claims in published maps and institutional affiliations.

Bionatura
Ibero-American Journal of Biotechnology and Life Sciences

Article

Taxonomic interpretation of non-heterocystous Cyanobacteria (Oscillatoriales) from eastern India with particular emphasis on *Lyngbya Plectonema* complex

Sreemanti Banerjee[1], Akanksha Singh[2], Ruma Pal[3]*

[1]Department of Botany, Diamond Harbour Women's University, Diamond Harbour Road, Sarisha, South 24 Parganas, Pin- 743368.
[2]Department of Biotechnology, Indian Institute of Technology Kharagpur, Kharagpur-721302.
[3]Department of Botany, University of Calcutta, 35 Ballygunge Circular Road, Kolkata-700019.
**Corresponding author- sreemantibanerjee@gmail.com*
Available from. http://dx.doi.org/10.21931/RB/2024.09.01.66

ABSTRACT

Filamentous non-heterocystous cyanobacterial taxa from 8 genera were collected from different ecological niches like high altitudes, plains and estuaries of eastern India. The systematic accounts of 23 taxa were investigated with a polyphasic approach considering morpho taxonomy, cultural behavior, and molecular phylogenetic analysis with 16S and 16S-23S Internal Transcribed Spacer (ITS) regions as molecular markers. The collected taxa were from the families Oscillatoriaceae, Phormidiaceae and Pseudanabaenaceae with 8 representative genera viz. *Lyngbya*, *Plectonema*, *Oscillatoria*, *Limnothrix*, *Leptolyngbya*, *Planktothrix*, *Desertifilum* and *Phormidium*. The 16S-23S ITS region-based molecular characterization of 13 species from Oscillatoriaceae, 6 species from Phormidiaceae, and 4 species from Pseudanabaenaceae were found to be congruent with earlier phylogenetic studies using other markers. Phylogenetic tree analysis revealed habitat-specific clustering of ITS sequences of the investigated taxa. The 16S molecular marker-based phylogenetic analysis, along with cultural studies of *the Lyngbya-Plectonema* clade, highlighted the need for morphotaxonomic reconsideration of *Lyngbya birgei* and *Plectonema tomasinianum* related to the formation of false branching. The present study affirmed that 98% sequence similarity in the ITS region can be considered as a threshold percentage for conspecificity determination in the *Lyngbya* genus.

Keywords: Cyanobacteria; ITS; Oscillatoriaceae; Phormidiaceae; Phylogenetic tree; Pseudanabaenaceae.

INTRODUCTION

The filamentous cyanobacteria without heterocyst and akinetes are generally grouped together in the order Oscillatoriales [1]. This large group has simple trachomatous members with or without the sheath. Besides different morphological traits like sheath morphology, cell shape, size and cross-wall constriction, several other characteristics were considered from time to time for proper identification of cyanobacterial taxa like nucleoid structure [2–4], fimbriae [5], membrane system architecture [6], composition of cell wall external structure [7,8], consequences of cyanophage infection [9] and polyphosphate bodies [10–12]. Monumental taxonomic works have been done to classify the group according to their morphological perspectives [13,14]. Both non-heterocystous and heterocystous genera were classified under the same order, Nostocales, where non-heterocystous filamentous cyanobacteria were grouped into the family Oscillatoriaceae with a total of 15 genera and 250 species [14]. The genera *Lyngbya*, *Phormidium*, and *Oscillatoria* dominated the group, having 65, 45, and 76 species, respectively. Relying solely on morphological traits, few misidentifications at the generic level were detected in

classical taxonomy after the intervention of molecular methods along with ultrastructure of thylakoids and cultural behavior studies.[1] Based on this, a number of genera like *Lyngbya*, *Oscillatoria, Leptolyngbya,* and *Phormidium* were reconsidered and split into many new genera to reduce confusion. However, the genus *Oscillatoria* is still understudied compared to others [15]. For cyanobacteria, 16S rDNA, 16S-23S ITS region, phycocyanin gene, *if* D, *psb*A, *rbcL*X, and *rpo*C1 are considered the significant molecular markers used for the determination of phylogenetic relationship in taxonomically complex group [16–20]. Though 16S rDNA is widely used for oscillations, the reliability of 16S rDNA has been restricted to higher taxonomic groups and has not been proven efficient at the sub-generic level because of its conserved nature.[21] In that context, the intergenic spacer region between the 16S-23S region was investigated to study the variation at the species level. The heterogeneities were noticed mainly in the size, secondary structure, and, most importantly, insertion and deletion of tRNA genes in multiple operons [22]. ITS region was less utilized in population genetics and molecular systematic studies for these variations.

Phylogenetic relationships using intergenic spacer sequences can be resolved by targeting the same operon in different species with the help of operon-specific primers. The first sequencing of the intergenic spacer region of *Microcystis* sp. was done to resolve phylogenetic relationships at population level [23]. Boyer et al. (2001)[24] compared the variations in the ITS region for the first time in five heterocystous genera. The ITS region should always be handled accurately to avoid complications associated with multiple non-identical operons. However, problems may arise if sequence data is assigned to morphologically misidentified samples. The presence of several cryptic species in *Microcoleus* was reported by using 16S and ITS sequence data [22]. Instead of directly constructing a phylogenetic tree, secondary structures of the ITS region should also be used for better resolution at the molecular level. Due to a few earlier trials worldwide, no such threshold similarity percentage of the ITS region is fixed for concluding conspecificity in the order Oscillatoriales.

MATERIALS AND METHODS

Sample collection

Cyanobacterial samples were collected from 23 sites in Eastern India (Figure 1). The latitude and longitude of the collection sites are represented in Table 1. The sites were located in northern hilly areas, suburb areas, lateritic soil areas, hot spring habitats, riverine plains, and also from mangrove regions, i.e., intertidal areas. The collection areas included aquatic habitats, moist soils and tree barks.

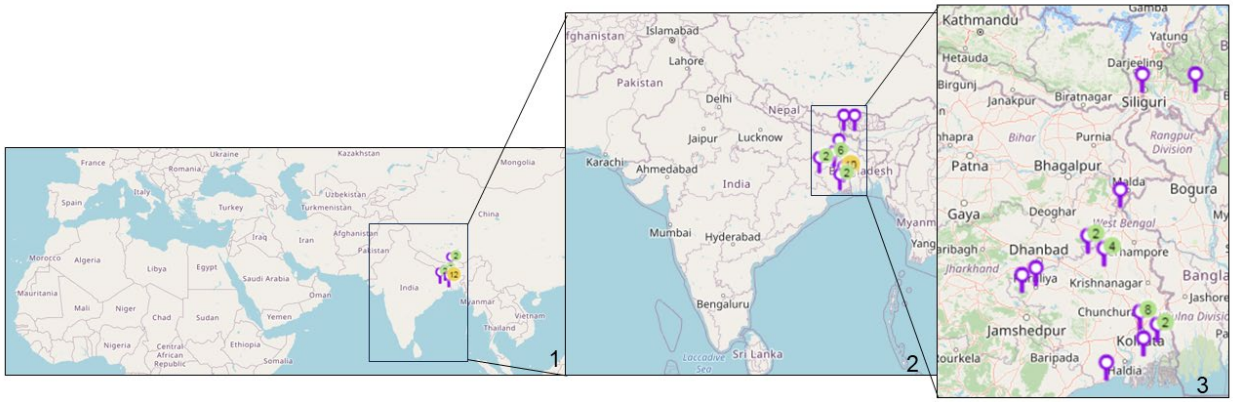

Figure 1: Map of sampling locations of Cyanobacteria in India. 1. Location sites are indicated. 2. Enlarged view of India showing the collection sites. 3. Enlarged view of eastern India showing the collection sites. (Map courtesy- Mapline, mapping software).

Immediate field vouchers were prepared at the sampling site using 4% formaldehyde in 25×50mm screw cap bottles (Tarson). The vouchers were deposited in the Calcutta University Herbarium for Algae (CUH/AL). The voucher numbers were assigned and are represented in Table 2. The remaining samples were cleaned thoroughly in double distilled water 2-3 times to remove debris from filaments. A portion of cleaned filaments was soaked in blotting paper, and approximately 100 mg of dried filaments were kept at -20ºC for molecular characterization purposes.

Site number	Names of collection sites	Latitude	Longitude
Site 1	Canning, South 24Parganas	22°19'58.62" N	88° 41' 12.624" E
Site 2	Canning, South 24Parganas	22° 19' 59.628" N	88° 41' 11.364" E
Site 3	Bakreswar, Birbhum	23° 52' 42.924" N	87° 22' 7.68" E
Site 4	Behala, Kolkata	22° 29' 21.912" N	88° 18' 55.908" E
Site 5	Dankuni, Howrah	22° 38' 5.532" N	88° 18' 8.748" E
Site 6	Dankuni, Howrah	22° 38' 11.364" N	88° 18' 18.792" E
Site 7	Kasba, Kolkata	22° 31' 19.38" N	88° 23' 18.96" E
Site 8	Saheb Bandh, Purulia	23° 19' 20.424" N	86° 22' 19.884" E
Site 9	Ballygunge, Kolkata	22° 31' 38.496" N	88° 21' 50.904" E
Site 10	Hasimara, Alipurduar	26° 40' 23.916" N	89° 24' 22.212" E
Site 11	Mahananda river, Siliguri	26° 39' 31.716" N	88° 24' 23.616" E
Site 12	Mahananda river, Maldah	24° 40' 45.48" N	87° 58' 3.18" E
Site 13	Hedua, Kolkata	22° 35' 14.82" N	88° 22' 7.608" E
Site 14	Dhakuria, Kolkata	22° 30' 43.38" N	88° 21' 35.784" E
Site 15	Bhubandanga, Birbhum	23° 40' 28.92" N	87° 41' 17.88" E
Site 16	Ajay River, Birbhm	23° 36' 55.764" N	87° 41' 47.292" E
Site 17	Kopai River, Birbhum	23° 41' 16.224" N	87° 38' 53.628" E
Site 18	Kopai River, Birbhum	23° 41' 19.968" N	87° 38' 53.844" E
Site 19	Baghmundi, Purulia	23° 11' 33.324" N	86° 6' 4.176" E
Site 20	Mathurapur, South 24Parganas	22° 5' 38.364" N	88° 25' 5.268" E
Site 21	Mandarmani, Purba Medinipur	21° 39' 49.5" N	87° 42' 21.996" E
Site 22	Bakreswar, Birbhum	23° 52' 47.46" N	87° 22' 2.712" E
Site 23	Duff Street, Kolkata	22° 35' 14.964" N	88° 22' 13.008" E

Table 1: Sample collection sites, along with their latitudes and longitudes.

Morphological characterization

The slides were prepared, and morphological details were studied using Carl Zeiss Axiostar microscope with 40X and 100X objective lenses. Photomicrographs were taken using Canon T2-T2 1, 6x SLR 426115. Morphological identifications were performed using Komarek and Anagnostidis (2005) and AlgaeBase [25].

Molecular characterization

The stored samples were subjected to genomic DNA extraction following phenol-chloroform extraction method [26]. Extracted DNA was stored in Tris-EDTA buffer at -20ºC. Partial 16S rDNA and 16S-23S ITS regions were amplified using suitable primers (Table 2) [27,28]. The amplifications were carried out in a thermal cycler machine (Biorad T100 PCR thermal cycler). The PCR cycle conditions were initial denaturation for 5 min at 94ºC, 35 cycles of 94ºC for 30 s, 45 s at 52ºC for ITS region and 58.5ºC for 16S rDNA region, 1 min

at 72ºC, and a final extension step for 10 min at 72ºC. The PCR products were visualized using a gel documentation system in 1% agarose gel (Vilber). The PCR products were subjected to purification and Sanger sequencing through a commercial sequencing service (Syngex India).

Phylogenetic analysis

To construct a phylogenetic tree, close relatives of the taxa were searched using the robust NCBI database using BLASTn queries (http://blast.ncbi.nlm.nih.gov). The collected sequences were visually inspected and then manually edited using BioEdit sequence alignment editor version 7.0.9.0 (Tom Hall, Ibis Biosciences, Carlsbad, USA). The sequences were submitted to NCBI, and accession numbers were assigned (Table 3, Table 4). The phylogenetic tree constructions were carried out in Molecular Evolutionary Genetics Analysis (MEGA) (version 7) [29]. The multi-sequence comparison by log expectation (MUSCLE) program aligned the sequences. The best evolutionary model for the used dataset was selected based on the lowest BIC value calculated. The tree was constructed by the maximum likelihood analysis (ML) using the model K2 + G and the neighbor-joining analysis (NJ) based on sequence differences with uniform rates in 1,000 bootstrap replications. The phylogenetic tree obtained was visualized using Tree Graph 2 [30].

The secondary structures of the 16S-23S internal transcribed spacer (ITS) were determined using Mfold version 2.3 with default parameters 31. According to Iteman et al. (2002) 32, different conserved and variable regions were identified.

Primer name	Sequence	References
ITSCYA236F	5′CTGGTTCRAGTCCAGGAT3′	27
ITSCYA225R	5′TGCAGTTKTCAAGGTTCT3′	27
CYA106F	5′CGG ACG GGT GAG TAA CGC GTG A3′	28
CYA781R	5′GAC TAC TGG GGT ATC TAA TCC CAT T3′	28

Table 2: Primers used for amplification and sequencing.

Cultural behavior studies

The selected samples were thoroughly cleaned in sterile double distilled water and cultured in BG11 medium ($NaNO_3$-1.5 g L^{-1}; $MgSO_4.7H_2O$-0.075 g L^{-1}; $CaCl_2.2H_2O$-0.036 g L^{-1}; Na_2CO_3 0.02 g L^{-1}; K_2HPO_4- 0.04 g L^{-1}) at 20°C under cool fluorescent lights at 20–30 µmol photons m^{-2} s^{-1} with 16:8 h light: dark. All the cultures were kept for 15 days, and morphology was studied after subsequent time intervals. Slides were prepared, and photomicrographs were taken under 40X and 100X objective lenses using the Carl Zeiss Axiostar microscope attached with Canon T2-T2 1, 6x SLR 426115.

RESULTS

Twenty-three samples were identified based on morphological characters and grouped under 8 genera, namely *Leptolyngbya*, *Planktothrix*, *Oscillatoria*, *Lyngbya*, *Phormidium*, *Limnothrix*, *Plectonema,* and *Desertifilum*. Among them, *Lyngbya* was found in rivers of the northern uphill and lateritic soil regions and the Gangetic plain associated with the coastal region. Genus *Oscillatoria* was collected from north hilly aquatic habitats and the areas surrounding populated cities, whereas *Plectonema* was recorded from the aquatic habitats of

lateritic soil areas. *Leptolyngbya* was found in the hot spring habitat and brackish mangrove region, whereas *Limnothrix* was detected only from the hot spring. Three genera like, *Planktothrix, Phormidium,* and *Desertifilum,* were solely found in suburban areas (Table 3). Photomicrographs of collected samples are represented in Figure 4-16 and 17-28. A total of 11 species were identified namely *Leptolyngbya valderiana* (Gomont) Anagnostidis et Komarek, *Limnothrix vacuolifera* (Skuja) Komárek ex G.McGregor, *Planktothrix pseudagardhii* Suda, *Phormidium autumnale* [Agardh] Trevisan ex Gomont, *Phormidium formosum* (Bory ex Gomont) Anagnostidis and Komárek, *Lyngbya birgei* G.M. Smith, *Lyngbya aestuarii* Liebman ex Gomont, *Lyngbya semiplena* J.Agardh ex Gomont, *Plectonema tomasinianum* Bornet ex Gomont, *Oscillatoria princeps* Vaucher ex Gomont and *Oscillatoria sancta* Kutzing ex Gomont. Taxonomic descriptions are provided in supplementary material.

Specimen (as deposited in NCBI GenBank)	Specimen (Morphologically)	Voucher Numbers	Habitat	GenBank Accession numbers
Leptolyngbya sp. RPL2	*L. valderiana*	CUH/AL/MW/CYANO-174	Mangrove (Brackish water)	MN640091
Leptolyngbya sp. RPL1	*L. valderiana*	CUH/AL/MW/CYANO-172	Mangrove (Brackish Water)	MN640090
Leptolyngbya sp. BKR	*Leptolyngbya* sp.	CUH/AL/FW/CYANO-103	Hotspring	MW238348
Limnothrix sp. BKR	*Limnothrix vacuolifera*	CUH/AL/FW/CYANO-104	Hotspring	MW393862
Planktothrix sp. DNK	*P. pseudagardhii*	CUH/AL/FW/CYANO-98	Suburb areas	MW238345
Planktothrix sp. DNK2	*P. pseudagardhii*	CUH/AL/FW/CYANO-96	Suburb areas	MW366802
Planktothrix sp. S41	*Planktothrix* sp.	CUH/AL/FW/CYANO-270	Suburb areas	MW393863
Phormidium sp. AKS1	*P. formosum*	CUH/AL/FW/CYANO-248	Suburb areas	MN817999
Desertifilum sp. RPL	*Desertifilum* sp.	CUH/AL/FW/CYANO-260	Suburb areas	MW366801
Phormidium sp. RPL	*P. autumnale*	CUH/AL/FW/CYANO-94	Suburb areas	MW238346
Plectonema sp. KAS	*P. tomasinianum*	CUH/AL/FW/CYANO-138	River (Lateritic soil area)	MN814325
Plectonema sp. KOP	*P. tomasinianum*	CUH/AL/FW/CYANO-121	River (Lateritic soil area)	MN814326
Plectonema sp. AJY	*P. tomasinianum*	CUH/AL/FW/CYANO-127	River (Lateritic soil area)	MN814324
Lyngbya sp. NB	*L. birgei*	CUH/AL/FW/CYANO-74	River (Northern Hilly area)	MT258376
Lyngbya sp. MHN	*L. birgei*	CUH/AL/FW/CYANO-161	River	MN818000
Lyngbya sp. SUND	*L. aestuarii*	CUH/AL/MW/CYANO-136	Mangrove (Brackish water)	MN817998
Lyngbya sp. MANI	*L. semiplena*	CUH/AL/MW/CYANO-246	Coastal region	MN630163
Lyngbya sp. RAB	*L. birgei*	CUH/AL/FW/CYANO-134	Freshwater	MN638845
Lyngbya sp. PRLA	*L. birgei*	CUH/AL/FW/CYANO-124	River (Lateritic soil area)	MK224842
Lyngbya sp. HDA	*L. birgei*	CUH/AL/FW/CYANO-120	Freshwater Pond	MN817997
Lyngbya sp. SHNTN	*L. birgei*	CUH/AL/FW/CYANO-111	River (Lateritic soil area)	MN630164
Oscillatoria sp. MND	*O. princeps*	CUH/AL/FW/CYANO-72	River (Northern Hilly area)	MW238347
Oscillatoria sp.	*O. Sancta*	CUH/AL/FW/CYANO-89	Suburb areas	MN630162

Table 3: List of specimens with their voucher numbers and GenBank accession numbers of 16S-23S ITS sequences.

Specimen (as deposited in NCBI GenBank)	Specimen (Morphologically)	Voucher Numbers	Habitat	GenBank Accession numbers
Plectonema sp. KAS	*P. tomasinianum*	CUH/AL/FW/CYANO-138	River (Lateritic soil area)	MT192753
Plectonema sp. KPY	*P. tomasinianum*	CUH/AL/FW/CYANO-121	River (Lateritic soil area)	MT192750
Plectonema sp. AJY	*P. tomasinianum*	CUH/AL/FW/CYANO-127	River (Lateritic soil area)	MT192748
Lyngbya sp. NB	*L. birgei*	CUH/AL/FW/CYANO-74	River (Northern Hilly area)	MT192720
Lyngbya sp. MHN	*L. birgei*	CUH/AL/FW/CYANO-161	River	MT192718
Lyngbya sp. RAB	*L. birgei*	CUH/AL/FW/CYANO-134	Freshwater	MT254899
Lyngbya sp. PRLA	*L. birgei*	CUH/AL/FW/CYANO-124	River (Lateritic soil area)	MT254898
Lyngbya sp. HDA	*L. birgei*	CUH/AL/FW/CYANO-120	Freshwater pond	MT254994
Lyngbya sp. SHNTN	*L. birgei*	CUH/AL/FW/CYANO-111	River (Lateritic soil area)	MW362745

Table 4: List of freshwater *Lyngbya* and *Plectonema* samples with their voucher numbers and GenBank accession numbers of 16S sequences

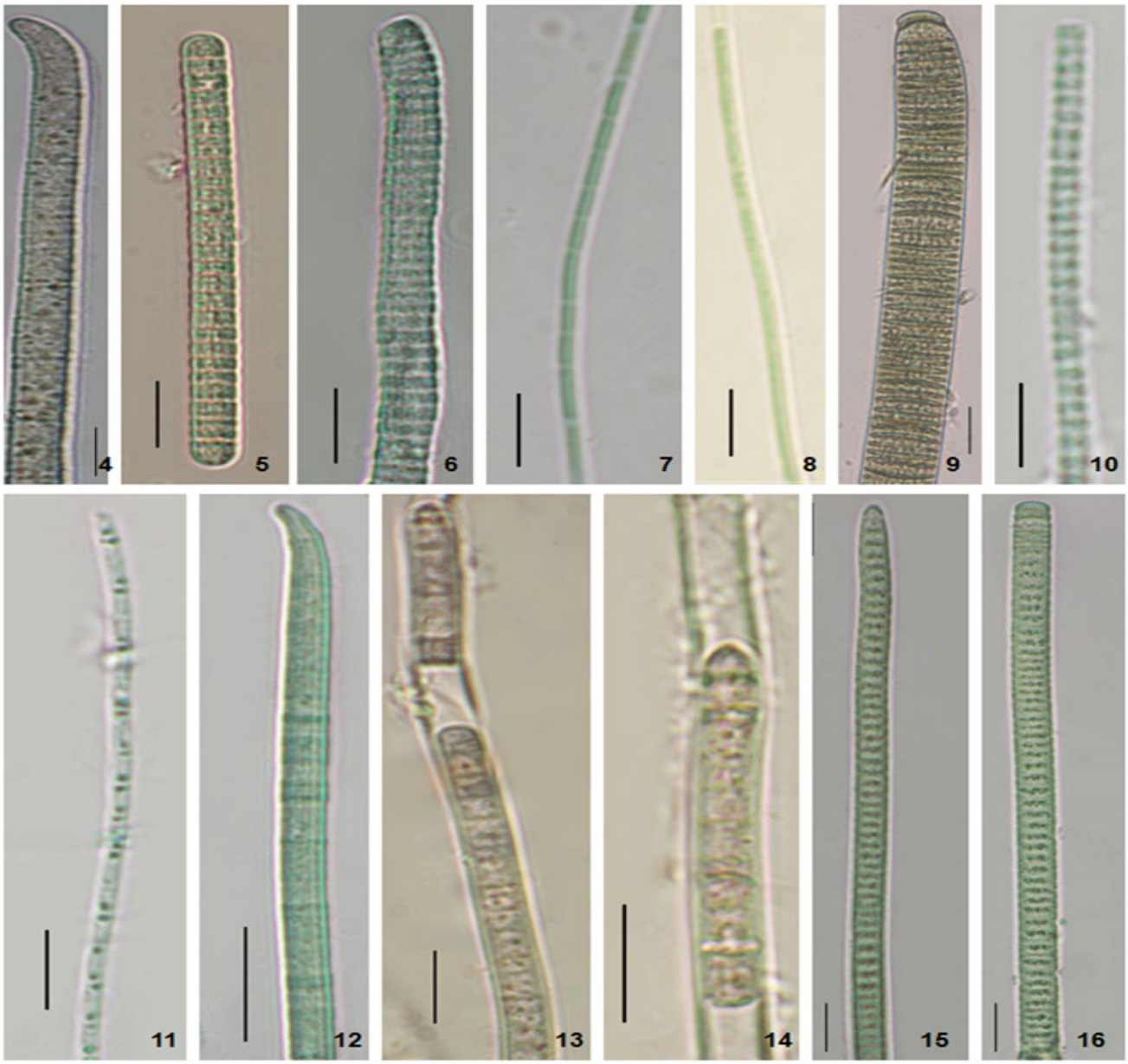

Figure 2: Photomicrographs of the specimens. 4. *Phormidium formosum* (*Phormidium* sp. AKS1). 5. *Planktothrix pseudagardhii* (*Planktothrix* sp. DNK). 6. *Planktothrix pseudagardhii* (*Planktothrix* sp. DNK2). 7. *Leptolyngbya valderiana* (*Leptolyngbya* sp. RPL1). 8. *Leptolyngbya valderiana* (*Leptolyngbya* sp. RPL2). 9. *Oscillatoria sancta* (*Oscillatoria* sp.). 10. *Leptolyngbya* sp. (*Leptolyngbya* sp. BKR). 11. *Limnothrix vacuolifera* (*Limnothrix* sp. BKR). 12. *Desertifilum* sp. (*Desertifilum* sp. RPL) 13-14. *Phormidium autumnale* (*Phormidium* sp. RPL). 15-16. *Planktothrix* sp. (*Planktothrix* sp. S41). Scale Bar- 5 µm.

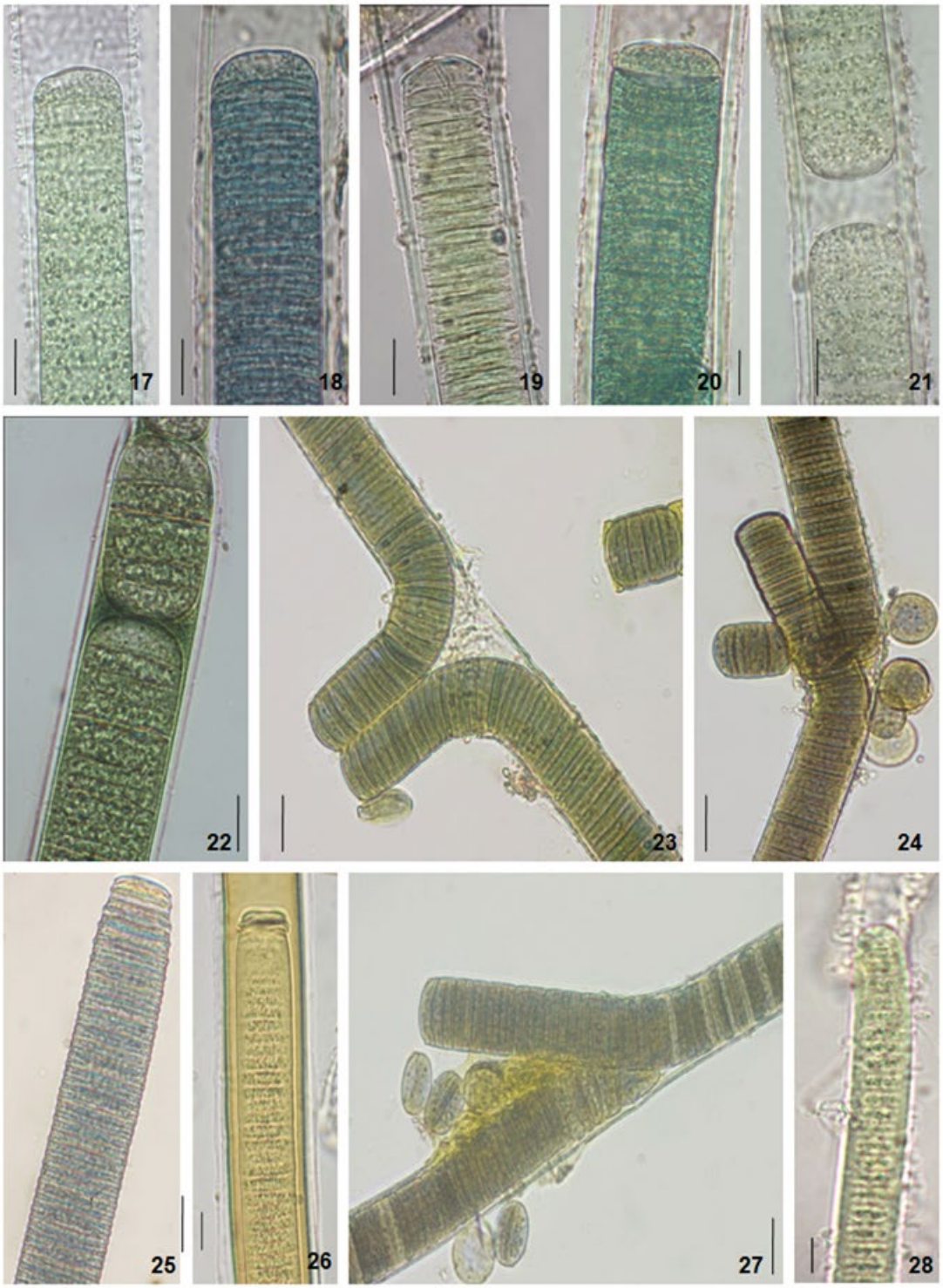

Figure 3: Photomicrographs of the specimens. 17. *Lyngbya birgei* (*Lyngbya* sp. PRLA). 18. *Lyngbya birgei* (*Lyngbya* sp. NB). 19. *Lyngbya birgei* (*Lyngbya* sp. SHNTN). 20. *Lyngbya birgei* (*Lyngbya* sp. RAB). 21. *Lyngbya birgei* (*Lyngbya* sp. MHN). 22. *Lyngbya birgei* (*Lyngbya* sp. HDA). 23. *Plectonema tomasinianum* (*Plectonema* sp. KOP). 24. *Plectonema tomasinianum* (*Plectonema* sp. AJY). 25. *Oscillatoria princeps* (*Oscillatoria* sp. MND). 26. *Lyngbya aestuarii* (*Lyngbya* sp. SUND). 27. *Plectonema tomasinianum* (*Plectonema* sp. KAS). 28. *Lyngbya semiplena* (*Lyngbya* sp. MANI). Scale Bar- 5 µm.

A phylogenetic study using 16S-23S ITS region

Based on morphology, the genera were grouped into Pseudanabaenaceae, Oscillatoriaceae, and Phormidiaceae. The phylogenetic trees were constructed within each family. The ITS length was around 250bp except for the MW238347 *Oscillatoria* sp. MND (morphologically identified as *O. princeps*) was almost 450bp. The similarity matrices of the sequences are represented in Supplementary Tables 1-6.

The Pseudanabaenaceae tree was constructed from a total of 34 sequences of ITS, including 4 from our study and 30 from the NCBI database (Fig. 29). The samples were resolved into 3 distinct clades with moderate to high bootstrap support (NJ/ML) values. The sequence similarities were represented in supplementary table 1. In clade 1 brackish water taxa MN640090 *Leptolyngbya* sp. RPL1(morphologically *L. valderiana*) and MN640091 *Leptolyngbya* sp. RPL2 (morphologically *L. valderiana*) formed a monophyletic clade with high bootstrap support with other saline *Leptolyngbya* sequences of the NCBI database (HQ891920, MF084983, MF084982, MF084981) and showed polyphyly with the experimental MW2383488 *Leptolyngbya* sp. BKR (morphologically *Leptolyngbya* sp.) from Hotspring. The MW2383488 *Leptolyngbya* sp. BKR formed monophyly with a hot-spring KM438181 *Leptolyngbya* sp. of Greece (clade 2). The sequences of *Albertania*, which was recently established as a new genus from *Leptolyngbya,* showed similarity with the *Leptolyngbya* sp. BKR and shared sister clade with the experimental taxa. Our experimental MW393862 *Limnothrix* sp. BKR (morphologically *Limnothrix vacuolifera*) sequence was well separated from the *Leptolyngbya* clades and formed a monophyletic clade with *Limnothrix*, *Geitlerinema*, and *Jaaginema* having high bootstrap values (clade 3).

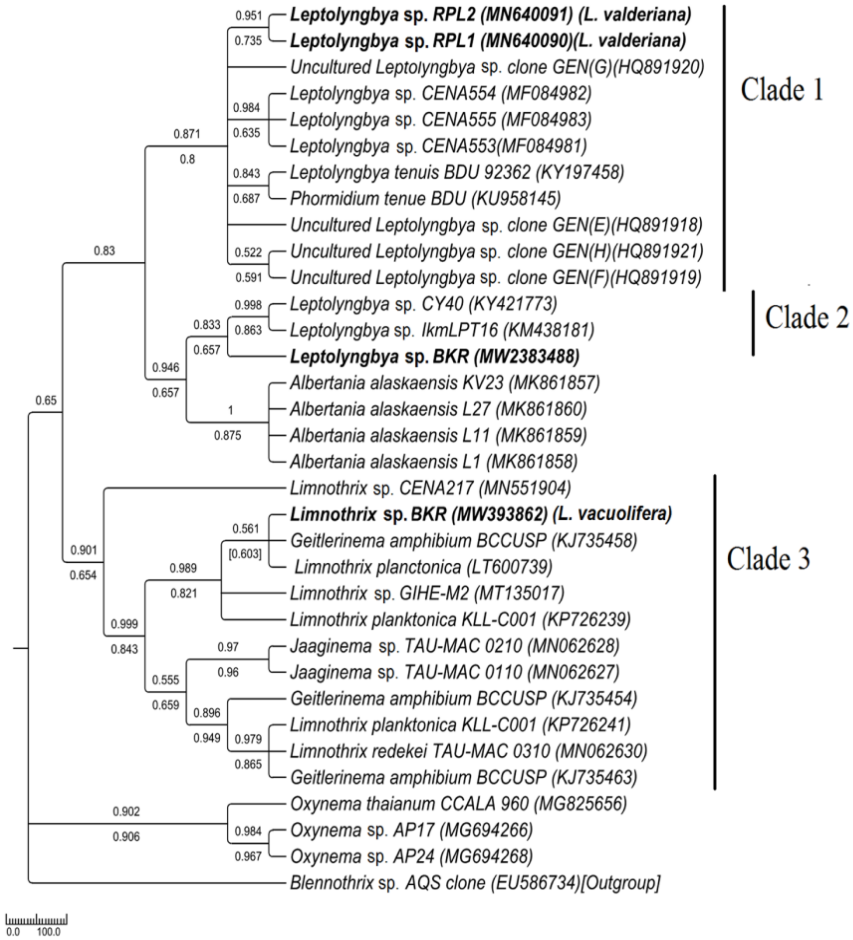

29

Figure 4: Phylogenetic tree of ITS sequences based on neighbor-joining and the maximum likelihood of the family Pseudanabaenaceae. Bootstrap values (NJ/ML) for nodes >50% were shown in the tree. Genbank accession numbers are provided.

The phylogenetic tree of Phormidiaceae was built up with 29 NCBI sequences along with 6 sequences of the current study (Fig. 30). Samples appeared to be divided into four clades of moderate to high bootstrap values—experimental MW238346 *Phormidium* sp. RPL (morphologically *Phormidium autumnale*) was placed in clade 1 with moderate to high bootstrap support and showed (90-91%) sequence similarity with its neighboring sister clades containing *Microcoleus* and *Phormidium autumnale* samples—the MN817999 *Phormidium* sp. AKS (morphologically identified as *Phormidium formosum*) was found to be very close to *the Planktothrix* clade (clade2) (having 60-70% similar sequences) and shown monophyly with the same instead of *the Phormidium* clade. The three *Planktothrix* samples were separated into two sub-clades within clade 2 and showed paraphyletic origin regardless of their morphological similarity. Experimental MW238345 *Planktothrix* sp. DNK (morphologically *Planktothrix pseudagardhii*) and MW393863 *Planktothrix* sp. S41 sequences were 91% similar and formed monophyletic clades with high bootstrap support with other *Planktothrix* sequences of the NCBI database (Supplementary Table 2)—another MW366802 *Planktothrix* sp. DNK2 (morphologically *Planktothrix pseudogardhii*) was separated and formed a distinct clade with *Planktothrix* samples from the NCBI database. MW366801 *Desertifilum* sp. RPL was found to form a monophyletic lineage with 99% similar *Desertifilum* sequences of NCBI databases consistent with their morphology and separated from clade 1 and clade 2.

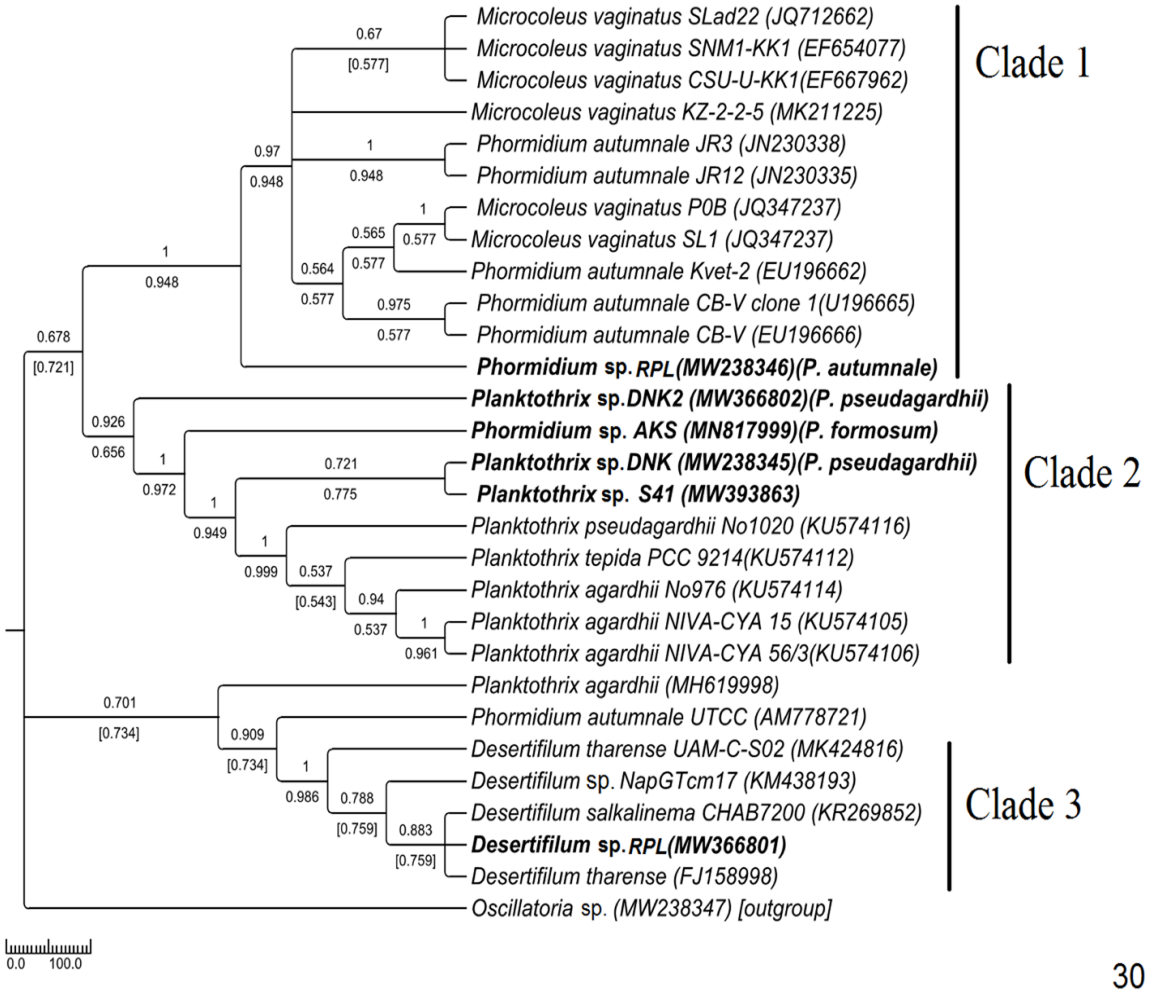

Figure 5: Phylogenetic tree of ITS sequences based on neighbor-joining and the maximum likelihood of the family Phormidiaceae. Bootstrap values (NJ/ML) for nodes >50% were shown in the tree. Genbank accession numbers are provided.

Phylogenetic relationships in Oscillatoriaceae were drawn using a total of 37 sequences, out of which 13 sequences were from the present study and 24 from the NCBI database (Fig. 31). Samples were divided into five clades of moderate to high bootstrap values. The experimental sample MN630162 *Oscillatoria* sp. (morphologically *Oscillatoria sancta*) formed a monophyletic clade (clade 2) with other *Oscillatoria sancta* sequences of the NCBI database with high bootstrap values. The sequences were 94-96% similar—another experimental MW238347 *Oscillatoria* sp. MND sequences from hilly regions (morphologically *Oscillatoria princeps*) formed a separate clade (clade 5) having high bootstrap values with *Oscillatoria* sequences collected from the NCBI database. The sequence of this strain's sister clades was 99% similar (Supplementary Table 3). It was well separated from the *Oscillatoria sancta* with 84% sequence similarity. Among the two brackish *Lyngbya* sequences, MN817998 *Lyngbya* sp. SUND (morphologically *L. aestuarii*) showed 81-82% sequence similarity with deposited sequences in NCBI and formed a monophyletic clade (clade 1) with the sequences. The MN630163 *Lyngbya* sp. MANI (morphologically *L. semiplena*) showed 97% similarity with *Neolyngbya irregularis*, which was also marine and formed a monophyletic clade (clade 3) with it (Supplementary Table 4). All the freshwater *Lyngbya* samples collected from high as well as low altitude regions (morphologically *L. birgei*) formed a single monophyletic clade (clade 4), which was separated from the marine *Lyngbya* clades, i.e., clade 1 and clade, 3. This monophyletic clade also contained *Plectonema* sequences along with *Lyngbya*.

Due to less availability of deposited sequences in GenBank, this clade mainly consists of sequences from the present investigation rather than from any online database. Though this clade contains sequences from two different genera, all the sequences were 99-100% similar (Supplementary Table 5). No threshold percentage for species discrimination had been recorded in the case of the 16S-23S ITS region. To attain better resolution in this clade 4, a 16S molecular marker-based phylogenetic tree was built (Fig. 32).

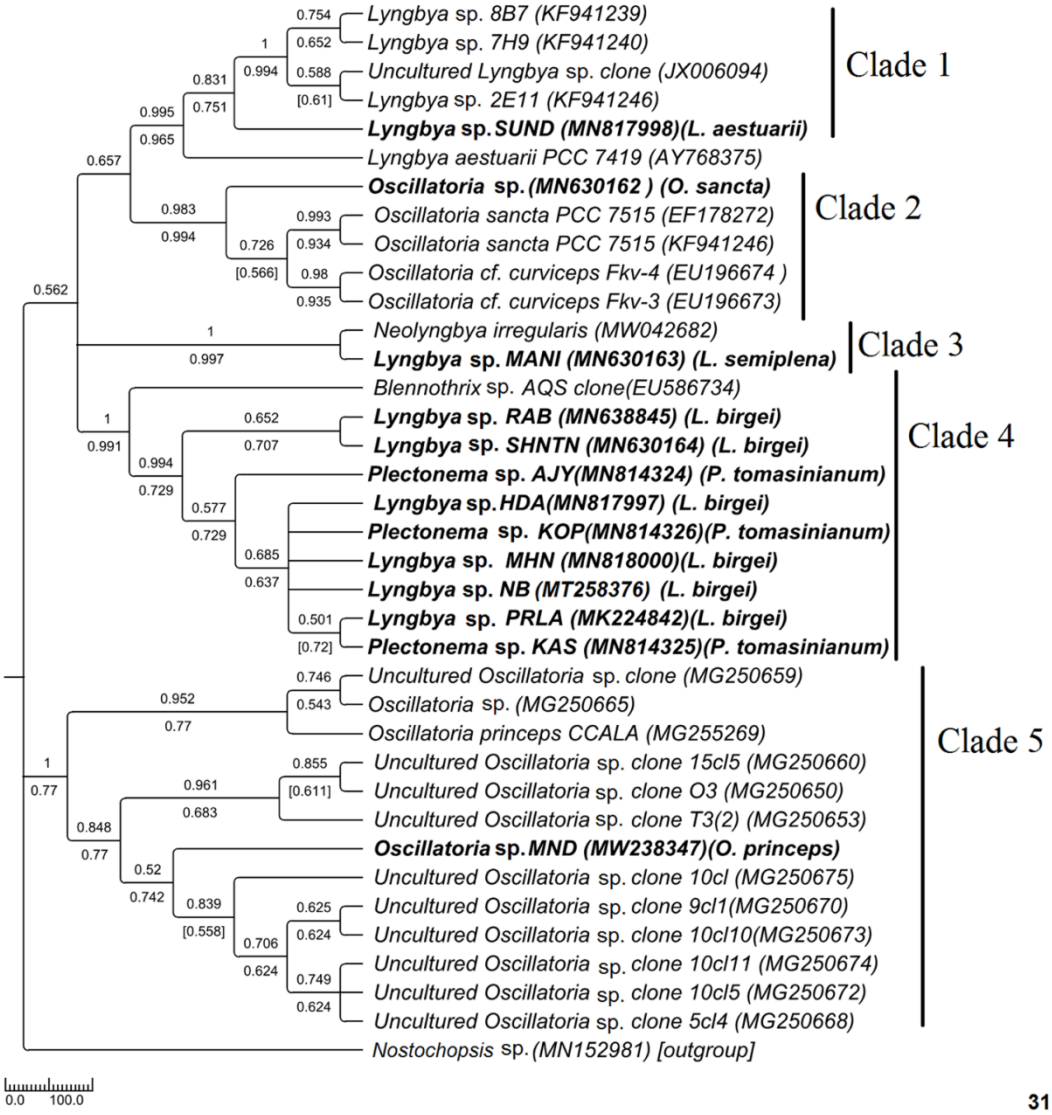

Figure 6: Phylogenetic tree of ITS sequences based on neighbor-joining and the maximum likelihood of the family Oscillatoriaceae. Bootstrap values (NJ/ML) for nodes >50% were shown in the tree. Genbank accession numbers are provided.

Phylogenetic study in Oscillatoriaceae using 16S rDNA region

The average sequence length in the tree was around 700bp. Samples were divided into two clades of moderate to high bootstrap values. This tree topology (Fig. 32) was more or less congruent with a phylogenetic tree with ITS sequence data. The non-availability of the same sequence in the NCBI database for 16S and ITS sequence data resulted in a difference in the topology of the phylogenetic tree. However, the basic topology remained the same, which supported the conspecificity of all freshwater *Lyngbya.* The 16S sequence similarity in *Lyngbya* and *Plectonema* ranged between 99-100%, similar to their similarity in the ITS region (Supplementary Table 6). In the 16S rDNA-based phylogenetic tree, *Plectonema* showed polyphyletic origin. MT192748

Plectonema sp. AJY (morphologically *Plectonema tomasinianum*) and MT192750 *Plectonema* sp. KPY (morphologically *Plectonema tomasinianum*) showed 98-99% similarity with *Microseira whole* sequences and formed a monophyletic clade with them, whereas MT192753 *Plectonema* sp. KAS (morphologically *Plectonema tomasinianum*) formed a clade with *Lyngbya* sp. NB has 100% sequence similarity.

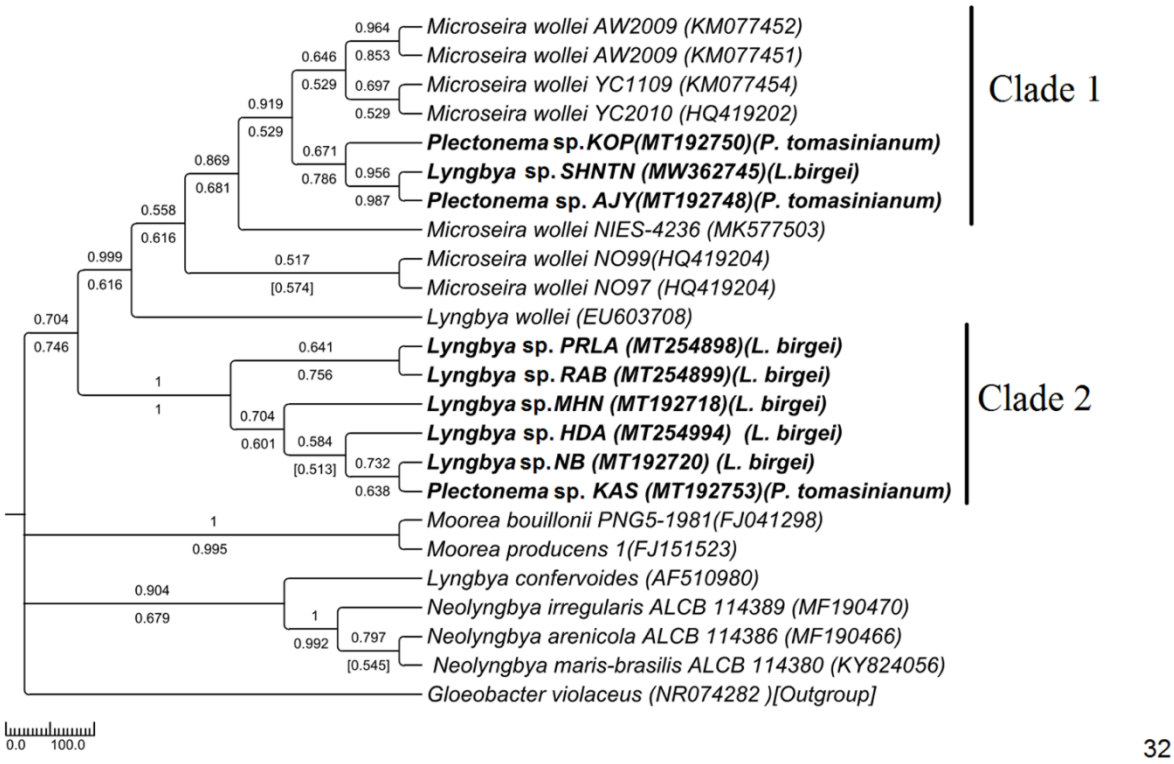

Figure 7: Phylogenetic tree of 16S sequences based on neighbor-joining and the maximum likelihood of the family Oscillatoriaceae. Bootstrap values (NJ/ML) for nodes >50% are shown in the tree. Genbank accession numbers are provided.

Cultural behavior study of *Lyngbya-Plectonema* complex

The cultural behavior of *Plectonema tomasinianum* samples and *Lyngbya birgei* were studied for further clarification. Surprising similarities in different growth stages were recorded among them. On the same note, *Lyngbya* samples formed false branching like *Plectonema* samples during the growth of filaments. The detailed changes are in Table 5, Figures 33-42, and Figures 43-57.

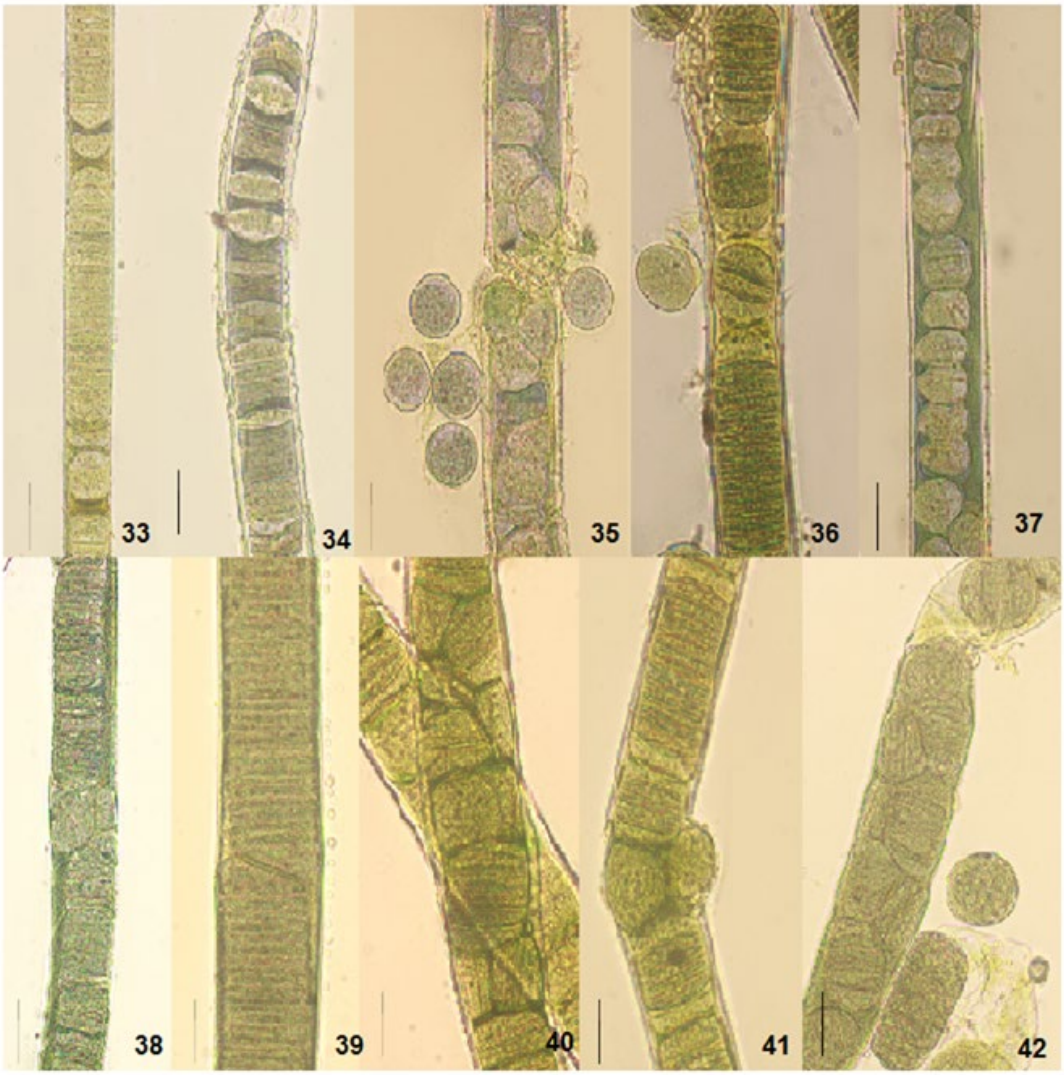

Figure 8: Light photomicrographs of *Lyngbya birgei* and *Plectonema tomasinianum* filaments at different growth phases in culture show the formation of separation discs and pseudohormogone formation. 33. Separation disc formation in *Lyngbya* sp. RAB filament. 34. Separation disc formation in *Lyngbya* sp. HDA filament. 35. Pseudohormogone formation in *Plectonema* sp. KAS. 36. Hormogone and pseudohormogone formation in *Plectonema* sp. KPY. 37. Pseudohormogone formation in *Plectonema* sp. AJY. 38. Cell division in different planes in *Lyngbya* sp. RAB. 39. Cell division in other planes in *Lyngbya* sp. HDA. 40. Cell division in different planes in *Plectonema* sp. KAS. 41. Cell division in different planes in *Plectonema* sp. KPY. 42. Cell division in other planes in *Plectonema* sp. AJY. Scale bar- 20 µm.

No. of days	*Lyngbya* sp. RAB	*Lyngbya* sp. HDA	*Plectonema* sp. KAS	*Plectonema* sp. KPY	*Plectonema* sp. AJY
3	Separation disc formation.	Separation disc formation.	Pseudo- Hormogonia formation.	Hormogonia formation.	Hormogonia formation.
6	Hormogonia formation continued, with cell division in different planes.	Diagonal fragmentations were noticed.	Cell division in different planes is initiated.	Cell division in different planes is initiated.	Cell division in different planes was observed with hormone formation.
9	Diagonal fragmentation followed by growth of trichome in a single sheath	Cell division in different planes, followed by growth of nascent trichomes.	Diagonal cell division followed by fragmentation of trichome.	The nascent trichome remained enclosed in the same sheath as the mother filament.	The nascent trichome remained enclosed in the same sheath as the mother filament.
12	Nascent filament growing with mother filament within the common sheath.	Nascent filament growing with mother filament within the common sheath.	Nascent filament growing with mother filament within the common sheath.	Nascent filament growing with mother filament within the common sheath.	Nascent filament growing with mother filament within the common sheath.
15	The nascent filament became mature and developed as a false branch within the same sheath, observed as a criss-cross structure.	False branches developed.	False branches developed.	False branches developed.	False branches developed.

Table 5: Variation in growth performances of *Lyngbya* and *Plectonema* in cultural conditions.

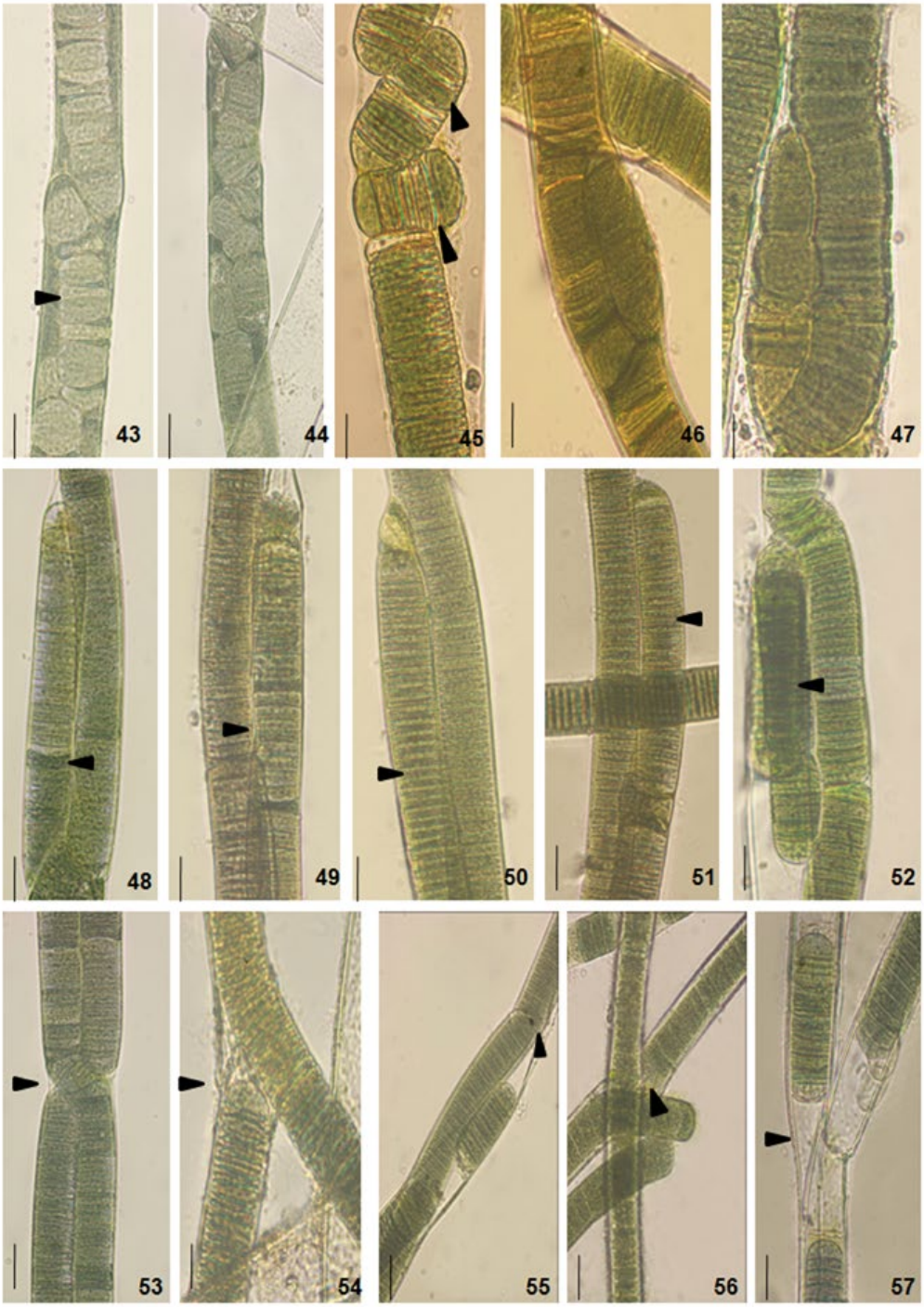

Figure 9: Light photomicrographs of *Lyngbya birgei* and *Plectonema tomasinianum* filaments at different growth phases in culture show diagonal fragmentation followed by nascent trichomes and false branch development initiation. Arrows indicate the changes. 43. Filament of *Lyngbya* sp. RAB. 44. Filament of *Lyngbya* sp. HDA. 45. Filament of Plectonema sp. KAS. 46. Filament of Plectonema sp. KPY. 47. Filament of *Plectonema* sp. AJY. 48. Filament of *Lyngbya* sp. RAB. 49. Filament of *Lyngbya* sp. HDA. 50. Filament of Plectonema sp. KAS. 51. Filament of Plectoneme sp. KPY. 52. Filament of *Plectonema* sp. AJY. 53. Filament of *Lyngbya* sp. RAB. 54. Filament of *Lyngbya* sp. HDA. 55. Filament of Plectoneme sp. KAS. 56. Filament of Plectonema sp. KPY. 57. Filament of *Plectonema* sp. AJY. Scale bar- 20 µm.

ITS secondary structure analysis

The 16S-23S ITS regions were subjected to the identification of conserved regio, followed by secondary structure analysis for freshwater *Lyngbya* and *Pleconema* samples. The amplified ITS region contained $tRNA^{Ala}$, $tRNA^{Ile}$, V_2, Box A and B helices. The lengths of individual helices are represented in Table 6. The secondary structures are provided in Supplementary Figure 1**.** No difference in secondary structures was noticed in all the investigated samples.

DISCUSSION

The current approaches to cyanobacterial systematics faced considerable challenges in building up conclusive results regarding the unity of morphological, cultural, and molecular data for phylogenetic interpretation [24]. In the present study, 23 taxa under 8 genera of the order Oscillatoriales were investigated with a polyphasic approach considering morphometry, cultural behavior, and ITS sequence-based molecular data in a need-based manner. As very few ITS sequence data of Oscillatoriales were available in the online database, we tried to incorporate our data as a reference value and constructed phylogenetic trees per the existing NCBI database.

To date, genera of non-heterocystous Oscillatoriales have yet to be well resolved by molecular approach. The *Leptolyngbya* is one of the most abundant and complicated genera of Pseudanabaenaceae due to its simple morphology with genetic variation[1]. A few *Lyngbya*, *Plectonema* and *Phormidium* members with very thin trichomes (0.5-3.5µm wide) were described as a new genus *Leptolyngbya*[33]. The monophyletic assemblage of this genus has not been proved yet. Polyphyletic assemblage based on 16S rDNA analysis was observed in the case of *Pseudanabaena*, *Leptolyngbya*, *Limnothrix*, and *Geitlerinema* [34,35]. In our present study, the polyphyletic origin of *Leptolyngbya* and *Limnothrix,* as well as habitat-specific clustering among species of *Leptolyngbya*, was noticed (Fig. 29). The sequences were clustered with other sequences with similar types of ecological preferences. Cyanobacterial habitat selectivity is a matter of debate to many researchers. The argument regarding endemism [36] or cosmopolitan distribution has existed for a long time[37]. However, present-day research has demonstrated that habitat specificity or nutrient requirement is related to genome size [38,39]. In the current study, genetic diversity among cyanobacteria dwelling in freshwater as well as extreme environments, like marine and hot springs, was studied based on ITS-based phylogenetic analysis for the very first time, which indicated that this molecular maker is capable of discriminating species belonging to different habitats. Morphologically ambiguous identification is inevitable in the family Phormidiaceae of Oscillatoriales due to its misleading nature of identifying criteria. The name of *Phormidium* was considered an invalid name due to more than 100 years of taxonomic confusion[40]. However, Casamatta et al. (2005)[41] did not agree with the fact totally but concluded that generic and subgeneric categorizations in this genus should not essentially correspond to systematic relations. The genus was revised and grouped using morphological and ultrastructural criteria to ease the identification process[1]. The 16S rDNA-based analysis showed a phylogenetically close *Microcoleus vaginatus* and *Phormidium autumnale* assemblage with almost indistinguishable morphological characters[34]. Both the taxa mainly differed in their sheath properties and filament size influenced by environmental factors; therefore, they are inconsistent in culture conditions and 16S rDNA-based phylogenetic study[33]. In the current ITS sequence-based study also, the *Microcoleus* and *Phormidium* formed a monophyletic assemblage that appeared as sister to the experimental genus *Phormidium* (morphologically *P. autumnal*), indicating congruency between 16S and ITS sequence-based interpretations (Fig. 30).

The genus *Planktothrix* was placed under Phormidiacae (after separation from *Oscillatoria*) because of their cellular characteristics and support from 16S rDNA sequencing[42]. In our study, the placement of MW238346

Phormidium sp. (morphologically *P. formosum*) with *Planktothrix* sequences (Fig. 30) justified polyphyly of *Phormidium* as proved by other authors also[42]. This kind of polyphyly may have resulted due to inadequate deposited sequences, and thus, more ITS sequence-based research should be done to enrich the sequence database. Paraphyly of *Planktothrix* was observed in our study (Fig. 30) as interpreted in earlier studies using 16S rDNA[42]. *Desertifilum* was considered a new genus under Phormidiaceae after being separated from *Microcoleus* and *Phormidium* based on 16S rDNA-based analysis coupled with morphological parameters[43]. In the current study, *Desertifilum* was in a monophyletic lineage consistent with their morphology and separated from the *Microcoleus-Phormidium* clade. The interpretation is congruent with the 16S rDNA-based study by the earlier workers. This is the first report of *Desertifilum* from eastern India.

Polyphyletic nature of *Oscillatoria* was also reflected in this ITS sequence-based study (Fig. 31). In the phylogenetic tree of Oscillatoriaceae, MN630162 *Oscillatoria* sp. (morphologically *O. sancta*) having apical cap was placed in monophyletic lineage with other *O. sancta* sequences with high sequence similarity and good bootstrap support whereas MW238347 *Oscillatoria* sp. MND (morphologically *O. princeps*) formed a well-supported clade with other *Oscillatoria* strains and was distantly placed from *O. Sancta*. As studied by Hasler et al. (2012)[, 34] *Oscillatoria sancta* having thickened apical cap formed well-supported lineage with other calyptrate taxa in 16S rDNA-based study. The origin of calyptra or their role in cyanobacteria has never been investigated[44]. Phylogenetic remoteness, as observed in our study, cannot be disregarded as both the sequences have shared a high level of similarity with their sister sequences having good bootstrap support. The genus *Oscillatoria* was not revised earlier; however, from our observation, it can be concluded that *Oscillatoria* having an apical cap showed a somewhat different evolutionary history from that of *Oscillatoria* without an apical cap. Further detailed investigation is needed in this regard.

For *Lyngbya*, brackish water and marine species were well separated, and their monophyletic assemblage with other ecologically consistent strains supported again that ITS-based sequence clustering can reflect ecological selectivity. Genetic divergence can reflect habitat preferences for ecologically distinct organisms[45]. In the phylogenetic tree of Oscillatoriaceae, freshwater *Lyngbya* sp. (morphologically *L. birgei*) formed a different monophyletic lineage than that of marine *Lyngbya* (Fig. 31). The morphological similarity was also tested at the molecular level because all the samples have shown 99-100% similarity. Surprisingly, *Plectonema* shared a common monophyletic lineage with the *Lyngbya* clade, having 99-100% sequence similarity. Though no threshold percentage value is available in the literature for species-level identification, the high-level sequence similarity of the ITS study may be considered further.

The ITS tree topology was compared with rDNA based phylogenetic tree (Fig. 32), and the topology was almost similar. However, two *Plectonema* samples (MT192748 *Plectonema* sp. AJY and MT192750 *Plectonema* sp. KPY) (morphologically *P. tomasinianum*) and MW362745 *Lyngbya* sp. SHNTN, all collected from rivers flowing over lateritic soil regions, formed a monophyletic clade with *Microseira wollei*, a nascent genus separated from *Lyngbya.* MT192753 *Plectonema* sp. KAS collected from similar habitats and having exactly similar morphology have been placed in *the Lyngbya* clade with 98% similar sequences. As per convention, more than 98% 16SrDNA similarity can be considered the same species[46]. Thus, in our present study, morphological identification of freshwater *Lyngbya* sequences from high to low altitudes became congruent with molecular characterization based on ITS and 16S sequence data. Both morphological and molecular details support that all freshwater *Lyngbya* belong to the same species. However, a problem in identifying *Plectonema* still needs to be resolved. Secondary structures (Table 6, Supplementary Figure 1) were also investigated, but no differences were noticed among the samples.

Plectonema was initially classified under Scytonemataceae[14,47] based on false branching formation, though no heterocyst was found. Genus *Lyngbya* was classified under Oscillatoriaceae by Geitler (1932), where the occasional occurrence of false branching was also noticed. Later on, the observation of other scientists inferred that false branching occurred facultatively in a tiny part of the population of *P. tomasinianum,* and the character was also overcredited, which should not be done because of its inconsistency[48–50]. Scarcity in the *P. tomasinianum* sequence in online databases led to the dilemma that existed for a long. In the present study, false branching in *Lyngbya* culture again confounded the generic discrimination between *Plectonema tomasinianum* and *Lyngya birgei.* Supporting the earlier workers, the current study also emphasized and proposed that this kind of plastic, pleomorphic character of cyanobacteria should not be considered as an autapomorphic character at the genus level.

CONCLUSIONS

The study marks the first-ever attempt to use ITS-based phylogenetic analysis on Indian non-heterocystous filamentous cyanobacteria. The results of our research demonstrate the impressive discriminatory ability of the 16S-23S ITS region in identifying and distinguishing cyanobacteria from various habitats. Our study highlights the novelty of this approach and its potential for revolutionizing the field of cyanobacterial research. Our research shows that species clustering in the ITS-based phylogenetic tree is habitat-specific. For instance, marine species of *Leptolyngbya* form a monophyletic clade with other marine *Leptolyngbya* sp., while hotspring taxa form a separate monophyletic clade with other hotspring *Leptolyngbya* species. Moreover, the study revealed the polyphyletic nature of *Planktothrix* and *Phormidium* in the phylogenetic tree of Phormidiaceae. The ITS-based species clustering supported earlier 16S rDNA-based studies, highlighting the significance of the ITS region in species identification.

We present a novel approach to differentiate various species of *Lyngbya* by proposing 98% sequence similarity as a threshold percentage of ITS sequence. Furthermore, this study emphasizes the need to re-evaluate the taxonomic status of *Lyngbya birgei* and *Plectonema tomasinianum* as they appear highly similar based on 16S rDNA and ITS sequence-based analysis and cultural behavior study. Our study offers valuable insights into the complexities of identifying these species and calls for more research in this area.

Supplementary Materials: The following pdf are available online

Figure S1: Secondary structures of 16S–23S internal transcribed spacer (ITS) sequences from the *Lyngbya* sp.HDA, *Lyngbya* sp.RAB, *Plectonema* sp. KOP, *Plectonema* sp. KAS and *Plectonema* sp. AJY., Table S1: A partial similarity matrix (P distance) generated using 16S-23S ITS region (Family- Pseudanabaenaceae), Table S2-A partial similarity matrix (P distance) generated using 16S-23S ITS region (Family- Phormidiaceae), Table S3-A partial similarity matrix (P distance) generated using 16S-23S ITS region (Family- Oscillatoriaceae-genus *Oscillatoria*), Table S4-A partial similarity matrix (P distance) generated using 16S-23S ITS region (Family- Oscillatoriaceae-genus *Lyngbya*(marine)), Table S5-A partial similarity matrix (P distance) generated using 16S-23S ITS region (Family- Oscillatoriaceae-genus *Lyngbya-Plectonema*(freshwater)), Table S6-A partial similarity matrix (P distance) generated using 16S region (Family Oscillatoriaceae-genus *Lyngbya-Plectonema*)

Author Contributions: "Conceptualization, Sreemanti Banerjee and Ruma Pal.; methodology, Sreemanti Banerjee.; software, Sreemanti Banerjee; validation, Sreemanti Banerjee, Akanksha Singh and Ruma Pal; formal analysis, Sreemanti Banerjee; investigation, Sreemanti Banerjee, Akanksha Singh; resources, Sreemanti Banerjee; data curation, Sreemanti Banerjee; writing—original draft preparation, Sreemanti Banerjee;

writing—review and editing, Ruma Pal; visualization, Sreemanti Banerjee; supervision, Ruma Pal; project administration, Sreemanti Banerjee; funding acquisition, Sreemanti Banerjee and Ruma Pal. All authors have read and agreed to the published version of the manuscript."

Funding: The present research has been funded by the Council for Science and Industrial Research (CSIR) - sanction no.-09/028(0964)2015-EMR1. CAS Phase VII and DST-FIST Level II, Department of Botany, University of Calcutta, supported the infrastructural facility.

Acknowledgments: The authors thank Prof. Sagarmoy Ghosh, Department of Microbiology, University of Calcutta, and Dr. Suparna Ghosh, Department of Microbiology, University of Calcutta, for their cooperation during the work.

Conflicts of Interest: The authors declare no conflict of interest. The funders had no role in the study's design, in the collection, analyses, or interpretation of data, in the writing of the manuscript, or in the decision to publish the results.

REFERENCES

1. Komarek J, Anagnostidis K. Cyanoprokaryota. II. teil: Oscillatoriales. In Süsswasserflora von Mitteleuropa. Büdel B, Gärdner G, Krienitz L, Schagerl M, editors. Vol. 19. München: Elsevier; 2005. 1–759 p.
2. Tschermak-Woess E, Schöller A. Verteilung und Aufteilung der DNS bei einigen Cyanophyceen, festgestellt durch ihre DAPI-Fluoreszenz. Plant Systematics and Evolution. 1982;140:207–23.
3. Cepák V. Morphology Of DNA containing structures (nucleoids) as a prospective character in cyanophyte taxonomy. J Physiol. 1993 Dec 20;29(6):844–52.
4. Cepák V, Kováčik L, Komárek J. DNA containing structures (nucleoids) in some cyano-phytes/cyanobacteria as revealed by DAPI fluorescent staining. Algological Studies/Archivfür Hy-drobiologie. 1991;Supplement Volumes:25–39.
5. Guglielmi G, Cohen-Bazire G. Etude taxonomique d'un genre de cyanobacterie oscillatoriacee: le genre Pseudanabaena Lauterborn. II. Analyse de la composition moleculaire et de la structure des phycobilisomes. Protistologica. 1984;20:393–413.
6. Golecki JR, Drews G. Supramolecular organization and composition of membranes. In: Carr N.G., Whitton B.A, editors. The Biology of Cyanobacteria. Blackwell Science; 1982. p. 125–41.
7. Weckesser J, Drews G, Mayer H. Lipopolysaccharides of Photosynthetic Prokaryotes. Annu Rev Microbiol. 1979 Oct;33(1):215–39.
8. Lounatmaa K, Vaara T, Österlund K, Vaara M. Ultrastructure of the cell wall of a Synechocystis strain. Can J Microbiol. 1980 Feb 1;26(2):204–8.
9. Mamkaeva KA, AL-MusAvI RA, Gromov BV. The effect of photosynthesis on the ultrastructure of a cyanophage during its intracellular growth. Mikrobiologiia. 1980;49:631–3.
10. Jensen TE, Baxter M. Imaging cell inclusions in air dried unfixed cyanobacteria with a transmission electron microscope at 75 kV. Microbios. 1985;28:145–50.
11. Baxter M, Jensen TE. Cell volume occupied by polyphosphate bodies during the polyphosphate overplus phenomenon in Plectonema boryanum. Cytobios. 1986;45:147–60.
12. Rippka R, Deruelles J, Waterbury JG, Herdman M, Stanier RY. Generic assignments, strain histories and properties of pure cultures of cyanobacteria. J Gen Microbiol. 1979;1–61.
13. Gomont M. Monographie des Oscillariées. Annales des Sciences Naturelles; Botanique. 1892;16:198–246.
14. Desikachary TV. Cyanophyta. Delhi: Indian Council of Agricultural Research; 1959. 1–686 p.
15. Casamatta DA, Vis ML, Sheath RG. Cryptic species in cyanobacterial systematics: a case study of Phormidium retzii (Oscillatoriales) using RAPD molecular markers and 16S rDNA sequence data. Aquat Bot. 2003 Dec;77(4):295–309.
16. Turner S. Molecular systematics of oxygenic photosynthetic bacteria. In 1997. p. 13–52.
17. Wilmotte A. Molecular evolution and taxonomy of the cyanobacteria. In: Bryant DA, editor. The Molecular Biology of Cyanobacteria. Boston: Kluwer Academic Press; 1994. p. 1–25.

18. Singh P, Singh SS, Elster J, Mishra AK. Molecular phylogeny, population genetics, and evolution of heterocystous cyanobacteria using nifH gene sequences. Protoplasma. 2013 Jun 23;250(3):751–64.
19. Mondal SK, Shit S, Kundu S. A comparative computational study of the 'rbcL'gene in plants and in the three prokaryotic families—Archaea, cyanobacteria and proteobacteria. Indian J Biotechnol. 2013;12:58–66.
20. Singh P, Fatma A, Mishra AK. Molecular phylogeny and evogenomics of heterocystous cyanobacteria using rbcl gene sequence data. Ann Microbiol. 2015 Jun 30;65(2):799–807.
21. García-Martínez J, Acinas SG, Antón AI, Rodríguez-Valera F. Use of the 16S–23S ribosomal genes spacer region in studies of prokaryotic diversity. J Microbiol Methods. 1999 May;36(1–2):55–64.
22. Boyer SL, Johansen JR, Flechtner VR, Howard GL. Phylogeny and genetic variance in terrestrial Microcoleus (Cyanophyceae) species based on sequence analysis of the 16s rrna gene and associated 16S–23S its region. J Phycol. 2002 Dec 19;38(6):1222–35.
23. Otsuka S, Suda S, Li R, Watanabe M, Oyaizu H, Matsumoto S, et al. Phylogenetic relationships between toxic and non-toxic strains of the genus Microcystis based on 16S to 23S internal transcribed spacer sequence. FEMS Microbiol Lett. 1999 Mar;172(1):15–21.
24. Boyer SL, Flechtner VR, Johansen JR. Is the 16S–23S rRNA Internal Transcribed Spacer Region a Good Tool for Use in Molecular Systematics and Population Genetics? A Case Study in Cyanobacteria. Mol Biol Evol. 2001 Jun 1;18(6):1057–69.
25. Guiry MD, Guiry GM. AlgaeBase. Worldwide electronic publication, National University of Ireland, Galway. 2021. http://algaebase.org.
26. Doyle JJ, Doyle JL. A rapid DNA isolation procedure for small quantities of fresh leaf tissue. Phytochemical Bulletin. 1987;19:11–5.
27. Valério E, Chambel L, Paulino S, Faria N, Pereira P, Tenreiro R. Molecular identification, typing and traceability of cyanobacteria from freshwater reservoirs. Microbiology (N Y). 2009 Feb 1;155(2):642–56.
28. Nübel U, Garcia-Pichel F, Muyzer G. PCR primers to amplify 16S rRNA genes from cyanobacteria. Appl Environ Microbiol. 1997 Aug;63(8):3327–32.
29. Kumar S, Stecher G, Tamura K. MEGA7: Molecular Evolutionary Genetics Analysis Version 7.0 for Bigger Datasets. Mol Biol Evol. 2016 Jul 1;33(7):1870–4.
30. Stöver BC, Müller KF. TreeGraph 2: Combining and visualizing evidence from different phylogenetic analyses. BMC Bioinform. 2010 Dec 5;11(1):7.
31. Zuker M. Mfold web server for nucleic acid folding and hybridization prediction. Nucleic Acids Res. 2003 Jul 1;31(13):3406–15.
32. Iteman I, Rippka R, de Marsac NT, Herdman M. rDNA analyses of planktonic heterocystous cyanobacteria, including members of the genera Anabaenopsis and Cyanospira. TheGenBank acces-sion numbers of the 16S rDNA gene sequences reported in this paper are AY038032–AY038037. Microbiology (N Y). 2002;148:481–96.
33. Stoyanov P, Moten D, Mladenov R, Dzhambazov B, Teneva I. Phylogenetic Relationships of Some Filamentous Cyanoprokaryotic Species. Evol Bioinform. 2014 Jan 23;10:EBO.S13748.
34. Hašler P, Dvořák P, Johansen JR, Kitner M, Ondřej V, Poulíčková A. Morphological and molecular study of epipelic filamentous genera Phormidium, Microcoleus and Geitlerinema (Oscillatoriales, Cyanophyta/Cyanobacteria). Fottea. 2012 Sep 1;12(2):341–56.
35. Perkerson III RB, Perkerson EA, Casamatta DA. Phylogenetic examination of the cyanobacterial genera Geitlerinema and Limnothrix (Pseudanabaenaceae) using 16S rDNA gene sequence data. Arch Hydrobiol Suppl Algol Stud. 2010 Jul 1;134:1–16.
36. Komárek J. Diversity of cyanoprokaryotes (cyanobacteria) of King George Island, maritime Antarctica - a survey. Arch Hydrobiol Suppl bd Algol Stud. 1999 Sep 16;94:181–93.
37. Mullins TD, Britschgi TB, Krest RL, Giovannoni SJ. Genetic comparisons reveal the same unknown bacterial lineages in Atlantic and Pacific bacterioplankton communities. Limnol Oceanogr. 1995 Jan 22;40(1):148–58.
38. Prabha R, Singh DP. Cyanobacterial phylogenetic analysis based on phylogenomics approaches render evolutionary diversification and adaptation: an overview of representative orders. 3 Biotech. 2019 Mar 15;9(3):87.

39. Prabha R, Singh DP, Somvanshi P, Rai A. Functional profiling of cyanobacterial genomes and its role in ecological adaptations. Genom Data. 2016 Sep;9:89–94.
40. Castenholz RW, Rippka R, Herdman M. Form genus IX. OscillatoriaVaucher 1803 (sensu Rippka, Deruelles, Waterbury,Herdman, and Stanier 1979). . In: Boone DR, Castenholz RW, editors. Bergey's Manual of Systematic Bacteriology. New York: Springer; 2001. p. 550–3.
41. Casamatta DA, Johansen JR, Vis ML, Broadwater ST. Molecular and morphological characterization of ten polar and near-polar strains within the Oscillatoriales (Cyanobacteria). J Phycol. 2005 Apr 17;41(2):421–38.
42. Komarek J, Komarkova J. Taxonomic review of the cyanoprokaryotic genera Planktothrix and Planktothricoides. Czech Phycology, Olomouc. 2004;4:1–18.
43. Dadheech PK, Abed RMM, Mahmoud H, Mohan MK, Krienitz L. Polyphasic characterization of cyanobacteria isolated from desert crusts, and the description of Desertifilum tharense gen. et sp. nov. (Oscillatoriales). Phycologia. 2012 May 23;51(3):260–70.
44. Whitton BA. Cyanobacterial diversity in relation to the environment. In: Algal toxins: nature, occurrence, effect and detection. Dordrecht: Springer; 2008. p. 17–43.
45. Nübel U, Garcia-Pichel F, Clavero E, Muyzer G. Matching molecular diversity and ecophysiology of benthic cyanobacteria and diatoms in communities along a salinity gradient. Environ Microbiol. 2000 Apr 21;2(2):217–26.
46. Yarza P, Yilmaz P, Pruesse E, Glöckner FO, Ludwig W, Schleifer KH, et al. Uniting the classification of cultured and uncultured bacteria and archaea using 16S rRNA gene sequences. Nat Rev Microbiol. 2014 Sep 14;12(9):635–45.
47. Geitler L. Cyanophyceae in Rabenhorst's Kryptogamen flora. Leipzing. 1932;1–1196.
48. McGregor GB, Sendall BC. Phylogeny and toxicology of Lyngbya wollei (Cyanobacteria, Oscillatoriales) from north-eastern Australia, with a description of Microseira gen. nov. J Phycol. 2015 Feb 11;51(1):109–19.
49. Seifert M, McGregor G, Eaglesham G, Wickramasinghe W, Shaw G. First evidence for the production of cylindrospermopsin and deoxy-cylindrospermopsin by the freshwater benthic cyanobacterium, Lyngbya wollei (Farlow ex Gomont) Speziale and Dyck. Harmful Algae. 2007 Jan;6(1):73–80.
50. Speziale BJ, Turner EG, Dyck LA. "Giant" Lyngbya. Aquatics. 1988;4–11.

Received: October 9th 2023/ **Accepte**d: January 15th 2024 / **Published:**15 February 2024

Citation: Banerjee S., Singh A., Pal R. Taxonomic interpretation of non-heterocystous Cyanobacteria (Oscillatoriales) from eastern India with particular emphasis on *Lyngbya Plectonema* complex. Revis Bionatura 2024; 9 (1) 66. http://dx.doi.org/10.21931/RB/2024.09.01.66

Additional information Correspondence should be addressed to sreemantibanerjee@gmail.com

Peer review information. Bionatura thanks anonymous reviewer(s) for their contribution to the peer review of this work using https://reviewerlocator.webofscience.com/

Bionatura ISSN. First 13909355 Ecuador. **Scopus coverage years**: from 2016 to the present

Bionatura
Ibero-American Journal of Biotechnology and Life Sciences

Article

Estudio químico y actividad antioxidante de la fracción lipídica de *Bactris gasipaes* Kunth (chonta) un fruto utilizado como alimento en la Amazonia ecuatoriana

Chemical Study and Antioxidant Activity of Lipid Fraction from *Bactris gasipaes* Kunth (peach palm) a fruit used as food in the Ecuadorian Amazon

*James Calva, Diana Sanchez & Vladimir Morocho**

Departamento de Química, Universidad Técnica Particular de Loja (UTPL), Calle M. Champagnat s/n, 1101608 Loja, Ecuador.
** Correspondence: svmorocho@utpl.edu.ec*
Available from. http://dx.doi.org/10.21931/RB/2024.09.01.67

RESUMEN

La fracción lipídica del fruto *Bactris gasipaes* (chonta) se obtuvo mediante el método soxhlet utilizando como disolvente hexano. Se realizó la caracterización química mediante cromatografía de gases acoplado a ionización de llama (CG-FID): Un total de12 ácidos grasos fueron identificados, siendo los compuestos mayoritarios los ácidos: oleico (51.75%), palmítico (28.52%), y linoleico (9.99%) respectivamente. Además, se evaluó las propiedades físicas del aceite vegetal, índices de acidez (0.003%), yodo (49.43cg/g), refracción (1.479) y de peróxidos (0.08 meqO2/kg). Finalmente, se valuó su actividad antioxidante mediante el método DPPH (78.32 µM ET/g) y ABTS (39.59 µM ET/g).

Keywords: *Bactris gasipaes*, DPPH, ABTS, CG- FID, ácido oleico.

ABSTRACT

The lipid fraction of the Bactris gasipaes (chonta) fruit was obtained by the soxhlet method using hexane as solvent. The chemical characterization was carried out employing gas chromatography coupled to flame ionization (CG-FID): A total of 12 fatty acids were identified, the main compounds being the acids: oleic (51.75%), palmitic (28.52%), and linoleic (9.99%) respectively. In addition, the physical properties of vegetable oil, acidity index (0.003%), iodine (49.43cg/g), refraction (1.479) and peroxides (0.08 meqO2/kg) were evaluated. Finally, its antioxidant activity was assessed by the DPPH method (78.32 µM ET/g) and ABTS (39.59 µM ET/g).

Keywords: *Bactris gasipaes*, DPPH, ABTS, CG- FID, oleic acid.

INTRODUCCIÓN

Bactris gasipaes es una palma perenne originaria de América Central, se sitúa generalmente en el trópico húmedo de América del Sur, se la conoce también como chonta, chontaduro, papunha, bobi, piire, pijuayo pejibaye, entre otros.[1]

La palma oscila entre los 20m a 25m de altura, se encuentra en zonas tropicales entre 24°C a 28°C se ha cultivado por los indígenas del trópico americano desde la época precolombina, particularmente para el

consumo de sus frutos. Se caracteriza por ser una especie adaptada al trópico húmedo, con lluvias entre 1.900 a 5.000 mm al año, esta produce dos productos de interés el palmito y su fruta [2].

Los frutos verdes o amarillos de *B. gasipaes* contienen más lípidos y proteínas que los rojos que son ricos en carotenoides siendo este último el pigmento orgánico involucrado en el refuerzo del sistema inmune además de la disminución del riesgo de padecer enfermedades, cardiovasculares, artritis e incluso cáncer. Todo ello como resultado de su capacidad antioxidante[3]. Estos frutos son empleados en la alimentación animal y humana, generalmente las comunidades obtienen harina, aceite pastoso[4], Adicional a ello esta palma representa una fuente significativa de hierro, niacina, retinol, riboflavina y tiamina.[5]

La fruta de la *B. gasipaes* representa un alimento funcional debido a su contenido de vitamina A, vitamina C, aminoácidos esenciales, omega 3, omega 6, y fibra dietaria, manifestada por su capacidad antioxidante, misma que se atribuye a la vitamina C, el tocoferol, los compuestos fenólicos, los antocianos, y el betacaroteno.[6]

Los ácidos grasos saturados (AGS) en su estructura química poseen enlaces químicos simples, entre los más comunes en la dieta son los C 14:0, C16:0, C18:0 encontrados en aceites de palma, siendo estructuras estables[7]. Los AGS son de síntesis endógena, necesarios para algunas funciones fisiológicas y estructurales, estos predominan en aceites con esqueleto lineal y numero par de carbonos y hacen triglicérido. Los que contienen un bajo peso molecular, es decir, inferiores a 14 carbonos se encuentra presentes en la leche de coco y palma[8].

Con el fin de aportar estudios, se identifica la composición química del aceite vegetal, así mismo, se evalúa la capacidad antioxidante[9] de origen natural que contiene la chonta, esta especie es considerada como un recurso vegetal de gran importancia económica, alimentaria, medicinal y de industria para varios países debido a que representa una de las plantas más útiles en las zonas rurales y pueblos indígenas muy aparte, se considera como un importante símbolo de identidad cultural, abundancia y alimentación.[10]

MATERIALES Y MÉTODOS

Área de estudio

El fruto se recolectó en las ferias libres de los productores locales de la parroquia Zurmi en la provincia de Zamora Chinchipe - Ecuador, en el mes de abril del 2021 con las siguientes coordenadas 04° 18’ 59.88” S, 79° 39’ 58.14” O. La muestra fue recolectada bajo el permiso de investigación MAE-DNB-CM-2016-0048.

Tratamiento post cosecha del fruto

Se seleccionaron los frutos en buen estado, realizamos una limpieza del fruto con agua destilada y se almacenó en refrigeración a -20°C para conservar las propiedades. Posteriormente se retiró las semillas del fruto, obteniendo así la pulpa con la cascara, la cual se deshidrató en una estufa de secado a 35°C durante 72 horas. Para la obtención del aceite vegetal ser realizó un proceso de molienda del fruto: la primera un molido manual de mesa, y posteriormente en un molino ultracentrífugo ZM200 disminuyendo el tamaño de las partículas, lo cual facilita la extracción del aceite.

Extracción del aceite fijo

Se realizó la extracción sólido-líquido, usando el método Soxhlet, para el cual se utilizó 100g de la chonta molida, para cada cartucho se usó 500mL hexano para la extracción del aceite, cada proceso de extracción se ejecutó durante 12 horas (este procedimiento se realizó por seis veces. Posteriormente se concentró el extracto líquido mediante el rotavapor, obteniendo de esta manera el aceite vegetal de la chonta, misma que fue almacenada en un frasco boeco a -4°C.

Determinación de las propiedades físico químicas del aceite de la chonta

Determinación el índice de yodo

El método que se empleó para encontrar el índice de yodo fue el (NTE INEN-ISO 3961: 2013) mediante titulación, "su principio se basa en solución de una porción para análisis en solvente y adición del reactivo de wijs". Posteriormente la adición de ioduro potásico y titulación del yodo liberado con una solución de tiosulfato sódico.

Determinación el índice de acidez

El método empleado para determinar el índice de acidez (NTE INEN-ISO 660, 2013), indica que la muestra se disuelve en una mezcla de solventes y los ácidos presentes se titulan con una solución de hidróxido sódico.

Determinación el índice de refracción

Se aplicó el método (NTE INEN-ISO 6320, 2013), mediante un refractómetro ABBE, marca BOECO GERMANY, que es un dispositivo electrónico que mide el índice de refracción de una muestra liquida a una temperatura especifica.

Determinación del índice de peróxidos

Mediante el método (NTE INEN-ISO 27107, 2013) en el cual la muestra se disuelve en ácido acético. El yodo liberado por los peróxidos se establece volumétricamente con una disolución patrón de tiosulfato sódico.

Caracterización química de los ácidos grasos

Mediante el método NTE INEN-ISO 5508:2014 se identificó y cuantifico los ácidos grasos del aceite vegetal de la *B. gasipaes* se utilizó un cromatógrafo de gases de serie Agilent 6890N acoplado a un detector de ionización de llama (FID) y una columna capilar de sílice fundida DB-23 (60 m '0.25 mm id.' 0.25 µm). El flujo de gas fue de 1,8 mL, se utilizó helio como gas transportador. El FID trabajo con 30 y 300 mL de gases H_2 y aire respectivamente. La inyección fue de modo Split (40:1). Las temperaturas del inyector y del detector fueron de 250 ° C. La temperatura máxima de la columna fue de 260 ° C.

Para la cuantificación se realizó un proceso de transesterificación de la muestra con solución metanólica de KOH (2N). Para la cuantificación de los ácidos grasos se utilizó un mix de estándares F.A.M.E. Mix, C4-C24 (certified reference) de marca Sulpeco. Para la integración se utilizó un programa MSD ChemStation.

Capacidad de disminución de DPPH

El ensayo de DPPH se realizó utilizando el radical libre 2,2-difenil-1-picrilhidrilo (DPPH-) basado en la técnica descrita por Brand Williams et al. [11] y Thaipong et al.[12] según lo descrito por Valarezo et al. [13] se utilizó Trolox como control positivo y metanol como blanco. Las muestras se evaluaron en un espectrofotómetro UV (Genesys 10S UV.Vis Spectrophotometer, Thermo Scientific, Waltham, MA, USA) a una longitud de onda de 515 nm. El porcentaje de disminución de radicales DPPH se calculó según la ecuación (1). SC_{50} es la concentración de AAG que proporcionó el 50% de disminución del DPPH.

$$(1)\ SC\ (\%) = \frac{(AAG - AMeOH)}{AAG} * 100$$

donde AAG es la absorbancia del DPPH- mezclado con AG y AMeOH es la absorbancia del DPPH mezclado con metanol.

Capacidad antioxidante por el método ABTS

El ensayo ABTS se realizó utilizando el catión radical del ácido 2,2′-azinobis-3-etilbenzotiazolina-6-sulfónico (ABTS-+) de acuerdo con el procedimiento reportado por Arnao et al. [11] y Thaipong et al. [12] , tal como lo describen Valarezo et al.[13] . Las muestras se evaluaron en un espectrofotómetro UV (Genesys 10S UV.Vis Spectrophotometer, Thermo Scientific, Waltham, MA, USA) a una longitud de onda de 734 nm. Se utilizó agua desionizada como blanco y trolox como control positivo. El porcentaje de capacidad de disminución del radical ABTS se calculó según la ecuación.

$$(2) Sc\ (\%) = \frac{(ASO - ASA)}{ASO} * 100$$

donde ASO es la absorbancia de ABTS-+ con la mezcla de disolventes y ASA es la absorbancia tras la reacción de ABTS-+ con la muestra.

RESULTADOS Y DISCUSIÓN

Propiedades Fisicoquímicas del fruto *Bactris gasipaes*

Se reportan las características fisicoquímicas del fruto, las mismas que se analizaron de acuerdo a los métodos analíticos de la AOAC (1992) (**Tabla 1**) y se compararon con las normas INEN para grasas y aceites.

Parámetro	Método	Unidad	Resul-tado	Requisito Norma NTE INEN	
				Mín.	Máx.
Índice de yodo	INEN 37	cg/g	49.43	44	60
Índice de acidez	AOAC 942.15ª	%	0.003	--	0.2
Índice de peróxido	INEN 277	meq O2/kg	0.08	--	10.00
Índice refracción	INEN 42	--	1.479	1.453	1.4595

Tabla 1: Resultados de propiedades fisicoquímicas del aceite vegetal de *B. gasipaes.*

El porcentaje obtenido de yodo en la muestra, comparado con el valor de referencia en la normativa, se encuentra dentro del rango indicado. Sin embargo, Mujica y colaboradores [14] mencionan que, el índice de yodo es una medida del grado de instauración de los ácidos grasos, este valor es indicativo del alto contenido de ácidos grasos insaturados establecidos precedentes en el aceite de la chonta, además, indica que el aceite es sensible a la oxidación, debido a que los índices de yodo son inferiores a 100 cg/g se les denomina como no secantes.

En lo referente a la acidez del aceite extraído con agua es mayor a 0.9%, el cual es usado para predecir condiciones de procesamiento y características finales del aceite. Este valor puede ser debido a la dificultad de separación de fases durante la etapa de decantación [15]. Por ende, se comprueba que el menor índice de acidez posible da como resultado un aceite de calidad, mientras que los altos niveles de acidez favorecen la formación de jabones, disminuyendo la eficiencia y desfavoreciendo la separación de fases. El índice de acidez expresado para el aceite de la chonta da como resultado un valor de 0.003% a temperatura ambiente, encontrándose dentro de los límites establecidos de las Normativas INEN 30 (--, 0.2%), aplicando el método oficializado AOAC 942.15 mediante titulación gastándose un volumen de 7.1 KOH. Según Córdova (2016), menciona que a mayor temperatura se obtiene mayor acidez en la relación agua y fruto.

Según, la norma NTE INEN-ISO 27107, 2013 especifica que el índice de peróxidos es el número de miliequivalentes de oxígeno por kilogramo de muestra determinado. De acuerdo con esta norma, este método oficializado es empleado en este estudio de caso.

El valor obtenido del índice de peróxido es de 0.08meq O2/kg. LA NTE INEN 30, especifica que la cantidad de peróxido total (meq O2/kg) debe encontrarse en un rango de (--,10). Si se compara el porcentaje de peróxido obtenido con el valor de referencia de la normativa se puede observar que se encuentra dentro del rango establecido, lo cual ratifica que los compuestos químicos que contiene el aceite son las adecuadas.

En las características fisicoquímicas del aceite del endospermo de la Pala Yagua (*Attalea cryptanther*) enfatiza que los bajos valores de peróxidos es una característica de grasas con alta resistencia a la oxidación, lo que favorece su fabricación de mantecas y margarinas [16]. Sin embargo, Mujica (2017) menciona que el aceite de la chonta contiene un valor de 9.32 meq O2/kg, llegando al límite establecido por la norma INEN 30, esto se le puede atribuir al deterioro del aceite por mecanismo u oxidación debido al contacto de la muestra con el oxígeno presente en el ambiente antes de realizar la prueba, concluyendo de esta manera que el aceite de chonta es sensible al proceso de oxidación.

El índice de refracción obtenido para nuestro aceite es de 1.479, si se compara el índice de refracción con el valor de referencia se encuentra superior a lo establecido por la norma, debido a que el índice de refracción aumenta con el grado de instauración de los ácidos grasos contenidos en el aceite. Además, en un estudio realizado en Venezuela sobre la evolución de las propiedades del aceite de la *B. gasipes* indica que el índice de refracción del aceite de la *Bactris gasipaes* es de 1.42 similar al resultado se ha obtenido en este estudio.[14]

Composición química d los acidos grasos del fruto *B. gasipaes*

Los ácidos grasos mayoritarios presentes en el aceite de la chonta (*Bactris gasipaes*) fueron: oleico (51.75%), palmítico (28.52%), linoleico (9.99%), en su mayoría fueron ácidos grasos monoinsaturados (58.01%) respecto a los ácidos grasos polinsaturados y a los ácidos grasos saturados. En contraste, con los estudios realizados en Colombia indican que el aceite extraído mediante soxhlet de la variedad *Bactris gasipaes var chichagui* en la cual los componentes principales fueron: ácido oleico (51.89%), palmítico (34.95%), palmitoleico (7.95%). Sin embargo, Restrepo, Estupiñán, & Colmenares (2016), mencionan que el estudio y la muestra de la chonta tiene un valor mayor de los ácidos grasos monoinsaturados (59.84%).[17]

CLASIFICACIÓN	PARÁMETRO	RESULTADO (%)
ÁCIDO GRASO SATURADOS	Ácido láurico	0.04
	Ácido miristico	0.12
	Ácido pentadecanoico	0.12
	Ácido palmítico	28.52
	Ácido heptadecanoico	0.03
	Ácido estearico	1.41
	Ácido araquidico	0.08
	Ácido behenico	0.08
ÁCIDOS GRASOS MONOINSATURADOS	Ácido palmitoleico	6.26
	Ácido oleico	51.75
ÁCIDO GRASO POLIINSATURADO	Ácido linoleico	9.99
	Ácido linolénico	1.60

Tabla 2: Ácidos Grasos del fruto *Bactris gasipaes.*

El aceite vegetal de la chonta presenta ácidos grasos similares a los del aceite de oliva, el aceite de oliva contiene ácidos grasos monoinsaturados (73.17%), poliinsaturados (10.75%), saturados (15.8%), siendo estables a la oxidación debido que es un ácido graso con un solo enlace [18]. Siendo el aceite de oliva [19] y el aceite de la chonta una fuente de energía para el sistema nervioso, presentando de esta forma, una acción antiinflamatoria y a su vez de disminuir la fracción transportada en LDL sin modificar o incrementar el contenido de las HDL.[8]

Estas proporciones ocurren de igual manera en aceites de origen vegetal como el de aguaje o morete (*Mauritia flexulosa*). Sin embargo, el aguaje tiene mayor cantidad de ácido oleico (75.63%), cuyo ácido es beneficioso en los vasos sanguíneos reduciendo el riesgo de sufrir enfermedades cardiovasculares.[20]

Evaluación de la actividad antioxidante del fruto de *Bactris gasipaes*

El resultado obtenido de IC_{50} expresada en ug/mL para el aceite de la chonta, se evidencia que mediante el método de captación del radical DPPH se adquirió como resultado el IC_{50} 364.4ug/mL con 78.32 uM ET/g de aceite, mientras que mediante el método de captación del radical ABTS se obtuvo el resultado de IC_{50} de 161.009ug/mL con 39.59ug ET/g.

	IC_{50} ug/ml	SD	µM ET/g extracto	SD
DPPH	364,40	0,026	78,32	2,92
ABTS	161,01	0,027	39,59	1,80

Tabla 3: Evaluación de la actividad antioxidante del fruto de *Bactris gasipaes.*

Un estudio previo demostró que el aceite de chonta en su evaluación de la capacidad antioxidante diluido en DMSO mediante el método DPPH, obtuvo un resultado de IC_{50} de 1018mg/l, en lo que se menciona que de acuerdo con los datos del IC_{50} del aceite de la chonta y al existir una relación inversamente proporcional, a mayor valor de IC_{50} menor actividad antiradical. [21] comparando los estudios se indica que se obtuvo un mejor resultado de actividad antioxidante mediante el método ABTS.

Por otro lado, Torres 2009 menciona en su estudio que la actividad antioxidante del aceite de fruto de *Anonna muricata* (Guanábana) obtuvo como resultado el IC_{50} en DPPH de 6938ug/ml y en ABTS de 8385 ug/ml, por lo tanto, el aceite *Batris gasipaes* presenta mayor actividad antioxidante[22]. Se realiza el método DPPH y ABTS debido a que estos métodos presentan buena estabilidad, aunque también muestran diferencias y así poder evidenciar con mayor precisión la actividad antioxidante que presenta la grasa de la chonta.

CONCLUSIONES

Las propiedades fisicoquímicas del aceite de la *Bactris gasipaes*, presentan los índices de yodo (49.43cg/g), acidez (0.003%), peróxidos (0.08 meq O2/kg) y refracción (1.479).

La caracterización química del aceite vegetal de la chonta (*B. gasipaes*) obtenido a partir de los frutos, se identificaron 12 compuestos, principalmente ácidos grasos monoinsaturados (58.01%). Además, este fruto presenta un gran valor nutricional debido a su contenido de ácidos grasos poliinsaturados (11.59%); siendo los ácidos de mayor concentración el oleico (51.75%) y linoleico (9.99%).

La actividad antioxidante del aceite de la *B. gasipaes* presenta un IC_{50} 364.50 ug/ml por el método DPPH, por otra parte, por el método ABTS se obtuvo un IC_{50} de 161.01 ug/ml. Demostrando tener una fuente natural de antioxidantes con potencial aplicación en la industria alimenticia. El aceite presento mayor actividad captadora de radicales mediante el método ABTS.

Agradecimientos

Agradecemos a la Universidad Técnica Particular de Loja por el financiamiento de la investigación.

REFERENCES

1. Yang, J. (2010). *Distribución, importancia económica y domesticación de la palma chonta (Bactris gasipaes)*. 26.
2. Pasquel, A., Del Castillo, A., Sotero, V., & García, D. (2002). Extracción del aceite de la cáscara de Bactris gasipaes HBK usando dióxido de carbono presurizado. *Revista Amazónica de Investigación Alimentaria*, *2*(1), 1–14.
3. Hooghiemstra, H., Cleef, A., Noldus, C., & M.Kappelle. (2012). Dinámica de la vegetación del Cuaternario superior y paleoclimatología del área del pantano La Chonta (Cordillera de Talamanca, Costa Rica). Revista de ciencia cuaternaria.
4. Mondragon Diaz, A. F. (2019). Determinación de las características agronómicas de 6 Ecotipos de Pijuayo para Palmito (Bactris Gasipaes K.) con posibilidades de propagación y desarrollo en la zona del Pongo de Caynarachi-San Martín.
5. Serrano, M., Umaña, G., & Sáenz, M. V. (Diciembre de 2011). Fisiología poscosecha, composición química y capacidad antioxidante de frutas de pejibaye (bactris gasipaes kunth) cv. Obtenido de Scielo: https://www.scielo.sa.cr/scielo.php?script=sci_arttext&pid=S0377-94242011000200006
6. Montealegre, Y. (enero de 2020). CARACTERIZACIÓN FISICOQUÍMICA Y NUTRICIONAL DE PASABOCAS DE CHONTADURO (Bactris gasipaes) EMPLEANDO PARA SU ELABORACIÓN DIFERENTES TECNOLOGÍAS DE SECADO. Obtenido de Repository: https://repository.unad.edu.co/bitstream/handle/10596/31888/ymontealegrer.pdf?sequence=1&isAllowed=y
7. Torrejón, C., & Uauy, R. (2011). Calidad de aceite, arterioesclerosis y enfermedad coronaria: Efectos de los ácidos grasos saturados y ácidos grasos trans. Revista Medica de Chile, 139(7), 924–931. https://doi.org/10.4067/S0034-98872011000700016.
8. Cabezas-Zábala, C. C., Hernández-Torres, B. C., & Vargas-Zarate, M. (2016). Aceites y aceites: efectos en la salud y regulación mundial. Revista de La Facultad de Medicina, 64(4), 761. https://doi.org/10.15446/revfacmed.v64n4.53684.
9. Jatunov, S., Quesada, S., Díaz, C., & Murillo, E. (2010). Carotenoid composition and antioxidant activity of the raw and boiled fruit mesocarp of six varieties of Bactris gasipaes. *Archivos latinoamericanos de nutrición*, *60*(1), 99.
10. Llumiquinga, M. (18 de Marzo de 2021). Análisis del estado actual de Bactris gasipaes Kunth en el Ecuador. Obtenido de ESPE: http://repositorio.espe.edu.ec/xmlui/bitstream/handle/21000/24215/T-ESPE-044451.pdf?sequence=1&isAllowed=y#:~:text=Bactris%20gasipaes%20Kunth%20se%20considera,alimentaci%C3%B3n%20(Mac%C3%ADa%2C%202004).
11. Brand-Williams, W.; Cuvelier, M.E.; Berset, C. Use of a free radical method to evaluate antioxidant activity. LWT Food Sci. Technol. 1995, 28, 25–30.
12. Thaipong, K.; Boonprakob, U.; Crosby, K.; Cisneros-Zevallos, L.; Hawkins Byrne, D. Comparison of ABTS, DPPH, FRAP, and ORAC assays for estimating antioxidant activity from guava fruit extracts. J. Food Compos. Anal. 2006, 19, 669–675.

13. Valarezo, E.; Rivera, J.X.; Coronel, E.; Barzallo, M.A.; Calva, J.; Cartuche, L.; Meneses, M.A. Study of Volatile Secondary Metabolites Present in *Piper carpunya* Leaves and in the Traditional Ecuadorian Beverage Guaviduca. *Plants* **2021**, *10*, 338.
14. Mujica, F., Viky, C., Rodriguez, M., Lopez, S., & Mendez, D. (2017). Evaluation of oil properties of fruit pulp pijiguao (Bactris Gasipaes H.B.K) for use in cosmetics industry. Ingeniería UC, 24(3), 314–326. Retrieved from https://www.redalyc.org/pdf/707/70754692006.pdf
15. Córdova, F. (2016). Producción De Biodiesel a Partir De Aceite Vegetal Extraído Del Fruto De La Palma Bactris Gasipaes (Chontaduro) (Universidad Libre). Retrieved from https://repository.unilibre.edu.co/bitstream/handle/10901/9818/Trabajo final Maestria Fausto.pdf?sequence=1
16. García-Pantaleón, D. M., González, J., Moreno-Álvarez, M. J., Belén-Camacho, D. R., Medina-Martínez, C., & Linares, O. (2006). Características fisicoquímicas del aceite del endospermo de la Palma Yagua (Attalea cryptanther). Aceites y Aceites, 57(3), 308–312.
17. Restrepo, J., Estupiñán, J. A., & Colmenares, A. J. (2016). Comparative study of lipid fractions from Bactris gasipaes Kunth (peach palm) obtained by soxhlet and supercritic CO2 extraction. Revista Colombiana de Química, 45, 5–9. https://doi.org/http://dx.doi.org/10.5446/rev.colomb.quim.v45nl.57199
18. Romero, L., Valdiviezo, C., & Bonilla, S. (2019). Characterization of sacha inchi seed oil (plukenetia volubilis) from "Canton San Vicente, Manabí, Ecuador", obtained by non-thermal extrusion processes. Revista de Ciencia de La Vida, 30(2), 77–87. https://doi.org/http://doi.org/10:17163/lgr.n30.2019.07
19. Valenzuela, A., & Nieto, S. (2003). Ácidos grasos omega-6 y omega-3 en la nutrición perinatal: su importancia en el desarrollo del sistema nervioso y visual. *Revista chilena de pediatría*, *74*(2), 149-157.
20. Restrepo, J., Arias, N., & Madriñán, C. (2018). Determination of the Nutritional Value, Fatty Acid Profile and Antioxidant Capacity of Aguaye pulp (Mauritia Flexuosa). Revista de Ciencias Naturales y Exactas, 20(1), 8. https://doi.org/10.25100/rc.v20i1.6109.
21. Martínez, A. (2011). Evaluación la actividad antioxidante de los aceites y de su fracción insaponificable de los frutos de: Mauritia flexuosa (Morete), Bactris gasipaes (Chonta), Plukenetia volubilis (Sacha inchi) y Oneocarpus batahua (Ungurahua). Universidad Politecnica Salesiana, 131.
22. Torres, J. (2019). Evaluación de ácidos grasos y actividad antioxidante in vitro del aceite de la semilla de *Annona muricata*.

Received: October 9th 2023/ **Accepte**d: January 15th 2024 / **Published:**15 February 2024

Citation: Calva J., Sanchez D. & Morocho V. Chemical Study and Antioxidant activity of lipid fraction from *Bactris gasipaes* Kunth (peach palm) a fruit used as food in the Ecuadorian Amazonic. Revis Bionatura 2024; 9 (1) 67. http://dx.doi.org/10.21931/RB/2024.09.01.67

Additional information Correspondence should be addressed to svmorocho@utpl.edu.ec
Peer review information. Bionatura thanks anonymous reviewer(s) for their contribution to the peer review of this work using https://reviewerlocator.webofscience.com/

Bionatura ISSN. First 13909355 Ecuador. **Scopus coverage years**: from 2016 to the present

Publisher's Note: Bionatura stays neutral concerning jurisdictional claims in published maps and institutional affiliations.

Bionatura
Ibero-American Journal of Biotechnology and Life Sciences

Article

Estrategia de intervención educativa para el abordaje del riesgo cardiovascular en pacientes con hipertensión arterial

Educational intervention strategy to address cardiovascular risk in patients with high blood pressure

Karen Rojas-Montenegro[1], Gustavo Cisneros-Cañas[1], Rosario Suárez de Terán[2], Ruben Cajilima-Vega[1], Cecilia Arteaga-Pazmiño[3], Evelyn Frias-Toral[4]*

[1]Área Biológica y Biomédica, Universidad Técnica Particular de Loja, Ecuador.
[2]Escuela de Medicina, Universidad Técnica Particular de Loja, Ecuador.
[3]Carrera de Nutrición y Dietética, Universidad de Guayaquil, Guayaquil, Ecuador.
[4]Escuela de Medicina, Universidad Espíritu Santo, Samborondón, Guayaquil, Ecuador.
** Correspondence: ceciliaarteagap@gmail.com*
Available from. http://dx.doi.org/10.21931/RB/2024.09.01.68

ABSTRACT

Cardiovascular diseases (CVD) are the leading cause of preventable death worldwide and nationally. Faced with this problem, educational strategies are essential in preventing and managing CVD. Aim: This study aimed to develop an academic intervention strategy to address cardiovascular risk (CVR) in patients with high blood pressure (HTN). A quasi-experimental study was carried out in which CVR and lifestyle habits were determined through the Globorisk and FANTASTIC Scale, respectively, before the educational intervention and after it, in a population of 97 patients of 40 to 79 years of age with primary HTN in the period from March to August 2021. The intervention consisted of educational strategies to promote healthy lifestyle habits and the prescription of an individualized eating plan according to the needs of the participants. Results: After the intervention, blood pressure control was obtained in 28.86% of the study population, body mass index decreased by 3.1%, CVR decreased by 11.34%, and healthy lifestyles improved by 9.15% (p=0.000) in all variables. Conclusions: In patients with HTN, educational interventions to promote healthy lifestyles improve CVR factors.

Keywords: Arterial hypertension; Cardiovascular risk; Healthy lifestyles; Primary health care.

RESUMEN

Introducción: Las enfermedades cardiovasculares (ECV) son la principal causa de muerte prevenible a nivel mundial y nacional. Frente a esta problemática, las estrategias educativas son esenciales en la prevención y manejo de las ECV. Objetivo: El objetivo de este estudio fue desarrollar una estrategia de intervención educativa para abordar el riesgo cardiovascular (RCV) en pacientes con hipertensión arterial (HTA). Métodos: Se realizó un estudio cuasi-experimental, en el que se determinó el RCV y hábitos de vida a través de la Escala Globorisk y FANTASTIC, respectivamente, previo a la intervención educativa y posterior a ésta, en una población de 97 pacientes de 40 a 79 años de edad con HTA primaria en el periodo de marzo a agosto del 2021. La intervención consistió en estrategias educativas para promover hábitos de vida saludables, y la prescripción de un plan de alimentación individualizado de acuerdo a las necesidades de los participantes. Resultados: Posterior a la intervención se obtuvo un control de la tensión arterial en el 28.86% de la población de estudio, el índice de masa corporal disminuyo en el 3.1%, el RCV disminuyó en un 11.34%, y los estilos de vida saludables mejoraron en un 9.15% (p=0.000) en todas las variables. Conclusiones: En los pacientes con HTA, las intervenciones educativas para promover estilos de vida saludables, mejoran los factores de RCV.

Keywords: Hipertensión arterial; Riesgo cardiovascular; Estilos de vida saludables, Atención primaria en salud.

INTRODUCCIÓN

Según la Organización Mundial de la Salud (OMS), la principal causa de muerte a nivel mundial son las enfermedades cardiovasculares (ECV), de las cuales, la cardiopatía isquémica ocupa el primer lugar y es responsable del 16% del total de muertes en el mundo[1]. El aumento de muertes por esta enfermedad se ha incrementado de forma exponencial, pasando de más de 2 millones de defunciones en 2000 a 8,9 millones en 2019[2]. Por otro lado, la incidencia de hipertensión arterial (HTA) ha aumentado en los últimos 40 años en adultos, partiendo de 594 millones en 1975 a 1130 millones en 2015[3,4]. Este incremento se ha observado especialmente en países de bajos y medianos ingresos bajos, relacionado con el aumento de los factores de riesgo cardiovascular (RCV) a los que están expuestos los individuos de países en situaciones de vulnerabilidad[4]. En Ecuador, según la encuesta STEPS, la prevalencia de HTA es del 20% en mayores de 19 años[5].

En 2018 se reportaron 5776 egresos hospitalarios por HTA primaria según el registro estadístico de Egresos Hospitalarios del Instituto Nacional de Estadísticas y Censos (INEC)[6]. En la ciudad de Loja se ha reportado una prevalencia de HTA de 7,9%[7].

Frente a la creciente incidencia y prevalencia de ECV, las guías para prevención de ECV del Colegio Americano de Cardiología y la Asociación Americana del Corazón (ACC/AHA) recomiendan realizar el manejo de los factores de RCV modificables en pacientes con HTA como estrategia preventiva de esta enfermedad[8]. La dieta y el ejercicio son factores modificables en la prevención primaria y secundaria de la ECV[9–13], por lo cual, la intervención en estas variables es esencial en el contexto de HTA y RCV.

La restricción de la sal dietética se ha descrito como un factor preventivo y una estrategia terapéutica en individuos con HTA[14,15]. Sin embargo, evidencia reciente sugiere que más allá de la restricción de sodio, el alto consumo de verduras, cereales integrales y frutas, ricos en compuestos bioactivos, antioxidantes, potasio y vitamina C, podrían modular de forma positiva los niveles de presión arterial[16–18]. Por otro lado, la combinación de ejercicio de fuerza 2-3 veces por semana a una intensidad moderada e intervención nutricional parecen ser eficaces en términos de reducción de la presión arterial[19], y con ello, en la modulación del RCV[20–22].

Las intervenciones de educación sanitaria en atención primaria y secundaria son estrategias diseñadas para promover estilos de vida saludables, en los que se involucra la dieta y la actividad física, que podrían ser efectivas en la modulación del RCV en pacientes con HTA[23].

El objetivo de este estudio fue desarrollar una estrategia de intervención educativa para el abordaje del RCV en pacientes con HTA.

MATERIALES Y MÉTODOS

Diseño y participantes: El presente estudio tuvo un diseño cuasi-experimental de tipo prospectivo en una muestra no probabilística de pacientes con diagnóstico de HTA en el periodo de marzo a agosto del año 2021 en la ciudad de Loja, Ecuador.

Se incluyeron a sujetos con diagnóstico de HTA primaria, que tuvieran otra patología asociada como: dislipidemias, diabetes, obesidad, hipotiroidismo; pacientes que manifestaron su voluntad de participar en el estudio y firmaron consentimiento informado. Los criterios de exclusión fueron: pacientes con diagnóstico de TA que presentaron deterioro cognitivo y personas con enfermedades degenerativas avanzadas (cáncer en estadios avanzados, enfermedades autoinmunitarias con compromiso cardiovascular).

Medidas e instrumentos

Variables sociodemográficas. La recolección de datos sociodemográficos se realizó a través de una entrevista en la consulta médica o en la visita domiciliaria.

Variables de estilo de vida. Se realizó la determinación de los estilos de vida con la escala de autoevaluación FANTASTIC. Se aplicó el cuestionario estilo de vida FANTASTIC que evalúa los estilos de vida desde una perspectiva multidimensional puesto que abarca situaciones con la familia y amigos, actividad física, nutrición, tabaco, alcohol, sueño y estrés, personalidad e introspección, trabajo, actividad diaria, y uso de drogas. Las categorías mencionadas se agrupan en 25 preguntas con tres opciones de respuesta con valor numérico de 0 a 2 para cada una de ellas, dando como resultado 5 categorías: de 0 a 39 zona de peligro, de 40 a 59 algo bajo, de 60 a 69 adecuado, de 70 a 84 buen trabajo, y de 85 a 100 excelente. La categoría "Excelente" es un indicador de que el estilo de vida del sujeto representa una influencia óptima para la salud; "Bueno" indica que el estilo de vida representa una influencia adecuada para la salud; "Regular" indica que el estilo de vida representa un beneficio para la salud, aunque también presenta riesgos; "malo y existe peligro" es un indicador de que el estilo de vida del sujeto representa muchos factores de riesgo [24].

Variables de riesgo cardiovascular. Se usó la Escala Globorisk [25] para determinar el RCV, previo a realizar la intervención educativa. Para la aplicación de la Escala Globorisk, previamente se realizó la medición de la presión arterial, siguiendo las recomendaciones de la guía del MSP de HTA del año 2019 [26], así como la medición del peso (kg) y de la talla (cm) según las normas de la OMS para determinar el índice de masa corporal (IMC [kg/m^2]), los mismos que fueron registrados en una base de datos de Excel.

Intervención educativa

Posterior a la aplicación inicial de las escalas, se realizó una charla educativa individualizada de aproximadamente 40 minutos el día de la consulta en la unidad operativa o en la visita domiciliaria. En la charla se abarcaron temas sobre alimentación adecuada y la importancia de la actividad física diaria, para lo cual, se utilizó material audiovisual y se incluyó a todos los pacientes en un grupo de WhatsApp que tuvo por nombre de "Corazones Saludables", a través del cual se realizó educación sanitaria a través de cápsulas informativas relacionadas con alimentación, actividad física, complicaciones de la HTA y cómo prevenirlas, y estilo de vida saludable. Adicionalmente, en esta primera fase, se proporcionó a todos los participantes un plan de alimentación modelo diseñado por un nutricionista.

Seguimiento

Los investigadores diseñaron una herramienta tecnológica que consistió en una aplicación móvil que llevaba el nombre de Corazones Saludables, por medio de la cual, los participantes tuvieron acceso a información sobre estilos de vida saludables. Además, se realizó la entrega de un calendario con frases motivacionales para el registro del cumplimiento de la actividad física. A través del seguimiento grupal e individual se obtuvo retroalimentación de la información socializada; el cumplimiento de los objetivos se valoró a través del registro fotográfico de la alimentación y la realización de actividad física.

Evaluación de intervención

Luego de cinco meses de la recolección de datos y la charla educativa iniciales, se realizó la reevaluación del RCV y del estilo de vida, a través de las escalas anteriormente mencionadas.

Análisis estadístico

Los datos recolectados pre y post intervención fueron ingresados en una matriz Excel y fueron analizados con el paquete estadístico SPSS® 27. Para el tratamiento estadístico de las variables cuantitativas se utilizaron medidas de tendencia central y desviación estándar o rango intercualítico según su distribución simétrica o

asimétrica, respectivamente; para las variables categóricas se utilizaron porcentajes y frecuencias. Para comparar el RCV y los estilos de vida antes y después de la intervención se utilizó la prueba t Student para muestras pareadas. Se consideró significativo un valor p <0,05.

Aspectos éticos

El estudio fue aprobado por el Comité de Ética e Investigación en Humanos de la Universidad Técnica Particular de Loja.

RESULTADOS

Un total de 97 pacientes con diagnóstico de HTA con una mediana de edad de 58 (40-79) años. El 63,9% (n=62) fueron mujeres y el 36,1% (n=35) fueron hombres. El hipotiroidismo y dislipidemias fueron prevalentes en el 24,7% (n=24) de los participantes y la diabetes mellitus tipo 2 en el 19,6% (n=19) (Tabla 1).

Variable	Total
Edad (años), mediana (RI)	58 (40-78)
Género, n (%)	
Femenino	62 (63,9)
Masculino	35 (36,1)
Peso (kg), media ± DE	75,9 ± 12,4
IMC (kg/m^2) media ± DE	31,8 ± 4,9
Diabetes, n (%)	62 (63,9)
Hipotiroidismo, n (%)	24 (24,7)
Dislipidemia	24 (24,7)
RI, rango intercuartílico; DE, desviación estándar; IMC, Índice de masa corporal	

Table 1: Características de la población de estudio.

Indicadores de riesgo cardiovascular previa intervención educativa

Respecto a la interpretación del IMC basal, el 6,2% (n=6) presentó normopeso, el 36,1% (n=35) sobrepeso, el 32% (n=31) obesidad grado I, el 17,5% (n=17) obesidad grado II, el 8,2% (n=8) obesidad grado III.

El perímetro abdominal de los sujetos estudiados fue 103,9 ± 10,7 cm. El 19,5% (n= 20) de los participantes presentó RCV aumentado.

El 14,4% (n=14) presentó RCV según la escala de autoevaluación de estilos de vida FANTASTIC, y el 46,4% (n=45) tenía descompensación de la presión arterial según la escala Globorisk. La puntuación media de RCV en la muestra fue de 7,2 ± 4,3%.

Previo a la intervención educativa, el 39,2% (n=38) presentó un RCV bajo, el 41,2% (n=40) tenía RCV intermedio, el 18,6% (n=18) RCV alto y el 1% (n=1) RCV muy alto (Tabla 2).

Presión Arterial	**Masculino**		**Femenino**			**TOTAL**
	n	%	n	%	n	**%**
Óptima	5	5,2	11	11,3	16	16,5
Normal	10	10,3	13	13,4	23	23,7
Normal Alta	3	3,1	10	10,3	13	13,4
HTA grado 1	12	12,4	18	18,6	30	30,9
HTA gado 2	3	3,1	7	7,2	10	10,3
HTA grado 3	2	2,1	3	3,1	5	5,2
Total	35	36,1	62	63,9	97	100
Total, no controlados	17	17,5	28	28,8	45	46,3
Riesgo Cardiovascular	Masculino		Femenino			TOTAL
	n	%	n	%	n	%
Bajo	8	8,2	30	30,9	38	39,2
Intermedio	14	14,4	26	26,8	40	41,2
Alto	12	12,4	6	6,2	18	18,6
Muy alto	1	1,0	0	0,0	1	1,00
Total	35	36,1	62	63,9	97	100,0
Total, RCV aumentado	13	13,4	6	6,1	19	19,5
Estilo de vida	Masculino		Femenino		TOTAL	
	n	%	n	%	n	%
Zona de peligro	1	1,0	0	0,0	1	1,0
Algo bajo	4	4,1	9	9,3	13	13,4
Adecuado	5	5,2	23	23,7	28	28,9
Buen trabajo	18	18,6	25	25,8	43	44,3
Estilo de vida (FAN-TASTIC)	7	7,2	5	5,2	12	12,4
Total	35	36,1	62	63,9	97	100,0
Total, estilo de vida de riesgo	5	5,1	9	9,2	14	14,4

HTA, hipertensión arterial; PAD, presión arterial diastólica; PAS, presión arterial diastólica, RCV, riesgo cardiovascular.

Tabla 2: Indicadores basales de presión arterial, riesgo cardiovascular y estilos de vida de la población estudiada.

Indicadores de riesgo cardiovascular posterior a intervención educativa

Posterior a la intervención educativa el 9,3% (n=9) presentó normopeso, el 37,1% (n=37) sobrepeso, el 30,9% obesidad grado I, el 17,5% (n=17) obesidad grado II, el 7,2% (n=7) obesidad grado III,

El perímetro abdominal de los sujetos estudiados después de la intervención fue de 102,4 ± 10,6 cm.

El 6,1% (n=6) presentó RCV según la escala de autoevaluación de estilos de vida FANTASTIC, el 17,5% (n=17) tenía descompensación de la presión arterial.

El 52,6% (n=52) presentó un RCV bajo, el 36,1% (n=35) tenía RCV intermedio, el 10,3% (n=10) RCV alto y el 1% (n=1) RCV muy alto. La puntuación media de RCV fue de 6,2 ± 3,6%.

Se encontró una diferencia estadísticamente significativa en los indicadores mencionados posterior a la intervención educativa, como se muestra en la Tabla 3.

Variables	Resultados Pre-Intervención Media ± DE	Resultados Pos-Intervención Media ± DE	Valor p
Riesgo cardiovascular, puntaje	7,2 ± 4,3	6,2 ± 3,6	0,000*
Estilo de vida, puntaje	70,4 ± 12,6	79,1 ± 10,2	0,000*
Peso, kg	75,9 ± 12,3	75,1 ± 12,2	0,000*
Perímetro abdominal, cm	103,9 ± 10,7	102,4 ± 10,6	0,000*
Índice de masa corporal, kg/m^2	31,7 ± 4,9	31,4 ± 4,8	0,000*
Tensión arterial sistólica, mmHg	133,1 ± 18,7	124,3 ± 10,9	0,000*
Tensión arterial diastólica, mmHg	82,3 ± 11,6	78,9 ± 7,4	0,000*
Categoría de riesgo cardiovascular, n (%)			
Bajo	38 (39,2)	51 (52,6)	0,000*
Intermedio	40 (41,2)	35 (36,1)	0,000*
Alto	18 (18,6)	10 (10,3)	0,000*
Muy alto	1 (1)	1 (1)	0,598
*Valor p estadísticamente significativo DE, desviación estándar			

Tabla 3: Indicadores de riesgo cardiovascular pre y post intervención educativa.

DISCUSIÓN

En la presente investigación se observó una mejoría significativa en los FRC modificables y en los estilos de vida saludables en sujetos con HTA posterior a una intervención educativa de 5 meses.

Respecto al puntaje de RCV, los resultados de esta investigación reportaron un valor medio de 7,2, contrastando con los reportados por Goyer et al., quienes identificaron una media de 16,0 en una población de 400 individuos [27]. Estas diferencias pueden estar relacionadas con el tipo de herramienta utilizada para valorar el RCV, puesto que en el estudio mencionado se utilizó la escala de Framingham. En una cohorte mexicana de pacientes con hipertensión arterial en seguimiento, el RCV intermedio, identificado en el 31,4% de los sujetos, fue menor al reportado en la misma categoría (41,2%) en la presente investigación. No obstante, el puntaje de RCV, valorado por la escala Globorisk, fue mayor en la población mexicana estudiada (12,3 vs. 7,2); las diferencias entre los estudios pueden estar influenciadas por el tamaño muestral [28].

La intervención educativa aplicada en esta investigación fue efectiva para reducir los puntajes de RCV (7,2 ± 4,3% vs. 6,2 ± 3,6%) y las categorías del mismo. Un impacto mayor se ha descrito en un estudio basado en un programa estructurado de estilos de vida saludables durante un año realizado en una unidad de atención primaria en Suecia, en el que se observó una mejoría del puntaje de RCV del 24,8% al 21,4% (disminución de 3,4 puntos) [29]. Las diferencias entre los valores obtenidos en este estudio y en la población sueca en pueden atribuirse a las discrepancias en el tiempo de seguimiento de ambos programas.

Por otro lado, las intervenciones en el estilo de vida, ya sea como complemento de la terapia con medicamentos o de forma independiente, en aquellos pacientes en los que los medicamentos pueden ser mal tolerados, tener un costo prohibitivo o ser ineficaces, pueden reducir significativamente la mortalidad cardiovascular y el riesgo de eventos cardíacos recurrentes [30].

Respecto a los estilos de vida, posterior a la intervención educativa realizada en este estudio, se evidenció un cambio positivo en las categorías de los 10 aspectos evaluados. Estos resultados fueron similares a los

descritos por Lidin et al., quienes reportaron una mejoría del 43% al 24% en los estilos de vida posterior a un año de una intervención con un programa estructurado multidisciplinario de estilos de vida [31].

Leiva et al., concluyeron que mientras mejoran los estilos de vida disminuyen los factores de riesgo para sufrir ECV [32]. En el presente estudio, se evidencia una mejora significativa en los estilos de vida posterior a la intervención con un programa educativo estructurado, y que, a su vez, logró una disminución del riesgo de sufrir enfermedades cardiovasculares y demás patologías relacionadas con estilos de vida no saludables. Este estudio se destaca por ser uno de los pioneros en evidenciar el impacto de programas de intervención educativa sobre el riesgo cardiovascular a nivel nacional.

No obstante, este estudio presenta limitaciones como el seguimiento a corto plazo de los pacientes y la ausencia de indicadores bioquímicos de RCV.

Con base en los resultados obtenidos y la fundamentación teórica de la literatura científica revisada, se recomienda un mayor énfasis en las intervenciones educativas sanitarias relacionadas con hábitos saludables para prevenir futuros ECV en pacientes con HTA a través de la modulación de los indicadores de RCV.

CONCLUSIONES

Las intervenciones educativas generaron cambios positivos en los estilos de vida de sujetos con HTA, y a la vez, mejoraron los indicadores de RCV en la población de estudio. Son necesarios más estudios en el área para ampliar el alcance de los resultados.

Author Contributions: KRM y GCC diseñaron el programa de intervención educativa y redactaron el apartado introductorio. KRM, GCC, RST CAP y EFT construyeron el apartado metodológico. KRM, GCC, RST realizaron el análisis estadístico. KRM, GCC, RST, CAP y EFT redactaron los resultados, discusión y conclusiones del artículo. Todos los autores revisaron y aprobaron la versión actual del manuscrito.

Funding: This research received no external funding.

Institutional Review Board Statement: UTPL-CEISH-2021-PD11.

Informed Consent Statement: Informed consent was obtained from all subjects involved in the study.

Data Availability Statement: This section provides details regarding where data supporting reported results can be found, including links to publicly archived datasets analyzed or generated during the study. Please refer to the suggested Data Availability Statements in the "Bionatura Research Data Policies" section at https://www.revistabionatura.com/policies.html. You might exclude this statement if the study did not report any data.

Conflicts of Interest: The authors declare no conflict of interest.

REFERENCES

1. Organización Mundial de la Salud. Las 10 principales causas de muerte. OMS. 2020. p. 1-14.
2. World Health Organization (WHO). WHO reveals leading causes of death and disability worldwide: 2000-2019. World Health Organization (WHO). 2020;(1):https://www.who.int/news/item/09-12-2020-who-revea.
3. Roth GA, Mensah GA, Johnson CO, Addolorato G, Ammirati E, Baddour LM, et al. Global Burden of Cardiovascular Diseases and Risk Factors, 1990–2019: Update From the GBD 2019 Study. Journal of the American College of Cardiology. 2020;76(25):2982. Doi: 10.1016/j.jacc.2020.11.010

4. Zhou B, Bentham J, Di Cesare M, Bixby H, Danaei G, Cowan MJ, et al. Worldwide trends in blood pressure from 1975 to 2015: a pooled analysis of 1479 population-based measurement studies with 19·1 million participants. Lancet (London, England). 2017;389(10064):37. Doi: 10.1016/S0140-6736(16)31919-5
5. Costa R, Gutiérrez A, Valdivieso D, Carpio L, Cuadrado F, Núñez J. Encuesta STEPS Ecuador 2018. 2018.
6. Instituto Nacional de Estadística y Censos. Ecuador - Estadísticas Hospitalarias Camas y Egresos 2018. 2018. 2018.
7. Freire WB, Ramírez-Luzuriaga MJ, Belmont P, Mendieta MJ, Silva-Jaramillo K, Romero N, et al. Encuesta Nacional de Salud y Nutrición 2012. Ensanut-Ecu 2012. Quito; 2014.
8. Arnett DK, Blumenthal RS, Albert MA, Buroker AB, Goldberger ZD, Hahn EJ, et al. 2019 ACC/AHA Guideline on the Primary Prevention of Cardiovascular Disease: Executive Summary: A Report of the American College of Cardiology/American Heart Association Task Force on Clinical Practice Guidelines. Circulation. 2019;140(11):e563-95. Doi: 10.1161/CIR.0000000000000677
9. Butler T, Kerley CP, Altieri N, Alvarez J, Green J, Hinchliffe J, et al. Optimum nutritional strategies for cardiovascular disease prevention and rehabilitation (BACPR). Heart. 2020;106(10):724-31. Doi: 10.1136/heartjnl-2019-315499
10. Delgado-Lista J, Alcala-Diaz JF, Torres-Peña JD, Quintana-Navarro GM, Fuentes F, Garcia-Rios A, et al. Long-term secondary prevention of cardiovascular disease with a Mediterranean diet and a low-fat diet (CORDIOPREV): a randomised controlled trial. The Lancet. 2022;399(10338):1876-85. Doi: 10.1016/S0140-6736(22)00122-2
11. Barrea L, Verde L, Suárez R, Frias-Toral E, Vásquez CA, Colao A, et al. Sex-differences in Mediterranean diet: a key piece to explain sex-related cardiovascular risk in obesity? A cross-sectional study. J Transl Med. 2024;22(1):44. Doi: 10.1186/s12967-023-04814-z
12. Barrea L, Verde L, Simancas-Racines D, Zambrano AK, Frias-Toral E, Colao A, et al. Adherence to the Mediterranean diet as a possible additional tool to be used for screening the metabolically unhealthy obesity (MUO) phenotype. J Transl Med. 2023;21(1):675. Doi: 10.1186/s12967-023-04546-0
13. Muscogiuri G, Verde L, Sulu C, Katsiki N, Hassapidou M, Frias-Toral E, et al. Mediterranean Diet and Obesity-related Disorders: What is the Evidence? Curr Obes Rep. 2022;11(4):287-304. Doi: 10.1007/s13679-022-00481-1
14. Grillo A, Salvi L, Coruzzi P, Salvi P, Parati G. Sodium Intake and Hypertension. Nutrients. 2019;11(9):1970. Doi: 10.3390/nu11091970
15. Suárez R, Diaz P, Sarmiento-Andrade Y, Cadena M, Alvarez L, Frias-Toral E. Evaluación del estilo de vida con el riesgo de diabetes mellitus tipo 2 en trabajadores universitarios ecuatorianos. Revis Bionatura. 2023;8(2):6. Doi: 10.21931/RB/2023.08.02.6
16. Cicero AFG, Veronesi M, Fogacci F. Dietary Intervention to Improve Blood Pressure Control: Beyond Salt Restriction. High Blood Pressure & Cardiovascular Prevention. 2021;28(6):547. Doi: 10.1007/s40292-021-00474-6
17. Borgi L, Muraki I, Satija A, Willett WC, Rimm EB, Forman JP. Fruit and Vegetable Consumption and the Incidence of Hypertension in Three Prospective Cohort Studies. Hypertension (Dallas, Tex : 1979). 2016;67(2):288-93. Doi: 10.1161/HIPERTENSIONAHA.115.06497
18. Grosso G, Laudisio D, Frias-Toral E, Barrea L, Muscogiuri G, Savastano S, et al. Anti-Inflammatory Nutrients and Obesity-Associated Metabolic-Inflammation: State of the Art and Future Direction. Nutrients. 2022;14(6):1137. Doi: 10.3390/nu14061137

19. Jurik R, Stastny P. Role of nutrition and exercise programs in reducing blood pressure: A systematic review. Journal of Clinical Medicine. 2019;8(9):1393. Doi: 10.3390/jcm8091393
20. Sharman JE, La Gerche A, Coombes JS. Exercise and Cardiovascular Risk in Patients With Hypertension. American Journal of Hypertension. 2015;28(2):147-58. Doi: 10.1093/ajh/hpu191
21. Voglhuber J, Ljubojevic-Holzer S, Abdellatif M, Sedej S. Targeting Cardiovascular Risk Factors Through Dietary Adaptations and Caloric Restriction Mimetics. Frontiers in Nutrition. 2021;8:726. Doi: 10.3389/fnut.2021.758058
22. Cáceres-Vinueza S, Frias-Toral E, Suárez R, Daher-Nader J, Flor-Muñoz E, Márquez-Vinueza M, et al. Anthropometric indexes and cardiovascular risk in Ecuadorian university students: A comparison with international references. Revis Bionatura. 2023;8(3):89. Doi: 10.21931/RB/2023.08.03.89
23. Ramôa Castro A, Oliveira NL, Ribeiro F, Oliveira J. Impact of educational interventions on primary prevention of cardiovascular disease: A systematic review with a focus on physical activity. The European Journal of General Practice. 2017;23(1):59. Doi: 10.1080/13814788.2017.1284791
24. Wilson DMC, Nielsen E, Ciliska D. Lifestyle Assessment: Testing the FANTASTIC Instrument. Canadian Family Physician. 1984;30:1863-4, 1866.
25. Hajifathalian K, Ueda P, Lu Y, Woodward M, Ahmadvand A, Aguilar-Salinas CA, et al. A novel risk score to predict cardiovascular disease risk in national populations (Globorisk): a pooled analysis of prospective cohorts and health examination surveys. The lancet Diabetes & endocrinology. 2015;3(5):339-55. Doi: 10.1016/S2213-8587(15)00081-9
26. Ministerio de Salud Pública. Hipertensión arterial: Guía de Práctica Clínica (GPC). Dirección Nacional de Normatización. 2019.
27. Goyer L, Dufour R, Janelle C, Blais C, L'Abbé C, Raymond É, et al. Randomized controlled trial on the long-term efficacy of a multifaceted, interdisciplinary lifestyle intervention in reducing cardiovascular risk and improving lifestyle in patients at risk of cardiovascular disease. Journal of behavioral medicine. 2013;36(2):212-24. Doi: 10.1007/s10865-012-9407-3
28. Martínez Morales HA. Comparación de la estimación del riesgo cardiovascular absoluto entre la escala Globorisk y la escala Framingham en pacientes de consulta externa de medicina interna del Hospital Central Dr. Ignacio Morones Prieto. 2020.
29. Lönnberg L, Ekblom-Bak E, Damberg M. Reduced 10-year risk of developing cardiovascular disease after participating in a lifestyle programme in primary care. En: Upsala Journal of Medical Sciences. Taylor and Francis Ltd; 2020. p. 250-6.
30. Brinks J, Fowler A, Franklin BA, Dulai J. Lifestyle modification in secondary prevention: Beyond pharmacotherapy. American Journal of Lifestyle Medicine. 2017;11(2):137-52. Doi: 10.1177/1559827616651402
31. Lidin M, Hellénius ML, Rydell-Karlsson M, Ekblom-Bak E. Long-term effects on cardiovascular risk of a structured multidisciplinary lifestyle program in clinical practice. BMC Cardiovascular Disorders. 2018;18(1):59. Doi: 10.1186/s12872-018-0792-6
32. Leiva AM, Petermann-Rocha F, Martínez-Sanguinetti MA, Troncoso-Pantoja C, Concha Y, Garrido-Méndez A, et al. Asociación de un índice de estilos de vida saludable con factores de riesgo cardiovascular en población chilena. Revista médica de Chile. 2018;146(12):1405-14. Doi: 10.4067/s0034-98872018001201405

Received: October 9th 2023/ **Accepte**d: January 15th 2024 / **Published:**15 February 2024

Citation: Rojas-Montenegro, K., Cisneros-Cañas, G., Suárez de Terán, R., Cajilima-Vega, R., Arteaga-Pazmiño C., Frias-Toral E. Estrategia de intervención educativa para el abordaje del riesgo cardiovascular en pacientes con hipertensión arterial. Revis Bionatura 2024; 9 (1) 68. http://dx.doi.org/10.21931/RB/2024.09.01.68

Additional information Correspondence should be addressed to ceciliaarteagap@gmail.com

Peer review information. Bionatura thanks anonymous reviewer(s) for their contribution to the peer review of this work using https://reviewerlocator.webofscience.com/

Bionatura ISSN. First 13909355 Ecuador. **Scopus coverage years**: from 2016 to the present

Bionatura
Ibero-American Journal of Biotechnology and Life Sciences

Article

Isolation, characterization and identification of *Klebsiella sp.* dor_27f isolated from textile effluents

Derly Ortiz-Romero[1], *Daniela Camacho-Valencia*[2,3], *Stamber Alvaro Ramírez-Revilla*[2,3]*

[1]*Universidad Católica de Santa María, Arequipa, Perú; dortiz@ucsm.edu.pe.*
[2]*Universidad Tecnológica del Perú, Arequipa, Perú; C26618@utp.edu.pe.*
[3]*Laboratorio de Calidad de Agua y Medio Ambiente, Universidad Tecnológica del Perú;*
* *Correspondence: sramirezr@utp.edu.pe; Tel.: +51974434314*
Available from. http://dx.doi.org/10.21931/RB/2024.09.01.72

ABSTRACT

This research study aimed to isolate and characterize a new bacterial strain from textile effluents. To do this, bacteria were cultured using the MSM medium, where a colony was isolated through six successive pickings. It then underwent a DNA extraction process using the phenol-chloroform-isoamyl alcohol methodology, and an electrophoresis was carried out to confirm the extraction. In addition, the isolated colony was identified as *Klebsiella sp*. by sequencing the 16S rRNA gene using bioinformatics tools. To observe its biotechnological potential, the bacterial strain was grown in an MSM broth enriched with Golden Yellow K2R azoic dye at a concentration of 50 mg/L, showing a percentage of decolorization of 74 % after 72 hours at 37 °C, indicating the potential of the isolated colony for the development of bio-remediation processes for effluents containing azoic dyes.

Keywords: Bacterial strain, *Klebsiella sp*., DNA extraction, decolorization, effluents.

INTRODUCTION

One of the main problems affecting the world's environment is water contamination due to industrial activity, which generates high amounts of polluting effluents that produce toxic effects. [1]. For example, the textile industry generates wastewater containing artificial recalcitrant or carcinogenic dyes [2-4].

Worldwide, around 10,000 types of dyes and pigments are used in a wide range of diverse industries, and approximately 7×10^5 tons of them are produced annually due to the industrialization and demand of the textile industry [5,6]. Among the dyes used in the industry, around 20 % remain unused (they do not fully penetrate the fabrics) and are released directly into the sewage system. This renders the water unfit for use and impedes light penetration into bodies of surface water, adversely affecting the aquatic environment [7-9].

Industrial dyes contain various structures, most composed of three reactive groups: azo, anthraquinon and phthalocyanin [6,10,11]. Numerous research studies have been carried out to perfect a treatment that allows the degradation of these textile dyes and colorings and the recovery of the natural water resource. A viable alternative is biological treatment since it is inexpensive, ecological, and functional compared to other chemical or physical treatments that require a lot of energy [6,11,12].

Some studies have used different bacteria for the biodegradation of reactive textile dyes, such as: *Alcaligenes faecalis*, *Bacillus cereus* and *Bacillus sp.* [6]; *Lysinibacillus sphaericus* and *Aeromonas hydrophila* [11]; *Micrococcus luteus* and *Bacillus subtilis* [4]; *Staphylococcus sp.* [13]; *Citrobacter freundii* [1]; *Planococcus* and *Bacillus* [14], *Pseudomonas* [15,16]; *Aeromonas* [17], *Bacillus* and *Lysinibacillus* [18]; *Paenibacillus polymyxa, Micrococcus luteus* and *Micrococcus* [19]. Other studies have used microorganisms such as *Galactomyces geotrichum* [20], *Phanerochaete chrysosporium* [21] and *Enterobacter* [22] for the same purpose.

This study focused on isolating, characterizing, and identifying a new bacterial strain from industrial textile dyes effluents. The strain was genetically assessed by 16S rRNA analysis and software. Finally, the isolated

bacteria were grown in a culture medium enriched with an azoic dye, and their decolorization capacity was evaluated.

MATERIALS AND METHODS

Culture medium

The mineral salts medium (MSM) consisted of the following components in (g/L): $Na_2HPO_4 \cdot 12H_2O$ (1.5), KH_2PO_4 (1.5), $(NH_4)_2SO_4$ (2.0), $MgSO_4 \cdot 7H_2O$ (0.2), $CaCl_2 \cdot 2H_2O$ (0.010), and $FeSO_4 \cdot 7H_2O$ (0.0010). The MSM was mixed with 0.010 g/L of the Golden Yellow K2R dye (Figure 1) and with agar (1.9% W/V) to isolate and maintain a pure culture. The media was sterilized at 121 °C for 20 min before use [23].

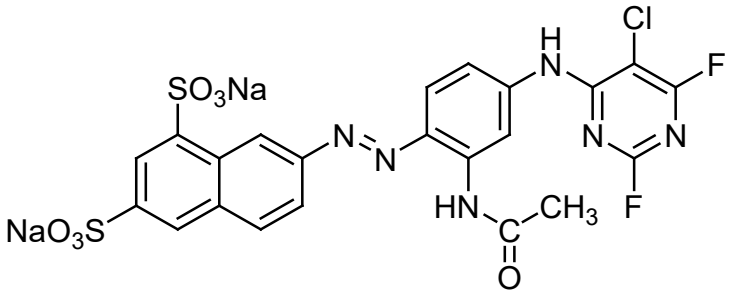

Figure 1: Chemical structure of the gold-yellow K2R dye.

Obtaining the sample

A sample of textile effluent was taken to the laboratory to isolate the bacteria. 1.5 mL of effluent was placed in each of the 10 Eppendorf tubes before being taken to the microcentrifuge and run at 10,000 RPM for 5 min. The supernatant was eliminated, and the pellets formed in each tube were gathered. Subsequently, 100 µL of the sample was seeded using a Drigalsky loop on a plate with MSM agar and the Golden Yellow K2R dye as the only carbon source. The sample was incubated at 37°C for 24 hours.

Picking

A colony was removed from the initial seeding. It was placed in an Eppendorf tube with 1 mL of Triton and vortexed for 5 min. Then, it was seeded with a cole loop on a new plate. A total of 6 pickings were made following the same procedure.

Antibiogram

To discover the sensitivity of the isolated bacteria to different antibiotics, a sample (of the pure culture in MSM broth) was seeded on nutritive agar using a sterile swab. Then, paper discs with the chosen antibiotics for gram-harmful bacteria such as neomycin, cefazolin, ceftriaxone, ampicillin/sulbactam, cotrimoxazole, amikacin, lincomycin were placed on the agar. Following the Bauer-Kirby disc diffusion procedure, antibiotics were impregnated on absorbent paper discs [24]. The discs were distributed symmetrically over the surface of the culture medium inoculated with the bacterial strain. After incubation for 48 hours at 37°C, the inhibition halos produced by the antibiotics were measured.

DNA extraction

An Eppendorf tube was filled with 100 µL of microbeads and 500 µL of sterile water, and a loop of bacteria was dissolved. Then, it was vortexed at maximum speed for 5 min. After that, 500 µL of a phenol-chloroform-isoamyl alcohol mixture was added during the vortexing, and lastly, it was placed in the microcentrifuge at 15,000 RPM for 10 min. The supernatant was recovered by adding 600 µL of isopropyl alcohol, mixed gently and then centrifuged at 15,000 RPM for 10 min. After discarding the supernatant, ethanol was applied to dry the pellet, and finally, it was re-suspended with 50 µL of sterile water, keeping the DNA at 4 °C. The technique used is a variant of the optimal method for bacterial DNA isolation by bead beating described by Fujimoto *et al.* [25].

Sequencing the 16s rrna gene of the 35-dor_27f bacteria

Once the DNA extraction had been verified, the 16S rRNA gene was amplified by the PCR method. The obtained product was purified and sent for sequencing to the Instituto de Biotecnología de ADN de Uchumayo using the FinchTV software. Sequencing analysis of the 16S rRNA gene was performed at the Laboratory of Molecular Biology, Harvard University, Cambridge, MA, USA.

Bioinformatic analysis by ncbi blast

For the bioinformatic analysis, the NCBI BLAST database was used. The previously obtained DNA sequence was inserted. Likewise, in order to obtain the phylogenetic tree, the BioEdit, Mega and Trie View Explorer software were used. The 16S rRNA gene sequence of bacterial strain 35-DOR_27F was inserted into the NCBI GenBank database for alignment and comparison with stored bacterial sequences to assess their degree of homology using the BLASTn algorithm [26]. BioEdit, Mega and Trie View Explorer software were used to obtain the phylogenetic tree.

Biotechnological potential studies

100 µL of the isolated bacterial strain was inoculated in 10 mL MSM broth with Golden Yellow K2R dye (50 mg/L). Incubation was carried out at 37 °C for 72 hours. Afterward, the broth was centrifuged at 6000 rpm for 20 min. Then, the supernatant was separated, and its absorbance was measured at 388 nm (corresponding to the λmax of the dye) in a Thermogenesis UV–visible spectrophotometer. For the biodegradation study, an Agilent Technologies Cary 60 UV-V spectrophotometer was used to quantify the absorbance of a 60 mg/L solution of the yellow dye K2R. The isolated strain was cultured in peptonized broth for 48 h at 37°C, and then 1 mL of inoculum was taken and placed in a flask containing 100 mL of a 50 mg/L solution of the dye in peptonized water. The percentage of decolorization was evaluated after 72 hours using Equation 1:

$$\%Decolorization = \frac{Inicial\ Abs - Final\ Abs}{Inicial\ Abs} \times 100 \quad \text{.....(1)}$$

RESULTS

Morphological and cultural characteristics

Gram-negative bacteria were isolated with the following characteristics: circular point shape, whole border, flat colony elevation, creamy consistency, smooth surface and transparent white pigmentation.

Antibiogram

Results of the susceptibility of the isolated bacteria are shown in Table 1. After 24 hours of incubation, the bacteria were sensitive to most chosen antibiotics except ampicillin/sulbactam. Amikacin was the antibiotic that presented the largest halo, indicating that the isolated bacteria have a greater sensitivity to said antibiotic.

Antibiotics	Halo diameter (cm)	Sensitive/ Resistant
Neomycin	2,0	Sensitive
Cefazoline	1,5	Sensitive
Ceftriaxone	1,4	Sensitive
Ampicillin/Sulbactam	-	Resistant
Cotrimoxazole	2,8	Sensitive
Amikacin	3,0	Sensitive
Lincomycin	1,8	Sensitive

Table 1. Samples resistance to antibiotics.

Figure 2 shows the inhibition halos for the different antibiotics with the isolated bacteria on nutrient agar. The biggest inhibition halo corresponds to the antibiotic amikacin.

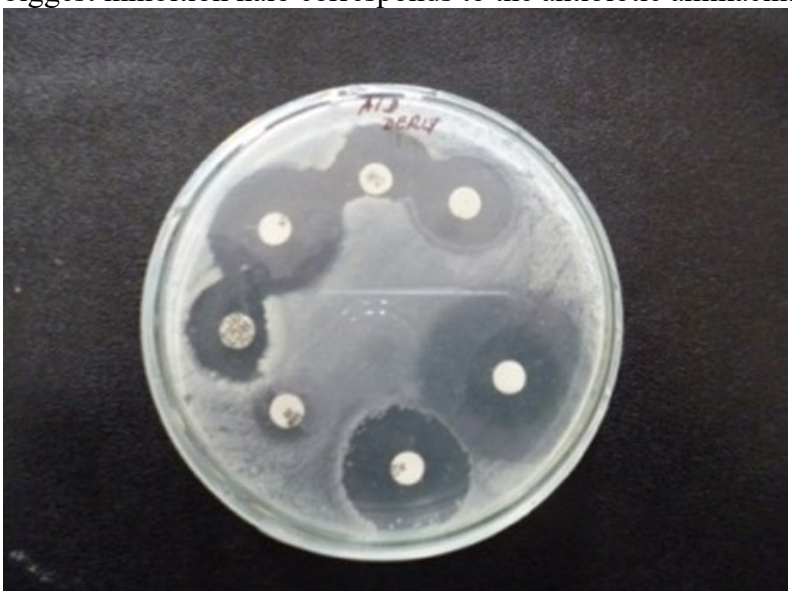

Figure 2: Antibiogram of the isolated bacteria.

The sequence of the 16s rRNA gene of the 35-dor_27f bacteria

Using the FinchTV software, it was possible to observe the sequence of the public and pyrimidine bases of the extracted DNA, which is shown in Figure 3.

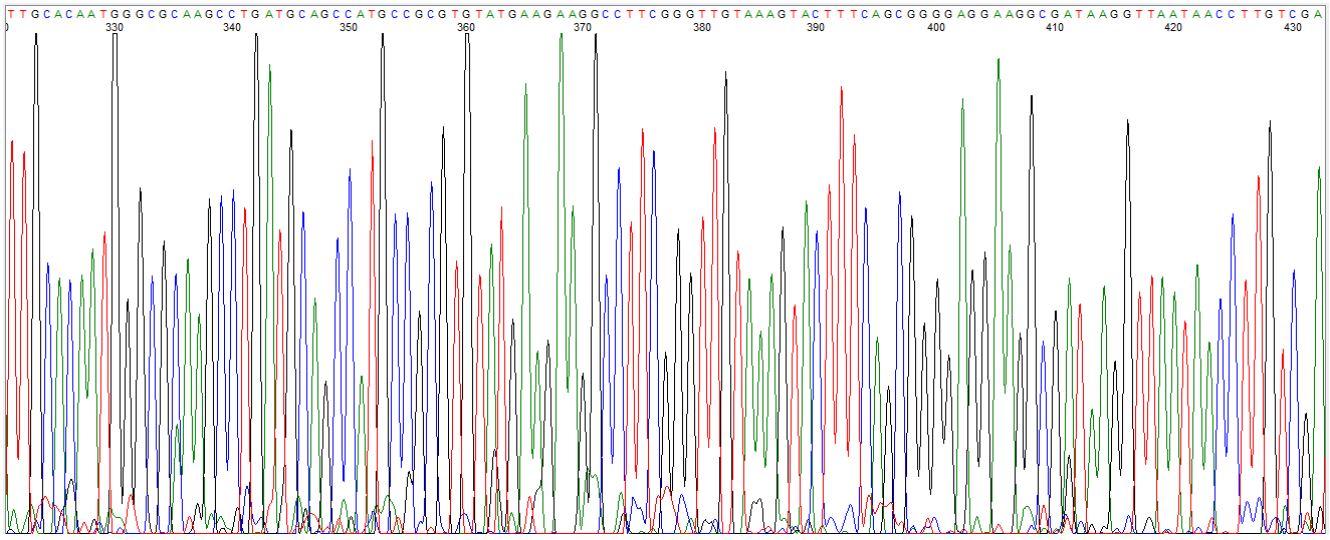

Figure 3: Visualization of the bacterial DNA sequence using FinchTV software.

Bioinformatic analysis using NCBI blast

After the sequence was obtained and the bioinformatic analysis using BLAST was performed, it was determined that the isolated strain shares a high percentage of similarity (99%) with *Klebsiella sp.*, which is cataloged as a species capable of decolorizing textile effluents. Figure 4 shows the results of the BLAST analysis with the greatest similarity to *Klebsiella sp.*, and Figure 5 shows the phylogenetic tree; notably, the bacterium encoded as DOR_27F is found at the same height as *Klebsiella sp.*, which indicates it could belong to this species.

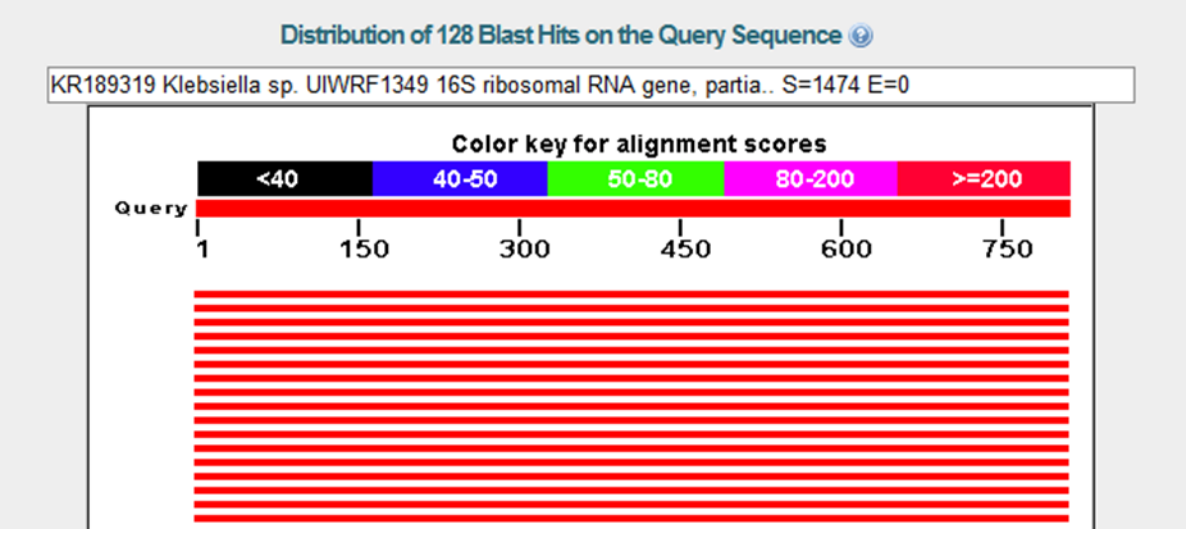

Figure 4: Analysis of the isolated bacteria using BLAST.

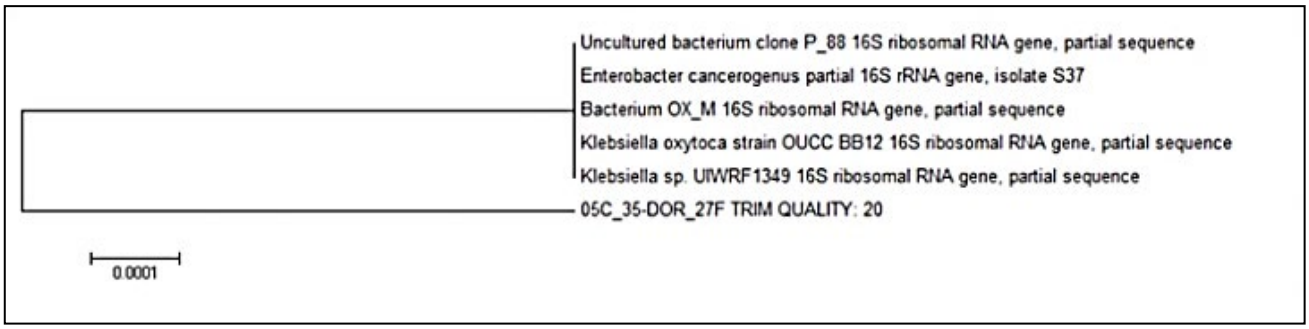

Figure 5: Phylogenetic tree of the isolated bacterium.

Biotechnological potential studies

The maximum absorption wavelength for a 60 mg/L solution of Golden Yellow K2R was 388 nm, with an absorbance of 0.9522. Figure 6 presents the spectrum obtained.

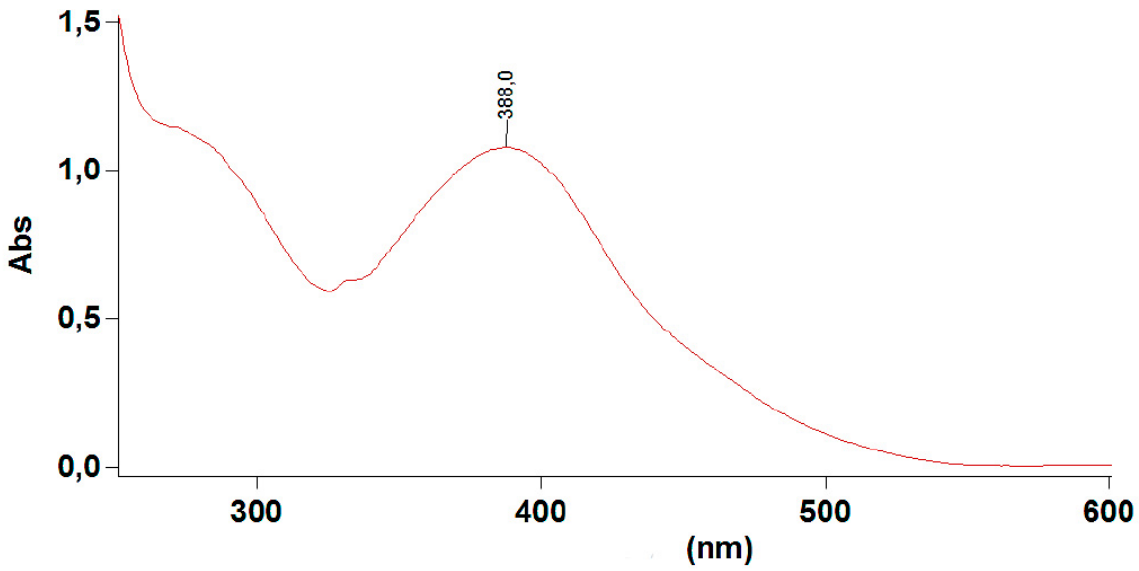

Figure 6: Spectral scanning of the Gold Yellow K2R.

After 72 hours of incubation, the results indicated that the decolorization of Golden Yellow K2R by the isolated strain identified *as Klebsiella sp.* was 74 %, suggesting that the isolated bacteria could be used in bioremediation processes.

DISCUSSION

Different bacterial species have been isolated from textile sources, demonstrating their bioremediation capacity against azoic dyes in solution. *Bacillus* and *Alcaligenes* stand out among the identified genera, as they are efficient when treating Novacron Super Black G dye [6]. In addition, *Alcaligenes aquatilis* proved effective in degrading synazol red 6HBN colorant (82%), suggesting it may be helpful in wastewater treatment [27]. Furthermore, *Bacillus subtilis*, *Bacillus megaterium*, *Erysipelothrix* and *Amphibacillus xylanus* were isolated and identified, and their degradation ability was studied against 7 azoic dyes. Results demonstrated that the dyes were decolorized (at least 50%) after 3 days of incubation. However, none of the isolates could decolorize novacron red [28]. Moreover, *Alishewanella sp*. has also shown decolorization capacity against Sumifex Tourqi blue (83%) after 6 days, thus showing its potential for removing azoic dyes [29].
In the present research study, the isolated bacterial strain corresponds to *Klebsiella sp.*, which was grown on MSM broth enriched with Golden Yellow K2R azoic dye and showed a decolorization of 74 %. Other studies report bacterial growth in agar enriched with different azoic dyes, such as Bezema Yellow S8-G and Bezema Red S2-B, showing decolorization rates of up to 90% [8].

CONCLUSIONS

A new bacterium obtained from textile effluents was isolated, and the code 35-DOR_27F was assigned. Sequencing the 16S rRNA gene was found to correspond to *Klebsiella* genus. Furthermore, after 72 hours of incubation, it exhibited a decolorization percentage of 74 % of the Golden Yellow K2R dye. This
the study indicates that this bacterium has promising characteristics for addressing pollution caused by textile effluents.

Author Contributions: "Conceptualization, D. Ortiz-Romero; methodology, D. Ortiz-Romero and D. Camacho-Valencia; software, D. Ortiz-Romero.; validation, S.A Ramírez- Revilla; formal analysis, D. Ortiz-Romero and D. Camacho-Valencia; investigation, D. Ortiz-Romero and S.A Ramírez- Revilla; data curation, D. Ortiz-Romero and S.A Ramírez- Revilla; writing—original draft preparation, D. Ortiz-Romero and D. Camacho- Valencia; writing—review and editing, D. Ortiz-Romero and S.A Ramírez- Revilla; supervision, S.A Ramírez- Revilla; project administration, D. Ortiz-Romero and S.A Ramírez- Revilla.; funding acquisition, S.A Ramírez- Revilla. All authors have read and agreed to the published version of the manuscript.

Conflicts of Interest: The authors declare no conflict of interest.

REFERENCES

1. Sunkar S, C. VN, K. R. Citrobacter freundii mediated degradation of textile dye Mordant Black 17. *Journal of Water Process Engineering*. 2015;8:28-34. doi:10.1016/j.jwpe.2015.08.006
2. Chung KT. The Significance of Azo-Reduction in the Mutagenesis and Carcinogenesis of Azo Dyes. Vol 114.; 1983.
3. Kawakami T, Isama K, Nakashima H, Tsuchiya T, Matsuoka A. Analysis of primary aromatic amines originated from azo dyes in commercial textile products in Japan. J Environ Sci Health A Tox Hazard Subst Environ Eng. 2010;45(10):1281-1295. doi:10.1080/10934529.2010.493827

4. Ito T, Shimada Y, Suto T. Potential use of bacteria collected from human hands for textile dye decolorization. Water Resour Ind. 2018;20:46-53. doi:10.1016/j.wri.2018.09.001
5. Aksu Z, Tezer S. Biosorption of reactive dyes on the green alga Chlorella vulgaris. Process Biochemistry. 2005;40(3-4):1347-1361. doi:10.1016/j.procbio.2004.06.007
6. Hossen MZ, Hussain ME, Hakim A, Islam K, Uddin MN, Azad AK. Biodegradation of reactive textile dye Novacron Super Black G by free cells of newly isolated Alcaligenes faecalis AZ26 and Bacillus spp obtained from textile effluents. Heliyon. 2019;5(7). doi:10.1016/j.heliyon.2019.e02068
7. Valli Nachiyar C, Namasivayam SKR, Kumar RR, Sowjanya M. Bioremediation of textile effluent containing Mordant Black 17 by bacterial consortium CN-1. Journal of Water Process Engineering. 2014;4(C):196-200. doi:10.1016/j.jwpe.2014.10.003
8. Karim ME, Dhar K, Hossain MT. Decolorization of Textile Reactive Dyes by Bacterial Monoculture and Consortium Screened from Textile Dyeing Effluent. Journal of Genetic Engineering and Biotechnology. 2018;16(2):375-380. doi:10.1016/j.jgeb.2018.02.005
9. Garzón-Pérez AS, Paredes-Carrera SP, Martínez-Gutiérrez H, Cayetano-Castro N, Sánchez-Ochoa JC, Pérez-Gutiérrez RM. Effect of combined microwave-ultrasound irradiation in the structure and morphology of hydrotalcite-like compounds al/mg-ch3coo and its evaluation in the sorption of a reactive dye. Revista Mexicana de Ingeniera Quimica. 2020;19(1):363-375. doi:10.24275/rmiq/Mat567
10. Axelsson J, Nilsson U, Terrazas E, Alvarez Aliaga T, Welander U. Decolorize the Reactive Red 2 and Reactive Blue 4 textile dyes using Bjerkandera sp. Strain BOL 13 in a continuous rotating biological contactor reactor. Enzyme Microb Technol. 2006;39(1):32-37. doi:10.1016/j.enzmictec.2005.09.006
11. Kumar SS, Shantkriti S, Muruganandham T, Murugesh E, Rane N, Govindwar SP. Bioinformatics aided microbial approach for bioremediation of wastewater containing textile dyes. Ecol Inform. 2016;31:112-121. doi:10.1016/j.ecoinf.2015.12.001
12. Saratale RG, Saratale GD, Chang JS, Govindwar SP. Bacterial decolorization and degradation of azo dyes: A review. J Taiwan Inst Chem Eng. 2011;42(1):138-157. doi:10.1016/j.jtice.2010.06.006
13. Durai S, Kumar NM, Saravanan D. Isolation of dye degrading bacteria from textile effluent. Available online www.jocpr.com Journal of Chemical and Pharmaceutical Research. 2015;7(3):2214-2218. https://www.researchgate.net/publication/305787431
14. Shah MP. Isolation and Screening of Dye Decolorizing Bacteria. J Appl Environ Microbiol. 2014;2(5):244-248. doi:10.12691/jam-2-5-7
15. Jadhav JP, Kalyani DC, Telke AA, Phugare SS, Govindwar SP. Evaluation of the efficacy of a bacterial consortium for the removal of color, reduction of heavy metals, and toxicity from textile dye effluent. Bioresour Technol. 2010;101(1):165-173. doi:10.1016/j.biortech.2009.08.027
16. Hussain S, Maqbool Z, Ali S, et al. Biodecolorization of reactive black-5 by a metal and salt tolerant bacterial strain Pseudomonas sp. RA20 isolated from Paharang drain effluents in Pakistan. Ecotoxicol Environ Saf. 2013;98:331-338. doi:10.1016/j.ecoenv.2013.09.018
17. Du LN, Li G, Zhao YH, et al. Efficient metabolism of the azo dye methyl orange by Aeromonas sp. strain DH-6: Characteristics and partial mechanism. Int Biodeterior Biodegradation. 2015;105:66-72. doi:10.1016/j.ibiod.2015.08.019
18. Anjaneya O, Souche SY, Santoshkumar M, Karegoudar TB. Decolorization of sulfonated azo dye Metanil Yellow by newly isolated bacterial strains: Bacillus sp. strain AK1 and Lysinibacillus sp. strain AK2. J Hazard Mater. 2011;190(1-3):351-358. doi:10.1016/j.jhazmat.2011.03.044

19. Moosvi S, Kher X, Madamwar D. Isolation, characterization and decolorization of textile dyes by a mixed bacterial consortium JW-2. Dyes and Pigments. 2007;74(3):723-729. doi:10.1016/j.dyepig.2006.05.005
20. Govindwar SP, Kurade MB, Tamboli DP, Kabra AN, Kim PJ, Waghmode TR. Decolorization and degradation of xenobiotic azo dye Reactive Yellow-84A and textile effluent by Galactomyces geotrichum. Chemosphere. 2014;109:234-238. doi:10.1016/j.chemosphere.2014.02.009
21. Enayatizamir N, Tabandeh F, Rodríguez-Couto S, Yakhchali B, Alikhani HA, Mohammadi L. Biodegradation pathway and detoxification of the diazo dye Reactive Black 5 by Phanerochaete chrysosporium. Bioresour Technol. 2011;102(22):10359-10362. doi:10.1016/j.biortech.2011.08.130
22. Chen G, Huang M hong, Chen L, Chen D hui. A batch decolorization and kinetic study of Reactive Black 5 by a bacterial strain Enterobacter sp. GY-1. Int Biodeterior Biodegradation. 2011;65(6):790-796. doi:10.1016/j.ibiod.2011.05.003
23. Brilon C, Beckmann W, Hellwig M, Knackmuss3t HJ. *Enrichment and Isolation of Naphthalenesulfonic Acid-Utilizing Pseudomonads*.; 1981
24. Of R, Technologists. *TECHNICAL SECTION ANTIBIOTIC SUSCEPTIBILITY TESTING BY A STANDARDIZED SINGLE DISK METHOD*. Vol 45.; 1966. https://academic.oup.com/ajcp/article
25. Fujimoto S, Nakagami Y, Kojima F. *Optimal Bacterial DNA Isolation Method Using Bead-Beating Technique*. Vol 3.; 2004. https://www.researchgate.net/publication/268409445
26. Zhang Z, Schwartz S, Wagner L, Miller W. *A Greedy Algorithm for Aligning DNA Sequences*. Vol 7. Mary Ann Liebert, Inc. Pp; 2000.
27. Ajaz M, Rehman A, Khan Z, Nisar MA, Hussain S. Degradation of azo dyes by Alcaligenes aquatilis 3c and its potential use in the wastewater treatment. AMB Express. 2019;9(1). doi:10.1186/s13568-019-0788-3
28. Mahbub KR, Mohammad A, Ahmed MM, Begum S. Decolorization of Synthetic Dyes Using Bacteria Isolated from Textile Industry Effluent. Asian Journal of Biotechnology. 2012;4(3):129-136. doi:10.3923/ajbkr.2012.129.136
29. Ajaz M, Elahi A, Rehman A. Degradation of azo dye by bacterium, Alishewanella sp. CBL-2 isolated from industrial effluent and its potential use in decontamination of wastewater. Journal of Water Reuse and Desalination. 2018;8(4):507-515. doi:10.2166/wrd.2018.065

Received: October 9th 2023/ **Accepte**d: January 15th 2024 / **Published:**15 February 2024

Citation: Ortiz-Romero D., Camacho-Valencia D., Ramírez-Revilla S. A. Isolation, characterization and identification of *klebsiella sp.* dor_27f isolated from textile effluents. Revis Bionatura 2024; 9 (1) **72**. http://dx.doi.org/10.21931/RB/2024.09.01.**72**

Additional information Correspondence should be addressed to sramirezrevilla@utp.edu.pe
Peer review information. Bionatura thanks anonymous reviewer(s) for their contribution to the peer review of this work using https://reviewerlocator.webofscience.com/

Bionatura ISSN. First 13909355 Ecuador. **Scopus coverage years**: from 2016 to the present

Bionatura
Ibero-American Journal of Biotechnology and Life Sciences

Article

Evaluating the protective effect of alpha-lipoic acid against gentamicin-induced gonadal toxicity indicated by histopathology.

Hozaifa Elsawah[1], Aziza Amin[2], Haitham Mokhimar[3], Mohamed Kandiel[4], Ayman Farid[5], and AbuBakr El-Mahmoudy[6]*

[1]*Department of Pharmacology, Faculty of Veterinary Medicine, Benha University, Egypt.*
[2]*Department of Pathology, Faculty of Veterinary Medicine, Benha University, Egypt. az-iza.amin@fvtm.bu.edu.eg.*
[3]*Department of Pharmacology, Faculty of Veterinary Medicine, Benha University, Egypt. hit-thammohamed@gmail.com.*
[4]*Department of Theriogenology, Faculty of Veterinary Medicine, Benha University, Egypt. mohamed.kandil@fvtm.bu.edu.eg.*
[5]*Department of Clinical Pathology, Faculty of Veterinary Medicine, Benha University, Egypt. ayman.samir@fvtm.bu.edu.eg.*
[6]*Department of Pharmacology, Faculty of Veterinary Medicine, Benha University, Egypt. a.elmahmoudy@fvtm.bu.edu.eg.*
** Correspondence: hozaifa2005@gmail.com. Postcode: 13736, Tel.: 0020132461411, Fax: 0020132463074.*
Available from. http://dx.doi.org/10.21931/RB/2024.09.01.73

ABSTRACT

Gentamicin induces gonadotoxicity in animal models, accompanied by oxidative stress. This study evaluated the histopathological protective effect of alpha-lipoic acid against gentamicin-induced gonadotoxicity. A parallel experimental study included 50 albino Wister rats, which were divided into 5 groups of ten according to the intraperitoneal intervention: group I received gentamicin, group II received gentamicin plus alpha-lipoic (100 mg/kg), group III received gentamicin plus a double dose of alpha-lipoic acid, group III received gentamicin plus oral vitamin E, and group IV received NaCl 0.9% (control). The animals were equally euthanized on days 15 and 16. Tests were dissected, prepared, and stained using a light microscope for histopathological examination. Rats exposed to gentamicin showed degeneration of seminiferous tubules, characterized by a significant decrease in germinal epithelial cells, impaired spermatogenesis, and a lack of spermatozoa in the lumen. An improvement in testes of animals co-treated with alpha-lipoic acid or vitamin E, including restoration of spermatogenesis and epithelial thickness. The histometric analysis also showed that the tubule epithelial thickness decreased when gentamicin was used, but this did not happen when alpha-lipoic acid or vitamin E was added simultaneously. The detrimental effects of gentamicin on testicular architecture are preventable through alpha-lipoic acid or vitamin E co-treatment.

Keywords: Alpha-lipoic acid; Gonads; Histometric; Gentamicin; Seminiferous tubule; Spermatogenesis.

INTRODUCTION

Infertility is a significant public health problem affecting 8–12% of couples worldwide; approximately 40–50% is due to male factor [1]. Some drugs can induce testicular dysfunction and interfere with spermatogenesis, such as gentamicin [2]. Gentamicin is an aminoglycoside antibiotic widely used to treat many infectious diseases,

including early-onset sepsis in neonates [3], urinary tract infections [4], and pneumonia [5]. Gentamicin decreased testicular weight, reduced sperm count, motility, and viability, and increased sperm head and tail abnormalities [6, 7]. These effects were associated with increased oxidative stress and altered histopathological structure [8, 9]. Oxidative stress was suggested as a possible mechanism of gentamicin-induced testicular damage [10]. There are many different ways that gentamicin can cause oxidative stress. Some of these are mitochondrial pathway-dependent oxidative stress [11], peroxidation of phosphoinositide by the gentamicin-iron complex [12], and lower levels of antioxidant enzymes in cells [10]. Noteworthy, oxidative stress is a significant cause of male infertility through damaging spermatogenic cells [13], as the sperm plasma membrane and testis tissue are rich in polyunsaturated fatty acids, which generally provide the sperm cells with the normal motility required for capacitation [14]. These polyunsaturated fatty acids are highly vulnerable to oxidative damage [15].

The alteration in testicular histopathological structure evaluated by a light microscope revealed intertubular space expansion with vacuolization, seminiferous tubule degeneration, and spermatogenic cell depletion [2, 9]. Moreover, cellular changes were also reported with a transmission electron microscope in rats treated with gentamicin, including primary spermatocytes and Sertoli cells [9]. Alpha-lipoic acid is a powerful antioxidant coenzyme that showed histopathological protection against adriamycin-induced testicular damage [16]. Also, it restored gentamicin-induced testis weight reduction, normalized gentamicin-induced impaired sperm parameters, and ameliorated gentamicin-induced oxidative stress [17, 18]. Additionally, it showed a nephroprotective effect when administered with gentamicin [19].

On the other hand, the potent antioxidant vitamin E protected against gentamicin-induced nephrotoxicity [20]. However, there were no studies on the potential histopathological protection of alpha-lipoic acid and vitamin E against gentamicin-induced testicular tissue damage. Consequently, our objective was to present histological and histometric data supporting the potential protective impact of alpha-lipoic acid and vitamin E against testicular histopathology alterations induced by gentamicin administration.

MATERIALS AND METHODS

Drug preparation

Gentamicin was provided as Garamycin® ampoules brand name with a strength of 80 mg/2 ml, Schering-Plough Corporation U.S.A. Alpha lipoic acid was provided as Thioamide® ampoules generic name with a 300 mg/ 10 ml strength, E.V.A. Pharmaceutical Industries, Cairo, Egypt. Both drugs were given intraperitoneally with a 25-gauge needle with a minimal volume for each drug. Vitamin E was provided as vitamin E 1000 mg® generic name: Pharco Pharmaceuticals, Cairo, Egypt. The Vitamin E capsules were diluted in sunflower oil to achieve 1 ml per rat and delivered orally using 18-gauge soft gavage tubes. NaCl 0.9% was obtained as a sterile solution in unit doses of 0.5 ml.

Animals and study design

A minimal sample size of 4 in each group was required to detect a mean difference in the seminiferous epithelium height of 30 µm between the gentamicin-treated group and any other group with 80% power and 0.05 alpha error. A parallel experimental study was conducted, including 50 albino Wister rats weighing 200 ± 20 gm and aged 2 weeks, obtained from the animal house of the veterinary medicine faculty. The animals were acclimatized without intervention for 2 weeks at room temperature (24º C), under a 12-hour light/12-hour dark cycle, and given water and feed as recommended [21]. The rats were divided into 5 groups of ten according to intervention as follows: group I received intraperitoneal gentamicin (36.5 mg/kg/day as a single dose), group

II received gentamicin plus alpha-lipoic acid (100 mg/kg/day as a single dose), group III received intraperitoneal gentamicin plus intraperitoneal alpha-lipoic acid (200 mg/kg/day as a single dose), group III received intraperitoneal gentamicin plus oral vitamin E (100 mg/kg/day as a single dose), and group IV served as control and received intraperitoneal NaCl 0.9%. After oral administration, the animal was kept upright for 5 minutes to avoid drug loss. Half the animals (5 rats from each group) were euthanized on day 15 (first euthanasia day), while the remaining animals were euthanized on day 60 (second euthanasia day). All animals were euthanized under anesthesia using isoflurane inhalation [22]. The study was conducted at the Departments of Pharmacology, Theriogenology, and Pathology, Faculty of Veterinary Medicine, Benha University. The faculty ethics committee approved the study with an ethical approval number of BUFVTM-080422.

Testis sampling

Immediately after euthanasia, one testis from each animal was dissected, weighed, and kept in Formation 10% (purchased from El Gomhouria Company for Trading Chemicals and Medical Appliances as formalin 34%). The formalin-preserved tissue samples were preserved in formalin for twenty-four hours and washed under running water. The washed models were dehydrated using different ascending ethanol concentrations, first using 50% concentration and finally 100% ethanol. The dehydrated tissues were fixed in xylol for 6 hours. The tissue samples were put in a soft paraffin container and left in an oven at 56°C for 12 hours. The pieces were then blocked in hard paraffin and cut into sections of about 5 microns in thickness. Paraffin was removed from the sections with absolute alcohol and washed with tap water. Sections were stained with Harris hematoxylin for 10 minutes and eosin for 5 minutes and then washed under slow-running water for 15 minutes to remove the excess stains [23]. The sections were dehydrated with two changes of absolute alcohol (five minutes each), then cleared with xylol. They were superimposed with Canada balsam and protected with cover slides to be fit for microscopical examination.

Histopathological examination

Digital photos were taken using a light microscope to evaluate the histological changes among groups after various treatments at x100, x200, and x400 magnifications. The examination included entire seminiferous tubules, spermatogenic cells and spermatogenesis, seminiferous tubule epithelium, interstitial space, subcapsular area, Sertoli cells, Leydig cells, and blood vessels.

Histometric evaluation

Cross-sections were obtained for many seminiferous tubules from different sites of one testis for each rat, and the average was calculated for each histometric measure. The following measures were obtained from the cross-sections using QuPath v.0.4.2 software [24]: 1 - Seminiferous tubule surface area (μm^2) was taken out by tracking the tubule's circumference. 2- Seminiferous epithelium height (µm) was achieved by measuring the height of the seminiferous epithelium in five different directions of each tubule and then calculating the average. 3 - Seminiferous tubule lumen area (μm^2) was achieved by obtaining the length and width of the lumen in each tubule, then calculating the lumen area as equal π multiplied by $(length/2)^2$ and $(width/2)^2$. 4 - Seminiferous epithelium area (µm2) was obtained as a difference between the seminiferous tubule surface area and lumen area [25-27]. Pixel was converted to µm at 400X magnification with a resolution of 0.25 µm/pixel[28].

Statistical analysis

Data are expressed as mean ± standard deviation (S.D.) and compared among groups using one-way ANOVA using IBM® SPSS® v.26 software. For post hoc pairwise comparisons, Tukey's test was used at a 0.05 level of significance. The mean difference (M.D.) ± standard error (S.E.) was used to show the difference between pairs in the post hoc comparison. The ANOVA assumptions were ensured, including normality, independence, and homoscedasticity [29].

RESULTS

Histopathological examination (first euthanasia day)

Typical tunica albuginea structure, intact seminiferous tubules, preserved interstitial tissue, and active spermatogenesis were observed throughout the study of gonads obtained from control group rats (Figure 1A).

Testes treated with gentamicin showed various pathological alterations as follows: some seminiferous epithelium had vacuoles in their cytoplasm (Figure 1B), a reduction of spermatogenic cells number that lined seminiferous tubules, accompanied by incomplete spermatogenesis and absence of sperm cells in the lumen of some tubules with mild inter-tubular edema (Figure 1C), prominent subcapsular blood vessels congested with subcapsular edema (Figure 1D) as well as inter-tubular edema (Figure 1E), were found. Furthermore, the seminiferous tubules had atrophy characterized by a decrease in the size of the tubules with increasing distance from one another, with variable degrees of degeneration of some seminiferous tubules (Figures F-H) in the form of a reduction of germinal epithelial cells.

In the meantime, an improvement in the testes of animals treated with gentamicin plus 100 mg/kg of alpha-lipoic acid for 2 weeks was detected. The microscopic analysis demonstrated relatively less pronounced histological alterations than the group administered with gentamicin alone over the same duration, as the majority of the seminiferous tubules were compact with one another, the tunica albuginea appeared to be expected (Figure 2A), and the spermatogenic layers appeared close to normal with typical spermatogenesis in most tubules (Figure 2B). Occasionally, the testes of only two cases showed mild degenerative changes in the spermatogenic cells of some seminiferous tubules in the form of swollen, pale, and vacuolated cytoplasm of the lining epithelium (Figure 2C).

The histopathological examination of the testes treated with gentamicin plus 200 mg/kg of the alpha-lipoic acid group revealed marked improvement with complete spermatogenic cells. Most of the seminiferous tubules restored their typical structure (Figure 2D), and the spermatogenesis processes are standard; only mild inter-tubular edema (Figure 2E), as well as degeneration of spermatogenic series, was demonstrated in some seminiferous tubules of the testes of one examined animal (Figure 2F).

On the other hand, microscopically examining the testes of animals treated with gentamicin plus vitamin E revealed less prominent changes than those treated with gentamicin alone. The majority of the seminiferous tubules were compact with one another, and the tunica albuginea approximated the typical structure in most examined animals (Figure 2G); hence, except for specific seminiferous tubules that had modest degeneration of the lining epithelial cells along with sub-capsular and inter-tubular edema, most of the seminiferous tubules recovered their standard histological architecture. The spermatogonia exhibited signs of degradation, characterized by the presence of cytoplasmic vacuoles and the shedding of many spermatocytes into the lumen of the seminiferous tubules, along with some seminiferous tubular epithelial necrosis with incomplete spermatogenesis (Figure 2H).

Histopathological examination (second euthanasia day)

The histopathological examination of testicular tissues in all investigated groups showed the standard histological structure of tunica albuginea, seminiferous tubules, and interstitial tissue (Figure 3A) with typical spermatogenesis (Figure 3B). However, mild degenerative changes in seminiferous tubules in association with mild sub-capsular and inter-tubular edema (Figure 3C & 3D) were demonstrated in some seminiferous tubules of rats treated with gentamicin alone

Histometric results

As shown in Table 1, the histometric evaluation of testes obtained from rats on the first euthanasia day revealed that seminiferous tubule diameter did not significantly differ among groups treated with gentamicin, gentamicin + 100 mg/kg of alpha-lipoic acid, and the control group. However, groups treated with gentamicin + 200 mg/kg of alpha-lipoic acid or gentamicin + vitamin E exhibited larger diameters with M.D. ± S.E. of 78.9 ± 11.4 104.6 ± 11.4, respectively, compared to the control.

Seminiferous tubule height was reduced in rats treated with gentamicin compared to the control (16.6 ± 4.1). However, the group treated with 100 mg/kg of alpha-lipoic acid showed a nonsignificant mean difference compared to the control. Moreover, groups treated with gentamicin + 200 mg/kg of alpha-lipoic acid or gentamicin + vitamin E had higher values than the control (21.5 ± 4.1, 23.9 ± 4.1, respectively).

Seminiferous tubule cross-sectional area did not significantly differ among groups treated with gentamicin, gentamicin + 100 mg of alpha-lipoic acid, and the control group. However, groups treated with gentamicin + 200 mg/kg of alpha-lipoic acid or gentamicin + vitamin E exhibited larger areas (47293.4 ± 2598, 53360.6 ± 2598, respectively) than the control group.

The luminal area was increased (10196.6 ± 2777.9), and the seminiferous epithelial area was reduced (4855.8 ± 2150.7) with gentamicin treatment compared to the control group. These changes were normalized with 100 mg/kg of alpha-lipoic acid co-treatment. However, higher values were obtained with vitamin E or 200 mg/kg of alpha-lipoic acid treatment.

The seminiferous epithelial area ratio and seminiferous epithelial height ratio were reduced with gentamicin treatment compared to the control group (0.134 ± 0.03, 0.065 ± 0.015, respectively). However, the proportions were normalized with 100 mg or 200 mg/kg of alpha-lipoic acid or vitamin E co-treatment, and there was no significant difference between the co-treated groups and the control group.

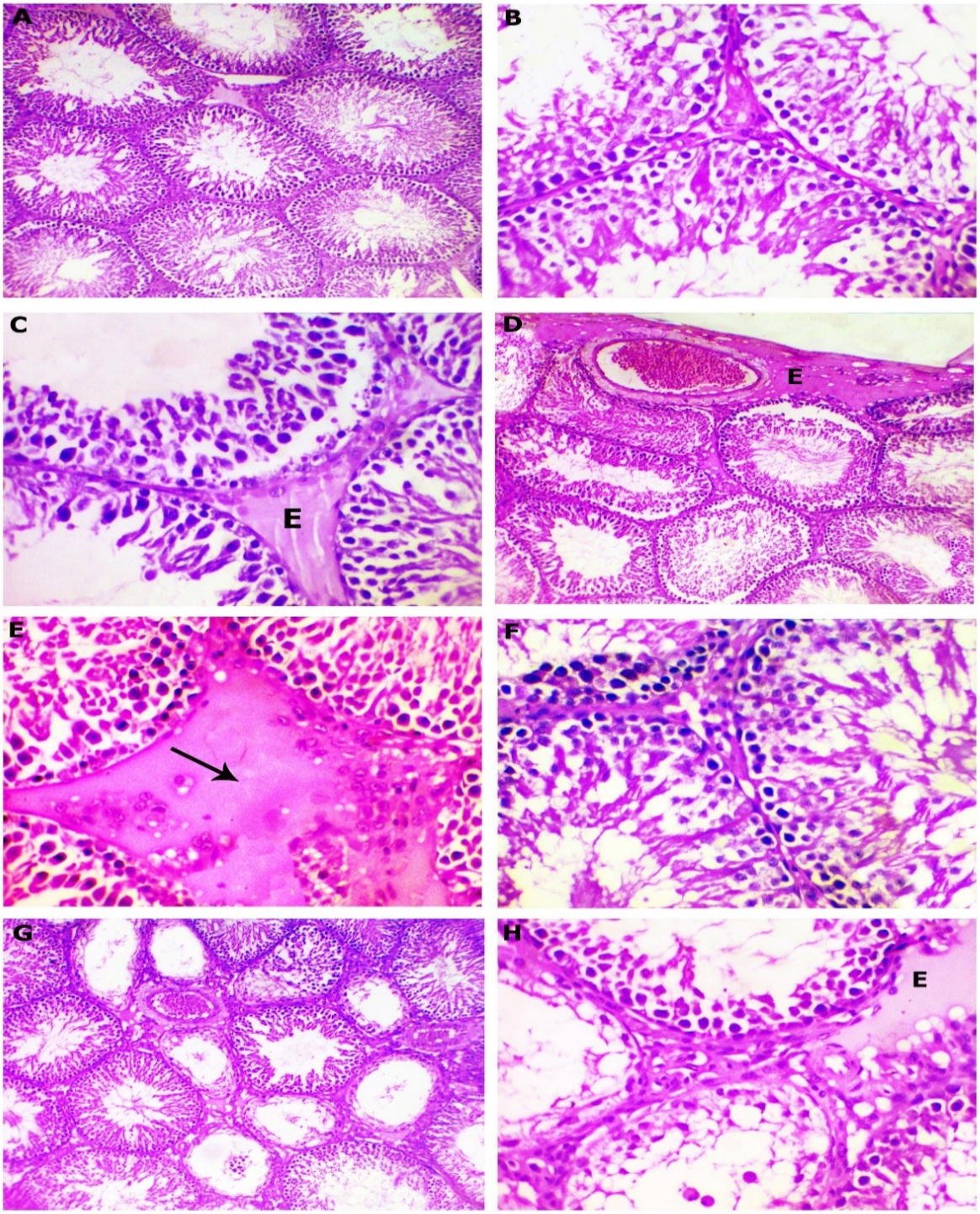

Figure 1: H&E stained section of testes obtained from rat, post administration of placebo (A) and gentamicin for 2 weeks (B-H), showing (A), typical histological structure of seminiferous tubules with active spermatogenesis (x100), (B) swollen, pale, and vacuolated cytoplasm of the lining epithelium of some seminiferous tubules (x400), (C) reduction in the number of spermatogonial cells lined seminiferous tubules with incomplete spermatogenesis and absence of spermatozoa in the lumen of some tubules with mild inter-tubular edema (E, x400), (D) marked congestion of subcapsular blood vessels with subcapsular edema (x100), (E) inter-tubular edema (arrow, x400), (F) degenerated germ cells (x400), (G), degeneration and necrosis of the lining epithelial cells of some seminiferous tubule (x100), (H), extensive degeneration of the lining epithelium of seminiferous tubules with mild inter-tubular edema (E, x400).

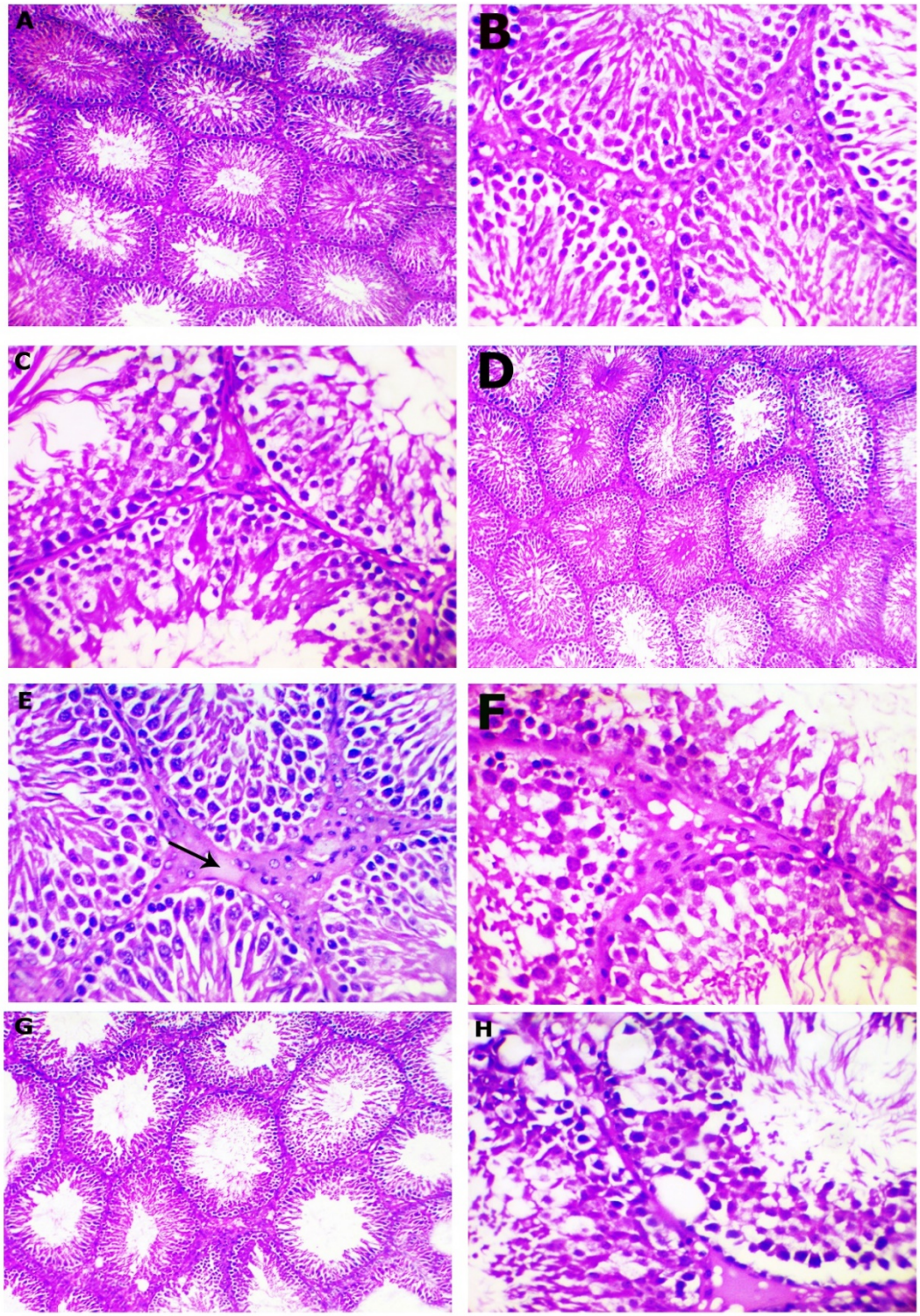

Figure 2: H&E-stained section of testes obtained from rat, post administration of gentamicin plus 100 mg A.L.A. (A-C), and gentamicin plus 200 mg A.L.A. (D-F) and gentamicin plus vitamin E (G-H) for 2 weeks, showing (A), normal seminiferous tubules and compact with each other (x100), (B), most of the seminiferous tubules showed regular spermatogenic layers and normal spermatogenesis (x400), (C), swollen, pale, and vacuolated cytoplasm of the lining epithelium of some seminiferous tubules (x400), (D), Most of the seminiferous tubules restored their typical histological structure (x100), (E), normal spermatogenesis with mild inter-tubular edema (arrow, x400), (G), the seminiferous tubules were compact with each other. The spermatogenic layers appeared somewhat normal (x100), (H), and cytoplasmic vacuolization with necrosis of some seminiferous tubular epithelium (x400).

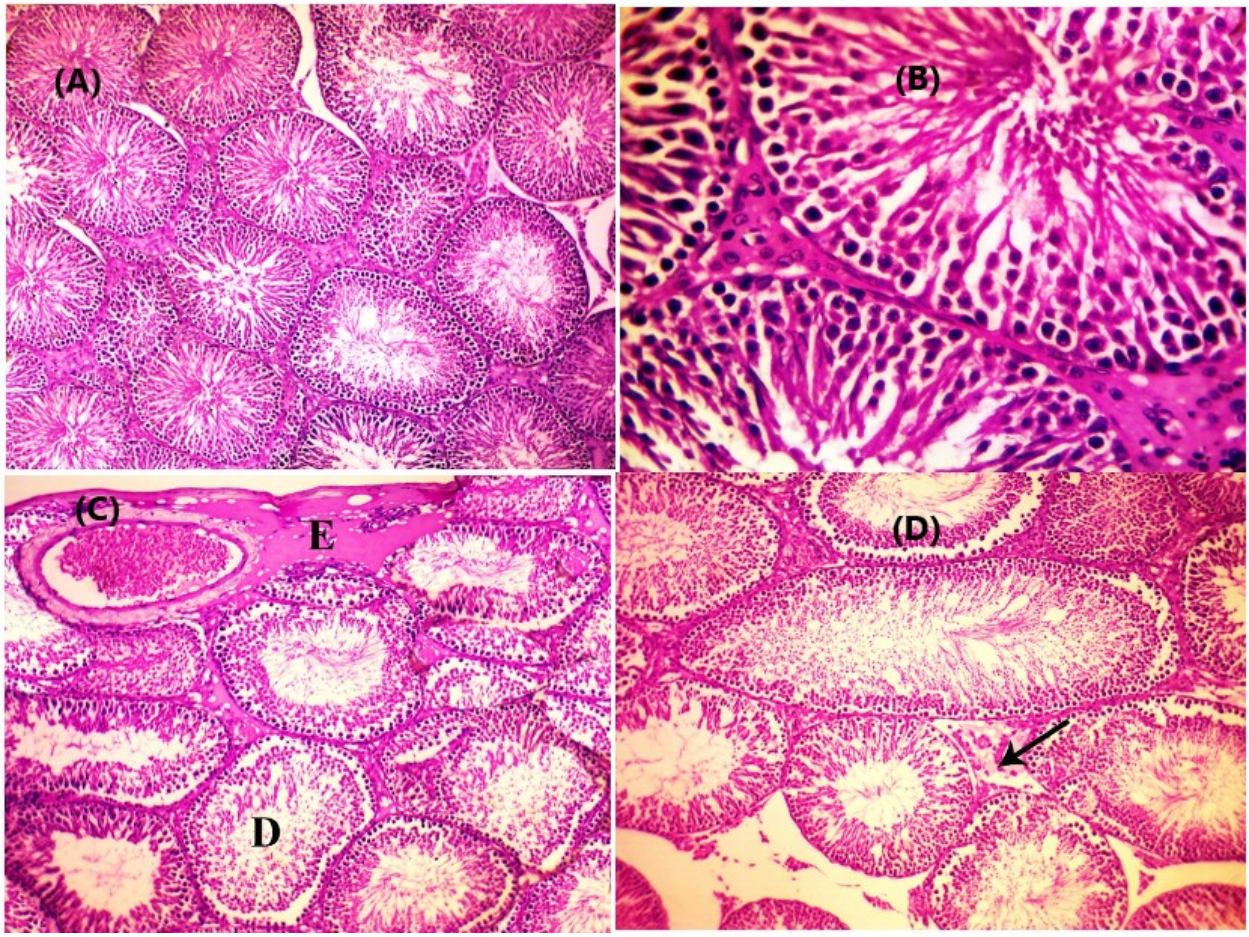

Figure 3: Testes of rats treated with gentamicin were obtained on the second euthanasia day; (A): Testes showed typical histological structures of seminiferous tubules and interstitial tissues. H&E stain x 100. (B): Testes of rats showing normal spermatogenesis. H&E stain x 400. (C): Testes of rats show sub-capsular edema "E" with degeneration of spermatogenic cells of some seminiferous tubules "D." H&E stain x 100. (D): Testes of rats show inter-tubular edema (arrow) with degeneration of spermatogenic cells of seminiferous tubules "D." H&E stain x 100.

Metrics	Control		Group I		Group II		Group III		Group IV	
	Mean	SD	Mean	SD	Mean	SD	Mean	SD	Mean	SD
STD	266.3[a]	12.8	271.0[a]	5.4	268.8[a]	14.9	345.2[b]	24.0	370.8[b]	25.4
SEH	56.7[a]	4.5	40.1[b]	2.6	63.5[a]	7.5	78.2[c]	8.9	80.6[c]	6.9
S. area	55552[a]	1501	60893[a]	2000	52681[a]	2966	92234[b]	7382	92234[b]	3853
L. area	19407[a]	1856	29604[b]	4479	17035[a]	2937	35206[bc]	5659	38439[c]	5683
SE. area	36145[a]	1846	31289[a]	3403	35646[a]	3911	67639[b]	3105	70474[b]	4230
A. ratio	0.651[a]	0.031	0.515[b]	0.063	0.676[a]	0.057	0.659[a]	0.033	0.648[a]	0.045
H. ratio	0.213[a]	0.009	0.148[b]	0.009	0.237[a]	0.034	0.227[a]	0.023	0.219[a]	0.030

Table 1: Histometric evaluation of rat testes treated with gentamicin with/without alpha-lipoic acid.

Group I was treated with gentamicin alone, group II was treated with gentamicin plus 100 mg/kg of alpha-lipoic acid; group III was treated with gentamicin plus 100 mg/kg of alpha-lipoic acid, group IV was treated with gentamicin plus vitamin E, A. ratio; area ratio equals lumen area divided by seminiferous tubule area, H. ratio; height ratio equals seminiferous epithelium height divided by seminiferous tubule diameter, L. area; lumen cross-sectional area (μ), S. area; seminiferous tubule area (μ^2), S.E. Area: seminiferous epithelium area (μ^2), S.E.H., seminiferous epithelium height (μ), S.T.D.; seminiferous tubule diameter (μ). A one-way ANOVA test was carried out, followed by post hoc Tukey's test for pairwise comparison; values in the same raw with different superscript letters indicate significant differences at 0.05 level.

DISCUSSION

This study is the initial investigation aimed at examining the histopathological evidence about the protective impact of alpha-lipoic acid against gonadotoxicity induced by gentamicin. In several studies, it has been observed that administering gentamicin leads to a reduction in testis weight, alteration of sperm parameters, a decline in serum testosterone levels, and an elevation in testicular oxidative stress. Some studies evaluated the testicular histopathological effect of gentamicin and found variable detrimental effects such as reduced germ cells, spermatogenic cell necrosis, seminiferous tubule degeneration with atrophy, incomplete spermatogenesis, interstitial space expansion, veins congestion, and decreased seminiferous epithelial thickness [2, 7, 9], which is consistent with the present study findings. Some antioxidants, such as lycopene, were histopathologically investigated for their potential protective effect against gentamicin-related testicular damage and showed favorable outcomes. [7]. Interestingly, each alpha-lipoic acid and vitamin E showed a promising protective effect against testicular adverse effects of gentamicin through morphological and biochemical evidence in recent studies [17, 18]. So, the histopathological effects of gentamicin alone compared to either the gentamicin-alpha-lipoic acid combination or the gentamicin-vitamin E combination were evaluated. A comparable protective effect of alpha-lipoic acid and vitamin E and a dose-dependent protection of alpha-lipoic acid on the histological structure of rat testes treated with gentamicin were observed compared to the control. However, with 100 mg/kg of alpha-lipoic acid, the spermatogenic layers appeared somewhat normal with typical spermatogenesis

in most tubules, which might be a sufficient dose to exhibit reliable protection. Consistently, only one recent study evaluated the protective effect of alpha-lipoic acid against the testicular harmful impacts of gentamicin, seeking morphological, hormonal, and histopathological evidence. The study reported good protection of alpha-lipoic acid on the histological structure of the testis. However, the study used alpha-lipoic acid with 600 mg/kg of oral suspension dose [17]. Our results showed that gentamicin harmed spermatogenesis, which could be mitigated with either alpha-lipoic acid or vitamin E treatment. In agreement with us, a study reported decreased sperm count, altered spermatogenesis, and spermatogonia necrosis among rats treated with 5 mg/kg of gentamicin [30]. In another study, alpha-lipoic acid could restore sperm count and abnormalities associated with gentamicin treatment [18]. The histometric analysis of the present research showed an increase in the seminiferous tubule diameters among rats co-treated with high-dose alpha-lipoic acid or vitamin E, accompanied by a rise in other metrics. However, the area and height ratios showed nonsignificant differences among all groups except those treated with gentamicin alone, which exhibited lower ratios. Consistently, the negative effect of gentamicin on seminiferous tubule epithelial height was demonstrated in the histopathological examination of the present study. In agreement with our findings, a very recent study evaluated the effect of gentamicin on the seminiferous tubule epithelial thickness and reported a significant reduction with gentamicin treatment [31]. Finally, it was noticed that gentamicin-induced testicular adverse effects were reversible as the testicular tissues are highly regenerative [32]. Consistently, the reversibility of the gentamicin effect on testes was demonstrated in testis weight and hormone levels [18, 33].

Limitations

The authors faced a few limitations: using NaCl 0.9% as a control treatment rather than the original solvent of drugs used due to the unavailability of these solvents in pure forms. Another limitation was the relatively small sample size used in this experiment. However, it provided sufficient power, which was 80%.

CONCLUSIONS

In summary, it can be concluded that both alpha-lipoic acid and vitamin E have a protective role in maintaining the testicular architecture, preserving the integrity of seminiferous tubule epithelial cells, and sustaining the process of spermatogenesis in the presence of gentamicin administration. The effects of both medications have a comparable nature, rendering them suitable for application in human investigations, mainly due to their established safety profiles.

Author Contributions: Conceptualization, A.E. and M.K.; methodology, H.E., A.A., and H.M.; software, A.A. and A.E.; validation, A.E. and M.K.; formal analysis, H.E. and A.A.; investigation, A.A.; resources, A.E. and A.A.; data curation, H.E. and A.A.; writing—original draft preparation, H.E. and A.A.; writing—review and editing, H.E., A.E., and A.F.; visualization, A.A.; supervision, A.E., M.K., A.F.; project administration, A.E.

Funding: This research received no external funding.

Institutional Review Board Statement: The study was approved by the ethics committee of the faculty of veterinary medicine with an ethical approval number of BUFVTM-080422.

Data Availability Statement: The data supporting this study's findings are available from the corresponding author upon request.

Acknowledgments: I would like to acknowledge the assistance of the academic staff of the pathology department in the histopathological examinations. Their contributions greatly enriched the depth and rigor of this study.

Conflicts of Interest: The authors declare no conflict of interest.

REFERENCES

1. Kumar N, Singh AK. Trends of male factor infertility, an important cause of infertility: A review of literature. Journal of human reproductive sciences. 2015;8(4):191.
2. Aly HA, Hassan MH. Potential testicular toxicity of gentamicin in adult rats. Biochemical and biophysical research communications. 2018;497(1):362-7.
3. Darlow CA, da Costa RM, Ellis S, Franceschi F, Sharland M, Piddock L, et al. Potential antibiotics for the treatment of neonatal sepsis caused by multidrug-resistant bacteria. Pediatric Drugs. 2021;23:465-84.
4. Goodlet KJ, Benhalima FZ, Nailor MD. A systematic review of single-dose aminoglycoside therapy for urinary tract infection: is it time to resurrect an old strategy? Antimicrobial agents and chemotherapy. 2019;63(1):e02165-18.
5. Siddiqui FG, Jung S, Ali A, Prakash A, Rais H, Kumar A. Ampicillin & Gentamicin V/S 3rd Generation Cephalosporin for the Management of Community-Acquired Pneumonia in Children; A Comparative Analysis. Journal of Pharmaceutical Research International. 2021:29-35.
6. Elsawah HK, Kandiel MM, Amin AA, Mokhimar HM, El Mahmoudy A. Gentamicin and amikacin adversely affect male infertility indicated by pharmacological, andrological and pathological evidence. International Journal of Basic & Clinical Pharmacology. 2020;9(2):218.
7. Aly H. Testicular toxicity of gentamicin in adult rats: Ameliorative effect of lycopene. Human & experimental toxicology. 2019;38(11):1302-13.
8. Kim SH, Lee IC, Baek HS, Shin IS, Moon C, Kim SH, et al. Melatonin prevents gentamicin-induced testicular toxicity and oxidative stress in rats. Andrologia. 2014;46(9):1032-40.
9. Khaki A, Ghaffari Novin M, Khaki A, Fathiazad F, Khabiri M, Hossinchi J. Ultra structural study of gentamicin and ofloxacin effect on testis tissue in rats: Light and transmission electron microscopy. Afr J Pharm Pharmacol. 2009;3(4):105-9.
10. Karaman M, Budak H, Çiftci M. Amoxicillin and gentamicin antibiotics treatment adversely influence the fertility and morphology through decreasing the Dazl gene expression level and increasing the oxidative stress. Archives of physiology and biochemistry. 2019;125(5):447-55.
11. Morales AI, Detaille D, Prieto M, Puente A, Briones E, Arévalo M, et al. Metformin prevents experimental gentamicin-induced nephropathy by a mitochondria-dependent pathway. Kidney international. 2010;77(10):861-9.
12. Lesniak W, Pecoraro VL, Schacht J. Ternary complexes of gentamicin with iron and lipid catalyze formation of reactive oxygen species. Chemical research in toxicology. 2005;18(2):357-64.
13. Dutta S, Sengupta P, Slama P, Roychoudhury S. Oxidative stress, testicular inflammatory pathways, and male reproduction. International Journal of Molecular Sciences. 2021;22(18):10043.
14. Tran LV, Malla BA, Kumar S, Tyagi AK. Polyunsaturated fatty acids in male ruminant reproduction-a review. Asian-Australasian journal of animal sciences. 2017;30(5):622-37.
15. Khosrowbeygi A, Zarghami N. Fatty acid composition of human spermatozoa and seminal plasma levels of oxidative stress biomarkers in subfertile males. Prostaglandins, Leukotrienes and Essential Fatty Acids. 2007;77(2):117-21.

16. Prahalathan C, Selvakumar E, Varalakshmi P. Protective effect of lipoic acid on adriamycin-induced testicular toxicity. Clinica chimica acta. 2005;360(1-2):160-6.
17. Yahya K, Hassan AH, Nadhem H. Evaluation the Effect of Gentamicin on Fertility of Male Rats & Probable Protective Role of Lipoic Acid. Indian Journal of Public Health Research & Development. 2019;10(6).
18. Elsawah H, Mokhimar HM, Kandiel MM, Amin A, Farid AS, El-Mahmoudy A. The ameliorative effect of α-lipoic acid on testicular dysfunction induced by gentamicin. Benha Veterinary Medical Journal. 2022;42(2):104-8.
19. Tahira A, Saleem U, Mahmood S, Hashmi FK, Hussain K, Bukhari NI, et al. Evaluation of protective and curative role of α-lipoic acid and selenium in gentamicin-induced nephrotoxicity in rabbits. Pakistan Journal of Pharmaceutical Sciences. 2012;25(1).
20. Derakhshanfar A, Bidadkosh A, Kazeminia S. Vitamin E protection against gentamicin-induced nephrotoxicity in rats: a biochemical and histopathologic study. 2007.
21. Olfert ED, Cross BM, McWilliam AA. Guide to the care and use of experimental animals: Citeseer; 1993.
22. Nakatsu N, Igarashi Y, Aoshi T, Hamaguchi I, Saito M, Mizukami T, et al. Isoflurane is a suitable alternative to ether for anesthetizing rats prior to euthanasia for gene expression analysis. The Journal of Toxicological Sciences. 2017;42(4):491-7.
23. Drury R, Wallington E. Carleton's Histological Techniques (6th edn.). Carleton's Histological Techniques (6th edn) New York, Toronto, U.S.A.: Oxford University Press; 1980. p. 126 - 7.
24. Bankhead P, Loughrey MB, Fernández JA, Dombrowski Y, McArt DG, Dunne PD, et al. QuPath: Open source software for digital pathology image analysis. Scientific reports. 2017;7(1):1-7.
25. Golalipour M, Azarhoush R, Ghafari S, Gharravi A, Fazeli S, Davarian A. Formaldehyde exposure induces histopathological and morphometric changes in the rat testis. Folia morphologica. 2007;66(3):167-71.
26. Montoto LG, Arregui L, Sánchez NM, Gomendio M, Roldan ER. Postnatal testicular development in mouse species with different levels of sperm competition. Reproduction. 2012;143(3):333.
27. Kumar A, Nagar M. Histomorphometric study of testis in deltamethrin treated albino rats. Toxicology reports. 2014;1:401-10.
28. Hein AL, Mukherjee M, Talmon GA, Natarajan SK, Nordgren TM, Lyden E, et al. QuPath digital immunohistochemical analysis of placental tissue. Journal of Pathology Informatics. 2021;12(1):40.
29. Emerson RW. ANOVA assumptions. SAGE Publications Sage CA: Los Angeles, CA; 2022. p. 585-6.
30. Fetouh FA, Azab AES. Ameliorating effects of curcumin and propolis against the reproductive toxicity of gentamicin in adult male guinea pigs: Quantitative analysis and morphological study. American Journal of Life Sciences. 2014;2(3):138-49.
31. Mardatillah M, Wurlina W, Yudaniayanti IS, Plumeriastuti H, Primarizky H, Hamid IS. Moringa oleifera leaf extract restored the diameter and epithelium thickness of the seminiferous tubules of rat (Rattus norvegicus) injected with gentamicin. Ovozoa: Journal of Animal Reproduction. 2022;11(1):15-21.
32. Koizumi T, Li ZG. Role of oxidative stress in single-dose, cadmium-induced testicular cancer. Journal of Toxicology and Environmental Health, Part A Current Issues. 1992;37(1):25-36.
33. Carageorgiou HK, Stratakis CA, Damoulis PD, Varonos DD, Messari ID, Sideris AC, et al. Reversible plasma testosterone levels reduction after gentamicin administration and freund's adjuvant arthritis in rats. Indian journal of physiology and pharmacology. 2005;49(4):443.

Received: October 9th 2023/ **Accepte**d: January 15th 2024 / **Published:**15 February 2024

Citation: Elsawah H., Amin A., Mokhimar H., Kandiel M., Farid A., El-Mahmoudy A. Evaluating the protective effect of alpha-lipoic acid against gentamicin-induced gonado toxicity indicated by histopathology. Revis Bionatura 2024; 9 (1) **73**. http://dx.doi.org/10.21931/RB/2024.09.01.**73**

Additional information Correspondence should be addressed to hozaifa2005@gmail.com

Peer review information. Bionatura thanks anonymous reviewer(s) for their contribution to the peer review of this work using https://reviewerlocator.webofscience.com/

Bionatura ISSN. First 13909355 Ecuador. **Scopus coverage years**: from 2016 to the present

Bionatura
Ibero-American Journal of Biotechnology and Life Sciences

Article

In silico design of CRISPR/Cas9 guide RNA for the knockout of the phytoene desaturase gene in sweet potato (*Ipomoea batatas* L.)

Diseño *in silico* de ARN guía CRISPR/Cas9 para la inactivación del gen fitoeno desaturasa en camote (*Ipomoea batatas* L.)

Mao Yupanqui-Celestino [1], Brayan Lugo [1], Giselle Jazmin Aguilar-Balabarca [1], Allison Esmeralda Lozano-Galindo [1], Desiderio Elías Cotos-Durán [1], Carlos Roberto Pesantes-Rojas [2], Miguel Angel Aguilar-Luna-Victoria [3], Ernesto Díaz-Ronceros [4], Linder Ramírez-Viena [5,]*

[1]*Escuela Profesional de Biología con mención en Biotecnología, Facultad de Ciencias, Universidad Nacional José Faustino Sánchez Carrión, Huacho, Perú.*
[2]*Escuela Profesional de Matemática Aplicada, Facultad de Ciencias, Universidad Nacional José Faustino Sánchez Carrión, Huacho, Perú.*
[3]*Escuela Profesional de Estadística e Informática, Facultad de Ciencias, Universidad Nacional José Faustino Sánchez Carrión, Huacho, Perú.*
[4]*Escuela Profesional de Ingeniería Electrónica, Facultad de Ingeniería Industrial, Sistemas e Informática, Universidad Nacional José Faustino Sánchez Carrión, Huacho, Perú.*
[5]*Departamento de Ciencias Naturales, Facultad de Educación, Universidad Nacional José Faustino Sánchez Carrión, Huacho, Perú*
** Correspondence: Linder Ramírez-Viena (lramirez@unjfsc.edu.pe).*
Available from. http://dx.doi.org/10.21931/RB/2024.09.01.74

ABSTRACT

This study aimed to design in silico guide RNA (sgRNA) for CRISPR/Cas9-mediated knockout of the phytoene desaturase (PDS) gene in sweet potato (*Ipomoea batatas* L.). The sequence of the coding region of the *IbPDS* gene is 1791 base pairs (bp) long, and these, in turn, are equivalent to 572 amino acids. The amino acid sequence of the IbPDS gene was compared with the homologous sequences of other nearby plant species, showing that it presents a close similarity with PDS of *Ipomoea triloba* and *Ipomoea nil* with 98.60% and 97.73%, respectively. CRISPR RGEN Tools provided 113 results for the *IbPDS* gene, filtering to 24 and selecting three sgRNA sequences for the design of the gene editing vector, which were sgRNA 1 (5'-ACCTCATCAGTCACCCTGTCNGG-3'), sgRNA 2 (5'- CCTCCAGCAGCAGTATTGGTTGGTTTGNGG -3') and sgRNA 3 (5'- CTGAACTCTCCTGGTTGGTTGTTNGG -3'). The predicted secondary structures of the selected sgRNAs present efficient sgRNA structures for gene editing of the target gene. The PMH-Cas9-3xsgRNA vector for CRISPR/Cas9-mediated knockout of the *IbPDS* gene was designed *in silico* with three sgRNA sequences and one Hygromycin resistance marker.

Keywords: Gene editing, sgRNA, *IbPDS*, gene editing vector, Hygromycin**.**

RESUMEN

Este estudio tuvo como objetivo el diseñó *in silico* de ARN guía (sgRNA) para la inactivación del gen fitoeno desaturasa (PDS) mediada por CRISPR/Cas9 en camote (*Ipomoea batatas* L.). La secuencia de la región codificante del gen *IbPDS* presenta una longitud de 1791 pares de base (bp) y estos a su vez equivalen a 572 aminoácidos. Se comparó la secuencia de aminoácidos del gen IbPDS con las secuencias homólogas de otras especies vegetales cercanas, demostrándose que presenta una similitud cercana con PDS de *Ipomoea triloba* e *Ipomoea nil* con 98.60% y 97.73%, respectivamente. CRISPR RGEN Tools proporcionó 113 resultados de

sgRNA para el gen *IbPDS*, filtrando a 24 secuencias y seleccionando tres secuencias de sgRNA para el diseño del vector de edición genética, los cuales fueron: sgRNA 1 (5'-ACCTCATCAGTCACCCTGTCNGG-3'), sgRNA 2 (5'- CCTCCAGCAGTATTGGTTTGNGG -3') y sgRNA 3 (5'- CTGAACTCTCCTGGTTT-GTTNGG -3'). La predicción de las estructuras secundarias de los sgRNA seleccionados presentan estructuras de sgRNA eficientes para la edición genética del gen diana. Se diseño *in silico* el vector pMH-Cas9-3xsgRNA, vector para la inactivación del gen *IbPDS* mediada por CRISPR/Cas9 con tres secuencias de sgRNA y un marcador de resistencia a Higromicina.

Palabras claves: Edición genética, sgRNA, *IbPDS*, vector de edición genética, Higromicina.

INTRODUCCIÓN

La edición genética es una de las tecnologías más importantes para la investigación moderna. Esta implica nucleasas específicas para generar mutaciones en regiones del genoma de organismos. Así mismo, ha aumentado su desarrollo en la edición genómica basada en CRISPR (Clustered Regulary Interspaced Short Palindromic Repeats) /Cas9 (CRISPR Associated Protein 9) que ha revolucionado por completo la biotecnología[1]. Actualmente, es usada para crear mutaciones dirigidas en el genoma del organismo de interés con resultados de amplia importancia en la biología funcional.

El sistema CRISPR/Cas9 de edición genética es capaz de cortar ADN cromosómico en regiones específicas. Posterior al corte, la célula utiliza mecanismos de reparación en el corte del ADN. Estas nucleasas inducen una rotura de doble cadena (DSB) en la secuencia del gen. El DSB se repara mediante mecanismos de recombinación homóloga (HDR) o de unión no homóloga propenso a errores (NHEJ), siendo este último el más predominante, debido a que genera pérdida de información genética a través de inserciones y deleciones (indels). Si esta se produce en regiones codificantes de un gen puede resultar en pérdida de su funcionalidad[2].

CRISPR/Cas9 tiene la capacidad de generar la pérdida o ganancia de funciones de genes, expresando características de interés en plantas[3]. Actualmente la técnica de inactivación de genes mediante CRISPR/Cas9 es la más usada por su fácil manipulación y alta precisión[4]. El mejoramiento de plantas mediado por la edición genética ha permitido añadir características genéticas de interés industrial en cultivos como especies oleaginosas ricas en ácidos grasos omega 3 y el arroz de alto rendimiento[5].

Los de ARN guías (sgRNA) permiten dirigir a la enzima Cas9 a regiones específicas del ADN, estas secuencias blanco serán cortadas de manera específica. Así el diseño *in silico* de sgRNA garantizará la síntesis correcta de una nueva molécula de ARN para redireccionar a la nucleasa hacia diferentes regiones del gen de interés. En ese sentido, CRISPR se distingue de las nucleasas porque no requiere diseñar una nueva enzima por cada secuencia que se desee editar con precisión. De manera que se obtiene una alta probabilidad de variaciones genéticas que puedan alterar a genes funcionales[6].

El camote (*Ipomoea batatas* L.) es una de las especies más cultivadas en Perú, lo que ha posicionado al país como el cuarto mayor exportador a nivel mundial. La concentración alta de almidón en sus raíces hace de estas una de las principales fuentes de nutrición humana[7]. El cloroplasto es la organela que lleva a cabo la síntesis de almidón por medio de cinco enzimas centrales, además, de codificar los carotenos de pigmentación, convirtiendo al genoma plastídico en un indicador cualitativo óptimo para pruebas de edición genética[8].

El gen fitoeno desaturasa (PDS) tiene como principal objetivo la biosíntesis de carotenoides y su función compromete muchos rasgos fenotípicos característicos como el color. Incluso, la secuencia de la proteína PDS se ha mantenido evolutivamente constante a lo largo del tiempo, lo que sugiere que este gen, en específico, es de gran aporte para los métodos de edición genética[9]. Es decir, que al inducir la disfuncionalidad del gen PDS permitirá determinar de forma rápida el grado de éxito en la edición genética, ya que compromete rasgos fenotípicos de gran notoriedad en la planta. Por lo tanto, el adecuado silenciamiento genético del gen PDS en *Ipomoea batatas*, considerada una planta de gran valor alimenticio y económico, aportará en el conocimiento global en edición genética, que es de gran interés científico, industrial y alimenticio[10].

Para el desarrollo de plantas editadas genéticamente es crucial presentar protocolos de regeneración de plantas a partir de diferentes explantes iniciales mediante el uso de metodologías de cultivo de tejidos vegetales, teniendo alternativas como la regeneración mediante callos[11,12], anteras[13], microsporas, protoplastos, callos embriogénicos[14], embriones somáticos, embriones cigóticos o directamente del explante inicial[15].

La obtención de características deseadas en las plantas mejoradas a partir de las ediciones genéticas dirigidas por CRISPR/Cas9 no transfiere transgenes al individuo, por lo que los individuos obtenidos por este método no pueden ser consideradas plantas transgénicas. Como resultado obtenemos plantas de múltiples aplicaciones comerciales. La técnica de edición libre de T-DNA puede impulsar los procesos de mejoramiento genético en plantas, por ello se verifica la respuesta de especies comerciales como la *Ipomoea batatas* al ser editadas genéticamente[16].

En este sentido, el presente estudio tiene como objetivo el diseño *in silico* de ARN guías específicos para la inactivación del gen fitoeno desaturasa del camote (*IbPDS*) mediante edición genética con el sistema CRISPR/Cas9.

MATERIALES Y MÉTODOS

Identificación de secuencias de aminoácidos del gen IbPDS

La secuencia de aminoácidos del gen fitoeno desaturasa del camote (*IbPDS*) estuvo basada en la secuencia presentada por Seo et al.[9], y se comparó con otras secuencias de aminoácidos de PDS en otros organismos que presentaron un porcentaje de similitud superior al 80%, las secuencias se obtuvieron de NCBI (http://www.ncbi.nlm.nih.gov/). Las secuencias se alinearon utilizando el programa Bioedit y se formó un árbol filogenético mediante el método de unión de vecinos (Neighbor-Joining) con 1000 repeticiones de análisis de arranque (Bootstrap) con el programa MEGA 11.

Diseño in silico de sgRNA para el gen IbPDS

El diseño de los sgRNA para la región de destino del gen *IbPDS* se realizó empleando la herramienta en línea CRISPR RGEN Tools (http://www.rgenome.net/) en el genoma *Ipomoea batatas* Pasi3. En este proceso se empleó la función Cas-Designer con el objetivo de realizar reconocimiento y mutación de cambio de marco en la secuencia objetivo. Las secuencias objetivos aptas RGEN (5' a 3') obtenidas se evaluaron con los criterios de contenido de GC entre 40% a 60%, puntuación fuera de cuadro mayor igual a 66 y desajustes de 1-0-0. Para las secuencias seleccionadas de Cas-Designer, se realizó una búsqueda potencial fuera del objetivo con la función Cas-OFFinder para evaluar su objetivo, número de objetivos encontrados, posición, desajuste y cromosoma objetivo de las secuencias on-target y off-target, seleccionado las secuencias sgRNA que posea 0 en desajustes y 1 en número de objetivos encontrados.

Predicción in silico de la estructura de sgRNA para IbPDS

La predicción de las estructuras de los sgRNA seleccionados se realizó empleando la herramienta en línea RNAfold webserver perteneciente The ViennaRNA Web Services (http://rna.tbi.univie.ac.at/#webservices). La predicción se enfocó a las estructuras secundarias de los sgRNA seleccionados en conjunto con un RNA scaffold establecido para la metodología de edición genética mediada por CRISPR/Cas9. La selección de los sgRNA basados en sus estructuras secundarias fue establecido por la formación de dos horquillas y tres bucles, en cada extremo, superior e inferior, respectivamente.

Diseño in silico del vector de inactivación del gen IbPDS mediada por CRISPR/Cas9

Con los sgRNA seleccionados se continuó con el diseño del vector edición genética del gen *IbPDS*, para esto se realizó el diseño *in silico* con el software Snapgene. Se descargo la secuencia del vector pMH-Cas9-gate (Plasmid #113742) de la plataforma virtual de addgene (https://www.addgene.org/) (Figura 1). El vector fue modificado según lo establecido por Mallet et al.[17], para la inserción de los tres sgRNA seleccionados mediante las reacciones de recombinación direccional mulisitio Gateway LR, opción integrada en el software Snapgene. Cada sgRNA previa a su inserción en el vector de destino se encuentran integrados con el promotor AtU6-26.

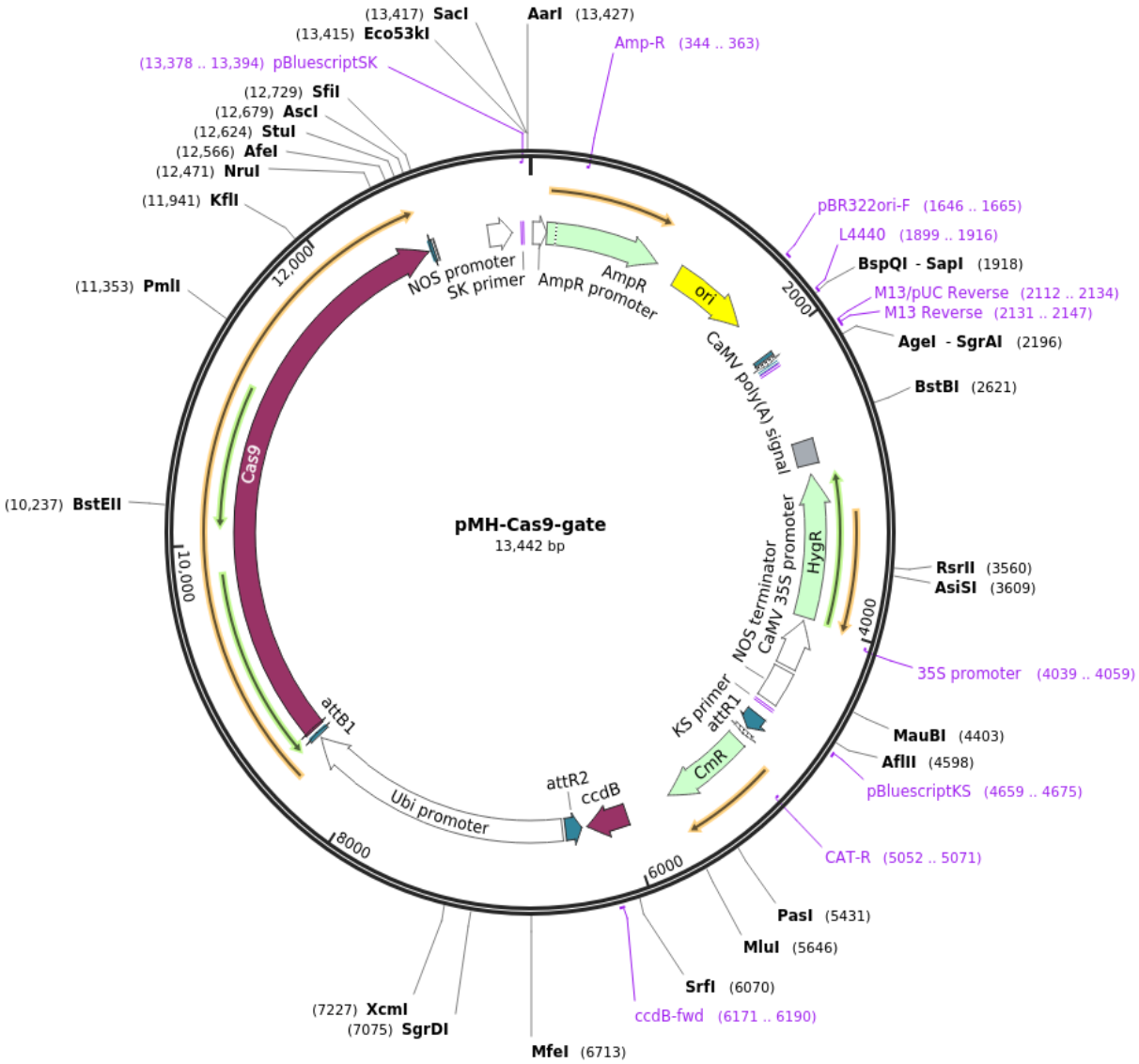

Figura 1: Mapa del vector de destino pMH-Cas9-gate que contiene los sitios Gateway.

RESULTADOS Y DISCUSIÓN

Identificación de secuencias de aminoácidos del gen IbPDS

La secuencia del fitoeno desaturasa del camote (*IbPDS*) presenta un tamaño total de 4741 bp, dividiéndose en 14 exones y 13 intrones, de los cuales 1791 bp representan su región codificante y estos a su vez equivalen a 572 aminoácidos, las cuales representan los datos obtenidos de Seo et al.[9]. La secuencia de aminoácidos de fitoeno desaturasa de camote presentó mayor porcentaje de similitud con *Ipomoea triloba* con 98.60%, seguido de *Ipomoea nil* con 97.73% y la secuencia que presentó menor porcentaje de similitud de las secuencias seleccionadas fue *Carica papaya* con 80.90% (Tabla 1). La cercanía de las secuencias de aminoácidos del gen fitoeno desaturasa en camote con *Ipomoea triloba* e *Ipomoea nil* se evidencia también en el árbol filogenético (Figura 2) y presentan similitud entre las tres especies con la presencia de gaps entre el aminoácido 15 y 23, en comparación con las otras secuencias que no presentan dicha característica (Figura 3). Este alto porcentaje de similitud entre las secuencias se atribuye a la divergencia evolutiva que presenta el camote con *Ipomoea triloba* e *Ipomoea nil*, específicamente este último presenta una divergencia del linaje que contiene con *Ipomoea triloba*, de esta manera considerando a *Ipomoea nil* como el posible ancestro común entre ambas especies[18].

N°	Accesión	Nombre científico	Abreviación del gen	Porcentaje de identidad (%)
1	XP_031092200.1	*Ipomoea triloba*	*ItPDS*	98.60
2	XP_019198822.1	*Ipomoea nil*	*InPDS*	97.73
3	VFQ70543.1	*Cuscuta campestris*	*CcPDS*	85.91
4	ABE99707.1	*Nicotiana benthamiana*	*NbPDS*	84.66
5	XP_019244024.1	*Nicotiana attenuata*	*NaPDS*	83.97
6	XP_009803390.1	*Nicotiana sylvestris*	*NsPDS*	84.14
7	AHN92038.1	*Lycium chinense*	*LcPDS*	83.79
8	XP_016498101.1	*Nicotiana tabacum*	*NtPDS*	83.97
9	KAH6821829.1	*Perilla frutescens*	*PfPDS*	82.24
10	KZV46264.1	*Dorcoceras hygrometricum*	*DhPDS*	83.10
11	XP_002264267.1	*Vitis vinifera*	*VvPDS*	82.90
12	XP_027125971.1	*Coffea arabica*	*CaPDS*	81.62
13	XP_006342880.1	*Solanum tuberosum*	*StPDS*	84.17
14	NP_001234095.1	*Solanum lycopersicum*	*SlPDS*	83.99
15	XP_021888908.1	*Carica papaya*	*CaPDS*	80.90

Tabla 1: Accesiones del gen PDS de especies vegetales seleccionadas para alineamiento múltiple de secuencias de aminoácidos para el gen *IbPDS*.

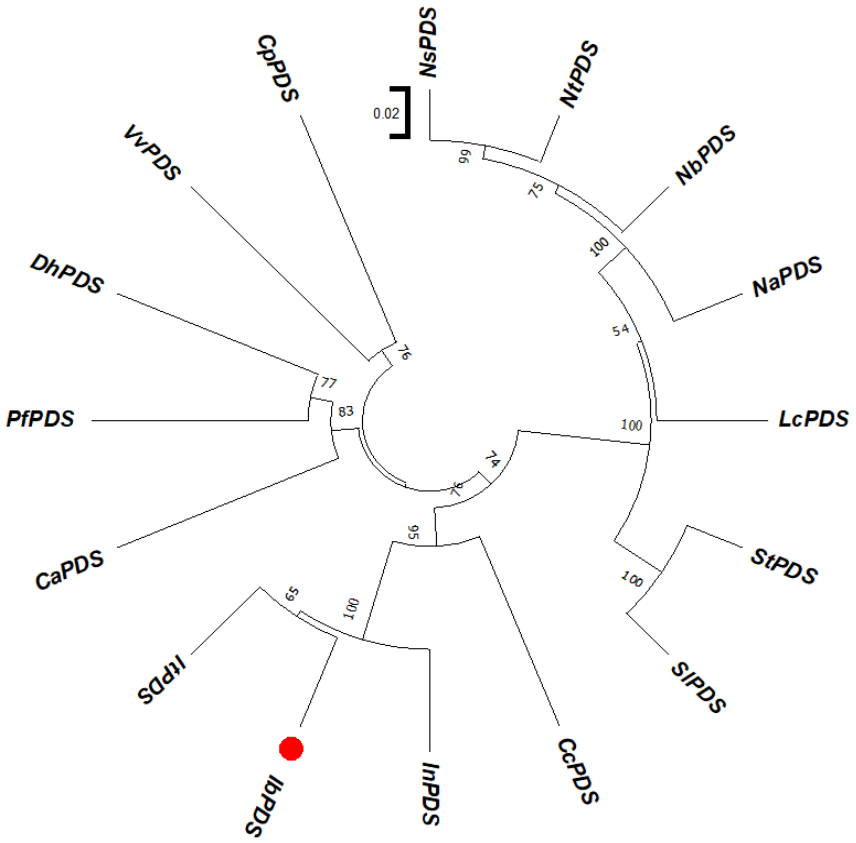

Figura 2: Análisis de árbol filogenético de unión de vecinos de la proteína PDS de camote y especies cercanas.

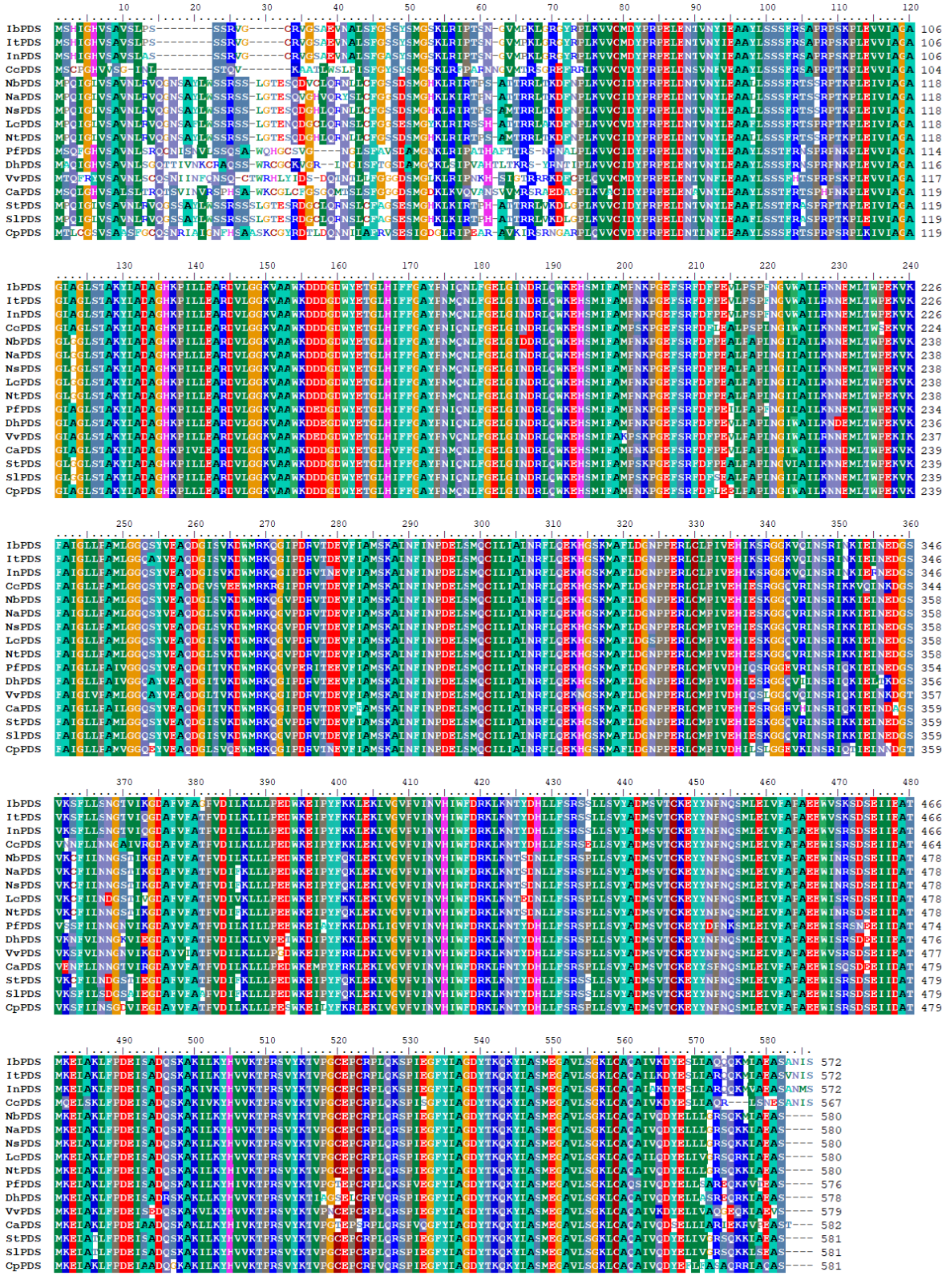

Figura 3: Comparación de las secuencias de aminoácidos de PDS de camote y especies cercanas.

Diseño in silico de sgRNA para el gen IbPDS

En el diseño *in silico* de los sgRNA se identificaron 113 secuencias candidatas para la edición genética en la región del gen *IbPDS*. Mediante el filtrado de las secuencias se redujo a un total de 24 sgRNA o RGENs

candidatos (Tabla 2), el filtrado aplicado estuvo constituido por la evaluación en 0 para Desajustes 1 y posterior se agregaron filtros adicionales en 0 para los Desajustes 1 y 2 en número de objetivos encontrados, permitiendo la reducción hasta de 19 sgRNA secuencias final.

Las consideraciones para la aplicación de filtros estuvieron basadas en Malik et al.[19], quienes mencionan que la eficacia de la escisión sgRNA se ve influida positivamente por el aumento del contenido de guanina (G) y citosina (C), pero no obstante el aumento del contenido GC disminuye las actividades de escisión notablemente. La elección de los valores de puntuación fuera de cuadro es importante elegir sitios de alta puntuación porque aumenta la probabilidad de obtener clones mutantes permanentes. Establecemos que el contenido de GC para este trabajo debe presentar un rango de 40-60% porque son valores eficientes demostrado por Bae et al.[20], siendo el primer filtro y seguido del segundo filtro mediante la aplicación discriminante de puntuación fuera cuadro de edición genómica, el cual debe presentar un valor superior a 66 como recomienda la herramienta en línea CRISPR RGEN Tools.

RGEN candidatos (5' a 3')	Posición	Posición de escisión (%)	Dirección	Contenido GC (%)	Puntuación fuera de cuadro	Desajustes		
						0	1	2
TTGCCGTCTTCCTCTAGAGTTGG	34	5	+	50	76.1	1	0	0
AACACGACAACCAACTCTAGAGG	44	4.9	-	45	71.8	1	0	0
GTGTTATGCCCAAATTAGGGAGG	146	16.2	+	45	67.6	1	0	0
TGTTATGCCCAAATTAGGGAGGG	147	16.3	+	40	75.4	1	0	0
GTTATGCCCAAATTAGGGAGGGG	148	16.4	+	45	75.1	1	0	0
TTATGCCCAAATTAGGGAGGGGG	149	16.5	+	45	69.7	1	0	0
CGGTACCCCCTCCCTAATTTGGG	154	15.9	-	55	72.1	1	0	0
CAGAACGAAATGAAGAGGACAGG	252	25.8	-	45	66.7	1	0	0
CCATTGGAAGTTGTTATTGCTGG	292	30.9	+	40	69.5	1	0	1
CCAGCAATAACAACTTCCAATGG	292	29.8	-	40	71.6	1	0	1
CCTCCAGCAGTATTGGTTTGTGG	363	36.9	-	50	75.1	1	0	0
GACGGGGACTGGTATGAGACTGG	430	44.7	+	60	66.5	1	0	0
CCGAATATACAGAACCTGTTTGG	478	49.5	+	40	73.4	1	0	1
TGATGCCTAGTTCTCCAAACAGG	492	49.8	-	45	73.4	1	1	0
GCATCAATGATCGCTTGCAGTGG	509	52.6	+	50	80.1	1	1	0
TTTGCGATGCCAAACAAACCAGG	550	56.7	+	45	73.9	1	0	0
CTGAACTCTCCTGGTTTGTTTGG	559	56.5	-	45	73.8	1	0	0
TCAAATCGGCTGAACTCTCCTGG	568	57.4	-	50	78	1	0	0
CTGTTGCCAGCAATGCTTGGTGG	691	70.8	+	55	73.6	1	0	0
ATGGGATATCTGTTAAGGACTGG	737	75.5	+	40	71.9	1	0	0
TAAGGACTGGATGAGAAAGCAGG	750	76.8	+	45	67.3	1	0	0
ACCTCATCAGTCACCCTGTCTGG	778	78.5	-	55	69.3	1	0	0
TGGCGGATTTCCGTCTAAAAAGG	914	92.1	-	45	74.8	1	0	0
ATCGGCAAGCAAAGCCTTTCTGG	934	94.1	-	50	66.4	1	0	0

Tabla 2: Secuencias de sgRNA para la edición del genómica en la región del gen *IbPDS*.

Secuencia objetivo	Cromosoma	Tamaño	Desajuste	Número de objetivos encontrados
AACACGACAACCAACTCTAGNGG	LG8	0	0	1
ACCTCATCAGTCACCCTGTCNGG	LG8	0	0	1
ATCGGCAAGCAAAGCCTTTCNGG	LG8	0	0	1
ATCGGCAAGCAAAGCCTTTCNGG	LG6	0	3	1
ATGGGATATCTGTTAAGGACNGG	LG8	0	0	1
ATGGGATATCTGTTAAGGACNGG	LG9	0	3	1
CAGAACGAAATGAAGAGGACNGG	LG8	0	0	1
CCTCCAGCAGTATTGGTTTGNGG	LG8	0	0	1
CGGTACCCCCTCCCTAATTTNGG	LG8	0	0	1
CTGAACTCTCCTGGTTTGTTNGG	LG8	0	0	1
CTGAACTCTCCTGGTTTGTTNGG	LG6	0	3	1
CTGTTGCCAGCAATGCTTGGNGG	LG8	0	0	1
CTGTTGCCAGCAATGCTTGGNGG	LG9	0	3	1
GACGGGGACTGGTATGAGACNGG	LG8	0	0	1
GTGTTATGCCCAAATTAGGGNGG	LG8	0	0	1
GTTATGCCCAAATTAGGGAGNGG	LG8	0	0	1
TAAGGACTGGATGAGAAAGCNGG	LG8	0	0	1
TCAAATCGGCTGAACTCTCCNGG	LG8	0	0	1
TGGCGGATTTCCGTCTAAAANGG	LG8	0	0	1
TGTTATGCCCAAATTAGGGANGG	LG8	0	0	1
TTATGCCCAAATTAGGGAGGNGG	LG8	0	0	1
TTATGCCCAAATTAGGGAGGNGG	LG9	0	3	1
TTGCCGTCTTCCTCTAGAGTNGG	LG8	0	0	1
TTGCCGTCTTCCTCTAGAGTNGG	LG9	0	3	1
TTTGCGATGCCAAACAAACCNGG	LG8	0	0	1

*Secuencias de color azul fueron las secuencias de sgRNA seleccionadas.
Tabla 3: Secuencias objetivo/fuera de objetivo para edición del genoma de región del gen *IbPDS*.

Los 19 sgRNA seleccionadas de la (Tabla 1) proporcionaron mediante la función Cas-OFFinder 50 secuencias objetivas (Tabla 2) con 323 sitios incisión probables en el genoma entre sitios objetivos y sitios fuera del objetivo que difieren en varios nucleótidos de los sitios en el objetivo. Mediante el filtro de las secuencias objetivos se redujo a 25 secuencias (Tabla 2), el filtro aplicado se considera las secuencias objetivo que pueden poseer "1" en número de objetivos encontrados. Además, se identificaron las 19 secuencias objetivo-finales que son equivalente a 19 sgRNA (Tabla 3), ya que poseen solo un sitio objetivo en el gen *IbPDS* ubicado en el cromosoma 8 y no poseen sitios fuera del objetivo. Cho et al.[21], mencionan que las RGEN pueden distinguir los sitios de interés de los que no lo son con desajustes de dos bases, pero no aquellos con un desajuste de una sola base. En su investigación trabajó con células K562 y demostró que dos RGENs indujeron indels en frecuencias del 75% (C4BPB) y del 60% (CCR5) en los sitios correspondientes en las células K562, además los

RGEN no pueden escindir eficientemente al DNA cromosómico si poseen desajustes de dos o más nucleótidos. Por otra parte, RGEN pueden distinguir los sitios objetivo de los sitios fuera del objetivo que difieren en al menos dos bases, permitiendo elegir sitios objetivo-únicos que no tengan secuencias homólogas en otras partes del genoma.

Predicción in silico de la estructura de sgRNA para IbPDS

Las estructuras secundarias de los tres sgRNA seleccionados fueron predichas presentando la formación de dos horquillas en el extremo superior y una doble horquilla en el extremo del tallo inferior (Figura 4). La determinación de estas estructuras secundarias es importante porque permite identificar las secuencias de sgRNA que pueden presentar variaciones estructurales que mermen la capacidad de reconocer y editar la región diana[22,23]. Sin embargo, dentro de estas potenciales variaciones, se establece la presencia de un motivo conservado en el sgRNA, que determina la formación de estructuras en forma de horquillas estables en posiciones establecidas, permitiendo la obtención de estructuras que están en concordancia con ser reconocido como un componente clave en el diseño de sgRNAs[24].

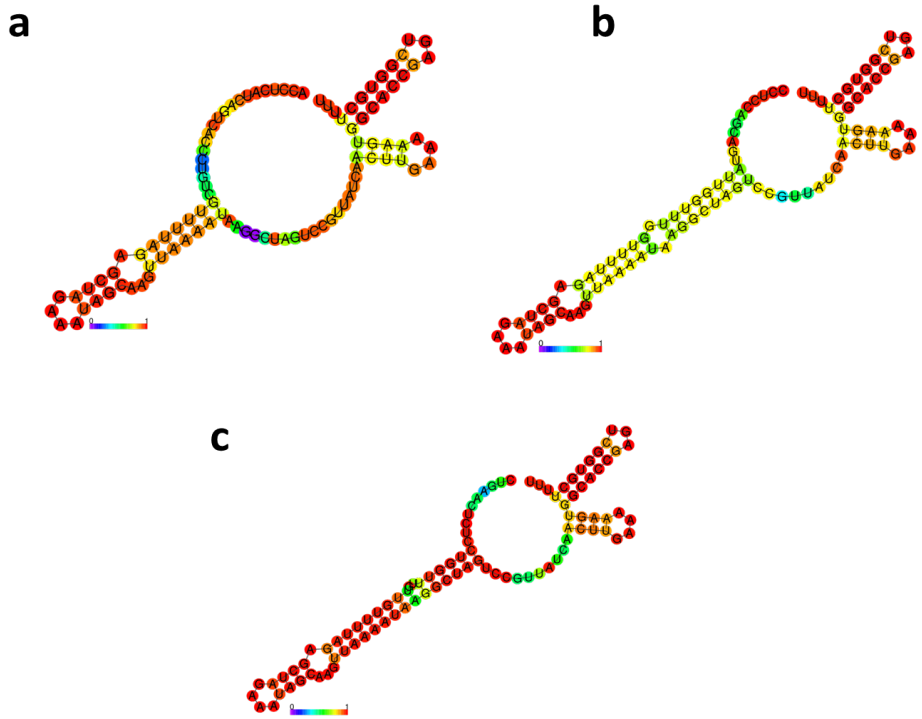

Figura 4: Estructuras secundarias de los sgRNA para la edición genética del gen *IbPDS*: (a) sgRNA 1, (b) sgRNA 2 y (c) sgRNA 3.

Diseño in silico del vector de inactivación del gen IbPDS mediada por CRISPR/Cas9

Se diseñó el vector de destino pMH-Cas9-3xsgRNA para la edición genética del gen *IbPDS*, la inserción de los tres sgRNA se realizó *in silico* mediante las reacciones de recombinación direccional mulisitio Gateway LR, específicamente en los sitios *att1* y *att2* del vector inicial. El vector presenta, a parte de los tres sgRNA, el marcador de selección de resistencia a Higromicina, el cual cuenta con el promotor 35S; también está presente la secuencia de la endonucleasa Cas9 con su promotor Ubi y terminador 35S (Figura 5). El vector de destino fue diseñado para la transformación genética de protoplastos de camote, según la metodología establecida por Nishimaki y Nozué[25], para la obtención de los protoplastos de camote y modificada para la aplicación del vector según la metodología establecida por Steiner[26], quienes establecieron metodologías para un alto rendimiento de obtención de protoplastos y la regeneración de pequeñas colonias a partir de los protoplastos hasta obtener plantas completas, así como una eficiencia de transformación cercano al 90%.

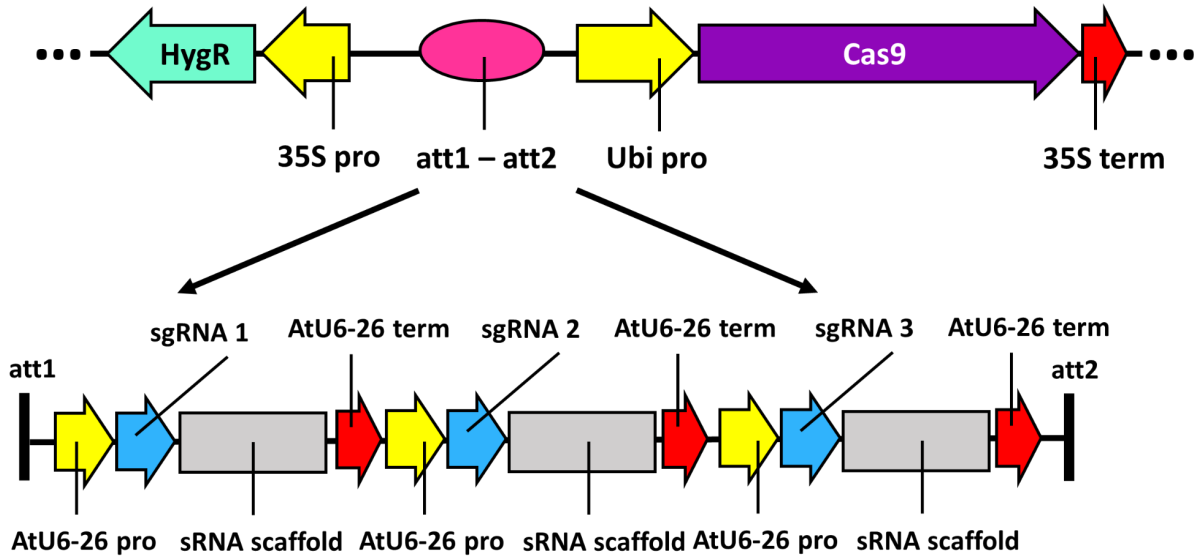

Figura 5: Mapa del vector de destino pMH-Cas9-3xsgRNA para la edición genética del gen *IbPDS*.

El diseño de vectores *in silico*, es una herramienta que permite predecir con precisión los sitios de restricción necesarios para la inserción de la máquina de edición genética, como es el caso de los tres sgRNA con sus respectivos promotores y terminadores. En otras investigaciones también utilizan SnapGene como herramienta para la construcción de un vector de expresión insertado con la secuencia de sgRNA pero en este caso emplearon un promotor T7 y otros promotores virales que codifican tanto el sgRNA como la proteína Cas12[27]. Este tipo de herramientas computacionales permite manipular las secuencias que codifican genes para la proteína Cas como para las resistencias a antibióticos, lo que representa una ventaja a tener en cuenta para las futuras etapas experimentales en laboratorio, evitando de esta manera futuros errores y por lo tanto reduciendo o evitando también perdidas en el uso de reactivos y tiempo por posibles fallos durante el clonamiento de este tipo de vectores[28]. Las herramientas del diseño de vectores *in silico* permiten además seleccionar y manipular diversos tipos de vectores, dependiendo del organismo a trabajar, así se presentan metodos efectivos para diseñar vectores de expresión transitoria o por métodos Gateway[29].

El uso de las herramientas computacionales o *in silico* son cruciales para prever la precisión y el éxito de la edición génica mediada por CRISPR/Cas9 del gen *IbPDS* en camote. Todas las herramientas utilizadas presentan el enfoque computacional, gracias a los avances y mejoras de algoritmos, el diseño de los sgRNA permite predecir la varianza individual relacionada con las actividades dentro y fuera del objetivo[30]. De esta manera los métodos *in silico* cubren las características más específicas, como el entorno de la cromatina, la accesibilidad y la expresión de exones, y ofrecen predicciones más precisas[31]. Considerando también la combinación del predictor de microhomología y la alineación local con la referencia puede allanar un nuevo camino para cuantificar las mutaciones inducidas en la secuencia del gen *IbPDS*[32]. El diseño *in silico* de sgRNA proporciona un paso clave para el sistema CRISPR y permite que los estudios CRISPR aprovechen la bioinformática y las técnicas computacionales, precisamente mediante el uso de estas herramientas computacionales se permite el diseño de sgRNA *in silico* con una alta eficacia en el objetivo y una reducción de los efectos fuera del objetivo[33].

CONCLUSIONES

Se diseñó *in silico* tres sgRNA para la inactivación del gen *IbPDS* mediada por CRISPR/Cas9. Se comparó la secuencia de aminoácidos de *PDS* de camote con otras especies vegetales y se demostró que presentan una similitud cercana con PDS de *Ipomoea triloba* e *Ipomoea nil* con 98.60% y 97.73%, respectivamente. La

predicción de las estructuras secundarias de los sgRNA seleccionados presentan estructuras de sgRNA eficientes en edición genética. Así mismo, se diseñó el vector pMH-Cas9-3xsgRNA, vector con las tres secuencias de sgRNA diseñadas. Este vector de edición genética fue diseñado mediante herramientas computacionales *in silico*, al igual que los sgRNA y las predicciones de estructuras secundarias. Estas herramientas son importantes en la predicción de la precisión y éxito de la edición genética del gen objetivo, mediante este enfoque permite a los estudios moleculares enfocados a edición genética aprovechar la bioinformática y técnicas computacionales para diseñar y predecir de manera práctica moléculas de ADN o proteínas.

Contribuciones de los autores: Conceptualización, MYC y BL; metodología, MYC, BL, GAB y ALG; software, MAALV y EDR; validación, DECD, CRPR, LRV; análisis formal, DECD, CRPR, MAALV y LRV; investigación, MYC, BL, GAB y ALG; conservación de datos, MYC y BL; redacción del borrador original, MYC, BL, GAB y ALG; redacción, revisión y edición, DECD, CRPR, EDR, MAALV y LRV; supervisión, LRV; Todos los autores han leído y aceptado la versión publicada del manuscrito.

Conflictos de intereses: Los autores declaran no tener ningún conflicto de intereses.

REFERENCIAS

1. Mojica, F.J.; Montoliu, L. On the Origin of CRISPR-Cas Technology: From Prokaryotes to Mammals. *Trends in Microbiology* **2016**, 24, 811-820.
2. Wang, H.; La-Russa, M.; Qi, L.S. CRISPR/Cas9 in Genome Editing and Beyond. *Annual Reviews in Biochemistry* **2016**, 85, 227-64.
3. Jain, A.; Zode, G.; Kasetti, R.B.; Ran, F.A.; Yan, W.; Sharma, T.P.; Bugge, K.; Seaby, C.C.; Fingert, J.H.; Zhang, F.; Clark, A.; Sheffield, A.C. CRISPR-Cas9–based treatment of myocilin-associated glaucoma. *Proc Natl Acad Sci USA* **2017**,114(42), 11199-11204.
4. Komor, A.; Kim, Y.; Packer, M.; Zuris, J.A.; Liu, D.R. Programmable editing of a target base in genomic DNA without double-stranded DNA cleavage. *Nature* **2016**, 533, 420-424.
5. Jaganathan, D.; Ramasamy, K.; Sellamuthu, G.; Jayabalan, S.; Venkataraman, G. CRISPR for Crop Improvement: An Update Review. *Front. Plant Sci.* **2018**, 9, 985.
6. Doudna, J.A.; Charpentier, E. Genome editing. The new frontier of genome engineering with CRISPR-Cas9. *Science* **2014**, 346, 1258096.
7. Oke, M.; Workneh, T.S. A review on sweet potato postharvest processing and preservation technology. *African Journal of Agricultural Research* **2013**, 8(40), 4990-5003.
8. James, M.G.; Robertson, D.S.; Myers, A.M. Characterization of the maize gene sugary1, a determinant of starch composition in kernels. *Plant Cell.* **1995**, 7(4), 417-29.
9. Seo, S.G.; Jang, H.R.; Shin, J.M.; Jun, B.K.; Shim, I-S.; Kim, S-H. Ectopic expression of ibPDS gene enhanced tolerance to oxidative stress in transgenic tobacco plants. *Plant Growth Regul* **2015**, 77, 245-253.
10. Wang, H.; Wu, Y.; Zhang, Y.; Yang, J.; Fan, W.; Zhang, H.; Zhao, S.; Yuan, L.; Zhang, P. CRISPR/Cas9-Based Mutagenesis of Starch Biosynthetic Genes in Sweet Potato (*Ipomoea Batatas*) for the Improvement of Starch Quality. *Int J Mol Sci.* **2019**, 20(19), 4702.
11. Hernández-Amasifuen, A.D.; Cortez-Lázaro, A.A.; Argüelles-Curaca, A.; Díaz-Pillasca, H.B. *In vitro* callogenesis of peach (*Prunus persica* L.) var. Huayco rojo from leaf explants. *Ciencia Tecnología Agropecuaria* **2021**, 23(1), e2032.
12. Hernández-Amasifuen, A.D.; Argüelles-Curaca, A.; Cortez-Lázaro, A.A.; Díaz-Pillasca, H.B. *In vitro* induction of callus from foliar explants in rocoto (*Capsicum pubescens* Ruiz & Pav.). *Granja* **2021**, 34(2), 127-135.
13. Hernández-Amasifuen, A.D.; Pineda-Lázaro, A.J.; Díaz-Pillasca, H.B. *In vitro* anther culture of rocoto (*Capsicum pubescens* Ruiz & Pav.). *Idesia* **2022**, 40(1), 115-121.
14. Pineda-Lázaro, A.J.; Hernández-Amasifuen, A.D.; Díaz-Pillasca, H.B. The efficient procedure of embryogenic callus formation from anther in *Capsicum pubescens* Ruiz & Pav. *Bionatura* **2023**, 8(1), 29.
15. Hernández-Amasifuen, A.D.; Pineda-Lázaro, A.J.; Díaz-Pillasca, H.B. *In vitro* micropropagation of sour orange (*Citrus aurantium* L.) from nodal segments. *Bionatura* **2021**, 6(4), 2216-2221.

16. Gao, X.; Chen, J.; Dai, X.; Zhang, D.; Zhao, Y. An Effective Strategy for Reliably Isolating Heritable and Cas9-Free Arabidopsis Mutants Generated by CRISPR/Cas9-Mediated Genome Editing. *Plant Physiol.* **2016**, 171(3), 1794-1800.
17. Mallett, D.R.; Chang, M.; Cheng, X.; Bezanilla, M. Efficient and modular CRISPR-Cas9 vector system for Physcomitrella patens. *Plant Direct.* **2019**, 3, 1-15.
18. Wu, S.; Lau, K.H.; Cao, Q.; et al. Genome sequences of two diploid wild relatives of cultivated sweetpotato reveal targets for genetic improvement. *Nat Commun* **2018**, 9, 4580.
19. Malik, A.; Gul, A.; Munir, F.; Amir, R.; Alipour, H.; Babar, M.M.; Bakhtiar, S.M.; Paracha, R.Z.; Khalid, Z.; Hayat, M.Q. Evaluating the cleavage efficacy of CRISPR-Cas9 sgRNAs targeting ineffective regions of Arabidopsis thaliana genome. *PeerJ* **2021**, 9, e11409.
20. Bae, S.; Kweon, J.; Kim, H. et al. Microhomology-based choice of Cas9 nuclease target sites. *Nat Methods* **2014**, 11, 705-706.
21. Cho, S.W.; Kim, S.; Kim, Y.; Kweon, J.; Kim, H.S.; Bae, S.; Kim, J-S. Analysis of off-target effects of CRISPR/Cas-derived RNA-guided endonucleases and nickases. *Genome Res.* **2014**, 24, 132-141
22. Robins, H.; Li, Y.; Padgett, R.W. Incorporating structure to predict microRNA targets. *Proc Natl Acad Sci USA* **2005**, 102(11), 4006-4009.
23. Konstantakos, V.; Nentidis, A.; Krithara, A.; Paliouras, G. CRISPR-Cas9 gRNA efficiency prediction: an overview of predictive tools and the role of deep learning. *Nucleic Acids Res* **2022**, 50(7), 3616-3637.
24. Wong, N.; Liu, W.; Wang, X. WU-CRISPR: characteristics of functional guide RNAs for the CRISPR/Cas9 system. *Genome Biol* **2015**, 16(1), 218.
25. Nishimaki, T.; Nozué, M. Isolation and culture of protoplasts from high anthocyanin-producing callus of sweet potato. *Plant Cell Rep* **1985**, 4(5), 248-251.
26. Steiner, J. Protoplast isolation and transformation in sweetpotato. Faculty of Engineering, Lund University, Lund, Suecia, **2022**.
27. Karlapudi, A.; Thirupati, C.; Srirrama, K.; Nageswaran, D.; Mikkili, I.; Ayyagari V. Design of CRISPR-Based Targets for the Development of a Diagnostic Method for SARS-CoV-2: An in Silico Approach. *EJMO* **2020**, 4(4), 304-308.
28. Hernández-Amasifuen, A.D.; Yupanqui-Celestino, M.; Pineda-Lázaro, A.J.; Delgado-Mera, E.; Ramírez-Viena, L.; Pesantes-Rojas, C.R.; Corazon-Guivin, M.A. *In silico* design of sgRNA for CRISPR/Cas9-mediated *FaRALF33* gene mutagenesis to decrease the infection process to *Colletotrichum acutatum* in strawberry. *J App Biol Biotech* **2024**, 12(3), 1-8.
29. Alburqueque-Vasquez, N.J.; Hernández-Amasifuen, A.D.; Pineda-Lázaro, A.J.; Fernández Ponce, J.N.; Guerrero-Abad, J.C.; García, L.; Corazon-Guivin, M.A. Response of the transcription factor BABY BOOM of Arabidopsis thaliana L. in the formation of embryogenic calluses of cocoa leaves (*Theobroma cacao* L.). *Scientia Agropecuaria* **2023**, 14(3), 359-366.
30. Canver, M.C.; Lessard, S.; Pinello, L.; Wu, Y.; Ilboudo, Y.; Stern, E.N. Variant-aware saturating mutagenesis using multiple Cas9 nucleases identifies regulatory elements at trait-associated loci. *Nat Genet* **2017**, 49, 625-34.
31. Lessard, S.; Francioli, L.; Alfoldi, J.; Tardif, J.C.; Ellinor, P.T.; Macarthur, D.G. Human genetic variation alters CRISPR-Cas9 on- and off-targeting specificity at therapeutically implicated loci. *Proc Natl Acad Sci USA* **2017**, 114, E11257-66.
32. Liu, G.; Yin, K.; Zhang, Q.; Gao, C.; Qiu, J.L. Modulating chromatin accessibility by transactivation and targeting proximal dsgRNAs enhances Cas9 editing efficiency in vivo. *Genome Biol* **2019**, 20, 145.
33. Zhang, Y.; Zhao, G.; Ahmed, F.Y.H.; Yi, T.; Hu, S.; Cai, T.; Liao, Q. In silico Method in CRISPR/Cas System: An Expedite and Powerful Booster. *Front Oncol* **2020**, 10, 584404.

Received: October 9th 2023/ **Accepte**d: January 15th 2024 / **Published:**15 February 2024

Citation: Yupanqui-Celestino M., Lugo B., Aguilar-Balabarca G. J., Lozano-Galindo A. E., Cotos-Durán D. E., Pesantes-Rojas C. R., Aguilar-Luna-Victoria M. A., Díaz-Ronceros E., Ramírez-Viena, L. *In silico* design of CRISPR/Cas9 guide RNA for the knockout of the phytoene desaturase gene in sweet potato (*Ipomoea batatas* L.). Revis Bionatura 2024; 9 (1) **74**. http://dx.doi.org/10.21931/RB/2024.09.01.**74**

Additional information Correspondence should be addressed to lramirez@unjfsc.edu.pe
Peer review information. Bionatura thanks anonymous reviewer(s) for their contribution to the peer review of this work using https://reviewerlocator.webofscience.com/

All articles published by Bionatura Journal are made freely and permanently accessible online immediately upon publication, without subscription charges or registration barriers.
Bionatura ISSN. First 13909355 Ecuador. **Scopus coverage years**: from 2016 to the present
Publisher's Note: Bionatura stays neutral concerning jurisdictional claims in published maps and institutional affiliations.